Geological Survey of Canada
Commission géologique du Canada

PAPER
ÉTUDE   85-1B

CURRENT RESEARCH PART B
RECHERCHES EN COURS PARTIE B

Canada

(Pages 1-302)

GEOLOGICAL SURVEY OF CANADA
PAPER 85-1B

COMMISSION GÉOLOGIQUE DU CANADA
ÉTUDE 85-1B

CURRENT RESEARCH
PART B

RECHERCHES EN COURS
PARTIE B

Issued in two sections/Publiée en deux volumes:
pages 1-302 and/et pages 303-637

1985

Cover

Folding in the Neruokpuk Formation along the Firth River.
These illustrations appear in report 27 by D.K. Norris (p. 223-229).

Plissement dans la formation de Neruokpuk le long de la rivière
Firth.   Ces illustrations apparaissent dans le rapport 27 par
D.K. Norris (p. 223-229).

GEOLOGICAL SURVEY OF CANADA
COMMISSION GÉOLOGIQUE DU CANADA

DIRECTOR GENERAL
DIRECTEUR GÉNÉRAL
R.A. Price

Administrative Services
Services administratifs
Y. P. Claude

Personnel Services
Services du personnel

Financial Services
Services financiers

Special Advisor
Conseiller spécial
J.A. Maxwell

CHIEF GEOLOGIST
GÉOLOGUE EN CHEF
J. G. Fyles

International Relations Unit
Services des relations internationales

Mineral Development Programs Unit
Service des programmes de mise en valeur des ressources minérales

Program Office
Bureau de planification
D. G. Benson

Special Projects
Projets spéciaux

CORDILLERAN GEOLOGY DIVISION
(Vancouver, B.C.)
DIVISION GÉOLOGIE DE LA CORDILLÈRE (Vancouver, C.-B.)
R. B. Campbell

Mainland Geology
Géologie continentale
Pacific Marine Geology
(Pacific Geoscience Centre)
Géologie marine du Pacifique (Centre géoscientifique du Pacifique)
Information Services
Services d'information

PRECAMBRIAN GEOLOGY DIVISION
DIVISION GÉOLOGIE DU PRÉCAMBRIEN
J. C. McGlynn

Bear-Slave
Bear-Slave
Northern Churchill
Churchill-Nord
Superior-Grenville
Supérieur-Grenville
Paleomagnetism
Paléomagnétisme
Geochronology
Géochronologie
Petrology
Pétrologie
Special Projects
Projets spéciaux

RESOURCE GEOPHYSICS AND GEOCHEMISTRY DIVISION
DIVISION GÉOPHYSIQUE ET GÉOCHIMIE APPLIQUÉES
A. G. Darnley

Resource Geochemistry
Géochimie appliquée
Resource Geophysics
Géophysique appliquée
Regional Geophysics
Géophysique régionale
Special Projects
Projets spéciaux
Technical Services
Services techniques

TERRAIN SCIENCES DIVISION
DIVISION SCIENCE DES TERRAINS
J. S. Scott

Paleoecology and Geochronology
Paléoécologie et géochronologie
Geomorphic Processes
Processus géomorphologiques
Sedimentology and Mineral Tracing
Sédimentologie et détection des minéraux
Engineering Geology
Géologie appliquée
Regional Projects
Projets régionaux

GEOLOGICAL INFORMATION DIVISION
DIVISION INFORMATION GÉOLOGIQUE
R. G. Blackadar

Scientific Editing
Publication Production
Rédaction scientifique et publication
Data Systems
Systèmes informatisés
Cartography
Cartographie
Library Services
Services de la bibliothèque
Technical Photography
Techniques photographiques
Publications
Publications

INSTITUTE OF SEDIMENTARY AND PETROLEUM GEOLOGY
(Calgary, Alta.)
INSTITUT DE GÉOLOGIE SÉDIMENTAIRE ET PÉTROLIÈRE Calgary, Alberta
W. W. Nassichuk

Petroleum Geology
Géologie pétrolière
Regional Geology
Géologie régionale
Coal Geology
Géologie du charbon
Paleontology (including Ottawa)
Paléontologie (incluant Ottawa)
Geological Information
Information géologique
Petroleum Resource Assessment Secretariat
Secrétariat d'évaluation des ressources pétrolières

ATLANTIC GEOSCIENCE CENTRE
(Darthmouth, N.S.)
CENTRE GÉOSCIENTIFIQUE DE L'ATLANTIQUE - Dartmouth, N.-É.
M. J. Keen

Eastern Petroleum Geology
Géologie pétrolière de l'Est
Environmental Marine Geology
Géologie du milieu marin
Regional Reconnaissance
Recherche régionale
Program Support
Planification

ECONOMIC GEOLOGY AND MINERALOGY DIVISION
DIVISION GÉOLOGIE ÉCONOMIQUE ET MINÉRALOGIE
D. C. Findlay

Mathematical Applications In Geology
Mathématiques appliquées à la géologie
Mineral Deposits Geology
Géologie des gîtes minéraux
Regional Metallogenic Studies
Études de la métallogénèse régionale
Regional Mineral Resource Assessment
Évaluation des ressources minérales régionales
Mineral Resource Information Services
Services d'information sur les ressources minérales
Analytical Chemistry
Chimie analytique
Mineralogy
Minéralogie

Separates

A limited number of separates of the papers that appear in this volume are available by direct request to the individual authors. The addresses of the Geological Survey of Canada offices follow:

601 Booth Street,
OTTAWA, Ontario
K1A 0E8

Institute of Sedimentary and Petroleum Geology,
3303-33rd Street N.W.,
CALGARY, Alberta
T2L 2A7

Cordilleran Geology Division
100 West Pender Street,
VANCOUVER, B.C.
V6B 1R8

Atlantic Geoscience Centre,
Bedford Institute of Oceanography,
P.O. Box 1006,
DARTMOUTH, N.S.
B2Y 4A2

When no location accompanies an author's name in the title of a paper, the Ottawa address should be used.

Tirés à part

On peut obtenir un nombre limité de "tirés à part" des articles qui paraissent dans cette publication en s'adressant directement à chaque auteur. Les adresses des différents bureaux de la Commission géologique du Canada sont les suivantes:

601, rue Booth
OTTAWA, Ontario
K1A 0E8

Institut de géologie sédimentaire et pétrolière
3303-33rd, St. N.W.,
CALGARY, Alberta
T2L 2A7

Division de la géologie de la Cordillère
100 West Pender Street
VANCOUVER, Colombie-Britannique
V6B 1R8

Centre géoscientifique de l'Atlantique
Institut océanographique de Bedford
B.P. 1006
DARTMOUTH, Nouvelle-Ecosse
B2Y 4A2

Lorsque l'adresse de l'auteur ne figure pas sous le titre d'un document, on doit alors utiliser l'adresse d'Ottawa.

GEOCHEMISTRY/GÉOCHIMIE

GEOPHYSICS/GEOPHYSIQUE

MARINE GEOSCIENCE/ÉTUDES GEOSCIENTIFIQUES DU MILIEU MARIN

MINERALOGY/MINÉRALOGIE

PALEONTOLOGY/PALÉONTOLOGIE

QUATERNARY GEOLOGY/GÉOLOGIE DU QUATERNAIRE

Inventory mapping and stratigraphic studies/Inventaire cartographique et stratigraphique

Paleoecology and geochronology/Paléoécologie et géochronologie

Sedimentology and geomorphology/Sédimentologie et géomorphologie

REGIONAL GEOLOGY/GÉOLOGIE RÉGIONALE

Appalachian region/Région des Appalaches

Arctic Islands/Archipel Arctique

Cordilleran region/Région de la Cordillère

Canadian Shield/Bouclier canadien

STRUCTURAL GEOLOGY/GÉOLOGIE STRUCTURALE

SCIENTIFIC AND TECHNICAL NOTES
NOTES SCIENTIFIQUES ET TECHNIQUES

FEDERAL-PROVINCIAL MINERAL DEVELOPMENT PROGRAMS 1984-89
AND OTHER FEDERAL PROGRAMS

PROGRAMMES FÉDÉRAUX-PROVINCIAUX DE MISE EN VALEUR DES
RESSOURCES MINÉRALES, 1984 à 1989, ET AUTRES PROGRAMMES FÉDÉRAUX

- 1 -

Anatomy of a ductile thrust zone: part of the northwest boundary of the Central Metasedimentary Belt, Grenville Province, Ontario (preliminary report)

Project 830009

S. Hanmer, R.H. Thivierge[1] and J.R. Henderson
Precambrian Geology Division

Abstract

The NW boundary zone of the Central Metasedimentary Belt in the Haliburton region is composed of at least two thrust sheets, each 3-4 km thick, bounded above and below by highly strained silicate gneisses and marble tectonic mélange. These are zones of ductile overthrusting towards the NW, along the direction of the extension lineation.

Résumé

La zone correspondant à la limite nord-ouest de la ceinture métasédimentaire Centrale dans la région de Haliburton contient au moins deux lambeaux tectoniques allochthones, épais de 3 à 4 km chacun. Des zones de gneiss silicatés et de mélange tectonique calcaire fort déformés, sous-jacents et sus-jacents par rapport aux lambeaux, sont les lieux privilégiés de chevauchements ductiles vers le nord-ouest, selon la linéation d'étirement.

---
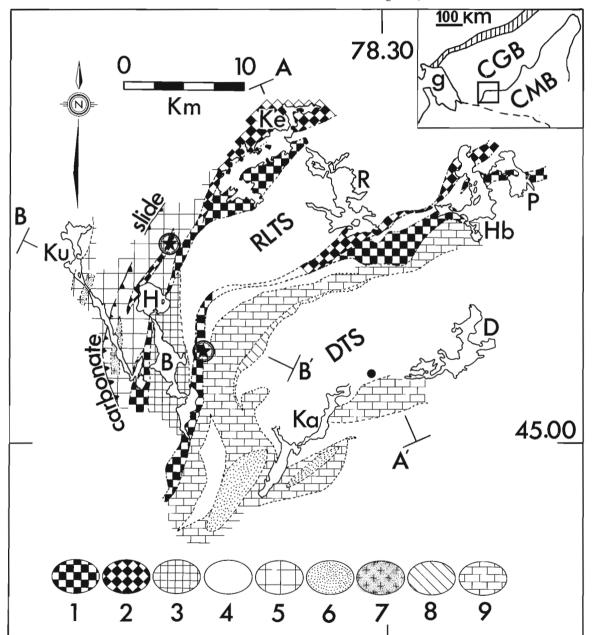
[1] Department of Geology, University of Ottawa, Ottawa, Ontario K1N 6N5

Introduction
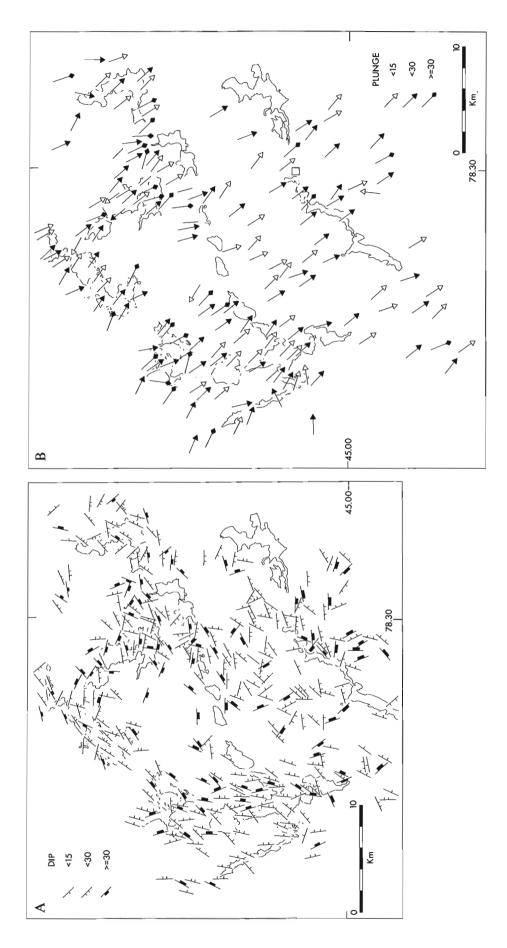
Recent 1:250 000 scale mapping in the Central Gneiss Belt (Wynne-Edwards, 1972) of the Grenville Province (Davidson et al., 1982; Culshaw et al., 1983; Davidson, 1984) has demonstrated the existence of regionally SE dipping major slices of gneiss, separated from each other by important shallow dipping ductile shear zones (see also Hanmer, 1984a) which are loci of overthrusting towards the NW. These findings raised the question of the tectonic nature of the northwestern boundary of the Central Metasedimentary Belt (Culshaw et al., 1983). An initial structural reconnaissance of the entire length of the boundary zone (Hanmer and Ciesielski, 1984) suggested that the boundary zone is a southeast dipping ductile shear, showing overthrust sense of displacement and characterized by very highly strained transposed gneisses and marble tectonic mélange. This very brief progress report concerns the second phase of this project: detailed structural mapping at 1:25 000 scale in selected parts of the Central Metasedimentary Belt boundary zone.

Field work in 1984 was located on the major deflection in strike direction of the boundary zone in the vicinity of Haliburton, Ontario (see also Culshaw, 1981; Easton and Bartlett, 1983; Easton and Van Kranendonk, 1984). Principal results are as follows:

1. The boundary zone in this region comprises two 4 km thick thrust sheets, composed mainly of homogeneous tonalitic gneiss, and bounded above and below by highly

Figure 1.1. A simplified map of tectonites in the Haliburton (dot) area. Location inset: CGB = Central Gneiss Belt; CMB = Central Metasedimentary Belt; vertical bars = Grenville Front Tectonic Zone; g = Georgian Bay; dashed line = limit of Paleozoic cover. (1) Straight gneiss (granitic and/or syenitic); (2) porphyroclastic gneiss; (3) regular quartzofeldspathic gneiss; (4) grey tonalitic gneiss; (5) irregular quartzofeldspathic gneiss; (6) meta-anorthosite; (7) late syntectonic leucogranite; (8) aluminous paragneiss (sillimanite-cordierite-garnet); (9) tectonic marble mélange. RLTS = Redstone Lake thrust sheet; DTS = Dysart thrust sheet; Lakes = Kennisis (Ke), Kushog (Ku), Halls (H), Boshkung (B), Kashagawigamog (Ka), Drag (D), Percy (P), Haliburton (Hb), Redstone (R). The toothed line is the carbonate slide. A and B are lines of section (see Fig. 1.4). Circled stars = U-Pb geochronology sampling sites (see text).

Figure 1.2. Simplified foliation (A) and extension lineation (B) maps of the Haliburton (square) area.

3

strained tectonites. These are overlain by a third sheet, the Glamorgan Gneiss (e.g. Easton and Bartlett, 1983), whose structural context remains equivocal. The Dysart thrust sheet (new name) underlies the Glamorgan Gneiss and is largely bounded by tectonic marble mélange. Beneath the Dysart thrust sheet, the Redstone Lake thrust sheet (new name) is generally bounded by anastomosing zones of transposed silicate tectonites forming large scale ductile "mesh structures" (Sibson, 1979).
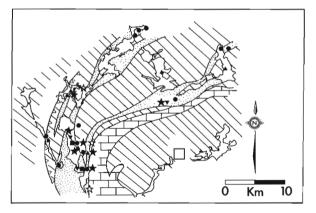
2. The entire boundary zone is underlain by a carbonate slide (ductile fault zone), up to 25 m thick in this region, lying within the irregular gneisses of the Central Gneiss Belt at 1-2 km depth below the tectonites at the base of the Redstone Lake thrust sheet.

3. The assemblage of kinematic indicators within the highly strained silicate tectonites and the carbonate slide give a consistent NW overthrust sense of movement along the remarkably constant 135° lineation direction.

4. The trend and plunge of the stretching lineation, as well as the dip of layering and of layer-parallel foliation do not vary with change in strike of the boundary zone.

The reader is referred to Hanmer and Ciesielski (1984) for terminology and to Hanmer (1984b) for a discussion of kinematic indicators.
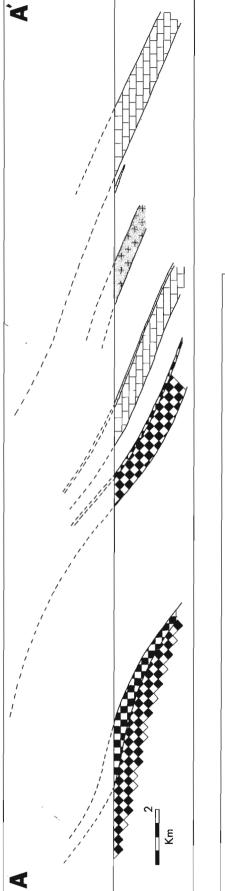
Field observations

Field results are presented in the form of maps of tectonite distribution (Fig. 1.1), foliation and lineation orientation (Fig. 1.2A, B), distribution of the assemblage of kinematic indicators (Fig. 1.3) and a series of schematic cross-sections (Fig. 1.4). In addition to the principal findings outlined above, we briefly draw attention to the following points arising from the fieldwork:
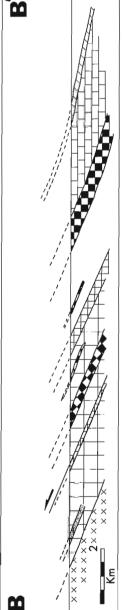
A. The Redstone Lake thrust sheet is a remarkably homogeneous, well foliated tonalitic body, carrying thin, generally concordant, sheets and discontinuous lenses of amphibolite. Such sheets and lenses indicate the high strain state of the thrust sheet itself (see below).

Figure 1.3. Distribution of kinematic indicators on a highly simplified tectonite map. Squares = 'C & S' planes (Berthé et al., 1979); triangles = shear band foliation (White et al., 1980); deltas = progressively rotated fold axial planes; solid circles = rotated winged feldspars (Hanmer, 1984b); open stars = Type 1 asymmetrical pull-aparts or "Turfs" (Hanmer, 1984b); solid stars = Type 2 asymmetrical pull-aparts or "Surfs" (Hanmer, 1984b). Highly strained tectonites (spotted), tectonic marble mélange (bricks) and homogeneous tonalitic gneiss (lined). Square = Haliburton.

Figure 1.4
Schematic cross-sections. See Figure 1.1 for legend and location. Arrow indicates carbonate slide.

4

B. The distribution of the straight and porphyroclastic gneisses on the underside of the Redstone Lake thrust sheet is discontinuous; their configuration is simplified in Figure 1.1. For example, the southeast shore of Boshkung Lake is lined by a discontinuous lens of straight gneiss. In detail, the configuration in the Halls Lake-Boshkung Lake area contains thin lenses of transposed straight and porphyroclastic gneisses set in a zone of generally highly deformed regular gneiss.

C. The straight and porphyroclastic gneisses on the upper side of the Redstone Lake thrust sheet become increasingly anastomosing northeastwards in the Haliburton-Percy Lakes area (Fig. 1.1). The tectonites separate slices of tonalitic gneiss from the lithologically identical, Redstone Lake thrust sheet below.

D. The tectonic marble mélange overlying the Redstone Lake thrust sheet and its bounding silicate tectonites contains map-scale tectonic inclusions of both tonalitic gneiss and meta-anorthosite (Fig. 1.1), of which the Dysart thrust sheet may simply be the largest. The Dysart thrust sheet is internally more complex than the underlying Redstone Lake thrust sheet. Although it is dominantly tonalitic major areas to the south and west (whose boundaries are not yet delimited) are underlain by granitic and syenitic gneisses. Its strain state is also variable. All stages from homogeneous tonalite cut by a branching network of (now) amphibolite veins, through well layered and visibly folded gneiss to perfectly concordant transposed gneiss are seen.

E. The underside of the Dysart gneiss is everywhere lined by a thin (100 m max.) band of sillimanite-garnet-cordierite paragneiss. This horizon appears to be continuous to a point due N of Haliburton and appears discontinuously at the same structural level along strike to a point south of Haliburton Lake. An identical lithology occurs in isolated outcrops on the islands of Haliburton Lake i.e. within the well developed "mesh structure" of anastomosing tectonite zones in the upper part of the Redstone Lake thrust sheet.

F. Little can be deduced from the field observations concerning relative timing of the various high strain tectonites and, consequently, about the relative timing of emplacement of the thrust sheets.

Age relations

Mapping variations in total strain state in complex gneisses which have undergone complex heterogeneous strain is not particularly fruitful unless control is available regarding the timing of events. For example, a straight gneiss formed early in a deformation can be folded and disrupted by subsequent strain increments. Therefore, Figure 1.1 is a representation of the distribution in space of zones of finite increments of high strain and not of total high strain.

O. van Breemen (GSC) has undertaken U-Pb dating of zircons from selected syntectonic granite and pegmatite sheets. The data will be published elsewhere, but late syntectonic granite from the porphyroclastic gneiss NE of Halls Lake along the underside of the Redstone Lake thrust sheet yields an age of 1060 Ma (+8/-7) while syntectonic incompletely transposed granite veins from straight gneiss east of Boshkung Lake along the topside of the same thrust sheet yield circa 1070 ma (Fig. 1.1).

Acknowledgments

We thank Danièle Spethmann and Bill Barclay for their field assistance and for braving the wildlife during the early part of the mapping. We also thank Bob and Joan Stinson of Willow Beach for their warm hospitality. Thanks to Tony Davidson and Paul Hoffman for critically reviewing the MS.

References

Berthé, D., Choukroune, P., and Jegouzo, P.
1979: Orthogneiss, mylonite and non-coaxial deformation of granites: the example of the South American shear zone; Journal of Structural Geology, v. 1, p. 31-42.

Culshaw, N.G.
1981: Precambrian geology of the Drag Lake area, Haliburton County, southern Ontario; Ontario Geological Survey, Map P. 2404, Geological Series Preliminary Map, scale 1:150 000.

Culshaw, N.G., Davidson, A., and Nadeau, L.
1983: Structural subdivisions of the Grenville Province in the Parry Sound-Algonquin region, Ontario; in Current Research Part B, Geological Survey of Canada, Paper 83-1B, p. 243-252.

Davidson, A.
1984: Identification of ductile shear zones in the southwestern Grenville Province of the Canadian Shield; in Precambrian Tectonics Illustrated, ed. A. Kroner and R. Greiling; E. Schweitz. Verlag (Stuttgart); p. 263-280.

Davidson, A., Culshaw, N.G., and Nadeau, L.
1982: A tectono-metamorphic framework for part of the Grenville Province, Parry Sound region, Ontario; in Current Research, Part A, Geological Survey of Canada, Paper 82-1A, p. 175-190.

Easton, R.M. and Bartlett, J.R.
1983: Precambrian geology of the Howland area, Haliburton, Peterborough and Victoria counties; Ontario Geological Survey, Map P. 2699, Geological Series Preliminary Map, scale 1:150 000.

Easton, R.M. and Van Kranendonk, M.
1984: Digby-Lutterworth area, Haliburton and Victoria Counties; in Summary of Field Work 1984, Ontario Geological Survey, Miscellaneous Paper 119.

Hanmer, S.
1984a: Structure of the junction of three tectonic slices; Ontario gneiss segment, Grenville Province; in Current Research, Part B, Geological Survey of Canada, Paper 84-1B, p. 109-120.
1984b: The potential use of planar and elliptical structures as indicators of strain regime and kinematics of tectonic flow; in Current Research, Part B, Geological Survey of Canada, Paper 84-1B, p. 133-142.

Hanmer, S. and Ciesielski, A.
1984: A structural reconnaissance of the northwestern boundary of the Central Metasedimentary Belt, Grenville Province, Ontario and Québec; in Current Research, Part B, Geological Survey of Canada, Paper 84-1B, p. 121-131.

Sibson, R.H.
1979: Fault rocks and structure as indicators of shallow earthquake source processes; in U.S. Geological Survey, Open File Report 79-1239, p. 276-304.

White, S.H., Burrows, S.E., Carreras, J., Shaw, N.D., and Humphreys, F.J.
1980: On mylonites in ductile shear zones. Journal of Structural Geology, v. 2, p. 175-187.

Wynne-Edwards, H.R.
1972: The Grenville Province; in Variations in Tectonic Styles in Canada, ed. R.A. Price and R.J.W. Douglas, Geological Association of Canada, Special Paper, 11.

Anatomy of a ductile transcurrent shear: the Great Slave Lake Shear Zone, District of Mackenzie, NWT (preliminary report)

Project 830008

S. Hanmer and S.B. Lucas[1]
Precambrian Geology Division

Abstract

The Great Slave Lake Shear Zone is a dextral transcurrent structure up to 25 km wide made up of four structural belts. With time, the locus of high strain rate moved outwards from the shear zone centre and metamorphic grade decreased from granulite to lower greenschist facies. The central part of the shear zone is dextral transpressive whereas the lateral or external parts are dextral transcurrent.

Résumé

Le cisaillement de Grand lac des Esclaves est une structure à décrochement dextre, comprenant quatre zones structurales dont la largeur peut atteindre jusqu'à 25 km. La localisation du taux de la déformation le plus élevé se déplace du centre vers l'extérieur du cisaillement au fur et à mesure que l'environnement métamorphique passe du faciès granulitique au faciès des schistes verts. La partie centrale de la zone decisaillement a subi une phase tectonique de transpression tandis que les flancs extérieurs ont connu une phase de décrochement. Dans les deux cas le sens du déplacement était dextre.

[1] Department of Geology, Brown University, Providence, R.I., U.S.A.

Introduction

The aeromagnetic map of the Canadian Shield west of Hudson Bay is dominated by a number of prominent NE-trending linear positive anomalies, each hundreds of kilometres in length (Geological Survey of Canada, 1984). A particularly striking example marks the SE margin of the Slave Craton at its contact with the western Churchill Province, on the SE side of Great Slave Lake. Clockwise deflection of the local N-S aeromagnetic grain in the Churchill Province suggests that such anomalies may coincide with major crustal-scale shear zones. Early mapping around the SE side of Great Slave Lake (Stockwell, 1932; Henderson, 1939; Wright, 1951, 1952) clearly indicated the main elements of the McDonald-Wilson fault system (Reinhardt, 1969; Hoffman et al., 1977), but did not identify any major ductile shear zones. Wright (e.g. 1968a, b) noted the existence of mylonites, but Reinhardt (1969) was the first to appreciate the extent of mylonite development. He mentioned that "mylonite zones up to four and five miles wide ...(are)... some of the widest zones of mylonitization so far recognized (anywhere)..." (Reinhardt, 1969, p. 20), but did not map them. He suggested that the mylonites were coeval with, and generated by, movement on the McDonald-Wilson fault system, and therefore did not attempt to relate them specifically to a ductile shear zone. However, identification of mylonite clasts in sedimentary rocks of the Great Slave Supergroup (Hoffman, 1968; Hoffman et al., 1977) suggests that the deposition and northwestward thrusting of the Great Slave Supergroup temporally separate the development of mylonites from activity on the McDonald-Wilson fault system.

Our fieldwork in 1984 (Fig. 2.1) comprised parts: A) systematic structural and lithological mapping at 1:25 000 scale in the McDonald-Laloche lakes area and B) initial systematic structural upgrading of Reinhardt's (1969) map. Our principal findings are:

1. A major crustal scale, NE-striking, ductile transcurrent shear zone, up to 25 km wide, outcrops in the McDonald-Laloche lakes area and extends to the SE shore of Great Slave Lake.
2. The shear zone comprises 4 belts of mylonitic rocks of different metamorphic grade and age of main preserved structure.
3. With time, metamorphic grade decreased from granulite facies to lower greenschist facies and the locus of maximum strain rate shifted laterally away from the core of the shear zone.
4. The shear zone is dextral with a subhorizontal movement vector throughout its deformation history.
5. The central part of the shear zone exhibits a transpressive strain regime whereas the outer parts are transcurrent.

Terminology

Mylonite Classification

Mapping in shear zones is fraught with terminological pitfalls (e.g. Zeck, 1974; White, 1982; Tullis et al., 1982). We adhere to the general definition of a mylonite given by Bell and Etheridge (1973, p. 347): "A mylonite is a foliated rock, commonly lineated and containing megacrysts, which occurs in narrow, planar zones of intense deformation. It is often finer grained than the surrounding rocks into which it grades". Attempts to refine this definition by introducing a reference to strain regime (White et al., 1980) are confuted by documented reports of mylonites produced during coaxial deformation events (Sylvester et al., 1978; Mawer, 1983; Law et al., 1984). Nevertheless the Bell and Etheridge definition presents a dialectical problem to the geologist since it depends upon the prior recognition of, at least, some

of the deformation boundary conditions of the rocks being described. In most cases the boundary conditions of the deformation are determined at a larger scale than that at which the rock descriptions are made.

The convention of mylonite typing according to the porphyroclast-matrix ratio (e.g. Higgins, 1971; Sibson, 1977), expressed here as vol. % of matrix, is well entrenched in the literature. The critical ratios are 20-50% for protomylonite, 50-90% for mylonite and > 90% for ultramylonites. The lower limit placed on protomylonites is a qualitative estimate of the minimum proportion of evenly distributed matrix at which an unequivocal porphyroclast/matrix distinction can be made in the field. This classification begs the question "What is a porphyroclast?": In his historical review of the literature, Higgins (1971, p. 7) stated that porphyroclasts are generally > 200 μ in size, implying that matrix grains are < 200 μ in diameter. This absolute grain size distinction between matrix and porphyroclast is a source of confusion in the light of Bell and Etheridge's general definition which is intentionally flexible with regard to grain size. Indeed, elsewhere in his glossary, Higgins (1971) gives a more practical definition of porphyroclast: "...a relatively large fragment...". Let the individual geologist determine the critical grain size according the local situation!

We have found, however, that this traditional classification fails to distinguish between strikingly different tectonites with sensibly different microstructural histories (Fig. 2.2); an obvious impediment to detailed mapping in shear zones. For example, a mylonitic tectonite (A) with 40% matrix containing porphyroclasts ranging in grain size from 10-0.5 mm is not discriminated from a rock (B) of similar porphyroclast-matrix ratio, but whose porphyroclasts are all about 0.5 mm in diameter. Both are protomylonites. Furthermore there are two 'end-member' microstructural routes from protolith to ultramylonite: (1) the classical protomylonite-mylonite-ultramylonite sequence resulting from a progressive decrease in the porphyroclast-matrix ratio independent of variation in porphyroclast grain size (e.g. Sibson, 1977 and Fig. 2.2D-F) and (2) the progressive decrease in uniform porphyroclast grain size at constant porphyroclast-matrix ratio, a very common feature of our study area (Fig. 2.2A-C). These two end-member routes are not mutually exclusive. We find it useful to add a mesoscopic textural qualifier which will allow inclusion of the range or uniformity of porphyroclast size in the classification of mylonites. We propose the use of the terms "hetero-porphyroclastic" (more briefly heteroclastic) and "homoporphyroclastic" (homoclastic) as adjectival qualifiers describing broad and narrow ranges of porphyroclast size respectively. Accordingly we consider case (A) to be an heteroclastic protomylonite while case (B) is an homoclastic protomylonite. The advantage of such qualifiers is that they themselves may be further qualified as relatively fine, medium or coarse, again with reference only to the size of the porphyroclasts. It follows that the sequence protomylonite ---> mylonite ---> ultramylonite (Fig. 2.2D-F) does not always apply, since in case (B) the porphyroblast/matrix distinction could vanish synchronously throughout the specimen or outcrop with increasing strain. In such a case the sequence would be fine homoclastic protomylonite ---> ultramylonite (Fig. 2.2B, C). Similar qualifiers can be applied in the case of both mylonites and ultramylonites.

Some tectonites, especially within the high grade part of the map area, are coarse- to medium-grained gneisses. It will be shown that these tectonites correspond to the mylonite definition of Bell and Etheridge (1973). However, they are distinctly coarser grained than the mylonitic tectonites of the lower grade portions of the area and often

(1) Chlorite – muscovite bearing mylonite and ultramylonite from variable prolith;

(2) biotite–bearing mylonite and ultramylonite from coarse leucogranite;

(3) finely homoclastic protomylonite from coarse leucogranite;

(4) as '3' plus abundant supracrustal assemblage and simple amphibolite inclusions;

(5) foliated coarse, biotite– or hornblende-bearing, K-feldspar megacrystic granite;

(6) irregular gneiss: low strain pod S of Hook Point, disrupted granoblastic straight gneiss at Laloche Lakes;

(7) supracrustal assemblage of paragneiss, amphibolite gneiss etc: see text;

(8) amphibolite gneiss;

(9) isotropic to poorly foliated, medium grained, homogeneous, biotite–hornblende leucocratic granite;

(10) isotropic, muscovite-bearing, leucocratic McDonald Granite. Lakes = McDonald (M); Laloche (L); Thubin (T); Gagnon (G). Informal names allocated to points = Finger (F); Hook (H); Scythe (S).

Figure 2.1 A simplified tectonite map of the Great Slave Lake Shear Zone. Dot-dash line = basement – Great Slave Supergroup contact.

9

(A) Coarse heteroclastic protomylonite derived from coarse (megacrystic ?) leucogranite, SE belt.

(B) Fine to medium homoclastic protomylonite derived from 'A'.

(C) Grey and pink fine homoclastic mylonites, the former after 'B' and the latter after clean leucogranite.

(D) Coarse heteroclastic protomylonite derived from aluminous paragneiss, NW belt. Mylonite terminology should not strictly be used to described this tectonite (see Fig. 2.7F), but we do so for the purpose of illustration.

(E) Coarse heteroclastic mylonite after 'D'.

(F) Ultramylonite after 'E', external belt.

Figure 2.2.   Illustration of mylonite terminology as used in this paper.
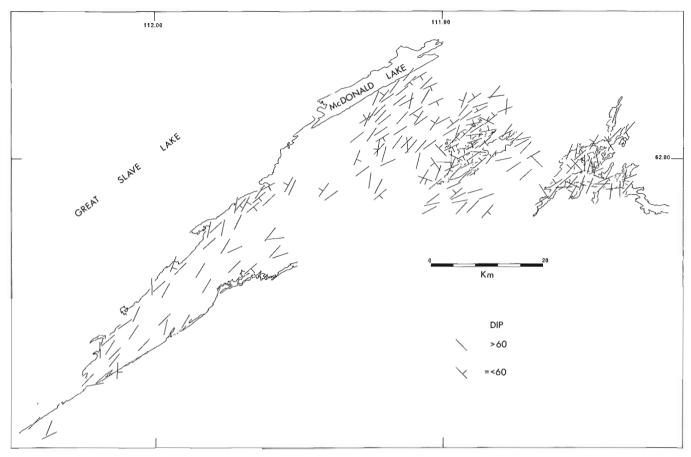
Figure 2.3. *Simplified foliation map of the Great Slave Lake Shear Zone plus part of Gagnon Lake: see text for description.*

show no porphyroclast/matrix grain size bimodality. We wish to distinguish them from the finer grained mylonites, but mylonite terminology leaves us in a quandry. Although used by some authors (e.g. White et al., 1982), the terms "coarse mylonite" or "coarse ultramylonite" may create confusion for those who still assume that mylonites and ultramylonites must be fine grained. The term "mylonite gneiss" has already been employed to designate protomylonites with large porphyroclasts (Higgins, 1971, p. 11 and p. 75). Therefore, we use the terms straight gneiss, block gneiss and irregular gneiss (see also Davidson et al., 1982; Hanmer and Ciesielski, 1984). Briefly, straight gneiss is a regular, rectilinearly banded tectonite (Fig. 2.6D, E). Block gneiss contains abundant inclusions of tectonically disrupted competent material, often amphibolite in a quartzofeldspathic matrix (Fig. 2.7E). Irregular gneiss is a gneiss with irregular shaped inclusions of variable size and mutual misorientation, often exhibiting internal intrusive and structural crosscutting relationships (Fig. 2.6A).

Supracrustal assemblage

The most important lithology in this assemblage is medium grained quartz-plagioclase-biotite gneiss, a rock of indeterminate origin. A common variant of this gneiss contains combinations of sillimanite, garnet, cordierite and K-feldspar (aluminous paragneiss). We have not yet observed the andalusite reported by Reinhardt (1969), but he may be referring to the terrane SE of Thubin Lake (see Fig. 2.1). On account of their aluminous composition and their spatial association with calcite marble and plagioclase-diopside-hornblende ± garnet calc-silicate horizons and lenses, examples of this variant are probably meta- (semi) pelites. Quartzitic layers occur but are very rare. Both the aluminous paragneiss and the quartz-plagioclase-biotite gneiss are commonly riddled with round, centimetre size isolated single feldspar inclusions, commonly of plagioclase. They may occur in trains and are visibly derived by the ductile degradation of pegmatite material (Fig. 2.7C, D). Alternatively, they occur evenly distributed throughout the rock volume (Fig. 2.2D, 2.7E), except for certain horizons marked by their total absence indicating a bulk compositional control over feldspar growth. Frequently, old plagioclase grain boundaries, marked by sillimanite inclusion trails, are overgrown by optically continuous plagioclase rims, themselves wrapped around by matrix sillimanite (Fig. 2.7F). Where porphyroblast development is extreme, lilac garnets attain unusually large (several centimetres) diameters. Thus both porphyroclasts and porphyroblasts occur; indeed the latter may themselves become porphyroclasts with progressive strain. It is obvious that classical mylonite terminology is ambiguous in such gneisses.

This paragneiss and quartz-plagioclase-biotite gneiss assemblage often contains concordant intercalations of variable thickness of well layered amphibolite gneiss and of medium grained, equigranular garnet leucogranite. The garnets of the leucogranite are markedly lilac. The gneissosity of the amphibolite gneiss reflects both grain size and compositional (diorite-amphibolite-hornblendite)

11
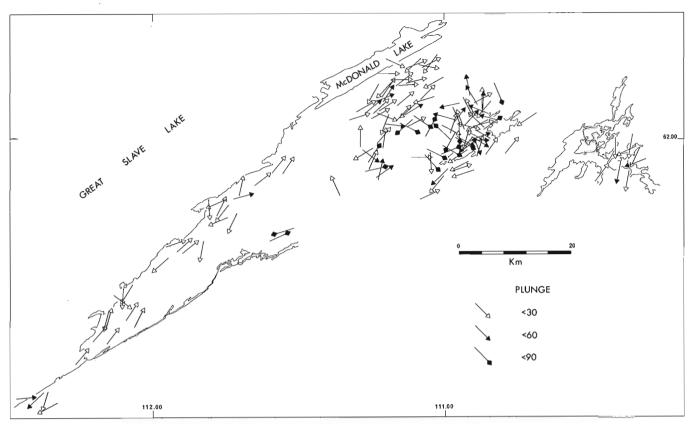
Figure 2.4. *Simplified extension lineation map of the Great Slave Lake Shear Zone: see text for description.*

variation on a centimetre to metre scale. The almost exclusive spatial association of such intercalated lithologies with the paragneisses suggests a genetic relationship. For example, are the amphibolite gneisses of supracrustal derivation? Is the garnet leucogranite the product of partial melting of aluminous metasediment? We refer to the complete association as the supracrustal assemblage.

Structural geometry

We divide the area into 4 structural belts, each characterized by similar lithologies, but structurally and metamorphically distinct. Since significant gaps remain in our mapping, we do not yet draw firm boundaries to the belts. The very narrow external belt occupies much of the shoreline of Great Slave Lake and projects inland along the SE margin of a granite terrane SE of McDonald Lake. The northwestern belt lies immediately SE of the external belt. The central belt occupies the ground around and to the NW of the Laloche Lakes. The southeastern belt, of which we have so far mapped only a small section, lies SE of the Laloche Lakes and the Laloche River. Several major areas of poorly foliated to isotropic granitic rocks either do not fall within the belts (e.g. SE of McDonald Lake) or require further mapping in order to assign them to one or other of the belts, e.g. the biotite hornblende granite between Hook and Scythe points and the Laloche River.

All of the structural belts show an upright, NE-striking main or regional foliation and layering and a shallow plunging extension lineation composed of smeared-out polycrystalline ribbons of feldspar or quartz, aligned crystals (biotite, sillimanite, hornblende) and isoclinal fold axes, except for the

central belt whose foliation and layering are highly variable in both strike and dip, especially in the vicinity of the Laloche Lakes (Fig. 2.3, 2.4). Similarly, the extension lineation is significantly steeper plunging than in the other belts. We will show below that the variable foliation orientation is due to a later disruption of the main deformation fabric. Where this disruption is least developed, the main foliation is upright and the extension lineation is steeply plunging. We present a map of lineation pitch for the area between McDonald Lake and the Laloche Lakes (Fig. 2.5) to filter out the effects of disruption and to highlight our observation that the central belt is characterized by lineations subparallel to dip, whereas the other belts show lineations subparallel to strike. The order in which the belts are now described reflects the relative timing of main deformation preserved in each.

Central belt

This belt is the most complex. It is composed of two parts: a southeastern zone of disrupted granoblastic straight gneiss, flanked to the northwest by a zone of straight gneiss. This is well illustrated by the maps of foliation orientation and lineation plunge and pitch (Figs. 2.3, 2.4, 2.5) which show a zone of variable foliation orientation and steeply plunging/pitching lineations in the Laloche Lakes area, bounded to the northwest by a zone of regular NE-striking upright foliation and equally steeply plunging lineations. The straight gneisses are derived by the deformation and transposition of a number of irregular protoliths ranging from homogeneous megacrystic granite to highly irregular quartzofeldspathic block gneiss, itself derived from a megacrystic granite parent, containing

misoriented inclusions (Fig. 2.6A). Rarely, the quartzo-feldspathic component is homogeneous and isotropic and may be a plutonic rock containing xenoliths. More typically, it is coarsely granoblastic, but nevertheless a well layered gneiss that strongly resembles the block gneisses produced by tectonic disruption and misorientation of competent lithologies in relatively incompetent quartzofeldspathic gneiss described from the Grenville Province in Ontario (Davidson et al., 1982; Hanmer and Ciesielski, 1984). For example, in the vicinity of the Laloche Lakes, aluminous paragneiss with garnet leucogranite intercalations, less aluminous nondescript quartz-plagioclase-biotite ± garnet gneiss and generally homogeneous amphibolite and calc-silicate form bands within a matrix of compositionally variable granitic-granodioritic gneiss derived from biotite-orthopyroxene foliated megacrystic granite (charnockite), medium grained homogeneous hornblende granite-granodiorite and white leucogranite with scattered lilac garnet. The charnockitic megacrystic granite can be traced progressively into mylonite of the same composition within which orthopyroxene is dynamically recrystallized and stable. However, much of the highly strained tectonite visibly derived from the megacrystic granite is a homogeneous, coarse- to medium-grained (1 mm +), granoblastic foliated granitic gneiss. It is derived from its protolith by extreme attenuation of recrystallized, layer – parallel ribbon aggregates derived from the K-feldspar megacrysts. With increasing deformation, the ribbons become difficult to distinguish mesoscopically, resulting in a seemingly bland granoblastic texture with no hand specimen or microscopic indication of the intense strains which the rock has undergone. However, the straight and parallel-sided bands of paragneiss plus trains of isolated feldspar porphyroclast from highly attenuated ductile degraded pegmatite are qualitative mesoscopic indicators of the high strains. Similar concordant bands of amphibolite may be deformed dykes and hence cannot be used in so simplistic a manner. However, where they are heterogeneously extended and are pulled apart, the extreme separation between fragments does provide a qualitative minimum indication of strain. No obvious protolith to the foliated hornblende granitic-granodioritic gneiss has been identified, but it shows mesoscopic to microscopic features similar to the deceptively bland granitic gneiss derived from the megacrystic granite.

The straight gneisses derived from the irregular protoliths described above have themselves been divided up into metre to kilometre size blocks by a combination
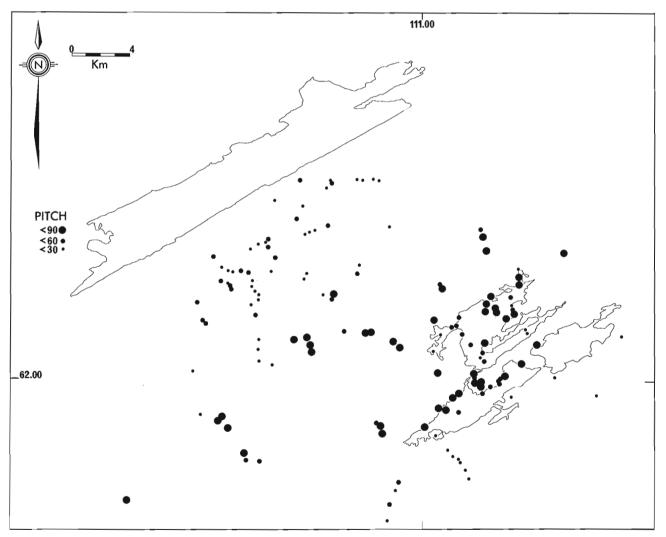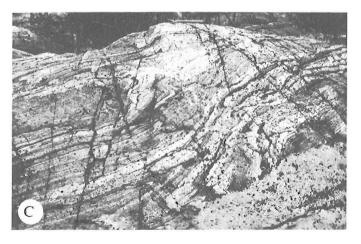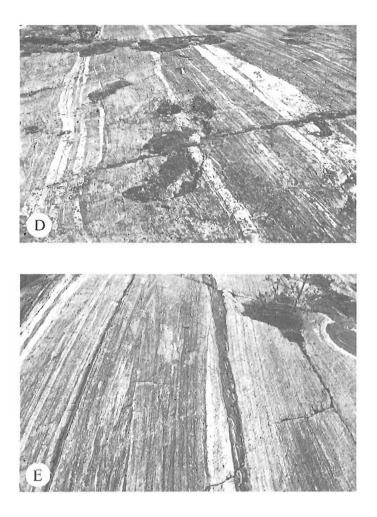
Figure 2.5. *Map of pitch of the extension lineation in the foliation plane in the McDonald Lake-Laloche Lakes area of the Great Slave Lake Shear Zone: see text for description.*
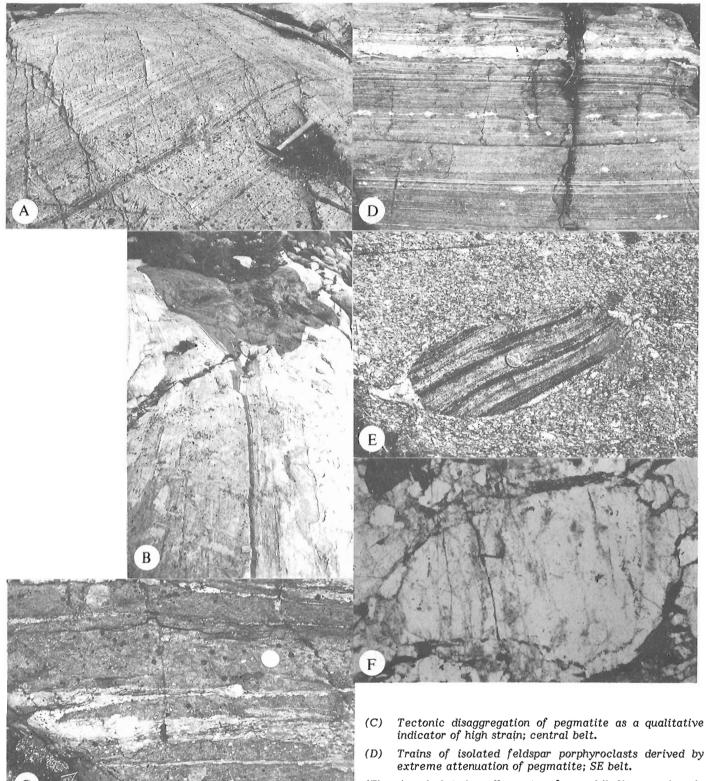
Figure 2.6

(A) Chaotic, mutually misoriented inclusions in irregular banded quartzofeldspathic gneiss. Note apparent "assimilation" of certain inclusions; central belt.

(B) Open folded, mildly foliated vein leucogranite sheet crosscutting straight gneiss; central belt.

(C) Isotropic vein leucogranite (bottom right) cuts folding of straight gneiss derived by transposition of garnet leucogranite sheets (white) in aluminous paragneiss (grey); central belt.

(D) Straight gneiss with transposed vein leucogranite, south boundary of central belt.

(E) Straight gneiss derived by transposition of vein leucogranite and amphibolite in aluminous paragneiss. Note fold, NW belt.

Figure 2.7.

(A) Medium to fine homoclastic protomylonite derived from coarse (megacrystic ?) leucogranite. Note the straight amphibolite layer; NW belt.

(B) Fine homoclastic protomylonite of granitic composition with highly attenuated amphibolite sheet; NW belt.

(C) Tectonic disaggregation of pegmatite as a qualitative indicator of high strain; central belt.

(D) Trains of isolated feldspar porphyroclasts derived by extreme attenuation of pegmatite; SE belt.

(E) An isolated pull-apart of amphibolite gneiss in feldspathic aluminous paragneiss as a qualitative indicator of high strain. Note quartzofeldspathic "pressure-shadows"; NW belt.

(F) Overgrowth of plagioclase on plagioclase core outlined by sillimanite inclusion trail (arrows) in feldspathic aluminous paragneiss similar to 'E'. It is equivocal to apply mylonite terminology to such tectonites. Plane polarized light. Field of view 2 mm; NW belt.

15
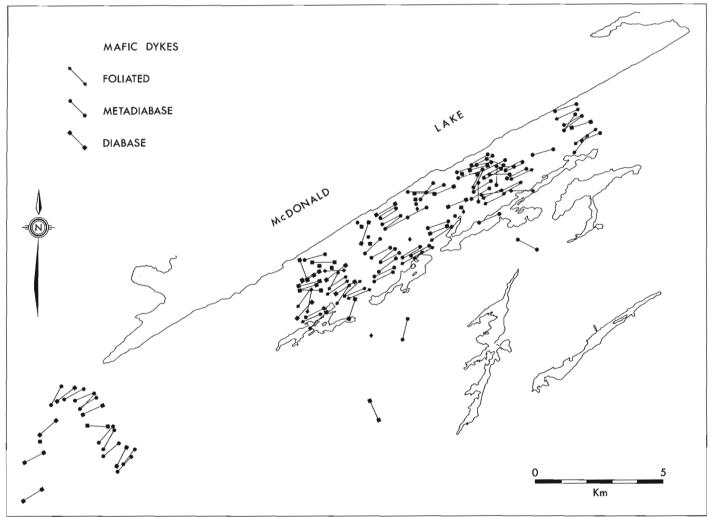
of folding, shearing and the emplacement of crosscutting granite. Folding of layering in the straight gneiss and continued intense shearing along the fold limbs resulted in shear bounded pods with NW-striking internal foliation enclosed by generally NE-striking, upright zones (10s to perhaps 100s of metres thick) of more intensely developed foliation, more highly attenuated layering and often a finer grain size than the same composition material within the pod. Alternatively, blocks have rotated between adjacent shears. Extension lineations within the shears are generally, but not everywhere, steeply plunging. The study of these shears is complicated by the existence of concordant (as opposed to the discordant shears described above) shear zones, visibly associated with the derivation of the straight gneisses from the irregular protoliths, but which are not always distinguishable from concordant syndisruption shears. These concordant shears formed under metamorphic conditions up to granulite facies (biotite-orthopyroxene – 2 feldspars-quartz) and can contain fine grained orthopyroxene bearing mylonite. Both orthopyroxene and biotite (lower metamorphic grade ?) bearing quartzofeldspathic mylonites occur in 1 m-1 km wide zones. While the granulite facies mylonites appear to be part of the relatively early main straight gneiss forming event(s), we cannot determine the time relations of the possibly lower grade concordant mylonite with any confidence, unless they are cut by later leucogranite veins (see below).

The disrupted granoblastic straight gneisses are succeeded to the northwest by granoblastic straight gneisses showing all the transposed features just described, but none of the disruption. Locally these gneisses shows the "greasy" appearance typical of granulites. Since these straight gneisses carry the steeply plunging lineation characteristic of the Laloche Lakes area, we suggest that they represent straight gneisses of the central belt which have escaped disruption.

With the exception of the discordant disrupting shears, all the central belt gneisses are crosscut by a widespread array of randomly oriented irregular veins and masses of white leucogranite (Fig. 2.6B, C), henceforth referred to as the 'vein leucogranite'. No major body of vein leucogranite has been recognized and veins range up to 10 m in width. The vein leucogranite is generally isotropic to poorly foliated, locally well foliated, variable in grain size and very rarely carries garnet-quartz aggregates, ranging up to fist-size.

Northwest belt

This belt is dominated by homoclastic protomylonite, in part visibly derived from a homogeneous pink leucocratic megacrystic ± biotite granite protolith (Fig. 2.7A, B). Towards the SW, the homoclastic protomylonite is also derived from both granite and a more complex gneissic

Figure 2.8. Map of upright mafic dykes emplaced into the McDonald Granite and part of the northwestern belt, SE of McDonald Lake. Bars = schematic representation of individual dykes observed; stations at bar centres.

protolith, part of which we have identified as a kilometre scale low strain pod SE of Hook point (Fig. 2.1). This gneissic protolith comprises an earlier foliated homogeneous grey-pink biotite granite with occasional centimetre to metre thick layers of hornblende diorite to granite, concordantly intruded by closely spaced, centimetre thick sheets of isotropic, leucocratic, pink pegmatite. The whole assemblage is then folded, imparting an axial plane foliation to the pegmatite layers. Intercalated decametre thick paragneiss layers are at least an order of magnitude thicker than the wavelength of the folds and so do not reflect the folding. This low strain pod is 4 km wide; at its NW edge the above described structures transpose into a single straight layering. The granitic homoclastic protomylonite, locally developing into metre thick bands of mylonite and even ultramylonite, generally contains dispersed, isolated elongate inclusions of homogeneous amphibolite, nondescript quartz-plagioclase-biotite-gneiss or aluminous paragneiss. However, there is a distinct strip several kilometres wide, extending from south of Hook point to east of McDonald Lake, wherein the density of dispersed metre to decametre sized inclusions is an order of magnitude greater (Fig. 2.1). We speculate that this strip may represent the deformed equivalent of a swarm of xenoliths in the granitic protolith.

The other major component of this belt is a set of extraordinarily long thin strips of supracrustal assemblage rocks, extending over distances of 20, possibly 30 kilometres, yet generally no wider than 500 to 1000 m (Fig. 2.1). The aluminous paragneiss component carries generally coarse sillimanite aligned parallel to the lineation and foliation and wrapped, often mimetically, around garnet augen. The garnets contain trails of sillimanite. Polycrystalline ribbons and single grains of variably pinnitized to fresh cordierite can be seen only in thin section. The presence of K-feldspar, the complete absence of muscovite plus the alignment of all the aforementioned minerals in the foliation and the lineation indicate that deformation occured under upper amphibolite facies (second sillimanite) conditions. The margins and internal layering of the strips of supracrustal assemblage rocks are concordant to the mylonitic foliation in the granitic homoclastic protomylonites and mylonites. The contacts of the thicker strips are, however, progressively intercalated with the granitic homoclastic protomylonites and mylonites. The homoclastic protomylonites and their associated mylonites therefore formed under the same metamorphic conditions as the aluminous paragneisses.

Southeast belt

This belt occupies most of the ground between the Laloche River and Thubin and Gagnon lakes (see Reinhardt, 1969). We have so far only mapped systematically in the area between Gagnon Lake and Laloche Lakes (see Fig. 2.1). There, the belt is remarkable in its compositional simplicity compared with the other belts. The belt comprises a well foliated leucocratic megacrystic biotite granite from which up to 5 km orthogonal thickness of fine homoclastic protomylonite have been derived. To the NW of the protomylonite a zone, 3-5 km thick, of mylonite, including a 1 km welt of ultramylonite, has been derived by further deformation of the protomylonites. Another zone, 2-4 km thick, of fine homoclastic protomylonite underlies the main parts of east and southwest Laloche Lakes. So far, only a narrow strip (1 km) of homoclastic protomylonite has been mapped on the SE side of the megacrystic granite. All boundaries are progressive and the progressive strain gradients have been walked out on several traverses. The mesoscopic resemblance between these homoclastic protomylonites and those seen to be derived from the homogeneous leucogranite protolith in the northwest belt is striking.

Highly attenuated, thin, continuous, parallel-sided inclusions of amphibolite and quartz-plagioclase-biotite-gneiss are fairly common in the homoclastic protomylonite underlying east and southwest Laloche Lakes and in the northwestern half of the mylonite-ultramylonite zone. These inclusions are set in mylonitic rocks indistinguishable in the field from those to the SE which are practically free of amphibolite inclusions. This disposition recalls a similar feature in the northwestern belt and suggests that the mylonite-ultramylonite zone here is centred upon the internal boundary of the contact zone of a major intrusive granite pluton. So far only one aluminous metasedimentary inclusion has been found within the homoclastic protomylonites of the southeastern belt (due west of Thubin Lake). This specimen carries plagioclase porphyroclasts containing inclusion trails of sillimanite and wrapped around by biotite and muscovite in the matrix. It would appear that the southeast belt was deforming, over part of its history, at temperatures below those of muscovite breakdown in the presence of quartz. The question remains as to whether it had earlier deformed at temperatures appropriate to the second sillimanite zones as in the northwest belt.

External belt

This belt is so named only for ease of reference (not to be confused with externides). It is uniform along its 80 km mapped strike length and varies in width from 1-2 km (Fig. 2.1). It comprises a belt of chlorite-muscovite grade mylonites to ultramylonites. All along the SE boundary of the external belt the granitic homoclastic protomylonites and porphyroclastic aluminous metasediments of the northwestern belt can be traced progressively into the external belt mylonites (Fig. 2.2D-F). The protomylonites are further mylonitized; the feldspar porphyroclasts of the metasediments are further reduced in size and proportion; the matrix to the porphyroclasts is reduced to an extremely fine grained phyllonite; the amphibolite sheets and inclusions are further thinned and attenuated. Metamorphic retrogression accompanies the visibly progressive structural reworking of the upper amphibolite facies gneisses and homoclastic protomylonites; sillimanite and biotite are replaced by muscovite and chlorite; the dark green to black amphibolites are replaced by muscovite and chlorite; the dark green to black amphibolites are replaced by a distinctive, brown-weathering rock containing chlorite and sericite. Clearly the external belt is later than the main structure and metamorphism of the northwestern belt and is not a coeval lower grade lateral equivalent. Locally, the dark ultramylonites are intruded by low angle crosscutting muscovite-bearing leucogranite mylonite (e.g. near Hook point).

Temporal relationships

All of the lithologies of both the northwestern and southeastern belts carry concordant, continuous, 10-50 cm thick sheets of generally pink vein leucogranite (Fig. 2.6D, E). Locally the sheets, or parts of them, are visibly crosscutting to the gneissosity of the surrounding tectonites. The fine grain size, plus feldspar porphyroclasts and quartz and especially feldspar ribbons, show that the sheets are highly strained and transposed granite veins, identical to the crosscutting leucogranite veins observed in the central belt. In places, and especially at the boundary of the central and southeastern belts, the progressive transposition can be walked out. Commonly these sheets appear to be more highly strained than the adjacent gneiss, i.e. the sheets are mylonites whereas the adjacent rocks are apparently homoclastic to intermediate protomylonites. In some cases this simply reflects a lower

plagioclase-K-feldspar ratio in the sheets (dispersed porphyroclasts in mylonitic granitic gneiss). In other cases, it reflects the introduction of new feldspar into the adjacent gneiss by porphyroblast growth (forming dispersed feldspar megacrysts in supracrustal gneisses) and/or by the tectonic degradation of syntectonic pegmatite sheets (porphyroclast trains). In any case, there is no simple correlation between age and apparent strain state at the hand specimen or outcrop scale. However, if the vein leucogranite is the same age in all the structural belts (excluding the external belt), the transposition of the vein leucogranite sheets suggests that the main deformation in the northwestern and southeastern belts is younger than that in the central belt. Furthermore, the lack of vein leucogranite crosscutting the discordant shears in the disrupted granoblastic straight gneiss of the central belt suggests that the disruption was itself post-vein leucogranite emplacement. Age relations between the northwestern and southeastern belts require further clarification.

In the boundary zone between the northwestern and central belts, there are several major coherent, concordant granitic bodies (Fig. 2.1). All are characterised by a highly variable strain state. Although they show a wide variation in strain state, including rare metre thick mylonitic bands, the sheets are generally isotropic to poorly foliated. Each shows clear intrusive relations with the highly deformed country rocks (crosscutting local contact, included rafts or xenoliths of well deformed country rock). One such body is a major zoned pluton measuring 40 by 5 km (Fig. 2.1), composed of texturally homogeneous, equigranular, medium grained granite-granodiorite. The NW half of the sheet is dominantly hornblende bearing, while the SE half carries mostly biotite. Lying parallel to, and NW of, this pluton is a major strip of a K-feldspar megacrystic equivalent of the hornblende-biotite granite. Further mapping is required to confidently assign these granitoids to the northwestern or central belts. Their significance lies in their evident late syntectonic nature.
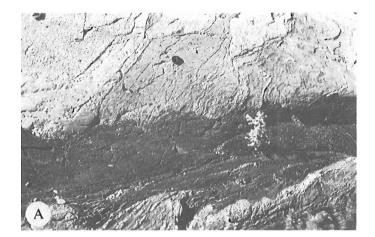
We have already shown that the mylonites of the external belt are younger than tectonites of the northwestern belt. The NW edge of the external belt is generally a faulted contact with the Great Slave Supergroup. However, SE of McDonald Lake the chlorite grade mylonites are in progressive contact with a large area of homogeneous, equigranular, isotropic, muscovite leucogranite (new name: McDonald Granite). A major elongate enclave (10 km) of now largely, but unevenly, retrograded coarse grained and foliated sillimanite-garnet-biotite-K-feldspar gneiss, is enclosed and intruded by the isotropic McDonald Granite (Fig. 2.1). Both the granite and the enclave are cut by a dense swarm of NE-trending, vertical mafic dykes. These range from pristine diabase, showing good ophitic texture, to chloritized and sericitized unfoliated metadiabase, to well foliated though annealed greenschist metabasite (Fig. 2.8). The diabase sheets occur throughout the McDonald Granite, while the foliated ones occur predominantly in the SE half of the granite outcrop (Fig. 2.8). Close to the foliated SE margin, the isotropic McDonald Granite contains misoriented, very well foliated xenoliths of fine grained homogeneous buff weathering leucogranite, locally crosscut by mafic dykes (Fig. 2.9A), as well as fine chlorite schist which we interpret as mylonite xenoliths in the isotropic McDonald Granite. Close to the mylonites of the external belt the McDonald Granite is itself strongly foliated to protomylonite, as are the diabase dykes. Within the contact zone, but not within the external belt mylonites themselves, late muscovite pegmatite dykes crosscut all the foliated rocks. Given the SE increase in the intensity of the retrogression of inclusions within isotropic McDonald Granite, and the SE increase in deformation of mafic dykes and of foliation intensity in the inclusions enclosed in isotropic granite, and the mylonitization of the SE margin of the granite itself,

we suggest that emplacement of the McDonald Granite is syntectonic with respect to the chlorite grade mylonitization in the external belt. This is supported by the occasional occurrence of leucocratic quartz-feldspar-muscovite mylonite sheets crosscutting at a low angle to the dark green ultramylonites (see above).

Both the granitic and supracrustal components of the structural belts contain amphibolite bodies ranging in continuous length from 1-100 m. They may be stubby pull-aparts, flattened isolated lenses or very long strips. The latter may be quite discrete or pervasively fractured and dilated with pegmatite filling the inter-fragment gaps (Fig. 2.9C, D). There are no preserved criteria to determine the pretectonic nature of the first two types of tectonic inclusion. However, the third type may have been basic dykes. In a few isolated cases this is demonstrably the case since branching apophyses and small scale crosscutting relationships are preserved (Fig. 2.9C). Such metamorphosed dykes must represent relatively late-syntectonic intrusions since they are emplaced into highly strained tectonites, but are themselves not highly strained. It is intriguing to note that all along the length of the northwestern belt half a dozen examples have been found of NE-striking, low to high angle crosscutting vertical diabase dykes; one even has a clear chilled margin. These dykes were emplaced into "cold" northwestern belt gneisses and are identical to diabase dykes intruding the McDonald Granite (Fig. 2.9B). By way of speculation, we wonder if there have been several periods of mafic dyke injection throughout the structural history of the map area.

Kinematics

As noted above, the principal finite extension direction of the central belt is oriented perpendicular to those of the other three belts. This also applies to the more discrete shears associated with the disruption of the central belt gneisses. All four belts present assemblages of kinematic indicators (see Hanmer, 1984a for definition); type examples of the commonest structures, e.g. rotated winged feldspars (Hanmer, 1984a), shear band foliations (Berthé et al., 1979a; White et al., 1980), rotated fold axial planes, Type I and Type II asymmetrical pull-aparts (Hanmer, 1984a; Hanmer in press), are given in Figure 2.10. Other structures include strain insensitive foliations (Means, 1981; Hanmer, 1984a, fig. 15.8F, 1984b), poorly developed 'C & S' planes (Berthé et al., 1979b), and heterogeneously extended oblique dykes (Hanmer, 1984a). Such kinematic indicators were all observed in the horizontal plane, and with few exceptions (i.e. local occurrences of sinistral shear bands; see Platt, 1984 and Harris and Cobbold, 1984 for discussion of kinematic significance), indicate a dextral flow. In the central belt the lineation is normal to the plane in which the kinematic indicators are observed, suggesting a component of shortening across the shear plane associated with the dextral transcurrent displacement, i.e. transpression (see Sanderson and Marchini, 1984). In the other three belts, kinematic indicators were observed in planes approximating the 'X/Z' plane of the finite strain ellipsoid; no evidence was noted for significant deviation from transcurrent, dextral simple shear.

The occurrence of an assemblage of dextral kinematic indicators, plus the major zones of homoclastic protomylonite through to ultramylonite in the northwestern, southeastern and external belts, indicates that these belts are the sites of important ductile dextral shear. The kinematics of the central belt require further discussion, beginning with the youngest structures. The discordant disrupting shears, as elements of an heterogeneous strain field (continuous and volume constant) and assuming that they have finite dimensions, must bend along their length; however, we have
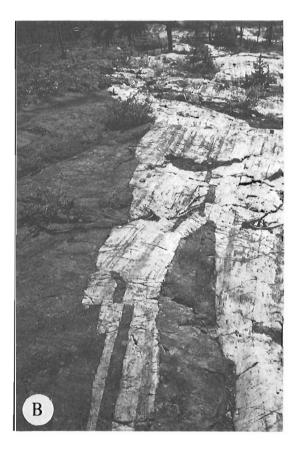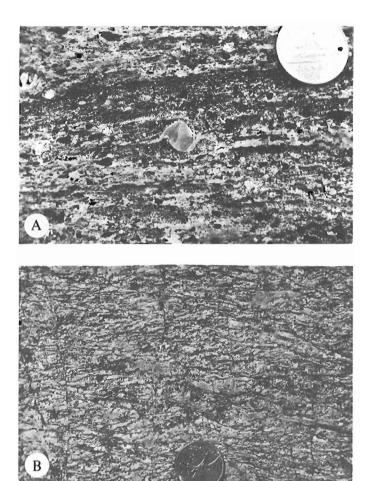
Figure 2.9.   *NE-striking mafic dykes.*

(A)   *Foliated metadiabase dyke crosscutting fine grained well foliated metagranite xenolith (grey) in isotropic McDonald Granite (white).*

(B)   *Branching diabase dyke crosscutting layering in fine homoclastic protomylonite; NW belt.*

(C)   *Discrete concordant amphibolite sheet with irregular, locally crosscutting contacts.   Note now deformed apophysis in left foreground.   Emplaced as a dyke into aluminous paragneiss; NW belt.*

(D)   *Highly deformed, fractured and pulled apart equivalent of 'C'; NW belt.*
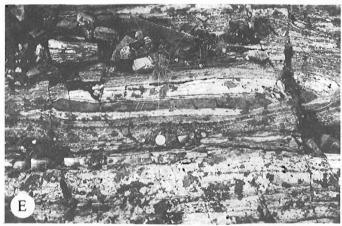
Figure 2.10. Dextral kinematic indicators, see text for discussion.

(A)   Rotated winged feldspar.

(B)   Shear band foliation.

(C) and (D)   Type 2 asymmetrical pull-aparts ("Surfs").

(E)   Type 1 asymmetrical pull-apart ("Turf").

(F)   Progressive rotation of fold axial planes with strain (tight folds to left, more open fold to right).

not observed this except at a very local scale. They could represent elements of an heterogeneous flattening field (Bell, 1981; Bell and Hammond, 1984), coaxial at the scale of the belt. However, while we have observed some indicators of dextral flow, we have not seen any sinistral kinematic indicators in the zone of disruption. Therefore, we envisage the zone of disrupted straight gneiss as a kilometre wide 'mesh structure' (Sibson, 1979), dominated by heterogeneous dextral shear accompanied by shortening across the bulk shear plane. By similar reasoning, we suggest that the pre-disruption transposition is also associated with dextral transpression. Although the deformation is heterogeneous and the number of kinematically significant observations is low, we have been able to follow a number of high grade mylonite zones over distances of kilometres without observing the variations in strike which the heterogeneous flattening model would predict.

Summary

A major crustal scale, up to 25 km wide, ductile, dextral shear zone lies along the southeastern margin of Slave Craton. We propose the name Great Slave Lake Shear Zone for this structure. It comprises four belts. With time the metamorphic grade decreased from granulite to lower greenschist facies, the locus of highest strain rate/strain softening shifted from the centre to the lateral parts of the shear zone, the width of the active zone of shear decreased and the strain regime changed from transpressive to transcurrent.

For the moment we cannot discriminate between the possibility that the Great Slave Lake Shear Zone might represent a single progressive event which occurred during a period of simple thermal decay resulting from erosional unroofing accompanied by on-going syntectonic acid and mafic magma injection, and an episodic, polyphase model.

Acknowledgments

References

Bell, T.H.
1981: Foliation development – the contribution, geometry and significance of progressive, bulk, inhomogeneous shortening; Tectonophysics, v. 75, p. 273-296.

Bell, T.H. and Etheridge, M.A.
1973: Microstructures of mylonites and their descriptive terminology; Lithos, v. 6, p. 337-348.

Bell, T.H. and Hammond, R.L.
1984: On the internal geometry of mylonite zones; Journal of Geology, v. 92, p. 667-686.

Berthé, D., Choukroune, P., and Jegouzo, P.
1979a: Orthogneiss, mylonite and non-coaxial deformation of granites: the example of the South American Shear Zone, Journal of Structural Geology, 1, p. 31-42.

Berthé, D., Choukroune, P. and Gapais, D.
1979b: Orientations prefèrentielles du quartz et ortho-gneissification progressive en régime cisaillant: l'exemple du cisaillement sud armoricain; Bulletin de Minéralogie, v. 102, p. 265-272.

Davidson, A., Culshaw, N.G. and Nadeau, L.
1982: A tectono-metamorphic framework for part of the Grenville Province, Parry Sound region, Ontario; in Current Research, Part A, Geological Survey of Canada, Paper 82-1A, p. 175-190.

Geological Survey of Canada
1984: Magnetic Anomaly Map of Canada, Map 1255A, 4th Ed.

Hanmer, S.
1984a: The potential use of planar and elliptical structures as indicators of strain regime and timematics of tectonic flow; in Current Research, Part B, Geological Survey of Canada, Paper 84-13, p. 133-142.

1984b: Strain – insensitive foliations in polymineratic rocks; Canadian Journal of Earth Sciences, v. 21, p. 1410-1414.

Hanmer, S.K. and Ciesielski, A.
1984: A structural reconnaissance of the northwest boundary of the Central Metasedimentary Belt, Grenville Province, Ontario and Quebec; in Current Research, Part B, Geological Survey of Canada, Paper 84-1B, p. 121-131.

Harris, L.B. and Cobbold, P.R.
1984: Development of conjugate shear bends during bulk simple shearing; Journal of Structural Geology, v. 7, p. 57-44.

Henderson, J.F.
1939: Taltson Lake, District of Mackenzie, NWT; Geological Survey of Canada, Map 525A.

Higgins, M.W.
1971: Cataclastic Rocks; USGS Professional Paper, 687, 97 pp.

Hoffman, P.F.
1968: Stratigraphy of the Lower Proterozoic (Aphebian), Great Slave Lake Supergroup East Arm of Grat Slave Lake, District of Mackenzie; Geological Survey, Paper 68-42, 93 p.

Hoffman, P.F., Bell, I.R., Hildebrand, R.S., and Thorstad, L.
1977: Geology of the Athapuscow Aulacogen, East Arm of Great Slave Lake, District of Mackenzie; in Report of Activities, Part A, Geological Survey of Canada, Paper 77-1A, p. 117-129.

Law, R.D., Knipe, R.J., and Dayan, H.
1984: Strain path partitioning within thrust sheets: microstructural and petrofabric evidence from the Moine Thrust Zone at Loch Eriboll, northwest Scotland; Journal of Structural Geology, v. 6, p. 477-498.

Mawer, C.K.
1983: State of strain in a quartzite mylonite, central Australia; Journal of Structural Geology, v. 5, p. 401-410.

Means, W.D.
  1981:   The concept of steady — state foliation;
          Tectonophysics, v. 78, p. 179-199.

Platt, J.P.
  1984:   Secondary cleavages in ductile shear zones;
          Journal of Structural Geology, v. 6, p. 439-442.

Reinhardt, E.W.
  1969:   Geology of the Precambrian rocks of Thubin
          Lakes map area in relationship to the McDonald
          Fault system, District of Mackenzie (75 E/12 and
          parts of 75 E/13 and 85 H/9); Geological Survey
          of Canada, Paper 69-21, 29 p.

Sanderson, D.J. and Marchini, W.R.D.
  1984:   Transpression;   Journal of Structural Geology,
          v. 6, p. 449-458.

Sibson, R.H.
  1977:   Fault rocks and fault mechanisms; Geological
          Society of London, Journal, v. 133, p. 191-213.

  1979:   Fault rocks and structure as indicators of shallow
          earthquake source processes; in: USGS Open File
          Report, 79/1239, p. 276-304.

Stockwell, C.H.
  1932:   Great Slave Lake — Coppermine River area, NWT;
          Geological Survey of Canada, Summary Report,
          Part. C, p. 37-63.

Sylvester, A.G., Oertel, G., Nelson, C.A., and Christie, J.M.
  1978:   Papoose Flat pluton: a granitic blister in the Inyo
          Mountains, California;   Geological Society of
          America Bulletin, v. 89, p. 1205-1219.

Tullis, J., Snoke, A.W., and Todd, V.R.
  1982:   Penrose Conference Report: significance and
          petrogenesis of mylonitic rocks;   Geology, v. 10,
          p. 227-230.

White, S.H.
  1982:   Fault rocks of the Moine Thrust Zone: a guide to
          their   nomenclature;   Textures   and
          Microstructures, v. 4, p. 211-221.

White, S.H., Burrows, S.E., Carreras, J., Shaw, N.D.,
and Humphreys, F.J.
  1980:   On mylonites in ductile shear zones;   Journal of
          Structural Geology, v. 2, p. 175-187.

White, S.H., Evans, D.J. and Zhong, D.L.
  1982:   Fault rocks of the Moine Thrust Zone:
          microstructures and textures of selected
          mylonites;   Textures and Microstructures, v. 5,
          p. 33-61.

Wright, G.M.
  1951:   Second preliminary map, Christie Bay, District of
          Mackenzie, NWT; Geological Survey of Canada,
          Paper 51-25.

  1952:   Second preliminary map, Reliance, District of
          Mackenzie, NWT; Geological Survey of Canada,
          Paper 51-26.

  1968a: Christie Bay, District of Mackenzie;   Geological
          Survey of Canada, Map 1122A.

  1968b: Reliance, District of Mackenzie;   Geological
          Survey of Canada, Map 1123A.

Zeck, H.P.
  1974:   Cataclastites, hemiclastites, holoclastites, blasto-
          ditto and mylo-blastites — cataclastic rocks;
          American   Journal   of   Science,   v. 274,
          p. 1064-1074.

Uranium and other trace and minor element concentrations in surface rocks and stream sediments from the Cypress Hills, Saskatchewan

Project 780015

W. Dyck and R.T. Bell[1]
Resource Geophysics and Geochemistry Division

Abstract

Surface rock samples from traverses of two buttes and a clay pit in the Cypress Hills near Eastend, Saskatchewan were collected and analyzed for 27 trace and minor elements.

The results show that most trace elements, particularly U, are markedly enriched in some coaly layers relative to others and the other rocks of the formations in general. U concentrations of up to 1200 ppm were encountered in seams in the Ravenscrag Formation of Anxiety Butte.

Excess U, relative to its daughter Ra, in one coaly layer suggests that U is accumulating or Ra depleting at a faster rate than its homologue; in another the reverse phenomenon was observed.
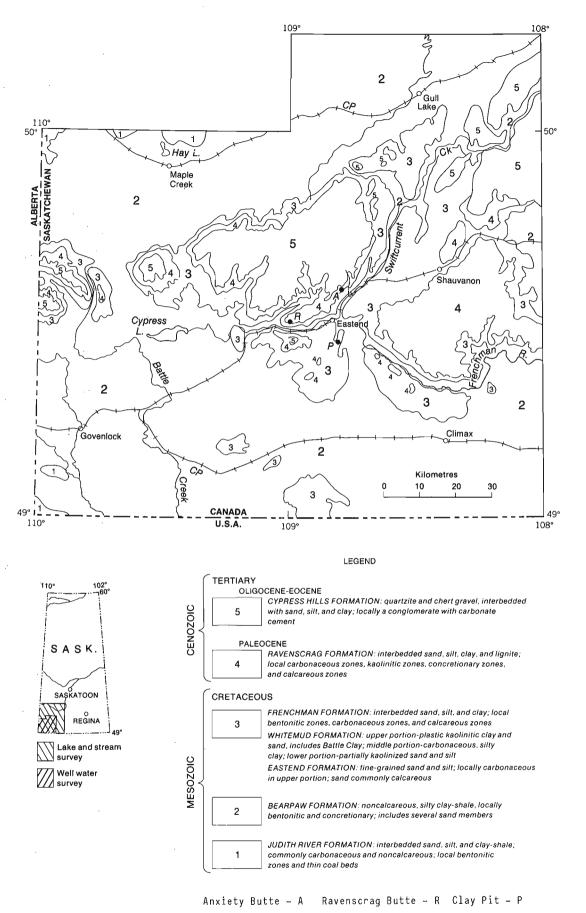
Résumé

Des échantillons de roches superficielles situés le long d'une ligne traversant deux buttes et une glaisière situées dans les collines Cypress près de Eastend, en Saskatchewan, ont été prélevés, et 27 éléments en traces et éléments mineurs en ont été analysés.

Les résultats obtenus révèlent que la plupart des éléments en traces, en particulier l'U, sont plus concentrés dans certaines couches charbonneuses que dans d'autres et par rapport à d'autres roches de l'ensemble des formations. Certaines couches de la formation de Ravenscrag de la butte Anxiety contiennent des concentrations d'U s'élevant jusqu'à 1 200 ppm.

La présence d'un surplus d'U, relativement à son produit de filiation Ra, dans une couche charbonneuse semble indiquer que l'accumulation d'U ou la décroissance de Ra, est plus rapide que son homologue; le phénomène inverse a d'ailleurs été observé dans une autre couche.

---

[1]Economic Geology and Mineralogy Division

2

5

CP

Gull
Lake

110°
50°

1

1

1

Hay L.

Maple
Creek

Ck

3

5

5

5

5

5

50°

ALBERTA
SASKATCHEWAN

2

5

5

3

4

3

5

4

3

Swiftcurrent

3

3

4

4

2

4

3

2

Shauvanon

A

Cypress
L.

5

4

3

4

3

4

R

5

3

3

4

Eastend

4

3

Frenchman R.

3

3

3

Battle

4

P

4

4

3

4

4

3

3

2

Govenlock

2

3

Climax

2

Kilometres

0   10   20   30

Battle   Creek

CP

3

3

2

3

3

49°
110°

CANADA
U.S.A.

109°

49°
108°

LEGEND

110°   102°
60°

SASK.

SASKATOON

REGINA

49°

Lake and stream
survey

Well water
survey

TERTIARY
OLIGOCENE-EOCENE

CENOZOIC

5   CYPRESS HILLS FORMATION: quartzite and chert gravel, interbedded
with sand, silt, and clay; locally a conglomerate with carbonate
cement

PALEOCENE

4   RAVENSCRAG FORMATION: interbedded sand, silt, clay, and lignite;
local carbonaceous zones, kaolinitic zones, concretionary zones,
and calcareous zones

CRETACEOUS

3   FRENCHMAN FORMATION: interbedded sand, silt, and clay; local
bentonitic zones, carbonaceous zones, and calcareous zones

WHITEMUD FORMATION: upper portion-plastic kaolinitic clay and
sand, includes Battle Clay; middle portion-carbonaceous, silty
clay; lower portion-partially kaolinized sand and silt

EASTEND FORMATION: fine-grained sand and silt; locally carbonaceous
in upper portion; sand commonly calcareous

MESOZOIC

2   BEARPAW FORMATION: noncalcareous, silty clay-shale, locally
bentonitic and concretionary; includes several sand members

1   JUDITH RIVER FORMATION: interbedded sand, silt, and clay-shale;
commonly carbonaceous and noncalcareous; local bentonitic
zones and thin coal beds

Anxiety Butte - A   Ravenscrag Butte - R   Clay Pit - P

Figure 3.1.   *Sample site location map (Geology after Macdonald and Broughton, 1980).*

Introduction

In an effort to explain the U and Rn anomalies discovered during the well water survey of the Cypress Hills area, Saskatchewan (Dyck et al., 1976), surface rocks from two buttes and a clay pit near the town of Eastend were collected and analyzed for 30 variables.

Uranium-rich coal seams (Cameron and Birmingham, 1970) and radioactive fossil bones (Bell et al., 1976) attest to the presence of U in the area. An airborne gamma-ray spectrometer survey of the area revealed higher radioactivity over some flanks of the hills (Cypress Hills Survey, 1976) which was traced to radioactive coal seams (K. Richardson, personal communication, 1984).

It was hoped that systematic sampling of the buttes would identify the radioactive seams and also give information on the relative radioactivity of the different formations. This report describes the results from 186 rock samples as well as the results of 22 stream sediment samples collected from the Frenchman River near Eastend.

Sampling and analytical methods

The approximate locations of the sampled sections are shown in Figure 3.1 by letters A, R, and P and dots. Samples were taken at about 1 m intervals from the bottom to the top of each section. Where notable physical changes in the rock occurred, the sample density was increased to reflect these changes. To obtain less weathered rock, the outer few centimetres were removed and discarded. Visible characteristics in rock type were recorded and matched with the known rock formations. Distance between sites, relative grain size and colour, were also recorded at each site. In situ gamma-ray activity was measured with a Rank Nucleonics and Controls Model NE148A scintillometer.

Stream sediments were collected along a 15 km section of the Frenchman River, starting just below the reservoir of the town of Eastend. These sediments were collected primarily for the purpose of determining whether the Rn and U fluctuations, observed in the stream water occur also in

Table 3.1. Sampling plus analytical precision of Cypress Hills rock data from 11 field duplicates (For units see Table 3.2)

Variable	1st duplicate Mean	1st duplicate Std. dev.	2nd duplicate Mean	2nd duplicate Std. dev.	Pooled data *Precision %	Pooled data Correlation coefficient	Precision % logtransformed data
As	21.1	30.1	16.5	18.6	107	0.98	*18
Se	0.6	0.8	0.5	0.6	82	0.99	25
F	305	71	315	60	19	0.85	4
U	5.8	6.7	6.0	5.2	64	0.94	40
Al	5.6	1.4	5.4	1.6	18	0.93	17
Ca	5.6	3.2	5.5	3.2	25	0.96	28
Mg	1.6	1.2	1.5	1.2	22	0.99	821
Fe	2.3	0.9	2.2	0.9	20	0.95	63
K	1.5	0.5	1.4	0.4	24	0.93	74
Be	3.6	3.9	3.3	3.0	41	0.99	19
La	52	38	57	45	51	0.92	17
Y	24	10	25	11	35	0.86	15
Ag	0.2	0.1	0.3	0.1	59	0.67	30
Pb	14	7	13	7	52	0.79	28
Zn	128	32	129	29	21	0.83	4
V	66	26	65	22	25	0.90	6
Mo	4.2	4.3	3.9	2.6	73	0.90	30
Cr	43	14	43	14	21	0.90	8
Cu	17	14	16	10	45	0.96	16
Co	8.9	8.3	7.5	5.8	119	0.65	41
Ni	14	7	16	8	29	0.95	12
Sr	213	175	180	110	66	0.95	7
Ba	558	214	580	255	34	0.87	11
Mn	425	353	372	382	87	0.82	28
Ti	3290	932	3190	1060	16	0.96	6

*% Precision $= \dfrac{2S}{C} \times 100$ where

S is the combined sampling and analytical variance

$$S^2 = \frac{1}{2N} \sum_{i=1}^{N} (X_{1i} - X_{2i})^2$$

C = pooled mean

N = no. of pairs

X_{1i} and X_{2i} are the values of the 1st and 2nd duplicates, respectively

the sediments. They are, however, also included in this report because the results provide some base for comparing the rock data.

A portion of each air-dried sample was ball-milled and analyzed for organic matter (loss on ignition – LOI) by heating one g samples in a furnace at 525°C for 4 hours.

U was determined on one g samples by neutron activation analysis by Atomic Energy of Canada Ltd.

Ra was determined by Rn emanometry. One g samples were dissolved in aqua regia, the solutions bottled for a specified time, degased, and the Rn emanations counted in an alpha counter using ZnS (Ag activated) cells.

Quantitative gamma-ray spectrometric determinations of K, U, and Th were carried out as described by Grasty et al. (1982). Because of the large sample requirement of the method, it was necessary, occasionally, to combine adjacent samples.

^{210}Po was determined by dissolving one g samples in strong acids, autoplating ^{210}Po onto Ni discs and counting the alpha-particle activity with a surface Barrier detector (Dyck and Bristow, 1984).

Arsenic and Se were determined by leaching one g samples with aqua regia, forming the hydride of the element with $NaBH_4$, atomizing the hydride in the silica tube, and reading the fluorescence with a Perkin-Elmer 300 atomic absorption spectrometer.

Fluoride was determined by sintering 250 mg samples with one g of a flux consisting of two parts Na_2CO_3 and one part KNO_3, dissolving the pellets in water, adjusting the pH of this solution to 6, and measuring the F ion activity with an ion selective electrode. The remaining elements in Tables 3.2 and 3.3 were determined by direct reading dc arc spectrometry (Timperley, 1974).

Sampling plus analytical precision

To obtain a measure of the sampling plus analytical precision of the methods, duplicate samples were collected from 11 sites. The results and the calculated precision are listed in Table 3.1. The correlation between duplicates is quite high but the precision is only fair to poor. Logtransformed data give higher precision than untransformed data for most variables. Mg, Fe, and K give

Table 3.2. Summary statistics of all rock samples from Ravenscrag and Anxiety Butte and the Clay pit (N = 186)

Variable	Units	Median	Geometric mean	Arithmetic mean	Std. dev.	Maximum	Minimum
LOI**	%	4.7	5.9	10.3	15.8	87.5	0.7
As	ppm	6.8	7.0	20.7	77.4	990	0.1*
Se	ppm	0.2	0.3	1.0	3.0	27.6	0.1*
F	ppm	320	318	335	107	625	85
U	ppm	3.3	4.0	8.1	42	565	0.5
Ra[1]	pCi/g	0.8	0.9	1.7	4.9	51	0.2*
eU[1]	ppm	3.0	3.7	8.6	44	469	0.4
eK[1]	%	1.7	1.3	1.7	0.74	3.4	0.1*
eTh[1]	ppm	8.9	9.5	10.6	5.4	30	2.0
Al	%	6.2	6.1	6.4	2.0	13	1.8
Ca	%	6.0	3.5	5.4	3.3	14	0.1*
Mg	%	1.2	1.1	1.5	1.1	4.3	0.1*
Fe	%	2.5	2.4	2.8	2.4	30	0.5
K	%	1.5	1.3	1.4	0.5	2.8	0.2
Be	ppm	2.4	2.5	3.0	2.9	22	0.5*
La	ppm	41	43	53	44	336	5*
Y	ppm	21	21	25	15	124	5*
Ag	ppm	0.2	0.2	0.3	0.3	1	0.2*
Pb	ppm	14	14	18	18	220	1*
Zn	ppm	124	116	125	46	260	21*
V	ppm	63	62	68	31	278	10
Mo	ppm	3.0	3.2	3.9	3.6	29	1.3*
Cr	ppm	45	42	47	20	128	4*
Cu	ppm	14	15	18	13	68	3
Co	ppm	4.8	4.2	7.4	13	127	1*
Ni	ppm	12	11	16	16	16	1*
Sr	ppm	135	146	182	140	820	31
Ba	ppm	531	532	686	1090	11400	80
Mn	ppm	229	189	366	478	3540	31*
Ti	ppm	3720	3520	3720	1080	8820	571

* Value given is half the detection limit of analytical method
** LOI = Loss on ignition
[1]N = 115 instead of 186

higher precision with untransformed data. This generally poor precision suggests that complex mathematical techniques for interpreting the data are not warranted.

Results and discussion

Summary statistics of all rock analyses are given in Table 3.2 and all sediment analyses in Table 3.3. Median values, broken down by LOI and rock formation, are given in Table 3.4. Profiles of 15 variables for each butte are plotted in Figures 3.2 and 3.3.

The unequal number of samples from the known rock formations makes the formation comparison in Table 3.4 difficult. However, the LOI sort of all rocks into >16% and <16% LOI groups shows clearly that most of the trace elements are enriched in the organic-rich (coaly) samples; as expected the more abundant elements are for the most part somewhat depleted (i.e. diluted) in the coaly samples. This correspondence is also evident in the profiles of a selected suite of variables in Figures 3.2 and 3.3. Superpositioning rock units or formations on the profiles, as shown in

Figures 3.2 and 3.3, does not help in classifying or discerning units. However, a noticeable change is observed in some of the trace element concentrations near lithological contacts. It is entirely possible that the weathering process has had an averaging effect on the composition of the units. This averaging effect is noticeable by comparing the stream sediment results to the low LOI rocks (Table 3.3 vs. Table 3.4); there is little difference between the two data sets.

Evidently the coal and lignite seams have acted, and may still act, as trace element getters, given the right ground water redox and salinity conditions. The fact that the coaly samples show an excess U relative to its daughter Ra or eU, suggests that at least some coals still act as trace element getters. This explanation does present a problem with respect to the uranium-rich ground waters that were observed in a number of wells during the regional well water survey. It was assumed there that the lignites were the source of the U in the waters. It is well known that in the zone of oxidation, U is generally mobilized more easily than Ra. Hence, the U-rich lignites are likely sources of U in the

Table 3.3. Summary statistics of stream sediment samples, Frenchman River (N = 22)

Variable	Units	Median	Geometric mean	Arithmetic mean	Std. dev.	Maximum	Minimum
Width	m	8.5	7.5	8.1	3.1	16	4
Depth	dm	5.5	5.9	6.2	2.1	10	3
Temperature	°C	17	17	17	1.3	19	15
LOI**	%	4.8	4.9	5.1	1.6	8.4	2.7
As	ppm	7.8	8.2	8.9	3.7	20	4.4
Se	ppm	0.2	0.2	0.3	0.20	1.1	0.1*
F	ppm	415	429	437	86	600	305
U	ppm	2.7	2.8	2.8	0.51	4.4	2.3
Ra	pCi/g	1.0	0.9	1.1	0.62	2.9	0.3*
eU	ppm	2.6	2.6	2.7	0.47	3.6	1.8
eK	%	1.8	1.8	1.8	0.19	2.1	1.4
eTh	ppm	6.5	6.4	6.6	1.6	9.3	4.4
Al	%	6.2	6.1	6.1	0.82	7.8	4.5
Ca	%	3.7	3.6	3.7	0.63	5.0	1.9
Mg	%	1.2	1.2	1.2	0.25	1.9	0.9
Fe	%	3.4	3.4	3.5	0.77	4.9	2.4
K	%	1.4	1.4	1.4	0.25	2.0	1.0
Be	ppm	2.8	2.7	2.7	0.23	3.0	2.2
La	ppm	37	35	36	11	58	19
Y	ppm	18	17	17	4.1	25	9
Ag	ppm	0.2	0.2	0.2	0·	0.2	0.2*
Pb	ppm	18	19	20	8.3	50	12
Zn	ppm	165	158	161	30	229	106
V	ppm	75	70	72	17	98	39
Mo	ppm	2.6	2.5	2.6	0.49	3.8	1*
Cr	ppm	57	54	55	13	79	29
Cu	ppm	15	14	15	4.4	23	8
Co	ppm	7.1	7.2	7.7	2.6	12	4
Ni	ppm	16	15	16	4.2	25	9
Sr	ppm	179	179	180	22	234	144
Ba	ppm	725	726	732	97	997	571
Mn	ppm	548	515	555	205	1010	151
Ti	ppm	3930	3950	4010	721	5760	2810

* Value given in half the detection limit of analytical method
** LOI = loss on ignition
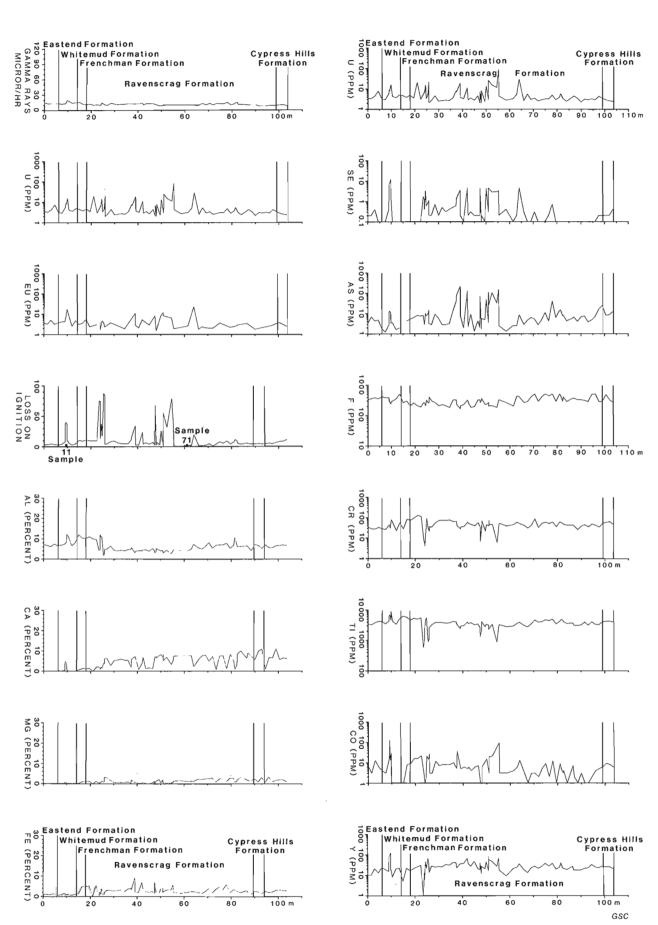
Figure 3.2. *Ravenscrag Butte surface rock element profiles as a function of distance from the bottom of the butte.*
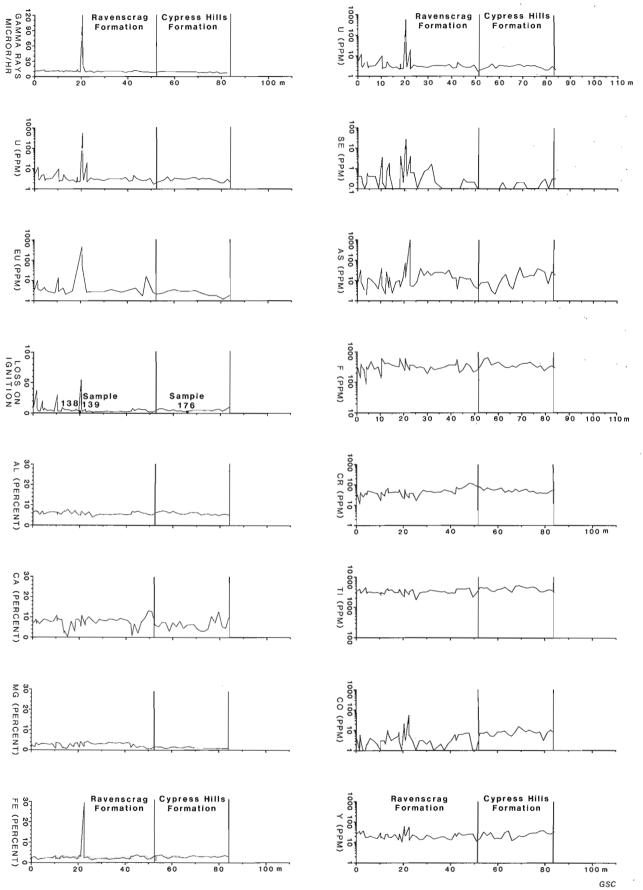
Figure 3.3. *Anxiety Butte surface rock element profiles as a function of distance from the bottom of the butte.*

Table 3.4. Median values of Cypress Hills rock samples sorted by loss on ignition and rock formation

Variable	LOI > 16.0% All formations	LOI ≤ 16.0% All formations	Till	Cypress Hills	Ravens-crag	Frenchman	Whitemud	Eastend
N	24	162	10	26	98	2	19	6
LOI	37.2	4.4	4.6	5.3	4.1	9.8	4.2	3.4
As	22.9	5.8	6.5	13	6.2	2.4	1.1	3.4
Se	3.2	0.2	0.3	0.1	0.2	0.1	0.1	0.2
F	230	337	446	343	319	278	352	365
U	11.3	3.2	3.4	3.0	3.1	4.1	4.2	3.4
Ra	1.2	0.8	0.7	0.9	0.8	0.8	1.0	0.7
eU	7.5	2.9	2.4	2.5	2.8	3.4	4.1	3.7
eK	1.1	1.7	1.8	1.6	1.8	0.7	1.4	2.3
eTh	9.0	8.8	8.3	7.2	8.6	21	18	11
Al	4.5	6.2	6.7	6.2	5.6	11	9.5	6.8
Ca	4.7	6.2	4.9	6.2	6.9	1.0	0.3	0.2
Mg	0.6	1.4	1.8	1.1	2.2	0.6	0.3	0.2
Fe	3.1	2.5	3.3	3.0	2.3	3.1	1.5	1.1
K	0.8	1.5	1.6	1.6	1.5	0.9	1.4	2.0
Be	5.8	2.2	2.4	2.3	2.0	2.7	3.1	3.3
La	95	38	36	38	40	38	32	48
Y	40	20	18	25	21	14	16	14
Ag	0.2	0.2	0.2	0.2	0.2	0.7	0.2	0.3
Pb	16	13	20	15	12	43	18	14
Zn	96	124	157	134	119	160	97	130
V	64	62	64	70	59	79	61	43
Mo	6.7	2.9	3.2	2.9	3.0	3.1	2.3	1.6
Cr	29	46	51	52	44	56	41	28
Cu	29	14	17	13	15	25	10	9
Co	15	4.3	7.3	7.6	3.3	4.5	1.3	4.5
Ni	25	12	18	14	12	19	4.3	7.5
Sr	344	126	238	189	116	126	48	100
Ba	523	531	618	660	484	368	474	673
Mn	94	241	535	590	224	174	41	36
Ti	2860	3760	4100	4000	3370	5920	4570	3440

Table 3.5. U and decay products of selected bulk rock samples.

Sample No.	Material	Location	Distance from bottom of butte, m	Rock formation	Loss on ignition %
11	coal	Ravenscrag	9.40	Whitemud	40.1
71	clay	Ravenscrag	61.50	Ravenscrag	3.7
138	coal	Anxiety	20.50	Ravenscrag	75.6
139	coaly-clay	Anxiety	20.65	Ravenscrag	8.3
176	Sand	Anxiety	66.00	Cypress Hills	3.1

U content, ppm, determined by:

Sample no.	U fluoro-metry	^{235}U delayed neutron counting	^{226}Ra-^{222}Rn emanometry	^{214}Bi gamma-ray spectrometry	^{210}Po alpha-particle spectrometry
11	9.4	9.7	8.8	7.4	4.7
71	2.6	4.4	3.4	2.6	1.7
138	1217	1160	491	476	331
139	8.0	8.6	49.8	45.8	40.8
176	1.9	3.3	3.3	2.9	2.4

ground water. However, such an explanation would leave the lignites deficient in U relative to its daughter, Ra. To shed more light on this problem, 5 samples were chosen for more detailed disequilibrium studies. The results are summarized in Table 3.5. They illustrate in miniature the complexity of geochemical processes in the surficial environment. Two samples (no. 138 and no. 139 Table 3.5), collected within 15 cm of each other display gross disequilibrium between U and its decay products. It looks very much as if U was leached from one site and redeposited in the other. Sample 139 is highly deficient and sample 138 has a large excess of U with respect to decay products. Thus, within 15 cm highly efficient U separation and concentration processes seem to be taking place. The results of sample 11 indicate that not all coals are highly enriched in U, and that the U in them is not always in disequilibrium with its decay products. Samples 71 and 176 show typical background contents.

The drop in the U content calculated from the ^{210}Po results can be explained by Rn loss from the samples in their natural setting. It should be remembered that the samples were taken within 10 cm of the surface, and Rn losses by emanation run around 20 to 60% for fine, weathered materials exposed to the atmosphere. Even though the results show clearly that separation of the U series is taking place, they do not tell which element is more mobile. We do know, however, from the chemical behaviour of the elements that the parent U is the most mobile homologue in a typical oxidizing environment. Quantitative determinations of ^{230}Th could resolve this question but these were not available. Obviously, a careful, even more detailed study of the disequilibrium of the U series in these lignites is needed to resolve this dilemma.

Conclusions

The analyses of the rocks from Cypress Hill buttes indicate that the lignite coal seams are enriched in most trace elements, particularly U, and could be the source of enriched ground waters. However, the observed disequilibrium in the U series in some samples suggests that some coals are absorbing U from waters and others serve as sources under present conditions.

References

Bell, R.T., Steacy, H.R., and Zimmerman, J.B.
1976: Uranium-bearing bone occurrence; Geological Survey of Canada, Paper 76-1A, p. 339-340.

Cameron, A.R. and Birmingham, T.F.
1970: Radioactivity in western Canadian Coals; Geological Survey of Canada, Paper 70-52, 35 p.

Cypress Hills Survey
1976: Geological Survey of Canada Geophysical series Map No. 35672G, Cypress Hills, Sask., Part of 72F, G, J, K.

Dyck, W. and Bristow, Q.
1984: Quantitative determination of ^{210}Po in geochemical samples; in Current Research, Part B, Geological Survey of Canada, Paper 84-1B, p. 41-46.

Dyck, W., Campbell, R.A., and Whitaker, S.H.
1976: Well water uranium reconnaissance, southwestern Saskatchewan; in Uranium in Saskatchewan, Saskatchewan Geological Society Special Publication No. 3, edited by C.E. Dunn, p. 157-168.

Grasty, R.L., Bristow, Q., Cameron, G.W., Dyck, W., Grant, J.A., and Killeen, P.G.
1982: Primary calibration of a laboratory gamma-ray spectrometer for the measurement of potassium, uranium and thorium. In Proceedings of the Symposium on Uranium exploration methods, Paris, 1st-4th June, NEA/OECD, Paris, p. 699-712.

Macdonald, R. and Broughton, P.
1980: Geological map of Saskatchewan; provisional edition. Saskatchewan Mineral Resources, Saskatchewan Geological Survey.

Timperley, M.H.
1974: Direct reading of dc arc spectrometry for rapid geochemical surveys. Spectrochimica Acta, Vol. 29B, No. 4, p. 95-110.

Ocean Drilling Program (ODP) site survey (Hudson 84-030) in the Labrador Sea: 3.5 kHz profiles

Project 840017

S.K. Chough[1], D.C. Mosher[2], and S.P. Srivastava
Atlantic Geoscience Centre, Dartmouth

Abstract

High resolution (3.5 kHz) profiles along the track of the detailed site survey reveal various large-scale bedforms and subsurface structures in the uppermost 80 m of the sedimentary sequence. Echo characteristics were analyzed and interpreted in terms of sedimentary processes.

On Belle Isle Bank, sediments have undergone erosion by the Labrador Current. On the slope mass-wasting processes dominate. At the southern margin of Gloria Drift two echo types suggest (1) thin-bedded turbidites and (2) pelagic settling on a gently rolling surface affected by bottom currents. The western margin of Eirik Ridge is dominated by sharp bottom echoes interpreted as the result of bottom current winnowing. The continental slope off Nain Bank is incised by several valleys. Four types of echo are recognized the most common reflecting the winnowing action of the Western Boundary Undercurrent.

In the Northwest Atlantic Mid-ocean Channel various echo characteristics result from the bedforms of turbidity current flows both in the channel and on the levees. Sedimentary layers thin progressively away from the channel axis.

Résumé

Des profils à haute résolution (3,5 kHz) qui suivent le tracé du levé détaillé du terrain révèlent diverses formes de relief et de structures de subsurface de grandes dimensions dans la partie supérieure (80 m) de la séquence sédimentaire. Les caractéristiques de l'écho ont été analysées et interprétées en fonction des processus sédimentaires.

Sur le banc Belle-Isle, les sédiments ont été érodés par le courant Labrador. Sur le talus, les phénomènes de mouvement de masse prédominent. Les deux types d'écho relevés au cours du sondage de la marge méridionale du drift Gloria laissent supposer la présence 1) de turbidites composées de minces couches et 2) de dépôts d'origine pélagique sur terrain onduleux qui seraient influencés par les courants de fond. Les échos prononcés qui caractérisent le sondage de la marge occidentale de la crête Eirik s'expliquent par le vannage accompli par les courants de fond. Le talus continental au large du banc Nain est entaillé de plusieurs vallées. Les échos sont de quatre types, dont le plus courant témoigne du vannage accompli par le courant sous-jacent de la limite occidentale.

Dans le fossé médio-océanique du nord-ouest de l'Atlantique, les formes de reflief qui résultent de coulées engendrées par des courants de turbidité, tant dans le fossé que sur les levées, donnent lieu à divers types d'échos. Les couches sédimentaires s'amincissent progressivement lorsque l'on s'éloigne de l'axe du fossé.

---

[1] Dept. of Oceanography, Seoul National Univeristy Seoul 151 Korea
[2] Dept. of Earth Sciences, Memorial University of Newfoundland, St. John's, Newfoundland A1B 3X5

Introduction

High resolution (3.5 kHz) reflection profiling serves as a means to delineate sedimentary processes that are operative on the seafloor (Damuth, 1975, 1980; Jacobi, 1976; Embley, 1980; Chough et al., 1985). It usually penetrates a few tens of metres into the subsurface revealing a depositional history of a few hundred thousand years in basins of moderate to high sedimentation rates (e.g. 1 to 10 cm/1000 years). High resolution profiles (ORE system), along with a 12 kHz echo sounder and air- and water-gun profiles, were obtained in the Labrador Sea during the **C.S.S. Hudson** cruise (84-030) along the entire survey track from the Strait of Belle Isle, across the Labrador Basin, to the continental slope off Nain Bank (Fig. 4.1). The survey was concentrated on the southern margin of the Gloria Drift (site 9), the western margin of the Eirik Ridge (site 5) and on the continental slope off Nain Bank, Labrador (site 2), as well as on several crossings of the Northwest Atlantic Mid-ocean Channel (NAMOC).

Echo characteristics of 3.5 kHz profiles were analyzed in detail, essentially following the scheme of Damuth (1980) and were interpreted in terms of sedimentary processes. The interpretation was made possible because many sedimentary features and their sedimentary processes, such as the Gloria Drift and Eirik ridge and the NAMOC have been previously identified by means of low-frequency seismic profiles and studies of sediment cores and surface samples (Jones et al., 1970; Davies and Laughton, 1972; Egloff and Johnson, 1975; Chough, 1978; Fillon and Full, 1984; Chough and Hesse, 1984).

Geological setting

The Labrador Sea was formed by seafloor spreading between late Cretaceous and Oligocene time (anomalies 33-13) (Srivastava, 1978; Srivastava et al., 1981). The extinct mid-Labrador Sea ridge runs approximately parallel to the axis of the basin. Sediment thickness in the central basin exceeds 2000 m, of which over one-third was deposited during the last 3-4 ma by mass-flow processes (mainly turbidity currents) channeled through the NAMOC (Chough and Hesse, 1976). The channel approximately parallels the Labrador Sea axis above the extinct mid-oceanic ridge in the central Labrador Sea (Chough, 1978). The Labrador Basin is also shaped by bottom currents overflowing from the Norwegian Sea. Large sedimentary drifts such as Eirik Ridge and Gloria Drift (Egloff and Johnson, 1975) dominate the continental rise south of Greenland and the central Labrador Basin, respectively (Fig. 4.1).

Echo characteristics

In describing echo characteristics of 3.5 kHz profiles we essentially followed the scheme of Damuth and Hayes (1977) and Damuth (1978, 1980). Our classification is summarized in Table 4.1. Type I echoes are distinct, whereas types II and III echoes are indistinct. Type IV echoes were not classified by earlier workers and consist of a combination of various types of echoes (types I, II, III) (Table 4.1). The echo characteristics are described generally along the survey track, i.e. Continental margin off Belle Isle Bank, basin floor and NAMOC, southern margin of Gloria Drift (site 9), western margin of Eirik ridge (site 5) and continental slope off Nain Bank (site 2) (Fig. 4.1).

Belle Isle Bank Margin

On the Belle Isle Bank (Fig. 4.1) the seafloor is characterized by indistinct echoes with prolonged subbottom reflectors (type IIB, Fig. 4.2), corresponding to the type IIB of Damuth (1980). The prolonged echoes are probably indicative of the lack of Holocene sediments, resulting from small-scale sand waves or iceberg scours that tend to scatter the acoustic energy.
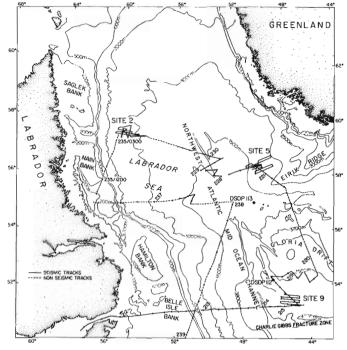
Figure 4.1. *Major physiographic features of the Labrador Sea; ship's tracks of* **CSS Hudson** *cruise 84-030 and Ocean Drilling Program (ODP) sites (9, 5 and 2).*

The Belle Isle Bank shelfbreak is characterized by indistinct echoes with irregular hyperbolae with varying vertex height (type IIIC, Fig. 4.2). Subbottom hyperbolae are present where sediments are perhaps less hard than the type IIB as described above. The irregular hyperbolae may result from various bedforms such as dunes and mounds.

Beyond the shelfbreak, the slope is dominated by indistinct echoes with prolonged subbottom reflectors (type IIB) and discontinuous subbottom reflectors (type IIIC). These echoes also occur in the slump and slide blocks that have slid downslope (type IVB, Fig. 4.2). Otherwise, the slope is smooth, dominated by the type IA echoes (Fig. 4.3) with no subbottom reflectors (Table 4.1). Individual slump blocks are up to about 30 000 m² in cross section.

Further downslope, depositional features (type IIID, Fig. 4.2) form a slightly rolling topography ranging in wavelength from 500 m to 5 km. Subbottom reflectors can be seen in each bedform. The hyperbolae of irregular overlapping mounds are tangential to the seafloor.

On the base-of-slope and rise, the seafloor is characterized by distinct echoes with many subparallel reflectors on a rolling topography (type IB-2, Fig. 4.3). These bedforms are believed to originate from bottom currents sweeping the rise, i.e. the Western Boundary Undercurrent (WBUC) (Carter and Schafer, 1983).

NAMOC and Basin floor

The natural levees of the NAMOC are characterized by two echo types: (1) indistinct, prolonged bottom echoes and often discontinuous subbottom reflectors (type IIA, Fig. 4.2); and (2) sharp bottom echoes with relatively continuous subbottom reflectors (type IB-1; Fig. 4.3), corresponding more or less to the type IB of Damuth (1980). In the former, the subbottom reflectors are fairly continuous, but wedge out in

Table 4.1.   Echo types

Damuth (1980)	This Cruise	Line Drawing	Type Section	Description	Occurrence	Interpretation
IA	IA		228/0439 – 228/0459	Continuous, sharp bottom echoes w/ no subbottom reflectors	NAMOC floor Continental slope and rise Belle Isle Bank	turbidity current scour; winnowed lag
IB	IB-1		214/0939 – 214/0959	Continuous, sharp bottom echoes w/ many continuous, sharp, parallel subbottom reflectors	Natural levees of NAMOC; basin plain	turbidity current overspill
	IB-2		213/0700 213/0720	Continuous, sharp bottom echoes w/ many subparallel subbottom reflectors on a rolling topography	lower continental slope and rise	bottom current
	IB-3			Continuous, sharp bottom echoes w/ numerous wedging subbottom reflectors (dunes)	continental slope; Gloria Drift and Eirik Ridge	bottom current
	IB-4		214/1639 – 214/1659	Continuous, sharp bottom echoes w/ only several parallel continuous discontinuous subbottom reflectors on a flat to gently rolling topography	Basin plain, Gloria Drift, Eirik Ridge	(hemi)pelagic settling and bottom current winnowing
IC	IC		228/0550– 228/0600	Continuous, sharp bottom echoes w/ one or two sharp unconformable wedging subbottom reflectors	NAMOC floor	turbidity current (Point bars)
IIA	IIA		229/0550 – 229/0610	Semi-prolonged bottom echoes w/ interstratent zones of semi-prolonged often discontinuous, subbottom reflectors	Natural levees of NAMOC	turbidity current overspill
IIB	IIB		214/0049 – 214/0109	Very prolonged bottom echoes w/ no subbottom reflectors,	Belle Isle Bank, Natural levee of NAMOC	glacial moraine proximal turbidite
IIIC	IIIC		212/1820 212/1930	Regular, overlapping hyperbolae w/ varying vertex elevations above the sea floor and no subbottom reflectors	Belle Isle Bank shelf break NAMOC floor	glacial moraine turbidity current
IIID	IIID, IB-3		213/0510 213/0530	Broad, single, gently rolling hyperbolae w/sharp bottom echo and several disconformable, migrating bottom reflectors	Base of slope	depositional lobes; weak contour currents
	IVA		212/2050– 212/2110	Large Block-like features (combined with hyperbolae) reflecting characteristics of types IB, IIA, and IIIC combined; internal reflectors are remnant.	NAMOC; continental slope	MASS flows
	IVB		233/720	Distinct bottom echoes w/ distinct subbottom reflectors (double IA type); transparent layer in between.	Small and broad valleys on the continental slope	debris flows and winnowed sediments in the slope depressions

Left margin groupings:
- Indistinct Echoes — Prolonged
- Indistinct Echoes — Hyperbolae
- Combined Echo Types

Vertical label: DISTINCTNESS OF ECHOES

35
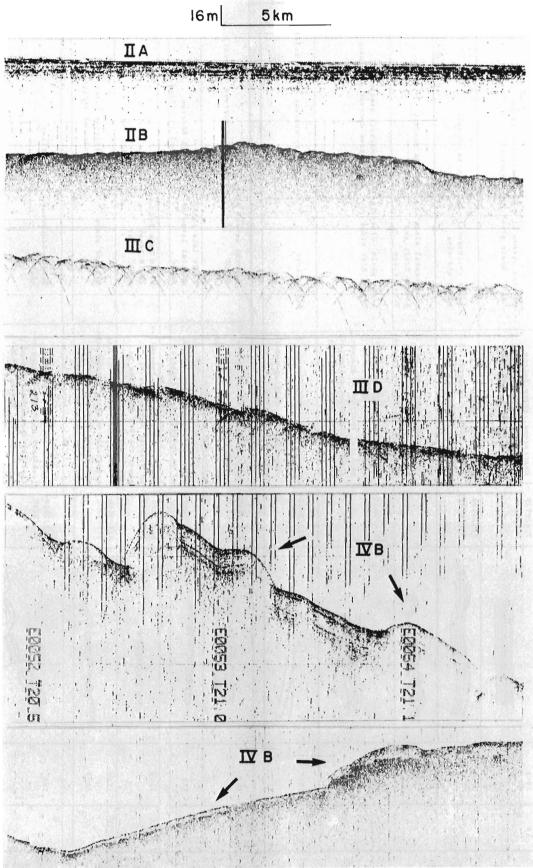
Figure 4.2. *Representative 3.5 kHz profiles of echo type. Refer to Table 4.1 for the description of echo characteristics.*
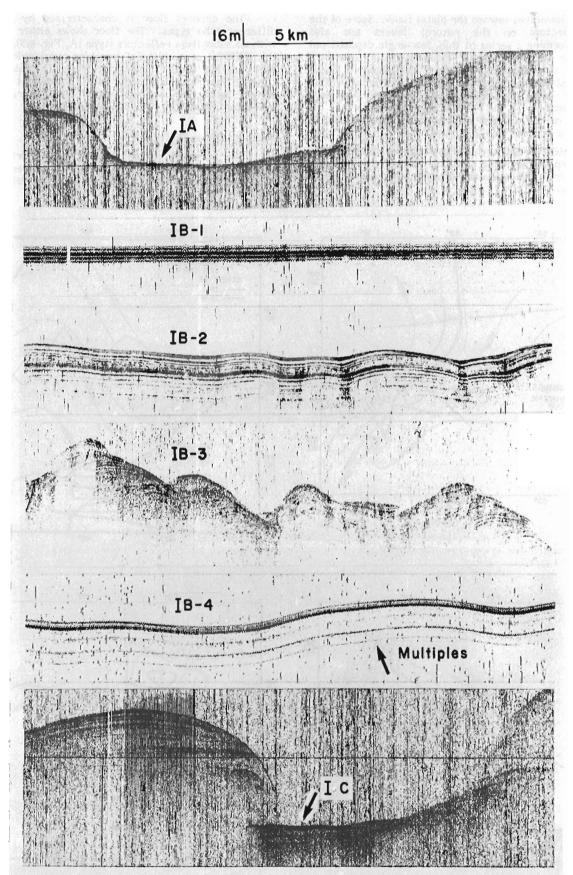
Figure 4.3. *Representative 3.5 kHz profiles of echo type. Refer to Table 4.1 for the description of echo characteristics.*

a few tens of kilometres toward the distal flank. Some of the type IB-1 reflectors on the natural levees are also discontinuous forming a series of thin, low-angle depositional wedges. Close to the channel, the subbottom reflectors become more discontinuous and less prolonged. These reflectors are similar to those of type IIA of Damuth (1980) in that they are semi-prolonged, often discontinuous subbottom reflectors. In the NAMOC crossings, the type IIA tends to occur on the eastern levee whereas the type IB-1 is prevalent on the western side (Fig. 4.4a).

The NAMOC walls are deeply incised, underlain by continuous sharp conformable wedging subbottom reflectors (Fig. 4.3, bottom). The walls are often chaotic due to slump and slide blocks.

The channel floor is characterized by a number of different echo types. The floor shows either sharp echoes with no subbottom reflectors (type IA, Fig. 4.3), especially in the thalweg, or consists of irregular overlapping hyperbolae with varying vertex elevations (type IIC, Table 4.1). The channel floor returns, in some cases, continuous sharp bottom echoes with one or two sharp unconformable wedging subbottom reflectors (type IC, Fig. 4.3).

Southern Gloria Drift (site 9)

The southern margin of the Gloria Drift (site 9) is dominated by type IB-4 and IB-1 echoes (Fig. 4.4b). Continuous sharp bottom echoes with several continuous
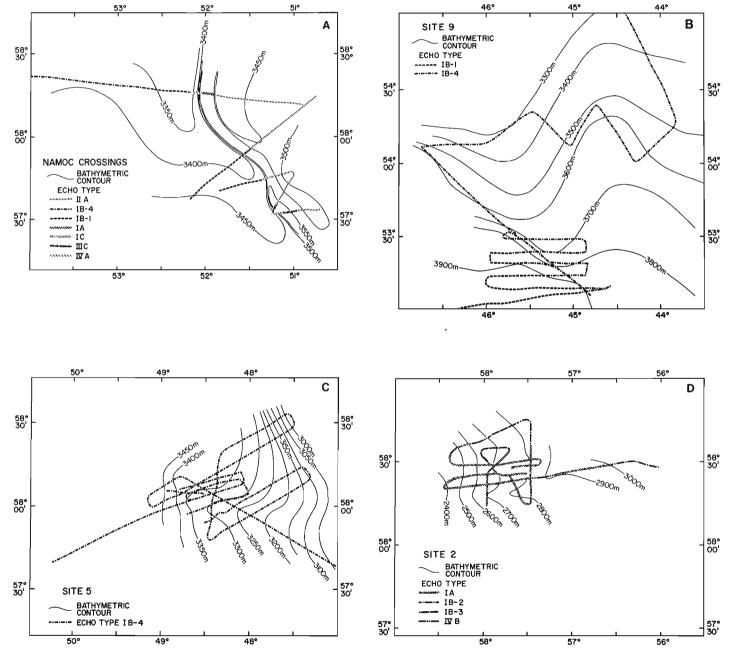
Figure 4.4. Distribution of individual echo types in survey sites 9, 5 and 2, as well as the NAMOC crossings.

parallel subbottom reflectors (type IB-4) of shallow (less than about 10 m) penetration prevail throughout the site. The seafloor is either smooth or gently rolling. In many crossings of the Gloria Drift the echo characteristics remain similar to those of the basin plain except those of large-scale sediment waves of up to a few kilometres in wave-length. On air-gun profiles these features are seen as large-scale climbing dunes (Fig. 4.5). Subbottom reflectors of these dunes tend to become thicker toward the trough, suggestive of bottom current winnowing. They are frequently accompanied by intermittent, discontinuous subbottom echoes in the trough. The bottom echoes sometimes form a transparent layer with sharp continuous reflectors underlying it.

The echo character of type IB-1 site 9 remains similar to that encountered in the NAMOC crossings as described above. Some subbottom reflectors are gently bent upward, forming a slightly transparent bulge (Fig. 4.6a). This is also evident in the air-gun profiles (Fig. 4.6b).

Western Eirik Ridge Margin site 5)

Type IB-4 (Fig. 4.3) dominates the western Eirik Ridge margin (Fig. 4.4c). It is characterized by sharp bottom echoes with a few weak subbottom reflectors forming transparent layers on a slightly rolling topography. The surface bedforms are rather smooth with hills and mounds. Further northeast, on the main body of Eirik Ridge, large-scale bedforms such as dunes and antidunes are well developed (Egloff and Johnson, 1975). Sediments of the ridge are poorly sorted, intensely bioturbated and mottled with rare wavy parallel laminations (Chough and Hesse, 1984).

Continental Slope off Nain Bank (site 2)

Continuous sharp bottom echoes with numerous wedging subbottom reflectors (type IB-3, Fig. 4.3) characterize the large-scale dunes (Fig. 4.4d). The dunes vary in scale, ranging in wavelength from a few hundred metres to 5 km. Individual sequences (layers) on the dunes are continuous or wedging on both stoss and lee sides forming large-scale climbing dunes. A strong sharp continuous bottom echo with a strong continuous subbottom reflector (type IVB; Fig. 4.2) occurs on the flanks of troughs and slope depressions. The top echo wedges out on the valley wall.

Sedimentary processes

Belle Isle Bank Margin

The sharp bottom echoes with prolonged subbottom reflectors on the Belle Isle Bank and the adjacent shelf (extending to the shelfbreak) suggest that the seafloor has undergone erosion. The erosion was probably enhanced by the southward-flowing Labrador Current winnowing fine-grained sediments into the depressions. The source sediments are probably glacial till and moraine deposits whose identity is still evident on the shelfbreak where the echoes yield regular overlapping hyperbolae with varying vertex elevations. The sediments also appear to have formed certain bedforms of large-scale dunes and waves in the process of transport.

The steep upper slope (slope gradient of 2°) is dominant by features indicative of mass flow processes such as sliding and slumping (type IVA). On the base of the slope depositional lobes (type IIID, Fig. 4.2) prevail. They consist of irregular or overlapping hyperbolae with vertices tangent to the seafloor. In this area, the WBUC plays a major role in shaping the seafloor (Carter and Schafer, 1983). The distinct bedforms of many subparallel subbottom reflectors (type IB-2) on the base-of-slope and rise are also believed to have been formed by the WBUC. Similar types of echo are also found on the lower slope of site 2 (Fig. 4.4d).

Southern Margin of Gloria Drift (site 9)

Site 9, on the southern margin of the Gloria Drift, is on the eastern margin of the natural levee of the NAMOC (Fig. 4.4b). Here, the levee extends more than 100 km from the channel. Turbidite layers interfinger with the hemipelagic layers or with the contourites of the Gloria Drift (Fig. 4.4b). The latter are characterized by transparent layers of minimal reflectivity on a slightly rolling topography. The facies change was also delineated both by air-gun and 3.5 kHz profiles. The channel levees of the NAMOC are dominated by a type IB-1 echo that is interpreted as turbidity current overspill. The lateral extent of spillover deposits seems to be confined by the topographic high of the adjacent seafloor and abut the hemipelagite and contourite of rolling topography.

100 m | 3 km
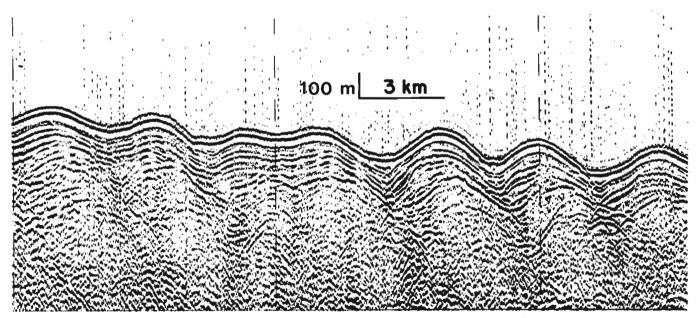
Figure 4.5.   *Air-gun profile of climbing dunes on the Gloria Drift.*

The contourites of the main body of the Gloria Drift show a distinct bottom echo with continuous subbottom reflectors and transparent sediments in between. They are characterized by large-scale bedforms such as dunes and climbing dunes.

The gently upward-bent reflectors in type IB-1 (Fig. 4.6) are perhaps due to the buoyancy of relatively lighter sediments filled with some kind of gas or of muddy sediments.

Western Eirik Ridge Margin (site 5)

Site 5 lies northwest of the main axis of Eirik Ridge south of Greenland. Deposition of sediments appears to be dominated by hemipelagic processes (type IB-4), i.e. settling of sediments on a slightly rolling topography at depths between 3200 and 3800 m. The influence of the WBUC seems to be minimal in this area.

NAMOC crossings

Outside the influence of NAMOC, the dominant sedimentation on the basin floor is hemipelagic settling, ice-rafting and bottom current transport (Fillon and Full, 1984). There appears to be very little of the central basin floor which remains outside the NAMOC influence. The levees of the channel extend for tens or hundreds of kilometres. They consist of turbidity current overspill deposits which produce types IB-1 and IIA on 3.5 kHz recordings. Damuth (1978) estimated that this type of record is produced by sediment containing low to moderate amounts of sand and silt. On NAMOC crossings (Fig. 4.4a), the echo type II is recognized on the eastern levee of the channel, whereas type IB-1 is seen only on the western levee. Type IB-1 echoes are characterized by a strong bottom echo with many sharp subparallel subbottom reflectors, that probably indicate deposits composed of relatively coarse beds of sand and silt. It is most likely that the Coriolis force pulls not only more
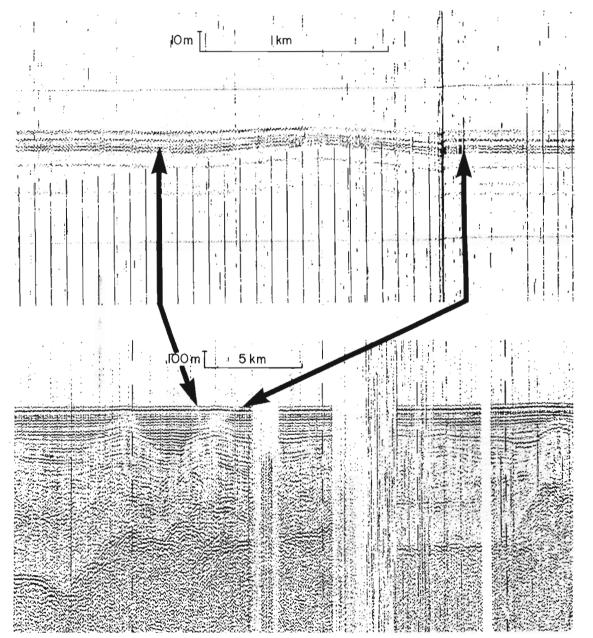
Figure 4.6. (a) 3.5 kHz and (b) air-gun profiles showing transparent sediment layer bulge.

40

sediments to the western levee (Chough and Hess, 1976), but also coarser sediments, thus accounting for the difference in echo types between the two levees. The discontinuity of type IIA reflectors on the eastern levee may indicate that spillover processes were intermittent, scouring the levee surface.

The channel walls are slumped onto the channel floor. The channel floor yields several different echo types depending on the morphology of the floor. The most common is type IA consisting of a sharp, continuous bottom echo with no subbottom reflectors. Type IIIC on the channel floor is interpreted as reflection of coarse material, in which the hyperbolae may be due to the diffraction of boulders or small-scale bedforms. The third echo type (Type IC), consisting of sharp continuous bottom echoes with one or two wedging subbottoms reflectors, may represent point bar sequences as found earlier by Chough and Hesse (1976).

Continental slope off Nain Bank (site 2)

The track lines of site 2, for the most part, run perpendicular to the continental slope, ranging in depth from 2600 to 3400 m (Fig. 4.4d). The seafloor morphology is complex, being incised by several depressions and valleys. The sedimentary features reflect this complex morphology in that four different types of echo are recognized.

The first echo type encountered was IB-2 which occurs at a depth of 3300 m. It results most likely from the influence of the WBUC. Type IA, a strong bottom reflector with no subbottom reflectors, dominates the rest of the site. It appears that winnowing processes have dominated the seafloor producing a hard, reflective bottom. In valleys and other depressions, type IVB occurs. It is described as a double IA type since two strong reflectors are seen separated by a transparent layer. Where the top reflector wedges out or terminates in a tongue-shaped lobe within valleys and depressions, the transparent layer of type IVB appears to represent the deposits of winnowed sediments or debris flow deposits.

The fourth type of echo in the site 2 area is type IB-3 (climbing dunes), which occurs in association with type IB-2 (subbottom reflectors on a rolling topography). Type IB-3 is very similar to the migrating waves described by Damuth (1980). This is seen on the northernmost part of site 2 on the crest of a broad ridge running downslope. Although the flow and boundary conditions that cause these bedforms are not clear at present, both types are interpreted as deposits of bottom currents (WBUC) flowing southward along the slope and rise as described by Carter and Schafer (1983).

Acknowledgments

References

Carter, L. and Schafer, C.T.
    1983:   Interaction of the Western Boundary Undercurrent with the continental margin off Newfoundland; Sedimentology, v. 30, p. 751-768.

Chough, S.K.
    1978:   Morphology, sedimentary facies and processes of the Northwest Atlantic Mid-ocean Channel between 61 and 52, Labrador Sea; Ph.D. Thesis, McGill University, 167 p.

Chough, S.K. and Hesse, R.
    1976:   Submarine meandering thalweg and turbidity currents flowing for 4000 km in the Northwest Atlantic Mid-ocean Channel, Labrador Sea; Geology, v. 4, p. 529-533.

Chough, S.K. and Hesse, R.
    1984:   Contourites from Eirik Ridge south of Greenland; Sedimentary Geology, v. 41.

Chough, S.K., Jeong, K.S., and Honza, E.
    1985:   Zoned facies of mass flow deposits in the Ulleung (Tsushima) Basin, East Sea (Sea of Japan); Marine Geology.

Damuth, J.E.
    1975:   Echo character of the western equatorial Atlantic floor and its relationship to the dispersal and distribution of terrigenous sediments; Marine Geology, v. 18, p. 17-45.

    1978:   Echo character of the Norwegian-Greenland Sea: relationship to Quaternary sedimentation; Marine Geology, v. 28, p. 1-36.

    1980:   Use of high-frequency (3.5-12 kHz) echograms in the study of near bottom sedimentation processes in the deep-sea: review; Marine Geology, v. 38, p. 51-75.

Damuth, J.E. and Hayes, D.E.
    1977:   Echo character of the east Brazilian continental margin and its relationship to sedimentary processes; Marine Geology, v. 24, p. 73-95.

Davies, T.A. and Laughton, A.S.
    1972:   Sedimentary processes in the North Atlantic: in Initial Reports of the Deep-Sea Drilling Project 12, U.S. Government Printing Office, Washington D.C., p. 905-1267.

Egloff, J. and Johnson, G.L.
    1975:   Morphology and structure of southern Labrador Sea; Canadian Journal of Earth Sciences, v. 12, p. 2111-2133.

Embley, R.W.
    1980:   The role of mass transport in the distribution and character of deep-ocean sediments with special reference to the North Atlantic; Marine Geology, v. 38, p. 23-50.

Fillon, R.H. and Full, W.E.
    1984:   Grain-size variations in North Atlantic non-carbonate sediments and sources of terrigenous components; Marine Geology, v. 59, p. 13-50.

Jacobi, R.D.
    1976:   Sediment slides on the northwestern continental margin of Africa; Marine Geology, v. 22, p. 157-173.

Jones, E.J.W., Ewing, M., Ewing, J.I., and Eittreim, S.L.
    1970:   Influences of Norwegian Sea overflow water on sedimentation in the northern North Atlantic and Labrador Sea; Journal of Geophysical Research, v. 75, p. 1655-1680.

Srivastava, S.P.
    1978:   Evolution of the Labrador Sea and its bearing on the early evolution of the North Atlantic; Geophysical Journal, v. 52, p. 313-357.

Srivastava, S.P., Falconer, R.K.H., and MacLean, B.
    1981:   Labrador, Davis Strait, Baffin Bay; geology and geophysics: a review; in Geology of the North Atlantic Borderlands, ed. J.W. Kerr and A.J. Ferguson; Canadian Society of Petroleum Geologists, Memoir 7, p. 333-398.

Stratigraphy, structure and timing of deformation of southwestern New World Island, Newfoundland

Colleen G. Elliott[1]

Abstract

The stratigraphy of southwestern New World Island, Newfoundland, consists of Lower to Middle Ordovician lavas, pyroclastic rocks and volcanogenic sandstones, and Caradocian argillites of the Summerford Group, overlain by the banded siltstones and feldspathic sandstones of the Sansom Formation, which is overlain in turn by Lower Silurian polymictic conglomerates of the Goldson Formation. These units are now overturned and dip steeply to the south. The deformational history of the area involved thrusting, four generations of folding, and later high-angle faulting. Deformation may have begun as early as Ashgillian times and continued through the early Silurian.

Résumé

La stratigraphie du sud-ouest de l'île New World, située à Terre-Neuve, est composée de laves formées entre les Ordoviciens inférieur et moyen, de roches pyroclastiques et de grès d'origine volcanique ainsi que d'argilites caradociennes du groupe Summerford, sur lesquels reposent des siltstones rubanées et du grès feldspathique de la formation de Sansom, qui à leur tour sont recouverts de conglomérats polygéniques du Silurien inférieur de la formation de Goldson. Ces unités qui ont subi un déversement plongent de façon abrupte vers le sud. L'histoire de la déformation de cette région comporte un charriage, quatre générations de plissements suivis de la formation de failles à angle presque droit. La déformation pourrait avoir commencé à l'Ashgillien pour se terminer après le début du Silurien.

---

[1] Department of Geology, University of New Brunswick, P.O. Box 4400, Fredericton, N.B., E3B 5A3

Introduction

New World Island is part of the Dunnage Zone of Williams (1978, 1979), which is composed of thick Lower Paleozoic volcanic and marine sedimentary units and clastic terrestrial sediments. The basic stratigraphy of the zone consists of Cambrian (?) and Lower Ordovician submarine volcanic rocks and volcaniclastic sediments, Caradocian black shales, Upper Ordovician and Silurian clastic sediments, and Silurian subaerial volcanic flows (Dean, 1978). A detailed review of the regional geology and past work in the Notre Dame Bay area of the Dunnage Zone can be found in Dean (1978). Kean et al. (1981) presented a more general overview of central Newfoundland regional geology.

New World Island and the surrounding area was mapped on a scale of 1:50 000 by Patrick (1956) and Williams (1963), and the Summerford Arm area (for location, see Fig. 5.1) was interpreted as a folded and highly faulted sequence comprising: unnamed Ordovician volcanic rocks, black slate and silicous argillite, Ordovician and Silurian clastic sediments, and Silurian conglomerate of the Goldson Formation (Williams, 1963).

McKerrow and Cocks (1981) interpreted the geology of southwestern New World Island in terms of large olistoliths that slid into an Ordovician basin of continuous turbidite and debris-flow conglomerate deposition complicated by contemporaneous high angle faulting. They interpreted the strata as a single north-younging sequence with no repetition due to large-scale folding or faulting.

The area discussed is the southwesternmost peninsula of New World Island between the village of Summerford and the eastern tip of Intricate Harbour (Fig. 5.1).

The following report gives a description of lithologies, and the revised stratigraphy, structural geology, and timing of deformation of southwestern New World Island.

Lithologies

Volcanic rocks

The volcanic rocks of southwestern New World Island are grey green to black, interlayered massive and pyroclastic units of four main lithological types: lavas, agglomerates, lapilli tuffs, and banded tuffs.

The lavas are massive or amygdaloidal basaltic flows that weather to purple, red, and orange. They have been mapped as pillow lavas by previous workers (Williams, 1963; Horne, 1968), but the author found no convincing pillows along Summerford Arm or along the Cottlesville road. Amygdules and veins are mostly filled with calcite, although chlorite filling is common and at one location just south of Rushy Pond, the lavas are intensely veined with chlorite and serpentine.

The agglomerates outcrop east of Reddetts Head and in two bands between Fudge Head and Green Cove. They consist of bombs, blocks, and angular fragments of mafic igneous rock in a sheared black and silver to green fine grained tuffaceous matrix. Clasts range in size from a few millimeters to tens of centimetres, tend to form discrete layers, and are elongate parallel to the regional cleavage (S_2).

Tuffs are light grey to green fragments in a calcareous matrix. Lapilli tuffs outcrop along the road to Cottlesville. They are composed of densely packed, millimetre to centimetre scale angular fragments in a light coloured matrix and show no layering on an outcrop scale. Banded tuffs are found in Green Cove, with massive lavas east of Farmer Head, along the road to Cottlesville, and interbedded with flows in eastern Intricate Harbour. The banded tuffs are composed of millimetre-sized fragments in a calcareous matrix in graded banda 1-5 cm thick. Rounded patches of almost pure calcite up to 3 cm across give the tuffs an amygdaloidal appearance in places, and locally the banded tuffs grade into tuffaceous limestone beds 1-4 metres thick.

Limestone lenses are associated with the volcanic rocks. They are pod shaped and range from one to five metres in width. The limestones are dirty, mottled light to dark grey, and are recrystallized to marble. On the east side of Reddetts Head a limestone lens in the volcanics contains trilobites and cephalopods of probable Tremadocian age (Horne, 1968). On the other side of Reddetts Head, Upper Llanvirnian to Llandeilian conodonts, brachiopods, ostracods, and chitinozoans were reported by Bergstrom et al. (1974).

Argillaceous rocks

The argillaceous rocks of southwestern New World Island are the most lithologically distinct units in the area. There are two types: black shale, and grey siliceous argillite. The black shales are fissile units of very fine grained carbonaceous detritus with minor grey silty or cherty laminae. They are sulphide rich and weather to red and yellow. These black shales are rich in graptolite faunas that range in age from late Llandeilo to late Caradoc (**N. gracilis** to **D. clingani** zones) (McKerrow and Cocks, 1981). The siliceous argillites are grey to green and are composed of millimetre to centimetre thick laminae of chert and fine silt. In places they are sulphide rich. They are non-fossiliferous but locally are interbedded with the black shales, thus the two are assumed to be equivalent units.

Arenaceous rocks

In the field, the arenaceous rocks were divided into volcanogenic sandstone, banded siltstone, undifferentiated sandstone, and turbiditic sandstones.

The volcanogenic sandstone is dark grey to black and weathers to grey and buff. It is composed of interbedded tuffaceous siltstone and fine grained dirty sandstone in lighter and darker layers 2-10 cm thick. In places it is highly brecciated and chloritized. It outcrops only at the intersection between the road to Cottlesville and the road to Rushy Pond, and contains a rich shelly fauna that includes brachiopods, corals and crinoids. The assemblage has been dated as Llanvirn by McKerrow and Cocks (1981).

Banded siltstones outcrop in two places along Summerford Arm, east and west of Green Cove. These are light grey, ochre, and dark grey on fresh surfaces, weathering to red, silver grey, and yellow. Bedding is highly disrupted laminae 0.1 cm to 10 cm thick. Convolute bedding is common and is restricted to single beds. There is a scattering of calcareous concretions up to 30 cm across. At the mouth of Green Cove the author found one solitary rugose-like coral that has not yet been dated, but no other fossils have been recorded in this unit. The unit coarsens to the northwest from dominantly shale and siltstone sized grains to siltstone interbedded with feldspathic sandstone and conglomerate. Conglomerate beds are up to 40 cm thick, and are graded to the northwest. The conglomerate is moderately well sorted and matrix supported with clasts 0.1-2 cm across. Clasts consist of vein quartz, black and red chert, sandstone, shales, and volcanic rock. The unit grades into mélange and pebbly mudstone to the northwest.
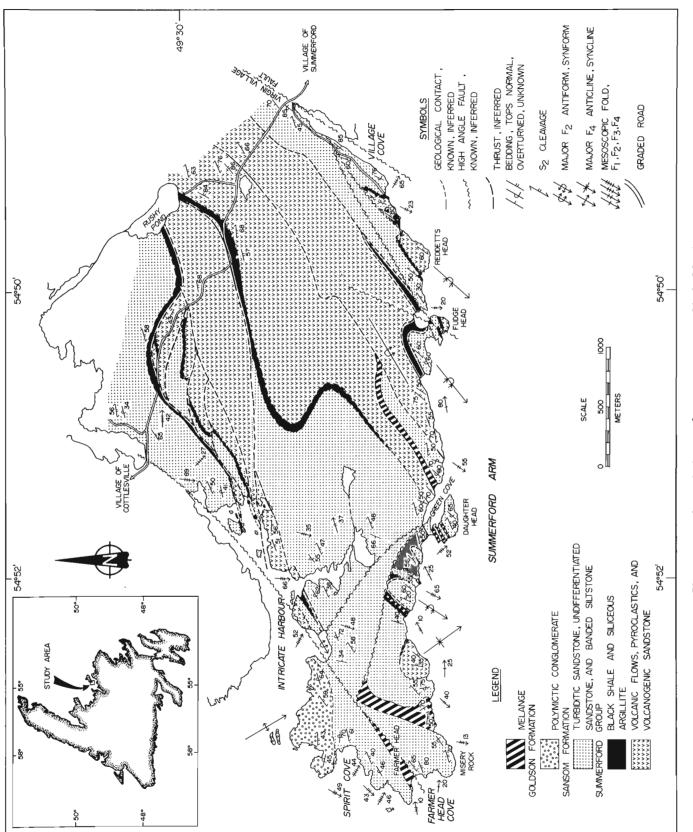
Figure 5.1. *Geological map of southwestern New World Island.*

45

The undifferentiated sandstone varies from interbedded shale, feldspathic sandstone, and conglomerate, to unbedded fine- to coarse-grained feldspathic sandstone. On the west side of Village Cove the two lithologies are transitional from feldspathic sandstone at the southwest to conglomerate with interbedded shales and feldspathic sandstone at the northeast. Bedding is on the centimetre to metre scale, can be massive or graded, and shows well defined Bouma sequences. Shale beds are laminated dark grey to silver and in places contain large (up to 3 cm long) clasts of red calcareous shale. The sandstone is dark grey, graded to massive, poorly sorted, and feldspathic, with subrounded to angular grains 0.1 mm to 1.5 cm in size. Conglomerate beds are massive to graded and poorly sorted with subrounded to angular grains 0.1 to 5.0 cm across and some angular shale clasts up to 20 cm long. Clasts include crystalline quartz, black chert, and lithic fragments of shale, feldspathic sandstone, and volcanic rocks. The matrix is feldspathic sandstone with trace amounts of sulphide minerals scattered throughout. Both the sandstone and the conglomerate weather to red, white, and grey. Outcrops of undifferentiated sandstone along Summerford Arm are medium- to very coarse-grained unbedded feldspathic sandstone of the same composition as those in Village Cove.

The turbiditic sandstones are fine- to coarse-grained grey feldspathic sandstones interbedded with thin argillaceous beds, and weather to buff, grey, and orange. Sandstone beds are 1 cm to more than 1 m thick and contain clearly defined Bouma sequences. Shale layers are 1-10 cm thick. The Bouma "A" layers range from fine to coarse sandstone and conglomerate with clasts up to 5 cm across. Clasts are poorly to moderately well sorted, subangular to subrounded quartz, feldspar, black chert, lithic fragments of sandstone, shale, limestone, and volcanic rocks. The matrix is feldspathic sandstone with trace amounts of sulphide minerals scattered throughout. Both the sandstone and the conglomerate weather red, white, and grey. Outcrops of undifferentiated sandstone along Summerford Arm are medium- to very coarse-grained unbedded feldspathic sandstone of the same composition as those in Village Cove.

The turbiditic sandstones are fine- to coarse-grained grey feldspathic sandstones interbedded with thin argillaceous beds, and weather to buff, grey, and orange. Sandstone beds are 1 cm to more than 1 m thick and contain clearly defined Bouma sequences. Shale layers are 1-10 cm thick. The Bouma "A" layers range from fine to coarse sandstone and conglomerate with clasts up to 5 cm across. Clasts are poorly to moderately well sorted, subangular to subrounded quartz, feldspar, black chert, lithic fragments of sandstone, shale, limestone, and volcanic rocks and trace amounts of disseminated sulphide minerals. The unit is not fossiliferous but it does contain round to oblate and prolate calcareous nodules up to 20 cm across in the long dimension. On Farmer Head, the turbidites contain channel fill sequences 8-10 m wide and 5-6 m thick with discordant bases and concordant tops composed of sandstone and conglomeratic fining upwards sequence. Turbiditic sandstones are conformably overlain by polymictic conglomerates at Farmer Head.

Polymictic conglomerate

Polymictic conglomerates outcrop at the mouth of Intricate Harbour and are intermixed with shale and feldspathic sandstone along Village Cove as described above. The lower contact with the turbiditic sandstone at the mouth of Intricate Harbour is depositional, with shallow channels of conglomerate cutting into the turbidites. The upper contact is not exposed, but the unit there must be at least 500 m thick.

The clasts are poorly sorted, angular to subrounded, matrix supported, and are a few millimetres to 50 cm across, with some limestone blocks up to 5 m across. Clasts are feldspathic sandstone, shale, green, grey, black, and red chert, mafic to volcanic rocks, quartz, felsic intrusive rocks, and limestone. The limestone clasts are rare grey to white irregular blocks up to 5 m across. They are highly fossiliferous, containing brachiopods, corals, algae, crinoids, and bryozoans that have been dated as Llandeilo and Caradoc (Horne and Johnson, 1970).

Beds are 3 cm to 2 m thick, may be massive to graded or reverse graded, and may have thin shaly interbeds. Away from the base of the unit beds become thicker and more often clast supported, and clasts become better sorted and rounded.

Mélange

The term 'mélange' is here used in a descriptive sense and applies to a medium- to fine-grained sedimentary matrix lacking well defined bedding and containing a heterogeneous assemblage of blocks and clasts of widely varying sizes. Mélange units on southwestern New World Island are intensely foliated sandstones, shales, and pebbly mudstones that contain no primary structures except for isolated bedding remnants. The matrix tends to have the same composition as adjacent sedimentary units although it is somewhat finer grained. Thus, on Daughter Head the mélange units have the composition of fine grained turbiditic sandstones but are highly sheared with isolated boudins of medium- to coarse-grained sandstone up to 20 cm long.

The mélange units at Green Cove, Daughter Head, and west of Daughter Head are concordant with surrounding units and tend to have abrupt contact or contacts that are gradational over the space of a few meters. East of Misery Rock (new informal name), mélange contact are unclear but are probably gradational, while on Farmer Head the contact with turbiditic sandstone is abrupt. In both cases the contact are structurally complex and the mélange units may or may not be concordant.

Intrusive rocks

Scattered throughout the map area are a series of grey to pink and buff felsic dykes. They are tens of centimetres to tens of metres wide, aphanitic to fine grained phaneritic and may or may not be porphyritic. Most have chilled contacts. Many show variations from andesitic to dacitic (Streckeisen, 1976), but most dykes can be classified as trondhjemites (Barker, 1979). Feldspar is unzoned albite (An_{0-10}) and may comprise from 36% to 60% of the rock by point count, depending on the intensity of alteration. Quartz content varies from none visible in thin section to 15%, but this estimate may be too low due to the difficulty in recognizing very fine interstitial quartz in the groundmass. Accessory minerals include chlorite (2-30%), white mica (0-23%), epidote (0-27%), carbonate (0-20%) and opaque minerals and apatite (1-16%). Chlorite, white mica, and epidote occur largely as alteration products of albite although some specimens contain large fresh crystals of epidote which may be primary.

Phenocrysts reach up to 3 mm in size and may be albite (often altered to chlorite, white mica, calcite, and/or epidote), or quartz. The groundmass in some cases has a spherulitic quench texture of albite ± quartz which attests to the hypabyssal nature of the dykes. Where quartz phenocrysts are present they are typically amoeboid and rimmed with quartz/albite symplectites.

Stratigraphy

Horne (1968, 1970) placed all the Ordovician strata in southwestern New World Island in the Summerford Group, which he divided into six units (labelled A, B, C, D, E, Z) primarily on the basis of contact relationships and primary structures. The stratigraphy proposed by Horne (1968, 1970) is considered inconsistent with field observations because: a) the lower, middle and upper volcanic units (units Z, B and D) are indistinguishable in the field and are probably the same unit, b) the Caradocian argillite unit (unit C) consists of graptolitic black shales in some places and of turbiditic siltstones and sandstones in other places, c) the chaotic unit (unit E) is turbiditic siltstone and sandstone in some places and graptolitic black shale in others, and d) the arkosic unit (unit A) is in places indistinguishable from the Upper Ordovician – Lower Silurian Sansom Formation.

Dean (1978) suggested a much simpler stratigraphy for the Summerford Group consisting of Lower and Middle Ordovician volcanic rocks and interbedded volcaniclastic sediments overlain by Caradocian black shales. On southwestern New World Island the Summerford Group is overlain by the Upper Ordovician – Lower Silurian (?) turbiditic sandstones and siltstones of the Sansom Formation which is overlain in turn by Lower Silurian polymictic conglomerates of the Goldson Formation. The undifferentiated sandstones are interpreted as being gradational between the Sansom Formation and the Goldson Formation. The undifferentiated sandstones are interpreted as being gradational between the Sansom Formation and the Goldson conglomerate. This ordering of lithologies is substantiated by field observation and fossil data from southwestern New World Island. Figure 5.2 shows the stratigraphy of the lithologies found on southwestern New World Island. The mélange units are not represented on the stratigraphic column because they are interpreted as secondary features representing the sites of intense deformation of pre-existing unlithified or lithified sediments.
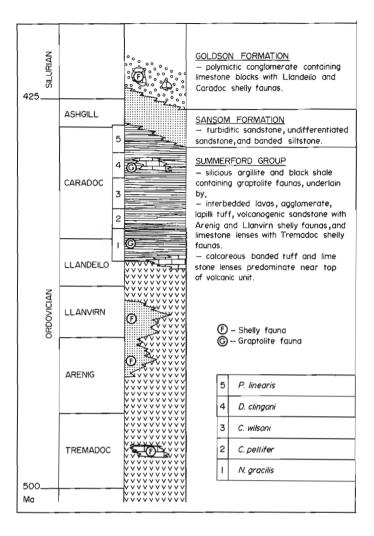
Structural Geology

On southwestern New World Island at least four generations of folds can be recognized on the basis of overprinting relationships. Early thrust faulting is thought to be responsible for the confusing repetition and rearrangement of strata across the peninsula. Late-stage high angle faults dissecting the area complicate the correlation of large-scale structures from one part of the area to another.

F_1
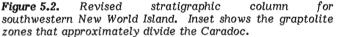
Folds of the earliest generation (overprinted by the S_2 cleavage and later fold generations), form tight folds with angular hinges and straight limbs, to isoclinal and intrafolial rootless folds. F_1 folds occur in all the bedded units of the area except in the Sansom Formation between Misery Rock and Spirit Cove, and the overlying Goldson Conglomerate.

F_2

Second generation folds are tight, with narrow hinges and planar to slightly curved limbs. They are plunging, inclined, may be upright or overturned, and have an axial planar cleavage (S_2). F_2 axes scatter in a broad, moderately southwest dipping girdle parallel to the trace of S_2. On outcrop scale F_2 folds are rare, but macroscopic folds in the area are interpreted as F_2 on the basis of the close relationship between S_2 orientations and those of the axial traces of macroscopic folds. The S_2 cleavage is penetrative on a microscopic scale and occurs throughout the area. The slaty cleavage is well defined in fine grained units, moderately well defined in coarse grained units, and only

Figure 5.2. Revised stratigraphic column for southwestern New World Island. Inset shows the graptolite zones that approximately divide the Caradoc.

locally visible in the massive lavas and coarse pyroclastic units. In thin section, S_2 is defined by a preferred orientation or bimodal fabric (Hobbs et al., 1976, p. 225) of elongate grains and slaty minerals, and by new growth of chlorite in sandy layers.

F_3

F_3 folds are morphologically similar to F_2 folds, but are only found at the mesoscopic scale and do not have a penetrative axial planar cleavage. They overprint the regional S_2 cleavage, have axial plane orientations roughly parallel to those of F_2, and tend to plunge moderately to the southwest. F_3 folds are common throughout the area but are best exposed at Farmer Head where F_3 folding was most intense.

F_4

F_4 folds are broad open warps that can be seen in outcrop to overprint the regional cleavage and all other fold generations. They are gentle folds with no related cleavage and they range in size from outcrop scale to kilometre scale. Axial planes dip steeply to the east southeast and fold plunge varies from gentle to steep towards the southeast. F_4 folding had little effect on the eastern part of the area and became more intense to the west near Farmer Head.

Late kinks

Scattered throughout the area are a series of small-scale kink bands. They are steeply dipping and overprint the regional cleavage, F_1, F_2, and F_3. A related crenulation cleavage (S_3) is locally developed. Kink bands are not common and insufficient data have been collected to properly interpret conjugate relationships and mean shortening direction. Overprinting relationships with F_4 are not clear, so kink bands are here grouped with F_4 folds although they may in fact pre- or post-date F_4 folding.

Thrusting

Outcrop-scale thrust ramps are abundant in the layered strata of southwestern New World Island. On a larger scale, mélange units similar to the movement zones described by Karlstrom et al. (1982) are found parallel to bedding in the zones between the repetitions of north-facing stratigraphic successions. Both structures are overprinted by the S_2 cleavage. These observations suggest that there was thrusting associated with the earliest deformation in the area, as has been recorded for eastern New World Island by Karlstrom et al. (1982).

Timing of Deformation

The youngest unit to show all four fold generations is the Upper Ordovician (Ashgillian) Sansom Formation. The youngest unit in the area, the Goldson Conglomerate, does not show the effects of intense deformation as do the finer grained sediments, but there is evidence that it has been deformed as early as F_2. A fracture cleavage (Hobbs et al., 1976, p. 216) is found in conglomerate beds and thin silty interbeds have a slaty cleavage which has the same orientation as the regional cleavage and is interpreted as S_2. Mesoscopic folds are rare, and those that exist are gentle warps in the style of F_4 that fold the S_2 cleavage. They have orientations similar to those of F_3 and F_4 and vergence is to the north and the south. Other evidence of pre-F_3 deformation is the presence of mesoscopic pre-S_2 thrust ramps.

Two felsic dykes in the conglomerates are displaced a few centimetres to one or two metres along bedding planes in a sinistral sense, but this may be related to flexural slip-type folding that resulted in the large southeasterly plunging F_4 antiform at the mouth of Intricate Harbour, rather than to F_1 or F_2 related thrusting.

It is possible that F_1 deformation took place prior to conglomerate deposition. The contact between the Sansom Formation and the Goldson Formation at Spirit Cove is conformable, but no F_1 fold closures have been found in the Sansom Formation at Farmer Head. This section represents the uppermost part of the Sansom Formation and it is possible that F_1 deformation ceased sometime during the deposition of that unit. This would mean that F_1 deformation in the base of the Sansom Formation may have taken place in unlithified sediments.

Another piece of evidence indicating folding prior to conglomerate deposition is the presence of a sandy siltstone clast containing a gentle fold in its primary layering. The external form of the clast itself is not folded, but it is possible that the fold was produced at some time during flattening of the clast after deposition.

On Farmer Head, metre-scale thrust ramps are folded by and found in the limbs of F_3 folds, and along Summerford Arm stratigraphically inferred thrust sheets are folded into macroscopic F_2 synclinoria that plunge to the southwest.

Table 5.1 Summary of the deformational history of southwestern New World Island. Vertical lines indicate relative duration of deformation events.

D_1 Ashgill(?)	Thrusting	F_1 folding SE/NW(?) compression	–mesoscopic folds in lithified and/or unlithified sediments. –formation of mélanges and thrust duplex.
post-Lower Silurian (Post-deposition of Goldson Cngl.)		F_2 folding SE/NW compression	–macroscopic NE/SW trending recumbent folds. –possible intrusion of some felsic dykes. –S_2 development ceases.
		F_3 folding SE/NW compression	–mesoscopic SW/NE plunging folds folding S_2. –steepening and overturning of strata. –intrusion of felsic dykes.
D_2		F_4 folding NE/SW compression	–mesoscopic and macroscopic NNW/SSE trending folds. –local kinking and formation of crenulation cleavage.
D_3 (?)	High angle faulting		

Mélange units on and near Daughter Head are crosscut by the S_2 cleavage. Thus thrusting took place early in the deformation history of the area, prior to or synchronous with F_2 folding.

At this time it can be confidently stated that F_1 deformation took place after the end of Caradocian times and that F_2, F_3, and F_4 deformation occurred later than early Silurian. F_1 deformation may have taken place in unlithified or semi-lithified sediments, but thrusting, F_2, F_3, and F_4 folding occurred after the deposition and lithification of the early Silurian Goldson Formation as indicated by the presence of thrust ramps and the S_2 cleavage in the conglomerates at the mouth of Intricate Harbour.

Synthesis

The depositional history of southwestern New World Island involved Lower to Middle Ordovician volcanism and volcaniclastic sedimentation, a Caradocian quiescence during which carbonaceous black shales were deposited, and the deposition of an Upper Ordovician-Lower Silurian coarsening upwards sequence of turbidite and debris flow conglomerate (Horne, 1968; McKerrow and Cocks, 1981).

The nature of the basement to this sequence is unclear but limestones and marine faunas in the lower Ordovician volcanic sequence indicate deposition in an oceanic environment above the carbonate compensation depth. The Ordovician volcanic rocks of the Dunnage Zone have been interpreted as island arc sequences (Kean and Strong, 1975; Dean, 1978; Williams, 1979) but recent geochemical analyses of some volcanic suites from the Bay of Exploits and from the Summerford Group on New World Island suggest the extrusives may be oceanic island basalts unrelated to subduction (Jacobi and Wasoski, personal communication, 1984).

Cessation of volcanism in Middle Ordovician times was followed by shale deposition in a restricted or starved basin that encompassed most of what is now the Dunnage Zone (Dean, 1978). This must have coincided with a tectonic quiescence and/or marine transgression which submerged the volcanic islands and prevented the production of terrigenous detritus and thus the deposition of coarser clastic marine sediment.

48

Thrusting, F_1 folding and mélange formation may have been initiated as early as Ashgillian times during the deposition of the coarsening upwards turbiditic flysch sequence of the Sansom Formation. This deformation continued through the deposition of the Lower Silurian Goldson Conglomerates.

F_2 mesoscopic and macroscopic folding was recumbent. S_2 cleavage development ceased before further northwest-southeast shortening produced upright F_3 folds which resulted in Type 3 (Thiessen and Means, 1980) coaxial overprinting of F_2 folds. Progressive deformation ended with the steepening and overturning of all strata.

F_4 folding and kinking was the result of later northeast-southwest compression that may have been related to the high angle strike-slip faulting in the area.

Table 5.1 summarizes the deformation history of southwestern New World Island. A single episode of progressive deformation is responsible for the sequence of events beginning with F_1 folding and thrusting and ending with F_3 folding. There are as yet no constraints on the duration of this deformation or on the timing of F_4 folding and high angle faulting.

Acknowledgments

References

Barker, F.
1979:   Trondhjemite: Definition, environment and hypotheses of origin; in Trondhjemites, Dacites and Related Rocks, ed. F. Barker; Elsevier, New York, N.Y. 659 p.

Bergstrom, S.M., Riva, J., and Kay, M.
1974:   Significance of conodonts, graptolites, and shelly faunas from the Ordovician of western and north-central Newfoundland; Canadian Journal of Earth Sciences, v. 11, p. 1625-1660.

Dean, P.L.
1978:   The volcanic stratigraphy and metallogeny of Notre Dame Bay, Newfoundland; Geology, v. 7, p. 1-12.

Hobbs, B.E., Means, W.D., and Williams, P.F.
1976:   An Outline of Structural Geology. John Wiley & Sons, New York, N.Y., 571 p.

Horne, G.S.
1968:   Stratigraphy and structural geology of southwestern New World Island area, Newfoundland; unpublished Ph.D. thesis, Columbia University, New York, N.Y.

1970:   Complex volcanic-sedimentary patterns in the Magog Belt of northeastern Newfoundland; Geological Society of America Bulletin, v. 81, p. 1767-1788.

Horne, G.S. and Johnson, J.H.
1970:   Ordovician algae from boulders in Silurian deposits of New World Island, Newfoundland. Journal of Paleontology, v. 44, no. 6, p. 1055-1059.

Karlstrom, K.E., van der Pluijm, B.A., and Williams, P.F.
1982:   Structural interpretation of the eastern Notre Dame Bay area, Newfoundland: regional post-Middle Silurian thrusting and asymmetrical folding; Canadian Journal of Earth Sciences, v. 19, p. 2325-2341.

Kean, B.F., Dean, P.L., and Strong, D.F.
1981:   Regional geology of the central volcanic belt of Newfoundland; in The Buchans orebodies: fifty years of geology and mining, ed. E.A. Swanson, D.F. Strong, and J.E. Thurlow; Geological Association of Canada, Special Paper 22.

Kean, B.F. and Strong, D.F.
1975:   Geochemical evolution of the Ordovician island arc of the central Newfoundland Appalachians; American Journal of Sciences, v. 275, p. 97-118.

McKerrow, W.S. and Cocks, L.R.M.
1981:   Stratigraphy of eastern Bay of Exploits, Newfoundland; Canadian Journal of Earth Sciences, v. 18, p. 751-764.

Patrick, T.O.H.
1956:   Comfort Cove, Newfoundland. Geological Survey of Canada, Paper 55-31. Map with marginal notes.

Streckeisen, A.
1976:   To each plutonic rock its proper name; Earth Science Reviews, v. 19, p. 1-33.

Thiessen, R.L. and Means, W.D.
1980:   Classification of fold interference patterns: a reexamination; Journal of Structural Geology, v. 2, no. 3, p. 311-316.

Williams, H.
1963:   Twillingate map-area, Newfoundland; Geological Survey of Canada, Paper 63-63, 30 p.

1978:   Tectonic-lithofacies map of the Appalachian orogen; Memorial University of Newfoundland; Map No. 1.

Vitrinite reflectance measurements from the South Whale Basin, Grand Banks, Eastern Canada, and implications for hydrocarbon exploration

M.P. Avery and J.S. Bell
Atlantic Geoscience Centre, Dartmouth

Abstract

Measurements made on samples from the Tern A-68 and Puffin B-90 offshore wells reveal a continuous increase in reflectance with significant oil generation levels reached at approximately 3350 m. Verrill Canyon shales now buried at 4700 m at Puffin B-90 are estimated to have reached this maturation level during Eocene time. Both wells also contain reworked vitrinite which is believed to have been sourced from nearby, but now buried, Upper Paleozoic rocks. Gas may have been generated from Mesozoic shales and from Upper Paleozoic coal-bearing units.

Résumé

Des mesures ont été réalisées sur des échantillons provenant des puits Tern A-68 et Puffin B-90. Elles révèlent une augmentation continuelle de la réflectance avec des niveaux de génération d'huile situés approximativement à 3350 m. Nous estimons que les argiles de la formation de Verrill Canyon, maintenant enfouies à 4700 m au puits Puffin B-90, ont atteint ce niveau de maturation durant l'Éocène. Les deux puits renferment également de la vitrinite remaniée. Nous pensons que celle-ci provient des proches, mais désormais enfouies, roches du Paléozoïque supérieur. Le gaz a pu être généré à partir des argiles du Mésozoïque et à partir des unités du Paléozoïque supérieur contenant du charbon.

Introduction

As part of the continuing studies of the thermal maturity of the sedimentary sequences encountered in petroleum exploration wells drilled on the eastern Canada offshore margin, organic maturation profiles have been determined for Amoco-Imperial-Skelly Tern A-68 and Amoco-Imperial Puffin B-90 wells, located in the South Whale Basin on the Grand Banks of Eastern Canada (Fig. 6.1).

Methods

Reflectance measurements have been made on vitrinite contained in the dispersed organic matter residues which were recovered as byproducts of palynological sample preparation, as described by Davies and Avery (1984). The organic residues were freeze-dried and mounted in acrylic lucite stubs. After polishing, the samples were examined under reflected light, and the reflectance in oil of the identified vitrinite grains was measured with a Zeiss Photomultiplier III reflectance microscope system, attached to a Zonax microcomputer equipped with software which permitted automated shutter control, online data acquisition, manipulation and display.

For each sample with surface area of approximately 32 mm^2 up to 99 readings were taken. Basic statistical information, such as the arithmetic mean and standard deviation of the readings, were continuously updated and displayed on the computer monitor as they were acquired. The software also provided a histogram display of the values as they were obtained from the photomultiplier. These histograms were later used to assist in the interpretation of primary and recycled vitrinite reflectance populations.
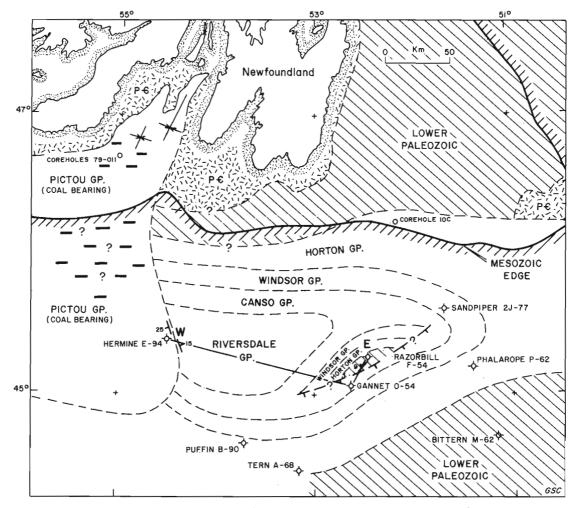
It is important to emphasize that the analysis was carried out on stubs containing a concentrate of grains of organic material, not polished rock surfaces. Although grain size, shape and edge characteristics can suggest whether a vitrinite particle is primary or reworked, the usual petrographic criteria for identifying reworked grains are more difficult to apply.

Results

The kerogen material from the Tern A-68 well (Fig. 6.2, Table 6.1) provided a very complete sample coverage for determining the thermal maturation profile. The average sample spacing over the 4189 m penetrated by the well was 150 m, providing adequate data for a detailed interpretation. The Puffin B-90 well (Fig. 6.3, Table 6.2) had similar sample coverage over the upper and lower sections but there was a sample break between 2557 and 4225 m.

Vitrinite reflectance increases log-normally with depth (Dow, 1977) and Figures 6.2 and 6.5 show this relationship as a best-fit line established by a least squares fit of the data.

Figure 6.1. *Schematic representation of a possible Paleozoic subcrop configuration beneath Mesozoic sequences of the southern Grand Banks.*

In both wells the Ro/depth line projects to the sea floor surface at a value of 0.22 Ro which suggests that the organics are now at their maximum burial depth since deposition, because newly deposited vitrinite (or its precursor huminite) has a reflectance of 0.2 Ro (Dow, 1977).

Both wells encountered very similar stratigraphic sequences with similar unconformities. These hiatuses do not involve large periods of time, so single maturation gradients can be applied to the entire well sections. A significant change in the complete histograms of the reflectance values was evident between the Early Eocene unonformity and the Avalon Unconformity. Vitrinite reflectance readings for this sequence were dominated by large populations of much higher reflectance than the primary populations (Tables 6.1 and 6.2).

Although the Puffin B-90 well was drilled to a greater depth than the Tern A-68 well, its vitrinite reflectance/depth profile is essentially identical. This is readily apparent when the various maturation levels are compared (Fig. 6.2 and 6.3).

The profile of reflectance values taken on the reworked vitrinite clasts above the Early Eocene unconformity in the Tern A-68 well shows a slightly negative or reversed gradient. Such a sequence could record the erosion of a normally matured section, and redeposition of its components in reverse order to their original stratigraphic position. Below this unconformity the 'reworked' profile abruptly increases in Ro and reverts to what may be a normal or positive gradient. This could indicate that the original pre-Mesozoic coalification level attained by the 'reworked' particles has been surpassed by the coalification imposed on them during their present burial. Alternatively, two separate source areas may have supplied the 'reworked' particles.

Discussion and conclusions

As noted above, the dispersed organic residue samples from Amoco-Imperial Skelly Tern A-68 contain a significant fraction of vitrinite flakes with anomalously high
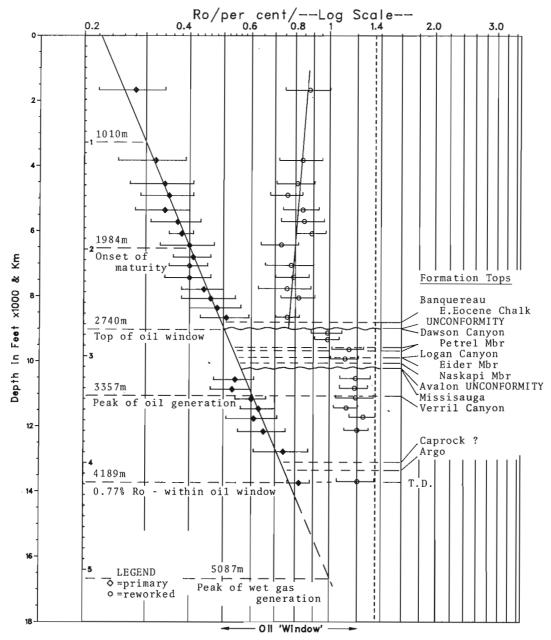
Figure 6.2. *Thermal maturation profile of the Amoco-Imperial Skelly Tern A-68 well.*

reflectance (Fig. 6.2). A similar, but less clearly defined, population was encountered in the samples from Amoco-Imperial Puffin B-90 (Fig. 6.3). It is likely that the Mesozoic and Cenozoic sequences penetrated by these wells contain vitrinite fragments that have been reworked from older Late Paleozoic units.

Jansa (1974) reported finding coal fragments in ditch cutting samples from the Missisauga, Logan Canyon and Banquereau formations at Puffin B-90. At the time, he did not speculate that any of these coal fragments might be reworked, but the vitrinite reflectance data reported here suggest that some of them may have been recycled. It is very likely that a source terrain for coal fragments existed to the northeast of the Tern A-68 and Puffin B-90 wells during Mesozoic and Tertiary time. King et al. (in press) cored grey shale with coal fragments, grey siltstone and grey

sandstone with carbonaceous stringers in Placentia Bay (Fig. 6.1). Barss (1979) separated palynomorphs from four of the cores. All were of Pennsylvanian age and cores 79-011 1-3, which contain shale with coal fragments, yielded spores of late Westphalian B-Westphalian D age (Barss, 1979). These seafloor outcorps are therefore assigned to the Pictou Group. Seafloor mapping suggests that Pictou Group sediments unconformably overlie Precambrian basement in Placentia Bay (King et al., in press). About 150 km to the south, the basal part of the Pictou Group is encountered in the Elf Hermine E-94 well (Howie, 1974) as illustrated in Figure 6.3. The dipmeter log indicates that the Pictou Group dips westward, whereas the underlying Upper Paleozoic section dips eastward (Fig. 6.1). Thus, in two areas of the western Grand Banks the Pictou Group appears to rest unconformably on older strata.

Figure 6.3. Thermal maturation profile of the Amoco-Imperial Puffin B-90 well.

Table 6.1. Summary of kerogen-based vitrinite reflectance data for the Tern A-68 well.

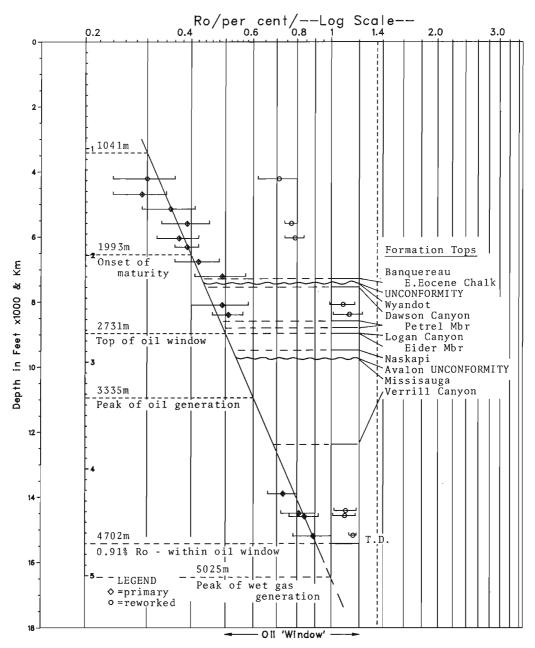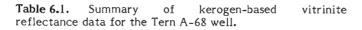| Depth interval in feet	Ro (stand. dev.) Primary	Reworked	Number of Readings Total	Primary	Reworked
1640-1670	.28 (.06)	.88 (.13)	56	30	16
3800-3830	.32 (.07)	.84 (.12)	66	31	31
4520-4550	.34 (.07)	.81 (.1)	71	39	23
4880-4910	.35 (.06)	.76 (.08)	25	13	11
5330-5360	.34 (.06)	.84 (.1)	58	46	7
5690-5720	.37 (.06)	.85 (.12)	57	35	18
6050-6080	.38 (.03)	.89 (.09)	49	29	7
6410-6440	.4 (.07)	.73 (.09)	42	33	5
6770-6800	.41 (.05)	--	43	34	--
7040-7070	.4 (.05)	.78 (.12)	41	23	14
7400-7430	.4 (.06)	.79 (.09)	45	32	11
7760-7790	.44 (.06)	.76 (.13)	46	33	9
8040-8070	.46 (.08)	.82 (.09)	54	40	14
8330-8360	.48 (.08)	--	50	46	--
8630-8660	.51 (.08)	.76 (.06)	41	25	12
9030-9160	--	.99 (.1)	99	--	74
9330-9360	--	.99 (.08)	99	--	50
9630-9660	--	1.14 (.12)	99	--	85
9930-9960	--	1.11 (.1)	99	--	88
10530-10560	.54 (.07)	1.19 (.12)	99	15	67
10830-10860	.53 (.07)	1.18 (.11)	99	30	53
11130-11160	.6 (.06)	1.19 (.15)	68	35	28
11430-11460	.63 (.07)	1.12 (.09)	62	55	6
11730-11760	.61 (.1)	1.25 (.11)	99	84	11
12130-12160	.65 (.1)	1.20 (.1)	95	64	17
12750-12780	.74 (.13)	--	17	13	--
13710-13740	.82 (.06)	1.20 (.15)	99	8	71

Table 6.2. Summary of kerogen-based vitrinite reflectance data for the Puffin B-90 well.

Depth interval in feet	Ro (stand. dev.) Primary	Reworked	Number of Readings Total	Primary	Reworked
4180-4210	.3 (.06)	.71 (.09)	37	16	16
4660-4690	.29 (.05)	--	23	22	--
5020-5140	.35 (.06)	--	19	15	--
5560-5590	.39 (.06)	.77 (.03)	30	26	3
5920-6040	.37 (.05)	.79 (.05)	46	28	3
6280-6310	.39 (.03)	--	23	13	--
6730-6760	.42 (.06)	--	42	28	--
7180-7210	.49 (.08)	--	20	10	--
7950-8090	.49 (.09)	1.08 (.09)	95	25	28
8360-8390	.51 (.05)	1.12 (.11)	91	3	59
13860-13890	.73 (.07)	--	50	49	--
14360-14440	.81 (.09)	1.10 (.08)	70	57	13
14560-14590	.84 (.08)	1.09 (.08)	71	50	21
15160-15190	.89 (.11)	1.15 (.01)	51	41	5

Table 6.3. Well and corehole information used to reconstruct the pre-Mesozoic subcrop configuration portrayed in Figure 6.1. Data sources were as follows: 1 - Howie, 1974; 2 - Howie and Barss, 1975; 3 - Operator's well history reports and logs; 4 - King et al. (in press).

| UNITS \ WELLS	Coreholes 79-011,1,3,6 [4]	Hermine E-94 [1]	Gannet O-54 [3]	Sandpiper 2J-77 [3]	Corehole 10 C [2]	Murre G-67 [3]	Phalarope P-62 [3]	Razorbill F-54 [3]	Bittern M-62 [3]	Jaeger A-49 [3]
PICTOU GROUP	ss, sh coal frags	1641.3 - 1709.9 Red ss, sh.								
RIVERSDALE GROUP		1709.9 - 2106.2 Red ss, cgl, sh, dol.								
CANSO GROUP		2106.2 - 2455.2 Red sh, ss.	1908.0-1972.3 Red sh, ss.							
WINDSOR GROUP		2455.2 - 3267.7 Halite,anhyd, dol, sh.	1972.3-2345.4 Anhyd,halite dol, sh.	3002.3-3264.1 Anhyd, sh. dol.						
HORTON GROUP			2345.4-3039.8 Red ss, cgl, sh.	3264.1-3525.3 Sh, ss.	Red. sh.	3157.7-3237.0 Red slates	2471.9-2942.2 Red sh,siltst, ss.			
LOWER PALEOZOIC						3237.0-3372.3 Met'c Qzites ? Lower Palz.	2942.2-3073.9 Sh, granite, ? Lower Ordovician	2621.3-3123.6 Sh, ss.	4718.0-4780.2 Red phylittes, ss.	893.1-935.7 Granite 376 ± 17 Ma
PRE-CAMBRIAN			3039.8-3048.0 Diorite sh, ss.				3073.9-3161.7 Met'cs.	3123.6-3135.2 Granite 661 ± 39 Ma	Depths given in metres below K.B.	
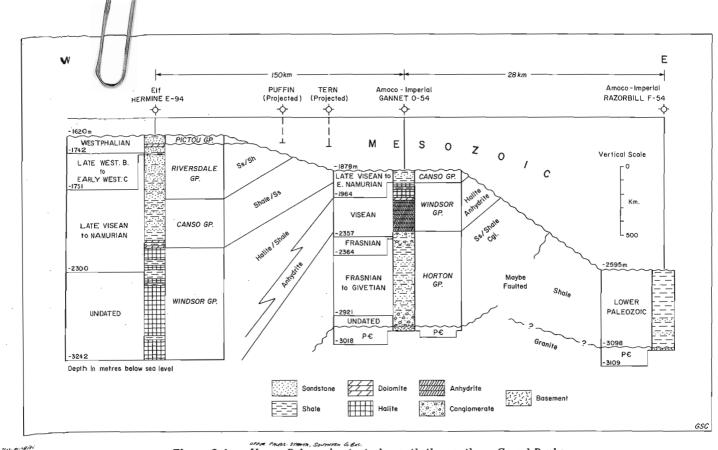
Figure 6.4.   *Upper Paleozoic strata beneath the southern Grand Banks.*

Additional evidence favouring this interpretation comes from the pre-Mesozoic subcrop configuration on the Southern Grand Banks. As illustrated in Figure 6.1, Upper Paleozoic rock units beneath the Pictou Group can be interpreted in terms of an east-west trending, faulted synclinorium. The configuration shown honours the known stratigraphic information (Table 6.3) and the few available dipmeter records.

The inferred unconformable overlap of Pictou Group is similar to its structural setting in the Sydney Basin and, indeed, the Pictou sediments encountered on the western Grand Banks most probably form the eastern offshore extension of this basin (Hacquebard, 1983; Keppie, 1982).

Hydrocarbon potential

The reflectance levels of the primary vitrinite populations of dispersed organic residue samples from Tern A-68 and Puffin B-90 suggest that the section has matured sufficiently for significant oil generation (Ro = 0.6) at depths below approximately 3350 m. What is not known is whether suitably rich sapropelic rocks are present to source oil. Maturation levels appropriate for significant wet gas generation (Ro = 1.0) would be reached at approximately 5000 m depth. If the bathyal Verrill Canyon Formation shale section in distal parts of the Grand Banks is as organic-rich as it is on the Scotian Shelf (Powell, 1982), significant gas generation could have occurred. Time-Temperature Index

calculations as described by Waples (1980), using age determinations of Barss et al. (1979) and today's thermal gradient, suggest that the basal shales in the Puffin B-90 well (i.e., Verrill Canyon Shales at 4701.5 m K.B.) reached a maturation level equivalent to 0.6 Ro in Early Eocene time. If appropriate source rocks had been present at this level, initial oil generation (0.5 Ro) would have occurred in Mid-Cretaceous time.

This study also defines a possible regional play involving gas generated from Late Paleozoic coal-bearing sequences. If the subcrop configuration portrayed in Figure 6.1 has some validity, there may be a coal-bearing sequence preserved beneath Mesozoic and Cenozoic rocks in the western part of the Grand Banks. If present, such a sequence may have matured sufficiently to have generated gas, which could be trapped in adjacent or overlying sandstone reservoirs, as has occurred in the southern North Sea and at Groningen in the Netherlands (Pegrum et al., 1975). No wells have yet been drilled to test this possibility.

Acknowledgments

References

Barss, M.S.
1979: Palynological analyses of samples submitted for age determinations by L.H. King, from Hudson 79011 cruise; Atlantic Geoscience Centre, Report No. EPGS-PAL.36-79MSB.

Barss, M.S., Bujak, J.P., and Williams, G.L.
1979: Palynological zonation and correlation of sixty seven wells, Eastern Canada; Geological Survey of Canada, Paper 78-24, 118 p.

Davies, E.H. and Avery, M.P.
1984: A system for vitrinite reflectance analysis on dispersed organic matter for offshore eastern Canada; in Current Research, Part A, Geological Survey of Canada, Paper 84-1A, p. 367-372.

Dow, W.G.
1977: Kerogen studies and geological interpretations; Journal of Geochemical Exploration, v. 7, p. 79-99.

Hacquebard, P.A.
1983: Geological development and economic evaluation of the Sydney coal basin, Nova Scotia; in Current Research, Part A, Geological Survey of Canada, Paper 83-1A, p. 71-81.

Howie, R.D.
1974: Report on the stratigraphic analysis of the Paleozoic section of the Elf Hermine E-94; Atlantic Geoscience Centre, Report No. EPGS-STRAT.1-74RDH.

Howie, R.D. and Barss, M.S.
1975: Upper Paleozoic rocks of the Atlantic provinces, Gulf of St. Lawrence and adjacent continental shelf; in Offshore Geology of Eastern Canada, Geological Survey of Canada, Paper 74-30, v. 2, p. 35-50.

Jansa, L.F.
1974: Report on the lithostratigraphy of the Amoco-I.O.E. A-1 Puffin B-90 well, Grand Banks, Newfoundland; Atlantic Geoscience Centre, Report No. EPGS-STRAT.4-74LFJ.

Jenkins, W.A.M.
1974: Age determinations in the interval 10,000 ft. to 10,949 ft. (T.D.) of the Amoco-I.O.E. A-1 Murre G-67 well, Grand Banks, Newfoundland; Atlantic Geoscience Centre, Report No. EPGS-PAL.8-7WAMJ.

Keppie, J.D.
1982: Tectonic Map of the Province of Nova Scotia; Department of Mines and Energy, Nova Scotia.

King, L.H., Fader, G.B., Jenkins, W.A.M., and King, E.L.
— Occurrence and regional setting of Lower Paleozoic sediments on the Grand Banks of Newfoundland; Canadian Journal of Earth Sciences. (in press)

Pegrum, R.M., Rees, G., and Naylor, D.
1975: Geology of the North-West European Continental Shelf, v. 2, The North Sea; Graham Trotman Dudley Ltd., London, 225 p.

Powell, T.G.
1982: Petroleum geochemistry of the Verrill Canyon Formation: a source for Scotian Shelf hydrocarbons; Bulletin of Canadian Petroleum Geology, v. 30, no. 2, p. 167-179.

Waples, D.
1980: Organic geochemistry for exploration geologists; Burgess Publishing Company, Minneapolis, 151 p.

Stress orientations from wellbore breakouts on the Scotian Shelf, Eastern Canada

A.J. Podrouzek[1] and J.S. Bell
Atlantic Geoscience Centre, Dartmouth

Abstract

Wellbore breakouts from 38 Scotian Shelf wells indicate that this region is presently subjected to anisotrophic horizontal stresses. The larger horizontal principal stress is oriented NE-SW, and the smaller horizontal principal stress lies parallel to the breakout elongation axes at right angles to this direction. In situ stresses may be locally different in parts of the Orpheus Graben.

Résumé

Cet article décrit une étude détaillée d'azimuts de cassures dans 38 puits d'huile dans la région du plateau de Scotian. Les azimuts indiquent que la direction de la contrainte horizontale maximale est nord-est — sud-ouest, et que la contrainte horizontale minimale est normale à cette direction. La situation peut-être différente dans certaines régions du graben Orpheus.

---

[1] GeoTech Surveys Ltd., 50 Johnson Crescent, Lower Sackville, Nova Scotia B4C 3A4

Method

In this study we have used wellbore breakouts to diagnose horizontal principal stresses of unequal magnitude and measure their azimuths. Breakouts are defined as intervals in boreholes which are noncircular because their walls have spalled so as to elongate one axis (Babcock, 1978). Such borehole elongation and the orientation of the long axes can be identified by four-arm dipmeter tools (Cox, 1970; Bell and Gough, 1983).

Breakouts are caused by localized compressive shear fracturing of the walls of boreholes due to amplification of the regional stress tensor by the borehole itself. When a vertical borehole is subjected to unequal (horizontal) stresses, acting approximately normal to its length, stress amplification on the borehole wall is greatest on that part of the wall which is at right angles to the greater stress. Kirsch (1898) analyzed the effect of uniaxial compression acting across an infinite slab with a small hole in it. He showed that, at the hole wall, radial and shear stresses vanish, as they must at a free surface, and the tangential stress σ_θ is:

$$\sigma_\theta = S - 2S\cos 2\theta$$

where S is the uniaxial stress and θ is measured from the direction of S. For biaxial horizontal principal stresses (Jaeger, 1962), the equation may be written:

$$\sigma_\theta = S_{Hmax} + S_{Hmin} - 2 (S_{Hmax} - S_{Hmin}) \cos 2\theta$$

where S_{Hmax} and S_{Hmin} equal the larger and smaller horizontal principal stresses respectively. If there is no horizontal stress anisotropy ($S_{Hmax} = S_{Hmin}$), in situ stresses will be doubled at the borehole wall, but this effect will be felt all round the borehole. On the other hand, if the horizontal principal stresses are unequal ($S_{Hmax} > S_{Hmin}$), σ_θ will have a maximum value ($3S_{Hmax} - S_{Hmin}$) on those sections of the borehole wall which are at right angles to S_{Hmax}. Bell and Gough (1979) proposed that shear fracturing there produces breakouts and elongates the borehole in a direction perpendicular to that of the larger horizontal principal stress. Subsequently, Gough and Bell (1982) applied Mohr-Coulomb fracture criteria to model an idealized breakout, and Zoback and others (in press) have modelled breakout failure zones under varying simulations of wellbore fluid pressure.

Wellbore breakouts have been analysed in several areas of North America, Europe, Asia, Afria and the East Pacific Ocean (see Bell and Gough, 1983; Cox, 1983; Newmark et al., 1984). In all areas where reliable independent measures of in situ stresses are available, the mean azimuths of borehole elongation are close to perpendicular to the larger horizontal principal stress in the region (Bell and Gough, 1983; Cox, 1983). There is, therefore, clear evidence that breakouts are reliable indicators of horizontal principal stress orientations, and that their presence documents stress anisotropy.

Breakout recognition criteria

Breakout recognition has been described at length by Babcock (1978), Bell and Gough (1981, 1983) and Cox (1983). Briefly, the four-arm dipmeter is a cylindrical tool with four electrode pads mounted on hydraulically extendable arms which monitor hole diameter as the tool is drawn up a borehole. Generally, these tools are raised at approximately 10 m/minute and the cable is torqued so as to rotate the tool clockwise. Rotation stops if one or both pads of a pair are trapped in a breakout. Simultaneous differential extension of the pairs of caliper arms completes breakout identification (Fig. 7.1).

In Western Canada, Fordjor et al. (1983) established the following breakout recognition criteria: (1) the log must record rotation of the tool below and above the breakout; (2) rotation must cease over the breakout interval, as shown by a record of constant azimuth for the No. 1 caliper arm; and (3) one pair of calipers must record the drill bit diameter and the other a larger value.

Scotian Shelf wells are drilled through less indurated rocks than Western Canadian wells of comparable depth, and generally exhibit more caving. Intervals in many wells were characterized by differential caliper extension, which was recorded with parallel traces and no cessation of tool rotation (Fig. 7.1). These zones are believed to represent washouts (Cox, 1983). We recognized breakouts in washed out zones when the caliper extension trace for the longer diameter recorded a morphology with greater relief than that recorded for the shorter diameter, as shown in Figure 7.1. We observed that the best developed breakouts occur typically in the deeper parts of the wells. Furthermore, the majority of the breakouts reported here were identified in the lower sections of dipmeter runs in intervals where the tools were rotating steadily. Frequently, there was limited tool torque near the tops of runs, so that the breakout recognition criteria there could not be met. Extensive caving, with boreholes often greatly exceeding drill bit diameter, was encountered in the shallower (Cenozoic) sections of many wells, which also prevented breakout recognition. It is probable that some genuine breakouts have been ignored because of resolution limitations of the four-arm dipmeter tool and its torquing capability, but we are confident that the data set presented here consists of true examples of the phenomenon.

Results and conclusions

Breakouts, together with caved intervals, are largely confined to shale, shale-rich or carbonate intervals on the Scotian Shelf in the wells we have examined. It appears that stress magnitudes and stress anisotropy on the Scotian Shelf are such that wellbore amplification produces localized shear stresses that exceed the cohesive strengths of shales, limestones and dolostones at many depths. For the most part, sandstone intervals in the Logan Canyon, Missisauga and Mic Mac formations do not exhibit breakouts. This is believed to
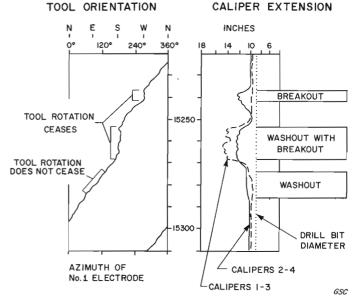

Figure 7.1. *Uncomputed 4-arm dipmeter log showing breakout and washout recognition criteria. The example is from the Sachem D-76 well.*

reflect their limited capacity to transmit anisotropic stress, because of relative lack of consolidation and, possibly, some strengthening by mudcake armouring of the hole walls. However, well-developed breakouts do occur in limestone and dolostone sequences in the Abenaki Formation. Some apparent breakouts were also observed in halite-rich sequences of the Argo Formation, but there was evidence in other wells of hole enlargement by salt solution. Plastic deformation of salt also could not be ruled out, so no breakouts were recorded in the Argo Formation.

Using the recognition criteria described above, consistent records of good and moderately developed breakouts have been recognized at burial depths between 376 m and 4873 m in wells on the Scotian Shelf. Within each breakout the azimuth of the greater diameter of the hole was measured at depth intervals ranging from 3 to 5 m. The shortest breakouts measured were 0.61 m long and the longest was 128 m. In all, 430 breakouts amounting to a total length of 5392.4 m, were identified in 38 wells (Table 7.1). Thirty two of these wells lie in the Scotian Basin and its sub-basins (Fig. 7.2). Two wells were drilled on the LaHave Platform and four wells are located in the Orpheus Graben (Fig. 7.2). As can be seen, the breakouts in wells in the Scotian Basin and on the LaHave Platform exhibit a remarkably consistent NW/NNW-SE/SSE orientation. This implies that this whole region is currently subjected to a regional anisotropic stress regime where S_{Hmin}, the lesser horizontal stress, is parallel to the mean breakout azimuths and oriented NW/NNW-SE/SSE and S_{Hmax}, the greater horizontal stress, is oriented NE/ENE- SW/WSW in a

Table 7.1.   Breakout analyses of wells from the Scotian Shelf

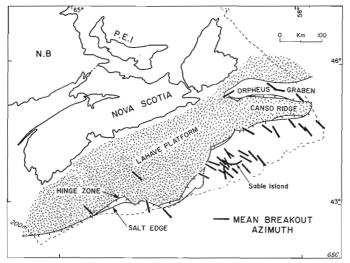| Location	Well	S_{Hmin} Mean Breakout Azimuth (Standard Deviation)	S_{Hmax} Azimuth
SCOTIAN BASIN			
42°51'43.98"N, 61°55'02.52"W	Acadia K-62	135.0° (10.5)	045 ± 11°
42°59'39.04"N, 62°28'51.32"W	Mohican I-100	164.2° (13.6)	074 ± 14°
43°41'27.20"N, 60°49'54.99"W	Demascota G-32	112.7° (10.8)	023 ± 11°
43°43'13.79"N, 60°05'21.93"W	Marmora C-34	130.0° (13.5)	040 ± 14°
43°44'19.17"N, 60°11'33.45"W	Onondaga F-75	168.5° (3.1)	079 ± 3°
43°45'07.30"N, 60°14'03.49"W	Onondaga B-96	116.5° (10.3)	027 ± 10°
43°49'35.78"N, 59°56'43.82"W	Intrepid L-80	129.7° (4.7)	040 ± 5°
43°50'06.73"N, 59°34'09.21"W	Eagle D-21	137.7° (13.5)	048 ± 14°
43°51'06.52"N, 60°37'13.89"W	Cohasset D-42	121.0° (21.3)	031 ± 21°
43°51'50.32"N, 60°36'18.23"W	Cohasset P-42	124.7° (10.3)	035 ± 10°
43°53'43.67"N, 60°13'38.13"W	Thebaud I-94	130.7° (10.8)	041 ± 11°
43°53'59.53"N, 60°12'19,34"W	Thebaud P-84	124.1° (7.2)	034 ± 7°
43°56'37.19"N, 60°29'58.55"W	Cohasset L-97	108.3° (11.4)	018 ± 11°
43°57'27.17"N, 60°07'37.81"W	Sable Island 3H-58	153.0° (7.1)	063 ± 7°
43°57'27.17"N, 60°07'37.81"W	Sable Island 4H-58	153.3° (10.0)	063 ± 10°
43°57'54.96"N, 60°06'38.16"W	Sable Island O-47	119.3° (24.7)	029 ± 25°
43°59'48.43"N, 59°06'51,63"W	Primrose N-50	141.8° (15.0)	052 ± 15°
43°59'56.13"N, 60°17'18.25"W	Migrant N-20	130.3° (10.4)	040 ± 10°
44°02'00.72"N, 59°36'37.37"W	Venture B-43	116.4° (16.0)	026 ± 16°
44°02'11.61"N, 59°32'03.50"W	Venture B-13	117.6° (7.9)	028 ± 8°
44°02'14.86"N, 59°34'24.72"W	Venture D-23	119.1° (10.0)	029 ± 10°
44°06'20.46"N, 59°21'27.45"W	Bluenose G-47	138.3° (7.2)	048 ± 7°
44°08'42.58"N, 59°37'32.11"W	Citnalta I-59	118.6° (11.0)	029 ± 11°
44°09'43.56"N, 60°04'09.34"W	Penobscot L-30	129.3° (21.6)	039 ± 22°
44°10'02.27"N, 60°00'34.53"W	Penobscot B-41	148.3° (6.7)	058 ± 7°
44°35'09.31"N, 57°41'58.40"W	Sachem D-76	143.7° (7.5)	054 ± 8°
44°36'20.50"N, 58°39'44.62"W	Chippewa G-67	150.8° (6.9)	061 ± 7°
44°38'08.86"N, 59°28'18.93"W	Mic Mac D-89	119.9° (16.3)	030 ± 16°
44°40'10.35"N, 58°55'10.83"W	Tuscarora D-61	128.3° (10.1)	038 ± 10°
44°41'40.33"N, 57°52'32.23"W	Hesper I-52	136.3° (8.9)	046 ± 9°
44°44'08.26"N, 57°20'46.62"W	Dauntless D-35	135.8° (19.9)	046 ± 20°
44°47'31.26"N, 58°11'19.24"W	Esperanto K-78	143.5° (8.4)	054 ± 8°
LAHAVE PLATFORM			
42°53'40.15"N, 64°13'45.83"W	Montagnais I-94	131.0° (15.4)	041 ± 15°
43°38'35.04"N, 62°48'17.04"W	Sambro I-29	129.1° (8.3)	039 ± 8°
ORPHEUS GRABEN			
45°19'27.56"N, 57°56'22.81"W	Adventure F-80	138.0° (4.3)	048 ± 4°
45°29'05.45"N, 58°32'28.72"W	Jason C-20	100.4° (4.1)	010 ± 4°
45°25'47.30"N, 60°04'46.97"W	Eurydice P-36	058.9° (17.0)	149 ± 17°
45°34'20.65"N, 58°47'13.07"W	Hercules G-15	124.7° (18.4)	035 ± 18°

Figure 7.2. *Mean breakout azimuths of Scotian Shelf wells. Breakouts were measured in 38 wells, but the results from several closely spaced wells are combined for this figure.*

perpendicular direction. This suggests that the LaHave Platform and the Scotian Basin form part of the Mid-American Stress province (Zoback and Zoback, 1980; Gough, 1984), which encompasses most of cratonic North America.

The situation may be different in the Orpheus Graben. Here two wells, Adventure F-80 and Hercules G-15, exhibit NW-SE breakouts, but Eurydice P-36 and Jason C-20 appear to be anomalous. At this time, it is not clear how significant these departures may be, but it is conceivable that the regional stress regime has been re-oriented locally around the southern margin of the Orpheus Graben along the offshore extension of the Chedabucto Fault (Keppie, 1982).

Acknowledgments

References

Babcock, E.A.
1978: Measurement of subsurface fractures from dipmeter logs; American Association of Petroleum Geologists Bulletin, v. 62, p. 1111-1126.

Bell, J.S. and Gough, D.I.
1979: Northeast-southwest compressive stress in Alberta: evidence from oil wells; Earth and Planetary Science Letters, v. 45, p. 475-482.

Bell, J.S. and Gough, D.I. (cont.)
1981: Intraplate stress orientations from Alberta oil wells; Evolution of the Earth, ed. R.J. O'Connell and W.S. Fyfe; American Geophysical Union and Geological Society of America, p. 94-104.

1983: The use of borehole breakouts in the study of crustal stress; in Hydraulic Fracturing Stress Measurements, M̄.D. Zoback and B.C. Haimson; National Academy Press, Washington, D.C., p. 201-209.

Cox, J.W.
1970: The high resolution dipmeter reveals dip-related borehole and formation characteristics; Proceedings, 11th Annual Logging Symposium, Society of Professional Well Log Analysts, Los Angeles, May 3-6, 1970.

1983: Long axis orientation in elongated boreholes and its correlation with rock stress data; Proceedings, 24th Annual Logging Symposium, Society of Professional Well Log Analysts, Calgary, June 27-30, 1983.

Fordjor, C.K., Bell, J.S., and Gough, D.I.
1983: Breakouts in Alberta and stress in the North American plate; Canadian Journal of Earth Sciences, v. 20, p. 1445-1455.

Gough, D.I.
1984: Mantle upflow under North America and plate dynamics; Nature, v. 311, p. 428-433.

Gough, D.I. and Bell, J.S.
1982: Stress orientations from borehole wall fractures with examples from Colorado, east Texas and northern Canada; Canadian Journal of Earth Sciences, v. 19, p. 1358-1370.

Jaeger, J.C.
1962: Elasticity, Fracture and Flow; 2nd edition, Wiley, New York, N.Y., 212 p.

Keppie, J.D.
1982: Tectonic map of the Province of Nova Scotia; Department of Mines and Energy, Nova Scotia.

Kirsch, G.
1898: Die Theorie der Elastizität und die Bedürfnisse der Festigketislehre: Zeitschrift des Vereines Deutscher Ingenieure, v. 42, p. 797-810.

Newmark, R.L., Zoback, M.D., and Anderson, R.N.
1984: Orientation of in situ stresses in the oceanic crust; Nature, v. 311, p. 424-428.

Zoback, M.L. and Zoback, M.D.
1980: State of stress in the conterminous Unived States; Journal of Geophysical Research, v. 85, p. 6113-6156.

Zoback, M.D., Moos, D., Mastin, L., and Anderson, R.N.
— Wellbore breakouts and in situ stress; Journal of Geophysical Research. (in press)

Clay minerals across the Tertiary-Quaternary boundary, northeastern Grand Banks of Newfoundland: preliminary results

Project 830056

M.P. Segall[1], J.V. Barrie[1], C.F.M. Lewis, and M.L.J. Maher[2]
Atlantic Geoscience Centre, Dartmouth

Abstract

The clay-sized minerals from six vibrocore sites have been analyzed using X-ray diffraction and SEM techniques. Although Late Pleistocene-Holocene sediments (commonly occurring as sand bodies <2 m thick) are generally clay-poor, minor quantities of illite, chlorite, quartz and feldspar in the <2 μm fraction do exist. These mineral phases probably reflect the mechanical weathering of continentally derived materials.

The relative abundances of clay minerals change significantly between the Late Pleistocene-Holocene and Tertiary marine sediments; this unconformable boundary exists on a regional scale. There is a marked downward increase (more than fivefold) in the amount of expandable minerals and kaolinite, and a notable decrease (more than threefold) in quartz and feldspar contents across the boundary. Relatively high Tertiary kaolinite contents (up to 1/6 of the clay mineral fraction) are indicative of an acidic leaching environment for this area. These results suggest a period of subaerial weathering for the uppermost Tertiary marine sediments. This was followed by deposition of sediments of northern latitude provenance (notably high illite and chlorite concentrations), possibly by ice rafting or glaciation.

Résumé

Les minéraux argileux prélevés à partir de six sondages vibrants ont été analysés par diffraction aux rayons X et au microscope électronique à balayage. Bien que les sédiments du Pléistocène supérieur et de l'Holocène (qui se présentent habituellement sous forme d'amas de sable inférieur à 2 m d'épaisseur) soient généralement pauvres en argile, on y trouve de faibles quantités d'illite, de chlorite, de quartz et de feldspath, de granulométrie inférieure à 2 μm. La présence des ces minéraux est peut-être le résultat d'une météorisation de matériaux en provenance du continent.

L'abondance relative de minéraux argileux est sensiblement différente entre les sédiments marins datant du Pléistocène supérieur et de l'Holocène et ceux de l'époque tertiaire; cette limite de discordance s'observe à l'échelle régionale. La quantité de minéraux gonflants et de kaolinite fait plus que quintupler à mesure que l'on descent, tandis la quantité de quartz et de feldspath diminue de plus de trois fois. La présence de quantités relativement élevées de kaolinite datant du Tertiaire (jusqu'à 1/6 de la fraction minérale argileuse) indique que l'environnement de cette région a subi un lessivage acide. Les sédiments marins du Tertiaire auraient donc connu une période de météorisation subaérienne. Cette période a été suivie par le dépôt de sédiments (notamment les concentrations élevées d'illite et de chlorite), en provenance des latitudes nordiques qui s'expliquerait par les glaces flottantes ou le remainiement de dépôts glaciaires antérieurs.

[1] C-CORE, Memorial University of Newfoundland, St. John's, Newfoundland A1B 3X5
[2] Golder Associates, St. John's, Newfoundland A1E 1C1

Introduction and geological setting

The Hibernia discovery area on the northeastern edge of the Grand Banks of Newfoundland is situated on an extensive wedge of Cretaceous-Tertiary sediments that lap onto older sequences of bedrock to the west (Fig. 8.1). Using shallow seismic reflection profiling (Huntec Deep Tow System), two major stratigraphic units have been defined (Fader and King, 1981): 1) the uppermost Late Pleistocene-Holocene sands and gravels which range from a maximum of 4 m in thickness to only a thin surficial cover; and 2) a lower, thick sequence of prograded Tertiary beds composed of fine sands, silts and clays, which is about 1.5 km thick (Arthur et al., 1982).

The uppermost thin unit of Late Pleistocene-Holocene sands and gravels has been described and divided into 5 surficial facies by Barrie et al. (1984): 1) sand ridge facies, 2) Grand Banks gravel facies, 3) boundary sand facies, 4) lag gravel and sand ribbons facies, and 5) continuous sand facies. In July 1983, 12 vibrocores were obtained from this same area (Lewis, 1984) (Fig. 8.1) and used to define the stratigraphy of the Late Pleistocene-Holocene sediments, the Tertiary-Quaternary unconformity, and the uppermost zone of Tertiary marine sediments.

The clay-sized minerals were examined from six vibrocore sites (Fig. 8.1) to determine the mineralogy in the <2 µm size fraction for the Hibernia area. The objective was to determine variations in mineralogy related to: source, current winnowing (transport), differential flocculation and coagulation within the marine environment, weathering, and diagenesis.

Methods

The clay mineralogy was analyzed using a combination of standard preparatory methods including those developed by Mehra and Jackson (1960), Cody and Thompson (1976), and Heath and Pisias (1979). These techniques involve: 1) the removal of silt by settling in the presence of sodium hexametaphosphate and subsequent flocculation with the addition of $MgCl_2$; 2) centrifuging and treatment with sodium citrate and sodium thiosulphate to remove amorphous free iron oxide; and 3) the use of a 10% talc internal standard. In addition, selected samples were treated by heating with concentrated HCl for 15 minutes. All samples were then allowed to settle using a vacuum apparatus onto 0.45 µm porous filters and mounted on glass slides. Selected samples were also heated at 110°C and 250°C for one hour to remove loosely-bound water from mineral phases. Untreated samples were also glycolated overnight before X-raying.

All samples were X-rayed using a Phillips X-ray diffractometer (XRD) (Model No. PW1130/96) at 1° 2θ per minute for the untreated, glycolated, heat and acid-treated slides. Slow scans of 1/4° 2θ per minute were run on the 0.33 to 0.35 nm area of the glycolated samples. CuK_α radiation was generated at 40 kV and 20 mA. Areas were determined using the peak height times peak width at half height method.

Selected samples were analyzed using scanning electron microscope and energy dispersive X-ray spectra (SEM/EDX) techniques. These methods were employed to verify results obtained from the XRD data.

Identification of clay-sized minerals

Analytical standards obtained from Wards Natural Science Limited were prepared with a talc internal standard in keeping with the above methodology and X-rayed to determine weighted peak-area percentages. It was found that weight ratios of clay minerals (i.e. chlorite, kaolinite, illite and montmorillonite) corresponded quite well to Biscaye's (1965) weighting factors. Thus, the following peaks and weighting factors were used: the area of 1.7 nm glycolated peak for montmorillonite; four times the 1.0 nm peak area (glycolated pattern) for illite; and twice the 0.7 nm chlorite/kaolinite peaks. The 0.7 nm chlorite/kaolinte peak was apportioned using Biscaye's (1965) ratio of 0.338 nm peak area divided by 0.358 nm plus 0.354 nm peak areas.

Because of the differences in crystal structure, the talc internal standard was considered inappropriate for abundance determination of quartz (0.426 nm), feldspar (0.325-0.318 nm), amphibole (0.848 nm), and pyroxene (0.299 nm). Ratios of feldspar (Ca and K), amphibole (hornblende) and pyroxene gave approximate weighting factors of 2 when varying known quantities were X-rayed with known quantities of clay minerals. A 2 µm sample of quartz was produced in the laboratory which gave acceptable peak areas. When apportioned and ratioed with clay and clay-sized minerals, the weighting factor for quartz ranged from 1.2 to 1.5. Although slightly lower than determined experimentally, a weighting factor of 1.3 was chosen for quartz, in keeping with results obtained by Mann and Müller (1980) for the western North Atlantic. The relative abundances of the clay-sized minerals in samples from the vibrocores are listed in Table 8.1 and are illustrated in Figure 8.2.

Precision of relative abundances

It must be stressed that the percentages calculated for these samples are semi-quantitative at best, and reflect only the relative abundances of identified minerals. Sources of error include: 1) lack of electronic precision in the X-ray circuits; 2) human error in area measurements; 3) slight changes in humidity and/or temperature; 4) the small size (approximately 45 cm^3) of the original sample; 5) the lack of successive runs on most samples for testing of consistency of results; and 6) the presence of mineral phases which cannot be accounted for. Per cent error noted in Table 8.1 is derived from the difference between the calculated sample weight, based on weighted peak areas, and the actual sample weight. Errors up to 40 per cent occur reflecting the semi-quantitative nature of the X-ray diffraction analytical technique.

Late Pleistocene-Holocene sediments

In general, Late Pleistocene-Holocene sediments are characterized as sands and gravels which consist of reworked earlier deposited glacial material or older underlying sequences (King and Fader, 1980; Fader and King, 1981; Barrie et al., 1984). Within these sediments are clay-sized components which generally amount to less than 2 per cent of the total sediment sample.

Figure 8.2 depicts the relative abundances of Late Pleistocene-Holocene clay-sized minerals determined by X-ray diffraction as a percentage of the total clay-size fraction for vibrocores 5 (0-1.89 m) and 6 (0-1.32 m) from a sand ridge. These sediments are characterized by high concentrations of illite accompanied by varying proportions of quartz, chlorite, feldspar and amphibole. Illite is the dominant clay-sized mineral (49%) at 1.32 m depth in vibrocore 6 (Fig. 8.3). Apatite is also present, as are quartz and feldspar. Illite and chlorite are general indicators of a northern latitude provenance suggestive of little weathering (Jackson et al., 1948; Chamley, 1979).

Vibrocore 16, from the boundary sand facies has clay-sized mineral suites typical of other Late Pleistocene-Holocene sediments. Illite, feldspar and chlorite comprise
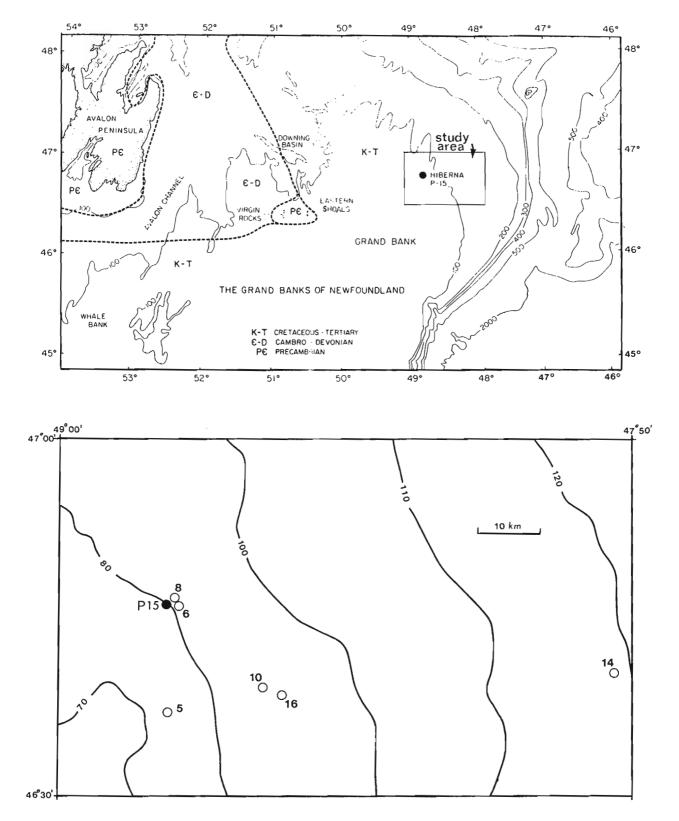
Figure 8.1.   Regional bedrock geology, bathymetry (m) and locations of vibrocore sites. The upper map after Barrie et al. (1984) shows locations os Hibernia P-15 well site and the study area.   The lower map shows detailed bathymetry (m) and locations of vibrocores within the study area.

Table 8.1. Hibernia clay mineralogy: relative abundances
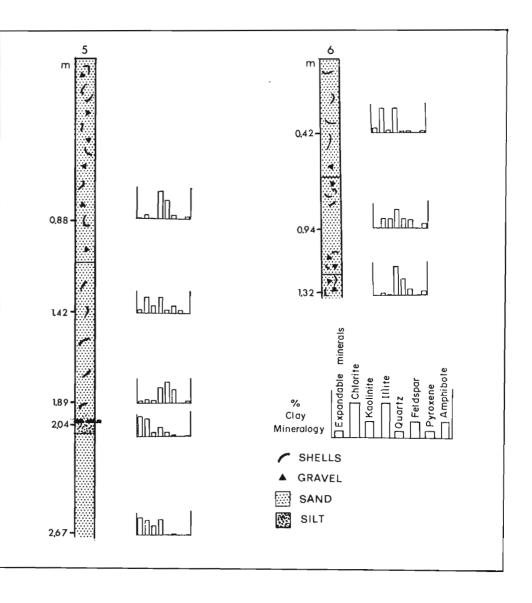
Sample	Bulk Mineralogy = 100%								
	E	C	K	I	Q	F	P	A	%Error
83-107-5-0.88	1	7	1	47	32	7	–	5	20
83-017-5-1.42	6	27	13	27	7	13	7	–	20
83-017-5-1.89	4	6	4	26	35	22	–	3	20
82-017-5-2.04	34	30	7	16	8	3	–	2	5
83-017-5-2.67	29	25	16	26	1	2	–	1	15
83-017-6-0.42	8	41	4	40	2	2	–	3	25
83-017-6-0.94	–	16	15	31	16	14	–	8	35
83-017-6-1.32	–	4	1	49	28	11	–	7	40
83-017-8-1.00	–	21	9	15	26	19	8	2	40
83-017-10-0.66	–	24	6	27	12	30	–	1	25
83-017-10-1.00	–	5	3	33	10	32	–	16	15
83-017-14-1.48	–	5	5	11	9	67	–	5	40
83-017-16-1.98	–	22	7	29	5	27	–	10	40

E - expandable minerals; I - illite; P - pyroxene;
C - chlorite; Q - quartz; A - amphibole
K - kaolinite; F - feldspar;

about equal amounts of approximately 25% each (Table 8.1). Farther to the east, in the continuous sand facies (Barrie et al., 1984) and in water depths greater than 110 m, angular well-crystallized sodic feldspar dominates a sample taken from vibrocore 14 at 1.48 m (Fig. 8.4). Feldspar comprises approximately 67% of the total clay-sized minerals. From the small number of vibrocore samples studied, it appears that clay-sized feldspar contents increase to the east in deeper waters, as does the angularity of clay-sized minerals in general. This could reflect the less energetic reworking of Holocene sediments in deeper water.

Piper and Slatt (1977) have also noted a high predominance of illite, chlorite, quartz and feldspar in samples collected from the Newfoundland continental shelf. They attribute the relatively high abundances of quartz and feldspar to the local bedrock of the continental source which contains more quartz and feldspar than clay minerals.

Uppermost Tertiary marine sediments

The uppermost Tertiary marine sediments differ from those of the Late Pleistocene-Holocene sediments having a higher content of fine sand, silt and clay particles. In the deeper sections of some vibrocores, a physially hard, dense surface which has been termed the Tertiary unconformity

Figure 8.2

Clay-sized mineralogy and lithology of Late Pleistocene-Holocene and uppermost Tertiary marine sediments for vibrocores 5 and 6. The Tertiary-Quaternary boundary is shown by the heavy dashed line on vibrocore 5.
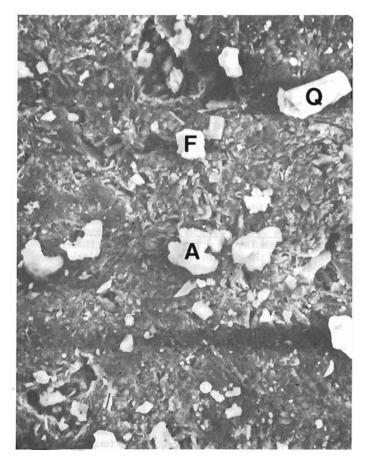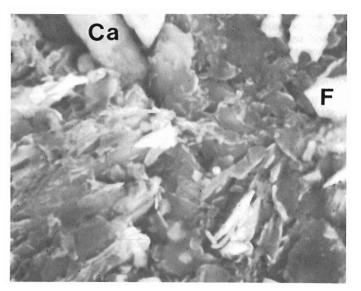
Figure 8.3. *SEM analysis, vibrocore sample 6 (1.32 m), showing the presence of apatite (A), feldspar (F), and quartz (Q) (x 2500). The majority of the small grains are illite.*

Figure 8.4. *SEM analysis, vibrocore sample 14 (1.48 m), showing the presence of calcite (Ca) and sodium feldspar (F) (x 2200).*

(Fader and King, 1981; Lewis and Barrie, 1981; Barrie et al., 1984) is encountered. Coring through this surface is difficult as indicated by the refusal of the vibrocorer. This dense unit is known acoustically by its greater sound velocity as determined in shallow seabed refraction surveys (Hunter et al., 1981). Although the sediments below the unconformity are dense and appear to be partially cemented, they slake in water when immersed for a period of 1-2 days.

At 2.04 m in vibrocore 5 (Fig. 8.2), there is a significant increase in the relative abundance of expandable minerals. These expandable minerals are considered to be predominantly swelling chlorite based on XRD data, but it is possible that iron rich smectites also exist. Quartz iron staining of the silt and sand-sized fraction suggests that there was abundant iron present which could have been leached from other mineral phases during a period of subaerial exposure. At 2.04 m in vibrocore 5 we see a moderate increase in kaolinite concentrations, while at 2.67 m, the relative abundance of kaolinite increases significantly to 16%. These high values provide evidence for the predominance of an acidic leaching environment under conditions of good drainage at a time of subaerial exposure. Kaolinite can form from K-feldspar, labradorite, illite, and montmorillonite with an increase in acidity to a pH of 4 and conditions of oxidation (Jackson et al., 1948). The absence of shells has been noticed from this interval, although they are prevalent in the Late Pleistocene-Holocene sediments. Acid dissolution during the weathering phase could be responsible for this absence. All of the preceeding aspects of the

uppermost Tertiary sediments indicate a chemically weathered zone. The density and strength of the Tertiary surface would likely be enhanced by dessication during subaerial exposure.

A mineralogical mixing of Late Pleistocene-Holocene (high illite, quartz and feldspar) and uppermost Tertiary (high kaolinite and expandable mineral phases) clay-sized components is possibly seen at 1.42 m in vibrocore 5. Although this interval lies within the Late Pleistocene-Holocene stratigraphic section, the presence of kaolinite and expandable mineral phases suggest that some Tertiary components have been introduced into the Late Pleistocene-Holocene sedimentary regime. For this to have occurred, the hard crust of the unconformity would have to be penetrated. Iceberg penetration as inferred from high resolution seismic reflection profiles (Lewis and Barrie, 1981) would destroy the original fabric of the soil, resulting in the release of Tertiary sediments.

Summary and conclusions

Preliminary results of clay-sized mineralogical analysis of Late Pleistocene-Holocene sediments and the uppermost Tertiary marine sediments suggest two geologically, geochemically, and geotechnically distinct units. Late Pleistocene-Holocene sediments are unconsolidated sands and gravels which are generally clay-poor. The clays which do exist consist of a dominant illite suite with feldspar increasing in relative abundance to the east. The predominance of clay-sized illite, chlorite and feldspar indicate derivation from a continental northern latitude provenance; while the eastward increase in feldspar content and angularity of particles could reflect variations of sediment reworking related to water depth.

The uppermost Tertiary marine sediments reflect an acidic, chemically weathered zone which was leached during conditions of subaerial exposure prior to the Late Pleistocene-Holocene marine transgression. Clay contents for this zone average 5%, with significant kaolinite abundances. Shells are absent from this interval. The weathering of this unit produced a hard, possibly desiccated crust which is difficult to penetrate. If this crust is disturbed

by iceberg penetration or by future installation of bottom-founded petroleum production facilities the underlying finer grained sediment could be subject to erosion by the present oceanographic regime.

References

Arthur, K.R., Cole, D.R., Henderson, G.G.L., and Kushner, D.W.
1982: Geology of the Hibernia discovery; American Association of Petroleum Geologists, Memoir 32, p. 181-195.

Barrie, J.V., Lewis, C.F.M., Fader, G.B., and King, L.H.
1984: Seabed processes on the northeastern Grand Banks of Newfoundland; modern reworking of relict sediments; Marine Geology, v. 27, p. 209-227.

Biscaye, P.E.
1965: Mineralogy and sedimentation of recent deep sea clay in the Atlantic Ocean and adjacent seas and oceans; Geological Society of America Bulletin, v. 76, p. 803-831.

Chamley, Herve
1979: North Atlantic clay sedimentation and palaeoenvironment since the Late Jurassic; in Proceedings of Maurice Ewing Symposium, American Geophysical Union, Washington, D.C., p. 342-361.

Cody, R.D. and Thompson, G.L.
1976: Quantitative X-ray powder diffraction analysis of clays using an orienting internal standard and pressed disks of bulk shale samples; Clays and Clay Minerals, v. 24, p. 224-231.

Fader, G.B. and King, L.H.
1981: A reconnaissance study of the surficial geology of the Grand Banks of Newfoundland; in Current Research, Part A, Geological Survey of Canada, Paper 81-1A, p. 45-81.

Heath, G.R. and Pisias, N.G.
1979: A method for the quantitative estimation of clay minerals in north Pacific deep-sea sediments; Clays and Clay Minerals, v. 27, p. 175-184.

Hunter, J.A.M., Waboso, C., Burns, R., and Good, R.
1981: Seabottom seismic reflection experiment; in C.F.M. Lewis. Report on Cruise BIO No. 81-012, CSS Baffin; Atlantic Geoscience Centre, Bedford Institute of Oceanography, Dartmouth, N.S., 24 p.

Jackson, M.L., Tyler, J.A., Willis, A.L., Bourbeau, G.A., and Pennington, R.P.
1948: Weathering sequence of clay-size minerals in soils and sediments; Journal of Physical Chemistry, v. 52, p. 1237-1260.

King, L.H. and Fader, G.B.
1980: Seabed conditions east of the Avalon Peninsula to the Virgin Rocks – their relationship to the feasibility of a pipeline from the Hibernia P-15 well site area to Newfoundland; Geological Survey of Canada, Open File 723.

Lewis, C.F.M.
1984: Sediment stability; coring on Grand Bank; in K.S. Manchester and B.D. Loncarevic. Report on Cruise 83-017, CSS Hudson; Atlantic Geoscience Centre, Bedford Institute of Oceanography, Dartmouth, N.S.

Lewis, C.F.M. and Barrie, J.V.
1981: Geological evidence of iceberg grounding and related seafloor processes in the Hibernia discovery area of Grand Bank, Newfoundland; in Symposium on Production and Transportation Systems for the Hibernia Discovery; Newfoundland Petroleum Directorate, St. John's, Newfoundland, p. 146-177.

Mann, U. and Müller, G.
1980: X-ray mineralogy of Deep Sea Drilling Project, Legs 51 through 53, western north Atlantic; in T. Donnelly, J. Francheteau et al., Initial Reports of the Deep Sea Drilling Project, v. 51, 52, 53, Part 2, U.S. Government Printing Office, Washington, D.C., p. 721-729.

Mehra, O.P. and Jackson, M.L.
1960: Iron oxide removal from soils and clays by dithionite-citrate system buffered with sodium bicarbonate; in Proceedings of the 7th National Conference on Clays and Clay Minerals, Clays and Clay Minerals, A. Swineford, ed., v. 7, p. 317-327.

Piper, D.J.W. and Slatt, R.M.
1977: Late Quaternary clay mineral distribution on the eastern continental margin of Canada; Geological Society of America Bulletin, v. 88, p. 267-272.

Coastal erosion and sedimentation in the Canadian Beaufort Sea

Project 830007

D.L. Forbes and D. Frobel
Atlantic Geoscience Centre, Dartmouth

Abstract

Sediments are supplied to the Beaufort Sea coast primarily from river and cliff sources. Mackenzie Delta is the major depositional feature, but has a predominantly erosional outer shoreline, despite high sediment supply and locally wide mudflats revealing sediment sink locations. Other features include cliffs, breached-lake embayments, flooded tundra flats, lagoons, estuaries, deltas, beaches, and barriers. Coastal surveys during 1984 included extensive oblique aerial video coverage, 22 beach profiles at 8 sites, sediment sampling, and 98 measurements of cliff recession at 11 sites. Beach deposits range from cliff-top gravels (up to 6.0 m above mean sea level) and gravel barriers (up to 2.2 m) to wide sandy spits and barrier islands with crest elevations as low as 0.4 m. Driftwood deposits occur as high as 6.0 m. Observed rates of cliff recession show high spatial and temporal variability, with 5-year means as high as 13 m/a.

Résumé

Les sédiments déposés sur la côte de la mer de Beaufort proviennent principalement des cours d'eau et des falaises. Le delta du MacKenzie constitue la principale zone de dépôt; il comporte cependant un littoral extérieur très exposé à l'érosion, malgré une forte alimentation en sédiments et la présence de vastes slikkes où les sédiments s'enfoncent à certains endroits. Parmi les autres éléments du relief, notons les falaises, les baies entaillées, les marécages de toundra inondées, les étangs, les estuaires, les deltas, les plages et les accumulations littorales. Les levés côtiers, effectués en 1984, comprenaient une couverture vidéo aérienne, 22 profils de plage à huit emplacements, l'échantillonnage de sédiments et 98 mesures visant à évaluer le retrait de 11 falaises. Les dépôts de plage sont composés de graviers provenant du haut des falaises (jusqu'à 6,0 m au dessus du niveau moyen de la mer) et d'accumulations littorales en gravier (jusqu'à 2,2 m) ainsi que de flèches littorales et d'îles barrières de sable dont la crête n'atteint pas 0,4 m de hauteur. Des dépôts de bois de dérive se trouvent à plus de 6 m. Le rythme de retrait des falaises varie considérablement dans l'espace et dans le temps, avec des moyennes aussi élevées que 13,4 m/a sur cinq ans.

Introduction

During 1984, the Geological Survey of Canada (GSC), in collaboration with Indian and Northern Affairs Canada (INAC), revived research activity in the Beaufort Sea coastal zone as part of the Northern Oil and Gas Action Plan (NOGAP). A renewed commitment to coastal research in the region is timely. Shorebase development in support of offshore exploration has already occurred in Tuktoyaktuk Harbour and McKinley Bay. Port facilities have been proposed at various times for Herschel Island, Stokes Point, King Point, and elsewhere. Additional requirements associated with offshore production may involve both pipeline shore crossings and extra port facilities. Demand for information on coastal geology and processes has increased rapidly as a result of these and other developments, including park planning and the Inuvialuit land claim settlement.

The Canadian Beaufort Sea coast possesses a range of coastal morphology and sediment types developed under varying seasonal runoff, wave, tide, surge, ice and thermal processes and a longterm rising trend in relative mean sea level (RSL). The present coast (Fig. 9.1) represents the landward limit of transgressive shoreline migration across the continental shelf over the past 20 ka or more (Blasco et al., 1983; Hill et al., in press). Geomorphological and tide-gauge data suggest that relative mean sea level is still rising rapidly (Forbes, 1980): the trend at the Tuktoyaktuk gauge (1962-1979 data), although not statistically significant, amounts to some 10 mm/a (Harper et al., 1985). Environmental conditions in the region include low mean annual air temperatures (-10°C at Tuktoyaktuk), thick permafrost and associated ground ice, a short open-water season averaging about 3 months (during which wave limitation by ice can still be important), very limited tidal range (0.5 m large tide at Tuktoyaktuk), important meteorological effects on water levels (with major storm surges raising levels substantially above normal higher high water), and 10%-exceedance deep-water significant wave heights of about 1.5 m (Huggett et al., 1975; Henry, 1975; Harper and Penland, 1982; Hall et al., 1983).

Early work along the Canadian Beaufort Sea coast (e.g. Mackay, 1960, 1963a, b; Rampton and Mackay, 1971; Public Works Canada, 1971a, b; Kerfoot and Mackay, 1972) was followed in the early 1970s and later by a number of reconnaissance surveys (e.g. McDonald and Lewis, 1973; McDonald et al., 1973; Lewis and Forbes, 1975; Lewis, 1977, unpublished notes; Lawrence et al., 1984) and more detailed site-specific studies (e.g. Carson et al., 1975; Hunter, 1975; Lewis, 1975; Rampton and Bouchard, 1975; Hollingshead et al., 1978; Forbes, 1981; Forbes and Lewis, 1983).

A field program was undertaken during the summer of 1984 with the following objectives:

1. Obtain low-level oblique airborne video of the coast for use in physical shore-zone classification.

2. Collect beach profile and sediment data at representative sites to supplement existing information.

3. Resurvey monumented cliff sections to determine erosion rates.

Video survey

The coastal video survey was undertaken to provide low-level aerial oblique imagery of the coast. Although oblique video lacks the quantitative photogrammetric potential of vertical photography, it has other advantages: these include an angle of view that is intelligible to untrained users and also provides coverage of high-angle cliff exposures; low cost; east of duplication; and opportunity for accompanying commentary. The commentary includes time and location data in addition to information on small-scale morphology, sediment characteristics, and other features that may be observable from the aircraft but difficult or impossible to see on the video record. It can also include a running description of physical shore-zone characteristics at all scales, with estimates of cliff height or beach width, and comments on processes. The commentary complements the video record and helps the viewer to assimilate visual data on the tapes, adding substantially to the value of the final product.

Figure 9.1 shows the extent of the 1984 video survey. The coverage includes part of eastern Liverpool Bay, the Tuktoyaktuk Peninsula including the north shore of Liverpool Bay, most of the Mackenzie Delta front including the older terrain of Richards Island and islands north of the delta (but excluding much of the active delta front facing Mackenzie Bay), and the entire Yukon coast. The survey was flown using a Bell-206 helicopter (G-VTK) out of Tuktoyaktuk. An attempt was made to keep altitude to 500 feet (150 m) and speed to 50 miles/h (25 m/s). The cameraman sat in the front port seat with the door removed, while the observer sat in the back port seat dictating commentary and monitoring the picture. The imagery was recorded on Sony U-matic (TM) 3/4-inch 20-minute tapes and subsequently copied to 3/4-inch 60-minute tapes for open-file release.
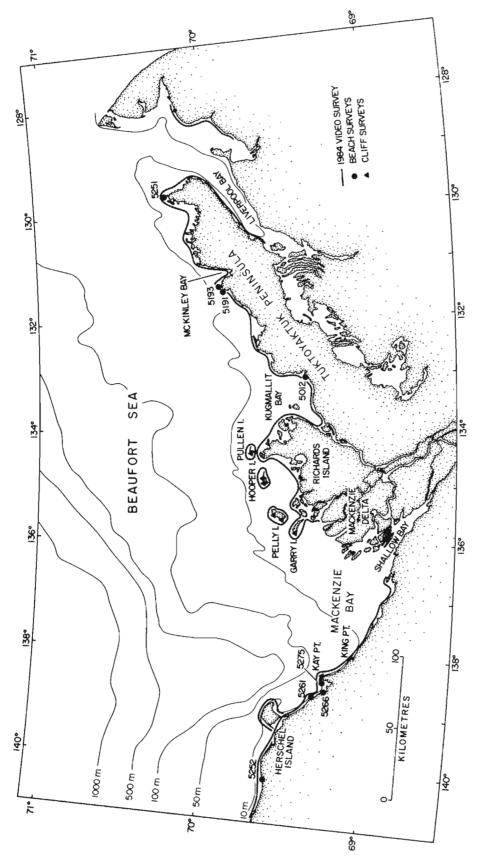
Coastal geomorphology

The major coastal morphological types in the Canadian Beaufort Sea (Fig. 9.2) are cliffs developed in ice-bonded Quaternary sediments, lagoons and complex embayments formed by transgressive breaching of lakes, estuarine drowned valleys flooded by the Holocene transgression, inundated tundra flats, fan deltas and deltas (including inter-tidal mudflats and deltaic supratidal flats), nondeltaic supratidal marsh flats, beaches and barriers.
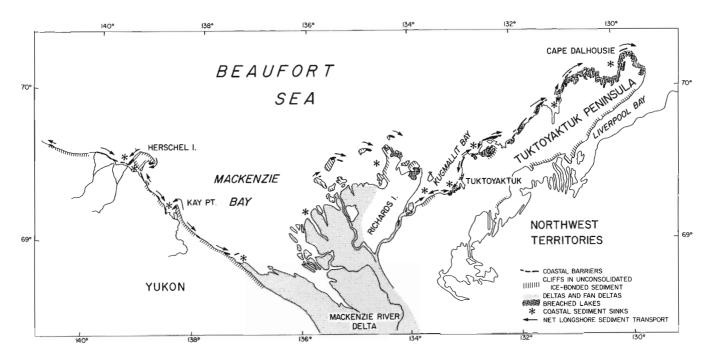
The dominant feature on the coast is the Mackenzie River delta (Mackay, 1963a; Johnston and Brown, 1965; Lewis, 1977). This large deposit occupies a depression that extends seaward into Mackenzie Bay to intersect the continental slope at about 400 m depth (Shearer, 1972). Active deltaic sedimentation occurs in Kugmallit Bay and across a broad front in Mackenzie Bay (Fig. 9.2). Despite very large sediment supply (some 10^{11} kg/a from Mackenzie River), representing about 95% of all sediment delivered to the Canadian Beaufort Sea (Harper and Penland, 1982; Harper et al., 1983; Blasco et al., 1983), the delta-front shoreline is largely erosional with some of the highest mean recession rates on the coast (Harper et al., 1985). However, wide mudflats on the west side of Richards Island (Fig. 9.3) and locally farther west indicate the locations of some important deltaic sediment sinks (Fig. 9.2).

Cliffs predominate on the Yukon coast, on the islands north of the Mackenzie Delta, on Richards Island and in southern Kugmallit Bay, locally along the north coast of Tuktoyaktuk Peninsula, and in Liverpool Bay. Materials exposed in coastal cliffs include a great variety of preglacial, glacial, and postglacial sediments and large quantities of ground ice (Fyles, 1966; Mackay, 1959, 1966, 1971; Mackay et al., 1972; Rampton, 1971, 1982; Rampton and Bouchard, 1975; Rampton and Mackay, 1971). Cliff erosion processes include surface runoff and gully development, basal wave cut, gravity failures, block failures, and retrogressive-thaw failures with associated mudflow development.
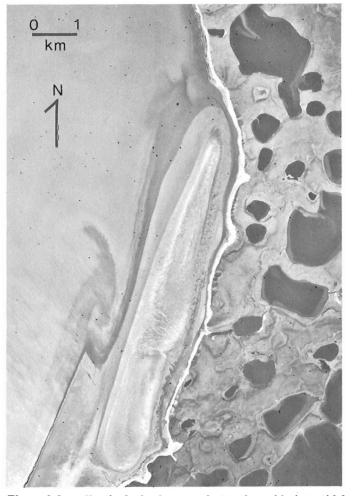
The complex indented shoreline associated with breached-lake features is a distinctive characteristic of northern Richards Island and much of the north coast of Tuktoyaktuk Peninsula (Mackay, 1963a). In areas of low relief, inundated tundra surfaces (including ice-wedge polygon features) attest to the rapid and ongoing marine transgression.

Figure 9.1. Canadian Beaufort Sea coast, showing extent of GSC video coverage and sites of 1984 beach and cliff surveys.

71

Figure 9.2. Beaufort Sea coast, showing major coastal morphological types, directions of net longshore sediment transport (inferred from coastal morphology), and major coastal sediment sinks (after Forbes and Lewis, in press).
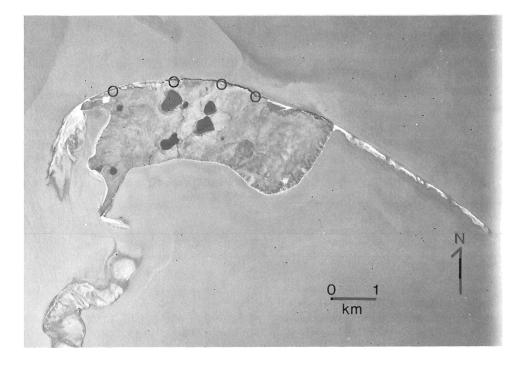
Figure 9.3. Vertical air photograph showing wide intertidal mud flats on the northwest shore of Richards Island: an important sink (Fig. 9.2) for sediment discharge from Mackenzie River. Note also the multiple bar system along the coast to the north. Part of NAPL photograph A22974-85 (1972).

Beach, spit, and barrier features (Fig. 9.2, 9.4) are developed in sands and gravels, fed from nearby cliff and inner-shelf sources, and reflect the characteristics of source deposits in the area. Gravels are abundant along the Yukon coast, on the islands north of Mackenzie Delta, in Kugmallit and Liverpool bays. Sand predominates on Richards Island and in the barrier islands of the north coast of Tuktoyaktuk Peninsula. Coastal dune development is limited and most barrier deposits (in sands and gravels) are characterized by extensive washover flats in the backshore. Tidal inlet development is limited and may be dominated by runoff and storm-surge processes. Extensive multiple-bar systems are prominent features of sand-dominated segments of the coast. Spit morphology provides some indication of net longshore transport directions and has been used in part to delineate the major coastal sediment sinks (Lewis and Forbes, 1975; Fig. 9.2). Flanking spits on Garry, Pelly, Hooper, and Pullen islands north of the Mackenzie Delta (Fig. 9.1, 9.4) reveal the dominance of southeasterly transport associated with waves approaching from the northwest. Similar reworking of abandoned artificial islands has provided additional confirmation of this process (Harper and Penland, 1982).

Beach surveys

Surveys were undertaken at a representative set of beach sites (Fig. 9.1) to complement information collected by Lewis and Forbes (1975) and Lawrence et al. (1984). The surveys were intended also to furnish data required for a joint INAC/GSC NOGAP contract project to carry out numerical estimation of nearshore waves and sediment transport at seven sites (Keith Philpott Consulting Ltd., 1985). Profiles were surveyed out to wading depth using either conventional rod and level or two rods with hand level and tape, and in deeper water with an acoustic sounder positioned by range markers and theodolite angles. Gravel sampling and analysis procedures followed conventions outlined by Kellerhals and Bray (1971). Sands and muds were sampled by sedimentation unit on the beach and using a Ponar grab sampler in nearshore waters. Analyses were carried out using settling tube and Sedigraph (TM) apparatus and READY software at the Atlantic Geoscience Centre.

Figure 9.4

Vertical air photograph showing Hooper Island (Fig. 9.1), with sites of cliff recession measurements (open circles) and flanking spits indicating net sediment transport toward the southeast. Part of NAPL photograph A 22974-120 (1972).

Table 9.1. Beach morphometry and driftwood elevations

Site	Geographical name	Sediment type	Foreshore slope (m)	Beach width (m)	Crest elevation (m)	Driftwood elevation (m)
5252	Komakuk Beach	gravel	0.18	70[1]	4.2[1]	3.7
5261	Stokes Point	gravel	0.14	700	1.9	1.2[2]
5266	Spring River	gravel	0.12	255	1.0	
5275	Kay Point	gravel	0.12	70	1.2	2.0[3]
5012	Tuktoyaktuk	gravel	0.11	50	2.0	2.4
5191	Atkinson Point	sand	0.01	90	0.5	2.5
5193	Atkinson Point	sand	0.08	530	1.0	
5251	Cape Dalhousie	sand	0.01	250	0.4	

[1] Includes gravel sedimentation on top of tundra cliff
[2] May not be highest driftwood
[3] Elevation at head of adjacent estuary; elevation at coast is 1.4 m (Forbes, 1981)
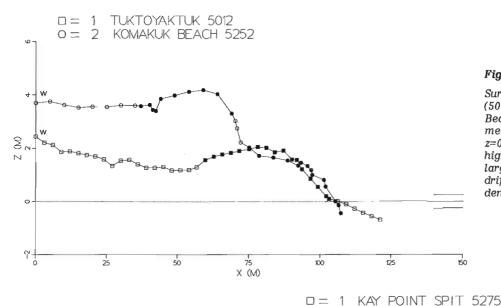
Beach morphology and sediments

Beach morphometric data are presented in Table 9.1, together with surveyed driftwood elevations that provide rough estimates of maximum storm-surge water levels. Representative beach profiles are plotted in Figures 9.5 and 9.6. Beaches in the region display a wide range of morphology and structure, reflecting long-term trends in relative sea level; ice, wave, and storm-surge regimes; sediment source characteristics; local sediment budget; and coastal recession (Forbes and Lewis, 1983).

Narrow fringing beaches at some sites are less than 50 m wide (Tuktoyaktuk 5012; see also Lawrence et al., 1984, Fig. 2). In contrast, sandy barrier islands on the Tuktoyaktuk Peninsula attain widths of over 500 m in places (Atkinson Point 5193). On the Yukon coast, the prograded sandy-gravel Spring River barrier (5266) is over 250 m wide; and a sand-gravel beach-ridge foreland up to 700 m wide has accumulated at Stokes Point (5261). On the other hand, transgressive gravel barriers attached to rapidly retreating coastal anchor points tend to be much narrower (Kay Point 5275).

Foreshore slope is correlated with grain size but is affected also by wave energy and other factors: it ranges from less than 0.01 at exposed sandy beachface sites on the eastern Tuktoyaktuk Peninsula to almost 0.2 on gravel beaches west of Herschel Island, where open-water fetch is more restricted by ice.

Despite this fetch limitation, the highest beach-crest elevation observed (4.2 m) was at Komakuk Beach (site 5252), where gravel extended some 35 m landward from the top of a low cliff and driftwood was present at 3.7 m (Table 9.1, Fig. 9.5). McDonald and Lewis (1973) reported gravel and driftwood on top of a 6-m cliff at a nearby site: this is the highest driftwood occurrence known to us in the Beaufort Sea (cf. Rimnitz and Maurer, 1979). Although ice-push may be responsible for the highest gravel and wood in the area, the 4.2-m gravel at Komakuk is believed to have been deposited by wave runup, possibly enhanced by an ice ramp.
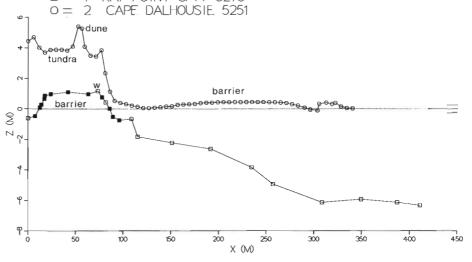
At Tuktoyaktuk, sand and gravel supplied by rapid cliff erosion along the west side of the community (Rampton and Bouchard, 1975; Shah, 1978) have formed a narrow fringing barrier and spit at site 5012 (Fig. 9.5). Beaches throughout

□ = 1 TUKTOYAKTUK 5012
○ = 2 KOMAKUK BEACH 5252

Figure 9.5

Surveyed beach profiles at Tuktoyaktuk (5012, R1, 1984/07/25) and Komakuk Beach (5252, R1, 1984/07/28). Datum is mean sea level (horizontal line at z=0 m); short horizontal lines indicate higher high water and lower low water at large tides. 'W' denotes storm-surge driftwood deposit; shaded symbols denote gravel.

Figure 9.6

Surveyed beach profiles at Kay Point spit (5275, R4, 1984/08/04) and Cape Dalhousie (5251, R1, 1984/07/24). Datum is mean sea level (horizontal line at z=0 m); short horizontal lines indicate higher high water and lower low water at large tides for Cape Dalhousie (range 0.5 m; range at Kay Point is 0.2 m). 'W' denotes storm-surge driftwood deposit; shaded symbols denote gravel.

□ = 1 KAY POINT SPIT 5275
○ = 2 CAPE DALHOUSIE 5251

the area are migrating landward with rising RSL and coastal recession: airphoto evidence suggests that the beach at site 5012 progressed landward more than 5 m between 1935 and 1950, and more than 30 m between 1950 and 1971 (Rampton and Bouchard, 1975, Fig. 13). The gravel storm ridge, with a crest elevation of about 2 m, is fronted by nearshore sand and peat (evidence of transgression) and backed by ponds and low ground with driftwood up to 2.4 m above mean sea level (Fig. 9.5). The beach contains sand-, pebble-, and cobble-size material, with sand preferentially removed from the swash zone to nearshore and backshore locations: a sample taken from the lower berm crest had a mean grain size of 17 mm and contained no sand.

The spit at site 5275 (Fig. 9.6) extends some 4.4 km southwest from Kay Point on the central Yukon coast (Fig. 9.1, 9.7). This feature displays the narrow foreshore beachface, extensive low washover flats, driftwood concentration near the barrier crest, and thin windblown deposits typical of many coarse grained barriers on the Beaufort coast (McDonald and Lewis, 1973; Lewis and Forbes, 1975; Forbes, 1981). The subaerial beach width ranges from 30 to 300 m. With a maximum crest elevation of about 1.2 m, the barrier at Kay Point is extensively overwashed during surge events (cf. driftwood elevation, Table 9.1). Forbes (1981) estimated that washover transport of sediment to the back-barrier lagoon amounted to some 10^4 m³/a, based on the mean 41 m landward migration of the barrier between 1952 and 1970 (McDonald and Lewis, 1973, Map no. 4).

Forbes and Lewis (1983) described a transgressive stratigraphic sequence observed in a borehole transect across Kay Point spit. The sequence included up to 5 m of barrier sand-gravel deposits over lagoon muds, with no observed preservation of estuarine facies seaward of the barrier, presumably because of the high rate of horizontal migration relative to the rate of change in RSL. Despite the general transgressive trend, parts of the spit show evidence of short-term local progradation, particularly at the distal end (Fig. 9.7B). Less obvious is the discontinuous subtidal backbarrier platform formed by distal spit extension, local progradation, or inlet migration. Some beach and nearshore profiles (e.g. Fig. 9.6) show evidence of a subtidal step and a convex shoreface profile extending seaward to approximately 6 m depth. Other profiles show broad bar-like shoals with relief of about 0.5 m in 2-3 m depths some 250-300 m off the beach. Nearshore sediments sampled off Kay Point spit include mud, sand, and gravel, with mean grain size ranging from 10 to 800 µm. Sediments in the beach show both distal (alongshore) and landward (cross-barrier) fining trends (McDonald and Lewis, 1973). Subsurface barrier crest sediments grade from sand-pebble-cobble gravel (mean size 6 mm) near the point to pebbly sand (mean size 0.9 mm) near the distal end of the spit (Hunter, 1975).

Barriers of the eastern Tuktoyaktuk Peninsula (e.g. Atkinson Point 5191 and 5193; Cape Dalhousie 5251) are developed in sand and differ substantially from the coarser deposits that predominate elsewhere. The composition of
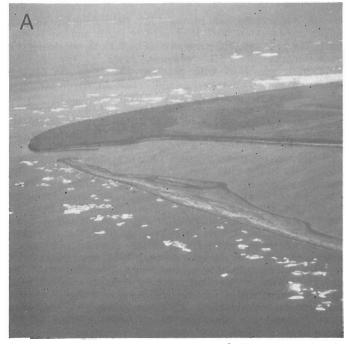
Figure 9.7A. Aerial oblique view of Kay Point, showing new tidal inlet at the proximal end of Kay Point spit and approximate locations of cliff segment 1 (dark area near point) and segment 2 (lighter area to right: cf. Lewis and Forbes, 1975, Fig. 1). Photo FZ-37110 (1984/07/28).
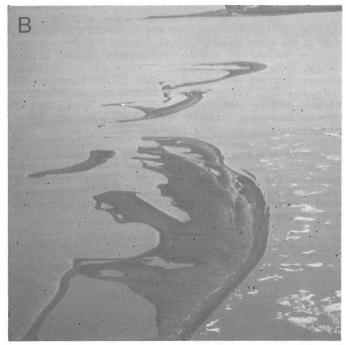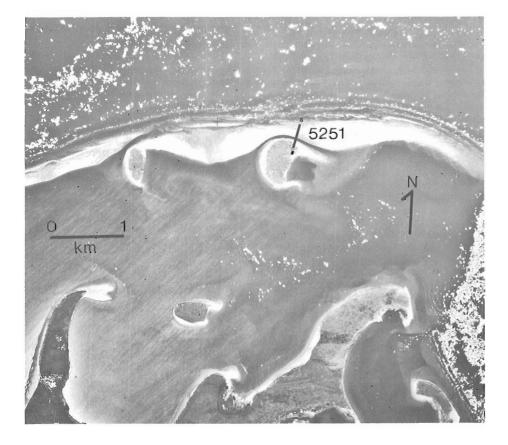
Figure 9.7B. Aerial oblique view of distal Kay Point spit (with Babbage estuary to the left), showing multiple recurve spit morphology and evidence for local short-term progradation; note also driftwood concentration near the barrier crest, extensive washover flats in the backshore, and small-scale reworking by waves in the estuary. Photo FZ-37112 (1984/07/28).

Figure 9.8

Vertical air photograph of breached-lake coast with tundra island remnants and sandy barrier island, Cape Dalhousie, eastern Tuktoyaktuk Peninsula. Note multiple parallel near-shore bars and location of surveyed profile (broken line). Part of NAPL photo A12702-410 (1950).

beaches in the eastern peninsula reflects the preponderance of sandy source materials in the area (Mackay, 1963a; Rampton, 1971). Wide low spits and barrier islands dominate much of the outer coast (Fig. 9.8), fronting a highly embayed shoreline formed by marine transgression across a lake-studded plain (Mackay, 1963a). Dunes occur on tundra surfaces, but are not well developed on the barriers. The latter, like their coarse grained counterparts elsewhere, are characterized by extensive washover flats. Swash bars are common foreshore features under open-water conditions. Multiple parallel nearshore bars are common on the outer coast (Fig. 9.8) and in Liverpool Bay. Spectacular transverse bar complexes are prominent lagoon-shore features (Fig. 9.9). The beach profile surveyed at Cape Dalhousie (Fig. 9.6) illustrates the barred foreshore and washover morphology common in the area. The high ground at the left is part of an island tundra surface (Fig. 9.8) with eolian dune development at the seaward edge.
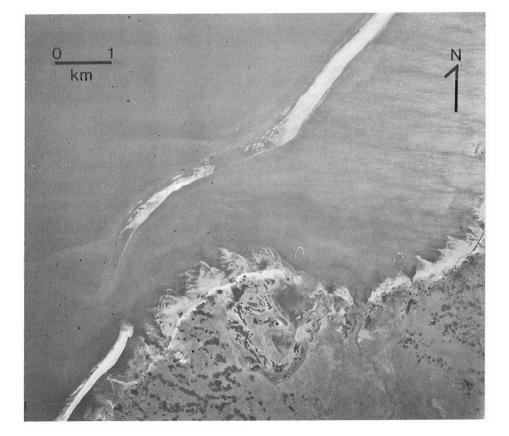
Beach stability

At Atkinson Point (5191 and 5193), three cross-barrier profiles established in 1973 (C.P. Lewis, unpublished notes) were resurveyed in 1984; at Kay Point (5275), 11 of some 30 profiles surveyed in 1974-1976 were reoccupied. Many lines showed very limited change over the decade. The stability of Atkinson Point spit (Fig. 9.10) is interesting in view of historical evidence of rapid retreat at the point (Richardson, 1851; Mackay, 1963a; Harper et al., 1985). At Kay Point, some lines showed little modification but changes at others were dramatic. At the proximal end of the spit, tidal inlet development (Fig. 7A) had destroyed five profile lines prior to the 1984 survey. Previously, a short-lived tidal inlet had been observed at the site in 1970, but was gone by 1972. Ice-thrust ridges close to 2 m high were observed on Kay Point spit in 1972 (McDonald and Lewis, 1973). Airphoto evidence reveals a net landward migration of the spit since the early 1950s (see above).

Cliff surveys

A major objective of the 1984 field program was to revisit monumented cliff sites at Kay Point and on Garry, Pelly, Hooper, and Pullen islands (Fig. 9.1) to obtain direct measurements of cliff recession rates. The results (Table 9.2), combined with previous measurements at the same sites (H. Kerfoot and C.P. Lewis, personal communications, 1984), provide valuable information on short- to medium-term erosion rates and a measure of calibration for regional surveys of cliff recession based on airphoto data (McDonald and Lewis, 1973; Harper et al., 1985). The tabulated data include the number of lines at each site (n), the mean distance (± one standard error) from monuments to the cliff edge, and the mean recession (± one standard error). In 1976 when the last survey was completed, the cliff network included over 200 monumented lines (H. Kerfoot, unpublished notes); 97 were resurveyed in 1984. Our failure to find any markers on Pullen Island and at three sites on Pelly Island was not surprising, given the very high recession rates through the mid-1970s: even assuming much lower mean rates for the interval 1976-1984, markers at most of these sites would have disappeared (Table 9.2). Cliffs at all survey sites are characterized by high ice content with varying proportions of massive ice and wedge ice. Although the measurements relate in all cases to the cliff top, they provide reasonable estimates of cliff-face retreat except where retrogressive-thaw headwall recession has been particularly rapid (Garry Island site 1, possibly some Pelly Island sites, and Pullen Island).

Kay Point sites 1 and 2 (Fig. 9.7) correspond, respectively, to segment-1 and lower segment-2 cliffs described by Lewis and Forbes (1975). Segment-1 cliffs are 5-10 m high and dominated by thermo-erosional block failure (undercutting and ice-wedge thaw) processes: airphoto evidence suggests that this section of the coast retreated roughly 30-90 m between 1952 and 1970 (McDonald and Lewis, 1973), with the most rapid erosion rates observed near
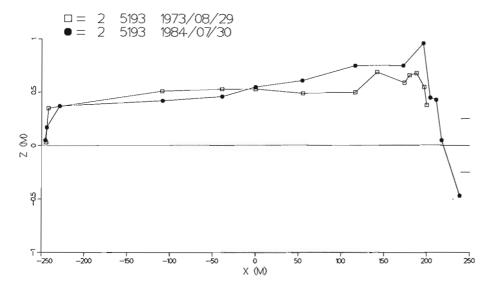
Figure 9.9

Vertical air photograph showing sandy barrier island system near Bols Point, east side of Hutchison Bay (Tuktoyaktuk Peninsula between Tuktoyaktuk 5012 and Atkinson Point 5191). Note nearshore bars on seaward side of barrier islands (including welded swash bars) and complex transverse bar system on lagoon shore. Part of NAPL photo A22386-42 (1971).

Table 9.2. Cliff erosion data

Site	n	1964 (m)	1971 (m)	1976 (m)	1984 (m)	64–71 (m/a)	71–76 (m/a)	76–84 (m/a)
					Distance			Mean erosion rate
Kay Point								
1	6			24.0	12.1			1.5
				±0.9	±1.4			±0.2
2	7			25.2	16.7			1.1
				±1.5	±3.2			±0.3
Garry Island								
1	14	41.3	28.5	20.9	12.8	1.8	1.5	1.0
		±2.9	±2.9	±0.8	±2.0	±0.3	±0.5	±0.2
2	14	31.7	25.3	21.8	12.8	0.9	0.7	1.2
		±1.4	±1.3	±1.5	±1.2	±0.1	±0.1	±0.1
Pelly Island								
1	15		49.3	21.7			5.5	
			±1.3	±1.0			±0.2	
2a	1		145.3	79.1			13.2	
2b	13		64.5	29.5			7.0	
			±0.7	±0.8			±0.2	
3a	5		77.7	38.4	10.0		7.9	3.5
			±0.2	±0.8	±2.6		±0.2	±0.3
3b	10		70.5	32.2			7.7	
			±2.3	±1.8			±0.2	
4	15		81.0	32.4			9.7	
			±2.2	±1.3			±0.6	
Hooper Island								
1	15		29.3	22.3	14.8		1.4	0.9
			±0.7	±0.7	±0.7		±0.1	±0.0
2	13		31.2	23.8	14.4		1.5	1.2
			±1.2	±0.7	±1.2		±0.1	±0.1
3	15		38.0	27.4	15.9		2.1	1.5
			±1.0	±1.0	±1.1		±0.1	±0.1
4	10		43.0	29.6	12.6		2.7	2.1
			±2.6	±1.6	±3.0		±0.4	±0.4
Pullen Island		1972	1976			72–76		
1	20	63.8	26.9			9.2		
		±1.7	±1.1			±0.2		

□ = 2 5193 1973/08/29
● = 2 5193 1984/07/30

Figure 9.10

Surveyed profiles across Atkinson Point spit (5193, R2) in 1973 (C.P. Lewis, unpublished notes) and 1984. Datum is mean sea level (horizontal line at z=0 m); short horizontal lines denote higher high water and lower low water at large tides; sea to right, McKinley Bay to left. Note remarkable stability of profile over 11 year interval.

the point. Segment-2 cliffs are 12-15 m high and characterized by surface wash, basal erosion, and gravity failure processes in the area of measurements reported here. Farther east, they rise to over 90 m and are dominated by retrogressive-thaw and mudflow processes. Air photographs record retreat of 25-30 m between 1952 and 1970 (McDonald and Lewis, 1973).

An observation of cliff retreat was also obtained at the Yukon-Alaska border. Ice-bonded pebbly mud deposits are exposed in a 6.5 m coastal cliff, with thermokarst and gully development extending back from the cliff edge along ice-wedges. Monument no. 1 of the International Boundary Commission was placed 61.9 m south of the cliff on 1912/07/30. As of 1972/07/17, the cliff top had retreated 43 m (McDonald and Lewis, 1973): this corresponds to a long-term (60 year) mean of 1.4 m/a. By 1984/07/28, a new monument had been established farther south, but what appeared to be the foundation of the original Monument no. 1 was 8.9 m from the cliff edge, suggesting a mean recession of about 0.8 m/a for the 12 years (1972-1984).

The cliff retreat data (Table 9.2) include evidence of significant reductions in the rate of erosion after 1976 at Pelly Island 3a and less pronounced reductions at Garry Island 1 and on Hooper Island. These changes may reflect a variety of factors affecting cliff erosion rates, including wave attack at the base of the cliffs, air temperature, precipitation, and feedback mechanisms in the erosion process. Retrogressive-thaw failures often exhibit a cyclic pattern of activity, stabilization, and reactivation, in part related to mudflow apron sedimentation and subsequent erosion of lower-apron deposits. This pattern was observed by Rampton and Bouchard (1975) at a major feature on the coast southwest of Tuktoyaktuk, where Rampton and Mackay (1971) had reported erosion rates of 6 to 9 m/a. Similar cyclicity has been noted on the Yukon coast, particularly southeast of King Point (D.G. Harry, personal communication, 1984) and at King Point itself, where previously stabilized failures had been reactivated by 1984. Rampton and Bouchard (1975) noted the high year-to-year variability of erosion processes and the importance of storm events at some sites. Low ice-rich cliffs such as those at Kay Point are susceptible to rapid erosion during major storms. At Tuktoyaktuk, the cliff at one site retreated over 13 m during an extreme storm in September 1970 (Public Works Canada, 1971b).

Conclusions

A reasonably complete picture of coastal morphology and sediments in the Canadian Beaufort Sea has emerged from surveys conducted over the past 20 years or so. Important conclusions include the recognition of sea-ice and ground-ice effects as major factors in the evolution of coasts in the region. Coastal recession rates show high spatial and temporal variability, the former related to varying sediment textures and ground-ice contents, the latter to varying climatic and oceanographic conditions and to feedback effects in the erosion process. In particular, retrogressive-thaw failures exhibit some cyclicity that may be largely feedback generated. Beaches developed in sands and gravels show substantial contrasts, suggesting the need for separate evaluation in future studies of coastal dynamics in the Beaufort Sea. Apart from sites where gravel deposition has occurred on top of low coastal cliffs west of Herschel Island, all beaches and barriers in the region have low crest elevations and barriers are characterized by extensive washover flats. Flanking spits on natural and artificial islands north of Mackenzie Delta attest to transport dominance by storm waves out of the northwest. Storm-surge effects are evident in the deposition of driftwood lines up to 3.7 m above mean sea level.

Work initiated under NOGAP during 1984 was designed to fill some of the major data gaps and synthesize existing data. This process has clarified future research requirements in the Canadian Beaufort coastal zone. These include direct observation of nearshore wave and sediment dynamics in order to calibrate the numerical models, continued on-site monitoring of selected beach and cliff sites to evaluate temporal variability of coastal erosion and sedimentation processes, and a shallow-marine survey program emphasizing sediment distribution and stratigraphy, scour processes, and the thickness of mobile sediment on the shoreface and inner shelf.

References

Blasco, S.M., Harper, J.R., and Forbes, D.L.
    1983: Sediment distribution and dynamics in the southern Beaufort Sea; in Proceedings, Workshop on Arctic Regional Coastal Erosion and Sedimentation (Calgary, 1983); Associate Committee for Research on Shoreline Erosion and Sedimentation, National Research Council, Ottawa, p. 1-2.

Carson, J.M., Hunter, J.A., and Lewis, C.P.
    1975: Marine seismic refraction profiling, Kay Point, Yukon Territory; in Report of Activities, Part B, Geological Survey of Canada, Paper 75-1B, p. 9-12.

Forbes, D.L.
    1980: Late-Quaternary sea levels in the southern Beaufort Sea; in Current Research, Part B, Geological Survey of Canada, Paper 80-1B, p. 75-87.

    1981: Babbage River delta and lagoon: hydrology and sedimentology of an Arctic estuarine system; unpublished Ph.D. dissertation, University of British Columbia, Vancouver, B.C., 554 p.

Forbes, D.L. and Lewis, C.P.
    1983: Transgressive coastal sedimentation, Yukon Beaufort Sea; Geological Association of Canada, Program with Abstracts, v. 8, p. A23.

    –   Coastal landforms and processes, southern Beaufort Sea: 1:1M map with accompanying notes and photographs; in Environmental Atlas of the Beaufort Sea, ed. B.R. Pelletier; Geological Survey of Canada, Miscellaneous Report. (in press)

Fyles, J.G.
    1966: Quaternary stratigraphy, Mackenzie Delta and Arctic coastal plain; in Report of Activities, Geological Survey of Canada, Paper 66-1, p. 30-31.

Hall, K., Baird, W., and Wright, B.
1983: Results of a ten year hindcast study for the Beaufort Sea; in Proceedings, Canadian Coastal Conference 1983 (Vancouver, 1983), ed. B.J. Holden; Associate Committee for Research on Shoreline Erosion and Sedimentation, National Research Council Canada, Ottawa, p. 107-122.

Harper, J.R. and Penland, P.S.
1982: Beaufort Sea sediment dynamics; unpublished report to Geological Survey of Canada, Dartmouth; Woodward-Clyde Consultants, Victoria, B.C.

Harper, J.R., Blasco, S.M., and Hill, P.R.
1983: Modern sediment dispersal and Holocene sediment budget of the Canadian Beaufort Sea; Geological Association of Canada, Program with Abstracts, v. 8, p. A30.

Harper, J.R., Reimer, P.D., and Collins, A.D.
1985: Canadian Beaufort Sea physical shore-zone analysis; unpublished draft report to Indian and Northern Affairs Canada, Ottawa, and Geological Survey of Canada, Dartmouth; Dobrocky-Seatech Limited, Sidney, B.C., 87 p., 3 appendices.

Henry, R.F.
1975: Storm surges; Beaufort Sea Project; Environment Canada, Technical Report 19, 41 p.

Hill, P.R., Mudie, P.J., Moran, K., and Blasco, S.M.
— A sea-level curve for the Canadian Beaufort Shelf; Canadian Journal of Earth Sciences. (in press)

Hollingshead, G.W., Skjolingstad, L., and Rundquist, L.A.
1978: Permafrost beneath channels in the Mackenzie Delta, N.W.T. Canada; in Proceedings, Third International Conference on Permafrost (Edmonton, 1978); National Research Council, Ottawa, p. 407-412.

Huggett, W.S., Woodward, F., Stephenson, F., Hermiston, F.V., and Douglas, A.N.
1975: Near bottom currents and offshore tides; Beaufort Sea Project; Environment Canada, Technical Report 16, 38 p.

Hunter, D.R.
1975: Three Arctic spits; unpublished B.Sc. dissertation, University of Waterloo, Waterloo, Ontario, 44 p.

Johnston, G.H. and Brown, R.J.E.
1965: Stratigraphy of the Mackenzie Delta, Northwest Territories, Canada; Geological Society of America, Bulletin, v. 76, p. 103-111.

Keith Philpott Consulting Limited
1985: Numerical estimation of sediment transport and nearshore profile adjustment at coastal sites in the Canadian Beaufort Sea — part of the Northern Oil and Gas Action Plan (NOGAP); unpublished interim report to Indian and Northern Affairs Canada, Ottawa, and Geological Survey of Canada, Dartmouth, 29 p., 3 appendices.

Kellerhals, R. and Bray, D.L.
1971: Sampling procedures for coarse fluvial sediments; Journal Hydraulics Division, American Society of Civil Engineers, v. 97, p. 1165-1180.

Kerfoot, D.E. and Mackay, J.R.
1972: Geomorphological process studies, Garry Island, Northwest Territories; in Mackenzie Delta Area Monograph, ed. D.E. Kerfoot; Brock University Press, St. Catherines, Ontario, p. 115-130.

Lawrence, M., Pelletier, B.R., and Lacho, G.
1984: Sediment sampling of beaches along the Mackenzie Delta and Tuktoyaktuk Peninsula, Beaufort Sea; in Current Research, Part A, Geological Survey of Canada, Paper 84-1A, p. 633-640.

Lewis, C.P.
1975: Sediments and sedimentary processes, Yukon Beaufort Sea coast; in Report of Activities, Part B, Geological Survey of Canada, Paper 75-1B, p. 165-170.

1977: Deltaic processes and delta morphology, Mackenzie Delta, N.W.T.; Geological Association of Canada, Program with Abstracts, v. 2, p. 32.

Lewis, C.P. and Forbes, D.L.
1975: Coastal sedimentary processes and sediments, southern Canadian Beaufort Sea; Beaufort Sea Project; Environment Canada, Technical Report 24, 68 p.

McDonald, B.C. and Lewis, C.P.
1973: Geomorphic and sedimentologic processes of rivers and coast, Yukon Coastal Plain; Canada, Environmental-Social Committee, Northern Pipelines, Task Force on Northern Oil Development, Report 73-39, 245 p.

McDonald, B.C., Edwards, R.E., and Rampton, V.N.
1973: Position of frost table in the nearshore zone, Tuktoyaktuk Peninsula, District of Mackenzie; in Report of Activities, Part B, Geological Survey of Canada, Paper 73-1B, p. 165-168.

Mackay, J.R.
1959: Glacier ice-thrust features of the Yukon coast; Geographical Bulletin, no. 13, p. 5-21.

1960: Notes on small boat harbours of the Yukon coast; Geographical Bulletin, no. 15, p. 19-30.

1963a: The Mackenzie Delta area, N.W.T.; Canada Department of Mines and Technical Surveys, Geographical Branch, Memoir 8, 202 p.

1963b: Notes on the shoreline recession along the coast of the Yukon Territory; Arctic, v. 16, p. 195-197.

1966: Segregated epigenetic ice and slumps in permafrost, Mackenzie Delta area, Northwest Territories; Geographical Bulletin, v. 8, p. 59-80.

1971: The origin of massive icy beds in permafrost, western Arctic coast, Canada; Canadian Journal of Earth Sciences, v. 8, p. 397-422.

Mackay, J.R., Rampton, V.N., and Fyles, J.G.
1972: Relic Pleistocene permafrost, western Arctic, Canada; Science, v. 176, p. 1321-1323.

Public Works Canada
1971a: Herschel Island: feasibility of a marine terminal; Engineering Programs Branch, Ottawa, 141 p., 19 plates.

1971b: Beaufort Sea storm, September 13-16, 1970: investigation of effects in the Mackenzie Delta region; Engineering Programs Branch, Ottawa, 22 p.

Rampton, V.N.
1971: Quaternary geology, Mackenzie Delta and Arctic Coastal Plain, District of Mackenzie; in Report of Activities, Part A, Geological Survey of Canada, Paper 71-1A, p. 173-177.

Rampton, V.N. (cont.)
1982: Quaternary geology of the Yukon coastal plain; Geological Survey of Canada, Bulletin 317, 49 p.

Rampton, V.N. and Bouchard, M.
1975: Surficial geology of Tuktoyaktuk, District of Mackenzie; Geological Survey of Canada, Paper 74-53, 17 p.

Rampton, V.N. and Mackay, J.R.
1971: Massive ice and icy sediments throughout the Tuktoyaktuk Peninsula, Richards Island, and nearby areas, District of Mackenzie; Geological Survey of Canada, Paper 71-21, 16 p.

Reimnitz, E. and Maurer, D.K.
1979: Effects of storm surges on the Beaufort Sea coast, northern Alaska; Arctic, v. 34, p. 339-344.

Richardson, J.
1851: Journal of a Boat Voyage through Rupert's Land and the Arctic Sea, in Search of the Discovery Ships Under the Command of Sir John Franklin; Longmans, Brown, Green, and Longmans, London, 2 v.

Shah, V.K.
1978: Protection of permafrost and ice rich shores, Tuktoyaktuk, N.W.T., Canada; in Proceedings, Third International Conference on Permafrost (Edmonton, 1978); National Research Council Canada, Ottawa, p. 870-876.

Shearer, J.M.
1972: Geological structure of the Mackenzie Canyon area of the Beaufort Sea; in Report of Activities, Part A, Geological Survey of Canada, Paper 72-1A, p. 179-180.

A preliminary report of alteration and fracture-filling mineralogy in the East Bull Lake pluton, District of Algoma, Ontario

D.C. Kamineni, G.F. McCrank, D. Stone, R.B. Ejeckam, and R. Sikorsky
Atomic Energy of Canada Limited, Ottawa

Abstract

The East Bull Lake pluton contains a variety of alteration minerals. Some of the more common ones are calcic amphiboles, biotite, epidote, adularia, quartz, calcite, sphene, sulphides, serpentine, chlorite, prehnite, pumpellyite, laumontite, gypsum, and iron hydroxides. The mode of occurrence and relevant experimental data related to the stability of the alteration minerals suggest that they were formed under pressure-temperature conditions of 1) epidote-amphibolite/greenschist facies, 2) prehnite-pumpellyite facies, 3) zeolite facies, and 4) low temperature rock-water interaction (<100°C).

Résumé

Le pluton de lac East Bull contient divers minéraux d'altération. Parmi les plus communs se trouvent les amphiboles calciques, la biotite, l'épidote, l'adulaire, le quartz, la calcite, le sphène, les sulfures, la serpentine, la chlorite, la prehnite, la pumpellyite, la laumontite, le gypse et les hydroxydes de fer. Le type de gisement et les données expérimentales concernant la stabilité des minéraux d'altération semblent indiquer qu'ils se sont formés dans des conditions de pression et de température entraînant la formation 1) d'un faciès à amphibolites avec épidote et à schistes verts, 2) d'un faciès à prehnite et à pumpellyite, 3) d'un faciès à zéolites et 4) l'interaction roche-eau à basse température (< 100°C)

Introduction

As a part of the concept assessment for the disposal of nuclear fuel waste in plutonic rocks, Atomic Energy of Canada Limited, in co-operation with the Geological Survey of Canada, is investigating a number of plutons in the Canadian Shield. The plutonic rocks under investigation are of granitic composition except for the East Bull Lake pluton which is a layered gabbro-anorthosite intrusion. Secondary minerals in fracture fillings, in alteration aureoles adjacent to fractures, and in unfractured rock masses are studied because these mineralogies are thought to be important in understanding the post-consolidation 'tectono fluid history' of plutons (Stone and Kamineni, 1982; Kamineni and Stone, 1983). In addition fracture fillings and pervasively distributed alteration products in the host rock of a disposal vault will play a key role in retarding the migration of radionuclides to the biosphere, because alteration and fracture-filling minerals, in general show higher sorption of radionuclides than do minerals in the unaltered host rock (Kamineni et al., 1983).

Four cored boreholes were drilled in the East Bull Lake pluton to investigate the shape, fracture characteristics, mineralogy and geohydrological parameters of the pluton. The holes also had specific targets that included geophysical anomalies and geological lineaments and faults. The borehole locations and orientations are given in Kamineni et al. (1984). Core samples recovered from the boreholes and samples collected on the surface were examined to characterize the alteration and fracture-filling minerals. This preliminary report contains a description of the postcrystallization secondary mineral assemblages found throughout the pluton and in specific structural sites. Visual specimen examination, optical microscopic examination, powder X-ray diffraction techniques and electron microprobe methods were used to identify the minerals.

Geological setting

The East Bull Lake pluton, located about 30 km north of Massey, Ontario, occurs within the Superior Structural Province. Supracrustal rocks of the Southern Structural province occur about 20 km south and 15 km west of the pluton. These supercrustal rocks contain deformations and metamorphic features related to the Penokean and Grenville orogenies (Zolnai et al., 1984). The intrusion was first mapped by Moore and Armstrong (1945), and subsequent petrological/geochemical investigations were made by Born (1978), Born and James (1978) and James et al. (1983).

The East Bull Lake pluton intrudes Archean plutonic and supracrustal rocks (McCrank et al., 1983). The pluton is cut by numerous mafic dykes, which are common throughout the region (see McCrank et al., 1983). A number of bulk rock K-Ar age determinations on these dykes cluster around 1.65 Ga (R. Stevens, GSC, personal communication), suggesting that these dykes probably record the Penokean event. Some other mafic dykes, which are generally unaltered and containing fresh olivine, pyroxenes and plagioclase, give a K-Ar bulk rock age of 1.2 Ga, indicating that they belong to the 'Sudbury swarm'. In addition, K-Ar age determinations of two samples from the troctolite zone (Kamineni et al., 1984) of the pluton gave 1.7 and 1.2 Ga (P. Hunt, GSC, personal communication). Recently, Krogh et al. (1984) reported a U-Pb age from two baddeleyite fractions as $2480 \pm^{10}_{5}$ Ma for a gabbro sample from this pluton. These preliminary age determinations suggest that the pluton experienced a complex tectonic-metamorphic history.

Kamineni et al. (1984) subdivided the pluton into 12 units, which range from anorthosite to granophyre dykes. The shape of the pluton is that of a layered lopolith that has a maximum depth of 780 m. The depth to width to length proportions are 1:4:20. The base of the pluton is composed of 400 m of anothosite that grades through gabbroic anothosite to rhythmically layered unit of anorthosite-gabbro. A troctolite unit, about 100 m thick, separates the rhythmically layered units from an upper series of gabbroic rocks described as layered gabbro, crescummulate gabbro and massive gabbro (Kamineni et al., 1984).

Petrological characteristics of gabbro–anorthosite

The various map units of the gabbro-anorthosite complex show differing mineral content, structures and textures, such as dendritic, pegmatitic, crescummulate and massive (Kamineni et al., 1984). The most common primary minerals are clinopyroxene and plagioclase, distributed in various proportions among the different gabbro units. The troctolite unit, in addition to plagioclase and clinopyroxene, also contains olivine and orthopyroxene. The latter, generally, is inverted pigeonite.

The anorthite content of plagioclase in the lower units (i.e. anorthosite, rhythmic layered unit and troctolite) varies between bytownite and labradorite, whereas in the upper units (layered gabbro, dendritic gabbro and massive gabbro etc.) it varies from labradorite to andesine. Clinopyroxene is invariably altered to calcic amphiboles throughout the pluton. It is present as relicts in some parts of the anorthosite and gabbro units, but fresh unaltered grains of both ortho-pyroxene and clinopyroxene are abundant in certain parts of the troctolite unit. Using the compositon of pyroxenes from the troctolite unit and the solvus geothermometric method of Kretz (1983), the temperature of crystallization is estimated to be 1050°C.
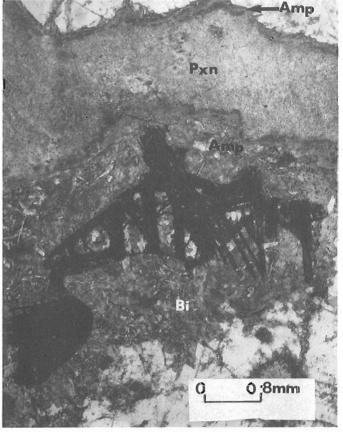

Figure 10.1. *Photomicrograph showing amphibole (Amp) rimming pyroxene (Pxn) crystal. Also note amphibole and biotite (Bi) rimming and replacing magnetite.*

Plagioclase generally is altered to various minerals such as epidote, prehnite, laumontite and kaolinite. This is more predominant in the wall rock adjacent to fractures and fracture zones. In large fracture zones, amphiboles are less dominant and plagioclase attains the composition of pure albite.

Textures and mineral associations of secondary minerals

Secondary minerals in the East Bull Lake pluton have several modes of occurrence, the most important being: (1) single phase fillings in mesoscopic and microscopic fractures, (2) anomalous concentrations in fracture haloes, (3) alteration coronas around primary minerals, and (4) irregular replacement habits along crystal cleavages and grain boundaries. Some of the important secondary minerals that occur in the East Bull Lake pluton are described below.

Calcic amphiboles

Three calcic amphiboles, i.e., hornblende, actinolitic hornblende, and actinolite, occur together in some rock units. The amphiboles are classified following the nomenclature of Leake (1978). Actinolitic hornblende and actinolite are generally concentrated in pyroxene cores whilst hornblende occurs as thin rims around pyroxene crystals (Fig. 10.1). In some cases, hornblende extends into microfractures in adjacent plagioclase crystals forming a bridge between two pyroxene crystals (Fig. 10.2). Although, hornblende generally occurs with the other calcic amphiboles, it can also occur independently near titanomagnetite grains. In such occurrences, it forms a rim around magnetite (Fig. 10.1) and also replaces magnetite along ilmenite cleavages (Fig. 10.3). The three amphibole types have distinct chemical and optical characteristics: hornblende is highly pleochroic from blue-green to dark brown, actinolitic hornblende has olive green to green pleochroism and actinolite has weak pleochroism from light green to faint yellow or colourless. Compositions of the three amphiboles determined from microprobe analysis of one sample are as follows:

Hornblende: $[Na_{0.5}K_{0.2}]$ $[Ca_{1.90}]$ $[Mg_{1.9}Fe_{3.50}Mn_{0.03}$ $Ti_{0.01}Al_{0.66}]$ $[Al_{1.74}Si_{6.26}]$ O_{22} $[OH, Cl]_2$

Actinolitic
Hornblende: $[Na_{0.27}K_{0.12}]$ $[Ca_{1.75}]$ $[Mg_{2.33}Fe_{2.75}$ $Mn_{0.05}Ti_{0.9}Al_{0.1}]$ $[Al_{0.8}Si_{7.2}]$ O_{22} $(OH)_2$

Actinolite: $[Na_{0.17}K_{0.01}]$ $[Ca_{1.9}]$ $[Mg_{3.25}Fe_{1.65}Mn_{0.03}$ $Al_{0.09}]$ $[Al_{0.21}Si_{7.79}]$ O_{22} $(OH)_2$
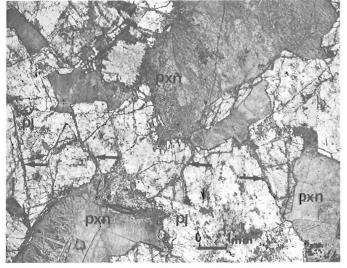
Figure 10.2. Photomicrograph showing microfractures (indicated by arrows) filled with hornblende, bridging pyroxene (Pxn) crystals separated by plagioclase (pl).

Figure 10.3. Photomicrograph showing amphibole replacing magnetite along ilmenite cleavages.

The compositions suggest that the Mg/Fe ratio of the amphiboles decreases according to: actinolite > actinolitic hornblende > hornblende. Al has the opposite relationship. A significant compositional characteristic of these amphiboles is that the hornblende commonly contains Cl ranging from 0.2 to 1.28%.

Biotite

This mineral is commonly present in most rocks in the pluton but is more common in the upper stratigraphic units. It has the same mode of occurrence as hornblende with some minor exceptions. Three modes of occurrence are recognized: (1) forming the outermost rim around some altered pyroxene grains that also have a rim of hornlende, (2) infilling microfractures as a bridge between two pyroxene crystals via plagioclase grains, and (3) rimming and replacing titamomagnetite.

Biotite contains 0.1 to 0.4% Cl.

Epidote and clinozoisite

Epidote and clinozoisite are distinguished by their differences in optical and chemical characteristics: epidote grains are yellowish in thin section under polarized light and contain relatively more Fe (total Fe as FeO ≈ 12%) and less Al (Al_2O_3 ≈ 25%) than clinozoisite. Clinozoisite is colourless in thin section and contains relatively less Fe (total Fe as FeO ≈ 8%) and slightly more Al (Al_2O_3 ≈ 28%) than epidote.

Epidote is a widespread fracture-filling mineral and easily recognized in the field. It occurs as a filling in both macrofractures and microfractures. It also forms as an alteration product of pyroxenes and plagioclase in the rock matrix. In altered pyroxenes, epidote is noted as tiny grains

dispersed in calcic pyroxenes that are replaced by calcic amphiboles. Some anorthosite layers contain epidote crystals formed by complete replacement of plagioclase.

Clinozoisite is noted in the subsurface in fractures of gabbroic units that generally contain calcite and chlorite. In the anorthositic rocks, clinozoisite needles of 2 cm in length are associated with quartz in fractures.

Garnet

Garnet, associated with actinolitic hornblende, actinolite and epidote, occurs in some fractures in core samples recovered from fault zones. Microprobe analysis of the garnet grains showed that they are of the andradite variety. Occurrence of andradite, exclusively, in fault zones is probably due to high oxygen fugacity, which appears to be the general case in these zones.
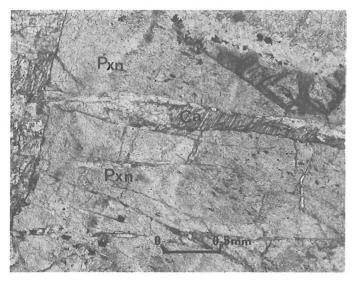
Adularia

This low-temperature K-feldspar polymorph occurs as a filling within fractures concentrated in the 'Folson Lake Fault' (McCrank et al., 1983). The adularia-filled fractures always crosscut epidote-filled fractures, suggesting that this mineral is younger than epidote. Microfractures filled with quartz cut adularia-filled fractures.

Apatite, calcite and sphene

These calcic minerals occur both in the rock matrix and in fractures of both gabbroic and anorthosite units. Apatite, as large crystals and slender needles (up to 5 mm long), commonly transects plagioclase and pyroxene crystals. It is commonly associated with quartz. The textural evidence suggests that apatite is a late mineral in the East Bull Lake pluton. It is also noted as a fracture filling in some microfractures and is commonly associated with calcite.

Calcite is a common fracture-filling in the East Bull Lake pluton, particularly in microfractures of large fracture zones. Most calcite fillings contain well developed crystals, some of which are elongated, possibly due to subsequent deformation (Fig. 10.4). Abundance of this mineral can generally be correlated with an increase in fracture

frequency and rock alteration. Microprobe analysis of calcites reveals that they are pure calcium carbonates with some Fe ($\approx 1\%$). Mn-rich calcite associated with laumontite is reported in one of the samples (R. Kerrich, Department of Geology, University of Western Ontario, personal communication, 1983).

Sphene commonly forms rims around titanomagnetite grains in the rock matrix, where it also replaces ilmenite lamellae. In microfractures, sphene is generally associated with epidote. The fracture-filling sphene shows variable composition, particularly with reference to aluminium and iron.

Sulphides

Sulphides comprising pentlandite, pyrrhotite and chalcopyrite most commonly occur in fractures in the basal anorthosite at depths greater than 300 m. Although the sulphides are essentially concentrated in fractures, some are dispersed in the rock matrix. Epidote is commonly present in the sulphide-filled fractures. Preliminary examination of drill core indicated that the sulphides occur approximately in one fracture every 80 m from 300 to 750 m depth.

Ilmenite

Ilmenite is identified in microfractures occurring within the 'Folson Lake Fault zone' (see McCrank et al., 1983; Kamineni et al., 1984). Microprobe study of ilmenites reveals that they are rich in Mn, which ranges from 2 to 10%.
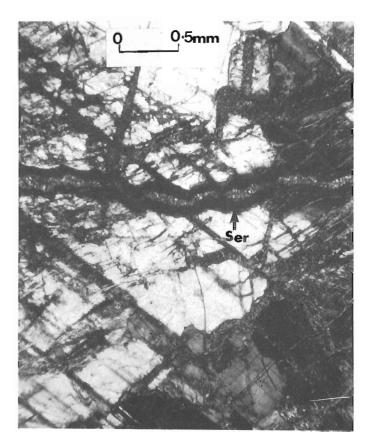
Figure 10.5. *Photomicrograph showing a serpentine-filled fracture (Ser) in troctolite unit.*

Figure 10.4. *Photomicrograph showing calcite-filled microfractures (Ca) transecting pyroxene crystals (Pxn). Note the twinning in calcite with twin planes oriented perpendicular to length. The twinning is probably due to deformation.*

Serpentine and chlorite
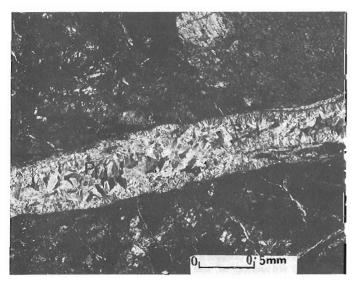
Serpentine is concentrated in the troctolite map unit, where it is very abundant in macroscopic fractures near the sheared top and bottom contacts. These serpentine-filled fractures are very extensive, correlatable in three boreholes (EBL-1, EBL-2 and EBL-3), which are about 500 m apart. Microscopic fractures cutting pyroxene and olivine are visible in thin sections (Fig. 10.5). Magnetite is commonly associated with serpentine and presumably formed as a by-product of the serpentinization of olivine.

Chlorite is abundant in large fracture zones such as the 'Folson Lake Fault zone' and in discontinuities in borehole EBL-2 (see Kamineni et al., 1984). In the fracture zones, chlorite may occur either as a filling in microfractures or as pods. The pods may represent pyroxene crystals replaced by chlorite. Though not abundant, chlorite also occurs sporadically in the altered rock matrix away from the fractures, where it is generally associated with calcic amphiboles. Chlorite commonly occurs as a microfracture filling in the anorthosite zone of the pluton. Chlorites have Mg/Fe ratios ranging from 0.45 to 0.90.

Prehnite, pumpellyite, albite and analcite

These minerals are found together in some fractures. Among these four minerals, prehnite and albite are more commonly distributed in fractures that cut amphibole- and epidote-filled fractures. Prehnite prisms are generally oriented perpendicularly to fracture walls, implying that they grew during extensional conditions (Fig. 10.6). Equigranular and elongated prisms of albite are concentrated at the centre of these fractures.
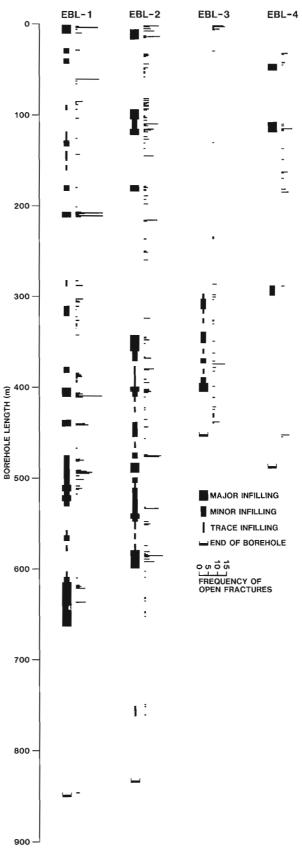
Albite is commonly present in the altered rock matrix in fracture zones.

Figure 10.6. *Photomicrograph showing prehnite crystals oriented normally to the fracture wall. The adjacent rock matrix is deformed, as indicated by cataclastic texture. This mode of occurrence by prehnite suggests growth under dilation in the extension direction of the fracture.*

Figure 10.7 *(opposite). The occurrence of laumontite in the four boreholes. Note that a good proportion of the open fractures are associated with laumontite-bearing fractures.*

OCCURRENCE OF LAUMONTITE AND FREQUENCY OF OPEN FRACTURES EAST BULL LAKE BOREHOLES

85

Laumontite

A calcium zeolite, laumontite, is an abundant fracture filling in the East Bull Lake pluton. It has a pale pink or buff colour and is flaky. This mineral is noted in all the rock units, but is more abundant in anorthositic rocks. Laumontite-bearing fractures vary from low dip (/30°) to subhorizontal attitudes indicating that they may owe their origin to the relief vertical stress in the rock. Calcite is a common associate.

The distribution of laumontite in subsurface is depicted in Figure 10.7. The figure also shows the occurrence of 'open fractures' – a majority of which are concentrated in the laumontite-bearing fracture zones.

Gypsum, clays and iron oxides

These fracture fillings are concentrated in specific zones in the boreholes.

Gypsum occurs only in fracture zones and is concentrated in fractures between 265 and 300 m in the EBL-3 borehole. There are two modes of occurrence: (1) filling smaller fractures within older fractures (Fig. 10.8), and (2) independently filling 1- to 2-mm thick fractures. In such occurrences, gypsum is found as thin sheet-like, fracture fillings, particularly in amphibolite dykes.

Clay fillings up to 2 mm thick have been identified in core samples collected from borehole EBL-2. These samples are extracted mainly from fractures at depth that are exposed at the surface as lineaments. Mineralogically, the clay fillings comprise essentially kaolinite, but indications of some amorphous species such as allophane and amogolite are noted in X-ray powder photographs. Kaolinite was also identified in some samples from the fractured lower contact of the serpentinized troctolite. Additionally, kaolinite is commonly noted at the surface in some subhorizontal fractures in the anorthosite unit.

Hydrated iron oxide fracture fillings, mostly limonite, goethite and hematite, are present in drill core and surface outcrops. The iron oxide minerals probably represent degradation products of infillings such as chlorite and epidote (Kamineni and Stone, 1983).

Discussion

The postconsolidation history of the East Bull Lake pluton can be deduced from the alteration minerals, and can provide information on the tectonic stability of the region as well. The chronology and composition of the fracture fillings can also assist in the definition of paleo-stress conditions.
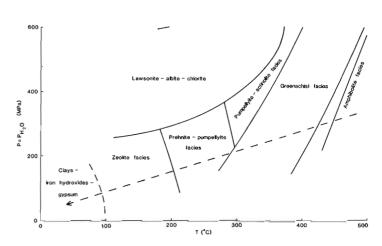
An estimate of the temperatures of formation can be obtained from experimental work related to the metamorphic stability of these minerals (see Table 10.1). The filling minerals indicate that the fractures were generated over a range of temperatures, probably as the pluton cooled after its

Figure 10.8. *Photomicrograph of core sample displaying thin gypsum-filled fractures transecting silicified gabbroic material in the 'Folson Lake Fault'.*

Table 10.1. Estimated temperatures of formation of the alteration minerals (after Turner, 1981)

Alteration Minerals	Temperature °C	Facies
Calcic amphiboles, biotite, sphene, epidote, andradite and quartz	300-450	Epidote-amphibolite/greenschist
Prehnite, pumpellyite, chlorite, tremolite, serpentine, adularia and quartz	200-300	Prehnite-pumpellyite
Laumontite, analcite and calcite	100-200	Zeolite
Clays, hydrous iron oxides and gypsum	<100	Water-rock interaction

Figure 10.9. *Pressure-temperature conditions for the formation of the alteration minerals present in the East-Bull Lake pluton. This diagram is a modified version of Figure 11-1 of Turner (1981). The arrow represents the probable path of alteration, which is corroborated by crosscutting relationships in the field and core specimens.*

consolidation phase. The mineral occurrences listed in Table 10.1 further suggest that the East Bull Lake pluton has been altered under variable metamorphic conditions. The variable metamorphic conditions may be related to thermal alteration along fractures caused by dyke emplacement and subsequent deformation of the pluton. Three distinct metamorphic facies can be inferred from the mode of occurrence of the minerals: (1) epidote-amphibolite/upper greenschist facies, (2) prehnite-pumpellyite facies, and (3) zeolite facies. These metamorphic facies represent progressively decreasing pressure-temperature conditions (Fig. 10.9). As the pressure and temperatures decreased, the spheres of influence of the three types of alteration were also reduced. For example, the early metamorphism is pervasive, and the alteration associated with it defines the ambient character of the pluton. Amphiboles, epidote and biotite form rims around grain boundaries (particularly pyroxenes and opaques) and in microfractures that transect plagioclase grains. Alteration assemblages belonging to the prehnite-pumpellyite and zeolite facies are confined to steep- and shallow-dipping fracture zones. Prehnite and the associated minerals are concentrated in major fracture zones, whereas laumontite is restricted to certain specific fractures with low angle dips (<30°). This suggests that the

TEMPERATURE (°C)

| MAGMATISM | FRACTURING AND HYDROTHERMAL METAMORPHISM | MAGMATISM mafic tholeiitic dykes (K-Ar age = 1.8 Ga) | FRACTURING AND FRACTURE-CONTROLLED METAMORPHISM | MAGMATISM Sudbury-type mafic dykes (K-Ar age = 1.2 Ga) | FRACTURING AND FRACTURE-CONTROLLED METAMORPHISM | FRACTURING ? WATER-ROCK INTERACTION |

1000 —

anorthosite

900 —

rhythmic layered gabbro

troctolite

800 —

layered gabbro

700 —
massive and dendritic gabbro

600 —

500 —
calcic amphiboles
biotite
sphene

400 —
epidote-quartz
chlorite

300 —
prehnite
pumpellyite
adularia
albite
chlorite

200 —
vermiculite
laumontite
analcite

100 —
calcite
gypsum
iron oxides
clays

0 —

TIME ⟶

Figure 10.10. *Schematic diagram representing magmatism, deformation (fracturing) and metamorphism (alteration) of the East-Bull Lake pluton. The X-axis representing time is not to scale.*

low grade metamorphism is fracture-controlled and retrogressive – presumably due to fluid circulation along either new fractures or reactivated older fractures. The gypsum iron oxide-hydroxide and clay-bearing fractures represent signatures of recent to present day water-rock interaction. The retrogressive nature of metamorphic alteration is supported further by crosscutting relations. For example, prehnite- and zeolite-bearing fractures commonly crosscut amphibole-bearing fractures, but not vice versa.

The inferred path of alteration, involving pressure-temperature gradients, is shown in Figure 10.9. This path defines the alteration conditions, and is confined to low-grade metamorphic conditions occurring below the pumpellyite-actinolite stability field. Seki (1966, 1969) suggested that the assemblage pumpellyite-actinolite is an indication of relatively high pressures. No such assemblage has been identified yet in the East Bull Lake pluton.

Figure 10.10 shows a schematic representation of various geological events inferred from the East Bull Lake pluton. The figure contains magmatic (intrusive), deformational (fracturing), and metamorphic (alteration) events. The scheme can be visualized, in general, as a temperature-time cooling curve for plutons, such as the type described by Kamineni and Stone (1983). The two dyke events labelled on the figure define thermal perturbations in an otherwise smooth curve.

References

Born, P.
1978: Geology of the East Bull Lake mafic intrusion, district of Algoma, Ontario; unpublished M.Sc. thesis, Laurentian University, Sudbury, Ontario.

Born, P. and James, R.S.
1978: Geology of the East Bull Lake layered anorthosite intrusion, District of Algoma, Ontario; in Current Research, Part A, Geological Survey of Canada, Paper 78-1A, p. 91-95.

James, R.S., Born, P., and Bigauskas, J.
1983: Geology of the East Bull Lake layered complex, District of Algoma, Ontario; in Current Research, Part B, Geological Survey of Canada, Paper 83-1B, p. 1-11.

Kamineni, D.C. and Stone, D.
1983: The ages of fractures in the Eye-Dashwa pluton, Atikokan, Canada; Contributions to Mineralogy and Petrology, v. 83, p. 237-246.

Kamineni, D.C., McCrank, G.F.D., Stone, D., Ejeckam, R.B., Flindall, R., and Sikorsky, R.
  1984: Geology of the central plateau of the East Bull Lake pluton, Northeastern Ontario; in Current Research, Part B, Geological Survey of Canada, Paper 84-1B, p. 75-83.

Kamineni, D.C., Vandergraaf, T.T., and Ticknor, K.V.
  1983: Characteristics of radionuclide sorption on fracture-filling minerals in the Eye-dashwa lakes pluton, Atikokan, Ontario; Canadian Mineralogist, p. 625-636.

Kretz, R.
  1983: Transfer and exchange equilibria in a portion of the pyroxene quadrilateral as deduced from natural and experimental data; Geochimica et Cosmochimia Acta, v. 46, p. 411-421.

Krogh, T.E., Davis, D.W., and Corfu, F.
  1984: Precise U-pb zircon and baddeleyite ages for the sudbury area; in The Geology and Ore Deposits of the Sudbury Structure, ed. E.G. Pye, A.J. Naldrett and P.E. Giblin; Ontario Geological Survey, Special volume 1, p. 432-446.

Leake, B.E.
  1978: Nomenclature of amphiboles, American Mineralogist, v. 63, p. 1023-1052.

McCrank, G.F.D., Stone, D., Kamineni, D.C., Zaychkivsky, B., and Vincent, G.
  1983: Regional geology of the East Bull Lake area, Ontario; in Current Research, Part A, Geological Survey of Canada, Paper 83-1A, p. 457-464.

Moore, E.S. and Armstrong, W.S.
  1945: Geology of the East Bull Lake area, Algoma district, Ontario; Ontario Department of Mines, Annual Report, 1943, v. 52, pt. 6.

Seki, Y.
  1966: Pumpellyite-bearing mineral assemblages and type of metamorphism. Journal of Japanese Association of Petrology, Mineralogy and Economic Geology, v. 55, p. 102-112.

  1969: Facies series in low-grade metamorphism; Journal of Geological Society of Japan, v. 75, p. 255-266.

Stone, D. and Kamineni, D.C.
  1982: Fractures and fracture infillings of the Eye-Dashwa lakes pluton, Atikokan, Ontario; Canadian Journal of Earth Sciences, v. 19, p. 789-803.

Turner, F.J.
  1981: Metamorphic petrology (second edition); mineralogical, field and tectonic aspects; McGraw Hill, Washington, New York and London, 524 p.

Zolnai, A.I., Price, R.A., and Helmstaedt, H.
  1984: Regional cross section of the Southern Province adjacent to Lake Huron, Ontario: implications for the tectonic significance of the Murray Fault Zone; Canadian Journal of Earth Sciences, v. 21, p. 447-456.

Rb-Sr age measurement on volcanic rocks from the Georges Brook Formation, La Poile Bay area, southwest Newfoundland

Project 830006

W.D. Loveridge and L.B. Chorlton
Precambrian Geology Division

Abstract

Volcanic rocks from the Georges Brook Formation, La Poile Bay area, southwest Newfoundland, have been dated by the Rb-Sr whole rock method. The isochron age of 452 ± 10 Ma (initial $^{87}Sr/^{86}Sr$ = 0.70749 ± 0.00035) confirms the pre-Devonian origin of these rocks.

Résumé

Des roches volcaniques de la formation de Georges Brook, située dans la région de la baie La Poile, dans le sud-ouest de Terre-Neuve, ont été datées par la méthode du rubidium-strontium sur des échantillons de roche entière. L'âge isochrone, établi à 452 ± 10 Ma (rapport $^{87}Sr/^{86}Sr$ initial = 0,70749 ± 0,00035), confirme l'origine prédévonienne de ces roches.
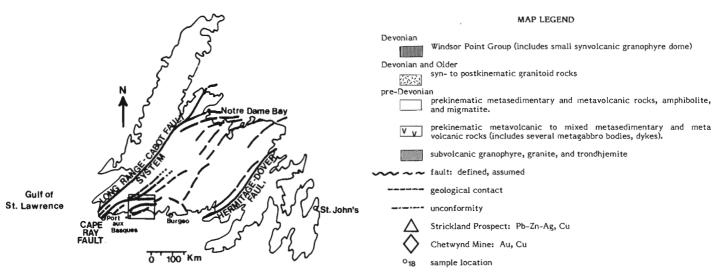
Figure 11.1: Geological setting and sample locations, La Poile Bay area, southern Newfoundland.

MAP LEGEND

Devonian
▨ Windsor Point Group (includes small synvolcanic granophyre dome)

Devonian and Older
▨ syn- to postkinematic granitoid rocks

pre-Devonian
☐ prekinematic metasedimentary and metavolcanic rocks, amphibolite, and migmatite.

V V prekinematic metavolcanic to mixed metasedimentary and metavolcanic rocks (includes several metagabbro bodies, dykes).

▨ subvolcanic granophyre, granite, and trondhjemite

~~~ fault: defined, assumed

‒ ‒ ‒ geological contact

‒·‒·‒ unconformity

△ Strickland Prospect: Pb–Zn–Ag, Cu

◇ Chetwynd Mine: Au, Cu

∘18 sample location

Introduction

The Georges Brook Formation (Chorlton, 1978) is the name applied to a calcalkaline sequence of metavolcanic and related rocks located at the southern end of the Newfoundland Central Mobile Belt in the La Poile Bay area (Fig. 11.1). The first regional map of the La Poile Bay area (Cooper, 1940, 1954) followed the discovery of significant Cu-Au mineralization[1] in Cinq Cerf Brook and the sinking of a mine shaft (Chetwynd Mine, Fig. 11.1), and later, of massive Pb-Zn-Ag and Cu mineralization near North Bay (Strickland Prospect, Fig. 11.1). Devonian plant fossils were found in sedimentary strata of low metamorphic grade at Billiards Brook (Dorf and Cooper, 1943) in the Cape Ray Fault zone much farther north (Fig. 11.1). General parallelism of the structural grain in all rocks of sedimentary and volcanic protolith persuaded Cooper that the wide belt of moderately high grade metamorphic rocks to the south of the Cape Ray Fault zone, and also rocks of relatively low grade south of the Bay d'Est Fault, were Devonian as well. The high grade rocks of the La Poile Bay area were therefore felt to be anomalous compared to the rest of the Newfoundland Appalachian system, where Devonian rocks generally exhibit low metamorphic grade (Williams et al., 1972).

More recent mapping (Chorlton, 1978, 1980a) challenged this interpretation, since the Devonian fossiliferous strata were found to lie unconformably over D_2 mylonites involving rocks immediately to the southeast. Contact relationships and petrofabrics have suggested that all of the metavolcanic, metasedimentary and amphibolitic rocks exposed southeast of the Cape Ray Fault, and on both sides of the Bay d'Est Fault (Fig. 11.1), are pre-Devonian, and belong to the same tectonic interval (Chorlton, 1980a, b, 1983, 1984). Volcanic rocks of the Georges Brook Formation were dated by the Rb-Sr whole rock method in an attempt to determine their approximate age.

Georges Brook Formation

Rock types and field relationships

The Georges Brook Formation consists of polydeformed, greenschist facies mafic, intermediate, and felsic volcanic rocks, volcaniclastic rocks of pyroclastic and sedimentary origin, and unseparated mafic and intermediate dykes and sills. Pyroclastic rocks comprise a large proportion of the total volume of volcanic rock. More detailed descriptions of the Georges Brook Formation can be found in Chorlton (1978, 1980b, 1984).

The depositional interval of the Georges Brook Formation spans the emplacement of the subvolcanic Roti Granite of Cooper (1954), and is in its latest stages coeval with the deposition of an extensive dacitic crystal tuff, of which an equivalent unit of higher metamorphic grade is exposed north of the Bay d'Est Fault (Chorlton, 1984). The throw on the steep Bay d'Est Fault decreases eastward toward Grandy's Brook (Fig. 11.1) where it resolves itself into a series of less prominent shear zones. The magnitude of the rise in metamorphic grade northward across the fault (from lower-middle greenschist facies to lower amphibolite facies near La Poile Bay) decreases eastward (from upper greenschist facies to lower amphibolite facies near Grandy's Brook). In the latter area, the progression of volcanic and sedimentary rock types, as well as their consistent northerly facing directions, continue with little interruption across the fault zone, suggesting equivalence of the rocks on both sides. In addition, the thick unit of dacitic crystal tuff appears in the same stratigraphic position (relatively young) north and south of the fault.

In general, the pre-Devonian volcanogenic rocks in the north and northwest half of the area shown in Figure 11.1 are more well-bedded and more thoroughly intermixed with metasedimentary rocks. They lack the abrupt facies changes and locally great flow thicknesses which characterize the Georges Brook Formation in the south. They have been interpreted as distal to the main centre of volcanism compared to the Georges Brook Formation, which resembles part of a central volcanic complex.

Geochemistry

Selected major and trace element geochemical criteria indicate that the flow rocks of the Georges Brook Formation are mainly calcalkaline, with subordinate tholeiites (Chorlton, 1980a, Appendix I). Mobile elements such as alkalis and strontium show substantial scatter, suggesting metasomatic alteration. Petrographic manifestations of alteration include intense sericitization of plagioclase in both mafic and felsic volcanic rocks, epidote veining, and local overprinting of mafic assemblages by fine grained biotite.

Alteration may have occurred both synvolcanically and during regional deformation. Alteration during the second phase of deformation, which was responsible for strong fabrics, major shear zones, and the steep Grand Bruit Fault (Fig. 11.1) in latest Silurian or early Devonian times might have been particularly significant in chemical redistribution. Although deformed and altered rocks could not be avoided in this dating project, rocks along the Grand Bruit Fault zone and a related ductile shear zone along the south side of the Highlands of Grand Bruit were avoided.

Analytical proceedures and results

Analytical proceedures for Rb-Sr isotopic analysis of whole rock samples were based on those described by Wanless and Loveridge (1972). Samples numbered 74 (Table 11.1, field no.) were analyzed in 1976 and those numbered 76 were analyzed in 1978. Due to the reconstruction of the mass spectrometer in 1977, analytical uncertainty was somewhat lower in 1978 than in 1976 (Table 11.1). Measured $^{87}Sr/^{86}Sr$ were normalized to a value of 0.7080 for the $^{87}Sr/^{86}Sr$ of the MIT isotopic Sr standard (Eimer and Amand $SrCO_3$, lot 492327). The ^{87}Rb decay constant and Rb and Sr isotopic compositions employed are those compiled by Steiger and Jager (1977).

The results of Rb-Sr analyses on eight samples, seven rhyolites and one basalt, are presented in Table 11.1 and plotted in Figure 11.2. The eight data points are collinear within analytical uncertainty, yeilding an isochron: age, 452 ± 10 Ma; initial $^{87}Sr/^{86}Sr$, 0.70749 ± 0.00035; MSWD, 1.75.

Although the one basalt data point ties down the lower end of the isochron, it does not unduly affect the age and initial ratio results. Regression of the seven rhyolite analyses, excluding the basalt data point, results in the identical age and initial ratio obtained from the eight data points, but with the analytical uncertainty approximately doubled.

Interpretation

We interpret the Rb-Sr whole rock isochron date of 452 ± 10 Ma as a minimum age for the volcanic activity in the La Poile Bay area. This age determination is consistent with the suggestion that the metasedimentary and metavolcanic belt as a whole is continuous with the fossil-dated Ordovician Baie d'Espoir Group to the east

---

[1] Interest in the gold potential of this area has been recently rekindled by confirmation of high tonnage, highly auriferous mineralization a few kilometres south of the original Cu-Au discovery zone (Northern Miner, 1985).

Table 11.1. Analytical data and localities, whole rock samples, Georges Brook Formation, Newfoundland

Sample no. This work	Field	Rock type	Rb pm	Sr ppm	$^{87}Rb/^{86}Sr$	$^{87}Sr/^{86}Sr$	UTM coordinates Easting	Northing
65	76-LC-65	basalt	0.142	242.2	0.0017	0.7075 ± 0.0003	402350	5279300
15	74-GB-15	rhyolite	45.85	130.5	1.016	0.7138 ± 0.0011	407400	5280500
32	74-GB-32	rhyolite	53.98	130.5	1.197	0.7156 ± 0.0011	406100	5281000
28	75-LC-28	rhyolite	70.86	131.5	1.556	0.7166 ± 0.0011	406200	5281700
227	76-LC-227	rhyolite	187.5	145.4	3.728	0.7320 ± 0.0003	397050	5276300
25	74-GB-25	rhyolite	95.61	72.67	3.806	0.7325 ± 0.0011	406800	5280600
215	74-GB-215	rhyolite	177.6	120.1	4.278	0.7343 ± 0.0011	397700	5278400
151	76-LC-151	rhyolite	152.9	85.53	5.168	0.7403 ± 0.0003	414350	5284400

Figure 11.2

Rb-Sr isochron, volcanic rocks from the Georges Brook Formation, southern Newfoundland.

(D. Kretchmar, personal communication, 1975; D. Prince, personal communication, 1977; Smyth, 1979; O'Brien, 1983), and with the recently mapped continuation of both assemblages with the conodont-dated Llandeilan Victoria Lake Group to the north-northeast (Kean, 1983). U-Pb zircon dates of 452+51/-13 Ma for the dacitic crystal tuff south of the Bay D'Est Fault and 458+29/-22 Ma for the crystal tuff north of the fault are in general agreement with the Rb-Sr isochron age.

The initial $^{87}Sr/^{86}Sr$ of 0.70749 ± 0.00035 is higher than would be expected for mantle derivation of the volcanic magma (cf. modern day ocean ridge basalts at 0.703). A continental crustal component within the magma is implied.

It must be cautioned that variable postvolcanic, syndeformational metasomatism might have affected many if not all of the samples analyzed. In addition, many calcalkaline magmatic complexes of this nature are interpreted by some as containing different mixtures of source material (eg. Burnham, 1979). Nevertheless, the observed systematics suggest generally closed system behaviour following isotopic homogeneity of Sr at about 452 Ma. We have interpreted this result as a minimum age, as the Rb-Sr systems may have been reset at about 452 Ma by the relatively mild effects noted above (e.g. Van Schmus et al., 1975).

References

Burnham, W.C.
1979: Magmas and hydrothermal fluids; in Geochemistry of Hydro-thermal Ore Deposits, 2nd edition, ed. H.L. Barnes, John Wiley and Sons. p. 71-137.

Chorlton, L.B.
1978: Geology of the La Poile area (110/9), Newfoundland; Government of Newfoundland and Labrador, Mineral Development Division, Report 78-5, 14 p.

1980a: Geology of the La Poile River area (110/16), Newfoundland; Government of Newfoundland and Labrador, Mineral Development Division, Report 80-3, 86 p.

1980b: Notes on the geology of Peter Snout (11P/13), Newfoundland; Government of Newfoundland and Labrador, Mineral Development Division, notes to accompany Map 80201, 7 p.

1983: Geology of the Grandy's Lake area (110/15), Newfoundland: Part I: Geology of the southern Long Range Mountains; Government of Newfoundland and Labrador, Mineral Development Division, Report 83-7, p. 1-116.

Chorlton, L.B. (con't)
1984: Geological development of the southern Long Range Mountains, southwest Newfoundland: a regional synopsis; Ph.D. thesis, Memorial University of Newfoundland, 579 p.

Cooper, J.R.
1940: La Poile – Cinq Cerf area, Newfoundland; Newfoundland Department of Mines, Open File Report, 123 p.

1954: The La Poile – Cinq Cerf map area, Newfoundland; Geological Survey of Canada, Memoir 254, 62 p.

Dorf, E. and Cooper, J.R.
1943: Early Devonian plants from Newfoundland; Journal of Paleontology, v. 17, p. 264-270.

Kean, B.F.,
1983: Geology of the King George IV Lake area (12A/4), Newfoundland; Government of Newfoundland and Labrador, Mineral Development Division, Report 83-4, 67 p.

Northern Miner
1985: Selco drilling impressive, Chetwynd looks good; Northern Miner, March 7, Section A, p. A1, A6.

O'Brien, S.J.
1983: Geology of the eastern half of the Peter Snout map area (115/13E), Newfoundland; in Current Research, M.J. Murray et al.; Government of Newfoundland and Labrador, Mineral Development Division, Report 83-1, p. 57-67.

Steiger, R.H. and Jager, E.
1977: Subcommission on geochronology: convention on the use of decay constants in geo- and cosmochronology; Earth and Planetary Science Letters, v. 36, p. 359-362.

Smyth, W.R.
1979: Reconnaissance of the Burgeo map area (11, west half), Newfoundland; in Report of Activities for 1978, ed. R.V. Gibbons; Government of Newfoundland and Labrador, Report 79-1, p. 54-57.

Van Schmus, W.R., Thurman, E.M., and Peterman, Z.E.
1975: Geology and Rb-Sr chronology of middle Precambrian rocks in eastern and central Wisconsin; Geological Society of America Bulletin, v. 86, p. 1255-1265.

Wanless, R.K. and Loveridge, W.D.
1972: Rubidium-strontium isochron age studies, Report 1; Geological Survey of Canada, Paper 72-23, p. 67-69.

Williams, H., Kennedy, M.J., and Neale, E.R.W.
1972: The Appalachian Structural Province; Geological Association of Canada, Special Paper 11, p. 182-261.

Structural reconnaissance of South Sansom Island, northeastern Newfoundland

EMR Research Agreement 179-04-81

Karl E. Karlstrom [1]
Precambrian Geology Division

Abstract

New mapping indicates that South Sansom Island is segmented by late high angle faults into a series of fault blocks within which three generations of folds are documented. Correlation of block to block stratigraphy is hindered by the absence of marker units in the greywacke sequences, but it is suggested that early thrusts accompanied F_1 isoclinal folding. F_1 folds and inferred thrusts are folded by F_2 folds with east-northeast-trending, steeply south-dipping axial plane cleavage. Structural data indicate the island is not a north-younging homoclinal sequence as proposed by other workers.

A new fossil locality on the southeast of the island gives a Caradocian to Ashgillian age for thin-bedded greywackes. These rocks are similar in lithology and faunal assemblage to rocks near Intricate Harbour, western New World Island. The newly dated greywackes structurally and stratigraphically overlie volcanics and fossiliferous limestones of probable Llandeilo age, suggesting a normal south-younging sequence within this fault slice. However, this upper Ordovician rock package structurally overlies Silurian (?) coarse grained turbidites, indicating an older over younger thrust.

Résumé

D'après les résultats de travaux cartographiques récents, l'île South Sansom est divisée par des failles à pendage élevé, d'origine récénte, en une série de blocs faillés à l'intérieur desquels on distingue trois générations de plis. Il est difficile d'établir des corrélations stratigraphiques entre les blocs, faute de repères dans les séquences de grauwacke; cependant, les auteurs supposent que des poussées orogéniques ont accompagné le plissement isoclinal F_1. Ces plis F_1 et failles de poussée sont à leur tour déformés par des plis F_2 dont le plan axial s'accompagne d'un clivage de direction est-nord-est et à pendage marqué vers le sud. Les données structurales contredisent les résultats d'autres études selon lesquels l'île serait une séquence homoclinale rajeunissant vers le nord.

D'après les observations réalisées dans une nouvelle localité de fossiles dans la partie sud-est de l'île, l'âge des couches minces de grauwacke se situerait entre le Cardocien et l'Ashgillien. Ces roches s'apparentent, par leur lithologie et leur assemblage faunal, aux roches trouvées près du havre Intricate, dans l'ouest de l'île New World. Les grauwackes que l'on vient de dater recouvrent, structuralement et stratigraphiquement, des calcaires volcaniques et fossilifères d'âge probablement llandeilien; cette observation semble indiquer l'existence, à l'intérieur de cette tranche de roches limitée par des failles, d'une séquence normale dont l'âge diminue vers le sud. Cependant, tout cet ensemble de roches de l'Ordovicien supérieur repose structuralement sur des turbidites à grains grossiers du Silurien (?), indiquant le chevauchement de couches plus anciennes sur des roches plus jeunes.

[1] Department of Geology, Northern Arizona University, Flagstaff, Arizona 86011

Introduction

This paper presents results of 1:12 500 mapping conducted on South Sansom Island (Fig. 12.1) in 1983 as part of ongoing mapping of the Comfort Cove (1:50 000) map sheet, northeastern Newfoundland by P.F. Williams and K.E. Karlstrom. The purposes of this paper are twofold: (1) to present preliminary interpretations of structure and stratigraphy of this area of Notre Dame Bay; and (2) to report a new fossil location on the southeastern part of the island which supports the interpretation of major fault repetition of stratigraphic units (Karlstrom et al., 1982).

Previous work on South Sansom Island includes reconnaissance mapping at 1:63 500 scale by Heyl (1936), at 1:17 000 scale by Horne (1968) and at 1:50 000 scale by McKerrow and Cocks (1981), but the island has remained poorly understood in spite of its obvious importance to regional interpretations, as a western extension of New World Island geology and as the original type area for the Sansom Formation, a regionally important flysch unit (Fig. 12.1).

Figure 12.2 is a simplified geological map of South Sansom Island showing lithological units, structural elements, and the positions of faults. Like much of Newfoundland's Dunnage Zone, structure is sufficiently complex and incompletely understood that it has not been possible to identify unmodified stratigraphic sections. Furthermore, a lack of marker units makes it difficult or impossible to piece together the fault-bounded and complexly folded segments of the stratigraphic section. Therefore, Figure 12.2 is presented as a lithological map (largely uninterpreted) to facilitate later, more detailed work.

The relative age succession of lithologies shown in the explanation to Figure 12.2 is the general stratigraphic succession throughout Notre Dame Bay (Williams, 1972; Dean, 1978; Keen et al., 1981). However, with the exception of the fossil dates on the southeastern part of the island, this stratigraphic succession cannot be established with evidence from South Sansom Island alone. My preliminary interpretation of Figure 12.2 assumes that local stratigraphy follows the regional succession, which suggests a structural complexity compatible with the observed mesoscopic and macroscopic structural features.

An alternative working hypothesis would be that stratigraphy is more complex and variable here than elsewhere in Notre Dame Bay and that the somewhat chaotic juxtaposition of lithologies shown in Figure 12.2 is in large part of sedimentary origin. This was the approach taken by McKerrow and Cocks (1981) who suggested that South Sansom Island is composed of north-younging olistostromal deposits. However, my mapping shows variable younging and a preponderance of east-northeast- and west-southwest-facing folds (Shackleton, 1958). Stratigraphic units are disrupted at all scales, as shown by macroscopic faults and folds

Figure 12.1. *Location and regional tectonic setting of South Sansom Island. Fossils (F) from the southeast corner of the island are similar to those found near Intricate Harbour (I.H.) on western New World Island. Paleocurrent trends in the northern part of the island appear similar to those reported by Arnott (1983) from rocks north of the Cobbs Arm Fault.*

Figure 12.2. *Simplified geological map of South Sansom Island based on 1:12 500 scale mapping and air photo interpretation. Lithological units are shown in their inferred stratigraphic sequence in the explanation, based on the regional stratigraphic sequence in the explanation, based on the regional stratigraphic succession in Notre Dame Bay (Dean, 1978; Keen et al., 1981). Abundant faults and the absence of marker beds make it difficult to verify this stratigraphy from South Sansom Island alone.*

(Fig. 12.2) and mesoscopic features such as bedding-parallel faults (Fig. 12.3A), faulted and disrupted folds (Fig. 12.3B), and intensely boudinaged movements zones (Fig. 12.3C). Major portions of this disruption postdated lithification as shown by faulted dykes, folded and boudinaged carbonate concretions (Fig. 12.3C) and folded volcanics (Fig. 12.2). These features, combined with a post-middle Silurian regional

structural complexity consisting of F_1-related thrusting, F_2 asymmetrical folding, and late transcurrent faulting (Karlstrom et al., 1982; Williams, 1984) support the structural interpretation shown in Figure 12.4 and appear to rule out the north-younging olistostrome interpretation for the island as a whole, although olistostromal deposits may be present locally.

A. *Gently dipping bedding-parallel fault in turbidites on the eastern side of the island. Beds young to the north (left) and the fault is interpreted as an overturned west-directed thrust (bed truncations below hammer are thus believed to be hanging wall cutoffs). Headland in the distance is the west coast of New World Island.*

B. *Disrupted turbidite sequences showing faulted folds; east side, South Sansom Island.*

C. *Movement zone showing disrupted siltstones and argillites on the east side of the island. The carbonate concretion just left of the pencil tip is folded into a tight rootless fold; the concretion under the right end of the pencil shows the lozenge-shape characteristic of boudinage. Both imply that deformation in the movement zone postdated lithification of the argillite matrix.*

Figure 12.3.

Lithological units

South Sansom Island was originally the type area for Heyl's (1936) "Sansom Graywacke and Quartzite", which was part of his Exploits Series (Ordovician) and included volcanics, limestones, argillites and conglomerates. The name Sansom Graywacke was retained by Horne (1968) and Kay (1976) for the New World Island area, but was restricted by Horne (1968) to "thick successions of rhythmically alternating graded greywacke and silty argillite". McKerrow and Cocks (1981) used the name Sansom Formation for rocks in a northeast-trending belt including South Sansom Island and central New World Island (Fig. 12.1). They reverted to Heyl's usage in that they included volcanics, limestones, and conglomerates as well as greywackes, but they considered these varied lithologies to be blocks in olistostromes interbedded with the turbidites.

For regional mapping, I prefer Horne's usage because it avoids uncertainties in interpreting the genesis of disrupted sequences (Karlstrom et al., 1982). However, with respect to South Sansom Island, none of the usages of the name Sansom Graywacke are satisfactory, and the island is a poor choice for the type locality of a regionally important flysch unit (Dean, 1978). The problem is that the island consists of a variety of argillite, sandstone, and conglomerate lithologies which, because of the island's structural complexity, are likely to be of quite different ages and depositional settings.

Clastic sedimentary rocks on South Sansom Island are divided into four lithological groups in Figure 12.2. (1) Dark grey, coarse grained polymictic conglomerate with abundant shale and sandstone clasts as well as granitoid and volcanic fragments; these resemble conglomerates of the New Bay Formation farther south (Hibbard, 1976). (2) Dark grey, thin-bedded and generally fine grained greywackes which resemble both rocks of the New Bay Formation and the Dark Hole Formation of southern New World Island (Kay, 1976). (3) Medium- to thick-bedded greywacke sequences containing alternating graded sandstones and argillites resembling Silurian ("Sansom-type") greywacke exposed in the Milleners Arm Formation of southern New World Island (McKerrow and Cocks, 1978). (4) Very coarse grained polymictic conglomerate containing mainly granite, volcanic, and chert fragments, but also containing metre-scale blocks of very coarse grained gabbro. These conglomerates resemble Silurian "Goldson-type" conglomerates of Horne (1967) and McKerrow and Cocks (1978).

Contacts between these turbidite lithologies are locally transitional, especially between units 2 and 3, and the varying lithologies are complexly juxtaposed (Fig. 12.2). Thus, it is not possible to identify an undisturbed type section of Sansom Graywacke on South Sansom Island, nor is it possible to definitely correlate most of these greywacke sequences with rocks elsewhere. The single exception is a newly dated turbidite on the southeast corner of the island which is described below.

The newly found upper Ordovician fossils on the southeastern corner of the island (Fig. 12.2, southern fossil locality) document a correlation with rocks near Intricate Harbour, on western New World Island (Fig. 12.1). This fossil locality is from unit 3 (above); dark grey,

Figure 12.4. Interpretive tectonic map of South Sansom Island showing generalized bedding form lines (long dashes), younging directions of bedding (arrows), major movement zones (closely spaced dashes), and two inferred thrusts (teeth on hanging wall). Equal area projections for subareas I-IV show poles to bedding (x = overturned; o = upright; . = younging unknown), F_1 and F_2 minor folds (+), average S_2 orientation (long-dash great circles), and girdles of poles to planes (short dashes) for various subareas. The upper synoptic diagram shows S_2 poles and F_1, F_2 minor folds; the lower synoptic diagram shows S_0 poles for the entire island.

medium-bedded greywackes. Fossils are from a 4 cm thick coarse grained sandstone layer within a complexly folded, rhythmically bedded sandstone-argillite sequence. Robert Neuman of the National Museum of Natural History, Washington, D.C., identified these fossils as follows (Neuman, written communications, 1983).

"Brachiopods are the most abundant fossils in the sample, followed by bryozoans and pelmatozoans (represented by disarticulated plates); there are also a few trilobite fragments, especially parts of trinucleid fringes, and 2 specimens of a high-spired gastropod.

The most abundant brachiopods are an unidentified species of **Sowerbyella** and an unidentified genus of dalmanellid. Specific and generic identifications, respectively, of these brachiopods require specimens that are better preserved than these. One or more specimens of the following brachiopod genera are also present: (alphabetical listing)

Christiania	rhynchonellid genus
Dolerorthis	indeterminable
Leangella	? **Schizophorella**
Leptaena	**Skenidioides**

These genera occur together in rocks of Caradocian and Ashgillian ages, except for the **Schizophorella**, an exclusively Ashgillian form, here questionably identified on one dorsal valve. Most of them were listed by McKerrow and Cocks (1981) from Intricate Harbour, a list that includes genera that are diagnostic of Ashgillian age.

Rocks having brachiopods of Caradocian age were not reported in the Intricate Harbour area by these authors, although they did report Caradocian algae-bearing limestone and graptolite-bearing pelites. Thus, although the brachiopods in the Sansom Island sample are not themselves diagnostic of Caradocian or Ashgill age, the latter seems more probable."

As shown in Figure 12.2 (southern fossil locality), the rocks containing these fossils are south of a major outcrop of volcanics which include pillow breccia and basaltic tuff. The volcanics themselves are folded and are structurally and stratigraphically overlain by limestone lenses which contain fossils of probable Llandeilo age (McKerrow and Cocks, 1981). The limestones are overlain by polymictic conglomerate followed by the newly dated greywackes. The lithological succession (Fig. 12.2) and the fossils in it suggest this package youngs to the south (c.f. McKerrow and Cocks, 1981, p. 758), although the abundance of mesoscopic bedding-parallel faults in the section plus tight to isoclinal folds in the greywacke indicate a highly disrupted section (Fig. 12.2, 12.4).

Dyke rocks on South Sansom Island include: (1) an isolated block on the northwest side of the island of porphyritic dacite which is surrounded by disrupted greywackes and argillites and which resembles blocks of Coaker dacite in the Dunnage Melange area; and (2) a suite of northwest-trending intermediate to felsic dykes which postdate folding but are locally faulted (Fig. 12.2). The latter may be related to Devonian granitoid plutonic rocks to the south.

Paleocurrent data

Rocks belonging to unit 3, medium- to thick-bedded turbidites, locally contain well preserved bottom structures. Groove casts and one flute cast were measured in scattered localities, as shown in Figure 12.5. These data cannot be restored to their prefolding orientation without better knowledge of the deformation history, as is true of all published paleocurrent measurements from New World Island (c.f. Arnott, 1983; Karlstrom et al., 1983). For comparison to date from Arnott (1983), I simply rotated beds to horizontal about their strike (which is how I assume Arnott "restored" paleocurrent data). Using this oversimplified and often misleading technique, measurements from South Sansom Island show a general east-west paleocurrent sense (the one flute cast shows easterly transport). Correlative rocks on New World Island, the Big Muddy Cove Group of Arnott (1983), show a similar sense and direction. This does not increase my confidence that this is a true paleocurrent direction, but it may tend to reinforce the correlation of rocks and deformational histories between South Sansom Island and north of the Cobbs Arm Fault Zone in central and western New World Island (Fig. 12.1).

Structural geology

South Sansom Island consists of a series of internally folded fault-bounded blocks. Figure 12.2 shows a network of northeast- and northwest-trending faults. The location of these faults are inferred from air photo lineaments, although many of the lineaments coincide with faults and fault zones mapped on the coastlines. The faults shown in Figure 12.2 are probably of several generations, some of which predate F_2 folding, but most of which postdate F_2.

Figure 12.4 is an interpretive form surface which shows folds of bedding, younging directions of beds, and the faults inferred to be of greatest significance to the overall rock distribution. This map shows three fold generations similar to those described by Karlstrom et al. (1982). F_1 folds are tight to isoclinal and are refolded. Their folded hinge surfaces have F_2 enveloping surfaces which trend roughly north-south for the northern parts of the island, and northwest on the southeast coast of the island. F_2 folds are open to tight with generally east-west trending axial plane cleavage, as shown by the synoptic diagram of S_2 (Fig. 12.4). F_2 folds vary in plunge and have variable facing direction reflecting the presence of macroscopic F_1 folds. F_2 folds are

Figure 12.5. *Scattered paleocurrent measurements from bottom structures in "Sansom-type" turbidites. Groove cast measurements are shown as lineations in bedding (directional sense unknown). One flute cast measurement (marked F, with current direction up-plunge) shows paleoflow towards the east. The "paleocurrent" rose diagram shows orientations of bottom structures if beds are simply rotated to horizontal about their strike.*

dominantly upward-facing on the south coast, dominantly east-facing on the west coast, and east- and west-facing on the east coast. Variable F_2 plunge and facing direction reflect F_1 and F_2 overprinting relationships which have produced an overall noncylindrical geometry for folded bedding (shown by the synoptic plot of poles to S_0 in Fig. 12.4). F_3 resulted in warping of refolded folds as shown on the southeast coast of the island and in the weak spread of the maximum of poles to S_2 (Fig. 12.4).

Major faults are as follows. (1) On the west coast, polymictic conglomerate, resembling Silurian Goldson conglomerate on New World Island, youngs continuously northeast (subarea III of Fig. 12.4) and underlies north-younging thin-bedded turbidites resembling Ordovician Dark Hole Formation. Neither of these units has been dated but if these lithological correlations can be considered stratigraphic correlations, this suggests an older over younger thrust which has been folded into its present steeply dipping orientation (Fig. 12.4). (2) Similarly, on the southeastern part of the island, the dated sequence – volcanics, Llandeilo limestone, conglomerate, Ashgill turbidites – structurally overlies a fault-bounded block of south-younging ("Sansom-type") thick-bedded turbidites which resemble Silurian units on New World Island, again suggesting a thrust. (3) Major parts of the island consist of highly disrupted turbidites, siltstones, and argillites (Fig. 12.3C). The most intense zones of disruption are shown in Figure 12.4. These zones are characterized by extreme boudinage of sandstone beds and blocks within an argillite matrix. These rocks closely resemble rocks of melange terranes such as the Dunnage Melange. The zones may have compound origin reflecting one or more fold and fault generation. However, some movement on the zones apparently postdated F_2 since they truncate mesoscopic and macroscopic F_2 folds (Fig. 12.4).

Conclusions

Major conclusions of this paper are as follows:

1. Fossils on southeastern South Sansom Island indicate that these turbidite sequences are Carodocian to Ashgillian, similar in age to turbidites near Intricate Harbour, western New World Island.

2. The island consists of fault-bounded blocks within which three fold generations can be documented. Because of the structural complexity of the island, South Sansom Island should not be considered the type locality for the Sansom Graywacke.

3. The island cannot be considered part of a north-younging stratigraphic section (c.f. McKerrow and Cocks, 1981) and the interpretation of the island as a series of olisto-stromes is difficult to reconcile with the observed geometry of rock units.

4. Two older over younger thrusts can be inferred if one assumes that the stratigraphic sequence here is similar to the stratigraphic sequence elsewhere in Notre Dame Bay. Both of these thrusts were folded subsequent to thrusting.

Acknowledgments

References

Arnott, R.J.
1983: Sedimentology of Upper Ordovician-Silurian sequences on New World Island, Newfoundland: separate fault-controlled basins?; Canadian Journal of Earth Sciences, v. 20, p. 345-354.

Dean, P.L.
1978: The volcanic stratigraphy and metallogeny of Notre Dame Bay, Newfoundland; Memorial University of Newfoundland, St. John's, Newfoundland, Geology Report 7, 204 p.

Heyl, G.R.
1936: Geology and mineral deposits of the Bay of Exploits area; Newfoundland Department of Natural Resources, Geologic Section Bulletin, no. 3, 66 p.

Hibbard, J.P.
1976: The southwest portion of the Dunnage Melange and its relationships to nearby groups; unpublished M.Sc. thesis, Memorial Unviersity of Newfoundland, 130 p.

Horne, G.S.
1968: Stratigraphy and structural geology of southwestern New World Island area, Newfoundland; unpublished Ph.D. thesis, Columbia University, 280 p.

Karlstrom, K.E., Van Der Pluijm, B.A., and Williams, P.F.
1982: Structural interpretation of the eastern Notre Dame Bay area, Newfoundland: regional post-Middle Silurian thrusting and asymmetrical folding; Canadian Journal of Earth Sciences, v. 19, p. 2325-2341.

1983: Sedimentology of Upper Ordovician - Silurian sequences on New World Island, Newfoundland: separate fault-controlled basins?: Discussion; Canadian Journal of Earth Sciences, v. 20, p. 1757-1758.

Kay, M.
1976: Dunnage melange and subduction of the Protacadic Ocean, northeast Newfoundland; Geological Society of America, Special Paper 175, p. 1-49.

Keen, B.F., Dean, P.L., and Strong, D.F.
1981: Regional geology of the Central Volcanic Belt of Newfoundland; in The Buchans Orebodies: Fifty years of Geology and Mining, ed. E.A. Swanson, D.F. Strong and J.G. Thurlow; Geological Association of Canada, Paper 22, p. 65-78.

McKerrow, W.S. and Cocks, L.R.M.
1978: A lower Paleozoic trench-fill sequence, New World Island, Newfoundland; Geological Society of America, Bulletin, v. 89, p. 1121-1132.

1981: Stratigraphy of eastern Bay of Exploits, Newfoundland; Canadian Journal of Earth Sciences, v. 18, p. 751-764.

Shackleton, R.M.
1958: Downward facing structures in the Highland Border; Geological Society London, Quarterly Journal, v. 113, p. 361-392.

Williams, H.
1972: Stratigraphy of the Botwood map-area, northeastern Newfoundland; Geological Survey of Canada, Open File 113, 103 p.

Williams, P.F.
1984: Deformation in the New World Island area, Newfoundland: late stage transcurrent faulting; Geological Society of America, Abstracts with Programs.

Geology of the southeastern Cape Breton Highlands, Nova Scotia

Project 730044

S.M. Barr[1], R.P. Raeside[1], and A.S. Macdonald[1]
Precambrian Geology Division

Abstract

The southeastern Cape Breton Highlands is composed of a series of elongate north-northeast trending granitoid plutons in the east and more northerly trending dioritic and tonalitic plutons in the west, which have been intruded by a variety of presumed Devonian granitoid bodies. Stratified rocks include siliciclastic, volcaniclastic and volcanic units some of which are continuous across the entire eastern Highlands. Metamorphic grade increases to the north from lower greenschist facies to upper amphibolite facies.

Résumé

Le sud-est des hautes-terres du Cap-Breton est constitué, dans l'est, d'une série de plutons granitoïdes allongés de direction nord-nord-est et, dans l'ouest, de plutons dioritiques et tonalitiques, à orientation nord plus prononcée, et dans lesquels font intrusion divers corps granitoïdes que l'on présume dater du Dévonien. Les roches stratifiées comprennent des unités silicoclastiques, volcanoclastiques et volcaniques, dont certaines s'étendent sans interruption à travers toute la partie est des hautes-terres. Le degré de métamorphisme s'accroît vers le nord, le faciès des schistes verts inférieur passant progressivement au faciès des amphibolites supérieur.

---

[1] Department of Geology, Acadia University, Wolfville, Nova Scotia B0P 1X0

Introduction

The Highlands of Cape Breton Island contain one of the largest segments of crystalline Precambrian and Paleozoic rocks in the Atlantic Canadian section of the Appalachian mountain belt. This segment is particularly significant, lying between Newfoundland and the mainland Appalachians, in an area where basement rocks are either buried beneath younger sedimentary cover or under water. Detailed mapping was begun in the central portion of the eastern Highlands (Raeside et al., 1984) as the first phase of remapping of the entire eastern and northern Highlands. In 1984, mapping was completed from the latitude of Wreck Cove to the southern limit of the Highlands where the Precambrian and Paleozoic crystalline rocks are overlain by Early Mississippian sedimentary rocks of the Horton and Windsor Groups. A 1:50 000 scale geological map has been compiled, a reduced version of which is shown in Figure 13.1.

Previous maps of this area (McLaren 1956a, b; Kelley 1957, 1960; Murray, 1977) are of reconnaissance nature and serve to outline the approximate positions of major rock types. No detailed descriptions of plutonic sequences, stratigraphy, structure or metamorphism were provided. On the geological map of Nova Scotia (Keppie, 1979) much of the map area is shown underlain by undivided gneiss and schist, undivided mafic gneiss and schist, marble and other undivided rocks of the George River Group and a variety of undated and questionably Hadrynian and Cambrian plutons. The area overlaps the area of detailed mapping of Jamieson and Craw (1983) and as a result of increased exposure incorporates some changes to the eastern edge of their mapping. The geology of the St. Ann's area has been described by Macdonald and Barr (1985).

GRANITOID ROCKS

DEVONIAN OR YOUNGER
  22 Microdiorite dykes

DEVONIAN
    Muscovite-bearing Suite (from north to south; no relative
      age sequence known or implied)
  21 East Branch Indian Brook pegmatite granite
  20 Cross Mountain granite/leucotonalite
  19 Oxford Lakes Granite
  18 North River Canyon granodiorite
  17 New Glen megacrystic granite
  16 Snake Cat Lake muscovite-biotite granodiorite
  15 Baddeck River biotite-muscovite granodiorite
  14 West Branch North River granite

SILURO-ORDOVICIAN(?)
  13 Cape Smoky granite
  12 Morrison Brook quartz monzonite
  11 Ingonish River Tonalite

LATE HADRYNIAN OR YOUNGER
  10 Kathy Road quartz diorite
   9 Timber Lake quartz diorite

LATE HADRYNIAN-EARLY CAMBRIAN
   8 Goose Cove Brook - Beinn Breagh Suite
   7 Murray Mountain quartz monzodiorite ⎤
   6 St. Ann's leucogranite   ⎥ St. Ann's Harbour -
   5 Indian Brook granodiorite   ⎥ Wreck Cove Suite
   4 Birch Plain granite   ⎦

LATE HADRYNIAN
   3 Wreck Cove Brook dioritic suite
   2 Gisborne Flowage quartz diorite
   1 North Branch Baddeck River leucotonalite

STRATIFIED ROCKS
MISSISSIPPIAN
   E Horton and Windsor Groups, undivided - sandstone, conglomerate,
      shale, limestone and evaporites

PRECAMBRIAN
   (no relative age known or implied)
   D undifferentiated metamorphic rocks of the Central Highlands
   C Price Point volcanic-sedimentary unit
   B Barachois River gneiss, and equivalent
   A5 upper clastic division ⎤
   A4 marble division   ⎥ Ingonish River
   A3 middle clastic division ⎬ metasedimentary
   A2 quartzite division   ⎥ unit
   A1 lower clastic division ⎦

Figure 13.1. *Geological map of the southeastern Cape Breton Highlands.*

Overview

The southeastern portion of the Cape Breton Highlands incorporates two of the major north-south trending belts identified in the east-central Highlands (Raeside et al., 1984). The package of pelitic, semipelitic, psammitic and calcareous metasedimentary rocks interbedded with tuffaceous and basaltic layers continues into the western part of the map area, where it is intruded by large dioritic bodies. The eastern belt of varied granitoid rocks also continues to the southern limit of the Highlands, but here incorporates isolated blocks of gneiss. Granitoid units are much more abundant than in the area to the north, and are also more abundant than previously reported.

Granitoid Units

Introduction

Granitoid rocks are a major component of the map area. Twenty-two units are recognized and assigned informal names based on local geographic features (Fig. 13.1). They are inferred to range in age from Late Hadrynian to Devonian, but few of the units are reliably dated and age interpretations are to a large extent speculative.

Late Hadrynian to Early Cambrian Units

North Branch Baddeck River leucotonalite (unit 1). The North Branch Baddeck River leucotonalite forms a large body in the southwestern corner of the map area. It was originally included by Jamieson and Doucet (1983) and Jamieson and Craw (1983) in the Baddeck Lakes complex; however, more detailed mapping has shown that the leucotonalite forms a relatively homogeneous unit in faulted contact with diorite to the east. This fault is one of the major north- to northeast-trending shear zones which are characteristic of the Cape Breton Highlands. To the north the leucotonalite is apparently in intrusive contact with the Central Highlands schist/gneiss and was intruded by the crosscutting West Branch North River syenogranite. As mapped by Jamieson and Doucet (1983), the western and southern contacts are all faulted.

A late Hadrynian age for the leucotonalite is based on an Rb-Sr whole-rock isochron which yielded an age of 752 ± 26 Ma (R.A. Jamieson, personal communication, 1984). This is the oldest age yet obtained from the Cape Breton Highlands.

The leucotonalite is a medium to coarse grained white rock with scattered mafic minerals. It consists of plagioclase (oligoclase-andesine) and quartz (up to 30%), with minor chloritized biotite and possibly amphibole. It is everywhere cataclased to mylonitized, especially near the faulted margins. In its northern part, the leucotonalite is more "gneissic" in appearance, with abundant biotite/chlorite and minor blue-green amphibole forming bands around plagioclase augen.

The North Branch Baddeck River leucotonalite is similar to leucotonalite in the Mabou Highlands (Barr and Macdonald, 1983) and has similarities to anorthosite bodies in the northern Highlands (Smith and Macdonald, 1983).

Gisborne Flowage quartz diorite (unit 2). The Gisborne Flowage quartz diorite was largely defined during mapping in the area north of the present map area and was described by Raeside et al. (1984). It extends only a few kilometres south into the present map area, where it wedges out within the Ingonish River metasedimentary unit. The age is not known, but the quartz diorite was apparently emplaced during the development of S_2 schistosity in the host rocks.

In the field the Gisborne Flowage quartz diorite is characterized by a distinctly "micaceous" appearance compared to other dioritic units and by the presence of numerous dykes of foliated grey granodiorite and granite pegmatite, as well as amphibolitic streaks, layers, and patches (xenoliths). The quartz diorite is medium grained, with a strong foliation, and consists of plagioclase (andesine), hornblende, and biotite, with minor (5-10%) quartz. Apatite and sphene are exceptionally abundant accessory minerals.

Wreck Cove Brook dioritic complex (unit 3). The Wreck Cove Brook dioritic complex extends into the eastern part of the present map area from the north (Raeside et al., 1984). Because of the inaccessibility of the area, this southern extension is not well mapped, and the relationship of the Wreck Cove Brook dioritic complex to the Barachois River "gneiss" is not known. The dioritic complex was intruded on the east by large granite and granodiorite bodies of Late Hadrynian and Siluro-Ordovician(?) ages and on the west by the Ingonish River Tonalite (Fig. 13.1). The dioritic complex is considered to be Late Hadrynian in age on the basis of an $^{40}Ar-^{39}Ar$ date of 560 Ma for hornblende from a pegmatite area (P.H. Reynolds, personal communication, 1984).

The dioritic complex consists primarily of medium grained quartz diorite but ranges even within a single outcrop, from diorite to granodiorite, from fine to coarse grained, and from equigranular to porphyritic or pegmatoid. Foliation is variably developed and generally trends northeast. The complex includes abundant amphibolitic screens and a variety of dyke rocks, including diorite (unit 22), Cape Smoky granite (unit 13), Birch Plain granite (unit 4), and diabase.

St. Ann's Harbour-Wreck Cove suite (units 4-7). The eastern part of the map area is divided into (inferred intrusive sequence from oldest to youngest) Birch Plain granite, Indian Brook granodiorite, St. Ann's leucogranite, and Murray Mountain quartz monzodiorite. The intrusive sequence is based primarily on observations of granitoid xenolithic material. The Late Hadrynian to Early Cambrian age is based on an Rb-Sr whole-rock isochron age of 517 ± 20 Ma for the St. Ann's leucogranite reported by Cormier (1979). The isochron also included one sample of the Indian Brook granodiorite, which is presumably similar in age but somewhat older. Overall similarity of these units to Late Hadrynian granitoid rocks to the south of St. Ann's Harbour supports the age interpretation. Near its western margin the Indian Brook granodiorite contains abundant xenoliths of the adjacent Barachois River gneiss, an indication of a Late Hadrynian or older age for the latter unit. The Price Point volcanic-sedimentary unit was also intruded by the granitoid rocks, based on local chilling of the Indian Brook granodioroite and apophyses of chilled granodiorite within the volcanic rocks adjacent to the contact, as well as the development of greenschist facies metamorphism in the Price Point unit.

Within the large map units of the St. Ann's Harbour-Wreck Cove belt, some variation in petrologic features is apparent, and more detailed studies of samples may result in further subdivision of the units. Petrological features of these units in the southeastern corner of the map area were previously described by Barr et al. (1982) as the St. Ann's Mountain pluton. Economic features of this area are described by Macdonald and Barr (1985).

The Birch Plain granite (unit 4) is medium grained, pink to red, with less than about 10% mafic minerals. It consists of microcline, plagioclase (oligoclase), quartz and biotite. Locally the granite is porphyritic, with microcline phenocrysts up to 3-4 cm in length. Amphibole is characteristically absent. Abundant large subhedral grains of

sphene are a prominent feature, and other accessory minerals (zircon, allanite) are common. The rocks are variably foliated and deformed. Sericite, epidote, and chlorite are abundant secondary minerals.

The Indian Brook granodiorite (unit 5) is also medium grained and pink to red, but contains 10-30% mafic minerals. It varies in both potassium feldspar and mafic mineral content, and is locally a granite. However, it differs from the Birch Plain granite in the characteristic presence of hornblende, which is typically more abundant than biotite. Foliation, deformation, alteration, and accessory minerals are similar to those in the Birch Plain granite. The Indian Brook granodiorite was not identified as a separate unit by Barr et al. (1982), and was included in part of the leucogranite and in part as separate bodies of hornblende-biotite granite and granodiorite.

The St. Ann's leucogranite (unit 6) is a distinctive medium to coarse grained pink rock containing only 1 or 2% mafic minerals (chloritized biotite). Essential minerals are plagioclase (albite-oligoclase), orthoclase(?) perthite, and quartz. Locally aplitic bodies are present within the leucogranite.

The Murray Mountain quartz monzodiorite (unit 7) forms the central part of the Murray Mountain peninsula (Fig. 13.1) and was largely mapped as hornblende granodiorite, quartz monzodiorite, quartz diorite, tonalite, and their altered equivalents by Barr et al. (1982). This reflects the variation in quartz and alkali feldspar content of the unit, which differs from the previously described units in its more mafic character. It appears to be the youngest unit, intruding both the Birch Plain granite and the Indian Brook granodiorite, but an upper age limit is not defined.

Goose Cove Brook-Beinn Breagh suite (unit 8). The belt of granitoid rocks extending south from approximately Goose Cove Brook is inferred to be similar in age to the St. Ann's Harbour-Wreck Cove suite largely because of the presence of slivers of leucogranite at the eastern margin of the belt. The leucogranite, however, is separated by the heterogeneous Barachois River gneiss from the Goose Cove Brook-Beinn Breagh granitoid rocks. In the south the Barachois River unit is largely metawacke, similar to that generally designated as George River Group farther to the south. The granitoid rocks intruded both this unit and probable George River Group correlatives to the west (Fig. 13.1). Their relation to the Timber Lake quartz diorite to the north is not known.

The Goose Cove Brook-Beinn Breagh suite appears, on the basis of limited sampling due largely to poor exposure, to consist of related but varied granodioritic rocks. They are more foliated in the north than in the south, but in all show strong deformational effects and recrystallization. Essential minerals are quartz (generally in interstitial masses of mosaic grains), microcline (also interstitial), plagioclase (large subhedral sericitized grains), and both hornblende and biotite. A characterisitc feature is the presence of large subhedral to euhedral grains of sphene, similar in size to the major minerals.

Late Hadrynian or younger units

Large bodies of dioritic rocks form much of the central and western map area, separated by metasedimentary rocks (Fig. 13.1). In places the metasedimentary septum consists only of a ridge of quartzite 2 km in width.

The western unit is termed the Kathy Road quartz diorite and is the most extensive unit in the map area. Although a varied unit, it is less heterogeneous on the outcrop scale than the Wreck Cove Brook dioritic suite. It consists mostly of medium to coarse grained quartz diorite, grading to diorite, tonalite and rarely hornblendite.

Amphibolitic bands are locally abundant, and large inclusions of gneissic or schistose rocks, some of mappable dimensions, are scattered through the body.

The dioritic rocks consist mainly of hornblende and plagioclase (andesine) in approximately equal abundance but locally more melanocratic and leucocratic variants are developed. Quartz averages 5-10% of the rock, and is interstitial to the major minerals. Biotite is rare or absent, in contrast to the Gisborne Flowage quartz diorite previously described. Pyroxene is also absent, and the main accessory minerals are apatite, sphene and opaque minerals, the latter two showing an obvious inverse correlation in their abundances. Epidote and sericite are the most abundant secondary minerals. Foliation is generally absent to moderate, but locally, especially near the western margin, is very strong. These samples are characterized by a "gneissic" appearance and elongate hornblende and plagioclase.

The Timber Lake quartz diorite (unit 10) to the east is petrographically similar to the Kathy Road body as described above, and the two units may be correlative.

The age of these dioritic rocks is largely speculative as contacts with other igneous units were not observed. Hornblende from the Kathy Road diorite has given Devonian $^{40}Ar-^{39}Ar$ ages but their significance is not clear (R.A. Jamieson, personal communication, 1984). Both units are intruded by inferred Devonian plutons (Fig. 13.1), and the Timber Lake body is probably also intruded by the Ingonish River tonalite of Ordovician (?) age. It may be an extension of the Wreck Cove Brook dioritic suite (Late Hadrynian) but is much less varied in composition and texture.

Siluro-Ordovician (?) units

Ingonish River Tonalite (unit 11). The Ingonish River tonalite extends from the Ingonish River area (Raeside et al., 1984) south into the central part of the present map area. It is a distinctive medium to coarse grained grey rock consisting primarily of plagioclase, hornblende and quartz. The proportion of hornblende varies so that in some areas the rock appears more leucocratic, but K-feldspar is characteristically absent. Foliation is well developed (although difficult to see in some coarse grained or leucocratic variants) and generally trends north to northeast.

Near its southern margin where it is intruded by the Cross Mountain granodiorite, the tonalite contains abundant biotite and microcline and locally grades to granodiorite, although retaining the characteristic "spotted" appearance. Near the western contact with the East Branch Indian Brook pegmatitic granite, no microcline is present, but the amphibole has apparently been replaced by masses of biotite flakes.

The Ingonish River tonalite is inferred to be Ordovician based on five whole-rock K-Ar ages which ranged from 485 to 420 Ma (A. Hayatsu, personal communication, 1984). These ages are similar to that of the Cape Smoky pluton, bodies of which have locally intruded the tonalite near its western margin (Raeside et al., 1984).

Cape Smoky pluton and Morrison Brook quartz monzonite (units 12 and 13). The Cape Smoky pluton is located for the most part north of the present map area, separated from the Birch Plain granite to the south by the small Morrison Brook quartz monzonite body (Fig. 13.1). The pluton consists of distinctive pink to red biotite granite to leucogranite. The petrology was described by Barr et al. (1979, 1982), although the presence in the south of a separate granite (now called the Birch Plain granite) was not recognized. The Cape Smoky granite contains significantly less biotite and consistently differs in texture (coarser grained, unfoliated) from the Birch Plain granite.

The Morrison Brook quartz monzonite is one of several small plutons peripheral to the Cape Smoky pluton, which are assumed to be of similar age (Raeside et al., 1984). The Morrison Brook quartz monzonite is chilled against the Birch Plain granite to the south.

The Cape Smoky pluton was originally dated by Cormier (1972) who reported a Rb-Sr isochron age of 453 ± 42 Ma (as recalculated by Keppie and Smith, 1978). It was redated by Cormier (1980), using new samples collected during the study by Barr et al. (1979), who obtained an identical age of 447 ± 37 Ma. Thus the Cape Smoky pluton and related plutons (and possibly the Ingonish River tonalite) may be evidence of an Ordovician thermal event in the Cape Breton Highlands.

Devonian units

An important result of the mapping in the central and eastern Cape Breton Highlands has been the recognition of numerous Devonian and Devono-Carboniferous plutons (Jamieson and Craw, 1983; Raeside et al., 1984; French and Barr, 1984).

The West Branch North River granite (unit 14) extends from the south and east into the present map area. It is a distinctive unfoliated medium to coarse grained pink to red syenogranite composed of microcline, albite-oligoclase, quartz, and very minor biotite. It has yielded an Rb-Sr isochron age of 401 ± 13 Ma (Jamieson and Craw, 1983).

A belt of predominantly muscovite-bearing plutons extends through the central part of the map area (Fig. 13.1). This belt continues north of the present map area through the Clyburn Brook pluton (Raeside et al., 1984) to the Warren Brook, Black Brook, and White Point plutons (Wiebe, 1975; Barr et al., 1982). The White Point pluton consists primarily of muscovite-biotite granite and granodiorite and has given an Rb-Sr isochron age of 386 ± 1 Ma (R.F. Cormier, personal communication, 1981). Associated pegmatites have yielded an age of 365 ± 12 Ma (Cormier, 1972; Keppie and Smith, 1978). It seems probable that all of the muscovite-bearing and associated plutons and dykes in this belt are also Devonian in age.

The Baddeck River granodiorite (unit 15) is characterized by abundant muscovite (up to 4%) and lessor amounts of biotite. It is generally medium grained, foliated, and white in colour. Relative amounts of microcline and oligoclase vary so the composition ranges from granite to granodiorite to leucotonalite. Myremekite is abundant in granitic varieties. Abundant accessory minerals include garnet, apatite, allanite, sphene, monazite, and zircon. Secondary minerals are sericite (predominantly in plagioclase), chlorite, and epidote. Evidence of deformation is ubiquitous, including bent twinning and cleavage in feldspars and micas, respectively, and development of undulatory extinction, subgrain boundaries, and granoblastic textures in quartz.

The Snake Cat Lake granodiorite (unit 16) appears to have a gradational relationship with the Baddeck River granodiorite, and the two units have in common most of the petrographic features described above. However, in the Snake Cat Lake body, biotite is more abundant than muscovite, and quartz forms prominent phenocrystic patches.

The New Glen megacrystic granite (unit 17) is gradational with the above two associated muscovite-bearing units, but lacks muscovite and contains large phenocrysts of microcline perthite.

Farther to the north, the North River Canyon granodiorite (unit 18) and Cross Mountain granite/leucotonalite (unit 20) are also typically muscovite-bearing.

Mineralogically they are similar to the Baddeck River unit, with variable amounts of microcline, sodic plagioclase, and biotite. The Cross Mountain body appears to be largely granite in the north and leucotonalite in the south.

The East Branch Indian Brook pegmatitic granite (unit 21) consists of large (up to 10 cm) grains of albite, microcline, quartz, muscovite, and biotite. Similar pegmatite occurs as dykes in the rock units to the north.

Devonian or younger units

Microdiorite and mafic dykes (unit 22). Dykes of fine grained diorite are common in the map area and were observed in most units. The majority are too small (1 to 3 m in width) to be shown on the scale of Figure 1, but several exceptionally large dykes were mapped on Indian Brook and Barachois River. They consist almost entirely of plagioclase and hornblende, and display a distinctive equigranular appearance except in chilled margins. Some have been mistakenly mapped as diorite plutons (e.g. Barr et al., 1982).

Mafic dykes are also numerous in the map area, but none are large enough to show on the scale of Figure 13.1. They may be of several different ages, but some are likely to be Devono-Carboniferous in age and related to mafic volcanism of the Fisset Brook Formation (Kelly and Mackasey, 1985).

Stratified units

Ingonish River metasedimentary unit (unit A)

Stratified rocks occur as keels and septa between many of the plutons. The most continuous unit is the Ingonish River metasedimentary unit, which continues into the map area from the north (Raeside et al., 1984). The unit is predominantly semipelitic to pelitic in composition with common metabasic layers, but it can be separated into five divisions by two lithologically distinct marker horizons, the marble division and the quartzite division (Fig. 13.2). It is not possible to estimate the true stratigraphic thickness of the division because of the extensive deformation although at least 4000 m can be measured.

The lower clastic division is at least 800 m thick and outcrops in the south, where metamorphic grade is in the greenschist facies, and in the central portion of the map area, at sillimanite grade conditions. It consists of a series of semipelitic phyllites and slated at the bottom and pelitic slates and phyllites interbedded with psammitic rocks at the top. Mafic rocks occur sporadically throughout the unit but are not laterally persistent. Small outcrops of calcsilicate rocks were observed in Barachois River in an area previously mapped as marble (Murray, 1977; Keppie, 1979) and in Goose Cove Brook (Milligan, 1970). Overlying the lower clastic division is the quartzite division which provides a prominent marker horizon across the southeastern Highlands. It occurs as a narrow ridge 30 km long and up to 1.5 km wide, but tapers both to the north and south. It is the only division which is continuous across the southeastern portion of the Highlands. The rock is typically a monotonous medium grained quartzite, but there are feldspathic quartzite and metabasic layers incorporated in it.

The middle clastic division is the most extensive division of the Ingonish River metasedimentary unit, and is up to 2 km thick. In the south at lower metamorphic grade it occurs as interbedded semipelitic schists and phyllites. It is cut off by the Kathy Road diorite in the North River area and to the north it occurs as semipelitic schist, typically migmatized, and commonly containing garnet, biotite, sillimanite ± staurolite. More pelitic and psammitic layers can also be recognized. Some metabasic layers locally

Figure 13.2. *Schematic stratigraphic section of the Ingonish River metasedimentary unit in the southeastern Cape Breton Highlands. The width of the column is a general indication of grain size.*

provide useful marker horizons although no single mafic layer has been traced throughout the outcrop area of the middle clastic division.

The upper two divisions – the marble division and the upper clastic division – were described by Raeside et al., (1984). No new outcrops of these divisions were encountered in the southeastern Highlands and as a result of drawdown of McMillian Lake the inferred outcrop area of these divisions has been reduced.

The rocks of the Ingonish River metasedimentary unit have been folded into a large syncline whose axial plane is oriented in a southwesterly direction near McMillian Lake, but swings to the south over most of the map area. Small scale lineations, for example fold hinges, are abundant in the psammitic rocks of the Ingonish River metasedimentary unit. In the McMillian Lake area, these plunge gently (10 to 30°) to the southwest, but in the remainder of the area they plunge very steeply (75 to 90°) to the south. This feature is ubiquitous throughout the unit and implies that the large gently plunging syncline observed in the north changes orientation into an extensive neutral fold in the south, of which only the east limb is now preserved.

Previous maps of the southeastern Highlands have shown much of the area underlain by rocks of the Ingonish River metasedimentary unit as George River Group. The use

of the term George River Group by Murray (1977) and Keppie (1979) follows that of Milligan (1970) who described the carbonate and siliciclastic rocks of the area south of Goose Cove Brook and considered them equivalent to the extensive Precambrian carbonate and quartzitic units elsewhere on Cape Breton Island. However, the stratified rocks of the southern Highlands can be better correlated to the Ingonish River metasedimentary unit, which lacks extensive carbonate and quartzitic sequences. The marble and quartzite, which does occur in the unit, is relatively much less abundant than in the George River Group of southern and central Cape Breton Island. It appears, therefore, that correlation between the George River Group and the Ingonish River metasedimentary unit is tenuous and that, at best, the Ingonish River metasedimentary unit must represent a deeper water, more argillaceous equivalent to the George River Group.

Barachois River gneiss (unit B)

A series of areas of outcrop of gneissic rocks exists in the predominantly plutonic eastern half of the map area. North of Goose Cove Brook these gneisses are typically dark grey K-feldspar augen gneisses, but more psammitic and some amphibolitic varieties have been noted. From Goose Cove Brook metamorphic grade decreases to the south, through a zone of sillimanite schists, garnet phyllites and biotite siltstones. The equivalent rocks exposed in the Big Hill inlier are lightly metamorphosed greywackes, presumably correlative with the greywackes exposed in the southern end of the Kelly's Mountain block (Barr et al., 1982). To the north, the Barachois River gneiss outcrops in the Ingonish Beach area (Raeside et al., 1984 – unit 7, pre-Ordovician felsic gneiss) and is probably equivalent to the coastal gneisses exposed around the White Point Pluton (Wiebe, 1972).

Price Point volcanic-sedimentary unit (unit C)

In the St. Ann's Harbour area, volcanic rocks of the Price Point volcanic-sedimentary unit consist primarily of andesitic to dacitic crystal-lithic tuffs. Minor flows of andesitic to dacitic composition occur in the western part of the unit. All have been metamorphosed to greenschist facies. Although previously considered to be correlative with the Fisset Brook Formation (Kelley, 1960; Keppie, 1979) these volcanic rocks are intruded by the Indian Brook granodiorite of probable Late Hadrynian age, and hence are interpreted to be Late Hadrynian.

The relative ages of each of these stratified units and those of the undifferentiated metamorphic rocks of the central Highlands (unit D) are unknown. In all cases the stratified units are bordered by intrusions, faults and unconformities. Similarly, the age of metamorphism and deformation is not defined. The trends of foliation exhibited by the Early Paleozoic and Precambrian plutons are generally parallel to those in the stratified units. Some of the Devonian plutons also show similar trends of foliation. It is therefore probable that some component of metamorphism and deformation was associated with the Acadian Orogeny. However, the west limb of the large syncline developed in rocks of the Ingonish River metasedimentary unit south of McMillan Lake has been removed by the intrusion of the Kathy Road quartz diorite, of presumed Late Hadrynian age, implying a Hadrynian or earlier age for the development of this fold. It appears, therefore, that broadly coaxial deformation has occurred at various times in the Late Hadrynian and Early Paleozoic.

References

Barr, S.M. and Macdonald, A.S.
1983: Geology of the Mabou Highlands, western Cape Breton Island, Nova Scotia; Geological Association of Canada, Programs with abstracts, v. 8, p. A5.

Barr, S.M., O'Reilly, G.A., and O'Beirne, A.M.
1979: Geochemistry of granitoid plutons of Cape Breton Island; Nova Scotia Department of Mines and Energy, Report 79-1, p. 109-141.

1982: Geology and geochemistry of selected granitoid plutons of Cape Breton Island; Nova Scotia Department of Mines and Energy, Paper 82-1, 176 p.

Bell, W.A. and Goranson, E.A.
1938: Bras d'Or sheet; Department of Mines and Resources, Map 359A.

Cormier, R.F.
1972: Radiometric ages of granitic rocks, Cape Breton Island, Nova Scotia; Canadian Journal of Earth Sciences, v. 9, p. 1074-1085.

1979: Rubidium/strontium isochron ages of Nova Scotian granitoid plutons; Nova Scotia Department of Mines, Mineral Resources Division, Report of Activities, Report 79-1, p. 143-147.

1980: New rubidium/strontium ages in Nova Scotia; Nova Scotia Department of Mines, Mineral Resources Division, Report of Activities, Report 80-1, p. 223-234.

French, V.A. and Barr, S.M.
1984: Age and petrology of the Gillanders Mountain Intrusive Complex, Lake Ainslie area, Cape Breton Island, Nova Scotia; Geological Association of Canada, Programs with Abstracts, v. 9, p. 63.

Jamieson, R.A. and Craw, D.
1983: Reconnaissance mapping of the southern Cape Breton Highlands – a preliminary report; in Current Research, Part A; Geological Survey of Canada, Paper 83-1A, p. 263-268.

Jamieson, R.A. and Doucet, P.
1983: The Middle River – Crowdis Mountain area, southern Cape Breton Highlands; in Current Research, Part A. Geological Survey of Canada, Paper 83-1A, p. 269-276.

Kelley, D.G.
1957: Baddeck, Nova Scotia; Geological Survey of Canada, Map 14-1956.

1960: St. Ann's, Nova Scotia; Geological Survey of Canada, Map 38-1960.

Kelley, D.M. and Mackasey, W.O.
1965: Basal Mississippian volcanic rocks in Cape Breton Island, Nova Scotia; Geological Survey of Canada, Paper 64-34, 10 p.

Keppie, J.D.
1979: Geological map of the Province of Nova Scotia; Nova Scotia Department of Mines and Energy, scale 1:500 000.

Keppie, J.D. and Smith, P.K.
1978: Compilation of isotopic age data of Nova Scotia; Nova Scotia Department of Mines, Report 78-4, 54 p.

Macdonald, A.S. and Barr, S.M.
1985: Geology and age of polymetallic mineral occurrences in volcanic and granitoid rocks, St. Ann's area, Cape Breton Island, Nova Scotia; in Current Research, Part B, Geological Survey of Canada, Paper 85-1B.

McLaren, A.S.
1956a: Cheticamp River; Geological Survey of Canada, Preliminary Map 55-36.

1956b: Ingonish; Geological Survey of Canada, Preliminary Map 55-35.

Milligan, G.C.
1970: Geology of the George River Series, Cape Breton; Nova Scotia Department of Mines and Energy, Memoir 7, 111 p.

Murray, D.L.
1977: The structural relationship between rocks of the George River and Fourchu Groups in the Ingonish River-Clyburn Brook area, Cape Breton Island, Nova Scotia; unpublished M.Sc. thesis, Queen's University, Kingston, Ontario, 271 p.

Raeside, R.P., Barr, S.M., and Jong, W.
1984: Geology of the Ingonish River-Wreck Cove area, Cape Breton Island, Nova Scotia; Nova Scotia Department of Mines and Energy, Report 84-1, p. 249-258.

Smith, P.K. and Macdonald, A.S.
1983: The geology of the Red River Anorthosite Complex, Inverness and Victoria Countries, Nova Scotia; Nova Scotia Department of Mines, Paper 83-1.

Wiebe, R.A.
1972: Igneous and tectonic events in northeastern Cape Breton Island, Nova Scotia; Canadian Journal of Earth Sciences, v. 9, p. 1262-1277.

1975: Origin and emplacement of Acadian granitic rocks, northern Cape Breton Island; Canadian Journal of Earth Sciences, v. 12, p. 252-262.

,

Preliminary report on the stratigraphy and sedimentology of the Huronian Bar River Formation, Ontario

D. Jean Wright[1]
Precambrian Geology Division

Abstract

The Bar River Formation is the uppermost preserved unit of the Huronian Cobalt Group. Near Bay Finn it can be subdivided into four members: 1) a basal laminated quartzite, 2) crossbedded quartzite, 3) quartzite and hematitic quartzite, and 4) interbedded quartzite, sandstone and siltstone. Members 1 and 4 are missing in the Flack Lake section.

Features indicating bimodal or multimodal paleocurrents are present throughout the formation in the form of herringbone crossbed sets, reactivation surfaces and multidirectional ripple crests. Desiccation cracks occur in the Flack Lake area. Paleocurrent measurements indicate predominantly northeastward sand transport in the Bay Finn area, and southerly transport in the Flack Lake area.

A preliminary interpretation is that the sediments of the Bar River Formation were deposited in a shallow marine environment by repeated buildup of sandy shoals across a shallow platform.

Résumé

La formation de Bar River est la plus haute unité conservée du groupe huronien de Cobalt. Près de la baie Finn, elle se subdivise en quatre niveaux: 1) un quartzite feuilleté à la base; 2) un quartzite à stratification oblique; 3) un quartzite et un quartzite à hématite et, 4) un niveau composé de quartzite, de grès et d'aleurolite interstratifiés. Les niveaux 1 et 4 sont absents dans la section du lac Flack.

Des marques présentes partout dans la formation témoignent de la nature bimodale ou multimodale des paléocourants; il s'agit de couches obliques en chevrons, de surfaces de réactivation et de crêtes de rides multidirectionnelles. On a observé la présence de fentes de dessication dans la région du lac Flack. Les mesures des paléocourants révèlent que le transport du sable se faisait surtout vers le nord-est dans la région de la baie Finn, et vers le sud dans la région du lac Flack.

L'interprétation provisoire des données suggère que les sédiments de la formation de Bar River se sont déposés dans un milieu marin peu profond à la suite de l'accumulation répétée de bancs sableux sur une plate-forme peu profonde.

---

[1] Department of Geology, University of Ottawa, Ottawa, Ontario K1N 6N5

Introduction

The Bar River Formation, which comprises mainly quartzites, is the uppermost preserved unit in the Cobalt Group of the Huronian Supergroup. Several authors have described it in regional reports, including Frarey (1977), Frarey and Cannon (1968), Wood (1975), Siemiatkowska (1978), Card (1976, 1978), and Card et al. (1978). It has been examined in more detail by Wood (1970) in the Flack Lake area, and by Card (1978) in the Bay Finn area, but there has never been a study of the formation covering all main areas of exposure.

Recent interest in apparently stratabound copper mineralization in the Cobalt Group (Chandler, 1984) has drawn attention to the need to understand the sedimentology of these rocks. The Bar River Formation, like many Huronian units, has been subject to several environmental interpretations. Frarey (1977) has suggested a fluvial origin for the unit. Wood (1970, 1976) favoured shoreline deposition with eolian influence, Card (1976, 1978) preferred a general marine shelf interpretation and a tidal marine regime with emergent sand shoals was suggested by Chandler (1984). Some of this conflict may be due to the fact that these authors worked on widely separated exposures of the formation. By examining as much of the unit as possible, this writer hopes to arrive at a model for the sedimentology of the Bar River Formation applicable to all exposures.

The Bar River Formation has been recognized in five locations (Fig. 14.1). Work done to date by this writer consists of stratigraphic and sedimentological examinations of the two most extensive exposures in the Flack Lake area and Bay Finn areas (Fig. 14.2).

Present study

Flack Lake area

In this area some 300-400 m of almost flat-lying Bar River quartzites remain. The lower contact with the Gordon Lake Formation is sharp but conformable, and the upper boundary is a modern erosion surface partially overlain by unconsolidated Cenozoic material (Wood, 1975; Siemiatkowska, 1978).

The formation is divisible into lower and upper intergradational members, based on lithology, bedding thickness and the abundance of sedimentary structures (Fig. 14.3). The lower member, (Siemiatkowska's (1978) lower massive orthoquartzite) approximately 175 m thick, consists of over 90% white quartzite with occasional thin beds, lenses and drapes of green siltstone. Bedding, where visible, is commonly of medium (10-30 cm) thickness, although some thick beds were observed. Sedimentary structures include parallel lamination with coarse lags and lenses, planar and trough crossbeds commonly with mud chip or rarely, granule lags, herringbone crossbed sets, overturned crossbeds, symmetrical and assymmetrical straight-crested ripples, desiccation and rare syneresis cracks. Planar crossbeds range in size from small to large scale, with those of medium scale being the most common. One isolated channel-like feature was observed on the Highway 639 roadcut near Mississagi Provincial Park. Others may be present, but unrecognized because of the homogeneity of the rocks and their commonly apparently featureless appearance. Pockets of poorly cemented coarse grained quartzite were observed associated with large scale crossbeds.

The upper member of which about 125 m in thickness are preserved, corresponds to Siemiatkowska's (1978) thinly-bedded, well-rippled quartzite and contains only quartzite apart from thin cracked skins of green and brown siltstone. Medium to thin bedding is well developed. Planar and trough crossbeds are common throughout the member and are commonly complexly interbedded. Within these packets, foreset dip azimuths vary by up to 270° and as many as four different orientations can be observed. Ripples are found on most bedding surfaces, with both asymmetrical and symmetrical forms represented. The ripple crests are straight or wavy, and the crest tops may be sharp or rounded. Wavelengths and amplitudes are low, with averages being approximately 3 cm and 0.8 cm respectively. Crests are generally continuous with tuning-fork bifurcations. The crest orientation is quite variable and interference patterns are common. A feature observed in this unit and also reported from the Lorrain and Gordon Lake formations (Frarey, 1977; Young, 1969; Wood, 1975) is the vermicular structure found in some ripple troughs. Despite its fossil-like appearance, it is probably the result of inorganic processes (Young, 1969; Wood, 1975), possibly infilling and disturbance of syneresis cracks.

Paleocurrent data, derived from planar crossbeds, trough crossbeds and ripple crests, indicate a predominantly southward transport direction (Fig. 14.4), somewhat different from Wood's (1970) polymodal interpretation. His interpretation of deposition in a marginal marine environment is not contradicated by these data.

Bay Finn area

Here the most complete section, over 900 m, of Bar River quartzite and siltstone is exposed in the core of the tightly folded Frazer Point Syncline. The lower contact with the Gordon Lake Formation is gradational over about 30 m. In this area the Gordon Lake Formation is made up of interbedded siltstone and greywacke. Through the transition zone the sandstone beds gradually become thicker and more frequent. The lower boundary of the Bar River Formation has been placed at the base of the first thick quartzite bed above which there is only minor siltstone (Card, 1978). The topographic expression of this boundary is commonly a marked increase in slope on passing up into the Bar River Formation. The upper boundary of the Bar River Formation is an angular unconformity, in places overlain by flat-lying Paleozoic strata (Card, 1978).

In the course of regional mapping, Card (1976) subdivided the Bar River Formation into five intergradational units. Here a somewhat modified version of this subdivision

KEY :
1 Flack Lake area (Wood, 1970)
2 Bay Finn area (Card, 1978)
3 Welcome Lake area (D. Long, per. com.)
4 McGiffin Lake area (Card et al, 1973)
5 Gordon Lake area (Frarey, 1977)

Figure 14.1. *Locations of Bar River Formation within the Huronian Belt.*

Figure 14.2. General geology 2a Flack Lake area, 2b Bay Finn area.

LEGEND

Undivided Paleozoic rocks	Bar River Formation
	Gordon Lake Formation
PRECAMBRIAN	Lorrain Formation
Proterozoic	
Undivided granitic rocks	Undivided Huronian rocks
Nipissing Diabase sills	Archean granitic rocks
Huronian Supergroup Cobalt Group	Geology after O.G.S. maps 2360, 2361 and 2419

is used. His two uppermost units have been combined into one and a local breccia unit has been included (Fig. 14.3). This modified division into 4 members in ascending order is as follows:

The laminated quartzite member (1), approximately 90 m thick, consists of fine- to medium-grained quartzite with silty laminae and lenses common near the base; it is white and locally red. Bedding is generally of medium thickness and sedimentary structures include coarse parallel laminae and planar crossbeds. Bedding tops, where visible, are commonly rippled. Laminations appear to dominate, but although exposure is good, lithology and surface texture of outcrops often make distinguishing sedimentary features difficult. The member varies laterally. On the northern limb of the McGregor Bay syncline, planar crossbedding is relatively abundant and interbedded with the laminated units, whereas on the eastern portion of the southern limb structures other than parallel lamination are rare. Near the base of the laminated quartzite member lies a previously unreported breccia lens. This lens, located about 500 m north of the western end of Bay Finn, is approximately 10 m thick and about 40 m long along strike and comprises angular clasts of transition zone and lamianted quartzite in a gritty green matrix. Clasts range in size from 1 cm to at least 10 cm. Although there are numerous faults in the area, the mixture of clast types suggests that this breccia is not of tectonic origin.

The crossbedded quartzite member (2), approximately 180 m thick, is white and locally blue and red. Sedimentary structures, where visible are planar crossbeds of medium scale with rippled bed tops. The colour in this unit is patchy and commonly discordant with sedimentary structures and bedding. Further evidence of the migration of iron-bearing fluids is found in red staining on joint surfaces. Cubic vugs, believed to be impressions of pyrite cubes, were found on joint surfaces at one location.

Figure 14.3. *Correlation of the members of the Far River Formation between the Bay Finn and Flack Lake areas.*

In the 230 m thick quartzite and hematitic quartzite member (3), the black, red, and blue colouring is more extensive and commonly concordant with bedding and sedimentary structures. These quartzites are medium to thinly bedded and sedimentary structures, commonly outlined in hematite, include trough crossbeds and planar crossbeds with herringbone sets and reactivation surfaces. Low wavelength, low amplitude symmetrical and asymmetrical ripples were observed on many bedding surfaces.

The interbedded siltstone, sandstone and quartzite member (4), has a different expression in different parts of the area. In the western portion it is confined to the top 400 m of the section. Typically it is made up of two or more cycles, each beginning with red to bluish, medium to thinly bedded quartzite followed by thinly interbedded fine sandstone and siltstone followed by red to white medium bedded quartzite. These cycles vary in thickness from about 50 to over 200 m, and the thickness of the component units is equally variable. An exceptionally thick (180 m) quartzite component in an upper cycle is Card's (1978) fifth unit. The only difference between this and other quartzite units in the member is thickness. This is not sufficient difference to warrant a separate division. The base of the cycle was observed to be erosional in one location. Other distinct contacts were not observed.

To the east, the silty portions thicken and the member interfingers with members lower in the section (Card, 1978). Sedimentary structures in the quartzites include planar corssbeds with reactivation surfaces and herringbone sets, symmetrical and asymmetrical ripples. The interbedded siltstone and sandstone portions show symmetrical and asymmetrical ripples, starved ripples and rare load structures, and common parallel lamination. Some of the siltstones are very dark in colour and appear to be iron-rich, containing hematite blebs and nodules. Paleocurrent measurements from planar crossbeds and ripple crests throughout the section indicate a polymodal current pattern with a stronger northeast component (Fig. 14.4). This is consistent with Card's (1978) observations and perhaps reflects basin circulation rather than paleoslope direction.

Discussion and conclusions

Similarity in lithology, stratigraphic context, bedding style and thickness and types and associations of sedimentary structures indicate a correlation between the Flack Lake area column and the middle two units in the Bay Finn area (Fig. 14.4). The basal and top members of the Bay Finn area are absent in the Flack Lake area, but the lack of the latter may be due to erosion. The presence of the laminated member and the lack of desiccation features in the Bay Finn area, and the difference in paleocurrent patterns in the two areas indicate differences in sedimentary history. Features indicating opposing and assymetrical currents abound (i.e. reactivation surfaces, herringbone crossbed sets, silty drapes on planar and trough crossbeds). This variability in current direction and strength is unlikely in a fluvial environment, 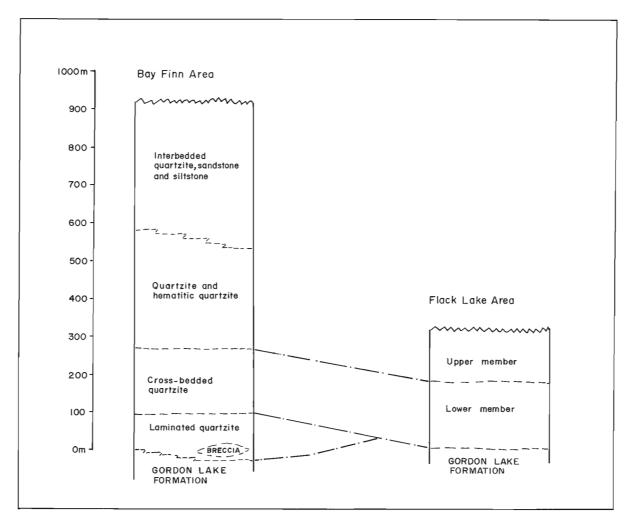and quite typical of a tidally influenced marine regime (Stride, 1982, p. 172). Similar combinations of structures in the lower Carboniferous Kinsale Formation were interpreted by deRaaf et al. (1977) as the result of wave action and wave generated currents on a shallow marine platform.

Wave formed ripples are ubiquitous in both areas. These are recognized as having symmetrical profiles and continuous, parallel crests, with bifurcations. The asymmetrical ripples are also interpreted as wave formed, because crests are also continuous and internal stratification is commonly discordant (deRaaf et al., 1977).

Figure 14.4. *Paleocurrent directions, Bar River Formation, based on measurements of ripples, trough and planar crossbeds.*

Although data collected to date do not lead to a unique interpretation, an environment similar to that suggested by Chandler (1984) and broadly similar to that modelled by deRaaf et al. (1977) shows promise. In deRaaf's (1977) model sandy longshore shoals build up on a muddy substrate. Shoals are built up by wave action and by wave generated currents in a marine environment with a high sediment supply. They are composed of intercalated parallel laminae and cross-bedded sandstones. The shoal may build up to the point of emergence. Where wave energy is lower, or in sheltered environments between shoals or below normal wave base, finer sediments may be deposited. In storm conditions, wave base deepens and laminated and rippled sandstones may be deposited in these locations.

The lower part (members 1 to 3) of the Bar River Formation in the Bay Finn area and the Flack Lake section may represent a higher energy portion of the shoal complex where sediments finer than sand are rarely deposited. The interbedded siltstone-sandstone and quartzite member could represent a deposit where wave energy was not so high. The lower sandy unit of this member would build up to the time when a seaward shoal developed. The seaward shoal would protect the area in its lee, allowing deposition of finer sediments, and would gradually build over it. This would give the quartzite (incipient shoal) sandstone-siltstone (inter-shoal area) and quartzite (shoal) cycles seen in the Bay Finn section. The thickness of the cycles would be dependent on energy conditions and sediment supply, perhaps functions of local geography.

Alternately the Bay Finn section may represent deeper conditions where more of the platform is below wave-base, allowing deposition of finer sediments. In this scenario, the Bar River Formation would be a transgressive sequence.

This interpretation is tentative and may undergo revision depending on the findings of the upcoming field season.

References

Card, K.D.
1976: Geology of the McGregor Bay – Bay of Islands area, Districts of Sudbury and Manitoulin; Ontario Division of Mines, Geoscience Report 138, 63 p.

1978: Geology of the Sudbury-Manitoulin area, Districts of Sudbury and Manitoulin: Ontario Geological Survey, Report 166, 238 p.

Card, K.D., McIlwaine, W.H., and Meyn, H.D.
1973: Geology of the Maple Mountain area, Districts of Timiskaming, Nipissing and Sudbury; Ontario Division of Mines, Geological Report 160, 131 p.

Chandler, F.W.
1984: Sedimentary Setting of an Early Proterozoic copper occurrence in the Cobalt Group, Ontario: a preliminary assessment; in Current Research, Part A, Geological Survey of Canada, Paper 84-1A, p. 185-192.

deRaaf, J.F.M., Boersma, J.R., and van Gelder, A.
1977: Wave-generated structures and sequences from a shallow marine succession, Lower Carboniferous, County Cork, Ireland; Sedimentology, v. 24, p. 451-483.

Frarey, M.J.
1977: Geology of the Huronian Belt between Sault Ste. Marie and Blind River, Ontario: Geological Survey of Canada, Memoir 383, 87 p.

Frarey, M.J. and Cannon, R.T.
1968: Notes to accompany a map of the geology of the Proterozoic rocks of Lake Panache-Collins Inlet map-areas, Ontario (41 I/3, H/4); Geological Survey of Canada, Paper 68-63, 5 p.

Johnson, H.D.
1978: Shallow Siliciclastic Seas: in Sedimentary Environments and Facies, ed. H.G. Reading; Elsevier, p. 207-258.

Siemiatkowska, K.M.
1978: Geology of the Endikai Lake area, District of Algoma; Ontario Geological Survey, Report 178, 79 p.

Stride, A.H.
1982: Offshore tidal sands-processes and deposits; Chapman and Hall, London, New York.

Wood, J.
1970: The Stratigraphy and sedimentation of the upper Huronian rocks in the Rawhide Lake – Flack Lake area, Ontario; unpublished MSc thesis University of Western Ontario, 235 p.

1975: Geology of the Rawhide Lake Area, District of Algoma; Ontario Division of Mines, Geoscience Report 129, 67 p.

Young, G.M.
1969: Inorganic origin of corrugated vermiform structures in the Huronian Gordon Lake Formation near Flack Lake, Ontario; Canadian Journal of Earth Sciences, v. 6, p. 795-799.

Geology and age of polymetallic mineral occurrences in volcanic and granitoid rocks, St. Ann's area, Cape Breton Island, Nova Scotia

EMR Research Agreement Number 269

Alan S. Macdonald[1] and Sandra M. Barr[2]
Economic Geology and Mineralogy Division

Abstract

Sulphide showings in the St. Ann's area include polymetallic quartz-calcite veins and barren pyritic occurrences in both granitoid and older volcanic rocks. The volcanic rocks consist of intermediate lithic-crystal tuffs and flows of calc-alkalic affinity which are probably Late Hadrynian in age as they have been intruded by a Late Hadrynian-Cambrian granitoid suite including granite, granodiorite, leucogranite, and quartz monzodiorite. Cu-Mo-Au-bearing veins are hosted mainly by the granitoid rocks and rarer Cu-Zn-Pb-Ag veins by the volcanic rocks, but both vein types exhibit similar orientations and morphological and textural features, suggesting a common origin. Most veins are located close to the eastern margin of the leucogranite. Muscovite from a vein swarm gave a K-Ar age of 517 $\pm$ 18 Ma, which is essentially the same as the Rb-Sr isochron age of the leucogranite.

Résumé

Les traces de sulfure dans la région de St. Ann's comportent des filons de quartz et de calcite polymétalliques et des venues pyritiques stériles dans des roches granitoides et des roches volcaniques plus anciennes. Les roches volcaniques se composent de tufs à blocs et à cristaux et de coulées calco-alcalines qui datent vraisemblablement de l'Hadrinien supérieur puisqu'ils sont pénétrés par un ensemble granitoïde, dont l'âge se situe entre la fin de l'Hadrinien et le Cambrien, composé de granite, de granodiorite, de leucogranite et de monzodiorite quartzifère. Les filons de Cu-Mo-Au se manifestent surtout dans les roches granitoïdes et les filons de Cu-Zn-Pb-Ag, plus rares, dans les roches volcaniques; toutefois, les orientations et les caractéristiques morphologiques et texturales des deux types de filons sont similaires, phénomène qui semble indiquer que tous les filons partagent une origine commune. La plupart des filons se situent près de la marge est du leucogranite. La datation par la méthode du K-Ar de la muscovite extraite d'un essaim de filons a donné un âge de 517 $\pm$ 18 Ma, essentiellement le même que l'âge établi à la suite de la datation du leucogranite par la méthode du Rb-Sr.

---

[1] R.R. 3 Wolfville, Nova Scotia B0P 1X0
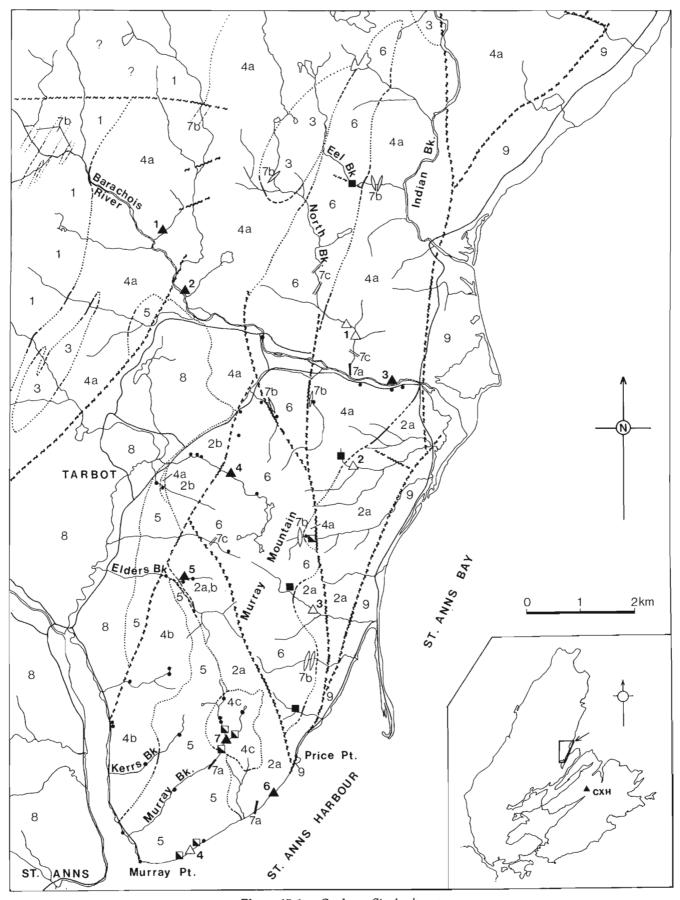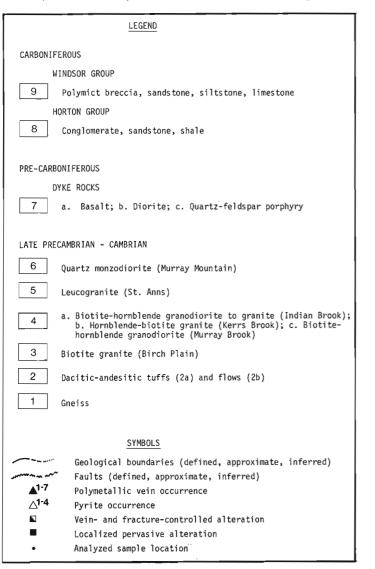[2] Department of Geology, Acadia University, Wolfville, Nova Scotia B0P 1X0

Figure 15.1. Geology, St. Ann's area.

Introduction

As part of regional mapping and petrological studies of granitoid intrusions and their host rocks in Cape Breton Island (Barr et al., 1979, 1982; Barr, 1982), detailed investigations of associated metallic mineral occurrences are also in progress. The Murray Mountain – Barachois River area near St. Ann's was selected for study because of its varied occurrences of vein-type Cu-Mo-Au-Zn-Pb-Ag mineralization hosted by both granitoid and volcanic rocks (Fig. 15.1). Originally of interest for their Au and Ag potential, the veins were first described by Douglas and Campbell (1941). Subsequent exploration focussed mainly on their Cu potential (e.g. Ransom, 1966), resulting in the drilling of the Murray Brook Cu-Mo occurrence, a mineralized quartz-calcite vein swarm in granodiorite displaying some of the characteristics of a porphyry copper deposit (Kirkham and Soregaroli, 1975). The granitoid rocks of the area were mapped and described by Barr et al. (1979, 1982). However, contact relations with the adjacent volcanic rocks, generally assumed to be of Devono-Carboniferous age and correlative with the Fisset Brook Formation (Kelley, 1960; Kelley and Mackasey, 1963; Keppie, 1979) were not established unambiguously.

For the present study, the Murray Mountain – Barachois River area was remapped at a scale of 1:10 000, and the map area was extended north of that described by Barr et al. (1979, 1982). This provided a clearer understanding of the

nature and relative ages of the granitoid units. It was established also that the granitoid rocks intrude the volcanic unit, thus showing that the geological situation is analogous to that at the important Coxheath Hills deposit in southeastern Cape Breton Island (Hollister et al., 1974; Kirkham and Soregaroli, 1975). In addition, veins and associated sulphides were examined and sampled for age determinations and mineralogical and fluid inclusion studies. This report presents preliminary results and conclusions from this project.

Price Point volcanic rocks

Volcanic rocks, herein referred to as the Price Point unit, flank and transect (in a graben-like structure) the granitoid rocks of Murray Mountain (Fig. 15.1). Although most contacts are faults, intrusive contacts are exposed locally with the Indian Brook granodiorite near where the Cabot Trail crosses the Barachois River and with the St. Ann's leucogranite near Price Point. A variety of granitoid dykes occur also in the volcanic rocks.

The volcanic rocks are essentially intermediate in bulk composition and consist mainly of crystal and lithic-crystal tuffs together with less abundant andesitic-dacitic flows. The only mafic rocks present appear to be dykes, of uncertain age but perhaps related to the volcanic package. No sedimentary rocks were observed in the sequence.

All of the volcanic rocks are moderately altered and generally consist of saussuritized feldspar, quartz, chlorite, epidote, actinolite, calcite, sericite, and opaque minerals. Although some locally are cut by quartz-calcite veins and mineralized with sulphides, the pervasive alteration is considered to be of low-grade metamorphic origin. However, no systematic foliation was recognizable in these rocks.

Initial geochemical studies of the andesitic-dacitic flows suggest that they belong to the calc-alkalic series (e.g. Fig. 15.2), and hence were presumably generated in an ensialic magmatic arc environment. More detailed descriptions of the geochemistry and tectonic implications of the volcanic rocks will be reported elsewhere.

Granitoid rocks

Granitoid rocks of the area are divided into six main units, intruded by dykes of diorite, quartz-feldspar porphyry, and aplite (Fig. 15.1). The largest unit is the Indian Brook granodiorite, composed of biotite-hornblende granodiorite gradational to granite, which extends to the north of the present map area (Barr et al., 1985). Towards its western margin, where it has intruded a belt of gneissic rocks (Fig. 15.1), it contains increasingly abundant strongly aligned xenoliths of the gneisses. Bodies of biotite granite which occur within the Indian Brook pluton in the western part of the map area (Fig. 15.1) are inferred to be part of the Birch Plain granite, a major pluton to the north which appears to have been intruded by the Indian Brook granodiorite (Barr et al., 1985).

Two small intrusions in the Murray Mountain area are considered to be related to the Indian Brook granodiorite. Although less mafic than much of the granodiorite, the Kerrs Brook hornblende-biotite granite is considered to be a variant of the Indian Brook unit because of the presence of amphibole, not a feature of the Birch Plain granite. The Murray Brook granodiorite is petrographically similar to the Indian Brook unit but is widely affected by alteration, veining, and mineralization.

The distinctive pink to red St. Anns leucogranite, with associated aplite, occurs in three separate bodies, intruding Indian Brook granodiorite, Kerrs Brook granite, and Murray Brook granodiorite (Fig. 15.1). Farther to the north and east,

---

LEGEND

CARBONIFEROUS

WINDSOR GROUP

9   Polymict breccia, sandstone, siltstone, limestone

HORTON GROUP

8   Conglomerate, sandstone, shale

PRE-CARBONIFEROUS

DYKE ROCKS

7   a. Basalt; b. Diorite; c. Quartz-feldspar porphyry

LATE PRECAMBRIAN - CAMBRIAN

6   Quartz monzodiorite (Murray Mountain)

5   Leucogranite (St. Anns)

4   a. Biotite-hornblende granodiorite to granite (Indian Brook);
     b. Hornblende-biotite granite (Kerrs Brook); c. Biotite-
     hornblende granodiorite (Murray Brook)

3   Biotite granite (Birch Plain)

2   Dacitic-andesitic tuffs (2a) and flows (2b)

1   Gneiss

SYMBOLS

⌒‿⌄⋅⋅   Geological boundaries (defined, approximate, inferred)
⌒⌄⌢⌄⌢   Faults (defined, approximate, inferred)
▲1-7   Polymetallic vein occurrence
△1-4   Pyrite occurrence
◣   Vein- and fracture-controlled alteration
■   Localized pervasive alteration
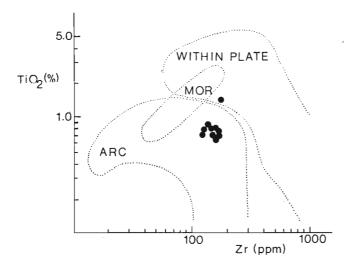•   Analyzed sample location

Figure 15.2. *Geochemical studies of 10 samples of flows indicate andesitic-dacitic compositions of calc-alkalic affinity, shown here by TiO$_2$ vs Zr (from Pearce, 1982).*

the central part of the map area is occupied by the Murray Mountain quartz monzodiorite, a narrow body, elongate north-south, of inhomogeneous fine grained porphyritic to medium grained subporphyritic quartz monzodiorite. This unit is inferred to be the youngest of the main intrusions, as it apparently intruded the Indian Brook granodiorite, and quartz monzodiorite dykes are also present in both the Murray Brook granodiorite and the St. Ann's leucogranite. Average analyses (compiled largely from Barr et al., 1982) for each of the main granitoid units (except the Birch Plain granite for which data are not yet available) are presented in Table 15.1 to illustrate the geochemical character of these rocks. As suggested by the petrographic data, the Kerrs Brook granite is somewhat less mafic than the Indian Brook granodiorite, with higher mean SiO$_2$ content and generally corresponding differences in the other oxides and elements, although K$_2$O and Rb are surprisingly lower in the granite than in the granodiorite. One sample of the granite has anomalously high Pb, Sb, and S values, perhaps reflecting the occurrence of lead mineralization within the body, although none has yet been identified. The Murray Brook granodiorite is similar in SiO$_2$ content and overall chemical character to the Indian Brook granodiorite, but with higher mean Al$_2$O$_3$, Na$_2$O, Cu, and S (although the latter two are largely the result of one anomalous sample), and lower K$_2$O, Ba, Rb, Th, and U. These differences may be related to the alteration and veining which have affected the small Murray Brook body. The St. Ann's leucogranite is a highly felsic unit, with a mean SiO$_2$ content of over 75%. It resembles other leucogranite units of similar age in the region (Barr et al., 1982) and has no obviously anomalous features. The Murray Mountain quartz monzodiorite is a surprisingly mafic unit to occur late in the intrusive sequence. However, it does not appear to display unusual chemical features (Table 15.1 and Barr et al., 1982).

Age relationships

Relative ages of the main lithological units as shown in Figure 15.1 have been reasonably well established on the basis of field relationships. Limited chronological control is provided by two radiometric ages. An Rb-Sr isochron using five samples of St. Ann's leucogranite, one of Indian Brook granodiorite, and one of a quartz-feldspar porphyry dyke has yielded an age of 515 ± 17 Ma (Cormier, 1980; Barr et al., 1982). Considering error limits, this overlaps marginally with the age of 553 ± 25 Ma reported for leucogranite on Kellys Mountain to the southeast (Cormier, 1972; Keppie and Smith, 1978), a unit which is probably correlative with the St. Ann's leucogranite. Hence a Late Hadrynian to Cambrian age seems well established.

In addition, as part of the present study, a K-Ar age of 517 ± 18 Ma (Appendix A) has been obtained for muscovite from a mineralized quartz-calcite vein in the St. Ann's leucogranite on Murray Brook. As similar veins also cut the Murray Mountain quartz monzodiorite, apparently the youngest of the main granitoid units, these radiometric age data suggest that the ages of all the units (except possibly the Birch Plain granite) are Late Hadrynian to Cambrian.

Quartz-calcite veins

Much of the mineralization and related localized alteration observed in the map area (Fig. 15-1) is spatially associated with quartz-calcite veins which occur in both granitoid and volcanic rocks (Table 15.2). Most commonly the veins are simple quartz or quartz-calcite bodies but locally they carry muscovite and (or) K-feldspar and sulphides. Generally the veins are 1 to 5 cm thick, with few attaining thicknesses of more than 20 to 30 cm; their lengths are rarely traceable over more than several metres. Although most are essentially tabular in form, numerous veins exhibit irregularities such as inclusions of wall rock, abrupt bifurcations and terminations, offsets, and locally curviplanar forms. Many appear to have been fractured and recemented by late calcite. The veins commonly occur in clusters or groups of one or, rarely, several distinct orientation(s) but vein densities are low and rarely exceed 1 or 2 per metre of host rock, even in the Murray Brook occurrence where veins are most abundant. The most common orientations are N to NNW, WNW, and W (Fig. 15.3), cutting across the regional NNE structural trend and paralleling some important fault directions (Fig. 15.1). Veins are distinctly more abundant in the granitoid rocks than in the volcanic rocks, but both groups have essentially similar orientations (Fig. 15.3) and morphological features. There are also mineralogical similarities, with both groups of veins containing quartz and calcite ± K-feldspar, pyrite, and chalcopyrite. However, some general differences exist, with muscovite and molybdenite apparently restricted to granitoid-hosted veins and sphalerite and galena more common in volcanic-hosted veins.

Initial fluid inclusion studies of the quartz-calcite veins indicate homogenization temperatures (uncorrected for pressure) in the range 245° to 266°C for rare primary(?) two-phase inclusions. Planar arrays of abundant small secondary inclusions with lower homogenization temperatures reflect the internal deformation displayed by the veins and associated sulphides.

Sulphide mineralization

Sulphide occurrences, although overlapping to some extent in their assemblages (Tables 15.2, 15.3), can be grouped into three main mineralogical types: pyrite, pyrite + chalcopyrite ± molybdenite, and sphalerite + galena ± chalcopyrite ± pyrite.

Most abundant is essentially barren pyritic mineralization which displays varied modes of occurrences (Table 15.3). Although some of this pyrite is clearly associated with quartz-calcite veins and related alteration, it is by no means certain that all of the pyrite occurrences are of the same age.

Figure 15.3. *Vein orientations in St. Ann's study area.*

The pyrite + chalcopyrite ± molybdenite association is found in calcite-bearing quartz veins in granodiorite along the Barachois River and in the more extensively developed vein swarm of Murray Brook which cuts both granodiorite and leucogranite. The sulphides occur mainly within the veins themselves but also to a limited extent within adjacent wall rocks as disseminations and fracture coatings. Pyrite in this assemblage occurs as isolated small grains to coarse grained aggregates which typically have been intensely fractured or shattered, then veined and partially replaced by chalcopyrite. Chalcopyrite has also infilled vugs within vein quartz and occupied late crosscutting quartz-calcite veinlets. Molybdenite is found only as smeared coatings on some fracture surfaces and as rare isolated flakes within quartz veins.

The association sphalerite + galena ± chalcopyrite + pyrite is best developed in quartz-calcite veins cutting volcanic rocks at Price Point and on Elders Brook (Fig. 15.1), but also occurs at the Barret-MacIntosh showing near Barachois River in a calcite-rich vein which is offset by the gold-quartz vein (Telford et al., 1968). Samples from Price Point and Elders Brook are quite similar, both containing fractured pyrite which has been veined and rimmed by sphalerite and chalcopyrite. The chalcopyrite veins and replaces the sphalerite and is also exsolved from it; both are crosscut by late stringers of galena and calcite. Tetrahedrite

Table 15.1. Means and standard deviations for chemical data* from the main granitoid units in the Murray Mountain – Barachois River map area

	Indian Brook Granodiorite (n=6)		Kerrs Brook Granite (n=6)		Murray Brook Granodiorite (n=4)		St. Anns Leucogranite (n=6)		Murray Mountain Qtz Monzodiorite (n=8)	
(%)	$\bar{x}$	s	$\bar{x}$	s	$\bar{x}$	s	$\bar{x}$	s	$\bar{x}$	s
SiO_2	66.7 ± 2.9		68.5 ± 1.4		66.4 ± 1.8		75.2 ± 2.0		57.1 ± 3.2	
TiO_2	0.43	0.16	0.31	0.05	0.25	0.05	0.17	0.04	0.79	0.22
Al_2O_3	14.4	1.6	14.9	0.4	16.0	1.1	11.8	1.0	17.2	1.3
Fe_2O_3	1.7	0.8	1.4	0.5	0.9	0.4	0.7	0.4	3.1	1.0
FeO	2.1	0.4	1.8	0.2	2.1	0.2	0.8	0.2	3.5	1.0
MnO	0.08	0.02	0.09	0.02	0.06	0.02	0.02	0.01	0.14	0.04
MgO	1.4	0.4	1.3	0.2	1.7	0.2	0.3	0.1	3.0	0.9
CaO	3.1	0.7	2.5	0.9	3.0	1.2	1.2	0.1	6.1	1.1
Na_2O	3.2	0.4	3.7	0.3	4.2	0.3	3.5	0.2	3.5	1.4
K_2O	3.9	0.4	3.3	0.2	2.1	0.3	4.5	0.2	2.5	0.4
P_2O_5	0.12	0.03	0.12	0.01	0.10	0.02	0.04	0.01	0.21	0.06
(ppm)										
Ba	525 ± 75		470 ± 77		359 ± 49		435 ± 262		387 ± 123	
Rb	127	10	87	6	51	9	157	32	68	16
Sr	253	107	310	15	218	47	67	56	474	163
F	570	106	486	202	475	101	365	34	605	48
Mo	2.0	0.5	1.8	0.6	1.4	0.3	2.0	0.4	1.8	0.5
Cu	40	42	13	15	110	186	8	5	75	38
Pb	9	5	28	49	4	3	15	4	12	6
Zn	51	12	57	11	45	5	27	11	76	20
S	50	47	77	68	103	132	45	22	88	77
Sn	2.7	0.3	2.2	0.8	1.7	0.7	5.3	2.2	1.9	0.5
W	1	-	1	-	1	1	1	-	1	-
U	2.5	0.6	1.8	0.2	1.1	0.5	3.2	0.4	1.4	0.8
Th	14	4	10	1	5	1	17	2	7	4
Ag	0.1	-	0.2	0.2	0.1	-	0.1	0.1	0.1	-
Sb	0.1	-	1.4	2.5	0.2	0.1	0.3	0.3	0.2	0.2
Bi	0.1	-	0.1	-	0.1	-	0.1	0.1	0.1	-
As	7	4	9	5	8	3	8	3	9	3
Au (ppb)	<10		<10		< 20		<20		<10	

* Major element and most trace element data compiled from the St. Ann's Mountain pluton of Barr et al. (1982), regrouped according to the map units of this study. Th, Ag, Sb, Bi, and Au are from previously unpublished data for these same samples (analyses for Th from Atomic Energy Commission, Ottawa; other elements by Chemex, Vancouver). n = number of samples analyzed.

has been reported from the Price Point occurrence, which apparently does have higher silver content than the Elders Brook showing (Table 15.2), but none was identified during the present study.

Alteration

Alteration observed within the area is of two types: 1) vein- and fracture-controlled alteration, and 2) localized pervasive alteration (Fig. 15.1). Vein- and fracture-controlled alteration usually forms bleached grey halos, 1-5 cm wide, adjacent to some quartz-calcite veins and related "dry" fractures. Rarely the halos reach 20 cm in width. The best developed are found within the St. Ann's leucogranite in an area 0.5-1 km northeast of Murray Point (Fig. 15.1), where several intersecting sets of closely spaced veins and fractures with associated halos create nearly pervasive patchworks of alteration. The altered rock consists of quartz, clay minerals, sericite, calcite, and pyrite.

Table 15.2. Summary data for polymetallic veins, Murray Mountain – Barachois River area

Map No.	Location	Host Rocks	Vein Material	#	Exposed Dimensions	Orientation	Sulphide Mineralogy[1]	Assay Value and Reference
1	Barachois River	granodiorite	quartz[2]	1	40cm x 10m	151/70E	py, cp	0.23oz Au[3] (Douglas and Campbell,
			calcite-quartz	1	10cm x 100m	000/90	sp, gn	- 1941)
2	Barachois River	granodiorite	quartz	6	1cm x 3-5m	015/45W	cp, py, mo, sp, ml	-
3	Barachois River	granodiorite	quartz-calcite	1	30cm x 30m	163/70E	cp, py, bn, cc, ml	0.04oz Au (Douglas and Campbell, 1941)
4	Schoolhouse Brook	quartz monzodiorite	quartz-calcite	2	5cm x 5-6m	174/75E	cp, py, ml	0.03, 0.09oz Au (Douglas and Campbell, 1941)
5	Elders Brook	andesite	quartz-calcite	1	15cm x 8m	013/45E	sp, cp, py, gn	0.47, 0.58oz Ag; trace Au (J. MacDonald, pers. comm.,1984)
6	Price Point	tuff	quartz-calcite	1	2-5cm x 10m	165/90	sp, cp, gn, py,?th	6.02oz Ag, trace Au (J. MacDonald, pers. comm.,1984)
7	Murray Brook	granodiorite leucogranite	quartz-calcite	swarm	1-15cm x 2-5m	e.g. 025/70W 090/65N 125/70N	py, cp, mo	i. 0.19% Cu, 0.027 Mo over 14m (Batchelor, 1967) ii. 0.04% Cu, 0.003 Mo (weighted average for 5 DDH's = 180m (Kervin, 1971)

[1] py = pyrite;   cp = chalcopyite;   bn = bornite;   ml = malachite;   cc = chalcocite;
mo = molybdenite; sp = sphalerite; gn = galena; th = tetrahedrite
[2] Barret-MacIntosh gold-quartz vein
[3] weighted average (oz/ton)

Table 15.3. Modes of occurrence of main pyritic showings, Murray Mountain – Barachois River area

Map No.	Location	Host Rocks	Modes of Occurrence
1	North Brook	granodiorite	Widespread disseminations and rare fracture coatings in relatively unaltered granodiorite
2	NE side, Murray Mtn.	tuff	Localized disseminations and fracture coatings near intrusive granodiorite contact
3	Eel Cove Bk. E side, Murray Mtn.	tuff	Coarse veining/infilling of intensely brecciated zone (>4m x 15m)
4	Murray Point	leucogranite	Disseminations within quartz veins and related alteration zones

Apparently more intense, green alteration halos, 10 to 20 cm in width, are associated with rare large quartz veins in the Indian Brook granodiorite. These halos are rich in chlorite, epidote, and pyrite. On Murray Brook, in the vicinity of the Cu-Mo occurrence, alteration appears as narrow pink selvages fringing many of the veins and related fractures which cut both granodiorite and leucogranite. These selvages consist of narrow zones, up to 3 cm wide, of K-feldspar enrichment within which biotite has apparently remained stable and unaltered. Pervasive reddening of the granitic host rocks between these altered zones is apparently due to hematitization.

Several areas of localized pervasive alteration, not obviously vein- or fracture-controlled, occur in granitoid rocks along the eastern side of Murray Mountain (Fig. 15.1), close to contacts with the volcanic country rocks. The rocks affected include granodiorite and quartz monzodiorite. Although poorly exposed, the alteration covers areas of at least several square metres and, where they can be seen, the limits of the alteration are irregular but relatively sharp. Quartz stringers can be found within these altered areas but they do not appear to control the distribution of the alteration. The altered rocks are pale grey to buff and consist essentially of quartz, clay minerals, and sericite with variable amounts of calcite and pyrite, and hence resemble the most common type of vein- and fracture-controlled alteration.

Another more isolated and different type of localized pervasive alteration occurs in Eel Brook, northwest of Indian Brook (Fig. 15.1) where quartz monzodiorite been strongly carbonatized and sheared over a width of at least 10 m. The rock now consists of calcite, clay minerals, quartz, chlorite, and hematite but apparently lacks any sulphides.

Conclusions

Price Point volcanic rocks in the St. Ann's area have been intruded by a suite of granitoid plutons of probably Late Hadrynian to Cambrian age. Hence the volcanic rocks are probably Late Hadrynian, and their age, combined with calc-alkalic chemical affinity and lack of associated sedimentary rocks, suggests that they are similar to volcanic rocks of the Fourchu Group of southeastern Cape Breton Island (e.g. Macdonald, 1983).

Mineralized quartz-calcite veins cut all of the main granitoid units and, to a lesser extent, the volcanic country rocks. All of these veins have similar geometric, textural, and mineralogical features, thus implying a common origin. Muscovite from one of the veins in the St. Ann's leucogranite has given a K-Ar age of 517 ± 18 Ma and hence may be essentially the same age as the host leucogranite. Most of the veins, with asociated alteration and polymetallic mineralization, are distributed in a zone extending from Murray Point north to Barachois River, paralleling the faulted and discontinuous eastern margin of the leucogranite. Favoured locations for these occurrences appear to be in granodioritic and volcanic rocks within approximately 1 km of the leucogranite, which seems likely to have exercised primary control over distribution of the polymetallic veins. A weaker NNE-trending pattern is also discernible, shown mainly by occurrences of barren pyrite and localized pervasive alteration which are distributed close to contacts between granodiorite or quartz monzodiorite and the volcanic rocks to the east (Fig. 15.1).

The volcano-plutonic environment of the St. Ann's area resembles that of the Coxheath Hills area (Hollister et al., 1974; Kirkham and Soregaroli, 1975) in age, rock types, and mineralization. Thus an environment of Late Hadrynian to Cambrian calc-alkalic magmatism and related "porphyry-type" Cu-Mo mineralization can be extended at least into the southeastern Cape Breton Highlands.

References

Barr, S.M.
1982: Geochemistry of granitoid plutons of Cape Breton Island, Nova Scotia; in Uranium in Granites, ed. Y.T. Maurice; Geological Survey of Canada, Paper 82-23, p. 55-59.

Barr, S.M., O'Reilly, G.A., and O'Beirne, A.M.
1979: Geochemistry of granitoid plutons of Cape Breton Island; Nova Scotia Department of Mines and Energy, Report 79-1, p. 109-141.

1982: Geology and geochemistry of selected granitoid plutons of Cape Breton Island; Nova Scotia Department of Mines and Energy, Paper 82-1, 177 p.

Barr, S.M., Raeside, R.P., and Macdonald, A.S.
1985: Geological mapping of the southeastern Cape Breton Highlands, Nova Scotia; in Current Research, Part B, Geological Survey of Canada, Paper 85-1B, Report 13.

Batchelor, E.W.
1967: Exploration report, Prices Point, Nova Scotia; Nova Scotia Department of Mines and Energy, Assessment report 11K/07A, 13-Q-36(03).

Cormier, R.F.
1972: Radiometric ages of granitic rocks, Cape Breton Island, Nova Scotia; Canadian Journal of Earth Sciences, v. 9, p. 1074-1086.

1980: New rubidium/strontium ages in Nova Scotia; Nova Scotia Department of Mines and Energy, Report 80-1, p. 223-234.

Douglas, G.V. and Campbell, C.O.
1941: Barasois and Indian Brook area; Nova Scotia Department of Mines, Report of Activities, 1940, p. 219-231.

Hollister, V.F., Potter, R.R., and Baker, A.L.
1974: Porphyry-type deposits of the Appalachian Orogen; Economic Geology, v. 69, p. 618-629.

Kelley, D.G.
1960: St. Anns map-area, Nova Scotia; Geological Survey of Canada, Map 38-1960.

Kelley, D.G. and Mackasey, W.O.
1963: Basal Mississippian volcanic rocks in Cape Breton Island, Nova Scotia; Geological Survey of Canada, Paper 64-34, 10 p.

Keppie, J.D.
1979: Geological map of the province of Nova Scotia; Nova Scotia Department of Mines and Energy.

Keppie, J.D. and Smith, P.K.
1978: Compilation of isotopic age data of Nova Scotia; Nova Scotia Department of Mines and Energy, Report 78-4.

Kervin, R.
1971: Prices Point project, Victoria County, Nova Scotia; Nova Scotia Department of Mines and Energy, Assessment report 1K/07A, 13-Q-36(05).

Kirkham, R.V. and Soregaroli, A.E.
1975: Preliminary assessment of porphyry deposits in the Canadian Appalachians; Report of Activities, Part A, Geological Survey of Canada, Paper 75-1A, p. 249-251.

Macdonald, A.S.
1983: Metallogenic studies, southeastern Cape Breton Island, Nova Scotia; Nova Scotia Department of Mines and Energy, Open File Report 527.

Pearce, J.A.
1982: Trace element characteristics of lavas from destructive plate boundaries; in Andesites, ed. R.S. Thorpe, Wiley, p. 525-548.

Ransom, P.
1966: Exploration report, Prices Point property, Nova Scotia; Nova Scotia Department of Mines and Energy, Assessment report 11K/07A, 13-Q-36(02).

Telford, W.M., Hope-Simpson, D., and Riddell, J.E.
1968: Report on geology of Brubec Block 1, Tarbotvale on Barachois River, Victoria County, Cape Breton, Nova Scotia; Nova Scotia Department of Mines and Energy, Assessment report 11K/07A, 13-Q-19(01).

Appendix A K-Ar age data

Material dated: Muscovite concentrate, -80/+200 mesh

Analytical data: ^{40}Ar = 0.2848 ppm

^{40}K = 8.165 ppm

K = 6.693%

Radiogenic ^{40}Ar/Total ^{40}Ar = 0.957

Radiogenic ^{40}Ar/^{40}K = 0.03481

Age = 517 ± 18 Ma

Constants used: λ_B = 4.72 x 10^{-10}/year

λ_e = 0.585 x 10^{-10}/year

^{40}K/K = 1.22 x 10^{-4} g/g

Regional sedimentology of the Namewaminikan Group, northern Ontario: Archean fluvial fans, braided rivers, deltas, and an aquabasin

EMR Research Agreement 176

Jonathan R. Devany [1] and Philip W. Fralick [1]
Precambrian Geology Division

Abstract

The Namewaminikan Group comprises the northern and central metasedimentary belts of the Beardmore-Geraldton Archean terrane of Superior Province. The northern metasedimentary belt is a conglomeratic product of braided rivers and fluvial fans. The central metasedimentary belt preserves well, in a largely homoclinal sequence, a coarsening-upward succession that was produced by a prograding clastic wedge.

The northern and central metasedimentary belts are the proximal and distal halves, respectively, of a once-continuous coarse clastic wedge or sheet. Proximally, this wedge has a basal conglomerate. Distally, fine-grained aquabasinal clastics are capped at different sites by deltaic facies: 1) rhythmically-bedded distributary mouth bar/distal bar couplets; 2) fan-delta slope resedimented conglomerates; and 3) fluvio-deltaic topsets of sandy braided river origin.

The clastic wedge section focussed folding within its least competent finer-grained and thinly bedded units, preferentially located at the base of the section, retaining most of a coarsening-upward, coarser and more competent succession.

Résumé

Le groupe de Namewaminikan forme les zones métasédimentaires nord et centre du terrain archéen de Beardmore et Geraldton de la province du lac Supérieur. La zone métasédimentaire nord est un produit conglomératique de rivières anastomosées et de cônes fluviaux. La zone métasédimentaire du centre a bien conservé, dans une séquence en grande partie monoclinale, une succession à granulométrie croissante vers le haut qui a été produite par un biseau clastique en progression vers la mer.

Les zones métasédimentaires nord et centre sont les moitiés proximale et distale respectivement d'un biseau ou couche clastique à texture grossière auparavant continu. La couche comporte un conglomérat à sa base, dans la partie proximale. Dans la partie distale, des sédiments clastiques à grains fins accumulés dans un bassin aqueux reposent par endroits sous des faciès deltaïques: 1) des couplets de sédiments à stratification rythmique, provenant d'une barre en avant d'une embouchure de rivière et d'une barre distale, 2) des conglomérats sédimentés à nouveau provenant du talus d'un delta et cône de déjection et, 3) des couches sommitales de nature fluvio-deltaïque accumulées dans une rivière sableuse à configuration anastomosée.

Les plis dans la couche clastique se sont formés dans les unités finement stratifiées à grains fins les moins compétentes, qui sont normalement situées à la base de la section. La couche clastique a donc conservé la plus grande partie d'une succession plus grossière et plus compétente, à granulométrie croissante vers le haut.

---

[1] Department of Geology, Lakehead University, Thunder Bay, Ontario P7B 5E1

Introduction

The Beardmore-Geraldton Belt (Fig. 16.1), an Archean metavolcanic-metasedimentary terrane within the Wabigoon Subprovince of Superior Province, lacks many features typical of Archean greenstone belts, such as granitic intrusives, a large-scale diapiric structural style and felsic volcanic centres. These features are present in the Onaman-Tashota area north of the Paint Lake Fault (Mackasey, 1975, 1976), a major structural and lithologic boundary within this part of the Wabigoon Subprovince. South of the Paint Lake Fault and its equivalents, long, linear east-striking belts of metasediments alternate with belts of mafic metavolcanics (Fig. 16.1; Stott, 1984a, b). The relative positions of these belts are thought to be the result of a regional fault or fold system.

The authors restrict the term "Beardmore-Geraldton (Archean) terrane" to the strip of rocks south of the Onaman-Tashota area and the Paint Lake Fault and equivalents, and north of the Quetico Subprovince. Towards Geraldton the nature of the terrane's northern contact changes (Beakhouse, 1982).

Two of the belts present in the Beardmore-Geraldton terrane, the northern metasedimentary belt (NMB) and the central metasedimentary belt (CMB) (Fig. 1; Mackasey, 1975, 1976) are herein designated as comprising the "Namewaminikan Group". This group and its component formations are in the process of being defined by J.R. Devaney (Misc thesis in preparation, Lakehead University). Tanton (1919) named these rocks the "Windigokan series".

During the summer of 1984 the northern and central belts, spanning a 60 km long area (Fig. 16.1; see also Mackasey, 1975, 1976), were mapped at various scales by the senior author. Field work was conducted near Beardmore and Jellicoe, west of Geraldton. Some of this paper's observations and conclusions do not apply to the Geraldton area; for instance, the central metasedimentary belt does not extend that far. Little mapping was done in Irwin Township because of access problems.

Figure 16.1. *Simplified geological map of the Beardmore-Geraldton area, modified from Stott (1984a, b). Upper right inset shows the study area, Dorothea to Colter Townships. NMB: northern metasedimentary belt; CMB: central metasedimentary belt; SMB: southern metasedimentary belt.*

The central metasedimentary belt contains thousands of north-facing stratigraphic top indicators, and only several south-facing sites. This belt also displays a consistent coarsening-north, hence coarsening-upward, pattern over a 34 km lateral extent, and is therefore not at all similar to the usual tightly to isoclinally folded metasedimentary sequences most typicaly of Archean metavolcanic-metasedimentary belts (Condie, 1981; Borradaile, 1982; Kehlenbeck, 1984).

The term "aquabasin" is used by the authors to refer to a lake, sea, or ocean, and implies a distinction from a fluvial basin. Such a term is useful for Precambrian terranes where the distinction between a lake, sea, or ocean is difficult to impossible to make. Also, "aquabasinal" is a useful adjective for describing nonfluvial subaqueously deposited (meta)sediments.

Hereafter the prefix "meta" will be omitted, as these greenschist facies rocks will be treated as a sedimentary rocks.

The northern metasedimentary belt

This belt is composed of massive to crudely bedded clast-supported polymict conglomerate interbedded with a relatively minor amount of sandstone. The conglomerate always contains a wide variety of clast lithologies: felsic (to intermediate) volcanics dominate, with lesser amounts of granitoid, mafic volcanic, felsic porphyry, chert, diorite/gabbro, and quartz clasts. Rare clasts display pre-erosion veining.

The gravel-sized clasts are nearly always oblate spheroids, flattened in the plane of the foliation. Average size of the deformed clasts, measured perpendicular to foliation, is in the 64-16 mm range. Average size of the ten largest clasts at a site varies widely, resulting in cobble-poor, cobble-rich, and bouldery conglomerate. Clast frameworks are poorly to moderately sorted and ungraded.

Crude bedding within the conglomerate is revealed by vaguely to well-defined sand lenses, fine pebble bands, and cobble bands. Sharp erosive bases are common and agree with rare north-topping sedimentary structures within the northern metasedimentary belt.

The interbedded pebbly sandstone and conglomerate matrices are coarse to medium/fine grained, moderately to poorly sorted feldspathic arenites. The strained beds are less than 0.5 m thick, massive or plane laminated, and less commonly planar crossbedded. Pebble bands are usually parallel to bed margins.

Outcrop-scale folds, excepting small kink folds, are very rare and are present mostly in this belt's eastern exposures.

Interpretation

The northern metasedimentary belt is the product of deposition by gravelly braided streams in a fluvial fan and/or braidplain environment. Outcrop-scale stratigraphic sections represent Scott-type profiles (Miall, 1977, 1978), the lithofacies suite being Rust's (1978) G$_{II}$ and the proximal facies of McGowen and Groat (1971), Boothroyd and Ashley (1975), and Boothroyd and Nummedal (1978). Identical Archean lithofacies and interpretations were given by Eriksson (1978) and Hyde (1980) for other Archean conglomeratic sequences. A fluvial fan (wet alluvial fan; Schumm, 1977) depositional paleoenvironmental is likely, considering the lithofacies, their commonly bouldery nature, and the lack of muddy debris flows. Areas of coarse massive conglomerate with little or no interbedded massive sandstone may be the result of sheet-flow fan conditions (process of Ballance, 1984).

Throughout this belt evidence of turbidite processes is totally lacking, except in parts of Irwin Township (Fig. 16.1), where graded wackes are present. These may represent original along-strike and regionally minor facies changes.

Most of the northern metasedimentary belt is next to a regional fault, the Paint Lake Fault. This belt's conglomerate clasts are coarsest and most oblate (elongate in two-dimensional exposures; measured long:short axis ratio) immediately along the Paint Lake Fault in Walters Township (Fig. 16.1). The various lithologies present as clasts within the belt, as well as conglomerate and sandstone similar to this belt (Moorhouse, 1939; Amukun, 1980) to this belt, are exposed within the Onaman-Tashota area's felsic volcanic centre, north of the Paint Lake Fault. The authors envisage fluvial fans being shed southward from the terrain north of such a regional fault, similar to Bruce's (1937) interpretation. Reactivation of this fault and subsequent transcurrent motions (e.g. Mackasey, 1975, p. 32, 34) may account for the deformation of the northern metasedimentary belt's conglomerate and sandstone.

An Archean basal conglomerate

In Legault Township (Fig. 16.1), the contact between the northern metasedimentary belt the mafic volcanic belt to the south is exposed in one small outcrop (Mackasey et al., 1976). The contact is a razor-sharp line on a flat surface. North of the contact mafic boulders, cobbles and pebbles are abundant (up to greater than 50% of the clasts by area) within the conglomerate. The fine grained matrix of the mafic clasts is rich in felsic clasts. In this outcrop the ten largest clasts are all of mafic composition. It is the only outcrop in the entire northern metasedimentary belt in which the ten largest clasts are not granitoids or felsic volcanics, and it is by far the coarsest conglomerate exposed in the belt. Immediately south of the contact the mafic volcanics appear highly strained and veined, as might be expected at such a lithologic contrast in a deformed terrane. About 25 m south of the contact mafic pillow lavas are well-exposed.

The mafic clasts in the outcrop's conglomerate were probably derived from the adjacent mafic volcanic belt. Tops at this site are to the north. The contact is interpreted to be a faulted or sheared unconformity and the outcrop's conglomerate a basal horizon of the northern metasedimentary belt.

The central metasedimentary belt

This belt is 1 to 2 km thick and 43 km long (Fig. 16.1), the easternmost 7 km being either felsic pyroclastics or reworked coarse volcaniclastics. Its homoclinal nature is poorly defined, with strata dipping moderately (40°-50°) to moderately steeply (60°-70°) northward. Mackasey (1975, 1976) mapped the belt's coarsening-north trend. More detailed sedimentological mapping also reveals thousands of north-facing top indicators, and only several south-facing ones.

The coarsening-north trend is surprisingly consistent over a 34 km lateral extent. The central metasedimentary belt's southern third contains mudstone (argillite/slate), sandstone, and ironstone. The middle third is sandstone-rich, with pebble bands, thin conglomerate beds, and very rare mudstone. Conglomerate and sandstone similar to the northern metasedimentary belt comprise the northern third of the central metasedimentary belt.

In Irwin and Walters townships (Fig. 16.1) the coarsening-north pattern is less well displayed. The northern half of the central metasedimentary belt in west Irwin Township contains an assemblage of graded sandstone and mudstone south of the typical conglomerate. Only one small outcrop of a fine grained conglomerate has been found in east Irwin Township. Farther east, in Walters Township, the conglomerate is in the middle of the central metasedimentary belt, fining south to sandstone and then mudstone. North of the conglomerate, graded sandstone (all tops north) is exposed.

Beatty Lake: a section through a prograded clastic wedge

Shoreline exposures at Beatty Lake in Leduc Township (Fig. 16.1, 16.2) offer a relatively well-preserved section through the belt's coarsening-northward sequence of clastic sediments.

The southern third of the central metasedimentary belt is an assemblage of mudstone, graded sandstone, rarely scoured fine grained sandstone, and very minor ironstone. In east central Beatty Lake graded sandstone (tops north) is interbedded with argillaceous matrix-supported conglomerate, graded (tops north) and ungraded clast-supported conglomerate, and plane laminated finer sandstone and siltstone.

Unit A. Figure 16.2 shows the location of units A, B and C. The succession will be described from base (south) to top (north), as defined by facing directions. Lithofacies codes and fluvial profile types are those of Miall (1978).

Near the base of unit A medium- to fine-grained well sorted sandstone is typical. This sandstone tends to be finer where rippled (Sr) and plane laminated (Sh, Fl), and coarser within planar crossbed (Sp) foreset laminae. Flasers and mud chips are also present in these pebble-free beds. About 1 m of section displays bimodal-bipolar ("herringbone") crossbedding, with four paleocurrent reversals.

Upward in the section, planar crossbeds are more common than trough crossbeds (St). The first pebbles that appear are less than 4 cm in size and are concentrated in planar crossbed toesets. Vague pebble bands become more common upward.

The bulk of this lithofacies assemblage is composed of planar crossbedded and Sh coarse/medium- to fine-grained sandstone, with lesser amounts of trough crossbeds and ripples. Pebbles are usually 2-6 cm in size (short axis).

The uppermost level of unit A contains coarse- to fine-grained pebbly sandstone, with pebbles up to 5 cm in size. One location had several 7-12 m clasts. Unit A's coarset fraction, the pebbles, define its coarsening-upward trend.

1. tightly to isoclinally folded (tops N and S) incompetent wackes
2. broad scours in fine grained sandstone (aquabasinal)
3. sandstone turbidites
4. siltstone/slate
5. resedimented conglomerates, sandstone tubidites and laminated sandstone/siltstone
6. bimodal-bipolar crossbedding
7. unit A; crossbedded sandstone assemblage (distal braided river)
8. unit conglomerate-sandstone assemblage (medial braided river)
9. unit C; conglomerate-dominant assemblage (medial braided river)
10. reactivation surface in planar crossbed
11. crudely graded conglomerate bed (bar/channel section)
12. bouldery conglomerate
13. mafic volcanics; and
14. off edge of map

Figure 16.2. Sedimentological highlights of Beatty Lake, west Leduc Township. Unless stated otherwise, stratigraphic tops are to the north. Map after Mackasey (1976).

Unit's A well-exposed crossbeds, mostly planar sets, give 73% (77 of 106) to the west to southwest. This agrees well with a correlative lithofacies assemblage 4.8 km to the east, where planar crossbedded and plane laminated coarse-to-medium-grained, moderately sorted sandstone has paleocurrents towards the west only. At this locality pebble bands are both horizontal and inclined, the former being gradational to thin conglomerate beds, and the latter defining foresets and toesets.

Unit B. The overlying lithofacies assemblage is composed of conglomerate and sandstone. Sections 4.8 m to 22.9 m thick contain 47 to 61% conglomerate. The conglomerates are massive to crudely bedded (Gm), the beds being several centimetres to several metres thick. D_{10} measurements (average size in (mm) of the ten largest clasts at a site) range from 111/176 to 141/222 (short axis/long axis; long axis lies within the foliation).

The conglomerate matrices and sandstones are coarse- to fine-grained and moderately to poorly sorted, with minor finer, better sorted beds. The sandstone beds are massive and plane laminated (Sm, Sh) with horizontal pebble bands. Plane laminated siltstone (Fl) is present at one locality.

Unit C. The uppermost and coarsest level of the sequence in northwest Beatty Lake (Fig. 16.2) is closely similar to the northern metasedimentary belt's conglomerate and sandstone in both lithofacies (Gm, Sm, Sh, Sp) and clast lithologies.

The lower part of unit C is generally more than 50% conglomerate; individual outcrop sections 4.9 m to 8.5 m thick vary from 21 to 87% massive to crudely crossbedded (Gm), with D_{10}s of 74/110 to 144/217. Outcrops higher in the section are composed of more than 90% conglomerate and have D_{10}s of 130/195 to 141/204. The uppermost conglomerate outcrop in the sequence is bouldery, with a D_{10} of 281/638.

Interpretation. The southernmost fine grained clastics and ironstones are the aquabasinal products of sediment gravity flows (turbidites) and settling from suspension. These may be of prodeltaic, submarine fan, or "abyssal" plain affinity; the probable context favours a prodeltaic paleoenvironment.

A rapid facies change from fluvio-deltaic braided river (see below) topsets to a gravelly fan-delta slope paleoenvironment (as discussed by Ethridge and Wescott, 1984; Nemec and Steel, 1984) explains the presence of resedimented conglomerates — fine-pebble normal-graded beds, argillaceous matrix-supported debris flows, disorganized beds, two possible inverse-graded beds, and one graded-stratified bed (lithofacies of Walker, 1978a) — and turbiditic sandstone in Figure 16.2. The D_{10} measurements of these resedimented conglomerates are finer grained than most of the nearby fluvial (see below) conglomerates in both the section stratigraphically above and exposures along strike, as would suit more distal clasts. Point counts and field observations show that the fluvial and resedimented conglomerates have the same provenance.

The bimodal-bipolar crossbedding should indicate an intertidal (shoreline) facies. This does not necessarily prove marine conditions, as very large lakes can have a tidal range. Also, storms and seiches can direct crossbeds shoreward and upstream within coastal distributaries.

The amount of conglomerate in the sections, stratification, sedimentary structures, grain size (especially the coarsest clasts), and sorting suggest:

1. for unit A, a Platte-type profile (distal braided fluvial), with possible minor transitions to a South Saskatchewan-type profile, and a minor intertidal unit;

2. for unit B, a Donjek-type profile (medial braided fluvial); and

3. for unit C, a Scott- to Donjek-type profile (proximal to medial braided fluvial).

Units A, B and C are very similar to the sections given by McGowen and Groat (1971) in their classic description and model of fluvial fan facies.

The fluvio-deltaic (fan-delta) lithofacies record the infilling of the adjacent adquabasin via the burial of the underlying sandstone, mudstone and ironstone. This coarsening-upward subaqueous to subaerial trend, with its increasingly proximal fluvial lithofacies assemblages, outlines a prograded clastic wedge.

Deltaic metasediments

Three outcrops in Sandra Township (Fig. 16.1), one a stream section over 30 m thick, contain well-exposed examples of rhythmic bedding. It is most unusual to find in Archean strata units like the ones described and interpreted below.

The Type B-Type A couplets outlined in Fig. 16.3 are 0.5 m to several metres thick. They recur rhythmically and form the major part of the sections. Medium- to fine-grained crossbedded sandstone forms a minor part of these sections. Ball-and-pillow structures and centimetre-scale and sand dykes are present in some Type B units. Paleocurrents from ripples, planar crossbeds, and one imbricate granule layer are broadly unimodal, to the east to southeast. (Three-dimensional exposure, although the best in the central metasedimentary belt, is too poor for detailed paleocurrent analysis).

Interpretation. The couplets are interpreted to be deltaic distributary mouth bar and/or distal bar deposits. No turbidites or other features typical of submarine fans are present. The sections' rhythmic nature, Type B-transition-Type A repeated vertically, does not suggest fluvial channels, where couplets would be prone to truncation by the initiation of new erosive channels. Interdistributary bay fill sequences usually coarsen rather than fine upward (Elliott, 1978). The couplets are too thin to represent deltaic lobes. One would expect turbidites and mudstone towards prodeltaic bottomsets, and fluvial facies as topsets; the couplets fit in between, in a delta front or slope paleoenvironment.

It is not known whether the fine grained Type A units are more distal in an axial-to-lateral sense (Elliott, 1978), as a result of distributary mouth avulsion and/or migration, or in a proximal-to-distal sense, with the Type A units representing finer grained background sedimentation periodically invaded from upslope by coarser Type B sands. The latter situation could be the result of a subaqueous channel incised into a delta slope, with couplets being the subaqueous equivalents of waning subaerial floods.

The couplets are part of a coarsening-upward sequence on two scales. Firstly, they are in the middle of the more than 1 km thick central metasedimentary belt, below (south of) the fluvial conglomeratic part of the sequence, with north-topping beds only. The couplets are finer grained and

better sorted than the fluvial sandstone above in the central belt section, as might be expected of a more distal deltaic succession. Secondly, the couplets are an integral part of the best exposed section, a more than 30 m thick subtly coarsening-upward sequence, the mud and finer sand fractions being gradually and irregularly lost upward.

Regional stratigraphy

The aquabasinal fine grained clastics and ironstones are mostly along the southern margin of the central metasedimentary belt. The deltaic and distal fluvial sandstone and conglomerate assemblages are in the middle of the belt. The fluvial conglomerate-rich sections are in the central belt's northern portion, with the exception of Walters and east Irwin townships (Fig. 16.1), where the former displays north-topping only turbiditic sandstone north of the fluvial conglomerate.

Bedding-foliation relationships and stratigraphic top indicators do not suggest any significant complication in the overall coarsening-upward trend. Objective criteria from all the central belt's lithofacies assemblages − per cent conglomerate in the sections, strained bed thicknesses, bed soles, sedimentary structures, D_{10} measurements, average grain size, and sorting − outline proximal-distal and north-facing patterns that crosscut the boundaries of the lithofacies assemblages and minor folding. Rare small scale folds in the central metasedimentary belt were mostly asymmetric, suggesting possibly the selective exposure of north-facing fold limbs.

The conglomerates of the central belt is of the same composition as that of the northern belt, as revealed by 31 point counts (500 non-matrix points per count) and field observations. The northern belt's braided river conglomerate clasts are coarser and more elongate (more oblate) than the central's. Distal features such as finer grained and better sorted conglomerate and sandstone, fluvial and aquabasinal sandstone-rich sections, mudstone interbedded with fluvial conglomerate, intraformational mud chip clasts, and abundant exposure of aquabasinal facies are all unique to the central metasedimentary belt.

The above points strongly suggest that the Namewaminikan Group's proximal northern metasedimentary belt and distal central metasedimentary belt once formed a continuous wedge or sheet of sediments, prograding with time probably southward into the adjacent aquabasin.

It is unclear whether the ironstone, mudstone (argillite/slate), and sandstone sporadically present for kilometres along strike in the upper (northern) part of the central belt represents a submergent (transgressive) phase, lacustrine deposits within a braidplain, or highly proximal inter-fan lakes.

The conglomerates of the Beardmore-Geraldton terrane's southern metasedimentary belt has the sampe provenance as that of the northern and central metasedimentary belts, based on field observations. The triad of metasedimentary belts mimics the central belt's proximal to the north trend. The lower aquabasinal portion
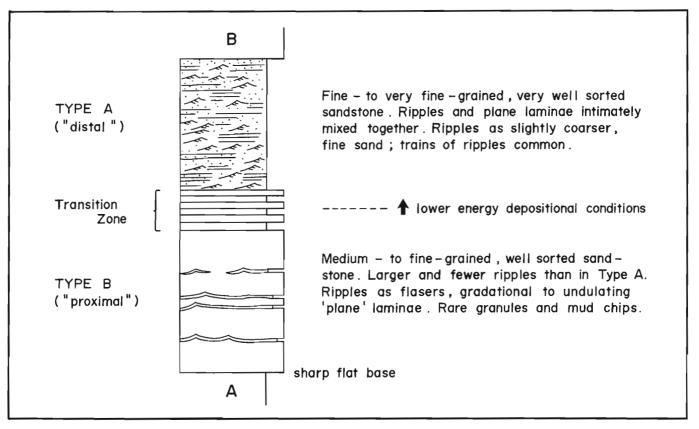

Figure 16.3. *Idealized couplet or rhythmite, interpreted to be of deltaic distributary mouth bar/diastal bar origin. Vertical scale varies from about 0.5 m to several metres.*

of the central belt is analogous to most of the southern belt, which was likely the ultradistal, turbiditic sandstone-rich component of northern-central-southern belt depositional systems tract. Earlier studies by Langford (1929), Ayres (1969), and Mackasey (1975, 1976) came to similar conclusions. The southern belt's stratigraphy is, however, relatively highly deformed (Kehlenback, 1983; Anglin and Franklin, 1985), and is the subject of other ongoing studies.

Structure and regional implications

Within the central metasedimentary belt's coarsening-northward section, folding appears to have been focussed within the least competent members of the sequence, the finer grained and more thinly bedded metasediments. These display tight to isoclinal folding, north- and south-facing stratigraphic tops, abundant quartz veining, and are usually near the inferred base of the section. Most of the central belt's section is of coarser and more thickly bedded conglomerates and sandstone that seems to have acted in a much more competent manner during deformation, leaving stratigraphic tops north throughout the rest of the relatively undisturbed central belt section, possibly the result of folds with highly asymmetric limbs.

The resedimented conglomeratic lithofacies assemblage (Fig. 16.2), with its great variety of lithologies and bed thicknesses, is a structural microcosm of the entire central metasedimentary belt. Small-scale folds are visible within the finer sandstone and siltstone, and these lithologies are often preserved as tectonic slivers rather than beds, in contrast to immediately adjacent north-younging beds of coarser clastics. Minor faulting disrupts the lateral continuity of some of the coarser beds.

The above helps explain why the central belt's stratigraphy as a whole youngs to the north, regardless of the minor folds. Such a facing is approximately perpendicular to the strike of bedding and foliation, unlike the Beardmore-Geraldton terrane's southern belt, where Kehlenbeck (1983) and Anglin and Franklin (1985) have mapped structural facing directions, which are supposed to show the younging of the sequence as a whole, that are to the east and west, along the approximate regional strike of bedding and foliation.

The points above also explain why, very surprisingly, a classical type of stratigraphy can be applied to an Early Precambrian meta-morphosed terrane. Goodwin (1977; see also Walker, 1978b) postulated the presence of a basin margin in this area, and an aquabasinal margin is easily inferred at Beatty Lake (Fig. 2), and probably extends along strike down the length of the central metasedimentary belt.

The authors have used the terms "Archean terrane" and "metavolcanic-metasedimentary belt/terrane" because, as suggested by M.M. Kehlenbeck (personal communication, 1983) and others, the Beardmore-Geraldton terrane may be more a regional zone of shear than an "Archean greenstone belt" proper (status quo in Condie, 1981). The lithotectonic style typical of Archean greenstone belts seems to be present in this area at the scale of the Wabigoon Subprovince as a whole, with the Beardmore-Geraldton terrane as a relatively minor strip of east-trending supracrustal rocks.

Acknowledgments

References

Amukun, S.E.
1980: Geology of the Conglomerate Lake area, District of Thunder Bay; Ontario Geological Survey, Report 197, 101 p.

Anglin, C.D. and Franklin, J.M.
1985: Gold mineralization in the Beardmore-Geraldton area of northwestern Ontario: structural considerations and the role of iron formation; in Current Research, Part A, Geological Survey of Canada, Paper 85-1A, p. 193-201.

Ayres, L.D.
1969: Early Precambrian stratigraphy of part of Lake Superior Provincial Park, Ontario, Canada, and its implications for the origin of Superior Province; unpublished Ph.D. dissertation, Princeton University.

Ballance, P.F.
1984: Sheet-flow dominated gravel fans of the non-marine middle Cenozoic Simmler Formation, central California; Sedimentary Geology, v. 38, p. 337-359.

Beakhouse, G.P.
1982: Kirby, Fulford, and McQueston Townships area, District of Thunder Bay; in Summary of Field Work, 1982, by the Ontario Geological Survey, ed. J. Wood et al.; Ontario Geological Survey, Miscellaneous Paper 106, p. 24-27.

Boothroyd, J.C. and Ashley, G.M.
1975: Processes, bar morphology, and sedimentary structures on braided outwash fans, north-eastern Gulf of Alaska; in Glaciofluvial and Glaciolacustrine Sedimentation, ed. A.V. Jopling and B.C. McDonald; Society of Economic Paleontologists and Mineralogists, Special Publication No. 23, p. 193-222.

Boothroyd, J.D. and Nummedal, D.
1978: Proglacial braided outwash: a model for humid alluvial fan deposits; in Fluvial Sedimentology, ed. A.D. Miall; Canadian Society of Petroleum Geologists, Memoir 5, p. 641-668.

Borradaile, G.J.
1982: Comparison of Archean structural styles in two belts of the Canadian Superior Province; Precambrian Research, v. 19, p. 179-189.

Bruce, E.L.
1937: The eastern part of the Sturgeon River area; Ontario Department of Mines Annual Report, v. 45, part 2, 1936, p. 1-59.

Condie, K.C.
1981: Archean Greenstone Belts; Elsevier, 434 p.

Elliott, T.
1978: Deltas; in Sedimentary Environments and Facies, ed. H.G. Reading; Elsevier, p. 97-142.

Eriksson, K.A.
1978: Alluvial and destructive beach facies from the Archean Moodies Group, Barberton Mountain Land, South Africa and Swaziland; in Fluvial Sedimentology, ed. A.D. Miall; Canadian Society of Petroleum Geologists, Memoir 5, p. 287-311.

Ethridge, F.G. and Wescott, W.A.
 1984: Tectonic setting, recognition and hydrocarbon potential of fan-delta deposits; in Sedimentology of Gravels and Conglomerates, ed. E.H. Koster and R.J. Steel; Canadian Society of Petroleum Geologists, Memoir 10, p. 217-235.

McGown, J.H. and Groat, C.G.
 1971: Van Horn Sandstone, west Texas: an alluvial fan model for mineral exploration; Bureau of Economic Geology, University of Texas at Austin, Report of Investigation No. 72, 57 p.

Miall, A.D.
 1977: A review of the braided river depositional environment; Earth-Science Reviews, v. 13, p. 1-62.

 1978: Lithofacies types and vertical profile models in braided river deposits: a summary; in Fluvial Sedimentology, ed. A.D. Miall; Canadian Society of Petroleum Geologists, Memoir 5, p. 597-604.

Moorhouse, W.W.
 1939: Geology of the south Onaman area; Ontario Department of Mines Annual Report, v. 47, part 8, 1938, 30 p.

Nemec, W. and Steel, R.J.
 1984: Alluvial and coastal conglomerates: their significant features and some comments on gravelly mass-flow deposits; in Sedimentology of Gravels and Conglomerates, ed. E.H. Koster and R.J. Steel; Canadian Society of Petroleum Geologists, Memoir 10, p. 1-31.

Rust, B.R.
 1978: Depositional models for braided alluvium; in Fluvial Sedimentology, ed. A.D. Miall; Canadian Society of Petroleum Geologists, Memoir 5, p. 605-625.

Schumm, S.A.
 1977: The Fluvial System; John Wiley and Sons, 338 p.

Stott, G.M.
 1984a: Lake Nipigon Sheet, Thunder Bay District; Ontario Geological Survey, Map P. 257 (Rev.), Compilation Series – Preliminary Map, scale 1:126 720.

 1984b: Geraldton Sheet, Thunder Bay and Cochrane Districts; Ontario Geological Survey, Map P. 241 (Rev.), Compilation Series-Preliminary Map, scale 1:126 720.

Tanton, T.L.
 1919: Canadian Northern railway between Nipigon and Longuelac, northern Ontario; Geological Survey of Canada, Summary Report, 1917, part E, 1E-6E.

Walker, R.G.
 1978a: Deep-water sandstone facies and ancient submarine fans: models for exploration for stratigraphic traps; American Association of Petroleum Geologists Bulletin, v. 62, p. 932-966.

 1978b: A critical appraisal of Archean basin-craton complexes; Canadian Journal of Earth Sciences, v. 15, p. 1213-1218.

Preliminary observations on stratiform copper occurrences in the basal Siyeh Formation of Proterozoic age, southern Alberta

EMR Research Agreement 310

Henry T. Koopman[1] and Pier L. Binda[1]
Economic Geology and Mineralogy Division

Abstract

Analyses for Cu, Pb, Zn, Co, and Ag in relevant horizons of a typical stratigraphic section of the upper Grinnell and lower Siyeh formations indicate at least two laterally continuous zones of anomalous metal concentrations. The most important is a zone 2-4 m-thick with Cu values of a few thousand ppm at the Grinnell/Siyeh boundary.

The facies sequence suggests a major marine transgression over the extensive mud flats of the Grinnell Formation producing a quiet, shallow-water reducing environment in the lower Siyeh Formation.

At the Grinnell/Siyeh contact both black argillites and arenites are mineralized, but copper values tend to be higher in the arenites. This, together with chalcopyrite rims around shale clasts and diagenetic sulphide 'ooids' in a clean arenite, suggest a syn-diagenetic base metal occurrence.

The stratigraphic position of the basal Siyeh copper occurrences is analogous to that of the ore shale of the Zambian Copperbelt, of the Kupferschiefer of central Europe, and of several other deposits.

Résumé

Des analyses de Cu, Pb, Zn, Co et Ag présents dans des horizons d'intérêt d'une section stratigraphique type de la partie supérieure de la formation de Grinnell et de la partie inférieure de la formation de Siyeh révèlent l'existence d'au moins deux zones latéralement continues de concentrations métalliques anormales. La plus importante est une zone de 2 à 4 m d'épaisseur dont les teneurs en Cu atteignent quelques miliers de ppm à la limite des deux formations.

D'après la séquence de faciès, on suppose qu'il s'est produit une transgression marine majeure sur les vastes <<mud flats>> de la formation de Grinnell; cet épisode a donné naissance à un paisible milieu réducteur d'eau peu profonde dans la partie inférieure de la formation de Siyeh.

Au contact des deux formations les argilites noires et les arénites sont minéralisées, mais les teneurs en cuivre sont généralement plus élevées dans les secondes. Ce phénomène, conjugué à la présence d'une bordure de chalcopyrite autour des clastes schisteux et d'oolithes sulfurées de nature diagénétique dans une arénite par ailleurs propre, semble indiquer l'existence d'un gisement syndiagénétique de métaux communs.

La position stratigraphique du cuivre à la base de la formation de Siyeh rappelle celle du schiste minéralisé de la <<Copper belt>> zambienne, du Kupferschiefer d'Europe centrale et de plusieurs autres gisements.

---

[1] Department of Geology, University of Regina, Regina, Saskatchewan S4S 0A2

Introduction

Field work carried out in the summers of 1983 and 1984, and Cu, Ag, Pb, Zn, and Co Atomic Absorption Spectroscopy (A.A.S.) analyses of more than 300 rock samples, have revealed the presence of a stratiform copper occurrence in arenites and shales of the lowermost Siyeh Formation in southern Alberta. The zone with anomalous copper values is 2 to 4 m thick and can be followed in outcrop for approximately 50 km from the Waterton Lakes National Park boundary to the West Castle River Valley. Minor base metal sulphides, which also appear to have considerable lateral continuity, occur higher in the section within the lower Siyeh Formation.

This report gives the first account of the stratigraphy, sedimentology, and sulphides of the upper Grinnell and lower Siyeh formations at South Drywood Creek, Alberta (Fig. 17.1), where the sedimentary layers are flat-lying, relatively undisturbed, and continuously exposed in a wide gully on the south side of the valley above Shell Oil gas well Waterton #30.

Within the 10 to 20 km-thick (Harrison, 1972) Middle-Proterozoic, Purcell Supergroup, stratabound and stratiform base metal deposits and sub-economic occurrences are present at various stratigraphic levels. Belt-Purcell rocks consist of alternating clastic and carbonate metasedimentary units occurring over an area of approximately 200 000 km² in the northwestern United States and adjacent southwestern Canada. Regional stratigraphic correlation of Belt-Purcell rocks is somewhat complicated by the intertonguing of sedimentary prisms from different source areas around the Belt-Purcell basin. Table 17.1 shows a tentative correlation of the Belt-Purcell stratigraphic units.

Ore deposits of the Purcell Supergroup are hosted in both shallow and deep water metasediments. The Sullivan lead-zinc-silver orebody in British Columbia is a hydrothermal synsedimentary deposit (Hamilton et al., 1982) hosted in deep water turbidite metasediments of the Aldridge Formation. On the other hand, shallow water metasediments of the middle Purcell Supergroup host stratiform and stratabound base metal occurrences which show no relation to hydrothermal exhalation. The copper-silver deposit at Spar Lake, Montana is hosted in the quartzites of the upper Revett Formation that represents sands deposited in subtidal or fluvial channels (Hayes, 1984). In the Coeur d'Alene district of Idaho, Ag (Pb-Zn-Cu) veins occur in complexly deformed rocks at the St. Regis/Revett and Burke/Prichard contacts (Crosby, 1984; Landis et al., 1984). In the United States, sub-economic copper showings have also been reported from green beds within red bed sequences of the upper Spokane Formation at Blacktail Mountain and a few other locations (Harrison and Lange, 1983; Connor et al., 1983; Braun and Lange, 1984).

In Canada, the Grinnell and Appekunny formations contain up to 6.4 per cent copper in thin white and green arenites at Yarrow Creek and Spionkop Creek, Alberta (Morton et al., 1974; Goble, 1970 and 1980). Collins and Smith (1977) investigated copper occurrences within thin lensing beds of white to greenish arenites of the upper Grinnell Formation at Grizzly Creek and Whistler Mountain in southern Alberta. A Cominco Ltd. drilling prospect north of Carbondale River, Alberta, revealed minor lead and zinc sulphides in black siltstones and grey dolomites of the Sheppard Formation (Carter, 1971).

Stratigraphy and depositional environment

In the Clarke Range of southwestern Alberta, rocks of the Purcell Supergroup occur as allochthonous sheets which have been thrust northeastward approximately 80 km (Mudge and Earhart, 1980) over the Cretaceous Belly River Formation. The thickness of exposed Purcell Supergroup strata in the southeastern Clarke Range is approximately 3500 m.

The Grinnell Formation consists of approximately 300 m of red and green argillites, red argillaceous arenites, intraformational conglomerates and white arenites (Fig. 17.2). The formation can be subdivided into a 225 m-thick, predominantly argillaceous lower unit consisting of redbeds with minor thin layers of white arenites, and a 75 m-thick upper unit in which thicker white quartz-arenite beds and green and grey argillites become predominant towards the top.

The Siyeh Formation conformably overlies the Grinnell Formation and can be subdivided into three units (Price, 1964). The lower unit, which can be correlated with the Empire Formation of Montana, consists of 120 m of black and green argillites interbedded with thin arenites and with buff-weathering dolomites in the upper portion. The middle unit comprises 275 m of dolomites with abundant stromatolites, molar-tooth structures and ooid-bearing beds. The upper unit, which can be correlated with the Snowslip Formation of the United States, is mainly terrigenous, consisting of 180 m of green and red argillites, siltstones, sandstones, and minor dolomites.

Figure 17.1. *Generalized geological map of the Akamina Synclinorium (after Price, 1965) with the location of the South Drywood Creek Section.*

Table 17.1. Tentative stratigraphic correlation chart of the Belt-Purcell Supergroup.

	Western Belt (1)	Kootenay-King Area (2)	Glacier Park (3)	Waterton-Flathead Area (4)	
Middle Proterozoic Belt - Purcell Supergroup	Pilcher Qtz.				
	Garnet Range Fm.		Top Not Exposed		
	McNamara Fm.	Roosville Fm.	McNamara Fm.	Roosville Fm.	
	Bonner Qtz.	Phillips Fm.	Bonner Qtz.	Phillips Fm.	
	Mount Shields Fm.	Gateway Fm.	Mount Shields Fm.	Gateway Fm. (Kintla Fm.)	
	Shepard Fm.	Sheppard Fm.	Shepard Fm.	Sheppard Fm.	
		Nicol Creek Fm.	Purcell Basalt	Purcell Lava	
	Snowslip Fm.	Van Creek Fm.	Snowslip Fm.	Upper	Siyeh Fm.
	Wallace Fm.	Kitchener Fm.	Helena Fm.	Middle	
			Empire Fm.	Lower	
	Ravalli Gr. St. Regis Fm.	Creston Fm.	Spokane Fm.	Grinnell Fm.	
	Revett Fm.		Greyson Fm. (Appekunny Fm.)	Appekunny Fm.	
	Burke Fm.				
	Prichard Fm.	Aldridge Fm.	Altyn Fm.	Altyn Fm.	
		Fort Steele Fm.		Waterton Fm.	
	Base		Not	Exposed	

(1) Winston, 1984; Harrison, 1972
(2) McMechan, 1981
(3) Earhart et al., 1984; Raup et al., 1983
(4) Price, 1962, 1965

Upper Grinnell Formation

The upper Grinnell Formation consists of repeated sequences composed of a maximum of 1 m of red argillite overlain by up to 40 cm of medium grained white quartz-arenite. These arenites display small scale crossbedding, rippled upper surfaces, and frequently have mud drapes with desiccation polygons preserved in the troughs (Fig. 17.3A). Preliminary examination of crossbedding measurements (102 in the Grinnell Formation) indicates multidirectional paleocurrents, however a few bidirectional structures resembling herringbone crossbedding were observed. Although some of the thinner arenite beds lense out over short distances, the thicker beds can be correlated over distances of a few kilometres. Upper surfaces of the argillite layers display abundant desiccation cracks that have been infilled by sand. Flakes of argillite are incorporated in the arenites to form intraformational mud-chip conglomerates (Fig. 17.3B).

The sedimentary sequences and structures suggest deposition on a low gradient mud flat which was cyclically subaerially exposed, and flooded by storms, with possible tidal influence.

Arenite layers increase in thickness, and become more abundant together with grey and green argillite, in the top 30 m of the formation. Intraformational conglomerates at the top of the Grinnell Formation contain abundant grey and green mud clasts (Fig. 17.3C). The top of the formation is capped by a 4 m-thick clean, white quartz-arenite. This medium grained arenite contains few visible structures except for some rippled surfaces. The increased amount of arenite in this interval suggests that the marine incursions became more frequent and of greater duration, until a stable strandline, possibly a barrier island system, was established.

Collins and Smith (1977) working mostly on outcrops approximately 20 km to the northwest of South Drywood Creek, suggested that barren arenites of the Grinnell Formation formed in river channels, whereas cycles of copper-bearing arenites and green and red argillites, were deposited by sheet floods. In the area that we have investigated so far, the only Grinnell Formation arenites that contain anomalous amounts of copper are the thick quartz-arenites at the top of the formation which we interpret as strandline deposits. Arenites of the Grinnell Formation lack the abundant trough crossbeds and channel geometry that are characteristic of fluvial deposits.

Lower Siyeh Formation

The lower 30 to 40 m of the Siyeh Formation (Fig. 17.2, 17.4) consist of black argillite passing upward to green argillite. Intercalated within the argillite are numerous rippled sand lenses which attain maximum thickness of 15 cm and contain fewer mud clasts than the arenites of the upper Grinnell Formation. Birdfoot and linear syneresis cracks formed by subaqueous dehydration of the mud (Whipple, 1980), are the characteristic sedimentary structures of this interval (Fig. 17.3D). Approximately 1.5 m above the base of the Siyeh Formation is a 30 to 60 cm-thick, laterally continuous arenite bed (Fig. 17.4) which contains diagenetic sulphide 'ooids' (Binda et al., 1985). The bed has a flat base and a rippled upper surface and, at places displays small-scale crossbedding with tangential foresets.

Rock units of the lower Siyeh Formation indicate a marine transgression over the mud flats of the Grinnell Formation. The sediments were deposited on a broad shelf under reducing conditions. The facies is indeed analogous to the anoxic facies that characterizes Phanerozoic transgressions discussed by Hallam (1981).

Above this argillaceous unit is a 35 m-thick sequence of interbedded buff-weathering dolomites, green to grey argillites, and minor arenite lenses. Also within this sequence are carbonate tempestites (Sepkoski, 1982) which are intraformational conglomerates formed by storm waves ripping up partially consolidated shelf muds (Fig. 17.3E). These layers are mound shaped and pinch and swell, reaching a maximum thickness of 60 cm and lensing out within a few metres to laminated argillaceous dolomite. Several dolomite layers within the interval have bulbous (hemispheroidal) stromatolites (Fig. 17.3F) up to 50 cm high. Approximately 10 m of interbedded green argillite and calcareous arenites overlie this first carbonate unit of the Siyeh Formation. The arenites are fine to coarse grained, attain maximum thickness of 30 cm, are predominantly horizontally bedded with some crossbedding, rippled upper surfaces, and contain minor argillite clasts.

Above this unit are 25 m of interbedded dolomites and green argillites. This unit is similar to the carbonate unit below, but it contains more stromatolitic beds.

The uppermost unit of the lower Siyeh Formation consists of 15 m of interbedded green argillites and beige calcareous arenites. The arenite layers are up to 75 cm thick, medium to coarse grained, predominantly horizontally bedded with minor crossbedding, ripples, and contain minor argillite clasts.

Continued transgression of the sea across the shelf resulted in less restricted conditions during the deposition of the interbedded carbonates and argillites. Micro-organisms were able to build stromatolites in these deeper waters.

Figure 17.2. *Simplified stratigraphic column of the upper Grinnell and lower Siyeh formations with Ag, Cu, Pb, Zn, and Co assay values.*

A - Rippled arenite with desiccated argillite drapes within the ripple troughs, upper Grinnell Formation.

B - White quartz-arenite overlain by red argillite. Note the red mud-chips which have been ripped up from desiccated mud surfaces. Visible in the top 10 cm of the white arenite are several desiccated argillite layers infilled by sandstone and partially disrupted, upper Grinnell Formation.

C - White quartz-arenite with green and grey mud clasts. At places, these clasts are rimmed, and have fractures filled by chalcopyrite, upper Grinnell Formation.

D - Sand-filled syneresis cracks in black argillites, lower Siyeh Formation.

E - Carbonate tempestite. Note the horizontal fabric of the mud clasts in the lower part of the bed, and random edgewise fabric in the upper part, lower Siyeh Formation.

F - Stromatolites, lower Siyeh Formation.

Figure 17.3. Sedimentary structures of the upper Grinnell and lower Siyeh formations.

py, ooid bed →

Siyeh Fm.
Grinnell Fm.

Figure 17.4

The Grinnell/Siyeh contact at South Drywood Creek.

The dolomites were deposited on this shallow subtidal shelf, under slightly restricted conditions, (Price, 1964). The two arenite-rich intervals within this upper section may represent minor progradation of nearshore sands.

Overlying the last arenite-argillite sequence of the lower Siyeh Formation, carbonate sedimentation resumed to form the stromatolitic and oolitic dolomites of the middle Siyeh.

The above interpretation of depositional environments of the upper Grinnell and lower Siyeh formations must be considered tentative at this stage. Sedimentological, petrographical, and geochemical studies in progress will undoubtedly improve the interpretation.

Base metal occurrences

The upper Grinnell Formation to lower Siyeh Formation transition is stratigraphically analogous to sequences that host some of the largest stratiform copper deposits in the world. Detailed stratigraphic sampling and geochemical analysis were done to test this comparison.

The five-element geochemical profile of the South Drywood section (Fig. 17.2) is typical of the upper Grinnell and Lower Siyeh section in the Waterton-Pincher Creek area. Essentially the same pattern is present in two other sections, one 5 km to the northwest, the other 6 km to the southeast of the South Drywood section. Care was taken in selecting sections in which diabase dykes are not present in outcrop, as dykes tend to produce local metal enrichments of no stratigraphic significance whereas the purpose of this study was to detect stratigraphically controlled and laterally continuous metal enrichments. Sampling was sporadic in parts of the section where no sulphides, or their oxidation products, were visible, and denser where malachite or limonite was seen, and also in stratigraphically more interesting parts of the section. For example, at the Grinnell/Siyeh contact, malachite, azurite, and limonite are clearly visible on weathered surfaces, and pyrite and chalcopyrite are visible in unweathered rocks. Unfortunately, the black argillite is recessive and covered at several places, therefore samples of this unit were difficult to obtain.

Several intervening sections were sampled and analyzed across the Grinnell/Siyeh contact zone where rocks just above and below the contact were observed to contain copper occurrences of the African Copperbelt-German Kupferschiefer type. In both mineral districts, in sedimentary sequences evolving from continental siliciclastic rocks to marine shales and carbonates, the most important and laterally continuous copper concentration occurs in black shales and arenites deposited during the first, major, regional marine transgression (Nicolini, 1962). Minor, local transgressions in rocks of the footwall and hanging wall of the "ore shale" produce occurrences of local significance (Binda and Mulgrew, 1974). In the Kupferschiefer and in Zaire, where footwall rocks consist of redbeds, footwall orebodies are lacking.

In the Waterton-Pincher Creek area, 2 to 4 m of black argillite and white to beige arenites at the Grinnell/Siyeh contact have copper values that are anomalous both in terms of average metal contents of sedimentary rocks of the same types and in terms of background values for the formations considered (Fig. 17.2). The highest Cu values detected so far do not exceed 4000 ppm, but the continuity of the copper-rich zone and its stratigraphic position are interesting features. Of the other metals, only Co appears to be slightly

anomalous. Mineralogical work in progress indicates that chalcopyrite is the main Cu mineral present. Pyrite is abundant throughout the Cu-bearing zone and in overlying rocks.

So far the main mineralogical interest has been focussed on the chalcopyrite-pyrite 'ooids' contained in a laterally-continuous arenite bed (Fig. 17.4) 1.5 to 2.0 m above the Grinnell/Siyeh boundary (Binda et al., 1985). These unmetamorphosed sulphide-coated grains may provide an important clue to the formation of sedimentary copper deposits. The sulphide 'ooids' nucleate around detrital grains of chalcopyrite, anatase, and intergrowths of the two minerals (Binda et al., 1985). Diagenetic nucleation of copper sulphides around detrital sulphide nuclei was suggested by Schneiderhöhn (1937) for the ores of central Africa. Batholomé (1974) dismissed Schneiderhöhn's suggestion and proposed instead a nucleation of sulphides around titanium oxides.

Other interesting sulphide textures include chalcopyrite rims around argillite clasts in the clean quartz-arenites at the top of the Grinnell Formation. They indicate movement of copper-rich solutions in the porous sand, and precipitation of sulphide at permeability barriers or favourable nucleation sites.

Approximately 50 m above the base of the Siyeh Formation is a 7-8 m-thick zone with anomalously high metal values in arenites interbedded with black argillites and with some stromatolitic dolomite. Although Cu values are lower here than at the Grinnell/Siyeh boundary, higher Pb and Ag values make this interval worthy of further study. No detailed mineralogical work has yet been done on these sulphides.

In all the zones with anomalous metal values shown in Figure 17.2, black argillites are present. Within these zones, however, arenites tend to contain more metal than the associated argillites. This may suggest movement of metal-rich fluids through more permeable arenites during early diagenesis.

Available analyses of samples from the upper Grinnell and lower Siyeh formations do not reveal copper grades approaching economic concentrations. However, the mineralized horizon at the base of the Siyeh Formation could well be continuous over a large area in the subsurface of the Akamina Synclinorium. Copper-rich zones of this type tend to have large lateral extent but only locally contain concentrations of ore grade (Brown, 1971; van Eden and Binda, 1972; Binda and Mulgrew, 1974; Rentzsch, 1974). Therefore blind orebodies conceivably could exist at depth in southwestern Alberta and southeastern British Columbia.

Acknowledgments

References

Bartholomé, P.
  1974: On the diagenetic formation of ores in sedimentary beds, with special reference to Kamoto, Shaba, Zaire; in Gisements Stratiformes et Provinces Cuprifères, ed. P. Bartholomé; Société Géologique de Beligique, Liège, p. 203-213.

Binda, P.L. and Mulgrew, J.R.
  1974: Stratigraphy of copper occurrences in the Zambian Copperbelt; in Gisements Stratiformes et Provinces Cuprifères, ed. P. Bartholomé; Société Géologique de Belgique, Liège, p. 215-233.

Binda, P.L., Koopman, H.T., and Schwann, P.L.
  1985: Sulphide ooids from the Proterozoic Siyeh Formation of Alberta, Canada; Mineralium Deposita, v. 20, p. 43-49.

Braun, E.R. and Lange, I.M.
  1984: Organic control of sandstone-hosted copper-silver mineralization in the Spokane Formation near Rogers Pass, western Montana; in Northwest Montana and Adjacent Canada, Montana Geological Society 1984 Field Conference and Symposium, ed. J.D. McBane, P.B. Garrison; Montana Geologic Society, p. 305-313.

Brown, A.C.
  1971: Zoning in the White Pine copper deposit, Ontonagon County, Michigan; Economic Geology, v. 66, p. 543-573.

Carter, K.M.
  1971: Final report, North Carbondale Project – 1970; Cominco Ltd. unpublished report, 6 p.

Collins, J.A. and Smith, L.
  1977: Genesis of cupriferous quartz arenite cycles in the Grinnell Formation (Spokane equivalent), Middle Proterozoic (Helikian) Belt-Purcell Supergroup, eastern Rocky Mountains, Canada; Bulletin of Canadian Petroleum Geology, v. 25, p. 713-735.

Connor, J.J., Domenico, J.A., Harrison, J.E., Reynolds, M.W., Rye, R.O., and Whelan, J.F.
  1983: Green-bed copper occurrences in upper part of the Spokane Formation at the Blacktail Mountain drilling site near Lakeside, Montana; in Guide to field trips, Belt Symposium II, ed. S.W. Hobbs; Department of Geology, University of Montana, Missoula, Montana, p. 105-114.

Crosby, G.M.
  1984: Locations of Coeur D'Alene orebodies in Belt stratigraphy; in The Belt, ed. S.W. Hobbs; Montana Bureau of Mines and Geology, Special Publication 90, p. 61-62.

Earhart, R.L., Mudge, M.R., and Connor, J.J.
  1984: Belt Supergroup lithofacies in the northern Disturbed Belt, northwest Montana; in Northwest Montana and Adjacent Canada, Montana Geological Society 1984 Field Conference and Symposium, ed. J.D. McBane, P.B. Garrison; Montana Geologic Society, p. 51-66.

Goble, R.J.
  1970: The Yarrow Creek – Spionkop Creek copper deposit, southwestern Alberta; unpublished M.Sc. thesis, University of Alberta, 116 p.

  1980: Copper sulfides from Alberta: Yarrowite Cu_9S_8 and Spionkopite $Cu_{39}S_{28}$; Canadian Mineralogist, v. 18, p. 511-518.

Hallam, A.
  1981: Facies interpretation and the stratigraphic record; W.H. Freeman and Co., 291 p.

Hamilton, J.M., Bishop, D.T., Morris, H.C., and Owens, O.E.
1982: Geology of the Sullivan orebody, Kimberley, B.C., Canada; in Precambrian Sulphide Deposits, H.S. Robinson Memorial Volume, ed. R.W. Hutchinson, C.D. Spence, and J.M. Franklin; Geological Association of Canada Special Paper 25, p. 597-665.

Harrison, J.E.
1972: Precambrian Belt basin of northwestern United States: its geometry, sedimentation and copper occurrences; Geological Society of America Bulletin, v. 83, p. 1215-1240.

Harrison, J.E. and Lange, I.M.
1983: Stratabound copper occurrences in green beds of the Belt Supergroup, Western Montana; in Guide to field trips, Belt Symposium II, ed. S.W. Hobbs; Department of Geology, University of Montana, Montana, p. 94-104.

Hayes, T.S.
1984: The relation between stratabound copper-silver ore and Revett Formation sedimentary facies at Spar Lake, Montana; in The Belt, ed. S.W. Hobbs; Montana Bureau of Mines and Geology Special Publication 90, p. 63-64.

Landis, G.P., Leach, D.L., and Hofstra, A.H.
1984: Silver-base metal mineralization as a product of metamorphism – Coeur D'Alene district, Shoshone County, Idaho: concepts of genesis; in The Belt, ed. S.W. Hobbs; Montana Bureau of Mines and Geology Special Publication 90, p. 68.

McMechan, M.E.
1981: The Middle Proterozoic Purcell Supergorup in the southwestern Rocky and southeastern Purcell Mountains, British Columbia and the initiation of the Cordilleran miogeocline, southern Canada and adjacent United States; Bulletin of Canadian Petroleum Geology, v. 29, p. 583-621.

Morton, R.D., Goble, R.J., and Fritz, P.
1974: The mineralogy, sulfur-isotope composition and origin of some copper deposits in the Belt Supergroup, southwest Alberta, Canada; Mineralium Deposita, v. 9, p. 223-241.

Mudge, M.R. and Earhart, R.L.
1980: The Lewis thrust fault and related structures in the Disturbed Belt, northwestern Montana; United States Geological Survey, Professional Paper 1174, 18 p.

Nicolini, P.
1962: L'utilisation des données sédimentologiques dans l'étude et la recherche des gisements stratiformes. Etablissements des <<courbes prévisionelles>>; Chroniques des Mines et Recherches Minieres, no. 309, p. 155-167.

Price, R.A.
1962: Fernie map-area, east half, Alberta and British Columbia; Geological Survey of Canada, Paper 61-24, 65 p.

1964: The Precambrian Purcell System in the Rocky Mountains of southern Alberta and British Columbia; Bulletin of Canadian Petroleum Geology, v. 12, p. 399-426.

1965: Flathead map-area, British Columbia and Alberta; Geological Survey of Canada, Memoir 336, 219 p.

Raup, O.B., Earhart, R.L., Whipple, J.W., and Carrara, P.E.
1983: Geology along Going-to-the-Sun Road, Glacier National Park, Montana; Glacier Natural History Association, West Glacier, Montana and Falcon Press, Helena, Montana, 62 p.

Rentzsch, J.
1974: The Kupferschiefer in comparison with the deposits of the Zambian Copperbelt; in Gisements Stratiformes et Provinces Cupriferes, ed. P. Bartholomé; Société Géologique de Belgique, Liège, p. 395-418.

Schneiderhöhn, H.
1937: Die Kupferlagerstatten von Northrhodesia und Katanga; Geologische Rundschau, v. 28, p. 282-291.

Sepkoski, J.J., Jr.
1982: Flat-pebble conglomerates, storm deposits, and the Cambrian bottom fauna; in Cyclic and Event Stratification, ed. G. Einsele, A. Seilacher; Springer-Verlag, p. 371-385.

van Eden, J.G. and Binda, P.L.
1972: Scope of stratigraphic and sedimentologic analysis of the Katanga sequence, Zambia; Geologie en Mijnbouw, v. 51, p. 321-328.

Whipple, J.W.
1980: Depositional environment of the Middle Proterozoic Spokane Formation – Empire Formation transition zone, west-central Montana; United States Geological Survey Open File Report 80-1232, 98 p.

Whipple, J.W., Connor, J.J., Raup, O.B., and McGimsey, R.G.
1984: Preliminary report on the Stratigraphy of the Belt Supergroup, Glacier National Park and adjacent Whitefish Range, Montana; in Northwest Montana and Adjacent Canada, Montana Geological Society 1984 Field Conference and Symposium, ed. J.D. McBane, P.B. Garrison; Montana Geologic Society, p. 33-50.

Winston, D., Woods, M., and Byer, G.B.
1984: The case for an intracratonic Belt-Purcell basin: tectonic, stratigraphic and stable isotopic considerations; in Northwest Montana and Adjacent Canada, Montana Geological Society 1984 Field Conference and Symposium, ed. J.D. McBane, P.B. Garrison; Montana Geologic Society, p. 103-118.

Statistical treatment of geochemical data with observations below the detection limit

Project 750094

C.F. Chung
Economic Geology and Mineralogy Division

Abstract

To estimate mean and variance of data with observations below detection limit, the maximum likelihood (ML) estimators are proposed. A FORTRAN-77 computer program has been developed for Newton's scoring method — the standard ML iterative procedure, to obtain the ML estimators.

Résumé

L'auteur propose d'établir des valeurs de calcul du maximum de vraisemblance en vue d'estimer la moyenne et la variance des données dont les observations se trouvent sous la limite de détection. Un programme d'ordinateur FORTRAN-77 a été mis au point pour la méthode de notation de Newton, soit le procédé d'itération normalement utilisé pour obtenir les valeurs de calcul du maximum de vraisemblance.

Introduction

When geochemical data to be statistically analyzed contain observations below the detection limit, this can cause severe problems during the application of standard statistical techniques to the data. For example, even simple statistics such as sample mean or variance, can not be readily estimated. In statistics, observations below detection limits are called singly truncated observations. These have been studied for well-known distribution functions such as the normal and lognormal (Cohen, 1950, 1957), and gamma (Broeder, 1955).

In this paper, the maximum likelihood estimation of two parameters, mean and variance of normal (and lognormal) distribution functions from data with truncated observations, are discussed. A computer program solving the maximum likelihood (ML) estimators of mean and variance has been developed and is listed in the Appendix A. As examples, the methods are applied to simulated data from the standard normal distribution and two real data sets (Franklin et al., 1975 and Goodfellow, 1981).

ML estimation of parameters for singly truncated data

Consider N observations, $y_1, y_2, \dots, y_N$ of a geochemical element. Suppose that there are n observations below the detection limit, say d, among them. Then by reordering the data according to increasing order, we have;

$$y_{1:N}, y_{2:N}, \dots, y_{n:N}, y_{n+1:N}, \dots, y_{N:N}$$

where $y_{k:N}$ denotes the k-th largest value among the N observations, $y_1, y_2, \dots, y_N$. Since the first n observations are below the detection limit d, the values for $y_{1:N}, \dots, y_{n:N}$ are unknown but we know that:

$$y_{i:N} < d \quad \text{for all } i = 1, 2, \dots, n.$$

Let us now suppose that the y_i's come from independent identically distributed random variables Y_i's with probability distribution function $F(y:r_1,\dots,r_k)$ and density function $f(y:r_1,\dots,r_k)$ where $r_1, \dots, r_k$ are the k unknown parameters of the distribution function. Then the likelihood function is:

$$L(y:r_1, \dots, r_k) = \binom{N}{n} F^n(d:r_1, \dots, r_k) \prod_{i=n+1}^{N} f(y_{i:N}:r_1, \dots, r_k) \tag{2.1}$$

Hence the log-likelihood function is:

$$logL(y,r_1, \dots, r_k) = nlogF(d:r_1, \dots, r_k) + \sum_{i=n+1}^{N} logf(y_{i:N}:r_1, \dots, r_k) \tag{2.2}$$

$$+ \, constant$$

The ML estimators $\hat{r}_1, \dots, \hat{r}_k$ for $r_1, \dots, r_k$ would be obtained by solving the following k equations:

$$\left(\frac{\partial logL}{\partial r_j} \right)_{r=\hat{r}} = \left(n \frac{1}{F(d:r)} \frac{\partial F(d:r)}{\partial r_j} + \sum_{i=n+1}^{N} \frac{1}{f(y_{i:N}:r)} \frac{\partial f(y_{i:N}:r)}{\partial r_j} \right)_{r=\hat{r}} = 0 \tag{2.3}$$

$$for \, j = 1, 2, \dots, k$$

where $r = (r_1, \dots, r_k)$ and $\hat{r} = (\hat{r}_1, \dots, \hat{r}_k)$.

However, the non-linear equations in (2.3) cannot be solved, in general, with respect to $\hat{r}$. Newton's scoring method - the standard ML iterative procedure, is commonly employed to obtain a solution for $\hat{r}$.

ML estimators for mean and standard deviation of normal distribution from singly truncated data

Suppose that Y_i's have a normal distribution with unknown mean μ and standard deviation σ. Then the distribution and density functions are;

$$f(y{:}\mu,\sigma) = \frac{1}{\sqrt{2\pi}\sigma} \, exp\,(-\frac{(y-\mu)^2}{2\sigma^2})\, and\, F(x{:}\mu,\sigma) = \int_{-\infty}^{x} f(y{:}\mu,\sigma)\,dy \qquad (3.1)$$

and traditionally $\phi(y) = f(y{:}0,1)$ and $\Phi(x) = F(x{:}0,1)$ are used to denote the standard distribution functions. By substituting ϕ and Φ for f and F, and μ and σ for $r_1,...,r_k$ for (2.2), the log- likelihood function is obtained from:

$$log\,L\,(y{:}\mu,\sigma) = n\,log\,\phi\,[\,(d-\mu)/\sigma] + \sum_{i=n+1}^{N} log\,\phi\,[\,(y_{i:N}-\mu)/\sigma] \qquad (3.2)$$

$$- (N\text{-}n)\,log\,\sigma + constant$$

By differentiating $log\,L$ with respect to μ and σ as in (2.3) and equating them to zero, we obtain:

$$-n\,\frac{\phi\,(\delta)}{\Phi\,(\delta)} + \sum_{i=n+1}^{N} x_i = 0,$$

$$n\,(1 - \delta\,\frac{\phi\,(\delta)}{\Phi\,(\delta)}) + \sum_{i=n+1}^{N} x_i^{\,2} = N \qquad (3.3)$$

where

$$\delta = (d-\hat{\mu})/\hat{\sigma}\,and\,x_i = (y_{i:N} - \hat{\mu})/\hat{\sigma}\,for\,i = n + 1,...,N.$$

To solve the equations in (3.3), Cohen (1955) has suggested another method for use instead of using Newton's scoring method. This new method is as follows: By combining two equations in (3.3) and after a few algebraic manipulations, we obtain;

$$\frac{1 - \delta\,(Y\,(\delta) - \delta)}{(Y\,(\delta) - \delta)^2} = \frac{v_2}{v_1^{\,2}} \qquad (3.4)$$

$$\hat{\sigma} = v_1/(Y\,(\delta) - \delta)$$

$$\hat{\mu} = d - \hat{\sigma}\,\delta \qquad (3.5)$$

where

$$Y\,(\delta) = \frac{n}{N-n}\,\frac{\phi\,(\delta)}{\Phi\,(\delta)},$$

$$v_2 = \frac{1}{N-n} \sum_{i=n+1}^{N} (y_{i:N} - d)^2, \qquad (3.6)$$

$$v_1 = \frac{1}{N-n} \sum_{i=n+1}^{N} (y_{i:N} - d)$$

The values of v_1 and v_2 can be computed from the observed data, $y_{n+1:N},...,y_{N:N}$ by (3.6). If we can solve equation (3.4) with respect to δ, we would obtain two ML estimators, $\hat{\mu}$ and $\hat{\sigma}$, of μ and σ from the equations (3.5). Again, equation (3.4) cannot be solved directly. It can be shown however, that the left hand side of (3.5) is an increasing function of δ, and for this reason using a simple iterative numerical algorithm implemented in the subroutine called, COHEN (listed in the Appendix A), equation (3.4) can be solved. Next $Y(\delta)$ is computed as in (3.6) and μ and σ are estimated by $\hat{\mu}$ and $\hat{\sigma}$ in (3.5).

Newton's scoring method is also implemented in the subroutine SINGLE and listed in Appendix A. Data containing observations truncated from both sides represent a special case that is described in the next section. The two subroutines COHEN and SINGLE should provide the identical ML estimators for mean and variance. However, as for all iterative procedures, sometimes neither of the procedures provides the estimators. Hence when one method fails to provide the estimators then the other methods should be tried to obtain the ML estimators for the singly truncated data.

ML estimators of μ and σ of normal distribution from doubly truncated data

Let $y_1, ..., y_N$ be a set of data containing observations truncated from both sides. Suppose that there are n_a observations below the detection limit, say a, and n_b observations above the maximum observable value b. By reordering the observations in increasing order, we obtain:

$$y_{1:N}, ..., y_{n_a:N}, y_{n_a+1:N}, ..., y_{N-n_b:N}, y_{N-n_b+1:N}, ..., y_{N:N}$$

where $y_i{:}N < a$ for $i = 1, 2, ... , n_a$,

         $y_j{:}N > b$ for $j = N-n_b + 1, ... , N$.

However, the exact values of the $y_{i:N}$ ($i \leq n_a$) and $y_{j:N}$ ($j \geq N-n_b + 1$) are unknown.

Let us assume that the y_i's come from independent identically distributed random variables Y_i's with distribution function $F(y{:}r)$ and density $f(y{:}r)$. Then the general log-likelihood function is:

$$\log L(y{:}r) = n_a \log F(a{:}r) + n_b \log [1 - F(b{:}r)]$$

$$+ \sum_{i=n_a+1}^{N-n_b} \log f(y_{i:n}{:}r) + constant$$

Hence, by substituting ϕ and Φ for f and F in (4.1), and μ and σ for r, as in (3.2), we obtain:

$$\log L(y{:}r) = n_a \log \Phi(\alpha) + n_b \log [1 - \Phi(\beta)] - n \log \sigma$$

$$+ \sum_{i=n_a+1}^{N-n_b} \log \phi [(y_{i:n} - \mu)/\sigma] + constant \tag{4.2}$$

where

$$\alpha = (a - \hat{\mu})/\hat{\sigma}, \beta = (b - \hat{\mu})/\hat{\sigma} \text{ and } n = N - n_a - n_b.$$

In order to obtain the ML estimators $\hat{\mu}$ and $\hat{\sigma}$ of μ and σ, Newton's scoring method based upon the Taylor expansion may be employed. The i-th estimators $\hat{\mu}_i$ and $\hat{\sigma}_i$ of μ and σ of the method are obtained by:

$$\begin{pmatrix} \hat{\mu}_i \\ \hat{\sigma}_i \end{pmatrix} = \begin{pmatrix} \hat{\mu}_{i-1} \\ \hat{\sigma}_{i-1} \end{pmatrix} - \begin{bmatrix} \begin{pmatrix} \dfrac{\partial^2 \log L}{\partial \mu^2} \\ \dfrac{\partial^2 \log L}{\partial \mu \partial \sigma} \end{pmatrix} \begin{pmatrix} \dfrac{\partial^2 \log L}{\partial \mu \partial \sigma} \\ \dfrac{\partial^2 \log L}{\partial \mu^2} \end{pmatrix}^{-1} \begin{pmatrix} \dfrac{\partial \log L}{\partial \mu} \\ \dfrac{\partial \log L}{\partial \sigma} \end{pmatrix} \end{bmatrix}_{\substack{\mu = \mu_{i-1} \\ \sigma = \sigma_{i-1}}} \tag{4.3}$$

where $\hat{\mu}_0$ and $\hat{\sigma}_0$ are initial estimates for μ and σ, and

$$\frac{\partial \log L}{\partial \mu} = \frac{n}{\sigma^2} \left\{ - \frac{n_a}{n} \sigma Y_1(\alpha) + \frac{n_b}{n} \sigma Y_2(\beta) + m_1 - \mu \right\}$$

$$\frac{\partial \log L}{\partial \sigma} = \frac{n}{\sigma^2} \left\{ - \frac{n_a}{n} \sigma \alpha Y_1(\alpha) + \frac{n_b}{n} \sigma \beta Y_2(\beta) - \sigma + \frac{1}{\sigma} (m_2 - 2\mu m_1 + \mu^2) \right\}$$

$$\frac{\partial^2 \log L}{\partial \mu^2} = \left(-\frac{n}{\sigma^2}\right)\left\{1 + \frac{n_a}{n}\left[Y_1^2(\alpha) + \alpha\, Y_1(\alpha)\right] - \frac{n_b}{n}\left[Y_2^2(\beta) - \beta\, Y_2(\beta)\right]\right\} \tag{4.4}$$

$$\frac{\partial^2 \log L}{\partial \mu \partial \sigma} = \left(-\frac{n}{\sigma^2}\right)\left\{\frac{2}{\sigma}(m_1 - \mu) - \frac{n_a}{n}\left[Y_1(\alpha) - \alpha\,(Y_1^2(\alpha) + \alpha\, Y_1(\alpha))\right] + \frac{n_b}{n}\left[Y_2(\beta) + \beta\,(Y_2^2(\beta) - \beta\, Y_2(\beta))\right]\right\}$$

$$\frac{\partial^2 \log L}{\partial \sigma^2} = \left(-\frac{n}{\sigma^2}\right)\left\{\frac{3}{\sigma^2}(m_2 - 2\mu m_1 + \mu^2) - 1 - \frac{n_a}{n}\alpha\left[2\,Y_1(\alpha) - \alpha\,(Y_1^2(\alpha) + \alpha\, Y_1(\alpha))\right]\right. \tag{4.5}$$

$$\left. + \frac{n_b}{n}\beta\left[2\,Y_2(\beta) + \beta\,(Y_2^2(\beta) - \beta\, Y_2(\beta))\right]\right\}$$

$$m_1 = \frac{1}{n}\sum_{i=n_a+1}^{N-n_b} y_{i:N} \;,\quad m_2 = \frac{1}{n}\sum_{i=n_a+1}^{N-n_b} y_{i:N}^2$$

$$Y_1(\alpha) = \frac{\phi(\alpha)}{\Phi(\alpha)} \; and \; Y_2(\beta) = \frac{\phi(\beta)}{1 - \Phi(\beta)}$$

This iterative procedure is programmed and implemented in subroutine DOUBLE in Appendix A. To obtain the ML estimators for singly truncated cases, the preceding procedures [(4.3), (4.4) and (4.5)] can also be utilized except that all the terms starting with n_b/n in the partial derivatives in (4.4) are zero, since $n_b = 0$. This special case for singly truncated data is also implemented in subroutine SINGLE in Appendix A.

Examples

1.   Simulated data

A set of 100 pseudo-random numbers from a standard normal random variable with mean 0 and variance 1, was simulated by using subroutine GGNML of IMSL Library (IMSL, 1984). The sample mean and variance using all 100 observations are, as shown in Table 18.1, 0.057 and 1.037, and, as expected, they are very close to the true values, 0 and 1. The next three columns of Table 18.1 show three singly truncated (left side) cases at 0.2, 0.5 and 0.8. For the case of left truncation at 0.5, 65 of 100 observations are below the detection limit of 0.5 and only 35 samples have observed values. Even then, the ML estimates of the mean and variance, 0.150 and 0.908 are close to the true values, 0 and 1. The last two columns show the ML estimates for doubly truncated cases.

Table 18.1

	all data	left trunc. at a=0.2	left trunc. at a=0.5	left trunc. at a=0.8	both trunc. at a=0.5 b=1.0	both trunc. at a=0.0 b=0.8
Total no. of observations	100	100	100	100	100	100
no. of obser. below a	NA	55	65	75	65	50
no. of obser. above b	NA	NA	NA	NA	19	25
no. of observations	100	45	35	25	16	25
ML estimate for mean	0.057	0.096	0.150	0.197	0.107	0.006
ML estimate for variance	1.037	0.995	0.908	0.840	1.055	1.430

2.   Nahanni area geochemical data (Goodfellow, 1981)

The data for these examples come from GSC Open file 868 which covers a geochemical reconnaissance survey of the Nahanni map area (NTS 105I). Only two elements, Mn and F, in stream waters from the northeastern quarter of NTS 105I are considered. There are 211 samples.

The first example is for Mn and from 211 samples, only 27 samples are above the detection limit of 10 ppb. When lognormality is assumed (i.e. the samples come from a lognormal distribution), then the ML estimates of mean and variance from the log-transformed data are -1.738 and 13.045. These estimates are completely different from the sample mean and variance, 1.955 and 0.934 computed from a data set which consists of all 27 log-transformed observed values (greater than the detection limit of 10 ppb) and 184 values set equal to the logarithm of 5 ppb (substituting half of the detection limit for the samples below the detection limit).

The element F is considered in the second example. Here 88 of 211 samples are below the detection limit of 25 ppb. The ML estimates for mean and variance from the log-transformed data are 3.325 and 0.682, whereas the sample mean and variance of the log-transformed 123 observations and 88 of log (12.5), are 3.295 and 0.634. These two sets of estimates are very close to each other, since the ML estimate for mean (3.325) is close to log (12.5)=3.219.

3.   Geochemical data from Sturgeon Lake area (Franklin, et al., 1975)

For these examples, two elements, Ni and Co measured by the atomic absorption method, are considered. For both elements, 10 ppb is the detection limit and there are 97 samples. For Ni, 54 of 97 samples are below the detection limit and for Co 39 samples are below the detection limit. Assuming lognormality, all observed data were transformed to logarithmic values.

The ML estimates for mean and variance are 2.028 and 1.434 for Ni, and 2.438 and 0.464 for Co, respectively. The sample mean and variance are 2.259 and 0.797 for Ni, and 2.359 and 0.518 for Co. While two estimates for Co are similar to each other, the estimates of the variance for Ni are quite different.

Concluding remark

The ML estimators for mean and variance of normal populations proposed in this paper serve to replace ad-hoc procedure used in the past, although the procedure does not provide an answer for testing the hypothesis of normality or lognormality required for the procedure.

An IBM-PC diskette containing the source program listed in Appendix A may be obtained on request from the author.

Acknowledgments

References

Broeder, G.G.
  1955:   On parameter estimation for truncated Pearson type III distributions; Annals of Mathematical Statistics, v. 26, p. 659-663.

Cohen, A.C.
  1950:   Estimating the mean and variance of normal populations from singly truncated and doubly truncated samples; Annals of Mathematical Statistics, v. 21, p. 557-569.

  1955:   Censored samples from truncated normal distributions; Biometrika, v. 42, p. 516-519.

Franklin, J.M., J. Kasarda and K.H. Poulsen
  1975:   Petrology & chemistry of the alteration zone of the Mattabi massive sulfide deposit; Economic Geology, v. 70, p. 63-79.

Goodfellow, W.D.
  1981:   Regional stream sediment and water geochemistry reconnaissance data, Yukon and Northwest Territories; Geological Survey of Canada, Open File 868, NGR 51-1981, NTS 105I.

A listing of the program to compute the ML estimates for
mean and variance of normal and lognormal populations.

```fortran
      PROGRAM MAIN
C******************************************************************
C  1.      THIS PROGRAM HAS BEEN DEVELOPED TO COMPUTE THE MAXIMUM
C     LIKELIHOOD ESTIMATORS FOR MEAN AND  STANDARD DEVIATION
C     OF NORMAL DISTRIBUTION FUNCTION FROM  DATA  CONTAINING
C     EITHER SINGLY OR DOUBLY TRUNCATED OBSERVATIONS.
C  2.      IT IS WRITTEN IN FORTRAN 77 AND PARTICULARLY  DESIGNED
C     FOR MICROSOFT FORTRAN COMPILER 3.2 ON DOS 2.0 (OR HIGHER)
C     ON IBM-PC.
C  3.      THIS MAIN PROGRAM SHOULD BE MODIFIED ACCORDING TO  THE
C     USER'S NEED.
C******************************************************************
      CHARACTER*1  IYES,LYES,YES
      CHARACTER*20 INNAME
      CHARACTER*40 INFORMAT
      DIMENSION X(500)
      DATA YES/'Y'/
C
20    WRITE(*,'(A\)')' INPUT FILE NAME ? '
      READ(*,'(A)')INNAME
      OPEN (3,FILE=INNAME)
      WRITE(*,'(A\)')' ENTER THE NUMBER OF THE DATA '
      READ(*,*)N
      WRITE(*,'(A\)')' ENTER THE FORMAT OF THE DATA '
      READ(*,'(A)')INFORMAT
      READ(3,INFORMAT)(X(I),I=1,N)
      WRITE(*,'(A\)')' IS THE LOG-TRANSFORMATION REQUIRED?(Y OR N) '
      READ(*,'(A)')LYES
      IF ( LYES.EQ.YES ) THEN
        WRITE(*,'(A\)')' ENTER REPLACEMENT VALUE FOR ZERO IN DATA '
        READ(*,*)ZZZ
        ZZ = ALOG(ZZZ)
        DO 50 I=1,N
          XX=X(I)
          IF ( XX.LE.0. ) THEN
            X(I) = ZZ
          ELSE
            X(I) = ALOG(XX)
          ENDIF
50      CONTINUE
      ENDIF
C
C * * * * * CALL SORT TO SORT THE DATA
C
      CALL SORT(X,N)
      CLOSE(3)
16    FORMAT(' NUMBER OF SAMPLE BELOW DETECTION LIMIT ',I6)
18    FORMAT(' ML ESTIMATES FOR MEAN AND VARIANCE ',2F15.5)
21      FORMAT(' NO SOLUTION HAS BEEN FOUND, TRY NEWTONS METHOD')

22    FORMAT(' USING THE COHENS METHOD')
23    FORMAT(' USING THE NEWTONS SCORING METHOD')
24    FORMAT(' NUMBER OF SAMPLES ABOVE OBSERVABLE VALUE ',I6)
100     WRITE(*,'(A\)')' ENTER THE LEFT  CENSORING VALUE '
      READ(*,*)A
      IF ( LYES.EQ.YES ) A = ALOG(A)
      WRITE(*,'(A\)')' ENTER THE RIGHT CENSORING VALUE '
      WRITE(*,'(A\)')' FOR NO RIGHT CENSORING, ENTER 999.0 '
      READ(*,*)B
      IF ( B.EQ.999.0 ) THEN
        N1 = 0
        WRITE(*,'(A\)')' SELECT COHENS(1) OR NEWTONS METHOD(2) '
        READ(*,*)IMETH
        IF(IMETH.EQ.1) THEN
C
C * * * * * CALL COHEN TO OBTAIN THE ML ESTIMATORS
C                 FOR SINGLY CENSORED DATA
C                 USING COHEN'S METHOD
C
          CALL COHEN(N,N1,A,X,U,S)
          IF ( S.LE.0. ) THEN
            WRITE(*,21)
            CALL SINGLE(N,N1,A,X,U,S)
            WRITE(*,23)
            WRITE(*,16)N1
            SS = S*S
            WRITE(*,18)U,SS
          ELSE
            WRITE(*,22)
            WRITE(*,16)N1
            SS = S*S
            WRITE(*,18)U,SS
          ENDIF
        ELSE
C
C * * * * * CALL SINGLE TO OBTAIN THE ML ESTIMATORS
C                 FOR SINGLY TRUNCATED DATA
C                 USING NEWTONS METHOD
C
          WRITE(*,21)
          CALL SINGLE(N,N1,A,X,U,S)
          WRITE(*,23)
          WRITE(*,16)N1
          SS = S*S
          WRITE(*,18)U,SS
        ENDIF
      ELSE
        IF ( LYES.EQ.YES ) B = ALOG(B)
        N1=0
        N2=0
C
C * * * * * CALL DOUBLE TO OBTAIN THE ML ESTIMATORS
C                 FOR DOUBLY CENSORED DATA
C                 USING NEWTONS METHOD
C
        CALL DOUBLE(N,N1,N2,A,B,X,U,S)
        WRITE(*,16)N1
        WRITE(*,24)N2
        SS = S*S
        WRITE(*,18)U,SS
      ENDIF
      WRITE(*,'(A\)')' WOULD YOU LIKE TO TRY ANOTHER CENSORING? '
      READ(*,'(A)')IYES
      IF(IYES.EQ.YES) GO TO 100
      WRITE(*,'(A\)')' WOULD YOU LIKE TO TRY ANOTHER DATA? '
      READ(*,'(A)')IYES
      IF(IYES.EQ.YES) GO TO 20
      STOP
      END
C================================================================
C
      REAL FUNCTION INVPHI(P)
C******************************************************************
C  1.    INVPHI   - FORTRAN 77 REAL FUNCTION
C  2.    FOR A GIVEN PROBABILITY P = PROB { N < X }, IT
C        COMPUTES X WHERE N IS THE STANDARD NORMAL
C        DISTRIBUTION. I.E.
C
C        INVPHI(P) = X WHERE P = PROB{ N < X } WHERE N ~ NORMAL(0,1)
C
C  3.    PARAMETERS:
C          IN   P    :  GIVEN PROBABILITY
C          OUT  INVPHI :  SEE THE ABOVE FORMULA
C  4.    SUBROUTINES OR FUNCTIONS REQUIRED:
C          NONE
C  5.    REFERENCES:
C          ABRAMOWITZ AND STEGUN ( 1964, (26.2.23) OF P.933)
C******************************************************************
      DATA CI/2.515517/, CJ/0.802853/, CK/0.010328/
      DATA DI/1.432788/, DJ/0.189269/, DK/0.001308/
C
      IF ( P.GT.0.5 ) THEN
        Q = 1.0 - P
      ELSE
        Q = P
      ENDIF
      TT = ALOG( 1.0/(Q*Q) )
      T = SQRT( TT )
      UP = CI + CJ*T + CK*TT
      DOWN = 1.0 + DI*T + DJ*TT + DK*T*TT
      INVPHI = T - UP / DOWN
      IF ( P.LT.0.5 ) INVPHI = -INVPHI
      RETURN
      END
C================================================================
C
      REAL FUNCTION PHI(X)
C******************************************************************
C  1.    PHI    - FORTRAN 77 REAL FUNCTION
C  2.    IT COMPUTES THE PROBABILITY OF STANDARD NORMAL DISTRIBUTION
C
C        FUNCTION:
C
C        PHI(X) = PROB { N < X } WHERE N ~ NORMAL( 0, 1 )
C
C  3.    PARAMETERS:
C          IN   X    :  SEE THE ABOVE FORMULA
C          OUT  PHI  :  PROBABILITY
C  4.    SUBROUTINES OR FUNCTIONS REQUIRED:
C          NONE
C  5.    REFERENCES:
C          ABRAMOWITZ AND STEGUN ( 1964, (26.2.17) OF P.932)
C******************************************************************
      DIMENSION B(5)
      DATA B/ 0.319381530, -0.356563782,  1.781477937,
     C        -1.821255978,  1.330274429/
      DATA PP/ 0.231641900/, PH/3.14159265359/
C
      IN = 0
      IF ( X.LT.0.0 ) THEN
        IN = 1
        X = -X
      ENDIF
      M = 5
      IF ( X.LT.9. ) THEN
        T = 1.0 / (1.0 + PP*X)
        ZX = (EXP(-X*X/2.0)) / SQRT(2.0*PH)
        TT = 1.
        BT = 0.
        DO 10 I = 1, M
          TT = TT * T
          BT = BT + B(I)*TT
10      CONTINUE
      ELSE
        ZX = 0.
        BT = 0.
      ENDIF
      PHI = 1.0 - ZX*BT
      IF ( IN.EQ.1 ) THEN
        PHI = 1.0 - PHI
        X = -X
      ENDIF
      RETURN
      END
C================================================================
C
```

```fortran
      REAL FUNCTION ZETA(X)
C******************************************************************
C  1.     ZETA - FORTRAN 77 REAL FUNCTION
C  2.     IT COMPUTES THE STANDARD NORMAL DENSITY DISTRIBUTION
C  FUNCTION
C******************************************************************
      DATA PH/3.14159265359/
      ZETA = EXP( -0.5*X*X ) / SQRT( 2.0*PH )
      RETURN
      END


C==================================================================
C
      REAL FUNCTION Y1(X)
C******************************************************************
C  1.     Y1 - FORTRAN 77 REAL FUNCTION
C  2.     IT COMPUTES THE RECIPROCAL OF MILL'S RATIO;
C  DENISTY FUNCTION OVER CUMULATIVE FUNCTION OF
C     NORMAL DISTRIBUTION FUNCTION.
C******************************************************************
      Y1 = ZETA(X)/PHI(X)
      RETURN
      END
C==================================================================
C
      REAL FUNCTION Y2(X)
C******************************************************************
C  1.     Y2 - FORTRAN 77 REAL FUNCTION
C  2.     VARIATION OF Y1 : Y2(X) = Y1(-X)
C******************************************************************
      Y2 = ZETA(X)/(1.0-PHI(X))
      RETURN
      END      '
C==================================================================
C
      REAL FUNCTION Y1P(X)
C******************************************************************
C  1.     Y1P - FORTRAN 77 REAL FUNCTION
C  2.     A FUNCTION OF Y1: SEE (4.4) IN TEXT
C******************************************************************
      Y1P = Y1(X)*Y1(X) + X*Y1(X)
      RETURN
      END
C==================================================================
C
      REAL FUNCTION Y2P(X)
C******************************************************************
C  1.     Y2P - FORTRAN 77 REAL FUNCTION
C  2.     A FUNCTION OF Y2: SEE (4.4) IN TEXT
C******************************************************************
      Y2P = Y2(X)*Y2(X) - X*Y2(X)
      RETURN
      END
C==================================================================
C
      REAL FUNCTION SINVAL(XN,X1,AN)
C******************************************************************
C  1.     SINVAL - FORTRAN 77 REAL FUNCTION
C  2.     IT COMPUTES THE LEFT SIDE OF FORMULA IN (3.4) IN TEXT
C  3.     FUNCTIONS REQUIRED: Y1 - PHI,ZETA
C******************************************************************
      Y = X1*Y1(AN)/XN
      SINVAL = (1.0 - AN*(Y-AN))/((Y-AN)*(Y-AN))
      RETURN
      END
C==================================================================
C
      SUBROUTINE SORT(X,N)
C******************************************************************
C  1.     SORT - FORTRAN 77 SUBROUTINE
C  2.     BUBBLE SORTING ALGORITHM IN INCREASING ORDER
C  3.     PARAMETERS:
C  4.     IN   N   : NUMBER OF VALUES TO BE SORTED IN ARRAY X
C              X   : ARRAY WHICH CONTAINS N VALUES. THIS ARRAY
C                    WILL BE REPLACED BY THE ORDERED ARRAY.
C              OUT  X   : THE N INPUT VALUES WILL BE ORDERED.
C******************************************************************
      DIMENSION X(N)
C
      NN = N-1
      DO 20 I = 1,NN
      II = I+1
      DO 10 J =II,N
      IF(X(I).GT.X(J))THEN
      TEMP = X(J)
      X(J) = X(I)
      X(I) = TEMP
      ENDIF
10    CONTINUE
20    CONTINUE
      RETURN
      END
C==================================================================
C
      SUBROUTINE COHEN(N,N1,A,X,PNU,SIGMA)
C******************************************************************
C  1.     COHEN - FORTRAN 77 SUBROUTINE
C  2.     IT COMPUTES THE ML ESTIMATES OF THE MEAN AND VARIANCE
C  OF A NORMAL DISTRIBUTION FUNCTION FROM A SET OF DATA
C  CONTAINING SINGLY TRUNCATED OBSERVATIONS.
```

```fortran
C  3.     PARAMETERS:
C         IN    N    : NO. OF VALUES IN SORTED ARRAY X.
C               A    : TRUNCATION VALUE. I.E. DETECTION LIMIT.
C               X    : INPUT ARRAY CONTAINING N SORTED VALUES
C                      IN INCREASING ORDER. THE FIRST N1 VALUES
C                      ARE BELOW DETECTION LIMIT A.
C         OUT   N1   : NO. OF VALUES BELOW A IN INPUT ARRAY X.
C                      IF(N1.EQ.0)THEN RETURN.
C               PNU  : ML ESTIMATOR OF MEAN.
C               SIGMA: ML ESTIMATOR OF STANDARD DEVIATION.
C  4.     SUBROUTINES AND FUNCTIONS REQUIRED:
C         - INVPHI
C         - Y1 - ZETA,PHI
C         - SLIKE - PHI
C  5.     REFERENCES:
C         SEE (3.4), (3.5), (3.6) OF TEXT
C******************************************************************
      REAL INVPHI
      DIMENSION X(N)
      DATA TOL/0.0001/
C
      DO 10 I=1,N
      IF(X(I).LT.A) N1=N1+1
10    CONTINUE
      IF(N1.EQ.0) RETURN
      WRITE(*,3) N, N1
      NN=N-N1
      XNN=FLOAT(NN)
      XN1=FLOAT(N1)
      NN1=N1+1
      R1=0.
      R2=0.
      DO 20 I=NN1,N
      XX=X(I)-A
      R1=R1+XX
      R2=R2+XX*XX
20    CONTINUE
      R1 = R1/XNN
      R2 = R2/XNN
      R = R2/(R1*R1)
C
C * * * * * STEP 0, SETTING UP INITIAL VALUES
C
      ISTEP = 0
      ALPHA = XN1/FLOAT(N)
      AN = INVPHI(ALPHA)
      Y = XN1*Y1(AN)/XNN
      YA = Y - AN
      SIGMA = R1/YA
      PNU = A - SIGMA*AN
      RR = (1.0 - AN*YA)/(YA*YA)
      CALL SLIKE(N,N1,A,X,PNU,SIGMA,SCORE)
      WRITE(*,2)
      WRITE(*,1)ISTEP,PNU,SIGMA,SCORE
1     FORMAT(3X,I4,3X,2F10.5,F12.5)
2     FORMAT(' ITERATION',3X,'MEAN',6X,'S.D.',3X,'LOG-LIKELIHOOD')
3     FORMAT(' NO. OF TOTAL OBSERVATIONS =',I5,/,
     *       ' NO. OF OBSERVATIONS BELOW DETECTION LIMIT =',I5)
C
C * * * * * ITERATION STARTS HERE
C
      XMIN = AN - 1.0
      XMAX = AN + 1.0
30    CONTINUE
      ISTEP = ISTEP+1
      IF(ABS(RR-R).LT.TOL.OR.ISTEP.GT.30)GO TO 50
      IF(RR.GT.R) THEN
      ADD = (XMIN - AN)/2.0
      XMAX = AN
      ELSE
      ADD = (XMAX - AN)/2.0
      XMIN = AN
      ENDIF
      AN = AN + ADD
      Y = XN1*Y1(AN)/XNN
      YA = Y - AN
      SIGMA = R1/YA
      PNU = A - SIGMA*AN
      RR = SINVAL(XNN,XN1,AN)
      IF(SIGMA.LE.0.0)GO TO 50
      CALL SLIKE(N,N1,A,X,PNU,SIGMA,SCORE)
40    WRITE(*,1)ISTEP,PNU,SIGMA,SCORE
      GO TO 30
C
50    RETURN
      END
C==================================================================
C
      SUBROUTINE SINGLE(N,N1,A,X,PNU,SIGMA)
C******************************************************************
C  1.     SINGLE - FORTRAN 77 SUBROUTINE
C  2.     IT COMPUTES THE ML ESTIMATES OF THE MEAN AND VARIANCE
C  OF A NORMAL DISTRIBUTION FUNCTION FROM A SET OF DATA
C  CONTAINING SINGLY TRUNCATED OBSERVATIONS.
```

148

```
C   3.    PARAMETERS:
C            IN     N    : NO. OF VALUES IN SORTED ARRAY X.
C            A      : LOWER TRUNCATION VALUE.-  LOWER DETECTION LIMIT.
C            X      : INPUT ARRAY CONTAINING N SORTED VALUES
C                      IN INCREASING ORDER. THE FIRST N1 VALUES
C                      ARE BELOW A.
C        OUT    N1   : NO. OF VALUES BELOW A IN INPUT ARRAY X.
C                      IF(N1.EQ.0 ) THEN  RETURN.
C            PNU  : ML ESTIMATOR OF MEAN.
C            SIGMA: ML ESTIMATOR OF STANDARD DEVIATION.
C   4.    SUBROUTINES AND FUNCTIONS REQUIRED:
C            - INVPHI
C            - Y1 - ZETA,PHI
C            - Y1P - Y1
C            - SLIKE - PHI
C   5.    REFERENCES:
C            SEE (3.7), (3.8) AND (3.9) OF TEXT
C****************************************************************
      REAL INVPHI
      DIMENSION X(N)
      DATA TOL/0.0001/
C
      IF ( N1.GT.0 ) GO TO 15
      DO 10 I=1,N
      IF(X(I).LT.A) N1=N1+1
10    CONTINUE
      IF(N1.EQ.0)RETURN
15    WRITE(*,3)N,N1
      NN=N-N1
      XNN=FLOAT(NN)
      XN1=FLOAT(N1)/XNN
      NN1=N1+1
      R1=0.
      R2=0.
      DO 20 I=NN1,N
      XX=X(I)
      R1=R1+XX
      R2=R2+XX*XX
20    CONTINUE
      R1 = R1/XNN
      R2 = R2/XNN
C
C * * * * * STEP 0, SETTING UP INITIAL VALUES
C
      ISTEP = 0
      ALPHA = XN1*XNN/FLOAT(N)
      A1 = INVPHI(ALPHA)
      YA = XN1*Y1(A1) - A1
      SIGMA = R1/YA
      SIG2 = SIGMA*SIGMA
      PNU = A - A1*SIGMA
      CALL SLIKE(N,N1,A,X,PNU,SIGMA,SCORE)
      WRITE(*,2)
      WRITE(*,1)ISTEP,PNU,SIGMA,SCORE
1     FORMAT(3X,I4,3X,2F10.5,F12.5)
2     FORMAT(' ITERATION',3X,'MEAN',6X,'S.D.',3X,'LOG-LIKELIHOOD')
3     FORMAT(' NO. OF TOTAL OBSERVATIONS =',I5,/,
     *        ' NO. OF OBSERVATIONS BELOW DETECTION LIMIT =',I5)
C
C * * * * * ITERATION STARTS HERE
C
30    CONTINUE
      ISTEP = ISTEP + 1
      YY1 = XN1*Y1(A1)
      YY1P = XN1*Y1P(A1)
      SIG2N = XNN/SIG2
      SS2 = R2 - 2.*PNU*R1 + PNU*PNU
C
      PL1 = (R1 - PNU - SIGMA*YY1)*SIG2N
      PL2 = (SS2/SIGMA - SIGMA*(1.+A1*YY1))*SIG2N
      SI1 = -( 1. + YY1P )*SIG2N
      SI2 = -( 2.*(R1-PNU)/SIGMA - YY1 + A1*YY1P )*SIG2N
      SI3 = -(3.*SS2/SIG2 - 2.*A1*(YY1-A1*YY1P) + 1.)*SIG2N
C
      DIV = SI1*SI3 - SI2*SI2
      HH = (-SI1*PL1 + SI2*PL2)/DIV
      HK = (SI2*PL1 - SI3*PL2)/DIV
C
      PNU = PNU + HH
      SIGMA = SIGMA + HK
      CALL SLIKE(N,N1,A,X,PNU,SIGMA,SCORE)
      WRITE(*,1)ISTEP,PNU,SIGMA,SCORE
      IF((ABS(HH).LT.TOL.AND.ABS(HK).LT.TOL).OR.(ISTEP.GT.30))GOTO 40
      A1 = (A-PNU)/SIGMA
      GO TO 30
40    RETURN
      END
C==============================================================
C
      SUBROUTINE DOUBLE(N,N1,N2,A,B,X,PNU,SIGMA)
C****************************************************************
C  1.    DOUBLE - FORTRAN 77 SUBROUTINE
C  2.    IT COMPUTES THE ML ESTIMATES OF THE MEAN AND VARIANCE
C    OF A NORMAL DISTRIBUTION FUNCTION FROM A SET OF DATA
C    CONTAINING DOUBLY TRUNCATED OBSERVATIONS.
C  3.    PARAMETERS:
C            IN     N    : NO. OF VALUES IN SORTED ARRAY X.
C            A      : LOWER TRUNCATION VALUE.-  LOWER DETECTION LIMIT.
C            B      : UPPER TRUNCATION VALUE - MAXIMUM OBSERVABLE VALUE.
C            X      : INPUT ARRAY CONTAINING N SORTED VALUES
C                      IN INCREASING ORDER. THE FIRST N1 VALUES
C                      ARE BELOW A AND THE LAST N2 VALUES ARE ABOVE B.
C        OUT    N1   : NO. OF VALUES BELOW A IN INPUT ARRAY X.
C            N2   : NO. OF VALUES ABOVE B IN INPUT ARRAY X.
```

```
C            IF(N1.EQ.0 .OR. N2.EQ.0) THEN  RETURN.
C            PNU  : ML ESTIMATOR OF MEAN.
C            SIGMA: ML ESTIMATOR OF STANDARD DEVIATION.
C  4.    SUBROUTINES AND FUNCTIONS REQUIRED:
C            - INVPHI
C            - Y1 - ZETA,PHI
C            - Y2 - ZETA,PHI
C            - Y1P - Y1
C            - Y2P - Y2
C            - DLIKE - PHI
C  5.    REFERENCES:
C            SEE (4.3), (4.4) AMD (4.5) OF TEXT
C****************************************************************
      REAL INVPHI
      DIMENSION X(N)
      DATA TOL/0.0001/
C
      DO 10 I=1,N
      IF(X(I).LT.A) N1=N1+1
      IF(X(I).GT.B) N2=N2+1
10    CONTINUE
      IF(N1.EQ.0.OR.N2.EQ.0)RETURN
      WRITE(*,3)N,N1,N2
      NN=N-N1-N2
      XNN=FLOAT(NN)
      XN1=FLOAT(N1)/XNN
      XN2=FLOAT(N2)/XNN
      NN1=N1+1
      NN2=N-N2
      R1=0.
      R2=0.
      DO 20 I=NN1,NN2
      XX=X(I)
      R1=R1+XX
      R2=R2+XX*XX
20    CONTINUE
      R1 = R1/XNN
      R2 = R2/XNN
C
C * * * * * STEP 0, SETTING UP INITIAL VALUES
C
      ISTEP = 0
      ALPHA = XN1*XNN/FLOAT(N)
      ALPHB = 1.0 - XN2*XNN/FLOAT(N)
      A1 = INVPHI(ALPHA)
      A2 = INVPHI(ALPHB)
      SIGMA = (B-A)/(A2-A1)
      SIG2 = SIGMA*SIGMA
      PNU = A - A1*SIGMA
      CALL DLIKE(N,N1,N2,A,B,X,PNU,SIGMA,SCORE)
      WRITE(*,2)
      WRITE(*,1)ISTEP,PNU,SIGMA,SCORE
1     FORMAT(3X,I4,3X,2F10.5,F12.5)
2     FORMAT(' ITERATION',3X,'MEAN',6X,'S.D.',3X,'LOG-LIKELIHOOD')
3     FORMAT(' NO. OF TOTAL OBSERVATIONS =',I5,/,
     *        ' NO. OF OBSERVATIONS BELOW DETECTION LIMIT =',I5,/,
     *        ' NO. OF OBSERVATIONS ABOVE OBSERVALE VALUE =',I5)
C
C * * * * * ITERATION STARTS HERE
C
30    CONTINUE
      ISTEP = ISTEP + 1
      YY1 = XN1*Y1(A1)
      YY2 = XN2*Y2(A2)
      YY1P = XN1*Y1P(A1)
      YY2P = XN2*Y2P(A2)
      SIG2N = XNN/SIG2
      SS2 = R2 - 2.*PNU*R1 + PNU*PNU
C
      PL1 = (R1 - PNU - SIGMA*(YY1-YY2))*SIG2N
      PL2 = (SS2/SIGMA - SIGMA*(1.+A1*YY1-A2*YY2))*SIG2N
      SI1 = -( 1. + YY1P - YY2P )*SIG2N
      SI2 = 2.*(R1-PNU)/SIGMA - YY1 + A1*YY1P + YY2 + A2*YY2P
      SI2 = -SI2*SIG2N
      SI3 = 3.*SS2/SIG2 - 2.*A1*(YY1-A1*YY1P) + 2.*A2*(YY2+A2*YY2P)
      SI3 = (-SI3 - 1.)*SIG2N
C
      DIV = SI1*SI3 - SI2*SI2
      HH = (-SI1*PL1 + SI2*PL2)/DIV
      HK = (SI2*PL1 - SI3*PL2)/DIV
C
      PNU = PNU + HH
      SIGMA = SIGMA + HK
      CALL DLIKE(N,N1,N2,A,B,X,PNU,SIGMA,SCORE)
      WRITE(*,1)ISTEP,PNU,SIGMA,SCORE
      IF((ABS(HH).LT.TOL.AND.ABS(HK).LT.TOL).OR.(ISTEP.GT.30))GOTO 40
      A1 = (A-PNU)/SIGMA
      A2 = (B-PNU)/SIGMA
      GO TO 30
40    RETURN
      END
C==============================================================
C
      SUBROUTINE SLIKE(N,N1,A,X,PNU,SIGMA,SCORE)
C****************************************************************
C  1.    SLIKE - FORTRAN 77 SUBROUTINE
C  2.    IT COMPUTES THE LOG-LIKELIHOOD FUNCTION OF A SET OF
C    DATA CONTAINING SINGLY TRUNCATED OBSERVATIONS  FROM
```

```
C      A NORMAL POPULATION WITH MEAN AND STANDARD DEVIATION.
C  3.    PARAMETERS:
C          IN        N   : NO. OF VALUES IN SORTED ARRAY X.
C          A    : LOWER TRUNCATION VALUE.- LOWER DETECTION LIMIT.
C          N1   : NO. OF VALUES BELOW A IN INPUT ARRAY X.
C          X    : INPUT ARRAY CONTAINING N SORTED VALUES
C                   IN INCREASING ORDER. THE FIRST N1 VALUES
C                   ARE BELOW A.
C          PNU  : MEAN.
C          SIGMA: STANDARD DEVIATION.
C      OUT    SCORE: VALUE OF THE LOG-LIKELIHOOD FUNCTION.
C  4.    SUBROUTINES AND FUNCTIONS REQUIRED:
C          - PHI
C  5.    REFERENCES:
C          SEE (3.2) OF TEXT
C********************************************************
       DIMENSION X(N)
       AA = (A - PNU )/SIGMA
       NN1=N1+1
       FA = PHI(AA)
       SCORE = FLOAT(N1)*ALOG(FA)-FLOAT(N-N1)*ALOG(SIGMA)
       DO 10 I=NN1,N
        XX=(X(I)-PNU)/SIGMA
        SCORE=SCORE - XX*XX/2.0
10     CONTINUE
       RETURN
       END
C===================================================
C
       SUBROUTINE DLIKE(N,N1,N2,A,B,X,PNU,SIGMA,SCORE)
C********************************************************
C  1.    DLIKE - FORTRAN 77 SUBROUTINE
C  2.    IT COMPUTES THE LOG-LIKELIHOOD FUNCTION OF A SET OF
C      DATA CONTAINING DOUBLY TRUNCATED OBSERVATIONS  FROM
C      A NORMAL POPULATION WITH MEAN AND STANDARD DEVIATION.
C  3.    PARAMETERS:
C          IN        N   : NO. OF VALUES IN SORTED ARRAY X.
C          A    : LOWER TRUNCATION VALUE.- LOWER DETECTION LIMIT.
C          B    : UPPER TRUNCATION VALUE - MAXIMUM OBSERVABLE VALUE.
C          N1   : NO. OF VALUES BELOW A IN INPUT ARRAY X.
C          N2   : NO. OF VALUES ABOVE B IN INPUT ARRAY X.
C          X    : INPUT ARRAY CONTAINING N SORTED VALUES
C                   IN INCREASING ORDER. THE FIRST N1 VALUES
C                   ARE BELOW A AND THE LAST N2 VALUES ARE ABOVE B.
C          PNU  : MEAN.
C          SIGMA: STANDARD DEVIATION.
C      OUT    SCORE: VALUE OF THE LOG-LIKELIHOOD FUNCTION.
C  4.    SUBROUTINES AND FUNCTIONS REQUIRED:
C          - PHI
C  5.    REFERENCES:
C          SEE (4.2) OF TEXT
C********************************************************
       DIMENSION X(N)
       AA = (A - PNU )/SIGMA
       BB = (B - PNU )/SIGMA

       NN1=N1+1
       FA = PHI(AA)
       FB = 1.0 - PHI(BB)
       SCORE = FLOAT(N1)*ALOG(FA)+FLOAT(N2)*ALOG(FB)
       SCORE = SCORE - FLOAT(N-N1-N2)*SIGMA
       DO 10 I=NN1,N2
        XX=(X(I)-PNU)/SIGMA
        SCORE=SCORE - XX*XX/2.0
10     CONTINUE
       RETURN
       END
```

APPENDIX B

A listing of a sample run. The data are contained in a diskette of A-drive and NAHANI.DAT is the name of the file. The underlined values represent values input through the keyboard.

```
INPUT FILE NAME ? A:NAHANI.DAT
ENTER THE NUMBER OF THE DATA 211
ENTER THE FORMAT OF THE DATA (20X,F5.0)
IS THE LOG-TRANSFORMATION REQUIRED?(Y OR N) Y
ENTER REPLACEMENT VALUE FOR ZERO IN DATA 1.0
ENTER THE LEFT  CENSORING VALUE 10.0
ENTER THE RIGHT CENSORING VALUE  FOR NO RIGHT CENSORING, ENTER 999.0 999.0
SELECT COHENS(1) OR NEWTONS METHOD(2) 1
NO. OF TOTAL OBSERVATIONS = 211
NO. OF OBSERVATIONS BELOW DETECTION LIMIT = 184
ITERATION   MEAN      S.D.    LOG-LIKELIHOOD
     0    -2.27206   4.02643   -99.63292
     1     1.76442    .84597  -190.71930
     2     1.00730   1.46169  -123.14790
     3      .09684   2.18142  -105.18840
     4     -.75248   2.84549  -100.55020
     5    -1.38771   3.33992   -99.54898
     6    -1.79049   3.65281   -99.44080
     7    -1.58050   3.48974   -99.45948
     8    -1.68321   3.56951   -99.44105
     9    -1.73626   3.61071   -99.43862
    10    -1.76323   3.63164   -99.43913
    11    -1.74971   3.62115   -99.43874
    12    -1.74297   3.61592   -99.43864
    13    -1.73962   3.61331   -99.43859
    14    -1.73794   3.61201   -99.43862
    15    -1.73710   3.61136   -99.43864
    16    -1.73752   3.61168   -99.43863
    17    -1.73773   3.61185   -99.43861
USING THE COHENS METHOD
NUMBER OF SAMPLE BELOW DETECTION LIMIT    184
ML ESTIMATES FOR MEAN AND VARIANCE        -1.73773      13.04543
WOULD YOU LIKE TO TRY ANOTHER CENSORING? N
WOULD YOU LIKE TO TRY ANOTHER DATA? N
Stop - Program terminated.
```

150

Stratigraphy and structure of the early Proterozoic Bell Island Group, District of Mackenzie

Project 820009

Ingrid Reichenbach[1]
Precambrian Geology Division

Abstract

The Bell Island Group includes the oldest supracrustal rocks of the Great Bear Magmatic Zone. These rocks lie unconformably on Hottah Terrane and are unconformably overlain by rocks of the Labine Group. The Bell Island Group is a complex sequence, up to 4 km thick, of sub-greenschist facies sedimentary rocks, subaerial basaltic to rhyolitic lava flows and ash-flow tuff, all overlain by pillow basalts and intruded by gabbro sills. The group outcrops from Conjuror Bay in the north to Beaverlodge Lake in the south. The rocks are broadly folded about gently plunging, north-trending axes and cut by northeast-trending dextral transcurrent faults. Prevalent brittle faults with both east-west and north-south trends are, for the most part, compatible with the same stress regime as the transcurrent faults.

Résumé

Le groupe de Bell Island comporte les roches supracorticales les plus anciennes de la zone magmatique de Great Bear. Ces roches reposent en discordance sur le terrain de Hottah et sont elles-mêmes recouvertes en discordance par les roches du groupe de Labine. Le groupe de Bell Island, dont l'épaisseur maximale atteint 4 km, présente une séquence complexe de roches sédimentaires au degré de métamorphisme immédiatement inférieur au faciès des schistes verts, de coulées subaériennes de lave basaltiques à rhyolitiques et de tuf volcanique, le tout reposant sous des basaltes en coussins et pénétré par des filons-couches de gabbro. Le groupe affleure de la baie Conjuror au nord jusqu'au lac Beaverlodge au sud. Les roches sont grossièrement plissées autour d'axes doucement inclinés à orientation nord et coupées par des décrochements dextres à orientation nord-est. Les nombreuses failles cassantes à orientation est-ouest et nord-sud se révèlent, pour la plupart, compatibles avec le même régime de contrainte que les décrochements.

---

[1] The Ottawa-Carleton Centre for Geoscience Studies, Department of Geology, Carleton University, Ottawa, Ontario K1S 5B6

Introduction

The Great Bear Magmatic Zone in western Wopmay Orogen (Fig. 19.1) has been interpreted as a continental magmatic arc (Hoffman and McGlynn, 1977; Hildebrand, 1981). Only in the vicinity of Hottah Lake are the oldest supracrustal rocks of the zone well exposed. These rocks have received no detailed study in the past, although they are of potential regional and volcanological significance. For example, if the rocks are compatible with a continental magmatic arc setting, they provide an excellent and rare opportunity to study the initiation of continental arc magmatism. Conversely, if the origin of these rocks is not compatible with a magmatic arc environment, their tectonic significance will improve the understanding of the regional tectonic evolution.

Geological mapping of these supracrustal rocks at 1:16 000 scale began during the summer of 1983 and was completed during the summer of 1984. This paper describes the units mapped and suggests probable correlations. Earlier work in this area includes that of Kidd (1936), McGlynn (1976, 1979), Wilson (1979) and Hildebrand et al. (1983, 1984).

Acknowledgments

Bell Island Group

The McTavish Supergroup comprises all the supracrustal rocks of Great Bear Magmatic Zone. The lowermost succession of rocks in the supergroup are here named the Bell Island Group after exposures on Bell Island in Hottah Lake. The group is a complex sequence of sub-greenschist facies sedimentary rocks, subaerial basaltic to rhyolitic lava flows and ash-flow tuff, all overlain by pillow basalts and intruded by gabbro sills. These rocks unconformably overlie an older sialic basement complex (Hottah Terrane). In the Hottah Lake area the top of the sequence is not exposed, but a similar succession found in the Conjuror Bay area lies unconformably beneath Moose Bay Tuff, the oldest cauldron complex in that area (Hildebrand, 1984). This upper unconformity marks an abrupt change from: (1) subaqueous to subaerial deposition and (2) tholeiitic to calc-alkaline magmatism. Therefore, the Bell Island Group is formally defined as the stratigraphic succession of supracrustal rocks, and associated sills, outcropping along the east shore of Hottah Lake, from the basal unconformity with Hottah Terrane to the base of the Moose Bay Tuff. For the purpose of this paper, the group will be subdivided into the following informal divisions: lower clastic sequence, mafic to intermediate lavas, bedded tuff, block and ash flows, ash-flow tuff, rhyolite flows, and pillow basalt sequence. Regional extent of the group is shown in Figure 19.1. The major units, calculated thicknesses and probable correlations are shown in Figure 19.2. The succession records a subaerial to subaqueous transition, both laterally and vertically. Outcrop in the Hottah Lake area is plentiful and maximum exposed thickness of the Bell Island Group is on the order of 4 km. The rocks are broadly folded about gently plunging, north-northwest-trending axes; these folds are cut by dextral transcurrent faults of northeast trend. Details of the structure will be discussed in another section.

Lower clastic sequence

The lower clastic sequence is poorly sorted, fining upwards arkose which overlies the deformed and metamorphosed basement. The basal contact is an erosional unconformity (Fig. 19.3) which is well exposed virtually everywhere the Bell Island Group outcrops. Thickness of the unit increases from about 1 m (section 8, Fig. 19.2) to 200 m (section 1, Fig. 19.2) from east to west. Coarse grained, poorly bedded to massive, polymictic, grain-supported conglomerate occurs at the base of the lower clastic sequence. It contains angular to subrounded clasts (up to 15 cm across) of silicic flow-layered lavas, vein quartz, basement granitoids, mafic sedimentary clasts and jasper, and angular potassium feldspar up to 4 cm (Fig. 19.4). Volcanic rocks account for at least one-third of the total fragments. Discontinuous beds (30 to 50 cm thick) contain vein quartz pebbles to near exclusion of anything else. Asymmetric ripples, sparse trough crossbeds and scours are present. The conglomerate is locally underlain by 1-5 m of inversely graded, medium grained sandstone to arkosic granulestone with discontinuous beds (1-15 cm thick), containing about 20% pebbles (up to 6 cm), locally imbricated. The medium grained beds contain pebble-lag deposits. Diffuse heavy mineral bands occur throughout and define trough crossbedding.

Overlying the conglomerate is an arkosic fining-upwards sequence of granulestone, and fine- to medium-grained, sandstone. Granulestone beds occur throughout, but decrease in occurrence upwards. The sequence is well bedded; individual beds fine upwards and are only 3-5 cm thick in the upper part of the unit. Trough cross beds are ubiquitous (Fig. 19.5) and indicate paleocurrents to the west-southwest. Local channels containing conglomerate are 4-5 m across by 1-2 m deep.
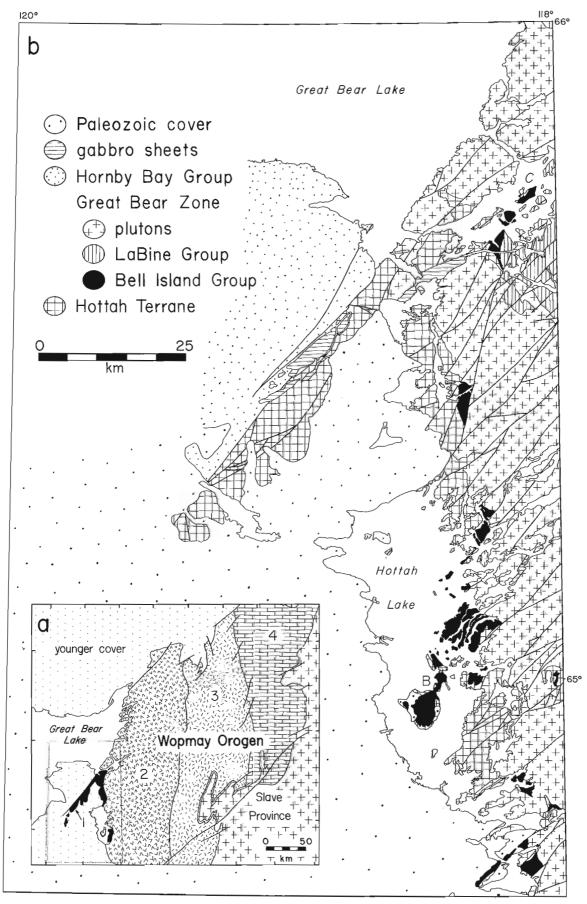
Locally, a well-bedded volcaniclastic unit marks the top of the lower clastic sequence. Beds, 1 mm to 3-4 cms thick, consist of alternating volcanogenic siltstone and wacke. The matrix of the wacke weathers dark grey and is attractively contrasted by angular red volcanic fragments and crystals of quartz, potassium feldspar and plagioclase. Clast size decreases upwards. Trough crossbedding, scours and slumps are common.

The lower clastic sequence is interpreted as a subaerial alluvial fan complex and is probably correlative with the lower member of the Conjuror Bay Formation (arkose, conglomerate, section 1, Fig. 19.2), which Hildebrand (1984) interpreted as marginal marine. Thus, the entire package may represent a fan to marginal marine transition with an alluvial fan to the east and marginal marine facies to the west. The predominance of volcanic fragments in this sequence suggests that sedimentation was synvolcanic.
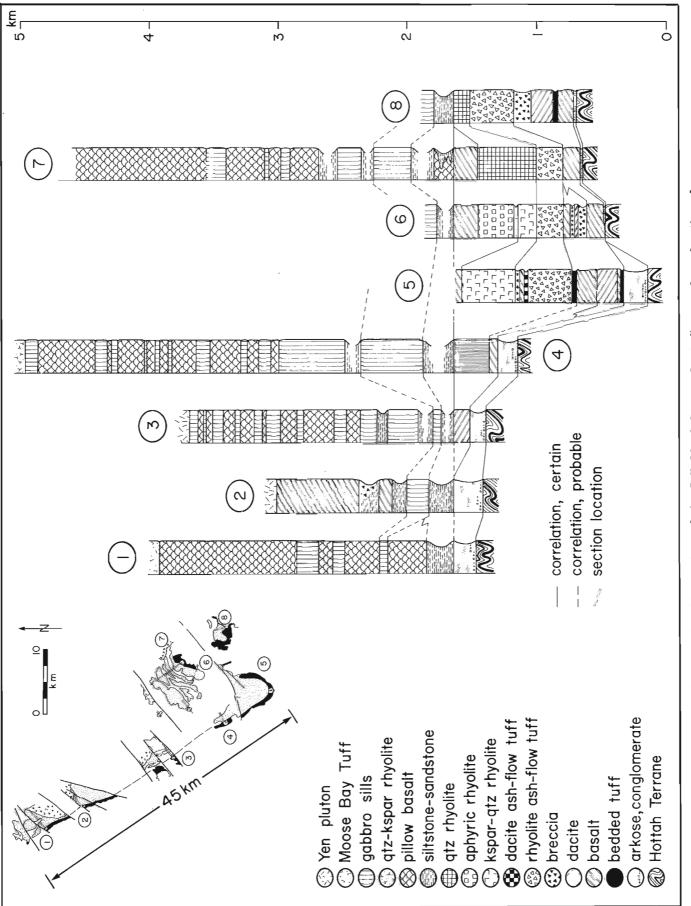
Mafic to intermediate lavas

A variety of lava flows and breccias conformably overlie and interfinger with the lower clastic sequence. Between sections 4 and 5 (Fig. 19.2) two separate basalt flows, probably filling paleovalleys, occur within the lower clastic sequence. Each is approximately 40 m thick and separated by an equal thickness of arkose. For the most part, however, lava flows are present only above the lower clastic sequence. Where they are in contact, rip-ups of sedimentary rocks occur in the basal portions of the lavas.

Except for a few of the overlying pillow basalts for which major element analyses are complete, names used for volcanic rocks are predominately field terms. The majority

Figure 19.1. (a) Generalized location map showing tectonic zones of Wopmay Orogen. 1, Hottah Terrane; 2, Great Bear Magmatic Zone; 3, Internal Zone; 4, External Zone. (b) Geological map showing the distribution of Hottah Terrane, Bell Island Group, Labine Group, Great Bear plutons and younger gabbro sills (after Hildebrand et al., 1983, 1984). B=Bell Island, C̲=Conjuror Bay.

Figure 19.2. Stratigraphic sections of the Bell Island Group. Inset diagram shows location of sections after strike-slip separation on the transcurrent faults is restored. Black, Hottah Terrane; dotted pattern, Bell Island Group; ticked pattern, younger rocks.

of the flows are aphyric and therefore difficult to quantitatively classify. Where phenocrysts are present, potassium feldspar, plagioclase and quartz ratios are used to assign names according to Streckeisen (1967); otherwise, some of the criteria used are textures, such as flow layering and devitrification features, and estimated density. Criteria for distinguishing flow units were basal and flow-top breccias, distribution of amygdules, discontinuities in outcrop and marker units (i.e. tuffs, breccias).

Aphyric lava flows mapped as dacite are the most abundant and outcrop in all areas where the Bell Island Group is exposed, except in the Conjuror Bay area. Some flows are at least 150 m thick and have well developed columnar jointing (Fig. 19.6). Basal portions are coarsely flow-layered parallel to bedding or have platy bases, becoming more massive higher in the flow. Weathering colour is highly variable, but in many places is a brick red to dark purplish brown. Quartz-filled amygdules are plentiful, in places stongly lineated. Flow-top breccias (Fig. 19.7) and striking devitrification features such as spherulites and perlitic fractures are common.

Associated with the dacite flows, but less voluminous, are basalt flows and two plagioclase-phyric flows mapped as andesite. The latter outcrop in eastern Bell Island and in the vicinity of section 4 (Fig. 19.2).

Figure 19.5. *Trough crossbeds, common in the upper part of the lower clastic sequence of the Bell Island Group. (GSC 204113-I)*

Figure 19.3. *Unconformity between Hottah Terrane and the overlying Bell Island Group, to the top of the photo. (GSC 204113-P)*

Figure 19.6. *Columnar jointed dacite flow on central Bell Island. (GSC 204113-U)*

Figure 19.4. *Conglomerate at the base of the lower clastic sequence of the Bell Island Group. (GSC 204113-E)*

Figure 19.7. *Flow top breccia with perlitic fractures in lava flow on central Bell Island. (GSC 204113-N)*

155

Bedded tuff

A good stratigraphic marker horizon is a sequence of light green weathering bedded tuff present almost continuously along eastern and southern Bell Island, central Bell Island and to the east of Bell Island. On east-central Bell Island it conformably overlies sandstone, but to the south interfingers with lava flows where it aids in separating flows. Maximum thickness of the unit is about 12 m. Well defined to diffuse bedding is defined by differences in grain size. Beds containing predominately ash-sized material alternate with lithic-rich layers containing lapilli- and block-sized fragments in an ash matrix. Beds generally range from several millimetres to 3 cm thick, although locally more massive beds are 0.5-2 m. Fragments include angular lithic clasts (less than 1 cm) of flow-layered volcanics and dark green cryptofelsite (originally glass) and crystals of potassium feldspar and clear quartz. Some coarser grained beds contain fragments up to 6 cm. Beds show normal and reverse grading.

Block and ash flows

A peculiar sequence of brick red weathering, monolithologic breccias occurs in east-central Bell Island. At its northern extent, it unconformably overlies the above described bedded tuffs: to the south, it interfingers with dacite flows. Length along strike is 2 km and total thickness is 53 m. The breccia comprises at least 8 units of variable thickness (1-10 m), each with sharp lower and upper contacts. The basal portion of each unit is light green weathering and consists of lapilli-sized red and green fragments in a locally thinly bedded ashy matrix. Excellent inverse grading of the basal portion is marked by a decrease in the amount of matrix and an increase in fragment size (Fig. 19.8). The predominant fragments are subangular to subrounded red boulders that are flow layered, spherulitic, aphyric and amygdaloidal. Fragment size is greater in the uppermost units, commonly 1.5 m across. Lower units also contain angular, dark green cryptofelsite fragments (up to 12 cm) and very sparse vein quartz and granitoid fragments. Upper beds appear massive because fragments are so large and matrix is sparse. The red and green fragments are interpreted to be of similar composition based on younger analogies. The red fragments were probably finely crystalline material that crystallized during cooling, and the green fragments probably formerly glassy material that devitrified at a later date. These units are interpreted as block and ash flows, and are similar to those described by Perret (1935) from Mt. Pelée.

Ash-flow tuff

Conformably overlying the mafic to intermediate lavas is a mineralogically zoned, lithic-poor, terracotta weathering, simple cooling unit of rhyolite ash-flow tuff. Maximum thickness is about 350 m (sections 5-8, Fig. 19.2). Just beneath the tuff is a locally exposed, light green weathering unit which is 2-4 m thick, well-bedded and inversely graded. It mantles the irregular surface of the underlying lava flow. Angular red volcanic fragments (less than 1 cm) and basement quartz are present. This unit may be an airfall tuff associated with the overlying ash-flow tuff.

The base of the ash-flow tuff has a distinctive, coarsely spherulitic(?) texture. Spherulites (up to 15 cm in diameter) occur in continuous contact with one another for several metres going upwards in the flow (Fig. 19.9). Flattened dark red weathering pumice defining a eutaxitic foliation is found only near the base and top of the tuff; pumice is usually 2-3 cm in diameter, although locally it is up to 20 cm in diameter by 5 cm thick. Near sections 6 and 7 (Fig. 19.2),
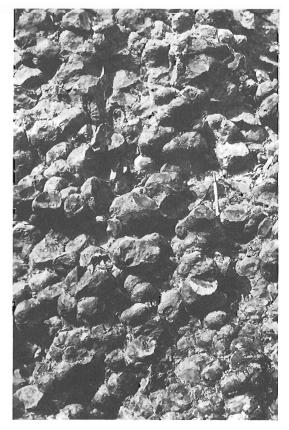

Figure 19.8. *Block-and-ash flow with very fine grained, ashy base and inverse grading marked by an increase in fragment size. (GSC 204113-T)*

Figure 19.9. *Coarse spherulites at the base of ash-flow tuff, northeast of Bell Island. (GSC 204113-M)*

a 10 m thick, light green weathering uppermost zone contains up to 20% highly flattened white pumice. Lithophysal cavities (up to 15 cm in diameter) filled with quartz euhedra are concentrated at the base and top of the tuff. Sparse (3%) angular lithic fragments (usually 5mm, but up to 6 cm) are predominately cognate. Mineralogically, the tuff is zoned, containing less than 1% clear, fractured quartz microphenocrysts near the base, and a maximum of 3-4% quartz (less than 5 mm) and 1% potassium feldspar (less than 1 cm) near the top.

Filling depressions in the irregular upper surface of this cooling unit is a dark brown weathering, lithic-rich, ash-flow tuff. Fractured quartz phenocrysts are sparse (less than 1%). Angular to rounded fragments (1-180 mm) account for up to one-third of the rock. Highly flattened orange and black pumice reach a maximum of 30 cm in diameter.

Rhyolite flows

A series of interfingering rhyolite flows and domes lies conformably above the ash-flow tuff. They are locally separated from the ash-flow tuff(s) by thin arkosic units and basalt flows. The rhyolites range from aphyric to porphyritic. Of the four distinct flows mapped, only two will be discussed here.

The most porphyritic flow, which occurs on central Bell Island (section 5, Fig. 19.2), contains 8% clear, euhedral quartz phenocrysts (2-3 mm) and 6% bladed to blocky potassium feldspar phenocrysts (8 mm). At the base of the flow is a monolithologic flow breccia, which grades into the massive internal lava. It contains amygdaloidal, flow-layered, quartz and potassium feldspar phyric blocks up to one metre across in a light green porphyritic, cryptofelsite matrix. The similarity between the mineralogy of this flow and the underlying ash-flow tuff, suggests that they may be comagmatic.

West of this flow is an aphyric, light grey weathering, finely flow-layered rhyolite (Fig. 19.10). This flow is unique in that its volcanic vent is well exposed. Intrusive to extrusive relationships are illustrated in Figure 19.11. Later faulting bisects the vent and is responsible for an approximately 60° rotation of the northwestern half. Intrusive rhyolite crosscuts bedding of the sedimentary rocks at low stratigraphic levels, and disturbs bedding in the immediate vicinity of the contact. When bedding is restored to the
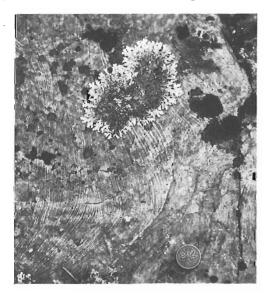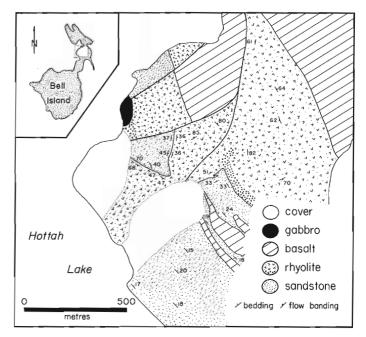
horizontal, the intrusive contact is near vertical. Upsection the contact turns abruptly and the rhyolite conformably overlies the sedimentary rocks. Prominent flow-layers in both the extrusive and intrusive rhyolite parallel the contact immediately adjacent to it, but become convoluted away from it. At the contact, the basal 8 cm of the flow is finely flow-layered, defined by light green and white laminations. In sharp contact with the laminations is a highly vesicular zone 12 cm thick, and then more fine flow-layering. At the base of the flow to the east of the volcanic plug is a light pink weathering flow breccia. It contains from 20-80% fragments (1-12 cm), identical in appearance to the aphyric rhyolite, in a light green matrix. Minor exotic basalt fragments are locally present. The contact with the overlying rhyolite is gradational. This rhyolite may be correlative with the aphyric rhyolite to the east in section 6 (Fig. 19.2). These rhyolites are locally overlain by quartz arenite or subaerial basalt flows.

Pillow basalt sequence

Overlying the rhyolites is a thick sequence of pillow basalts, intercalated sedimentary rocks and breccias, and gabbro sills. They have a lateral extent of 45 km when separation along the transcurrent faults is restored (Fig. 19.2). Exposed thickness, including sills, approaches 3.5 km; original total thickness is unknown, since the sequence is truncated by younger Great Bear plutons.

Sedimentary rocks, most common in the lower portion of the pillow basalt sequence, are very poorly exposed. Thicknesses of 100-200 m are estimated. In contrast to the sedimentary rocks at the unconformity, these units are predominantly planar-bedded, and contain continuous layers 1-15 cm in thickness of siltstone, ashstone, fine grained sandstone and recessively weathering calcareous rock. These layers are internally well-bedded to thinly laminated. Many beds show evidence of soft sediment deformation such as mud rip-ups, slump folds, boudinaged layers and contorted bedding. Low angle crossbedding and ripples are present locally. Where the sedimentary rocks are intruded by gabbro sills the rocks are metamorphosed to the albite-epidote-hornfels facies. The sedimentary structures, lithologies and

Figure 19.10. *Finely flow-layered rhyolite from the vicinity of Figure 19.11. (GSC 204113-L)*

Figure 19.11. *Geological map illustrating rhyolite vent on central Bell Island. Later faulting bisects the vent and has rotated the northwestern half approximately 60°.*

157

association with pillow basalts suggests subaqueous deposition, most likely marginal marine. The sedimentary rocks described here are similar to the upper member of the Conjuror Bay Formation (Hildebrand, 1984) and are probably correlative.

One to two kilometres of pillow basalts are intercalated with and overlie these sedimentary rocks. Contacts between the pillow basalts and underlying lava flows are exposed locally. The lower contact of the pillows with the sedimentary rocks is irregular, with bits of sediment squeezed up between basal pillows. Pillow breccias are common near the contacts and elsewhere in the pillow pile (Fig. 19.12). Hyaloclastite horizons occur locally. Shoreline exposures of the pillows in both cross-section and 3-dimension are excellent. The texture of the pillows varies considerably from nearly aphyric to extremely plagioclase glomeroporphyritic. Phenocrysts and amygdules occur both internally and in the chilled selvages.

The aggregate thickness of gabbro sills is about equal to that of the pillow basalts they intrude. Gabbros form dykes in the basement, oblique sheets in the lower units of the Bell Island Group and sills where they intrude the pillow basalt pile. The sills are more abundant and somewhat thicker near the base of the pillow basalt sequence and may have been high level magma chambers feeding upper parts of the pillow basalt sequence. Textures in the sills vary from

Table 19.1 Chemical analyses of pillow basalts and gabbro sills, Bell Island Group

Sample	83-61	83-56	83-68	83-78	83-60
SiO_2	51.81	53.12	50.33	49.88	50.56
TiO_2	1.20	1.06	1.19	1.18	1.14
Al_2O_3	14.31	15.03	14.40	15.80	14.22
Fe_2O_3	2.40	1.96	2.70	2.26	2.70
FeO	10.34	9.37	10.06	9.03	10.12
MgO	7.05	7.92	6.53	6.99	7.85
MnO	0.25	0.20	0.36	0.21	0.39
CaO	7.92	8.37	10.57	11.39	9.40
Na_2O	4.16	1.02	3.37	2.11	1.73
K_2O	0.29	1.59	0.29	0.90	1.64
P_2O_5	0.15	0.12	0.14	0.14	0.16

Analyses recalculated to 100% on a volatile-free basis

Figure 19.12. *Pillow basalts and associated breccias.* (GSC 204113-O)

Figure 19.13. *Plagioclase glomeroporphyritic gabbro sill.* (GSC 204113-F)

fine grained diabasic to coarse grained plagioclase-glomeroporphyritic (Fig. 19.13). Local pegmatite zones contain pyroxene needles up to 8 cm long. Some sills have calcite-filled amygdules. The plagioclase clots are randomly distributed throughout the sills, although in one location in northeastern Hottah Lake the sills have spectacular alternating phenocryst-rich and phenocryst-poor layers.

In thin section, the majority of the basalts and gabbros have ophitic to subophitic intergrowths of plagioclase and pyroxene, along with magnetite. Olivine has not been observed. The glomeroporphyritic samples contain euhedral to subhedral crystals, in clusters up to 4 cm in size. The light green weathering cores of the clots comprise completely saussuritized plagioclase(?) crystals, surrounded by nearly continuous 1-3 mm rims of unaltered plagioclase.

Table 19.1 presents five analyses of nonporphyritic pillow basalts and gabbros, recalculated to 100% on a volatile-free basis. Total combined CO_2 and H_2O content of these samples ranges from 2.1-4.3 weight per cent. These are olivine and quartz normative tholeiitic basalts. Based on the high total iron content, the rocks represent a somewhat evolved magma. The coupled nature of the Na_2O and K_2O values suggests potassium introduction and sodium loss, which may be a feature of later alteration.

The pillow basalts and gabbro sills are interpreted as comagmatic based on their identical, distinctive, glomeroporphyritic textures. In the Canadian Shield, they are similar to the leopard rocks in the Labrador Trough described by Baragar (1967), however, Cenozoic analogues are unknown by the author. A thick pillow basalt pile, intruded by gabbro sills, occurs in the Conjuror Bay area (Bloom Basalt of Hildebrand, 1984) and is probably correlative with the above described sequence as first suggested by Hoffman and McGlynn (1977).

The highest stratigraphic unit of the Bell Island Group is a finely flow-layered, potassium feldspar- and quartz-phyric rhyolite flow with local brecciated zones (section 4, Fig. 19.2). A gabbro sill intrudes the flow, but no other contacts with underlying rocks were found. Stratigraphic position is based on relative location with respect to other units after separation along the transcurrent faults is restored.

Structure

Rigorous structural interpretations and reconstructions for the Bell Island Group are severely limited due to a lack of kinematic indicators and piercing points, unknown fault plane

orientations and reactivation of pre-existing structures. The oldest deformational structures recognized in rocks of the Bell Island Group are broad gently plunging folds having north-trending axes and minor subsidiary folds on their limbs. The folding affects most of the rocks of the Great Bear Zone, although to the north and notheast the regional trend of the fold axes is more to the northwest. Strain fabric attributed to the folding has only been recognized in bedded tuff: a low angle cleavage that forms an angle of 30-40° with the bedding plane and is steeper than bedding on both fold limbs.

These folds, and all the rocks of the Bell Island Group, are segmented by right-lateral, northeast-trending transcurrent faults typical of those found throughout Wopmay Orogen and interpreted to result from east-west compression (Hoffman and St-Onge, 1981; Tirrul, 1984). The faults, however, are not related to the folds as different strain regimes are necessary to explain their nearly perpendicular respective orientations (Anderson, 1951; Wilcox et al., 1973).

Brittle faults of east-west and north-south orientation affect virtually all the rocks of the Bell Island Group. For instance, in areas with good stratigraphic control, east trending faults having small amounts of displacement are prevalent (Fig. 19.14). For the most part, dips of the fault planes could not be measured. These faults must postdate folding since many of them cut fold axes. The faults could be interpreted as subsidiary strike-slip faults associated with the major transcurrent movements. However, assuming strike-slip displacement, the offset is both sinistral and dextral, which is incompatible with the dextral displacement along the transcurrent faults. A more reasonable interpretation is that they are normal faults, formed perpendicular to the north-south extension direction during transcurrent faulting. It is possible that some of these normal faults are reactivated synvolcanic faults.

Other faults trending north-northeast terminate at an oblique angle to a minor transcurrent fault cutting Bell Island (Fig. 19.14). Relative offset between the faults cannot be

accounted for by dextral strike-slip movement alone. One north-trending fault brings basement rocks over rocks of the Bell Island Group and may be a reverse or thrust fault. Several of the faults have locally developed north-south, steep cleavages along their traces.

One explanation for these faults is that they are earlier structures truncated by the transcurrent fault, but no comparable structures are found to the north on the other side of the fault. A preferred explanation is that both the transcurrent faults and the faults at an oblique angle to them are synchronous. An estimate of the strike-slip separation along the transcurrent fault ranges from 1km in the northeast to close to zero in the southwest. Thus, one model might be that these faults are due to the termination of the transcurrent fault by splaying. The compressional structures (cleavages, reverse faults) of the secondary faults are compatible with this model, according to which the faults occur in an area of compression (cf. Chinnery, 1961). However, left-stepping dextral strike-slip faults also produce compression in the step-over area (Segall and Pollard, 1980; Rodgers, 1980). Unfortunately, there is neither exposure to the south of Bell Island, nor aeromagnetic data, where the left-stepping transcurrent fault would likely continue.

In conclusion, these north-northeast-trending faults are compatible with a syn-transcurrent fault origin. Similarly trending faults that formed obliquely to the transcurrent faults occur elsewhere in the Bell Island Group. These are also interpreted as transcurrent-related structures. Another fabric attributed to the east-west compression is a nearly vertical, north-south cleavage that is well developed only in bedded tuff.

Many of the transcurrent faults that cut rocks of the Bell Island Group have a component of dip-slip movement. Perhaps this is a result of reactivation by a period of normal faulting which is recognized in rocks of the younger Hornby Bay Group (Hoffman and McGlynn, 1977).

No structures have clearly been recognized as synvolcanic. However, Figure 19.2 illustrates that the subaerial lavas are clearly restricted to the southern extent of the Bell Island Group, in contrast to the overlying pillow basalts which are found as far north as Conjuror Bay. A possible interpretation is that the subaerial lavas were erupted in local areas of subsidence. Synvolcanic subsidence is clearly substantiated by the overlying thick pile of pillow basalts which necessitate extension, perhaps with associated normal faulting, during their eruption. Subsidence may have begun during early subaerial volcanism and culminated during, or shortly after, the extrusion of the thick pillow basalt pile. Any synvolcanic structures have likely been reactivated during later episodes of deformation and their origin obscured.

References

Anderson, E.M.
1951: The Dynamics of Faulting; Edinburgh, Oliver and Boyd, 206 p.

Baragar, W.R.A.
1967: Wakuach Lake map-area, Quebec-Labrador; Geological Survey of Canada, Memoir 344.

Chinnery, M.A.
1961: The deformation of the ground around surface faults; Seismological Society of America, Bulletin, v. 51, p. 355-372.

Hildebrand, R.S.
1981: Early Proterozoic Labine Group of Wopmay Orogen: remnant of a continental volcanic arc developed during oblique convergence, in Proterozoic Basins of Canada, ed. F.H.A. Campbell; Geological Survey of Canada, Paper 81-10, p. 133-156.

Figure 19.14. *Simplified geological map of southern Bell Island illustrating faults.*

Legend:
- cover
- gabbro
- rhyolite
- ash-flow tuff
- basalt
- andesite/dacite
- sandstone
- Hottah Terrane

0   2
km

Bell Island

Hildebrand, R.S. (cont.)
  1984: Geology of the Rainy Lake-White Eagle Falls area, District of Mackenzie: Early Proterozoic cauldrons, stratovolcanoes, and subvolcanic plutons; Geological Survey of Canada, Paper 83-20, 42 p.

Hildebrand, R.S., Bowring, S.A., Steer, M.E., and Van Schmus, W.R.
  1983: Geology and U-Pb geochronology of parts of the Leith Peninsula and Riviere Grandin map areas, District of Mackenzie; in Current Research, Part A, Geological Survey of Canada, Paper 83-1A, p. 329-342.

Hildebrand, R.S., Annesley, I.R., Bardoux, M.V., Davis, W.J., Heon, D., Reichenbach, I.G., and Van Nostrand, T.
  1984: Geology of the early Proterozoic rocks in parts of the Leith Peninsula map area, District of Mackenzie; in Current Research, Part A, Geological Survey of Canada, Paper 84-1A, p. 217-221.

Hoffman, P.F. and McGlynn, J.C.
  1977: Great Bear Batholith: volcano-plutonic depression; in Volcanic Regimes in Canada, ed. W.R.A. Baragar, L.C. Coleman and J.M. Hall; Geological Association of Canada, Special Paper 16, p. 170-192.

Hoffman, P.F. and St-Onge, M.R.
  1981: Contemporaneous thrusting and conjugate transcurrent faulting during the second collision in Wopmay Orogen: implications for the subsurface structure of post-orogenic outliers; in Current Research, Part A, Geological Survey of Canada, Paper 81-1A, p. 251-257.

Kidd, D.F.
  1936: Rae to Great Bear Lake, Mackenzie District, N.W.T.; Geological Survey of Canada, Memoir 187.

McGlynn, J.C.
  1976: Geology of the Calder River (86F) and Leith Peninsula (86E) map areas, District of Mackenzie; in Report of Activities, Part A, Geological Survey of Canada, Paper 76-1A, p. 359-361.

McGlynn, J.C. (cont.)
  1979: Geology of the Precambrian rocks of the Riviere Grandin and in part of the Marion River map areas, District of Mackenzie; in Current Research, Part A, Geological Survey of Canada, Paper 79-1A, p. 127-131.

Perret, F.A.
  1935: The eruption of Mt. Pelée 1929-1932; Carnegie Institution of Washington, Publication No. 458, p. 1-125.

Rodgers, D.A.
  1980: Analysis of pull-apart basin development produced by en echelon strike-slip faults; International Association of Sedimentology, Special Publication 4, p. 27-41.

Segall, P. and Pollard, D.D.
  1980: Mechanics of discontinuous faults; Journal of Geophysical Research, v. 85, p. 4337-4350.

Streckeisen, A.L.
  1967: Classification and nomenclature of igneous rocks; Neues Jahrbuch fur Mineralogie Monatshefte, v. 107, p. 144-150.

Tirrul, R.
  1984: Regional pure shear deformation by conjugate transcurrent faulting, externides of Wopmay Orogen, NWT; Geological Association of Canada, Program with Abstracts, v. 9, p. 111.

Wilcox, R.E., Harding, T.P., and Seely, D.R.
  1973: Basic wrench tectonics, American Association of Petroleum Geologists, Bulletin, v. 57, p. 74-96.

Wilson, A.
  1979: Petrology and Geochemistry of the Upper Hottah Lake Sequence, Hottah Lake, District of Mackenzie, Northwest Territories; unpublished B.Sc. thesis, McMaster University, Hamilton, Ontario.

The Elzevir batholith: emplacement history with respect to the Grenville Supergroup and Flinton Group, southeastern Ontario

Project 830009

J.N. Connelly[1]
Precambrian Geology Division

Abstract

The Elzevir batholith margin and surrounding metavolcanic rocks of the Hermon Group (Grenville Supergroup) contain a single, dominant planar and linear fabric parallel to the batholith contact. The fabric is synchronous with the regional fabric in both the Grenville Supergroup and the overlying Flinton Group. Foliation in the metavolcanic rocks is cut by both deformed and undeformed dykes related to the Elzevir batholith, suggesting that deformation was synchronous with emplacement. It is proposed that the Elzevir batholith was emplaced as a radially expanding diapir into a regionally deforming terrane. Foliation trajectory patterns, including foliation triple points, result from interference between the regional strain and the strain caused by the expanding batholith. The Flinton Group may have been tectonically juxtaposed to the Elzevir batholith, after its crystallization, perhaps during the late stages of regional deformation. Discordance between the lineations in these rocks and those in the Northbrook gneiss to the southeast may mark a tectonic break.

Résumé

La bordure du batholite Elzevir ainsi que les roches volcaniques métamorphisées environnantes du groupe d'Hermon (supergroupe de Grenville) comportent une fabrique simple, à prédominance plane et linéaire, parallèle à la zone de contact du batholite. La fabrique est synchrone avec la fabrique régionale, tant dans le supergroupe de Grenville que dans le groupe de Flinton sus-jacent. La foliation des roches volcaniques métamorphisées est entrecoupée par des dykes déformés et non déformés associés au batholite Elzevir, ce qui laisse supposer que la déformation s'est produite en même temps que la mise en place. Le batholite se serait formé tel un diapir en expansion radiale dans un terrain subissant une déformation à l'échelle régionale. La configuration de la foliation, y compris des points triples de foliation, résulte de l'interférence entre la déformation régionale et celle causée par le batholite en expansion. Le groupe de Flinto peut avoir été juxtaposé tectoniquement au batholite Elzevir, après sa cristallisation, probablement au cours des dernières étapes de la déformation régionale. Le manque de concordance entre la linéation de ces roches et celle que l'on retrouve dans le sud-est du gneiss de Northbrook peut-être attribuable à une cassure tectonique.

---

[1]Department of Geological Sciences, Queen's University, Kingston, Ontario K7L 3N6

Introduction

This study examines the structural and metamorphic relationships between the Elzevir batholith and its host metavolcanic and metasedimentary rocks within the Central Metasedimentary Belt of the Grenville Province in southeastern Ontario (Fig. 20.1). The main objectives are to investigate the strain variations within and around this batholith, to establish the structural, metamorphic and tectonic history of the area, and to correlate and integrate previous work. Field work toward these ends was undertaken from June to August 1984.

Geological setting

The area is underlain by rocks of the Grenville Supergroup and its proposed basement, the Kaladar complex, which Chappell (1978) described as a composite mafic intrusive body that is, at least in part, older than adjacent metavolcanic rocks. The Grenville Supergroup is represented by metavolcanic rocks of the Hermon Group and overlying metasedimentary rocks of the Mayo Group. Mafic metavolcanic rocks of the Tudor Formation (Hermon Group) form the dominant host rock of the Elzevir batholith (Fig. 20.2). Metarhyolite within the Hermon Group has given a zircon U-Pb age of 1286 ± 15 Ma[1] (Silver and Lumbers, 1966), and volcanic rocks of the Tudor Formation a whole-rock Rb-Sr isochron age of 1250 ± 90 Ma (Bell and Blenkinsop, 1980). The overlying Mayo Group comprises marble and clastic metasedimentary rocks.

The Grenville Supergroup has been intruded by three distinct plutonic suites, a biotite tonalite-granodiorite suite, a granite suite and a diorite-syenite suite (Fig. 20.2). U-Pb ages for the first two are 1226 ± 25 Ma[1] and 1104 ± 25 Ma[1] respectively (Silver and Lumbers, 1966); whole-rock Rb-Sr isochron ages for the same two suites are 1240 ± 50 Ma and 1060 ± 30 Ma respectively, and for the diorite-syenite suite, 1020 ± 50 Ma (Bell and Blenkinsop, 1980).

The Grenville Supergroup and intrusive rocks of the tonalite-granodiorite and granite suites were considered to be overlain unconformably by metasedimentary rocks of the Flinton Group (Thompson, 1972; Psutka, 1976; Moore and Thompson, 1980). The Flinton Group consists of quartzite pebble conglomerate, psammite, quartzite, pelitic schist, calcite and dolomite marble, and calcareous psammite, and is divided into six formations. It is preserved in long, narrow synclines. Two other units, the Ore Chimney and Skootamatta formations, sparsely distributed at the base of the Flinton Group, are separated from it by a minor unconformity. All units are crosscut by pegmatite dykes, one of which has given a zircon U-Pb age of 1030 ± 20 Ma[1] (Silver and Lumbers, 1966), providing a minimum age for the Flinton Group.

Four major phases of deformation are considered to have affected this area (Venkitasubramanyan, 1969; Thompson, 1972; Psutka, 1976; Chappell, 1978; Moore and Thompson, 1980). Thompson (1972) proposed that deformation had occurred prior to Flinton Group deposition, as indicated by foliated xenoliths within the Elzevir batholith and a related dyke that cuts foliated Hermon Group metavolcanic rocks. He suggested that this deformation (D_x) may have been synchronous with intrusion of the Elzevir batholith.

According to Thompson (1972), the first post-Flinton deformation (D_1) caused isoclinal folding, and was responsible for the dominant fabric (termed S_1 in this paper) throughout the area, producing strong foliation and lineation. Metamorphic textures suggest that D_1 was accompanied by and outlasted the peak metamorphic conditions in the area. Thompson suggested that the Elzevir batholith may have behaved as a relatively rigid body during D_1.

The second post-Flinton deformation (D_2) may have produced the structural grain in the area by refolding D_1 structures and planar elements into their present orientation (Venkitasubramanyan, 1969; Thompson, 1972; Chappell, 1978; this study). Only minor recrystallization occurred during this
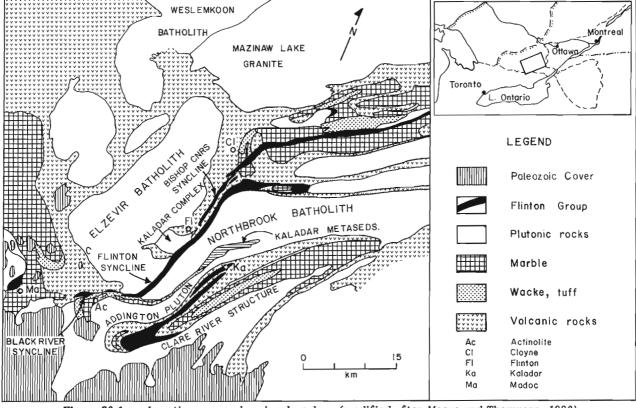

Figure 20.1. *Location map and regional geology (modified after Moore and Thompson, 1980).*

---

[1] U-Pb ages recalculated according to constants of Steiger and Jager (1977)

event, and no pervasive fabrics formed. D_3 deformation is credited with warping the pre-existing structures into map-scale open folds about northwest-southeast axial planes (Fig. 20.1; Thompson, 1972).

Results of field work

Elzevir batholith

The tonalitic Elzevir batholith consists of rocks containing dominant plagioclase and quartz, minor biotite, epidote and muscovite, and subordinate microcline, carbonate, titanite, apatite, amphibole, tourmaline and zircon. An intrusive relationship between the batholith and the Grenville Supergroup is well established by the presence of dykes and xenoliths. In contrast there is no evidence of intrusion into the Flinton Group. On this basis, and also because there is angular discordance between bedding in the Flinton Group and Grenville Supergroup, previous authors have interpreted the contact between the two supracrustal units to be an unconformity. Dykes cut across foliation within Tudor Formation metavolcanic rocks, but are also folded and deformed parallel to the foliation (Fig. 20.3, 20.4). A single planar fabric element is intensely developed within the margin parts of the Elzevir batholith. It dips steeply and

Figure 20.3. *Elzevir dyke crosscutting strongly foliated metavolcanic rocks.*

Figure 20.2. *Geology of the study area. Outlined areas A and B give the locations of Figures 20.9 and 20.10.*

Figure 20.4. *A pinched Elzevir dyke within the foliation of metavolcanic rocks.*

163

strikes parallel to the contact. Toward the core of the batholith, tectonic fabrics are either weakly developed with no systematic orientation, or are absent. The foliation is defined by a planar preferred orientation of biotite and muscovite (Fig. 20.5). Lineations, defined by elongate mineral aggregates, are generally steep and lie in the plane of foliation.

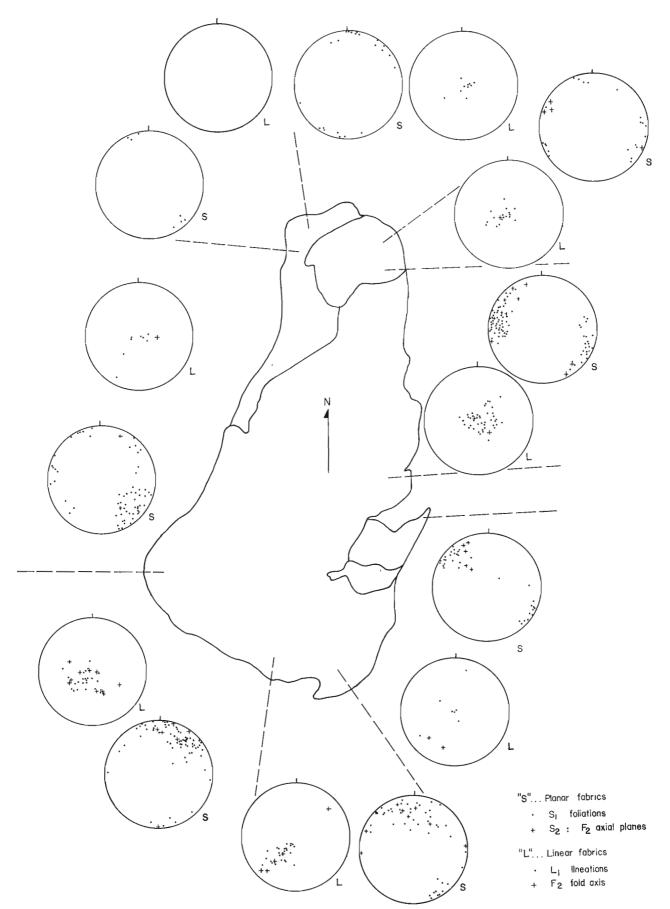**Figure 20.5.** *Elzevir granodiorite; symmetrical foliation observed in the marginal parts of the batholith.*

Figure 20.6. *Generalized foliation trajectory map. Geological contacts correspond to those in Figure 20.2. Marginal numbers here and in Figure 20.7 are UTM co-ordinates from topographic maps NTS 3lC/11 and /14. Areas marked 'L' are characterized by constrictional strain.*

164

Host rocks

One dominant fabric consisting of a strong foliation and lineation is observed in the host rocks. Near the batholith it is concordant to the steep Elzevir fabric (Fig. 20.6, 20.7). Conformity of the foliation to the batholith contact is demonstrated in Figure 20.8, in which orientations of planar and linear fabric elements in each of eight domains around the margin of the batholith are shown in lower hemisphere stereographic projection. Away from the batholith this fabric merges with the northeast regional trend that prevails to the east, south and southwest (Fig. 20.6). Attempts to define two fabrics with crosscutting relationship were unsuccessful; there is no direct evidence to suggest that any tectonic fabric existed prior to S_1. In areas where the Elzevir-parallel foliation and the regional foliation converge, the two become parallel, as detailed by mapping in the Harlowe Road area (Fig. 20.9). Although it is difficult to map the relative intensities of L versus S fabric elements, it is apparent that two domains, to the northeast and southwest of the Elzevir batholith, are dominated by constrictional strain (Fig. 20.6). These areas are marked by a strong, steeply plunging lineation and weak to negligible foliation. The character of the fabric elements varies with metamorphic grade and rock type. Planar fabric elements in the metavolcanic rocks within the lower grade areas west and northwest of the batholith are defined by chlorite (with or without amphibole). In the higher grade areas to the south and east they are defined by preferred orientation of amphibole without chlorite. The dominant D_1 foliation and lineation in the Flinton Group rocks are concordant to the fabric in the metavolcanic rocks, but are defined by

Figure 20.7. *Generalized map showing variation in plunge of L_1 lineations.*

Figure 20.8. *Lower hemisphere stereographs of linear (L) and poles to planar (S) fabric elements around the Elzevir batholith. Only measurements proximal to the batholith are plotted.*
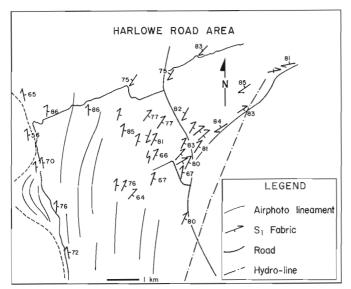
"S"... Planar fabrics

    · S_1 foliations

    + S_2 : F_2 axial planes

"L"... Linear fabrics

    · L_1 lineations

    + F_2 fold axis

Figure 20.9. S_1 fabric map of the Harlowe Road area. See Figure 20.2 for location.

preferred orientation of muscovite and deformed pebbles as well as amphibole. Many localities show S_1 overprinted by randomly oriented amphibole or biotite metacrysts. This relationship is consistent with Thompson's (1972) conclusion that metamorphism in the Flinton Group peaked, or at least continued, after the main fabric-forming deformation (D_1).

The D_1 fabrics have been affected by D_2, thought to be responsible for the final orientation of S_1 and L_1. Although S_2 foliation is rare, S_1 is folded into tight northeast trending folds that are coaxial with L_1 elongation.

In addition to this polyphase history, there is a distinct break in lineation orientations between the southeast Elzevir batholith margin and the Northbrook gneiss to the east-southeast (Fig. 20.7), a tonalitic orthogneiss similar in composition to the Elzevir tonalite. The steep lineation that dominates the area surrounding the Elzevir batholith changes abruptly to shallow, whereas the foliations on either side of this break have parallel strikes.

Discussion

Thompson (1972) concluded that pre-Flinton fabrics were locally preserved in and around the Elzevir batholith but were transposed into the regional S_1 trend south and east of the batholith so that they are now parallel to the dominant fabric within the Flinton Group. Given that the dominant fabric within the Tudor metavolcanic rocks is conformable to S_1 in the Flinton Group, and that both supracrustal units have a similar metamorphic history, it seems more reasonable to suggest that Tudor and Flinton fabrics are the same age. Accepting this, it becomes apparent that the Elzevir batholith could not have been a rigid body during D_1: the metavolcanic rocks southwest of the batholith have been flattened parallel to the Elzevir contact, in an area where strain shadow effects would be expected if the batholith had behaved rigidly (Fig. 20.10). The Elzevir-parallel fabric found around the batholith suggests that shortening has occurred perpendicular to the contact in response to a lateral expansion of the intrusion. The foliations within the Elzevir margin are symmetrical flattening foliations. This suggests that asymmetrical simple shear was not operative along the margins at this time. The Elzevir dyke relationships suggest that the dykes were emplaced late during the deformation that created the Elzevir-parallel foliation.

Figure 20.10. S_1 fabric orientation in the area southwest of the Elzevir batholith. See Figure 20.2 for location.

The implications of these observations are twofold: (1), if the fabrics in the Grenville Supergroup and Flinton Group are the same, and Elzevir dykes crosscut this fabric, the Flinton Group could not have been deposited unconformably on the Elzevir batholith, and (2), as no dykes are observed in the Flinton Group, it seems unlikely that the Flinton Group could have been juxtaposed against the batholith during its final stages of crystallization. The Elzevir batholith may have been intruded into its final position as a diapir expanding into a regionally deforming terrane. The radial expansion created the contact-parallel fabric close to the batholith, while regional shortening produced the northeast-southwest fabric to the south and east.

Brun and Pons (1981) have described the Sierra Morena pluton in southern Spain as a diapirically emplaced pluton within a regionally deforming terrane. They described the regional fabric as merging with the pluton-parallel fabric where the two meet at low angles, and as forming foliation triple points where they meet at high angles. The areas dominated by constrictional strain, southwest and northeast

of the Elzevir batholith, may be foliation triple points. The foliation patterns and areas of constrictional strain may be interpreted as a result of interference between the strain caused by the expanding diapir and the regional strain. If the Elzevir batholith stopped expanding before regional deformation was complete, the Flinton Group may have been emplaced tectonically next to the already crystalline batholith during a later stage of regional deformation. Although this conclusion contradicts that of Thompson (1972), it is consistent with his observations. The basal contact of the Flinton Group is nowhere clearly exposed and further work will be required to investigate this zone for more direct evidence concerning the relationship between the Grenville Supergroup, the Flinton Group and the Elzevir batholith.

The lineation discordance between the Flinton Group and the Northbrook gneiss to the east-southeast may represent a large-scale tectonic break. The foliation in the Northbrook gneiss, compared with the generally massive structure of the interior of the Elzevir batholith, represents an abrupt change in strain intensity.

Conclusions

The Hermon Group metavolcanic rocks of the Grenville Supergroup adjacent to the Elzevir batholith possess strong planar and linear fabric elements parallel to the batholith contact. Within the batholith margins there are also strong planar and linear fabric elements that are concordant to those in the surrounding metavolcanic rocks. Away from the batholith on its south and east sides, fabric elements trend northeast and appear to be synchronous with the fabric in the Flinton Group. Deformed and undeformed Elzevir dykes cut across this fabric in the Hermon Group. These relationships suggest that the Elzevir batholith was emplaced as a radially expanding diapir into a regionally deforming terrane. Furthermore, if these post-Flinton fabrics were created in part by the emplacement of the batholith, the Flinton Group cannot have overlain the batholith unconformably. It is proposed that the Flinton Group was tectonically emplaced against the Elzevir batholith after final crystallization, possibly during the late stages of the regional D_1 deformation.

Acknowledgments

References

Bell, K. and Blenkinsop, J.
1980: Whole-rock Rb-Sr studies in the Grenville Province of southeastern Ontario and western Quebec – a summary report; in Current Research, Part C, Geological Survey of Canada, Paper 80-1C, p. 152-154.

Brun, J.P. and Pons, J.
1981: Strain patterns of pluton emplacement in a crust undergoing non-coaxial deformation, Sierra Morena, southern Spain; Journal of Structural Geology, v. 3, p. 219-229.

Chappell, J.F.
1978: The Clare River structure and its tectonic setting; unpublished Ph.D. thesis, Carleton University, Ottawa, Ontario, 184 p.

Moore, J.M., Jr. and Thompson, P.H.
1980: The Flinton Group: a late Precambrian metasedimentary succession in the Grenville Province of eastern Ontario; Canadian Journal of Earth Sciences, v. 17, p. 1685-1707.

Psutka, J.F.
1976: Provenance of the plutonic pebbles in the Kaladar metaconglomerate and geology of the associated metasediments; unpublished B.Sc. thesis, Carleton University, Ottawa, Ontario, 62 p.

Silver, L.T. and Lumbers, S.B.
1966: Geochronological studies in the Bancroft – Madoc area of the Grenville Province, Ontario, Canada; Geological Society of America, Special Publication 87, p. 156 (abstract).

Steiger, R.H. and Jager, E.
1977: Subcommission on geochronology: convention on the use of decay constants in geo- and cosmochronology; Earth and Planetary Science Letters, v. 36, p. 359-362.

Thompson, P.H.
1972: Stratigraphy, structure and metamorphism of the Flinton Group in the Bishop Corners – Madoc area, Grenville Province, eastern Ontario; unpublished Ph.D. thesis, Carleton University, Ottawa, Ontario, 268 p.

Venkitasubramanyan, G.S.
1969: Large scale superimposed folds in Precambrian rocks of the Actinolite – Kaladar area, southeastern Ontario; unpublished Ph.D. thesis, Queens University, Kingston, Ontario, 222 p.

An occurrence of pre-McConnell nonglacial sediments, Selwyn Mountains, Northwest Territories

Project 800001

L.E. Jackson, Jr., G.M. MacDonald[1], A.E. Foscolos[2], and A.H. Clarke[3]
Terrain Sciences Division, Vancouver

Abstract

Nonglacial sediments that predate the McConnell Glaciation have been found in the O'Grady Lake area, Northwest Territories, near the Yukon boundary. The marls, siltstones and gravels were probably deposited in a lacustrine environment. The constituent assemblages of fossil pollen and molluscs indicate an interglacial or Neogene climate during deposition. The sediments have been tilted; however, their limited exposure precludes a definite explanation of this disturbance.

Résumé

Des sédiments non glaciaires antérieurs à la glaciation de McConnell ont été trouvés dans la région du lac O'Grady, dans les Territoires du Nord-Ouest, près de la frontière du Yukon. Les marnes, <<siltstones>> et graviers ont probablement été déposés en milieu lacustre. Les assemblages de pollens et de mollusques fossiles qu'ils renferment indiquent que la sédimentation a eu lieu sous un climat interglaciaire ou néogène. Les sédiments ont subi un basculement, mais le peu qui affleure ne permet pas aux auteurs de se prononcer avec certitude sur la cause de cette perturbation.

[1] Department of Geography, McMaster University, Hamilton, Ontario L8S 4M1
[2] Institute of Sedimentary and Petroleum Geology, Calgary, Alberta T2L 2A7
[3] Ecosearch Inc., Mattapoisett, Massachusetts, U.S.A.

Introduction

Exposures of nonglacial sediments predating the last (McConnell) glaciation are rare in areas of southern Yukon Territory that were glaciated during that glacial episode. Those that have been described are restricted to broad low-lying areas such as Liard Plain (Klassen, 1978). While broad lowland valleys are topographically suited for accumulating glacial and interglacial deposits, the area of mountainous divide between Yukon Territory and Northwest Territories would seem singularly unsuited for preserving unconsolidated deposits older than the last glaciation. Newly discovered preglacial or interglacial deposits in the O'Grady Lake area of the Selwyn Mountains provide paleoenvironmental information.

Acknowledgments

We would like to express their appreciation to A.R. Cameron and A.R. Sweet of the Institute of Sedimentary and Petroleum Geology, Calgary, Alberta, for supporting analyses. Thanks are expressed to Mark Pawson for his work as field assistant. We also gratefully acknowledge critical review by R.J. Fulton whose comments improved this report; all interpretations are the responsibility of the authors.

Setting

The sediments described occur on the west side of a roughly elliptical intramontane depression, 16 km east of the Yukon-Northwest Territories border (Fig. 21.1). O'Grady Lake (approximately 1280 m elevation) lies in its southeastern quadrant. This depression will be referred to as the O'Grady basin. The O'Grady basin forms the headwaters of Natla River. The section to be discussed is exposed along the outside of a bend in an unnamed tributary of Natla River (Fig. 21.2) at approximately 1370 m elevation. Peaks adjacent to the O'Grady basin rise to 2290 m. Vegetation in the area is dominated by dwarf birch (**Betula gladulosa**). The site lies approximately 150 m above the upper limit of boreal forest in this area.
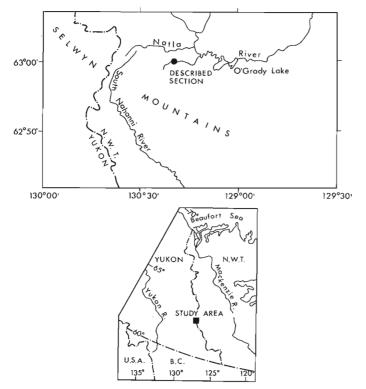

Figure 21.1. Location map of study site.

General geology

The uplands surrounding the O'Grady basin are composed of Devonian to Mississippian clastics which have been complexly folded and intruded by Cretaceous-age felsic plutons (Green et al., 1967; Blusson, 1971; Gordey, 1981). The O'Grady basin is underlain by unconsolidated glacial and alluvial deposits.

The area was intensely glaciated during the McConnell glaciation which ended locally by approximately 10 000 BP (Jonasson et al., 1983; MacDonald, 1983). During this episode, ice flowed north into the basin from an ice centre somewhere over the South Nahanni River basin to the south (L.E. Jackson, Jr., unpublished data).

Section description

The nonglacial deposits are obscured by colluvium and underlie a 13.5 m-high steep slope (Fig. 21.2). The slope is unconformably capped by terraced glaciofluvial gravels. The colluvium is composed of sediments reworked from the underlying section and glaciofluvial gravels eroded from the top of the slope. The only surficial indication of these deposits was the presence of scattered fragments of lignified wood within the overlying colluvium. The first trench through the colluvium was made in 1980; this was widened and deepened in 1982. Figure 21.3 depicts the stratigraphy and lithology of the sediments. Although approximately 12 m of section was revealed, this proved to be an apparent thickness. The beds dip at from 24 to 27° towards the east so that their true thickness is approximately 3 m. The nonglacial sediments included interbedded marls, claystone, siltstone, and deeply weathered gravels. The gravels are composed of siltstone and sandstone clasts. Lignified wood and stringers of lignite are abundant. Discontinuous lenses of goethite concretions are associated with lignite lenses. Marls above 200 cm were locally rich in gastropod remains, whereas the lower marl between 0 and 50 cm was barren. These nonglacial sediments are unconformably overlain by a few metres of colluvium and terraced glaciofluvial gravels. The base of the nonglacial deposits was not observed.

The fine grained and marly nature of the sediments, along with the presence of lignified wood and plentiful fresh water molluscs, indicates a nearshore lacustrine depositional environment. The two gravelly beds probably represent sporadic influxes of coarse sediment carried by small streams entering the lake.

A number of analyses were carried out in order to extract paleoenvironmental information from these deposits and to determine their age. These are discussed below.
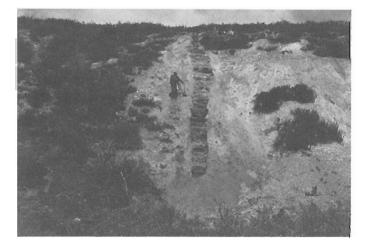

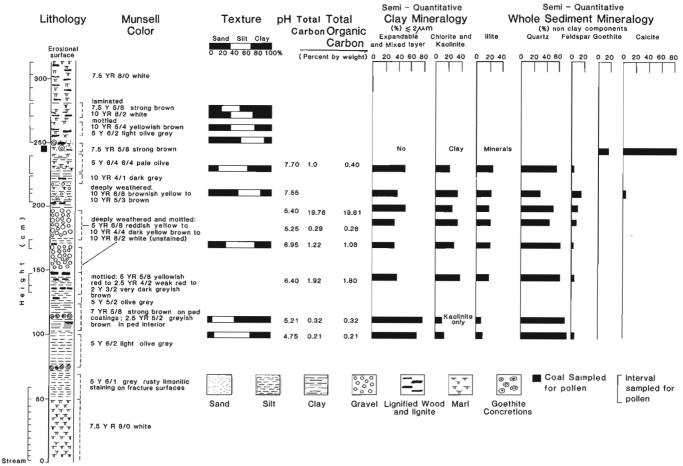*Figure 21.2. The section described in the text.*

Figure 21.3 (stratigraphy chart)

Lithology | Munsell Color | Texture | pH | Total Carbon | Total Organic Carbon | Semi – Quantitative Clay Mineralogy (%) ≤ 2μm | Semi – Quantitative Whole Sediment Mineralogy (%) non clay components

Texture: Sand Silt Clay 0 20 40 60 80 100%

Clay Mineralogy columns: Expandable and Mixed layer | Chlorite and Kaolinite | Illite

Whole Sediment Mineralogy columns: Quartz | Feldspar | Goethite | Calcite

Total Carbon / Organic Carbon (Percent by weight)

Erosional surface

300 —
7.5 YR 8/0 white

laminated
7.5 Y 5/8 strong brown
10 YR 8/2 white
mottled
10 YR 6/4 yellowish brown
5 Y 6/2 light olive grey

250 —
7.5 YR 5/8 strong brown

5 Y 6/4 6/4 pale olive — 7.70 | 1.0 | 0.40

10 YR 4/1 dark grey

deeply weathered:
10 YR 6/8 brownish yellow to
10 YR 5/3 brown — 7.55

200 —
5.40 | 19.76 | 19.61

deeply weathered and mottled:
5 YR 6/8 reddish yellow to
10 YR 4/4 dark yellow brown to
10 YR 8/2 white (unstained) — 5.25 | 0.29 | 0.28
6.95 | 1.22 | 1.08

150 —
mottled: 5 YR 5/8 yellowish red to 2.5 YR 4/2 weak red to 2 Y 3/2 very dark greyish brown — 6.40 | 1.92 | 1.80

5 Y 5/2 olive grey

7 YR 5/8 strong brown on ped coatings; 2.5 YR 5/2 greyish brown in ped interior — 5.21 | 0.32 | 0.32

100 —
5 Y 6/2 light olive grey — 4.75 | 0.21 | 0.21

5 Y 6/1 grey rusty limonitic staining on fracture surfaces

50 —
7.5 YR 8/0 white

Stream 0 —

Legend: Sand | Silt | Clay | Gravel | Lignified Wood and lignite | Marl | Goethite Concretions | ■ Coal Sampled for pollen | Interval sampled for pollen

No Clay Minerals
Kaolinite only

Figure 21.3. *Stratigraphy and lithology of the described section.*

Palynology

Twenty-four samples were taken from intervals indicated in Figure 21.3. Separation of palynomorphs and analysis were carried out by G.M. MacDonald at the University of Toronto. Palynomorph extraction was facilitated through the use of sodium pyrophosphate suspension and sieving technique outlined by Cwynar et al. (1979). Absolute pollen concentrations were calculated through the use of the **Lycopodium** spore method described by Stockmar (1972). Only three samples yielded palynomorphs. Preservation of palynomorphs in these samples is generally poor, the per cent contents of identifiable palynomorphs are illustrated in Figure 21.4.

Interpretation of the palynological data is hampered by a lack of knowledge regarding the preglacial or interglacial paleoenvironmental history of the Mackenzie and Selwyn mountains. Attempts to compare and correlate the sparse data from the O'Grady Lake section with the possibly age-equivalent, but geographically distant, Porcupine River section described by Lichti-Federovich (1973) or Eocene Old Crow palynoflora (Hopkins and Norris, 1974; Hopkins et al., 1975) would be questionable. Additional constraints to the interpretation of the O'Grady Lake section lie in a lack of detailed knowledge regarding the depositional setting of the pollen grains and their poor preservation. On the basis of the pollen assemblages obtained from the O'Grady Lake section, however, a few generalizations regarding paleoenvironmental conditions may be drawn. These interpretations are aided through comparison of the fossil pollen spectra with a suite of modern pollen surface samples from the region (MacDonald, 1983).

The high relative frequency of **Picea** and **Pinus** in comparison with **Betula**, which is exhibited in the lower two samples, indicates the presence of a boreal type forest, occurring under slightly warmer conditions than those today. This view is consistent with the marly nature of the sediment. The pollen assemblage derived from the upper sample is markedly different from the lower two (Fig. 21.4). The increase in the relative importance of **Betula**, Cyperaceae, and Gramineae in respect to **Picea** and **Pinus** suggests a setting dominated by a cooler climate similar to present conditions. The significant decrease in absolute pollen concentrations might reflect an increase in sedimentation rate and a decrease in vegetation cover.

Paleontology

Mollusc remains were collected from marly beds and small coquina lenses over the upper 100 cm of the section. Four genera were present; three of these were identified to the species level. These are **Physa jennessi** Dall, **Sphaerium nitidum** Clessin, **Sphaerium (Musculium)** cf. **lacustre** (Muller), and **Valvata** sp. The identification of **S. lacustre** is somewhat uncertain. Only one or two fragmentary specimens were present.

P. jennessi and **S. nitidum** and the genus **Valvata** are wide ranging in the low arctic and subarctic parts of Canada. **S. lacustre** ranges throughout the boreal forest region but not north of treeline (Clarke, 1981). These taxa indicate a northern environment, probably a boreal forest environment based upon the occurrence of **S. lacustre**. This corroborates the palynological data.
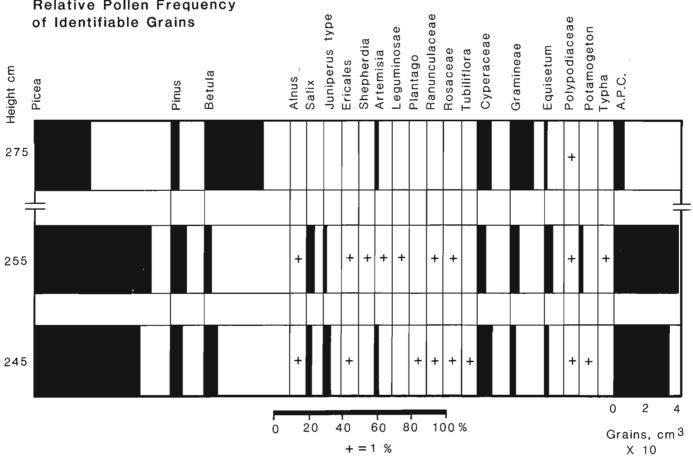
171

O'Grady Lake Section
Relative Pollen Frequency
of Identifiable Grains

Height cm

Picea · Pinus · Betula · Alnus · Salix · Juniperus type · Ericales · Shepherdia · Artemisia · Leguminosae · Plantago · Ranunculaceae · Rosaceae · Tubiliflora · Cyperaceae · Gramineae · Equisetum · Polypodiaceae · Potamogeton · Typha · A.P.C.

275

255

245

0 20 40 60 80 100 %
+ = 1 %

0 2 4

Grains, cm3
X 10

Figure 21.4. Per cent content of identifiable palynomorphs from the three productive horizons.

Coal petrology and palynology

Lignite occurs as discrete angular chunks of lignified wood up to 10 cm in maximum dimension and thin lenses or partings. No identification of the wood was possible. Petrographic and palynologic studies of the coal were undertaken to determine coal rank, burial depth, and autochthoneity of coal through comparison of coal and sediment palynomorphs. The latter determination was necessary because the lenticular nature of the coal stringers and the presence of discrete chunks of lignified wood in this section made it unclear as to whether they were coalified in place or allochthonous.

Reflectance studies of the lignite were carried out by A.R. Cameron of the Institute of Sedimentary and Petroleum Geology, Calgary. Coal rank was found to be at the bottom of the lignite range — too low to permit any determination of past maximum burial depth. The woody tissue within the lignite was found to fluoresce under ultraviolet irradiation, indicating that some unaltered cellulose may still be preserved within cell walls.

Pollen was separated from one coal stringer (Fig. 21.3) and analyzed by A.R. Sweet of the Institute of Sedimentary and Petroleum Geology, Calgary; the taxa identified are listed in Table 21.1. The palynomorph preservation permits only a crude estimate of its age as Cenozoic and sheds no light upon whether the coal is autochthonous or allochthonous.

Sediment texture, chemistry, and mineralogy

During initial (1980) excavation of the section, one of the most striking features exposed was a coloured bed of strong brown (7.5 YR 5/8) claystone between 100 and 120 cm above the base of the exposure (Fig. 21.3). This bed was suspected to be the B horizon of a paleosol (Jackson et al., 1982). Sediment texture, chemistry, and mineralogy of the highly coloured bed were investigated because paleosols have proven to be valuable in interpreting paleoclimate (e.g., Foscolos et al., 1977).

Weight percentages of sand, silt, and clay were determined for the coloured bed and other fine grained units elsewhere in the section. The coloured bed is significantly richer in clay than both the sediments that directly overlie it and underlie it (Fig. 21.3). The mineralogy of whole sediment (less than 2 mm) and clay fraction (less than 2 µm) samples was determined by X-ray diffraction (XRD) (Fig. 21.3). Relative semiquantitative mineral percentages were determined from relative XRD peak heights (Fig. 21.5). With the exception of the coloured bed and the iron concretion-bearing horizon, the whole sediment fractions are dominated by quartz (30 to 75 % of the sediment). Feldspar content ranges from 2 to 15%. Calcite is confined to marly bands and goethite is confined to the concretion-bearing horizon. The balance of the whole sediment fraction is clay minerals; their percentages are not plotted in the whole sediment fraction but can be determined by subtracting the total contents of nonclay minerals from 100%.

Table 21.1. Identifiable taxa extracted from coal

Alnus sp. (rare)
Betula sp. (rare to scarce)
Corylus sp. (scarce)
Cupressaceae – Taxodiaceae pollen (common)
Deltoidospora sp. (rare)
Ericaceous pollen (rare to scarce)
Iridaceous (?) pollen (scarce)
   (a small, monocolpate, reticulate grain with spines
   on the muri)
Laevigatosporites sp. (common)
   (probably spores of Polypodiaceous ferns)
Miscellaneous tricolpate pollen (scarce)
Miscellaneous bisaccate pollen (scarce)
   (including **Pinus, Abies,** and possibly **Picea**)

The clay size (less than 2 μm) fraction, with the exception of the coloured bed, is composed of quartz, kaolinite, chlorite, illite, and a low swelling 2:1 layered clay. The semiquantitative relative percentages of clay minerals in the clay size fraction are presented in Figure 21.3. The quartz content of the clay size fraction is not shown but can be determined by subtracting clay totals from 100%. Diffractograms of clay fraction samples from the coloured bed and underlying unit are shown in Figure 21.5. Quartz is confirmed by the d_{100} 0.333 nm peak; traces of chlorite is from the d_{001} peak at 1.40 nm; illite by a d_{001} peak at 1.00 nm in the specimens. The illite is interstratified with chlorite as indicated by shoulder trailing off to 1.40 nm from the illite peak following heating to 550°C. The low swelling 2:1 layered (vermiculitic) clay is identified by its expansion to 1.40 nm under both calcium and potassium glycerol solvation. The low swelling 2:1 layered clay collapses to 1.00 nm at 0% relative humidity and upon heating to 550°C.

The coloured bed also contains kaolinite and illite, trace amounts of feldspar, and no chlorite. The 2:1 layered clay in the coloured bed is a high swelling (montmorillonitic) variety that expands to 1.80 nm following Ca and glycerol solvation. A low cation exchange capacity is indicated by the shifting of the d_{001} peak for this mineral to 1.40 nm following Ca solvation under a 50% relative humidity, and to 1.00 nm following treatment with K solution and exposure to 0% relative humidity atmosphere. Its overall behaviour indicates it is an alteration product of the low expandable 2:1 layered clay present in the underlying sediment.

With the predictable exception of the marly horizons, saturated paste extracts of these sediments were found to be acidic. The coloured bed and underlying sediment were especially acidic at pH 5.21 and 4.75, respectively. The coloured bed is significantly enriched in total amorphous iron (Jackson, 1965). The amorphous Al_2O_3/Fe_2O_3 ratio is 1.5 in the underlying sediment and 0.8 in the coloured bed. Total organic carbon (Foscolos and Barefoot, 1970) is also elevated in the coloured bed with respect to the underlying sediment. Conversely, it is depleted in water soluble calcium and potassium. Sodium is present in trace amounts in both horizons.

The tentative conclusions following initial field description in 1980, and on the basis of the above analyses, were that the coloured bed is a paleosol. The colour, enrichment of iron, loss of chlorite presumably by acid solutions from higher in the now eroded profile, alteration of the low expansive 2:1 (vermiculitic) clay of the underlying sediment to a high expansive 2:1 (montmorillonitic) clay in the coloured band, and enrichment in clays and organics are indicative of pedogenesis (Jackson et al., 1982). However, re-excavation of the trench in 1982 and further examination of the coloured band in monolith revealed that the dark colour is present only on the outside of peds. Thus the

apparent enrichment of iron is probably only a ped surface phenomenon. Since the bed dips at more than 20°, iron deposition could have resulted from lateral rather than vertical flow of soil water from the surface. Chlorite dissolution and removal of potassium from the low expanding 2:1 layered silicate could also have occurred in this way (J. Dormaar, personal communication, 1982). The other chemical and textural properties may have simply been initial properties of the bed.

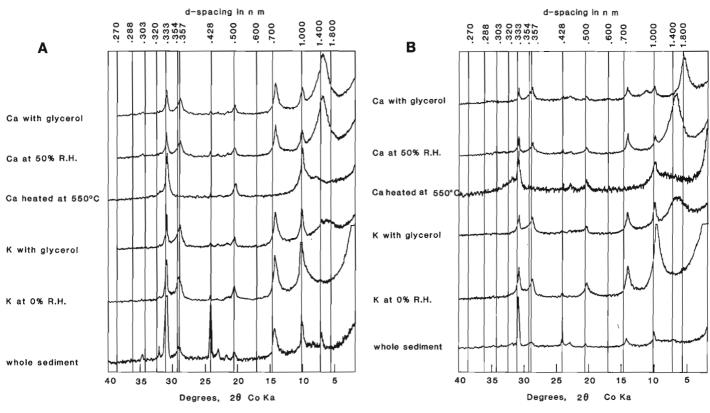In conclusion, identification of the coloured bed as a paleosol remains conjectural.

Age

The Paleogene climate of the interior of British Columbia and northern Yukon was warm-temperate to subtropical (Rouse et al., 1970; Hopkins et al., 1972, 1975; Hopkins and Norris, 1974). It supported a broadleaf evergreen forest. The boreal forest pollen assemblage in the noncoal sediments contrasts sharply with described Paleogene assemblages, suggesting a late Neogene or Quaternary age. It is unlikely that the assemblage described from the O'Grady basin could reflect a Paleogene montane climate because warm-temperate forests existed in the northern Rocky Mountain Trench during this time (Hopkins et al., 1972). Although it is not known when the extant species of molluscs recognized in these sediments first appeared, they are northern-ranging and again suggest a Neogene or Quaternary age for these sediments.

Whereas faunal evidence suggests a maximum Neogene age for these sediments, geomorphic evidence suggests that they predate the last glaciation by a significant degree. First, no granitic pebbles are present in the gravels exposed in the section, despite extensive exposures of granitic rocks only 6 km upstream today. This suggests that extensive changes in drainage patterns have occurred and/or the granites had not been unroofed at the time these sediments were deposited. Either or both possibilities suggest a considerable minimum age for these deposits. Secondly, the occurrence of partially lithified sediments beneath an erosional unconformity capped by a thin cover of unconsolidated colluvium and glaciofluvial sediments demands significant burial followed by uplift or a change in local base level and erosion. This sequence of events would require an unknown but presumably significant period of time and supports the first line of geomorphic evidence. Whatever the absolute age of these sediments, however, their constituent pollen and mollusc assemblages indicate interglacial if not preglacial climatic conditions during deposition. Thus they must date from or predate marine oxygen isotope stage 5 (more than about 70 000 years; Kukla, 1977) which marked the last interglacial period.

Possible causes of bedding inclination

If the sediments exposed in this section are Quaternary or late Neogene in age, then tilting of these sediments is geologically recent. Three causes for this tilting are likely: glacial overriding, landsliding, and tectonic activity. The passage of glacial ice has disturbed both bedrock and unconsolidated sediments in many areas (e.g., Moran et al., 1980). As previously noted, the limited exposures of these sediments indicate a homoclinal dip. Consequently, glacially induced folding can be ruled out; however, low angle thrusting cannot. Although the general direction of ice flow into the basin was at about 90° to the direction of dip, the local detailed history of ice flow in the basin is not apparent and exposures of the base of this sequence are nonexistent. Similarly, the sediments could just as easily be part of an erosional remnant of a large landslide and have been tilted during movement. Exposures are simply inadequate to reject

A

d-spacing in n m
.270 .288 .303 .320 .333 .354 .357 .428 .500 .600 .700 1.000 1.400 1.800

Ca with glycerol

Ca at 50% R.H.

Ca heated at 550°C

K with glycerol

K at 0% R.H.

whole sediment

40 35 30 25 20 15 10 5

Degrees, 2θ Co Kα

B

d-spacing in n m
.270 .288 .303 .320 .333 .354 .357 .428 .500 .600 .700 1.000 1.400 1.800

Ca with glycerol

Ca at 50% R.H.

Ca heated at 550°C

K with glycerol

K at 0% R.H.

whole sediment

40 35 30 25 20 15 10 5

Degrees, 2θ Co Kα

Figure 21.5

X-ray diffractograms of sediments discussed in the text: A. sediments underlying the coloured band; B. the coloured band.

this hypothesis. Deformation due to neotectonic activity would not be unexpected because the Selwyn and Mackenzie mountains are one of the most seismically active regions in the Canadian north (Basham et al., 1977). Holocene faulting has been identified in the Mackenzie Mountains and earthquake activity has been implicated in sturtzstrom activity in that area (Eisbacher, 1979).

References

Basham, P.W., Forsyth, D.A., and Wetmiller, R.J.
1977: The seismicity of northern Canada; Canadian Journal of Earth Sciences, v. 14, p. 1646-1667.

Blusson, S.L.
1971: Sekwi Mountain map area, Yukon Territory and District of Mackenzie; Geological Survey of Canada, Paper 71-22, 17 p.

Clarke, A.H.
1981: Freshwater molluscs of Canada; National Museum of Canada, 417 p.

Cwynar, L.C., Burden, E., and McAndrews, J.H.
1979: An inexpensive sieving method for concentrating pollen and spores from fine grained sediments; Canadian Journal of Earth Sciences, v. 16, p. 1115-1120.

Eisbacher, G.H.
1979: Cliff collapse and rock avalanches (Sturtzstroms) in the Mackenzie Mountains, Northwestern Canada; Canadian Geotechnical Journal, v. 16, p. 309-334.

Foscolos, A.E. and Barefoot, R.R.
1970: A rapid determination of total organic and inorganic carbon in shales and carbonates; Geological Survey of Canada, Paper 70-11.

Foscolos, A.E., Rutter, N.W., and Hughes, O.L.
1977: The use of pedological studies in interpreting the Quaternary history of central Yukon Territory; Geological Survey of Canada, Bulletin 271, 48 p.

Gordey, S.P.
1981: Geology of the Nahanni map area, Yukon Territory and District of Mackenzie; Geological Survey of Canada, Open File 780.

Green, L.H., Roddick, J.A., and Blusson, S.L.
1967: Geology, Nahanni; Geological Survey of Canada, Map 8-1967.

Hopkins, W.S. and Norris, D.K.
1974: An occurrence of Paleogene sediments in the Old Crow structural depression, Northern Yukon Territory; in Report of Activities, Geological Survey of Canada, Paper 74-1, Part A, p. 315-316.

Hopkins, W.S., Jr., Hughes, O.L., and Milner, M.
1975: Some coal-bearing Eocene sediments and comments on their combined microflora, Cliff Creek, Yukon Territory; in Report of Activities, Part C, Geological Survey of Canada, Paper 75-1C, p. 37-39.

Hopkins, W.S., Jr., Rutter, N.W., and Rouse, G.E.
  1972: Geology, paleogeology and palynology of some Oligocene rocks in the Rocky Mountain Trench of British Columbia; Canadian Journal of Earth Sciences, v. 9, p. 460-470.

Jackson, L.E., Jr., Foscolos, A.E., and MacDonald, G.M.
  1982: An interglacial or preglacial paleosol from the Selwyn Mountains, N.W.T., Canada; Abstracts, American Quaternary Association, Seventh Biennial Conference, p. 109.

Jackson, M.L.
  1965: Free oxides, hydroxides and amorphous alumino-silicates; in Methods of Soil Analysis, ed. C.A. Black; Part 1, p. 578-603; American Society of Agronomy, p. 578-603.

Jonasson, I.R., Jackson, L.E., Jr., and Sangster, D.F.
  1983: A Holocene zinc deposit, Howards Pass, Yukon/N.W.T.; Journal of Geochemical Exploration, v. 18, p. 189-194.

Klassen, R.W.
  1978: A unique stratigraphic record of late Tertiary-Quaternary events in southeastern Yukon; Canadian Journal of Earth Sciences, v. 15, p. 1884-1886.

Kukla, G.J.
  1977: Pleistocene land-sea correlations 1. Europe; Earth Science Reviews, v. 13, p. 307-374.

Lichti-Federovich, S.
  1973: Palynology of six sections of late Quaternary sediments from the Old Crow River, Yukon Territory; Canadian Journal of Botany, v. 51, p. 533-564.

MacDonald, G.M.
  1983: Holocene vegetational history of the upper Natla River area, Northwest Territories, Canada; Arctic and Alpine Research, v. 15, p. 169-180.

Moran, S.R., Clayton, L., Hooke, R. Le.B., Fenton, M.M., and Andriashek, L.D.
  1980: Glacier bed landforms of the Prairie of North America; Journal of Glaciology, v. 25, p. 457-476.

Rouse, G.E., Hopkins, W.S., Jr., and Piel, K.M.
  1970: Palynology of some late Cretaceous and early Tertiary deposits in British Columbia and adjacent Alberta; Geological Society of America, Special Paper 127, p. 213-246.

Stockmar, J.
  1972: Tablets with spores used in absolute pollen analysis; Pollen et spores, v. 13, p. 615-621.

Permafrost growth in recently drained lakes, Western Arctic Coast

Project 680047

J. Ross Mackay[1]
Terrain Sciences Division

Abstract

A study of permafrost growth in lakes that have drained recently along the Western Arctic Coast has been carried out from 1971 to 1984. The sublake bottom sediments are mainly sands. Bench marks on the drained lake bottoms have been repeatedly surveyed and ground temperatures measured. The uplifts of the bench marks have been used to estimate the uplifts from the volume change of water to ice as permafrost aggrades beneath the drained lake bottoms. The temperature measurements have been used to estimate freezing conditions in the basal part of aggrading permafrost and apparent thermal diffusivities. The results show that: the growth rate of ice-bonded permafrost is less than that of non ice-bonded permafrost; the zone between the 0°C isotherm and the isotherm where nearly complete freezing of pore water occurs can be many metres in thickness; and the apparent thermal diffusivities give good indications as to the depths at which phase changes occur. There is field evidence to suggest that the downward movement of water in summer from the thawed active layer with freezing in the still frozen active layer and top of permafrost may contribute to lake bottom uplift. The uplift of bench marks appears to be greatest when the winter snow depth is the least.

Résumé

Les auteurs ont réalisé, entre 1971 et 1984, une étude de la croissance du pergélisol dans des lacs qui se sont asséchés récemment le long de la côte ouest de l'Arctique. Les sédiments sous-lacustres se composent essentiellement de sables. Les repères de nivellement mis en place sur les fonds des lacs asséchés ont été maintes fois relevés, et les températures du sol mesurées. À l'aide des mesures données par les repères de nivellement, les chercheurs ont calculé les élévations de hauteur résultant du changement de volume de l'eau à mesure de la croissance du pergélisol les lacs. À l'aide des températures mesurées, ils ont évalué les conditions de gel à la base du pergélisol en progression ainsi que les diffusivités thermiques apparentes. Les résultats ont établi les faits suivants: le taux de croissance du pergélisol limité par la glace est inférieur à celui du pergélisol qui ne l'est pas; la zone entre l'isotherme de 0°C et celui où l'eau interstitielle gèle presque entièrement peut avoir un grand nombre de mètres d'épaiseur; et, les valeurs de la diffusivité thermique apparente donnent une bonne indication des profondeurs auxquelles surviennent les changements de phase. Certains éléments observés sur le terrain semblent indiquer que le mouvement descendant de l'eau en été à partir de la couche active dégelée et le gel survenant dans la couche active encore gelée et au sommet du pergélisol peuvent contribuer au soulèvement des fonds lacustres. Il semble que l'élévation des repères de nivellement soit d'autant plus appréciable que l'épaisseur de la neige est faible en hiver.

[1] Department of Geography, University of British Columbia, Vancouver, British Columbia V6T 1W5

Introduction

In the Tuktoyaktuk Peninsula and Richards Island region of the Western Arctic Coast, lakes cover from 20 to 40% of the total area. The region is in the zone of continuous permafrost with depths ranging from about 400 to 600 m. The mean annual ground temperature at the depth of zero annual temperature change is in the -6°C to -10°C temperature range. When the lakes of the Western Arctic Coast drain naturally – a common event – permafrost commences to aggrade downward on the exposed drained lake bottoms. This report discusses some aspects of permafrost growth in the lake bottoms of recently drained lakes as studied during the 1971 to 1984 period. In the absence of names, the drained lakes will be referred to by numbers (Fig. 22.1).

Figure 22.1. *Location map. The locations of drained lakes are indicated by numbers in the absence of names.*

Field measurements

Several methods have been used in the field study of permafrost growth on drained lake bottoms. The lake bottom uplifts resulting from permafrost growth have been determined from repetitive surveys of bench marks of different lengths anchored in holes drilled into permafrost. The datum bench marks have been located landward of the predrainage lake shorelines, because such sites are underlain by thick permafrost and so should be unaffected by permafrost growth on the drained lake bottoms. Most of the bench marks have "antiheave rings" (Mackay, 1973) for that portion embedded in permafrost in order to minimize frost heave by freeze-thaw in the active layer. At the time of installation, the ground level of each bench mark was recorded so that any long term frost heave could be detected. Some bench marks have been frost heaved, and the data have been omitted, unless a correction could be made for the amount of frost heave. A Wild NA2 automatic engineer's level with a parallel plate micrometer reading directly to 0.01 cm and Wild GPLE 3 m invar staves with supporting struts have been used in all levelling. All surveys have been closed at least once. Temperatures have been measured with thermistor cables in cased holes. Some permafrost depths have been determined by drilling.

Lake 1

Lake 1, prior to drainage, was about 700 m long, 600 m wide (Fig. 22.2), with a maximum depth of about 3 m. The lake drained rapidly by erosion of ice wedges at the outlet between 18 July 1971 and 5 August 1972 as shown by

Figure 22.2. *Lake 1 showing a residual pond on the drained lake bottom, the former shoreline, and the locations of bench marks (BM). Photo taken in 1976.*

air photographs. Bench marks (BM) were installed between 1976 and 1980 as shown in Figure 22.2. Bench marks 6, 7, and 8 are landward of the former lake shore where permafrost prior to drainage was deep. From 1978 to 1984, the greatest variation in height among BM 6, 7, and 8 was less than 1 mm so all three are stable and BM 7, being in the middle, has been used as the datum BM.

Lake bottom uplift

Prior to lake drainage, a bowl-shaped talik (unfrozen zone) would have underlain Lake 1. After drainage, the merging of downward aggrading permafrost with upward aggrading permafrost from beneath the talik would then occur first near shore and last near the lake centre (Mackay, 1984). The bench mark uplift (Table 22.1) would then cease first near the shore and last near the lake centre. This trend is clearly shown in two profiles. First, a profile from BM 1 to BM 2 by the residual pond shows that BM 1 and BM 12 are essentially stable, thus indicating little freezing of

Table 22.1. Uplift (ΔH) of the bench marks of Lake 1

Bench Mark	Period	Uplift (ΔH) cm/y (approx.)	Comment
A	1978 to 1984	2.1	10 m from residual pond; 3 m-long bench mark
1	1978 to 1983	∿ 0.0	On lake flat 75 m from former shoreline
2	1978 to 1984	4.0	By residual pond
2A	1978 to 1984	3.9	By residual pond; 7 m-long bench mark
3	1978 to 1984	5.0	By residual pond
4	1978 to 1984	5.0	By residual pond
5	1978 to 1984	3.0	By residual pond
6	1978 to 1984	∿ 0.0	Located inland from former shoreline; 0.5 m from BM 7
7	1978 to 1984	datum	Located inland from former shoreline
8	1978 to 1984	∿ 0.0	Located inland from former shoreline; 0.5 m from BM 8
9	1978 to 1984	1.0	On lake flat 40 m from former shoreline
10	1978 to 1984	∿ 0.0	On lake flat 110 m from former shoreline
11	1980 to 1984	3.2	By residual pond; 14.5 m-long bench mark
12	1980 to 1984	∿ 0.0	30 m from residual pond; 8.5 m-long bench mark
13	1980 to 1984	2.9	In residual pond; 9.5 m-long bench mark

water at depth. The uplifts of BM A (2.1 cm/year), BM 2 (4.0 cm/year), and BM 2A (3.9 cm/year) show that freezing is occurring at depth. Second, a profile from datum BM 7 to BM 4 by the residual pond shows a slight heave for BM 9 (1 cm/year), no heave for BM 10 (0.0 cm/year), and heave for BM 4 (5.0 cm/year). The uplift data then suggest that downward and upward aggrading permafrost have merged for the nearshore sites (BM 1, 9, 10, and 12) and permafrost is actively aggrading by and in the residual pond (BM 2, 2A, 3, 4, 5, 11, and 13).

Ground temperatures

Ground temperatures have been measured at BM A, BM 2A (Fig. 22.3), BM 11 (Fig. 22.4), BM 12, and BM 13 (Fig. 22.5). Permafrost beneath the residual pond is shown in Figure 22.6. The depth of the residual pond fluctuates each summer from a maximum in the June snowmelt period to a minimum during summer dry periods and, in addition, a gradual year-to-year shoaling has accompanied lake bottom uplift. In 1984, mean water depths were only 30 to 40 cm as compared to 50 cm or more in 1976. In 1976, permafrost beneath the pond (Fig. 22.6) was about 3.5 m deep as compared to about 4.5 just inland from the shoreline of the pond. By 1984, permafrost had grown to a greater depth beneath the pond as compared to beneath the shoreline. Summer temperatures beneath the pond at BM 13 (Fig. 22.5) have been consistently colder than at BM 2A (Fig. 22.3) and BM 11 (Fig. 22.4) on the shoreline. The reasons for the warmer ground temperatures at the shoreline are uncertain, but they may in part reflect differences in snow cover.

Figure 22.3.   Temperature profiles at BM 2A.

Figure 22.4.   Temperature profiles at BM 11.

Figure 22.5. *Temperature profiles at BM 13.*

Figure 22.6. *The growth of permafrost, defined by the 0°C isotherm, is shown for the residual pond of Lake 2, Figure 22.2.*

In 1976, Lake 1 had been drained for only four or five years so the vegetation around the lake shore was too low to trap much drifting snow in winter. As the vegetation grew taller and more abundant, the pond ice became windswept in winter and snow accumulated in drifts along the shoreline. The warmer ground temperatures at the shoreline may then reflect a deep insulating snow cover (Mackay and MacKay, 1974).

Freezing zones

It is well known that the pore water in a soil freezes at a temperature somewhat below 0°C. In the finer grained soils and in soils with saline pore water, freezing is over an extended temperature range. The end result, in so far as standard nomenclature is concerned, is ambiguity and confusion, as discussed by van Everdingen (1976). Miller (1972) has referred to the zone between the first pore ice and a growing ice lens as the "frozen fringe". The "frozen fringe" has been measured in the laboratory, but since the specimens are small and the temperature gradients are steep, the frozen fringe is a very narrow zone. For example, in a typical experiment, Loch and Kay (1978) used a temperature gradient of 0.6°C/cm across an 8 cm-long cell and measured a frozen fringe varying from 0.23 to 0.39 cm in thickness. Similar temperature gradients have been used in many other laboratory experiments, mainly with fine grained frost

susceptible soils. Under field conditions, the temperature at which pore water first begins to freeze can be identified by a rapid increase in the temperature gradient on the cold side of 0°C, in going from positive to negative temperatures. Figures 22.3 and 22.4 show no change in temperature gradient across the 0°C isotherm. The temperature profiles for 25 July 1983 and 24 June 1984 for the freezing point depression zone of Figure 22.4 are reproduced at a larger scale in Figure 22.7 with an interpretation of the freezing zones. The sediments are believed to be sands. Three freezing zones can be identified. Zone 1 is the lower zone of unfrozen pore water. The temperature limits are defined by 0°C and the freezing point depression, identified by a steepening of the otherwise linear temperature gradient. Zone 2 is the middle zone of partially frozen pore water identified by a steepening temperature gradient. This zone corresponds to the "frozen fringe". Zone 3 is the upper zone of largely frozen pore water identified by a nearly linear temperature profile. The temperature profile for 24 June 1984 in Figure 22.7 shows that zone 1 had a thickness of about 2.1 m and zone 2 (i.e. the frozen fringe) about 1.3 m. In other words, although permafrost was about 9 m thick on 24 June 1984, the bottom 3.4 m had some unfrozen pore water. Because the thickness of zones 1 and 2 should increase with the depth of aggrading permafrost, it seems possible that if aggrading permafrost were several hundred metres thick, zones 1 and 2 might be tens of metres thick.

The temperature profiles of Figures 22.3, 22.4, and 22.7, and to a lesser extent Figure 22.5, show that the downward growth of permafrost, as defined by the 0°C isotherm, exceeds the downward growth of ice-bonded permafrost as indicated by the presence of pore ice. For example, from 25 July 1983 to 24 June 1984 the growth of permafrost at BM 11 (Fig. 22.7) was 1.2 m, that of the freezing point depression for pore water (i.e. zone 2) was about 0.4 m, and that of the zone of ice-bonded permafrost (i.e. zone 3) was about 0.3 m.

Upward freezing

When downward and upward aggrading permafrost surfaces are about to merge, the temperature in the unfrozen zone between them quickly approaches 0°C (Fig. 22.8), because cooling is from two directions. The temperature profiles for BM 2A (Fig. 22.3) and BM 11 (Fig. 22.4) show a rapid decrease in the temperature gradients below 0°C,

Figure 22.7. *Temperature profile for the bottom of BM 11 (cf. Fig. 22.4) showing the three zones where pore water is unfrozen, partially frozen, and mostly frozen.*

Figure 22.8. *Schematic diagram to show the unfrozen zone between downward and upward aggrading permafrost where freezing is in a closed system. In a frost-susceptible soil the growth of ice lenses may result in water loss and consolidation of the unfrozen zone. In a nonfrost-susceptible soil, pore water expulsion may result in water gain and artesian pressures in the unfrozen zone.*

Figure 22.9. *Bench mark uplift for Lake 1.*

an indication of upfreezing from below. The uplifts of bench marks can be used in conjunction with temperature measurements to study the freeze-through of downward and upward aggrading permafrost. For example, the cumulative uplifts for BM A, 2A, 11, and 13, all of which exceed 7.5 m in length and so are securely anchored in permafrost, are plotted in Figure 22.9. Only BM A, where the downward and upward growing permafrost surfaces were merging, shows a decreasing rate of uplift.

Pore and segregated ice

An estimate can be made at some sites of the amount and type of ice that freezes as permafrost aggrades downward, because the amount of lake bottom (bench mark) uplift is known from survey and the growth of ice-bonded permafrost from temperature measurements. If it is assumed that the in situ freezing of pore water results in a 9% volume expansion and that additional pore water can migrate to the freezing plane and freeze, then for time (t) and to a first approximation:

$$z = \Delta P - \Delta H \qquad (1)$$

$$0.09nz + z + 1.09 \Delta W = \Delta P \qquad (2)$$

$$0.09nz + 1.09 \Delta W = \Delta H \qquad (3)$$

where

  z is the thickness of the soil frozen in time t

  n is the porosity of the unfrozen soil

  ΔP is the thickness of ice-bonded permafrost frozen in time t

  ΔH is the ground surface (bench mark) uplift in time t

  ΔW is the thickness of water that migrates to layer z during freezing

  $0.09nz$ is the uplift from the in situ freezing of pore water

  $1.09 \Delta W$ is the uplift from the freezing of ΔW to form segregated ice

The porosities of the soils are unknown, but for discussion purposes a reasonable value of n = 0.4 will be used. For BM 2A and the 1978 to 1983 period ($\Delta H = 0.22$ m, $\Delta P = 1.0$ m) the uplift from pore ice would be 3 cm and that from segregated ice 17 cm. For BM 11 for the 1980 to 1984 period ($\Delta H = 0.13$ m, $\Delta P = 1.25$ m) the uplift from pore ice would be 4 cm and from segregated ice 9 cm. For BM 13 for the 1980 to 1983 period ($\Delta H = 0.12$ m, $\Delta P = 2.5$ m) the uplift from pore ice would be 9 cm and from segregated ice 2 cm. The data show that uplift from water (ΔW) added to the system to grow segregated ice is far more important, in relative terms, than the uplift from the in situ freezing of pore water. For example, in situ freezing of pore water equivalent to a 10 cm water layer would produce an uplift of only 0.9 cm whereas an influx of 10 cm of water to grow segregated ice would produce an uplift of 10.9 cm, a 12:1 greater efficiency.

Lake 2

Prior to drainage, Lake 2 was 1300 m long with a maximum width of about 600 m (Fig. 22.10). The lake drained in 1962 or 1963 according to local reports and the estimate is supported by age dated willows which had commenced growth by 1964. The maximum lake depth in 1972 was about 2.0 m and when allowance is made for ten years of lake bottom uplift, the maximum water depth prior to drainage was about 2.5 m. Bench marks were installed in 1971 and 1973.

Lake bottom uplift

Bench mark 85 (Fig. 22.10) which is inland from the former lake shore and 2.3 m above it was stable for the 1971 to 1979 period and has been used as the datum bench mark. The uplift of the bench marks that have been stable, with the exception of BM 86 which may have been frost heaved a few centimetres in the 1971 to 1979 period, are shown in Figure 22.11. The mean annual rate of uplift of the bench marks decreased from the side of the lake to the centre, that is, from BM 86 to BM 87.

181

Figure 22.10. *Lake 2 showing the locations of bench marks and temperature cable. The lake outlet prior to drainage was along a small creek labelled (2) but in 1962 or 1963 the lake drained catastrophically through the channel labelled (1). Photo taken in 1974.*
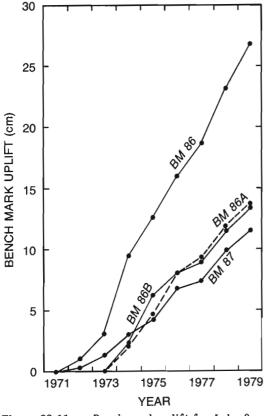

Figure 22.11. *Bench mark uplift for Lake 2.*

Ground temperatures

In 1977 three holes were drilled through permafrost and temperature cables installed at the location shown in Figure 22.10. The temperature profiles (Fig. 22.12) for one cable show that in March 1978, downward aggrading permafrost was 14 m deep, but the curvature in the profile below 0°C (cf. Fig. 22.8) shows that the top of upward aggrading permafrost was at a depth of about 25 m. As the temperature profiles show, the merging of downward aggrading permafrost with upward aggrading permafrost had started by July 1978 and was effectively completed a year later by July 1979.

The predrainage depth to permafrost at the site of the temperature cable of Figure 22.12 is unknown, but in 1978, after 15 years of drainage, upfreezing had only reached a depth of 25 m. Judging by the very rapid 10 m of upfreezing from 1978 to 1981, the 1962/1963 depth to permafrost was likely in excess of 40 to 50 m.

Lake 3

Prior to drainage, Lake 3 measured 1000 m by 300 m (Fig. 22.13). The lake drained before 1963, as age dated by willows growing on the drained lake bottom and after 1950, when a lake was present on 1950 air photographs. The original lake depth is unknown, but in 1969, maximum depths below the former shoreline were about 1.25 m.

Lake bottom uplift

Bench marks were installed on the drained lake bottom in 1971 and 1973 (Fig. 22.13). Bench mark 88 is on the old shoreline and BM 94 is inland from the old shoreline.

TEMPERATURE (°C)

Figure 22.12. *Temperature profiles for Lake 2 at the location of the temperature cable given in Figure 22.10.*

Because the 1971 to 1981 maximum difference in elevation of these two bench marks on opposite sides of the drained lake was only 1.4 mm, the two bench marks are therefore stable. Bench mark 88 has been used as the datum bench mark. As some of the bench marks were frost heaved a few centimetres during the survey period, the frost heave component has been deleted from the uplift data in Table 22.2. The uplifts plotted in Figure 22.14 are for bench marks that showed no evidence of frost heave during the survey period which was 1971 to 1981 for BM 89 and BM 91 and 1973 to 1981 for BM 92A.

Ground temperatures

A profile across the middle of Lake 3 in 1977 shows a maximum depth of 1 m about 20 years after lake drainage (Fig. 22.15). When allowance is made for lake bottom uplift at about 2 cm/year (Table 22.2), the predrainage depth would have been about 1.5 m. A water depth of 1.5 m approximates, rather closely, the mean annual winter ice thickness for the region. It seems likely, therefore, that prior to lake drainage the lake ice froze to the bottom over much of the lake each winter and the mean annual lake bottom temperature was likely about $1.5°C \pm 0.5°C$. The predrainage steady state temperature distribution beneath Lake 3, given simplifying assumptions (Johnston, 1981), can be estimated. Lake 3 is long and narrow, so it can be likened to a river. If the mean annual ground temperature was -6°C, the undisturbed permafrost thickness 500 m, and the mean annual lake bottom temperature +1.5°C, then the lake bottom isotherms would resemble those in Figure 22.16.

In 1977, two holes were drilled to a depth of 30 m, one by BM 89 and the other by BM 91 (Fig. 22.13). Both holes were entirely in permafrost. Temperature profiles for the

Figure 22.13. *Lake 3 showing the locations of bench marks, temperature cable, and outlet (marked with an arrow). Photo taken in 1974.*

Table 22.2. Uplift (ΔH) of the bench marks of Lake 3

Bench Mark	Period	Uplift (ΔH) cm/y (approx.)
88	1971 to 1981	datum
89	1971 to 1981	1.5
90	1971 to 1981	0.2
91	1971 to 1981	1.0
91A	1973 to 1981	1.0
92	1971 to 1981	1.4
92A	1973 to 1981	1.8
93	1971 to 1981	1.2
93A	1973 to 1981	∿ 0.0
94	1971 to 1981	∿ 0.0

Figure 22.14. Bench mark uplift for Lake 3.

Figure 22.15. Cross profile of Lake 3 through BM 91 and the temperature cable (Fig. 22.13) as surveyed in 1977.

hole by BM 91 are given in Figure 22.17. Because the temperature at a depth of 23 m remained nearly constant at -2.5°C for two years, -2.5°C is very close to the temperature at the depth of "zero" annual temperature change (Lunardini, 1981).

Figure 22.16. Steady state temperature profile prior to lake drainage at the cross profile of Figure 22.15 with simplifying assumptions (see text).

Figure 22.17. Temperature profiles for Lake 3 at the location of the temperature cable given in Figure 22.13.

Discussion

This discussion focuses on aspects of permafrost growth common to Lakes 1, 2, and 3 and to other lakes whose locations are given in Figure 22.1.

Rate of permafrost growth

The minimum time since lake drainage is known for Lakes 1 to 6. Stefan's formula (Johnston, 1981), which involves several simplifying assumptions, can be used to estimate permafrost growth:

$$z = \sqrt{\frac{-2Tkt}{Q}} = b\sqrt{t} \tag{4}$$

where

z is the depth of permafrost
t is the time since permafrost commenced to grow
T is mean annual ground surface temperature, °C
k is the thermal conductivity of the frozen soil
Q is the volumetric latent heat of fusion of the frozen soil
b is Stefan's constant

The rate of permafrost growth is:

$$\frac{dz}{dt} = \frac{b}{2\sqrt{t}} \tag{5}$$

The values of Stefan's "b", calculated for five of the drained lakes, are given in Table 22.3. On theoretical grounds, the range in value of "b" for different soils will be about 2:1 (Brown, 1964). The value of "b" is very responsive to the volumetric latent heat (Q), being small where the water content is high and large where the water content is low. The value of "b" for Lake 4 comes from the centre of Illisarvik, an experimental drained lake site (Mackay, 1984). Temperature profiles for Lake 5, which drained in about 1953, are plotted in Figure 22.18. Permafrost growth is in saturated sands. The very gentle temperature gradient in the range from 0°C to -0.1°C is similar to that observed at Lakes 1 and 4. Lake 6 drained shortly before 1950 and growth is in sands beneath a saturated sedgy lake bottom. In summary, the rather consistent value of Stefan's "b" of about $3.0 \ m \cdot y^{-\frac{1}{2}}$ for sands and about $1.5 \ m \cdot y^{-\frac{1}{2}}$ for high ice content soils enables estimates to be made of permafrost growth in recently drained lakes along the Western Arctic Coast.

Although thickness of permafrost is unknown for Lake 3, an estimate can be made using a "b" value of $3.0 \ m \cdot y^{-\frac{1}{2}}$ for sands because Lake 3 is underlain by sands. In 1978, Lake 3 had drained no more than 27 years ago because the lake had water in 1950. From equation 4, using "b" of $3.0 \ m \cdot y^{-\frac{1}{2}}$ and a maximum of t = 27 years, permafrost might have grown to about 16 m. However, in 1978 the temperature at a depth of 23 m was -2.5°C (Fig. 22.17). The most likely explanation for the low temperature at 23 m is that the top of permafrost was not much more than 20 m or more in depth prior to drainage (Fig. 22.16) and freeze-through of permafrost was completed a few years prior to 1978.

Thermal diffusivity

The thermal diffusivity of a soil is defined as:

$$\alpha = \frac{k}{c} \tag{6}$$

Table 22.3. The value of Stefan's "b" has been calculated from measurements of the depth of permafrost (z) and the time (t) since lake drainage (see text).

Lake	Stefan's "b" $m \cdot y^{-\frac{1}{2}}$	Comment
1 (BM 2A)	1.5	Pore ice and much segregated ice
1 (BM 11)	1.8	Pore ice and segregated ice
1 (BM 13)	2.7	Mainly pore ice
2	3.2	Site at temperature cable; pore ice in sands
4	3.1	Lake centre; pore ice in sands
5	3.0	Pore ice in sands
6	3.0	Pore ice in sands

TEMPERATURE (°C)

Figure 22.18. Temperature profile for a site near a residual pond of Lake 5.

where

α is the thermal diffusivity
k is the thermal conductivity
c is the volumetric heat capacity

The thermal diffusivity (α) is an index of the rapidity with which a material will respond to a temperature change. The thermal diffusivity appears in the heat conduction equation (Johnston, 1981) as applied to ground temperatures:

$$\frac{\partial T}{\partial t} = \alpha \frac{\partial^2 T}{\partial z^2} \tag{7}$$

where

T is temperature
t is time
z is depth in the ground

The thermal diffusivity may be estimated from the propagation of a temperature wave into the ground where temperatures at depth are known for two different times. The time and space derivatives of equation 7 can be obtained by finite difference methods and the thermal diffusivity calculated (McGaw et al., 1978). However, if there is a phase change, the volumetric heat capacity (c) must be replaced by an apparent heat capacity to take care of the phase change (Smith, 1976; McGaw et al., 1978).

The apparent thermal diffusivities for the temperature cables at Lakes 2 and 3 have been calculated from their temperature profiles for the winter of 1977/1978. For Lake 2, the apparent thermal diffusivities at 10 m and 18 m were both $12 \times 10^{-7} m^2/s$, a value typical of a fine grained frozen soil (Johnston, 1981, p. 121). By contrast, at 14 m,

where freeze-through of permafrost was taking place, the apparent thermal diffusivity had decreased to $2 \times 10^{-7} m^2/s$ because of a phase change increasing the apparent heat capacity (equation 6). The apparent thermal diffusivity for Lake 3 at 11 m was $12 \times 10^{-7} m^2/s$ and at 15 m, $15 \times 10^{-7} m^2/s$, both being in the range of that of a frozen sand (Johnston, 1981, p. 123). Thus, the calculated values for the apparent thermal diffusivities can be helpful in determing the temperature range at which a phase change occurs as permafrost is growing.

Synchronous lake bottom uplift

Although Lakes 2 and 3 are 25 km apart, the uplift patterns of their bench marks seem similar, particularly for the small 1976 to 1977 uplifts for five of the seven bench marks involved (Fig. 22.11, 22.14). In the following discussion, nonparametric statistics have been used, because the data are limited. In order to evaluate synchronous lake bottom uplift, the uplift of each bench mark has been ranked by year, from the least to the greatest. Then the ranks have been compared using Spearman's rank correlation coefficient where two ranks were compared and Kendall's coefficient of concordance (Siegel, 1956) where four rankings were compared. The statistical evidence (Table 22.4) suggests that lake bottom uplift of the bench marks in Lakes 2 and 3 has followed the same general pattern for the 1970s.

The apparently synchronous uplift of the bench marks at Lakes 2 and 3 might be explained by several mechanisms, of which active layer frost heave of the bench marks is one possibility. The four bench marks selected for comparison, however, have shown little variation in height above ground level over the observation period. The greatest change was for BM 86 which showed a maximum variation of 7 cm above ground level from 1971 to 1979 during which period the surveyed uplift (Fig. 22.11) was 27 cm. Bench marks 87, 89, and 91 varied no more than several centimetres above ground level during the same periods. Therefore, frost heave of the bench marks during the freeze-back period cannot explain the apparent similar uplift patterns of the bench marks of Lakes 2 and 3.

Propagation of a temperature wave

If the apparent synchronous yearly uplift of bench marks at Lakes 2 and 3 resulted from the freezing of unfrozen pore water at depth, then the propagation of the yearly summer and winter temperature waves down to the depth of freezing must also be in phase. In periodic heat flow, the propagation of a temperature wave into the ground is later than its occurrence at the ground surface (Ingersoll and others, 1954) by:

$$t = \frac{z}{2}\sqrt{\frac{P}{\pi\alpha}} \qquad (8)$$

where

t is the lag in time
z is depth
P is the period of one year for the annual wave
α is the thermal diffusivity

For Lake 2, Stefan's "b" (Table 22.3) is about $3.2 \ m \cdot y^{-\frac{1}{2}}$. From 1971 to 1978, permafrost would have grown from about 9 m to 14 m, and the phase lag (t) would have increased from 4 or 5 months in 1971 to about 6 months in 1978. For Lake 3, data have already been presented to show that freeze-through of permafrost had been completed by 1978. Even if this inference is incorrect, from Figure 22.17, the depth of permafrost certainly exceeded 30 m which means that the lag (t) where freezing might take place would be more than 12 months. Therefore, the propagation of a temperature wave could not result in synchronous freezing of water at depth for Lakes 2 and 3, because the lag in time (t) would be out-of-phase by much more than 6 months. In addition, the depth of "zero" annual temperature change for Lake 3 was at about 23 m in 1978 (Fig. 22.17), so seasonal variations in temperature would have had virtually no effect at any freezing depths much greater than 23 m. Consequently, the propagation of year-to-year seasonal changes in temperature cannot explain the apparently synchronous uplift of the bench marks of Lakes 2 and 3.

Summer uplift

In recent years, evidence has accumulated to show that during the winter period, unfrozen pore water can migrate upward from the top of permafrost and the bottom of the frozen active layer to increase the ice content in the upper part of the active layer. Conversely, in summer there may be a reverse movement with water moving downward from the thawing active layer to refreeze in the subjacent frozen ground of the active layer and top of permafrost (e.g. Parmuzina, 1978; Mackay, 1981, 1983; Cheng, 1982a,b; Chizhov et al., 1983; Wright, 1983).

It is evident that if there is a downward migration of water in summer with refreezing at depth, then short bench marks anchored only in the active layer should be uplifted more than long bench marks anchored deeply in permafrost. In order to test the theory, repetitive surveys were carried out at Lake 1 in the summer of 1978 with the result that short bench marks were found to be uplifted more than long bench marks. In the summer of 1981, two very short bench marks were installed entirely in the active layer, BM 2B being located at 0.5 m from BM 2 and 1 m from BM 2A. Bench mark 11A was installed 0.5 m from BM 11. During the 40 day thaw period from 6 June to 16 July 1981, BM 2B, which was anchored only in the active layer, was uplifted 7.0 mm; BM 2, which was anchored in the top of permafrost, was uplifted 6.9 mm; and BM 2A, which penetrated permafrost (Fig. 22.19), was uplifted 5.2 mm. During the same period, BM 11A, which was only in the active layer, was uplifted 8.3 mm whereas BM 11 which penetrated permafrost, was uplifted only 5.4 mm. The field evidence for the summer uplift of short bench marks at Lake 1 is in agreement with the summer uplift of heavemeters at Lake 4, Garry Island, and Inuvik (Mackay, 1981, 1983). At Lake 3, in the one year period from 1980 to 1981, the 25 m-deep steel pipe which held the temperature cable (Fig. 22.17) showed no measurable
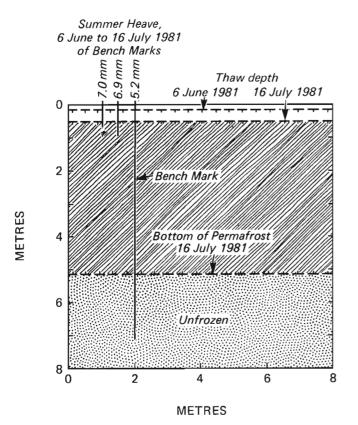
Table 22.4. Comparison of the uplift (ΔH) of bench marks, ranked by year, using Spearman's rank correlation coefficient for ranking two bench marks and Kendall's coefficient of concordance for ranking four bench marks.

Bench marks	Period	Level of Significance[1] 5%	Level of Significance[1] 1%
Lake 2 (BM 86 and 87)	1971 to 1979	S	S
Lake 3 (BM 89 and 91)	1971 to 1981	S	NS
Lakes 2 and 3 (BM 86, 87, 89, and 91)	1971 to 1978[2]	S	S

[1] S is significant and NS not significant.
[2] The period is 1971 to 1978 and not to 1979, because of lack of comparability of data in 1979 between Lakes 2 and 3.

Figure 22.19. Bench mark uplift for Lake 1. The 7 m-long bench mark that penetrates permafrost is BM 2A which heaved 5.2 mm between 6 June and 16 July 1981. The bench mark that heaved 6.9 mm is BM 2 and that which heaved 7.0 mm is BM 2B (see text).

uplift but nearby BM 91, which was 2 m long, was uplifted 0.55 cm, thus suggesting a near surface cause of the uplift. In summary, although the evidence for differential summer uplift of short bench marks and heavemeters as compared to long bench marks has now been measured at four different field sites and seems well established, the magnitudes of the summer uplifts so far measured seem insufficient to explain the apparently synchronous uplifts of bench marks at Lakes 2 and 3.

Year-to-year uplift variations

The apparent synchroneity of the year-to-year uplift patterns for Lakes 2 and 3 suggests a climatic control, such as temperature, if summer bench mark uplift is a contributing cause. Because winter ground temperatures and early summer moisture are greatly influenced by snow depth, a comparison has been made with uplift and with snow depth as measured in March at a snowcourse at Garry Island, Northwest Territories (Mackay and MacKay, 1974). The results, given in Table 22.5, suggest that uplift and snow depth are inversely correlated, as expected if snow depth were a contributing cause. In other words, maximum uplift is associated with cold winter ground temperatures (i.e. little snow) and vice versa.

Lake depths prior to drainage

Many of the lakes of the Western Arctic Coast are probably thermokarst in origin where the lake depths result mainly from the thaw of excess ice. If this assumption is correct, then if a lake basin is still present after the bed of a

Table 22.5. Comparison of the uplift (ΔH) of bench marks and snow depth at Garry Island, N.W.T., ranked by year, using Spearman's rank correlation coefficient for ranking one bench mark with snow depth and Kendall's coefficient of concordance for ranking two bench marks with snow depth.

Bench marks	Period	Level of Significance[1]	
		5%	1%
Lake 2 (BM 86 and 87)	1971 to 1979	S	NS
Lake 2 (BM 86A and 86B)	1973 to 1979	NS	NS
Lake 3 (BM 89 and 91)	1971 to 1978	S	NS
Lake 3 (BM 92A)	1973 to 1978	S	NS

[1] S is significant and NS not significant.

drained thermokarst lake has undergone complete freeze-through, the missing volume reflects that of the excess ice thawed during the formation of the thermokarst lake basin. It is therefore instructive to note that there are hundreds of old drained lake basins, presumably of thermokarst origin, along the Western Arctic Coast. Many of the lakes drained at least several thousand years ago, as shown by the accumulation of thick deposits of peat in ice-wedge polygons with large ice wedges. A few thousand years is a sufficiently long period for lakes such as Lakes 1, 2, 3, and 4 to freeze through completely. Even if thermal equilibrium has not been completely established at the end of a few thousand years, any additional lake bottom uplift from the freezing of unfrozen pore water would likely be small. However, since hundreds of old drained thermokarst lakes still have basins that lie well below the adjacent terrain, either there was considerable excess ice prior to lake development or else lakes developed in existing basins. In view of the numerous present and past thermokarst lakes along the Western Arctic Coast, many being found in flat terrain, the most likely explanation is that considerable excess ice was thawed to create basins (cf. Harry and French, 1983; Lawson, 1983). The lakes under discussion (i.e., Lakes 1 to 6) will likely have residual lake basins after lake bottom uplift ceases, so excess ice was likely present prior to lake formation.

Conclusions

A study of permafrost growth in lakes that have drained recently along the Western Arctic Coast shows that the rate of growth can be estimated from Stefan's formula. The value of Stefan's "b" for the freezing of saturated sands is about $3 \text{ m} \cdot \text{y}^{-\frac{1}{2}}$ and that for a high ice content permafrost about $1.5 \text{ m} \cdot \text{y}^{-\frac{1}{2}}$. Ground temperature profiles for the basal part of permafrost aggrading in saturated sands show no change in gradient across the 0°C isotherm. The basal part of aggrading permafrost can be divided into three zones: a lower zone where the pore water is unfrozen; a middle zone where the pore water is partially frozen; and an upper zone where the pore water is mostly frozen. The temperature boundaries vary from site to site and also with time, at any given site. The bottom of the lower zone, by definition, is 0°C. For the sites under study, the temperature boundary between the lower and middle zones is at about -0.05° to -0.10°C and that between the middle and upper zones is at about -0.20° to -0.25°C. For permafrost that is only 5 to 10 m in thickness, the middle and lower zones may each have

a thickness greater than 1 m. As permafrost aggrades – whether downward or upward – the rate of growth of the 0°C isotherm (i.e., permafrost) exceeds the rate of growth of the middle zone where most of the pore water freezes. In other words, the rate of growth of non ice-bonded permafrost exceeds that of ice-bonded permafrost. The propagation of seasonal temperature waves can be used to calculate the apparent thermal diffusivity of the ground. The apparent thermal diffusivity approaches zero in the zone where most of the pore water freezes.

As permafrost aggrades in recently drained lake bottoms, the volume expansion of water to ice causes lake bottom uplift. The uplift of drained lake bottoms can be estimated from the uplift of bench marks referenced to stable datum bench marks inland from the former lake shores. The uplift of bench marks referenced to a stable datum can take place by at least three different mechanisms. First, bench marks can be frost heaved, as shown by a progressive year-to-year uplift relative to ground level. This type of frost heave results from freeze-back of the active layer in the fall and winter months. Second, bench marks that are securely anchored in permafrost can be uplifted as part of the general lake bottom uplift caused by freezing of water at depth. Third, bench marks can undergo summer uplift by the downward movement of pore water from the thawed active layer with refreezing in the subjacent frozen active layer and top of permafrost. All three types of bench mark uplift have occurred at the drained lake sites, but only the second and third types reflect lake bottom uplift. If the amount of bench mark uplift is known from survey and the downward growth of permafrost is known from temperature measurements, then an estimate can be made of the type and growth of ice that contributes to uplift. For freezing of a given thickness of water, the greatest uplift occurs where segregated ice grows from the migration of pore water.

A comparison of bench mark (lake bottom) uplift for two drained lakes 25 km apart shows an apparently similar year-to-year pattern of uplift, despite different lake bottom permafrost temperatures. The uplifts can be correlated with year-to-year snow depths. The reason for the apparent similarity in behaviour is uncertain, but, at present, uplift from the downward movement of water in summer seems the most likely explanation. More data, however, are required before firm conclusions can be drawn.

The uplift pattern of drained lakes can be used to estimate the prelake occurrence of excess ice for those lakes that are of thermokarst origin. There are thousands of drained lakes along the Western Arctic Coast and many of the lakes are generally believed to be of thermokarst origin. Of these drained thermokarst lakes, hundreds have thick peat deposits and large ice wedges indicative of drainage at least a few thousand years ago, a time sufficient to cause freeze-through of permafrost in all but the larger lakes. If freeze-through has occurred sufficiently long ago that lake bottom uplift, to a first approximation, has ceased, then the depths of the drained thermokarst basins beneath the adjacent lands give some measure of the excess ice that melted to produce the basins. Since the bottoms of many old thermokarst lakes still lie below the levels of the adjacent land, the missing volumes can be attributed in part to the thaw of excess ice in lake development.

References

Brown, W.G.
1964: Difficulties associated with predicting depth of freeze or thaw; Canadian Geotechnical Journal, v. 1, p. 215-216.

Cheng, G.
1982a: The forming process of thick layered ground ice; Scientia Sinica (Series B), v. 25, p. 777-788.

Cheng, G. (cont.)
1982b: Effect of uni-direction accumulation of unfrozen water in seasonally frozen and thawed ground; Kexue Tongbao (Scientific Bulletin), v. 27, p. 984-989.

Chizhov, A.B., Chizhova, N.I., Morkovina, I.K., and Romanov, V.V.
1983: Tritium in permafrost and ground ice: Permafrost, Fourth International Conference, Proceedings, Fairbanks, Alaska; National Academy Press, Washington, D.C., p. 147-151.

Harry, D.G. and French, H.M.
1983: The orientation and evolution of thaw lakes, southwest Banks Island, Canadian Arctic; Permafrost, Fourth International Conference, Proceeding, Fairbanks, Alaska; National Academy Press, Washington, D.C., p. 456-461.

Ingersoll, L.R., Zobel, O.J., and Ingersoll, A.C.
1954: Heat Conduction, with Engineering, Geological, and Other Applications; The University of Wisconsin Press, Madison, Wisconsin, 325 p.

Johnston, G.H. (editor)
1981: Permafrost Engineering, Design and Construction; John Wiley and Sons, Toronto, 540 p.

Lawson, D.C.
1983: Ground ice in perennially frozen sediments, northern Alaska; Permafrost, Fourth International Conference, Proceedings, Fairbanks, Alaska; National Academy Press, Washington, D.C., p. 695-700.

Loch, J.P.G. and Kay, B.D.
1978: Water redistribution in partially frozen, saturated silt under several temperature gradients and overburden loads; Soil Science Society of America Journal, v. 42, p. 400-406.

Lunardini, V.J.
1981: Heat transfer in cold climates; Van Nostrand Reinhold Company, New York, 731 p.

Mackay, J.R.
1973: The growth of pingos, Western Arctic Coast, Canada; Canadian Journal of Earth Sciences, v. 10, p. 979-1004.

1981: Active layer slope movement in a continuous permafrost environment, Garry Island, Northwest Territories, Canada; Canadian Journal of Earth Sciences, v. 18, p. 1666-1680.

1983: Downward water movement into frozen ground, western arctic coast, Canada; Canadian Journal of Earth Sciences, v. 20, p. 120-134.

1984: Lake bottom heave in permafrost; Illisarvik drained lake site, Richards Island, Northwest Territories; in Current Research, Part B, Geological Survey of Canada, Paper 84-1B, p. 173-177.

Mackay, J.R. and MacKay, D.K.
1974: Snow cover and ground temperatures, Garry Island, N.W.T.; Arctic, v. 27, p. 287-296.

McGaw, R.W., Outcalt, S.I., and Ng, E.
1978: Thermal properties and regime of wet tundra soils at Barrow, Alaska; Proceedings, 3rd International Conference on Permafrost, Edmonton, Alberta; National Research Council of Canada, Ottawa, v. 1, p. 47-53.

Miller, R.D.
  1972: Freezing and heaving of saturated and unsaturated soils; Highway Research Record Number 393, p. 1-11, Washington, D.C., Highway Research Board, National Research Council.

Parmuzina, O. Yu.
  1978: Cryogenic texture and some characteristics of ice formation in the active layer (In Russian); in Problems of Cryolithology, v. 7, ed. A.I. Popov; Moscow University Press, Moscow, U.S.S.R. p. 141-164. Translated: Polar Geography and Geology, v. 4, 1980, p. 131-152.

Siegel, S.
  1956: Nonparametric statistics for the behavioral sciences; McGraw-Hill, New York, 312 p.

Smith, M.W.
  1976: Permafrost in the Mackenzie Delta, Northwest Territories; Geological Survey of Canada, Paper 75-28, 34 p.

van Everdingen, R.O.
  1976: Geocryology terminology; Canadian Journal of Earth Sciences, v. 13, p. 862-867.

Wright, R.K.
  1983: Relationships between runoff generation and active layer development near Schefferville, Quebec; Permafrost, Fourth International Conference, Proceedings, Fairbanks, Alaska; National Academy Press, Washington, D.C., p. 1412-1417.

Geochronology of retrogressed granulites from Wilson Lake, Labrador

K.L. Currie and W.D. Loveridge
Precambrian Geology Division

Abstract

A U-Pb upper concordia intercept age of 1699 ± 3 Ma on zircon from granulite gneiss from the north shore of Wilson Lake, Red Wine Mountains, Labrador, dates the period of high grade metamorphism in the area. A Rb-Sr date of 1014 ± 31 Ma on biotite from the same specimen provides evidence for a Grenvillian thermal event. Duplicate K-Ar dates of 2239 ± 28 and 2201 ± 48 Ma on the same biotite concentrate that yielded the 1014 ± 31 Ma Rb-Sr date, indicate the presence of excess argon in this mineral.

These dates suggest an Aphebian or older protolith for the Red Wine Mountains region, metamorphosed and intruded at great depth at about 1700 Ma. A second (Grenvillian) period of metamorphism was of retrograde character, even though it reached amphibolite grade, and can only be detected in structurally disturbed zones.

Résumé

Une datation à l'U-Pb basée sur l'intercept supérieur concordia évaluant à 1 699 ± 3 Ma l'âge d'un zircon provenant d'un gneiss à granulite de la rive septentrionale du lac Wilson, dans les monts Red Wine au Labrador, permet de dater la période de métamorphisme à degré élevé qu'a connu cette région. La datation au Rb-Sr, évaluation à 1 014 ± 31 Ma, l'âge d'une biotite prélevée d'un même échantillon, confirme qu'un événement thermique s'est produit au Grenvillien. Une double datation au K-Ar donnant 2 239 ± 28 et de 2 201 ± 48 Ma à partir du même concentré de biotite dont l'âge a été évalué à 1 014 ± 31 Ma selon la méthode au Rb-Sr indique la présence d'un excédent d'argon dans ce minéral.

Ces datations laissent supposer que, dans la région des monts Red Wine, une roche-mère de l'Aphébien ou plus ancienne, s'est métamorphisée et s'est introduite à grande pronfondeur il y a environ 1 700 Ma. Une seconde période de métamorphisme à charactère régressif s'est produite au Grenvillien; elle a toutefois atteint le faciès des amphibolites. Le métamorphisme n'est observable que dans les zones ayant subi des dérangements structuraux.

Geological setting

Wilson Lake lies near the southeastern margin of the Red Wine Mountains, (Fig. 23.1), a roughly rectangular massif of granulite-grade metamorphic rocks including sapphirine-quartz and hypersthene-sillimanite-quartz assemblages, as well as various younger intrusive rocks (Gittins and Currie, 1978; Emslie et al., 1978). The Wilson Lake region exhibits transitions from these very high grade assemblages to lower-grade assemblages possibly of younger age. These transitions take place in the vicinity of major structural dislocations. Gittins and Currie (1978) argued that the various sapphirine-bearing assemblages (sapphirine-quartz, sapphirine-cordierite-corundum) demonstrated a history of alteration and metamorphism subsequent to the high-grade event which produced the sapphirine-quartz assemblages. They further argued that the structural complexity of the granulite gneiss suggested an extensive premetamorphic history.

The regional geological setting of the granulite facies rocks, and even their regional extent, remains essentially unknown. Recent geological mapping suggests that correlative rocks underlie a very broad tract of central Labrador (Thomas and Wood, 1983; Nunn, 1982; Thomas et al., 1981), probably hundreds of kilometres in extent. Radiometric dating reported by Emslie (1981) and Thomas et al. (1981) suggests that this region underwent a period of high-grade metamorphism, reaching granulite facies, accompanied by intrusive activity at about 1660 Ma. However no evidence of any Grenvillian metamorphism (±1000 Ma) was found in these studies, even though the Wilson Lake region is shown on most geological compilations as falling well inside the Grenville province (Douglas, 1970; Wynne-Edwards, 1972). The present study was intended to help unravel the metamorphic history of the Wilson Lake region, and by implication to help date the broad tract of similar rocks in central Labrador. Since particular interest centred on the presumed polymetamorphic history of the gneiss, and the possibly identical protoliths of the sapphirine-quartz and amphibolite grade assemblages, a single block of gneiss (sample no. 78135) weighing about 40 kg was collected from a cliff face on the north shore of Wilson Lake (Fig. 23.2). The material consisted of a greyish pink, leucocratic gneiss with characteristic thin, black mafic seams. The fine grained quartzo-feldspathic matrix shows very little foliation, although the salic layers may be boudined and intricately small folded. The mafic seams tend to pinch out and disappear in such regions of boudinage and small folding. Locally the mafic seams contain visible muscovite. In thin section the matrix consists of granoblastic aggregates of quartz, tartan-twinned microcline and plagioclase (oligoclase). The presence of microcline is characteristic of the retrograded gneisses in this region. The high-grade rocks contain orthoclase, or fine bleb perthite. The mafic seams consist mainly of biotite, muscovite, magnetite-ilmenite intergrowth, and relicts of sillimanite and cordierite. In gneisses which have not been retrograded, biotite, muscovite and cordierite do not occur. Zircon occurs in the mafic layers as brownish, rounded grains. Sapphirine does not occur in this specimen, but relicts of sapphirine surrounded by cordierite occur within a few metres of the sample site, and retrograded gneiss similar to the specimen

Figure 23.1. *Regional setting of the Wilson Lake area. The assemblage sapphirine + quartz occurs throughout the Red Wine Mountain block (stippled area). Retrogressed granulites occur as far west as Michikamau Lake. The position of the Grenville Front (inset) is often taken as the southern margin of the Naskaupi Fold belt, along a major mylonite zone, but its position south of Michikamau Lake is unknown.*

can be traced continuously into gneisses in which the characteristic mafic seams consist of hypersthene, sillimanite, sapphirine and magnetite-ilmenite. It thus seemed possible that appropriate dating methods applied to this sample could reveal two or more ages of metamorphism.

Analytical procedures and results

Techniques for the concentration of zircon and the extraction and analysis of lead and uranium are described in Sullivan and Loveridge (1980). Results of U-Pb analysis on zircon are listed in Table 23.1 and displayed in a concordia diagram (Fig. 23.3). A description of the zircon morphology is presented in the appendix. The method of Davis (1982) was used for linear regression of the U-Pb data and error estimation.

The +105 and -105 +74 μm zircon size fractions were first handpicked to obtain 100% zircon and then divided into less and more magnetic splits using the magnetic pin technique of Krogh (1982). The -74 +62 μm fractions on the other hand, were first separated into less and more magnetic magnetic fractions using a Frantz isodynamic separator, and then were handpicked for purity.

The six zircon fractions analyzed yielded data points forming a linear trend (Fig. 23.3). Four data points (1, 2, 4 and 6) are collinear within analytical uncertainty defining a chord which cuts the concordia curve at 1699 ± 3 and 179 + 82/ -78 Ma; the two data points which do not fit this pattern (3 and 5) resulted from analyses of the more magnetic splits of the coarser (+149 and -149 +74 μm) fractions. These two points clearly lie to the right of the chord defined by the other four points and have $^{207}Pb/^{206}Pb$ ages of 1707 ± 2 and 1709 ± 2 Ma respectively, both of which are greater than the upper intercept age given by the chord.

Biotite was separated from the same sample of gneiss that yielded the zircon. Results of K-Ar analyses on the biotite were published by Stevens et al. (1982, pub. no. GSC 80-201) and are listed in Table 23.2 for reference.

Figure 23.2. *Geology of the Wilson Lake area.*

A_{hg} *gneissic granulite and sodic charnockite, contains sapphirine + quartz in pelitic portions*

P_{mg} *modified granulite with contorted banding, development of retrograde biotite, with the assemblage hypersthene + sillimanite*

P_{bc} *gabbroic to ultramafic hypersthene-diopside granulite gneiss, with retrogressed biotite-hornblende zones, minor actinolitic schist*

P_{og} *oxide-rich zones; titaniferous hematite and magnetite with interstitial sapphirine, cordierite, sillimanite and hypersthene*

P_{gg} *Wilson Lake complex; muscovite-biotite gneiss and migmatite, locally gradational to P_{mg} and A_{hg}*

The location of the dated sample (78135) is shown by a star

Table 23.1. Analytical data, zircon fractions from sample 78135

Fraction no.	Size and magnetics	Weight mg	U ppm	Pb* ppm	Measured $^{206}Pb/^{204}Pb$	Isotopic abundance, $^{206}Pb=100$ ^{204}Pb	^{207}Pb	^{208}Pb	Isotopic ratios $^{206}Pb/^{238}U$	$^{207}Pb/^{235}U$	$^{207}Pb/^{206}Pb$	Age, Ma $^{207}Pb/^{206}Pb$
1	-74+62, m-1°	0.70	228.7	70.48	547.3	0.0295	10.801	13.009	0.29268	4.1960		1696
2	-74+62, n-1°	1.88	119.7	36.45	1086	0.0255	10.739	11.904	0.29145	4.1753		1695
3	+105, m	2.04	283.2	87.08	784.3	0.1136	12.012	17.747	0.28717	4.1412		1707
4	+105, n	1.19	253.6	75.47	1894	0.0156	10.572	13.620	0.28014	4.0011		1689
5	-105+74, m	0.70	467.6	140.08	1199	0.0581	11.261	15.896	0.27979	4.0383		1709
6	-105+74, n	0.82	407.9	118.56	2000	0.0248	10.713	13.605	0.27431	3.9233		1692

Grain size is in µm.

m = magnetic, n = non mag. at 1° slope, fractions 1 and 2; for 3-6 see text.

Pb* = radiogenic Pb.

Isotopic abundances of Pb presented after subtraction of Pb blank.

Rb-Sr analyses on the same biotite concentrate were performed using techniques similar to those described by Wanless and Loveridge (1972) and results are presented in Table 23.2.

The initial $^{87}Sr/^{86}Sr$ for this biotite is not known but a reasonable range of values might be from 0.705 to 0.715 considering the c. 700 Ma of existence of the gneiss prior to formation of the biotite. The Rb-Sr age and uncertainty of 1014 ± 31 Ma includes the uncertainity due to the above range of initial $^{87}Sr/^{86}Sr$; if the initial $^{87}Sr/^{86}Sr$ was greater than 0.715, the age would be lower than stated.

Interpretation

The U-Pb age measurements on zircon yield a bimodal distribution of data points, with points 3 and 5 from the more magnetic splits of the coarser zircon fractions falling to the right of the chord defined by the other four points. The more magnetic split of the finer fraction yields a point (1) which falls on the chord.

The morphology of all zircon fractions is generally similar with approximately 80% of zircon grains being rounded and equidimensional to ovoid with rounded crystal facets, suggesting crystallization (Pidgeon and Bowes, 1972; Pidgeon and Aftalion, 1972) during the period of high grade metamorphism which affected the rocks. The remaining 20% of zircon crystals and fragments show a more euhedral form, typically with partially rounded terminations but with generally parallel sides. The proportion of more euhedral zircon was somewhat greater in the +149 µm, less magnetic fraction (4). Euhedral to subhedral zircon cores were seen only in a few members of the more magnetic splits of the coarser zircon fractions (3 and 5); they were not seen in the finer fractions nor in the less magnetic splits of the coarser fractions.

We attribute the bimodal distribution of the zircon data to the presence of these zircon cores in fractions 3 and 5. A small component of inherited lead within the cores would cause the observed shift to the right of the two data points. The common lead contents of these two fractions (3.1 and 5.9% respectively; note ^{204}Pb contents, Table 23.1) are greater than those of the other four fractions (0.9 to 1.6%) but this is probably due to the greater incidence of black speck inclusions in fractions 3 and 5.

Since the zircon population is composed of about 80% metamorphic zircon, we interpret the upper intercept age of 1699 ± 3 Ma as dating the period of high grade metamorphism. The period of crystallization of the more euhedral zircon component probably does not differ significantly in time from that of the metamorphic zircon (cf. Pidgeon and Aftalion, 1972). This is further indicated by the results from fraction 4 which contains a higher proportion of euhedral zircon but yields a data point collinear with the other three. The presence of an older component in these gneisses is indicated by the existence of rare zircon cores in fractions 3 and 5. It is conceivable that very rare zircon cores may have been present in zircon from fractions other than 3 and 5 even though they were not found in the representative portions subjected to detailed microscopic examination. If this were the case, the measured age could be a slight overestimate for the age of high grade metamorphism.

Discussion

The best defined age measured in the present study is the upper intercept age of 1699 ± 3 Ma on zircon. Since the four points defining the chord all lie relatively close to the upper intercept, assumptions about the subsequent metamorphic history of the rock only slightly affect this
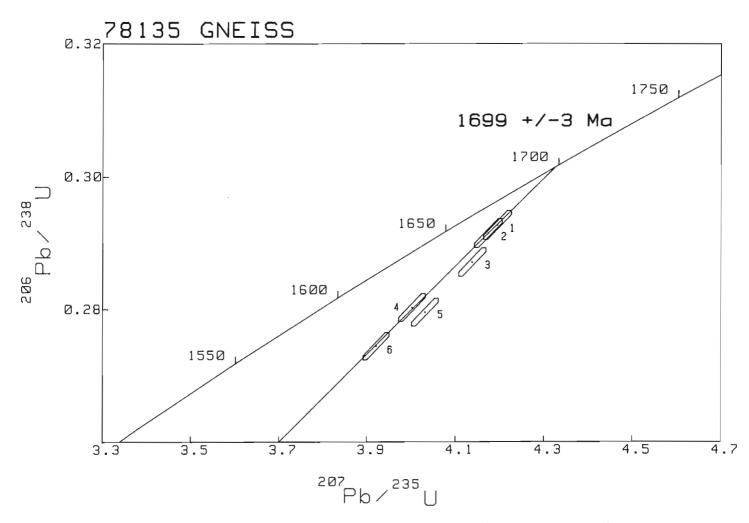
Figure 23.3. *Concordia diagram showing the results of U-Pb analyses of zircon concentrates from 78135.*

Table 23.2   Rb-Sr and K-Ar age results, 78135 biotite

Rb	425.2 ppm	K			6.48%
Sr	55.77 ppm	$^{40}Ar/^{40}K$, Ar%	i		0.2578, 99.6%
			ii		0.2502, 99.8%
$^{87}Rb/^{86}Sr$	22.04 ± 0.33				
		Age	i		2239 ± 28 Ma
$^{87}Sr/^{86}Sr$	1.0297 ± 0.0004		ii		2201 ± 48 Ma
*Age	1014 ± 31 Ma				
*See discussion of initial $^{87}Sr/^{86}Sr$ in text.					

date, which is marginally older than the 1660 Ma age reported by Emslie (1981) for the granulite grade metamophism 60 km to the north, or the 1654 ± 22 Ma age of the North Pole Brook intrusive suite (Thomas et al., 1981) which is probably related to this episode. Emslie (1981) suggested that these ages were too young to be related to the 1700 Ma Hudsonian orogeny in this region, but the closure time for such high grade metamorphism may be substantially later in the core of a high-grade zone than on its margins (this study). It is unlikely that the lower intercept age of 179 Ma is geologically meaningful.

We interpret the Rb-Sr age on biotite of 1014 ± 31 Ma to date closing of the biotite Rb-Sr system after the formation of biotite from the original assemblage hypersthene + potash feldspar, and presumably to approximately date the rest of the associated minerals such as muscovite, cordierite, and the local sapphirine + corundum segregations. This age represents the first evidence for a Grenvillian thermal event in the granulite facies terrane, although the coexistence of contrasting metamorphic assemblages demonstrated that post-granulite-facies metamorphism was required, and the widespread occurrence

of biotite giving Grenville K-Ar ages in the surrounding region (Wanless, 1969; Dallmeyer and Rivers, 1983) made it probable that Grenville metamorphism must be involved. Because of the extremely high grade of the gneisses affected by Grenville metamorphism, this metamorphic event was essentially of retrograde character in the Red Wine Mountains, even though the mineral assemblages show that it reached amphibolite facies. Like most retrograde metamorphism, the effects appear most prominently along major dislocations where water had access to the rocks. The absence of such effects from the central parts of the Red Wine Mountains massif thus suggests that these rocks probably were little affected by either Grenvillian deformation or metamorphism.

From the above remarks, it seems clear that the K-Ar biotite ages of 2201 and 2239 Ma cannot represent geological events, but rather indicate the presence of substantial excess argon in the biotite. Assuming that the true age of the biotite only slightly exceeds the 1014 Ma value found by Rb-Sr measurement, the biotites contain roughly twice the expected amount of argon. The region south of the boundary of the Grenville province has been known for many years to contain excess argon in biotite, and to a lesser extent in amphibole (Wynne-Edwards, 1972; Dallmeyer and Rivers, 1983; Wanless et al., 1969, 1970). Recently Dallmeyer and Rivers (1983) made a detailed study to the west of the Red Wine Mountains, and concluded that the presence of excess argon indicated the presence of a pervasive intragranular gas phase derived from degassing of underlying Archean rocks. The oldest ages found by them (2066 Ma for biotite) were comparable to those observed at Wilson Lake, but around Wilson Lake, the gneisses appear to be the oldest rocks, with no evidence of any basement. It seems reasonable, therefore, to suggest that the gneiss itself may be the Archean basement.

The structural significance of excess argon in biotite is poorly understood at present, but two suggested alternatives have some relevance to the Wilson Lake region. The excess argon might be retained due to (1) a massive, low-porosity character of the rock, or (2) deep burial, for example by piling of nappes on top, to prevent the escape of argon. The first alternative seems improbable for this region since the rocks show a pronounced cataclastic foliation and underwent hydrothermal alteration between the time of granulite facies metamorphism and the 1014 Ma event (Gittins and Currie, 1978). The second alternative seems reasonable for the very high grade metamorphism at c. 1700 Ma, but less plausible for the moderate amphibolite facies conditions associated with the Grenvillian metamorphism. Both alternatives suggest that the accumulation of excess argon was most probable during the older high-grade metamorphism, and that the younger metamorphism may actually have partially dissipated some of this excess. Since the residual excess is still substantial, this lends weak support to the hypothesis that the original protolith was Archean rather than Proterozoic (Gittins and Currie, 1978). The presence of excess argon may also help to explain previous difficulties in detecting Grenville metamorphism in this region.

In summary, the data indicate a protolith, possibly of Archean age, raised to exceptionally high metamorphic grade at 1699 ± 3 Ma. Since the marginal Wilson Lake region yields an approximately Hudsonian (c. 1700 Ma) age, younger ages in the core of the Red Wine block (Emslie, 1981; Thomas et al., 1981) may suggest that rocks in the core stayed at high grade for a substantial length of time, perhaps as much as 50 Ma. The high grade rocks of this study were remetamorphosed during the Grenville orogeny to amphibolite grade, but due to the retrogressive character of this second metamorphism, it can only be detected in favourable locations. There is no reliable isotopic evidence of any event younger than the Grenville orogeny.

References

Dallmeyer, R.D. and Rivers, T.
1983: Recognition of extraneous argon components through incremental-release $^{40}Ar/^{39}Ar$ analysis of biotite and hornblende across the Grenvillian metamorphic gradient in southwestern Labrador; Geochemica et Cosmochimica Acta v. 47, p. 413-428.

Davis, D.W.
1982: Optimum linear regression and error estimation applied to U-Pb data; Canadian Journal of Earth Sciences, v. 19, no. 11, p. 2141-2149.

Douglas, R.J.W.
1970: Geology and Economic Minerals of Canada; Geological Survey of Canada, Economic Geology Report 1.

Emslie, R.F.
1981: Exceptionally high grade metapelitic gneisses in the Red Wine Mountains, southern Labrador; Geological Association of Canada Abstracts 6, p. A-17.

Emslie, R.F., Hulbert, L.J., Brett, C.P., and Garson, D.F.
1978: Geology of the Red Wine Mountains, Labrador; the Ptarmigan complex; in Current Research, Part A, Geological Survey of Canada, Paper 78-1A, p. 129-134.

Gittins, J. and Currie, K.L.
1978: Petrologic studies of sapphirine-bearing granulites around Wilson Lake, Labrador; in Current Research, Part A, Geological Survey of Canada, Paper 78-1A, p. 77-82.

Krogh, T.E.
1982: Improved accuracy of U-Pb zircon dating by selection of more concordant fractions using a high gradient magnetic separation technique; Geochimica et Cosmochimica Acta. v. 46, p. 631-635.

Nunn, G.A.G.
1982: Regional geology east of Michikamau Lake, central Labrador; Newfoundland Mineral Development Division, Report 82-1, p. 149-167.

Pidgeon, R.T. and Aftalion, M.
1972: The geochronological significance of discordant U-Pb ages of oval-shaped zircons from a Lewisian gneiss from Harris, outer Hebrides; Earth and Planetary Science Letters, v. 17, p. 269-274.

Pidgeon, R.T. and Bowes, D.R.
1972: Zircon U-Pb ages of granulites from the Central Region of the Lewisian, northwestern Scotland; Geological Magazine, v. 3, p. 247-258.

Stevens, R.D., Delabio, R.N., and Lachance, G.R.
1982: Age determinations and geological studies, K-Ar isotopic ages, Report 15; Geological Survey of Canada, Paper 81-2.

Sullivan, R.W. and Loveridge, W.D.
1980: Uranium-lead age determinations on zircon at the Geological Survey of Canada; current procedures in concentrate preparation and analysis; in Loveridge W.D., Rubidium – strontium and uranium-lead isotopic age studies, Report 3; in Current Research, Part C, Geological Survey of Canada, Paper 80-1C, p. 161-246.

Thomas, A., Jackson, V., and Finn, G.
1981: Geology of the Red Wine Mountains and surrounding area, central Labrador; Newfoundland Mineral Development Division, Report 81-1, p. 111-120.

Thomas, A. and Wood, D.
  1983:   Geology of the Winokapau Lake area, Grenville Province, central Labrador; in Current Research, Part A, Geological Survey of Canada Paper 83-1A, p. 305-312.

Wanless, R.K.
  1969:   Isotopic age map of Canada; Geological Survey of Canada, Map 1256A.

Wanless, R.K. and Loveridge, W.D.
  1972:   Rubidium-strontium isochron age studies, Report 1; Geological Survey of Canada, Paper 72-23.

Wanless, R.K., Stevens, R.D., and Loveridge, W.D.
  1969:   Anomalous parent-daughter isotopic relationships in rocks adjacent to the Grenville Front near Chibougamau, Quebec; Eclogae geoligicae Helvetia, v. 63, p. 345-364.

  1970:   Excess radiogenic argon in biotites; Earth and Planetary Science Letters, v. 7, p. 167-168

Wynne-Edwards, H.R.
  1972:   The Grenville Province; in Variations in Tectonic Style in Canada; ed. R.A. Price and R.J.W. Douglas; Geological Association of Canada, Special Paper 11, p. 263-334.

APPENDIX

Sample location and description of zircon concentrates.
Sample no. 78135, latitude 53°20'53"N, longitude 62°53'30"W.

Fraction 1: The -74 +62 μm size fraction was separated into relatively magnetic and non magnetic fractions by repeated passes through a Franz Isodynamic Separator. Both fractions were then hand picked to produce concentrates of clear, whole zircon grains. The more magnetic fraction consisted of 100% clear rounded to rounded-euhedral zircon grains of a very pale straw colour, a few of which contained small bubble inclusions.

Fraction 2: The -74 +62 less magnetic fraction was similar to the above except that the grains were essentially clear of inclusions.

Fraction 3: The +105 size fraction was first hand picked to obtain 100% pure zircon and was then magnetically separated using the magnetic pin technique of Krogh (1982) and a high intensity, rare earth, cobalt magnet. The more magnetic fraction consisted of 100% clear zircon of rounded to rounded-euhedral shape, ranging from colourless to light tan with a few crystals showing a red-orange colour in reflected light. Ten to fifteen percent contained black speck inclusions and a few grains contained euhedral to subhedral zircon cores. Some bubble inclusions were noted.

Fraction 4: The +105 less magnetic fraction was separated as above and was generally similar in appearance to fraction 3. Some of the larger crystals were more prismatic and euhedral than noted in other fractions of this sample and no zircon cores were seen. The less magnetic grains were less strongly coloured and contained fewer black speck inclusions, although fine bubble inclusions were noted in about 10%.

Fraction 5: The -105 +75 μm size fraction was hand picked to produce a concentrate of the whole clearest zircons. This was then magnetically separated using the high gradient magnetic field and pin technique. The more magnetic concentrate consisted of 100% zircon of rounded to rounded euhedral outline, more coloured and less clear than the less magnetic fraction described below. Approximately 25% contained black speck inclusions and euhedral to subhedral zircon cores were notes in rare grains.

Fraction 6: The -105 +74 μm less magnetic fraction consisted to 100% rounded to rounded-euhedral zircon, mostly clear and ranging from colourless to slightly yellow-tan with a hint of red-orange in some. Some 10-15% of the grains contained small black speck inclusions and up to 5% showed distinct fine zoning in transmitted light. Bubble inclusions were noted in up to 20% of the grains.

Deep electromagnetic mapping of sedimentary formations in Southern Ontario

Project 810003

A.K. Sinha, D.C. Gresham, and L.E. Stephens
Resource Geophysics and Geochemistry Division

Abstract

Deep transient electromagnetic (EM) soundings were carried out in two areas in Southern Ontario to evaluate the possibility of mapping gently dipping sedimentary formations. In both locations, the depths to an electrically conductive shale horizon changed systematically and were mapped along two profiles.

The first test area was chosen around the village of Copetown, about 75 km southwest of Toronto. There, a buried river valley, which cuts through a shale formation, was mapped beneath a fairly resistive glacial till cover. The interpreted depths of the conductive shale horizon underlying the till ranged from 85 m to about 150 m which generally agreed well with shallow seismic reflection data gathered earlier. In the second area, seven EM soundings were performed along a 50 km long east-west profile passing through Kitchener. The separations between the sounding points varied from 5 to 10 km. The interpreted depths of dolomite, shale and limestone horizons generally agreed with known geological information. Hence, electromagnetic mapping of gently dipping sedimentary strata appears to be a practical method for obtaining subsurface geological information when drillhole data are inadequate or not available.

Résumé

Des sondages électromagnétiques transitoires en profondeur ont été réalisés dans deux régions du sud de l'Ontario pour évaluer la possibilité de cartographier les formations sédimentaires faiblement inclinées. Aux deux endroits, la profondeur d'un horizon de schiste argileux conductif augmente de façon constante et a été porté sur carte en fonction de deux coupes.

La première zone étudiée se trouve près du village de Copetown, à environ 75 km au sud-ouest de Toronto. On y a cartographié une vallée fluviale enfouie; cette dernière entaille une formation de schiste argileux et se situe sous une couverture de till moyennement résistant. Les profondeurs relevées du schiste argileux conductif sous-jacent au till varient entre 85 et environ 150 m, ce qui correspond bien en général aux données obtenues antérieurement par sismique réflexion à faible profondeur. Dans la seconde zone étudiée, sept sondages électromagnétiques ont été effectués le long d'un profil est-ouest de 50 km qui traverse Kitchener. Les points de sondage étaient espacés de 5 à 10 km. Les profondeurs relevées des horizons de dolomite, de schiste argileux et de calcaire correspondent en général aux renseignements géologiques connus. Il ressort donc de cette étude que la cartographie d'une strate sédimentaire de faible inclinaison à partir de levés électromagnétiques, constitue une méthode pratique pour obtenir des renseignements géologiques souterrains lorsque les données recueillies au moyen de trous de sondage sont insuffisantes ou non disponibles.

Introduction

Electromagnetic (EM) methods have been successfully used for a wide variety of geophysical investigations including mineral exploration, engineering studies, geothermal exploration and permafrost mapping. In the last decade, several attempts have also been made to apply EM sounding techniques for geological mapping. Patra (1970) suggested the use of central frequency sounding method to map a two-layer ground with possible application in groundwater prospecting. Ryu et al. (1972) used the multifrequency EM dipole sounding method to map unconsolidated sediments in Santa Clara Valley in California using the polarization characteristics of the measured field. Later, Koefoed and his associates (Koefoed and Biewinga, 1976; Biewinga, 1977) used a similar system for groundwater surveys in arid regions using the mutual coupling ratios of two loops for interpretation.

The Geological Survey of Canada has investigated the possibility of using multifrequency and transient EM systems for deep geological mapping since 1982. A survey with both multifrequency and transient EM systems over the permafrost terrain in the Mackenzie Delta indicated that both methods can be used to map the permafrost and other geological formations down to depths of 700 m (Sinha and Stephens, 1983). Transient EM data were shown to be less influenced by near surface inhomogeneities and generally had better lateral resolution than multifrequency data.

EM surveys were undertaken in 1983 and 1984 to investigate the possibility of using deep EM sounding techniques for mapping gently dipping sedimentary formations in Southern Ontario. The purpose of the surveys was to determine the depths and thicknesses of different formations at several discrete sounding stations down to several hundred metres from the surface, thereby aiding in the detailed mapping of the terrain. Since much of Southern Ontario is covered with glacial till and other Quaternary sediments, geological mapping of the subsurface strata has been carried out in the past using drillhole information from a limited number of oil and gas wells scattered throughout Southern Ontario. Sanford (1969) has compiled a geological map of Southern Ontario based mainly from drillhole information. However, in areas with few drillholes, the uncertainties in the map may be quite significant. The purpose of this project was to determine if deep penetration ground EM systems could be used to obtain additional information in such areas. This was to be done by comparing the geophysical results with drillhole information whenever the holes were close to the sounding stations. This paper presents results from two survey areas: a profile across a buried river valley near Copetown, about 75 km southwest of Toronto and another profile passing through the Kitchener area (Fig. 24.1).

The area around Copetown was selected because it lies directly across an ancient river valley filled with glacial till. The pre-glacial valley was cut through dolomite and shale

Figure 24.1. *Location of deep EM soundings in Southern Ontario.*

formations by an eastward flowing river. The presence of the buried valley has been known at this site for some time and the area has recently been studied using gravity and shallow reflection seismic methods (J.A. Hunter, personal communication, 1984) prior to our survey.

The presence of electrically resistive glacial till and Middle Silurian dolomites (Amabel Group) overlying electrically conductive Lower Silurian and Upper Ordovician shales (Cataract Group and Queenston Formation) which had been cut by the river valley provide a good electrical contrast that can be detected by EM methods. The Meaford-Dundas Formation of Upper Ordovician age consisting of shale with limestone and dolomite is electrically more resistive than the overlying Queenston Formation.

The river valley is narrow at the western end but becomes wider and deeper towards the east. The survey measured the depth to the conductive shale layers that had been cut by the river showing that the thickness of the resistive overburden decreased from about 150 m at the centre of the valley to about 85 m towards north and south over a distance of 2.5 km. Six transient EM soundings were carried out along a north-south line in order to map the thickness variation of unconsolidated sediments in the east-west trending valley. Two of the sounding stations had to be offset towards the east because of the presence of power lines.

Seven transient EM soundings were performed along a generally east-west trending profile near Kitchener with the separations between the sounding points varying from 5 to 10 km (Fig. 24.1). This line of profile was selected because our data could be compared to a published geological section (Sanford, 1969) which had been derived from information provided by a small number of irregularly spaced drillholes in the vicinity of the profile. The conductive shale formations of the Cataract Group provided good electrical contrast with the overlying dolomite formations in the area. The geological section indicated that the depth to the shale layers increased from about 100 m at the eastern end to about 250 m at the western end of the profile, 50 km away. The purpose of our survey was to trace all the formations based on the variation of their electrical resistivities and to compare the results with the generalized geological section. The agreement was good at most locations.

A Geonics EM-37 tranient EM system was used at both locations. The transient system was used because of its superior depth penetration and lateral resolution compared to frequency-domain or direct current electric systems. The latter generally requires the current electrode separations to be about five times the depth penetration desired (McNeill, 1980). In populated areas like Southern Ontario, that would make direct current sounding quite impractical. The depth penetration of the EM-37 system with a transmitter loop of size 300 m x 300 m carrying a current of 20A would be approximately 400-500 m in most areas of Southern Ontario.

Geological setting

The subsurface geology of the area is relatively simple. It consists of a succession of dolomite, shale and limestone of Silurian and Ordovician age, dipping gently toward the west. The Salina, Guelph and Amabel Formations of Late and Middle Silurian age are at the top of the sequence and are mostly dolomite containing anhydrite and gypsum lenses along with numerous bioherm reefs. These are underlain by the Cataract Group of Early Silurian age which are mostly shales and brown and grey dolomite. Upper Ordovician shales with minor siltstone, dolomite and limestone underlie the Cataract Group. The Queenston shales at the top of the Upper Ordovician sequence are underlain by Meaford-Dundas Formation of interbedded siltstone, limestone and dolomite.

These are underlain by the Blue Mountain and Collingwood formations which are mostly shales. Beneath these is the Trenton Group of Middle Ordovician age which is mostly shales. Beneath these is the Trenton Group of Middle Ordovician age which is mostly limestones with minor amounts of shale. These Paleozoic formations overlie an electrically resistive Precambrian basement. The depth to the basement generally increases from about 300 m near Toronto to about 1 km near Sarnia, 250 km to the west.

Geonics EM-37 transient EM system

The instrument used for the survey was the Geonics EM-37 transient EM system. The transmitter in the system powered by a gasoline generator consists of a square or rectangular wire loop varying in size from 40 m x 40 m to 300 m x 600 m. The receiver consists of a multi-turn loop which can be oriented in three orthogonal directions for measuring the decay of three components of the induced magnetic field. A steady current is passed through the transmitter long enough for the turn-on transients in the ground to dissipate. The current is then abruptly terminated in a linear ramp fashion. The rapid reduction of the current produces a rapid decrease of the primary field flux. In accordance with Faraday's law of electromagnetic induction, this produces an electromotive force (emf) in the ground which tries to keep the field strength constant at every point just after the turn-off. This emf causes currents to flow in ground conductors. These currents decay with time in a manner depending on the electrical and geometrical characteristics of the ground. The decaying currents generate a secondary magnetic field, whose time rate of change is recorded by the receiver coil. The receiver records the decay of the field at 20 logarithmically equi-spaced time channels during the transmitter off-time. The current is 'off' for a time equal to the 'on' period of the current. During the 'off' period the decay voltages are measured in the absence of the primary field which makes the system insensitive to small errors in distance and orientation between the transmitter and the receiver in contrast to frequency domain systems where the secondary fields are always measured in the presence of a much stronger primary field.

The upper half of Figure 24.2 shows the set-up for the central transient EM sounding, where the transmitter is a square loop and the receiver is placed at the centre. At the end of the 'off' period, the current is turned 'on' again rapidly but in the negative sense. The lower half of Figure 24.2 shows the currents and induced magnetic fields measured by the system. The transmitter can be operated with two base frequencies of 30 and 3 Hz.

With a base frequency of 30 Hz, the time channels represent samples from 0.087 to 7 ms after the transmitter turn-off. With the lower base frequency of 3 Hz, the channel times range from 0.87 to 70 ms. Since the last ten channels at 30 Hz coincide with the first ten channels at 3 Hz, the use of both frequencies produces a total 30 measurements at each sounding station. The system has been described in detail by Sinha (1983).

The EM-37 can be used in either a profiling or a sounding mode. In the profiling mode, the transmitter loop is generally rectangular and the measurements are made along profiles normal to the longer side of the transmitter loop which is laid parallel to the general direction of the geological strike. In the sounding mode used during the present survey, the transmitter loop is square with the receiver at the centre. Normally, two loop sizes are used at each sounding point. The larger loop with its larger dipole moment allows reliable measurements to greater depths, while the smaller loop is most sensitive to near-surface materials.
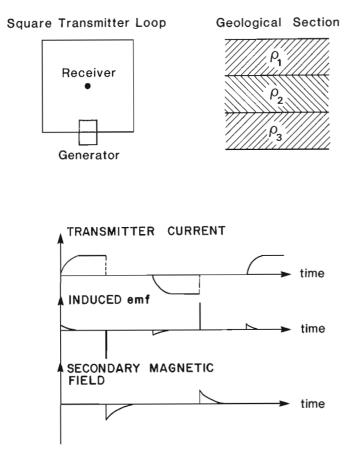
Square Transmitter Loop   Geological Section

Figure 24.2. *Schematic of the transient EM sounding set-up showing the transmitter pulse and secondary effects.*
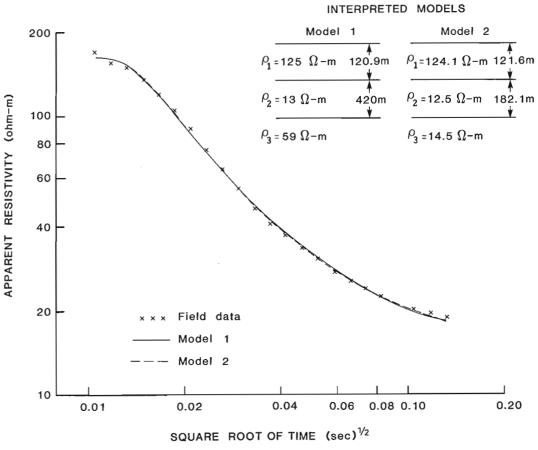
Interpretation techniques

In the sounding mode, the EM-37 measures the decay of the vertical component of the induced magnetic field at 20 channels for each base frequency (30 or 3 Hz). The measured voltage is highest in the earlier channel and decreases gradually in later channels. It can be shown, however, that the measured decay amplitudes are relatively insensitive to changes in the resistivity of subsurface layers. It has therefore been found useful to transform the decay voltages into apparent resistivity values much like what is done in direct current or magnetotelluric methods. After the current is turned off in the transmitter, eddy current intensity is highest near the ground under the transmitter. Hence, the emf in the receiver in early channels is influenced mainly by the resistivity of the upper layers. As time increases, the induced eddy currents gradually diffuse into the ground, and the decay voltages in later channels are influenced increasingly by the resistivities of the deeper layers. After a certain period of time, the subsurface current pattern stablizes. During this "late time" the equations describing the magnetic field components are greatly simplified and can be expressed uniquely in terms of the electrical parameters of the ground and the dipole moment of the transmitter. The apparent resistivity values can thus be derived easily from the measured decay voltages in late times.

The interpretation of the field data in terms of a layered model can be accomplished by graphical or analytical techniques. In the graphical technique, the measured apparent resistivity values for each channel are plotted against the square root of time for that channel on a log-log graph paper. The field plots are then compared with a catalogue of previously computed master curves plotted on log-log graphs with the same cycle length until a good match

Figure 24.3

Interpretation of a transient EM sounding curve in the Copetown area with a square transmitter loop 300 m x 300 m in size. Note that there may be more than one model consistent with the field data.

INTERPRETED MODELS

Model 1	Model 2
$\rho_1 = 125$ Ω-m 120.9m	$\rho_1 = 124.1$ Ω-m 121.6m
$\rho_2 = 13$ Ω-m 420m	$\rho_2 = 12.5$ Ω-m 182.1m
$\rho_3 = 59$ Ω-m	$\rho_3 = 14.5$ Ω-m

× × × Field data
——— Model 1
— — — Model 2

SQUARE ROOT OF TIME (sec)$^{1/2}$

is obtained. In the analytical case, an inversion of the field data is attempted which provides a solution for the data in the least square sense assuming a layered earth model. A combination of the two generally provides the optimum results.

To interpret the field data, an analytical inversion is performed first. The analytical model is refined further by changing one or more parameters at a time until the response of the model matches the field data. This procedure is normally carried out interactively on a graphics screen. Figure 24.3 shows the interpretation performed on the sounding data from a location near Copetown. The figure shows two possible interpretations of the field data. Although the resistivities of the first two layers and the thickness of the top layer are almost identical in the two models, the second layer thickness and the third layer resistivities are quite different. This is due to the phenomenon of equivalence and is a fundamental problem in all potential field technique methods. In such cases, unique interpretation may be impossible unless other independent information is available.

Interpretation of field data

Copetown profile

Six soundings were carried out on a north-south profile in order to produce a section showing the variation in thickness and resistivity of the unconsolidated sediments filling the east-west trending valley and the Paleozoic sediments below the top resistive layer. Two sounding stations (C4 and C5, Fig. 24.1) were offset towards the east because of the presence of power lines in their vicinity. Figure 24.4 shows the interpreted section along the profile. Sounding stations 1 through 4 were north of the centre of the valley while station 5 was very close to the deepest point of the valley. Sounding station 6 was about 4.5 km south of the centre. Difficulty with access to cultivated fields and the presence of a number of high voltage power lines in the area prevented any more soundings in the area. In all locations except at station 6, two loop sizes were used, generally 75 m and 300 m on the sides. The data from each loop were interpreted independently and the interpretations are indicated in Figure 24.4. A shallow reflection seismic survey (Hunter, personal communication, 1984) was also carried out along the line in 1982 and the thickness of the unconsolidated sediments from seismic data are indicated by dashed lines.

The depths of interfaces mapped by using small and large loop transmitters are almost identical except at station 5 where the bottom of the conductive layer is not resolved in the small loop data. The large loop data provide an additional interface at a depth of 88 m. The discrepancy can be explained by the principle of equivalence whereby the two layers of 291 and 37 ohm-m resistivity may be combined to form one layer of resistivity 99 ohm-m as observed by the small loop data. The discrepancy between the seismic and EM data at station 4 may be explained by the fact that the EM sounding station was about 500 m east of the seismic survey line and the valley was also dipping towards east. Hence, the measured depth to the shale formation would be greater at the EM sounding station than at the corresponding point on the seismic survey line. The resistivities of the dolomite and the unconsolidated sediments are too similar to be resolved by EM methods. However, the Queenston shale which has a resistivity of about 10 ohm-m as compared to about 100 ohm-m for the overlying sediments is mapped very clearly. There is some discrepancy between the top layer

NORTH   **SOUTH**

Numbers indicate resistivities in Ω-m

— — — — — Overburden depth from seismic survey

Figure 24.4. *Interpretation of the Copetown profile data. The numbers on the left of the sounding positions are from the large loop (300 m) and the ones to the right are from the small loop (75 m). The locations of interfaces are indicated by horizontal dashes.*

resistivity values obtained by using the small and large loops in that the values from the large loop are consistently higher than those using the smaller loop. This map be explained by the way the apparent resistivity values are obtained from the decay amplitudes. The formula for obtaining apparent resistivity values assume the late time conditions to prevail at all measurement times. In reality, however, the data at early channels with the large loop may not be taken at late times while the requirement may be better satisfied with the smaller loop data since the onset of late time is related to the size of the loop. Hence, the apparent resistivity values measured with the smaller loop are likely to be more accurate. In this area the top layer resistivity varies from 77 to 99 ohm-m in the profile which is reasonably uniform. The layer underlying the Queenston Formation is somewhat more resistive. This agrees with geological information that the Queenston Formation is underlain by Meaford-Dundas formation which contains shales with intervals of siltstone, limestone and dolomite and hence is more resistive than the Queenston Formation.

Kitchener profile

The Kitchener profile consisted of seven deep EM soundings with the station separations varying from 5 to 10 km. Although two loop sizes were used at each station, data from the smaller loop were not used since they were noisy. There were no drillholes in the vicinity of the profile but it was situated along a generalized geological section (Sanford, 1969) derived from isolated drilling data. Figure 24.5 shows the interpretation of EM soundings superimposed on the generalized section. Boundaries between layers are marked by horizontal dashes and the resistivities of the layers in ohm-m are indicated by numbers.
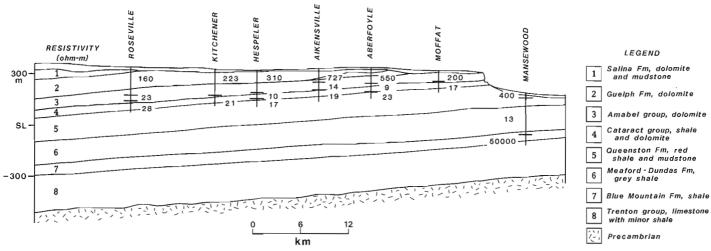
Figure 24.5. *Interpretation of the Kitchener profile data and its comparison with the generalized geological section.*

The Guelph Formation and Amabel Group are both dolomite and cannot be distinguished by EM methods. The resistivity contrast between the Amabel Group and the underlying shale and dolomite of the Cataract Group gives a good indication of this boundary at each of the stations. The EM interpretation indicates that this boundary is shallower than on the geological section at Roseville and Aikensville, but the interpretation agrees well with the geological section at the other stations. Delineation of the boundary between Cataract Group and Queenston Formation is somewhat uncertain due to the low electrical resistivity contrast, although the EM interpretation at four stations indicates a thickness for the Cataract Group similar to the geological section. The electrical contrast between the Queenston and Meaford-Dundas formations is poor, both being relatively good conductors. Consequently, this contact was not detected at all. At the Mansewood station Queenston and Meaford-Dundas formations are detected below resistive glacial till and soil and above the highly resistive Trenton Group consisting of resistive limestone with minor shales.

It should be noted here that the geological section is only approximate, based on limited drillhole data. Hence, some of the discrepancies may be attributed to the errors in the geological section.

Concluding remarks

Electromagnetic mapping techniques have most commonly been used in mineral exploration in the past. the availability of deep EM sounding systems, both multi-frequency and transient, has opened up the possibility of their use in general geological mapping in sedimentary terrains. This study indicates the potential of using EM techniques to map areas where no detailed geologic data exist either because the bedrock geology is concealed by overburden or drillholes are too sparsely distributed. The technique is most successful when the formations are subhorizontal and there is a sufficient contrast in the electrical resistivities of the different formations.

References

Biewinga, D.T.
1977: Electromagnetic depth sounding experiment; Geophysical Prospecting, v. 25, no. 1, p. 13-28.

Koefoed, O. and Biewinga, D.T.
1976: The application of electromagnetic frequency sounding to groundwater problems; Geoexploration, v. 14, p. 229-241.

McNeill, J.D.
1980: Applications of transient electromagnetic techniques; Technical Note TN-7, Geonics Ltd., Toronto, 17 p.

Patra, H.P.
1970: Central frequency sounding in shallow engineering and hydro-geological problems; Geophysical Prospecting, v. 18, no. 2, p. 236-254.

Ryu, J., Morrison, H.F., and Ward, S.H.
1972: Electromagnetic depth sounding experiment across Santa Clara valley; Geophysics, v. 37, no. 2, p. 351-374.

Sanford, B.V.
1969: Geology of the Toronto-Windsor area, Ontario; Geological Survey of Canada, Map 1263A.

Sinha, A.K.
1983: Deep transient electromagnetic soundings over the McClean Uranium deposits; in Uranium Exploration in the Athabaska Basin, Saskatchewan, Canada, ed. E.M. Cameron; Geological Survey of Canada, Paper 82-11, p. 273-280.

Sinha, A.K. and Stephens, L.E.
1983: Deep electromagnetic sounding over the permafrost terrain in the Mackenzie Delta, N.W.T., Canada; Permafrost: Fourth International Conference Proceedings, National Academy Press, Washington, D.C., p. 1166-1171.

The basal contact of the Road River Group - a proposal for its location in the type area and in other selected areas in the Northern Canadian Cordillera

Project 650024

W.H. Fritz
Institute of Sedimentary and Petroleum Geology, Ottawa

Abstract

The suggested location of the base of the Road River Group is consistent with the concept that the group comprises basinal dark grey to black shale, siltstone and platy limestone. Within the Richardson Trough (type area), the Road River overlies light- to medium-brown, Middle Cambrian sandstone (Slats Creek Formation), and light grey, Lower Cambrian limestone (Illtyd Formation).

Within the Selwyn Basin, the Road River lies immediately above medium grey, wavy bedded, Lower Cambrian limestone (Sekwi Formation, northeast); maroon Precambrian and Lower Cambrian shale (Upper "grit unit", northwest); medium grey to light brownish grey, Upper Cambrian (?) and Lower Ordovician (?) siltstone and shale (Kechika Group, west); and medium grey to light brownish grey, Upper Cambrian and Lower Ordovician silty limestone (Rabbitkettle-Kechika Formation, southeast).

Road River strata within the Kechika Trough overlie medium grey to medium brownish grey siltstone, shales and limestone of Lower Ordovician age (Kechika Group). On the Cassiar Platform, Road River strata overlie medium grey to greenish grey siltstones, shales and volcanics of Upper Cambrian and Lower Ordovician age (Kechika Group).

Résumé

L'emplacement suggéré de la base du groupe de Road River est compatible avec l'hypothèse voulant que le groupe se compose de schiste argileux, d'aleurolite et de calcaire feuilleté decouleur gris foncé à noir accumulés dans un bassin. Dans la fosse de Richardson, la région type, le groupe de Road River recouvre un grès brun clair à brun moyen du Cambrien moyen (la formation de Slats Creek) et un calcaire gris clair du Cambrien inférieur (la formation d'Illtyd).

Dans le bassin de Selwyn, la formation de Road River repose directement sur du calcaire gris moyen à stratification ondulée du Cambrien inférieur (la formation de Sekwi, au nord-est), du schiste argileux couleur bordeaux du Précambrien et du Cambrien inférieur (l'"unité de grit" supérieur, au nord-ouest), de l'aleurolite et du schiste argileux gris moyen à gris brunâtre clair du Cambrien supérieur et de l'Ordovicien inférieur (la formation de Rabbitkettle-Kechika, au sud-est).

Dans la dépression de Kechika, les couches de Road River sont sus-jacentes à de l'aleurolite, à des schistes argileux et à du calcaire limoneux gris moyen à gris brunâtre moyen de l'Ordovicien inférieur (le groupe de Kechika). Sur la plate-forme des Cassiars, les couches de Road River reposent sur des aleurolites, des schistes argileux et des roches volcaniques gris moyen à gris verdâtre du Cambrien supérieur et de l'Ordovicien inférieur (le groupe de Kechika).

Introduction

Since Jackson and Lenz's (1962) definition of the Road River Formation in the Richardson Trough (Fig. 25.1), a number of important developments have taken place that bear upon its correlation. These have been brought to the writer's attention by geologists who have mapped and/or measured the Road River in different areas. As might be expected, more than one opinion is held on how the base of the Road River should be correlated. Ensuing discussions have shaped the contents of this paper, and therefore it is appropriate that some of their aspects be presented before proceeding with the writer's preferred correlation.

Geologists with experience within the Richardson Trough have suggested three positions for the base of the Road River that are founded upon mappability within the type region and beyond. While agreeing that two of the positions represent a major departure from the North American Stratigraphic Code (Oriel, 1983), they argue that the vagueness of the original description, plus the practicality of their suggested contacts, make all three possibilities viable.

One option is to locate a contact at least 865 m below the original base of the Road River, where it coincides with the base of the Slats Creek Formation (Fig. 25.2). Using this contact would include a major body of light coloured (Slats Creek) sandstone within the Road River, a rock type that is rare within the type Road River or within the group elsewhere.

The second possibility is to raise the base approximately 2000 m, so that it coincides with the base of the original Upper member of the Road River Formation. By removing the Lower member (platy limestone) and allowing the Upper member (graptolitic shale) to represent the whole of the formation, the thickness of the type Road River would be reduced by roughly two thirds.

The third interpretation places the base at the base of the Jackson and Lenz Lower member, or, in other words, where it was originally defined.

In the present correlation, the first two options were not considered because they depart too far from the Code. The third posibility is favored over the other two, but it features a weak lithological contact. A more visible contact, near that of the third interpretation, is championed here because the writer believes it can be more readily demonstrated in the field (see discussion under Richardson Trough). This minor change is believed to be consistent with the Code.

The above three interpretations come from geologists who have worked within and outside the type area, whereas one strongly held opinion has come from geologists working mainly outside the type area. This interpretation is virtually the same as the second one mentioned above, but is supported for different reasons.

Those working outside the type region hold that the lengthy account of graptolitic shale (Upper member) in the type description gives the impression that the type Road River is characterized by graptolitic strata. The short, imprecise description of the Lower member is viewed as implying a much lower degree of importance. Also, until recently, the isolation of the type area has precluded visits to type Road River outcrops. The result has been a widespread mapping of the Road River with reference only to the type Upper member. Currently, the amount of published Road River data from outside the type region (Richardson Trough) greatly exceeds that from within. This being so, it can be argued that if agreement between the larger "regional reality" and the Road River within the type region is to be achieved, it is necessary to restrict the name Road River to

the upper member in the type area, and to redraw the base of the Road River within the Richardson Trough. This change in the type area is unacceptable under the Code, which states (Oriel, 1983, Article 19g): "Undesirable restrictions – When a unit is divided into two or more of the same rank as the original, the original name should not be used for any of the divisions. Retention of the old name for one of the units precludes use of the name in a term of higher rank. Furthermore, in order to understand an author's meaning, a later reader would have to know about the modification and its date, and whether the author is following the original or the modified usage. For these reasons, the normal practice is to raise the rank of an established unit when units of the same rank are recognized and mapped within it."

After deliberation, the writer concluded that a major change in the type Road River would not enhance its mappability within or outside the Richardson Trough. A major change to fit the "regional reality" concept is likewise unnecessary, because emphasis could (and should) be placed upon the lithological character of the group, which permits the use of a highly diachronous base to meet regional variation. Encouragement for this flexible approach is found in the Code (Oriel, 1983, Article 22e), which states: "The boundaries of most lithostratigraphic units may transgress time horizons...", and also that "...concepts of time or age play no part in defining lithostratigraphic units nor in determining their boundaries..."
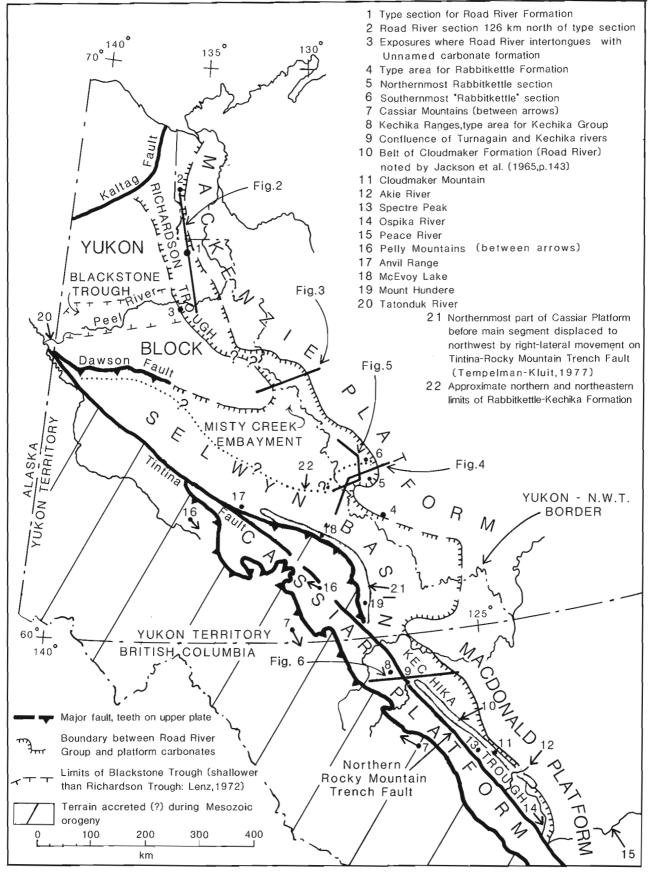
Acknowledgments

The wide usage of the term Road River, and the map unit's complex depositional history, make it virtually certain that future correlations for the group will pass through a period of volatility. In an attempt to anticipate some of these changes, the mentioned discussions were held with those closest to the subject. Additional discussions were held with others on points of logic and presentation. Those who participated in the discussions are: M.P. Cecile, H. Gabrielse, S.P. Gordey, A.C. Lenz, R. Ludvigsen, R.W. Macqueen, B.S. Norford, D.K. Norris, B.R. Pratt, D.J. Tempelman-Kluit, R.I. Thompson, S.R. Westrop, and J.O. Wheeler.

The writer thanks those mentioned, and wishes to add that the naming of any one of the above does not indicate his agreement with the views in this paper. Illustrations were drafted by H. McLaughlin.

Location of base within the type area

In their initial description of the Road River Formation in the Richardson Trough, Jackson and Lenz (1962, p. 32) stated that "More detailed work will probably show that this formation can be subdivided into an upper predominantly shaly unit [member] , and a lower predominantly calcareous unit [member] ". At the type section on a tributary of the Road River (Fig. 25.1, loc. 1), only the Upper member was measured and described. At this location, the Lower member is cut by numerous faults. Jackson and Lenz noted that their knowledge of the Lower member was supplemented by a section measured on the Road River 17 km south of the type section. Unfortunately, data from this section were omitted from their paper. However, they did state that the base of the Road River Formation "is well exposed on the Road River and other localities in the Richardson Mountains, where a thick sequence of limestones generally present in the lower part of the formation is apparently conformably underlain by shale, siltstone, and sandstone of Cambrian Age." An estimate of the thickness of the Lower member can be obtained by subtracting the thickness of the Upper member at the type section (loc. cit., 910 m) from the total thickness of the formation (2652 m)
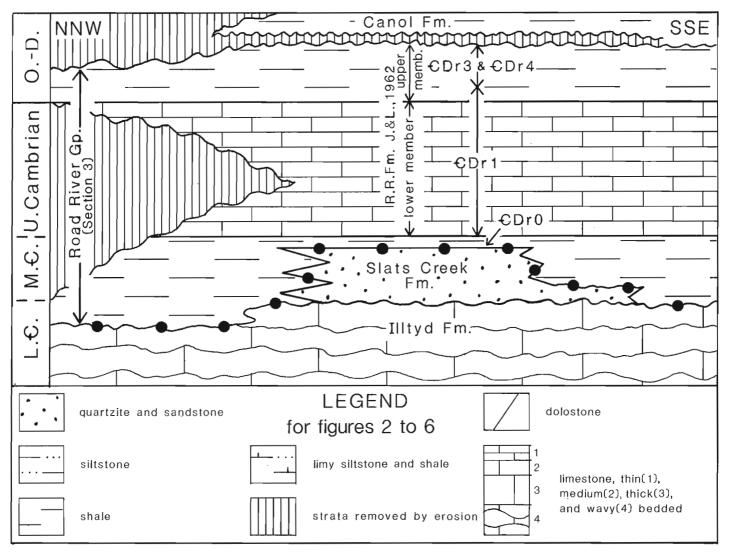
Figure 25.1. *Locality map showing distribution of Road River Group, major geologic features, and outcrop areas (numbered) mentioned in text. Locations of cross-sections shown in Figures 25.2 to 25.6 are also given.*

The numbered outcrop areas shown on the map:

1 Type section for Road River Formation
2 Road River section 126 km north of type section
3 Exposures where Road River intertongues with Unnamed carbonate formation
4 Type area for Rabbitkettle Formation
5 Northernmost Rabbitkettle section
6 Southernmost 'Rabbitkettle' section
7 Cassiar Mountains (between arrows)
8 Kechika Ranges, type area for Kechika Group
9 Confluence of Turnagain and Kechika rivers
10 Belt of Cloudmaker Formation (Road River) noted by Jackson et al. (1965, p.143)
11 Cloudmaker Mountain
12 Akie River
13 Spectre Peak
14 Ospika River
15 Peace River
16 Pelly Mountains (between arrows)
17 Anvil Range
18 McEvoy Lake
19 Mount Hundere
20 Tatonduk River
21 Northernmost part of Cassiar Platform before main segment displaced to northwest by right-lateral movement on Tintina-Rocky Mountain Trench Fault (Tempelman-Kluit, 1977)
22 Approximate northern and northeastern limits of Rabbitkettle-Kechika Formation

Legend:

— Major fault, teeth on upper plate
— Boundary between Road River Group and platform carbonates
— Limits of Blackstone Trough (shallower than Richardson Trough: Lenz, 1972)
— Terrain accreted (?) during Mesozoic orogeny

0 100 200 300 400
km

given by Jackson and Lenz at Rock River, located 17 to 25 km from the type section. The result is a thickness of 1742 m for the Lower member, or nearly twice that of the Upper member. This thickness for the Lower member is in fair agreement with the 2040 m reported by Norford (1964, p. 110) and the 2000 m measured and estimated by Cecile et al. (1982) at Rock River.

The Lower member, known to contain the graptolite Dictyonema sp., was tentatively placed in the Ordovician, although Jackson and Lenz (1962, p. 32, 33) recognized that the genus Dictyonema extends into the Cambrian. A later report (Berry and Norford, 1976) listing Dictyonema sp. and other graptolites associated with early Upper Cambrian (Dresbachian) trilobites within a 273 m interval low in the Lower member provided a firm, Late Cambrian age for that part of the map unit. Recent collections of earliest Ordovician conodonts by Cecile (personal communication) from near the Lower-Upper member boundary at the Rock River section, suggest that nearly all of the Lower member is within the Upper Cambrian. Dresbachian trilobites in float (GSC locs. 90526-90528) originating from the lower part of the Lower member are known from localities 9 km south of the type section (Fritz, manuscript report).

No variations from the original concept of the Road River Formation were noted in the Lexicon of Canadian Stratigraphy in 1981 (Cecile and Morrow, p. 152). A minor change at the base of the Road River in the type area, and an amplification of the Road River concept in the Richardson Trough, were recorded on geological maps by D.K. Norris (1981a-c, 1982a,b). No explanatory text accompanied the change. Norris divided strata in the type Road River into three map units, and added new strata in a fourth. He continued to rank the Road River as a formation. In the present paper, the undesignated map units of Norris are ranked as formations, and the Road River Formation is raised to group level.

Figure 25.2. Schematic cross-section locating base of Road River Group (solid circles) in Richardson Trough. Road River Formation as originally defined by Jackson and Lenz (1962) is located at centre of figure. Section 3 (Fritz, manuscript) is near left margin. Numbered map units (ЄDr0, ЄDr1, etc.) are those of Norris (1981a). In this paper, base of the Road River is revised near type area by lowering it from base of Lower member of Jackson and Lenz (1962) to base of Norris' map unit ЄDr0, and rank of Road River is changed from formation to group. Position of cross-section is indicated in Figure 25.1.

Recommendation for minor change in base of Road River at type area A lowering of the base of the Road River to include a thin (150+ m) map unit of black shale (Fig. 25.2, Norris map unit ЄDrO) is here formally recommended. The revised base is in accordance with mapping by Norris (1981a), who recognized the following map units within the Road River in the type area (ascending order): black shale (formation), ЄDrO; black shale and limestone (formation), ЄDrl; medium grey siltstone and dark grey limestone (formation), ЄDr3; and black shale and limestone (formation), ЄDr4. Most of the second formation (ЄDr1) equates with the Lower member of Jackson and Lenz (1962), and the remaining part of the second plus all of the third and fourth (ЄDr3, ЄDr4) equate with their Upper member. By a minor lowering of the base of the Road River, Norris established a more mappable base that is located at the top of the Slats Creek Formation. Above is the dark coloured basinal succession, and below is a thick succession of Slats Creek sandstone.

A stratigraphic section (Fritz, in Norris, manuscript report, Section 106L10; located on GSC map 1524A, lat. 66°38', long. 135°50'30") illustrates the Road River-Slats Creek contact 9 km south of the type Road River section. Below this contact is 715+ m of thin and medium bedded, rust, light brown, and light grey weathering Slats Creek sandstone. The upper contact of the Slats Creek is covered, but is readily mappable because float strongly reflects the lithological change below. At an outcrop several hundred metres north of the section, 41 m of the lowest strata in the black shale formation (ЄDrO) is exposed. At this location, sparse (10 per cent), thin interbeds of limy, very fine grained sandstone and a few lenses (45 cm wide, 15 cm thick) of dark grey, finely laminated limestones are present in the black shale. Abundant sponge spicules were seen at some levels. Except for the lime content, the sandstone in the interbeds resembles that in the Slats Creek below.

Most of the black shale formation in this section has been deeply weathered to dark soil, but more resistant, platy, dark grey limestone (25 per cent) and black shale outcrop in the interval from 99 to 126 m above the base. At 152 m above the base, platy limestone float is abundant, and remains so for a considerable distance up-section. It is likely that the top of the black shale formation is at or near the 152 m level. The previously mentioned early Upper Cambrian fossils (GSC locs. 90526-90528) probably came from the limestone talus above the 152 m level.

Location of base elsewhere in the Richardson Trough

At a thin Road River section (Fritz, in Norris, manuscript report; located on GSC map 1520 A, lat. 67°51'15", long. 135°50'00") 126 km north of the type section, the underlying Slats Creek Formation and the lower two Road River formations (ЄDr0, ЄDr1) are missing (Fig. 25.2). At this location, 102 m of shale belonging to the upper Road River is unconformably overlain by Permian siltstone and unconformably underlain by dark, Lower Cambrian shale and platy limestone. In mapping the base of the Road River at this locality, Norris (1981c) applied the same criteria used in locating the base in the type area, but to strata of a different age. The continuous succession of dark grey to black shale and platy limestone was traced downward to a major lithological change – the top of a wavy parting, thin- to thick-bedded limestone succession belonging to the Lower Cambrian Illtyd Formation. The contact between the light grey, resistant Illtyd and the dark, recessive Road River is as obvious here as is the Slats Creek-Road River contact in the type area.

In an area 95 km south of the type area (where the Peel River crosses the Richardson Trough) the Road River-Slats Creek contact is like that mentioned in the type area.

A short distance to the south, however, the Road River intertongues with a laterally equivalent unnamed carbonate formation (Norris, 1981a; GSC map 1528A, ЄDb), and the age of the basal contact changes depending upon which tongue is mapped. This intertonguing relationship not only once marked the western edge of the Richardson Trough (now eroded and/or covered by younger strata), but is locally exposed over the adjacent Yukon Block, where the Road River is generally younger than the Unnamed carbonate (Norford, 1964, Fig. 4; Jackson, 1966, Fig. 4). The dark grey, thin bedded Road River can be readily separated from the underlying Ordovician or Silurian, nearly white weathering Unnamed carbonate unit.

The Richardson Trough was probably physically linked to the Selwyn Basin through a corridor that extended to the southeast (Lenz, 1972). This corridor cannot be accurately traced today, because its likely route was through a now uplifted area presently underlain mainly by Precambrian and Quaternary strata. This area is 100 km long and averages 35 km wide (Norris, 1982a,b, between 65°00' and 65°30'N), and it contains sparse outcrops of Road River strata and of light coloured carbonate. Recently, Cecile (1982) and Pugh (1983) viewed the light coloured carbonate as representing remnants of a once continuous body of shallow water carbonate that completely separated the Richardson Trough and Selwyn Basin. If this concept can be substantiated, it follows that the Road River nomenclature should be restricted to the Richardson Trough and adjacent margins, and that a different nomenclature should be applied in the Selwyn Basin and beyond. The writer believes the original concept of a connection between the two basins is more likely because:

1. The two basins are aligned along a structural and depositional trend.

2. Strata assigned to the Road River Group in both basins are not only similar as a whole, but are similar at the formation level as well.

3. Individual outcrops of light coloured carbonate used to support the separation concept record only part of the total time allotted to Road River deposition.

4. The complex record of faulting between the two basins leaves open the possibilities of a shifting corridor, more than one corridor, an intermittent corridor, etc.

Northeastern Selwyn Basin (including Misty Creek Embayment) and adjacent Mackenzie Platform

Blusson (1974) applied the name Road River Formation to the strata covering a wide part of this area. The base of the Road River was placed at the top of the Lower Cambrian Sekwi Formation (Fig. 25.3). The same contact for the base of the Road River Formation was used by Aitken et al. (1973, p. 75) and was recognized by Cecile and Morrow (1981, p. 152). This basal contact is typically abrupt, with dark grey or black shale and platy limestone of the Road River Group overlying medium-grey weathering, wavy bedded limestone of the Sekwi Formation. A rather abrupt, northeastward interfingering of Road River basinal strata with lighter coloured carbonates on the Mackenzie Platform has been illustrated by Aitken et al. (1973, Fig. 3).

Later workers were less sure of the limits of the Road River, and hesitated to use the name. Fritz (1976, 1978, 1979a) referred to strata equivalent to the Road River (in sense of Norris, 1981a) as "post-Sekwi dark shale and platy limestone", and showed that the contact between the Sekwi Formation and the overlying basinal strata is diachronous, ranging in age from the middle to the uppermost part of the Lower Cambrian **Bonnia-Olenellus** Zone.
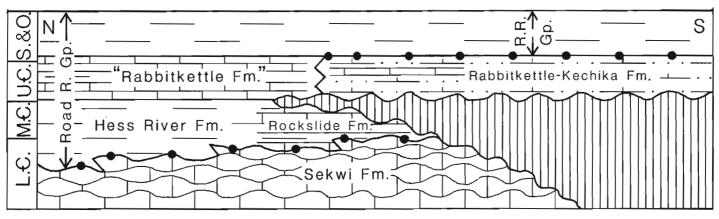
Figure 25.3. *Schematic cross-section locating base of Road River Group (solid circles) in northeastern Selwyn Basin (Misty Creek Embayment). Figure has been modified from Cecile (1982). Unnamed carbonate unit at left margin is formation mapped to north as ƐDb by Norris (1982a). For description of this map unit see Macqueen (1974, p. 323; 1975). Position of cross-section is indicated in Figure 25.1.*

Cecile (1978, 1982; in Goodfellow et al., 1980) studied the Road River strata in the Misty Creek Embayment and erected three, new, widespread formations, two of which equate with the Upper member of Jackson and Lenz (1962), and one with the black shale (formation) that was added by Norris (1981a, ƐDr0). Cecile (1982, Fig. 4) also extended the use of the term Rabbitkettle Formation into the area from the south, and equated it with the lower member of Jackson and Lenz (1962). Cecile (1982, p. 20) considered placing all four formations in the Road River Group when he stated "It is natural then to consider up-grading Road River Formation to a group that might include all basin strata [all four formations] in the Misty Creek Embayment, including the Hess River Formation, because of its lithological affinity to the rest of the succession." However, Cecile (1982, p. 20, 23) decided to delay using Road River in the northeastern Selwyn Basin and adjacent Mackenzie Platform because of problems encountered in correlating with a type section having a faulted base, and also with strata to the south, where others had applied a "different usage" of the Road River concept.

Figure 25.3 shows the Road River-Sekwi contact as the recommended base for the Road River in the northeastern Selwyn Basin. This base, however, is not enthusiastically accepted by all workers, some of whom favor a placing the base at the top of Cecile's "Rabbitkettle Formation."

Figures 25.3 and 25.5 show strata (their name placed in quotes) that Cecile (1982) has recognized as Rabbitkettle Formation, and which the writer believes should be placed under a new name. These strata are mainly dark grey, platy, relatively clean limestone and interbeds of dark grey siltstone and black shale. They are similar in lithology and age to the type Lower member of the Road River Formation, and are unlike strata in the type Rabbitkettle Formation to

the south. In the type area (east margin of southern Selwyn Basin) the Rabbitkettle is predominantly medium grey, limy siltstone and silty limestone, which are discussed in the next section of this paper.

A few workers disagree with the writer's assessment of the "Rabbitkettle Formation", and some others, although in agreement with the lithologic appraisal, still believe the name Rabbitkettle should be carried into the northeastern Selwyn Basin. Both groups point to the value of recognizing a widespread Rabbitkettle in the Selwyn Basin as the formation immediately underlying the Road River Group. In their correlation, the base of the Road River lies close to the Cambrian-Ordovician boundary over a wide area in the Selwyn Basin, and therefore agrees more closely in age with the basal strata in north-central British Columbia and on the northern Cassiar Platform. Although this correlation fits with, and indeed is part of, the "regional reality" concept, it fails to reflect the original Road River concept, the manner in which that concept was followed in the Richardson Trough, or the most obvious approach to correlating the type Road River into the Selwyn Basin.

Southern Selwyn Basin and adjacent Mackenzie Platform

Gabrielse et al. (1973, Fig. 8) assigned upper Middle Ordovician through Silurian, dark, basinal strata near the margin of the southern Selwyn Basin and the Mackenzie Platform to the Road River Formation, and showed these strata interfingering with carbonate formations to the east. They (op. cit., p. 48) excluded 300 m of underlying, dark grey, basinal strata from the formation because of an intervening unconformity. Ludvigsen (1982, p. 6) lowered the base of the Road River by 300 m, so that it is now located where dark shale and platy limestone (above) changes to the medium grey, limy siltstone and silty limestone (below). The latter

strata belong to the Rabbitkettle Formation near its type area, which Gabrielse et al. (1973, p. 51) state "can be traced northwesterly almost to Pelly River in Nahanni map-area...and southerly through Coal River map-area into northern Rocky Mountains...". The strata to which the Rabbitkettle was traced in the Northern Rocky Mountains have been assigned to the Kechika Group (Taylor and Stott, 1973), a group almost as widespread as the Road River Group. It is known that the two groups are in part time equivalent, and that to the south the Road River overlies the Kechika Group (see section on north-central British Columbia). Because the Rabbitkettle Formation in the southern Selwyn Basin (also informally called "wavy banded silty limestone") and the Kechika Group in north-central British Columbia are parts of what was once one laterally continuous lithological unit, the two names are here hyphenated and used to represent one formation in order to better illustrate their relationship in the southern Selwyn Basin.

In defining the base of the Road River within the Selwyn Basin, the northern boundary of the Rabbitkettle-Kechika formation is of considerable importance, because at that boundary the Rabbitkettle-Kechika begins to laterally displace part of the Road River (Fig. 25.5). Using criteria mentioned later, the northern boundary of the Rabbitkettle-Kechika was approximately located in Figure 25.1 (loc. 22) by a west and northwest trending line. At the eastern edge of the Selwyn Basin (Fig. 25.1, locs. 5, 6), the southernmost published "Rabbitkettle" (partial) section (Fritz, 1979a, Section 36) and the northernmost published Rabbitkettle section (Fritz, 1981, Section 3) serve to locate the line. The remainder of the line cannot be accurately located because Lower and Middle Paleozoic erosion has removed "Rabbitkettle" and Rabbitkettle-Kechika strata in areas where these map units might be expected to come together. The southern and southwestern limits used to position the line are tempered by outcrops of Kechika-like strata in the southern Dawson and northern McQuesten map areas (D.J. Tempelman-Kluit and S. Gordey, personal communication).

Figure 25.4.   Schematic cross-section locating base of Road River Group (solid circles) in southern Selwyn Basin and adjacent edge of Mackenzie Platform.   Position of cross-section is indicated in Figure 25.1.

Figure 25.5.   Schematic cross-section locating base of Road River Group (solid circles) in northern and southern Selwyn Basin.   Position of cross-section is indicated in Figure 25.1.

211

North of the dotted line, the Rabbitkettle-Kechika is absent and the Road River comprises black shale and dark grey, platy limestone ranging from Early Cambrian through Silurian in age. The graptolite shale, fine, planar laminae in the limestone and marginal penecontemporaneous slump folds and slump breccias testify to the slope and basin environment of the Road River. A sub-Franconian regional unconformity noted by Gabrielse et al. (1973, p. 48), is locally present, but is generally weak and is within the Road River Group.

South of the dotted line, the Road River resembles Road River strata to the north, but is represented only by Lower or Middle Ordovician to Silurian strata. South of the line, the Upper Cambrian and some Lower Ordovician Road River strata that occur in the north are replaced by the Rabbitkettle-Kechika. As in the type Kechika area in the Kechika Mountains in northern British Columbia, the Rabbitkettle-Kechika comprises argillaceous limestone, limy siltstone, and shale that are medium grey with hues of green or brown. Limestone is present in variable amounts and is usually more argillaceous or silty than that found in the Road River. It occurs in plates, wavy beds, and nodules, the latter often producing a "swiss cheese" texture on the weathering surfaces. Black shale is generally lacking in the Rabbitkettle-Kechika formation.

Few prominent environmental indicators are apparent in the Rabbitkettle-Kechika or in the Kechika Group to the south. Of interest, however, is the map unit's relationship to the outer edge of the carbonate shelf. Unlike the Road River, this map unit does not terminate abruptly against the platform carbonates, but grades over a wider area into the carbonates, or passes over the carbonates for a considerable distance onto the platform. This distribution, plus the higher clastic content in the Rabbitkettle-Kechika formation and the Kechika Group, suggests that their different appearance relative to the Road River is caused by a higher terrestrial clastic content. The sub-Franconian unconformity mentioned earlier is strongly developed immediately beneath the Rabbitkettle-Kechika formation in the southern Selwyn Basin (Fig. 25.5).

North-central British Columbia

The Northern Rocky Mountain Trench Fault, known to have a large right-lateral displacement (Gabrielse, 1985) passes through the middle of north-central British Columbia, where it juxtaposes contrasting rock types (Fig. 25.6). In the area west-southwest of the fault (southern Cassiar Platform) the Road River Group overlies and laterally interfingers with the Kechika Group. Near the westernmost outcrops, the Road River may directly overlie the light coloured limestone (Cambrian) of the Atan Group (Gabrielse, personal communication). Throughout the area, the incompetent Road River and Kechika are highly deformed, and depositional relationships are mainly obscured. Existing maps show the two groups as one or two map units (Gabrielse, 1962, 6a = K., 6b mostly = R.R.; 1963a, 5 = K. & R.R.; 1963b, 4a = K., parts 4b & 4c = R.R.), but maps in preparation separate the black shale and dark grey, platy limestone of the Road River from the medium grey silty shale and limestone of the Kechika (Gabrielse, personal communication). Minor, greenish grey weathering, igneous, extrusive rocks and sills are also present in the Kechika.

Locally, the Road River laterally displaces Lower Silurian dolostone of the Sandpile Formation. Fossils known thus far from the Road River are Early Ordovician (Arenig) to Middle Silurian in age (H. Gabrielse, personal communication). Fossils from the base of Kechika are latest Late Cambrian (Trempealeauan) in age (Gabrielse, 1969, p. 6).

East-northeast of the Northern Rocky Mountain Trench Fault, in the Kechika Trough, the Road River and Kechika groups have been mapped as two units. In this area there are various exposures where typical Kechika underlies the Road River, and the contrasting rock types are similar to those in the area west-southwest of the Fault.

In a preliminary report on Road River strata, Jackson et al. (1965, p. 143) state that the Cloudmaker Formation (= Road River Group) outcrops in a narrow belt that starts at the confluence of the Turnagain and Kechika rivers and extends southeastward for 320 km (Fig. 25.1, loc. 10). This suggests that the Road River can be readily mapped along trend, and also that the group was deposited in a continuous, elongate trough. In this belt, and at points 200 km (Cloudmaker Mountain) and 255 km (Akie River) from the northwest end (Fig. 25.1, locs. 11, 12), the Road River is 360 and 380 m thick, respectively, and is underlain by a thick succession of Mount April Formation strata (= Kechika Group of Jackson et al.). From these two localities, the Road River-Kechika contact extends 10 to 20 km northeastward to where the lower Road River is laterally displaced by dolostone of the Skoki Formation (Cecile and Norford, 1979).

Recent mapping and isolated observations by Gabrielse (1977, 1981) along and near the belt, and by Taylor and Stott (1973) to the northeast, indicate that sub-basins and ridges exist in and near the trough, and that the Road River map pattern will be more complex than formerly envisioned. A second notable observation by Gabrielse (personal communication) is that Late Precambrian to Devonian fine clastics, which will be difficult to separate from the Road River, occur in and near the trough. As for the Road River-Kechika contact, it is presently unclear as to whether the Kechika once extended everywhere below the Road River (as shown in Fig. 25.6). In this mobile area, a local lack of Kechika deposition, or Kechika erosion in pre-Road River time, would leave no Road River-Kechika contact and require different criteria to establish the base of the Road River.

A region in which locating the base of the Road River is but part of a larger problem lies between the narrow belt outlined by Jackson et al. (1965) and the Northern Rocky Mountain Trench Fault. In this area, Gabrielse (1977, Ware W 1/2 map area) mapped extensive regions as Road River, and adjacent extensive regions as Kechika. Both regions are crossed by a 60 km long, northwesterly trending line of unusually large, white limestone mounds containing Middle Cambrian fossils (Fritz, 1979b, Pl. 13.3, fig. 6). The stratigraphic relationship of the mounds to the base of the Kechika and Road River groups is unknown.

The southern end of the 320 km long belt of Road River mentioned by Jackson et al. (1965) is immediately east of Ospika River (Fig. 25.1, loc. 14). At this location, Gabrielse (1975, p. 11) has mapped "...the southernmost exposures of lower Paleozoic facies typical of the Road River Formation". Gabrielse's map of the area shows the Mount April Formation (= Kechika Group) underlying the Road River. A short distance farther south, near Peace River, the Northern Rocky Mountain Trench Fault cuts across the inner margin of Road River (basinal deposition), and still farther south, only the platformal carbonate equivalent of Road River is exposed.

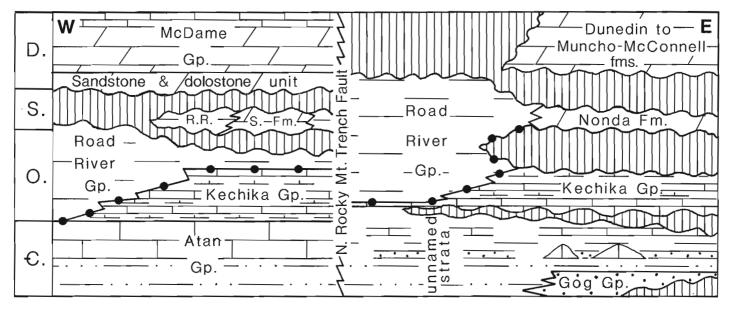## Northern Cassiar Platform and adjacent Selwyn Basin

Gabrielse and Wheeler (1961, p. 4, 5) first recognized the close similarity of the lower Paleozoic strata in the Pelly Mountains (northern Cassiar Platform) to those on trend in the southeast in the Cassiar Mountains (southern Cassiar Platform). The Kechika Group was correlated from the

Cassiar to the Pelly mountains, where it was described as including a black, graptolitic shale of Ordovician and Early Silurian age at the top (Templeman-Kluit et al., 1976, p. 97; Gordey, 1981, p. 8). This shale should now be assigned to the Road River.

In an attempt to correlate the Kechika from the Pelly Mountains eastward (across the Tintina Fault), Tempelman-Kluit et al. (1974) noted Kechika-like strata in the Anvil Range, at outcrops near McEvoy Lake, and at Mount Hundere (Fig. 25.1, locs. 17-19). In the Anvil Range, Middle Ordovician to Lower Silurian black shale (Road River Group) "probably overlies" Kechika-like strata unconformably, but no contact was observed (Tempelman-Kluit, 1972, p. 8). A sub-Silurian unconformity has probably removed the Road River near McEvoy Lake and at Mount Hundere (Abbott, 1977, Fig. 6).

Northwest Selwyn Basin and adjacent Yukon Block

In this area, the boundary between the Selwyn Basin and the Yukon Block is defined by the Dawson Fault, which separates basinal clastics to the south from shelf carbonates to the north (Green, 1972; Thompson and Roots, 1982). South of the fault, Middle Ordovician to Upper Silurian chert and black shale of the Road River Group unconformably overlie Upper Proterozoic and Lower Cambrian(?) maroon shale and gritty clastics of the "grit unit" of these authors. At some localities, the Road River overlies mafic flows that "may be intercalated" within the "grit unit" (Thompson and Roots, 1982, p. 410).

At the Yukon-Alaska boundary, the depositional trend of strata on the Yukon Block turns abruptly northward and away from the east-west trending Dawson Fault. Near the

Figure 25.6. *Schematic cross-section locating base of Road River Group (solid circles) in north-central British Columbia. Southern Cassiar Platform (left) and Kechika Trough (right) have common boundary at Northern Rocky Mountain Trench Fault. Road River Group (R.R.) and Sandpile Formation (S. Fm.) are abbreviated. Position of cross-section is indicated in Figure 25.1.*

Figure 25.7. *Regional correlation for base of Road River Group (solid circles).*

Tatonduk River, the shelf-basin transition is exposed north of and away from the pervasive shearing of the Dawson Fault. Within the slope and basin succession, Lower Ordovician strata at the base of the Road River are reported (Brabb, 1967, Fig. 13) to unconformably overlie early to latest Upper Cambrian platy limestone of the Hillard Formation. A short distance to the northeast, the Hillard and part of the Road River abruptly change facies into the white, thick bedded limestone of the Jones Ridge Formation (shelf facies). An Upper Ordovician tongue of the Road River that is approximately 18 m thick projects for at least a short distance eastward over the Jones Ridge Formation (op. cit., p. 19).

Summary

Figure 25.7 is a sketch illustrating the writer's concept of the correlation of the base of the Road River Group from the northern part of the Richardson Trough to the south end of the Kechika Basin, a distance of 1400 km. Beginning in the Richardson Trough, a minor revision is suggested, which would locate the base at the top of the Slats Creek Formation, whereas elsewhere in the trough the base is placed at the top of the Illtyd Formation. In the northeastern Selwyn Basin, the Road River overlies the Sekwi Formation. In the southern Selwyn Basin, however, stratigraphic relations are quite complex. Strata equivalent to the lower part of the Road River Group have been removed by erosion; strata equivalent to the medial part have been displaced by the Rabbitkettle-Kechika formation; and strata in the upper part overlie the Rabbitkettle-Kechika and extend southward through the southern Selwyn Basin. In the Kechika Trough, the Road River-Kechika contact generally serves as the base of the Road River. Key factors underlying this concept are the suppression of the Rabbitkettle Formation in the northeastern Selwyn Basin, and the recognition of a close link between the Rabbitkettle in the southern Selwyn Basin and the Kechika Group in the Kechika Trough.

The Road River-Kechika contact, which serves as a base for the Road River on the Cassiar Platform and adjacent Selwyn Basin, and the Road River – "grit unit" contact that serves as the base in the northwestern Selwyn Basin, are not shown in Figure 25.7.

References

Abbott, J.G.
1977: Structure and stratigraphy of the Mt. Hundere area, southeastern Yukon; Masters Thesis, Department of Geosciences, Queen's University, 111 p.

Aitken, J.D., Macqueen, R.W., and Usher, J.L.
1973: Reconnaissance studies of Proterozoic and Cambrian stratigraphy, Lower Mackenzie River area (Operation Norman), District of Mackenzie; Geological Survey of Canada, Paper 73-9, 178 p.

Berry, W.B.N. and Norford, B.S.
1976: Early Late Cambrian dendroid graptolites from the northern Yukon: Geological Survey of Canada, Bulletin 256, p. 1-12.

Blusson, S.L.
1974: Geology, Operation Steward (Northern Selwyn Basin) Yukon and District of Mackenzie, N.W.T. (106 A, B, C; 105 N, O), scale 1:250,000; Geological Survey of Canada, Open File Report 205.

Brabb, E.E.
1967: Stratigraphy of the Cambrian and Ordovician rocks of east-central Alaska; U.S. Geological Survey, Professional Paper 559-A. 30 p.

Cecile, M.P.
1978: Report on Road River stratigraphy and the Misty Creek Embayment, Bonnet Plume (106B), and surrounding map-areas, Northwest Territories; in Current Research, Part A, Geological Survey of Canada, Paper 78-A, p. 371-377.

1982: The Lower Paleozoic Misty Creek Embayment, Selwyn Basin, Yukon and Northwest Territories; Geological Survey of Canada, Bulletin 335, 78 p.

Cecile, M.P. and Norford, B.C.
1979: Basin to platform transition, Lower Paleozoic strata of Ware and Trutch map areas, northeastern British Columbia; in Current Research, Part A, Geological Survey of Canada, Paper 79-1A, p. 219-226.

Cecile, M.P. and Morrow, D.W.
1981: Road River Formation; in Lexicon of Canadian stratigraphy, volume 2, Yukon Territory and District of MacKenzie; Canadian Society of Petroleum Geologists, 240 p.

Cecile, M.P., Hutcheon, I.F., and Gardner, V.
1982: Geology of the northern Richardson Anticlinorium (map areas 106L/12, 13; 116I/9, 16) Geological Survey of Canada, Open File 875.

Fritz, W.H.
1976: Ten stratigraphic sections from the Lower Cambrian Sekwi Formation, Mackenzie Mountains, northwestern Canada; Geological Survey of Canada, Paper 76-22, 42 p.

1978: Fifteen stratigraphic sections from the Lower Cambrian of the Mackenzie Mountains, northwestern Canada; Geological Survey of Canada, Paper 77-33, 19 p.

1979a: Eleven stratigraphic sections from the Lower Cambrian of the Mackenzie Mountains, Northwestern Canada; Geological Survey of Canada, Paper 78-23, 19 p.

1979b: Cambrian stratigraphy in the northern Rocky Mountains, British Columbia; in Current Research, Part B, Geological Survey of Canada, Paper 79-1B, p. 99-109.

Fritz, W.H.
1981: Two Cambrian stratigraphic sections, eastern Nahanni map area, Mackenzie Mountains, District of Mackenzie; in Current Research, Part A, Geological Survey of Canada, Paper 81-1A, p. 145-156.

Gabrielse, H.
1962: Geology Kechika, British Columbia; Geological Survey of Canada, Map 42-1962.

1963a: McDame map-area, Cassiar District, British Columbia; Geological Survey of Canada, Memoir 319, 138 p.

1963b: Geology Rabbit River; Geological Survey of Canada, Map 46-1962.

1969: Geology of Jennings River map-area, British Columbia (104-0); Geological Survey of Canada, Paper 68-55, 37 p.

1975: Geology of Fort Grahame E 1/2 map-area, British Columbia; Geological Survey of Canada, Paper 75-33, 25 p.

1977: Geology of Toodoggone and Ware map areas, British Columbia (94E, 94F W 1/2), scale 1:250,000; Geological Survey of Canada, Open File Report 483.

Gabrielse, H. (cont.)
1981: Stratigraphy and structure of Road River and associated strata in Ware (west half) map area, northern Rocky Mountains, British Columbia; in Current Research, Part A, Geological Survey of Canada, Paper 81-1A, p. 201-207.

1985: Major dextral transcurrent displacements along the Northern Rocky Mountain Trench and related lineaments in north-central British Columbia; Geological Society of America, Bulletin, v. 96, p. 1-14.

Gabrielse, H. and Wheeler, J.O.
1961: Tectonic framework of southern Yukon and northwestern British Columbia; Geological Survey of Canada, Paper 60-24, 37 p.

Gabrielse, H., Blusson, S.L., and Roddick, J.A.
1973: Geology of Flat River, Glacier Lake, and Wrigley Lake map-areas, District of Mackenzie and Yukon Territory; Geological Survey of Canada, Memoir 366, 153 p.

Goodfellow, W.D., Jonasson, I.R., and Cecile, M.P.
1980: Nahanni Integrated Multidisciplinary Pilot Project. Geochemical Studies Part 1: Geochemistry and mineralogy of shales, cherts, carbonates and volcanic rocks from the Road River Formation, Misty Creek Embayment, Northwest Territories; in Current Research, Part B, Geological Survey of Canada, Paper 80-1B, p. 149-161.

Gordey, S.P.
1981: Stratigraphy, structure and tectonic evolution of southern Pelly Mountains in the Indigo Lake area, Yukon Territory; Geological Survey of Canada, Bulletin 318, 39 p.

Green, L.H.
1972: Geology of Nash Creek, Larsen Creek, and Dawson map-areas, Yukon Territory; Geological Survey of Canada, Memoir 364, 157 p.

Jackson, D.E.
1966: Graptolitic facies of the Canadian Cordillera and Arctic Archipelago; Bulletin of Canadian Petroleum Geology, v. 14, no. 4, p. 469-485.

Jackson, D.E. and Lenz, A.C.
1962: Zonation of Ordovician and Silurian graptolites of northern Yukon, Canada; Bulletin of American Association of Petroleum Geologists, v. 46, no. 1, p. 30-45.

Jackson, D.E., Steen, G., and Sykes, D.
1965: Stratigraphy and graptolite zonation of the Kechika and Sandpile Groups in northeastern British Columbia; Bulletin of Canadian Petroleum Geology, v. 13, no. 1, p. 139-154.

Lenz, A.C.
1972: Ordovician to Devonian history of northern Yukon and adjacent district of Mackenzie; Bulletin of Canadian Petroleum Geology, v. 20, no. 2, p. 321-361.

Ludvigsen, R.
1982: Upper Cambrian and Lower Ordovician trilobite biostratigraphy of the Rabbitkettle Formation, western District of Mackenzie; Royal Ontario Museum, Life Sciences Contributions, no. 134, 188 p.

Macqueen, R.W.
1974: Lower and Middle Paleozoic studies, northern Yukon Territory; in Report of Activities, Part A, Geological Survey of Canada, Paper 74-1A, p. 323-326.

1975: Lower and Middle Paleozoic sediments, northern Yukon Territory; in Report of Activities, Part C, Geological Survey of Canada, Paper 75-1C, p. 291-301.

Norford, B.C.
1964: Reconnaissance of the Ordovician and Silurian rocks of northern Yukon Territory; Geological Survey of Canada, Paper 63-39, 139 p.

Norris, D.K.
1981a: Geology Trail River, Yukon-Northwest Territories, Geological Survey of Canada, Map 1524A.

Norris, D.K.
1981b: Geology Eagle River, Yukon Territory; Geological Survey of Canada, Map 1523A.

1981c: Geology Fort McPherson, District of Mackenzie, Geological Survey of Canada, Map 1520A.

1982a: Geology Wind River, Yukon Territory; Geological Survey of Canada, Map 1528A.

1982b: Geology Snake River, Yukon-Northwest Territory, Geological Survey of Canada, Map 1529A.

Oriel, S.S. (Chairman)
1983: North American Stratigraphic Code; American Association of Petroleum Geologists, Bulletin, v. 67, no. 5, p. 841-875.

Pugh, D.C.
1983: Pre-Mesozoic geology in the subsurface of Peel River map area, Yukon Territory and District of Mackenzie; Geological Survey of Canada, Memoir 401, 61 p.

Taylor, G.C. and Stott, D.F.
1973: Tuchodi Lakes map-area, British Columbia; Geological Survey of Canada, Memoir 373, 37 p.

Tempelman-Kluit, D.J.
1972: Geology and origin of the Faro, Vangorda, and Swim concordant zinc-lead deposits, central Yukon Territory; Geological Survey of Canada, Bulletin 208, 73 p.

1977: Stratigraphic and structural relations between the Selwyn Basin, Pelly-Cassiar Platform, and Yukon Crystalline Terrane in the Pelly Mountains, Yukon; in Report of Activities, Part A: Geological Survey of Canada, Paper 77-1A, p. 223-227.

Tempelman-Kluit, D., Abbott, G., and Read, B.
1974: Stratigraphy and structure of Pelly Mountains; in Report of Activities, Part A, Geological Survey of Canada, Paper 74-1, p. 43, 44.

Tempelman-Kluit, D.J., Gordey, S.P., and Read, B.C.
1976: Stratigraphic and structural studies in the Pelly Mountains, Yukon Territory; in Report of Activities, Part A, Geological Survey of Canada, Paper 76-1A, p. 97-106.

Thompson, R.I. and Roots, C.F.
1982: Ogilvie Mountains Project, Yukon; Part A; a new regional mapping program; in Current Research, Part A, Geological Survey of Canada, Paper 82-1A, p. 403-411.

Two new middle Givetian rhynchonellid genera, Pine Point Formation, Great Slave Lake, District of Mackenzie

Project 700034

Paul Sartenaer [1]
Institute of Sedimentary and Petroleum Geology, Calgary

Abstract

Two new middle Givetian genera are proposed: **Droharhynchia** and **Homeocardiorhynchus,** with type species, respectively, **D. intermissa** (Crickmay, 1963), and **H. pityinus** n. sp.. Both species are found in the Bituminous limestone member of the Pine Point Formation.

In a forthcoming paper by A.W. Norris, T.T. Uyeno, and P. Sartenaer, the brachiopods and conodonts of the middle Givetian Bituminous limestone member of the Pine Point Formation, on the south side of the Great Slave Lake, will be described. It has been considered advisable to publish promptly the two new rhynchonellid genera in order to make them available for further research and discussion.

Résumé

L'auteur propose deux nouveaux genres du Givétien moyen: **Droharhynchia** et **Homeocardiorhynchus,** dont les espèces types sont **D. intermissa** (Crickmay, 1963) et **H. Pityinus** n. sp., respectivement. Les deux espèces sont trouvées dans le calcaire bitumineux de la formation de Pine Point.

A.W. Norris, T.T. Uyeno et P. Saternaer publieront sous peu une description des brachiopodes et des conodontes du calcaire bitumineux mi-givétien de la formation de Pine Point sur la rive sud du Grand lac des Esclaves. L'auteur a jugé opportun de publier une description des deux nouveaux genres de rhynchonelles afin de les mettre à la disposition des chercheurs à des fins de recherche et de discussion.

---

[1] Royal Institute of Natural Sciences of Belgium, Brussels

Droharhynchia n. gen.

Derivatio nominis. The name is formed by the inversion of the two first syllables of the original genus name **Hadrorhynchia** in allusion to the fact that, until now, this form has been included in that genus.

Type species. Hadrorhynchia intermissa Crickmay, 1963. This species is illustrated by photographs and by two transverse serial sections in the original publication. Photographs of five specimens, and complete serial sections of one specimen may be found in McLaren (1962, figs. 1a-f, 2a-c, 3a-c, 4a-c, 5a-f, fig. 16 **in textu** p. 60) under the name **H. sandersoni** (Warren, 1944).

Description. Small to medium sized. Half-circular to half-elliptical, and in some species, half-barrel shaped contour in frontal view. Transversely subelliptical to subcircular in ventral and dorsal views. Not inflated. Front margin uniplicate. Strongly inequivalve, the pedicle valve being very low. Cardinal line long and slightly undulated. Postero-lateral margins concave near the commissure. Commissure generally sharp, with the exception of the top of the tongue and, in some cases, of the lateral commissures that merge in the wall of the shell if the frontal end of the fold and the margin of the lateral flanks are curved downwards. Lateral commissures located very low anteriorly. Commissure deeply crenulated by the costae.

Contour of pedicle valve. A more or less regular half-ellipse with small, minor axis in longitudinal median sections; in transverse median sections, a very flattened half-ellipse hardly invaginated by the sulcus. Ventral flanks very slightly convex, sometimes almost flat, sloping gently toward the lateral commissures, and becoming steeper near the postero-lateral commissures. Anterior end of the flanks standing out as characteristic spurs. Well marked sulcus, clearly separated from the flanks, beginning at a variable distance from the beak (30 to 60 per cent of the length of the shell or 22 to 45 per cent of the unrolled length of the valve). Moderately deep to deep sulcus (three to five times the height of the costae where it passes to the tongue) with flat bottom, starting with a width of about one quarter the width of the shell, widening rapidly, and reaching its greatest width (60 to 70 per cent of the width of the shell) at the junction of the frontal and lateral commissures. Tongue high with sharp borders, standing out clearly, having the shape of an isosceles trapezium generally vertical at its crest, and commonly recurved posteriorly. The top of the tongue is never the top of the shell. Beak thickset, sub-erect, not overhanging the cardinal line. Ventral interarea long (varying from 44 to 71 per cent of the width of the shell, most of the valves varying from 52 to 60 per cent), and high (generally between 1 and 1.5 mm), limited by distinct ridges. Foramen large, oval. Disjunct deltidial plates observed in transverse serial sections.

Brachial valve uniformly convex. Curve of the valve is one quarter of a circle or one quarter of an ellipse in longitudinal median sections. Dorsal flanks steep and sometimes abrupt to vertical near the commissure. Fold high with convex top, well marked, clearly delimited, beginning a short distance from the beak, and rising abruptly.

Top of pedicle valve located approximately where the sulcus starts. Greatest thickness of brachial valve located at a point between 60 and 80 per cent of the length of the shell forward of the ventral beak; in some cases it is reached at the frontal commissure, in others not, and in the latter case, the valve curves gently or steeply from this point toward the commissure. Width variable but always the largest dimension; greatest width is usually located at a point between 50 and 60 per cent of the length of the shell anterior

of the ventral beak. Thickness is the smallest dimension. Thickness of pedicle valve varies from between 25 to 32 per cent of the thickness of the shell. Apical angle varies from 108° to 125°.

Costae simple, regular, well marked, moderately high, angular, usually with rounded tops, starting either level with the sulcus and fold, or, more commonly, posteriorly; in the latter case they begin close to the beak, but do not reach it. Median ventral and lateral dorsal costae clearly lower than the others. Width of median costae at the front usually varies from between 1.5 to 2 mm, but may reach 2.5 mm. Number of costae few: generally three to four on the fold, two to three in the sulcus, and five to nine on the flanks. Crest of ventral median costae and bottom of dorsal and ventral median furrows in some cases marked near the frontal commissure by narrow, flat or even slightly curved strips. When sharply curved, costae on the fold are thickened at the point of inflexion. In one specimen out of five, a parietal costa may be observed on one side and, very exceptionally, on both sides. Also very exceptionally, an adventitious costa may be present on an external median costa. No radial costellae. Growth lines commonly preserved, especially on the anterior part of the shell.

Shell moderately thick. Dental plates of moderate thickness and concave anteriorly, with lengths varying from 2 to 3 mm; they diverge in their extreme posterior parts and are subparallel (some with the shape of parentheses) anteriorly. Ventral umbonal cavities clearly present. Teeth small, robust, short (0.45 to 0.5 mm), and wide. Denticula well developed. Septum blade-shaped, thin, decreasing in height and thinning anteriorly, with a length about one fifth of the length of the shell, or about 30 per cent of the unrolled length of the brachial valve. Thin, divided hinge plate with a median, narrow, somewhat deep septalium dividing it into two rather flat (in some cases slightly convex, in others slightly concave) parts. Dental sockets small, short, with low inner socket ridges, snugly conforming to the shape of the teeth. Crural bases inconspicuous, passing abruptly forward into delicate, short (about 0.7 mm), triangular crura in transverse serial sections, and curving strongly ventrally at their distal ends. Although the type species collection is rather abundant, no good observations of the muscle scars have been made.

PLATE 26.1

Homeocardiorhynchus pityinus n. gen., n. sp.

A. 1-5. Ventral, dorsal, frontal, apical, and lateral views, x1, Holotype, GSC 75985. GSC loc. C-94688. Bituminous limestone member of the Pine Point Formation; 0.93 km southwest of Pine Point at 61°00'21"N, 114°16'15"W, south shore of Great Slave Lake, N.W.T. Collectors: A.W. Norris and P. Sartenaer, 1981.

B. Camera lucida drawings of serial transverse sections; distances are in millimetres forward from the crest of the pedicle umbo. Paratype A, GSC 5986. GSC loc. 5675 (same locality as GSC loc. C-94688). l: 17.8 mm; w: 19 mm; t: 12.8 mm. Black bituminous limestone of Pine Point Formation; half a mile west of Pine Point, south shore of Great Slave Lake, N.W.T. Collectors: E.J. Whittaker and E.M. Kindle, 1917.

C. Three transverse serial sections of the same specimens shown in figure B., magnified two times and showing various stages of the cardinal process in the septalium and on the hinge plate.

A

1 2 3 4 5 x 1

B

1.25 1.65 1.75 1.95 2.2 2.3 2.45

2.6 2.75 2.9 3 3.45

3.8 4.15 4.3 4.4

4.6 4.75 4.95 5.25 5.45 x 3.5

C

2.6 2.75 2.9 x 7

219

Diagnostic characters. Small to medium sized. Transversely subelliptical to subcircular. Strongly inequivalve. Dorsal flanks commonly abrupt to vertical near the commissure. Anterior ends of ventral flanks standing out as spurs. Well marked sulcus and fold starting at some (variable) distance from the beak. Wide and moderately to very deep sulcus. High fold. High, trapezoidal, and clearly conspicuous tongue. High and long ventral interarea separated from the flank by a ridge. Few, simple, regular, well marked costae starting some distance from the beak; they are commonly sharply curved near the commissure. No radial costellae. Thin, blade-shaped septum. Narrow, variably deep septalium. Subparallel dental plates.

Comparisons. When the genus **Hadrorhyncha** McLaren (1961) was erected with **Pugnoides sandersoni** Warren (1944) as the type species, McLaren (1961, 1962) included a form later assigned to **Hadrorhynchia intermissa** Crickmay (1963), which is here treated as a new genus. Thus, the new genus, **Droharhynchia**, has characters belonging to both, and others that are only valid for one of them. No new description of **Hadrorhynchia** has been given. Therefore, it must be clear that, in the following comparison, **Hadrorhynchia** is considered as a late Givetian genus encompassing its type species, and **H. alta** Cooper and Dutro, 1982 and **H. mclareni** Cooper and Dutro, 1982.

Droharhynchia n. gen. resembles the genus **Hadrorhynchia** in the following characteristics: contour in frontal view; uniplicate frontal commissure; strongly inequivalve aspect; commissure, clearly crenulated by the costae; convexity of the pedicle valve; anterior end of the flanks standing out as characteristic spurs; wide sulcus; high tongue with sharp borders, standing out clearly; thickset beak; the long and high ventral interarea clearly separated from the ventral flanks by a ridge; the location of the greatest thickness; the steep dorsal flanks, in some cases very steep to vertical near the commissure; height being the smallest dimension, and length the largest; the similar values of apical angle; the simple, regular, well marked, and angular costae; the similar number of median costae, ventral umbonal cavities clearly present; the small, stout, short, and wide teeth; the septum decreasing in height and thinning anteriorly; and in its small, short dental sockets, with low inner socket ridges. However, many characteristics make **Droharhynchia** distinct from **Hadrorhynchia**: its smaller size; the transversely subelliptical to subcircular outlines of its pedical and brachial valves (generally subcircular to subpentagonal for **Hadrorhynchia**); the fact that the sulcus and fold generally start nearer to the beak, and, thus, are marked and separated from the flanks by a greater distance, beginning with smaller width, and widening rapidly; the costae start nearer to the beak; there are a higher number of lateral costae; narrow strips are present on the crest of the ventral median costae and are in some cases present in the bottom of the dorsal and ventral median furrows (it is generally the case for **Hadrorhynchia**); the lack of radial costellae; the internal structures are thinner; the ventral umbonal cavities are wider and differently shaped; a septalium is present (a crural trough in **Hadrorhynchia**); and the crural bases are weak.

Species attributed to the genus. At present only the type species is attributed to the new genus.

Homeocardiorhynchus n. gen.

Derivatio nominis. Ὅμοῖος, α, ον (Greek) = similar; καρδια, ας (Greek, feminine) = heart; ρυγχος (Greek, neuter) = beak. The name has been chosen to draw attention to the shape of the shell and to the similar thicknesses of the valves.

Type species. **Homeocardiorhynchus pityinus** n. gen., n. sp. πιτυινος, η, ον (Greek) = made out of pine, related to pine; to draw attention to the type locality of the species near Pine Point on the southern shore of Great Slave Lake, N.W.T.

As the genus is monospecific, the description of the genus applies to the species.

Description. Medium sized. Subcordiform in ventral and dorsal views. Contour is a flat ellipse with truncated margin or a horizontally lying barrel with a thin bulge visible in frontal profile. Inequivalve, but commonly only slightly, the brachial valve being not much higher than the pedicle valve, which in turn is not high. Both valves have similar slight convexity longitudinally and transversely, with the convexity of the pedicle valve being slightly less. Postero-lateral margins are commonly very slightly concave near the commissure. Cardinal line long and slightly undulated. Commissure sharp, clearly crenulated by the costae, merging in the wall of the shell where costae are thickened at their extremities; in some specimens, narrow, flat, clearly delimited strips, a few millimetres long, may be observed in the middle and at the ends of the costae and the furrows. This thickening gives the impression that the flanks are bent at right angles at their extreme lateral margins.

Although not particularly inflated, the ventral umbonal region stands out clearly, because the antero-lateral part of the flanks slope gently, but their postero-lateral part is steep. Contour of pedicle valve is a more or less regular half-ellipse in longitudinal median sections, and a very flat half-lens hardly invaginated by the sulcus in transverse median sections. Sulcus pronounced only in the anterior part of the shell, beginning imperceptibly at a point between 51 and 68 per cent of the length of the shell or between 45 and 56 per cent of the unrolled length of the valve. Low sulcus (one to three times the height of the costae where it passes to the tongue) with flat bottom, starting with a width varying from 24 to 41 per cent of the width of the shell, widening slowly, and reaching its greatest width (56 to 64 per cent of the width of the shell) at the junction of the frontal and lateral commissures. Tongue low with sharp borders, standing out clearly, trapezoidal, tending to become vertical at its crest. Beak thickset, sub-erect to erect, resorbed by a circular foramen. Ventral interarea high (1.2 to 1.6 mm) and long (about two thirds of the width of the shell), made out of two parts having the shape of propeller blades, and separated by a ridge from the ventral flanks. Strong deltidial plates observed in transverse serial sections.

Brachial valves low to moderately high. Curve of the valve resembles a more or less flattened ellipse in longitudinal medial sections. Fold low with convex top, marked only in the anterior part of the shell, and beginning imperceptibly at a considerable distance from the beak.

Top of pedicle valve located posteriorly at a point about one third of the length of the shell forward of the beak. Greatest thickness of brachial valve located at a point between 37 and 55 per cent of the length of the shell posterior to the frontal commissure; from this point the valve curves toward this commissure, and, thus, the highest part of the tongue is never the highest part of the shell. Length and width are about equal. Maximum width occurs at a point between 57 and 64 per cent of the length of the shell anterior to the ventral beak. Thickness of brachial valve generally greater than that of pedicle valve. Apical angle varies from 105° to 120°.

Costae low, regular, simple. Number of costae few: three on the fold, two in the sulcus, and six to eight on the flanks for the type species. Median dorsal and lateral ventral costae higher and angular, with rounded tops. Median ventral

and lateral dorsal costae with lower and almost flat, slightly rounded tops. Median costae originate anterior to the beginning of sulcus and fold and are commonly 2 to 3 mm wide at the anterior margin. Lateral costae restricted to the margins of the flanks. Internal ventral lateral costa on each side of the sulcus, always higher and more conspicuous than the other lateral costae. No parietal costae. Fine growth lines commonly preserved.

Shell material of medium thickness. Dental plates moderately thick, with anterior margin concave and varying in length from 3 to 4 mm, distinctly and widely separated from each other, and becoming subparallel anteriorly. Ventral umbonal cavities clearly developed. Teeth stout, 1.2 to 1.5 mm wide. Denticula very stout. Septum moderately thick, continuing to one third the length of the shell. Moderately thick, divided hinge plate, the two parts of which extend far inward with increasing concavity. Rather deep septalium, as wide as deep. Very short (about 0.75 mm) cardinal process extending only slightly over the septalium at its highest point, and protruding a little over the hinge plate. Dental sockets wide, moderately deep, with low, inner socket ridges. Crural bases appear to be absent. As a matter of fact, the inner rims of the hinge plates extend beyond the septalium in the form of flanges to which the hinge plates remain attached as they become progressively shorter and curve dorsally; thus, transverse serial sections show two heads with flagella shifting from horizontal to vertical. Where flagella have disappeared, the crura have the shape of a Phrygian cap, and curve ventrally in their distal part. The material at hand does not show ventral and dorsal muscle scars.

Diagnostic characters. Medium sized. Subcordiform. Slightly inequivalve: brachial valve low to moderately high, commonly only slightly higher than the pedicle valve. Sulcus and fold starting imperceptibly at some distance from the beak and only conspicuously marked in the anterior part of the shell. Low, flat-bottomed sulcus. Low fold. Low tongue. High and long ventral interarea. Length and width similar. A few low, regular, simple costae restricted to the anterior part of the shell. Very short cardinal process. No true crural bases. The two parts of the hinge plate extend beyond the septalium. Crura with characteristic shape.

Comparisons. **Homeocardiorhynchus** n. gen. resembles the genus **Nemesa** Schmidt, 1941 of late middle Eifelian age, in the following features: subcordiform contour; uniplicate frontal commissure; the fact that the sulcus and fold start imperceptibly a long distance from the beak, and are only conspicuous on the anterior parts of the shell; the low and wide sulcus; the low fold; trapezoidal tongue, standing out clearly, with sharp borders, and tending to become vertical at its crest; its long and high ventral interarea, clearly separated from the ventral flanks by a ridge, and composed of two parts having the shape of propeller blades; the fact that there are no parietal costae; the fact that the greatest thickness is never located at the top of the tongue; and the similar values of apical angle. However, many characters make **Homecardiorhynchus** distinct from **Nemesa**: its larger size; the fact that it is commonly slightly inequivalve; the

similar convexity of both its valves; the different contour in frontal view (half-oval or half-circular for **Nemesa**); the fact that the commissure is always crenulated by the costae; the fact that the ventral umbonal region stands out; its projecting beak, suberect to erect, (erect to slightly incurved for **Nemesa**); the presence of lateral costae; and the higher (although low), longer, and usually more median costae.

The very poor transverse serial sections of **Nemesa nemesana** Schmidt, 1941, found in the literature (Schmidt, 1941, pl. 7, fig. 22-24; Schmidt in Schmidt and McLaren, 1965, fig. 476, 1a-h in textu p. H593; Mohanti, 1972, fig. 37 in textu p. 179), prevents assessment of all the differences between the two genera, but dental plates and a cardinal process are not present in **Nemesa**.

Species attributed to the genus. Outside the type species, it is possible that ?**Nemesa skalensis** Biernat, 1966, from the Skala Beds of probable early Givetian age in the Holy Cross Mountains, belong to the genus, but more information is needed on the internal characters.

References

Biernat, G.
1966: Middle Devonian brachiopods of the Bodzentyn syncline (Holy Cross Mountains, Poland); Palaeontologie Polonica, no. 17.

Crickmay, C.H.
1963: Significant new Devonian brachipods from Western Canada; Evelyn de Mille Books, Calgary, 63 p.

McLaren, D.J.
1961: Three new genera of Givetian and Frasnian (Devonian) rhynchonelloid brachiopods; Royal Institute of Natural Sciences of Belgium, Bulletin t. XXXVII, no. 23.

1962: Middle and early Upper Devonian rhynchonelloid brachiopods from Western Canada; Geological Survey of Canada, Bulletin 86.

Monhanti, M.
1972: The Portilla Formation (Middle Devonian) of the Alba syncline, Cantabrian Mountains, Prov. Leon, northwestern Spain: carbonate facies and rhynchonellid palaeontology; Leidse Geologische Mededlingen, Deel 48, Aflevering 2, p. 135-205.

Schmidt, H.
1941: Die mitteldevonischen Rhynchonelliden der Eifel; Abhandlungen der Senckenbergischen Naturforschenden Gesellschaft 459.

Schmidt, H. and McLaren, D.J.
1965: Palaeozoic **Rhynchonellacea**; in Treatise on Invertebrate Paleontology, directed and edited by R.C. Moore; Part H (Brachiopoda), v. 2, p. H552-H597.

Warren, P.S.
1944: Index brachiopods of the Mackenzie River Devonian; Royal Society of Canada, Transactions, Third Series, v. 38, Sec. 4, p. 105-135, Pl. 1-3.

The Neruokpuk Formation, Yukon Territory and Alaska

Project 690005

D.K. Norris
Institute of Sedimentary and Petroleum Geology, Calgary

Abstract

The Neruokpuk Formation is composed of a monotonous succession of slaty argillites, poorly sorted quartz arenites, argillaceous limestones, and chert. It has an exposed thickness in excess of 13 400 m. The entire succession is no higher than the greenschist facies in Canada. Paleontological data suggest that the formation may be as young as Paleozoic in Alaska, although it may be no younger than Hadrynian in Canada. It would appear to be the deep water, slope equivalent of the platformal, upper part of the Tindir Group 450 km to the south.

Because of seemingly abrupt lateral facies changes, unconformities within the succession and the lack of a set of distinctive markers, many uncertainties exist in the correlation of rock units between Canada and Alaska.

Résumé

La formation de Neruokpuk dans le nord du Yukon et le nord-est de l'Alaska comporte une succession monotone d'argilites schisteuses, de quartzarénites mal triées, de calcaires argileux et de chert. La partie qui affleure a plus de 13 400 m d'épaisseur. Au Canada, la succession entière n'a pas été métamorphisée au delà du faciès des schistes verts. Les données paléontologiques laissent croire que la formation pourrait dater du Paléozoïque en Alaska, bien qu'elle ne remonte vraisemblablement qu'à l'Hadrinien au Canada. Elle s'est formée sur un talus en eau profonde et semble être l'équivalent de la partie supérieure du groupe de Tindir qui s'est accumulé sur une plate-forme et qui se situe à 450 km au sud.

En raison des changements latéraux vraisemblablement abrupts de faciès et de discordances dans la succession et de l'absence d'une série de repères caractéristiques, la corrélation des unités lithostratigraphiques au Canada et en Alaska est encore très incertaine. Il faudra entreprendre des études sédimentologiques et stratigraphiques détaillées pour expliquer le milieu de sédimentation de cette partie de la plaque nord-américaine ancestrale, améliorer les connaissances actuelles en ce qui concerne l'âge de la formation, reconstituer l'histoire et le style structuraux du soulèvement de Romanof, vérifier l'hypothèse voulant que la formation soit entièrement allochtone et qu'elle fasse partie d'un terrain accumulé, reconstituer l'histoire pré-ellesmérienne de la plaque de l'Alaska arctique et déterminer la profondeur minimale de la croûte cristalline sous la formation.

Definition

The Neruokpuk Formation was originally defined by Leffingwell (1919, p. 103-105) as a thick sequence of sedimentary rocks consisting "chiefly of quartzite schist" in the Franklin Mountains in northeastern Alaska. Contact relations with both over-and underlying units were not defined, the thickness of the formation was not determined, and the age of the sequence was considered to be pre-Carboniferous.

The United States Geological Survey, in its investigation of northern Alaska for the Office of Naval Petroleum and Oil Shale Reserves, greatly extended Leffingwell's definition to apply "to all the pre-Mississippian rocks in northeastern Alaska, except for those carbonates exposed in the cores of the Shublik and Sadlerochit Mountains" (Dutro et al., 1972, p. 808). This extension allowed for the inclusion of a wide variety of sedimentary and volcanic rock units of Late Devonian and older ages. Norris et al. (1963) mapped the continuation of this stratigraphic assemblage in northern Yukon Territory, called it the Neruokpuk Formation, and perpetuated the concept of including all rocks of pre-Carboniferous age within it. Thus, graptolite-bearing clastics coeval with the Lower and Middle Paleozoic Road River Formation in the Barn Mountains were embraced within the extended definition of the Neruokpuk.

New lithostratigraphic and biostratigraphic control has resulted in the identification of formations and groups within the extended Neruokpuk that are clearly not part of it; they have quite correctly been reassigned to their proper places within the stratigraphic succession. These include, for example, the Endicott and Lisburne groups in the headwaters of the Okpilak and Jago rivers, and the Katakturuk Dolomite along the Hulahula River and Old Man Creek (Sable, 1977, p. 6). To eliminate further confusion, Reiser et al. (1978) proposed that the Neruokpuk be restricted to its original definition set forth by Leffingwell, but that it be Precambrian in age. Norris (1981a,b) restricted the formation even further by excluding the thick, volcaniclastic succession (CWMv) and its underlying shale and siltstone unit (CWMs) in the British Mountains, and the graptolite-bearing clastic sequence (OSH) in the Barn Mountains.

Areal extent

The Neruokpuk Formation is exposed for a strike distance of approximately 310 km, from the Canning River in northeastern Alaska almost to the Babbage River in northern Yukon Territory. It comprises a tectonically segmented band in Romanzof Uplift up to 65 km wide, reaching its maximum width in the vicinity of the International Boundary, and plunging beneath younger rocks at both its eastern and western extremities.

Subdivisions

Because of seemingly abrupt lateral facies changes, unconformities within and above the formation, and structural repetition of diverse ages, as many as six different sequences and twelve members (Dutro et al., 1972) have been identified in the Neruokpuk of Alaska. Some of them cannot be recognized with certainty in the Yukon. It was necessary, therefore, to establish an independent, informal breakdown of the Yukon assemblage, with the expectation that detailed sedimentological and stratigraphic investigations in Canada would resolve many of the apparent ambiguities.

The Neruokpuk Formation in the northern Yukon has been subdivided into seven informal lithostratigraphic units (Norris, 1981a,b) based on gross lithologic content, that is, the dominance of slaty argillite, quartzite and limestone, or some combination of them. The units can be quite distinctive (Fig. 27.1, 27.2). Some of them may be the lateral equivalents of others and some may recur in the succession as simple stratigraphic rather than structural repetitions (c.f. Limestone member of Dutro et al., 1972).

In spite of both large- and small-scale deformation of the Neruokpuk, the whole of the stratigraphic succession dips generally southwest. Thus, on a regional scale, the stratigraphically highest of the seven informal units mentioned above occurs in the direction of the southwest flank of Romanzof Uplift, and the stratigraphically lowest in the direction of the northeast flank. The total exposed thickness of the Neruokpuk is estimated to be greater than 13 400 m (Table 27.1), setting a minimum depth to the top of the crystalline basement in this part of the Cordilleran Orogenic System.

Brief descriptions of the seven informal lithostratigraphic units comprising the Neruokpuk Formation in the British Mountains in northern Yukon Territory are included in Table 27.1, along with their tentative correlation with units in Alaska. Neither schists as referred to by Leffingwell (1919, p. 103) nor semischists as described by Dutro et al. (1972) have been found in the formation in Canada, although slaty cleavage parallel and subparallel to bedding is abundant in the argillites. The entire succession would appear to be metamorphically no higher than greenschist facies. Moreover, no unconformities have been conclusively demonstrated to exist between or within the seven units.

Age

The Neruokpuk Formation in Alaska has been considered to be as young as Devonian and as old as Precambrian (Dutro et al., 1972), based on fossils collected from some units, the relative stratigraphic position of units unconformably beneath known Lower Carboniferous rocks (Endicott Group of Visean age), and the hosting of granite of the Jago stock, dated radiometrically (Hb) at 431 Ma (Reiser, 1970), in the Quartzite and semischist member.

In Canada, no fossils have been found in the Neruokpuk. The only reliable evidence for its age rests with its unconformable relations to the overlying Visean Endicott Group (Fig. 27.3) and with its hosting granite dated radiometrically (Hb) as old as 341 Ma at Mt. Sedgwick, at the southeastern limit of exposure of the Neruokpuk (Norris, 1981b). Insofar as the granite at Mt. Sedgwick is overlain nonconformably by the Visean Kekiktuk Formation (350 Ma), it is clear that the radiometric age obtained for the granite is a minimum number. Its intrinsic age is, therefore, greater, perhaps closer to 431 Ma (Early Silurian Llandoverian), the age of the Jago stock. The granite intrusions observed both low (Sedgwick) and high (Jago) in the Neruokpuk successions would indicate that much, if not all, of the Neruokpuk should be Ordovician or older.

The reported occurrence of an Upper Ordovician graptolite along the International Boundary (Dutro et al., 1972) at the headwaters of Craig Creek, was investigated in the field by the author in 1972 and again with H.N. Reiser, United States Geological Survey, in 1973. A careful examination of the strongly foliated, micaceous argillites there failed to uncover additional fossil material, let alone graptolites. Moreover, it was not possible to corroborate the presence of "black slate associated with volcanic rocks" (Dutro et al., 1971) in which the graptolite was reported to have been found at this locality.

The age of the Neruokpuk in Canada may be constrained further because the overlying, thick volcaniclastic and carbonate assemblage (CWMv) is known to contain both Lower and Upper Cambrian trilobites in northeastern Alaska (Dutro et al., 1972). If it may be

correctly assumed that these trilobites and the limestone masses[1] containing them are indigenous to the volcaniclastic assemblage, the age of the unit ranges from Early to Late Cambrian, and spans more than 30 Ma. Moreover, the assemblage, with its associated shale and siltstone unit (CWMs), appears to rest with angular unconformity on the second youngest unit of the Neruokpuk (PN4). The Neruokpuk would appear to have been deposited, deformed by high-angle contraction faults, and bevelled prior to deposition of CWMs and the lower part of CWMv in the Early Cambrian. The Neruokpuk is, therefore, Precambrian in age, and the identification of pre-Carboniferous contraction faulting suggested by Reed (1968, p. 75) is confirmed.

On the other hand, if it may be assumed that the limestone masses within the volcaniclastic assemblage are olistoliths, the assemblage can range in age between latest Cambrian and earliest Carboniferous, and may perhaps even be associated with the Ellesmerian orogenic event. Verification of this hypothesis would come from the discovery of faunas younger than latest Cambrian in some of these limestones.

The fact that echinoderm columnals have been reported from the Calcareous siltstone and sandstone member in Alaska (Dutro et al., 1972) may indicate a Paleozoic age for at least part of the restricted Neruokpuk sequence.

Figure 27.1. *Isoclinal folding in rusty weathering, slaty argillites of Unit PNO of the Neruokpuk Formation on the northeast flank of Romanzof Uplift. View is to the northwest across the lower Firth River. Photo DKN 3-1-71. See Norris (1981a)*

---

[1] Some of the limestone masses are tuffaceous (W.P. Brosgé, personal communication, 1985)

The problem is that the latter unit reportedly overlies the Quartzite and semischist member there (Dutro et al., 1972), whereas its possible equivalent in Canada appears to underlie it (Table 27.1). The correlation of stratigraphic units between Alaska (Dutro et al., 1972) and Canada (Norris, 1981a,b) is clearly uncertain and is by no means resolved.

Depositional setting

The thick, monotonous succession of argillites, poorly sorted quartz arenites, argillaceous limestones and chert appears to represent a deep water, slope sequence, deposited in large part by turbidity currents. Redbeds are few, conglomerates are rare, and algal biostromes and ripple marks are unknown. The deposits appear to indicate a protracted period of tectonic quiescence represented by mud, muddy limestone and silica accumulation, punctuated by pulses of quartz-rich clastics, shed, as Reed (1968, p. 25) has suggested, from a provenance that was sedimentary and perhaps metamorphic in nature.

The writer hypothesizes that the paleogeographic setting for the slope deposits comprising the Neruokpuk was the extreme northwest corner of the ancestral North American plate, and that the sediments may have been

Figure 27.2. Folded limestone and slaty argillite of Unit PN3 of the Neruokpuk Formation in the core of Romanzof Uplift. View is to the west across the Firth River, a few kilometres above Glacier Creek. Photo DKN 2-10-71. See Norris (1981a)

deposited at least in part on oceanic crust. He further hypothesizes that the Neruokpuk may be Late Precambrian (Hadrynian) in age, and, therefore, that it is the thick, distal, slope equivalent of the platformal deposits of the upper Tindir Group, now 450 km to the south, across the suture between the Arctic Alaska and North American plates.

There is substantial evidence for a late Precambrian age for the Tindir Group (see Allison and Moorman, 1973) whereas there is no direct evidence for a presumed late Precambrian age for most if not all of the Neruokpuk. That the two successions are more or less coeval is purely a hypothesis.

The provenance for the Tindir as well as for the Neruokpuk is presumed to have been the Precambrian craton to the east and south. At that time, the Arctic Alaska plate occupied either a medial position in the ancestral Canada Basin, and formed one flank of the Richardson-Hazen Trough (Norris, 1983), or it was juxtaposed against what is now the northwest margin of the North American plate (Carey, 1959, p. 198). In the latter instance, the trough either did not exist or it was considerably narrower. Whatever the precise relative position of the Arctic Alaska plate, more than 13.4 km of clastics and carbonates were deposited beyond a continental shelf edge in the position of the Arctic

Table 27.1.   Neruokpuk Formation; Tentative correlation of rock units

Yukon Territory			Alaska
Unit (Norris, 1981a, b)	Lithology	Thickness m/ft	Unit (Dutro et al., 1972; Reiser et al., 1980)
PN6	(Interbedded) Dark grey weathering sandstone; and olive grey and pale red, slaty argillite? Not examined on the ground.	>1000 m/ 3000 ft	Not recognized in Alaska
PN5	(Interbedded) Limestone, black, fine crystalline, yellowish weathering; and argillite, slaty, olive grey, locally red.	>1300 m/ 4300 ft	Limestone member; and Argillite and limestone member
PN4	(Interbedded) Sandstone, olive grey, fine- to medium-grained quartz; argillite, slaty, olive grey, locally red; and chert, olive grey. Top not seen.	>5100 m/ 16 200 ft	Quartzite and semischist member (Neruokpuk Schist of Leffingwell (1919) and Ferruginous sandstone member; and Calcareous siltstone and sandstone member
PN3	(Interbedded) Argillite, slaty, olive grey; limestone, dark grey, fine crystalline; and siltstone, variably calcareous, olive grey.	>1000 m/ 3000 ft	Calcareous siltstone and sandstone member (H.N. Reiser pers. comm., 1973)
PN2	(Interbedded) Argillite, slaty, olive grey; sandstone, quartz fine- to coarse-grained; and limestone, argillaceous, fine crystalline.	>3000 m/ 10 000 ft	Grey phyllite and chert member; Red and green phyllite member; Limestone member; and Slate, argillite, quartzite and chert member
PN1	(Interbedded) Slaty argillite, argillaceous limestone and sandstone? Not examined on the ground.	>1000 m/ 3000 ft	Red and green phyllite member; and Limestone member
PN0	Argillite, dark grey, rusty weathering; and sandstone, fine grained, brown weathering. Base not seen.	>1000 m/ 3000 ft	Slate and quartzite member

Figure 27.3. *Angular unconformity between vertical to steeply south-dipping Neruokpuk strata of Unit PN2 and gently north-dipping conglomerate, shale and limestone of the Endicott and Lisburne groups on the northeast flank of Romanzof Uplift. View is to the northwest across the lower Malcolm River. Photo DKN 3-12-71. See Norris (1981a)*

Alaska plate. They were destined to be on its leading edge when the plate began to rotate to its present position relative to the North American plate. Part of these slope deposits remains to comprise the backbone of Romanzof Uplift, but doubtless much of it was subducted as the two plates collided and sutured in the mid-Cretaceous (Norris, 1984).

Acknowledgments:

The writer is especially indebted to L.D. Dyke, who made many of the measurements on the Neruokpuk in Canada, and to W.P. Brosgé for critically reading the manuscript. Many of Brosgé's suggestions for clarifing the correlation of rock units of the Neruokpuk between Alaska and Yukon Territory are incorporated in Table 27.1.

References

Allison, C.W. and Moorman, M.A.
   1973:   Microbiota from the Late Proterozoic Tindir Group, Alaska; Geology, v. 1, no. 2, p. 65-68.

Carey, S.W.
   1959:   Continental Drift, A symposium; Geology Department, University of Tasmania, Hobart, 1958.

Dutro, J.T., Jr., Reiser, H.N., Detterman, R.L., and Brosgé, W.P.
   1971:   Early Paleozoic Fossils in the Neruokpuk Formation, northeast Alaska; United States Geological Survey, Open-File report 499.

Dutro, J.T., Jr., Brosgé, W.P., and Reiser, H.N.
   1972:   Significance of recently discovered Cambrian fossils and reinterpretation of the Neruokpuk Formation, northeastern Alaska; American Association of Petroleum Geologists, Bulletin, v. 56, no. 4, p. 808-815.

Leffingwell, E. de K.,
   1919:   The Canning River Region northern Alaska; United States Geological Survey, Professional Paper 109.

Norris, D.K.
   1981a: Geology Herschel Island and Demarcation Point Yukon Territory; Geological Survey of Canada, Map 1514A, scale 1:250 000.

   1981b: Geology Blow River and Davidson Mountains Yukon Territory – District of Mackenzie; Geological Survey of Canada, Map 1516A, scale 1:250 000.

Norris, D.K. (cont.)

1983: Porcupine Virgation – the structural link among the Columbian, Innuitian and Alaskan orogens; Abstract in Geological Association of Canada Program with Abstracts, v. 8, Victoria, p. A51.

1984: Post-Valanginian restructuring of the northern Cordillera and contiguous Canada Basin; Abstract in Abstracts with Programs 1984, 80th Annual Meeting Cordilleran Section Geological Society of America, Anchorage, v. 16, no. 5, p. 326.

Norris, D.K., Price, R.A., and Mountjoy, E.W.

1963: Geology northern Yukon Territory and northwestern District of Mackenzie; Geological Survey of Canada Map 10-1963, scale 1:1 000 000.

Reed, B.L.

1968: Geology of the Lake Peters Area northeastern Brooks Range, Alaska; United States Geological Survey, Bulletin 1236.

Reiser, H.N.

1970: Northeastern Brooks Range – a surface expression of the Prudhoe Bay section; in Proc. of the geological seminar on the North Slope of Alaska; American Association of Petroleum Geologists, Pacific Section, p. K1-K13.

Reiser, H.N., Brosgé, W.P., Dutro, J.T., Jr., and Detterman, R.L.

1980: Geologic map of the Demarcation Point Quadrangle, Alaska; United States Geological Survey, Map I-1133.

Reiser, H.N., Norris, D.K., Dutro, J.T., Jr., and Brosgé, W.P.

1978: Restriction and Renaming of the Neruokpuk Formation, northeastern Alaska; in Changes in Stratigraphic Nomenclature by the United States Geological Survey, 1977, United States Geological Survey, Bulletin 1457-A, p. A106-107.

Sable, E.G.

1977: Geology of the western Romanzof Mountains, Brooks Range, northeastern Alaska; United States Geological Survey, Professional Paper 897.

Preliminary results of palynological studies of the Permian and lowermost Triassic sediments, Sabine Peninsula, Melville Island, Canadian Arctic Archipelago

Project 810038

John Utting
Institute of Sedimentary and Petroleum Geology, Calgary

Abstract

Well preserved palynomorphs have been found in samples from the uppermost part of the Canyon Fiord Formation (Lower Permian?); the Belcher Channel (Lower Permian), Sabine Bay (Lower Permian), and Assistance (Lower Permian) formations; "Unit A" (Lower or Upper Permian); and the Trold Fiord (Upper Permian) and lower Bjorne (Lower Triassic) formations. Pollen and spores occur in all formations, and acritarchs in all except the Canyon Fiord and Bjorne. In general terms, the Permian assemblages contain abundant, striate disaccate pollen (**Protohaploxypinus** spp.), polyplicate pollen (**Vittatina** spp. and **Weylandites** spp.), and trilete spores. Monosaccate pollen (**Cordaitina** spp.) occurs occasionally. The Lower Triassic assemblages contain abundant striate disaccate pollen (**Protohaploxypinus** spp. and **Taeniaesporites** spp.), non-striate disaccate pollen (**Falcisporites** sp. and **Klausipollenites** spp.), colpate pollen (**Gnetaceaepollenites** spp.), and trilete spores (**Kraeuselisporites** spp. and **Lundbladispora** spp.). Present also is the cyst-like microfossil **Tympanicysta stoschiana**. The assemblages are unlike those of Gondwana and Cathaysia. They appear to be more similar to those described from the northeast European part of Russia than those of Western Europe.

The Thermal Alteration indices of the palynomorphs are low (2- to 2+ on a five point scale), suggesting suitable conditions for the generation of liquid hydrocarbons.

Résumé

Des palynomorphes bien conservés ont été trouvés dans des échantillons provenant de la partie supérieure de la formation de Canyon Fiord (Permien inférieur?); des formations de Belcher Channel, de Sabina Bay et d'Assistance, toutes du Permien inférieur; de l'"unité A" (Permien inférieur ou supérieur); de la formation de Trold Fiord (Permien supérieur) et de la partie inférieure de la formation de Bjorne (Trias inférieur). Toutes ces formations contiennent du pollen et toutes, sauf celle de Canyon Fiord et de Bjorne, contiennent des acritarches. En général, les assemblages permiens contiennent une quantité abondante de pollens bi-ailé strié (espèces de **Protohaploxypinus**), de pollen polyplicaturé (espèces de **Vittatina** et de **Weylandites**) et des spores trilètes. On trouve du pollen à ballonet (espèces de **Cordaitina**) par endroits. Les assemblages du Trias récent contiennent d'abondantes quantités de pollen bi-ailé strié (espèce de **Protohaploxypinus** et de **Taeniaesporites**), de pollen bi-ailé non strié (espèce de **Falcisporites** et espèces de **Klausipollenites**), de pollen à sillons (espèces de **Gnetaceaepollenites**) et de spores trilètes (espèces de **Kraeuselisporites** et de **Lundbladispora**), ainsi qu'un microfossile en forme de kyste, **Tympanicysta stoschiana**. Ces assemblages sont différents de ceux de Gondwana et de Cathaysia; ils ressemblent plus à ceux qui proviennent de la partie nord-est européenne de la Russie qu'à ceux de l'Europe occidentale.

Les palynomorphes ont de faibles indices d'altération thermique (de 2- à 2+ sur une échelle de cinq points), ce qui porte à croire que les conditions favorisaient la formation d'hydrocarbures liquides.

Introduction

During the summer of 1984, seventy-four samples were collected from Permian and lower Triassic formations in the Tingmisut Lake and Hiccles Creek areas in the southeast part of the Sabine Peninsula of Melville Island (Fig. 28.1, 28.2). Units sampled include the uppermost part of the Canyon Fiord Formation; the Belcher Channel, Sabine Bay, and Assistance formations; "Unit A"; and the Trold Fiord and lower Bjorne formations (Fig. 28.3). Preservation of palynomorphs is generally good; damage by the growth of pyrite crystals on pollen and spore exines is slight, and the Thermal Alteration indices are low (2- to 2+ on the five point scale of Hunt, 1979). Identifications made are mainly at the generic level, reflecting the large number of undescribed species present, and the fact that further taxonomic study is necessary.

In the following section, the stratigraphy in the Tingmisut Lake area is summarized (in ascending order) and a general description given of the palynological assemblages (Fig. 28.4).

Stratigraphy and palynological assemblages

Canyon Fiord Formation

The lowest beds of the formation, according to Tozer and Thorsteinsson (1964), consist of light grey to white, quartzose, medium grained sandstone, with some grains of black chert and much carbonate cement. A Middle Pennsylvanian brachiopod fauna was collected by Tozer and Thorsteinsson from this unit. The overlying beds consist of reddish brown, interbedded sandstone and conglomerate, overlain by red shale containing grey limestone concretions up to 0.08 m in diameter. The total thickness approaches 600 m.

No macrofaunal data are available from the middle and upper part of the formation. In the Canyon Fiord area of Ellesmere Island, Thorsteinsson (1974), reported that the oldest fossils (mainly fusulinaceans) were of Bashkirian age and the youngest were probably Sakmarian, although an Asselian age could not be ruled out.

In the investigation of this formation during the summer of 1984, only the middle and upper parts were studied. Most of the formation, with its dominantly red-brown colour, is not suitable for palynological analysis; however, in the uppermost part, about 10 m below the base of the Belcher Channel Formation, approximately 8 m of alternating grey, grey-khaki and purplish shale occur. Samples from this unit yielded poor to fairly well preserved assemblages of pollen and spores.

Striate disaccate pollen (**Protohaploxypinus** spp.) and polyplicate pollen (**Vittatina** spp. and **Weylandites** spp.) are common, with rare, monosaccate pollen (**Cordaitina** sp.) and occasional trilete spores (**Leiotriletes** sp., **Lophotriletes** sp., **Punctatisporites** sp., and **Raistrickia** sp).

The age of this material is uncertain, but the abundance of polyplicate grains and striate disaccate grains indicates that it may be Early Permian (Asselian or Sakmarian).

The organic matter consists mainly of small to medium sized (approx. 30-50 µm) coaly fragments, along with some woody and exinous fragments. The abundance of land derived pollen and spores, along with the lack of any marine palynomorphs, suggests a nonmarine environment of deposition for the interval sampled. The fact that the coaly fragments are small to medium sized may be the result of transportation, possibly in a fluviatile regime, prior to deposition. The fine grained grey sediments at the top of the formation are poorly exposed, but the colour change can be

Figure 28.1.　Location of study area.

traced along strike for several hundred metres, suggesting that the beds are laterally extensive, and that they may represent deposition in a lacustrine environment.

The spores and pollen are light yellow-brown to medium brown suggesting a Thermal Alteration Index of 2+.

Belcher Channel Formation

The original description by Tozer and Thorsteinsson (1964, p. 102), included beds, now assigned to the Belcher Channel Formation, in the lower Sabine Bay Formation. They pointed out (p. 229) that further work on Ellesmere and Axel Heiberg islands would probably necessitate revision of the stratigraphy and that the upper, essentially nonmarine part should be included in the Sabine Bay Formation, whereas the lower, marine part correlated with the Belcher Channel Formation of the northeastern Arctic islands. The lithology of the Belcher Channel Formation at the sample locality is essentially a quartzose, bioclastic limestone, within which is a calcareous, quartzose sandstone at least 20 m thick. The total thickness is in the order of 90 m. In the limestone units occur brachiopods, bryozoans and fusulinids, which, according to Tozer and Thorsteinsson (1964), indicate an Early Permian age. In other parts of the Sverdrup basin, the formation has a possible age range from latest Carboniferous (Gzhelian) to earliest Artinskian, (Nassichuk and Wilde, 1977, Textfigure 4), but Nassichuk (1965), pointed out that in the southern part of Sabine Peninsula only the uppermost part of

Figure 28.2. Sample localities.

the formation may be represented. Fusulinids collected by Nassichuk from near the top of the formation were identified by Thorsteinsson as **Parafusulina** sp., and an early Artinskian age was suggested (Nassichuk, 1970).

Within the limestone units occur very thin, argillaceous intercalations that were sampled for palynomorphs. These intercalations contain assemblages with striate disaccate pollen (**Protohaploxypinus** spp. and **Striatoabieites** sp.), polyplicate pollen (**Vittatina** spp. and **Weylandites** spp.), and a variety of trilete spores (**Apiculatisporis** sp., **Calamospora** sp., **Cyclogranisporites** sp., **Dictyotriletes** sp., **Kraeuselisporites** spp., **Leiotriletes** sp., **Lophotriletes** sp., and **Raistrickia** sp.). Monosaccate pollen is rare, but includes **Cordaitina** sp. and **Florinites luberae** Samoilovich 1961. Acritarchs (**Micrhystridium** spp.) occur occasionally, and scolecodonts are rare.

The organic matter consists of a high proportion (approx. 50%) of finely dispersed organic debris along with approximately equal proportions of small to medium sized, coaly, woody and exinous material. The occurrence of this type of organic matter, and the fact that land derived pollen and spores are abundant and acritarchs occur occasionally, suggest a high energy, shallow marine environment of deposition.

The colour of the spores is yellow-brown to dark orange, indicating a Thermal Alteration Index of 2.

SYSTEM	N. AMERICAN SERIES	STAGE	FORMATION	SAMPLE NOS.	PALYNOMORPHS PRESENT	T.A.I.
TRIASSIC / LOWER		Griesbachian	Bjorne	C-099221-/C-099227	√	2
PERMIAN / UPPER	Guadalupian	Capitanian	Trold Fiord	C-099228-C-099246	√	2 to 2+
		Wordian				
	Leonardian	Roadian	¹"Unit A"	C-099249	√	2
			Assistance	C-099247 C-099248 C-099250 /C-126251-C-126256	√	2-
PERMIAN / LOWER		Artinskian	Sabine Bay	C-126257-C-126278	√	2-
			Belcher Channel	C-126284-C-126294	√	2+
	Wolfcampian	Sakmarian	Uppermost(?) Canyon Fiord	C-126279-C-126283	√	2+
		Asselian				

Major hiatus........——————   Minor hiatus......../ / / / /

Figure 28.3. *Correlation table indicating the approximate ages of beds sampled in the Tingmisut Lake area, Sabine Peninsula, Melville Island.* ¹*"Unit A" used in the sense of Nassichuk (1965).* √*Indicates palynomorphs present.*

Sabine Bay Formation

This formation consists mainly of medium grained, generally grey to buff, cross-bedded, quartzose sandstone. It contains occasional, thin beds of carbonaceous mudstone and coal (0.05 m); varicoloured chert pebbles are commonly present. Exposure of the formation, especially the lower part, is generally poor and discontinuous in the Hiccles Creek area. Near the presumed base occurs a bed with large (0.80 m), calcareous, nodular concretions that contain occasional brachiopods and trace fossils (**Zoophycus?** sp.); the latter were observed also near the top of the formation. The Sabine Bay Formation may be divided into a lower unit, which is so unindurated that sections may be dug easily with a shovel, and an upper part, which is well indurated, and forms prominent cliffs. According to Nassichuk (1965), the total maximum thickness is approximately 120 m.

The age of the formation is uncertain but, near the base, Nassichuk (1970), recorded **Sverdrupites** sp., and suggested an Artinskian age.

The thin, argillaceous, carbonaceous beds yielded very well preserved pollen and spores and occasional acritarchs. The assemblages contain a variety of taxa, including striate disaccate pollen (**Protohaploxypinus** spp., **Striatopodocarpites** spp., and **Hamiapollenites** sp.), and non-striate disaccate pollen (**Alisporites** spp., **Pityosporites** spp., **Sulcatisporites** spp., and **Triadispora** spp.), polyplicate pollen (**Vittatina** spp. and **Weylandites** spp.), trilete spores (**Apiculatisporis** spp., **Calamospora** spp., **Cyclogranisporites** spp., **Densoisporites** spp., **Foveosporites** spp., **Kraeuselisporites** spp., **Leiotriletes** spp., **Lophotriletes** spp., **Neoraistrickia** spp., **Nevesisporites** sp., **Punctatisporites** spp., **Raistrickia** spp., and **Verrucosisporites** sp.), and the monolete spore **Speciososporites** sp. Acritarch genera include **Micrhystridium** and **Veryhachium**. Also present are reworked Late Devonian specimens including **Ancyrospora** sp. and **Cyrtospora cristifer** (Luber) Van der Zwan 1979, along with **Pustulatisporites** sp. and **Retusotriletes** sp., which may also be of Late Devonian age.

The organic matter consists of abundant (50-80%) medium to large sized (approx. 50-170 µm) coaly fragments along with some woody and exinous fragments. Finely dispersed organic matter is rare. The medium to large size of the coaly fragments, the abundance of land derived pollen and spores, and the presence of occasional acritarchs, indicate a fairly low energy, marine environment of deposition such as a delta front.

The pollen and spores are yellow-orange in colour and the Thermal Alteration Index is estimated to be 2-.

Assistance Formation

The Assistance Formation is recognized in the sense of Nassichuk (1965), rather than that of Tozer and Thorsteinsson (1964). It consists of grey sandstone, ironstone concretionary bands and grey mudstone. The total thickness is in the order of 30 m.

Exposure is extremely poor due to the recessive nature of the beds and a cover of solifluction debris. In the Hiccles Creek area, Nassichuk (1965) recorded typical Assistance ammonoids. In the type section of the Assistance Formation (Grinnell Peninsula, Devon Island), the ammonoid fauna indicates a probable Late Artinskian age (Nassichuk, 1970).

Samples collected from the rare exposures yielded well preserved, diverse assemblages of pollen and spores. Acritarchs are common and occasional scolecodonts occur.

SYSTEM	FORMATION	ASSEMBLAGE CHARACTERISTICS
TRIASSIC	Lower Bjorne	*Taeniaesporites noviaulensis*, *Protohaploxypinus* spp., *Striatoabieites richteri*, *Falcisporites zapfei*, *Klausipollenites staplinii*, *Gnetaceaepollenites steevesi*, *Kraeuselisporites* sp., *Lundbladispora obsoleta*, *Lundbladispora* sp., *Proprisporites pocockii*, *Tympanicysta stoschiana*.
UPPER PERMIAN	Trold Fiord	*Protohaploxypinus* spp., *Striatoabieites* spp., *Abiespollenites* sp., *Alisporites* sp., *Limitisporites* sp., *Sulcatisporites* sp., *Triadispora* sp., *Vitreisporites* sp., *Vittatina* spp., *Weylandites* spp., *Cordaitina* sp., *Florinites luberae*, *Apiculatisporis* spp., *Cyclogranisporites* spp., *Diatomozonotriletes* sp., *Kraeuselisporites* spp., *Lophotriletes* sp., *Neoraistrickia* sp., *Nevesisporites* sp., *Micrhystridium* spp., *Veryhachium* spp.
-?-?-?-	"Unit A"	*Aletes(?)* common. *Vittatina* spp., *Weylandites* spp., *Florinites luberae*, *Sulcatisporites* sp., *Apiculatisporis* sp., *Calamospora* sp., *Cyclogranisporites* sp., *Diatomozonotriletes* sp., *Kraeuselisporites* sp., *Leiotriletes* sp., *Punctatisporites* spp., *Micrhystridium* spp., *Veryhachium* spp.
LOWER PERMIAN	Assistance	*Protohaploxypinus* spp., *Striatoabieites* spp., *Abiespollenites* sp., *Triadispora* sp., *Pityosporites* sp., *Vittatina* spp., *Weylandites* sp., *Florinites luberae*, *Apiculatisporis* sp., *Diatomozonotriletes* sp., *Kraeuselisporites* spp., *Lophotriletes* sp., *Neoraistrickia* spp., *Nevesisporites* sp., *Punctatisporites* sp., *Raistrickia* sp., *Verrucosisporites* sp., *Micrhystridium* spp., *Veryhachium* spp.
	Sabine Bay	*Protohaploxypinus* spp., *Striatopodocarpites* spp., *Hamiapollenites* sp., *Alisporites* spp., *Pityosporites* spp., *Sulcatisporites* spp., *Triadispora* sp., *Vittatina* spp., *Weylandites* spp., *Apiculatisporis* spp., *Calamospora* spp., *Cyclogranisporites* spp., *Densoisporites* spp., *Foveosporites* spp., *Kraeuselisporites* spp., *Leiotriletes* spp., *Lophotriletes* spp., *Neoraistrickia* spp., *Nevesisporites* sp., *Punctatisporites* spp., *Raistrickia* spp., *Verrucosisporites* sp., *Speciososporites* sp., *Micrhystridium* spp., *Veryhachium* spp.
	Belcher Channel	*Protohaploxypinus* spp., *Hamiapollenites?* sp., *Striatoabieites* sp., *Vittatina* spp., *Weylandites* spp., *Apiculatisporis* sp., *Calamospora* sp., *Cyclogranisporites* sp., *Dictyotriletes* sp., *Kraeuselisporites* spp., *Leiotriletes* sp., *Lophotriletes* sp., *Raistrickia* sp., *Cordaitina* sp., *Florinites luberae*, *Micrhystridium* spp.
	Uppermost Canyon Fiord	*Protohaploxypinus* spp., *Hamiapollenites?* sp., *Striatoabieites* sp., *Vittatina* spp., *Weylandites* spp., *Cordaitina* sp., *Striomonosaccites* sp., *Leiotriletes* sp., *Lophotriletes* sp., *Punctatisporites* sp., *Raistrickia* sp.

Figure 28.4. *Summary of palynomorph assemblages.*

The assemblages contain striate disaccate pollen (**Protohaploxypinus** spp. and **Striatoabieites** spp.) and non-striate disaccate pollen (**Abiespollenites** sp., **Triadispora** sp., and **Pityosporites** sp.), polyplicate pollen (**Vittatina** spp. and **Weylandites** spp.), monosaccate pollen **Florinites luberae** Samoilovich, 1961, and a variety of trilete spores (**Apiculatisporis** sp., **Diatomozonotriletes** sp., **Kraeuselisporites** sp., **Lophotriletes** sp., **Neoraistrickia** spp., **Nevesisporites** sp., **Punctatisporites** sp., **Raistrickia** sp., and **Verrucosisporites** sp.). Acritarch genera include **Micrhystridium** and **Veryhachium**. Scolecodonts occur rarely. Present are some specimens of spores which are possibly derived from the Late Devonian or, more rarely, the Lower Carboniferous (e.g. **Densosporites rarispinosus** Playford 1963).

The organic content consists largely of abundant, medium to large sized (approx. 50-170 µm) coaly and woody fragments (75%) but there is a significant amount of exinous and finely dispersed debris. This type of organic matter, along with the presence of abundant land derived pollen and

spores, acritarchs and scolecodonts, suggests a nearshore marine environment of deposition, with the presence of abundant nutrients.

The colour of the spores is yellow-orange, indicating a Thermal Alteration Index of 2-.

"Unit A"

"Unit A", recognized by Nassichuk (1965), consists mainly of bioclastic limestone and is about 90 m thick. He suggested that the upper and lower contacts are disconformable. This conclusion was based mainly on litho-stratigraphic criteria, as the abundant fauna of brachiopods and bryozoans has yet to be studied; a late Early or early Late Permian age was tentatively suggested, based mainly on the relative stratigraphic position of the unit.

Argillaceous intercalations suitable for palynological samples are rare in "Unit A", but one sample, from approximately 5 m above the base, was found to contain fairly well preserved palynomorphs. These consisted of

abundant alete grains of uncertain affinity. Polyplicate pollen was common (**Vittatina** spp. and **Weylandites** spp.); present also was monosaccate pollen (**Florinites luberae**), non-striate disaccate pollen (**Sulcatisporites** sp.), and trilete spores (**Apiculatisporis** sp., **Diatomozonotriletes** sp., **Kraeuselisporites** sp., **Leiotriletes** sp., and **Punctatisporites** sp.). In addition, the acritarchs **Micrhystridium** spp. and **Veryhachium** spp. occur. Occasional reworked spores occur, including **Cyrtospora cristifer** (Luber) Van der Zwan 1979; these were probably derived from Late Devonian rocks.

The organic matter consists of small, medium and large sized (approx. 30-170 µm) coaly and woody fragments (approx. 50%), and finely dispersed organic debris with a small amount of exinous material. The variety of size ranges of the coaly and woody material, the abundance of land derived pollen and spores, and the presence of acritarchs, indicate a high energy, nearshore marine environment of deposition.

The colour of the spores is yellow to orange, suggesting a Thermal Alteration Index of 2- to 2.

Trold Fiord Formation

The Trold Fiord Formation consists of green, glauconitic sandstone, black chert and minor limestone bands. Occasional, thin, grey mudstone intercalations occur, and these were sampled for palynomorphs. Exposure of the formation is incomplete; approximately 65 m of actual outcrop were measured, although the formation as a whole is much thicker. Nassichuk, who referred to this formation as "Unit B" in 1965, estimated its thickness to be in the vicinity of 230 m; Thorsteinsson (1974, p. 66) later assigned "Unit B" to the Trold Fiord Formation. The formation contains an abundant fauna of brachiopods, but present in addition are bryozoans, pelecypods, gastropods, and rare cephalopods. Well preserved trace fossils (**Zoophycus**? sp.) are common.

Macrofaunal data concerning the age of the Trold Fiord Formation on Melville Island are limited, but brachiopods collected by Nassichuk and studied by R.E. Grant indicate a Guadalupian age (Thorsteinsson, 1974). No evidence of any Dzulfian or Changhsingian rocks has yet been found in this area, suggesting that a significant hiatus is present between the Permian and Triassic.

Palynomorphs found in the Trold Fiord Formation include pollen and spores, acritarchs and occasional scolecodonts. Present are striate disaccate pollen (**Protohaploxypinus** spp. and **Striatoabieites** spp.) and non-striate disaccate pollen (**Abiespollenites** sp., **Alisporites** sp., **Limitisporites** sp., **Sulcatisporites** sp., **Triadispora** sp., and **Vitreisporites** sp.), polyplicate pollen (**Vittatina** spp. and **Weylandites** spp.), and occasional monosaccate pollen (**Cordaitina** sp. and **Florinites luberae** Samoilovich 1961). There is a variety of trilete spores, including **Apiculatisporis** spp., **Cyclogranisporites** spp., **Diatomozonotriletes** sp., **Kraeuselisporites** spp., **Lophotriletes** sp., **Neoraistrickia** spp., and **Nevesisporites** sp. Acritarchs include **Micrhystridium** spp. and **Veryhachium** spp. Scolecodonts occur rarely. In addition, a number of reworked species occur, including **Cornispora varicornuta** Staplin and Jansonius in Staplin, 1961, of Late Devonian (Famennian) age, and **Densosporites** sp. and **Murospora** sp. of Early Carboniferous age.

The organic matter consists mainly of finely dispersed organic debris, which sometimes occurs in coagulated lumps; small to medium sized (approx. 30-50 µm) woody and coaly fragments and exinous material constitute the remainder. The presence of abundant, finely dispersed organic matter,

occurring in association with land derived pollen and spores, acritarchs and scolecodonts, suggests deposition in a high energy, nearshore marine environment, with abundant nutrients.

The colour of the spores is pale yellow-brown, suggesting a Thermal Alteration Index of 2.

Bjorne Formation

The Bjorne Formation was named by Tozer (1961; and in Fortier et al., 1963), and has its type section on the Bjorne Peninsula, southern Ellesmere Island. It is mainly composed of sandstone, and is a basin margin equivalent of the mid-basin, marine Blind Fiord Formation. The oldest beds of the Blind Fiord Formation are regarded as representing the base of the Triassic (Tozer, 1967), and the oldest beds of the Bjorne Formation are approximately synchronous (Tozer, personal communication in Thorsteinsson, 1974, p. 73).

In the Hiccles Creek section there are approximately 15 m of crossbedded, fine grained, buff sandstone with occasional thin, grey, shaly intercalations. Trace fossils occur on some bedding planes near the base of the section.

The contact with the underlying Trold Fiord Formation is not exposed at this locality, and, therefore, it is not certain that these beds represent the oldest part of the formation.

Well preserved palynomorphs occur in samples taken from the grey shale beds, and include pollen, spores and the cyst-like microfossil **Tympanicysta stoschiana** Balme 1980. The assemblage contains striate disaccate pollen [**Taeniaesporites noviaulensis** Leschik 1956, **Protohaploxypinus** spp., and **Striatoabieites richteri** (Klaus) Hart 1965], non-striate disaccate pollen [**Falcisporites zapfei** (Potonié and Klaus) Leschik 1956 and **Klausipollenites staplinii** Jansonius 1962], plicate pollen (**Gnetaceaepollenites steevesi** Jansonius 1962), and trilete spores (**Kraeuselisporites** sp., **Lundbladispora obsoleta** Balme 1970, **Lundbladispora** sp., and **Proprisporites pocockii** Jansonius 1962). Reworked spores include **Cyrtospora cristifer** (Luber) Van der Zwan 1979 and **Hystricosporites**? sp.; these are probably of Late Devonian age.

The organic matter consists mainly of small, medium and large sized (approx. 30-170 µm) coaly and woody fragments, with the remainder comprising exinous material. The facts that only land derived pollen and spores were found, and that there is considerable variety in the size of the coaly and woody fragments, suggest deposition in a continental (fluviatile?) environment.

The spores are yellow-brown and the Thermal Alteration Index is estimated as 2.

Conclusions

It is difficult to reliably compare the Permian Melville Island assemblages with those from other parts of Canada, because although illustrations have been given in publications by Barss (1967) and Bamber and Barss (1969), the only material accompanied by systematic descriptions is that of Jansonius (1962). The latter described assemblages from the Belloy Formation of the Peace River area of Western Canada, and suggested a Leonardian-Guadalupian age. The presence of striate disaccate pollen and polyplicate pollen is documented, but in general the assemblages lack variety, and reliable comparisons are difficult. **Vittatina striata** Jansonius, which is common in the Belloy Formation, occurs in all of the Permian formations of Melville Island.

236

In East Greenland, Balme (1980), recorded assemblages that contain abundant specimens of **Vittatina** spp. and which he suggested may be younger than Guadalupian. In contrast to the Upper Permian assemblages of Melville Island, the Greenland material has low diversity and trilete spores are rare.

The assemblages from the Bjorne Formation are similar to those recorded by Jansonius (1962), from rocks of probable Griesbachian age from the Toad-Grayling Formation of the Peace River area of Western Canada, and by Fisher (1979), from his palynofloral zone 1 of Griesbachian age from the Canadian Arctic Archipelago. Also, there are many similarities to the **Protohaploxypinus** – Association of East Greenland described by Balme (1980), and assigned to the Griesbachian.

At the specific level, the Melville Island Permian assemblages are unlike those of Gondwana and Cathaysia. Neither are they like those from Western Europe. They have a number of features in common with assemblages described from the northeast European part of Russia by Varyukhina (1971), and Molin and Koloda (1972); for example, there are many qualitative similarities and, quantitatively, species of **Vittatina** and striate disaccate pollen are abundant and trilete spores common at both localities. According to Meyen (1982), the northeast European part of Russia contains Angaran and sub-Angaran plants; this area is marginal to the Angara paleofloristic province and is termed the Pechora province. A detailed comparision of the Canadian with the Russian material will probably enable relatively precise biostratigraphic correlations to be made. At present, insufficient work has been carried out on the marine fauna of the Melville sections to provide detailed biostratigraphic control; it is hoped that the study of conodont and foraminifera samples, collected by A.C. Higgins and P.H. von Bitter, simultaneously with the study of palynology samples from the Belcher Channel to Trold Fiord formations, will partially remedy this situation.

The environment of deposition deduced for the Permian formations in the southwestern part of the Sabine Peninsula is, with the exception of the uppermost part of the Canyon Fiord Formation, nearshore marine. The uppermost part of the Canyon Fiord Formation is possibly lacustrine. No marine palynomorphs were found in the Triassic Bjorne Formation and a continental (fluviatile?) environment is suggested.

The Thermal Alteration indices in the study area are low and vary from 2- to 2+. The variation appears to be more the result of lithological differences than depth of burial. For example, the Thermal Alteration Index is only 2- in the Sabine Bay and Assistance formations, which consist mainly of sandstone and mudstone respectively, but 2 to 2+ in the overlying Trold Fiord Formation, which consists mainly of glauconitic sandstone, black chert and minor limestone bands. These levels of maturation suggest that conditions may have been suitable for the generation of liquid hydrocarbons.

The occurrence of reworked Upper Devonian spores in the Permian and Lower Triassic rocks is not surprising in view of the abundance of Upper Devonian rocks present on Melville Island. The presence of occasional Lower Carboniferous spores in the Assistance and Trold Fiord formations is more problematical, as no Lower Carboniferous rocks are known from this part of the Arctic Archipelago; there is a hiatus between the Upper Devonian (Famennian) and the Upper Carboniferous (Moscovian). The Thermal Alteration indices of both the Upper Devonian and Lower Carboniferous material is 2+ (spores are light brown), indicating that the sediments from which they were derived had not been subjected to any great depth of burial.

References

Balme, B.E.
1980: Palynology of Permian-Triassic boundary beds at Kap Stosch, East Greenland; Meddelelser om Grønland, Upgivne af, Kommissionen for videnskabelige undersøgelser i Grønland, Bd. 200, nr. 6, p. 1-37.

Bamber, E.W. and Barss, M.S.
1969: Stratigraphy and palynology of a Permian section, Tatonduk River, Yukon Territory; Geological Survey of Canada, Paper 68-18, p. 1-38.

Barss, M.S.
1967: Carboniferous and Permian spores of Canada; Geological Survey of Canada, Paper 67-11, p. 1-94.

Fisher, M.J.
1979: The Triassic palynofloral succession in the Canadian Arctic Archipelago; American Association of Stratigraphic Palynologists, Contributions Series No. 5B, p. 83-100.

Fortier, Y.O., Blackadar, R.G., Glenister, B.F., Greiner, H.R., McLaren, D.J., McMillan, N.J., Norris, A.W., Rootes, E.F., Souther, J.G., Thorsteinsson, R., and Tozer, E.T.
1963: Geology of the north-central part of the Arctic Archipelago, Northwest Territories (Operation Franklin); Geological Survey of Canada, Memoir 320, p. 1-671.

Hunt, J.M.
1979: Petroleum Geochemistry and Geology; Freeman and Co., San Francisco, p. 1-617.

Jansonius, J.
1962: Palynology of Permian and Triassic sediments, Peace River area, western Canada; Palaeontographica Abt. B, 110, p. 35-98.

Meyen, J.V.
1982: The Carboniferous and Permian floras of Angaraland (a synthesis); International Publishers Lucknow (India), Biological Memoirs, v. 7(1), p. 1-109.

Molin, V.A. and Koloda, N.A.
1972: Verkhnepermskie sporovopyl'tsevye kompleksy severa russkoi platformy; Akademiia Nauk. SSSR, Geologicheskii Institut "Nauka" Leningrad, p. 1-76.

Nassichuk, W.W.
1965: Pennsylvanian and Permian rocks in the Parry Islands Group, Canadian Arctic Archipelago; in Report of Activities, Field, 1964; Geological Survey of Canada, Paper 65-1, p. 9-12.

1970: Permian Ammonoids from Devon and Melville islands, Canadian Arctic Archipelago; Journal of Paleontology, v. 44, no. 1, p. 77-97.

Nassichuk, W.W. and Wilde, G.L.

1977: Permian fusulinaceans and stratigraphy at Blind Fiord, southwestern Ellesmere Island; Geological Survey of Canada, Bulletin 268, p. 1-59.

Thorsteinsson, R.

1974: Carboniferous and Permian stratigraphy of Axel Heiberg Island and western Ellesmere Island, Canadian Arctic Archipelago; Geological Survey of Canada, Bulletin 224, p. 1-115.

Tozer, E.T.

1961: Triassic stratigraphy and faunas, Queen Elizabeth Islands, Arctic Archipelago; Geological Survey of Canada, Memoir 316, p. 1-116.

Tozer, E.T. (cont.)

1967: A standard for Triassic time; Geological Survey of Canada, Bulletin 156, p. 1-103.

Tozer, E.T. and Thorsteinsson, R.

1964: Western Queen Elizabeth Islands, Arctic Archipelago; Geological Survey of Canada, Memoir 332, p. 1-242.

Varyukhina, L.M.

1971: Spory i pyl'tsa krasnotsvetnykh i uglenosnykh otloshchenii permi i triasa severo-vostoka evropeiskoi chasti SSSR; Adademiia Nauk. SSSR, Komi Filial, Geologicheskii Institut. "Nauka" Leningrad, p. 1-159.

Stratigraphic subdivision of the Isachsen and Christopher formations (Lower Cretaceous), Arctic Islands

Project 750083

Ashton F. Embry
Institute of Sedimentary and Petroleum Geology, Calgary

Abstract

The Isachsen Formation, a Lower Cretaceous sandstone-dominant unit, is herein divided into three members, named in ascending order: Paterson Island, Rondon and Walker Island. The Paterson Island and Walker Island members are sandstone-dominant units of delta front and delta plain origin and are separated by the shale-siltstone-dominant Rondon Member, which is of offshore marine shelf origin. The Christopher Formation, a Lower Cretaceous, shale-siltstone-dominant unit, which overlies the Isachsen Formation, is divided into two members, named in ascending order: Invincible Point and Macdougall Point. Both members are of offshore marine shelf origin, and the boundary between the two is placed at the top of a widespread sandstone-siltstone interval that occurs in the middle of the Christopher Formation.

Résumé

La formation d'Isachsen, unité à dominance de grès du Crétacé inférieur, se divise ici en trois membres, nommés dans l'ordre ascendant: Paterson Island, Rondon et Walker Island. Les membres Paterson Island et Walker Island sont des unités où prédomine le grès, d'origine deltaïque (front et plaine); ces deux membres sont séparés par le membre de Rondon où prédominent le schiste argileux et le siltstone d'origine sous-marine (plate-forme continentale). La formation de Christopher, unité du Crétacé inférieur où prédomine le schiste argileux et le siltstone, et qui surmonte la formation d'Isachsen, comporte deux membres, nommés dans l'ordre ascendant: Invincible Point et Macdougall Point. Les deux membres sont d'origine sous-marine (plate-forme continentale) et la limite entre les deux se situe au sommet d'un intervalle étendu de grès et de siltstone qui traverse le milieu de la formation de Christopher.

Introduction

The Isachsen and Christopher formations were recognized and defined by Heywood (1955, 1957) on the basis of fieldwork on northern Ellef Ringnes Island in 1952 and 1953. Subsequent fieldwork permitted the recognition of these units over much of the Arctic Islands, and the combined thickness of the formations commonly exceeds 1500 m. The Isachsen Formation is composed mainly of fine- to very coarse-grained, quartzose sandstone, with interbeds of siltstone, shale and coal. The overlying Christopher Formation comprises predominantly medium to dark grey shale and siltstone, with only minor sandstone content.

The two formations make up the bulk of the Lower Cretaceous succession in the Arctic Islands, and occur mainly within the Sverdrup Basin, Eglinton Graben and Banks Basin (Fig. 29.1). Small, isolated occurrences are also present as outliers on Lower Paleozoic strata to the south and east of the Sverdrup Basin. Numerous subsurface and surface sections are available for the formations (Fig. 29.1) and regional correlations have indicated that both formations can be subdivided into members that extend over much of the study area. In this paper, three members within the Isachsen and two within the Christopher are defined and described. Stratigraphic tops for these units in selected wells across the area are listed in the appendix. Chip samples, taken at 3 m intervals from the type sections of these new members, can be examined at the Institute of Sedimentary and Petroleum Geology in Calgary, Alberta, Canada.

Previous work

The Isachsen and Christopher formations were defined by Heywood (1955, 1957) from exposures on northern Ellef Ringnes Island. The Isachsen is a prominent sandstone unit that lies between two shale-siltstone units (Deer Bay and Christopher formations) whereas the Christopher is a shale-siltstone unit lying between two sandstones (Isachsen and Hassel formations). Fieldwork during Operation Franklin in 1955 extended the two formations eastward to Amund Ringnes and Axel Heiberg islands (Fortier et al., 1963). Subsequent fieldwork in the late fifties and early sixties further extended the formations and demonstrated their occurrence on Ellesmere, Melville, Prince Patrick, Mackenzie King, Eglinton and Banks islands (Thorsteinsson and Tozer, 1962; Tozer, 1963; Tozer and Thorsteinsson, 1964). More recently, the formations have been described by Stott (1969), Nassichuk and Christie (1969), Plauchut and Jutard (1976), Balkwill and Roy (1977), Miall (1979), Balkwill et al., (1982) and Balkwill (1983) as part of regional mapping studies in various parts of the Arctic Islands.

In a few cases (McLaren, 1963; Balkwill, 1983), the Isachsen Formation was subdivided into informal members on the basis of weathering pattern, but these units were of local extent only. On the other hand, the Christopher Formation has been divided into two informal members over much of its extent (Plauchut and Jutard, 1976; Balkwill and Roy, 1977; Balkwill, 1983). This subdivision is based on the occurrence of a medial sandstone and siltstone unit in the Christopher, the top of which is used as the boundary between the two informal members.

Present work

As part of a regional study of the Mesozoic succession in the Arctic Islands the author has examined numerous surface and subsurface sections of the Isachsen and Christopher formations. Correlation of these sections has led to the recognition of three, widespread members in the Isachsen and two in the Christopher.

A distinctive unit of medium- to dark-grey shale and siltstone of marine origin occurs within the sandstone-dominant Isachsen Formation over most of the formation's

Figure 29.1. Distribution of Isachsen and Christopher formations and control points. Key to numbered wells listed in appendix: 1. North Sabine H-49, 2. Drake Point F-16, 3. Skybattle Bay C-15, 4. Wallis A-73, 5. Hoodoo Dome H-37, 6. Helicopter J-12, 7. Romulus C-42, 9. Pedder Point D-49, 10. Castel Bay C-68.

extent in the Sverdrup Basin. The existence of this unit was first noted by Balkwill et al. (1982) in a well on Lougheed Island. The delineation of this shale-siltstone unit within the Isachsen Formation allows the formation to be divided into three members: a lower sandstone, a medial shale-siltstone and an upper sandstone. These three members are formally defined herein and have been named, in ascending order, Paterson Island, Rondon, and Walker Island members.

Figure 29.2 illustrates the general stratigraphy of these three members. In some areas of the Arctic Islands (north-eastern Sverdrup, southeastern basin margin, Banks Basin) the Rondon Member is absent due to facies change to sandstone, and in these areas the Isachsen Formation is undivided. In the northwestern portion of the Sverdrup Basin (Mackenzie King Island), the Walker Island Member is absent due to facies change to shale and siltstone and the Paterson Island Member comprises the entire Isachsen Formation in this area (Fig. 29.2).

For the Christopher Formation, an interval of inter-bedded very fine grained sandstone, siltstone and shale can be recognized in the mid-portion of the formation on Ellesmere, Axel Heiberg, Amund Ringnes, Ellef Ringnes and King Christian islands. To the southwest, this interval consists mainly of coarse siltstone with only minor sandstone, but is still clearly recognizable on Lougheed, Melville, Eglinton and Banks islands. The sandstone or coarse siltstone unit is abruptly overlain by soft, clay-rich shale. This boundary is readily delineated in surface and subsurface sections, and is also a good seismic reflector over portions of the western Sverdrup (A. Densmore, personal communication, 1982). Following Balkwill (1983) this boundary is used to divide the Christopher into two members, which are formally defined herein and are named, in ascending order, the Invincible Point and Macdougall Point members.

Paterson Island Member, Isachsen Formation

Definition

The Paterson Island Member consists predominantly of fine- to very coarse-grained, pebbly sandstone with interbeds of carbonaceous siltstone, shale and coal. The type section is in the Sun Skybattle Bay C-15 well (77°14'12"N, 105°05'57"W; spudded April 1, 1971, abandoned November 23, 1971; T.D. 3658 m, K.B. 33.5 m) between 1111 m (3644 ft) and 1263 m (4144 ft), and is 152 m thick (Fig. 29.3). The name is taken from Paterson Island, which lies to the south of Lougheed Island.

Boundaries

The Paterson Island Member overlies either the Deer Bay or Mackenzie King formations, with the contact varying from unconformable on the basin margin to conformable in the basin centre. The contact is placed at the base of the first sandstone unit above which sandstone is predominant. The Paterson Island Member is usually conformably overlain by the Rondon Member of the Isachsen Formation except in the northwestern Sverdrup, where it is overlain by the Christopher Formation (Fig. 29.2). The contact is placed at the top of the highest sandstone unit above which shale and siltstone are predominant.

Lithology

In the type section (Fig. 29.3) the Paterson Island Member consists mainly of units of fine- to very coarse-grained, pebbly, quartzose sandstone that have abrupt basal contacts, and which fine upward into units of carbonaceous shale, siltstone, very fine grained sandstone, and coal. The sandstone units are up to 35 m thick, and the intervening argillaceous intervals are between 2 and 10 m thick. This lithological association is typical for the Paterson Island Formation, with the sandstones in outcrop commonly

Figure 29.2. *Schematic stratigraphic cross-section, Isachsen Formation, Sverdrup Basin.*

Figure 29.3. *Lithology (from samples) and gamma ray curve for type sections of Paterson Island, Rondon, Walker Island members. Isachsen Formation, Skybattle Bay C-15 well.*

exhibiting trough and planar crossbedding. Ripple cross-lamination, root casts, and parallel lamination occur in the very fine grained sandstone and siltstone units. In the basin centre area, where the basal contact of the member is conformable, coarsening-upward cycles of shale, siltstone and very fine- to coarse-grained siltstone occur in the basal portion of the member.

Thickness and distribution

The Paterson Island Member occurs over most of the Isachsen Formation's extent in the Sverdrup Basin, with the exception of the areas previously noted. The member is

usually thin (<20 m) on the basin margins and thickens basinward to a maximum recorded thickness of 880 m on eastern Ellef Ringnes Island.

Age

Late Valanginian pelecypods occur in the basal portion of the member in basinal sections (Balkwill, 1983), and the overlying Rondon Member is dated as Barremian. Thus, within the basin, the member is late Valanginian to early Barremian in age. Seismic records indicate that much of the marginward thinning of the member is due to onlap onto a basal unconformity (A. Densmore, personal communication, 1982) and thus marginal sections have a far shorter age range (mainly late Hauterivian to early Barremian).

Environment of deposition

The bulk of the member is interpreted to be of delta plain origin, with both channel and overbank environments represented (fining-upward cycles, coal). The coarsening-upward cycles in the basal portion of the member in basinal sections are of delta front origin.

Rondon Member, Isachsen Formation

Definition

The Rondon Member comprises interbedded medium- to dark-grey shale, siltstone and very fine grained sandstone. The type section is in the Sun Skybattle Bay well between 1064 m (3490 ft) and 1111 m (3644 ft), and is 47 m thick (Fig. 29.3). The name is taken from Cape Rondon, on the east coast of Lougheed Island.

Boundaries

As previously described, the Rondon Member conformably overlies the Paterson Island Member. The Rondon is conformably overlain by the Walker Island Member of the Isachsen Formation, with the contact placed at the base of the first sandstone unit above which sandstone is predominant (Fig. 29.3).

Lithology

The Rondon Member is composed predominantly of dark grey, silty shale and siltstone with minor interbeds of very fine- to fine-grained sandstone. In outcrop, the sandstones are usually burrowed and ripple crosslamination is also present. Shales and siltstones are parallel laminated to burrowed. The lithotypes are commonly arranged in coarsening-upward cycles 5 to 10 m thick.

Thickness and distribution

The Rondon Member occurs over most of the Sverdrup Basin except in the areas previously noted. It is very thin (5-10 m) along the basin margin, and usually falls within the 30 to 70 m thickness range within the basin.

Age

The strata comprising the Rondon were previously tentatively dated as Aptian on the basis of micropaleontology (Balkwill et al., 1982). More recent palynological studies have indicated that the Rondon is Barremian in age (McIntyre, personal communication, 1984; Kosta, personal communication, 1985).

Environment of deposition

The rock types and flora of the Rondon indicate an offshore marine shelf environment of deposition.

Walker Island Member, Isachsen Formation

Definition

The Walker Island Member is made up of interbedded very fine- to coarse-grained sandstone, siltstone, shale and minor coal. The type section is in the Sun Skybattle Bay C-15 well between 924 m (3032 ft) and 1064 m (3490 ft), and is 140 m thick (Fig. 29.3). The name is taken from Edmund Walker Island, which lies immediately south of Lougheed Island.

Boundaries

As previously described, the Walker Island conformably overlies the Rondon Member. The member is conformably overlain by the Christopher Formation, with the contact placed at the top of the highest sandstone bed above which shale and siltstone predominate.

Lithology

The Walker Island Member is composed predominantly of very fine- to coarse-grained sandstone with interbeds of medium- to dark-grey, carbonaceous siltstone, shale and minor coal. Coarsening-upward cycles up to 30 m thick occur in the lower and uppermost portions of the member, with fining-upward cycles and associated coal occurring in the mid-portion of the member. Individual sandstone units are up to 25 m thick, and shale-siltstone units are usually less than 10 m thick. Sandstones capping the coarsening-upward cycles are commonly horizontally bedded to ripple crosslaminated. Trough and planar crossbeds occur in sandstone units that fine upward.

Thickness and distribution

The member has the same distribution as the underlying Rondon Member and occurs over most of the Sverdrup. On the basin margins, the member is 20 to 100 m thick. It thickens to a maximum of about 500 m on eastern Ellef Ringnes Island.

Age

No age-diagnostic fossils have been identified from the Walker Island Member, but it is bracketed by a Barremian age below and an Aptian age above. Thus the member is tentatively dated as late Barremian to early Aptian. Stratigraphic relationships suggest that the top of the member becomes younger toward the basin margins.

Environment of deposition

The lithotypes and cyclicity of the member indicate that its lower and middle portion represent a regressive delta front to delta plain succession. The coarsening-upward cycles of the uppermost portion represent transgressive delta front to marine shelf deposits.

Invincible Point Member, Christopher Formation

Definition

The Invincible Point Member comprises mainly dark grey shale and siltstone with interbeds of very fine grained sandstone. The type section is in the Panarctic North Sabine H-49 well (76°48'15"N, 108°45'11"W; spudded May 2, 1974, abandoned July 8, 1974; T.D. 3787 m, K.B. 60 m) between 1435 m (4708 ft) and 1856 m (6088 ft), and is 421 m thick (Fig. 29.4). The name is taken from Invincible Point on the eastern side of Sabine Peninsula, Melville Island.

Synonyms

1. Lower unit, Christopher Formation, Banks and Eglinton islands, Plauchut and Jutard (1976).
2. Lower member, Christopher Formation, King Christian Island, Balkwill and Roy (1977).
3. Lower member, Christopher Formation, Amund Ringnes Island, Balkwill (1983).

Figure 29.4. *Lithology (from samples) and gamma ray curve for type section of Invincible Point Member, Christopher Formation; North Sabine H-49 well.*

Boundaries

The Invincible Point Member conformably overlies the Isachsen Formation, and the contact is placed at the base of the lowest shale-siltstone unit above which shale and siltstone are predominant. The member is conformably overlain by the Macdougall Point Member of the Christopher Formation. The contact is placed at the base of a dark grey to black, clay-rich shale unit, which abruptly overlies sandstone or siltstone of the uppermost Invincible Point.

Lithology

At the type section (Fig. 29.4), the Invincible Point Member is composed of medium- to dark-grey, silty shale and siltstone with interbeds of very fine- to fine-grained, silty sandstone. The sandstone units are usually less than 4 m thick and occur in the lower and uppermost portions of the member. Basinward from the type section, sandstone units become less common and occur mainly in the lowermost and uppermost portions of the member. Sandstone units in the uppermost portion of the member are most common and thickest in the south-central portion of the basin (southern Axel Heiberg, Amund Ringnes). These sandstone units are up to 15 m thick and usually contain thin beds of shale and siltstone. Hummocky crossbedding, ripple crosslamination and burrows are the main sedimentary structures in these sandstones as seen in outcrop and/or core. Glauconite is a common assessory mineral. In the southwestern part of the basin, sandstones are rare in the uppermost portion of the member, but coarse siltstones occur in this interval.

Petrified wood and a variety of concretions occur within the shale and siltstone units, and pelecypods and ammonites occur most frequently in the uppermost portion of the member.

Thickness and distribution

The member has been delineated over the extent of the Christopher Formation although its identification in the Eglinton Graben and Banks Basin must be regarded as tentative. The maximum recorded thickness of the member is about 850 m on southern Axel Heiberg Island.

Age

The basal beds of the member range in age from Barremian on Mackenzie King Island, to Aptian over most of the Sverdrup, to early Albian on Banks Island (Plauchut and Jutard, 1976; Balkwill, 1983). The uppermost beds are dated as latest early Albian, based on ammonite evidence (Balkwill, 1983).

Environment of deposition

The rock types and fauna of the member indicate an offshore marine shelf environment of deposition. The sedimentary structures of the sandstone units suggest that the sands were deposited below fair weather wave-base by storm-generated currents.

Macdougall Point Member

Definition

The Macdougall Point Member consists predominantly of dark grey shale and siltstone with minor interbeds of very fine- to fine-grained sandstone. The type section is in the Panarctic North Sabine well between 899 m (2950 ft) and 1435 m (4708 ft), and is 536 m thick (Fig. 29.5). The name is taken from Macdougall Point, on the western side of Sabine Peninsula, Melville Island.

Figure 29.5. *Lithology (from samples) and gamma ray curve for type section of Macdougall Point Member, Christopher Formation; North Sabine H-49 well.*

Synonyms

1. Upper unit, Christopher Formation, Banks and Eglinton islands, Plauchut and Jutard (1976).
2. Upper member, Christopher Formation, King Christian Island, Balkwill and Roy (1977).
3. Upper member, Christopher Formation, Amund Ringnes Island, Balkwill (1983).

Boundaries

The Macdougall Point Member conformably overlies the Invincible Point Member, as previously stated. The Hassel Formation conformably overlies the Macdougall Point, with the contact placed at the base of the first sandstone unit above which sandstone is the predominant rock type.

Lithology

The Macdougall Point is composed mainly of dark grey to black shale and siltstone with interbeds of very fine- to fine-grained sandstone occurring in the uppermost portion of the member. The basal portion of the member consists of very dark to black, clay-rich shale. Silt content increases upward. A variety of concretions occur throughout the member.

Thickness and distribution

The member has been identified over the extent of the Christopher Formation. The maximum recorded thickness is 536 m (type section).

Age and environment of deposition

Ammonites and foraminifera from the member indicate a Middle Albian age (Balkwill, 1983; Wall, 1983).

The lithotypes and fauna of the member indicate an offshore marine shelf to prodelta environment of deposition.

References

Balkwill, H.R.
1983: Geology of Amund Ringnes, Cornwall and Haig-Thomas islands, District of Franklin; Geological Survey of Canada, Memoir 390.

Balkwill, H.R. and Roy, K.J.
1977: Geology, King Christian Island, District of Franklin; Geological Survey of Canada, Memoir 386.

Balkwill, H.R., Hopkins, W.S. Jr., and Wall, J.H.
1982: Geology, Lougheed Island, District of Franklin; Geological Survey of Canada, Memoir 395.

Fortier, Y.O., Blackadar, R.G., Glenister, B.F., Greiner, H.R., McLaren, D.J., McMillan N.J., Norris, A.W., Roots, E.F., Souther, J.G., Thorsteinsson, R., and Tozer, E.T.
1963: Geology of the north-central part of the Arctic Archipelago, Northwest Territories (Operation Franklin); Geological Survey of Canada, Memoir 320.

Heywood, W.W.
1955: Arctic piercement domes; Canadian Institute of Mining and Metallurgy, Bulletin, v. 48, p. 59-64.

1957: Isachsen Area, Ellef Ringnes Island, District of Franklin, Northwest Territories; Geological Survey of Canada, Paper 56-8.

McLaren, D.J.
1963: Meteorologist Peninsula dome, Ellef Ringnes Island; in Fortier et al., Geology of the north-central part of the Arctic Archipelago, Northwest Territories; Geological Survey of Canada, Memoir 320, p. 552-558.

Miall, A.D.
1979: Mesozoic and Tertiary Geology of Banks Island, Arctic Canada; Geological Survey of Canada, Memoir 387.

Nassichuk, W.W. and Christie, R.L.
1969: Upper Paleozoic and Mesozoic stratigraphy in the Yelverton Pass region, Ellesmere Island, District of Franklin; Geological Survey of Canada, Paper 68-31.

Plauchut, B.P. and Jutard, G.G.
1976: Cretaceous and Tertiary stratigraphy Banks and Eglinton islands and Anderson Plain, Northwest Territories; Bulletin of Canadian Petroleum Geology, v. 24, p. 321-371.

Stott, D.F.
1969: Ellef Ringnes Island, Canadian Arctic Archipelago; Geological Survey of Canada, Paper 68-16.

Thorsteinsson, R. and Tozer, E.T.
1962: Banks, Victoria and Stefansson islands, Arctic Archipelago; Geological Survey of Canada, Memoir 330.

Tozer, E.T.
1963: Mesozoic and Tertiary stratigraphy, western Ellesmere Island and Axel Heiberg Island, District of Franklin; Geological Survey of Canada, Paper 63-30.

Tozer, E.T. and Thorsteinsson, R.
1964: Western Queen Elizabeth Islands, Arctic Archipelago; Geological Survey of Canada, Memoir 332.

Wall, J.H.
1983: Jurassic and Cretaceous foraminiferal biostratigraphy in the eastern Sverdrup Basin, Canadian Arctic Archipelago; Bulletin of Canadian Petroleum Geology, v. 31, p. 246-281.

Stratigraphic tops from selected wells, Isachsen and Christopher formations.
Location of wells shown on Figure 29.1.

Panarctic Drake F-16
    Christopher Formation
        Macdougall Point Member   spud
        Invincible Point Member   131 m   (430 ft)
    Isachsen Formation
        Walker Island Member   425 m   (1395 ft)
        Rondon Member   527 m   (1728 ft)
        Paterson Island Member   565 m   (1854 ft)
    Deer Bay Formation   576 m   (1890 ft)

Panarctic North Sabine H-49
    Christopher Formation
        Macdougall Point Member   899 m   (2950 ft)
        Invincible Point Member   1435 m   (4708 ft)
    Isachsen Formation
        Walker Island Member   1856 m   (6088 ft)
        Rondon Member   1992 m   (6535 ft)
        Paterson Island Member   2025 m   (6645 ft)
    Deer Bay Formation   2063 m   (6767 ft)

Sun Skybattle Bay C-15
    Christopher Formation
        Macdougall Point Member   240 m   (787 ft)
        Invincible Point Member   638 m   (2092 ft)
    Isachsen Formation
        Walker Island Member   924 m   (3032 ft)
        Rondon Member   1064 m   (3490 ft)
        Paterson Island Member   1111 m   (3644 ft)
    Deer Bay Formation   1263 m   (4144 ft)

Dome Wallis A-73
    Christopher Formation
        Invincible Point Member   spud
    Isachsen Formation
        Walker Island Member   344 m   well
        Rondon Member   556 m   logged
        Paterson Island Member   616 m   in
    Mackenzie King Formation   1078 m   metres

Panarctic Hoodoo Dome H-37
    Christopher Formation
        Invincible Point Member   spud
    Isachsen Formation
        Walker Island Member   412 m   (1352 ft)
        Rondon Member   600 m   (1970 ft)
        Paterson Island Member   652 m   (2138 ft)
    Mackenzie King Formation   1132 m   (3714 ft)

Panarctic Helicopter J-12
    Isachsen Formation
        Walker Island Member   spud
        Rondon Member   455 m   (1492 ft)
        Paterson Island Member   552 m   (1810 ft)
    Mackenzie King Formation   1315 m   (4314 ft)

Panarctic Romulus C-42
    Christopher Formation
        Macdougall Point Member   246 m   (807 ft)
        Invincible Point Member   436 m   (1429 ft)
    Isachsen Formation
        Walker Island Member   813 m   (2667 ft)
        Rondon Member   869 m   (2850 ft)
        Paterson Island Member   875 m   (2870 ft)
    Deer Bay Formation   900 m   (2952 ft)

Panarctic Pedder Point D-49
    Christopher Formation
        Macdougall Point Member   285 m   (936 ft)
        Invincible Point Member   326 m   (1068 ft)
    Isachsen Formation
        Walker Island Member   604 m   (1982 ft)
        Rondon Member   1058 m   (3471 ft)
        Paterson Island Member   1085 m   (3560 ft)
    Deer Bay Formation   1165 m   (3823 ft)

Panarctic Castel Bay C-68
    Christopher Formation
        Macdougall Point Member   1453 m   (4767 ft)
        Invincible Point Member   1500 m   (4920 ft)
    Isachsen Formation undivided   1688 m   (5537 ft)
    Awingak Formation   1862 m   (6110 ft)

Stratigraphy of the Saunders Group in the central Alberta Foothills - a progress report

Project 810039

T. Jerzykiewicz
Institute of Sedimentary and Petroleum Geology, Calgary

Abstract

A new stratigraphic subdivision of the mid-Campanian — Early Paleocene nonmarine Saunders Group is presented. Six cyclothems related to major orogenic pulses in the Cordillera have been distinguished. Each cyclothem consists of two parts: a lower one containing thick and numerous channel sandstone layers, and an upper one composed mainly of overbank mudrock with coaly mudstone and/or coal. The Saunders sequence shows an overall coarsening-upward trend manifested by a predominance of channel sandstone units within the lower part of each cyclothem giving way to an upward increase in the number of conglomerate units. The succession was deposited during the final infilling of the foreland basin. The former subdivision of the Saunders Group into Brazeau and Paskapoo formations has been maintained but modified by introduction of the Coalspur Formation. It comprises the Entrance conglomerate, alternating beds of sandstone and mudrock below the Coalspur coal zone, and the coal zone itself. Both stratigraphic classifications, the traditional and the new one, are compared. The Coalspur coal zone, which corresponds to the upper part of the Fifth Cyclothem, can be correlated along the Foothills between the Athabasca and Blackstone rivers over a distance of about 100 km. The Cretaceous-Tertiary boundary has been discovered at the base of the Coalspur coal zone.

Résumé

L'auteur traite d'une nouvelle subdivision stratigraphique du groupe de Saunders d'origine non marine et datant du Campanien moyen — Paléocène inférieur. Il identifie six cyclothèmes associés aux principales poussées orogéniques de la Cordillère. Chaque cyclothème comprend deux parties: une partie inférieure qui contient de nombreuses couches épaisses de grès fluviatile et une partie supérieure composée principalement de pélite de plaine d'inondation dans laquelle s'intercalent du mudstone charbonneux ou du charbon, ou les deux. L'étude de la séquence de Saunders révèle que les grains ont tendance à être plus gros vers le haut, ce qui se traduit par une prédominance d'unités de grès fluviatile dans la partie inférieure de chaque cyclothème, lesquelles laissent graduellement la place à un nombre croissant d'unités de conglomérat. Cette succession s'est déposée au cours du dernier remplissage du bassin de l'avant-pays. L'ancienne subdivision en deux formations du groupe de Saunders (Brazeau et Paskapoo) est maintenue bien qu'elle soit modifiée par l'introduction de la formation de Coalspur. Cette dernière comprend le conglomérat Entrance, les couches alternantes de grès et de pélite sous la zone de charbon Coalspur ainsi que la zone de charbon elle-même. Les deux classifications stratigraphiques, l'ancienne et la nouvelle, font l'objet d'une comparaison. La zone de charbon Coalspur, qui correspond à la partie supérieure du cinquième cyclothème, peut être corrélée sur une distance d'environ 100 kilomètres avec les Foothills situées entre les rivières Athabasca et Blackstone. La limite Crétacé-Tertiaire a été repérée à la base de la zone de charbon Coalspur.

Introduction

The name Saunders Group was first introduced by Allan and Rutherford (1923), as a general term for the post-Wapiabi sequence of nonmarine clastics in the Saunders Creek and Nordegg coal basins. Since that time, numerous attempts have been made to subdivide the Saunders Group in the central Foothills into smaller stratigraphic units. As a result, several names have been applied to various parts of the Saunders sequence in central Foothills, for example, Lower, Upper and Coal-bearing Saunders, Brazeau and Paskapoo formations and Coalspur beds (for a comprehensive reference see Jerzykiewicz and McLean, 1980 and Fig. 7).

The Saunders Group is considered to be a synorogenic sequence of clastics deposited in the foreland basin that developed during deformation and uplift of the Rocky Mountains, probably east of the Omineca Crystalline Belt (Bally et al., 1966; Price and Mountjoy, 1970; Eisbacher et al., 1974; Walker, 1982). Large scale cyclicity within the Saunders Group is believed to be related to major orogenic pulses in the Cordillera (McLean and Jerzykiewicz, 1978). Some of these pulses and periods of tectonic quiesence must have been synchronous over much of the Cordilleran belt, as the units of coarse clastics and coal-bearing intervals reflecting them are laterally persistent.

The Entrance conglomerate and Coalspur coal zone are the most persistent lithostratigraphic units within the Saunders Group. Some other, less lithologically distinct units of coarse clastics, however, are laterally continuous enough to be used for mapping purposes (Lang, 1947; Douglas, 1958; Ollerenshaw, 1968).

The present paper is an attempt to establish a new stratigraphic subdivision of the Saunders Group based on cyclicity. The subdivision of the lower part of the Saunders Group is based on observations along the Blackstone River 30 km northwest of Nordegg. Subdivision of the uppermost part of the Saunders Group, containing the Coalspur coal zone and the High Divide Ridge conglomerate, is based on data collected in the Hinton-Coalspur-Coal Valley area (Fig. 30.1).

Acknowledgments

Blackstone River section

Figure 30.2 is a three-dimensional geological map of the northeast limb of the Sunbeam Syncline located about 30 km northwest of Nordegg (Fig. 30.1). Here, between the

Figure 30.1

Location map.

Figure 30.2. *Standard section of the Saunders Group along the Blackstone River.*

Ancona and Brazeau thrusts, the Saunders Group is exposed in closely spaced outcrop sections along the Blackstone River and Chungo Creek banks (Fig. 30.2, localities 1-19; Plate 30.1, fig. 1). This almost continuous section, about 1300 m thick, was measured in detail from the Wapiabi Formation at the base (Fig. 30.2, locality 1) to the Brazeau Thrust at the top (Fig. 30.2, locality 19). It contains all stratigraphically important units, including the lower contact of the Saunders Group, a prominent tuff horizon (locality 7), the Entrance conglomerate (locality 14) and the lower part of the Coalspur coal zone correlatives (localities 15-19). A minor part of the section above the Entrance conglomerate is covered, and the interval embracing the Cretaceous-Tertiary boundary is covered by a bridge over the Blackstone River.

The entire Saunders succession can be characterized in terms of sandstone beds cyclically interbedded with various mudrocks. The scale of cyclicity can be expressed by the thickness of sandstone units compared with the thickness of the interbedded mudrocks. Three orders of cyclicity can be observed in the Saunders sequence (Fig. 30.3). Small scale cyclicity or cyclicity of the third order (C in Fig. 30.3) is expressed by the alternation of low- and high-energy sediments within both overbank and channel deposits. The overbank deposits are composed of mudrock interbedded with very fine grained sandstone to siltstone of leveé origin and sandstone layers of crevasse splay or sheet flood origin. Many channel deposits are composed of vertically stacked fining-upward cycles, reflecting changes in current energy.

Medium scale cyclicity (B in Fig. 30.3) is expressed by an alternation of intervals built up mainly of channel sandstone layers or overbank deposits. The thickness of the intervals is in the order of tens of metres. Large scale cyclicity, or cyclicity of the first order (A in Fig. 30.3), is shown by the entire Saunders sequence.

Rocks of the Saunders Group can be said to represent six large cycles or cyclothems (Fig. 30.4). Each cyclothem is composed of two parts: a lower one, containing thick and numerous channel sandstone layers; and an upper one composed predominantly of overbank mudrocks, coaly mudstone, and/or coal.

The detailed characteristics of the six cyclothems represented by the Saunders Group are presented below. The uppermost portion of the Saunders sequence, containing the upper part of Cyclothem Vb and Cyclothem VIa, is absent in the Blackstone River section because of the Brazeau Thrust. This part of the Saunders Group was measured in the Coalspur – Hinton area (Fig. 30.1).

First Cyclothem

Part a   The lower contact of the Saunders Group is drawn below the first, very thick (up to 10 m), vertically stacked channel sandstone sequence containing chert-granule and/or chert-pebble conglomerate (locality 2; Plate 30.1, fig. 2, 5). The sequence is composed of: several thick, multistoried channel sandstone units; thinner and fine grained splay sandstone units; and overbank deposits containing mudstone, siltstone and very fine grained sandstone. Channel and splay sandstone units make up 27.5 per cent[1] of the total.

The channel facies are up to 12 m thick and, as a rule, are composed of several stacked channel units. The lower contact of most channels is erosional and very abrupt (Plate 30.1, fig. 2). The channel lag deposit contains plant debris, intraformational mud chips, chert and quartzite granules and/or pebbles (Plate 30.1, fig. 6). Both tabular-planar and trough crossbedding are present, but very commonly the lower part of the channel unit is massive and/or shows low angle, inclined or parallel bedding. Ripple-drift crossbedding is predominant in the upper part of the channel units as well as in the upper part of the splay facies.

The overbank deposits that separate the channels are usually about three times thicker than the channel facies. They contain nonlaminated, greenish grey to dark grey mudstone, silty to sandy mudstone, laminated siltstone, and very fine grained sandstone that commonly contains upright rootlets. Coal is absent; coaly shale and coaly mudstone are very rare. Thin bentonite beds up to 0.2 m thick begin to appear in the uppermost portion of Part a. The first bentonite bed occurs 234 m above the base of the Saunders Group at this locality.

---

[1] Percentage values mentioned in the text refer to the thickness of sandstone and/or mudrock unit in a given part of the measured section

PLATE 30.1

Figures 1. Blackstone River. Downstream overview from locality 6. Arrow indicates locality 3.
2. Thick channel sandstone layers in the lower part of the First Cyclothem. White arrow indicates lower contact of the Saunders Group at mouth of Brown Creek. Locality 2.
3. Overbank deposits with minor channel sandstone units of the First Cyclothem. Blackstone River bank between localities 6 and 7.
4. Silicified tuffs. Locality 6.
5. Chert-granule conglomerate. Locality 3.
6. Channel lag deposit containing plant debris and mud chip conglomerate. Locality 2.

Figure 30.3

Three orders of cyclicity in the Saunders Group.

Part b   This part of the cyclothem is composed of 84.5 per cent overbank deposits, mainly various kinds of mudstone (localities 6 and 7; Plate 30.l, fig. 4).   Greenish grey and dark grey to almost black, structureless, silty mudstones are most common. Coaly mudstone and shale with some tiny laminae and lenses of coal occur at the top. Laminated siltstone to very fine grained sandstone layers of levée type underlain by fine- to medium-grained sandstone units of splay origin are common, forming numerous cycles. Bentonite and other rocks of volcanic origin (Plate 30.l, fig. 4) are common throughout Part b. The interval between 531 m and 542 m above the base of the section is predominantly composed of silicified tuffs, exhibiting a distinct lamination of alternating dark- and light-coloured lamina sets.   They are correlative with the silicified tuffs described by Jerzykiewicz and McLean (l977) in the Coal Valley Mine. Except for one unit, thick channel sandstones are absent. A pinching out, multistoried channel layer occurs almost immediately above the tuff interval.   Other channel sandstone units are rare and rather thin (less than 2.5 m).

Second Cyclothem

Part a   The Second Cyclothem starts with a prominent, approximately 10 m thick, laterally persistent, multistoried, channel sandstone layer.   The total quantity of channel sandstone layers increases to 33.7 per cent (Fig. 4).   The channel units are numerous but thinner (averaging 2 m) than those in the First Cyclothem.   They contain slightly finer material. Intraformational debris within channel lag units is usually present, but the chert-granule or chert-pebble conglomerate that is characteristic of the channels in the First Cyclothem is absent. Overbank deposits are composed of dark mudstone and well developed, numerous levée siltstone to very fine grained sandstone sequences. They are very commonly underlain by splay sandstone units. Bentonite beds are thin and very rare.

Part b   The upper part of the Second Cyclothem is composed of 88.3 per cent overbank deposits, with coaly shale, and one 0.25 m thick layer of coal.

Figure 30.4. *Simplified stratigraphic column of the Saunders Group in the central Alberta Foothills between Athabasca and Blackstone rivers.*

251

Figure 30.5

Nomenclature and correlation of coal seams within the Coalspur coal zone between Athabasca and Blackstone rivers. Compilation after Manalta Coal Ltd., Mercoal and McLeod Projects, unpublished reports, 1981, and Dentherm Resources Ltd., Coalspur Project, unpublished report, 1982; McAndrew, 1931, and the author's observations.

Third Cyclothem

Part a   Part a of the Third Cyclothem displays a significant increase in the amount of channel sandstone units (up to 61.8 per cent). Vertically stacked channel units predominate, with some more than 10 m thick (Plate 30.2, fig. 1). The lower part of most channel sandstones shows parallel bedding and parting lineation indicating upper flow regime conditions (Plate 30.2, fig. 2). Above, both trough and tabular-planar large scale crossbedding occur. In addition, large tree trunks occur within channel lag deposits.

Part b   Thin layers of coaly mudstone, coaly shale and coal (up to 0.3 m) occur in the lower and upper portion of this part of the cyclothem. The total amount of the overbank deposit is 73.8 per cent. Splay sandstone beds are rare and thin.

Fourth Cyclothem

Part a   Part a of the Fourth Cyclothem displays a further increase in both the total amount of sandstone (71.3 per cent) and the thickness of vertically stacked channel units (15 m), (Plate 30.2, fig. 3). In addition, evidence of very strong episodic floods is displayed. Overbank deposits are reduced to 28.7 per cent. Bentonites are absent.

Part b   The upper part of the cyclothem is composed of 56.0 per cent overbank deposits. Thin coaly mudstone, coaly shale, and bentonite beds are common throughout. Coal beds up to 0.25 m, and up to 0.5 m thick, occur in the middle and upper portion, respectively, of this part.

Fifth Cyclothem

Part a   The base of this cyclothem is drawn at the base of the 12 m thick Entrance conglomerate. This laterally persistent unit, best developed in the Athabasca River area,

also has equivalent beds containing pebble conglomerate at the base in the Blackstone River area (Plate 30.3, fig. 3, 4). All of Part a is composed of several, thick, channel sandstone layers, splay sandstone units and overbank deposits. The total amount of channel and splay sandstone units is 55.6 per cent.

Part b   This part of the cyclothem is referred to as the Coalspur or Coal Valley coal zone. The coal zone is laterally persistent and can be traced between the Athabasca and Blackstone rivers (Fig. 30.1, 30.5; Plate 30.3, fig. 2). It contains the following mineable coal seams: Mynheer, Upper Silkstone, McPherson, Arbour and Val d'Or (Fig. 30.6). Overbank deposits comprise 66.5 per cent of the upper part of the cyclothem. They consist of mudstone, shale and siltstone. Bentonites are common and sometimes thick. Splay sandstone units predominate over channel units. A laterally persistent, multistoried channel sandstone, over 10 m thick, occurs 50 m above the Mynheer coal (localities 17, 18). The Mynheer coal seam is considered to be the base of the Coalspur coal zone. The Cretaceous-Tertiary boundary occurs at the base of the Mynheer coal.

Sixth Cyclothem

Part a   The lower contact of this cyclothem is placed below the first, very thick, vertically stacked channel sandstone sequence occurring above the Coalspur coal zone. This lowermost part of the Paskapoo Formation (Fig. 30.7) is almost entirely composed of channel sandstone. Large-scale trough crossbedding is predominant. The High Divide Ridge conglomerate (Fig. 30.7) forms a local, very coarse grained facies of the lower Paskapoo Formation in the Athabasca River area. These cobble-size, quartzite conglomerates, which built up the prominent High Divide Ridge, are the youngest Paskapoo deposits preserved in the Central Foothills. The thickness of the High Divide Ridge conglomerate can be estimated at greater than 300 m (Jerzykiewicz, 1985).

PLATE 30.2

Figures 1. Contact between the Second and Third cyclothems. Note vertically stacked channel units at the base of the Third Cyclothem. Locality 9.
2. Parting lineation. Arrows are parallel to current. Locality 9.
3. Contact between the Third and Fourth cyclothems. Note large number of sandstone layers in lower part of the Fourth Cyclothem. Locality 11.

PLATE 30.3

Figures 1. Mudrock and coal bed of the Fifth Cyclothem (Coalspur coal zone). Chungo Creek bank at locality 16.
2. Uppermost part of the Saunders Group exposed in the Blackstone River section. Coalspur coal zone cut by Brazeau Thrust.
3. Entrance conglomerate sample taken from the place indicated by arrow.
4. Conglomeratic sandstone layer with pebble conglomerate (Entrance conglomerate) at base. Locality 14.

A. Dentherm Resources Ltd., drillhole CRD 8137.
B. Road cut section in Coalspur.

C. Abandoned open pit on hill about 800 m southeast of Highway 47 in Coalspur.

Figure 30.6.   Coal seams of the Coalspur coal zone in the vicinity of Coalspur.

Figure 30.7. *Lithostratigraphic correlation chart.*

AGE	CENTRAL FOOTHILLS			SOUTHERN FOOTHILLS	CENTRAL PLAINS	NORTHWEST-CENTRAL PLAINS
	Allan and Rutherford, 1923	Douglas, 1958	This Report — CYCLOTHEMS / FORMATIONS	Carrigy, 1971	Gibson, 1977 / McLean, 1971	Kramers and Mellon, 1972
TERTIARY	UPPER SAUNDERS (SAUNDERS GROUP)	PASKAPOO FM — UPPER	High Divide Ridge congl. — PASKAPOO FM — VI a	PORCUPINE HILLS FM	PASKAPOO	"PASKAPOO" FM
	COAL-BEARING SAUNDERS	PASKAPOO FM — LOWER	VAL D'OR — COALSPUR — MYNHEER — COALSPUR b, V	WILLOW CREEK FM	ARDLEY — SCOLLARD — NEVIS FM (EDMONTON GROUP)	ARDLEY "ZONE" (WAPITI GROUP)
		Sandstone and conglomerate	FM Entrance congl. — a			UPPER
CRETACEOUS	LOWER SAUNDERS (SAUNDERS GROUP)	BRAZEAU FM — UPPER	BRAZEAU FM — IV b/a, III b/a, II b/a	KNEEHILLS TUFF / ST. MARY RIVER FM	KNEEHILLS TUFF / BATTLE FM / WHITEMUD FM / HORSESHOE CANYON FM	KNEEHILLS TUFF / MIDDLE
		BRAZEAU FM — MIDDLE				
		BRAZEAU FM — LOWER	b — I — a	BEARPAW FM / BELLY RIVER FM	BEARPAW FM / JUDITH RIVER FM	LOWER
	WAPIABI FORMATION				LEA PARK FM	SMOKY GROUP

Hinton – Coalspur – Coal Valley area

Stratigraphic correlation between the Blackstone River section and the Coalspur coal zone in the Hinton – Coalspur – Coal Valley area (Fig. 30.1) is possible due to the large lateral extent of the Entrance conglomerate and of some of the coal seams. In both areas, the Entrance conglomerate occurs about 150 m below the first Tertiary coal bed (Mynheer coal seam in the Hinton – Coalspur – Valley area, and Seam 1 in the Blackstone River section) (Fig. 30.5). Correctness of the stratigraphic correlation between these two areas has been confirmed by palynology (A.R. Sweet, personal communication, 1984). Hence, the Coalspur coal zone can be considered as part of the Fifth Cyclothem of the Saunders Group. The upper part of this cyclothem, containing economically important coal seams, is being exploited in the Coal Valley Mine. The Coalspur coal zone, known also as the Coal Valley coal zone (Energy Resources Conservation Board, Reserves of Coal, unpublished report, 1983), has lately been the object of extensive drilling programs in numerous localities in the area between Hinton and Coal Valley (Manalta Coal Ltd., Mercoal and McLeod Projects, unpublished reports, 1981, and Dentherm Resources Ltd., Coalspur Project, unpublished report, 1982). Figure 30.5 is a compilation based on these exploration drilling programs and on the description of drillholes and test pit sections by McAndrew (1931). Despite some local variations and changes in coal seam nomenclature, the uppermost Val d'Or and the lowermost Mynheer coal seams are recognizable in the whole area between Hinton and Coal Valley over a distance of about 70 km (Fig. 30.1, 30.5). The coal zone is also known to appear in some isolated outcrops farther to the northwest and southeast, far beyond the Blackstone River and Chungo Creek sections (Erdman, 1950; Douglas, 1958).

The lateral extension of the Coalspur coal zone beyond the area discussed requires further research. However, data available from the Hinton – Coalspur – Valley area indicate that these beds are mappable, and may be treated as a formation within the Saunders Group. The Coalspur Formation, previously named the Coalspur beds after MacKay (1949) (Jerzykiewicz and McLean, 1980) is herein proposed as the name for the 450 m thick unit that includes the Entrance conglomerate, alternating units of sandstone, mudrock and bentonite below the coal zone, and the Coalspur coal zone itself. The lower boundary of the formation is drawn below the Entrance conglomerate bed and the upper one is set at the base of the lowest prominent sandstone layer above the highest thick coal seam, that is, Val d'Or seam of the Coalspur coal zone. The age of the Coalspur Formation is of latest Maastrichtian to earliest Paleocene. The Cretaceous-Tertiary boundary has been defined at the base of the Coalspur coal zone, that is, at the base of the lowest Mynheer coal (Jerzykiewicz et al., 1984). As defined, therefore, the Coalspur Formation corresponds to the Fifth Cyclothem within the Saunders Group, and is underlain by the Brazeau Formation (cyclothems I to IV), and overlain by the Paskapoo Formation (Cyclothem VI, Fig. 30.7).

The Coalspur Formation (or the Fifth Cyclothem) is correlative with the Scollard Formation as defined by Gibson (1977) in the central Plains. The upper part of the Coalspur coal zone, containing the economically most important Val d'Or, Arbour and McPherson coal seams, has been described from several old pits and road cuts in the vicinity of Robb and Coalspur (Jerzykiewicz and McLean, 1980; Jerzykiewicz and Langenberg, 1983). The Arbour – Val d'Or coal seams and contiguous strata exposed along Highway No. 47 at Coalspur, and the McPherson seam in an abandoned open pit on the hill about 800 m to the southeast of the highway, can be correlated with subsurface data in the area (Fig. 30.6).

The lower part of the Coalspur coal zone containing the Mynheer coal seam has lately been the subject of a detailed palynological study in the search for the Cretaceous-Tertiary boundary. Two cored boreholes were drilled by Luscar Sterco (1977) Ltd. for the Geological Survey of Canada over Pit #42-2 in the Coal Valley mine site (Fig. 30.1), in order to obtain a continuous core of the lower portion of the Mynheer coal seam. This portion of the Mynheer seam is not mined because of the presence of bentonite partings.

Using palynological evidence, the Cretaceous-Tertiary boundary was found to be at the base of the Mynheer coal seam. Analysis of this level for iridium, performed by J.F. Lerbekmo (U. of Alberta), showed an anomaly across 6 cm of the coal, reaching a maximum of approximately 6 ppb in the lowest 2 cm (Jerzykiewicz et al., 1984).

Concluding remarks

The lithology of the Saunders sequence is rather monotonous. Sedimentary facies are repeated many times throughout the sequence so that the recognition of stratigraphic units in isolated outcrops is very difficult. Hence, application of the general term "Saunders Group", for the total sequence of nonmarine clastics from the Wapiabi contact at the base to the High Divide conglomerate at the top, is justified. It should be subdivided into a lower part, i.e. the Brazeau Formation, beginning at the Wapiabi contact at the base, to the base of the Entrance conglomerate, and an upper part containing two formations, namely, the Coalspur and the Paskapoo formations (Fig. 30.7).

The Coalspur Formation has well defined boundaries. The lower one is drawn at the base of the Entrance conglomerate, and the upper one is set at the base of the lowest prominent sandstone layer above the highest thick coal seam (Val d'Or) of the Coalspur coal zone. The Coalspur Formation, previously named the "Coalspur beds" after MacKay (1949) (Jerzykiewicz and McLean, 1980) is recognized as being about 450 m thick from the vicinity of Hinton southeast to Nordegg area.

The range of lateral extension of the Coalspur Formation along the Foothills belt beyond the Athabasca River to the northwest and the North Saskatchewan River to the southeast requires more study.

The stratigraphic subdivision of the Saunders Group into the cyclothems introduced in this paper should help in the understanding of the depositional history of the entire sequence. It shows the overall coarsening-upward trend manifested by an increasing proportion of channel sandstone units within the lower "a" parts of each cyclothem (Fig. 30.3, 30.4). The conglomerates also show a coarsening-upward trend. They are rare and of granule size in cyclothems I to IV, of pebble size at the base of the Fifth Cyclothem (the Entrance conglomerate), and of cobble size at the top of the Saunders sequence, forming a prominent, at least 300 m thick interval, of High Divide Ridge conglomerate.

The Saunders Group is a coarsening-upward sequence deposited during the final infilling of the foreland basin, controlled by uplift of the Rocky Mountains. The rate of subsidence, corresponding to tectonic pulses within the Rocky Mountains, was not constant, because there are well developed upper "b" parts of the cyclothems with coaly mudstone and coal-bearing intervals.

According to the stratigraphic classification used in this report, the Fifth Cyclothem corresponds to the Coalspur Formation, which represents one depositional cycle within the Saunders Group. It is mappable over the entire study area. The rest of the cyclothems are mappable in the Blackstone River area, but their further mapping as well as age determination both require more work.

Palynological work by P.R. Gunther (1970) and P.R. Gunther and L.V. Hills (1972) confirmed the mid-Campanian to Early Paleocene age of the Blackstone River section and allowed for some correlations with the Plains area. The samples collected for palynological investigation along the Blackstone River section are now the subject of a detailed study by A.R. Sweet (personal communication, 1985). Some of the results, such as the position of the Cretaceous-Tertiary boundary; the age of the Coalspur Formation; the correlation of the pebbly sandstone unit at base of the Fifth Cyclothem with the Entrance conglomerate; and the position of the Campanian-Maastrichtian boundary above the tuff horizon, have been used in this report. However, further palynological investigations are needed in order to establish the age of the cyclothems recognized within the Saunders Group along the Blackstone River.

References

Allan, J.A. and Rutherford, R.L.
1923:   Saunders Creek and Nordegg coal basins, Alberta, Canada; Scientific and Industrial Research Council of Alberta, Geology Division Report 6.

Bally, A.W., Gordy, P.L. and Stewart, G.A.
1966:   Structure, seismic data and orogenic evolution of southern Canadian Rocky Mountains; Bulletin of Canadian Petroleum Geology, v. 14, p. 337-381.

Carrigy, M.A.
1971:   Lithostratigraphy of the uppermost Cretaceous (Lance) and Paleocene strata of the Alberta Plains; Research Council of Alberta, Bulletin 27, 161 p.

Douglas, R.J.W.
1958:   Chungo Creek map-area, Alberta (83 C/9); Geological Survey of Canada, Paper 58-3.

Eisbacher, G.H., Carrigy, M.A., and Campbell, R.B.
1974:   Paleodrainage pattern and late orogenic basins of the Canadian Cordillera; in Tectonics and Sedimentation, ed. W.R. Dickinson; Society of Economic Paleontologists and Mineralogists, Special Publication 22: 146-166.

Erdman, O.A.
1950:   Alexo and Saunders map areas, Alberta; Geological Survey of Canada, Memoir 254, 100 p.

Gibson, D.W.
1977:   Upper Cretaceous and Tertiary coal-bearing strata in the Drumheller-Ardley region, Red Deer River Valley, Alberta; Geological Survey of Canada, Paper 76-35.

Gunther, P.R.
1970:   Megaspore Palynology of the Brazeau Formation (Upper Cretaceous), Nordegg Area, Alberta; M.Sc. Thesis, The University of Calgary, 128 p.

Gunther, P.R. and Hills, L.V.
1972:   Megaspores and other palynomorphs of the Brazeau Formation (Upper Cretaceous), Nordegg area, Alberta; Geoscience and Man, v. 4, p. 29-48.

Jerzykiewicz, T.
1985:   Tectonically deformed pebbles in the Brazeau and Paskapoo formations, central Alberta Foothills, Canada; Sedimentary Geology, v. 42, p. 159-180.

Jerzykiewicz, T. and Langenberg, W.
1983:   Structure, stratigraphy and sedimentary facies of the Paleocene and Lower Cretaceous coal-bearing strata in the Coalspur and Grande Cache areas, Alberta; The Canadian Society of Petroleum Geologists Conference, The Mesozoic of Middle North America, Field Trip Guidebook No. 9, 63 p.

Jerzykiewicz, T. and McLean, J.R.
1977: Bedded volcanic chert near Coalspur, central Foothills, Alberta; in Report of Activities, Part B, Geological Survey of Canada, Paper 77-1B, p. 149-155.

1980: Lithostratigraphical and sedimentological framework of coal-bearing Upper Cretaceous and Lower Tertiary strata, Coal Valley area, central Alberta Foothills; Geological Survey of Canada, Paper 79-12, 47 p.

Jerzykiewicz, T., Lerbekmo, J.F. and Sweet, A.R.
1984: The Cretaceous-Tertiary boundary, central Alberta Foothills; 1984 Canadian Paleontology and Biostratigraphy Seminar, Programme with Abstracts, p. 4.

Kramers, J.W. and Mellon, G.B.
1972: Upper Cretaceous-Paleocene coal-bearing strata, northwest-central Alberta Plains; in Proceedings of the First Geological Conference on Western Canadian Coal, ed. G.B. Mellon, J.W. Kramers and E.J. Seagel; Research Council of Alberta, Information Series 60, p. 109-124.

Lang, A.H.
1947: Brûlé and Entrance map-areas, Alberta; Geological Survey of Canada, Memoir 244.

MacKay, B.R.
1949: Coal areas of Alberta; Geological Survey of Canada Atlas, to accompany estimate of coal reserves prepared for the Royal Commission on Coal, 1949.

McAndrew, R.T.
1931: Coal Mining at Drinnan, Alberta; The Canadian Mining and Metallurgical Bulletin No. 236, p. 1375-1395.

McLean, J.R.
1971: Stratigraphy of the Upper Cretaceous Judith River Formation in the Canadian Great Plains; Saskatchewan Research Council, Geology Division Report 11, 96 p.

McLean, J.R. and Jerzykiewicz, T.
1978: Cyclicity, tectonics and coal: some aspects of fluvial sedimentology in the Brazeau-Paskapoo formations, Coal Valley area, Alberta, Canada; in Fluvial Sedimentology, ed. A.D. Miall; Canadian Society of Petroleum Geology, Memoir 5, p. 441-468.

Ollerenshaw, N.C.
1968: Preliminary account of the geology of Limestone Mountain map-area, southern Foothills, Alberta; Geological Survey of Canada, Paper 68-24.

Price, R.A. and Mountjoy, E.W.
1970: Geologic structure of the Canadian Rocky Mountains between Bow and Athabasca Rivers – a progress report; in Structure of the south Canadian Cordillera, ed. J.O. Wheeler; Geological Association of Canada, Special Paper 6, p. 7-25.

Walker, R.G.
1982: Clastic units of the Front Ranges, Foothills and Plains in the area between Field, B.C. and Drumheller, Alberta; International Association of Sedimentologists 1982 Congress, Guidebook to Field Excursion 21A, 160 p.

Fossil fungal fructifications from Bonnet Plume Formation, Yukon Territory

R.M. Kalgutkar
Institute of Sedimentary and Petroleum Geology, Calgary

Abstract

Three samples from the Bonnet Plume Formation of the Yukon Territory have yielded fungal fruiting bodies assignable to **Callimothallus pertusus** Dilcher 1965, a new species of **Paramicrothallites**, **Plochmopeltinites masonii** Cookson 1947, and cleistocarps, possibly of **Meliola** type. **Callimothallus pertusus** is the most common, and it may be inferred that the assemblage reflects humid, subtropical conditions at the time of deposition. The age of the deposit is within the range of Late Paleocene to Middle Eocene.

Résumé

L'analyse de trois échantillons prélevés dans la formation de Bonnet Plume au Yukon a permis d'identifier des carpophores de champignons assimilables aux **Callimothallus pertusus** Dilcher 1965, nouvelle espèce de **Paramicrothallites**, aux **Plochmopeltinites masonii** Cookson 1947, et aux cléistocarpes, possiblement de type Meliola. Les **Callimothallus pertusus** étant les plus répandus, on peut conclure que cet assemblage s'est déposé dans des conditions humides et subtropicales. Le dépôt date de le période située entre le Paléocène supérieur et l'Éocène moyen. L'étude stratigraphique détaillée des spores dispersées de ces champignons est en cours.

Introduction

In the course of palynological analysis of the samples from Bonnet Plume Basin, Yukon Territory, dispersed fungal material, containing a variety of spores, fragments of mycelia and detached fruiting bodies, was observed. The fruiting structures resemble thyriothecia of the Microthyriaceae, and cleistocarps of the Meliolaceae.

The purpose of this study is to describe the morphology of the thyriothecia and the cleistocarps, compare their affinities with similar forms reported from other localities, and comment on possible paleoecological implications.

Recently, fossil fungi have attracted the attention of palynologists and paleobotanists as an important source of information that may have significant potential in assessing the geological record of the plants and their environment. The fossil fungal record, however fragmentary, may contribute substantially to our understanding and unravelling of fungal phylogeny. Pirozynski and Weresub (1979) have presented a comprehensive analysis of the classification and nomenclature of fossil fungi, and, while discussing the history of the Ascomycetes and the development of their pleomorphism, they remarked that, "only in the fossil record can we find less equivocal evidence of ancestral linking groups most of which, because of their rapid evolution, have failed to survive to the present".

A large amount of literature on fossil fungi is based on the documentation of dispersed spores, detached mycelial hyphae, and scattered fruiting bodies recovered principally from Cenozoic sediments [Cookson, 1947a,b; Graham, 1962; Wilson, 1962; Varma and Rawat, 1963; Clarke, 1965; Wolf, 1966a,b, 1967a,b,c,d; Srivastava, 1968; Kar et al., 1970; Sheffy and Dilcher, 1971; Elsik, 1974, 1975, 1976; Elsik and Jansonius, 1974; Jansonius, 1976; Petros'yants, 1976; Kemp, 1978; Kexue Chubanshe (Science publishers), 1978; Smith, 1980; Sepulveda and Norris, 1982]. However, studies have also been made of fossil fruiting bodies found associated with their host tissue (Edwards, 1922; Cookson, 1947a,b; Chitaley, 1951, 1957; Godwin and Andrew, 1951; Rao, 1954, 1959; Tilgner, 1954; Dilcher, 1963, 1965; Ramanujam, 1963; Venkatachala and Kar, 1968; Jain and Gupta, 1970; Alvin and Muir, 1970; Kar et al., 1970; Vishnu-Mittre, 1973; Selkirk, 1975).

The importance of fungal remains to paleoecological studies has been stressed by many authors (Cookson, 1947a; Graham, 1962; Dilcher, 1963, 1965; Wolf, 1967a; Venkatachala and Kar, 1968; Kar et al., 1970; Selkirk, 1975; Elsik, 1976, 1980). Graham (1962) presented an extensive compilation of information on fossil fungal spores and inferred that environments of the past can be interpreted from the flora recorded in a given sediment because "organisms are limited in ecological amplitude and their distribution patterns change with environmental variations". He pointed out the importance of host specificity in determining the type of vegetation. Some fungi are confined to a specific host of a specific vegetation type. The significance of host specificity in parasitism of some fossil fungi has been suggested by Dilcher (1965). The extant Meliolales are invariably obligate parasites of vascular plants, and appear to be very restricted in their parasitism (Hansford, 1961). Dilcher (1965) found that **Meliola anfracta** and various microthyriaceous forms flourished in close association and suggested a form of fungal parasitism upon fungi, although he could not prove it conclusively. Wolf, who published a series of papers (1966a,b; 1967a,b,c,d) on the distribution and population count of fungal spores in African lake sediments, indicated that the pattern of spore distribution shows an overall trend toward a decline in numbers with an increase in profile depth and, as in the case of pollen in the deposits, the population of fungal spores differs at different profile depths, reflecting vegetational changes caused by changes in climate.

The occurrence of epiphyllous fungi has been correlated with moist and humid climates favourable to the lavish growth of forest vegetation and ground vegetation flourishing under the canopy of trees. Edwards (1922) cited the importance of rainfall rather than temperature in the distribution of epiphyllous microthriaceous fungi from the Tertiary rocks of Scotland. Cookson (1947a), in her study of fossil fungi from Tertiary deposits in Kergulen Archipelago and in New Zealand, indicated that the abundance of some fungi in warm-temperate and tropical zones is primarily due to high humidity rather than high temperatures. Hansford (1961) pointed out that at least a minimum level of humidity is required for the growth of modern Meliolales, which seem to be absent from the arid areas of the subtropics (Alexopoulos and Mims, 1983, p. 316). Dilcher (1965), while working on epiphyllous fungi were found on compression fossils of Eocene angiosperm leaves, deduced that the majority of them belonged to the Ascomycetes, and seem to have appeared in association with the evolution of angiosperm hosts since none of them has been reported from below the Upper Cretaceous. Their modern counterparts appear to thrive in humid, tropical and subtropical environments. This may suggest that the region in Tennessee where the fossils were found was characterized by a similar climate (Dilcher, 1963; Stewart, 1983, p. 39). Venkatachala and Kar (1968), in their study of the Tertiary sediments in Kutch, India, have commented that the abundance of epiphyllous Hemisphaeriales and Pseudosphaeriales probably suggests the dependence of these forms on broad leaved angiosperms, and that the evolution and diversification of the fungi is directly correlated with the evolution and luxuriance of angiosperms in the Tertiary. Kar et al., (1970) investigated assemblages of algal and fungal remains from the Tura Formation of Garo Hills, Assam, India, and concluded that the abundance of epiphyllous fungi may suggest the prevalence in the past of a moist and humid climate in the region.

Lange (1978), in his study of Tertiary epiphyllous fungal forms from Australian environments, assessed the habitat indicator value of the fossils from the geographic, climatic, and vegetational relationships of modern forms. The sites at which samples containing callimothalloid and cribitoid shields were found represented a habitat range from equatorial to about 28°S, with rainfalls ranging from 6000 to 1600 mm per annum, indicating humid tropical and subtropical environmental conditions.

However, Dilcher (1965) and Selkirk (1975) pointed out that ecological interpretations suggesting warm, moist conditions based on the presence of fossil microthyriaceous fungi should be treated with caution. They further indicated that although most fossil epiphyllous fungi have been found associated with warm or subtropical vegetation, isolated fruiting bodies do occur over a wide latitudinal range in Pleistocene deposits of North America (Rosendahl, 1943) and under a wide range of climatic conditions in Britain (Godwin and Andrew, 1951).

More recent studies of fossil fungi have been directed toward an attempt at correlating the results of fungal discoveries with stratigraphy. Varma and Rawat (1963) gave a good account of diporate fungal spores in the Tertiary horizons of India, and tried to demonstrate the value of these spores to stratigraphic studies. They were not sure of the identity of the material they were studying and found diporate grains with limited vertical range and wide horizontal distribution. However, they were the first to establish the significance of characteristic fungal spores in

stratigraphic interpretations. Based on a study of about 700 samples, they made a qualitative and quantitative assessment of those grains by calculating their frequency of appearance in various rock units, and plotting a stratigraphic distribution for their correlation. The distribution of spores from Middle Eocene to Miocene correlated well in the two regions about 1440 km apart, but an inter-regional study was not done. Jansonius (1976) found several similar species with similar ranges in the Arctic Lower Tertiary. Clarke (1965) recorded nine species of dispersed fungal spores from the Upper Cretaceous of Vermejo Formation in central Colorado, and pointed out that fungal spores have the potential of being useful in stratigraphic interpretations, because they exhibit observable morphological differences and are dispersed in a similar way as other spores and pollen. Elsik and Jansonius (1974) described **Ctenosporites, Granatisporites** and **Pesavis** from the Cenozoic of the Pacific Northwest and Arctic region, and suggested that these forms may eventually be used to date sediments in which normal palynological fossils are rare. Elsik (1976) pointed out that the data outlining detailed distribution and ranges of characteristic

fungal spores such as **Striatetracellaeites, Fusiformisporites, Striadiporites, Striasporonites,** and the verrucate **Verrusporonites,** will probably allow interpretation of phylogenetic relationships. Jansonius (1976) presented a short but impressive paper including qualitative and quantitative information on the fungal spores in the Paleocene-Eocene deltaic sediments of the Mackenzie Delta region of the Canadian Arctic, which elucidated the importance of fungal fossils in stratigraphic correlation. He emphasized that several characteristic species and genera of fungal spores with short ranges are important indicators of age in stratigraphic studies. He also mentioned the common occurrence of microthyriaceous fruiting bodies in the Paleogene strata of northern Canada, with special reference to **Callimothallus pertusus** and its easily recognizable ascomata.

Although the paleoecological and stratigraphic importance of fossil fungal discoveries have yet to be fully established, continued investigations may further our understanding of the occurrences and ranges of different

Figure 31.1. *Location and lithologic sequence of Section 77-LBA-W4 in the Bonnet Plume Formation, Yukon Territory (NTS 106E). Sample horizons with fungi are indicated by numbers.*

fungal spores and fruiting bodies. The results can be applied to the study of the stratigraphy of an area, and the evolution of plants, and can be used to interpret floristic changes in concurrence with palynological findings.

Materials and methods

Abundant fungal remains, consisting of a variety of spores, fragments of vegetative hyphae, portions of mycelia and a few fructifications, were found to occur in three (samples from GSC locs. C-68304, C-68305 and C-68329) out of 18 samples from Section 77-LBA-W4 of the uppermost part of the Bonnet Plume Formation, located on Peel River, 65°54'N, 135°04'W (Fig. 31.1). Fungal material in these samples is well preserved and proportionally better represented than the pollen and other spores. Sample C-68329 contains more fructifications than the other samples.

The age of the upper part of the Bonnet Plume Formation was defined as Paleocene by Rouse and Srivastava (1972). A more recent study of the uppermost beds of this formation established the presence of species additional to those reported by Rouse and Srivastava. **Pistillipollenites mcgregorii** Rouse 1962, and **Caryapollenites inelegans** Nichols and Ott 1978, are present in samples from GSC locs. C-68304, C-68305, and C-68329; **C. wodehousei** Nichols and Ott 1978, **Tilia vescipites** Wodehouse 1933, and cf. Acanthaceae A in Rouse (1977) are present in samples from GSC locs. C-68304 and C-68305; and **Momipites triradiatus** Nichols 1973, **Caryapollenites imparalis** Nichols and Ott 1978, **Momipites coryloides** Wodehouse 1933, emend. Nichols 1973 and **Pterocarya stellatus** (R. Potonié) Martin and Rouse 1966 are present in a sample from GSC loc. C-68329.

The presence of **Pistillipollenites mcgregorii** Rouse 1962 and **Caryapollenites inelegans** Nichols and Ott 1978 in samples from GSC locs. C-68304, C-68305 and C-68329 restricts their age to within the range of Late Paleocene to Middle Eocene. The presence of the above species and the additional occurrence of **Caryapollenites inelegans** Nichols and Ott 1978, **C. wodehousei** Nichols and Ott 1978, and **Tilia vescipites** Wodehouse 1933 in samples from C-68304 and C-68305 is suggestive of a Late Paleocene or very earliest Eocene age (A.R. Sweet, personal communication).

The standard palynomorph preparation techniques were followed to recover microfossils from the samples, except that the samples containing the fungal matter were treated with care during oxidation with Schulze's solution. The procedure included treatment with hydrochloric and hydrofluoric acids, oxidation with Schulze's solution, base treatment with ammonium hydroxide and separation of organic contents with zinc bromide. Residues were mounted on slides using polyvinyl alcohol and bioplastic media. Slides of unsieved, +45 µm, -45 µm, +20 µm and -20 µm fractions were prepared. The coordinates for the figured specimens were taken using Leitz Ortholux transmitted light microscope No. 717633. Slides bearing the figured specimens are permanently stored in the type collection, Geological Survey of Canada, Ottawa. Sample residues and relevant slides are kept with the Geological Survey of Canada at the Institute of Sedimentary and Petroleum Geology in Calgary.

Description and discussion of form-taxa

Although dispersed fungal fructifications are not generally found with associated mycelia and spores, they can be referred to extant taxonomic groups with greater accuracy than can dispersed spores, due to their more complex morphology. Indeed, quite a few families belonging to the Ascomycetes, such as Meliolaceae, Microthyriaceae,

and Micropeltaceae are recognizable by the characteristics of non-sporic, easily fossilizable organs (Pirozynski and Weresub, 1979).

The following fossil forms described in this study are classified according to the system of classification adopted by Cookson (1947), Dilcher (1965), Selkirk (1975) and Alexopoulos and Mims (1983, p. 393).

<div align="center">

Class: Ascomycetes
Subclass: Loculoascomycetidae
Order: Microthyriales
Family: Microthyriaceae
Genus: **Callimothallus** Dilcher 1965
Callimothalus pertusus Dilcher 1965
Plate 31.1, figures 1-4

</div>

Description: Ascomata flattened, subcircular to round, radiate, non-ostiolate, porate, with entire and partially crenate margin (figs. 1, 2). Ascomata pseudoparenchymatous, 50-70 µm in diameter, consisting of radially arranged rows of cells. Central cells squarish, mostly isodiametric, dark and thick walled, about 5-6 µm in diameter, (fig. 3). Radiating cells extend outward from central cells. Marginal cells more or less rectangular and elongated, about 3-6 µm wide x 7-9 µm long. Individual cells forming the ascomata are generally porate. Pores 1-2 µm in diameter, usually emerging at extreme proximal end of the cells (fig. 4).

Comments: All dispersed ascomata encountered in this investigation were well preserved and distinctly porate. Elsik (1980) pointed out that the porate condition in **Callimothallus** is required for at least a number of the cells, to separate it from **Phragmothyrites**. If the porate nature is well represented, even fragments of the thyriothecium are identifiable as **Callimothallus**. Jain and Gupta (1970) described **Callimothallus quilonensis** from the Miocene in the Western Ghats of South India which, although morphologically similar to **C. pertusus**, is differentiated from it in having pores only in the peripheral cells and a complete lack of them in the central cells. Kar et al., (1970) described **Callimothallus assamicus** from Tertiary sediments of Assam, India, and distinguished it from **C. pertusus** and **C. quilonensis** by the presence of pores in almost all its cells except for a few in the periphery. Elsik (personal communication) pointed out that **C. assamicus** has pores restricted to a small area of

---

PLATE 31.1

Figures 1. **Callimothallus pertusus**, C-68329, P 2096-55i, 40.9 x 115.0, GSC 75869, x 500.
2. **C. pertusus**, showing a cluster of three thyriothecia, C-68329, P 2096-55i, 46.2 x 107.0, GSC 75870, x 500.
3. **C. pertusus**, central group of thick-walled cells, C-68329, P 2096-55i, 43.9 x 107.4, GSC 75871, x 1000.
4. **C. pertusus**, pores emerging at proximal end of the cells, C-68329, P 2096-55i, 40.9 x 115.0, GSC 75872, x 1000.
5. **Paramicrothallites canadensis** sp. nov. showing central tissue of thin-walled cells, C-68329, P 2096-55d, 43.0 x 118.7, GSC 75873, x 500.
6. **P. canadensis** sp. nov. showing ostiole, C-68329, P 2096-55g, 10.3 x 99.2, GSC 75874, x 500. Holotype.
7. **P. canadensis** sp. nov. showing disintegrating cells of the ostiole, C-68305, P 2096-63b, 41.3 x 115.0, GSC 75875, x 500.
8. **Plochmopeltinites masonii**, showing plectenchyma and ostiole, C-68329, P 2096-55g, 41.0 x 105.7, GSC 75876, x 1000.

In the explanation of figures the species name is followed by GSC locality number, the slide number, stage co-ordinates, the GSC type number and the magnification. Stage co-ordinates were obtained using Leitz Ortholux transmitted light microscope No. 717633.

PLATE 1

central cells and the marginal cells are elongated. Kemp (1978) recorded **Callimothallus** cf. **C. assamicus** from the early Tertiary sediments at Deep Sea Drilling Site 254, on the Ninetyeast Ridge, Indian Ocean.

The holotype of **Pseudosphaerialites senii** described by Venkatachala and Kar (1968) from Eocene deposits in Kutch, India, resembles **Callimothallus pertusus** not only in its overall size, shape and pseudoparenchymatous nature, but more characteristically in being apparently porate (Kar et al., 1970; Elsik, 1980). Similarly, **Microthyriacites sahnii**, described by Rao (1959) from Tertiary deposits of India, bears a close resemblance to **Callimothallus pertusus** in its gross morphology, in the absence of an ostiole, and especially in having "most of the cells with a single clear area almost like an aperture", similar to the pores in **C. pertusus.**

Genus: **Paramicrothallites** Jain & Gupta 1970
Paramicrothallites canadensis sp. nov.
Plate 31.1, figures 5-7
Holotype: Plate 31.1, fig. 6

Diagnosis: Ascomata characterized by distinguishable, dark coloured, pseudoparenchymatous, irregularly rectangular rows of cells on the outside of the central region (fig. 6).

Description: Ascomata subcircular, radiate, ostiolate, with more or less entire margin. Ascomata consists of radiating rows of cells, pseudoparenchymatous, with a central group of squarish, thin-walled cells and slightly thick-walled, brownish, irregularly rectangular cells outside the central region (fig. 5, 6). Bordering the ostiole, the inner cells of the radiating rows seem somewhat loosely arranged. Except for the thickened walls, the ostiole is not surrounded by any specialized cells. Thyriothecia one-layered, flattened, 55 to 115 μm in diameter. Central tissue about 9 to 19 μm in diameter, and fully formed ostiole about 19 μm in diameter (fig. 6).

Comments: Paramicrothallites is segregated from other dispersed forms of ascomata by its simple type of ostiole, without any specialized bordering cells. The ostiole is probably formed lysigenously from the dissolution of the central group of thin-walled cells (fig. 7) which probably become indistinct and gradually disintegrate during the development of the thyriothecia.

Dilcher (1965) described **Microthallites lutosus** and **M. spinulatus** from Lower Eocene deposits in western Tennessee, U.S.A. Both had two-layered stroma, but **M. lutosus** was non-ostiolate whereas **M. spinulatus** was ostiolate. Jain and Gupta (1970) proposed the new genus **Paramicrothallites** to include fossil dispersed ostiolate forms of **Microthallites**, and **M. spinulatus** was thus made the type species of **Paramicrothallites.**

Paramicrothallites canadensis sp. nov. resembles **Paramicrothallites spinulatus** (Dilcher) Jain and Gupta (1970), and **Paramicrothallites menonii** Jain and Gupta (1970), in its shape, radiating cell pattern, and in the presence of an ostiole that is not encircled by any specialized cells.

However, **P. spinulatus** and **P. menonii** can be distinguished from **P. canadensis** sp. nov. in their lack of a matrix of darkened rows of cells exterior to the central region eventually developing into an ostiole, and in their generally smaller size. The presence of a one-layered stroma, as in **P. menonii**, or a two-layered stroma with basal echinations on the margins, as in **P. spinulatus**, are diagnostic in separating the specimens found in attached condition, but in dispersed fruiting bodies found in palynological preparations, these characteristics are not always present due to the possibility of their loss during deposition and preservation.

Genus: **Plochmopeltinites** Cookson 1947
Plochmopeltinites masonii Cookson 1947
Plate 31.1, figure 8; Plate 31.2, figures 1, 2, and 3

Description: Ascomata composed of thin, sinuous, intertwined plectenchyma with more or less rounded, entire, irregularly sinuate margin and an irregular central ostiole (Pl. 31.1, fig. 8; Pl. 31.2, fig. 1).

Ascomata brown, glabrous, with diameter ranging from 59 to 125 μm. Small thyriothecia, mostly incomplete structures, probably due to partial distortion during the process of preservation. Ostiole varies from 9 to 20 μm in diameter, usually bordered by a ring of small, thick-walled cells. Thickening usually conspicuous as a complete, dark ring around the ostiole (Pl. 31.2, fig. 2) about 5 to 7 μm in thickness. Two specimens (Pl. 31.2, fig. 3) found in the sample seem to be similar to ascomal or covering membrane or "scutellum" described by Cookson (1947a). They are composed of prosenchymatous plectenchyma consisting of slender, rather loosely woven tissue of elongated hyphae lying more or less parallel to one another, and with central strands somewhat thicker than those of the periphery. Specimens in Plate 31.2, figure 3 were about 113.0 and 134.0 μm in diameter.

Comments: **Plochmopeltinites masonii** is easily distinguishable from other peltate genera by its characteristic fruiting bodies, consisting of thin, sinuous, extended hyphae and a well developed, central bordered ostiole. Most of the diagnostic characters of **Stomiopeltis plectilis** Dilcher 1965 and **Stomiopeltites cretacea** Alvin and Muir 1970 strongly resemble those of **Plochmopeltinites masonii**. Elsik (1980) indicated that the dispersed thyriothecia of **Stomiopeltites** are equivalent to ascomata included in **Plochmopeltinites**. This association ignores the respective non-radial and radial cell pattern of these genera.

Cookson (1947a) included **Plochmopeltinites** in the subfamily Plochmopeltinae of the family Micropeltaceae, based mainly on the structure of the ascomal membrane or "scutellum" characterized by a sinuous plectenchyma, and did not recognize the taxonomic significance of the radial structure of the ascomata. Dilcher (1965) described **Stomiopeltites plectilis** and included it in the subfamily Stomiopeltoideae of the family Micropeltaceae. The fungus was found on well preserved leaves from Lower Eocene deposits in western Tennessee, U.S.A. Alvin and Muir (1970) described **Stomiopeltites cretacea** and included it in the subfamily Stomiopeltoideae of the family Micropeltaceae. They found thyriothecia and pycnidia with conspicuous epicuticular mycelium on well preserved shoot fragments of a conifer from the Wealden (Lower Cretaceous) near Hanover Point, Compton Bay, Isle of Wight. They pointed out that the thyriothecium of **Plochmopeltinites masonii** differs from that of **Stomiopeltites cretacea** in being radiate, and therefore **P. masonii** cannot be classified as being in the family

---

PLATE 31.2

Figures 1. **Plochmopeltinites masonii,** C-68329, P 2096-55g, 41.0 x 105.7, GSC 75877, x 500.
2. **P. masonii,** showing dark ring around the ostiole, C-68329, P 2096-55d, 27.5 x 112.2, GSC 75878, x 1000.
3. **P. masonii,** ascomal membranes, C-68305, Slide 2096-63j, 43.9 x 100.9, GSC 75879, x 500.
4. cf. **Meliola** sp., with branched mycelial tissue, C-68329, P 2096-55c, 30.8 x 109.0, GSC 75880, x 500.
5. cf. **Meliola** sp., peridium of irregularly angular to polygonal cells, C-68329, P 2096-55b, 18.7 x 115.5, GSC 75881, x 500.

PLATE 2

1

2

3

4

5

Micropeltaceae, which is distinguished from the family Microthriaceae by the strictly non-radiate structure of the flattened ascomata.

Selkirk (1975) described **Plochmopeltinites masonii** from Kiandra, New South Wales, and followed Alvin and Muir in assigning it to the family Microthyriaceae. Sepulveda and Norris (1982) described two specimens of **Plochmopeltinites** from the Eocene and Oligocene of Patagonia, southern Argentina. Similar specimens attributed to **Plochmopeltinites masonii** have been described by Norris (in press), from the western Canadian Arctic, ranging from Eocene to Miocene.

<div align="center">

Unidentified Inflated Fruiting Bodies
cf. **Meliola** sp.
Plate 31.2, figures 4, 5

</div>

Some twenty specimens of inflated fruiting bodies were seen. Although found in detached condition they resemble closely the cleistocarps of Ascomycetes. They appear to suggest the fruiting bodies (ascocarps) of the extant Meliolales, showing similarity in the presence of a dark coloured mycelium, a well defined peridium, and the lack of an ostiole and perithecial appendages. The lack of characteristic appendages separate them from cleistothecia of Erysiphales.

Description: The cleistocarps are black or dark brown, globose, and without ostioles. The mycelium around the perithecium is composed of dark coloured, septate, reticulately branched hyphae with cylindrical cells (fig. 4). The external layer of the peridium is dark coloured, made up of irregularly angular to polygonal cells without any characteristic appendages (fig. 5). Outer cells of the peridium appear thicker walled than the inner cells. Cleistocarps are about 75 to 105 µm in diameter.

Comments: Studies of fossil Ascomycetes with cleistocarps are fragmentary, and only a few records have been published so far. Hutchinson (1955) described and reviewed the genus **Sporocarpon**. More recently, Baxter (1960) and Davis and Leisman (1962) found small, non-ostiolate spherical bodies associated with hyphae resembling the cleistothecia of Ascomycetes, and described the genera **Sporocarpon**, **Dubiocarpon** and **Mycocarpon**. Of these, **Mycocarpon**, with its appendages and surrounding hyphae, appeared more closely related to an extant Erysiphales (Stewart, 1983, p. 37). Another fruiting body resembling a sclerotium was originally described by Rothwell (1972) as **Palaeosclerotium**. Dennis (1976), on further investigation of these structures from the Pennsylvanian of Illinois, showed that they contained asci and ascospores and were similar to cleistothecia of Ascomycetes (Stewart, 1983, p. 37).

Dilcher (1965) recorded several fragmentary specimens and a few well preserved colonies of **Meliola anfracta** on the upper epidermis of **Sapindus** sp., and randomly scattered colonies of **Meliola spinksii** on the lower surface of **Chrysobalanus**. The colonies of **M. anfracta** were found growing in close association with various forms of microthyriaceous fungi, whereas colonies of **M. spinksii** were free from such an association. In the present investigation, cleistothecia were found dispersed with thyriothecia of microthyriaceous fungi in the samples studied.

General discussion

Fossil microthyriaceous fungi have been recorded in rocks ranging in age from Early Cretaceous to Recent, but they are found most commonly in Tertiary sediments, especially those of Eocene and younger ages. The occurrence and evolution of microthyriaceous fungi may have accompanied the emergence and rapid spread of the angiosperms (Dilcher, 1965; Venkatachala and Kar, 1968).

Although there is no evidence to suggest that they existed on plants prior to the origin of angiosperms, or emerged and evolved concurrently in association with angiosperms, they occur most abundantly in post-Cretaceous strata, suggesting the dependence of these fungi on the broad-leaved angiosperms. However, both fossil and modern forms of microthyriaceous fungi have been reported on both gymnosperm and angiosperm plants. Alvin and Muir (1970) commented that there is no reason why the group should not have occurred widely in pre-angiosperm floras, and that they have merely been overlooked.

Rouse (1977), commenting on the climate in the Arctic during the Paleogene, indicated that the pattern of distribution of palynomorphs suggests a marked warming during the middle-Late Paleocene, the early-Middle Eocene climate being essentially subtropical. As previously noted in this paper, the samples containing fungal material range in age between Late Paleocene and Middle Eocene. This suggests that the sites in the Bonnet Plume Formation containing these samples were probably characterized by a humid and subtropical climate. This may explain the presence of microthyriaceous and Meliola-like fructifications in these samples, the modern forms of which have been found predominantly in humid, tropical and subtropical environments.

However, as was pointed out earlier, Rosendahl (1943) and Godwin and Andrew (1951) have reported microthyriaceous fruiting bodies from relatively cool, high latitude localities, and under a wide range of climatic conditions. Therefore, paleoecological interpretations based upon the distribution of a few fossil microthyriaceous fruiting bodies are not perfectly conclusive without broadly based supportive palynological studies, since our knowledge of the ecology of both modern and fossil epiphyllous fungi is limited (Dilcher, 1965; Selkirk, 1975).

It may be concluded that the continuing study of well preserved fungal spores and fructifications will demonstrate their importance in helping trace the evolution of plants, changes in their distribution with environmental variations, and their stratigraphic distribution.

Acknowledgments

References

Alexopoulos, C.J. and Mims, C.W., editors
　　1983: Introductory Mycology; Wiley Eastern Ltd., New Delhi India, 632 p.

Alvin, K.L. and Muir, M.D.
　　1970: An epiphyllous fungus from the Lower Cretaceous; Biological Journal of the Linnean Society, v. 2, p. 55-59.

Baxter, R.W.
　　1960: **Sporocarpon** and allied genera from the Americal Pennsylvanian; Phytomorphology, v. 10, p. 19-25.

Chitaley, S.D.
　　1951: Further report on the fossil microflora from the Mohgaonkalan beds of Madhya Pradesh, India; The Proceedings of the 37th Indian Science Congress, Banglore, v. 3, p. 159.

Chitaley, S.D. (cont.)
1957: Further report on the fossil microflora from the Mohgaonkalan beds of Madhya Pradesh, India; The Proceedings of the National Institute of Science, India, v. 23, p. 69-79.

Clarke, R.T.
1965: Fungal spores from Vermejo Formation coal beds (Upper Cretaceous) of Central Colorado; Mountain Geologist, v. 2, p. 85-93.

Cookson, I.C.
1974a: Fossil fungi from Tertiary deposits in the southern hemisphere, Part I; The Proceedings of the Linnean Society of New South Wales, v. 72, p. 207-214.

1974b: Plant microfossils from the lignites of Kerguelen Archipelago; British, Australian and New Zealand Antarctic research expedition, 1929-1931, Reports, Series A, v. 2, p. 127-142.

Davies, B. and Leisman, C.A.
1962: Further observations on **Sporocarpon** and allied genera; Torrey Botanical Club, Bulletin, v. 89, p. 97-109.

Dennis, R.L.
1976: **Palaeosclerotium**, a Pennsylvanian age fungus combining features of modern ascomycetes and basidiomycetes; Science, v. 192, p. 66-68.

Dilcher, D.L.
1963: Eocene epiphyllous fungi; Science, v. 142, p. 667-669.

1965: Epiphyllous fungi from Eocene deposits in western Tennessee, U.S.A.; Palaeontographica B, v. 116, p. 1-54.

Edwards, W.N.
1922: An Eocene microthyriaceous fungus from Mull, Scotland; British Mycological Society, Transactions, v. 8, p. 66-72.

Elsik, W.C.
1974: Fossil fungal spores and Cenozoic palynostratigraphy; photocopied handout at the 7th Annual Meeting of the American Association of Stratigraphic Palynologists, October 15-19, Calgary, Alberta, p. 1-17.

1975: Fossil fungal spores; Paleogene palynology, Cenozoic palynology short course, Louisiana State University.

1976: Microscopic fungal remains and Cenozoic palynostratigraphy; Geoscience and Man, v. 115, p. 115-120.

1980: Classification and geological history of the microthyriaceous fungi; The Proceedings of the 4th International Palynological Conference, Lucknow, India (1976-77), v. 1, p. 331-342.

Elsik, W.C. and Jansonius, J.
1974: New genera of Paleogene fungal spores; Canadian Journal of Botany, v. 52, p. 953-958.

Godwin, H. and Andrew, R.
1951: A fungal fruit body common in post-glacial peat deposits; New Phytology, v. 50, p. 179-183.

Graham, A.
1962: The role of fungal spores in palynology; Journal of Paleontology, v. 36, p. 60-68.

Hansford, C.G.
1961: The Meliolineae, A monograph; Sydovia Annales Micrologici, Series II, supplement 2, p. 1-806.

Hutchinson, S.A.
1955: A review of the genus **Sporocarpon** Williamson; Annals of Botany, v. 69, p. 425-437.

Jain, K.P. and Gupta, R.C.
1970: Some fungal remains from the Tertiaries of the Kerala coast; Palaeobotanist, v. 18, p. 177-182.

Jansonius, J.
1976: Palaeogene fungal spores and fruiting bodies of the Canadian Arctic; Geoscience and Man, v. 15, p. 129-132.

Kar, P.K., Singh, R.Y., and Sah, S.C.D.
1970: On some algal and fungal remains from Tura Formation of Garo Hills, Assam; Palaeobotanist, v. 19, p. 146-154.

Kemp, E.M.
1978: Microfossils of fungal origin from Tertiary sediments on the Ninetyeast Ridge, Indian Ocean; Bureau of Mineral Resources, Bulletin, Australia, no. 192, p. 73-81.

Keuxe Chubanshe (Science Publishers)
1978: Early Tertiary spores and pollen grains from the coastal region of the Bohai; Chinese Academy of Sciences, Peking, China, p. 1-666 (in Chinese, English translation).

Lange, R.T.
1978: Southern Australian Tertiary epiphyllous fungi, modern equivalents in the Australasian region, and habitat indicator value; Canadian Journal of Botany, v. 56, p. 532-541.

Norris, G.
— Systematic and stratigraphic palynology of Eocene and Paleocene strata in Imperial Nuktak C-22 well, Mackenzie Delta region, District of Mackenzie, Northwest Territories; Geological Survey of Canada, Bulletin 340. (in press)

Petros'yants, M.A.
1976: Fossil fungal remains in Turonian deposits in the northeastern VST-VRT and Aval regions; Trudy of the All Union Petroleum Scientific Research Institute of Geological Exploration, issue 192, p. 42-53 (in Russian, English translation).

Pirozynski, K.A. and Weresub, L.K.
1979: The classification and nomenclature of fossil fungi; The Whole Fungus, B. Kendrick (ed.), published by the National Museum of Canada for the Kananaskis Foundation, v. 2, p. 653-688.

Ramanujam, C.G.K.
1963: Thyriothecia of Asterineae from the South Arcot Lignite, Madras; Current Science, v. 32, p. 327-328.

Roa, A.R.
1954: Fungal remains from some Tertiary deposits of India; The Proceedings of the 41st Indian Science Congress, Hyderabad (Deccan), v. 3, p. 165-166.

1959: Fungal remains from some Tertiary deposits; Palaeobotanist, v. 7, p. 43-46.

Rosendahl, C.O.
1943: Some fossil fungi from Minnesota; Torrey Botanical Club, Bulletin, v. 70, p. 126-138.

Rothwell, G.W.
1972: **Palaeosclerotium pusillum** gen. et sp. nov., a fossil eumycete from the Pennsylvanian of Illinois; Canadian Journal of Botany, v. 50, p. 2353-2356.

Rouse, G.E.
1977: Paleogene palynomorph ranges in western and northern Canada; American Association of Stratigraphic Palynologists, Contribution, series no. 5A, p. 48-61.

Rouse, G.E. and Srivastava, S.K.
1972: Palynological zonation of Cretaceous and Early Tertiary rocks of the Bonnet Plume Formation, northwestern Yukon, Canada; Canadian Journal of Botany, v. 9, p. 1163-1179.

Selkirk, D.R.
1975: Tertiary fossil fungi from Kiandra, New South Wales; The Proceedings of the Linnean Society of New South Wales, v. 100, p. 70-94.

Sepulveda, Eliseo G. and Norris, G.
1982: A comparison of some Paleogene fungal palynomorphs from Arctic Canada and from Patagonia, southern Argentina; Ameghiniana, v. 19, p. 319-334.

Sheffy, M.V. and Dilcher, D.L.
1971: Morphology and taxonomy of fungal spores; Palaeontographica B, v. 133, p. 34-51.

Smith, P.H.
1980: Trichothyriaceous fungi from the Early Tertiary of southern England; Palaeontology, v. 23, p. 205-212.

Srivastava, S.K.
1968: Fungal elements from the Edmonton Formation (Maestrichtian), Alberta, Canada; Canadian Journal of Botany, v. 46, p. 1115-1118.

Stewart, W.N.
1983: Paleobotany and evolution of plants; Cambridge University Press, Cambridge, London, 405 p.

Tilgner, W.
1954: Fruit bodies in brown coal; Micropalaeontologist, v. 8, p. 40-41.

Varma, C.P. and Rawat, M.S.
1963: A note on some diporate grains recovered from Tertiary horizons of India and their potential marker value; Grana Palynologica, v. 4, p. 130-139.

Venkatachala, B.S. and Kar, R.K.
1968: Palynology of the Tertiary sediments in Kutch-2. Epiphyllous fungal remains from the bore-hole no. 14; Palaeobotanist, v. 17, p. 179-183.

Vishnu-Mittre
1973: Studies of fungal remains from the Flandrian deposits in the Whittlesey Mere region, Hunts, England; Palaeobotanist, v. 22, p. 89-110.

Wilson, L.R.
1962: A Permian fungus spore type from the Flowerpot Formation of Oklahoma; Oklahoma Geological Notes, v. 22, p. 91-96.

Wolf, F.A.
1966a: Fungus spores in East African lake sediments; Torrey Botanical Club, Bulletin, v. 93, p. 104-113.

1966b: Fungus spores in East African lake sediments II; Elisha Mitchell Science Society, Journal, v. 82, p. 57-61.

1967a: Fungus spores in East African lake sediments IV; Torrey Botanical Club, Bulletin, v. 94, p. 31-34.

1967b: Fungus spores in East African lake sediments V; Mycologia, v. 59, p. 397-404.

1967c: Fungus spores in East African lake sediments VI; Elisha Mitchell Science Society, Journal, v. 83, p. 113-117.

1967d: Fungus spores in East African lake sediments VII; Torrey Botanical Club, Bulletin, v. 94, p. 480-486.

New stratigraphic units, Middle Jurassic to lowermost Cretaceous succession, Arctic Islands

Project 750083

Ashton F. Embry
Institute of Sedimentary and Petroleum Geology, Calgary

Abstract

Bajocian to Valanginian strata (Middle Jurassic to lowermost Cretaceous) in the southern and western portions of the Sverdrup Basin consist of alternating units of shale-siltstone and sandstone. The stratigraphic nomenclature for these strata is well established in this area, and the only addition proposed in this paper is the formalization of a previously recognized sandstone member in the argillaceous Deer Bay Formation, herein named the Glacier Fiord Member. To the north and west, the sandstone units disappear due to facies change and the entire succession consists of siltstone and shale. This thick shale-siltstone unit is herein named the Mackenzie King Formation. In some areas, the formation can be divided into three members – McConnell Island, Ringnes and Deer Bay – all of which have formation status in the southeastern Sverdrup Basin.

Résumé

Les couches déposées entre le Bajocien et le Valanginien (du Jurassique moyen au Crétacé très inférieur) dans les parties méridionales et occidentales du bassin Sverdrup sont composées d'unités alternantes de schiste argileux-siltstone et de grès. La nomenclature stratigraphique de ces couches est bien établie dans cette région; il est cependant proposé d'y ajouter le membre de grès de la formation argileuse de Deer Bay qui a déjà été identifié et qui serait officiellement appelé membre de Glacier Fiord. À cause du changement de faciès, les unités de grès disparaissent vers le nord et l'ouest où la succession se compose entièrement de siltstone et de schiste argileux. Cette importante unité de schiste argileux-siltstone est appelée formation de Mackenzie King. À certains endroits, la formation se divise en trois membres (McConnell Island, Ringnes et Deer Bay) lesquels constituent des formations de la partie sud-est du bassin Sverdrup.

Introduction

The Middle Jurassic (Bajocian) to lowermost Cretaceous (Valanginian) succession within the Mesozoic strata of the Arctic Islands, is an interval that has been plagued by stratigraphic nomenclatural problems. These strata are widespread in the Arctic Islands, occurring in both Sverdrup and Banks basins (Fig. 32.1) and numerous surface and subsurface control points are available for them. The strata are readily delineated over most of the area because they usually occur between two regional sandstone units, the Sandy Point Formation below and the Isachsen Formation above (Fig. 32.2). In the southern and eastern portions of the Sverdrup Basin, the succession consists of alternating sandstone and shale-siltstone units, and a reasonable stratigraphic nomenclatural system has been established on the basis of both early reconnaissance work (Souther, 1963; Tozer, 1963) and more recent subsurface-surface regional syntheses (Balkwill, 1983; Embry, 1984). The only proposed addition to the nomenclature of the strata in this area is the assignment of a formal name to a sandstone unit high in the succession. This sandstone unit has been described and mapped by previous workers (Tozer, 1963; Balkwill, 1983) and is herein named the Glacier Fiord Member of the Deer Bay Formation (Fig. 32.2).

To the northwest, in the Sverdrup Basin, the sandstone units disappear due to facies change to shale and siltstone, and the succession consists almost entirely of these two rock types (Fig. 32.2). Previous workers have given this thick interval of argillaceous strata a variety of names, none of which is deemed suitable for reasons discussed below. In this paper a new formal name, Mackenzie King Formation, is proposed for the Bajocian-Valanginian shale-siltstone unit of the Arctic Islands. Tops for the stratigraphic units of the Bajocian-Valanginian interval in selected wells (Fig. 32.1) are listed in the appendix.

Previous work

The nomenclatural problems for this interval stem mainly from the early reconnaissance fieldwork, at which time authors did not have the benefits of subsurface data and a regional framework. Heywood (1955, 1957) conducted fieldwork on northwestern Ellef Ringnes Island in 1952 and 1953. He defined the Deer Bay Formation from exposures of medium- to dark-grey shale that underlie the sandstone-dominant Isachsen Formation. Unfortunately, Heywood did not observe the base of the formation and did not designate a type section. Fossils collected from the Deer Bay strata by Heywood were all of Valanginian age.

In 1955, a shale unit, which lies between the sandstone-dominant Awingak Formation (Upper Jurassic) and the Isachsen Formation, on Axel Heiberg Island, was assigned to the Deer Bay Formation (Souther, 1963). This usage was later extended to other portions of Axel Heiberg Island (Fricker, 1963; Tozer, 1963).

Tozer and Thorsteinsson (1964) mapped Mackenzie King Island in 1958. The entire Bajocian-Valanginian shale-siltstone unit that outcrops on the island was assigned to the

1. Emerald K-33;
2. Cape Norem A-80;
3. Skybattle Bay C-15;
4. Wallis K-62;
5. Kristoffer Bay B-06;
6. Helicopter J-12;
7. Char G-07;
8. West Amund I-44;
9. Halcyon O-16;
10. Orksut I-44.

Figure 32.1. Distribution of Bajocian-Valanginian strata and control points. Key to numbered wells listed in appendix.

Figure 32.2. *Schematic stratigraphic cross-section, Bajocian-Valanginian strata, Sverdrup Basin.*

Mould Bay Formation, a sandstone-dominant unit with a type section on Prince Patrick Island. This assignment was made on the erroneous interpretation that the interval on Mackenzie King consists mainly of sandstone. In fact, it is almost entirely shale and siltstone.

In 1967, Stott (1969) mapped Ellef Ringnes Island and placed the base of the Deer Bay Formation at the top of a Callovian (late Middle Jurassic) sandstone that he assigned to the Wilkie Point Formation (Hiccles Cove Formation of Embry, 1984). Subsequent drilling in the Ellef Ringnes Island area further complicated the matter, because over most of the area it was found that shale and siltstone were continuous from the base of the Isachsen Formation to the top of an Aalenian sandstone unit usually referred to as Jaeger (Sandy Point Formation of Embry, 1984). Henao-Londono (1977) referred the entire shale-siltstone unit to the Deer Bay Formation. Thus the term Deer Bay became commonly applied to two different shale units, one between the Isachsen and Awingak formations, and the other between the Isachsen and Sandy Point formations. The Lower Cretaceous shale originally described as Deer Bay by Heywood was common to both these units.

Balkwill (1983) attempted to resolve this problem of dual usage by recognizing three, separate stratigraphic units within the Bajocian-Valanginian argillaceous succession: the Deer Bay and Ringnes formations and the "Upper Savik". Each unit consists mainly of shale and siltstone, but the units were distinguished from one another on the basis of colour,

silt content and the character of associated concretions. This subdivision allowed Balkwill (1983) to redefine the Deer Bay Formation as the Upper Jurassic-Lower Cretaceous shale unit that lies between the Isachsen Formation and either the Awingak Formation or its shale-siltstone equivalent, the Ringnes Formation. However, as noted by Balkwill (1983), a drawback to this nomenclatural scheme was that the three shale-siltstone units could not always be objectively delineated in subsurface sections.

The sandstone unit that occurs in the Deer Bay Formation and which is given formal nomenclature in this paper, was first described by Tozer (1963). He outlined its distribution on southern Axel Heiberg Island and dated it as Early Valanginian. Balkwill (1983) recognized the same unit on southern Amund Ringnes Island and mapped it as Member D of the Deer Bay Formation.

Present work

The writer's surface and subsurface studies of the Bajocian-Valanginian interval has led to the assignment of the thick, argillaceous succession that comprises the interval in the northwestern Sverdrup to a single formation. Because the name Deer Bay has been redefined as discussed above, and the term Mould Bay was inappropriate in the first place, a new name, Mackenzie King Formation, is proposed for this rock unit. It is acknowledged that separate shale-siltstone units can be distinguished in most outcrop sections and in

some wells (Upper Savik, Ringnes and Deer Bay of Balkwill, 1983) and these units are given member status (McConnell Island, Ringnes, Deer Bay members) (Fig. 32.2). Formation status for these units in the northwestern Sverdrup is presently inappropriate because of the difficulty of objectively delineating them in subsurface sections. However, it is important to note that the type Ringnes and Deer Bay are still valid at these localities, although they are members rather than formations as originally defined.

The sandstone member of the Deer Bay Formation was examined on southern Axel Heiberg Island in 1983. It is a readily recognizable unit in this area as described by Tozer (1963). Because it is such a distinctive unit in the Deer Bay Formation and is a potential hydrocarbon reservoir in the subsurface, it is herein formally named the Glacier Fiord Member of the Deer Bay Formation.

The relationships of the newly defined units with previously designated units are shown in Figure 32.3.

Mackenzie King Formation

Definition

The Mackenize King Formation consists mainly of medium- to dark-grey shale and siltstone with a few, very fine grained, sandstone interbeds. The type section is in the Cape Norem A-80 well (77°29'13"N, 110°27'05"W; spudded April 19, 1970, abandoned August 27, 1970; T.D. 2970 m, K.B. 14 m) between 192 m (630 ft) and 1009 m (3310 ft),

and is 817 m (2680 ft) thick (Fig. 32.4) The name is taken from Mackenzie King Island upon which the type well was drilled. Chip samples taken at 3 m intervals from the type section can be examined at the Institute of Sedimentary and Petroleum Geology, in Calgary, Alberta.

Synonyms

1. Deer Bay Formation, northern Ellef Ringnes, Heywood (1955, 1957).
2. Mould Bay Formation, Mackenzie King and northwestern Melville, Tozer and Thorsteinsson (1964).
3. Deer Bay Formation, Ellef Ringnes, Stott (1969), Henao-Londono (1977).
4. Wilkie Point and Mould Bay formations, Banks Island, Miall (1979).
5. Upper Savik, Ringnes Formation and Deer Bay Formation, central Amund Ringnes, Balkwill (1983).

Boundaries

The Mackenize King Formation usually conformably overlies the Sandy Point Formation, and the contact is placed at the lowest shale-siltstone unit above which shale and siltstone are predominant. In the central portion of the Sverdrup Basin, the Sandy Point is absent due to facies change, and the Mackenzie King conformably overlies the

NORTHWESTERN ELLEF RINGNES		CENTRAL RINGNES ISLANDS MACKENZIE KING ISLAND				AXEL HEIBERG ISLAND SOUTHERN AMUND RINGNES				
Stott 1969	This paper Embry 1984	Tozer and Thorsteinsson 1964	Henao 1977	Balkwill 1983	This paper	Tozer 1963	Balkwill 1983	This paper Embry 1984		
Isachsen Fm.	Isachsen Fm.	Isachsen Fm.		Isachsen Fm.						CRETACEOUS
Deer Bay Fm.	Deer Bay Mbr. (Mackenzie King Fm)	Mould Bay Fm.	Deer Bay Fm.	Deer Bay Fm.	Deer Bay Mbr. (Formation)	Sandstone Mbr. / Deer Bay Fm.	Mbr. D / Deer Bay Fm.	Glacier Fiord Mbr. / Deer Bay Fm.	VALANGINIAN	
									BERRIASIAN	
									TITHONIAN	
	Ringnes Mbr.			Ringnes Fm.	Ringnes Mbr. (King Formation)	Awingak Fm.	Awingak Fm.	Awingak Fm.	KIMMERIDGIAN	
								Ringnes Fm.	OXFORDIAN	JURASSIC
Wilkie Point Fm.	Hiccles Cove Fm.		Upper Savik Mbr.	Upper Savik Mbr.	McConnell Island Mbr. (Mackenzie King Fm)	Upper Savik Mbr.	Upper Savik Mbr.	McConnell Island Fm.	CALLOVIAN	
	McConnell Island Fm.								BATHONIAN	
									BAJOCIAN	
	Sandy Point Fm.	Wilkie Point Fm.	Savik Fm.	Jaeger (Savik Fm.)	Sandy Point Fm. / Jameson Bay Fm.	Jaeger (Savik Fm.)	Jaeger (Savik Fm.)	Sandy Point Fm.	AALENIAN	

Figure 32.3. *Past and present nomenclature of Bajocian-Valanginian strata, Sverdrup Basin.*

Jameson Bay Formation (Fig. 32.2). The contact at these localities is placed at the base of a soft, clay-rich shale unit that abruptly overlies the uppermost siltstones of the Jameson Bay Formation. In a few sections on the north-western and southwestern margins of the Sverdrup and on south-central Banks Island, the Mackenzie King conformably overlies the Hiccles Cove Formation. The contact is placed at the base of the first shale-siltstone unit above which shale and siltstone are predominant (Fig. 32.2).

The Mackenzie King Formation is overlain by the Isachsen Formation. The contact varies from conformable within the Sverdrup Basin, to unconformable on the basin flanks and on Banks Island, and is placed at the base of the first sandstone unit above which sandstone is predominant.

The name Mackenzie King ceases to be used in sections in which the Awingak Formation can be recognized (Fig. 32.2).

Lithology

In the type section, the three members of the Mackenzie King Formation can be distinguished (Fig. 32.4). The basal member, the McConnell Island, consists of soft, light to medium green-grey shale and siltstone with ironstone concretions. The overlying Ringnes Member consists of dark grey to black, silty shale and siltstone with dolomitic concretions. The Deer Bay Member, which comprises the bulk of the formation, consists of medium- to dark-grey,

Figure 32.4. Lithology (from samples) and gamma-ray curve for type section of Mackenzie King Formation; Cape Norem A-80 well.

273

silty shale and siltstone with interbeds of very fine grained sandstone in the uppermost portion. This lithologic subdivision of the Mackenzie King characterizes the formation over its extent, although basinward, the shales of the McConnell Island Member become darker and are difficult to distinguish from the Ringnes strata. Sandstone units become more common in the Deer Bay Member toward the basin margins, and consist of very fine- to fine-grained, burrowed sandstone. Marine fossils, mainly pelecypods, occur in all members.

Thickness and distribution

The Mackenzie King Formation occurs mainly in the northwestern portion of the Sverdrup Basin (Fig. 32.1) and is bounded by facies change to the southeast and erosion to the northwest. The formation was penetrated in a well on south-central Banks Island but its distribution in this area is probably limited, as it is absent in surrounding wells. The thickest occurrences of the formation occur on eastern Ellef Ringnes Island and central Amund Ringnes Island, where it is about 1350 m thick.

Age

Pelecypods and ammonites collected from surface exposures range in age from Callovian to Valanginian (Balkwill, 1983) but the lowermost beds have not yielded macrofossils. Stratigraphic relationships suggest the basal beds are Bajocian and Bathonian in age (Embry, 1984). The ages of the members are interpreted to be: McConnell Island – Bajocian to Callovian; Ringnes – Oxfordian to Kimmeridgian; Deer Bay – Tithonian to Valanginian (Balkwill, 1983).

Environment of deposition

The rock types and fauna of the formation are indicative of an offshore marine shelf to prodelta environment of deposition.

Glacier Fiord Member, Deer Bay Formation

Definition

The Glacier Fiord Member consists of very fine- to medium-grained sandstone. The type section is located on southern Axel Heiberg Island, 5 km east-northeast of the head of Glacier Fiord (78°37'20"N, 89°46'W) on the north side of a prominent glacier. The member is named for Glacier Fiord, which is close to the type section.

Synonyms

1. Sandstone member, Deer Bay Formation, south Axel Heiberg Island, Tozer (1963).

2. Member D, Deer Bay Formation, southern Amund Ringnes Island, Balkwill (1983).

Boundaries

The Glacier Fiord Member is conformably underlain and overlain by shale and siltstone of the Deer Bay Formation. The lower contact of the member is placed at the base of the first sandstone unit above which sandstone becomes predominant. The upper contact is placed at the top of the highest sandstone above which shale and siltstone are predominant.

Lithology

At the type section, the member displays a coarsening-upward trend. The basal 6 m are composed of light grey, very fine grained, burrowed sandstone. The overlying 22 m comprise interbedded burrowed sandstone and very fine- to fine-grained, hummocky to horizontally bedded sandstone. The upper 12 m consist of white, massive to horizontally bedded, fine- to medium-grained sandstone. Balkwill's (1983) description of the member on southern Amund Ringnes

Figure 32.5. *Lithology (from outcrop) for type section of Glacier Fiord Member, Deer Bay Formation; Glacier Fiord area, southern Axel Heiberg Island.*

is similar, and he records thin, chert-pebble beds in the uppermost portion. Northward, the massive to hummocky crossbedded strata disappear, and the member is composed entirely of burrowed, very fine grained sandstone.

Thickness and distribution

The member occurs on southern Axel Heiberg Island (Tozer, 1963) and southern Amund Ringnes Island (Balkwill, 1983). The member is limited in the north by facies change to shale and siltstone and in the south by truncation beneath the sub-Isachsen Formation unconformity. The member probably extends along the eastern and southern margins of the basin and it has been encountered in one well south of Ellef Ringnes Island and one well on Fosheim Peninsula, Ellesmere Island (Fig. 32.1, appendix). Coarse grained siltstones stratigraphically equivalent to the member occur in a number of wells. The maximum recorded thickness is 40 m (type section).

Age environment of deposition

Pelecypods from below, within, and above the member are Early Valanginian in age (Tozer, 1963; Balkwill, 1983).

The lithotypes, sedimentary structures, and fauna indicate a shallow marine shelf environment. Burrowed sandstones were probably deposited below storm wave base, and the hummocky to horizontally bedded sandstones deposited above storm wave base.

References

Balkwill, H.R.
1983: Geology of Amund Ringnes, Cornwall and Haig Thomas islands, District of Franklin; Geological Survey of Canada, Memoir 390.

Embry, A.F.
1984: The Wilkie Point Group (Lower-Upper Jurassic), Sverdrup Basin, Arctic Island, in Current Research, Part B, Geological Survey of Canada, Paper 84-1B, p. 299-308.

Fricker, P.E.
1963: Geology of the Expedition Fiord area, western central Axel Heiberg Island, Canadian Arctic Archipelago; McGill University, Axel Heiberg Island Research Reports, Geology, No. 1.

Henao-Londono
1977: Correlation of producing formations in the Sverdrup Basin; Bulletin Canadian Petroleum Geology, v. 25, p. 969-980.

Heywood, W.W.
1955: Arctic piercement domes; Bulletin Canadian Institute Mining Metallurgy, v. 48, p. 59-64.

Heywood, W.W.
1957: Isachsen Area, Ellef Ringnes Island, District of Franklin, Northwest Territories; Geological Survey of Canada, Paper 56-8.

Miall, A.D.
1979: Mesozoic and Tertiary Geology of Banks Island, Arctic Canada; Geological Survey of Canada, Memoir 387.

Souther, J.G.
1963: Geological traverse across Axel Heiberg Island from Buchanan Lake to Strand Fiord: in Geology of the north-central part of the Arctic Archipelago, Northwest Territories (Operation Franklin), ed. Y.O. Fortier; Geological Survey of Canada, Memoir 320.

Stott, D.F.
1969: Ellef Ringnes Island, Canadian Arctic Archipelago; Geological Survey of Canada, Paper 68-16.

Tozer, E.T.
1963: Mesozoic and Tertiary stratigraphy, western Ellesmere Island and Axel Heiberg Island, District of Franklin; Geological Survey of Canada, Paper 63-30.

Tozer, E.T. and Thorsteinsson, R.
1964: Western Queen Elizabeth Islands, Arctic Archipelago; Geological Survey of Canada, Memoir 332.

APPENDIX

Stratigraphic tops from selected wells, formations of Bajocian-Valanginian succession, Arctic Islands. Location of wells shown on Figure 32.1.

	metres	feet
BP Emerald K-32		
Mackenzie King Formation	447	(1466)
Hiccles Cove Formation	798	(2618)
McConnell Island Formation	975	(3200)
Sandy Point Formation	1003	(3290)
Elf Cape Norem A-80		
Mackenzie King Formation	192	(630)
Sandy Point Formation	1009	(3310)
Sun Skybattle Bay C-15		
Deer Bay Formation	1263	(4144)
Awingak Formation	1571	(5154)
Ringnes Formation	1674	(5492)
McConnell Island Formation	1711	(5612)
Sandy Point Formation	1767	(5797)
Dome Wallis K-62		
Mackenzie King Formation	1084	(3558)
Jameson Bay Formation	1755	(5758)
Panarctic Kristoffer Bay B-06		
Mackenzie King Formation	372	(1220)
Jameson Bay Formation	1106	(3630)
Panarctic Helicopter J-12		
Mackenzie King Formation	1316	(4316)
Sandy Point Formation	3139	(10300)
Panarctic Char G-07		
Deer Bay Formation	985	well
Glacier Fiord Member	1014	
underlying Deer Bay Formation	1043	logged
Awingak Formation	1314	
Ringnes Formation	1415	in
McConnell Island Formation	1439	
Sandy Point Formation	1477	metres
Panarctic West Amund I-44		
Mackenzie King Formation	spud	
Sandy Point Formation	687	(2254)
Panarctic Halcyon O-16		
Deer Bay Formation	1239	(4066)
Glacier Fiord Member	1244	(4083)
underlying Deer Bay Formation	1273	(4178)
Awingak Formation	1519	(4983)
Ringnes Formation	1806	(5925)
Hiccles Cove Formation	1847	(6060)
Sandy Point Formation	1880	(6169)
Deminex Orksut I-44		
Mackenzie King Formation	1457	(4781)
Hiccles Cove Formation	1813	(5948)
Cape de Bray Formation (Devonian)	1828	(5998)

New occurrences of <u>Kolmodinia</u> Martinsson (Ostracoda) from the Silurian (Wenlock) of the Mackenzie Mountains, Northwest Territories

Project 720072

M.J. Copeland
Institute of Sedimentary and Petroleum Geology, Ottawa

Abstract

The genus **Kolmodinia** Martinsson, 1962 has previously been known only from Upper Wenlock and Middle Ludlow strata of the Island of Gotland, Sweden. The two incomplete specimens previously described, **K. grandis** (Kolmodin) and **K.** cf. **grandis** (Kolmodin), were considered by Martinsson as possibly beyrichiacean in morphology. The three new specimens described here (**K. spinosa, K. martinssoni** and **K. kolmodini**) are more complete and the genus is referred to the Drepanellacea (Drepanellidae).

Résumé

Le genre **Kolmodinia** Martinsson, 1962, n'a été relevé que dans les couches du Wenlock supérieur et du Ludlow moyen sur l'île de Gotland en Suède. Les deux spécimens incomplets précédemment décrits, **K. grandis** (Kolmodin) et **K.** cf. **grandis** (Kolmodin), possédaient vraisemblablement, selon Martinsson, une morphologie de beyrichiacéen. Les trois nouveaux spécimens qui sont décrits dans cet article (**K. spinosa, K. martinssoni** et **K. kolmodini**) sont plus complets et appartiennent au genre des Drepannellacea (Drepanellidae).

278

Introduction

During examination of acid residues for Late Ordovician to Middle Silurian silicified ostracodes, three specimens of the ostracode genus **Kolmodinia** were found. These specimens were recovered from three stratigraphic sections: AV2 and AV4 (measured by Chatterton and Perry in 1978 and 1979) and AV7 (measured by Chatterton and Over in 1983), about 10 to 12 km east of Avalanche Lake (63°23'N, 127°02'30"W), Northwest Territories (see Chatterton and Perry, 1983, 1984). Two, **Kolmodinia spinosa** n. sp. (GSC 72628) and **Kolmodinia martinssoni** n. sp. (GSC 80852), are from near the base of the Delorme Formation (odonto-pleurid trilobite assemblage "j", of Chatterton and Perry, 1983, 1984) and are of early Wenlock age. The other, **Kolmodinia kolmodini** n. sp. (GSC 81000), occurs in strata of Road River Group lithology and is probably of late Wenlock age (Chatterton, personal communication, December 1984). The author is indebted to B.D.E. Chatterton of the University of Alberta for permission to study this material. All specimens are deposited in the National Type Fossil Collection, Geological Survey of Canada, Ottawa.

Discussion

Only two specimens of this genus have been described previously, both from the Island of Gotland (Sweden): **Kolmodinia grandis** (Kolmodin) from the Upper Wenlock Mulde Beds at Djupvik, and **Kolmodinia cf. grandis** (Kolmodin) from the Middle Ludlow Eke Beds at Lau Backar (Martinsson, 1962, p. 354, 355, Fig. 7). Both of those specimens are incomplete, but Martinsson concluded, "The present evidence seems to be sufficient for including the genus among the palaeocope ostracodes. If it can be proved to be a beyrichiacean, which is most probable at present, it cannot be regarded as a beyrichiid but as a representative of a new family".

None of the five specimens now known bears what could be considered a beyrichiacean crumina. Instead, the anterior lobe typically bears a pronounced tubercle at or slightly above mid-height of the valve, well removed from a velar position. Martinsson (1962) remarked that "The tubercle of this [anterior lobal] element is hollow in Kolmodin's specimen". Whether this statement is meant as an observation of that specimen's external and/or internal morphology is uncertain, as it is obvious from the illustration only that the anterior lobal tubercle of the specimen from Djupvik bears a pronounced depression (hole?) in external view.

PLATE 33.1

Figures   1-3. **Kolmodinia spinosa** n. sp.

> Lateral, dorsal and interior views of a right valve; x 70; holotype; GSC 72628; locality AV4 - 126Tm, Delorme Formation; early Wenlock.

     4, 5. **Kolmodinia martinssoni** n. sp.

> Lateral and interior views of a right valve; x 35; holotype; GSC 80852; locality AV2 - 255 to 260 m, lower Delorme Formation; early Wenlock. Note the 'aperture' of the hollow tubercle on the anterior lobe, figure 5.

     6-8. **Kolmodinia kolmodini** n. sp.

> Lateral, dorsal and interior views of a left valve; x 35; Holotype; GSC 81000; locality AV7 - 312 m, Road River Group; probably late Wenlock.

All of the Avalanche Lake specimens are free valves, but only one (Plate 33.1, figs. 4, 5) has the hollow tubercle of the anterior lobe connecting directly with the interior of the valve via an irregularly oval 'aperture', somewhat reduced in diameter from that of the exterior of the tubercle. The other two specimens show no indication of the 'aperture' on the interior wall surface. If the anterior lobal tubercle was a sealed-off chamber in the valve wall it may have provided buoyancy to an otherwise relatively heavy carapace. The interior 'aperture' would then indicate that the interior wall of the anterior lobal tubercle was extremely thin and subject to chemical or physical destruction. It is equally possible that any interior 'aperture' present on the other two specimens could have been obliterated during the process of silicification. The conclusion that the presence or absence of an 'aperture' connecting the anterior lobal tubercle chamber to the interior of the valve has dimorphic significance is extremely tenuous.

The hingeline of the Avalanche Lake specimens is certainly palaeocopid, but the hinge mechanism is unknown because it is obscured by the coarseness of the silicification of the valves. Also, the closure of the valves and lack of duplicature indicate a palaeocopid condition.

Martinsson's speculation as to the beyrichiacean nature of **Kolmodinia** is interesting but questionable. As Martinsson remarked, the extreme dorsal position and isolation of L2 does occur within the Beyrichiacea, such as on the kloedeniine genus **Kloedenia**. It appears more likely, however, that **Kolmodinia** belongs within the apparently non-dimorphic Drepanellacea, and is closely allied with such genera as **Drepanella** and **Scofieldia** of the Drepanellidae.

In his diagnosis of **Kolmodinia**, Martinsson indicated that "There is one tumid anterior element with a character-istic tubercle, one tumid posterior element, two smaller cusps above those lobal elements, and one major cusp between them". It would seem, however, that a generally broad, continuous, marginal ridge, typical of most drepanellids, is present around the margin of the valve, wraps around L1 and L3, may fuse dorsally with L1, extends above the hingeline anteriorly and posteriorly, and is separated dorsally by S1 and S2, which meet ventral to L2. L2, the "major cusp" of Martinsson, also extends above the hingeline. In this diagnosis, therefore, the ends of the broad, marginal ridge form the anterior and posterior dorsal cusps, whereas the positions of these cusps on **Scofieldia** is occupied by the dorsal extensions of L1 and L3, and on **Drepanella** only the anterior end of the marginal ridge extends to the dorsal margin of the valve. The prominent, hollow tubercle on the anterior lobe of **Kolmodinia** is not present on other drepanellids.

Paleontology

<div align="center">

Order Palaeocopida Henningsmoen, 1953
Suborder Beyrichicopina Scott, 1961
Superfamily Drepanellacea Ulrich and Bassler, 1923
Family Drepanellidae Ulrich and Bassler, 1923
Genus **Kolmodinia** Martinsson, 1962

</div>

Type species.   **Beyrichia grandis** Kolmodin, 1879

<div align="center">

Kolmodinia spinosa n. sp.
Plate 33.1, figures 1-3

</div>

Description. Trilobate, hinge long, relatively straight, hidden in lateral view by dorsal cusps of the marginal ridge and preadductorial lobe (L2). Preplete, posterior cardinal angle with a short acroidal process, anterior cardinal angle rounded. L1 and L3 separated by combined S1 and S2 crossing the valve somewhat diagonally, extending to the marginal ridge and separated dorsally by the small

median lobe. Anterior lobe (L1) subcircular, with large, near median, circular tubercle; posterior lobe (L3) rounded, subtriangular with posterodorsal spinose process; both lobes superimposed on the broad marginal ridge, which is expressed as an anterior and posterior shelf, lateral to the lobes and extending dorsally as anterior and posterior dorsal cusps. Neither the tubercle on the anterior lobe nor the spinose process on the posterior lobe is indicated on the interior of the valve. L2 dorsal, surrounded by S1 and S2 and extending above the hingeline. Domicilium separated from the marginal ridge by a channel-like rounded groove. Elevated portions of the valve coarsely granular, depressed areas (sulci, supra marginal channel, etc.) less granular.

Measurements of holotype, GSC 72628 (in mm): L: 1.3, H: 0.75.

Number of specimens studied: one

Type. Holotype, GSC 72628.

Occurrence. Delorme Formation, Avalanche Lake area, Northwest Territories, Section AV4 - 126Tm. Brachiopods and ostracodes from this unit have been described (as from Avalanche Lake locality 2; 300 to 330 ft, (90 to 99 m)) by Lenz (1977) and Copeland (1978).

Remarks. This is the only known species of **Kolmodinia** that possesses a short, posterior, acroidal process and an attenuated posterior dorsal process of L3. It is represented only by a relatively small specimen, which may be juvenile.

Kolmodinia martinssoni n. sp.
Plate 33.1, figures 4, 5

Description. Trilobate, hinge long, relatively straight, hidden in lateral view by dorsal cusps of broad marginal ridge and L2. Preplete, anterior margin more narrowly rounded than posterior. L1 and L3 separated by deep, narrow, inclined S1 and S2 that join ventral of L2. On the interior, S1/S2 form a ridge that is elevated almost as high as the plane of valve closure. L1 large, semicircular, with marginal ridge above the hingeline, and large, dorso-median, circular tubercle. L3 ovate to semicircular, extended anteroventrally beneath the combined, median sulcus. Both lobes superimposed on a broad ridge marginal to L1 and L3 and extending dorsally as anterior and posterior dorsal cusps. L2 nearly circular, extending dorsally as a low cusp. The tubercle on the anterior lobe is indicated on the interior as an ovate hollow 'aperture'. Along the anterior margin, L1 is separated from the marginal ridge by a channel. All parts of the valve coarsely granular.

Measurements of holotype, GSC 80852 (in mm): L: 2.45, H: 1.60.

Number of specimens studied: one.

Type. Holotype, GSC 80852.

Occurrence. Delorme Formation, Avalanche Lake area, Northwest Territories, Section AV2 - 255 to 260 m.

Remarks. **K. martinssoni** n. sp. differs from other species of the genus in having L1 an inclined oval lobe, the tubercle of L1 more dorsal in position, and S1/S2 much more narrow and deep.

Kolmodinia kolmodini n. sp.
Plate 33.1, figures 6-8

?Kolmodinia cf. **grandis** (Kolmodin), Martinsson, 1962, p. 354, Figure 7B

Description. Trilobate, hinge long, straight, hidden in lateral view by dorsal cusps of broad marginal ridge and L2. Amplete, L1 nearly circular, separated from ovate L3 by deep S1/S2 which surround L2 and extend to the marginal ridge. L1 with large, circular anterodorsal tubercle. Wide marginal ridge along free margin, wrapping around L1 and L3 and extending dorsally as cusps above L1 and L3.

Measurements of holotype, GSC 81000 (in mm): L: 2.8, H: 1.8.

Number of specimens studied: one.

Type. Holotype, GSC 81000.

Occurrence. Road River Group, Avalanche Lake area, Northwest Territories, Section AV7 - 312 m.

Remarks. It is doubtful whether **K.** cf. **grandis** of Martinsson should be compared specifically with **K. grandis** (Kolmodin) because of the poor condition of the type specimen. The present specimen is much more similar to the specimen referred by Martinsson to **K.** cf. **grandis**, and for that reason is compared with it. The L2 of Martinsson's specimen is larger than that of the present specimen, but otherwise both are comparable. The broad, marginal ridge of the Avalanche Lake specimen is complete, whereas that of the Gotland specimen is broken. Lack of a marginal ridge on either of the Gotland specimens is possibly the reason Martinsson was unsure of the systematic position of the genus. **K. kolmodini** is much larger and lacks the posterodorsal projection on L3 of **K. spinosa**; it is also somewhat larger than **K. martinssoni** but is much smaller than **K. grandis**. Also, **K. kolmodini** differs from **K. martinssoni** in having more prominent dorsal cusps on the marginal ridge, much broader sulcation and less prominent L1.

References

Chatterton, B.D.E. and Perry, D.G.
  1983:   Silicified Silurian odontopleurid trilobites from the Mackenzie Mountains; Palaeontographica Canadiana, no. 1.

  1984:   Silurian cheirurid trilobites from the Mackenzie Mountains northwestern Canada; Palaeontographica Beiträg zur Naturgeschichte der Vorzeit, Abteilung A, Band 184, Lieferung 1-4, p. 1-78, 35 plates.

Copeland, M.J.
  1978:   Some Wenlockian (Silurian) Ostracoda from southwestern District of Mackenzie; in Current Research, Part B, Geological Survey of Canada, Paper 78-1B, p. 65-72.

Lenz, A.C.
  1977:   Llandoverian and Wenlockian brachiopods from the Canadian Cordillera; Canadian Journal of Earth Sciences, v. 14, no. 7, p. 1521-1554.

Martinsson, A.
  1962:   Ostracodes of the Family Beyrichiidae from the Silurian of Gotland; Publications from the Palaeontological Institution of the University of Uppsala, Number 41 (also: Bulletin of the Geological Institutions of the University of Uppsala, volume XLI).

Lower Paleozoic stratigraphy of northwestern Melville Island, District of Franklin

M.J. Robson[1]
Institute of Sedimentary and Petroleum Geology, Calgary

Abstract

The Lower Paleozoic succession in the Canrobert Hills comprises three formations: the Canrobert, the Ibbett Bay and the Blackley.

The resedimented carbonate rocks of the Canrobert Formation (Upper Cambrian? to Lower Ordovician) are interpreted as slope deposits. They are overlain by black shales and cherts of the Ibbett Bay Formation which ranges in age from the early Ordovician to Middle Devonian, and is interpreted as a deep water basinal deposit. Above the Ibbett Bay, the Blackley Formation, comprising siltstones, mudrocks, and turbidite packages, forms the local base of the Middle Devonian clastic wedge that represents the closing phase of sedimentation in the Franklinian Geosyncline.

Résumé

La succession du Paléozoïque inférieur dans les collines Canrobert comprend trois formations: celles de Canrobert, d'Ibbett Bay, et de Blackley.

On suppose que les calcaires et dolomites resédimentés de la formation de Canrobert de (Cambrien supérieur? Ordovicien inférieur) ont été déposés dans une zone de talus. Ils reposent sous des schistes argileux et des cherts foncés de la formation d'Ibbett Bay (Ordovicien inférieur au Dévonien moyen) mise en place, selon les auteurs, dans un profond bassin de sédimentation. La formation de Blackley, caractérisée par ses <<siltstones>>, <<mudrocks>> et dépôts de courant de turbidité, constitue la base régionale du bisean clastique (Dévonien moyen) qui correspond à la phase finale de l'épisode de sédimentation du géosynclinal de Franklin.

---

[1] Department of Geology, University of Western Ontario, London N6A 5B7

Introduction

A Lower Paleozoic, deep water basinal sequence on northwestern Melville Island has been divided into three formations: the Cambrian(?) to Middle Ordovician Canrobert Formation, the Middle Ordovician to lower Middle Devonian Ibbett Bay Formation, and the Middle Devonian Blackley Formation. These formations outcrop in the Canrobert Hills north of Ibbett Bay.

A detailed stratigraphic study of the formations was carried out in 1984, and samples were collected for graptolites, trilobites and microfossils. Two sections through the Canrobert and Blackley formations and three sections through the Ibbett Bay Formation were studied at three different localities (Fig. 34.1).

The field stratigraphic study is part of a Master's program at the University of Western Ontario. Guidance and advice have been provided by A. Lenz and by H.P. Trettin of Calgary, Alberta. Field work was carried out as part of the Melville project, a two-year, air-supported field program of the Geological Survey of Canada led by R.L. Christie, Calgary. The author especially appreciates the help given by Dr. Trettin during the first weeks of the field program. Sabine Fuelgen assisted cheerfully throughout the season.

Tentative age determinations for graptolites were provided by A. Lenz.

Canrobert Formation

The Canrobert Formation comprises the oldest exposures on Melville Island. The unit consists of light coloured, resistant limestone and dolostone. The lowest outcrops lie in the core of an anticline, and the base is not exposed. A trilobite collected near the lowest exposures at locality 2 is Ordovician in age (W.H. Fritz, personal communication, 1985).

The section at locality 2 is 463 m thick. The lower 365 m include light greyish yellow, flaggy weathered, interbedded calcareous and dolomitic mudrocks. The calcareous beds pinch and swell, and fine crosslaminae commonly occur in the dolomitic mudrock. The calcareous beds seem to have undergone synsedimentary deformation that has produced boudinage structures. Where this feature is well developed, there is commonly a transition into in situ breccias 0.5 to 4 m in thickness. The laminae in the dolostone are contorted around the solid clasts of limestone.

Above this lower section is a 57 m thick interval of chaotic, poorly sorted, matrix supported conglomerate. The matrix is a calcareous mudrock; clasts are subangular to

subrounded, pebble to cobble sized fragments of chert and massive or flat-laminated carbonate mudrock. No bedding is present in the conglomerate, and its lateral extent is not known.

The uppermost 41 m of the section are predominately medium-grey weathered, thin bedded dolostone with minor black chert or argillaceous mudrock layers. This dolostone and chert also forms clasts in 60 to 150 cm thick beds of flat-pebble conglomerates. The conglomerate is clast supported, well sorted, and has a laminated, crosslaminated, or massive carbonate mudrock matrix.

Toward the top of the unit, a few 6 to 16 m thick intervals of black graptolitic mudrock and bedded chert suggest a gradual transition into the overlying Ibbett Bay Formation. The presence of **Isograptus** and **Tetragraptus** below the last conglomerate, which marks the upper contact, gives the upper age of the Formation as Arenigian.

At Giddy River (locality 3), the outcrops cover a stratigraphic thickness of 369 m. The limestones and dolostones are generally finer grained than those at locality 2, and no conglomerates or in situ breccia beds were found in the studied interval.

The lower 165 m consists of greyish brown, poorly bedded limestone. Packages of thin beds, 0.7 to 2 m thick, appear to form lenses that pinch out along strike. The next 204 m include alternating recessive and resistant units. The recessive units comprise 12-15 m of medium grey to yellow-grey limestone with discontinuous internal colour layering. The pinching and swelling of these beds is similar to that found in the boudinage beds at locality 2. The limestones are massive and resistant, with brownish grey weathered surfaces. Internal laminae, where present, are poorly developed. These massive units contain bioclastic "patches" that appear promising for biostratigraphic purposes.

The exact location of the upper contact of the Canrobert Formation at Giddy River is unknown because of the lack of paleontological control and the absence of conglomerates. The contact is tentatively placed at the change in rock type from massive, brownish grey limestone with bioclastic intervals to the finely laminated, dolomitic mudrock of Unit A, Ibbett Bay Formation (Table 34.1).

The presence of ripple crosslamination in dolo-arenites, and of both carbonate pebbles and black chert pebbles in the same conglomerates indicate that the carbonates of the Canrobert Formation are allogenic. The presence of very fine laminae in the dolomitic mudrocks suggests deposition from a nepheloid layer. Synsedimentary boudinage structures, and the presence of large lobes of slumped beds are attributed to downslope drag, and the thick conglomerate unit appears to be gravity emplaced. The Canrobert Formation is interpreted to be a slope deposit, the more distal version of which is at Giddy River, in the northern part of the study area. The sediments, therefore, evidently were derived from areas to the south.

Ibbett Bay Formation

The Ibbett Bay Formation is conformable above the Canrobert Formation. **Tetragraptus** and **Isograptus** are found near the base (Tozer and Thorsteinsson, 1964), and the upper contact of the formation is placed 200 m above the last occurrence of **Monograptus yukonensis**. The age range of the formation is thus Early Ordovician to late Early Devonian.

The Ibbett Bay Formation is here divided into five members, which form a sequence of alternating recessive, dark units, and more competent, light weathering units (Table 34.1, Fig. 34.2). These members appear to be mappable. The following rocks are present: thick units of

Figure 34.1. *Numbers 1, 2, 3 indicate localities of measured sections, northwestern Melville Island. Locality 3 lies on Giddy River.*

mudrocks (graptolitic shales); dolomitic mudrocks and sediment gravity flows of dolomitic material (both variably replaced by black cherts); calcareous or dolomitic concretions; and bedded black cherts. The rocks range from deeply weathered to crumbling, recessive material, and outcrops are poor.

The formation ranges in thickness from 800(?) m at Giddy River to 1175 m at locality 2, and is about 1300 m thick in the section at locality 1.

The Ibbett Bay Formation, characterized by its dark colour, pelagic fauna, primary and replacement chert, minor resedimented carbonates, and conformable relationships with the Canrobert Formation, is interpreted as a deep water basinal succession.

Figure 34.2. *Stratigraphic sections of lower Paleozoic formations, northwestern Melville Island. Units of the Ibbett Bay Formation are described in Table 34.1.*

283

Table 34.1. Generalized stratigraphy of the Ibbett Bay Formation

Unit	Lithology	Approximate thickness of unit in metres	Total thickness from base in metres
A	Mudrock: recessive, black, cherty, argillaceous (cherts apparently secondary).	60	60
B	Dolomitic mudrock: light coloured, resistant; fine laminae flat or crinkled due to soft sediment deformation.	190	250
C_1	Bedded dolostone and dolomitic sediment gravity flows (10-20 cm): conglomeratic base, minor argillaceous mudrock; variable silicification (25-40% at locality 1, 80-90% at locality 2). At Giddy River: diplograptids, colonial corals.	100	350
C_2	Mudrock: recessive, black, argillaceous; **Monograptus spiralis** toward top.	75	425
D	"Mottled dolostone": light coloured resistant marker; discontinuous inter laminae of darker, fine and coarse grained, lighter material; transition above and below into black argillaceous mudrock.	100	525
E_1	Mudrock: black, argillaceous, laminated; forms poor outcrops.	100	625
E_2	Mudrock: black, argillaceous; with concretionary beds, medium grey, resistant, 10 cm to 1 m thick; and some interbeds of lighter coloured carbonate mudrock. **Monograptus yukonensis.**	170	795
E_3	Mudrock: black, argillaceous; and bedded cherts; some rusty zones.	200	995

Blackley Formation

The Blackley Formation was most recently described by Embry and Klovan (1976). Based on 1984 fieldwork, the unit can described as follows: deeply weathered, light- to medium-grey, argillaceous and silty mudrock and sandstone, with fine- to medium-grained, rust coloured, sideritic(?) sandstones occurring as thin or irregular beds. Micaceous sandstones with pinkish grey weathered surfaces form the bases of turbidite packages. The lower sandstones have scoured bases. The turbidite cycles consist of fine sand to silt grade B-C-D or C-D Bouma sequences. The sandstones form the only prominent outcrops in the formation.

The Blackley Formation was examined in two places; at each locality, a thickness of about 210 m is exposed, and the unit is very deeply weathered. At locality 1, the basal 130 m are characterized by arhythmic alternations of 2 to 10 cm thick grey mudrock or siltstone with thin, sideritic sandstone beds. The upper 80 m comprise resistant sandstone beds, up to 1.5 m in thickness, separated by covered intervals of similar thickness. The topographic relationships suggest that the Blackley Formation is 670 m thick.

The contact between the Blackley Formation and the underlying Ibbett Bay Formation is transitional over about 2 m at locality 2. The basal 65 m consist predominantly of deeply weathered, light grey to yellowish grey, argillaceous and silty mudrock with interbeds of sideritic arenite. Any small-scale grain size variations, sedimentary structures or cyclicity are obscured. Fine grained sandstones and siltstones with fining-upward cycles are exposed from 65 m to 100 m. The upper 110 m have sporadic beds of sandstone in deeply weathered argillaceous strata.

Surface sampling of the Blackley Formation by Tozer and Thorsteinsson (1964) and by Embry and Klovan (1976) has not yielded fossils. A Givetian age is based on spores found in cores from Banks Island (Miall, 1976).

Embry and Klovan (1976) interpreted the Blackley Formation as "a submarine fan composed mainly of turbidites". It represents the earliest deposits of the Middle and Upper Devonian clastic wedge that forms the uppermost sequence in the Franklinian Geosyncline. Data are too few at present to comment on source direction.

Conclusions

Lower Paleozoic time on northwestern Melville Island is represented in part by the Canrobert Formation, the Ibbett Bay Formation, and some of the Blackley Formation.

The sequence consists of a slope deposit, followed by strata accumulated in a deep but not starved basin. More distal representatives lie to the north of proximal members. The Middle Devonian Blackley Formation represents the local beginning of the final sedimentary phase of the Lower Paleozoic geosyncline.

References

Embry, A.F. and Klovan, J.E.
1976: The Middle-Upper Devonian clastic wedge of the Franklinian Geosyncline, Bulletin of Canadian Petroleum Geology, v. 24, p. 485-639.

Miall, A.D.
1976: Proterozoic and Paleozoic geology of Banks Island, Arctic Canada; Geological Survey of Canada, Bulletin 258.

Tozer, E.T. and Thorsteinsson, R.
1964: Western Queen Elizabeth Islands, Arctic Archipelago; Geological Survey of Canada, Memoir 332.

Lochkovian (Early Devonian) rugose corals from Prince of Wales and Baillie Hamilton islands, Canadian Arctic Archipelago

Project 680093

A.E.H. Pedder
Institute of Sedimentary and Petroleum Geology, Calgary

Abstract

Lochkovian rugose corals from the Canadian Arctic Archipelago are illustrated for the first time. Tryplasma sp. and Lythophyllum thorsteinssoni sp. n. are described from the delta or pesavis Zone, in the upper member of the Drake Bay Formation on northwestern Prince of Wales Island. Adinophyllum smithi gen. et sp. n. (family Mucophyllidae) is described from beds equivalent to either the eurekaensis or delta Zone of the same member and region. Stylopleura julli Pedder, Mochlophyllum sp., Lekanophyllum sp. and Lyrielasma sp. are illustrated and discussed from beds equivalent to the eurekaensis Zone, in the middle unit of the Sophia Lake Formation on eastern Baillie Hamilton Island. Corals from all three locations are well dated on evidence provided by brachiopods, trilobites, conodonts and graptolites. The unnamed species of Mochlophyllum and Lekanophyllum are the oldest known representatives of these genera.

Résumé

Les coraux rugosa (Lochkovien) prélevés dans l'archipel Arctique canadien sont illustrés pour la première fois. Les Tryplasma sp. et les Lythophyllum thorsteinssoni n. sp. sont décrits à partir de la zone à delta ou à pesavis, dans le membre supérieur de la formation de Drake Bay dans la partie nord-ouest de l'île Prince de Galles. L'Adinophyllym smithi n. gen. et sp. (Mucophyllidae fam.) décrit, provient de couches équivalentes soit de la zone à eurekaensis, soit de celle à delta du même membre dans la même région. Les Stylopleura julli Pedder, Mochlophyllum sp., Lekanophyllum sp. et Lyrielasma sp. sont illustrés et commentés en fonction de couches équivalentes à la zone à eurekaensis, dans l'unité traversant le centre de la formation de Sophia Lake située dans la partie orientale de l'île Baillie Hamilton. Les coraux provenant de ces trois endroits ont pu être datés avec précision grâce aux preuves fournies par les brachiopodes, les trilobites, les conodontes et les graptolites. Les espèces non désignées des genres Mochlophyllum et de Lekanophyllum constituent les représentants les plus anciens de ces genres.

Introduction and acknowledgments

Lochkovian Rugosa have been made known from several northern regions of the world, including Yukon Territory, Novaya Zemlya, Pay Khoy and Chernyshev ranges, and the northern to polar Urals, but until now, none has been described from the Canadian Arctic Archipelgao.

The known Lochkovian coral faunas from the Canadian Arctic Islands are small, and any discussion of their zoogeographic or evolutionary significance would be premature. However, it is interesting to note that they include only one species common to any other region, and that neither of the two most abundant Lochkovian genera – **Carlinastraea** and **Neomphyma** – is represented in them. Furthermore, two of the three cystiphyllid genera present are confined to younger rocks elsewhere, and the only mucophyllid genus present is apparently endemic to the region.

The author is indebted to R. Thorsteinsson and R.E. Smith for making collections available for study, and to Q.H. Goodbody for accompanying him on Baillie Hamilton Island in 1983. Transport and logistic support in the Arctic Islands were provided by the Polar Continetal Shelf Project for all of the collectors and their assistants. Identifications in animal groups, other than corals, were made mostly by colleagues, as follows: brachiopods by J.G. Johnson and R.E. Smith, trilobites by A.R. Ormiston, conodonts by T.T. Uyeno, and graptolites by R. Thorsteinsson.

Biostratigraphy

Drake Bay Formation. This formation was established by Mayr (1978, p. 23-29) for a predominantly dolostone and silty argillaceous limestone unit with minor amounts of graptolitic shale, occurring on western Prince of Wales Island, where it attains a maximum thickness of about 1550 m, and western Russell Island. Essentially, it is a western carbonate equivalent of the clastic Peel Sound Formation of the eastern regions of the same two islands. Two members of the Drake Bay Formation were recognized by Mayr. The Upper member contains Lochkovian brachiopods (Johnson, 1975; Smith, 1980), trilobites (A.R. Ormiston in Smith, 1980), conodonts (T.T. Uyeno in Smith, 1980, personal communication, 1982) and at least one occurrence of the early Lochkovian graptolite **Monograptus uniformis** (R. Thorsteinsson in Smith, 1980, p. 4). The Upper member also contains Pragian brachiopods, trilobites and conodonts (Ormiston, 1969), and a bed near the top of the formation on northwestern Prince of Wales Island has yielded the late Pragian graptolite **Monograptus yukonensis** (Thorsteinsson and Uyeno, 1981, p. 15). Much of the Lower member of the Drake Bay Formation is unfossiliferous dolostone. However, a conodont, identified as **Pedavis** sp. aff. **thorsteinssoni**, is present in the basal beds of the formation on western Prince of Wales Island (Thorsteinsson and Uyeno, 1981, p. 27), and is considered indicative of late Ludlow time.

Tryplasma sp. and **Lythophyllum thorsteinssoni** sp. n. are described from 18.6 m above the base of an incomplete exposure of the upper part of the Drake Bay Formation. From the same section, Johnson (1975) described **Quadrithyris** Zone brachiopods from both below (GSC loc. C-8214 to C-8217) and above (GSC loc. C-8219) the corals. T.T. Uyeno (personal communication, 1982) isolated **Ozarkodina remscheidensis remscheidensis** from 17 m below (GSC loc. C-8215) and 4 m above (GSC loc. C-8219) the coral bearing bed. He also identified an undetermined subspecies of **Pedavis pesavis** 18 m (GSC loc. C-8214) and 17 m (GSC loc. C-8215) below the same horizon. The age of these two corals is evidently either that of the **delta** or **pesavis** conodont zone.

Adinophyllum smithi gen. et sp. n. occurs 3.5-7.5 m above the base of an 11.5 m thick exposure (Section 10 of Smith, 1980) of the Upper member of the Drake Bay Formation. Brachiopods occur abundantly in the section, but Smith (1980, p. 7) noted that they do not include key **Quadrithyris** Zone genera. Some weight was attached to the presence of the trilobite **Basidechenella laticaudata**, identified by A.R. Ormiston, which, it was said, "could indicate an age of conodont fauna 3". In present zonal terminology, the old conodont fauna 3 is the **delta** Zone. Conodonts, identified by T.T. Uyeno (in Smith, 1980, Fig. 6) as **Ozarkodina remscheidensis remscheidensis** and **O. remscheidensis** cf. **repetitor**, have been obtained from 2.5 m below (GSC loc. C-26911) and 2.5 m above (GSC loc. C-26913) the type stratum of **Adinophyllum smithi**. On these data, the age of **Adinophyllum smithi** is approximately middle Lochkovian (**eurekaensis** or **delta** Zone equivalent).

Sophia Lake Formation. This formation was proposed by Thorsteinssson (in Thorsteinsson and Uyeno, 1981, p. 7-8) for planar bedded limestones and lesser amounts of dolostone, quartzose siltstone and sandstone, shale and, on Devon Island only, gypsum and gypsiferous shale. Outcrops are confined to an arcuate belt in the Sophia Lake area of eastern Cornwallis Island, the Griffin Inlet region of southwestern Devon Island, and the eastern coastal area of Baillie Hamilton Island (Thorsteinsson and Uyeno, 1981, Fig. 5). The type section, which is situated 6 km south of Sophia Lake, near the head of Read Bay, previously comprised Member D of the Read Bay Formation.

The Sophia Lake Formation on Baillie Hamilton Island was referred to as "unnamed Gedinnian limestones" by Ormiston (1967, p. 62). The same Baillie Hamilton outcrops were tentatively assigned to the Stuart Bay Formation by Thorsteinsson and Kerr (1968) and to the Sutherland River Formation by Kerr and others (1977).

Thorsteinsson (1984, p. 273) and Smith (1980, p. 7) recognized a threefold division of the Sophia Lake Formation (Unnamed Lochkovian carbonate of Smith) on Baillie Hamilton Island. The lower unit is about 135 m (Smith, 1980, Section 11) to 190 m (Thorsteinsson, 1984, p. 273) thick, and consists of thin planar limestones with minor amounts of shale and siltstone. A shale near the base of the unit has yielded the early Lochkovian graptolite **Monograptus uniformis angustidens** Pribyl, identified as **M.** cf. **M. uniformis** in Kerr and others (1977, p. 285). The important Lochkovian trilobite **Warburgella rugulosa canadensis** Ormiston ranges through all but the lowest 6 m of the unit. The large, early Lochkovian brachiopod fauna described by Smith (1980) from the unit includes **Orbiculoidea** sp., **Tyersella** sp., **Schizophoria fossula fossula** Smith, **Salopina submurifer** Johnson, Boucot and Murphy, **Gypidula pelagica pyraforma** Smith, **Leptaena nassichuki** Smith, **Iridistrophia johnsoni** Smith, **Barbaestrophia bieleri** Smith, **Strophonella** sp. cf. **S. plasi** Havlíček, **Mesodouvillina equicosta** Smith, **M. tuberosa** Smith, **Ancilotoechia gutta rotunda** Smith, **A.** sp., **Tadschickia(?) crassiforma crassiforma** Smith, **T.(?) crassiforma producta** Smith, **Atrypa nieczlawiensis** Kozlowski, **Notoparmella gilli** Johnson, **N. costalata** Smith, **Arctispirifer canadensis** Smith, **Coelospira exilicosta orbita** Smith, **Protathyris(?)** sp., **Cyrtina** sp., **Ambocoelia** sp., **Howellella** sp. and **Acanthospirifer macdonaldi** Smith. Abundant conodonts have been obtained from the lower unit of the Sophia Lake Formation on Baillie Hamilton Island (Kerr and others, 1977; Uyeno in Smith, 1980; and in Thorsteinsson and Uyeno, 1981). The most important for zonation are **Icriodus woschmidti hesperius** Klapper and Murphy, 163 m above the base of the unit at Washington Point, and **Ozarkodina paucidentata**

Murphy and Matti, **O. remscheidensis repetitor** (Carls and Gandl) and **Amydrotaxis** sp. n. in the uppermost 4 m of the unit, one to two km southwest of Surprise Point (Smith's Section 11).   **O. remscheidensis remscheidensis** (Ziegler) ranges through the upper part of the lower unit. On the basis of the occurrence of **Monograptus uniformis angustidens** near the base of the unit, and of published conodont ranges (Klapper and Johnson, 1980, tables 1, 2; Murphy and Matti, 1982), the bulk of the lower unit of the Sophia Lake Formation on Baillie Hamilton Island is equivalent to the **hesperius** and at least some part of the overlying **eurekaensis** zones of Nevada.

The middle unit of the Sophia Lake Formation on Baillie Hamilton Island consists of about 140 m (Thorsteinsson, 1984, p. 273) to 260 m (Smith, 1980, Section 12) of medium to thin bedded, slightly silty lime-mudstones with subordinate shaly beds.   Faunally, it is characterized by abundant colonial corals, especially favositids, as well as stromatoporoids, bryozoa and brachiopods. The exact stratigraphic position of the Sophia Lake Formation corals described in this paper is not known, but they are certainly from within the lower 100 m of the middle unit.   Genera and species occurring in this part of the formation are **Amphipora** sp., **Favosites** sp., **Cladopora** sp., **Alveolites** sp., **Aulopora** sp., **Stylopleura julli** Pedder, **Mochlophyllum** sp., **Lekanophyllum** sp., **Lyrielasma** sp., **Orbiculoidea** sp., **Schizophoria fossula fossula** Smith, **Gypidula pelagica pyraforma** Smith, **Iridistrophia johnsoni** Smith, **Mesodouvillina equicosta** Smith, **Cymostrophia**(?) sp., **Ancillotoechia gutta rotunda** Smith, **Tadschikia**(?) **crassiforma crassiforma** Smith, T.(?) **crassiforma producta** Smith, **Atrypa nieczlawiensis** Kozlowski, **Spinatrypa**(?) sp., **Meristina**(?) sp., **Cyrtina** sp., **Ambocoelia** sp., **Howellella** sp., **Acanthospirifer macdonaldi** Smith, **A. norfordi** Smith, **Conocardium** sp., **Warburgella rugulosa canadensis** Ormiston, **Ozarkodina remscheidensis remscheidensis** (Ziegler), **O. remscheidensis** cf. **repetitor** (Carls and Gandl), O. sp. 7 of Uyeno, and **Oulodus** sp.   Although the cystimorph genera **Mochlophyllum** and **Lekanophyllum** have not been reported previously in beds as old as Lochkovian (McLean, 1976a), the overall composition of this fauna, and its position above beds equivalent to part of the **eurekaensis** Zone, demand an approximate age assignment equivalent to the middle **eurekaensis** Zone of Nevada.

Smith (1980, p. 17) noted that corals in the middle unit of his Section 12 occur in very silty, slightly argillaceous lime-mudstone-wackestone, and appear to be in growth position. In this paper most of the corals described from the middle unit of the Sophia Lake Formation are from a silt-free lime-packstone, with only subordinate wackestone, and show unmistakable signs of preburial transport and damage.

The upper surface of the upper unit of the Sophia Lake Formation on Baillie Hamilton Island is a present-day erosion surface. According to Thorsteinsson (1984, p. 273), about 440 m of the unit are preserved. Most of the unit consists of thin to very thin bedded, silty lime-mudstones and minor amounts of dolomitic limestone. Features such as lime-mud intraclasts, ripple marks and an impoverished low diversity fauna, dominated by leperditicopid ostracodes, point to a shallow subtidal to intertidal environment. Smith (1980, p. 7) speculated that the unit is not significantly younger than the lower units, and thought that it is also probably equivalent to the **eurekaensis** Zone ("conodont fauna 2").

Figure 35.1.   *Map of the central part of the Canadian Arctic Archipelago with locations of GSC locs. C-8220, C-8234, C-26912 and C-91484.*

Systematic paleontology

Family TRYPLASMATIDAE Etheridge, 1907
Genus **Tryplasma** Lonsdale, 1845

Cyathophyllum subgenus **Tryplasma** Lonsdale, 1845, p. 613.

Type species.   **Cyathophyllum (Tryplasma) aequabile** Lonsdale, 1845, p. 613-614, Pl. A, figs. 7, 7a. The occurrence of the figured specimen was given by Lonsdale as Silurian; Kakva River, east side of the North Ural Mountains. Smaller, unfigured specimens, that "possibly belonged to a distinct species", were said to be from the Silurian or Devonian, Petropavlofsk (**sic**), northernmost Russo-Uralian mines. All of these specimens are missing, and presumed lost, although Rosen and Wise's (1980, p. 148-150) discussion of Murchison's Russian corals suggests this is not necessarily the case.

A neotype, designated and figured by Ivanovskiy and Shurygina (1975, p. 15, Pl. 1, figs. 1a, b) and refigured by Hill (1981, figs. 40, 2a, b), is from the **Favosites regularissimus** Zone on the left bank of Kakva River, 2.5 km above the Karpinsk Highway.   The **F. regularissimus** Zone on Kakva River corresponds to some part of the Vagran Suite of older literature and to the Karpinsk Horizon of recent work (Khodalevich and others, 1982).   Its age is approximately middle Zlichovian to early Dalejan, on the evidence of conodonts (loose range chart accompanying Khodalevich and others, 1982) and goniatites (Chlupáč and Turek, 1983, p. 137-138).

Remarks. A correct synonymy and diagnosis of **Tryplasma** is given in Hill (1981, p. 98). The genus is represented by many named species, ranging in age from Late Ordovician to Early Devonian. It is essentially cosmopolitan, but is not known in the Devonian of the Eastern North Americas Realm.

Tryplasma sp.
Figures 35.2, 35.3

Material. One specimen, GSC 68647, from GSC loc. C-8220.

Description. Corallum solitary, ceratoid; estimated length along the convex side 35 mm; mean diameter at base of calice 15 mm. The peripheral stereozone is 2.5 mm thick and mostly septal in origin. Septa are essentially undifferentiated and consist of blunt spines that only just project into the lumen; about 60 of these spines are visible in a transverse section taken from immediately below the calice. The fine structure is holacanthine, but not well preserved. There are no dissepiments. The tabulae, which are complete and typically flat, are separated from each other by 1.0 to 2.5 mm, and are coated with as much as 0.8 mm of sclerenchyme.

Remarks. This specimen is not a typical example of **Tryplasma**, because of its short, holacanthine and peripherally contiguous septa. It almost certainly represents an unnamed species, but does not constitute sufficient material on which to base a new taxon.

It resembles two poorly known species – **Tryplasma anastasiae** Cherepnina (1970, p. 112-113, Pl. 40, figs. 1a, b) from the early Pragian Yakushin Beds of the Mountain Altay of central Asia, and **T. yanbianense** (He, 1978, p. 170, Pl. 82, figs. 5a, b), from beds said to be equivalent to the late Pragian or early Zlichovian Ganxi Formation, in Szechwan Province, southern China. **T. anastasiae** has less sclerenchyme and a narrower stereozone than the species from Prince of Wales Island, and is said to have rhabdacanthine septa. **T. yanbianense** is larger than the species from Prince of Wales Island and yet has fewer septa (49 septa at a diameter of 22 mm). Also, its septal spines are longer than those of the Prince of Wales specimen.

Family MUCOPHYLLIDAE Hill, 1940

Diagnosis. Family of predominantly solitary corals with horizontal skeletal elements restricted to broad tabulae and peripheral platform (diaphragmatophorous). Two included genera, **Mucophyllum** and **Stylopleura**, are known to have flaring calices at maturity. Septa are radially arranged and not amplexoid. In the unexpanded region of the corallite, the septa are either short and narrowly cuneate, leaving wide interseptal loculae, or they are broad and contiguous, forming a septal stereozone of variable width. In the unexpanded region of a corallite, the trabecular structure is either simple holacanthine (probably secondary), or compound rhabdacanthine; in the expanded part of the corallite, the trabecular structure is entirely rhabdacanthine. Development of long, hollow, supporting rootlets, and absence of septal fossulae, are characteristic of the family.

Included genera. **Mucophyllum** Etheridge, 1894 (=**Mycophyllum** Lang, Smith and Thomas, 1940); **Pseudamplexus** Weissermel, 1897 (=**Pselophyllum** Počta, 1902; **Pseliophyllum** Lang, Smith and Thomas, 1940 and ?**Pseudotryplasma** Ivaniya, 1958); **Kungejophyllum** Sultanbekova, 1971; **Stylopleura** Merriam, 1974; **Adinophyllum** gen. n.; ?**Pseudamplexophyllum** Shurygina, 1968.

Figures 35.2, 35.3. **Tryplasma** sp., both figured specimen GSC 68647, x3.
2, 3. *Longitudinal and transverse sections.*

Remarks. It is not known whether the Mucophyllidae were derived from the Tryplasmatidae by loss of peripheral sclerenchymal tissue, or from the Kodonophyllidae (sensu Hill, 1981, p. 171-175) by development of rhabdacanthine trabecular structure and loss of amplexoid septal ridges. The present author favours the first of these hypotheses, and envisages a similar composition for the Mucophyllidae as that cited by Hill (1981, p. 175-178). However, two genera, **Briantia** Barrois (1889, p. 44-45) and **Ningqiangophyllum** Cao (1975, p. 184), that were tentatively attributed to the Mucophyllidae by Hill, should be excluded from the family. The long, axially dilated and rotated septa, and highly arched tabulae of **Briantia**, and its probable junior synonym **Symphyphyllum** Spasskiy (in Bulvanker and others, 1968, p. 14), necessitate classification with the Kodonophyllidae. Although **Ningqiangophyllum** Cao (1975, p. 184) is a junior homonym of **Ningqiangophyllum** Ge and Yu (1974, p. 171), a substitute name is not required, because **N. tenuiseptatum**, the type species of **Ningqiangophyllum** Cao, is a species of **Pilophyllia** Ge and Yu, 1974 (multiple spellings in Ge and Yu – **Pilophylloia** on p. 170, **Pilophylloides** on p. 170, and **Pilophyllia** on the legend to Plate 78 – are considered stabilized by the use of **Pilophyllia** in Hill, 1981, p. 173). Species of **Pilophyllia** have long, adaxially attenuate, amplexoid septa and broadly arched, closely spaced tabulae, and, because of these morphological features, are better classified with the Kodonophyllidae than the Mucophyllidae.

Genus **Stylopleura** Merriam, 1974

Stylopleura Merriam, 1974, p. 34-35.

Type species. **Stylopleura berthiaumi** Merriam, 1974, p. 35, Pl. 3, figs. 6-20. See Pedder (1985, p. 588) for occurrence.

Stylopleura julli Pedder
Figures 35.4-35.14

Stylopleura sp., Pedder in Jackson and others, 1978, p. 38, Pl. 27, figs. 1-5.
Stylopleura julli Pedder, 1985, p. 589-592, Pl. 70.1, figs. 2-7, 9, 11-23.

Material from Baillie Hamilton Island. Two colonies, GSC 75987, 75988; two silicified fragments recovered from acid residue, GSC 75989, 75990. All from GSC loc. C-91484.

Remarks. The holotype and paratypes of **Stylopleura julli** are from Lochkovian beds, assigned to the **eurekaensis** and **delta** zones, in the headwaters area of Royal Creek, Yukon Territory. The material from Baillie Hamilton Island is more silicified and suffered greater preburial damage than the types. Most of the original description of the species applies

Figures 35.4-35.6. *Stylopleura julli* Pedder, all figured specimen GSC 75987, x2.5.
  4. *Subcalicular transverse section.*
  5. *Longitudinal section of two corallites.*
  6. *Transverse section, mostly near and above calicular bases.*

289

to the new material, although there are some taxonomically insignificant differences. Colonies from Baillie Hamilton Island consist of larger clusters of corallites, and individual corallites are known to have grown to a length of 8 cm or more. Diameters of the unexpanded and expanded calices are comparable in both sets of material, as are the numbers of septa (49 septa at 10 mm diameter, 56 septa at 23 mm diameter and 66 septa at 47 mm diameter in specimens from Baillie Hamilton Island). Silicified fragments from acid residues, such as the specimen depicted in Figure 35.8, show peripherially situated, superposed series of funnel shaped tabular depressions, which may, or may not, lead into hollow supporting rootlets. Further examination of Yukon material has revealed similar depressions, although none was recorded in the original description of the species. Spacing of the tabulae is more variable in specimens from Baillie Hamilton Island (two to eleven in a vertical distance of one cm), and one calicular section, illustrated by Figure 35.14, shows a gerontic rejuvenescent phenomenon, in which a part of the otherwise rhabdacanthine platform is replaced by a series of thin, nontrabecular walls that mimic presepiments.

Genus **Adinophyllum** nov.

Type species. **Adinophyllum smithi** sp. n. Upper member (Lochkovian; equivalent to the **eurekaensis** or **delta** Zone) of the Drake Bay Formation; GSC loc. C-8234, northwestern Prince of Wales Island.

Diagnosis. Solitary genus of mucophyllid corals having a calice approaching the shape of an inverted cone. Septa rhabdacanthine, long and greatly expanded; predominantly contiguous in the subcalicular region. Tabulae few or entirely lacking.

Remarks. **Adinophyllum** is closely related to **Pseudamplexus**, but differs from it by having greatly enlarged septa that essentially displace the tabularium. At present, the type species is the only species attached to the new genus.

The name derives from the Greek words, **adinos** meaning thick or crowded, and **phyllon** meaining a leaf.

Adinophyllum smithi sp. n.
Figures 35.15-35.27

Type series. Holotype, GSC 75991 from GSC loc. C-26912. Paratype, GSC 75992 from GSC loc. C-8234.

Figures 35.7-35.14. (opposite)

Stylopleura julli Pedder

7. *Figured specimen GSC 75989, silicified fragment showing change from spinose septal structure below mature calice, to the nonspinose rhabdacanthine septal structure of the mature, expanded calice, x5.*
8. *Figured specimen GSC 75990, silicified fragment showing lateral, funnel shaped depressions on the tabulae, and short septal spines, x5.*
9, 10. *Figured specimen GSC 75988, longitudinal sections of the distal parts of mature corallites, x2.5.*
11. *Figured specimen GSC 75988, transverse section of part of a mature, expanded calice with four offsets; same corallite as one depicted in Figures 10, 14, x2.5.*
12, 13. *Figured specimen GSC 75987, longitudinal sections, x2.5.*
14. *Figured specimen GSC 75988, transverse section discussed in text; same corallite as one depicted in Figures 10, 11, x2.5.*

Description. Corallum solitary, trochoid, large, attaining a maximum diameter of at least 50 mm, and a length of 75 mm measured along the convex side. The well preserved exterior of the holotype bears septal furrows and interseptal ridges of about the same amplitude, as well as fine growth rings. Scars of two broken radiciform processes were present, close to the apical tip of the holotype, before it was sectioned. Calice deep, accounting for two thirds of the length of the corallum, and shaped like an inverted cone. The distal region of the calice is excentric due to the greater length of the septa on the convex side of the coral.

Near the rim of the calice, minor and major septa are undifferentiated, and are separated by shallow, adaxially open, interseptal loculi. As the coral enlarges and the calice migrates away from the proximal tip of the corallum, the septa thicken, and the minor septa, which are mostly less than 3.0 mm long, become engulfed by contiguous major septa. Adaxially, some major septa fuse with others, or, like the minor septa, are themselves engulfed by other pairs of major septa. In this way, the lower part of the corallum fills with septal skeleton. Thin sections of early stages (mean diameters 5.0, 7.5 and 10.5 mm) of the holotype have been prepared, but poor preservation obscures the boundaries between contiguous septa, so that it is not possible to count septa accurately in these stages. In later stages of the holotype, numbers of septa at given mean diameters are 43 x 2 at 26 mm, 48 x 2 at 33 m, and 49 x 2 at 42 mm. Despite inadequacies of the preservation, especially in the paratype, it is clear that the trabecular structure is rhabdacanthine in the thickened parts of the septa.

A few peripherally situated partitions are suspended between adjacent septa in the most distal part of both specimens. As the material has been prepared, the partitions are visible only in transverse sections (left hand side of Fig. 35.15), and it is not known whether they are true dissepiments. Their alignment suggests a rejuvenescent feature. Concave tabulae may be present (none in the holotype; six in the paratype, Fig. 35.26) above the level where the subcalicular diameter is 25 mm or more. Some of these tabulae are overlain by thick septal skeleton, others bear only a thin layer (0.1-0.15 mm thick) of apparently structureless sclerenchyme.

Remarks. The trivial name is a patronym for R.E. Smith, who collected the type specimen and described the accompanying brachiopod fauna.

Family CYSTIPHYLLIDAE Milne Edwards and Haime, 1850
Subfamily CYSTIPHYLLINAE Milne Edwards and Haime, 1850
Genus **Lythophyllum** Wedekind, 1925

Lythophyllum Wedekind, 1925, p. 32-33.
Nardophyllum Wedekind, 1925, p. 36.
Plagiophyllum Wedekind and Vollbrecht, 1931, legend to Pl. 17 (Pl. 3 of reprints); 1932, p. 113-114, 115.
Lytophyllum Wedekind and Vollbrecht, 1932, p. 115 (**nomen vanum**).
Lithophyllum Lang, Smith and Thomas, 1940, p. 78 (**nomen vanum**).
Wedekindophyllum Stumm, 1949, p. 39 (**nomen substitutum** for "Lithophyllum (as **Lythophyllum**) Wedekind, 1925 (not Mueller, 1859), p. 32").
Dansikophyllum Ulitina, 1963, p. 5, 15, in part (**nomen nudum**).

15

16

17

18

19

20

21

22

23

24

Patridophyllum Ulitina, 1963, p. 5, 15 (nomen nudum).
Patridophyllum Ulitina in Sytova and Ulitina, 1966, p. 207 (nomen nudum).
Patridophyllum Ulitina, 1968, p. 86.

Type species of Lythophyllum, Lytophyllum, Lithophyllum (Lang, Smith and Thomas, 1940) and Wedekindophyllum. Lythophyllum marginatum Wedekind, 1925, p. 33, Pl. 6, figs. 32, 33. Lower Stenophyllumschichten, middle Middle Devonian; Dachsberg, near Gerolstein, Eifel region, Germany. Birenheide (1964, p. 33) considered this species to be a junior synonym of Cystiphyllum macrocystis Schlüter, 1889, which he incorrectly (Weyer, 1971) referred to Plasmophyllum. In current terminology, the type stratum of Lythophyllum marginatum is probably in the early Givetian Loogh Schichten.

Type species of Nardophyllum and Plagiophyllum. Nardophyllum exzentricum Borchers in Wedekind, 1925, p. 36-37, Pl. 9, fig. 59. Beds overlying the upper Stenophyllumschichten, middle Middle Devonian; Plateau Berndorf, near Hillesheim, Eifel region, Germany. This species was also considered synonymous with Cystiphyllum macrocystis Schlüter, 1889, by Birenheide (1964, p. 33). In current terminology, the type stratum of Nardophyllum exzentricum is certainly Givetian and presumably in the Cürten Schichten.

Type species of Patridophyllum. Patridophyllum paternum Ulitina, 1968, p. 86-88, Pl. 18, figs. 1a-d; Pl. 19, figs. 1a, b. Upper Eifelian Stage; right bank of the Arpa River, near the village of Danzig, Nakhichevan ASSR, Soviet Union. Mamedov (1983, loose fig. 5) and Spasskiy (1983, Table 1) assign the type horizon to the late Dalejan or early Eifelian (patulus Zone) Sharurskaya Suite.

Remarks. In previous Canadian cystiphyllid systematics (McLean, 1976a, 1976b; Pedder and McLean, 1982), Lythophyllum was put in synonymy with Cystiphylloides Chapman, 1893. Here, Cystiphylloides is reserved for fasciculate species, and Lythophyllum is used for solitary cystiphyllid species that have distinct centric or excentric septal crusts, and weak, or nonexistant septal crests.

The synonymy given above is not necessarily complete. Genera that might be added include Skoliophyllum Wedekind (1937, p. 50, 52) and Praenardophyllum Spasskiy (1955, p. 99), both with type species characterized by progressively offset calices. Comanaphyllum H. Flügel (in Flügel and Flügel, 1961, p. 388-389) may belong here also, although the type species apparently lacks proper septal crusts. Pseudozonophyllum Wedekind (1924, p. 25-28) and Paralithophyllum Wedekind (1925, p. 35-36) are other possible synonyms, but their type species are not strictly determinable.

Figures 35.15-35.24. (opposite)

Adinophyllum smithi gen. et sp. n., all holotype GSC 75991.

15, 19-21. Transverse sections through calice, x2.
    16. Longitudinal section below calice, x3.
17, 23, 24. Transverse sections below calice, x4.
    18. Part of transverse section showing rhabdacanthine septal structure, x10.
    22. Part of the exterior surface of the corallum, x5.

Stumm (1949, p. 39) introduced the name Wedekindophyllum because he believed that Lythophyllum Wedekind (1925) should be spelled Lithophyllum and that it is therefore a homonym of Lithophyllum Müller (1859, p. 62). He was wrong on two counts. Firstly, the change of spelling is illegal, and secondly, Lithophyllum Müller (1859, p. 62) is, itself, a nomen nullum, being a misspelling of Lithophyllium (Müller, 1858, p. 154, 155; 1859, p. 52). Lithophyllium Müller in a radiolarian genus.

Lythophyllum thorsteinssoni sp. n.
Figures 35.28-35.36

Type series. Holotype, GSC 68187 and paratypes GSC 68188-68191, all from GSC loc. C-8220.

Diagnosis. Ceratoid to subcylindrical species of Lythophyllum with a maximum known length of 65 mm and mean diameter of 16 mm. Septal crusts centric and up to 1.4 mm thick. Tabularium distinct from dissepimentarium.

Description. Corallum solitary, ceratoid in early stages, subsequently subcylindrical with minor rejuvenescences. Absence of radiciform processes, and pronounced twisting of the direction of growth, indicate that the coral was not firmly attached to the substrate. Length, measured along the predominately convex side, and maximum mean diameter of the largest specimen, 65 mm and 16 mm, respectively. The exterior of the corallum bears fine and coarser growth rings; septal furrows and interseptal ridges are not present. Calice shallow, less deep than wide, with gently sloping sides and an undulant, subhorizontal base.

Septal apparatus weak, comprising irregularly spaced septal crusts, that are centric rather than excentric, and cover entire calical surfaces. The septal crusts have a maximum observed thickness of 1.4 mm, and, at the periphery, locally incorporate short, but coarse, and commonly contiguous monacanths. The longest peripheral monacanths project only 0.2 mm into the lumen, and they are not differentiated into major and minor orders of septa.

Most of the dissepiments are large and steeply inclined towards the axis. On the whole, compared with other species of the genus, the dissepiments are well differentiated from the tabulae. Although the tabularium is dominated by broad, gently sloping, convex plates, a few of the tabulae are complete and flat. The tabularium occupies between one half and two thirds of the total diameter of the corallum.

Remarks. Lythophyllum thorsteinssoni resembles several European and Asian species more than other North American species. Soshkina (1936, p. 27-33, figs. 7-20) erected three species – Lythophyllum minimum, L. aconicum and L. platycalix – on material from a single bed, said to be Eifelian, exposed on Malyi Patok River, on the western slope of the Northern Urals. In 1949 (p. 52, Pl. 13, figs. 1a-f), she proposed yet another name – Nardophyllum vermiforme – for a similar specimen from the same bed and locality. All four species were put in synonymy by Ivanovskiy and Shurygina (1980, p. 17) under the name Zonophyllum minimum (Soshkina). The synonymy seems correct, although the species is better retained in Lythophyllum. L. minimum Soshkina is similar to L. thorsteinssoni, especially in size (adult length 30-70 mm; adult diameter 11-15 mm), but has more, and therefore on average, smaller dissepiments.

The new species also resembles Lochkovian specimens identified as Pseudomicroplasma devonica (Soshkina) by Sytova (1968, p. 59-60, Pl. 3, figs. 4a, b) and Lavrusevich (1968, p. 126, Pl. 12, figs. 6a, b) from the Borshchov Horizon of Podolia and the Shishkat Horizon of central Tadzhikistan.

Figures 35.25-35.27. **Adinophyllum smithi** gen. et sp. n., all paratype GSC 75992, x2.
　　　25, 27. Transverse sections.
　　　26. Longitudinal section intersecting six tabulae.

Figures 35.28-35.36. **Lythophyllum thorsteinssoni** sp. n., all x3.
　　　28, 31. Paratype, GSC 68188, transverse and longitudinal sections.
　　　29, 32, 35, 36. Holotype, GSC 68187, three transverse and a longitudinal section.
　　　30, 33. Paratype, GSC 68189, transverse and longitudinal sections.
　　　34. Paratype, GSC 68191, longitudinal thin section.

Compared with **L. thorsteinssoni**, the Russian forms have much fewer and thinner septal crusts, and they have a peripheral stereozone that is independent of the septal crusts. Like the poorly known type specimen of **Microplasma devonicum** Soshkina (1937, p. 79-80, 99, Pl. 15, figs. 5, 6), which is probably from the Zlichovian to Dalejan Karpinsk Horizon (**Favosites regularissimus** Zone according to Ivanovskiy and Shurygina, 1975, p. 35) on the right bank of Kakva River, 2.5 km above the Kakva Ferry, on the eastern slope of the central Urals, Sytova's and Lavrusevich's specimens have been considered to be solitary examples of **Loboplasma** by Pedder and McLean (1982, p. 69).

The coral named **Pseudomicroplasma minima** by Goryanov (in Bulvanker and others, 1968, p. 26-27, Pl. 10, figs. 2a, b), from the Pragian Talbulak Horizon of central Tadzhikistan, resembles **Lythophyllum thorsteinssoni** in some respects, but it is much smaller (maximum diameter said to be 7 mm) and may have significantly weaker septal crusts and a stronger peripheral stereozone. In any event, Goryanov's name appears to be an uncorrected primary homonym of **Pseudomicroplasma minima** Cherepnina (1967, p. 170-171, Pl. 3, figs. 3, 4) which is from the Eifelian Shiverta Beds of the Gornoy Altay, and is not similar to **L. thorsteinssoni.**

Lythophyllum distortum (Jin and He, 1982, p. 144, Pl. 36, figs. 1a-f) from the Dalejan Dale Member of the Sipai Formation of Xiangzhou xian (county), Guangxi Province, southern China, also resembles the new species. It is, however, larger (maximum mean diameter at least 22 mm), has thinner, excentric septal crusts and a relatively narrower dissepimentarium with more steeply inclined and elongate dissepiments.

The trivial name is a patronym for R. Thorsteinsson, distinguished arctic geologist and collector of the type series.

Subfamily DIGONOPHYLLINAE Wedekind, 1923
Genus **Mochlophyllum** Wedekind, 1923

Mochlophyllum Wedekind, 1923, p. 31, 35.
Bothriophyllum Vollbrecht, 1926, p. 220 (nomen imperfectum).
Uralophyllum Soshkina, 1936, p. 44-45.

Type species of **Mochlophyllum**. **Cyathophyllum maximum.** Originally, Wedekind (1923, p. 35) gave neither authorship nor reference to identify the species. However, in 1925 (p. 39) he indicated that it is "Mesophyllum" maximum Schlüter (1889, p. 70). This species was founded as **Actinocystis maxima** by Schlüter in 1882 (p. 207) and has been revised under the name **Plasmophyllum (Mesophyllum) maximum maximum** by Birenheide (1964, p. 43-44, Pl. 7, figs. 30, 31; Pl. 8, fig. 32; Pl. 15, fig. 74; Pl. 28, fig. 136). The lectotype (Birenheide, 1964, p. 42) is one of Schlüter's syntypes, sectioned by Wedekind and first illustrated by Vollbrecht (1926, Pl. 15, fig. 2). According to Birenheide, it is from the Rechert or Nims Horizon of the Junkerberg Schichten (Eifelian) on the south slope at Auberg, Gerolsteiner Mulde, Eifel region, Germany.

Type species of **Uralophyllum**. **Uralophyllum unicum** Soshkina, 1936, p. 45-49, 73, figs. 43-46. Lower Middle Devonian (Soshkina, 1936, Table 1), Bed 5; Outcrop 8, River Malyi Patock, western slope, northern Urals. Later, Soshkina (1952, p. 81) assigned the type horizon to the Biya Beds. Sapel'nikov and Mizzens (1980, table on p. 34, 35) equate the Biya Beds with the **patulus** conodont zone, which straddles the Dalejan-Eifelian boundary. In the most recent revision of **U. unicum** by Ivanovskiy and Shurygina (1980, p. 19, Pl. 4, figs. 2a, b) the species is referred to the genus **Digonophyllum.**

37   **38**

Figures 35.37, 35.38. Mochlophyllum sp., both figured specimen GSC 68838, x3.
37, 38. Longitudinal and transverse sections of an abraded specimen.

295

Remarks. The generic name **Bothriophyllum** is invalid for want of a named species. Essentially, **Mochlophyllum** differs from **Digonophyllum** by possessing abundant discrete, crossbar carinae, and differs from **Mesophyllum** by having substantially expanded septa in the axial region.

<center>

Mochlophyllum sp.
Figures 35.37, 35.38

</center>

Material. One specimen, GSC 68838, from GSC loc. C-91484.

Remarks. The single available specimen represents a new species, but is incomplete, due to both preburial abrasion and present-day damage, and is also affected by dolomite replacement. It is characterized by having well developed septa, an elongated fossula surrounded by sclerenchyme that thickens septa and tabulae alike, discrete, crossbar carinae and some lateral dissepiments.

This occurrence is the earliest known of the genus, and is the only Canadian occurrence known to the author.

<center>

Genus **Lekanophyllum** Wedekind, 1924

</center>

Lekanophyllum Wedekind, 1924, p. 29-34 (in part, includes a species of **Mesophyllum**).

Type species. **Lekanophyllum punctatum** Wedekind, 1924, p. 30, 34, figs. 36-38. "**Dohmophyllum**-Stuffe", Middle Devonian; "Schurf" on the south slope, Auburg, Gerolsteiner Mulde, Eifel Region, Germany. Birenheide (1968, p. 23) assigned the type horizon to the Eifelian Junkerberg Schichten.

Remarks. A full synonymy and diagnosis of **Lekanophyllum** is given in Pedder and McLean (1982, p. 75).

<center>

Lekanophyllum sp.
Figures 35.39-35.42

</center>

Material. Two specimens, GSC 75993, 75994, both from GSC loc. C-91484.

Remarks. Other than differences in apparent adult diameters (19 mm in GSC 75994; 29 mm in GSC 75993), the specimens have similar morphology and presumably are conspecific. The species is probably new, but both specimens are far from complete and it would be inappropriate to found a new taxon on them. They are entirely typical of **Lekanophyllum**, despite being the earliest known examples of the genus.

<center>

Family PTENOPHYLLIDAE Wedekind, 1923
Subfamily PTENOPHYLLINAE Wedekind, 1923
Genus **Lyrielasma** Hill, 1939

</center>

Lyrielasma Hill, 1939, p. 243-244.

Type species. **Cyathophyllum subcaespitosum** Chapman, 1925, p. 112, Pl. 13, figs. 15-16b. "Silurian (Yeringian)"; Cave Hill, Lilydale, Victoria, Australia. The name is a junior primary homonyn of **Cyathophyllum subcaespitosum** Meek, 1873, p. 470; 1877, p. 60-61, Pl. 5, figs. 4-4b, and has been replaced by **Lyrielasma chapmani** Pedder, 1967, p. 5. The age of the Lilydale Limestone is Pragian (Philip and Pedder, 1967; Strusz, 1972).

Figures 35.39-35.42. Lekanophyllum sp., all x3.
    39, 40. Figured specimen GSC 75993, longitudinal and transverse sections of an abraded specimen.
    41, 42. Figured specimen GSC 75994, transverse and longitudinal sections of an abraded specimen.

Diagnosis. Ptenophyllid genus with fasciculate corallum produced by nonparricidal marginarial budding. Septa of both orders normally complete, variably carinate, expanded peripherally to form a narrow to broad stereozone. Trabeculae moderately coarse, horizontal to only slightly elevated adaxially. Dissepimentarium narrow, with inwardly sloping surface; presepiments rare, normally absent. Tabularium typical of family.

Remarks. Most specimens of **Lyrielasma chapmani** from the type locality are single corallites, but this is believed to be due to post mortem damage sustained in a high energy environment. The type specimen is fasciculate (Pedder, 1967, Pl. 1, figs. 9, 13) and Philip (1962, Pl. 28, fig. 6) has illustrated a topotype with abundant offsets.

<div align="center">

Lyrielasma sp.
Figures 35.43-35.46

</div>

Material. Three specimens, GSC 75995-75997, from GSC loc. C-91484.

Remarks. The material from Baillie Hamilton Island suffered severe preburial damage, and also has been adversely affected by stylolitization. It probably represents a new species, although it is similar, especially in respect to the short minor septa and dissepimentarial morphology, to **Lyrielasma crassiseptatum**, described by Cherepnina (1970, p. 115, Pl. 40, figs. 4a, b; Pl. 41, fig. 1) from the early Pragian Yakushin Beds of the Mountain Altay region of central Asia. One obvious difference between the two is that whereas the Canadian species has 20x 2 to 23 x 2 septa at corallite diameters of 7.5 to 9.0 mm, **L. crassiseptatum** is reported to have no more than 18 x 2 septa in corallites with diameters as large as 10.0 mm.

Most of the described species of **Lyrielasma** fall within the range of Pragian to Middle Devonian, and consequently are younger than the species found on Baillie Hamilton Island. However, Lochkovian occurrences of **Lyrielasma** are known in the Elmside Formation of New South Wales (Picket in Bradley, 1982, p. 49) and in the Beck Pond Limestone of Maine (Oliver, 1960, p. 10-12, Pl. 2, figs. 1-6; Pl. 3, figs. 1-5). Specimens identified as species of **Weissermelia** by Guo (1978, p. 56, Pl. 15, figs. 6a-7b), from the supposedly Late Silurian Bateraobao Group in the region northwest of Bailingmiao in Inner Mongolia, resemble **Lyrielasma** more than **Weissermelia**, but their age is not beyond doubt, and may also be Lochkovian.

Locality register

GSC loc. C-8220. Drake Bay Formation, Upper member, 18.6 m above base of section, 195.2 m below top of section; **delta** or **pesavis** Zone. East side of Drake Bay, northwestern

---

Figures 35.43-35.46

Lyrielasma sp., all x4.

43. *Figured specimen GSC 75996, transverse and oblique sections.*
44. *Figured specimen GSC 75995, slightly oblique transverse section of an abraded and stylolitized corallite.*
45. *Figured specimen GSC 75995, longitudinal section of an abraded corallite and offset, both affected by stylolites.*
46. *Figured specimen GSC 75997, transverse and longitudinal section of abraded and stylolitized corallites.*

Prince of Wales Island; 73°29'40"N latitude, 100°35'45"W longitude; UTM Zone 14x, 449700 mE, 8156750 mN. Collected by R. Thorsteinsson, 1970. **Favosites** sp., **Tryplasma** sp., **Lythophyllum thorsteinssoni** Pedder. Samples (GSC loc. C-8214, C-8215) from 17-18 m below have yielded **Protocortezorthis carinatus** Smith?, **Schizophoria** sp., **Plicogypa thorsteinssoni** (Johnson), **Iridistrophia** (?) sp., **Cymostrophia**(?) sp., **Machaeraria** sp., **Atrypa** sp., **Ozarkodina remscheidensis remscheidensis** (Ziegler), **Pedavis pesavis** subsp. n. A sample (GSC loc. C-8219) from 4 m above has yielded **Schizophoria** sp., **Plicogypa thorsteinssoni** (Johnson), **Leptaena** sp., **Cymostrophia** sp., **Machaeraria** sp., **Atrypa** sp., **Nucleospira** sp., **Undispirifer** sp., **Ozarkodina remscheidensis remscheidensis** (Ziegler).

GSC loc. C-8234. Drake Bay Formation, Upper member, approximately 6.0-7.5 m above base of section, 4.5-6.0 m below top of section; **eurekaensis** or **delta** Zone. Unnamed creek between Cape John Dyer and Harrison Point, northwestern Prince of Wales Island; 73°26'15"N latitude, 101°17'30"W longitude; UTM Zone 14x, 427250 mE, 8150850 mN. Collected by R. Thorsteinsson, 1970. **Adinophyllum smithi** Pedder, **Protocortezorthis quadriforma** Smith, **Gypidula dyerensis** Smith, **Iridistrophia thorsteinssoni** Smith, **Mesodouvillina** sp., **Cymostrophia** sp., **Asymmetrochonetes spinalonga** Smith, **Ancillotoechia magnaplica** Smith, **Atrypa** sp. cf. **A. nieczlawiensis** Kozlowski, **Howellella** sp., **Cyrtina maclennani** Smith, **Basidechenella laticaudata** Ormiston, **Pedavis pesavis** subsp. n., **Pelekysgnathus** sp. n., **Ozarkodina wurmi** (Bischoff and Sannemann), **O. remscheidensis remscheidensis** (Ziegler), **O. remscheidensis** cf. **repetitor** (Carls and Gandl) form approaching **Pandorinellina optima** Moskalenko.

GSC loc. C-26912. Drake Bay Formation, Upper member, 3.5 m above base of section, 8.0 m below top of section; **eurekaensis** or **delta** Zone. Same geographical location as GSC loc. C-8234. GSC loc. C-26912 collected by R.E. Smith, 1973. **Adinophyllum smithi** Pedder. A sample (GSC loc. C-26911) from 2.5 m below has yielded **Crania** sp., **Schizophoria protonevadensis** Smith, **Salopina submurifer** Johnson, Boucot and Murphy, **Skenidioides** sp., **Gypidula dyerensis** Smith, **Iridistrophia thorsteinssoni** Smith, **Mesodouvillina** sp., **Asymmetrochonetes spinalonga** Smith, **Machaeraria obesa** Smith, **Ancillotoechia magnaplica** Smith, **Spirigerina** sp., **Atrypa** sp., **Nucleospira** sp., **Undispirifer laeviplicatus** (Kozlowski), **Cyrtina maclennani** Smith, **Ambocoelia** sp., **Ozarkodina remscheidensis remscheidensis** (Ziegler), **O. remscheidensis** cf. **repetitor** (Carls and Gandl), **Pedavis** sp. A sample (GSC loc. C-26913) from 2.5 m above has yielded **Protocortezorthis quadriforma** Smith, **Schizophoria protonevadensis** Smith, **Gypidula dyerensis** Smith, **Iridistrophia thorsteinssoni** Smith, **Mesodouvillina** sp., **Cymostrophia** sp., **Leptaena** sp., **Ancillotoechia magnaplica** Smith, **Atrypa** sp., **Nucleospira** sp., **Undispirifer laeviplicatus** (Kozlowski), **Cyrtina maclennani** Smith, **Ambocoelia** sp., **Ozarkodina remscheidensis remscheidensis** (Ziegler), **O. remscheidensis** cf. **repetitor** (Carls and Gandl), **Pedavis** sp.

GSC loc. C-91484. Sophia Lake Formation, near base of middle unit; **eurekaensis** Zone equivalent. Unnamed stream, 1.7 km inland from the east coast of Baillie Hamilton Island and 11 km south of Surprise Point; 75°53'05"N latitude, 94°28'00"W longitude; UTM Zone 15x, 460100 mE, 8423500 mN. Collected by A.E.H. Pedder, 1983. **Amphipora** sp., undet. bulbous stromatoporoid, **Favosites** sp., **Cladopora** sp., **Alveolites** sp., **Aulopora** sp., **Stylopleura julli** Pedder, **Mochlophyllum** sp., **Lekanophyllum** sp., **Lyrielasma** sp., undet. trepostomatous bryozoan, **Conocardium** sp., **Ozarkodina remscheidensis remscheidensis** (Ziegler), **Oulodus** sp.

References

Barrois, C.E.
1889: Faune du calcaire d'Erbray (Loire Inférieure); Société géologique du Nord, Mémoires, tome 3, pt. 1. p. 1-348.

Birenheide, R.
1964: Die "Cystimorpha" (Rugosa) aus dem Eifeler Devon; Senckenbergischen Naturforschenden Gesellschaft, Abhandlungen ⁵07.

1968: Die Typen der Sammlung Wedekind aus der Gattung **Plasmophyllum** (Rugosa; Mitteldevon); Senckenbergiana lethaea, Band 49, p. 1-37.

Bradley, G.M.
1982: Elmside Formation; in The Silurian System in New South Wales, ed. J.W. Pickett; Geological Survey of New South Wales, Bulletin 29, p. 49-50.

Bul'vanker, E.Z., Goryanov, V.B., Ivanovskiy, A.B., Spasskiy, N.Ya., and Shchukina, V.Ya.
1968: Novye predstaviteli chetyrekhluchevykh korallovykh polipov SSSR; in Novye vidy drevnikh rasteniy i bespozvonochnykh SSSR, vypusk 2, chast' 1, ed. B.P. Markovskiy; Vsesoyuznyy Nauchno-Issledovatel'skiy Geologicheskiy Institut (VSEGEI), Izdatel'stvo "Nedra", Moskva, p. 14-45, 304-343.

Cao Xuan-duo
1975: Rugosa; in Early Paleozoic stratigraphy of the western part of Dabashan, ed. The Geological Press; Geological Publishing House, Beijing, p. 179-195, 298, 300-321, 323 (Chinese).

Chapman, F.
1925: New or little-known fossils in the National Museum. Part XXVIII. — Some Silurian rugose corals; Royal Society of Victoria, Proceedings, new ser., v. 37, p. 104-118.

Cherepnina, S.K.
1967: Novye vidy srednedevonskikh rugoz Gornogo Altaya; in Nekotorye voprosy geologii zapadnoy Sibiri, ed. V.A. Khakhlov; Izdatel'stvo Tomskogo Universiteta, Tomsk, p. 168-175.

1970: Novye rugozy iz nizhnedevonskikh otlozheniy Gornogo Altaya; in Novye vidy paleozoyskikh mshanok i korallov, ed. G.G. Astrova and I.I. Chudinova; Izdatel'stvo "Nauka", Moskva, p. 112-116, 165.

Chlupáč, I. and Turek, V.
1983: Devonian goniatites from the Barrandian area, Czechoslovakia; Ustředního Ustavu Geologického, Rozpravy, svazek 46.

Flügel, E. and Flügel, H.
1961: Stromatoporen und Korallen aus dem Mittel-Devon von Feke (Anti-Taurus); Senckenbergiana lethaea, Band 42, p. 377-409.

Ge Zhi-zhu and Yu Chang-min
1974: Silurian corals; in A handbook of the stratigraphy and paleontology in southwest China, ed. Nanking Institute of Geology and Paleontology Academia Sinica; Science Press, Beijing, p. 165-173 (Chinese).

Guo Sheng-zhe
1978: Late Silurian tetracorals from northern Bailingmiao of the Autonomous Region of Inner Mongol; Professional Papers of Stratigraphy and Palaeontology, no. 6, p. 50-68 (Chinese).

He Yuan-xiang
1978: Subclass Rugosa; in Atlas of fossils of southwest China. Sichuan volume, Part 1. From Sinian to Devonian, ed. Chengdu Institute of Geology and Mineral Resources; Geological Publishing House, Beijing, p. 98-179, 555-568 (Chinese).

Hill, D.
1939: The Devonian rugose corals of Lilydale and Loyola, Victoria; Royal Society of Victoria, Proceedings, new ser., v. 51, p. 219-256.

1981: Treatise on invertebrate paleontology. Part F. Coelenterata. Supplement 1. Rugosa and Tabulata, ed. C. Teichert; Geological Society of America and University of Kansas Press, Boulder and Lawrence, xl + 762 p. (2v.).

Ivanovskiy, A.B. and Shurygina, M.V.
1975: Reviziya rugoz Urala; Akademiya Nauk SSSR, Sibirskoe Otdelenie, Instituta Geologii i Geofiziki, Trudy, vypusk 218.

1980: Reviziya devonskikh rugoz Urala; Akademiya Nauk SSSR, Paleontologicheskogo Instituta, Trudy, tom 186.

Jackson, D.E., Lenz, A.C., and Pedder, A.E.H.
1978: Late Silurian and Early Devonian graptolite, brachiopod and coral faunas from northwestern and arctic Canada; Geological Association of Canada, Special Paper no. 17.

Jin Shan-yu and He Jin-han
1982: The Devonian rugose corals of Guangxi, their sequence and systematic descriptions; in The Devonian biostratigraphy of Guangxi and adjacent area, ed. Bai Shun-liang, Jin Shan-yu and Ning Zhong-shan; Beijing University Press, p. 109-148, 160-165, 188-202.

Johnson, J.G.
1975: Devonian brachiopods from the **Quadrithyris** Zone (Upper Lochkovian), Canadian Arctic Archipelago; Geological Survey of Canada, Bulletin 235, p. 5-57.

Kerr, J.W., McLaren, D.J., and Thorsteinsson, R.
1977: Canadian Arctic Archipelago; in The Silurian-Devonian Boundary, ed. A. Martinsson; International Union of Geological Sciences, ser. A, no. 5, p. 281-288.

Khodalevich, A.N., Breyvel', M.G., Antsygin, N.Ya., Bogoyavlenskaya, O.V., Breyvel', I.A., Zenkova, G.G., Nasedkina, V.A., Petrova, L.G., Shurygina, M.V., and Yanet, F.E.
1982: O granitse nizhnego i srednego devona na vostochnom sklone Urala; in Biostratigrafiya pogranichnykh otlozheniy nizhnego i srednego devona. Trudy polevoy sessii Mezhdunarodnoy podkomissii po stratigrafii devona Samarkand, 1978, ed. B.S. Sokolov and M.A. Rzhonsnitskaya; Nauka, Leningradskoe Otdelenie, p. 148-151.

Klapper, G. and Johnson, J.G.
1980: Endemism and dispersal of Devonian conodonts; Journal of Paleontology, v. 54, p. 400-455.

Lang, W.D., Smith, S., and Thomas, H.D.
1940: Index of Palaeozoic coral genera; British Museum (Natural History), London, vii + 231 p.

Lavrusevich, A.I.
1968: Rugozy postludlovskikh otlozheniy doliny r. Zeravshan (Tsentral'nyy Tadzhikistan); in Biostratigrafiya pogranichnykh otlozheniy silura i devona, ed. B.S. Sokolov and A.B. Ivanovskiy; Akademiya Nauk SSSR, Sibirskoe Otdelenie, Institut Geologii i Geofiziki, Izdatel'stvo "Nauka", Moskva, p. 102-130.

Lonsdale, W.
1845: Description of some characteristic Palaeozoic corals of Russia. Appendix A, p. 591-634; in Murchison, R.I., de Verneuil, E. and von Keyserling, A.; The geology of Russia in Europe and the Ural Mountains, v. 1, John Murray, London, 700 p.

Mamedov, A.B.
1983: Zonal'noe raschlenenie srednego devona Zakavkaz'ya po brakhiopodam; in Nizhniy yarus srednego devona na territorii SSSR, ed. V.N. Dubatolov; Akademiya Nauk SSSR, Sibirskoe Otdelenie, Institut Geologii i Geofiziki, Trudy, vypusk 562, p. 112-130.

Mayr, U.
1978: Stratigraphy and correlation of Lower Paleozoic formations, subsurface of Cornwallis, Devon, Somerset, and Russell islands, Canadian Arctic Archipelago; Geological Survey of Canada, Bulletin 276.

McLean, R.A.
1976a: Genera and stratigraphic distribution of the Silurian and Devonian family Cystiphyllidae Edwards and Haime; in Report of Activities, Part B, Geological Survey of Canada, Paper 76-1B, p. 295-301.

1976b: Middle Devonian cystiphyllid corals from the Hume Formation, northwestern Canada; Geological Survey of Canada, Bulletin 274.

Meek, F.B.
1873: Preliminary paleontological report, consisting of lists and descriptions of fossils, with remarks on the ages of the rocks in which they were found, etc., etc.; United States Geological Survey of the Territories, embracing portions of Montana, Idaho, Wyoming, and Utah, Annual Report 6 (1872), p. 429-518.

1877: Palaeontology; in Report of the geological exploration of the fortieth parallel, Clarence King, Geologist-in-Charge; Government Printing Office, Washington, v. 4, pt. 1.

Merriam, C.W.
1974: Silurian rugose corals of the central and southwest Great Basin; United States Geological Survey, Professional Paper 777 (imprint 1973).

Müller, J.P.
1858: Einige neue bei St. Tropez am Mittelmeer beobachtete Polycystinen und Acanthometren aus den Abbildungen. Königliche Preussische Akademie der Wissenschaften zu Berlin, Monatsberichte, Gesammtsitzung vom 11. Februar 1858, p. 154-155.

1859: Über die Thalassicollen, Polycystinen und Acanthometren des Mittelmeers. Königliche Preussische Akademie der Wissenschaften zu Berlin, Abhandlungen, Physikalisch-Mathematische Klasse, 1858, p. 1-62.

Murphy, M.A. and Matti, J.C.
1982: Lower Devonian conodonts (**hesperius-kindlei** Zones), central Nevada; University of California Publications in Geological Sciences, v. 123.

Oliver, W.A., Jr.
1960: Devonian rugose corals from northern Maine; United States Geological Survey, Bulletin 1111-A.

Ormiston, A.R.
1967: Lower and Middle Devonian trilobites of the Canadian Arctic Islands; Geological Survey of Canada, Bulletin 153.

1969: A new Lower Devonian rock unit in the Canadian Arctic Islands; Canadian Journal of Earth Sciences, v. 6, p. 1105-1111.

Pedder, A.E.H.
1967: **Lyrielasma** and a new related genus of Devonian tetracorals; Royal Society of Victoria, Proceedings, new ser., v. 80, p. 1-29.

1985: Lower Devonian rugose corals of Lochkovian age from Yukon Territory; in Current Research, Part A, Geological Survey of Canada, Paper 85-1A, p. 587-602.

Pedder, A.E.H. and McLean, R.A.
1982: Lower Devonian cystiphyllid corals from North America and eastern Australia with notes on the genus **Utaratuia**; Geologica et Palaeontologica v. 16, p. 57-110.

Philip, G.M.
1962: The palaeontology and stratigraphy of the Siluro-Devonian sediments of the Tyers area, Gippsland, Victoria; Royal Society of Victoria, Proceedings, new ser., v. 75, p. 123-246.

Philip, G.M. and Pedder, A.E.H.
1967: The age of the Lilydale Limestone (Devonian), Victoria; Journal of Paleontology, v. 41, p. 795-798.

Rosen, B.R. and Wise, R.F.
1980: Revision of the rugose coral **Diphyphyllum concinnum** Lonsdale, 1845 and historical remarks on Murchison's Russian coral collection; British Museum (Natural History), Bulletin, Geology ser., v. 33, p. 147-155.

Sapel'nikov, V.P. and Mizzens, L.I.
1980: Novoe b probleme granitsy nizhnego i srednego devona na Urale; in Paleontologiya i biostratigrafiya srednego paleozoya Urala, ed. G.N. Papulov and V.P. Sapel'nikov; Academiya Nauk SSSR, Ural'skiy Nauchnyy Tsentr, Sverdlovsk, p. 23-38.

Schlüter, C.A.F.
1882: Neue Korallen des Mitteldevon der Eifel; Verhandlungen des Naturhistorischen Vereines der Preussischen Rheinlande und Westfalens, Jahrg. 39 — Sitzungsberichte der niederrheinischen Gesellschaft für Natur- und Heilkunde in Bonn, p. 205-210.

1889: Anthozoen des rheinischen Mittel-Devon; Geologischen Specialkarte von Preussen und den Thuringischen Staaten, Abhandlungen, Band 8, Heft 4, p. 259-465 (reprint pagination 1-207).

Smith, R.E.
1980: Lower Devonian (Lochkovian) biostratigraphy and brachiopod faunas, Canadian Arctic Islands; Geological Survey of Canada, Bulletin 308.

Soshkina, E.D.
1936: Korally Rugosa srednego devona Severnogo Urala; Akademiya Nauk SSSR, Polyarnoy Komissii, Trudy, vypusk 28, p. 15-76.

1937: Korally verkhnego silura i nizhnego devona vostochnoga i zapadnogo sklonov Urala; Akademiya Nauk SSSR, Paleozoologicheskogo Instituta, Trudy, tom 6, vypusk 4.

1949: Devonskie korally Rugosa Urala; Akademiya Nauk SSSR, Paleontologicheskogo Instituta, Trudy, tom 15, vypusk 4.

1952: Opredelitel' devonskikh chetyrekhluchevykh korallov; Akademiya Nauk SSSR, Paleontologicheskogo Instituta, Trudy, tom 39.

Spasskiy, N.Ya.
1955: Korally Rugosa i ikh znachenie dlya stratigrafii srednego devona zapadnogo sklona Urala; in Stratigrafiya paleozoyskikh otlozheniy Timana i zapadnogo sklona Urala, ed. M.V. Kulikov; Vsesoyuznogo Neftyanogo Nauchno-Issledevatel'skogo Geologo-Razvedochnogo Insituta (VNIGRI), Trudy, novaya seriya, vypusk 90, p. 91-224.

1983: Analiz rasprostraneniya srednedevonskikh rugoz Zakavkaz'ya; in Nizhniy yarus srednego devona na territorii SSSR, ed. V.N. Dubatolov; Akademiya Nauk SSSR, Sibirskoe Otdelenie, Institut Geologii i Geofiziki, Trudy, vypusk 562, p. 164-170.

Strusz, D.L.
1972: Correlation of the Lower Devonian rocks of Australasia; Geological Society of Australia, Journal, v. 18, p. 427-455.

Stumm, E.C.
1949: Revision of the families and genera of the Devonian tetracorals; Geological Society of America, Memoir 40.

Sytova, V.A.
1968: Tetrakorally skal'skogo i borshchovskogo gorizontov Podolii; in Siluriysko-devonskaya fauna Podolii, ed. Z.G. Balashov; Izdatel'stvo Leningradskogo Universiteta, Leningrad, p. 51-71.

Sytova, V.A. and Ulitina, L.M.
1966: Rugozy isen'skoy i biotarskoy svit; in Stratigrafiya i fauna siluriyskikh i nizhnedevonskikh otlozheniy Nurinskogo sinklinoriya, ed. A.A. Bogdanov; Materialy po geologii Tsentral'nogo Kazakhstana, tom 6, p. 198-253.

Thorsteinsson, R.
1984: A sulphide deposit containing galena, in the Lower Devonian Disappointment Bay Formation on Baillie Hamilton, Island, Canadian Arctic Archipelago; in Current Research, Part B, Geological Survey of Canada, Paper 84-1B, p. 269-274.

Thorsteinsson, R. and Kerr, J.W.
1968: Cornwallis Island and adjacent smaller islands, Canadian Arctic Archipelago; Geological Survey of Canada, Paper 67-64.

Thorsteinsson, R. and Uyeno, T.T.
1981: Stratigraphy and conodonts of Upper Silurian and Lower Devonian rocks in the environs of the Boothia Uplift, Canadian Arctic Archipelago; Geological Survey of Canada, Bulletin 292 (imprint 1980).

Ulitina, L.M.
  1963:   Korally podotryada Cystiphyllina iz devona Zakavkaz'ya (semeystva Zonophyllidae, Dansikophyllidae i Digonophyllidae); Akademiya Nauk SSSR, Paleontologicheskiy Institut, Moskva, 18 p.

  1968:   Devonskie korally tsistifilliny Zakavkaz'ya; Akademiya Nauk SSSR, Paleontologicheskogo Instituta, Trudy, tom 113.

Vollbrecht, E.
  1926:   Die Digonophyllinae aus dem unteren Mittel-Devon der Eifel. Eine morphologisch-chronologische Studie. I. Teil; Neues Jahrbuch für Mineralogie, Geologie und Paläontologie, Abteilung B, Beilage-Band 55, p. 189-273.

Wedekind, R.
  1923:   Die Gliederung des Mitteldevons auf Grund von Korallen; Gesellschaft zur Beförderung der gesamten Naturwissenschaften zu Marburg, Sitzungsberichte, 1922, no. 4, p. 24-35.

  1924:   Das Mitteldevon der Eifel. Eine biostratigraphische Studie. I. Teil. Die Tetrakorallen des unteren Mitteldevon; Gesellschaft zur Beförderung der gesamten Naturwissenschaften zu Marburg, Schriften, Band 14, Heft 3.

Wedekind, R. (cont.)
  1925:   Das Mitteldevon der Eifel. Eine biostratigraphische Studie. II. Teil. Materialien zur Kenntnis des mittleren Mitteldevon; Gesellschaft zur Beförderung der gesamten Naturwissenschaften zu Marburg, Schriften, Band 14, Heft 4.

  1937:   Einführung in die Grundlagen der historischen Geologie. II. Band. Mikrobiostrigraphie die Korallen- und Foraminiferenzeit; Ferdinand Enke Verlag, Stuttgart, viii + 136 p.

Wedekind, R. and Vollbrecht, E.
  1931:   Die Lytophyllidae des mittleren Mitteldevon der Eifel. I. Teil. Das Tatsachenmaterial; Palaeontographica, Band 75, p. 84-110.

  1932:   Die Lytophyllidae des mittleren Mitteldevon der Eifel. II. Teil. Die systematische Erfassung des Tatsachenmateriales; Palaeontographica, Band 76, p. 95-115.

Weyer, D.
  1971:   Nomenklatorische Bemerkungen zum Genus **Plasmophyllum** Dybowski, 1873 (Anthozoa, Rugosa, Silur). Deutsche Gesellschaft für geologische Wissenschaften, Berichte, Reihe A, Band 16, p. 13-17.

Figure 31.1. Lake Ontario – upper St. Lawrence – Ottawa valley region showing approxiamte extent of glacial lake coverage, Champlain Sea shoreline, and locations of sites discussed in text.

NOTE TO CONTRIBUTORS

Submissions to the *Discussion* section of *Current Research* are welcome from both the staff of the Geological Survey and from the public. Discussions are limited to 6 double-spaced typewritten pages (about 1500 words) and are subject to review by the Chief Scientific Editor. Discussions are restricted to the scientific content of Geological Survey reports. General discussions concerning branch or government policy will not be accepted. Illustrations will be accepted only if, in the opinion of the editor, they are considered essential. In any case no redrafting will be undertaken and reproducible copy must accompany the original submissions. Discussion is limited to recent reports (not more than 2 years old) and may be in either English or French. Every effort is made to include both *Discussion* and *Reply* in the same issue. *Current Research* is published in January and July. Submissions should be sent to the Chief Scientific Editor, Geological Survey of Canada, 601 Booth Street, Ottawa, Canada, K1A 0E8.

AVIS AUX AUTEURS D'ARTICLES

Nous encourageons tant le personnel de la Commission géologique que le grand public à nous faire parvenir des articles destinés à la section *discussion* de la publication *Recherches en cours*. Le texte doit comprendre au plus six pages dactylographiées à double interligne (environ 1500 mots), texte qui peut faire l'objet d'un réexamen par le rédacteur en chef scientifique. Les discussions doivent se limiter au contenu scientifique des rapports de la Commission géologique. Les discussions générales sur la Direction ou les politiques gouvernementales ne seront pas acceptées. Les illustrations ne seront acceptées que dans la mesure où, selon l'opinion du rédacteur, elles seront considérées comme essentielles. Aucune retouche ne sera faite aux textes et dans tous les cas, une copie qui puisse être reproduite doit accompagner les textes originaux. Les discussions en français ou en anglais doivent se limiter aux rapports récents (au plus de 2 ans). On s'efforcera de faire coincider les articles destinés aux rubriques *discussions* et *reponses* dans le même numéro. La publication *Recherches en cours* paraît en janvier et en juillet. Les articles doivent être renvoyés au rédacteur en chef scientifique: Commission géologique du Canada, 601, rue Booth, Ottawa, Canada, K1A 0E8.

CURRENT RESEARCH PART B
RECHERCHES EN COURS PARTIE B

Canada

Notice to Librarians and Indexers

The Geological Survey's twice-yearly *Current Research* series contains many reports comparable in scope and subject matter to those appearing in scientific journals and other serials. All contributions to Current Research include an abstract and bibliographic citation. It is hoped that these will assist you in cataloguing and indexing these reports and that this will result in a still wider dissemination of the results of the Geological Survey's research activities.

Avis aux bibliothécaires et préparateurs d'index

La série *Recherches en cours* de la Commission géologique paraît deux fois par année; elle contient plusieurs rapports dont la portée et la nature sont comparables à ceux qui paraissent dans les revues scientifiques et autres périodiques. Tous les articles publiés dans les Recherches en cours sont accompagnés d'un résumé et d'une bibliographie, ce qui vous permettra, nous l'espérons, de cataloguer et d'indexer ces rapports, d'où une meilleure diffusion des résultats de recherche de la Commission géologique.

GEOLOGICAL SURVEY OF CANADA
PAPER 85-1B

COMMISSION GÉOLOGIQUE DU CANADA
ÉTUDE 85-1B

CURRENT RESEARCH
PART B

RECHERCHES EN COURS
PARTIE B

1985

Cover

Folding in the Neruokpuk Formation along the Firth River.
These illustrations appear in report 27 by D.K. Norris (p. 223-229).

Plissement dans la formation de Neruokpuk le long de la rivière
Firth. Ces illustrations apparaissent dans le rapport 27 par
D.K. Norris (p. 223-229).

SCIENTIFIC AND TECHNICAL REPORTS
RAPPORTS SCIENTIFIQUES ET TECHNIQUES

QUATERNARY GEOLOGY/GÉOLOGIE DU QUATERNAIRE

Inventory mapping and stratigraphic studies/Inventaire cartographique et stratigraphique

Paleoecology and geochronology/Paléoécologie et géochronologie

Sedimentology and geomorphology/Sédimentologie et géomorphologie

REGIONAL GEOLOGY/GÉOLOGIE RÉGIONALE

Appalachian region/Région des Appalaches

STRUCTURAL GEOLOGY/GÉOLOGIE STRUCTURALE

SCIENTIFIC AND TECHNICAL NOTES
NOTES SCIENTIFIQUES ET TECHNIQUES

Le Front de Grenville dans la région de Chibougamau (Québec)

André Ciesielski et Eric Ouellet [1]
Division de la Géologie du Précambrien

Résumé

La zone tectonique du front de Grenville (ZTFG) a été cartographiée sur 60 km. Il s'agit d'une discontinuité lithotectonique marquant la limite entre les séries volcano-sédimentaires archéennes de la province du lac Supérieur (appelées autochtone Archéen) et un grand bloc d'orthogneiss migmatisés et d'amphibolites. Ce dernier, connu sous le nom de parautochtone Archéen, gît coincé entre les nappes granulito-anorthositiques de la province de Grenville et l'autochtone Archéen. Dans la partie sud de la carte géologique, les roches volcano-sédimentaires autochtones qui se prolongent de façon continue dans le parautochtone, accusent un changement, du faciès des schistes verts au faciès des amphibolites, et sont marquées par la présence de failles et de plis orientés N 10° à 20°. Dans le secteur nord, la ZTFG se distingue surtout par la présence de failles et de contacts tectoniques entre roches volcaniques et orthogneiss. Le parautochtone est considéré comme le socle des séries volcano-sédimentaires de la province du lac Supérieur. Sa remontée s'est effectuée de façon inverse et senestre sur l'authochtone avec une venue des nappes grenvilliennes qui n'ont vraisemblablement pas atteint la ZTFG dans la région de Chibougamau.

Abstract

The Grenville Front Tectonic Zone (GFTZ) was mapped over a distance of 60 km. A lithotectonic break separates the Archean volcanic-sedimentary rocks of the Superior Province (called the Archean autochthon) from a large block of amphibolites and migmatized orthogneiss, the Archean parautochthon, which lies between the granulite-anorthosite nappes of the Grenvile Province and the Archean autochthon. In the southern part of the geological map, autochthonous volcano-sedimentary rocks extend continuously into the parauthochthon; they exhibit a facies transition from greenschist to amphibolite, as well as faults and folds oriented 10 to 20° N. In the northern section, the GFTZ is characterized by the presence of faults and tectonic contacts between the volcanic rocks and the orthogneiss. The parautochthon is considered to represent the basement of the volcano-sedimentary series of the Superior Province. It was inversely and sinistrally displaced over the authochthon by the Grenvile nappes which probably did not reach the GFTZ in the Chibougamau area.

---

[1] Université du Québec à Chicoutimi G7H 2B1

Introduction

La zone tectonique du front de Grenville (ZTFG) est située à 35 km au sud-est de la ville de Chibougamau, au Québec (fig. 36.1). Il s'agit d'une discontinuité lithotectonique constituée par une zone de transition étroite à orientation N 10°, où les séries volcano-sédimentaires et plutoniques de type archéen de la province du lac Supérieur[1] passent de façon abrupte à des orthogneiss et à des amphibolites. La zone sud de la carte géologique (fig. 36.2) montre les séries volcaniques du groupe de Roy (Hébert, 1979; Gobeil et Racicot, 1983; Cimon, 1977) qui passent du faciès des schistes verts dans la province du lac Supérieur au faciès des amphibolites de l'autre côté de la ZTFG (Laurin, 1955; Gilbert, 1959), selon des failles et des contacts tectoniques grossièrement orientés nord-nord-est; la transition s'effectue avec l'apparition de linéations, de plis serrés déca- et kilométriques et de foliations orientées N 10° qui reprennent une direction ouest-sud-ouest une fois passés sa ZTFG. La section nord de la carte géologique, pour sa part, montre une discontinuité encore plus nette entre les séries volcano-sédimentaires et les orthogneiss (Imbault, 1959; Longley, 1959; Neale, 1959); elle est marquée par une série de failles, de zones transposées et de contacts tectoniques à orientation nord-nord-est au centre et est-nord-est vers le nord.

Le front de Grenville

Une interprétation des cartes aéromagnétiques du champ total et du relief éclairé (Commission géologique du Canada, 1984) permet d'établir assez clairement la présence, le long de la discontinuité recoupant les roches de la province du Supérieur (ZTFG), d'une entité à caractéristiques magnétiques relativement homogènes par rapport au reste; cette dernière a été reconnue un peu plus au nord-est par Rivers et Chown (sous presse) qui ont convenu de lui donner le nom de "parautochtone Archéen". À la hauteur de Chibougamau, cette "plage magnétique", se compose d'orthogneiss leucocrates à caractère orthomigmatitique par endroits et déformés lors d'une première phase de façon à donner de grandes structures serrées à axes grossièrement orientés nord-sud qui ont été reprises par une deuxième phase de déformation plus ample à axes est-ouest, ainsi que de séries métavolcano-sédimentaires (présumées de type archéen de la province du Supérieur) en méga-enclaves (Grenier, 1953; Deland et Grenier, 1959). Dans la région de la ZTFG et dans le parautochtone, des datations au Rb/Sr effectuées sur des échantillons roche totale ont donné, dans le cas des orthogneiss, des âges variant de 2,7 à plus de 3,0 Ma (Frith et Doig, 1975; Baker, 1980). Le parautochtone Archéen est littéralement coincé entre les complexes de granulites et d'anothosites de la province de Grenville et ce qui est convenu d'appeler le front de Grenville (fig. 36.1). Ce dernier, bien que délimité sur les cartes aéromagnétiques par une discontinuté qui tronque les séries volcano-sédimentaires et plutoniques de la province du Supérieur (définies comme l'autochtone Archéen), est plus difficile à délimiter sur le terrain. Cette zone peut se caractériser par des failles séparant des lithologies très différentes, par des discontinuités tectoniques remobilisées, ou non, par des zones de transpositions, ou par des passages graduels de roches souvent difficiles à distinguer, particulièrement quand les effets du métamorphisme grenvillien décroissent vers le Supérieur et oblitèrent toute trace de métamorphisme kénoréen. La ZTFG peut se définir de façon tectonique,
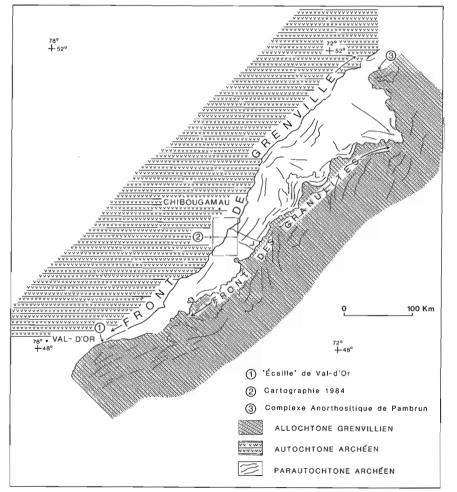

Figure 36.1. *Carte synthétique du parautochtone Archéen. Ce dernier est coincé entre les nappes grenvilliennes (front des Granulites) et l'autochtone Archéen. Les lignes fines du parautochtone correspondent à des patrons structuraux visibles sur les cartes aéromagnétiques. Les deux lignes perpendiculaires au front et touchant la région cartographiée sont des anomalies négatives dont les roches ne sont pas visibles sur le terrain.*
1. Écaille de Val-d'Or
2. Superficie cartographiée à l'été 1984
3. Massif anorthositique de Pambrun

---

[1] Abrégé dans le texte en "du Supérieur", ou "province du Supérieur" pour respecter la nomenclature des géologues du Québec.

lithologique, géochronologique ou métamorphique; à tout endroit de la ZTFG, un ou plusieurs de ces paramètres s'applique et permet, malgré des imprécisions et des interprétations évidentes, de délimiter ce grand accident qui tronque la fosse du Labrador et les provinces du Supérieur, de Churchill et de Nain. Immédiatement au sud de la ZTFG, on retrouve une zone à laquelle on a donné le nom de front des Granulites; cette dernière entre en contact avec les séries volcano-sédimentaires du Supérieur dans la région de Val d'Or selon un patron en forme d'écaille semi-circulaire (fig. 36.1). Le front se caractérise par une série de lobes dont la présence résulte d'un épisode de tectonique tangentielle par écaillage jusqu'au contact, à la hauteur du massif anorthositique de Pambrun (Chown, 1971, 1979), avec le parautochtone Aphébien qui est corrélé avec les roches sédimentaires de la fosse du Labrador (fig. 36.1; Rivers, 1983; Rivers et Chown, sous presse).

Contexte lithométamorphique de la ZTFG dans la région de Chibougamau

La ZTFG dans la région de Chibougamau est caractérisée par le passage abrupt entre les séries volcano-sédimentaires de type archéen et les orthogneiss, également de type archéen mais faiblement remaniés par l'orogénèse Grenvillienne. Le contact est généralement marqué par des failles ou par des zones de transpositions, ou simplement par des discontinuités lithotectoniques sur lesquelles des linéations sont souvent bien développées. La carte géologique à la figure 36.2 illustre deux domaines différents séparés au centre par le massif de Ladauversière, massif intrusif Archéen associé au groupe de Roy. La moitié nord de la carte se distingue de la moitié sud:
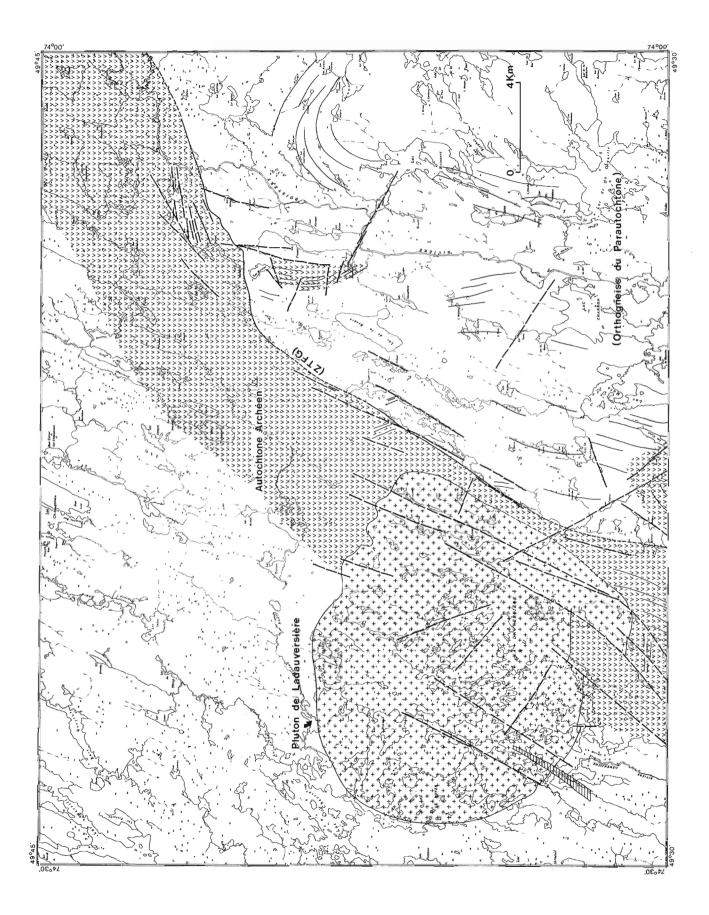
- par la présence beaucoup plus importante au sud de métabasites à laves en coussins formant des enclaves dans les orthogneiss;

- par un métamorphisme des séries volcaniques et sédimentaires de type archéen, présumé de type grenvillien et de nature beaucoup plus intense et pénétrante au nord;

- par une différence marquée, de part et d'autre du massif de Ladauversière, dans la nature des laves et des sédiments archéens qui font face à la ZTFG; et,

- par un réseau de failles de part et d'autre de la ZTFG beaucoup plus important au centre et au sud.
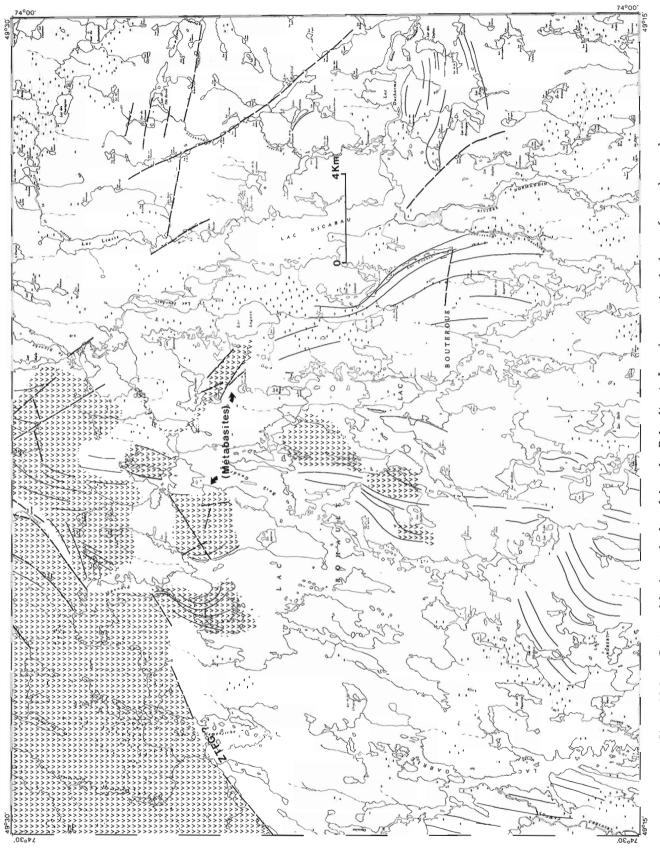
Dans le secteur central et nord de la carte géologique, la position exacte du front de Grenville est déterminée à quelques endroits (au nombre de sept) où des contacts tectoniques entre les lithologies différentes sont visibles. Dans la zone sud de la région, les basaltes à débit en coussins de la formation d'Obatogamau (base du groupe de Roy) contiennent des grenats dans les bordures figées, à moins de deux kilomètres d'une faille qui sépare des amphibolites à coussins résiduels (fig. 36.3) et des orthogneiss leucocrates. Ces derniers exhibent des caractéristiques tantôt paramigmatitiques (fig. 36.4a,b), tantôt orthomigmatitiques et, dans ce dernier cas, renferment de nombreuses enclaves de métabasites (métavolcaniques) et de roches plutoniques de nature intermédiaire ou acide. Au centre de la carte, le pluton tonalitique de Ladauversière est bordé du côté est par une mince bande de roches volcaniques qui conserve le faciès des schistes verts et se trouve en contact avec les orthogneiss leucocrates (Bellavance, 1984) selon des failles orientées N 10° à 20°. Le pourtour exact du pluton est déterminé à partir de la topographie; les tonalites forment une légère dépression causée par l'érosion différentielle. Immédiatement au nord du massif, les roches volcaniques en contact tectonique avec les orthogneiss contiennent des grenats sur environ un kilomètre, situation d'ailleurs analogue à la moitié sud de la carte.

La partie nord de la carte géologique (canton de Dollier) est relativement différente, en raison du fait que le métamorphisme, présumé grenvillien, s'étend dans les séries volcano-sédimentaires a contenu andésitique généralement plus élevé qu'au sud, sur une distance beaucoup plus grande et aussi parce que les assemblages à grenat et amphiboles (fig. 36.5) sont plus développés, (voir l'isograde "grenat" dans le canton de Dollier ouest dans Cimon, 1977 et Allard, 1967). Certains affleurements montrent des structures coussinées dont la polarité a été préservée ainsi que des brèches de sommet de coulée (fig. 36.6a,b,c), des métaconglomérats (fig. 36.7) caractérisés par des structures de granoclassement et des dykes antémétamorphiques, le tout porté au faciès des amphibolites (Baker, 1980). Le métamorphisme de contact du pluton de Ladauversière ne s'étend que sur quelques centaines de mètres et n'interfère pas avec celui du front de Grenville (Hébert, 1979); au nord, la faible influence du pluton de Chibougamau sur les anorthosites du lac Doré et sur les roches volcano-sédimentaires à proximité du front de Grenville ne se remarque que dans des variations subtiles de la chimie de certain minéraux typomorphes (Kline, 1984).

Des côtés sud-est et centre-est, les orthogneiss sont identiques à ceux du nord et contiennent des enclaves déca- et kilométriques de roches métavolcaniques associées quelques fois à des pegmatites et souvent caractérérisées par des contacts tectoniques avec les gneiss. La présence dans ces derniers de métabasites d'origine volcanique, beaucoup plus déformées et métamorphisées dans le parautochtone que du côté de la province du Supérieur de la ZTFG, semble indiquer une origine commune pour ces deux entités géologiques. Des vestiges métamorphisés et déformés de roches de la province du lac Supérieur dans les gneiss du parautochtone Archéen ont déjà été décrites par Allard (1978, 1979) et Avramtchev (1975). Outre les métabasites communes, ces auteurs décrivent des méta-anorthosites qui ont une filiation directe avec celles du lac Doré. Au nord du lac Mistassini, Chown (1971) a remarqué la présence, le long du front de Grenville, d'anorthosites et de gabbros associés, qui forment des écailles coincées entre l'autochtone et le parautochtone Archéen et que l'on a corrélé avec les complexes anorthositiques de la province de Grenville; le style de déformation et la position interdisent toute filiation avec les roches du complexe du lac Doré. À l'est de la région de Val-d'Or, Sethuraman (1979, 1984) décrit des séries volcano-sédimentaires de type archéen portées au faciès des granulites et localisées près de la limite entre la zone considérée comme l'allochtone Grenvillien et le parautochtone Archéen. Bien qu'aucune filiation directe avec les séries volcano-sédimentaires de la région de Val-d'Or ne soit connue, l'origine archéenne de ces roches est incontestable.

Dans la partie nord de la carte, soit dans la région du lac Dollier, la stratigraphie des roches archéennes basée sur des section types effectuées plus à l'ouest (Charbonneau et coll., 1983; Cimon, 1977; Hébert, 1976, 1979) est difficile à établir étant donné la présence de failles à orientation est-nord-est qui provoquent une carbonatisation responsable de la dégradation des affleurements, et du métamorphisme au faciès des amphibolites présent le long de la ZTFG. Les raisons d'un "métamorphisme différentiel" surimposé le long du front de Grenville sont nécessairement reliées non seulement à la tectonique de l'époque et au rôle de l'eau, mais aussi aux différences de compositions originales des lithologies et à l'altération syngénétique variable des roches volcaniques archéennes qui peut provoquer l'apparition des grenats à cause d'un chimisme particulier. La présence près du front de dykes à kyanite et quartz orientés N 55° et recoupant des séries volcaniques métamorphisées au faciès des amphibolites, semble indiquer un lessivage des roches déjà relativement riches en alumine et une nouvelle concentration de cette dernière dans la zone; l'épisode de

49°45'   74°00'

4 Km

0

(Orthogneiss du Parautochtone)

Autochtone Archéen

(ZTFG)

Pluton de Ladauversière

74°30'   74°30'
49°45'   49°30'

Figure 36.2. *Carte géologique de la région de Rohault et Lemoine montrant des méga-enclaves de métabasaltes (vvv) noyées dans les orthogneiss du parautochtone et souvent bordées de failles. L'autochtone Archéen se compose des suites volcano-sédimentaires classiques de l'Abitibi. Le pluton de Ladauversière accuse une composition tonalitique; les orthogneiss migmatisés sont de composition tonalito-granodioritique. Le dyke de diabase dans le massif de Ladauversière s'aligne parallèle aux failles de "Mistassini".*

Figure 36.3. *Débit coussiné dans des métabasaltes portés au faciès des amphibolites. On note des grenats dans la bordure figée et dans le centre des coussins. La déformation est relativement faible.*
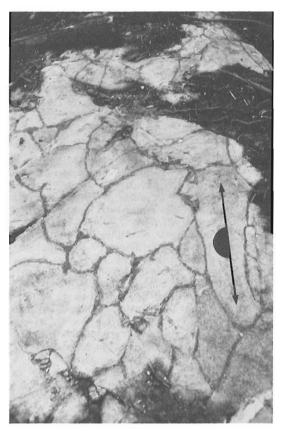

Figure 36.5. *Grenats sinusoidaux dans une roche volcanogénique de composition intermédiaire. La phase de déformation locale F_1 est parallèlle au front de Grenville et parallèlle aux séries de failles à orientation N 70°. La phase F_2 est reliée à la phase de déformation Z_2, et si on considère les grenats comme des indicateurs cinématiques, le mouvement horizontal apparent le long de Z_2 serait senestre.*

Figure 36.4a. *Orthogneiss tonaltiques bien foliés montrant des enclaves variées de compositions principalement intermédiaires à quartz modal.*

Figure 36.4b. *Orthogneiss montrant un taux de mobilisation élevé dû au fort pourcentage de biotite dans la roche.*

métamorphisme de fracturation de haute pression apparaissant à la fin ou après l'épisode de métamorphisme thermique causé par la formation de la ZTFG, est relié à la deuxième phase de déformation Z_2 (plissements, foliations et fracturations) localisée sur la ZTFG à la figure 36.8a. Des assemblages à kyanite et quartz ont déjà été décrits près de la ZTFG dans des métasédiments de la province du lac Supérieur, dans le groupe d'Opémisca (Baker, 1980), dans des métabasites situées dans le parautochtone Archéen (Chown, 1979) et dans des métasédiments à caractère granulitique (Lumbers, 1975). Plus au sud dans la province de

Grenville, Lumbers (1971, 1975) a aussi décrit des assemblages à kyanite, mais dans des contextes différents et éloignés de la ZTFG, et il n'appert pas que ces deux types d'occurences soient liées au même phénomène.

La question des dykes de diabase est intéressante à maints égards et on peut en tirer une chronologie du métamorphisme grenvillien. Dans les orthogneiss du parautochtone, on décrit souvent des dykes de diabase métamorphisés de façons diverses, jusqu'au faciès des amphibolites à grenat; ces dykes, presque toujours orientés
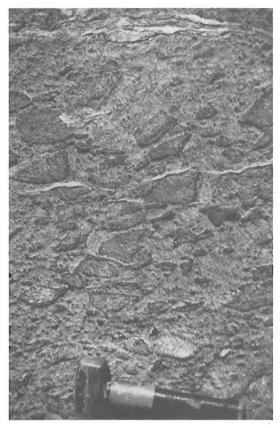
Figure 36.6a. *Métabasite au faciès des amphibolites de composition intermédiaire, exhibant un débit coussiné à polarité conservée. Le sommet pointe vers le sud et correspond au flanc sud de l'anticlinal de Chibougamau (Daigneault et Allard, 1984). L'allongement des coussins est parallèle au système de failles à orientation N 70° (au nord de la carte géologique).*

Figure 36.6c. *Roche identique montrant le détail de la brèche. Les cailloux sont anguleux et représentent cette fois un sommet de coulée massive.*

Figure 36.6b. *Roche identique montrant une brèche de sommet de coulée métamorphisée qui se compose de coussins à taille réduite dans une matrice de hyaloclatites.*

Figure 36.7. *Métaconglomérats de la formation de Stella (base du groupe d'Opémisca), métamorphisés au faciès des amphibolites. La déformation a étiré les cailloux de granite dans le plan perpendiculaire à la photographie. La matrice contient des assemblages à amphibole, grenat et biotite.*

vers le nord ou le nord-nord-est (Remick, 1970; Deland et Grenier, 1959; Laurin, 1955; Gilbert, 1959), s'alignent parallèles aux failles "de Mistassini" identifiées par Allard (1981). Du côté situé dans la province du Supérieur, des dykes de lamprophyres ont été observés dans les séries volcaniques de la région de Rohault (Wagner, 1978), mais ces derniers s'avèrent être anté-kénoréens; dans la ZTFG, le métamorphisme des dykes de diabase est aussi variable et les

Figure 36.8a. *Schéma tectonique simplifié de la région de Chibougamau. Le symbole S_1 n'apparaît pas sur la carte, étant plus à l'ouest et la phase de déformation S_2 tourne autour du pluton de Ladauversière. Les phases Z_1 et Z_2 sont causées par le mouvement senestre le long du front de Grenville. La phase de déformation P_1 peut se confondre avec la phase P_2 puisqu'elle tourne du nord vers le nord-est et même vers l'est, phénomène dû à l'influence du front de Grenville et des systèmes de failles n'ayant rien à voir avec P_2 dont l'existence est d'ailleurs spéculative. L'étendue du métamorphisme grenvillien au sein du parautochtone demeure inconnue.*

orientations observées sont congruentes avec le système Z_1 de failles orientées N 10° à 20° (fig. 36.8a). On considère que la zone d'extension du métamorphisme dans les dykes corespond à la fin de l'influence exercée par l'épisode de métamorphisme grenvillien. Bien qu'il y ait un rapport certain entre le métamorphisme des dykes et celui de la province de Grenville le long de la ZTFG, Deland (1956) décrit dans la région du lac Surprise, à l'extérieur et au sud-ouest de la carte géologique, un isograde "grenat" vraisemblablement relié au métamorphisme grenvillien et des dykes de diabases non métamorphisés à direction nord-est. L'inconsistance du métamorphisme des dykes ne met pourtant pas en doute l'influence de l'orogénie Grenvillienne; leurs orientations sont conformes à l'orientation N 10° à 20° des plus importantes failles régionales et établissent du fait l'âge protérozoïque du système. Il est possible qu'il y ait plus d'une famille de dykes dont il sera difficile d'établir la chronologie. Il est toutefois certain que des dykes anté-kénoréens et post-volcaniques existent du côté situé dans la province du Supérieur, dans les gneiss et métabasites du parautochtone (fig. 36.9a,b) et se distinguent des dykes protérozoïques en ce qu'ils sont systématiquement plissés et métamorphisés.
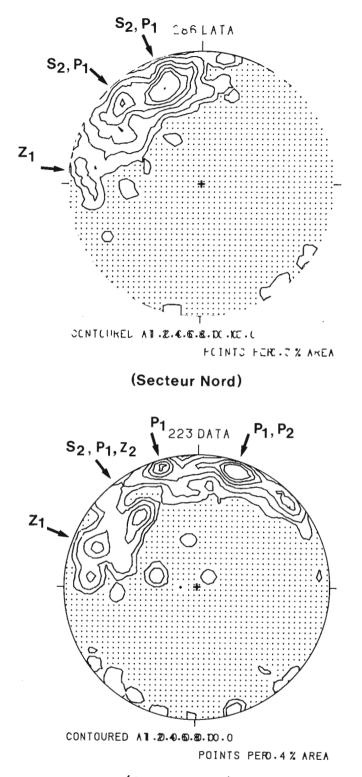
Contexte structural de la ZTFG

Au nord et au centre de la carte géologique, le front de Grenville se définit par une discontinuité lithologique. Au sud, la continuité apparente des roches, compte tenu du

manque d'affleurements, fait que l'on est obligé placer le front à l'endroit ou les premières discontinuités structurales apparaissent; il s'agit d'un changement des attitudes des foliations archéennes qui passent d'est-ouest à nord-nord-est. La structure des roches volcaniques est compliquée par la présence du massif de Ladauversière autour duquel, dans la partie sud, vont tourner les foliations archéennes ainsi que les failles majeures à orientation nord-nord-est ayant rejoué au Grenvillien mais datant d'âges antérieurs (Racicot et coll., 1984). Plus au sud, le front est caractérisé par la présence de grands plis repris dont les axes de première phase s'alignent presque parallèles au front; ils sont particulièrement discernables sur la carte des conducteurs Input (Ministère des Richesses Naturelles du Québec, 1977) qui permet d'observer le changement d'attitude des conducteurs volcaniques de type archéen selon des plis et des orientations nord-est en passant la ZTFG. L'autochtone Archéen, par contre, présente des foliations constantes et une déformation conforme aux plis de deuxième phase reconnus par Daigneault et Allard (1984).

En règle générale, on considère que la déformation comprend plusieurs phases dont deux dans l'autochtone de la province du Supérieur, S_1 et S_2, deux le long de la ZTFG, Z_1 et Z_2, et au moins deux dans le parautochtone Archéen, P_1 et P_2 (fig. 36.8a,b).

À proximité de la ZTFG, les foliations rebroussent vers le nord et se trouvent coincées dans le système de failles de Mistassini orientées N 10° à 20°. Ce modèle simple observé
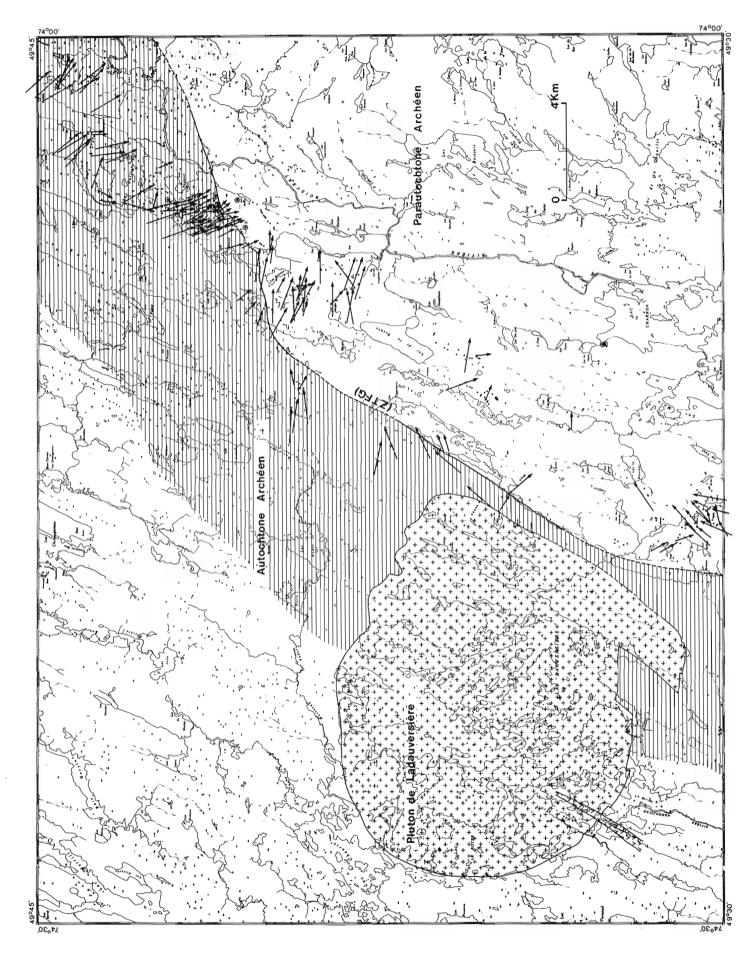
(Secteur Nord)

Figure 36.9a. *Dyke de diabase anté-kénoréen et post-volcanique dans le parautochtone Archéen, folié par la phase de déformation P_1 et, métamorphisé au faciès des amphibolites et replissé en P_2 selon une orientation de N 130°.*
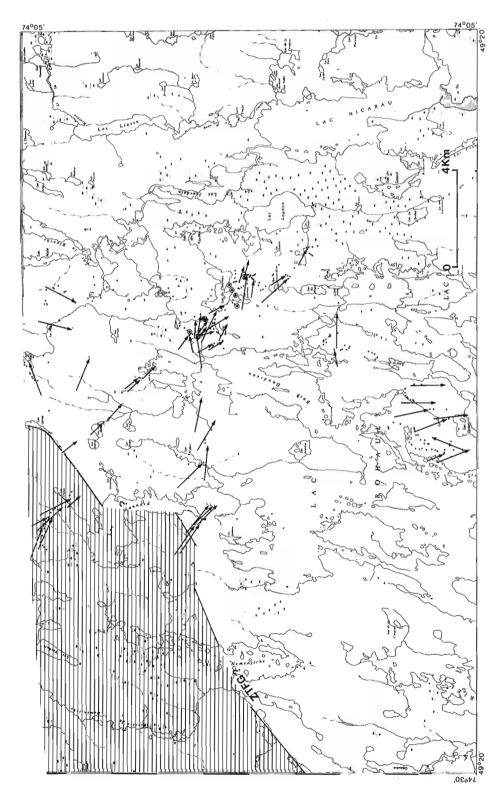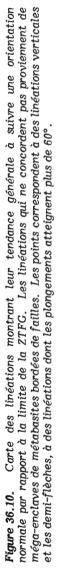

(Secteur Sud)

Figure 36.8b. *Stéréogrammes montrant la disposition des différentes familles de foliations et pendages, leur situation géographique et leurs relations aux phases tectoniques. Les phases de déformation S_2, Z_1 et P_1 peuvent se confondre aux abords immédiats du front de Grenville. La phase P_1 passe vers le nord-est en approchant du front et peut même avoir des orientations semblables à P_2 dans les méga-enclaves bordées de failles. On ne fait que spéculer l'existence de P_2. La phase Z_2 n'est pas apparente parce que son pendage, que l'on suppose fort et vers le sud-est, n'est pas visible sur le terrain.*

Figure 36.9b. *Détail du même dyke montrant des morceaux de métabasites arrachés aux murs composés de métavolcanites archéennes (DIBS = diabase).*

dans la région du lac Dollier (Baker, 1980), au nord de la carte, change radicalement d'aspect au sud dans la région du lac Mannard où le système de failles orienté N 10° à 20° a tendance à se déformer et à suivre des foliations orientées vers le sud-ouest et même vers l'ouest (Deland, 1956; Remick, 1970).

Des foliations reliées à des déformations cassantes à caractère local le long de la ZTFG, se trouvent surimposées aux foliations existantes, particulièrement dans la région nord où on observe des foliations reliées à un système de
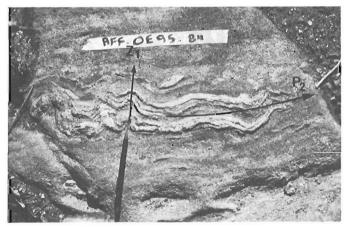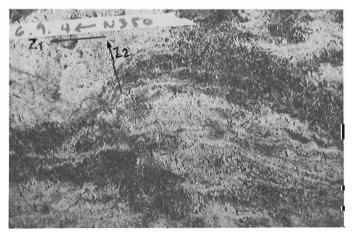
Figure 36.10. *Carte des linéations montrant leur tendance générale à suivre une orientation normale par rapport à la limite de la ZTFG. Les linéations qui ne concordent pas proviennent de méga-enclaves de métabasites bordées de failles. Les points correspondent à des linéations verticales et les demi-flèches, à des linéations dont les plongements atteignent plus de 60°.*

313

failles à orientation N 70° (fig. 36.12). Dans la région centrale, on observe des foliations de crénulations marquées par des microplis à orientation N 55° (Z_2) et probablement reliées de façon conjuguée au système de failles majeures orientées N 10° à 20° (fig. 36.8b). Cette foliation surimposée se retrouve également dans le secteur nord du complexe anorthositique de type archéen du lac Doré, dans des séries volcaniques en contact avec le front de Grenville (Avramtchev, 1975; Allard, 1976), et correspond à la troisième phase de déformation reconnue par Daigneault et Allard (1984). Dans le parautochtone Archéen, les foliations reprennent leurs attitudes est-ouest quand il y a continuité lithologique, puis se développent selon de grands plis à axes grossièrement nord-sud apparemment repris par une phase serrée localement mais à expression régionale plus ample et à axe est-ouest (fig. 36.11). Les foliations parasites reliées au front de Grenville disparaissent alors. Des systèmes de failles à orientation nord-ouest, nord et nord-est sans filiation avec les failles de Mistassini, recoupent la ZTFG ainsi que les foliations du parautochtone.

Les foliations locales n'ont pas été reportées sur la carte géologique; en général elles suivent mal les plus importantes tendances structurales dans le parautochtone Archéen, particulièrement au sud, en raison d'une grande hétérogénéité lithologique et d'une plus grande complexité

Figure 36.11. *Orthogneiss du parautochtone montrant les plis P_2 à orientation N 95° repris par la première phase de déformation Z_1 à orientation N 15°.*

Figure 36.12. *Métabasites de composition intermédiaire à débit coussiné caractérisées par un étirement des bordures figées à N 350° correspondant à la phase Z_1, et une orientation surimposée des amphiboles à N 65° correspondant à la phase Z_2.*

Figure 36.13. *Indicateur de mouvement donnée par un dyke ultrabasique dans des amphibolites à grenat en enclaves dans les orthogneiss du parautochtone. La composante horizontale serait dextre.*

structurale (Laurin, 1955; Gilbert, 1959). L'attitude des linéations (fig. 36.10) est un bon indice de l'influence du front de Grenville dans la région. Ces dernières, bien que pas parfaitement anisotropes, donnent une idée du sens de la déformation. En effet les linéations, puisqu'il ne s'agit pas de linéations du type intersection (la déformation se situe dans la catazone et les schistosités sont absentes), se doivent d'être du type rotation ou étirement. Dans le premier cas, bien qu'il existe quelques indicateurs de mouvement (fig. 36.13) il n'est pas permis de coupler des indicateurs de cisaillement ou de mouvements horizontaux avec les linéations; il y a, en effet, absence marquée de mylonites ou de roches apparentées. Au contraire, tout porte à croire que les mouvements se sont fait surtout dans le sens vertical avec un déplacement du parautochtone vers le nord-ouest en chevauchement sur l'autochtone Archéen selon un mouvement senestre engendrant un déplacement de quelques kilomètres le long du front. Ce mouvement senestre se reconnaît à la morphologie des séries volcano-sédimentaires rebroussées le long du front (Allard, 1978). Des mouvements identiques ont également été signalés dans la région de Val-d'Or, immédiatement à l'ouest du lac Matchi-Manitou, le long de failles qui délimitent la ZTFG (Marquis, 1980); en outre, la morphologie de certains isogrades de métamorphisme de type archéen dans des roches métasédimentaires impliquées dans la ZTFG près de Val-d'Or, semble aussi indiquer un mouvement senestre le long du front (A. Indares, comm. pers.).

La position du front de Grenville dans la région sud de la carte géologique est difficile à déterminer puisqu'il n'existe aucune discontinuité lithologique permettant de distinguer les séries autochtones du parautochtone Archéen. Le métamorphisme étant graduel, soit du faciès des schistes verts dans les séries volcaniques au faciès des amphibolites là où les orthogneiss apparaissent dans le parautochtone archéen, la position de la ZTFG sera déterminée à partir de critères structuraux. Les gneiss autochtones de type archéen passent sans interruption dans le parautochtone et il est pratiquement impossible de distinguer un orthogneiss archéen d'un autre orthogneiss archéen repris par l'orogénie Grenvillienne, particulièrement lorsqu'il y a absence d'horizons métabasiques. Le front se situe donc là où les foliations cessent d'être orientées est-ouest pour remonter vers le nord.

Discussions

Le front de Grenville a été cartographié sur une distance de 60 km dans la région de Chibougamau. Le passage de l'autochtone au parautochtone Archéen se fait abruptement selon des discontinuités lithotectoniques ou de façon graduelle; ainsi les séries volcano-sédimentaires, dans les schistes verts dans la province du Supérieur, apparaissent beaucoup plus déformées dans le faciès des amphibolites, et assimilées dans les orthogneiss en passant la ZTFG. L'origine des ces derniers qui forment la majorité des roches du parautochtone demeure obscure. Les datations au Rb/Sr ont établi que les orthogneiss sont 300 millions d'années plus vieux que les séries volcano-sédimentaires de la province du Supérieur âgées d'environ 2,7 milliards d'années. Le métamorphisme est aussi polyphasé, passant du faciès des schistes verts au faciès des amphibolites sur de courtes distances et d'âges grenvilliens (Baker, 1980) à kénoréens (Frith et Doig, 1975). Les âges le long du Front sont très variables et vont de 2,2 millions d'années jusqu'au début de l'orogénèse Grenvillienne vers 1,0 millions d'années.

Le type de déformation le long du front, le métamorphisme thermique de type contact ainsi que la déformation qui affecte les enclaves d'autochtone Archéen dans les orthogneiss, et particulièrement des foliations horizontales dans de grandes enclaves d'anorthosites appartenant au complexe du lac Doré (Allard, 1978, 1979), semblent établir que le parautochtone Archéen constitue un socle des séries volcaniques, sédimentaires et plutoniques de la province du Supérieur remonté en chevauchement vers le nord-ouest selon un mouvement senestre. Le modèle mis de l'avant dans Thomas et Gibb (1983), bien qu'apparemment conforme à la réalité du terrain, ignore le style structural tangentiel de la province de Grenville qui suppose un angle de chevauchement le long de la ZTFG plus faible ainsi que des foliations horizontales à une moins grande profondeur dans le parautochtone que dans la partie située dans la province du Supérieur.

La position des isogrades de métamorphisme est très variable le long de la ZTFG. L'apparition du grenat, par exemple, se fait de façon tout à fait discontinue dans les roches volcaniques de l'autochtone Archéen et est relié à un chimisme particulier de la roche interagissant avec un isograde (Allard, comm. pers.). La morphologie spaciale des isogrades demeure inconnue et il est clair que la forme du chevauchement le long du front est variable et fonction des différents contextes géologiques. En outre, la déformation dans le parautochtone diffère de celle de l'autochtone et si les orthogneiss représentent vraiment le socle des séries volcaniques de la province du Supérieur, on pourrait s'attendre à retrouver des traces résiduelles laissées par la deuxième phase de déformation des séries volcaniques dans le parautochtone, mais tel n'est pas le cas. Il faudrait plutôt invoquer l'effet dû au chevauchement qui aura amené en surface des roches d'assez grande profondeur de façon à ce que ces dernières oblitèrent la structure de surface, ou un déplacement du parautochtone assez considérable pour mettre en place, face à face, des roches structuralement étrangères l'une à l'autre, phénomène d'ailleurs peu probable.

Les cartes aéromagnétiques du champ total et du relief éclairé montrent des effets de réverbération ou de surimpression dans le parautochtone immédiatement au nord du front des Granulites. On peut interpréter ceci comme la trace des nappes grenvilliennes qui auraient laissé des empreintes magnétiques après érosion. Il est probable que ces nappes n'aient pas rejoint la ZTFG dans la région de Chibougamau.

Le front de Grenville se distingue par la présence de cette grande plage de parautochtone Archéen coincée entre les granulites et les roches volcaniques de la province du Supérieur. La situation est très différente ailleurs le long du front, même à l'intérieur du parautochtone Archéen (Chown, 1979). À l'extérieur du contexte géologique de ce dernier, on pourra retrouver:

— des roches huroniennes en contact avec des gneiss granulitiques de nature hybride (Lumbers, 1978; Davidson et coll., 1979; Davidson, 1984);

— des roches équivalentes au groupe de Pontiac coincées entre des roches plutoniques de type archéen et des gneiss granulitiques (Lumbers, 1978);

— le groupe de Pontiac, proprement dit, retectonisé en passant le front et en contact avec des gneiss granulitiques;

— des roches de la fosse du Labrador en contact avec leurs équivalents métamorphisés dans la province de Grenville (Rivers, 1983); et,

— des roches plutoniques et gneissiques d'origine archéenne et protérozoïque en contact dans des zones hautement tectonisées selon de grands chevauchements (Gower et coll., 1980; Gower et Owen, 1984).

Si on compare de façon préliminaire le parautochtone Archéen avec un autre socle présentant quelques affinités pétrologiques, comme le domaine du lac Bienville situé au Québec, au nord de la rivière La Grande (Ciesielski, 1984; Card et Ciesielski, sous presse), on note dans ce dernier l'absence évidente de séries volcano-sédimentaires. De petites différences structurales et pétrologiques existent et l'origine et le métamorphisme des enclaves de métabasites se présentent de façon tout à fait différente. En l'occurence, le parautochtone est aussi un socle orthogneissique, mais accuse une remontée certainement moins considérable que celle du domaine du lac Bienville et a eu lieu 1,5 million d'années plus tard, dans un contexte différent de tectonique tangentielle à la fois ductile et cassante et sans venue magmatique majeure.

Il semble donc que les recherches futures les plus utiles sur la ZTFG devront porter sur:

— les différents types de métamorphisme grenvillien le long de la ZTFG et leur influence sur l'autochtone et le parautochtone Archéen, tout en établissant la façon dont ils se distinguent des métamorphismes typiquement kénoréens, et en particulier sur la présence ou l'absence d'un isograde "grenat" dans la région du Front, ainsi que son origine;

— la morphologie des différents isogrades de type archéen et grenvillien, ou les deux, et leur rapport à la tectonique, et plus particulièrement sur l'existence de rebroussements d'isogrades profonds de type Kapuskasing;

— la déformation dans le parautochtone Archéen et son rapport à la déformation dans l'autochtone, ainsi que son rapport avec la morphologie de la ZTFG;

— la déformation cassante et son rapport aux types de lithologies archéennes le long de la ZTFG; et,

— la géochronologie des différentes entités impliquées le long de la ZTFG, et une autre tentative d'établir l'âge du métamorphisme grenvillien, afin de confirmer les dates obtenues par Baker (1980).

Remerciements

Bibliographie

Allard, G.O.
1967: Geology of Northwest Quarter of Rinfret Township, Abitibi-East and Roberval Counties; Ministère des Richesses Naturelles du Québec, PR 567.

1976: Doré Lake Complex and its importance to Chibougamau Geology and Metallogeny; Ministère des Richesses Naturelles du Québec, DPV 368.

1978: Pétrologie et potentiel économique du prolongement du sillon de roches vertes de Chibougamau dans la Province de Grenville; Ministère des Richesses Naturelles du Québec, DPV 604.

1979: Prolongement du Complexe du Lac Doré dans la Province de Grenville à l'est de Chibougamau; Ministère des Richesses Naturelles du Québec, DPV 685.

1981: Quart sud-ouest du canton de Rinfret et partie du quart sud-est du canton de Lemoine-Relation avec le Front de Grenville; Ministère de l'Énergie et des Ressources du Québec, DPV 759.

Avramtchev, L.
1975: Géologie du quart nord-est canton de McCorkill; ministère des Richesses Naturelles du Québec, RP 611.

Baker, D.J.
1980: The Metamorphic and Structural History of the Grenville Front near Chibougamau, Quebec; Unpub. Ph. D. Thesis, University of Georgia, Athens, Georgia, 344 p.

Bellavance, Y.
1984: Étude pétrographique et structurale du batholite de Ladauversière; Projet de fin d'étude, inédit, Université du Québec à Chicoutimi, 70 p.

Card, K.D. and Ciesielski, A.
—   Subdivisions of the Superior Province of the Canadian Shield; 5e Geoscience Canada. (sous presse)

Charbonneau, J.M. et Dupuis-Hébert, L.
1983: Lithostratigraphie de la région des lacs Lamarck et La Trêve, Québec; dans Ministère de l'Énergie et des Ressources du Québec, DV 83-11, p. 35-46.

Chown, E.H.
1971: Région de la Rivière Savane, Territoire de Mistassini, Comtés de Roberval et Chicoutimi; Ministère des Richesses Naturelles du Québec, RP 146.

1979: Structure and Metamorphism of the Otish Mountain Area of the Grenvillian Foreland Zone, Quebec; Geological Society of America Bulletin, Part 2, v. 90, p. 178-196.

Ciesielski, A.
1984: Pétrologie des gneiss du domaine du lac Bienville, sous-province archéenne d'Ungava, Québec: rapport d'étape; dans Recherches en cours, partie B, Commission géologique du Canada, Étude 84-1B, p. 1-10.

Cimon, J.
1977: Quart Nord-Ouest du Canton de Dollier; Ministère des Richesses Naturelles du Québec, DPV 504.

Commission géologique du Canada
1984: Cartes aéromagnétiques du champ total à relief éclairé inédites; Cartes aéromagnétiques du champ total no. NL 18-M et NL 19-M.

Daigneault, R. et Allard, G.O.
1984: Évolution Tectonique d'une Portion du Sillon de Roches Vertes de Chibougamau; Canadian Institute of Mining and Metallurgy, Special v. 34, p. 212-228.

Davidson, A., Britton, J.M., Bell, K., and Blenkinsop, J.
1979: Regional Synthesis on the Grenville Province of Ontario and Western Quebec; in Current Research Part B, Geological Survey of Canada Paper 79-1B, p. 153-172.

Davidson, A.
1984: Tectonic Boundaries within the Grenville Province of the Canadian Shield; Journal of Geodynamics, v. 1, p. 433-444.

Deland, A.N.
1956: The boundary between the Temiscaming and Grenville Subprovinces in the Surprise Lake area, Quebec; Proceedings of the Geological Society of America v. 9, p. 127-141.

Deland, A.N. et Grenier, P.E.
1959: Région d'Hazeur-Druillettes, district électoral d'Abitibi-est; Ministère des Mines du Québec, RG 87.

Frith, R.A. and Doig, R.
1975: Pre Kenoran Tonalitic Gneisses in the Grenville Province; Canadian Journal of Earth Sciences, v. 12, p. 844-849.

Gilbert, J.E.
1959: Région de Rohault, districts électoraux d'Abitibi-est et de Roberval; Ministère des Mines du Québec, RG 86.

Gobeil, A. et Racicot, D.
1983: Carte lithostratigraphique de la région de Chibougamau; Ministère de l'Énergie et des Ressources du Québec, MM-83-02, 14 p.

Gower, C.F. and Owen, V.
1984: Pre-Grenvillian and Grenvillian lithotectonic regions in eastern Labrador-correlations with the Sveconorwegian Orogenic Belt in Sweden; Canadian Journal of Earth Sciences, v. 21, p. 678-693

Gower, C.F., Ryan, A.B., Bailey, D.G., and Thomas, A.
1980: The position of the Grenville Front in Eastern and Central Labrador; Canadian Journal of Earth Sciences, v. 17, p. 784-788.

Grenier, P.E.
1953: Preliminary Report on Gamache Area, Abitibi-East County; Ministère des Mines du Québec, PR 284

Hébert, C.
1976: Demie sud du canton de Fancamp; Ministère des Richesses Naturelles du Québec, DPV 429.

1979: La Dauversière (SW) et Rohault (NW), Rapport Final; Ministère de l'Énergie et des Ressources du Québec, DPV 723.

Imbault, P.E.
1959: Région de Queylus, Districts électoraux d'Abitibi-Est et de Roberval; Ministère des Mines du Québec, RG 83.

Kline, S.W.
1984: Metamorphic Mineralogy of The Dore Lake Complex in the vicinity of the Grenville Front; Canadian Institute of Mining and Metallurgy Special v. 34, p. 198-211.

Laurin, A.F.
1955: Preliminary Report on Ducharme-Bouteroue Area, Roberval and Abitibi-East Counties; Ministère des Mines du Québec PR 310.

Longley, W.W.
1959: Région de Rinfret, Chibougamau, Districts électoraux d'Abitibi-est et de Roberval; Ministère des Mines du Québec, RG 81.

Lumbers, S.B.
1971: Geology of the North Bay Area, Districts of Nipissing and Parry Sound; Ontario Department of mines Geol. Rep. 94.

1975: Geology of the Burwash Area, Districts of Nipissing, Parry Sound and Sudbury; Ontario Division of Mines Geol. Rep. 116.

1978: Geology of the Grenville Front Tectonic Zone in Ontario; Geological Association of Canada-Mineralogical Association of Canada Annual Meeting, Field Trips Guidebook p. 347-361.

Marquis, R.
1980: Étude tectono-stratigraphique à l'est de Val-d'Or: Essai de corrélation structurale entre les roches métasédimentaires des groupes de Trivio et de Garden Island et application à l'exploration aurifère; Mémoire de maîtrise inédit, Université du Québec à Montréal, 175 p.

Ministère des Richesses Naturelles du Québec
1977: Levé EM (Input). Région de Ladauversière. Questor Surveys Ltd., Ministère des Richesses Naturelles du Québec, DP-496.

Neale, E.R.W.
1959: Région de Dollier-Charron, Districts électoraux d'Abitibi-Est et de Roberval; Ministère des Mines du Québec, RG 82.

Racicot, D., Chown, E.H., and Hanel, T.
1984: Plutons of the Chibougamau-Desmaraisville Belt: A preliminary survey; Canadian Institute of Mining and Metallurgy Special v. 34, p. 178-197.

Remick, J.H.
1970: Géologie de la région de Bressani-Chambalon, comté d'Abitibi-Est; Ministère des Richesses Naturelles du Québec, RP 581.

Rivers, T.
1983: Progressive metamorphism of pelitic and quartzofeldspathic rocks in the Grenville Province of western Labrador-tectonic implications of bathozone 6 assemblages; Canadian Journal of Earth Sciences, v. 20, 1791-1804.

Rivers, T. and Chown, E.H.
–   The Grenville Orogen in Eastern Quebec and Western Labrador-Definition, Identification and Tectonometamorphic Relationships of Autochtonous and Allochtonous Terranes; Geological Association of Canada Special Paper. (in press)

Sethuraman, K.
1979: Géologie du Projet Echouani; cartes non publiées, Campbell Chibougamau Mines Ltd.

1984: Discovery of an Archean Volcanogenic Environment in the Grenville Structural Province, Echouani Area, Quebec, Canada; Canadian Institute of Mining and Metallurgy Special v. 34, p. 473-482.

Thomas, M.D. and Gibb, R.A.
1983: Convergent Plate Tectonics and Related Faults in the Canadian Shield; International Basement Tectonics Association Publication no. 4, p. 115-134.

Wagner, W.R.
1978: Geology of the Chibex Gold Deposit, Chibougamau, Quebec; Mémoire de maîtrise, inédit, Université du Québec à Chicoutimi, 105 p.

Recent intertidal molluscs from the east-central coast of Ellesmere Island, Northwest Territories

Janis E. Dale [1]
Terrain Sciences Division

Abstract

Twenty-nine species of recent molluscs were collected along the east coast of Ellesmere Island in the intertidal and nearshore area. All were cold water species adapted to habitation in a harsh intertidal environment, with ice cover 10 months of the year and exposure to ice gouging and melt runoff the remaining two months. Five species of molluscs were new to Ellesmere Island.

The greatest mollusc densities were found in the midtidal zone (approximately 1 m above lowest low tide) where large numbers of mobile gastropods dwelled. Larger sedentary forms were more common lower or in protected intertidal areas. Some of the recent species have existed in the area for more than 8000 years.

Résumé

Vingt-neuf espèces de mollusques récents ont été recueillis dans la zone intertidale du littoral oriental de l'île Ellesmere. Toutes les espèces observées sont adaptées à l'eau froide dans un habitat soumis à un milieu intertidal rigoureux, recouvert de glace dix mois par année et exposés au frottement des glaces et aux eaux de fonte au cours des deux autres mois. Cinq espèces de mollusques ont été découvertes pour la première fois sur l'île Ellesmere.

Les plus grandes densités de mollusques ont été observées au centre de la zone intertidale (à environ 1 m au-dessus de la marée basse) où se sont installés un grand nombre de gastropodes mobiles. Les gastropodes sédentaires sont plus nombreux dans la partie inférieure des zones intertidales ou dans les zones intertidales protégées. Certaines espèces récentes existent dans la région depuis plus de 8 000 ans.

---

[1] Department of Geography, Queen's University, Kingston, Ontario K7L 3N6

Introduction

This report introduces a species list of recent intertidal molluscs collected along the east coast of Ellesmere Island. Collections were taken near Cape Herschel (78° 35'N, 74° 35'W) and at Alexandra Fiord (78° 53'N, 75° 45'W) from 1 June to 20 July, 1983 (Fig. 37.1). The only previously published faunal records for the area were made by Grieg (1909), who examined specimens dredged from shallow water during the first year of the Second Norwegian Arctic Expedition in the "Fram", 1898-1902. More recently Macpherson (1971) and Lubinsky (1980) have recorded the ranges of molluscs found in the Arctic. Ellis (1960, 1966) and Ellis and Wilce (1961) described fauna found in the subtidal and intertidal environments of Baffin Island, and Thomson (1982) studied the community structure of marine benthos in Lancaster Sound and Baffin Bay in the subtidal environment. Thorson (1936), Vibe (1939, 1950), and Madsen (1936, 1940) examined fauna along the west coast of Greenland in latitudes comparable to those of this study.

This report is contribution No. 21 from the Cape Herschel project.

Collection sites

Six locations were examined in the vicinity of Cape Herschel and Alexandra Fiord (Fig. 37.1). All sites experienced macrotidal, semi-diurnal tides with a mean tidal range of 2.9 m and a large range of 4.5 m (M. Krawetz, personal communication, 1983). A high potential for ice movement and corresponding sediment redistribution exists as a result of such large influxes of water. The sites varied in exposure to wave and sea ice action, as well as freshwater and sediment input. They ranged from low, broad intertidal flats to steep, rocky shorelines (Table 37.1).

The study was confined to the intertidal zone because of logistical limitations. This zone had not been studied previously in any detail in the Canadian High Arctic. Reconnaissance began in early June when the approximate limits of the intertidal zone could be determined by the presence of coastal sediments and shell debris in the sea ice. Molluscs that had been frozen into the sea ice during freezeup or that were subject to ice push activity became exposed at the ice surface as the sea ice ablated.

The intertidal ice cover had deteriorated by 1 July 1983, exposing the substrate during low tide and permitting random collections of live fauna. In addition, random cores were taken with a total surface area of 100 cm² to an average depth of 10 cm. The cores were sieved through a 0.5 mm screen (1.0 ϕ) and the fauna was preserved whole in buffered 10% formalin for 24 hours and then transferred to isopropyl alcohol. Estimates of mollusc density were calculated from the core results.
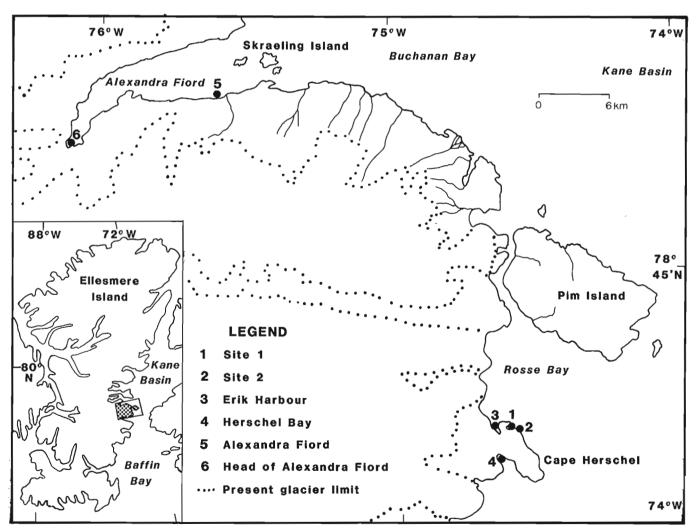

Figure 37.1. Location map, east-central coast of Ellesmere Island.

Table 37.1. Collection site characteristics

Sites	Aspect	Intertidal width (km)	Slope	Freshwater input	Shoreline	Intertidal characteristics
SITE 1	NE sheltered	0.8	Gradual	Ice; small stream	Bedrock	Boulder and sediment mounds with pool; silts on the upper flat and in pools; coarser sands and gravels seaward.
SITE 2	NE Exposed	0.10	Narrow bench, then steep	Ice	Bedrock	Large boulder and sediment mounds with pools; tidal channel with silt at shoreline; coarser sands seaward.
ERIK HARBOUR	N Sheltered	1.0	Gradual	Ice; small streams	Partially vegetated zone and beach	Broad intertidal zone with boulder mounds, tidal channels; fines with underlying gravels at high tide mark.
HERSCHEL BAY	SE Sheltered, except S winds	1.5	NA Under ice	Ice; small streams	Sandy Beach	Numerous ballycatters, indicative of boulder mounds.
ALEXANDRA FIORD	N Exposed	0.10	Gradual to boulder ridge, then steep	Ice; river to east	Bedrock and delta	Silts at shore coarsening seaward to sands at boulder ridge, <0.8 m ALLT; pools, sediment mounds, some boulders on inner flat.
HEAD OF ALEXANDRA FIORD	N Sheltered	1.0	Gradual	River	Delta sands	Sorted sands observed under ice.

Ice action affects the study sites throughout the season to varying degrees. The area has a solid cover of sea ice up to 10 months of the year, from approximately October to July (M. Krawetz, personal communication, 1983). From observations made in 1983, the presence of fast ice helped delay thawing of the frozen substrate at the inception of breakup, thus inhibiting larval settlement and faunal activity. Some infaunal benthos such as the **Mya truncata** and **Serripes groenlandicus** lived within the icefoot zone and were probably frozen within the substrate most of the winter. Once the coastal fast ice had ablated, offshore ice and multi-year ice continued to raft into the intertidal zone. Ice gouging of the substrate by this ice not only disrupted the sediment by dislodging the fine fractions, but also crushed fragile molluscs and barnacles on exposed sediment and rock surfaces. Ice melt resulted in lowered salinity and appeared to inhibit faunal activity (Dale, 1982).

Balanus crenatus (Bruguière, 1789), **Balanus balanus** L., and various species of macroalgae were also collected at the lower edge of the intertidal zone in protected crevices on boulders. Shell debris from the barnacles was found throughout the area at all sites indicating larger subtidal populations.

Observations and results

Twenty-eight species were collected in 1983, and one gastropod was sampled in 1979 (BS-79-24). The 29 species include 13 gastropods and 16 bivalves. Table 37.2 lists the family, genus, and species names, as well as the condition when collected (living or dead). Twelve species were collected live and thus are able to colonize the intertidal zone for at least a brief period. These species are **Margarites helicinus, Cingula castanea, Oenopota bicarinata, Cylichna alba, Retusa obtusa, Crenella faba, Musculus discors, Axinopsida orbiculata, Serripes groenlandicus, Macoma calcarea, Mya truncata,** and **Hiatella arctica.** The remaining species may have been transported into the intertidal zone from deeper sites by ice or wave action.

The table also includes collection site information and previous records for the area. The most common species found and the number of sites where collected are as follows: **Mya truncata** (6), **Hiatella arctica** (6), **Portlandia arctica** (5), **Cylichna alba** (5), **Oenopota bicarinata** (4), **Astarte borealis** (4), and **Axinopsida orbiculata** (4). Six of the molluscs were represented by single specimens: **Buccinum** cf. **hydrophanum, Buccinum** sp., cf. **Colus** sp., **Crenella faba,** cf. **Yoldiella** sp., and **Bathyarca glacialis.** These six plus **Cingula castanea** and **Retusa obtusa** were present at only one of the six sites.

The greatest number of live species was collected in the low broad intertidal zone where the accumulation of fine sediment enhanced living conditions (e.g., Site 1 (10 species), and Erik Harbour (8) (Table 37.2)). Fewer species were present on the coarser, steeper substrate at Site 2 (7) and the exposed narrow tidal flat at Alexandra Fiord (5). Unfavourable ice conditions hampered collection at Herschel Bay (4) and the delta at the head of Alexandra Fiord (3). In general, the sediments coarsen across the intertidal zone in a seaward direction. Finer sediments drape the upper flats where poorly drained pools have developed from ice microrelief structures. It is difficult to determine whether change in tidal height or grain size is the primary control on mollusc presence and frequency.

Cores were taken at Site 1, Site 2, and Alexandra Fiord in order to estimate mollusc densities (Table 37.3). The highest density of molluscs (41 organisms/100 cm^2) was obtained at Site 1, a narrow sheltered inlet which inclined gently seaward. This concentration was recorded on the slope of a fine grained sediment mound in the midflat region

Table 37.2. Intertidal species list (Gastropoda, Bivalvia), Eastern Ellesmere Island, N.W.T.[1]

Family, Genus, Species	Condition[2]	Site 1	Site 2	Erik Hbr.	Collection sites (cf. Fig. 37.1) Herschel Bay	Alex. Fd.	Head Alex Fd.	Grieg's samples (1909)
GASTROPODA								
LEPETIDAE								
Lepeta caeca (Müller, 1776)	D			X		X		
TROCHIDAE								
Margarites helicinus (Phipps, 1774)	L	X	X	X				X
Margarites umbilicalis[3] (Broderip & Sowerby, 1829)	L				X			X
RISSOIDAE								
Cingula castanea (Møller, 1842)	L	X						
TRICHOTROPIDAE								
Trichotropis borealis Broderip & Sowerby, 1829	D	X						X
BUCCINIDAE								
cf. **Colus** sp.	D					X		
Buccinum sp.	D					X		X
Buccinum cf. **hydrophanum** Hancock, 1846	D						X	
TURRIDAE								
Oenopota arctica (A. Adams, 1855)	D	X				X		
Oenopota bicarinata (Couthouy, 1838)	L	X		X		X	X	
Oenopota turricula (Montagu, 1803)	D					X		
CYLICHNIDAE								
Cylichna alba Brown, 1827	L	X	X	X	X	X		
RETUSIDAE								
Retusa obtusa (Montagu, 1807)	L	X						
BIVALVIA								
NUCULANIDAE								
Portlandia arctica (Gray, 1824)	D	X		X	X	X	X	
cf. **Yoldiella** sp.	D			X				
Yoldiella cf. **intermedia** (M. Sars, 1865)	D	X		X				
ARCIDAE								
Bathyarca glacialis (Gray, 1824)	D			X				
MYTILIDAE								
Crenella faba (Müller, 1776)	L		X					
Musculus discors (Linné, 1767)	L		X	X				X
ASTARTIDAE								
Astarte sp.	D	X		X	X	X		
Astarte borealis (Schumacher, 1817)	D	X		X	X	X		X
Astarte montagui (Dillwyn, 1817)	D	X		X				X
Astarte striata (Leach, 1819)	D			X				
THYASIRIDAE								
Axinopsida orbiculata (G.O. Sars, 1878)	L	X	X	X	X			
CARDIIDAE								
cf. **Clinocardium** sp.	D	X		X				
Serripes groenlandicus (Bruguière, 1789)	L	X				X		X
TELLINIDAE								
Macoma calcarea (Gmelin, 1791)	L	X		X				
MYIDAE								
Mya truncata Linné, 1758	L	X	X	X	X	X	X	X
HIATELLIDAE								
Hiatella arctica Linné, 1767	L	X	X	X	X	X	X	X

[1] Samples deposited at the National Museum of Natural Sciences, Ottawa, Canada. Accession No. IZ 1984-117
[2] L = Live; D = Dead
[3] Collected by W. Blake, Jr., 7.5 m below the sea ice surface (BS-79-24)

on 15 July 1983 and included **Axinopsida orbiculata** which accounted for 58% of the specimens, **Cylichna alba** 24%, and **Oenopota bicarinata** 17%. Replicate sampling at Site 1 showed that a faunal bloom occurred between 7 July and 15 July 1983, with average mollusc densities rising from 9.2/100 cm² to 17.3/100 cm². Increases in the number of **Axinopsida Oenopota** and **Cylichna** accounted for the rise in density.

The largest densities of molluscs were found in the midflat region at approximately 1 m above lowest low tide (ALLT). In general, at this tidal height, fine sediment had accumulated and sediment mounds with intervening tidal pools had developed. The largest mollusc populations were always at 1 m ALLT, even at more exposed collection sites where ice and wave action discouraged fine sedimentation and disrupted tidal pool development. However, within this tidal range the faunal distribution was highly variable due to the paucity of fauna found at some sites and, as illustrated by the high variations in standard deviations calculated from the mollusc densities (Table 37.3).

The smaller molluscs such as **Oenopota, Cylichna,** and **Axinopsida** were found in great numbers in the midflat region. The larger molluscs such as the infaunal **Mya** and **Hiatella** were found more commonly at the lower edge of the flats. Alexandra Fiord was an exception with **Mya** and **Hiatella** inhabiting the midflat zone. A discontinuous boulder ridge at the lower edge of these flats probably helped protect the inner zone from severe ice gouging and enhanced

Table 37.3. Core results, species numbers, and densities

Location		Site description	Sample date in 1983	Axinopsida orbiculata	Cylichna alba	Hiatella arctica	Mya truncata	Oenopota bicarinata	Total fauna per 100 cm²	Average density per 100 cm²
					Number of each species per 100 cm²					
Site 1	83-JD-46	Midtidal sediment mound	July 6	5	3	–	–	2	10	
	83-JD-53	Silts between boulder mounds	July 7	2	5	–	–	–	7	
	83-JD-54	Silts and sands, side of boulder mound	July 7	1	3	–	–	–	4	
	83-JD-55	Silts, runnel between boulder mounds	July 7	5	3	1	–	3	12	
	83-JD-57	Silts and sands, side of sediment mound	July 7	7	3	1	–	2	13	
										9.2 std = 3.7
Site 1	83-JD-109	Same site as 83-JD-46	July 15	24	10	–	–	7	41	
	83-JD-117	Same site as 83-JD-55	July 15	11	4	5	–	3	23	
	83-JD-95	Low intertidal sands, some gravels	July 15	3	2	–	–	–	5	
	83-JD-94	Low intertidal, tidal channel	July 15	–	–	–	–	–	–	
										17.3 std = 18.7
Site 2	83-JD-83a	Inner pool, silts by icefoot	July 14	–	–	–	–	–		
	83-JD-83b	Low intertidal pool, landward of boulder ridge	July 14	–	–	–	–	–		
	83-JD-81	Silts, side of boulder mound, low intertidal	July 14	–	–	–	–	–		
	83-JD-82	Same as 83-JD-83b	July 14	–	–	–	–	–		
	83-JD-80	Silts and clay, low intertidal	July 14	–	–	–	–	–		
	83-JD-91	Same as 83-JD-81	July 14	–	1	1	–	–	2	
										0.3 std = .82
Alexandra Fiord										
	83-JD-102A	Midtidal pool	July 17	–	1	–	1	–	2	
	83-JD-102B	Low intertidal, seaward of boulder ridge	July 17	–	–	–	–	–		
	83-JD-110C	Shoreward side of boulder ridge	July 17	–	1	–	–	–	1	
	83-JD-111D	Midtidal pool	July 17	–	–	–	2	–	2	
	83-JD-11A	Fluvial delta, midtidal	July 18	–	–	–	–	–	–	
	83-JD-11B	Fluvial delta, low intertidal	July 18	–	–	–	–	–		
	83-JD-112C	Pool, shoreward side of boulder ridge	July 18	–	–	2	1	–	3	
										1.14 std = 1.2

sedimentation of fine material. The paucity and small size of the live **Mya** and **Hiatella** sampled, however, illustrates the continued severity of conditions resulting in short life spans and slow growth (see Hewitt and Dale, 1984 for further analyses of these same samples). In more suitable subarctic, intertidal environments **Mya truncata** specimens can reach a maximum age of 40 years and shell lengths up to 8.7 cm (Hewitt and Dale, 1984). The maximum age and length attained by **Mya truncata** collected live in this study was 16 years at 4.2 cm (Hewitt and Dale, 1984). A great number of larger empty valves were found on these same flats, probably washed up from the subtidal area by wave and ice action. A sizable walrus population in the area feeds on this species, making empty shells available for transport to the intertidal area in Alexandra Fiord.

Conclusions

All the molluscs collected are recognized as northern species. **Cingula castanea, Cylichna alba, Retusa obtusa, Oenopota arctica,** and **Oenopota turricula** are new to Ellesmere Island; the latter two were considered previously to occupy a range to northern Baffin Island. Twelve of the species collected are shallow-water forms capable of intertidal habitation. They can withstand a harsh marine environment with ice cover for 10 months of the year and exposure to ice gouging and freshwater input during the remaining two months. In this high arctic locale, the greatest densities are found in the midtidal zone around 1 m ALLT where large numbers of the smaller, more mobile gastropods dwell, such as **Oenopota** and **Cylichna** and the tiny bivalve **Axinopsida**. Larger sedentary forms such as **Mya, Hiatella,** and **Serripes** are found lower or in protected sites in the intertidal areas like Alexandra Fiord. The relatively small size of **Mya truncata** at this latter locale reflects their short life span and slow growth rate in what must be a marginally habitable environment (Hewitt and Dale, 1984).

Several of these recent species have been collected in raised strandlines on Ellesmere Island and their ages determined by radiocarbon dating. **Mya truncata** at the head of Alexandra Fiord have been dated at 7000 ± 70 BP (GSC-3288; Blake, 1982) and **Hiatella arctica** near Cape Herschel were dated at 8930 ± 100 BP (GSC-2519; Blake, 1981). As well as **Mya** and **Hiatella**, samples of **Portlandia arctica** (Blake, 1981), **Serripes groenlandicus, Macoma calcarea,** and **Clinocardium ciliatum** collected on Ellesmere Island, have had ages ranging from 8000 BP to the present (Blake, 1975). These findings appear to indicate fairly continuous habitation by these molluscs in high arctic waters. Again, this reflects their ability to adapt to severe and variable environmental conditions.

Acknowledgments

References

Blake, W., Jr.
  1975: Radiocarbon age determinations and postglacial emergence at Cape Storm, southern Ellesmere Island, Arctic Canada; Geografiska Annaler, Series A, v. 57, p. 1-71.

  1981: Neoglacial fluctuations of glaciers, southeastern Ellesmere Island, Canadian Arctic Archipelago; Geografiska Annaler, Series A, v. 63, p. 201-218.

Blake, W., Jr. (cont.)
  1982: Coring of frozen pond sediments, east-central Ellesmere Island: a progress report; in Current Research, Part C, Geological Survey of Canada, Paper 82-1C, p. 104-110.

Dale, J.E.
  1982: Physical and biological zonation of subarctic tidal flats at Frobisher Bay, southeast Baffin Island; unpublished M.Sc. thesis, McMaster University, Hamilton, 267 p.

Ellis, D.V.
  1960: Marine infaunal benthos in North America; Arctic Institute of North America, Technical Paper, no. 5, 53 p.

  1966: Some observations on the shore fauna of Baffin Island; Arctic, v. 14, p. 224-236.

Ellis, D.V. and Wilce, R.J.
  1961: Arctic and subarctic examples of intertidal zonation; Arctic, v. 14, p. 229-236.

Grieg, J.A.
  1909: Brachiopods and molluscs with a supplement to the echinoderms. Report of the Second Norwegian Arctic Expedition in the "Fram" 1898-1902; Videnskabs-Selskabet i Kristiania, No. 20, 38 p.

Hewitt, R.A. and Dale, J.E.
  1984: Growth increments of modern **Mya truncata** L. from the Canadian Arctic, Greenland, and Scotland; in Current Research, Part B, Geological Survey of Canada, Paper 84-1B, p. 179-186.

Lubinsky, I.
  1980: Marine bivalve molluscs of the Canadian central and eastern Arctic: faunal composition and zoogeography; Canadian Bulletin of Fisheries and Aquatic Sciences, Bulletin 207, 111 p.

Macpherson, E.
  1971: The marine molluscs of Arctic Canada; Publications in Biological Oceanography, No. 3, National Museums of Canada, Ottawa, 149 p.

Madsen, H.
  1936: Investigations on the shore fauna of East Greenland with a survey of the shores of other arctic regions; Meddelelser om Grønland, v. 100, no. 8, 79 p.

  1940: A study of the littoral fauna of Northwest Greenland; Meddelelser om Grønland, v. 124, no. 3, 24 p.

Thomson, D.H.
  1982: Marine benthos in the eastern Canadian High Arctic: multivariate analyses of standing crop and community structure; Arctic, v. 35, no. 1, p. 61-74.

Thorson, G.
  1936: The larval development, growth, and metabolism of Arctic marine bottom invertebrates compared with those of other seas; Meddelelser om Grønland, v. 100, no. 6, 155 p.

Vibe, C.
  1939: Preliminary investigations on shallow water animal communities in the Upernavik- and Thule-Districts (Northwest Greenland); Meddelelser om Grønland, v. 124, no. 2, 42 p.

  1950: The marine mammals and the marine fauna in the Thule District (Northwest Greenland) with observations on ice conditions in 1939-41; Meddelelser om Grønland, v. 150, no. 6, 115 p.

A regional marine multiparameter survey south of Newfoundland

Projects 730081, 810031

Ron Macnab, B.D. Loncarevic, R.V. Cooper [1], P.R. Girouard,
M.D. Hughes, and Fan Shouzhi [2]
Atlantic Geoscience Centre, Dartmouth

Abstract

A combined hydrographic-geophysical survey cruise has completed the regional mapping of the offshore south of Newfoundland. Good quality bathymetric, magnetic, and gravity data were collected at a line spacing of ten nautical miles, using a combination of satellite navigation and rho-rho Loran-C.

A number of secondary trials and experiments were carried out in conjunction with this survey: intercomparison of two modern sea gravimeters, a Bodenseewerk KSS-30 and a LaCoste and Romberg with modified electronics; evaluation of GPS for routine survey positioning; test and development of a microcomputer-based data logging system; and measurements of ship's magnetic effect.

Résumé

Un équipage chargé de réaliser des levés hydrographiques et géophysiques a terminé la cartographie régionale du fond océanique situé au sud de Terre-Neuve. On a recueilli, selon un espacement linéaire de dix milles marins, des données bathymétriques, magnétiques et gravimétriques de bonne qualité en utilisant la navigation par satellite et le système rho-rho Loran-C.

Des expériences et essais secondaires ont été réalisés parallèlement: comparaison de deux gravimètres océaniques (un Bodenseewerk KSS-30 et un LaCoste and Romberg aux composantes électroniques modifiées), évaluation du GPS pour le positionnement en ce qui concerne les levés ordinaires, essai et mise au point d'un système d'enregistrement des données sur micro-ordinateur et mesure de l'effet magnétique du navire.

---

[1] Earth Physics Branch, Ottawa
[2] Institute of Oceanology, Academia Sinica, Tsingtao, P.R.C.

Introduction

In late 1984, hydrographers and geophysicists sailed for five weeks aboard **CSS Baffin** to conduct a regional survey in an area covering some 77 000 km^2 south of Newfoundland. Survey tracks are shown in Figure 38.1. The operation was a continuation of the offshore survey program that has contributed to the mapping of a large segment of the Canadian East Coast Offshore since 1964 (Macnab, 1983a; Miller et al., 1983).

Seagoing staff represented the following three agencies of the Federal Government: the Atlantic Region of the Canadian Hydrographic Service (CHS); the Gravity, Geothermics, and Geodynamics Division of the Earth Physics Branch (EPB); and the Atlantic Geoscience Centre (AGC) of the Geological Survey of Canada.

The primary purpose of the survey was to measure systematically the large-scale features of the bathymetry, the magnetic field, and the gravity field on the continental shelf and part of the slope. Detailed bathymetric measurements are planned for future hydrographic surveys, while high-resolution magnetic data will be collected by airborne methods.

Secondary purposes of the cruise were: to carry out a preliminary assessment of GPS (Global Positioning System) as a means of routine survey positioning; to perform an intercomparison between two sea gravimeters, a standard Bodenseewerk KSS-30, and a modified LaCoste & Romberg Straight-Line system; to carry out tests and development of CIGAL, a new computer-based data acquisition and logging system.

Survey navigation

The main navigation system used in the survey was BIONAV – the Bedford Institute of Oceanography Integrated Navigation System – which combines satellite data from a Marconi NNSS receiver and range data from an Austron Loran-C system operating in rho-rho mode (Wells and Grant, 1981). Except for some internal real-time processing problems discussed below, the quality of navigation was excellent throughout the survey, with positional accuracies estimated to be 150 m or better.

Shipboard data processing

Geophysical data were processed mainly by means of the Atlantic Geoscience Centre's standard seagoing software package, SHIPAC (Macnab, 1983b). Some additional software was provided by Earth Physics Branch, while preliminary navigation checks and bathymetric processing were handled largely by Canadian Hydrographic Service routines.

Figure 38.1. *Ships' tracks from combined hydrographic-geophysical surveys off Newfoundland and Nova Scotia in 1979, 1982, and 1984. Tracks illustrated by the heavy solid lines represent the cruise described in the text.*

Recorded on magnetic tape by three separate logging devices, three sets of potential field observations (from a towed proton precession magnetometer and the two sea gravimeters) were transferred to disc files in the shipboard computer for error checks and corrections, display, and merging with navigation and bathymetry.

Departing from previous years' practice of using Eotvos corrections calculated in real time by BIONAV, a new off-line procedure was initiated: corrections were calculated at one-minute intervals from recorded positional data, then treated with a ten-point filter that compensated for the known delay factor in BIONAV while eliminating minor navigational noise.

The calculated and filtered Eotvos corrections were plotted on a daily basis as a further check on the navigation, in order to satisfy the stringent positioning requirements of gravity measurements. In these daily plots, potential problems in navigation manifested themselves in various forms, most often as spikes that signalled discontinuities in course or speed. In the assessment of navigation data, extensive use was made of the geographic display package MAPGEN (Evenden, 1982). This software made it extremely simple to generate fix plots at a variety of scales to pinpoint positions that required correction or deletion.

As an example of the sort of analyses carried out on the navigation data, Figure 38.2 shows a plot of the Eotvos correction over the first half of a survey day. The plot is reasonably smooth from 0000 to about 0500. There then follow two abrupt drops, corresponding to major course changes at 0500 and 0600. The remainder of the plot features several spikes in the Eotvos corrections; their apparent width is a result of the ten point filtering described above.

These spikes are improbable-looking, as changes of this magnitude and duration would have to be caused by small transients in course or speed; ships as a general rule don't move through the water in this fashion. The apparent transients are also manifest in Figure 38.3, which is a plot of one-minute BIONAV positions over the period 0851-0950 of the same day. Small irregularities in the spacing or alignment of these fixes correspond to spikes in the Eotvos correction at 0855, 0910, 0929, and 0941. These are not due

to ship's motion, but are artifacts introduced by the navigation system, which applies stepwise instead of graduated corrections to compensate for Loran-C overland phase lag. Repair in these cases consisted of simple deletion of offending fixes.

Additional software introduced on this cruise facilitated the automated and rapid analysis of data discrepancies at track crossover positions. Developed in large part by John Halpenney (EPB), these programs facilitated routine and frequent reviews of accumulated data, and contributed to the early detection of several instrumental and processing problems.

Table 38.1 describes the statistics of the crossover discrepancies of the various data sets for the entire cruise (the number of crossovers is not identical in all cases because of interruptions in logging, etc.). These crossover discrepancies were evaluated before the drift of the gravimeters could be determined. On completion of the survey, the harbour check shows a drift of +2.33 mGal in 32 days for the KSS-30 instrument. Using drift-corrected gravimeter readings somewhat reduces the means and standard deviations given in Table 38.1. A histogram of crossover discrepancies for the LaCoste & Romberg meter is shown in Figure 38.4.

A preliminary review of the data

The processing of geophysical data on a daily basis had two major benefits: (i) crossovers were evaluated on a regular basis in order to assess the overall quality of the survey; and (ii) the preliminary values of bathymetry, gravity and magnetic anomalies could be 'posted' in time to produce contoured maps of these quantities before leaving the ship.

Figure 38.2. Eotvos correction for the first half of Day 310, calculated at one-minute intervals and then subjected to ten-point filtering. Major changes at 0510 and 0600 reflect deliberate alterations in ship's cruise. Prominent spikes in the last six hours are caused by software faults in the real-time navigation software.
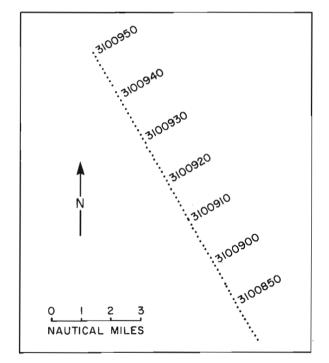

Figure 38.3. Plot of ship's positions at one minute intervals from 0.841 to 0950, Day 310 (positions were derived in real time by the BIONAV integrated navigation system). Irregularities in the spacing and alignment of the positions are evident at 0855, 0910, 0929, and 0941. These are caused by faults in the real-time navigation software, and give rise to spikes in the Eotvos corrections, as seen in Figure 38.2.

Table 38.1. Statistics on measurement discrepancies at track crossover points

Parameter	Number of points	Mean	Standard Deviation
Bathymetry	121	0.38	2.12
Magnetics	121	3.38	35.53
Gravity -L & R	124	-0.07	1.07
Gravity -KSS-30	119	0.72	1.78

The central part of the survey area covered the Laurentian Channel from the Cabot Strait to the edge of the Continental Shelf. Eight survey lines were extended over the slope of the Continental Shelf to interline earlier surveys. Similarly, three survey lines were extended to the east to connect with various surveys of the Grand Banks. These two survey extensions are not discussed in the comments that follow.

Bathymetry

Main physiographic features of the area are labelled in Figure 38.1. More detailed maps will be produced at a later date when interlining and detailed surveys are completed by Canadian Hydrographic Service.

The Laurentian Channel is the major physiographic feature of the survey area. The channel separates the Nova Scotia Shelf from the Newfoundland Shelf and the Grand Banks. Portions of the two shelves covered by the survey include the Banquereau Bank on the Nova Scotia Shelf and St. Pierre and Burgeo Banks on the Newfoundland Shelf. These banks have a smooth, flat surface with wave-cut benches established during the Pleistocene lowering of the sea level. The bottom is probably hard sand, as it is opaque to the 12 kHz sounder acoustic signal.

Between the Banquereau Bank and the Island of Cape Breton is an area of disturbed topography with erosional deeps reminiscent of karst topography. Interlining of a one to two mile line spacing will be required to properly contour this area.

On the Newfoundland side the St. Pierre and Burgeo banks are separated by a deep, fiord-like channel extending from Hermitage Bay into the Laurentian Channel. To the north is the Cabot Strait, the entrance to the Gulf of St. Lawrence.

The Nova Scotia side of the Laurentian Channel is steeper and appears to be still eroding. This is also the deeper side of the channel, with the bottom slowly rising towards the Newfoundland side. The deepest area in the channel (more than 530 m) is in Cabot Strait, and the next deepest area (490 m) occurs to the southeast some 160 km from the edge of the shelf. The bottom then shallows towards the mouth of the channel, where the sill depth is 418 m.

The gravity field

The gravity field (Fig. 38.5) is characterized by a pronounced change in character along the northeast edge of the Laurentian Channel. To the east (St. Pierre Bank) the gravity field is smooth with broad anomalies of small to moderate amplitude, while to the west anomalies are large with some of the steepest gradients recorded on the continental shelf.

Figure 38.4. Histogram of discrepancies in gravity readings acquired by the modified LaCoste and Romberg Straight Line system at track crossover points. Cell width = 0.5 mGal; mean = -0.070; standard deviation = 1.066.

The three main anomalies are: the Orpheus anomaly, which comprises a band of negative anomalies in the centre of the map; a strong positive anomaly extending eastward from the south edge of the Banquereau Bank and a strong negative anomaly north of the Orpheus anomaly.

The Orpheus anomaly is a band of deep negative anomalies extending eastward across the western ridge of the Laurentian Channel. It was interpreted earlier as the manifestation of a deep sediment-filled trough (Loncarevic and Ewing, 1967). The present survey revealed that within this general band there are several localized intense negative anomalies with one reaching -63 mGal. Speculation about the nature of these negative anomalies should take into account the results of exploration drilling in the area by oil companies. The Orpheus anomaly appears to be truncated at the Newfoundland side of the Laurentian Channel. In tectonic terms, it can be speculated that the Laurentian Channel is fault-controlled on the Newfoundland side, and that the channel was cut by a river along the downthrown side of this fault.

To the south, the Orpheus anomaly is flanked by a strong, elongate anomaly reaching a peak of +76 mGal. This anomaly parallels the shelf break but its lack of continuity suggests that it is not simply an 'edge effect' anomaly. The strong gradients over the anomaly suggest a relatively shallow source. The nature of the rock material causing this anomaly is interesting as there is no associated magnetic anomaly (see the next section) and thus an igneous intrusive can be ruled out.

To the north of the Orpheus anomaly is a broad, almost circular negative anomaly, within which is a confined area reaching -60 mGal. This interesting anomaly may represent an extension of Canso granitic intrusions though it would be the only known occurrence north of the Cobequid Fault – Orpheus Anomaly trend.

The magnetic field

The magnetic anomaly map (Fig. 38.6) shows two provinces relative to the zero nanoTesla contour. To the south of the Orpheus anomaly the field is smooth and there are no local anomalies, indicating a considerable depth to basement. There is no pronounced magnetic field gradient
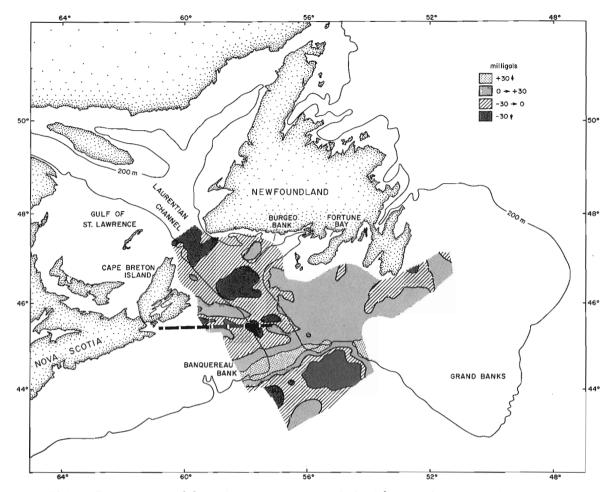
Figure 38.5. *Regional map of free air gravity anomaly, derived from cruise observations. The dashed line trending across the end of the Scotian Shelf represents the axis of the Orpheus gravity anomaly.*

associated with the shelf break and, as already mentioned, there is no magnetic anomaly associated with the +75 mGal shelf edge gravity anomaly.

The character of the magnetic field changes to the north of the Orpheus anomaly. The magnetic contours are quite convoluted and a large number of isolated anomalies occur in this area, the most intense of which reach a peak amplitude of +800 nT. On less generalized versions of Figure 38.6, there appears to be east-west structural trends but this impression cannot be confirmed since the contouring of most isolated anomalies is based on a single track. One to two mile line spacing is required to confirm the existence of any systematic structural trends.

There is no strong visual correlation between either bathymetry or gravity and the magnetic field. The only possible exception is a rather broad 400 nT anomaly in the middle of the Laurentian Channel coincident with the deepest part of the channel. To the extent that these anomalies reflect seaward extension of the land geology, their interpretation may benefit from study of the origin of onshore anomalies.

Sea gravimeter intercomparison

A standard Bodenseewek KSS-30 and a LaCoste & Romberg Straight Line system with modified electronics (Valliant et al., 1985) were operated side-by-side throughout

the survey, thus giving us an excellent opportunity to evaluate the relative performance of each instrument. Conclusions can be stated only in qualitative terms at this stage, as a detailed anlaysis is not yet complete.

In general terms, both instruments performed satisfactorily. Where comparisons were made, records from the two devices showed a remarkable similarity, reproducing faithfully even the smallest variations of the gravity field. As the weather deteriorated late in the season, the comparative record reflected the character of the two instruments. Output from the Straight-Line system continued to be relatively smooth, reflecting a higher degree of filtering than in the KSS-30. Another effect of the different digital filter design was a time delay in the KSS-30 of about 2 minutes relative to the Straight-Line system.

Over the five weeks of operation there was a gradual separation of the two records, indicating a small drift in one or the other (or both) gravimeters.

The design of the survey was such that over 130 cross-over points are available for the evaluation of the reliability of each instrument, as well as the comparison of their relative performance. These cross-overs were well distributed in time, space, direction of travel, weather conditions and gravity gradients. When completed, the evaluation should therefore provide a reliable indication of instrument performance under the operational survey conditions.
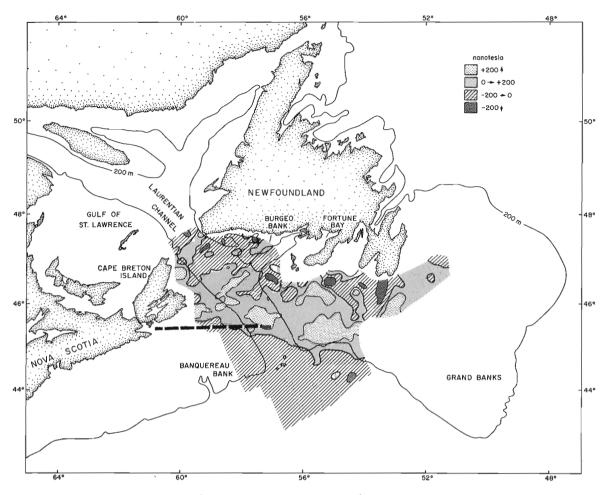
Figure 38.6. *Regional map of magnetic anomaly, derived from cruise observations. The dashed line trending across the end of the Scotian Shelf represents the axis of the Orpheus gravity anomaly.*

Preliminary analysis of the cross-overs indicates a mean of +0.1 mGal and +0.8 mGal for the Straight-Line and KSS-30 gravimeters, respectively, thus indicating that the KSS-30 may have had some positive drift. The standard deviation was just over 1 mGal for the Straight-Line and around 1.7 mGal for the KSS-30. These figures must be viewed with caution, especially that for the KSS-30. An arbitrary time shift of 3 minutes was applied to the KSS-30 output to allow for the time delay of its filter. One way of checking if this assumption is correct is to separate the cross-overs into two groups (according to the gravity gradient of the cross-over point) and to calculate the standard deviation for each group. Then one can find a better estimate of the time delay by minimizing the cross-over discrepancy within the group of high gradient cross-overs. This work is presently in hand.

An evaluation of GPS

The equipment available for this evaluation consisted of a Texas Instruments Model 4100 GPS receiver connected to a Hewlett Packard Model 9826 computer. The equipment was supplied and operated by NORTECH CO., of Calgary, Alberta using proprietory software in the HP 9826.

GPS-derived positions, courses, and velocities were fed from the HP 9826 to the KSS-30 gravimeter. In addition to being logged on the KSS-30 recorder, these data were used by the meter's internal computer to calculate Eotvos corrections in real time. Results of these calculations, along with original GPS data, were then compared with BIONAV output.

A general conclusion at this stage is that GPS is not adequate for routine gravity survey control for the following reasons:

1. There is a large scatter of independent fixes and the calculated velocity and course are very noisy. Clever predictive filtering might overcome this problem.

2. The equipment configuration employed aboard **CSS Baffin** did not provide real-time navigation (fix output was delayed by 10 to 16 seconds). The slow response of the HP 9826 computer programmed in BASIC and the generally experimental nature of the software were inadequate for the demands placed on them.

3. The constantly changing constellation of satellites requires manual dropping of satellites with elevations below 5° and a manual acquisition of new satellites as they rise above the horizon. (This may be overcome by later improved versions of receiving equipment and software for processing of fixes.)

4. As a consequence of a continuously variable constellation, the accuracy of fixes is constantly changing. It should be noted that a lock on four satellites is not necessarily better than three. If two of four satellites had

330

Figure 38.7. *CIGAL (Computer Integrated Geophysical Acquisition and Logging) system block diagram.*
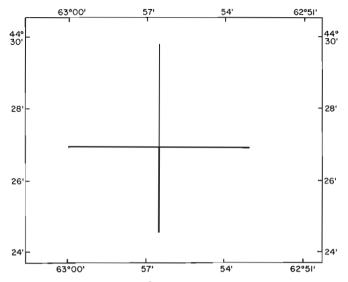

Figure 38.8. *Pattern of north-south and east-west lines executed during magnetometer heading tests. Length of each track segment is approximately five nautical miles.*

converging azimuths, then the scatter of fixes increased, as did the number of iterations necessary to calculate a fix, and the HP 9826 program frequently crashed if the two aximuths became exactly equal.

5. Hourly updating of Satellite ephemeris by the ground control station(s) causes a jump in position as well as loss of several fixes during the updating (this may be an inherent problem with the system and may be present even in the operational configuration after 1986).

6. Availability of GPS is unpredictable, but the United States Department of Defense has made it clear that the system is still in an experimental stage, and has not been released for general use. At the present time, therefore, users operate at their own risk. The system is sufficiently complex that it may take several years before it reaches the reliability of the TRANSIT system. In passing, it may be mentioned that the best of TRANSIT passes with satellites at optimum elevation and the ship on steady course in calm seas agreed very well with NAVSTAR and appeared to be of the same order of accuracy.

CIGAL

The development of CIGAL (Computer Integrated Geophysical Acquisition and Logging) was initiated in mid-1984 to replace the 20 year old BIODAL (BIO Data Logger). In BIODAL, the central controller is hardwired and is thus inflexible. The controller for CIGAL, on the other hand, is a programmable microcomputer; simple changes in software will allow the system to accommodate itself to changing operational needs.

A proposed system block diagram is shown in Figure 38.7. All inputs to CIGAL are via RS-232C or IEEE-488 communication channels; instruments or sensors with non-standard outputs will be interfaced to CIGAL via special microcomputer-based interfaces. CIGAL development is planned to occur in two phases. In Phase I, software will be written to accept gravity, magnetic, and bathymetric data. Position and time will also be accepted, but their availability will depend on parallel developments by

other groups. Output formats to be developed in Phase I include video displays (numerical and graphical), optional hard-copy plots, printouts, and storage on magnetic tape cartridges. Phase II developments will include more advanced input features, such as an event status logger, and an electronic logbook.

The CIGAL features that were developed and tested in connection with this cruise included gravimeter input and all Phase I output formats.

Ship's magnetic effect

A long-standing rule of thumb in the operation of marine magnetometers is that the disturbance caused by the magnetization of the ship's hull will be less than 10 nT if the sensor is towed at a distance of two ship lengths astern (Bullard and Mason, 1961).

A series of measurements were undertaken early in the cruise to confirm that this principle also applied to a ship like **CSS Baffin.** A cross pattern was executed that consisted of intersecting east-west and north-south tracks. Each leg of the pattern was traversed twice and in opposite directions (see Fig. 38.8).

Total magnetic field profiles for the two sets of tracks are shown in Figures 38.9 and 38.10. All data were obtained with the magnetometer sensor towed two ship lengths astern.

The north-south profiles show a nearly constant offset of 30 nT, with higher values observed on the southbound traverse. This is reasonably consistent with the theory behind current practice. Assuming the 30 nT offset can be split equally between northbound and southbound tracks, this implies a field disturbance in the order of 15 nT. This is 50% higher than suggested by the rule of thumb, and may be due to the increased steel content of the **Baffin's** icebreaking hull.

The east-west profiles show an unexpected crossover, so that readings on the eastbound traverse are higher than the westbound readings at one end, and lower at the other. The reason for this is not clear. It could arise from a lateral

Figure 38.9. *Magnetometer observations acquired on north and south traverses of pattern shown in Figure 38.8. The dashed line near 44.45 indicates the point of intersection with the east-west lines.*
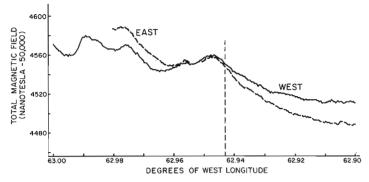

Figure 38.10. *Magnetometer observations acquired on east and west traverses of pattern shown in Figure 38.8. The dashed line near 62.94 indicates the point of intersection with the north-south lines.*

displacement of the magnetometer sensor from the ship's track, compounded by high spatial variability of the local magnetic field. Evidence of the latter can be seen in Figure 38.9; due to operational constraints, the experiment was carried out in shallow water, where inhomogeneities in the sub-bottom material would give rise to more pronounced irregularities in the magnetic field at the sea surface.

Temporal variations in the magnetic field could also be responsible for the unexpected observations on the east-west profiles. One could postulate a change in the magnetic field throughout part or all of the 75 minutes that it took to execute these profiles (including 15 minutes for the ship to reverse course). On the north-south profiles, however, the constant offset would seem to indicate a relatively stable magnetic field. This pair of profiles was initiated within only 35 minutes of the end of the east-west pair. It may not be realistic to expect that a temporal change should occur only during the first set of passes, and not the second.

Further investigation will be necessary to clear up this ambiguity, and to determine the feasibility of implementing a method to apply heading corrections to magnetometer data. Further trials, of course, should be conducted in a deep-water site with low magnetic gradient.

References

Bullard, E.C. and Mason, R.G.
1961: The magnetic field astern of a ship; Deep Sea Research, v. 8, p. 20-27.

Evenden, G.I.
1982: MAPGEN: an interactive, flexible, expandable software system for generation of publication-quality maps; First Annual Conference on the Management, Analysis, and Display of Geoscience Data, Mathematical Geologists of the United States, Golden, Colorado.

Loncarevic, B.D. and Ewing, G.N.
1967: Geophysical study of the Orpheus gravity anomaly; in World Petroleum Congress (7th:1967:Mexico City), Proceedings; v. 2, Origin of Oil, Geology and Geophysics, New York: Elsevir, p. 827-835.

Macnab, R.F.
1983a: Multiparameter mapping off the east coast of Canada: in Current Research, Part A, Geological Survey of Canada, Paper 83-1A, p. 163-171.

1983b: SHIPAC: a software package for the shipboard processing of marine geophysical survey data; in Current Research, Part B, Geological Survey of Canada, Paper 83-1A, p. 327-330.

Miller, R.O., Macnab, R., Amos, C.L., and Fader, G.B.
1983: Canadian East Coast multiparameter surveys, 1982; in Current Research, Part B, Geological Survey of Canada, Paper 83-1B, p. 331-334.

Valliant, H.D., Halpenny, J., and Cooper, R.V.
1985: A microprocessor-based controller and data acquisition system for LaCoste and Romberg air-sea gravity meters; Geophysics, v. 50.

Wells, D.E. and Grant, S.T.
1981: An adaptable integrated navigation system: BIONAV: Proceedings of Colloquium III on Petroleum Mapping and Surveys in the 80's, The Canadian Petroleum Association, Banff, Alberta.

Geology of the mid-Cretaceous volcanic units near Kingsvale, southwestern British Columbia

Project 800029

D.J. Thorkelson [1]
Cordilleran Geology Division, Vancouver

Abstract

Mid-Cretaceous Spences Bridge Group volcanic rocks unconformably overlie older plutonic rocks, and metamorphosed volcanic rocks of the Triassic Nicola Group. The Spences Bridge section comprises about 50% calcalkaline lavas, of andesitic to rhyolitic composition, and 50% clastic rocks. Overlying this package is a pile of locally conformable amygdaloidal andesite with minor intercalated clastic rocks. This rather homogeneous upper unit, herein called the amygdaloidal andesite unit, has been called Kingsvale Group by other authors. It is proposed that the name Kingsvale Group should be discontinued, leaving the amygdaloidal andesite unit without a proper name.

New K-Ar ages of 91.7 ± 3.3 Ma for the amygdaloidal andesite unit, and 94.4 ± 3.4 Ma for the Spences Bridge Group suggest no hiatus between these units.

Résumé

Les roches volcaniques du groupe de Spences Bridge datant du Crétacé moyen reposent en discordance sur des roches plutoniques plus anciennes et des roches volcaniques métamorphisées du groupe triasique de Nicola. La coupe de Spences Bridge comprend environ 50 % de lave calco-alcaline, dont la composition varie d'andésitique à rhyolitique, et 50 % de roches clastiques. Au-dessus de cet ensemble, on distingue un empilement d'andésite amygdaloïde concordante à la géologie locale et dans laquelle s'intercalent quelques roches clastiques. D'autres auteurs ont donné à cette unité supérieure plutôt homogène, appelée unité d'andésite amygdaloïde, le nom de groupe de Kingsvale. Il est proposé d'abandonner cette dernière appellation ou, en d'autres termes, de ne pas attribuer de nom propre à cette unité.

De nouvelles datations de 91,7 ± 3,3 millions d'années de l'unité d'andésite amygdaloïde, obtenues par le méthode du K-Ar, et des datations de 94,4 ± 3,4 millions d'années du groupe de Spences Bridge semblent indiquer qu'il n'existe aucune lacune stratigraphique entre ces deux unités.

---

[1] Department of Geological Sciences, University of British Columbia, Vancouver, B.C. V6T 2B4

Introduction

Fieldwork on the Cretaceous Kingsvale and Spences Bridge volcanic groups, undertaken in the summer of 1984, was concentrated in the north-central Hope (92H) and south-central Ashcroft (92I) map areas. The purpose of the project was to examine the Kingsvale Group in its type area near Kingsvale, British Columbia, and to determine its relationship with the underlying Spences Bridge Group. This study was necessary due to confusion regarding the application of correct nomenclature for Cretaceous rocks in southwestern British Columbia. During the course of fieldwork it became evident that Rice (1947) mistakenly redefined the upper part of the Spences Bridge Group as Kingsvale Group. The writer is grateful to A.J. Arthur and J.A. O'Brien for valuable discussions in the field, and to J.W.H. Monger of the Geological Survey of Canada who suggested the project and offered many stimulating ideas.

Field relations and structures

The most comprehensive mapping by the writer was completed in the vicinity of Kingsvale, about 25 km southwest of Merritt, British Columbia. A simplified version of this map is shown in Figure 39.1. The area is underlain by several mappable bedrock units, which have been condensed to the four units shown. Quaternary surficial deposits are generally thin except along Midday Creek and the northern part of the Coldwater River.

Unit 1 consists of Triassic Nicola Group volcanic rocks and plutonic intrusives of uncertain age, forming the basement to the overlying Cretaceous rocks. The Nicola volcanics are metamorphosed to lower greenschist grade or higher, and in places possess a schistose fabric. The plutonic rocks comprise two main lithologies, agmatitic granodiorite to diorite, and locally mylonitic alkali feldspar granite. Field relations indicate that the Nicola Group volcanics were intruded by the granodiorite; the alkali feldspar granite later intruded both. These intrusive rocks were clearly emplaced prior to the deposition of unit 2, as they do not cut units 2, 3, or 4. Minor volumes of younger plutonic rocks are also included in this unit.

Unit 2 is the Cretaceous Spences Bridge Group, as defined by Drysdale (1914). It consists roughly of 50% lavas, which vary in composition from basaltic andesite to rhyolite, and 50% clastic rocks.

Unit 3, which was called Kingsvale Group by Duffell and McTaggart (1952), and later authors, consists of mostly dark amygdaloidal and dense andesite, with some interbedded clastic rocks. Vesicles are commonly filled with chlorite, calcite, zeolites and quartz. For reasons which are discussed later, the writer has chosen to use the lithologic term "amygdaloidal andesite unit" to represent this rather homogeneous volcanic package. This unit conformably overlies the Spences Bridge Group, the contact being best exposed about 4 km east of Spius Creek. J.W.H. Monger (personal communication) has also suggested that a conformable relationship between the Spences Bridge Group and the amygdaloidal andesite unit may exist along much of their contact on the southwest slope of the Nicola Valley. However, Devlin (1981) concluded that an angular unconformity separates the units near Soap Lake, south of Spences Bridge. These apparently conflicting field relations can be explained by localized deformation which occurred either concurrently with deposition of the Spences Bridge Group, or during a brief hiatus prior to extrusion of the amygdaloidal andesite unit.

Unit 4 is correlated on lithologic grounds with the Eocene Kamloops Group. These rocks comprise hornblende-needle dacite, and conglomerate containing clasts of
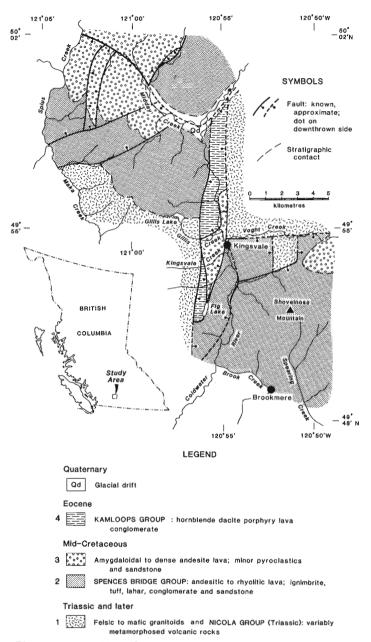

Figure 39.1. *Simplified geological map in vicinity of Kingsvale, British Columbia.*

this porphyry. Although everywhere in the map area this unit is bounded by faults, Monger (1981) found flows of similar lithology overlying the amygdaloidal andesite unit on the Nicoamen Plateau to the northwest.

As shown in Figure 39.1, the present distribution of rock units is largely due to normal faulting. Although the faults have a wide variety of orientations, the greatest offsets occur on faults trending almost due north. The fault zone through which the Coldwater River runs contains blocks of unit 4 juxtaposed against unit 1, giving probable vertical offset of a few thousand metres. The age(s) of faulting is uncertain but the time of latest movement on the faults with greatest offset is probably Eocene or later.

Rocks of the Spences Bridge Group and perhaps those of the amygdaloidal andesite unit have been gently folded, as shown by opposing dips, but the geometry of these folds is uncertain. Although folding is evident in some places, faulting and deposition over uneven terrain may account for

many of the irregularities in bedding attitudes. To the northwest, in the Ashcroft map area, Drysdale (1914) stated that the Spences Bridge rocks were folded into a broad synclinorium, trending northwest. This concept was restated by Duffell and McTaggart (1952). Monger (1985) applied the name Nicoamen Syncline to the structure, extended its length, and suggested the Cretaceous as time of deformation. If this syncline continues southeastward into the Hope map area, the evidence is limited. Present bedding attitudes and outcrop patterns probably reflect Tertiary extensional faulting more than the postulated syncline development. Consequently, if the Nicoamen Syncline does extend through the area mapped by the writer, its geometry has been substantially altered.

The only igneous intrusions observed to cut the Cretaceous volcanics are felsic and mafic dykes. These dykes are seldom encountered within the map area of Figure 39.1, but are extremely abundant a few kilometres to the south of Brookmere on Mt. Thynne, where they trend northward. The dykes contain hornblende which is rare in both Cretaceous units, but common in the Eocene volcanics. The striking parallelism between the trend of these dykes and the faults with greatest offset suggests that the orientation of crustal extension in this area during Eocene time was east-west.

Stratigraphy

The Cretaceous volcanics have a complex and laterally discontinuous stratigraphy. A simplified stratigraphic column is shown in Figure 39.2. The Spences Bridge Group rocks were deposited on a surface having moderate topographic relief. In some places, paleotopographic highs are evident, where older plutonic rocks are exposed as windows within a Cretaceous section.

The lowest Spences Bridge unit is acid andesite lava. Like many of the lavas in this group, it is dense plagioclase-augite porphyry. Overlying this flow-rock in many places is coarse conglomerate or breccia, containing predominantly basement clasts, especially granitoids. In some places, due to paleotopography, the lowest lava is absent and the conglomerate sits directly on basement rocks. Although clasts of basement rocks are commonly found within the various Spences Bridge clastic units, they constitute a majority of the rock only in this pseudo-basal conglomerate. The thickness of this lithology varies within a kilometre from less than a metre to over 60 m. It seems likely that it was deposited in fans as a result of exposed fault escarpments.

Above this conglomerate, the Spences Bridge Group comprises a pile of both felsic and mafic lavas, and interbedded clastic rocks. The lavas are generally hard and non-amygdaloidal, although some amygdaloidal flows do exist. The mafic lavas are frequently columnar jointed, with subtle planar flow banding perpendicular to jointing, suggesting that they were quite fluid during extrusion. The felsites typically exhibit well developed curviplanar flow banding along which fracturing has been facilitated (Fig. 39.3). This flow banding is often steep, bears no relation to bedding, and is undoubtedly due to high viscosity at the time of extrusion. Less commonly, felsic lavas are columnar joined, and similar to their mafic counterparts in their overall morphology (Fig. 39.4).

Nonwelded ignimbrite, typically unsorted and poorly bedded, easily constitutes the largest fraction of the clastic rocks, but welded ignimbrite, air fall tuff and lahar are also common. Figure 39.5 shows a thick section of bedded air fall tuff.

The chemical compositions of the rocks vary considerably, but no overall magmatic trend is discernible. The Spences Bridge Group is a typical composite volcanic package, probably having formed as a stratovolcano or set thereof, the feeders to which are not evident in the study area. Since no single fault block contains both the lower and upper stratigraphic bounds to the package, only a minimum thickness of 2400 m can be determined.

In the study area, the amygdaloidal andesite unit sits conformably on both lavas and clastic rocks of the Spences Bridge Group. Most of this unit consists of amygdaloidal to dense andesite lava flows. Many of these rocks are extremely altered, owing to their high porosity and probable extensive deuteric alteration from exsolving volatiles during extrusion. Columnar jointing is absent, and obvious flow banding is uncommon. These flows are very similar in lithology and chemistry to the few amygdaloidal flows within the Spences Bridge Group. Minor amounts of clastics are intercalated with the lavas. Only a minimum thickness of 600 m for the amygdaloidal andesite unit could be determined due to the lack of an upper stratigraphic limit.
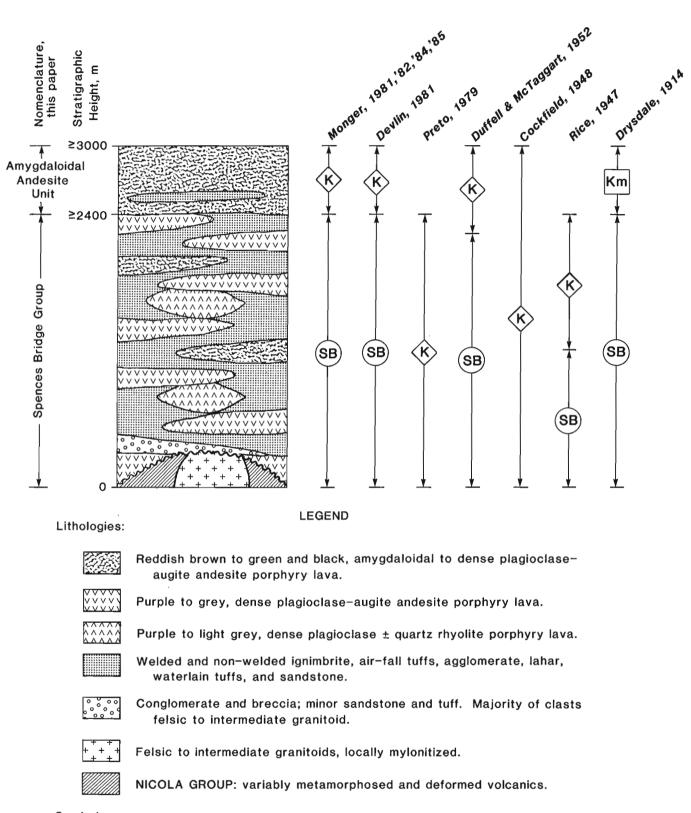
Chemistry

Twelve Spences Bridge Group and 11 amygdaloidal andesite unit rocks were chemically analyzed. All samples are subalkaline, and are shown plotted on a tholeiitic/calcalkaline discrimination diagram (Fig. 39.6). All the amygdaloidal andesite unit analyses indicate an obvious calcalkaline nature. The Spences Bridge rocks show a probable calcalkaline trend, although iron enrichment occurs in some samples of high silica content. From the same analyses, the rocks have been categorized on a potash vs. silica diagram (Fig. 39.7). As shown, the majority of the samples are low to medium potassium, basaltic to acid andesites, with only the Spences Bridge Group including rhyolites. No dacites are present, but this is a likely result of too few analyses. It should also be noted that almost all the amygdaloidal andesite unit samples fall within the chemical field defined by the Spences Bridge Group. The lack of a single basalt in either of these rock groups conflicts strongly with the work of Devlin (1981) whose classifications, based on refractive index, showed basalt to be the dominant rock type. A poor correlation between his tests and this classification scheme is the probable cause of discrepancy.

Petrography

The Spences Bridge Group lavas have a consistent mineralogy. Plagioclase phenocrysts, typically about 2 mm long, are ubiquitous. Dark green clinopyroxene phenocrysts, generally smaller and less abundant than plagioclase, are present in all andesites, but absent from rhyolites. Orthopyroxene, distinguishable from monoclinic pyroxene only in thin section, is present as a phenocryst in many of the rocks. Quartz phenocrysts are found only in some rhyolites.

In thin section, the plagioclase phenocrysts commonly show complex zoning. Most form isolated crystals, but may be clustered as glomerophenocrysts, some with pyroxene. Opaques, probably magnetite, are ubiquitous in thin section as microphenocrysts and are also common members of these crystal clumps. Plagioclase microlites are also ubiquitous. They may be randomly oriented or constitute a moderately trachytic fabric. Both clino- and orthopyroxene occur in the plagioclase-pyroxene glomerophenocrysts, but may also form pyroxene (only) clumps, or isolated crystals. Clinopyroxene is typically contact-twinned; orthopyroxene may be twinned either by contact or by interpretation. Both pyroxenes occur as microphenocrysts. Quartz is restricted to silica-rich rhyolite, and has suffered resorption as indicated by extreme embayment.

The magmatic mineralogy of the amygdaloidal andesite unit lavas is similar to that of the Spences Bridge Group andesites. Indeed, descriptions of both hand specimens and
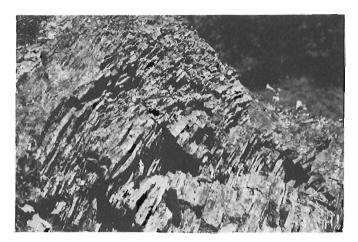
Figure 39.2. *Schematic stratigraphic section of the Cretaceous rocks near Kingsvale, British Columbia, showing the nomenclature of this paper and that of previous authors. Correlations of previous authors' descriptions with this section are based on areal mapping, stratigraphic and petrologic studies. "Monger '84" refers to Monger and McMillan (1984).*

Figure 39.3. *Typical steeply dipping curviplanar flow banding and subsequent fracturing in Spences Bridge Group rhyolite, near peak of Shovelnose Mountain.*

Figure 39.4. *Columnar joints in Spences Bridge Group plagioclase rhyolite porphyry near peak of Shovelnose Mountain. This morphology is rare in rhyolites, but common in Spences Bridge andesites.*

Figure 39.5. *Well bedded air fall tuffs, 5 km northwest of Gillis Lake.*

Figure 39.6. *Iron-enrichment classification of Spences Bridge and amygdaloidal andesite unit rocks (after Miyashiro, 1974). FeO* refers to total iron as FeO.*

Figure 39.7. *Silica and potash classification of Spences Bridge and amygdaloidal andesite unit rocks (after Taylor, 1969). Note almost complete overlap of the chemical fields defined by each group.*

thin sections for some rocks from each unit are interchangeable. However, many of the amygdaloidal andesite unit rocks lack phenocrysts of either plagioclase or pyroxene, exhibit strong plagioclase microlite alignment, and contain serpentine-after-olivine (?) pseudomorphs. The former presence of olivine, and the conspicuous lack of plagioclase phenocrysts in these rocks but not in Spences Bridge andesites, may be due to higher magma volatile contents, as evidenced by the abundant filled vesicles. The depolymerizing effects of such water contents could have suppressed the liquidus temperatures of plagioclase and pyroxene, extended the stability of olivine (Kushiro, 1975), and reduced the viscosity, giving different mineralogies and textures from similar dry magma compositions.

Age and history of nomenclature

The Spences Bridge Group and amygdaloidal andesite unit have been studied by several workers. Unfortunately, the nomenclature used to describe these rocks has been so inconsistent that it is difficult to determine which package of rocks a particular author is addressing. Figure 39.2 shows the correlations between previous authors' terminology and the stratigraphy discussed earlier.

337

Drysdale (1914) originally defined the Spences Bridge Group from fieldwork near Spences Bridge. He clearly described the composite nature of the group and reported an age of Jura-Cretaceous, based on plant fossils. On lithologic grounds, he included the amygdaloidal andesite unit within the Tertiary Kamloops Group.

Rice (1947) mapped the east half of the Hope map sheet, and encountered both packages of volcanics. The amygdaloidal andesite unit is poorly exposed in this area, and as a result he neither recognized it as a distinct unit, nor classified it consistently. However, the Spences Bridge Group is well exposed there, and Rice studied this unit in moderate detail. He correctly correlated, on lithologic grounds, some of the lavas with Spences Bridge rocks, as defined by Drysdale. Fossils from the type locality of the Spences Bridge Group were re-examined by W.A. Bell (Rice, 1947, p. 25) who assigned them an Aptian age which Rice adopted for the age of the Spences Bridge rocks in his area. But Rice identified a second, composite volcanic package whose breccias contained clasts of Spences Bridge lavas. He interpreted those breccias to be a younger, erosional product of the Spences Bridge rocks. Within those clastic rocks, near Kingsvale, he found a fossil locality which yielded 15 varieties of fossil plants, including 4 angiosperms. Bell examined the flora and concluded that they were Albian (younger) (Rice, 1947, p. 26). Rice then applied the name Kingsvale Group to this composite package.

Fieldwork by the writer revealed that the Spences Bridge Group includes Rice's Kingsvale rocks. The usage of the term Kingsvale Group should therefore be discontinued, for three reasons: firstly, the volcanic breccias which Rice believed to be erosional detritus from the Spences Bridge Group are largely non-welded ignimbrite, tuff and agglomerate, that is, simply pyroclastics of the Spences Bridge Group. Some epiclastic rocks are present, but they constitute a normal part of the volcanic pile. Secondly, since these volcaniclastic and epiclastic rocks occur throughout the Spences Bridge section, Rice's attempt to correlate all such lithologies with the rocks hosting the fossils at Kingsvale is clearly in error. Thirdly, Rice correctly identified Spences Bridge lavas in the vicinity of Fig Lake. These rocks, however, overlie the clastic rocks hosting the Kingsvale fossil locality. Assuming that Bell's fossil ages are correct, it can be concluded that the Spences Bridge Group was deposited over several million years, spanning the Aptian-Albian boundary.

Cockfield (1948), in his report on the eastern half of the Ashcroft sheet, directly north of Rice's map area, followed Rice's nomenclature. He mapped almost all the Spences Bridge rocks plus the amygdaloidal andesite unit as Kingsvale Group.

Duffell and McTaggart (1952) mapped the west half of the Ashcroft map area. They found a fossil locality high in the Spences Bridge Group section which contained plant fossils similar to those found by Rice at Kingsvale. As a result, they placed the Spences Bridge-Kingsvale contact at the base of these clastic rocks hosting the Albian fossil flora. Since the amygdaloidal andesite unit directly overlies these clastic rocks, Duffell and McTaggart included both the uppermost Spences Bridge beds and the amygdaloidal andesite unit in their Kingsvale Group map unit.

Preto (1979), in his report on the Nicola Group in the east part of the Hope map area, mapped Spences Bridge rocks as Kingsvale Group, evidently following Rice's lithologic descriptions and mapping. He reported an age of 112 Ma as determined by Rb-Sr geochronometry, which correlated well with Bell's fossil ages.

Devlin (1981), Monger (1981, 1982, 1985), and Monger and McMillan (1984), used the Kingsvale name to refer specifically to the amygdaloidal andesite unit, and correctly included the Albian fossil-bearing clastic rocks in the Spences Bridge Group. However, their usage of Kingsvale Group for the amygdaloidal andesite unit should not be followed. Consequently, this unit is still not properly named.

G.E. Rouse examined microflora from the Squianny Creek strata which unconformably overlie the amygdaloidal andesite unit south of Spences Bridge (Devlin, 1981, p. 36). He assigned an Upper Cretaceous age to these rocks thereby establishing a minimum age for the amygdaloidal andesite unit. This coincides well with the 82.0 Ma (Campanian) date from a dyke cutting the amygdaloidal andesite unit, which may or may not be a feeder to that unit (Monger and McMillan, 1984). The amygdaloidal andesite unit therefore falls between the Albian age of the upper Spences Bridge Group, and the broader Upper Cretaceous age of the Squianny Creek rocks.

New ages

Two new potassium-argon dates have been obtained from Cretaceous andesites with known stratigraphic positions. One sample from low in the amygdaloidal andesite unit pile, yielded an age of 91.7 ± 3.3 Ma; the other, from high in the Spences Bridge Group section, yielded a 94.4 ± 3.4 Ma age. Both rocks are from locations east of Spius Creek and northwest of Gillis Lake. Complete data sets are shown in Table 39.1.

The overlap of these ages, as indicated by the margins of error, suggests no hiatus in deposition between the Spences Bridge Group and the amygdaloidal andesite unit. This finding complements the locally conformable contact which these units share. Further continuity within the entire Cretaceous volcanic pile is provided by similar chemistry and mineralogy, and the presence of amygdaloidal flows within the Spences Bridge section which strongly resemble typical amygdaloidal andesite unit lithologies. Existing evidence indicates that these volcanic packages are different products of the same magmatic flux.

Table 39.1. New (1985) isotopic age determinations

	Amygdaloidal Andesite unit	Spences Bridge Group
Sample number	MVT84-152I	MVT84-322B
Type	Whole rock	Whole rock
Lat. N.	50°00'53"	49°48'32"
Long. W.	121°03'23"	121°01'17"
K (wt. %)	1.21 ± 0.01	0.713 ± 0.002
Radiogenic ^{40}Ar (x $10^{-6}cm^3/g$)	4.426	2.687
Percentage of total ^{40}Ar	87.1	89.6
Age (Ma)	91.7 ± 3.3	94.4 ± 3.4

Analyses by K. Scott (K) and J. Harakal (Ar), Department of Geological Sciences, University of British Columbia. K was determined in duplicate by atomic absorption using a Techtron AA4 spectrophotometer and Ar by isotope dilution using an AEI MS-10 mass spectrometer and high-purity ^{38}Ar spike. Errors reported are for one standard deviation. The constants used were: $K_e = 0.581 \times 10^{-10}$ year^{-1}, $K = 4.962 \times 10^{-10}$ year^{-1}, and $^{40}K/K = 0.01167$ at%.

References

Cockfield, W.E.
1948: Geology and mineral deposits of Nicola map-area, British Columbia; Geological Survey of Canada, Memoir 249, 164 p.

Devlin, B.D.
1981: The relationships between the Cretaceous Spences Bridge and Kingsvale Groups in southcentral British Columbia; unpublished B.Sc. thesis, University of British Columbia, 57 p.

Drysdale, C.W.
1914: Geology of the Thompson River Valley below Kamloops Lake, British Columbia; Geological Survey of Canada, Summary Report 1912, p. 115-150.

Duffell, S. and McTaggart, K.C.
1952: Ashcroft map-area, British Columbia; Geological Survey of Canada, Memoir 262, 122 p.

Kushiro, I.
1975: On the nature of silicate melt and its significance in magma genesis: regularities in the shift in the liquidus boundaries involving olivine, pyroxene, and silica minerals; American Journal of Science, v. 275, p. 411-431.

Miyashiro, A.
1974: Volcanic rock series in island arcs and active continental margins; American Journal of Science, v. 274, p. 321-355.

Monger, J.W.H.
1981: Geology of parts of western Ashcroft map area, southwestern British Columbia; in Current Research, Part A, Geological Survey of Canada, Paper 81-1A, p. 185-189.

1982: Geology of Ashcroft map area, southwestern British Columbia; in Current Research, Part A, Geological Survey of Canada, Paper 82-1A, p. 293-297.

1985: Structural evolution of the southwestern Intermontane Belt, Ashcroft and Hope map areas, British Columbia; in Current Research, Part A, Geological Survey of Canada, Paper 85-1A, p. 349-358.

Monger, J.W.H. and McMillan, W.J.
1984: Bedrock geology of Ashcroft (92I) map area; Geological Survey of Canada, Open File 980.

Preto, V.A.
1979: Geology of the Nicola Group between Merritt and Princeton; British Columbia Ministry of Energy, Mines and Petroleum Resources, Bulletin 69, 90 p.

Rice, H.M.A.
1947: Geology and mineral deposits of Princeton map area, British Columbia; Geological Survey of Canada, Memoir 234, 136 p.

Taylor, S.R.
1969: Trace-element chemistry of andesites and associated calc-alkaline rocks; Oregon Department of Geology and Mineral Industries Bulletin, v. 65, p. 43-63.

Cross-sections through Sylvester Allochthon and underlying Cassiar Platform, northern British Columbia

Project 770016

Tekla A. Harms[1]
Cordilleran Geology Division, Vancouver

Abstract

Structural cross-sections of the Sylvester Allochthon and the immediately underlying Cassiar Platform autochthon in Cry Lake map area show that thin Silurian and Devonian carbonate at the top of the autochthonous assemblage is deformed into southwest-verging duplex which has the basal Sylvester Fault as its roof thrust. Above the basal Sylvester Fault, the allochthon comprises a stack of nested, fault-bounded slices.

Résumé

L'analyse de coupes structurales de l'allochtone Sylvester et de l'autochtone sous-jacent Cassiar Platform dans la région de Cry Lake révèle qu'une mince couche de carbonate du Silurien et du Dévonien surmontant l'assemblage autochtone se transforme vers le sud-ouest en un duplex qui comporte la faille basale Sylvester à son sommet. Au-dessus de cette faille, l'allochtone comprend un empilement de copeaux tectoniques qui sont limités par des failles et qui s'emboîtent.

---

[1] Department of Geosciences, University of Arizona, Tucson, AZ

Introduction

In Cry Lake and McDame map areas, northern British Columbia, the basal Sylvester Fault is a regional, subhorizontal structural surface which separates underlying North American miogeoclinal strata of the Cassiar Platform from overlying accreted exotic oceanic assemblages of the Sylvester Allochthon, Slide Mountain Terrane. Although the Sylvester Fault is undeformed, both the allochthon and the autochthon are involved in separate, complex deformational systems (Harms, 1984).

UNITS
NORTH AMERICAN MIOGEOCLINE
(SECTIONS A – A' & B – B''')

"BLACK CLASTIC"

McDAME GROUP

UNNAMED SILURIAN/DEVONIAN

SILURIAN–MISSISSIPPIAN SHALE FACIES

KECHIKA GROUP

SYLVESTER ALLOCHTHON

Figure 40.1. Structure sections through a portion of the Sylvester Allochthon and underlying Cassiar Platform. Cross-section B-B''' shows a duplex system in Siluro-Devonian and McDame units with the Sylvester Allochthon forming the roof thrust, and a sole thrust above the Kechika Formation. In cross-section A-A' the southwest verging duplex system continues below the Sylvester Allochthon to its western flank. Section C-C'''' is a composite section from the centre to the east side of the Sylvester Allochthon in Cry Lake map area. Deeper portions of this section are somewhat interpretive. Legend for allochthonous rocks includes ages (in brackets) where known.

Sub-Sylvester Autochthon deformation

The North American stratigraphic sequence which structurally underlies the Sylvester Allochthon (Fig. 40.2) is part of the regional Cassiar Platform miogeoclinal assemblage (Gabrielse, 1963, 1979). At its base is a relatively thick Proterozoic to Ordovician sequence of clastics and less abundant carbonate strata of the Ingenika, Atan and Kechika groups, the latter capped by a thin, distinctive, black graptolitic shale. Overlying are two thinner carbonate units, an unnamed Siluro-Devonian unit and

UNITS
SYLVESTER ALLOCHTHON
(SECTION C – C''')

GABBRO

ULTRAMAFICS OR SERPENTINITE

SILICEOUS TECTONITE

BLACK BANDED CHERT (1D-1M)

TONALITE (1P)

NIZI FORMATION (m-uM)

LAYERED BASALT WITH TUFF AND CHERT (P)

PILLOWED AND MASSIVE BASALT WITH MINOR CHERT (mM)

RED & GREY CHERT WITH EXTENSIVE BASALTIC INTRUSIONS (M-P)

GREYWACKE AND VOLCANIC CONGLOMERATE

BLACK SILICEOUS ARGILLITE WITH LS (1M)

the Middle Devonian McDame Group. Below the Sylvester Allochthon, in Cry Lake map area, the sequence is capped by a very thin Upper Devonian to Middle Mississippian gun-steel grey or black shale. In the region of Cassiar townsite, in McDame map area, and below the northwest end of the allochthon in Wolf lake map area (Poole et al., 1960) the shale unit thickens and includes conglomerate, chert arenite, and minor barite horizons. Although originally mapped as a Lower Sylvester Group unit (Gabrielse, 1963) it forms the top of the autochthonous stratigraphy (Gabrielse and Mansy, 1980) and is part of the informal 'Black Clastic', correlative with the Earth Group (Gordey et al., 1982a). In Cry Lake map area, below the southwest end of the Sylvester Allochthon along Turnagain River, the Paleozoic platformal sequence changes abruptly into an off-platform shale facies in which only thinner Atan carbonate persists (Gabrielse, 1979 and personal communication).

The base of the Sylvester Allochthon lies at the top of the miogeoclinal sequence, above the 'gun-steel' or 'Black Clastic' shales throughout its outcrop length. Previous regional scale mapping in Cry Lake map area (Gabrielse, 1979) represented the Siluro-Devonian and McDame carbonate immediately below the Sylvester as undeformed. However, just east of the base of the allochthon, the entire miogeoclinal section is involved in a large-scale overturned southwest-verging structure (Gabrielse, 1979; Gabrielse and Mansy, 1978), whose projection must be truncated by the base of the Sylvester.

Detailed mapping in and around the southern end of the Sylvester Allochthon in Cry Lake map area during 1983 and 1984 has shown a predominantly southwest verging duplex exists in the relatively thin Siluro-Devonian and McDame carbonate at the top of the miogeoclinal sequence. The duplex is developed between two décollement horizons; one in the 'gun-steel', 'Black Clastic' shales at the base of the Sylvester Allochthon, the second in thin black graptolitic shale at the top of the Kechika Group (Fig. 40.2). The duplex system is shown in cross-sections A-A' and B-B''' (Fig. 40.1). These cross-sections are not balanced with respect to units below the décollement at the top of the Kechika Group. As not detailed mapping was conducted below that horizon no folds or faults within or below the Kechika Group are shown, although they must exist (Mansy, 1980). Some changes in unit thicknesses will be noted in section B-B''' (e.g., between km 10 and 11). Unit thickening is the result of mesoscopic intraformational buckle-folding (Fig. 40.3) which is localized within some horses in the duplex. Several large exposures along or near section B-B''' reveal thrust ramps of the duplex cutting upsection to the southwest and establish the vergence of the system (Fig. 40.4). The duplex system, still southwest vergent, emerges below the western flank of the Sylvester in the Cassiar area (section A-A') and must be continuous beneath the allochthon. However, in the Cassiar region, thicker 'Black Clastic' shales are included with thinner Siluro-Devonian and McDame carbonate in the duplex.

Several implications result from recognition of the duplex structure. First, the Sylvester Allochthon is the roof of the duplex system. Thrust faults within the duplex system are asymptotic to the basal Sylvester Fault which rides in a décollement horizon. This implies that emplacement of the allochthon and development of the southwest-verging duplex system are coeval. Furthermore, the Siluro-Devonian and McDame duplex, above the Kechika décollement, must presumably also roof a system of large scale structures within the thicker lower Paleozoic and Proterozoic strata below. Thus, the apparent contradiction of regional deformation of the miogeocline section versus the consistent subhorizontal structural position of the base of the Sylvester at the top of the miogeocline section is resolved. Second, although southwest verging, the Siluro-Devonian and McDame duplex system, if cogenetic with emplacement of the Sylvester, must be part of a general displacement towards the craton of allochthonous and autochthonous assemblages. Therefore, the duplex must have formed by a process of wedging and delamination as the duplex stack thickened. The duplex system is buttressed to the east against the thick southwest-verging thrust nappe of a complete overturned Proterozoic and Paleozoic miogeoclinal section (km 20-21, section B-B'''). In this area, northeast-vergent "back-thrusting" has occurred. Finally, the shale-out transition, which occurs below the Sylvester to the west (km 1, section B-B'''), has been telescoped and occurs across a duplex fault.

Sylvester Allochthon

Cross-section C-C''' (Fig. 40.1) is a composite section from the east-centre of the Sylvester Allochthon to its eastern contact within Cry Lake map area. The section illustrates the characteristic structural style of the Sylvester Allochthon (Harms, 1984). With the exception of the jagged, intrusive tonalite contacts, all unit contacts within the section are faults. Furthermore, units shown in the cross-section are lithotectonic units rather than formations; they commonly represent a few related or repeated lithologies and may also include imbricate slices (e.g., red and grey chert unit). Many of the units across the line of section have recently been dated (see Fig. 40.1 legend). The repeated
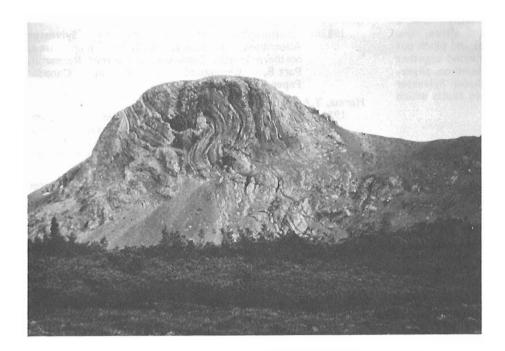
NORTH AMERICAN STRATIGRAPHY

Figure 40.2. *North American stratigraphy of the Cassiar Platform below the Sylvester Allochthon. Décollement horizons for the Siluro-Devonian and McDame duplex system are shown.*

344

Figure 3. *Mesoscopic buckle folding in Siluro-Devonian carbonates resulting in localized unit thickening.*

Figure 4. *View southeast across the Major Hart River showing a thrust within the McDame Group cutting upsection to the southwest.*

juxtaposition of older-over-younger and of initially depositionally incompatible lithologies (i.e., chert and limestone) emphasizes the complexity of the structural stacking and confirms the tectonic nature of Sylvester "stratigraphy". Folding in chert and cleavage in argillite are common within lithotectonic slivers; however, the faults bounding these slices are generally undeformed, planar, and subparallel with layering within the unit. Although otherwise indistinguishable, some of the sliver-bounding faults significantly predate emplacement of the allochthon; others are younger and presumably are related to emplacement of the allochthon (Harms, 1985).

Mapping during 1984 revealed the possibility of a second-order grouping of the fault-bounded slices. Although in variable relative structural positions, lithotectonic slices are associated with only a limited number of other slices for considerable distances along strike. Across strike the second-order structural units are lensoidal, fault-bounded, and interleaved in a structural style similar to that of the first order lithotectonic slices. In section C-C''' four such second-order structural units are outlined by contacts with barbs. Reconnaissance study in the Cassiar region (the generous co-operation and assistance of the staff of Brinco, Cassiar is gratefully acknolwedged) suggested that, as at the western end of section C-C''' (km 1-2), the bases of some of the second order units are not uncommonly marked by discontinuous ultramafic or serpentinite slivers.

Lithotectonic slices, to the depth they can be drawn in section C-C''', suggest a shingle-like imbrication. This is, however, a local feature only, the result of the regional, probably isostatic, synclinal shape of the Sylvester Allochthon. Mapping on the west side of the Allochthon around Cassiar substantiates the Gordey et al. (1982b) cross-section from the central region of the allochthon;

345

fault-bounded slices in the Sylvester regionally form a subhorizontal pancake stack. Lithotectonic slices, and second-order groupings of slivers, are lensoidal and pinch out along strike and up and down dip. They are nested together rather than strictly imbricate. Low in the allochthon, sliver-bounding faults may be asymptotic to the basal Sylvester Fault, higher in the allochthon they merge into faults which bound the second-order structural units.

References

Gabrielse, H.
1963: McDame map area, British Columbia; Geological Survey of Canada, Memoir 319, 138 p.

1979: Geology of Cry Lake (104I) map area; Geological Survey of Canada, Open File 610.

Gabrielse, H. and Mansy, J.L.
1978: Structural style in northeast Cry Lake map-area, north central British Columbia; in Current Research, Part A, Geological Survey of Canada, Paper 78-1A, p. 33-34.

1980: Structural style in northeast Cry Lake map-area, north central British Columbia; in Current Research, Part A, Geological Survey of Canada, Paper 80-1A, p. 33-35.

Gordey, S.P., Abbott, J.G., and Orchard, M.J.
1982a: Devono-Mississippian (Earn Group) and younger strata in east-central Yukon; in Current Research, Part B, Geological Survey of Canada, Paper 82-1B, p. 93-100.

Gordey, S.P., Gabrielse, H., and Orchard, M.J.
1982b: Stratigraphy and structure of Sylvester Allochthon, southwest McDame map area, northern British Columbia; in Current Research, Part B, Geological Survey of Canada, Paper 82-1B, p. 101-106.

Harms, T.A.
1984: Structural style of the Sylvester Allochthon, northeastern Cry Lake map area, British Columbia; in Current Research, Part A, Geological Survey of Canada, Paper 84-1A, p. 109-112.

1985: Pre-emplacement thrust faulting in the Sylvester Allochthon, northeast Cry Lake map area, British Columbia; in Current Research, Part A, Geological Survey of Canada, Paper 85-1A, p. 301-304.

Mansy, J.L.
1980: Structure of the Turnagain River pendant in northeastern Cry Lake map area, British Columbia; in Current Research, Part A, Geological Survey of Canada, Paper 80-1A, p. 351-352.

Poole, W.H., Green, L.H., and Roddick, J.A.
1960: Geology of Wolf Lake map area; Geological Survey of Canada, Map 10-1960.

Petrology, chemistry and radiogenic isotope (K-Ar, Rb-Sr, and U-Pb) study of the Emerald Lake pluton, eastern Yukon Territory

Project 770044

Hans Smit [1], Richard Lee Armstrong [1], and Peter van der Heyden [1]
Institute of Sedimentary and Petroleum Geology, Calgary

Abstract

Emerald Lake pluton is a mid-Cretaceous, saturated, metaluminous, alkaline to calc-alkaline, epizonal syenite to granite which intrudes Paleozoic sedimentary rocks of the Selwyn Basin. The pluton has abundant K-feldspar megacrysts and consequent high potassium content throughout. Three phases have been distinguished: a Main phase, a Blue Trachytic phase, and a Biotite phase. There is a chemical gradation from Blue Trachytic phase through the Main phase to the more differentiated Biotite phase. Aplite dykes intruding the pluton are even more differentiated.

Age determinations using three methods indicate an age of about 92 Ma for the pluton (92 ± 3 Ma by K-Ar; 83 ± 2 to 102 ± 6 Ma by Rb-Sr; and 91 ± 1 Ma by U-Pb).

Sulphide mineralization within the pluton is probably related to late stage deuteric fluids. No economic mineral zoning or mineralization halos were demonstrated.

Résumé

Le pluton, saturé, métalumineux et de nature alcaline à calo-alcaline, du lac Emerald date du Crétacé moyen; sa composition varie de la syénite épizonale au granite et il pénètre les roches sédimentaires d'âge paléozoïque du bassin de Selwyn. Ce pluton contient des mégacristaux de feldspath potassique en abondance et a, par conséquent, une teneur élevée en potassium. On y distingue trois phases: une phase principale, une phase trachytique bleue et une phase à biotite. Le passage de la phase trachytique bleue à la phase à biotite plus différenciée, en passant par la phase principale, comporte une gradation chimique. Les dykes d'aplite qui pénètrent le pluton présentent une différenciation encore plus marquée.

Les datations utilisant trois méthodes différentes fixent l'époque de formation du pluton a environ 92 millions d'années (92 ± 3 millions d'années selon la méthode du K-Ar; 83 ± 2 à 102 ± 6 millions d'années selon la méthode du Rb-Sr; et 91 ± 1 millions d'années selon la méthode de l'U-Pb).

La minéralisation en sulfures au sein du pluton est probablement associée à l'action des eaux deutériques à la dernière phase d'évolution. Aucune zonation de minéraux économiques ni auréole de minéralisation n'ont été relevées.

---

[1] Department of Geological Sciences, University of British Columbia, Vancouver, B.C. V6T 2B4

Introduction

Emerald Lake pluton is located 70 km northwest of Macmillan Pass in eastern Yukon (Fig. 41.1), in the Arrowhead Lake 1:50 000 map area (105 O/11), where it underlies an area (centred at 63°35'N, 131°15'E) of higher topographical relief (elevations 1110-2250+ m). The pluton underlies about 26 km² and outcrops in a T-shaped valley and on surrounding rugged, glaciated ridges north of Emerald Lake, with a small satellite plug (1 km²) to the east on Horn Peak (Fig. 41.2).

History of study

Reconnaissance mapping by the Geological Survey of Canada (Blusson, 1974) listed the western part of the pluton as syenite and the Horn peak outlier as granodiorite. The pluton

Figure 41.1.   *Location map.*

is part of a claim block owned by AGIP of Canada Ltd. (Grapes, 1982). The original claims were staked in 1979 on the basis of a radiometric anomaly. Subsequent discoveries of copper, molybdenum, gold and tungsten mineralization in the pluton and country rocks led to further claims in 1980 and 1981 and continued detailed mapping and exploration in 1983.

The Niddery Lake 1:250 000 map sheet (105 O) was recently remapped by the Geological Survey of Canada (Cecile, 1984). Field work for this study was completed as part of this remapping in 1983. Representative samples were studied petrographically, and mineral separates and rocks analyzed for Rb, Sr, and Sr isotopes, K and radiogenic Ar, and U and Pb isotopes during the winter of 1983-1984 at the University of British Columbia. Chemical analyses were performed by Cominco Ltd. at their research laboratory in Vancouver. Descriptive and procedural details are reported in Smit (1984).

Regional geology

Emerald Lake pluton intrudes pervasively deformed, Paleozoic sedimentary rocks of the Selwyn Basin. From east to west it intrudes Lower Cambrian argillite and quartzite, Ordovician through Silurian chert, graptolitic shale, argillite, and quartzite, and Devonian Earn Group cherts, cherty shale and bedded, locally cross laminated, quartzite. Many other stocks of granite to granodiorite occur in the region.

Geology of the pluton

The Emerald Lake pluton is an heterogeneous alkali feldspar megacrystic to equigranular, coarse grained syenite to granite, typically a quartz syenite (Fig. 41.3). Three phases distinguished are: the Main phase in the pluton's central and eastern parts (75% of the pluton's surface area); the Biotite phase in the south central portion (8% of the area); and the Blue Trachytic phase which makes up the pluton's western margin and Horn Peak outlier (17% of the area).

Main phase quartz syenite and granite comprises pink to white orthoclase megacrysts with large hornblende crystals and finer grained plagioclase, orthoclase, quartz, and minor biotite (Fig. 41.4a). Biotite phase quartz monzonite is finer grained than Main phase, with fine- to medium-grained
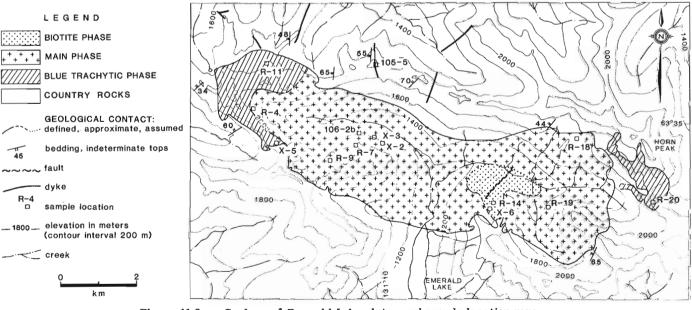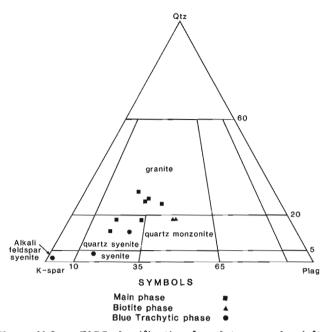

Figure 41.2.   *Geology of Emerald Lake pluton and sample location map.*

Figure 41.3. *IUGS classification for pluton samples (after Streckeisen, 1974). Mineral modes estimated from handsamples.*
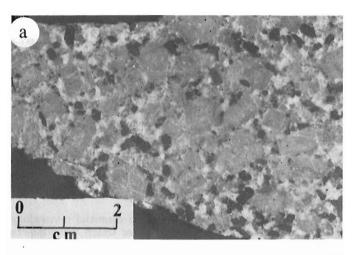
Centimetre-scale, rarely metre-scale vugs characterize all phases; these are most common in the western half of the pluton. They contain quartz, tourmaline, orthoclase, biotite, and locally sulphides. Quartz crystals longer than 0.5 m have been found.
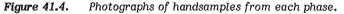

biotite present but little hornblende (Fig. 41.4b). Blue Trachytic phase alkali feldspar syenite, syenite, and granite is a bluish grey rock with poor to well developed trachytoid texture and finer grained orthoclase, plagioclase, hornblende, minor biotite and uncommon quartz. It is generally more mafic than the other phases (Fig. 41.4c).

Flow banding and segregation layers are widespread and especially common in more mafic parts of the Main phase in the western part of the pluton. All phases contain mafic plutonic inclusions which are up to a metre across, but mostly smaller. There are some inclusions of the country rock close to contacts. Most are unaltered and less than a metre across, rarely several metres across. Few sedimentary inclusions occur more than 100 m from the pluton's border. Those farther inside the pluton tend to be more metamorphosed.

Contacts between the Main and the Blue Trachytic phases are commonly gradational over a few to several metres, and are even more gradational between the Main and Biotite phases. In the southwest dykes similar in appearance to the Main phase were observed intruding the Blue Trachytic phase. No intrusive relationships were observed between the Main and Biotite phases. Intraphase contacts within the heterogeneous Main phase vary from sharp to gradational.

Contacts between intrusion and country rocks are sharp or rarely gradational over a few centimetres. The pluton remains coarse grained up to its margin and the country rocks have not been notably deformed by the intrusion, but contact metamorphism produced biotite-grade hornfels and calc-silicate assemblages in limestone horizons.

Satellite dykes rarely intrude country rock more than a few metres from the pluton margin except along the pluton's southwest margin where they penetrate 100-200 m and some along the north and east sides of the pluton which extend northeasterly 3 km from the margin (Cecile, 1984). Aplitic and rare pegmatitic dykes intrude all phases. Locally dykes are alkali feldspar-rich or consist of trachytoid alkali feldspar megacrysts in a more mafic matrix. Granodiorite and quartz-eye porphyry dykes occur within the country rock envelope, but were never observed within the pluton.

a) Main phase
b) Biotite phase
c) Blue Trachytic phase

Figure 41.4. *Photographs of handsamples from each phase.*

Centimetre-scale veins are scattered throughout the pluton but are locally abundant and are mineralogically similar to the vugs. The veins did not noticeably alter their wallrock. The same mineralogy also may be found coating fractures within the pluton. Economic elements within the vugs, veins, and fractures include copper, molybdenum, bismuth, tungsten, and gold.

Petrography

Fourteen thin sections and hand samples were examined for mineral assemblages, textures, and modes. (Fig. 41.2 shows sample locations.) Mineral modes are summarized in Appendix 41.1a.

The typical quartz syenite of the pluton contains 10-60 per cent orthoclase megacrysts (0.3 to >4 cm in size), 0-35 per cent plagioclase, 5-20 per cent mafics, 0-20 per cent quartz, and 0-20 per cent finer grained groundmass orthoclase and accessory minerals magnetite, zircon, titanite, apatite, pyrite, and allanite. Mafic minerals show the typical Bowen reaction series with hornblende, which could be due to an increase in volatiles content and alkalies during magma crystallization.

All pluton samples have the same essential mineralogy except R-20 from the Horn Peak outlier which lacks quartz or plagioclase and Biotite phase samples which are characterized by allanite. Otherwise the phases only vary in texture and in compositional details. Main phase is characterized by larger, more euhedral, and more abundant hornblende, more abundant quartz and coarser grained matrix than other phases. Resorption textures in Main phase samples are more common than in the Blue Trachytic phase and plagioclase has higher anorthite content in the Main phase (An_{38-44}) than in the Blue Trachytic phase (An_{44-48}).

In the Biotite phase, biotite replacement of hornblende is common, plagioclase is more abundant, and of lower An content (An_{32-33}) and clinopyroxene or calcic plagioclase cores are absent. It generally has fewer megacrysts and greater reabsorption of megacrysts than other phases, typical of more differentiated magmas. The matrix is finer grained than the Main phase and much more leucocratic.

The Blue Trachytic phase is distinguished by alignment of megacrysts. It also has more anorthite-rich plagioclase, less quartz, and more mafics than other phases. Clinopyroxene cores in the hornblende and more calcic plagioclase cores, which could be incompletely reacted, early crystallizing phases, or restite are also distinctive. The Blue Trachytic phase is the least differentiated, based on more common relic mineralogy and less common reabsorption or reaction textures among network silicates.

Chemistry

Twelve samples of the main phases and a sample of an aplitic dyke from within the pluton (sample 106-2b), and of a granodioritic dyke from outside the pluton (sample 105-5), were analyzed for major and minor elements (Appendix 41.1).

High potash content (6-9 weight per cent K_2O) is the most distinctive feature of the pluton's composition compared with average content for syenites (4.2 weight per cent) and granites (4.0 weight per cent; Le Maitre, 1976) and is difficult to explain in the petrogenesis of these rock types (Stewart, 1979). In the Emerald Lake pluton it may be due to alkali feldspar accumulation, consistent with petrogenic textures, and thus not be a measure of the primary magma composition. Na_2O is below average (1.9-3.0 weight per cent) compared to an average of 5.2 weight per cent for syenites and 3.7 weight per cent for granites (Le Maitre, 1976). Other major element contents are typical of worldwide averages for these rock types. The aplite dyke is higher in SiO_2 (76.9 weight per cent), and similar in K_2O composition to the pluton, while the granodiorite dyke contains more cafemic oxides and comparatively less K_2O.

All samples are quartz normative. More siliceous Biotite phase and dyke rocks are corundum normative, whereas the rest are clinopyroxene normative (Appendix 41.1d). In most variation diagrams granodiorite dyke composition plots off the smooth trends or fields established by other samples (Smit, 1984). The compositions show a gradation consistent with normal fractional crystallization from least differentiated Blue Trachytic phase through Main and Biotite phases to the most differentiated aplite dyke. There is a general decrease in normative diopside and a late appearance of normative corundum with differentiation.

The total alkali-silica plot (Fig. 41.5a) shows that the Blue Trachytic rocks are alkaline, the Main phase rocks are transitional, and the Biotite phase and the aplite dykes are subalkaline. The AFM plot (Fig. 41.5b) shows that all samples, except the granodiorite dyke, follow a normal calc-alkaline differentiation trend and lie below the tholeiitic/calc-alkaline dividing line of Irving and Baragar (1971). The Main and Blue Trachytic phases are metaluminous (molar ratio $Al_2O_3/CaO+Na_2O+K_2O$ = A/CNK <1), the Biotite phase and granodiorite dyke are transitional and the aplite dyke is peraluminous (A/CNK >1). None of the samples are peralkaline (molar ratio Al_2O_3/Na_2O+K_2O >1 for all samples). A plot of FeO against Fe_2O_3 (Fig. 41.5c) shows that samples plot in both the I-type and S-type granitoid fields of Hine et al. (1978). A plot of Na_2O against K_2O (Fig. 41.5d) shows samples plot outside the I and S range due to the very high K_2O contents.

Compositional fields for the O'Grady Batholith, another high potassium granite in the Selwyn plutonic suite southeast of Macmillan Pass (Anderson, 1983, and personal communication) are included in Figure 41.3 for comparison.

Average trace element abundance for all phases shows a general homogeneity within the pluton. F, Cl, and Sr plots (Smit, 1984) show general linear decreases with increasing SiO_2, which follow magmatic differentiation, but with generally more scatter than that found in major element plots. Rb and Li plots show no trends. Cl, B, Rb, and Sr are enriched within the pluton compared to crustal averages.

Implicit in the pluton's radiometric signature and differentiated, syenitic composition are enrichments in lithophile elements K, Th and U (e.g. Day, 1963). In the Emerald Lake pluton, thorium contents are greater than average crustal abundance. Uranium is below detection limit (20 ppm) except for samples R-7 and R-20 (39 and 23 ppm U) which have 15-20 times average crustal abundance of U.

Concentrations of most metals of economic interest in the pluton are close to average (Day, 1963) but W and Mo are somewhat higher. Gold, silver, and tin contents were all below detection limits (10 ppb for gold; 0.4 ppm for silver; 20 ppm for tin). No zoning pattern for the metals is evident as concentrations are low and most variations are not statistically significant. Only two samples showed statistically higher amounts of more than one of the metals, but neither are more than 2 standard deviations greater than the mean. Both were collected from near areas of known mineralization; however other samples near mineralized areas show no enrichment, and therefore no mineralization halos could be demonstrated.
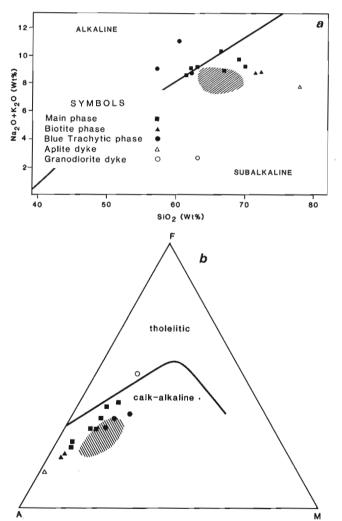
Table 41.1. K-Ar data

Sample	Latitude	Longitude	Material analyzed	%K	Radiogenic ^{40}Ar x 10^{-6} cc/gm	%Radiogenic Ar in ^{40}Ar Extracted	K-Ar Date Ma ± σ
X-5	63°34'36"	131°18'24"	Biotite	5.73	20.913	91.3	91.5 ± 3.2
X-5	63°34'36"	131°18'24"	Hornblende	0.977	3.580	86.6	91.9 ± 3.2

K is determined in duplicate by atomic absorption using a Techtron AA4 spectrophotometer and Ar by isotope dilution using an AEI MS-10 mass spectrometer and high purity ^{38}Ar spike. The constants used are:

$$K\lambda e = 0.581 \times 10^{-10}a^{-1}, \quad K\lambda\beta = 4.962 \times 10^{-10}a^{-1},$$

$$^{40}K/K = 0.01167 \text{ atom percent.}$$

Decay constants are those recommended, by the IUGS Subcommission, on Geochronology (Steiger and Jäger, 1977). Errors reported are for one standard deviation or the standard error of the mean unless otherwise noted.

a. Alkali against SiO_2; Alkaline and subalkaline fields after Irving and Baragar (1971).

b. AFM plot; Tholeiitic and calc-alkaline fields after Irving and Baragar (1971).

c. Fe plot; I- and S-type granitoid fields from Hines et al. (1978).

d. Alkali plot; I- and S-type granitoid fields from Hines et al. (1978).

Figure 41.5. Geochemistry plots; oblique line shading shows distribution of analyses from the O'Grady batholith (Anderson, 1983, and personal communication).

Figure 41.6.   *Rb-Sr Isochrons*

a.   Isochrons for sample X-6 (83 Ma, solid line) and errorchron for sample X-5 (91 Ma, dotted line). Aplite dyke whole rock data point is also shown.   Small dashed box in bottom-left corner is area covered by Fig. 41.6b.

b.   Isochrons for sample X-6 and X-2 (102 Ma, dot and dashed line), and errorchron for sample X-5. Isochron for sample X-5 without biotite (156 Ma, dashed line) also shown, as well as whole rock data points.

Table 41.2a. Rb-Sr Data

Sample	Sample Type	Latitude	Longitude	ppm Sr ± 5%	ppm Rb ± 5%	Rb/Sr ± 2%	$^{87}Sr/^{86}Sr$ Observed ± 0.0001 (Unless Noted)
X-2	W. R.	63°34'36"	131°14'54"	769	353	0.458	0.7173
X-2	Hbld	"	"	145	27.3	0.188	0.7161
X-2	Plag	"	"	767	26.5	0.035	0.7154
X-2	K-spar	"	"	1082	664	0.613	0.7178
X-5	W. R.	63°34'36"	131°18'24"	692	353	0.510	0.7184
X-5	Bi	"	"	72.6	1012	13.94	0.7679
X-5	Hbld	"	"	78.9	29.7	0.377	0.7171
X-5	Plag	"	"	935	411	0.440	0.7177
X-5	K-spar	"	"	1026	614	0.598	0.7186
X-6	W. R.	63°33'42"	131°11'24"	468	315	0.674	0.7188
X-6	Bi	"	"	114	957	8.42	0.7456
X-6	Plag	"	"	389	69.7	0.179	0.7172
X-6	K-spar	"	"	673	544	0.809	0.7190
R-7	W. R.	63°35'00"	131°19'12"	503	450	0.896	0.7195
R-18	W. R.	63°34'48"	131°09'06"	973	281	0.289	0.7168
R-19	W. R.	63°33'42"	131°09'30"	622	355	0.571	0.7177
R-20	W. R.	63°33'54"	131°06'12"	903	450	0.498	0.7167
106-2b	W. R.	63°34'42"	131°15'06"	195	399	2.05	0.7228
105-5	W. R.	63°35'42"	131°15'00"	301	107	0.355	0.7201 ± 0.0003

Table 41.2b. Summary of Rb-Sr Isochrons

Sample	Number of points	MSWD	Age	Initial Ratio	True Isochron ?
X-2	4	0.6	102 ± 6	.7153 ± 1	yes
X-5	5	5.1	91 ± 4	.7161 ± 1	no
X-5 (-Bi)	4	3.0	156 ± 30	.7149 ± 6	yes
X-6	4	1.3	83 ± 2	.7165 ± 1	yes
X-6 (-Bi)	3	0.7	76 ± 5	.7166 ± 1	yes

Rb and Sr concentrations were determined by replicate analysis of pressed powder pellets using X-ray fluorescence. U.S. Geological Survey rock standards were used for calibration; mass absorption coefficients were obtained from Mo Kα Compton scattering measurements. Rb/Sr ratios have a precision of 2% (1 σ) and concentrations a precision of 5% (1 σ). Sr isotopic composition was measured on unspiked samples prepared using standard ion exchange techniques. The mass spectrometer, Vacuum Generators Isomass 54R, has data acquisition digitized and automated using a Hewlett-Packard HP-85 computer. Experimental data have been normalized to a $^{86}Sr/^{88}Sr$ ratio of 0.1194 and adjusted so that the NBS standard SrCO$_3$ (SRM987) gives a $^{87}Sr/^{86}Sr$ ratio of 0.71020 ± 2 and the Eimer and Amend Sr a ratio of 0.70800 ± 2. The precision of a single $^{87}Sr/^{86}Sr$ ratio is 0.00010 (1 σ). Rb-Sr dates are based on a Rb decay constant of $1.42 \times 10^{-11}a^{-1}$. The regressions are calculated according to the technique of York (1967 and 1969).

Isotopic study

K-Ar dating

Sample X-5, from the biotite and hornblende-bearing Blue Trachytic phase yielded concordant K-Ar isotope ages of 91.5 ± 3.2 Ma (biotite) and 91.9 ± 3.2 Ma (hornblende; Table 41.1).

The identical isotope ages determined for both minerals indicate rapid cooling between hornblende and biotite blocking temperatures for the southwestern part of the pluton after emplacement, consistent with intrusive relations, dyke abundance, vugs and mineralized fractures found there. These dates are within the time interval suggested by Godwin et al. (1980) and reported by Anderson (1983) for the intrusion of the Selwyn plutonic suite.

Rb-Sr dating and Sr isotope geochemistry

Nine samples were selected on the basis of spread in Rb/Sr ratio, good geographic coverage of the pluton, and representation of all petrologic types. The samples analyzed

represent the Main phase (X-2, R-18, R-9, R-7); Biotite phase (X-6); Blue Trachytic phase (X-5, R-20); aplite dykes (105-5); and granodiorite dyke (106-2b).

Whole-rock data do not define an isochron, as has been found for Rb-Sr in other whole-rock suites from plutons in the Selwyn Mountains and Anvil Range (Godwin et al., 1980; Wood and Armstrong, 1982; Anderson et al., 1983; Pigage and Anderson, in press).

Mineral separates from one sample of each phase were also analyzed, e.g., the Main phase, sample X-2 (plagioclase, orthoclase, hornblende); Biotite phase, sample X-6 (plagioclase, orthoclase, biotite); Blue Trachytic phase, sample X-5 (plagioclase, orthoclase, hornblende, biotite). Mineral separates resulted in well defined isochrons for samples X-2 and X-6.

Sample X-2, Main phase, gave an isochron age of 102 ± 6 Ma and an initial $^{87}Sr/^{86}Sr$ ratio of 0.7153 ± 0.0001. Sample X-6, Biotite phase, yielded an isochron age of 83 ± 2 Ma and an initial ratio of 0.7165 ± 0.0001. If the biotite is not included in the sample X-6 isochron calculation similar results are obtained (76 ± 6 Ma with an initial ratio of 0.7166 ± 0.0001). Sample X-5, Blue Trachytic phase, gave an errorchron (Brooks et al., 1972) with an isotopic "age" of 91 ± 4 Ma and an initial ratio of 0.7161 ± 0.0001. If the biotite is not included in the isochron calculation, an isochron age of 156 ± 30 Ma is obtained with an initial ratio of 0.7149 ± 0.0006 (see Fig. 41.6 and Table 41.2). These results suggest a significant departure from initial isotopic equilibrium and closed system assumptions implicit in the method.

The other whole rock data plot within the isochrons, except for R-20 from the Horn Peak outlier which plots below. R-18 and R-19 data are close to the X-2 isochron, while R-7 analysis is close to both the X-5 and X-6 isochrons. The aplite dyke analysis plots close to both the X-5 and the X-6 isochrons and its possible isotope age must be between 76-89 Ma depending on its initial ratio. The granodiorite dyke analysis is distinct from the field for the Emerald Lake pluton.

Rb-Sr whole-rock mineral isochron ages range from 83-102 Ma for the pluton, but their average, 92 Ma, is identical to the 92 Ma K-Ar isotopic age. Intrusive relationships, which do not indicate large time intervals between solidification of the three phases, are supported by somewhat similar Rb-Sr and K-Ar isotopic ages for the Main and Biotite phases but are contradicted by the significantly younger isotopic age for the Biotite phase. Either the phases were intruded over an extended period (there is no field evidence of this) or else the phases are coeval, but open system Sr behavior (e.g. slow cooling, later alteration, weathering) has produced the anomalously younger isotopic ages.

High and variable $^{87}Sr/^{86}Sr$ initial ratios (0.7153-0.7165) for the constituent phases support open system Rb-Sr behavior and lack of initial ratio homogenization in a radiogenic, sialic crustal environment (White and Chappell, 1983). Blue Trachytic phase, distinguished by relict clinopyroxene and plagioclase cores, yields the poorest isochron, an anomalously older age and the lowest $^{87}Sr/^{86}Sr$ initial ratio. These data support the possibility that a more primitive magma, with lower Sr initial ratio, intruded

Table 41.3. U-Pb data

Sample HS X-5   Zircon; Hand Picked Bulk Sample

ppm U	ppm Pb	206	207	208	204	Meas. $\frac{206}{204}$	Mole % Blank Pb	Rad. Pb Rad+Com Pb	Common Pb Age
		Radiogenic plus common Pb							
1305.3	20.3	100	6.2941	14.9657	0.0948	793	0.9	0.941	95

$^{206}Pb/^{238}U$	$^{207}Pb/^{235}U$	$^{207}Pb/^{208}U$	$^{206}Pb/^{238}U$ Date		$^{207}Pb/^{235}U$ Date	$^{207}Pb/^{206}Pb$ Date
0.01461 ± 0.00008	0.0987 ± 0.0009	0.04900 ± 0.00034	93.5 ± 0.5 Ma		95.6 ± 0.8 Ma	147.6 ± 16.4 Ma

Errors 1σ

Isotopic composition of blank: $^{206}Pb/^{204}Pb = 17.75$, $^{207}Pb/^{204}Pb = 15.57$, $^{208}Pb/^{204}Pb = 37.00$

Isotopic composition of common Pb based on S-K curve: $^{206}Pb/^{204}Pb = 11.152$, $^{207}Pb/^{204}Pb = 12.998$, $^{208}Pb/^{204}Pb = 31.23$ at 3.7 Ga with $^{235}U/^{204}Pb = 9.74$, $^{232}Th/^{204}Pb = 37.19$

Zircons were separated from finely crushed 20 to 40 kg rock samples using wet shaking table, heavy liquids, and a magnetic separator. They were acid washed in strong aqua regia, sized using nylon mesh screens, and hand-picked as required. Chemical dissolution and mass spectrometry follow the procedures of Krogh (1973). We use a mixed $^{208}Pb-^{235}U$ spike and measure Pb and U on an automated Vacuum-Generators Isomass 54R solid source mass spectrometer. Automation and data reduction are done with a dedicated Hewlett-Packard HP-85 computer.

U-Pb and Pb-Pb date errors were obtained by summing the variances that arise from twenty four independent variables used in the date calculation. Only the decay constants, natural abundance ratios, and atomic weights are considered known constants.

U decay constants and isotopic ratio are: $^{238}U\lambda = 0.155125 \times 10^{-9} a^{-1}$
$^{235}U\lambda = 0.98485 \times 10^{-9} a^{-1}$
$^{238}U/^{235}U == 137.88$

through old, radiogenic sialic crust and was heterogeneously enriched in radiogenic Sr (Armstrong et al., 1977). Throughout fractionation, emplacement and crystallization, magma of the Emerald Lake pluton (and other members of the Selwyn plutonic suite) has been affected by selective anatexis of, contamination by, and(or) assimilation of the Precambrian basement which underlies the Selwyn Basin.

U-Pb dating

Zircon was separated from sample X-5, Blue Trachytic phase, for U-Pb dating (Table 41.3). The zircons were colourless to light orange and euhedral. A $^{238}U-^{206}Pb$ date of 93 ± 1 Ma and a $^{235}U-^{207}Pb$ date of 96 ± 1 Ma were obtained on hand picked material. The slight discordance suggests a small component of inherited radiogenic lead and a lower concordia intercept of approximately 91 ± 1 Ma may be estimated.

The U-Pb date corresponds well with the 92 Ma K-Ar and the 91 Ma Rb-Sr dates obtained for the same sample, X-5. This concordance supports the inference of rapid post-emplacement cooling deduced from concordant K-Ar dates for mineral phases with different closing temperatures.

Emerald Lake pluton, granitoid classifications and the Selwyn plutonic suite

Emerald Lake pluton's petrography suggests that it is an I-type granitoid (Chappell and White, 1974; White and Chappell, 1983). It has dark green hornblende with clinopyroxene cores, chocolate-brown biotite with few inclusions, calcic plagioclase cores, accessory magnetite, titanite, apatite, and zircon, and mafic igneous-type inclusions. These criteria indicate an igneous protolith.

Geochemically Emerald Lake pluton has mixed I-, S-, and A-type characteristics. Compositional diversity (e.g. SiO_2 = 56-71 weight per cent), higher cafemic, Ti and P oxide and Sr contents, lower Rb/Sr ratio and metaluminous and diopside-normative nature are typical of Cordilleran I-type plutons (Chappell and White, 1974; White and Chappell, 1983; Miller and Bradfish, 1980; Pitcher, 1982). Low $Na_2O:K_2O$ ratios and high $^{87}Sr/^{87}Sr$ initial ratios (greater than 0.0708) are attributes of S-type plutons. High K_2O and Th content, radiometric anomaly and miarolitic cavities suggest some A-type characteristics (e.g., Collins et al., 1982) for the pluton, but it lacks the more typical granophyric texture, interstitial biotite, sodic mafic mineralogy, high F content and overall alkaline or peralkaline composition. These classifications are probably not suitable for the Emerald Lake pluton and other members of the Selwyn plutonic suite (Anderson et al., 1983).

The Emerald Lake pluton is part of the Selwyn plutonic suite on the basis of geographic location and age. The suite comprises 85 to 96 Ma old monzonite to granodiorite plutons in the Selwyn and Mackenzie Mountains (Anderson, 1983; Pigage and Anderson, in press; Godwin et al., 1980). The distinctive potash rich chemistry of the Emerald Lake pluton is similar to that found in the O'Grady batholith in western Northwest Territories (Anderson, 1983). The two plutons are similar mineralogically but the Emerald Lake pluton has somewhat less Na_2O, is more syenitic, and exhibits a greater compositional spectrum. Both have abundant K-feldspar megacrysts, abundant titanite, magnetite, clinopyroxene cores in hornblende, chocolate brown biotite, and both lack mafic dykes. O'Grady batholith is finer grained and more equigranular, has smaller hornblende crystals, and lacks mafic segregations and layering, but the textural differences are most likely due to different emplacement histories and depths and do not indicate major chemical differences.

Skarn mineralization containing chalcopyrite, magnetite, pyrrhotite, arsenopyrite, and minor gold is associated with the O'Grady batholith (Smit, 1983), but no mineralization has been reported within the O'Grady batholith.

Anderson (1983) divided plutons in southeast Selwyn Mountains into two groups, hornblende bearing plutons with mainly I-type characteristics devoid of tungsten mineralization and mica-bearing plutons without hornblende, having many S-type features, and local associated tungsten skarns. The mineralogy of the mica-bearing plutons, which contain muscovite, garnet, and andalusite is dissimilar to Emerald Lake pluton. Hornblende-bearing plutons other than the O'Grady have similar mineralogy to the Emerald Lake pluton but are different in mineral proportions and chemistry. Coexistence of both hornblende and associated tungsten mineralization suggests that Emerald Lake pluton is transitional or outside the two groups which Anderson recognized. It and the O'Grady pluton are examples of the complex petrogenesis of the Selwyn plutonic suite.

Summary and conclusions

The Emerald Lake pluton is a saturated, metaluminous, alkaline to calc-alkaline, high level quartz syenitic intrusive body of mid-Cretaceous age (92 ± 3 Ma by K-Ar, 83 ± 2 to 102 ± 6 Ma by Rb-Sr, probably a bit less than 93 ± 1 Ma by U-Pb). All 3 dating methods agree on an age of about 92 Ma for the pluton. It intrudes Paleozoic sedimentary rocks of the Selwyn Basin. Three internally heterogeneous phases are distinguished; a Main phase which has pink to white K-feldspar megacrysts and coarse grained hornblende, a more leucocratic Biotite phase where biotite predominates over hornblende, and a Blue Trachytic phase with aligned K-feldspar megacrysts and a more mafic matrix. Differentiation trends and common mineralogy indicate a single parental magma for all the phases.

The magma intruded as batches of crystal mush enriched in K-feldspar crystals and later phases intruded and mixed with earlier, slightly differently differentiated and/or contaminated phases to various degrees. There is no field evidence to suggest large time intervals between successive phases.

Strain due to diapiric rise resulted in alignment of orthoclase megacrysts in the upper parts of the diapir giving it a trachytoid texture. Late differentiates formed aplitic dykes and residual volatile-rich fluids created filled fractures, vugs, and coated open joints.

All the phases are rich in orthoclase accounting for distinctively high K_2O content. Compositional variation (e.g. an increase in K_2O and Na_2O with respect to SiO_2 and an increase in biotite and quartz with differentiation) suggest a regular differentiation sequence from least differentiated Blue Trachytic phase through transitional Main and Biotite phases to most differentiated phase. Orthoclase-rich dykes in the intrusion or in the country rock are likely related, but proximal, more mafic granodiorite dykes appear to be unrelated.

Different Sr isotope initial ratios between phases can be explained by different degrees of incorporation of Precambrian basement during emplacement. One anomalous mineral isochron may be the consequence of early formed or pre-melt residual minerals, which are observed as clinopyroxene cores in hornblende and calcic plagioclase cores. U-Pb analyses also suggest some contamination by older radiogenic lead.

The Horn Peak outlier (sample R-20), is somewhat different from the rest of the intrusion, with less radiogenic Sr, and no quartz or plagioclase present. It may have had a somewhat different differentiation or contamination history than the main body, though its general chemical and petrographical similarity and proximity would argue for a common origin.

Late stage highly differentiated post-intrusion fluids moved through fractures and open joints and precipitated veins and vugs of quartz, orthoclase, tourmaline, and biotite gangue and bismuth, copper, gold, molybdenum, and tungsten mineralization. Some of the late stage fluids escaped into the country rock where they produced small veinlets in clastic rocks and local skarn in carbonate beds.

Abundant and widespread dykes, common vugs, veins and mineralized joint surfaces and evidence for rapidly closed U-Pb, Rb-Sr and K-Ar isotopic systems suggests that the southwestern part of the pluton cooled soon after emplacement due to increased permeability through hydrofracturing and release of volatile-rich, residual magmatic fluids.

Acknowledgments

References

Anderson, R.G.
1983:   Selwyn plutonic suite and its relationship to tungsten mineralization, southeastern Yukon and District of Mackenzie; in Current Research, Part B, Geological Survey of Canada, Paper 83-1B, p. 151-163.

Anderson, R.G., Armstrong, R.L., Parrish, R., and Bowman, J.R.
1983:   Potential of SE Selwyn plutonic suite for W-skarn deposits; (abstract), Geological Association of Canada, Program with Abstracts, v. 8, p. A2.

Armstrong, R.L., Taubeneck, W.H., and Hales, P.O.
1977:   Rb-Sr and K-Ar geochronometry of Mesozoic granitic rocks and their Sr isotope composition, Oregon, Washington, and Idaho; Geological Society of America, Bulletin, v. 88, p. 397-411.

Blusson, S.L.
1974:   Geology, Operation Stewart (northern Selwyn Basin) Yukon and District of Mackenzie, N.W.T. (106A, B, C; 105N, O); Geological Survey of Canada, Open File 205.

Brooks, C., Hart, S.R., and Wendt, I.
1972:   Realistic use of the two-error isochron as applied to rubidium-strontium data; Reviews of Geophysics and Space Physics, v. 10, no. 2, p. 551-577.

Cecile, M.P.
1984:   Geology of Southwest and Central Niddery Lake (105O-4,5,6,11); Geological Survey of Canada, Open File 1118.

Chappell, B.W. and White, A.J.R.
1974:   Two contrasting granite types; Pacific Geology, v. 8, p. 173-174.

Collins, W.J., Beams, S.D., White, A.J.R., and Chappell, B.W.
1982:   Nature and origin of A-type granites with particular reference to southeastern Australia; Contributions to Mineralogy and Petrology, v. 80, p. 189-200.

Day, F.H.
1963:   The Chemical Elements in Nature; G.G. Harrap and Co., London, 372 p.

Godwin, C.I., Armstrong, R.L., and Thompson, K.M.
1980:   K-Ar and Rb-Sr dating and the genesis of tungsten at the Clea tungsten skarn property, Selwyn Mountains, Yukon Territory; Canadian Institute of Mining and Metallurgy, Bulletin, v. 73, no. 821, p. 90-93.

Grapes, K.
1982:   Emerald Lake; Yukon Exploration and Geology, 1982, Department of Indian and Northern Affairs, Whitehorese, p. 163-164.

Hine, R., Williams, I.S., Chappell, B.W., and White, A.J.R.
1978:   Contrasts between I- and S-type granitoids of the Kosciusko Batholith; Journal of the Geological Society of Australia, v. 25, p. 219-234.

Irving, T.N. and Baragar, W.R.A.
1971:   A guide to the chemical classification of the common volcanic rocks; Canadian Journal of Earth Science, v. 8, p. 523-528.

Krogh, T.E.
1973:   A low-contamination method for hydrothermal decomposition of zircon and extraction of U-Pb for isotopic age determinations; Geochimica et Cosmochimica Acta, v. 37, no. 3, p. 485-494.

Le Maitre, K.W.
1976:   The chemical variability of some common igneous rocks; Journal of Petrology, v. 17, p. 589-637.

Miller, C.F. and Bradfish, L.J.
1980:   An inner Cordilleran belt of muscovite-bearing plutons; Geology, v. 8, p. 412-416.

Pigage, L.C. and Anderson, R.G.
—   The Anvil plutonic suite, Faro, Yukon Territory; Canadian Journal of Science. (in press)

Pitcher, W.S.
1982:   Granite type and tectonic environment; in Mountain Building Processes, ed. K.J. Hsu; Academic press, London, p. 19-40.

Smit, H.
1983:   Sulphide mineralogy of the Nat claims, eastern N.W.T.; unpublished paper, University of British Columbia.

1984:   Petrology, chemistry and isotope analysis of the Emerald Lake pluton, eastern Yukon; B.Sc. thesis, University of British Columbia.

Steiger, R.H. and Jäger, E.
1977:   Subcommission on geochronology: convention on the use of decay constants in geo- and cosmochronology; Earth and Planetary Science Letters, v. 36, p. 359-362.

Stewart, D.B.
1979:   The formation of siliceous potassic rocks; in The Evolution of the Igneous Rocks, ed. H.S. Yoder, p. 339-350.

Streckeisen, A.
    1974:   Classification and nomenclature of plutonic rocks; Geol. Rundsch., v. 63, no. 2, p. 773-786.

White, A.J.R. and Chappell, B.W.
    1983:   Granitoid types and their distribution in the Lachlan Fold Belt, southeastern Australia; in Circum-Pacific Plutonic Terranes, ed. J.A. Roddick; Geological Society of America, Memoir 159, p. 21-34.

Wood, D.H. and Armstrong, R.L.
    1982:   Geology, chemistry, and geochronometry of the Cretaceous South Fork Volcanics, Yukon Territory; in Current Research, Part A, Geological Survey of Canada, Paper 82-1A, p. 309-316.

York, D.
    1967:   The best isochron; Earth and Planetary Science Letters, 2, p. 472-482.

Appendix 1a Mineral modes

Sample	Megacry. %	X-spar %	x	Plag %	(An)	Qtz. %	Mafics % Hbld	% Bi	Rock name (IUGS System)
R-4	50	60		15	(38)	10	15	<1	Quartz syenite
R-9	40	50		15	(44)	15	15	5	Quartz syenite
R-18	30	40		20	(38)	20	20	2	Granite
R-19	30	40		30	(38)	20	8	2	Granite
X-2	40	45		20	(38)	20	14	1	Granite
X-3	10	35		15	(40)	20	20	5	Granite
R-14	10	40		35	(33)	15	2	8	Quartz Monzonite
X-6	15	40		35	(32)	15	2	8	Quartz Monzonite
R-11	50	60		10	(48)	<5	25	3	Syenite
R-20	60	75		0	-	0	20	5	Alk. Feld. Syenite
X-5	30	50		20	(44)	10	15	5	Qtz. syenite

Appendix 1b Chemical composition: Major elements

Sample	R-1	R-7	R-9	R-18	R-19	X-2	X-3	R-14	X-6	R-11	R-20	X-5	106-2b	105-5	Phase Averages		
															Main	Biotite	Blue Trac.
PHASE	Main	Main	Main	Main	Main	Main	Main	Biotite	Biotite	Blue Trach.	Blue Trach.	Blue Trac.	Dyke	Dyke			
Lat.	63° 31' 30"	63° 35' 00"	63° 34'19"	63° 34' 48"	63° 33' 42"	63° 34' 36"	63° 34' 41"	63° 11' 24"	63° 11'	63° 35' 42"	63° 33' 54"	63° 34' 36"	63° 34' 42"	63° 35' 42"			
Long.	131° 15' 47"	131° 19' 12"	131° 16' 41"	131° 09' 06"	131° 09' 30"	131° 14' 54"	131° 15' 07"	131° 11' 24"	131° 11'	131° 18' 47"	131° 06' 12"	131° 18' 24"	131° 15' 06"	131° 15' 00"			
SiO_2	60.40	68.37	66.00	62.34	69.28	65.57	61.00	71.00	70.41	56.22	59.85	61.22	76.89	62.06	64.71	70.71	59.10
TiO_2	0.83	0.34	0.52	0.67	0.32	0.49	0.66	0.22	0.24	0.82	0.72	0.70	0.09	0.75	0.55	0.23	0.75
Al_2O_3	13.91	14.62	14.34	15.42	14.51	14.66	15.27	14.39	14.66	14.86	14.24	15.17	12.08	16.24	14.68	14.52	14.76
Fe_2O_3	2.63	1.26	1.02	0.94	0.87	1.45	2.06	0.50	0.56	2.71	1.05	1.21	0.17	0.44	1.46	0.53	1.66
FeO	4.74	2.16	3.38	4.53	2.16	3.02	4.38	1.80	1.87	4.38	4.74	4.45	0.93	6.25	3.48	1.83	1.66
MnO	0.10	0.04	0.08	0.11	0.05	0.07	0.11	0.04	0.05	0.12	0.12	0.11	0.02	0.24	0.47	0.04	0.12
MgO	2.54	0.62	1.42	1.48	0.62	1.20	1.68	0.46	0.55	3.59	2.52	2.54	0.15	1.82	1.37	0.50	2.88
CaO	4.38	2.08	3.04	3.80	2.00	3.21	3.95	1.76	1.93	6.28	4.38	4.34	0.66	5.44	3.21	1.84	5.00
Na_2O	1.86	2.96	2.23	2.29	2.74	2.28	2.70	2.82	2.83	2.13	2.00	2.24	1.75	1.94	2.44	2.83	2.12
K_2O	6.71	6.69	6.57	6.71	6.29	6.62	6.20	5.86	5.87	6.73	8.97	6.41	5.82	2.58	6.54	5.86	7.37
P_2O_5	0.36	0.09	0.24	0.30	0.09	0.22	0.34	0.05	0.06	0.57	0.49	0.25	0.02	0.14	0.23	0.06	0.44
L.O.I.	1.06	0.58	0.89	0.72	0.85	0.63	1.24	0.74	0.57	1.08	0.90	0.96	1.51	1.61	0.85	0.65	0.98
CO_2	0.02	<0.01	<0.01	0.12	0.07	<0.01	0.08	0.05	<0.01	0.04	0.14	<0.01	0.37	0.21	0.05	0.03	0.06
Total	99.54	99.81	99.73	99.43	99.85	99.42	99.68	99.69	99.60	99.53	100.12	99.608	100.46	99.72	100.04	99.62	99.69

Appendix 1c Chemical composition: Minor elements

Cu (ppm)	44	17	18	10	15	16	14	14	8	42	17	22	49	23	19	19	27
Zn (ppm)	22	18	20	11	28	22	14	16	24	33	22	36	10	78	19	20	30
Mo (ppm)	3	5	3	5	5	5	4	7	5	2	4	7	3	9	4	6	4
Pb (ppm)	4	7	4	8	13	15	5	11	12	15	13	14	8	15	8	12	14
As (ppm)	2	b.d.	b.d.	3	2	3	b.d.	b.d.	2	8	b.d.	b.d.	33	55	2	b.d.	b.d.
W (ppm)	b.d.	b.d.	2	2	7	5	8	6	2	3	2	10	2	2	4	4	7
U (ppm)	b.d.	39	b.d.	b.d.	b.d.	b.d.	b.d.	b.d.	b.d.	b.d.	23	b.d.	47	b.d.	b.d.	b.d.	b.d.
Th (ppm)	23	67	23	18	35	24	24	36	21	16	35	29	42	b.d.	31	28	27
S (ppm)	480	100	120	280	120	400	60	80	60	690	160	220	1790	670	223	70	356
F (ppm)	320	290	350	200	280	320	450	295	260	345	300	390	180	245	316	274	345
Li (ppm)	30	30	37	51	76	62	49	89	90	70	11	44	54	36	48	90	42
Cl (ppm)	600	350	650	1100	500	550	500	200	200	800	800	900	b.d.	550	607	200	833
B (ppm)	20	30	10	b.d.	b.d.	30	b.d.	20	b.d.	70	b.d.	70	100	b.d.	16	15	48
Rb (ppm)	295	400	317	250	316	346	319	310	307	280	410	317	372	99	320	308	336
Sr (ppm)	923	469	721	935	577	697	715	410	459	811	879	652	185	276	720	435	792

b.d. = below detection limit

Detection Limits:
Cu, Zn, Mo, Pb, As, W   2ppm
U   20 ppm
Th, S, F, Li, Cl, B, Rb, Sr   10 ppm

In all samples:
Au < 10 ppb
Ag < 0.4 ppm
Sn < 20 ppm

Appendix 1d Normative mineralogy

Sample	R-4	R-7	R-9	R-18	R-19	X-2	X-3	R-14	X-6	R-11	R-20	X-5	106-2b	105-5	Phase Averages		
Chem. Series	Alkaline	Calc-alk	Calc-alk	Calc-alk	Calc-alk	Alkaline	Alkaline	Calc-alk	Calc-alk	Alkaline	Alkaline	Calc-alk	Calc-alk	Calc-alk	Main	Biotite	Blue Trach.
Quartz	11.58	20.09	18.85	12.06	23.42	18.41	10.60	26.97	25.73	2.37	2.31	10.22	42.62	22.70	16.43	26.35	4.97
Corundum	0.00	0.00	0.00	0.00	0.00	0.00	0.00	0.37	0.32	0.00	0.00	0.00	1.76	0.71	0.00	0.34	0.00
Orthoclase	40.18	39.82	39.26	40.16	37.56	39.58	37.18	35.00	35.01	40.28	53.45	38.37	34.60	15.52	39.11	35.00	44.0
Albite	15.95	25.23	19.08	19.63	23.42	19.52	23.19	24.12	24.17	18.25	17.06	19.20	14.90	16.71	20.86	24.14	18.17
Anorthite	9.92	6.90	9.92	12.13	8.80	10.33	11.40	8.49	9.26	11.25	3.41	12.56	3.16	26.54	9.91	8.88	9.07
Diopside	7.99	2.44	3.21	4.20	0.53	3.60	5.20	0.00	0.00	13.39	12.67	6.27	0.00	0.00	3.88	0.00	10.78
Ortho-px	7.79	2.76	6.66	8.28	4.11	4.92	7.10	3.77	4.05	7.16	6.92	9.56	1.47	14.98	5.84	5.80	7.88
Magnetite	3.86	1.84	1.50	1.38	1.27	2.13	3.03	0.73	0.82	3.98	1.53	1.78	0.25	0.65	2.14	0.78	2.43
Ilmenite	1.60	0.65	1.00	1.29	0.61	0.94	1.27	0.42	0.46	1.58	1.38	1.35	0.17	1.45	0.97	0.44	1.43
Apatite	0.85	0.21	0.57	0.71	0.21	0.52	0.80	0.12	0.14	1.35	1.15	0.59	0.05	0.33	0.55	0.13	1.03
Pyrite	0.28	0.06	0.06	0.17	0.06	0.06	0.23	0.06	0.06	0.40	0.11	0.11	1.02	0.40	0.10	0.06	0.21

Norms are calculated and names given following the procedure outlined in Irvine and Baragar (1971).

U-Pb zircon age of the Jubilee Stock in the Michipicoten Greenstone Belt near Wawa, Ontario

R.W. Sullivan, R.P. Sage[1], and K.D. Card
Precambrian Geology Division

Abstract

A U-Pb study of zircon from the subvolcanic Jubilee Stock yields a linear trend of data points giving a concordia intercept age of 2745 ± 3 Ma. This result is in good agreement with previously obtained U-Pb zircon ages for related lower cycle volcanics and supports the view that associated gold mineralization is contemporaneous with volcanism and plutonism.

Résumé

Une datation par la méthode de l'U-Pb d'un zircon prélevé dans le stock hypovolcanique Jubilee a permis de constater une tendance linéaire des données qui fixe à 2 745 ± 3 millions d'années l'âge correspondant à l'intercept concordia. Ce résultat concorde avec les âges obtenus antérieurement par la méthode de l'U-Pb du zircon contenu dans des roches volcaniques de cycle inférieur et confirme l'opinion selon laquelle la minéralisation associée de l'or serait contemporaine au épisodes de volcanisme et de plutonisme.

[1] Ontario Geological Survey, Ministry of Natural Resources, 77 Grenville St., Toronto, Ontario M5S 1B3

Figure 42.1. Geological sketch map of part of the Michipicoten greenstone belt showing locations of samples for which U-Pb zircon and Rb-Sr isochron age determinations have been made. Map compiled from Ontario Division of Mines (1971) and Card (1981).

Introduction

The Jubilee Stock is a small felsic pluton in the Michipicoten greenstone belt of the Superior Province in the southern part of the Canadian Shield (Fig. 42.1). It intrudes a sequence of felsic and intermediate metavolcanic rocks, and geological relationships suggest that the intrusion and the volcanics are closely associated in time and genesis. Goodwin (1966) suggested that the felsic volcanics and intrusive stocks of the Michipicoten belt are cogenetic and coeval. Sage (1979) postulated that the Jubilee Stock occupies the central part of a volcanic caldera, and furthermore, that there is a genetic connection between the plutonic-volcanic complex and gold mineralization in the area. In light of the foregoing, and because Turek et al. (1982, 1984) who have carried out extensive radiometric age studies in the area, did not obtain a U-Pb zircon age on the stock, it was considered advisable to attempt to date its age of emplacement.

Previous geological and geochronological studies

Early geological investigations in the Michipicoten belt were carried out by, among others, Collins and Quirke (1926), Gledhill (1927), and Goodwin (1966). Attoh (1980) conducted a stratigraphic study in part of the belt, and Sage (1979, 1980, 1981) is currently mapping a large part of the belt in detail. As a result of these studies the volcanic-sedimentary sequence has been subdivided into a number of major cycles. The more recent work has also given an indication of the complex structure of the belt, with recognition of overturned sequences and possible recumbent folds or nappes and thrusts.

Early geochronological investigations in the area by the Geological Survey of Canada (Leech et al., 1963, Lowdon et al., 1963; Wanless et al., 1974) resulted in publication of several K-Ar ages ranging from 800 Ma to 2500 Ma. Brooks et al. (1969) obtained two Rb-Sr isochron ages from Michipicoten volcanics of 2650 ± 100 Ma and 2500 ± 100 Ma. Recently, Turek et al. (1982, 1984) have published a number of Rb-Sr and high precision U-Pb zircon ages from volcanic and plutonic rocks in and around the Michipicoten belt. These data, summarized in Table 42.1, demonstrate that felsic volcanics in the lower part of the section are 2744 ± 10 Ma and 2749 ± 2 Ma old and felsic volcanics near the top of the sequence are 2696 ± 2 and 2698 ± 11 Ma old. Felsic plutons within the belt (internal granites) yielded U-Pb zircon ages of 2722 ± 1 and 2737 ± 6 Ma and granitic rocks surrounding the belt (external granites) yielded U-Pb zircon ages ranging from 2662 ± 5 Ma to 2888 ± 2 Ma.

The presence of 2888 Ma felsic plutonic rocks suggests that an older volcanic-plutonic cycle may be present in the area. This conjecture is strengthened by recent lead isotopic determination on galena from a base metal occurrence in mafic metavolcanics about 10 km east of Wawa which yield a Pb-Pb model age of about 2950 Ma (R. Thorpe, personal communication, 1985)

Geology of the Jubilee Stock

The Jubilee Stock is exposed over an area of approximately 6 km by 1.3 km in the southern part of the Michipicoten belt where it intrudes felsic and intermediate fragmental volcanics of the lower volcanic cycle (Fig. 42.1). The contacts between the pluton and the volcanics are irregular and not sharply defined; apophyses of the intrusion extend out into the wall rocks; the eastern margin is an intrusion breccia consisting of angular, sharp-bordered volcanic rock fragments in a fine grained igneous matrix; volcanic fragments are prevalent throughout the stock and locally constitute up to 50 per cent of the intrusion. The abundance of volcanic xenoliths and lack of assimilation indicates that the complex is a high-level subvolcanic intrusion; Sage (1979) noted that the stock is partly enclosed by a ring fracture occupied by quartz-feldspar porphyry and suggested that the intrusion occupies the centre of a caldera.

The Jubilee Stock, like its host volcanics, is foliated and it has imposed a hornfelsic thermal aureole on the surrounding metavolcanics. The intrusion is composed of fine- to medium-grained, equigranular to locally porphyritic granodiorite and diorite. The rock consists of 10% to 30% quartz, 40% to 55% plagioclase (An_{30}), 10% to 20% biotite and minor amphibole, opaque minerals, and accessories including brown zircon. Some carbonate, epidote, and chlorite alteration is present. Chemically the rock is calc-alkaline.

There are a number of gold occurrences associated with the Jubilee Stock and its thermal aureole (Studemeister et al., in press). Gold occurs within sulphide-bearing quartz lenses cutting and concordant with andesitic to dacitic tuffaceous units about the margins of the stock. The gold deposits are considered to represent either vein

Table 42.1. Summary of recent U-Pb Zircon and Rb-Sr Isochron age determinations, Michipicoten Belt, Ontario

Rock Unit	U-Pb Zircon (Ma)	Rb-Sr (Ma)	Reference
1) Felsic volcanic; upper cycle	2696 ± 2		Turek et al., 1982
2) Felsic volcanic, upper cycle	2698 ± 11		Turek et al., 1984
3) Felsic volcanic; lower cycle	2744 ± 10	2680 ± 490	Turek et al., 1982
4) Felsic volcanic; lower cycle	2749 ± 2	2530 ± 90	Turek et al., 1982
		2285 ± 70	
5) Granite stock; internal	2737 ± 6	2560 ± 220	Turek et al., 1982
6) Gautcher Lake stock; internal	2722 ± 1		Turek et al., 1982
7) Northern granite; external	2662 ± 5		Turek et al., 1984
8) Southern granite; external	2694 ± 3		Turek et al., 1984
9) Southwestern granite; external	2698 ± 1		Turek et al., 1984
10) Hawk Lake trondhjemite; external	2747 ± 7		Turek et al., 1982
11) Hawk Lake granite; external	2888 ± 2		Turek et al., 1984
12) Jubilee Stock; internal		2560 ± 270	Turek et al., 1982
	2745 ± 3		this paper

See Figure 42.1 for locations of isotopic age determinations

Table 42.2. Analytical data for U-Pb analyses of zircon from the Jubilee Stock, near Wawa, Ontario

Sample Description	Fraction No.	Weight mg	U ppm	Pb* ppm	Measured $^{206}Pb/^{204}Pb$	Isotopic Abundances** $^{206}Pb=100$			$^{206}Pb/^{238}U$	$^{207}Pb/^{235}U$	$^{207}Pb/^{206}Pb$ Age (Ma)
						^{204}Pb	^{207}Pb	^{208}Pb			
-149 +105 μm, NM +2°, A	1	1.63	179.1	108.1	19206	0.0028	19.038	15.436	0.52202	13.679	2743
-105 +74 μm, NM .0°	2	3.23	227.9	127.1	32397	0.0005	18.938	13.006	0.49118	12.821	2736
-74 +62 μm, NM -0.5°	3	1.60	223.1	123.3	19850	0.0020	18.955	12.527	0.48876	12.758	2736
-149 +105 μm, M +2°	4	2.64	277.3	156.1	13351	0.0054	18.926	16.571	0.48346	12.572	2730

Note: NM, M = non magnetic, magnetic at given angle
A = abraded
* Radiogenic lead
** Corrected for lead blank

Figure 42.2

Concordia diagram showing results of U-Pb analyses of four zircon fractions from the Jubilee Stock, near Wawa, Ontario. Error boxes are at the 2 sigma level. No geological significance is placed on the lower intercept age of 300 Ma.

deposits (Gledhill, 1927) or gold-bearing cherty tuffs about a volcanic edifice built above the Jubilee Stock (Studemeister, 1985).

Geochronology of the Jubilee Stock

The general techniques of zircon fraction preparation, chemistry and mass spectrometric analysis are described in Sullivan and Loveridge (1980) and van Breemen et al. (in press). Regression analysis was done using the methods of Davis (1982).

The zircon concentrate was brown and had a full size distribution of +149 to -44 μm. Microscopic examination showed a range of morphologies from euhedral clear internally simple, through euhedral with zoning, some with large inclusions and central cores, to subhedral more rounded zircons with clearer overgrowths. This population is interpreted as consisting of primary igneous zircon plus zircon with varying proportions of primary zircon and relict zircon in the form of cores and inclusions.

Four zircon fractions were prepared for analysis. Only clear, euhedral zircons were hand picked, complex zircons with inclusions or overgrowths were avoided. One fraction (1) was abraded using the technique developed by Krogh (1982). Analytical results are listed in Table 42.2 and plotted on a concordia diagram (Fig. 42.2).

The four discordant data points are not collinear within analytical error but define a linear trend, and with the one abraded fraction (1) plotting close to the concordia curve,

result in a low-error upper intercept age of 2745 ± 3 Ma. This result is interpreted as the age of emplacement of the Jubilee Stock.

Even though there is an apparent older zircon component in the sample population, careful hand picking has resulted in obtaining only single-age zircons for analyses. A normal discordancy model with surface correlated lead loss is invoked to explain the data array. No work was done on the zircons with cores. No geological significance is placed on the lower intercept age of 300 Ma.

Discussion of the U-Pb zircon age of the Jubilee Stock

The U-Pb zircon age of 2745 ± 3 Ma for the Jubilee Stock obtained in the study is essentially identical to the U-Pb zircon ages of 2744 ± 10 and 2749 ± 2 Ma obtained by Turek et al. (1982) for the lower cycle volcanics. It is also about the same age as some of the external granites near Hawk Lake (2747 ± 7 Ma) and only slightly older than other internal granites (2737 ± 6 Ma, 2722 ± 1 Ma) dated by Turek et al. (1982).

The 2745 ± 3 Ma age is considered to represent the age of emplacement and crystallization of the Jubilee Stock, and as such supports the geological interpretation that the intrusion and its host volcanics are coeval and probably cogenetic. The fact that the volcanic and plutonic activity are essentially synchronous also supports a syngenetic origin for the gold mineralization.

References

Attoh, K.
1980: Stratigraphic relations of the volcanic-sedimentary succession in the Wawa Greenstone Belt, Ontario; in Current Research, Part A, Geological Survey of Canada, Paper 80-1A, p. 101-106.

Brooks, C., Krogh, T.E., Hart, S.R., and Davis, G.L.
1969: The initial $^{87}Sr/^{86}Sr$ ratios of the upper and lower series Michipicoten metavolcanics, Ontario, Canada; Annual Report of the Director, Department of Terrestrial Magnetism, Carnegie Institution of Washington Yearbook, p. 422-424.

Card, K.D.
1981: Central Superior Province Compilation, preliminary geological maps 41N (Michipicoten) and 42C (White River), scale 1:250 000; Geological Survey of Canada, Open File 729.

Collins, W.H. and Quirke, T.T.
1926: Michipicoten Iron Ranges; Geological Survey of Canada, Memoir 147, 173 p.

Davis, D.W.
1982: Optimum linear regression and error estimation applied to U-Pb data; Canadian Journal of Earth Sciences, v. 19, p. 2141-2149.

Gledhill, T.L.
1927: Michipicoten gold area, District of Algoma, Ontario; Ontario Department of Mines Annual Report, v. 36, p. 1-49.

Goodwin, A.M.
1966: The relationship of mineralization to stratigraphy in the Michipicoten area, Ontario; in The relationship of mineralization to Precambrian stratigraphy in certain mining areas of Ontario and Quebec, Geological Association of Canada, Special Paper 3, p. 37-73.

Krogh, T.E.
1982: Improved accuracy of U-Pb zircon ages by the creation of more concordant systems using an air abrasion technique; Geochimica et Cosmochimica Acta, 46, p. 637-649.

Leech, G.B., Lowdon, J.A., Stockwell, C.H., and Wanless, R.K.
1963: Age determinations and geological studies; Geological Survey of Canada, Paper 63-17, 140 p.

Lowdon, J.A., Stockwell, C.H., Tipper, H.W., and Wanless, R.K.
1963: Age determinations and geological studies; Geological Survey of Canada, Paper 62-17.

Ontario Division of Mines
1971: Manitouwadge-Wawa sheet, Geological Compilation Series; scale 1:253 440, Ontario Division of Mines Map 2220.

Sage, R.P.
1979: Wawa area, District of Algoma; in Summary of Field Work, 1979, Ontario Geological Survey M.P. 90, p. 48-53.

1980: Wawa area, District of Algoma; in Summary of Field Work, 1980, Ontario Geological Survey M.P. 96, p. 47-50.

1981: Josephine area, District of Algoma; in Summary of Field Work, 1981, Ontario Geological Survey M.P. 100, p. 37-40.

Studemeister, P.A.
1985: Gold-bearing quartz around felsic stocks in Ontario; Canadian Mining and Metallurgical Bulletin, v. 78, p. 43-47.

Studeimeister, P.A., Koza, H., and Gignac, D.
— The distribution of gold occurrences on the Dunraine Property near Wawa, Ontario (Canada); Mining Engineering Transactions. (in press)

Sullivan, R.W. and Loveridge, W.D.
1980: Uranium-lead age determinations on zircon at The Geological Survey of Canada: Current procedures in concentrate preparation and analysis; in Current Research, Part C, Geological Survey of Canada, Paper 80-1C, p. 161-246.

Turek, A., Smith, P.E., and Van Schmus, W.R.
1982: Rb-Sr and U-Pb ages of volcanics and granite emplacement in the Michipicoten belt, Wawa, Ontario; Canadian Journal of Earth Sciences, v. 19, p. 1608-1626.

1984: U-Pb zircon ages and the evolution of the Michipicoten plutonic-volcanic terrane of the Superior Province, Ontario; Canadian Journal of Earth Sciences, v. 21, p. 457-464.

van Breemen, O., Davidson, A., Loveridge, W.D., and Sullivan, R.W.
— U-Pb zircon geochronology of Grenville tectonites, granulites and igneous precursors, Parry Sound, Ontario; Canadian Journal of Earth Sciences. (in press)

Wanless, R.K., Stevens, R.D., Lachance, G.R., and Delabio, R.N.D.
1974: Age determinations and geological studies, K-Ar Isotopic Ages, Report 12; Geological Survey of Canada, Paper 74-2, 72 p.

A U-Pb age on zircon from a quartz syenite intrusion, Amer Lake map area, District of Keewatin, NWT

Project 760025

Subhas Tella, W.W. Heywood and W.D. Loveridge
Precambrian Geology Division

Abstract

U-Pb analysis of zircon from a quartz syenite intrusion, Amer Lake map area, District of Keewatin, yielded an upper concordia intercept age of 1850 + 30/-10 Ma, in agreement with a K-Ar age of 1833 ± 32 Ma on hornblende from the same specimen. This is interpreted as the age of magmatic intrusion which is probably coeval with the lower Proterozoic (late Aphebian) Dubawnt Group alkaline igneous activity in the Baker Lake region.

Résumé

Une analyse par la méthode de l'uranium-plomb (U-Pb) du zircon extrait d'une intrusion de syénite quartzique dans la région du lac Amer, dans le district de Keewatin, a produit, sur la courbe de type concordia, une intersection haute de 1 850 +30/-10 Ma; ce résultat concorde avec l'âge de 1 833 ± 32 Ma obtenu par la méthode du potassium-argon sur du hornblende provenant du même spécimen. Les auteurs considèrent que cette intersection haute correspond à l'âge de l'intrusion magmatique, qui est probablement contemporaine de l'activité ignée de nature alcaline du groupe de Dubawnt datant du Protérozoïque inférieur (fin de l'Aphébien), survenue dans la région de Baker Lake.

Geological setting

The sample area (Fig. 43.1) lies within the Armit Lake Block of the Churchill Structural Province (Heywood and Schau, 1978) 15 to 20 km south of the Amer and Meadowbank faults. The area is chiefly underlain by granulite, the oldest rock unit, and various granitic rock types (Tella, 1984). A few gneisses are recognizably of sedimentary origin. Minor amounts of amphibolite also occur. The rock sampled (WN-227-76) is a quartz syenite that is characteristically massive, unfoliated and unmetamorphosed, which suggests it is younger than the other granitoid rocks and also the Amer group. The bulk of the granitoid rocks are older than the Amer group, the major metasedimentary rock sequence in the Amer Lake map area; however, aplite and pegmatite are known to intrude quartzite at the base of the group. A K-Ar age of 1729 ± 41 Ma (Stevens et al., 1982, publication no. 81-188) was obtained on muscovite from a pegmatite. Units of the Amer group outcrop 10 km south of the sample site but the quartz syenite is not known to be in contact with the group.

The quartz syenite is a pink, medium- to coarse-grained, massive to cataclastic, porphyritic to equigranular rock. Microscopically this rock can be seen to be composed of 70 to 80 per cent potash feldspar, chiefly as string perthite with minor amounts of microcline. Quartz forms 5 to 15 per cent. Diopside forms from a trace to 15 per cent, but is only locally present. It is commonly altered to chlorite and carbonate. Rare sodic amphibole comprises a trace to 3 per cent. Sphene, apatite (commonly forming large crystals), opaque minerals, zircon and rare fluorite, form the accessory minerals. Secondary epidote is present in trace amounts.

Analytical procedures

The initial U-Pb analysis on zircon from WN-227-76 took place in 1978 (fractions 1 and 4) and these were supplemented by analyses of fractions 2 and 3 in 1985.

Procedures used for the concentration and preparation of zircon fractions, the chemical extraction of U and Pb from zircon, and the isotopic analysis of U and Pb evolved over this period of time but a general description is given in Sullivan and Loveridge (1980). Exceptions to this description are as follows. In 1978, zircon fractions were not handpicked to ensure 100% purity. Sieving and magnetic separation procedures were employed to ensure that the purity of the fractions analyzed was greater than 90%. Weights of zircon fractions analyzed, 5-20 mg in 1978, decreased to 1-2 mg in 1985. Both fractions analyzed in 1985 were handpicked and fraction 2 was abraded (Krogh, 1982).

Mass spectrometric procedures in use in 1978 are as described by Sullivan and Loveridge (1970), whereas analyses undertaken in 1985 were performed on a Finnigan-MAT 261 mass spectrometer in the multicollector mode. In this mode, ion beams composed of each of the four lead isotopes are collected and measured simultaneously in four separate

Figure 43.1. *Geological sketch map. Amer Lake area, showing sample location.*

Faraday cups. A more accurate measure of the minuscule ^{204}Pb abundance is obtained, at essentially the same time, by stepping the magnetic field in order to measure the ^{204}Pb/^{207}Pb ratio on an associated electron multiplier.

Lead contamination introduced during the chemical extraction procedures was less than 1% of the zircon lead present. The common lead component of the zircon lead itself ranged from 2.7 to 3.9%. The isotopic composition assumed for the common lead component was that of a 1850 Ma Stacey and Kramers (1975) model lead.

U-Pb ages have been calculated using the uranium decay constants and isotopic composition recommended by Steiger and Jaeger (1977). Linear regression of the U-Pb data and error estimation (95% confidence level) is based on Davis (1982).

Results and discussion

The results of the U-Pb analyses are presented in Table 43.1 and displayed on a concordia diagram (Fig. 43.2). The four tightly grouped data points are collinear and 6 to

Table 43.1. Analytical data, zircon fractions from sample WN-227-76

		WN-227-76			
Fraction number		1	2	3	4
Fraction size, μm		+149	+149	+149	+149
Magnetic or n.m., angle		nm-1.5°	m-1°	nm-1°	m-1.5°
Handpicked, abraded			a	hp	–
Weight, mg		15.63	1.469	1.712	8.58
Uranium ppm		497.5	747.1	586.2	667.4
Radiogenic Pb ppm		164.9	245.4	190.9	216.1
Meas. ^{206}Pb/^{204}Pb		1789	1397	1727	1244
Abundances (^{206}Pb=100)	^{204}Pb	0.0514	0.0627	0.0489	0.0732
	^{207}Pb	11.895	12.034	11.841	12.130
	^{208}Pb	11.850	12.376	11.806	12.891
Atomic Ratios	^{206}Pb/^{238}U	0.31771	0.31449	0.31200	0.30957
	^{207}Pb/^{235}U	4.9067	4.8505	4.8094	4.7547
	^{207}Pb/^{206}Pb	0.11200	0.11186	0.11180	0.11139
Ages, Ma	^{206}Pb/^{238}U	1779	1763	1751	1739
	^{207}Pb/^{235}U	1803	1794	1787	1777
	^{207}Pb/^{206}Pb	1832	1830	1829	1822

Figure 43.2. Concordia diagram showing the results of U-Pb analyses of zircon from WN-227-76.

10% discordant defining a chord which cuts the concordia curve at 1850 + 30/-10 Ma and 594 + 354/-208 Ma. The relatively high uncertainty associated with the ages results from the tight grouping of the data points.

Uranium contents are relatively high, 497 to 747 ppm (Table 43.1), but discordancy of data points due to lead loss was held to a minimum by selecting for analysis the most nonmagnetic zircon of the largest grain size available. The abraded fraction (2), the most magnetic of the four zircon fractions has the highest measured U content. The data point from this fraction is collinear with the other three points, indicating that the zircon interiors are not obviously different from the bulk zircon (i.e. no inherited lead component).

Although the zircon in these fractions consisted mostly of fragmented anhedral grains, a few grains were subhedral to euhedral. These were specifically handpicked to constitute fraction 3. The results from fraction 3 are comparable to those from the other fractions, indicating that the subhedral to euhedral, and anhedral grains, do not form different populations.

Previously, a K-Ar age of 1833 ± 32 Ma was obtained on hornblende from this same specimen (Tella and Heywood, 1978). The present U-Pb zircon age of 1850 + 30/-10 Ma is in agreement with the K-Ar age. This is interpreted as the age of quartz syenite intrusion which is probably coeval with the lower Proterozoic (late Aphebian) Dubawnt Group alkaline magmatic activity in the Baker Lake region (Blake, 1980).

References

Blake, D.H.
1980: Volcanic rocks of the Paleohelikian Dubawnt Group in the Baker Lake-Angikuni Lake area, District of Keewatin, N.W.T.; Geological Survey of Canada, Bulletin 309, 39 p.

Davis, D.W.
1982: Optimum linear regression and error estimation applied to U-Pb data; Canadian Journal of Earth Sciences, v. 19, p. 2141-2149.

Heywood, W.W. and Schau, Mikkel
1978: A subdivision of the northern Churchill Structural Province; in Current Research, Part A, Geological Survey of Canada, Paper 78-1A, p. 139-143.

Krogh, T.E.
1982: Improved accuracy of U-Pb zircon ages by the creation of more concordant systems using an air abrasion technique; Geochemica et Cosmochimica Acta, v. 46, p. 637-649.

Stacey, J.S. and Kramers, J.D.
1975: Approximation of terrestrial lead isotope evolution by a two stage mode; Earth and Planetary Science Letters, v. 26, p. 207-221.

Steiger, R.H. and Jaeger, E.
1977: Subcommission on Geochronology: convention on the use of decay constants in geo- and cosmochronology; Earth and Planetary Science Letters, v. 36, p. 359-362.

Stevens, R.D., Delabio, R.N., and Lachance, G.R.
1982: Age determinations and geological studies, K-Ar isotopic ages, Report 16; Geological Survey of Canada, Paper 82-2.

Sullivan, R.W. and Loveridge, W.D.
1980: Uranium-lead age determinations on zircon at the Geological Survey of Canada; current procedures in concentrate preparation and analysis; in Loveridge, W.D., Rubidium-strontium and uranium-lead isotopic age studies. Report 3; in Current Research, Part C, Geological Survey of Canada, Paper 80-1C, p. 161-246.

Tella, S.
1984: Geology of the Amer Lake (NTS 66H), Deep Rose Lake (NTS 66G), and parts of the Pelly Lake (NTS 66F) map areas, District of Keewatin, N.W.T.; Geological Survey of Canada, Open File 1043.

Tella, S. and Heywood, W.W.
1978: The structural history of the Amer Mylonite Zone, Churchill Strutural Province, District of Keewatin; in Current Research, Part C, Geological Survey of Canada, Paper 78-1C, p. 79-88.

APPENDIX

Zircon selection and morphology

Fractions 1 and 4:

The +149 µm concentrate was passed through a Frantz electromagnetic separator at a slope of -1° and the resultant less magnetic component was again separated at -1.5°. The less and more magnetic pair from this second separation constituted fractions 1 and 4 respectively. Zircon grains were fragmented anhedral, generally equidimensional, with a small percentage being subhedral to euhedral. Zircon was mostly clear to c. 15% translucent and c. 20% had external and/or internal orange stains.

Fraction 2:

From the +149 µm concentrate that was more magnetic when passed through the Frantz at a slope of -1°, a quantity of fragmental anhedral grains was handpicked. The general population was heavily stained with orange; the most lightly stained component was selected by hand picking, but all grains still exhibited some staining. The handpicked zircons were then abraded (Krogh, 1982). The resultant fraction consisted of well rounded grains, pale tan in colour, with varying degrees of orange staining.

Fraction 3:

From the unused residuals of fractions 1 and 4, the subhedral to euhedral grains and broken grains were individually hand picked. Most grains exhibited some orange staining and most were clear, but c. 20% were translucent.

A U-Pb age on zircon from a dacite porphyry, Amer Lake map area, District of Keewatin, NWT

Project 760025

Subhas Tella, W.W. Heywood and W.D. Loveridge
Precambrian Geology Division

Abstract

A U-Pb study on zircon from a dacite porphyry, Amer Lake area, yielded a U-Pb upper concordia intercept age of 2798 + 24/-21 Ma, which establishes an Archean age for some of the supracrustal rocks in this part of the Churchill Structural Province.

Résumé

La datation par la méthode de l'uranium-plomb (U-Pb) du zircon extrait d'un porphyre dacitique de la région du lac Amer a produit, sur la courbe de type concordia, une intersection haute de 2 798 +24/-21 Ma; ce résultat établit ainsi l'âge archéen de certaines des roches supracortiales de cette partie de la province structurale de Churchill.

Geological setting

The sample area (Fig. 44.1) forms part of the Armit Lake Block of the Churchill Structural Province (Heywood and Schau, 1978). The oldest rocks in the area consist of metamorphosed layered rocks, commonly intermediate to mafic volcanic rocks, quartzite, and schists chiefly of sedimentary origin. Associated with these rocks are ultrabasic rocks which elsewhere in the Amer Lake map area are known in part to be of extrusive origin. These layered rocks are intruded by a weak to well foliated granite to quartz monzonite and also by a porphyritic granite. Preliminary results of bedrock mapping in the Amer Lake area (NTS 66H) were previously reported (see Tella, 1984, for a detailed bibliography).

The present sample, WN-503-78, is associated with mafic metavolcanic rocks that structurally underlie quartzite and phyllitic schist. The dacite porphyry is structurally above the mafic volcanic rocks but is considered to be a part of the mafic sequence. It is a fine grained, yellowish grey dacite that is mottled with greenish grey and displays a weak schistosity. Vitreous quartz phenocrysts, up to 4 mm long, are readily visible megascopically. Thin sections show highly altered sub- to anhedral plagioclase phenocrysts or clusters of crystals up to 2 mm, as well as the quartz. The latter are commonly well rounded and some display a caries texture, suggesting a tuffaceous origin. The plagioclase (An_{12}) is chiefly altered to chlorite and calcite. A few plagioclase clusters contain small amounts of sodic amphibole, probably riebeckite. The matrix is a very fine grained, slightly schistose matte of white mica, chlorite, untwinned plagioclase, and rarer calcite, quartz, apatite, zircon and pyrite.

Rare fractures are filled with fresh plagioclase (An_{11}), quartz, epidote and chlorite.

Analytical procedures and results

The analytical procedures used for the preparation of zircon concentrates and the extraction and isotopic analysis of lead are described in Sullivan and Loveridge, 1980.

Analytical results are listed in Table 44.1 and displayed on a concordia diagram (Fig. 44.2). A description of the zircon morphology of the fractions analyzed is presented in the Appendix. The sample location is shown in Figure 44.1 and co-ordinates are given in the Appendix.

The zircon fractions analyzed yielded three well spaced but relatively discordant data points, collinear within analytical uncertainty, defining a chord which cuts the concordia curve at 2798 + 24/-21 Ma and 1513 + 41/-40 Ma.

Table 44.1. Analytical data, zircon fractions from sample WN-503-78

Sample number		WN-503-78		
Fraction number		1	2	3
Fraction size, µm		-105 +74	-105 +74	+105
Magnetic or nm, angle		nm-2°	mag-2°	–
Weight, mg		5.18	3.17	2.14
Uranium, ppm		109.4	149.8	196.9
Radiogenic Pb, ppm		56.13	67.39	82.44
Meas. $^{206}Pb/^{204}Pb$		1706	1417	1058
Abundances (^{206}Pb=100)	^{204}Pb	0.01130	0.00225	0.0538
	^{207}Pb	17.892	16.400	16.197
	^{208}Pb	13.884	12.234	13.975
Atomic Ratios	$^{206}Pb/^{238}U$	0.45407	0.40673	0.38070
	$^{207}Pb/^{235}U$	11.116	9.1821	8.1489
	$^{207}Pb/^{206}Pb$	0.17754	0.16372	0.15524
Ages, Ma	$^{206}Pb/^{238}U$	2413	2200	2080
	$^{207}Pb/^{235}U$	2533	2356	2248
	$^{207}Pb/^{206}Pb$	2630	2495	2404

Archean/Aphebian (undifferentiated) Helikian

Archean Supracrustals Aphebian

LEGEND

7 PORPHYRITIC GRANITE

6 GRANITE, GRANODIORITE, QUARTZ MONZONITE

5 ULTRABASIC ROCKS, CHIEFLY PERIDOTITE

4 WHITE ORTHOQUARTZITE

3 GNEISS DERIVED FROM SEDIMENTARY AND VOLCANIC ROCKS

2 SCHISTS DERIVED FROM SEDIMENTARY AND VOLCANIC ROCKS

1 METAMAFIC VOLCANIC ROCKS

● SAMPLE LOCATION (WN-503-78)

FAULT

THRUST FAULT

Figure 44.1. *Geological sketch map, Amer Lake area, showing sample locations.*

Figure 44.2

Concordia diagram showing the results of U-Pb analyses of zircon fractions from sample WN-503-78.

Uranium contents are not high, ranging from 109 to 197 ppm (Table 44.1) with the lower uranium data points being consistently less discordant than the higher uranium ones.

Discussion

The U-Pb age of 2798 + 24/-21 Ma establishes an Archean age for some of the supracrustal rocks in this part of the Churchill Structural Province. The lower intersection of the chord with concordia, 1513 + 41/-40 Ma, is lower than most K-Ar ages on biotite from the general area and probably marks the time at which sufficient radiation damage had accumulated in the zircon crystals to allow lead loss due to minor environmental influences. As such it is not interpreted as the age of a specific event.

References

Heywood, W.W. and Schau, Mikkel
1978: A subdivision of the northern Churchill Structural Province; in Current Research, Part A, Geological Survey of Canada, Paper 78-1A, p. 139-143.

Sullivan, R.W. and Loveridge, W.D.
1980: Uranium-lead age determinations on zircon at the Geological Survey of Canada; current procedures in concentrate preparation and analysis; in Loveridge W.D., Rubidium – strontium and uranium-lead isotopic age studies. Report 3; in Current Research, Part C, Geological Survey of Canada, Paper 80-1C, p. 161-246.

Tella, S.
1984: Geology of the Amer Lake (NTS 66H), Deep Rose Lake (NTS 66G), and parts of the Pelly Lake (NTS 66F) map areas, District of Keewatin, NWT; Geological Survey of Canada, Open File 1043.

Appendix

WN-503-78: latitude 65° 17'30"N; longitude 96°25'W

Fractions 1 and 2: The -140 +200 μm concentrate was separated into less and more magnetic splits using a Frantz Isodynamic Separator. The fractions which were handpicked from each of these splits for analysis, were morphologically similar consisting of c. 100% hyacinth euhedral zircon crystals and fragments. Terminations were generally rounded but rarely sharp, and zoning was noted in occasional grains. Clear rod and bubble shaped inclusions were evident. Highly rounded and red-orange or clear zircons were excluded from the fractions analyzed.

Fraction 3: In the +140 μm fraction, 100% clear euhedral zircon, hyacinth in colour with a few clear colourless and red-orange grains, was handpicked. Bubble and rod shaped clear inclusions and some dark inclusions were noted. No magnetic separation was made on this fraction.

Glacial features of the west-central Canadian Shield

J.M. Aylsworth and W.W. Shilts
Terrain Sciences Division

Abstract

A small scale map of selected glacial features (eskers, related outwash and meltwater features, rogen moraine, and drift-free areas) was compiled for approximately 650 000 km^2 of the Canadian Shield lying between 60° and 66° N and west of Hudson Bay. It combines data obtained by airphoto interpretation of selected glacial sediment characteristics of 37 1:250 000 NTS map areas and surficial geology mapping of 28 additional sheets. This map is presented along with preliminary discussion of regional glacial sedimentation patterns.

A widespread, integrated system of trunk and tributary eskers suggests stagnation of the Keewatin Ice Sheet while it still covered a large area. In addition, distribution of constructional glacial landforms suggests that erodibility of bedrock and character of resulting sediment significantly influenced the type and pattern of glacial sedimentation. This influence may have been as great a control on the nature and distribution of landforms as glacier dynamics.

Résumé

Les auteurs ont porté sur une carte à petite échelle des formes du relief glaciaire (eskers, plaines alluviales et autres éléments formés par les eaux de fonte, moraine de Rogen et régions dépourvues de sédiments glaciaires) qui couvrent environ 650 000 km^2 du Bouclier canadien, entre les 60e et 66e degrés de latitude nord, à l'ouest de la baie d'Hudson. Ils ont groupé des données obtenues par photo-interprétation de certaines caractéristiques des sédiments glaciaires observées dans 37 régions cartographiées à 1/250 000 et par cartographie des formations en surface de 28 autres régions. Les auteurs accompagnent la présentation de cette carte d'un exposé préliminaire des modelés de sédimentation glaciaire régionaux.

L'existence d'un réseau étendu et intégré d'eskers principaux et secondaires semble indiquer que l'inlandsis du Keewatin a connu une phase stationnaire au moment où il recouvrait encore une vaste région. En outre, d'après la répartition des formes construites du relief glaciaire, il semble que la facilité d'érosion de la roche en place et les caractéristiques des sédiments qui en ont résultée aient profondément influé sur la nature et la forme de la sédimentation glaciaire, au point, peut-être, de contrôler la nature et la répartition des formes de relief à l'instar de la dynamique des glaciers.

Introduction

Preliminary results of a reconnaissance airphoto interpretation of selected glacial features of much of the west-central part of the Canadian Shield have been combined with more detailed mapping carried out near Hudson Bay by the authors and colleagues. The resulting map reveals distinctive patterns of deposition and erosion that may have considerable significance in interpretation of the history and dynamics of the western part of the Laurentide Ice Sheet.

In this paper we present a preliminary small-scale map (Fig. 45.1) and a limited discussion of the meaning of the patterns of deposition and erosion that it reveals.

Background

Most of the study area was mapped at a general reconnaissance level by Geological Survey of Canada personnel in the late 1950s and early 1960s (Fyles, 1955; Lee, 1959; Craig, 1964, 1965). These early maps were restricted to depicting or symbolizing the most prominent geomorphic features, such as major esker ridges, and only portray rogen moraine, sometimes termed ribbed moraine (Cowan, 1968; Hughes, 1964), in a fraction of the area actually covered by it. No attempt was made to differentiate drift-covered from drift-free areas. These works were compiled onto the Glacial Map of Canada (Prest et al., 1968).

Since the Glacial Map of Canada was published, more detailed surficial geology maps (1:125 000 and 1:250 000) have been produced for much of the District of Keewatin. These maps, in published or unpublished form, cover approximately 40% of the area of the present mapping project. For the remaining 60%, major glacial features have been compiled from interpretation of 1:60 000 scale air photographs on 1:250 000 scale maps under contract to Terrain Analysis and Mapping Services Ltd., Stittsville, Ontario. Information from these maps was plotted at 1:1 000 000 and further generalized for presentation here (Fig. 45.1).

General distribution pattern

In Figure 45.1 it is possible to discern four zones of sedimentation patterns that are roughly concentric about the Keewatin Ice Divide:

Zone 1

The innermost zone, characterized by the absence of eskers and rogen moraine (Lundqvist, 1969) occupies southern Keewatin and extends about 50 km on either side of the Keewatin Ice Divide (Lee et al., 1957). The characteristic glacial landscape of Zone 1 comprises till plains with areas of low till hummocks and virtually no oriented depositional features. It is almost completely devoid of glaciofluvial deposits, except for minor outwash in some valleys. The location of the ice divide (Fig. 45.2), which forms the axis of the region, is clearly defined by striation orientations.

Zone 2

Zone 2 is 200-250 km wide, surrounds Zone 1 on three sides, and is characterized by the presence of well developed rogen moraine and esker-outwash systems.

Rogen moraine comprises sinuous ridges trending roughly perpendicular to ice flow (Cowan, 1968; Shilts, 1977) and occurs in linear belts or trains parallel to major directions of ice movement. The trains of rogen ridges radiate from the Keewatin Ice Divide like the spokes of a wheel. In the areas between rogen trains, drift forms featureless or drumlinized or fluted till plains (see GSC maps 7-1979; 8, 9-1980; 1-1984; 2, 5-1985). Individual drumlins may occur within rogen moraine trains and individual large ridges may be fluted. Where rogen moraine is best developed, its distribution is little influenced by topography, occurring both in depressions and on uplands, but where the belts become more widely separated, down ice from the ice divide, rogen moraine generally occurs preferentially in depressions.

Distribution of rogen moraine about the Keewatin Ice Divide is not uniform. It is rare west of Dubawnt Lake and east of Baker Lake (indicated by ? on inset map, Fig. 45.1) where large areas are devoid of glacial deposits or are covered by a featureless till veneer, and northwest of Dubawnt Lake where an extensive drumlin field occurs. The northern boundary of the southwestern-most field of rogen moraine is remarkably distinct against the featureless till plain west of Dubawnt Lake. In general the down-ice margin of the zone of rogen moraine is abrupt although isolated, small, linear trains occur in the inner half of the next zone.

Eskers also begin near the boundary between Zone 1 and Zone 2 and, like the rogen moraine trains, radiate from the region of the Keewatin Ice Divide. A typical esker system begins as a series of hummocks or short segments which pass downstream into continuous large eskers joined by areas of outwash or meltwater channels. Along a section measured across the southwestern part of Zone 2, eskers are spaced approximately 13 km apart, with spacing varying from 2 to 27 km. Throughout most of the area eskers are sharp ridged, up to 40 m high, with occasional conical knobs projecting well above the average elevation of the esker crest. Along their length they may be periodically interrupted by bulges where the single ridge splits into multiple ridges which coalesce downstream. Above marine limit they are commonly flanked by outwash in terraces disrupted by kettle lakes. North of Thelon River eskers are associated with prominent outwash terraces and the tops of the eskers are in some places flat, planed off by meltwater flowing on a stagnant ice floor into which the esker ridge was frozen (Shilts, 1984).

Below marine limit, eskers are commonly reworked by wave action in the offlap phase of the Tyrrell Sea. This has had the effect of subduing their relief to the extent that they rarely project more than 10 m above the adjacent terrain. Sonar profiles show them to retain their relief and sharp crest where they are submerged in deep lakes (W.W. Shilts, unpublished data).

Zone 3

Zone 3, which lies west of Zone 2, is characterized by an intricate dendritic pattern of eskers, and continuous drift cover. It forms a 200 to 300 km-wide belt of glacial sediment, commonly till, which thins to a discontinuous veneer in the outer part of the zone. Large esker systems are known to extend into Hudson Bay and wave-reworked eskers, bearing erratics common to the Keewatin mainland, occur within the Bay on Coats Island (Shilts, 1982), suggesting that an area similar to Zone 3 may lie east of Zone 2, submerged by Hudson Bay.

Within Zone 3 rogen moraine occurs only as isolated, short, narrow, linear trains, lying in depressions and closely associated, in space, if not in time or genesis, with eskers. Within the rogen areas, individual ridges are much smaller and depart considerably in shape from the "classical" rogen moraine (Lundqvist, 1969) of Zone 2 (S. Paradis, personal communication, 1985).

Compared to the 13 km spacing of eskers in Zone 2, spacing between eskers decreases to approximately 8 km (3-15 km range) 200 km downstream (southwest) from the
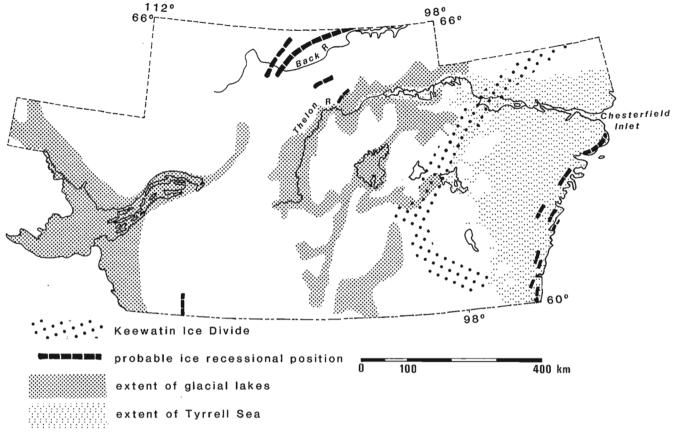
Figure 45.1. *Distribution of selected glacial features on the west-central Canadian Shield.*

377

Figure 45.2. *Glacial geology features discussed in the text.*

section that was measured in Zone 2. Although numbers of eskers and their tributaries increase in Zone 3, the overall size (height and width) decreases in this zone.

In the outer part of Zone 3 the esker systems become more discontinuous and disorganized, and esker distributaries are common. Short esker segments are commonly oriented in various directions and areas of crevasse fillings are associated with disruption of the esker system.

Within the northwestern portion of this zone a prominent ice recessional position (Fig. 45.2) is marked by a chain of ice-contact deltas or fans, other outwash features, and esker distributaries which extends parallel to and north of the Back River. In the vicinity of this feature, short parallel esker segments abound between the major systems.

Zone 4

The outermost zone of the Canadian Shield part of the study region is characterized by extensive bedrock outcrops that are nearly bare of drift. Although the transition from Zone 3 to 4 is abrupt in the southern part of the study area, long trains of drift project into major lowlands along the northern part of the boundary. The abrupt transition from drift to no drift in the south parallels 110° longitude and then curves northeastward south of the Eastern Arm of Great Slave Lake. It corresponds roughly to the eastern boundary of the Fort Smith Belt, a northward-trending zone of radioactive gneisses and intrusive rocks (Charbonneau, 1980; Fig. 45.3). The transition zone north of Great Slave Lake corresponds with the eastern edge of the Bear/Slave

Structural Province (Fig. 45.3). The long trains of relatively continuous drift cover that extend northwestward along lowlands developed in the crystalline bedrock of the Bear/Slave Province, are probably trains of debris eroded and transported from the poorly consolidated sedimentary rocks of Thelon Basin (Fig. 45.3).

Esker pattern

The eskers radiating outwards from the Keewatin Ice Divide consist of networks of tributaries which form dendritic patterns similar to a simplified Horton system. These esker systems can be traced as far as 600 km and continuous lengths of individual eskers can be traced for up to 75 km. In many places, discontinuous segments are linked by meltwater channels, usually scoured through drift to bedrock or filled by outwash.

Tributary eskers join the main esker preferentially from the left; that is, from the north on those eskers deposited by eastward-flowing meltwater east of the Keewatin Ice Divide and from the south on those eskers deposited by westward-flowing meltwater west of the divide (Fig. 45.1). This observation is best illustrated by the esker system trending northwestward from Dubawnt Lake where, in a distance of 300 km, 9 tributaries join from the south and none from the north. Similarly, between its origin near Yathkyed and Henik lakes and Hudson Bay most tributaries of the Maguse River esker system join the trunk stream on its north side. In most cases the orientation of the tributary esker changes abruptly as it approaches the main esker and the tributary joins the main esker at right angles.

Figure 45.3. *Bedrock geology features discussed in the text.*

western limit of Canadian Shield

Bear/Slave Structural Province

Dubawnt Group: sedimentary & volcanic rocks

In some locations clusters of short, parallel esker ridges occur between trunk eskers, and distributary ridges fan out from trunk eskers. One such cluster occurs along the coast south of Chesterfield Inlet. There are several areas with similar clusters in eastern Keewatin and somewhat similar features, although more disorganized and associated with crevasse fillings, occur near the western edge of Zone 3. The eastern clusters may mark the position of the ice front during slowing of glacier melt-back and thus may correlate with similar positions northwest of the Keewatin Ice Divide (see above, Zone 3) (Fig. 45.2).

Implication of patterns

Even at the reduced scale of these figures, the resolution of major geomorphic features is considerably enhanced over the only previous compilation, the Glacial Map of Canada (Prest et al., 1968). The following are only preliminary comments based on an initial analysis of data currently on hand.

Esker systems

In an earlier paper, Shilts (1984, p. 218) described in some detail the characteristics of a typical esker of the western Canadian Shield; esker systems were described as reflecting

"... what appears to have been a fully integrated Horton system of tributaries and trunk streams, regularly bifurcating upstream into lower order tributaries until the deposits disappear near the Keewatin Ice Divide. This pattern may be

interpreted in at least three ways: 1) The whole system may have functioned subglacially in sub-ice tunnels extending from the centre of a thin, stagnant glacier to its retreating margins, which lay at one time some 300-500 km away. Although this model has some merit, the very size of the ice sheet at the inception of esker deposition would seem to argue against it, the thicker ice near the divide being too plastic at the base to maintain open tunnels. In addition, it is hard to image how the Horton system could have developed so fully within a solid mass of ice; topographic irregularities at the base of the ice would have exercised greater influence on esker trends than is evident from the Horton pattern. 2) The esker may have been deposited by streams flowing in short tunnels near the margin of the glacier, continuity being maintained by up-ice migration of the heads of the tunnels by melting (St-Onge, 1984, p. 274). Although this model is more compatible with observed sedimentation features and probable dynamic conditions in the retreating ice, it does not explain well the Horton pattern of tributaries. It is hard to imagine how a subglacial tunnel would bifurcate regularly as it melted up ice without some external control. 3) The most attractive model of glacial meltwater drainage in this region is presently one in which an integrated system of drainage channels developed on the surface of the glacier, the meltwater plunging to the base of the glacier to flow in a subglacial tunnel the last few kilometres of its course before issuing from the

retreating glacier front (similar to the model suggested by St-Onge, 1984, p. 273). This system would have developed quite late in the glacial cycle, when most of the glacier was below the equilibrium line. The tunnels near the ice edge would have extended themselves headward by melting, as in the preceding model, but their headward migration would have followed roughly the traces of the surface drainage, thus accounting for the regular bifurcation upstream. ' This hybrid model best explains both the Horton drainage pattern and the manifest evidence of subglacial origin of esker sediments."

The dendritic pattern of the eskers provides the most compelling evidence of the stagnant nature of the ice sheet. It is difficult to conceive of a dendritic meltwater system developing and maintaining itself on the surface of an active ice sheet; it is similarly difficult to conceive of tributary eskers joining the main esker at right angles within vigourously moving ice. The reason for the preferred direction of approach of tributaries (from the left) is unknown. Perhaps it reflects the influence of Coriolis force on the movement of water on a large featureless plain – the surface of the ice sheet (a hypothesis that requires most of the ice cover over the area of this study to be below the equilibrium line).

Disruptions in the esker pattern are thought to indicate temporary halts in the retreat of the ice front, possibly the result of climate deterioration. The most prominent of these zones lies in an arc north of Back River (Fig. 45.2) and is accompanied by an extensive outwash complex. When areas of numerous disorganized short esker segments, crevasse fillings, and esker distributaries, which occur in the outer portion of Zone 3, are linked, they seem to extend this marginal position in a single arc across the western part of the study area. Clusters of esker distributaries and short parallel esker segments in eastern Keewatin may also record positions of temporary halts of the ice front. The most prominent of them may be contemporaneous with the western position, the rapid retreat of the ice which fronted the more than 150 m deep water of the Tyrrell Sea, accounting for the asymmetry of their locations with respect to the ice divide.

The height and width of an esker ridge is roughly proportional to the amount of debris supplied to its conduit while it is flowing near or at the base of a glacier. Assuming that basal conduit length and duration of meltwater flow are similar for most eskers in this region, the diminishing size of the eskers with distance from the ice divide may reflect a regularly decreasing amount of basal debris in the glacier. Particularly in Zone 4, the small size and low frequency of eskers and the paucity of drift suggest that the ice was relatively clean. This implies 1) that there was little erosion of the generally hard crystalline bedrock of Zone 4 and 2) that most debris carried by ice through the region was derived from the inner zones and was mostly deposited before reaching Zone 4.

If the assumption that the well developed dendritic esker systems developed in stagnant ice is correct, then the stagnant ice sheet would have covered zones 2 and 3. Ice over Zone 1 may have remained active while the outer zones were stagnant, although eventually it too would have become stagnant, thinning until only remnant ice blocks remained in lake basins. The absence of well developed, dendritic, esker systems over southern and western parts of Zone 4 may indicate that retreat of the ice sheet within this area was accomplished by back melting of active ice, but, alternatively, may only reflect the paucity of basal debris in stagnant ice. Much of the northern portion of Zone 4 contains well developed dendritic esker systems. The reason

that eskers were developed in the northern part of Zone 4 may be that dispersal trains of debris from the east penetrated along the lowlands and provided sediment to the meltwater streams in this area. To the south, a lack of debris in the ice may have prevented the development of esker ridges. A third alternative suggested to the authors is that the lack of eskers in Zone 4 may be related to retreat of the ice front in a proglacial lake. This does not seem to be likely because eskers are well developed below marine limit east of the ice divide, and they occur both below and above lacustrine limits west of the divide (Fig. 45.2).

Rogen moraine

Rogen moraine is confined to a well defined belt around the Keewatin Ice Divide. Thus, distribution of fields of rogen moraine appears to be directly related to the position of the ice divide, and, therefore, to the glacier dynamics in the region adjacent to the ice divide. In Sweden, Lundqvist (1969), observed that rogen moraine occurred only above marine limit and then only in valleys or other depressions. In contrast, on the western Canadian Shield rogen moraine occurs with equal frequency above and below marine limit, and where best developed, is found both in depressions and on topographically positive areas. Furthermore, both rogen moraine and drumlins or flutings occur in long, narrow trains radiating in the direction of ice flow outward from the region of the ice divide. The two types of landform trains pass laterally one into the other, and individual trains commonly can be traced back to specific outcrops of particular bedrock lithologies (Shilts, 1977) or specific areas of coarse unconsolidated sediments.

In general, rogen moraine is composed of coarse, bouldery or gravelly debris that is relatively undeformable, even when saturated. Conversely, at the few sites checked in eastern Keewatin, trains of drumlins or flutings appear to be underlain by more clay- and silt-rich drift that deforms readily when saturated. It is possible that the dynamic conditions in glacier ice near the ice divide were such that either drumlins or rogen moraine could be formed where a sufficient subglacial thickness or basal load of debris was available. Because of the lateral alternation of one feature with the other, and their compositional peculiarities, it is possible that wherever the basal debris load reached a sufficient amount, trains of either drumlins or ribbed moraine formed, with the type of feature formed dependent largely on the local physical characteristics of the debris.

The reason for the abrupt down-ice termination of the rogen patterns is not known. Drumlins are most abundant in Zone 2 but continue to occur through Zone 3; rogen moraine, on the other hand, is concentrated in Zone 2 and occurs only sporadically and in depressions in the other zones.

Drift cover

The lack of drift and apparent lack of erosion within Zone 4 may reflect the resistant nature of the underlying bedrock, the dynamics of the ice, or a combination of both. A prolific source of debris is available in the easily eroded sedimentary rocks of the Thelon Basin. This debris, however, was largely depleted before the ice passed from Zone 3. Possibly the crystalline rock that underlies the Bear/Slave Province and Fort Smith Belt was largely resistant to erosion and so did not yield much autochthonous debris. Although the absence of drift in Zone 4 probably reflects the resistant nature of the underlying bedrock, it is possible that ice dynamics may have been influenced by local topography, particularly south of Great Slave Lake where the relief is rugged and the trend of valleys is perpendicular to the direction of movement of ice. As the elevation of this area is 300 m higher than that at the centre of the ice sheet and

isostatic depression at the time would have accentuated this difference, the ice sheet may have been thin enough over this area to be frozen to its bed, preventing erosion. Another possible explanation of the lack of evidence of erosion is that ice within the valleys oriented transverse to the direction of ice movement, may have been largely stationary so that most regional ice flow occurred above the base of the ice sheet. If this was the case, little erosion could have occurred.

Conclusions

1. The pattern of esker distribution described herein strongly suggests that the last stages of Wisconsin Glaciation west of Hudson Bay consisted of the backwasting of a large, thin, stagnant ice sheet centred on the District of Keewatin. The diameter of this relatively dormant ice mass may have exceeded 1500 km.

2. The pattern of rogen moraine distribution is primarily associated with the configuration of the Keewatin Ice Divide. The trains of rogen moraine and associated drumlins that radiate from the ice divide region are also associated with areas of outcrop of specific bedrock lithologies or unconsolidated sediment, suggesting that the erodibility of the substrate and characteristics of the eroded material in transport have a strong influence on the nature and distribution of resulting landforms.

3. Large areas where drift cover is thin or absent may be resistant to glacial erosion and may also be located beyond the zone of deposition of easily entrained bedrock debris (principally in the Thelon Basin) which lies near or on the Keewatin Ice Divide.

4. Finally, although the regional patterns of drift deposition and landform development may be related to some extent to regional dynamic conditions at the base of the Keewatin ice sheet when it was actively flowing, there is little doubt that the lithology and topography of outcrops over which the glacier passed exerted an important influence on its deposits.

References

Charbonneau, B.W.
1980:   The Fort Smith radioactive belt, Northwest Territories; in Current Research, Part C, Geological Survey of Canada, Paper 80-1C, p. 45-47.

Cowan, W.R.
1968:   Ribbed moraine: Till-fabric analysis and origin; Canadian Journal of Earth Science, v. 5, p. 1145-1159.

Craig, B.G.
1964:   Surficial geology of east-central District of Mackenzie, Geological Survey of Canada, Bulletin 99, 41 p.
1965:   Glacial Lake McConnell, and the surficial geology of parts of Slave River and Redstone River map-areas, District of Mackenzie; Geological Survey of Canada, Bulletin 122, 33 p.

Fyles, J.G.
1955:   Pleistocene features; in Geological notes on central District of Keewatin, Northwest Territories by G.M. Wright; Geological Survey of Canada, Paper 55-17, p. 3-4.

Hughes, O.L.
1964:   Surficial geology, Nichicun-Kaniapiskau map-area, Quebec; Geological Survey of Canada, Bulletin 106, 20 p.

Lee, H.A.
1959:   Surficial geology of southern District of Keewatin and the Keewatin Ice Divide, Northwest Territories; Geological Survey of Canada, Bulletin 51, 42 p.

Lee, H.A., Craig, B.G., and Fyles, J.G.
1957:   Keewatin Ice Divide; Geological Society of America Bulletin, v. 68, no. 12, pt. 2, p. 1760-1761 (abstract).

Lundqvist, J.
1969:   Problems of the so-called Rogen moraine; Sveriges geologiska undersokning, Ser C NR 648 (Arsbok 64 NR 5), 32 p.

Prest, V.K., Grant, D.G., and Rampton, V.N.
1968:   Glacial Map of Canada; Geological Survey of Canada, Map 1253A, 1:5 000 000 scale.

St-Onge, D.A.
1984:   Surficial deposits of the Redrock Lake area, District of Mackenzie; in Current Research, Part A, Geological Survey of Canada, Paper 84-1A, p. 271-277.

Shilts, W.W.
1977:   Geochemistry of till in perennially frozen terrain of the Canadian Shield – application to prospecting; Boreas, 6, p. 203-212.
1982:   Quaternary evolution of the Hudson/James Bay Region; Naturaliste Canadien, v. 109, p. 309-332.
1984:   Esker sedimentation models, Deep Rose Lake map-area, District of Keewatin; in Current Research, Part B, Geological Survey of Canada, Paper 84-1B, p. 217-222.

Further evidence of late glacial climatic fluctuations from Newfoundland: pollen stratigraphy from a north coast site

Project 690064

Joyce Brown Macpherson[1] and T.W. Anderson
Terrain Sciences Division

Abstract

A 4.6 m core of lake sediment from near the coast of Notre Dame Bay, north-central Newfoundland, consisted of basal silty clay, clay gyttja within which was a 15 cm layer of silty clay, and gyttja. Pollen analysis of the lowest 0.7 m of the core revealed early (13.2 ka BP) pioneer to sparse herb – low shrub vegetation, followed by reversion to sparse herb tundra associated with deposition of the silty clay, and indicating cooling. Rapid development of richer shrub tundra after 10.5 ka BP indicates renewed warming. Timing and sequence of these events are similar to those reported from south Newfoundland and the Maritime Provinces; correlation with ocean surface temperature fluctuations is indicated.

Résumé

Les auteurs ont examiné une carotte de 4,6 m d'un sédiment lacustre prélevé prés de la côte de la baie Notre Dame, dans le centre nord de Terre-Neuve. Cet échantillon était constitué, à sa base, d'argile silteuse, puis de gyttja argileuse à l'intérieur de laquelle se trouvait une couche de 15 cm d'argile silteuse, et de gyttja. L'analyse pollinique des 70 cm formant la base de la carotte indique qu'il existait au début (13,2 ka B.P.) une végétation constituée d'herbes nouvelles à éparses et de petits arbustes; on observe ensuite un retour à la toundra à herbes éparses qui correspond au dépôt de la couche d'argile silteuse et qui indique un refroidissement du climat. Le développement rapide d'une toundra à arbustes plus abondants après 10,5 ka B.P. témoigne d'un adoucissement du climat. Les périodes et la séquence de ces événements s'apparentent à celles qui ont été rapportées pour le sud de Terre-Neuve et les provinces de l'Atlantique; une corrélation est également établie avec les variations de la température superficielle des océans.

[1] Department of Geography, Memorial University of Newfoundland, St. John's, Newfoundland A1B 3X9

Introduction

Evidence indicating a late glacial climatic oscillation has recently been presented by Anderson (1983) from a site on the Burin Peninsula, southern Newfoundland, and by Mott (1985) and Mott et al. (1984) from more than twenty sites in the Maritime Provinces. A reversion to colder conditions following deglaciation and/or postglacial warming is indicated in the interruption of organic sedimentation by mineral deposition and by revertences in late glacial pollen stratigraphy dated 11.3 to 10.7 ka BP in Newfoundland and approximately 11 to 10 ka BP in the Maritime Provinces.

This report presents similar evidence from a second lake site in Newfoundland, 280 km north of Anderson's South Burin lake site, near the coast of Notre Dame Bay, and compares the evidence from the two sites. The pollen profile from the second site, which lies 3 km south of the community of Leading Tickles South, is the first to be published from a terrestrial site in north-central Newfoundland. A pollen profile from a core of marine sediment from Notre Dame Channel, north of the Leading Tickles site, has recently been published (Scott et al., 1984), but it lacks the resolution of the profile to be described.

The site

The Leading Tickles site (49°28'17"N, 55°28'23"W; Fig. 46.1) is a small (ca. 1.5 ka) rock-basin lake (105 m a.s.l.) located near the northern tip of the peninsula between Seal Bay and Osmonton Arm, arms of Notre Dame Bay. The lake is the second of a series of lakes that drain northwestward to Seal Bay, 1 km distant. There is no evidence of postglacial marine inundation above about 75 m in the general area. The surface of the peninsula, above steep coastal slopes, consists of highly irregular rock-knob and basin topography with a patchy veneer of till. Weathering has removed glacial striae from naturally exposed rock surfaces, but recently exposed surfaces reveal two sets of striae and chattermarks, the stronger set indicating south-north ice movement probably related to an island ice cap; the weaker (and probably later) set trending southeast-northwest and indicating local flow from the peninsula towards Seal Bay. These observations are in conformity with those of Heyl (1936, 1938, quoted in Jenness 1960) and Lundqvist (1965).

The site lies in the Northshore ecoregion of Damman (1983), where the principal tree species are **Picea mariana** and **Abies balsamea**. In addition, **Betula** and other hardwood trees occur within the catchment basin, and **Populus tremuloides** was observed in the vicinity. The proportion of hardwood trees in the forest near the site is higher than for the ecoregion in general and is related to the local presence of base-rich bedrock and till (Dean and Strong, 1975; P.L. Dean, personal communication, 1985). The forest of the Northshore ecoregion is in marked contrast with the treeless blanket bogs which dominate the Hyper-oceanic Barrens ecoregion in which Anderson's South Burin site lies. The contrast is related to climatic differences, particularly during the growing season. The oceanic influence along the south coast is evident in cool summer temperatures (fewer than 1100 degree-days above 5°C), abundant annual precipitation (greater than 1500 mm), and frequent fog; the north coast is markedly more continental, with warmer, drier, and sunnier summers (more than 1200 degree-days above 5°C; less than 1200 mm annual precipitation) (Banfield, 1983).

Stratigraphy and radiocarbon dates

The Leading Tickles core was obtained by Macpherson in July 1982, from the deepest point in the basin at a water depth of 3.3 m, using a modified Livingstone-type corer with a diameter of 5 cm. The stratigraphy of the core is given in Table 46.1.

Figure 46.1: *Locations of Leading Tickles and South Burin lake sites, Newfoundland. The grey line is the inferred limit of Late Wisconsinan ice from Grant (1977).*

This represents a typical postglacial sequence, with the exception of the 15 cm layer of silty clay within the silty clay gyttja near the base. The sediments are noncalcareous throughout. Two radiocarbon dates were obtained from the silty clay gyttja: 13 200 ± 300 BP (GSC-3608) from the base (433-443 cm), and 10 500 ± 140 BP (GSC-3610) from immediately above the silty clay layer (405-414.5 cm). Sediment accumulated at a mean rate of 0.01 cm/year between the two dated segments (Fig. 46.2).

Early organic sedimentation at the South Burin site was also interrupted by the deposition of a layer of silty clay between about 11.3 and 10.7 ka BP (Anderson, 1983; Anderson in Blake, 1983). The core from this site fails to show the typical postglacial sequence of the Leading Tickles core, as detrital gyttja directly overlies material interpreted as till. As the southern part of Burin Peninsula extends beyond the Late Wisconsinan ice margin (Tucker and McCann, 1980), the till must be of pre-Late Wisconsinan age, and a depositional hiatus or erosional interval may have intervened between its deposition and that of the gyttja, the base of which is dated at 13 400 ± 140 BP (GSC-3559).

This date is statistically indistinguishable from the basal date from the Leading Tickles core, as are dates from immediately above the anomalous silty clay layer in each core, suggesting that organic sedimentation began initially, and later resumed, at about the same time at each site.

Pollen analysis and zonation

Sediment samples (1 mL) were extracted from the Leading Tickles core at 5 cm intervals between 390 and 420 cm (additional samples were taken at the contact

Table 46.1

Sediment type	Depth below sediment-water interface (cm)
dark brown gyttja, becoming lighter below 375 cm	0-400
silty clay gyttja	400-414.5
grey silty clay	414.5-430
silty clay gyttja with fibrous layers	430-443
laminated grey thixotropic silty clay, with darker bands down to 450 cm	443-460
stiff grey silty clay on a gritty base; could be penetrated with auger but too cohesive to core	460-530

Depth-time scales

Figure 46.2. Depth-time scales for basal sediments, Leading Tickles and South Burin Peninsula sites.

between silty clay and clay gyttja) and at 2.5 cm intervals between 420 and 450 cm. Measured volumes of a suspension of exotic **Eucalyptus** pollen were added to the samples before treatment with KOH and HF, followed by acetolysis. Most samples also required disaggregation and filtration following the method of Cwynar et al. (1979). The sum of land pollen (tree, shrub, and herb pollen, including Cyperaceae) exceeded 300 for samples between 390 and 405 cm; was 100 or greater for samples between 410 and 437.5 cm; and was less than 100 for samples at greater depths. To attain even such low sums required the counting of multiple slides. **Eucalyptus** counts were used to calculate fossil pollen concentrations, from which pollen influx values were derived, using the mean rate of sediment accumulation.

Abbreviated pollen percentage and influx diagrams are given in Figure 46.3. Where the pollen sum is less than 50 the presence of a taxon is indicated, rather than a percentage value given. Tree and shrub taxa contribute significantly to the pollen sum at all but the lowest levels. However, when total land pollen influx is plotted against interpolated radiocarbon years BP for both the Leading Tickles and South Burin cores (Fig. 46.4), it will be noted that pollen influx in the Leading Tickles core was extremely low (21 grains/cm^2/year or less) until shortly before 10.5 ka BP. These values are only slightly greater than those of 6-8 grains/cm^2/year quoted by Fredskild (1973) for high arctic north Greenland, where vegetation cover is less than 3%. For this reason, all tree, low arctic and boreal shrub pollen (**Betula, Alnus,** and **Myrica**) present before 10.5 ka BP is considered exotic. The local pollen influx (herbs and some shrubs) is then seen to be closer to north Greenland values (Fig. 46.5). After 10.5 ka BP, influx values at the Leading Tickles site increased and approached those which had prevailed for most of the preceding period at the South Burin site: 400 to 500 grains/cm^2/year. The South Burin influx values also include exotic tree pollen (Anderson, 1983); if these are excluded (Fig. 46.5) total influx falls within the range of 180 to 320 grains/cm^2/year reported by Fredskild for the low arctic dwarf-shrub heath of coastal south Greenland. It should be noted that in Figures 46.4 and 46.5 the influx curves have not been extrapolated above the highest dated core segment.

With these considerations in mind, it is possible to identify three pollen assemblage zones in the Leading Tickles profile; the zone boundaries coincide with stratigraphic changes.

Zone 1 occurs below 430 cm, in the basal clay and lower clay gyttja. The most frequent pollen taxon at the base is Gramineae (up to 62%), followed by **Artemisia**, other Compositae, and Chenopodiineae. Percentage values for Cyperaceae, **Oxyria digyna/Rumex,** Caryophyllaceae, **Salix** and **Sphagnum** increase in the clay gyttja; **Pediastrum** is also abundant here. Pollen concentrations are below 1000 grains/mL in the basal clay, rising to a mean of more than 2000 grains/mL in the clay gyttja.

Zone 2 (414.5-430 cm) coincides with the layer of silty clay within the clay gyttja. The most marked change in the local pollen component is a sharp decline in **Salix**, which is absent from some samples. Cyperaceae and **Sphagnum** decrease more gradually. Certain, mainly herbaceous, taxa appear only in this zone, or are represented more continuously than in zones 1 or 3: Rosaceae (probably **Dryas**), Ranunculaceae, Chenopodiineae, Saxifragaceae, **Filipendula,** and Gentianaceae. Of the far-travelled grains, **Betula** and **Myrica** decrease whereas **Alnus** increases. **Pediastrum** is sharply reduced. Pollen concentrations decrease to about 2000 grains/mL at the top of the zone.

Zone 3 (390-414.5 cm) occurs in the upper clay gyttja and gyttja. It is marked by pronounced increases in influx values for almost all taxa shown, with the exception of **Sphagnum** and **Oxyria**-type pollen which appears for the last

Figure 46.3. *Abbreviated pollen percentage and influx diagrams for the base of the Leading Tickles core.*

time at the base of the zone. Other herbs, apart from Cyperaceae, occur discontinuously, and their percentage representation is more reduced because of the great increase in shrub pollen. However, the proportion of **Alnus** declines. **Lycopodium** and Filicales increase and **Pediastrum** resumes its former abundance in the clay gyttja, declining in the gyttja. **Nuphar** is present in the topmost sample. Pollen concentrations rise from 5000 grains/mL at the base of the zone to more than 100 000 grains/mL at the top of the analysed part of the core.

Vegetation and climate reconstruction

Zone 1 represents the colonization of the area adjacent to the site by an increasingly diverse assemblage of plants. Though much of the surface was devoid of vegetation, sheltered areas near streams and the pond itself, which were protected by snow in winter, may have supported a cover of **Sphagnum** and probably other mosses, and **Cyperaceae**. This reduced the flux of mineral particles into the pond and increased the flux of organic material. Apparently the water was sufficiently free of turbidity for part of the summer for **Pediastrum** to flourish. Dwarf shrubs, predominantly willow, with some heaths and probably also **Dryas**, were present in protected areas, together with grasses and other herbs. The appearance and composition of the vegetation are believed to have resembled those of Edlund's (1983) Zone 2 of the high arctic or those of north Greenland described by Fredskild (1973).

Pollen assemblage Zone 2 is less easy to interpret, partly because this zone coincides with the silty clay layer within the silty clay gyttja. If, as is possible, the clay layer was deposited rapidly, then rates of influx of contemporary pollen within this zone would be higher than those indicated in Figures 46.3, 46.4, and 46.5, and some apparent decreases in influx might disappear or be reversed. Adjustment of influx rates cannot, however, affect the apparent representation of taxa which are absent, such as **Salix**. It is useful, nevertheless, to consider the consequences of rapid deposition of the clay, if, for example, this had been caused by degradation of permafrost and resulting in downslope flow of surface mud. There would probably be a change in total pollen concentration at the base of Zone 2, and there is not. The proportion of deteriorated grains, previously deposited on the surface, and redeposited with the clay, would increase (Lowe, 1984), and it does not; the ranges of percentages of indeterminable (i.e., deteriorated) grains (calculated outside the sum, and not plotted in Figure 46.3) are 11.8 to 17.5% in Zone 2 as compared with 7.1 to 18.7% in Zone 1. Concentrations of pine pollen, the grain of most distant origin and that most likely to give an unambiguous signal of surface disturbance in the basin, would probably be variable, whereas in fact they show marked consistency. Thus the evidence does not support permafrost degradation as a likely source for the silty clay layer.

386

Other Compositae · Urtica type · Oxyria digyna-Rumex · Umbelliferae · Chenopodineae · Thalictrum · Epilobium · Ranunculaceae · Caryophyllaceae · Rosaceae · Saxifragaceae · Cyperaceae · Filicales · Lycopodiaceae · Nuphar · Sphagnum · Pediastrum · Pollen zones

3

2

1

Other herbs | Cyperaceae | Lycopodiaceae (170, 66, 81, 96) | Filicales (57, 87, 112, 77) | Total shrubs (980, 1144, 547, 301) | Total herbs (85, 114) | Pediastrum (83, 581, 1132, 342, 210, 1333)

3

2

1

During the deposition of this layer **Pediastrum** was suppressed, indicating that the lake water remained turbid throughout the melt season, and thus suggesting a longer period of runoff. In the context of an environment similar to the modern high arctic, more prolonged runoff implies snow cover that was either more extensive or of longer duration. More extensive snow cover would have provided greater winter protection for dwarf shrubs, which could be expected to increase. However, willow declines, as do Cyperaceae and **Sphagnum**, also found in areas protected by winter snow. This evidence suggests that snowbeds, which formerly melted early enough in summer to allow the plants which they protected to produce pollen, became more permanent. Edlund (1983) noted marked vegetational contrasts at the margins of permanent snowbeds in the Queen Elizabeth Islands, and related diversity of plant communities to effective growing season. The greater diversity of herbs in Zone 2 than in Zone 1 does not negate this argument, for it can be accounted for by the greater availability of permanently moist sites for certain Ranunculaceae, **Thalictrum**, Umbelliferae, and saxifrages. Edlund's work suggests that a decrease in mean July temperatures of only about 1°C could account for the observed changes in pollen assemblages.

The presence of permanent snowbeds during this period is attested to by evidence in a sample from a thin layer of sediment at 415 cm at the transition from Zone 2 to Zone 3. The scale of the pollen diagram did not permit the pollen assemblage of this sample to be plotted, but it contained an anomalously high concentration of pollen (8000 grains/mL) with more than 60% far-travelled grains, including

11.5% "Coryloid" (probably deteriorated **Myrica**), a much greater proportion than in adjacent samples. The dark grey colour of the matrix of the sample lightened on exposure, indicating deposition of sulphides under reducing conditions. This thin layer of sediment could well have resulted from the final melting of snowbeds and the discharge of accumulated pollen and other organic debris into the lake.

This event heralded a marked change in the vegetation. Within Zone 3 willows, heaths, and sedges increased immediately and dwarf birch, **Myrica Gale**, ferns, and clubmosses arrived within a few centuries, eventually displacing willow. Typical tundra herbs all but disappeared. The lake became decreasingly turbid and **Pediastrum** flourished until soils within the catchment basin were stabilized by vegetation; **Nuphar** arrived after organic mud had accumulated on the lake bottom. The vegetation of this zone is interpreted as being similar in appearance to the low arctic dwarf-shrub heath of coastal south Greenland (Fredskild, 1973), with a transition to tall-shrub tundra in the final centuries.

Discussion and conclusions

The three-fold sequence of vegetational changes identified at the Leading Tickles site is of similar trend to the sequence from the South Burin site (Table 46.2). During the first stage, beginning by about 13.5 ka BP, pioneer plants became established, and vegetation developed to shrub tundra at the south coast site and to a very sparse herb dwarf-shrub tundra at the north coast site. Reversion to sparse herb

Figure 46.4. *Total pollen influx in basal sediments, Leading Tickles and South Burin Peninsula sites.*

tundra at the north coast site corresponds to a similar reversion to herb-shrub tundra at the south coast site dated at 11.3 ka BP; the reversion in both cases is ascribed to cooler summers with longer-lasting snowbeds. Finally, at about 10.5 ka BP, the major postglacial warming led to the development of tall-shrub tundra at both sites.

The late glacial vegetation is inferred to have been more abundant and somewhat more diverse at the south coast site than at the north coast site, the reverse of the present situation. Ruddiman and McIntyre's synthesis (1981) of oceanic conditions during this period refers to warming south of the Grand Banks by 13 ka BP; air from southerly sources would have been relatively warm and moist at the south coast but had to pass over the island's residual ice cap, which disappeared only shortly before 11.4 ka BP (Macpherson, in Blake, 1983), to reach the north coast site.

Winds from the southwest carried pollen from distant sources to the two sites. The South Burin site presumably received tree pollen from mainland Quebec and Atlantic Canada, whereas the Leading Tickles site received, in addition, shrub pollen from the south coast. For example, the late glacial profiles for **Betula** and **Myrica** at the Leading Tickles site mirror those in the South Burin diagram, but low influx estimates indicate that these plants were absent from the vicinity of the site. Similarly, the **Picea** curve in the South Burin profile shows a decline beginning about 11 ka BP, and the **Alnus** curves at both sites show increases about the same time, corresponding with the late glacial vegetation recession identified by Mott (1985) in mainland Atlantic Canada. That these patterns may be recognized suggests that the summer cooling which led to the reversion of vegetation in Newfoundland was not caused by a change in mean wind direction, but by a cooling of the surface waters offshore Atlantic Ocean. General circulation modelling shows that the climatic oscillation may be related to fluctuations in salinity and in the production rate of deep water correlated with fluctuations in extent of ice cover in the North Atlantic (Broecker et al., in press). The association of the **Alnus** rise with other evidence of climatic cooling in the Leading Tickles core suggests that cooling may have been almost synchronous throughout the region.

Table 46.2. Pollen zones, chronology, inferred vegetation and environmental conditions at the Leading Tickles and South Burin sites

Leading Tickles: north coast			South Burin Peninsula: south coast		
Pollen zone	Inferred vegetation	Environmental conditions	Pollen zone	Inferred vegetation	Environmental conditions
3: **Betula–Myrica**	shrub tundra	warming trend	3: **Betula-**Lycopodiaceae	shrub tundra	warming trend
——— 10.5 ka BP ———			——— 10.7 ka BP ———		
2: Herbs	sparse herb tundra	cooling; long-lasting snowbeds; more open ground	2: **Oxyria digyna-Alnus***	herb tundra	cooling; long lasting snow-beds; more open ground
			——— 11.3 ka BP ———		
1: Gramineae-Herbs-**Salix**	development of sparse herb-low shrub tundra	deglaciation; initial warming; much open ground	1: **Salix**-Cyperaceae-Ericaceae	development of low shrub-herb tundra	initial warming
——— 13.2 ka BP ———			——— 13.4 ka BP ———		
*of distant origin					

388

Leading Tickles: north coast

South Burin Peninsula: south coast

Figure 46.5. *Pollen influx by groups of taxa in basal sediments, Leading Tickles and South Burin Peninsula sites. Note the difference in the scales for influx.*

For those events for which we have radiocarbon dates – the initial warming about 13.5 ka BP, the cooling at 11.3 ka BP, and the final warming at 10.5 ka BP – the correlation with similar events in the oceanic record (Ruddiman and McIntyre, 1981) is inescapable.

References

Anderson, T.W.
1983: Preliminary evidence for Late Wisconsinan climatic fluctuations from pollen stratigraphy in Burin Peninsula, Newfoundland; in Current Research, Part B, Geological Survey of Canada, Paper 83-1B, p. 185-188.

Banfield, C.E.
1983: Climate; in Biogeography and Ecology of the Island of Newfoundland, ed. G.R. South; Junk, The Hague, p. 37-105.

Blake, W. Jr.
1983: Geological Survey of Canada Radiocarbon Dates XXIII, Geological Survey of Canada, Paper 83-7, 34 p.

Broecker, W.S., Peteet, D., and Rind, D.
     –   Does the ocean-atmosphere system have more than one stable mode of operation?; Nature. (in press)

Cwynar, L.C., Burden, E., and McAndrews, J.H.
     1979: An inexpensive sieving method for concentrating pollen and spores from fine-grained sediments; Canadian Journal of Earth Sciences, v. 16, p. 1115-1120.

Damman, A.H.W.
     1983: An ecological subdivision of the island of Newfoundland; in Biogeography and Ecology of the Island of Newfoundland, ed. G.R. South; Junk, The Hague, p. 163-206.

Dean, P.L. and Strong, D.F.
     1975: Point Leamington map-area: map and explanatory text; Geological Survey of Canada, Open File 375.

Edlund, S.A.
     1983: Bioclimatic zonation in a High Arctic region: central Queen Elizabeth Islands; in Current Research, Part A, Geological Survey of Canada, Paper 83-1A, p. 381-390.

Fredskild, B.
     1973: Studies in the vegetational history of Greenland; Meddelelser om Grønland, bd. 198, nr. 4, p. 1-245.

Grant, D.R.
     1977: Glacial style and ice limits, the Quaternary stratigraphic record, and changes of land and ocean level in the Atlantic Provinces, Canada; Géographie physique et Quaternaire, v. XXXI, p. 247-260.

Jenness, S.E.
     1960: Late Pleistocene glaciation of eastern Newfoundland; Bulletin of the Geological Society of America, v. 71, p. 161-180.

Lowe, J.J.
     1984: A critical evaluation of pollen-stratigraphic investigations of pre-Late Devensian sites in Scotland; Quaternary Science Reviews, v. 3, p. 405-432.

Lundqvist, J.
     1965: Glacial geology in northeastern Newfoundland; Geologiska Foreningens i Stockholm Förhandlingar, v. 87, p. 285-306.

Mott, R.J.
     1985: Late-glacial climatic change in the Maritime Provinces; in Climatic Change in Canada 5: Critical Periods in the Quaternary Climatic History of Northern North America, ed. C.R. Harington; Syllogeus No. 55, p. 281-300.

Mott, R.J., Grant, D.R., Stea, R., and Occhietti, S.
     1984: The Allerød/Younger Dryas oscillation in North America – fact or fiction; Sixth International Palynological Conference, Calgary, Abstracts, p. 112.

Ruddiman, W.F. and McIntyre, A.
     1981: The North Atlantic Ocean during the last deglaciation; Palaeogeography, Palaeoclimatology, Palaeoecology, v. 35, p. 145-214.

Scott, D.B., Mudie, P.J., Vilks, G., and Younger, D.C.
     1984: Latest Pleistocene-Holocene paleoceanographic trends on the continental margin of eastern Canada: foraminiferal, dinoflagellate and pollen evidence; Marine Micropaleontology, v. 9, p. 181-218.

Tucker, C.M. and McCann, B.
     1980: Quaternary events on the Burin Peninsula, Newfoundland and the islands of St. Pierre and Miquelon, France; Canadian Journal of Earth Sciences, v. 17, p. 1462-1479.

Diatom dispersal phenomena: diatoms in rime frost samples from Cape Herschel, central Ellesmere Island, Northwest Territories

Project 720078

Sigrid Lichti-Federovich
Terrain Sciences Division

Abstract

The presence of marine and freshwater diatoms in rime frost samples collected in two successive years, clearly shows the significance of atmospheric diatom dispersal. Floristic similarity between all samples, based mainly on the abundance of the principal element, **Nitzschia cylindrus** (Grunow) Hasle, overrides any spatial or temporal differences as well as dissimilarities due to variation in substrate. A positive causal relationship exists with two meteorological variables, fog and southwesterly wind.

Résumé

La présence de diatomées d'eau salée et d'eau douce dans des échantillons de givre prélevés au cours de deux années successives fait clairement ressortir l'importance de la dispersion des diatomées dans l'atmosphère. Les similitudes observées au point de vue de la flore entre tous les échantillons, qui tiennent surtout à l'abondance de l'élément principal, **Nistzschia cylindrus** (Grunow) Hasle, l'emportent sur toute différence spatiale ou temporelle, de même que sur toute différence attribuable à la variation du substrat. Une relation de cause à effet est établie avec deux variables météorologiques, soit le brouillard et le vent du sud-ouest.

Introduction

The aim of this paper is to aid our understanding of the complexities involved in the study of diatom dispersal and to attain a clearer insight into the role of wind transport as one of its mechanisms.

Atmospheric transport of diatoms in polar regions has been convincingly demonstrated by the discovery of marine-derived diatoms and diatom fragments in the surface snow from arctic ice caps (Lichti-Federovich, 1984; and unpublished data). Since, however, the resultant data were based on a time span of several months, this investigation was subject to interpretative limitations.

Therefore it was hoped that a more tightly controlled investigation with regard to meteorological variables would resolve some of the ambiguities and uncertainties posed by the process of diatom dispersal. The following study is based on rime frost samples and thus is concerned with certain aspects of short term diatom dispersal phenomena.

This report is Contribution No. 24 from the Cape Herschel project.

Material and methods

The diatoms, which form the basis of this report, were recovered from rime frost samples collected by W. Blake, Jr. in east-central Ellesmere Island during June 1983 and 1984. The collection sites include two granite boulders located south and southeast of the base camp on the Cape Herschel peninsula; other samples were collected from radio antenna and various support structures at the Cape Herschel base (Fig. 47.1 and 47.2).

Table 47.1 lists the dates on which the collections were made and the prevailing meteorological conditions. It should be noted that all 1983 meteorological data were compiled from instantaneous readings taken at specific times (0630 and 1830 hours) within the approximated rime frost formation time interval. The 1984 wind data were extrapolated from a continuous chart (anemograph). All other 1984 meteorological information is given as instantaneous readings at 12 hour intervals within the rime frost formation time span.

In each case field procedures included removal of the ice into a plastic bag (1983 samples) or a low stainless steel pan covered with aluminum foil (1984 samples). Subsequent melting at room temperature and removal of meltwater into precleaned, tightly capped, plastic bottles was followed by storage under dark conditions at or near outdoor temperatures.

After initial treatment with hydrogen peroxide and potassium dichromate, followed by repeated washings with distilled water, the meltwater residue was concentrated on a 25 mm diameter, 0.8 µm nuclepore filter. The filter then was either mounted with Hyrax for light microscopy at 250x and 400x magnification using a Leitz Ortholux or prepared for SEM examination with a Cambridge Instruments Stereoscan 180 at 20 kv.

Limitations

As with most scientific enquiries, certain limitations must be acknowledged. In general, the greatest restrictive aspect in aerobiological investigations arises in the evaluation of diatom analytical data on a highly detailed comparative basis, since the results of such assays are based on a system in flux, nonstationary, ever changing.

More specifically, for this study, since the time of initial onset of rime frost formation was unknown, meteorological conditions such as wind velocity and direction had to be abstracted for a 24 hour period.

Another methodological limitation affecting the quantitative evaluation of the results is that the diatom valves and frustules were fragmented. Nevertheless, quantitative determination, on a comparative basis, with each fragment counted as one unit regardless of size, retains some measure of validity.

In addition to this numerical ambiguity, underestimation of the minute **Nitzschia cylindrus**, resulting in somewhat lower sum totals as well as lower percentage values, is imposed by optical difficulties, especially with samples examined under 250x magnification. One must also take into account the lack of transparency and the textural irregularity of a 0.8 µm nuclepore filter when examined using transmitted light. Such implied underrepresentation of **N. cylindrus** is also supported by visual examination of 0.8 µm nuclepore filters utilizing scanning electron microscopic techniques. Without any doubt, investigation by scanning electron microscopy convincingly established the marked predominance of this diatom. Essentially, however, it is a matter of balance or reasonable trade off, which an investigator dealing with time consuming scientific techniques attempts to reach between time expended (person hours) and the scientific value of the results obtained.

Notwithstanding these restrictions, this study clearly indicates that on a broad delineatory basis, uniform comparable results can be obtained.

Results and discussion

Approaching atmospheric dispersal studies on an evaluatory basis, the immediate perception is one involving a system of immense lability, a system influenced by incessant change. Considering the many variables operative — meteorological factors such as wind direction and velocity, precipitation duration and intensity, as well as dispersal distance, sources of origin, and diatom content of the atmosphere modified by seasonal changes — it is deemed rather unlikely to obtain valid spatio-temporal correlates.

The present investigation, however, was able to eliminate a few uncertainties and to introduce some measure of scientific control and environmental uniformity.

Experimental consistency relates to the following (Table 47.1):

1. All rime frost samples (excluding those from rock) were collected from a diatom-free surface above ground. Such above-surface sampling ensures that all diatoms originate from the aerial plankton. In particular the smooth metal surface of the antenna, devoid of adhering diatoms, represents a convincing means of demonstrating the impact of atmospheric transport as a diatom dispersal mechanism.

2. Although the rime frost samples were derived from two successive years, they were collected within the same week, thus eliminating floristic differences due to seasonal variation.

3. In addition, the formation of rime frost represents a short term phenomenon, in this example representing meteorological conditions operative within a 36 hour maximum time span.

Diatom analytical results of these rime frost samples were therefore awaited with a great deal of anticipation to see whether these methodological and meteorological uniformities translated into semblances expressed as diatom floristic correlates. Since, however, as mentioned previously, scientific assays with regard to aerobiological investigations are subjugated to such immense flux, detailed systematic evaluation of the various samples was omitted in favour of emphasizing the most immediate observable floristic similarity or difference.

Figure 47.1. Aerial view of Cape Herschel, Ellesmere Island showing rime frost collection sites.

Figure 47.2. Radio tower, Cape Herschel Base, with string attached to the antenna (arrow) and support steel cables from which rime frost was collected. (Photograph by W. Blake, Jr.)

Diatom floristic similarities and/or differences between 1) 1983 rime frost samples collected from rock and antenna; 2) 1984 rime frost samples; and 3) 1983 and 1984 rime frost samples rests upon floristic composition, diatom frequency, and key species.

Although diatom analysis of these rime frost samples on a comparative basis indicates some heterogeneity, the most immediate, most important factor, which holds for all rime frost samples, is that diatom floristic similarity overrides any quantitative/qualititative variance due to spatio-temporal differences.

Floristic similarity, with some reservation, also holds for the diatom associations characterizing the two rime frost samples collected from granite boulders. In both cases there is a high relative abundance of **N. cylindrus**; however diatom diversity and frequency increase in the samples from rock. These discrepencies between rime frost samples from antenna and those from rock can be explained in terms of autochthonous epilithic diatoms within encrustations or attached to the outer surfaces of rock.

Floristic composition

The diatom complex of each rime frost sample represents an admixture of fresh water and marine elements, thus reflecting different origins or biotopes and varying dispersal distances. The freshwater diatoms, predominantly aerophilous taxa, may have derived from short distance semi-aquatic, nival, or terrestrial sources such as ephemeral meltwater pools or as algal detrital matter from marginal areas of lakes and ponds. Several such ponds, both temporary and permanent, are close to the sampling sites.

This general view is also supported by Blake's description of the low-lying area or pass west and southwest from the base as a veritable "quagmire" in the spring (W. Blake, Jr., personal communication, 1985). This pass, which connects Herschel and Rosse bays, not only contains a

large shallow lake, but may be considered as a major source area for these diatoms with its numerous aero-aquatic habitats such as meltwater pools and puddles, standing water in depressions on rock outcrops, and shallow streams.

The marine component, on the other hand, taking into consideration the prevailing wind direction, must have been transported at least 0.8 km.

Diatom frequency

All rime frost samples are characterized by a relative abundance of diatoms. For example, the sum total of diatoms, including diatom fragments, of sample 11-1983 (DT-84-13) comprises 614/50 mL (x25 objective) and of sample 20-1984 (DT-84-17) is 868/50 mL (x40 objective), thus in each case exceeding 1000 diatom units/100 mL meltwater. The lower numerical value for sample 11-1983 may in part be due to microscopic examination under lower magnification (see limitations). These numerical values, as reflections of the diatom load of the atmosphere, gain added significance when considering the short time interval (not exceeding 36 hours) representing the period from initial rime frost formation to sample collection.

Key species

Nitzschia cylindrus (Grunow) Hasle (Plate 47.1, fig. 1-12) is the most abundant species in the rime frost diatom assemblages. This predominance necessitates its ecological and distributional characterization.

Antarctic distribution. As a member of the antarctic sea ice community, **N. cylindrus** is reported by Krebs (1977) from fast ice, intermittent and grounded pack ice, shore ice, drifting sea ice, and from brown ice slush at Arthur Harbor. Clarke and Ackley (1983) listed this taxon's abundant occurrence in Weddell Sea pack ice at 44-58 cm depth. Furthermore, **N. cylindrus** represents one of the major

Table 47.1. Characterization of rime frost samples from Cape Herschel, Ellesr

Location	Elevation (m/a.s.l.)	Field/Lab Numbers	Sample material	Volume of meltwater (mL)	Temperature (°C)	Wind direction	Wind speed (m/s)	Other meteorological data	Time interval from frost formation to time of collection	Date/Time of collection
1983 Rime frost collection										
Plateau behind base 78°36.3'N, 74°43.5'W	200	#4-1983 DT-84-11	Rime frost from south-facing rock	100	min. -2.2 max. 0.1	11th 1900 h SW 12th 0700 h SW 12th 1900 h SW 13th 0700 h SW 13th 1900 h SW	10.9 2.2 13.5 1.0 5.2	clear some fog; trace of precipitation fog; blowing snow (48 mm) sun dimly visible; precipitation (10 mm) trace of precipitation	12 h minimum	13.6.83
Base 78°37.0'N, 74°41.4'W	70	#11-1983 DT-84-13	Rime Ice from support string of radio antenna	100	min. -1.6 max. 0.5	25th 1900 h SW 26th 0700 h SW 26th 1900 h SW 27th 0700 h SW	13.5 12.0 6.2 0.52	trace of precipitation fog; new snow (0.85 mm) fog; new snow (0.51 mm) fog; new snow (1.0 mm)	at least 12 h, more likely 24-36 h	27.6.83 0900-1000 h
High plateau 78°35.5'N, 74°40.0'W	260	#12-1983 DT-84-12	Rime frost (melting) from rock	100	min. -1.6 max. 2.6	27th 1900 h SW 28th 0700 h S 28th 1900 h N 29th 0700 h N 29th 1900 h N	5.2 7.8 0.52 3.6 2.6	some fog trace of precipitation trace of precipitation precipitation (1.5 mm) rain since 1100 hrs; snow above 200 m (2.0 mm)	12 h minimum	29.6.83
1984 Rime frost collection										
Base 78°37.0'N, 74°41.4'W	70	#20-1984 DT-84-17	Rime frost from steel cable	265	min. -2.5	27th 0700 h SW	10.4	light snow (0.5 mm); changed to S wind during day	approximately 36 h	28.6.84 1200 h
Base 78°37.0'N, 74°41.4'W	70	#21-1984 DT-84-18	Rime frost from metal struts of radio tower	280	max. 2.0	27th 1900 h SW 28th 0700 h SW	5.7 9.9	fog; precipitation (0.8 mm) fog; trace of precipitation		
Base 78°37.0'N, 74°41.4'W	70	#22-1984 DT-84-19	Rime frost from support string of radio antenna	530		28th 1200 h SW	10.4			

PLATE 47.1

Nitzschia cylindrus (Grunow) Hasle.

figures 1, 2, 3, 7, 8, 10. Scanning electron micrographs of external view of frustule.

figures 4, 6, 12. Scanning electron micrographs of oblique view of partially separated frustule.

figures 5, 8, 9, 11. Scanning electron micrographs of inside view of valve.

constitutents of the ice-algal population of Weddell Sea ice floes, frazil ice, and congelation ice (Garrison et al., 1983; Clarke et al., 1984). These recent findings substantiate Fukushima and Meguro's (1966) observation that **N. cylindrus** represents the dominant species in surface type as well as bottom type plankton ice around the Antarctic peninsula.

South polar distribution of **N. cylindrus** as numerically important cryoplanktonic species includes the following oceanic regions: Antarctic and Southern oceans (Guillard and Kilham, 1977), Southwestern Atlantic and Indian oceans (El-Sayed and Hampton, 1981; El-Sayed et al., 1983; Fryxell et al., 1983). Krebs (1977, 1983) based the importance of **N. cylindrus** as a cryoplanktonic species on its abundant occurrence in intertidal and shallow subtidal areas of Arthur Harbor, where it also characterizes the clayey ooze of offshore sediments.

Arctic distribution. Relevant north polar distribution of **N. cylindrus** listed by Hasle (1965), using various source references, include the following areas: Arctic Ocean, Barents Sea, Franz Josef Land, North Norwegian fiords, Denmark Strait, Greenland, Canadian Arctic, Baffin Bay, Davis Strait, Hudson Bay, Hudson Strait, Cape Wankerema, and the northern waters of the U.S.S.R. as well as the North Pacific and Sub-Antarctic basins as cited by Guillard and Kilham (1977).

Considering the distributional aspects of **N. cylindrus** as a sea ice diatom and phytoplankton element in Arctic Canada, foremost mention need be made of the useful compilation of its occurrences by Hsiao (1983) who enumerated the following localities: Arctic Ocean and Robeson Channel at the northern tip of Ellesmere Island; coastal and oceanic areas surrounding the central arctic islands such as Lancaster Sound, Barrow Strait, Wellington Channel, Resolute Passage, and Austin Channel; the waters surrounding Baffin Island, specifically Eclipse Sound, Baffin Bay, Cape Eglinton, Davis Strait, Brevoort Harbour and vicinity, Frobisher Bay, Igloolik, and Creswell Bay, as well as the Beaufort Sea and Eskimo Lakes in the southwestern part of the Canadian Arctic.

Similar to antarctic habitat associations, high concentrations of **N. cylindrus** are reported also from various arctic sea ice and plankton communities. Usachev (1946), for example, described the quantitative dominance of this taxon in ice floes from coastal sections of the U.S.S.R. and the Kara Sea. Its ice-linked occurrence is further documented by Grainger and Hsiao (1982), who recorded optimal occurrence of **N. cylindrus** in the bottom 5 cm of sea ice during May at Frobisher Bay. According to Cross (1982), **N. cylindrus** ranked as the third most abundant species in diver-collected ice cores from Pond Inlet during the period of May 12th to July 2nd, 1979. This rating was based on 41 samples from 12 ice edge and fast ice stations.

Its abundant occurrence is also reported as a member of the ice plankton community; it grows extensively in brines among ice crystals during winter and early spring in the seasonally ice-covered areas of the Bering and Chukchi seas (Saito and Taniguchi, 1978).

Other numerically significant planktonic occurrences of **N. cylindrus** have been observed by Cleve (1896) in Davis Strait and Baffin Bay, who described it as characteristic species of polar sea plankton most abundant during May, and by Polunin (1934), who noted its abundant representation in the spring plankton of Hudson Bay.

Detailed observations by Bursa (1961) of seasonal phytoplankton successions at Igloolik, north of Melville Peninsula, Northwest Territories, denote a more than three-fold increase of the initial ice-linked populations of **Achnanthes taeniata** and **Nitzschia cylindrus** between April 26th and May 5th, with the first increase for **N. cylindrus** recorded as 17 200 cells/L. This under-ice spring growth occurred despite minimal light conditions. By June 19th surface diatom populations had reached a maximum and by July 2nd optimal growth conditions had descended to the 10 m level.

One can hypothesize that the **N. cylindrus** dominance (31% in sample 20-1984) relates to seasonal bloom and is further aided by its dispersive and floating abilities optimized by the small size and lightness of its frustule. Furthermore, its colonial, ribbon-like growth habit suggests the possibility of multitudinous dissemination. In either case, incorporation of **N. cylindrus** into the atmosphere, by either splash droplets from sea spray, bursting sea foam and white cap bubbles, or uptake as sloughed off minute ice algal particulates, must have occurred through turbulent wave and wind action.

This marked influx of **N. cylindrus** raises a number of perplexing questions. For example, it is rather intriguing to speculate on the postdepositional fate of these diatoms. Aside from an occasional occurrence in surface snow from two arctic ice caps, never to my knowledge has **N. cylindrus** been found in samples collected from arctic lakes and ponds. In the light of its abundance in the rime frost samples, the apparent absence of this taxon in water samples and in surface lake and pond upper sediments from Cape Herschel (Table 47.2) is difficult to understand. This is especially true as **N. cylindrus**, although numerically insignificant, has been documented by Fukushima (1967) from three antarctic inland lakes.

There are two possible explanations for the apparent lack of **N. cylindrus**, in particular, and the scarcity of marine diatoms in general: 1) rapid dissolution of the exceedingly small **N. cylindrus** frustules under hostile environmental conditions and 2) the dilution effect manifested by the influx of marine diatoms and their fragments into a freshwater biotope inhabited by an unprecedented number of authochthonous freshwater diatoms

Table 47.2. Surficial lake and pond samples from Cape Herschel examined for the presence of **Nitzschia cylindrus**

Location	Field No.	Lab. No.	Sample material
'Camp Lake' 78°37.1'N, 74°41.5'W	Diat. coll. #4-1977	DT-77-136	water and surface sediment
	Diat. coll. #12-1977	DT-78-8	
'Beach ridge pond' 78°37.2'N, 74°42'W	Diat. coll. #41-1979	DT-80-36	pond water and bottom sediment
'Col Lake' 78°36.2'N, 74°40'W	Diat. coll. #1-1979	DT-80-27	black lake sediment and water
	Diat. coll. #2-1979	DT-80-28	brownish sediment and water
'Willow pond' 78°37.2'N, 74°42'W	BS-80-2 (1: 0 cm and up into ice)	DT-80-91	frozen core, top of sediment and up into ice

with active growth potential. Furthermore, the comparatively lower diversity and frequency of diatoms characterizing the antarctic lakes may have helped facilitate immediate observation and ready recognition of this minute diatom during routine light microscopic examination.

In summary, it can be stated that these rime frost samples are characterized not only by a high relative abundance of diatoms, but also by compositional similarities and most noticeably by the marked predominance of **N. cylindrus.**

This diatom floristic semblance of the 1983 and 1984 rime frost samples suggests a causal interrelation with physical parameters. Table 47.1 shows an identifiable correlation with wind direction and the occurrence of fog (except for June 29th, 1983). The occurrence of sea fog, usually associated with some precipitation and southwesterly wind, is the most significant meteorological factor prevailing during the 1983 and 1984 collection periods.

However, as yet, there are no means of ascertaining whether these diatoms acted as a nucleating agent for the supercooled mist and fog droplets, whether they were removed from the atmosphere by precipitation, or whether direct impaction of wind dispersed diatoms onto the freezing surface took place during the process of rime frost build up.

In this context, it is of interest to mention the various electron microscope studies of fog nuclei documenting combustion particles, soil particles, and sea salt as nucleating agents (Kuroiwa, 1951, 1953, 1956; Yamamoto and Ohtake, 1955).

Concluding remarks

The most important result of this study is the demonstration of aerial transport as an effective mechanism of diatom dispersal, shown by the presence of these algae in rime frost collected from above-ground diatom free surfaces.

These discoveries not only verify the significance of atmospheric dispersal, but they also illuminate the fundamental issue concerning the nature of the colonization process with regard to diatoms, i.e. active versus passive dispersal. Rime frost analyses and assays conducted on precipitation samples (study in progress) indicate that the passive mode of diatom dissemination carries unprecedented impact. Thus, it is reasonable to challenge Hustedt's (1943) concept of active diatom dispersal which ascribes to the passive mode a rather insignificant function. Wind dispersed diatoms serve as massive inoculum, the significance of this process being evidenced by the cosmopolitan distribution of most diatoms within certain limitations, i.e., restrictions imposed by microenvironmental factors characterizing specific biotopes.

Although this study elucidates some aspects of diatom dispersal phenomena, these findings do not allow a firm conclusion to be drawn with regard to point source of origin or dispersal distance of diatoms. Nor does this study indicate the actual mechanism involved in the removal of these diatoms from the atmosphere. Furthermore, resolving the question of the fate of **N. cylindrus,** present in such significant numbers, and that of other marine diatoms, poses a challenge for future investigations.

Acknowledgments

References

Bursa, A.S.
1961: The annual oceanographic cycle at Igloolik in the Canadian Arctic. II. The phytoplankton, "Calanus" Series, No. 17; Journal of the Fisheries Research Board of Canada, v. 18, no. 4, p. 563-615.

Clarke, D.B. and Ackley, S.F.
1983: Relative abundance of diatoms in Weddell Sea pack ice; Antarctic Journal of the United States, v. 18, no. 5, p. 181-182.

Clarke, D.B., Ackley, S.F., and Kumai, M.
1984: Morphology and ecology of diatoms in sea ice from the Weddell Sea; Cold Regions Research and Engineering Laboratory, Report 84-5, 41 p.

Cleve, P.T.
1896: Diatoms from Baffins Bay and Davis Strait; collected by M.E. Nilsson; Bihang till kungliga Svenska Vetenskaps-Akademiens Handlingar, v. 22, no. 4, p. 3-22.

Cross, W.E.
1982: Under-ice biota at the Pond Inlet ice edge and in adjacent fast ice areas during spring; Arctic, v. 35, no. 1, p. 13-27.

El-Sayed, S.Z. and Hampton, I.
1981: Phytoplankton ecology and krill distribution in the southern ocean; Antarctic Journal of the United States, v. 16, no. 5, p. 138-139.

El-Sayed, S.Z., Weber, L.H., and Kopczynska, E.E.
1983: Phytoplankton studies in the sector between Africa and Antarctica; Antarctic Journal of the United States, v. 18, no. 5, p. 188-190.

Fryxell, G.S., Buck, K.R., and Theriot, E.C.
1983: Phytoplankton from the southwestern Atlantic and Indian Oceans; Antarctic Journal of the United States, v. 18, no. 5, p. 186-188.

Fukushima, H.
1967: A brief note on diatom flora of Antarctic inland waters; Proceedings of the Symposium on Pacific-Antarctic Sciences, Japanese Antarctic Research Expedition, Scientific Reports, Special Issue No. 1, p. 253-264.

Fukushima, H. and Meguro, H.
1966: The plankton ice as basic factor of the primary production in the Antarctic Ocean; Antarctic Record, v. 27, p. 99-101.

Garrison, D.L., Buck, K.R., and Silver, M.W.
1983: Studies of ice-algal communities in the Weddell Sea; Antarctic Journal, v. 18, no. 5, p. 179-181.

Grainger, E.H. and Hsiao, I.C.
1982: A study of the ice biota of Frobisher Bay, Baffin Island 1979-1981; Canadian Manuscript Report of Fisheries and Aquatic Sciences, No. 1647, 128 p.

Guillard, R.R.L. and Kilham
1977: The ecology of marine planktonic diatoms; in The Biology of Diatoms, ed. D. Werner; Botanical Monographs, v. 13, University of California Press, Berkeley and Los Angeles, 498 p.

Hasle, G.R.
1965: **Nitzschia** and **Fragilariopsis** species studied in the light and electron microscopes. III. The Genus **Fragilariopsis**; Skrifter Utgitt av Det Norske Videnskaps-Akademi i Oslo I. Matematisk-Naturvidenskapelig Klasse, Ny Serie No. 21, 49 p., 17 pl.

Hsiao, S.I.C.
1983: A checklist of marine phytoplankton and sea ice microalgae recorded from Arctic Canada; Nova Hedwigia, v. 8, p. 225-313.

Hustedt, F.
1943: Die Diatomeen einiger Hochgebirgsseen der Landschaft Davos in den Schweizer Alpen; Internationale Revue der gesamten Hydrobiologie und Hydrographie, v. 43, p. 124-197, 225-280.

Krebs, W.N.
1977: Ecology and presentation of neritic marine diatoms, Arthur Harbor, Antarctica; unpublished Ph.D. thesis, University of California, Davis, California, 216 p.

1983: Ecology of neritic marine diatoms, Arthur Harbor, Antarctica; Micropaleontology, v. 29, no. 3, p. 267-297.

Kuroiwa, D.
1951: Electronmicroscope study of fog nuclei, Journal of Meteorology, v. 8, p. 157-160.

1953: Electron microscope study of fog nuclei (on the condensation nuclei of cloud particles); Low Temperature Science, v. 10, p. 39-52.

1956: The composition of sea-fog nuclei as identified by electron microscope; Journal of Meteorology, v. 13, p. 408-410.

Lichti-Federovich, S.
1984: Investigation of diatoms found in surface snow from the Sydkap Ice Cap, Ellesmere Island, Northwest Territories; in Current Research, Part A, Geological Survey of Canada, Paper 84-1A, p. 287-301.

Polunin, N.
1934: The flora of Akpatok Island, Hudson Strait; Journal of Botany, v. 72, p. 197-204.

Saito, K. and Taniguchi, A.
1978: Phytoplankton communities in the Bering Sea and adjacent seas. II. Spring and summer communities in seasonally ice-covered areas; Astarte, v. 11, no. 1, p. 27-35.

Usachev, P.I.
1946: Biological indicators of the origin of the ice-floes in the Kara Sea and of Brothers Laptev and the Straits of the Franz-Josef-Land Archipelago; Akademiya Nauk SSSR, Institut Okeanologii, Trudy, v. I, p. 113-150.

Yamamoto, G. and Ohtake, T.
1955: Electron microscope study of cloud and fog nuclei. II. Science Reports; Tôhoku University, Fifth Series, v. 7, p. 10-16.

Temporal distribution and significance of Late Pleistocene fossils in the western Champlain Sea basin, Ontario and Quebec

Project 740068

Cyril G. Rodrigues [1] and S.H. Richard
Terrain Sciences Division

Abstract

After the final major retreat of the Laurentide Ice Sheet from the Ottawa-St. Lawrence Lowlands cold subarctic water, salinity 30 to 34‰, occupied the deeper parts of the western Champlain Sea basin and cold lower salinity water (<30‰) was present at shallower depths. Warmer boreal water, salinity less than 20‰, migrated into the basin at shallow depths along the south side of the Champlain Sea during the middle part of the marine episode and does not appear to have penetrated west of 74°47'W. The cold, high salinity water retreated from the western Champlain Sea basin during the later part of the marine episode and was replaced by lower salinity water (<20‰) which eventually turned fresh. Freshwater was also present in the western Champlain Sea basin during the middle part of the marine episode, probably as a surface layer and preceded the outflow of freshwater from Lake Algonquin via the North Bay outlet.

Résumé

Après le recul final de l'inlandsis laurentidien des basses terres de l'Outaouais et du Saint-Laurent, des eaux subarctiques froides dont le degré de salinité a atteint 30 à 34 ‰, occupaient les parties les plus profondes de la partie ouest de la mer de Champlain alors que des eaux froides à degré de salinité plus faible (<30 ‰) couvraient les parties les moins profondes du bassin. Vers le milieu de l'épisode marin, des eaux boréales plus chaudes à degré de salinité inférieur à 20 ‰ ont occupé les parties les moins profondes du bassin dans la partie sud de la mer de Champlain. Elles ne semblent pas avoir pénétré plus à l'ouest que 74°47'O. Les eaux froides de haute salinité se sont retirées de la partie ouest du bassin de la mer de Champlain durant la dernière partie de l'épisode marin et elles ont alors été remplacées par des eaux beaucoup moins salifères (<20‰) qui sont par la suite devenues des eaux douces. Durant le milieu de l'épisode marin, une tranche d'eau douce couvrait probablement la partie ouest du bassin de la mer de Champlain et ceci, bien avant l'arrivée dans le bassin des eaux douces en provenance du lac Algonquin par l'émissaire de North Bay.

---

[1] Department of Geology, University of Windsor, Windsor, Ontario N9B 3P4

Introduction

Radiocarbon age determinations on marine shells, wood, and gyttja are commonly used to estimate the timing of deglaciation and marine inundation of areas covered by ice during the Late Pleistocene. Since 1963 the Radiocarbon Dating Laboratory of the Geological Survey of Canada has made 73 radiocarbon age determinations on pelecypod shells, cirriped plates, marine algae, and whale bones from late glacial and postglacial sediments west of 74°W in the Champlain Sea basin (Fig. 48.1). This paper presents the radiocarbon dates and describes the temporal distribution and significance of some marine and freshwater fossils in the western Champlain Sea basin on the basis of the radiocarbon age determinations.

Acknowledgments

Radiocarbon dates

The 73 radiocarbon dates are arranged in groups and listed in Tables 48.1, 48.2, and 48.3. Remarks for the 17 previously unpublished radiocarbon dates are listed in Table 48.4. The locations of sites where the dated materials were collected, together with the dates, are shown in Figures 48.2, 48.3, and 48.4. The finite ages reported here are in conventional ^{14}C years before 1950 (BP) and are based on the 2σ criterion, i.e., there is a 95.5% probability that the correct age in conventional radiocarbon years lies within the stated limits of error. All radiocarbon age determinations reported by the Geological Survey of Canada during the period 1963 to 1972 quoted an age error calculated by using the counting errors of sample, background, and standard, the error in the half-life, and an error to account for the average variation of ±1.5% in the ^{14}C concentration of the atmosphere during the past 1100 years. Since 1973, the correction for fluctuations of atmospheric ^{14}C is no longer applied to GSC radiocarbon age determinations (Lowdon and Blake, 1973).

For some samples $^{13}C/^{12}C$ ratios have been determined and a correction for isotopic fractionation has been applied to the date. The corrected age differed from the uncorrected age by 0 to ±100 years. The $\delta^{13}C$ values, related to the PDB standard, are reported in Tables 48.1, 48.2, and 48.3 for those dates that have been corrected.

Temporal distribution of fossils

Selected taxa

The oldest radiocarbon dates for **Macoma balthica** (Linné) are from the Clayton (No. 1), Cantley (No. 2), and White Lake (No. 3) sites in Ottawa valley (Table 48.1, Fig. 48.2). The dates from the Clayton site are 600 to 700 years older than those from the Cantley and White Lake sites. The youngest date for samples containing only shells of **Macoma balthica** is 10 460 ± 160 years, outer fraction, for material from the Glen Nevis site (No. 21; Table 48.1, Fig. 48.2). We consider the inner fraction date of 10 740 ± 170 years to be a more reliable estimate of the age of the **Macoma balthica** shells. Thus, the date of 10 600 ± 140 years for shells from the Cazaville site (No. 22, Table 48.1) is the youngest radiocarbon age determination on a sample of **Macoma balthica**. At site 48 (Table 48.3, Fig. 48.2) a monospecific **Macoma balthica** macrofaunal

Figure 48.1 *Location map of the western part of the Champlain Sea basin. The study area is west of 74 W.*

assemblage overlies an assemblage characterized by **Portlandia arctica** (Gray). The date of 10 500 ± 210 years for **Portlandia arctica** from the Saint-Stanislas-de-Kostka site (No. 48) is a maximum age for the monospecific **Macoma balthica** assemblage. A sample from the Russell site (No. 42) containing **Macoma balthica** and **M. calcarea** (Gmelin) yielded a date of 10 000 ± 320 years (Table 48.2, Fig. 48.3). Therefore, **Macoma balthica** was present in the western Champlain Sea basin ca. 12 700 years and from 12 200 to 10 000 years on the basis of the radiocarbon dates.

Radiocarbon age determinations on shells of **Hiatella arctica** (Linné) range from 11 400 ± 140 to 10 100 ± 130 years (Table 48.2, Fig. 48.3). The species was also present in the sample from the Meach Lake site (No. 35) which was dated at 11 600 ± 150 years (Table 48.2, Fig. 48.3). **Hiatella arctica** is present at sites above the elevation of site 35, thus the species may have migrated into the western Champlain Sea basin before 11 600 years ago. Four radiocarbon age determinations on shells of **Mya arenaria** Linné range from 11 100 ± 100 to 10 500 ± 100 years (Table 48.3, Fig. 48.4). Additional ^{14}C dates are required to determine the total range of the species in the western Champlain Sea basin.

Balanus hameri (Ascanius) appears to have a restricted range in the western Champlain Sea basin. The species was dated at 11 000 ± 90 years at both the Navan and Rivière-Beaudette sites (Nos. 20 and 44, respectively; Table 48.3, Fig. 48.4), and 10 800 ± 90 years (inner fraction) at the Bearbrook site (No. 33). The dated samples are from the base of marine sequences exposed in sand and gravel pits.

Table 48.1. Radiocarbon age determinations on shells of **Macoma balthica** (Linné)

Site Number	Site Name	Elevation (m. a.s.l.)	Laboratory Number	Age (years BP)	δ^{13}C (‰)	Reference
1	Clayton	168	GSC-1859	12 800 ± 220		Richard, 1974
			GSC-2151	* 12 800 ± 100	-0.2	Richard, 1978
				‡ 12 700 ± 100	-0.2	Richard, 1978
2	Cantley	194	GSC-1646	12 200 ± 160		Romanelli, 1975
		195	GSC-3844	11 800 ± 170		This paper
3	White Lake	170-171	GSC-3110	* 12 100 ± 100	-0.6	Rodrigues and Richard, 1983
				† 12 200 ± 100	-0.5	Rodrigues and Richard, 1983
				‡ 12 100 ± 100	-0.6	Rodrigues and Richard, 1983
4	Martindale	176	GSC-1772	11 900 ± 160		Lowdon and Blake, 1973
5	Maitland	103	GSC-1013	11 800 ± 210		Lowdon and Blake, 1970
6	Val-des-Bois	180	GSC-2769	11 800 ± 100	-1.8	Richard, 1980
7	Merrickville	118-120	GSC-3523	11 800 ± 100	-0.7	Rodrigues and Richard, in press
8	Farrellton	180	GSC-3812	11 700 ± 100	-1.4	This paper
9	Douglas	120	GSC-3872	11 700 ± 120	-3.6	This paper
10	Saint-Sixte	145	GSC-2863	11 500 ± 200	-4.8	Richard, 1980
11	Mayo	182	GSC-2878	11 500 ± 210	-0.6	Richard, 1980
12	Val-Paquin	195-198	GSC-3865	11 500 ± 130	-1.7	This paper
13	Shawville	170	GSC-3670	11 400 ± 190	1.7	Blake, 1983
14	Sparrowhawk Point	83	GSC-3788	11 300 ± 100	-2.7	This paper
15	Almonte	154	GSC-1672	11 200 ± 160		Richard, 1975
16	Perkins	178-180	GSC-3835	11 200 ± 100		This paper
17	Calumet	160	GSC-2703	11 100 ± 120		Richard, 1980
18	Westmeath	158	GSC-1664	11 000 ± 160	-1.6	Lowdon and Blake, 1979
19	Twin Elm	97	GSC-588	10 880 ± 160		Mott, 1968
20	Navan	95	GSC-3743	* 10 700 ± 100	-1.7	Rodrigues and Richard, in press
				‡ 10 800 ± 90	-1.8	Rodrigues and Richard, in press
21	Glen Nevis	79	GSC-119	* 10 460 ± 160		Dyck and Fyles, 1964
				‡ 10 740 ± 170		Dyck and Fyles, 1964
22	Cazaville	55	GSC-2423	10 600 ± 140		Richard, 1978

* Outer fraction
† Middle fraction
‡ Inner fraction

The dates for **Portlandia arctica** range from 11 900 ± 100 to 10 500 ± 210 years (Table 48.3, Fig. 48.2). The species is also present at the Cantley site (No. 2) in the unit containing **Macoma balthica** which was dated at 12 200 ± 160 years (Romanelli in Lowdon and Blake, 1973). **Portlandia arctica** also occurs at the Bearbrook site (No. 33) with **Hiatella arctica** which has been dated at 10 200 ± 110 and 10 200 ± 90 years, outer and inner fractions, respectively (Table 48.2). Therefore, the range of **Portlandia arctica** in the study area is 12 200 to 10 200 years.

There is only one date for **Macoma calcarea**, 10 600 ± 100 years (Table 48.3), and for **Mya truncata** Linné, 10 300 ± 100 years (Table 48.3); there are no dates for **Mytilus edulis** Linné from the western Champlain Sea basin. Approximate ranges for these species, however, can be inferred from their occurrence at some of the dated sites. **Macoma calcarea** occurs at the Glenroy site (No. 45; Table 48.3, Fig. 48.4) in the **Hiatella arctica** shell bed that underlies clayey sand containing **Mya arenaria** which has been dated at 10 700 ± 100 years; this is a minimum age for the

shells of **Macoma calcarea** in the shell bed. **Macoma calcarea** also occurs in the **Hiatella arctica** shell bed at the Bearbrook site (No. 33; Table 48.2, Fig. 48.3). Therefore, the approximate range for **Macoma calcarea** in the study area is 10 700 to 10 200 years. At the Rivière-Beaudette site (No. 43) **Mya truncata** occurs below **Mya arenaria**, which was dated at 11 100 ± 100 years (Table 48.3, Fig. 48.4), and also occurs at the Bearbrook site (No. 33, Table 48.2) in the **Hiatella arctica** shell bed. Therefore, the approximate range for **Mya truncata** in the western Champlain Sea basin is 11 100 to 10 200 years.

Mytilus edulis is present at the Cantley site (No. 2, Fig. 48.2) in the unit containing **Macoma balthica** which was dated at 12 200 ± 160 years (Romanelli in Lowdon and Blake, 1973). Large numbers of specimens of **Mytilus edulis** were observed at the Perkins site (No. 16, Fig. 48.2) in the upper part of the clay unit underlying crossbedded sand which contained **Macoma balthica**. The date of 11 200 ± 100 years for these shells of **Macoma balthica** is a minimum age for the **Mytilus edulis** shells at the Perkins site. **Mytilus edulis** is also

Table 48.2. Radiocarbon age determinations on shells of **Hiatella arctica** (Linné) and marine shells

Dated Material	Site Number	Site Name	Elevation (m a.s.l.)	Laboratory Number	Age (years BP)	$\delta^{13}C$ (‰)	Reference
Hiatella arctica	23	Buckingham	180	GSC-2763	11 400 ± 140	1.9	Richard, 1980
	24	Newington	106	GSC-2108	11 200 ± 100		Richard, 1975
	25	Rigaud	160	GSC-2296	11 200 ± 90	1.7	Richard, 1978
	26	Montebello	167	GSC-2590	11 100 ± 120	2.3	Richard, 1980
	27	Kars	98	GSC-2312	10 900 ± 100	1.7	Cronin, 1976
	28	Rivière-du-Lièvre	146	GSC-2621	10 700 ± 100	1.1	Lowdon and Blake, 1978
	29A	Saint-Lazare-de-Vaudreuil	84	GSC-2265	10 600 ± 130	1.1	Lowdon and Blake, 1979
	30	Sainte-Justine-de-Newton	74	GSC-2391	10 500 ± 110	1.5	Richard, 1978
	31	Cazaville	71-72	GSC-3882	* 10 300 ± 90	-0.1	This paper
					† 10 500 ± 90	1.2	This paper
	32	Beaver Crossing	67	GSC-2453	10 500 ± 80	1.6	Lowdon and Blake, 1979
	33	Bearbrook	69	GSC-3907	* 10 200 ± 110	-0.8	Rodrigues and Richard, in press
					† 10 200 ± 90	0.3	Rodrigues and Richard, in press
	34	Deschênes	94	GSC-2189	10 100 ± 130	1.3	Richard, 1978
‡Marine Shells	35	Meach Lake	169	GSC-842	11 600 ± 150		Lowdon and Blake, 1970
	36	Lascelles	166	GSC-1612	11 500 ± 150		Lowdon and Blake, 1975
	37	Mahon Lake	167	GSC-982	11 300 ± 180		Lowdon and Blake, 1970
	38	Stittsville	130	GSC-2448	11 300 ± 120		Gadd, 1978
	39	Crysler	70	GSC-2614	10 900 ± 100	-2.1	Lowdon and Blake, 1980
	40	Pembroke	139	GSC-90	10 870 ± 130		Dyck and Fyles, 1963
	41	Ottawa	64	GSC-623	10 720 ± 150		Lowdon et al., 1967
	19	Twin Elm	104	GSC-587	10 620 ± 200		Mott, 1968
	42	Russell	70	GSC-1553	10 000 ± 320		Lowdon and Blake, 1973

* Outer fraction
† Inner fraction
‡ More than one species dated or dated material not identified to specific level

Table 48.3. Radiocarbon age determinations on marine and freshwater pelecypod shells and marine cirriped plates

Dated Material	Site Number	Site Name	Elevation (m a.s.l.)	Laboratory Number	Age (years BP)	δ¹³C (‰)	Reference
Mya arenaria	43	Rivière-Beaudette	56–57	GSC-3741	11 100 ± 100	-2.2	This paper
	44	Rivière-Beaudette	59	GSC-3809	10 900 ± 100	-2.7	This paper
	45	Glenroy	79–80	GSC-3845	10 700 ± 100	-2.7	This paper
	30	Sainte-Justine-de-Newton	76	GSC-3475	10 500 ± 100	-0.9	Blake, 1982
Mya truncata	30	Sainte-Justine-de-Newton	75	GSC-2261	10 300 ± 100	1.5	Richard, 1978
Balanus hameri	44	Rivière-Beaudette	56	GSC-3702	11 000 ± 90	1.4	This paper
	20	Navan	93	GSC-3706	11 000 ± 90	1.4	Rodrigues and Richard, in press
	33	Bearbrook	67	GSC-3983	* 10 800 ± 90	-0.2	This paper
Portlandia arctica	14	Sparrowhawk Point	76	GSC-3767	11 900 ± 100	0.2	This paper
	46	Saint-Pierre-de-Wakefield	160–162	GSC-3834	11 700 ± 150	-1.1	This paper
	47	Twin Elm	105	GSC-3641	11 200 ± 200	-2.8	Blake, 1983
	48	Saint-Stanislas-de-Kostka	42	GSC-3853	10 500 ± 210	-0.4	This paper
Macoma calcarea	29B	Saint-Lazare-de-Vaudreuil	82	GSC-3614	10 600 ± 100	-1.1	Blake, 1983
Lampsilis sp.	9	Douglas	120	GSC-3852	11 400 ± 400	-6.3	This paper
Lampsilis radiata	49	Vankleek Hill	61	GSC-3235	10 300 ± 90		Lowdon and Blake, 1981
Lampsilis sp.	50	Bourget	53	GSC-1968	10 200 ± 90		Gadd, 1976
Lampsilis siliquoidea	51	Saint-Stanislas-de-Kostka	47	GSC-2414	9 750 ± 150		Richard, 1978
Balaena mysticetus	52	White Lake	170	GSC-2269	11 500 ± 90	-13.5	Lowdon and Blake, 1979
Delphinapterus leucas	53	Pakenham	107	GSC-2418	10 400 ± 80		Lowdon and Blake, 1979
Bones of white whale	54	Ottawa	91	GSC-454	10 420 ± 150		Dyck et al., 1966
Marine algae	19	Twin Elm	98	GSC-570	10 800 ± 150		Mott, 1968

* Inner fraction

abundant at the Navan site (No. 20) below shells of **Macoma balthica** which were dated at 10 700 ± 100 and 10 800 ± 90 years, outer and inner fractions respectively (Table 48.1, Fig. 48.2). The species occurs in the same unit as the dated **Hiatella arctica** shells from the Bearbrook site (No. 33; Table 48.2, Fig. 48.3). Therefore, a range of 12 200 to 10 200 years is inferred for **Mytilus edulis** in the study area.

Dates for congeners of the freshwater pelecypod **Lampsilis** from sites below about 62 m in the eastern part of the study area range from 10 300 ± 90 to 9750 ± 150 years (Table 48.3, Fig. 48.4). In the western part, **Lampsilis** sp. from the base of a deltaic unit at about 120 m elevation at the Douglas site (No. 9; Table 48.3, Fig. 48.4) was dated at 11 400 ± 400 years. The temporal distribution of cirriped and pelecypod species is shown in Figure 48.5. Marine algae (kelp) from the Twin Elm site (No. 19) yielded a date of 10 800 ± 150 years (Table 48.3, Fig. 48.4). Dates for whale bones from the White Lake (No. 52), Pakenham (No. 53), and Ottawa (No. 54) sites range from 11 500 ± 90 to 10 400 ± 80 years (Table 48.3, Fig. 48.4).

Cirriped and pelecypod associations

The solid portion of the range of each species in Figure 48.5 is based on radiocarbon age determinations of samples containing only that species. The dated species is the most abundant one in the interval from which the sample was collected except at Mayo (No. 11, Table 48.1) where **Hiatella arctica** and **Macoma balthica** (the dated species) appear to be equally abundant. Thus, the solid portions of the ranges represent the temporal distribution of assemblages characterized by the dated species, i.e., associations of Rodrigues and Richard (1983). The **Macoma balthica** association appears to be the first macrofaunal association to colonize the western Champlain Sea basin and was accompanied by the **Portlandia arctica** and **Hiatella arctica** associations from 11 900 and 11 400 years, respectively. The **Mya arenaria** association was present in the eastern part of the study area from 11 100 years to at least 10 500 years. The **Balanus hameri, Hiatella arctica, Macoma balthica, Mya arenaria,** and **Portlandia arctica** associations inhabited different parts of the western Champlain Sea basin from 11 000 to 10 800 years. More than one macrofaunal association was also present in the study area between 10 800 years and the end of the marine episode ca. 10 100 years.

Foraminiferal and ostracode associations accompany the cirriped and pelecypod associations. Successions of the macrofaunal and microfaunal associations were recognized from marine sequences exposed in ridges and in cored sections from the deeper parts of Ottawa valley (Rodrigues and Richard, 1983; in press; Rodrigues, 1984).

Table 48.4. Remarks for previously unpublished radiocarbon dates. Laboratory numbers and other data are listed in Tables 48.1-48.3

Dated Material	Site Number	Site Name	Age (years BP)	Remarks
Portlandia arctica	14	Sparrowhawk Point	11 900 ± 100	Base of marine clay overlying varved clay that contains **Candona** sp.
Macoma balthica	14	Sparrowhawk Point	11 300 ± 100	Lower part of laminated sand overlying marine clay
Macoma balthica	2	Cantley	11 800 ± 170	Lower part of marine clay overlying outwash gravel and sand
Macoma balthica	8	Farrellton	11 700 ± 100	Fossiliferous clay near marine limit
Macoma balthica	9	Douglas	11 700 ± 120	Clasts of fossiliferous sandy clay at base of deltaic sand
Lampsilis sp.	9	Douglas	11 400 ± 400	Base of deltaic sand underlain by clay
Portlandia arctica	46	Saint-Pierre-de-Wakefield	11 700 ± 150	Fossiliferous clay near marine limit
Macoma balthica	12	Val-Paquin	11 500 ± 130	Fossiliferous fine grained sand near marine limit
Macoma balthica	16	Perkins	11 200 ± 100	Fossiliferous crossbedded sand overlying deformed marine clay
Mya arenaria	43	Rivière-Beaudette	11 100 ± 100	Fossiliferous horizontally bedded sand overlain by cross-bedded sand
Balanus hameri	44	Rivière-Beaudette	11 000 ± 90	Pebbly clayey sand at base of marine sequence overlying gravel and sand
Mya arenaria	44	Rivière-Beaudette	10 900 ± 100	Pebbly sand near top of marine sequence
Balanus hameri	33	Bearbrook	† 10 800 ± 90	Pebbly clayey sand at base of fossiliferous sequence; see Table 48.2 for dates from top of sequence
Mya arenaria	45	Glenroy	10 700 ± 100	Clayey sand overlying **Hiatella arctica** shell bed
Portlandia arctica	48	Saint-Stanislas-de-Kostka	10 500 ± 210	Marine clay overlain by sand containing **Lampsilis** sp.
Hiatella arctica	31	Cazaville	* 10 300 ± 90 † 10 500 ± 90	Fossiliferous diamicton

* Outer fraction
† Inner fraction

Table 48.5. Paleosalinity, relative temperature, and substrate types for some late glacial and postglacial macrofaunal associations from the western Champlain Sea basin

Macrofaunal Association	Salinity (%oo)	Relative Temperature	Substrate
Mya arenaria	<20	Warm boreal water	Clayey sand Pebbly sand
Macoma balthica	10–32		Clay Sandy clay Clayey sand
Hiatella arctica	20–32	Cold subarctic water	Sand Pebbly sand
Portlandia arctica	20–34		Clay
Balanus hameri	30–34		Pebbly clay Pebbly sand

The successions are related to decreasing salinity, increasing temperature in the eastern part of the study area, and variations in substrate type; the ranges for these parameters for some macrofaunal associations are listed in Table 48.5. The presence of more than one association during the marine episode and the successions of associations in the ridges and in cored sections from the deeper parts of the basin are related, in part, to salinity stratification of the Champlain Sea. Cold subarctic water, salinity 30 to 34%oo, occupied the deeper parts of the basin and was overlain by cold, lower salinity water (<30%oo) at shallower depths. Cold subarctic and warmer boreal waters, salinity less than 20%oo, were contemporaneous at least between 11 100 and 10 500 years on the basis of the overlapping ranges of the boreal **Mya arenaria** association and the other pelecypod associations (Fig. 48.5). The warm water migrated into the basin at shallow depths along the south side of the Champlain Sea and does not appear to have penetrated west of 74°47'W, i.e., the western limit of **Mya arenaria** (Rodrigues and Richard, 1983). Cold, high salinity water occupied the deeper parts of the western Champlain Sea basin until at least 10 800 years, i.e., the youngest date for the **Balanus hameri** association (Table 48.3). As the sea shoaled, the high salinity water retreated from the basin and was replaced by lower salinity water which eventually became fresh ca. 10 100 years. The **Lampsilis** association, characterized by congeners of **Lampsilis**, colonized the freshwater which covered the eastern part of the study area.

Figure 48.2. Positions of sites from which radiocarbon dates have been obtained for **Macoma balthica** (Linné) and **Portlandia arctica** (Gray).

Figure 48.3. *Positions of sites from which radiocarbon dates have been obtained for **Hiatella arctica** (Linné) and marine shells (see footnote 3, Table 48.2).*

The date for **Lampsilis** sp. from the Douglas site (No. 9, Fig. 48.4) indicates that a freshwater surface layer was present in the western part of the study area ca. 11 400 years. Meltwater from the retreating Laurentide Ice Sheet and outflow from the Lake Ontario basin are possible sources of the freshwater. The Douglas date for the freshwater pelecypod shells is older than the estimate of 10 400 years of Karrow et al. (1975) for the outflow of freshwater from Lake Algonquin into the Champlain Sea basin via the North Bay outlet.

Discussion

Some workers (e.g., Karrow et al., 1975; Dreimanis, 1977; Karrow, 1981; Clark and Karrow, 1984; Anderson et al., 1985) have pointed out that the arrival of marine water in the western Champlain Sea basin, based on radiocarbon age determinations on marine shells, conflicts with the timing of events in the Lake Ontario basin. They reasoned that the older radiocarbon dates for marine shells are "too old." For example, Clark and Karrow (1984) and Anderson et al. (1985) concluded that marine water arrived in the western part of the Champlain Sea basin later than 12 100 years ago and between 11 700 and 11 400 years ago, respectively. A detailed discussion of the reliability of marine shell dates is beyond the scope of this paper; however, it is appropriate to comment on some of the radiocarbon dates reported here.

There is good agreement between the oldest radiocarbon age determinations on marine shells from the valleys north of Ottawa River, upper St. Lawrence valley, and Champlain valley. The oldest dates from the northern valleys are 11 900 ± 160 (site 4) and 11 800 ± 100 years (site 6, Fig. 48.2) In upper St. Lawrence valley the oldest dates are 11 800 ± 210 years for shells from a beach deposit at the Maitland site (No. 5, Fig. 48.2) and 11 900 ± 100 years for shells from the base of a marine clay unit that overlies varved clay at the Sparrowhawk Point site (No. 14, Fig. 48.2). The Maitland and Sparrowhawk Point dates are comparable to the date of 12 000 ± 200 years reported by Kirkland and Coates (1977) for marine shells from downtown Massena (Fig. 48.1). The oldest dates from Champlain valley are 11 900 ± 120 years (GSC-2338) and 11 800 ± 150 years (GSC-2366; Lowdon and Blake, 1979) for shells of **Macoma balthica** from sites near Peru and Plattsburg, respectively (Fig. 48.1).

The highest fossiliferous beach deposits near Clayton (Fig. 48.1) are at an elevation of 170 m. The radiocarbon dates for shells of **Macoma balthica** from the beach deposits are 12 800 ± 220 years, 12 800 ± 100 years (outer fraction), and 12 700 ± 100 years (inner fraction) from the Clayton site (No. 1, Fig. 48.2) and 12 100 ± 100 years (outer fraction), 12 200 ± 100 years (middle fraction), and 12 100 ± 100 years (inner fraction) from the White Lake site (No. 3, Fig. 48.2). The difference between the dates from the sites is puzzling. The collagen fraction of a whale bone from a beach deposit at site 52, at the same elevation as the dated shells from the Clayton (No. 1) and White Lake (No. 3) sites, yielded a date of 11 500 ± 90 years (Table 48.3, Fig. 48.4). The date for the whale bone is significantly different from the dates for the marine shells. If it is assumed that sea level fell after a high

Figure 48.4. *Positions of sites from which radiocarbon dates have been obtained for **Balanus hameri** (Ascanius), **Macoma calcarea** (Gmelin), **Lampsilis** spp., **Mya** spp., marine algae, and whale bones.*

stand during the early part of the marine episode, then it would be expected that the beach deposits at successively lower elevations should be progressively younger. A rise of sea level would modify the trend of younger ages at lower elevations. Thus, a high stand of sea level ca. 11 500 years may explain, in part, the discrepancy between the dates for the marine shells and whale bone which are at the same elevation along the western rim of the Champlain Sea basin.

The younger dates for freshwater shells from sites 49 and 50, elevation 61 and 53 m, respectively (Table 48.3, Fig. 48.4), overlap dates for marine shells from sites 33 (**Hiatella arctica**) and 42 at an elevation of about 70 m (Table 48.2, Fig. 48.3). The overlap indicates that the dates for the freshwater shells are too old compared with the marine shell dates.

In spite of the problems discussed above, the radiocarbon dates for marine shells are generally consistent. For example, the dates for marine shells from the base and top of the marine sequences at site 14 (Tables 48.1 and 48.3), site 20 (Tables 48.1 and 48.3), site 33 (Tables 48.2 and 48.3), and site 44 (Table 48.3) are older at the base and younger at the top of the sequences. The dates for marine shells from the base and top of the marine sequence and for marine algae from the middle part of the sequence at site 19 (Tables 48.1, 48.2, and 48.3) also show the same trend. We believe that the radiocarbon dates presented here can be used to reconstruct a relative sequence of events for the period of marine inundation of the western Champlain Sea basin even if there are discrepancies between the absolute ages and the dates for marine shells.

Conclusions

The **Macoma balthica** and **Portlandia arctica** associations colonized the western Champlain Sea basin between 12 800 and 11 600 years and were accompanied by the **Balanus hameri, Hiatella arctica, Mya arenaria,** and **Mya truncata** associations during the middle (11 600 to 10 800 years) and later part (10 800 to 10 100 years) of the marine episode. The presence of more than one macrofaunal association during most of the marine episode is related to stratification of the marine water and variations in the substrate. After the Laurentide Ice Sheet retreated from the Ottawa-St. Lawrence Lowlands, cold subarctic water, salinity 30 to 34‰, was present in the deeper parts of the basin and was overlain by cold, lower salinity water (<30‰) at shallower depths. Warmer boreal water, salinity less than 20‰, migrated into the basin at shallow depths along the south side of the Champlain Sea and penetrated as far west as 74°47'W, i.e., the western limit of the **Mya arenaria** association. Cold subarctic and warmer boreal waters were contemporaneous at shallow depths in the western Champlain Sea basin from 11 100 years to at least 10 500 years. The cold, high salinity water retreated from the western Champlain Sea basin after 10 800 years and was replaced by lower salinity water (<20‰) which eventually turned fresh ca. 10 100 years. The **Lampsilis** association characterizes the freshwater deposits overlying marine sediments in some parts of the basin. Freshwater was present near the western rim of the basin during the middle part of the marine episode ca. 11 400 years, i.e., about 1000 years before the estimated time of outflow of freshwater from Lake Algonquin via the North Bay outlet.

409

Figure 48.5. *Temporal distribution of some fossils in late glacial and postglacial sediments of the western Champlain Sea basin (see text).*

References

Anderson, T.W., Mott, R.J., and Delorme, L.D.
  1985: Evidence for a pre-Champlain Sea glacial lake phase in Ottawa valley, Ontario, and its implications; in Current Research, Part A, Geological Survey of Canada, Paper 85-1A, p. 239-245.

Blake, W., Jr.
  1982: Geological Survey of Canada radiocarbon dates XXII; Geological Survey of Canada, Paper 82-7, 22 p.

  1983: Geological Survey of Canada radiocarbon dates XXIII; Geological Survey of Canada, Paper 83-7, 34 p.

Clark, P. and Karrow, P.F.
  1984: Late Pleistocene water bodies in the St. Lawrence Lowland, New York, and regional correlations; Geological Society of America Bulletin, v. 95, p. 805-813.

Cronin, T.M.
  1976: An Arctic foraminiferal fauna from Champlain Sea deposits in Ontario; Canadian Journal of Earth Sciences, v. 13, p. 1678-1682.

Dreimanis, A.
  1977: Correlation of Wisconsin glacial events between the eastern Great Lakes and the St. Lawrence Lowlands; Géographie physique et Quaternaire, vol. XXXI, p. 37-51.

Dyck, W. and Fyles, J.G.
  1963: Geological Survey of Canada radiocarbon dates II; Radiocarbon, v. 5, p. 39-55.

  1964: Geological Survey of Canada radiocarbon dates III; Radiocarbon, v. 6, p. 167-181.

Dyck, W., Lowdon, J.A., Fyles, J.G., and Blake, W., Jr.
  1966: Geological Survey of Canada radiocarbon dates V; Radiocarbon, v. 8, p. 96-127.

Gadd, N.R.
  1976: Surficial geology and landslides of Thurso-Russell map area, Ontario; Geological Survey of Canada, Paper 75-35, 18 p.

  1978: Mass flow deposits in a Quaternary succession near Ottawa, Canada: diagnostic criteria for subaqueous outwash: Discussion; Canadian Journal of Earth Sciences, v. 15, p. 327-328.

Karrow, P.F.
  1981: Late-glacial regional ice-flow patterns in eastern Ontario: Discussion; Canadian Journal of Earth Sciences, v. 18, p. 1386-1390.

Karrow, P.F., Anderson, T.W., Clarke, A.H., Delorme, L.D., and Sreenivasa, M.R.
  1975: Stratigraphy, paleontology, and age of Lake Algonquin sediments in southwestern Ontario, Canada; Quaternary Research, v. 5, p. 49-87.

Kirkland, J.T. and Coates, D.R.
  1977: The Champlain Sea and Quaternary deposits in the St. Lawrence Lowlands, New York; in Amerinds and their Paleoenvironments in Northeastern North America, ed. W.S. Newman and B. Salwen; Annals of the New York Academy of Sciences, v. 288, p. 498-507.

Lowdon, J.A. and Blake, W., Jr.
  1970: Geological Survey of Canada radiocarbon dates IX; Radiocarbon, v. 12, p. 46-86.

  1973: Geological Survey of Canada radiocarbon dates XIII; Geological Survey of Canada, Paper 73-7, 61 p.

Lowdon, J.A. and Blake, W., Jr. (cont.)
1975:   Geological Survey of Canada radiocarbon dates XV; Geological Survey of Canada, Paper 75-7, 32 p.

1978:   Geological Survey of Canada radiocarbon dates XVIII; Geological Survey of Canada, Paper 78-7, 20 p.

1979:   Geological Survey of Canada radiocarbon dates XIX; Geological Survey of Canada, Paper 79-7, 58 p.

1980:   Geological Survey of Canada radiocarbon dates XX; Geological Survey of Canada, Paper 80-7, 28 p.

1981:   Geological Survey of Canada radiocarbon dates XXI; Geological Survey of Canada, Paper 81-7, 22 p.

Lowdon, J.A., Fyles, J.G., and Blake, W., Jr.
1967:   Geological Survey of Canada radiocarbon dates VI; Radiocarbon, v. 9, p. 156-197.

Mott, R.J.
1968:   A radiocarbon-dated marine algal bed of the Champlain Sea episode near Ottawa, Ontario; Canadian Journal of Earth Sciences, v. 5, p. 319-324.

Richard, S.H.
1974:   Surficial geology mapping: Ottawa-Hull area (Parts of 31 F, G); in Report of Activities, Part B, Geological Survey of Canada, Paper 74-1B, p. 218-219.

Richard, S.H. (cont.)
1975:   Surficial geology mapping: Ottawa Valley Lowlands (Parts of 31 G, B, F); in Report of Activities, Part A, Geological Survey of Canada, Paper 75-1A, p. 417-418.

1978:   Age of Champlain Sea and "Lampsilis Lake" episode in the Ottawa-St. Lawrence Lowlands; in Current Research, Part C, Geological Survey of Canada, Paper 78-1C, p. 23-28.

1980:   Surficial geology; Papineauville-Wakefield region, Québec; in Current Research, Part C, Geological Survey of Canada, Paper 80-1C, p. 121-128.

Rodrigues, C.G.
1984:   Faunal successions in Late Pleistocene sediments of the Ottawa-St. Lawrence Lowlands; 1984 Canadian Paleontology and Biostratigraphy Seminar, Programme with Abstracts, p. 7-8.

Rodrigues, C.G. and Richard, S.H.
1983:   Late glacial and postglacial macrofossils from the Ottawa-St. Lawrence Lowlands, Ontario and Quebec; in Current Research, Part A, Geological Survey of Canada, Paper 83-1A, p. 371-379.

—   An ecostratigraphic study of Late Pleistocene sediments of the western Champlain Sea basin, Ontario and Quebec; Geological Survey of Canada, Paper 85-22. (in press)

Romanelli, R.
1975:   The Champlain Sea episode in the Gatineau River Valley and Ottawa area; Canadian Field-Naturalist, v. 89, p. 356-360.

Applications of till geochemistry in southwestern New Brunswick: acid rain sensitivity and mineral exploration

Project 800027

I.M. Kettles and P.H. Wyatt
Terrain Sciences Division

Abstract

A systematic till sampling program was undertaken in southwestern New Brunswick to quantify regional variations in drift composition in order to provide baseline data that might be used in assessing the effects of acid rain. The distribution of two groups of sediment compositional characteristics — (1) texture and carbonate content of tills and (2) concentrations of naturally occurring trace and minor elements in tills — were mapped. Results show that tills in this area are fine grained, averaging 41% sand, 35% silt, and 24% clay. The carbonate minerals appear to have leached to depths greater than 1.5 m. Sites with anomalous concentrations of various trace elements correspond, on a regional scale, to major lithological units in the underlying bedrock. U-rich till, for example, is found overlying Devonian granites and Carboniferous conglomerates derived in part from these granitic sources.

Résumé

Des chercheurs ont entrepris un programme d'échantillonnage systématique du till dans le sud-ouest du Nouveau-Brunswick, pour quantifier les variations régionales de la composition des matéraux de transport glaciaire et ainsi recueillir des données fondamentales qui pourraient servir à évaluer les effets des pluies acides. Pour ce faire, ils ont porté sur une carte la répartition de deux groupes de caractéristiques de la composition des sédiments: (1) texture et teneur en carbonate du till et (2) concentration des oligo-éléments et des éléments accessoires naturels dans le till. Les résultats démontrent que le till de cette région a une texture à grains fins et qu'il renferme en moyenne 41 % de sable, 35 % de silt et 24 % d'argile. Les minéraux carbonatés semblent avoir été lessivés jusqu'à des profondeurs supérieures à 1,5 m. Les endroits où divers oligo-éléments se présentent en concentrations anormales correspondent, à l'échelle régionale, à d'importantes unités lithologiques dans le socle sous-jacent. Par exemple, on rencontre du till riche en uranium sur des granites dévoniens et des conglomérats carbonifères dérivés en partie de ces sources granitiques.

Introduction

In August, 1982 a program of systematic sampling of till and other glacial sediments was carried out along Saint John River valley in southwestern New Brunswick (Fig. 49.1). This study is part of an ongoing research project designed to quantify regional variations in drift composition in order to provide baseline data that might be used in assessing the effects of acid rain. For this purpose, the distribution of two groups of sediment compositional characteristics were mapped: (1) texture and carbonate content of tills and (2) concentrations of naturally occurring trace and minor elements. The former properties are related to potential buffering capacity; the latter might be harmful if released into the environment by acid leaching or exchange reactions. This particular part of the Appalachian Highlands was chosen because it is underlain by interbedded noncalcareous and calcareous sedimentary rock, as well as by carbonate-poor crystalline rock. In this respect, the region is similar to the Frontenac Arch and adjacent West and Central St. Lawrence Lowland areas in eastern Ontario where a similar study was undertaken between 1980 and 1982 (Shilts, 1982; Kettles and Shilts, 1983a,b).

Bedrock geology

The study area (Fig. 49.1) is located within the Chaleur Uplands along Saint John River valley to the west and within the more rugged Miramichi Highlands to the southeast (Bostock, 1970). Local relief varies from less than 30 m in the Chaleur Uplands south of Bristol to several hundred metres in the Miramichi Highlands.

Approximately 75 per cent of the study area is underlain by unmetamorphosed to low-grade metamorphic Paleozoic sedimentary rock (Anderson, 1968; Potter et al., 1979; Fig. 49.2) composed of:

1. slate and argillite interbedded with greywacke sandstones, including locally important limestone units (Cambro-Ordovician age);

2. thinly bedded arenaceous to highly calcareous slate (Silurian age);

3. slate, greywacke, sandstone, and minor conglomerate (Siluro-Devonian age);

4. minor outcrops of slate, shale, and conglomerate (Devonian age); and

5. red to grey unmetamorphosed conglomerate, sandstone, and grit (Carboniferous age).

The remainder of the area is underlain by Devonian granite, quartz monzonite, granodiorite, and syenite as well as minor areas of andesite and basalt, numerous diabase sills and dykes, and isolated bodies of granophyre. In some places granite bodies are deeply weathered and are referred to as "recomposed" granite (Anderson, 1968).

Glacial geology

Pre-Wisconsinan or Early Wisconsinan tills have been recognized in the subsurface at scattered locations along Saint John River valley (Rampton and Paradis, 1981). Elsewhere the till is thought to be Late Wisconsinan, deposited from ice flowing to the south-southeast (Gadd, 1973; Rampton and Paradis, 1981). Till is exposed most commonly in roadside ditches less than 1.5 m deep. It is usually stony, with most erratics being locally derived, and contains a large component of silt- and clay-sized material in the matrix (<2 mm). Most of the near surface till has been oxidized to a tan colour but in the deepest exposures some grey till was observed. Where till is underlain by Carboniferous red conglomerate east of Hartland, the matrix is red-brown. At a road construction site in this area, there occurs a veneer of red-brown gravelly sand overlying till, which appears to be laterally continuous over several hundred metres.

Early Quaternary mapping in this region was undertaken by Lee (1957, 1959, 1962). More recently, Rampton and Paradis (1978) and Gadd (1973) have mapped deposits north and south of 46°N at a scale of 1:250 000. This work indicated that the till cover over much of the study area is thin (< 0.5 m) and discontinuous. Thicker till (0.5 to 1.5 m) has been deposited in a northwest-southeast trending strip approximately 30 km wide extending from Bath in the northwest to Saint John River west of Fredericton. Along the southeastern margin of the field area and south of Saint John River, thick (>1.5 m) end moraine deposits consisting of sand, gravel, and till are common.

Glaciofluvial sand and gravel, generally greater than 1.5 m thick, have been deposited along Saint John River and tributary valleys. A discontinuous esker system west of the Saint John can be traced southward from the Bath area over approximately 35 km. South of Saint John River, parts of several large esker systems are commonly associated with end moraine deposits.

Methods

Sample collection

More than 170 samples were collected from road and stream cuts, as well as from sand and gravel pits, over an area of approximately 6000 km². Till was collected wherever possible because, as the debris load carried by the last glacier, it serves as the source or parent material for soils and postglacially produced sediments. Care was taken to sample below the postglacial solum and below signs of frost disturbance to ensure that samples were uncontaminated. An attempt was made to collect samples every 3-5 km, but the sampling pattern was dependent upon the degree of road access.

Figure 49.1. *Location and physiography of the study area in Saint John River valley, southwestern New Brunswick.*

Sample preparation and analyses

The silt plus clay fraction (<63 μm) of the samples collected was analyzed for carbonate content (calcualted as %CaCO₃ equivalent) using a Leco Carbon Analyzer. The clay-sized fraction (<2 μm) was separated by centrifugation and analyzed by Bondar-Clegg Ltd. for Cu, Pb, Zn, Co, Ni, Ag, Cr, Mo, Cd, Fe, Mn, and Hg using standard atomic absorption techniques after treatment with a hot (HNO₃-HCl) leach. As and U were analyzed using colorimetric and fluorimetric techniques, respectively. Textural composition of the <2 mm fraction was determined using standard sieve and hydrometer procedures.

Data reduction

Sample site locations were coded according to the UTM grid system and classified according to sediment type. This information and all results of laboratory analyses were stored on computer files using the SIR format (Burns, 1985).

Carboniferous
red and grey conglomerate, sandstone, shale, minor volcanic flows and tuffs.

Devonian
granite, quartz monzonite granodiorite, gabbro, diorite, diabase, granophyre, and related rocks.
basalt, andesite
grey to green sandy slate, sandstone conglomerate.

Silurian and Devonian
grey to green slate, greywacke, minor conglomerate.

Silurian
grey to green to red arenaceous to calcareous slate, greywacke and related rocks, manganiferous iron formation, limestone.

Cambro-Ordovician
grey to green slate, greywacke, argillite, basic lava.

Figure 49.2. *Bedrock lithologies underlying the study area, southwestern New Brunswick (after Anderson, 1968; Potter et al., 1979).*

415

Geochemical and textural data for a representative sample from each site were plotted and contoured using a computer package (APPMAP) developed by D.J. Ellwood of the Geological Survey of Canada.

Results and discussion

Carbonate distribution

Carbonate content of the samples collected was, on average, very low (<1%); only five samples had contents greater than 2%, and these ranged from 2.8 to 15.9. In contrast, samples collected in Ontario over the eastern part of the Frontenac Arch contain substantial amounts of carbonate minerals, even samples collected at depths of less than 1.5 m. (Although there is abundant marble within the Frontenac Arch, the carbonate in till was largely derived from Paleozoic rocks in the Central St. Lawrence Lowland and glacially transported up to 70 km onto the Canadian Shield (Shilts, 1982; Kettles and Shilts, 1983a,b)). This apparently anomalous degree of depletion of carbonate in the surficial sediment of the New Brunswick study area may be explained in terms of till geochemistry and the effects of weathering on the till and groundwater systems.

In another part of the Appalachian Highlands – the Eastern Townships of Quebec – Shilts (1978, 1984) examined in detail the effects of weathering on till. In one stratigraphic section near Thetford Mines, 10 m of hard, olive grey till is weathered to a brown to tan colour to a depth of 2 m below the surface. Where unoxidized, the till contains a noticeable amount of sand- and granule-sized pyrite cubes and fragments, derived from local schists, which in badly oxidized material completely disintegrate. Reflecting the close relationship of leaching to oxidation in this low carbonate terrain, %CaCO$_3$ equivalent of unoxidized till is 2-4% compared to a trace or less in overlying, oxidized material.

Till in the study area was not observed to contain visible pyrite by which to gauge the content of sulphide or the intensity of weathering. Nevertheless, like other till in the Appalachian region, in unoxidized form it likely contains high background levels of sulphide minerals which would produce a weathering pattern similar to that observed for till composed of similar lithologies near Thetford Mines.

Most samples collected for this study were taken at depths of less than 1.5 m from the surface in tan coloured, presumably oxidized, till. In such an oxidizing environment the sulphide and carbonate minerals are likely to have been destroyed. The differences in weathering patterns (particularly depth of carbonate leaching) between till from Frontenac Arch and New Brunswick are probably related to 1) the greater relative abundance of sulphide minerals, the weathering of which may lower the pH of near surface groundwaters, enhancing carbonate dissolution (W.W. Shilts, personal communication, 1978) or 2) the much greater original carbonate content in tills of the Frontenac Arch, which may buffer groundwaters, slowing the leaching process (Merritt and Muller, 1959).

In addition, these results illustrate that an understanding of the effects of weathering on till and groundwater geochemical systems is required before analytical results can be interpreted reliably. Standard sampling procedures and routine analytical techniques must be modified in response to the specific geochemical system under study.

Textural properties

In Figure 49.3, computer contoured maps illustrate regional variations in textural composition. Till samples (n = 141) average 41% sand (64-2000 μm), 35% silt (4-64 μm), and 24% clay (<4 μm) (<2 mm fracton) with ranges of 10 to 84%, 8 to 54%, and 3 to 45%, respectively. In general, the till has high concentrations of clay-sized material in the area northwest of Juniper and south of Hartland and Millville.

The till of this area of New Brunswick is much more fine grained than the till collected over the Frontenac Arch area which averages 67% sand, 26% silt, and 7% clay (n=1080). The large component of fine grained material in the New Brunswick till should increase buffering capacity because it enhances the internal surface area (reaction surface) of the sediment, increasing its potential for reaction with ground or surface waters containing abnormal levels of protons.

Trace element distribution patterns

Computer contoured maps illustrating distribution patterns of trace elements in till are presented in Figure 49.4. Sites where glacial sediment contains anomalously high concentrations (above 90th percentile) of trace elements are located on Figure 49.5. For comparison, occurrences of high or anomalous levels of trace elements in stream and spring sediments (-80 mesh), analyzed using the techniques listed in Table 49.1 (Austria, 1971, 1977, 1979a, b, 1980a-h), have also been depicted on Figure 49.5, as have locations of known mineral occurrences in bedrock (Picklyk et al., 1978).

Areas with anomalous levels of various trace elements in till are generally related to bedrock lithology (cf. Fig. 49.2). For example, till with high uranium content is found overlying Devonian intrusive rocks – the Pinder-Keswick granitic body in particular – and is also found over Carboniferous conglomerates derived in part from this granitic source. Highest concentrations of most elements – Cu, Pb, Ni, Co, Zn, Fe, Hg, and Mn – are associated with sedimentary rocks.

Trace element data from this study indicate that there is good correspondence between the distribution patterns of Mn and Fe in till. Three anomalies, labelled 'A', 'B', and 'C', are prominent at the same location on both maps (Fig. 49.4). High concentrations of one or more of the following elements, Zn, Pb, Cu, Co, Ni, Cr, As, and Hg, are associated with each of these anomalies.

The anomalously high levels of Mn and Fe may reflect primary mineralogical composition of the sediment. Fe and Mn mineralization commonly coexists in manganiferous hematite in Silurian rocks (Anderson, 1968), and at another site near Glassville, high concentrations of Mn and Fe in till do correspond to sites with known mineralization of this type. In this case, however, enhanced levels of these trace elements are thought to be artifacts of weathering. The high concentrations of Fe and Mn are accompanied by high levels of one or more trace elements which often indicate the presence of secondary alteration products such as manganese hydroxides and oxides in the clay-sized fraction of the sample (Shilts, 1973). In addition, at least one of the samples collected within each anomalous area is composed of glaciofluvial sand and gravel. High trace element levels are particularly common in the fine grained component (<2μm) of sand and gravel because it is composed primarily of weathering products (mixed-layer clays, secondary Fe and Mn oxides and hydroxides) formed by postdepositional decomposition of primary (mainly silicate) minerals.

Elsewhere in the study area, areas with high levels of various trace elements in till, particularily those associated with sulphide mineralization, can sometimes be correlated. Prominent anomalies of Cu and Zn, accompanied by high levels of Mo and Hg, are found in sediment southeast of Woodstock around the Gibson granite stock. In this area

numerous known occurrences of Cu, Pb, Zn, and Mo sulphide mineralization in pyrite veins hosted by Cambro-Ordivician greywacke and slate have been documented (Anderson, 1968).

Anomalous concentrations of many trace elements are found in the Millville area. In the northwestern part of the area Cr, Ni, As, Pb, and Hg correlate, as do Ag, U, Pb, and Cu to the northeast.

The lack of correlation between till and stream sediment anomalies (Fig. 49.5) may be explained by the following factors: 1) Sampling density for each type of sediment varies independently throughout the area. Systematic sampling for both the stream and till surveys was undertaken at a reconnaissance scale and stream sediment and till samples are commonly spaced more than 6 km apart. 2) Stream and spring sediment anomalies are particularly abundant in the southern part of the study area south of Saint John River and around the Millville area to the east (Fig. 49.5). Though no Fe data are available for stream and spring sediments, high levels of Mn commonly coincide with high concentrations of U, Zn, Pb, and Mo. As mentioned previously Cu, Pb, Zn, and Mo are strongly adsorbed and co-precipitated by manganese hydroxides and oxides especially in sand and gravel samples. It is possible then that some high concentrations of trace elements in these sediments may reflect chemical changes due to scavenging by secondary minerals rather than to primary mineralogical composition.

Correspondence between sites of known minerali-zation and those with anomalous levels in either type of sediment – till or stream is also generally limited (Fig. 49.5). Known mineral occurrences and old workings in this area are generally small, limited to veins or lenticular beds in the bedrock. During glacial erosion metal-rich debris derived from these small mineralized zones would have been quickly diluted by debris from the surrounding metal-poor rock. On a regional scale, therefore, the mineralogical composition of the drift would, in most cases, more closely approximate the average composition of the surrounding bedrock rather than the mineralized zone.

Conclusions

1. Using field and laboratory methods similar to those used in a study on the Frontenac Arch of southern Ontario we were unable to discern patterns of carbonate distribution over southwestern New Brunswick. Carbonate minerals present in Appalachian tills appear to be leached more intensely and to a greater depth than they are in till of the Frontenac Arch and St. Lawrence Lowlands, a phenomenon noted by Merritt and Muller (1959). Before terrain sensitivity can be evaluated, it is important to consider the abundance of carbonate and other major or minor mineral components in unweathered till which, when weathered, may cause changes in the pH of near surface groundwater. As in the Quebec Appalachians, carbonate minerals of New Brunswick tills appear to have been depleted to depths greater than 1.5 m, possibly leaving the drift more susceptible to the effects of acid loading. A better indication of the naturally occurring patterns of carbonate enrichment in till could be obtained by sampling unweathered sediment found locally in stratigraphic sections along major streams, or by coring in areas of thick sediment accumulation.

Figure 49.3. *Textural compostion (<2 mm fraction) of till in Saint John River valley, southwestern New Brunswick.*

ZINC
IN
CLAY-SIZED FRACTION

PPM	%TILE
191	MAX
153	95
142	90
134	75
120	50
47	MIN

168 SAMPLES

CHROMIUM
IN
CLAY-SIZED FRACTION

PPM	%TILE
115	MAX
106	95
96	90
86	75
76	50
33	MIN

168 SAMPLES

LEAD
IN
CLAY-SIZED FRACTION

PPM	%TILE
65	MAX
47	95
39	90
33	75
26	50
9	MIN

168 SAMPLES

SILVER
IN
CLAY-SIZED FRACTION

PPM	%TILE
2.40	MAX
0.20	98
0.10	90
0.05	MIN

168 SAMPLES

COPPER
IN
CLAY-SIZED FRACTION

PPM	%TILE
175	MAX
101	95
86	90
67	75
57	50
14	MIN

168 SAMPLES

NICKEL
IN
CLAY-SIZED FRACTION

PPM	%TILE
194	MAX
120	95
108	90
97	75
86	50
15	MIN

168 SAMPLES

SITES

COBALT
IN
CLAY-SIZED FRACTION

PPM	%TILE
43	MAX
31	95
28	90
23	75
20	50
11	MIN

168 SAMPLES

418

Figure 49.4. *Geochemistry of till and other surficial sediments (<2 μm fraction) in Saint John River valley, southwestern New Brunswick.*

419

Figure 49.5. *Location map of sites with (1) anomalous concentrations (>90th percentile) of trace elements in till and other surficial sediments (<2 μm); (2) high or anomalous concentrations of trace elements in stream and spring sediments (-80 mesh); and (3) known mineral occurrences (Canmindex). Areal distribution and sources of trace element data for each sample medium is shown in Table 49.1.*

Table 49.1. Areal distribution of trace element data for till and other glacial sediments (this study) and stream and spring sediments

Area	NTS	Geochemical analyses (<2 μm) for till and other glacial sediment	Reference	Geochemical analyses (–80 mesh) for stream and spring sediments	Reference
Fosterville	21G/13	Cu, Pb, Zn, Co, Ni, Ag Cr, U, Mo, Mn, Fe, Cd, As, Hg*	this study	Cu, Pb, Zn, Mn, Mo, Sb	Austria, 1971, 1980c
				U	Austria, 1979b
Canterbury	21G/14	"	"	Cu, Pb, Zn, Mn, Mo, Sb	Austria, 1971, 1980a, b
				U	Austria, 1977, 1979b
Burtts Corner	21J/2	"	"	U	Austria, 1979b
Millville	21J/3			Cu, Pb, Zn, Mn, Mo, Sb	Austria, 1980d,e
				U	Austria, 1977, 1979b
Woodstock	21J/4	"	"	Cu, Pb, Zn, Mn, Mo	Austria, 1980f
				U	Austria, 1979a,b
Florenceville	21J/5	"	"	U	Austria, 1979b
Coldstream	21J/6	"	"	Cu, Pb, Zn, Mn, Fe, Sb	Austria, 1980g,h
				U	Austria, 1977, 1979a
Juniper	21J/11	"	"		
Perth-Andover	21J/12	"	"		
		*Cu, Pb, Zn, Co, Ni, Ag, Cr, Mo, Mn, Fe, Cd by atomic absorption techniques; As by colorimetric methods; U by fluorimetric techniques		*Cu, Pb, Zn and Mn by atomic absorption techniques; Mo, Sb by colorimetric methods; U by neutron activation techniques.	

Tills in this area are fine grained, having on average 24% clay and 35% silt. Even in areas where the carbonate content is low, the large internal surface area of this sediment may increase its capacity to buffer acid rain.

2. Distribution patterns of trace element concentrations in the drift of southwestern New Brunswick are illustrated in Figure 49.4. Computer contoured maps show areas of metal-rich till which may form potential sources of groundwater pollution should the metals be mobilized by adverse pH conditions. Similar to the Frontenac Arch area, sites with anomalous concentrations of various trace elements correspond, on a regional scale, to major lithological units in the underlying bedrock. Uranium-rich till, for example, is found overlying Devonian granites and related rocks whereas Ni and Co anomalies are in this case commonly associated with Paleozoic sedimentary rocks.

3. Because trace element concentrations appear to be controlled in some cases by mineralization as well as by average bedrock composition, information obtained in this type of study (Fig. 49.4, 49.5) may also be applied to mineral exploration.

References

Anderson, F.D.
1968: Woodstock, Millville, and Coldstream map-areas, Carleton and York Counties, New Brunswick; Geological Survey of Canada, Memoir 353, 69 p.

Austria, V.B.
1971: The Cu, Pb, Zn, Mn, Mo, and Sb content of stream and spring sediments, York County, New Brunswick; New Brunswick Department of Natural Resources Mineral Resources Division, Report of Investigation 14.

1977: Uranium content of stream and spring sediments; New Brunswick Department of Natural Resources, Mineral Resources Division, MP 77-23 (Canterbury (21G/14), MP 77-24 (Millville (21J/3), MP 77-25 (Coldstream (21J/6).

1979a: Uranium content of stream and spring sediments, Woodstock East (21J/4E); New Brunswick Department of Natural Resources, Mineral Resources Division, MP 79-52.

1979b: Distribution trend of uranium in stream sediment, southwestern New Brunswick (21G, 21J); New Brunswick Department of Natural Resources, Mineral Resources Division, MP 79-142.

1980a: Stream and spring sediment geochemistry maps, Canterbury West (21G/14W); New Brunswick Department of Natural Resources, Mineral Resources Division, MP 80-19a-e.

1980b: Stream and spring sediment geochemistry maps, Canterbury East (21G/14E); New Brunswick Department of Natural Resources, Mineral Resources Division, MP 80-20a-e.

1980c: Stream and spring sediment geochemistry maps, Fosterville East (21G/13E); New Brunswick Department of Natural Resources, Mineral Resources Division, MP 80-23a-e.

1980d: Stream and spring sediment geochemistry maps, Millville East (21J/3E); New Brunswick Department of Natural Resources, Mineral Resources Division, MP 80-24a-f.

1980e: Stream and spring sediment geochemistry maps, Millville West (21J/3W); New Brunswick Department of Natural Resources, Mineral Resources Division, MP 80-25a-f.

1980f: Stream and spring sediment geochemistry maps, Woodstock East (21J/4E); New Brunswick Department of Natural Resources, Mineral Resources Division, MP 26a-f.

1980g: Stream and spring sediment geochemistry maps, Coldstream West (21J/6W); New Brunswick Department of Natural Resources, Minerals Resources Division, MP 80-27a-g.

1980h: Stream and spring sediment geochemistry maps, Coldstream East (21J/6E); New Brunswick Department of Natural Resources, Mineral Resources Branch, MP 80-28a-h.

Bostock, H.S.
1970: Physiographic subdivisions of Canada; in Geology and Economic Minerals of Canada, ed. R.J.W. Douglas; Geological Survey of Canada, Economic Geology Report No. 1, p. 10-30.

Burns, R.K.
1985: Data storage and processing in Terrain Sciences Division; in Current Research, Part B, Geological Survey of Canada, Paper 85-1B, Note.

Gadd, N.R.
1973: Quaternary geology of southwest New Brunswick, with particular reference to Fredericton area; Geological Survey of Canada Paper 71-34.

Kettles, I.M. and Shilts, W.W.
1983a: Reconnaissance geochemical data for till and other surficial sediments, Frontenac Arch and surrounding areas, Ontario; Geological Survey of Canada, Open File 947.

1983b: Drift composition of Frontenac Arch area, Ontario: Implications for evaluating effects of acid rain; Abstracts with Programs, Geological Society of America, v. 15, p. 612.

Lee, H.A.
1957: Surficial geology of Fredericton, York and Sunbury counties, New Brunswick; Geological Survey of Canada, Paper 56-2.

1959: Surficial geology of Grand Falls, Madawaska and Victoria counties, New Brunswick; Geological of Canada, Map 24-1959.

1962: Surficial geology of Canterburgy, Woodstock, Florenceville and Andover map areas, York, Carleton and Victoria counties; New Brunswick; Geological Survey of Canada, Preliminary Paper 62-12.

Merritt, R.S. and Muller, E.H.
1959: Depth of leaching in relation to carbonate content of till in central New York state, American Journal of Science, v. 257, p. 465-480.

Picklyk, D.D., Rose, D.G., and Lawrence, R.M.
1978: Canadian Mineral Occurrence Index (Canmindex) of the Geological Survey of Canada; Geological Survey of Canada, Paper 78-8.

Potter, R.R., Hamilton, J.B., and Davies, J.L.
1979: Geological map – New Brunswick; New Brunswick Department of Natural Resources, Geological Map NR-1.

Rampton, V.N. and Paradis, S.
1981: Quaternary geology of Woodstock map area (21J), New Brunswick; New Brunswick Natural Resources, Map Report 81-1, 37 p.

Shilts, W.W.
1973: Drift prospecting; geochemistry of eskers and till in permanently frozen terrain; District of Keewatin, Northwest Territories; Geological Survey of Canada, Paper 72-45.

1978: Detailed sedimentological study of till sheets in a stratigraphic section, Samson River, Quebec; Geological Survey of Canada, Bulletin 285, 30 p.

1982: Potential effects of acid rain on glaciated terrain; in Groundwater as a Geomorphic Agent, ed. R.G. LaFleur; Binghamton Symposia in Geomorphology; International Series, no. 13, Allen and Unwin, Inc., Boston.

1984: Till geochemistry in Finland and Canada; Journal of Geochemical Exploration, v. 21, p. 95-117.

Radiocarbon dating with accelerator mass spectrometry: results from Ellesmere Island, District of Franklin

Projects 570148 and 750063

W. Blake, Jr.
Terrain Sciences Division

Abstract

Radiocarbon dating by means of accelerator mass spectrometry (AMS) has two great advantages over conventional dating: 1) much smaller samples can be handled and 2) counting time is significantly shorter. Three examples are given for Holocene-age material from east-central Ellesmere Island. The results demonstrate the potential use of this technique as a powerful research tool in studies of Quaternary chronology. Individual fragments of marine shells as small as 0.1 g have been dated successfully at the IsoTrace Laboratory, University of Toronto. In the case of an aquatic moss from a lake sediment core, an increment 0.5 cm thick could be used instead of a 5 cm-thick slice, thus allowing a much more precise estimate of the onset of organic sedimentation.

Résumé

La datation par le carbone radioactif exécutée au moyen d'un spectromètre de masse accélérateur (AMS), comparée à la méthode classique, présente deux avantages marqués. Premièrement, elle peut s'éxécuter sur des échantillons beaucoup plus petits. Deuxièmement, le temps de comptage est beaucoup plus court. L'auteur démontre ces phéomènes à l'aide de trois datations faites sur des échantillons de l'Holocène recueillis dans le centre-est de l'île Ellesmere. Les résultats établissent que cette technique peut constituer un outil de recherche puissant dans l'étude de la chronologie du Quaternaire. Des fragments de coquilles marines pas plus grosses que 0,1 g ont pu être datés avec succès au laboratoire IsoTrace de l'Université de Toronto. Dans le cas d'une mousse aquatique provenant d'une carotte de sédiment lacustre, on a pu utiliser une constante de progression de 0,5 cm au lieu d'une épaisseur de 5 cm; cette mesure a permis de dater avec beaucoup plus de précision le début de la sédimentation organique.

Introduction

The advent of radiocarbon dating by means of accelerator mass spectrometry (AMS) has opened up many new possibilities for refining the chronology of events during the last 40 000 to 50 000 years. Already a considerable body of literature devoted to AMS has come into existence, and several international conferences have been held since 1978. The development of this method has been described by Muller (1977), who used a cyclotron rather than a Van de Graaf accelerator, and by Bennett et al. (1977), Nelson et al. (1977), Doucas et al. (1978), and Stuiver (1978). For a recent review of accelerators and dating the reader is referred to Possnert and Olsson (1984).

A number of early reports suggested that ages beyond the limits attainable by decay counting in conventional proportional or scintillation counters were to be expected, and a figure of 100 000 years appeared in a number of articles (e.g., Gribbin, 1979). In the proceedings of the first conference devoted to dating with accelerators, Haynes (1978) listed one of the advantages of AMS to be the "extension of the datable time range to approximately 90 000 B.P. or twice the conventional range of 45 000 B.P.". It seems clear, however, that the greatest advantages of AMS, at least initially, are: 1) that extremely small samples (milligrams instead of grams) can be accommodated and 2) that the counting time required is much shorter.

This report discusses three examples of the promising results that can be expected by means of AMS. The conventional age determinations reported here were carried out in the Radiocarbon Dating Laboratory at the Geological Survey of Canada, where two proportional counters are in operation (Dyck, 1967; Lowdon, 1985). The accelerator dates were obtained from the IsoTrace Laboratory, University of Toronto, where the machine in use is one of six around the world that have been manufactured by General Ionex Corporation, Newburyport, Massachussetts (Litherland, 1984). The AMS results constitute part of a series of 'Crown' samples, whose ages have been determined as one 'task' under a developmental contract, funded in part by the Department of Energy, Mines and Resources.

This report is Contribution No. 22 from the Cape Herschel project.

Sample descriptions and results

Over the last few years my field work has been concentrated in east-central Ellesmere Island, especially in the narrow ice-free coastal zone along Smith Sound, and along the opposite shore in Inglefield Land, Greenland (Fig. 50.1). The main research objective has been to attempt to decipher the glacial history, in particular to determine when glacier ice last flowed southward from Kane Basin through Smith Sound toward Baffin Bay. Raised marine deposits, which normally constitute a major source of datable material, are relatively scarce because of the rugged fiord terrane. Likewise, there are considerable expanses of bare rock and felsenmeer, hence a major effort has been devoted to coring pond and lake sediments as a way of obtaining chronological information (Blake, 1978, 1981, 1982a; Smol, 1983; Hyvärinen, 1985).

Figure 50.1. *LANDSAT image showing Smith Sound and southern Kane Basin. Numerals refer to sites discussed in the text: 1 - MacMillan Glacier; 2 - north side of Cape Herschel; 3 - Proteus Lake. The image shows the development of the 'North Water' on April 4, 1973 (image E-10255-18054, spectral band 7).*

Although raised beaches are rare, the presence of shelly till in lateral moraines indicates that fiord-bottom sediments have been picked up and incorporated into the basal ice by advancing outlet glaciers from the Central Ellesmere Island Icecap. In the field area the most striking example of this phenomenon encountered up to now is on the south side of Leffert Glacier (Fig. 50.1). Abundant mollusc shells and crustose coralline algae in an ice-cored lateral moraine along a nunatak are as young as 2280 ± 140 years (GSC-3515; Blake, 1984a, b), and they are located more than 6 km behind the present position of the glacier snout. At an elevation of 160 to 180 m the shells are well above the highest dated molluscs of Holocene age, which occur at approximately 105 m a.s.l. The presence of these shells in the lateral moraine means that approximately 2000 radiocarbon years ago the snout of Leffert Glacier was at least 7 km west of its present position.

To the south of Leffert Glacier is another outlet tongue, MacMillan Glacier (Fig. 50.1), and in 1983 and 1984 marine shells were collected from the surface and side of a small terrace adjacent to a stream flowing along the north side of the glacier (Fig. 50.2). The site is 2.7 km west of the nearest bay of Baird Inlet at an elevation of approximately 145 m a.s.l., as determined by repeated measurements with a surveying altimeter. As this terrace was close to being at the same elevation as a perched delta near Cape Herschel, there was a chance that the shells might date from the initial incursion of the sea in early Holocene time.

The first determination, on **Hiatella arctica** shells excavated from the till-like material and sand comprising the terrace, as well as from the adjacent stream channel, gave an age of 25 700 ± 890 BP (GSC-3897). This somewhat surprising age, representing a time when it could be expected that the coastal fringe of bare ground was inundated by glacier ice, suggested that the fragments comprising the dated sample might have been derived from different sources. The field situation was such that shells in till could readily have become mixed with shells of Holocene age, and **Hiatella arctica** is a particularly robust species, one which commonly occurs in till in eastern Ellesmere Island and elsewhere in the Arctic.

For this reason a second sample, consisting of a single barnacle fragment (**Balanus balanus**), and weighing only 0.35 g, was submitted to the IsoTrace Laboratory. The age of a portion of this fragment, weighing 64.0 mg after pretreatment, was determined to be 7640 ± 60 BP (TO-71; Table 50.1). This result demonstrates that Holocene shells are indeed present in the terrace adjacent to MacMillan Glacier. Because the sample is well above the elevation at which materials of this age might be expected, based on several dated samples near Cape Herschel and in Alexandra Fiord (Blake, 1978, 1982a, b), we can conclude that fiord-bottom sediments were dragged or ploughed upward as MacMillan Glacier advanced. The ice-marginal stream later reworked the fiord-bottom material, so that the terrace today includes both till, or colluviated till, and patches of washed sediment. We can conclude further that at the time the barnacles were living the front of MacMillan Glacier was several kilometres west of its present position.

The second dated site is near our base station on Cape Herschel peninsula. A small pond ('Moraine Pond') is held up by a moraine ridge along the north slope of the peninsula (Fig. 50.3). Abundant marine shells and shell fragments are present on the ground surface at the western end of the pond. They are presumed to derive by slope wash from marine sediments slightly higher up the slope, and some may have been brought to the surface by frost action. Two small pockets of raised beach occur above the level of the pond,

Figure 50.2. Aerial view eastward from MacMillan Glacier along the north side of Baird Inlet, July 9, 1984. The shell collection site is indicated by the arrow. 201464-O

Table 50.1.   Radiocarbon age determinations, east-central Ellesmere Island

Sample elevation m a.s.l.	Dated material[1]	Field sample No.	Laboratory dating No.[3]	δ¹³C ‰	Age (Corrected for δ¹³C)[4,5]	Sample weight (g)	(mg)	Counter (L)	Pressure (atm)	Counting time (days)[6]	Comments
145	**Hiatella arctica**	83-BS-289+ 84-BS-160	GSC – 3897	+0.7	25 700 ± 890	6.7	–	2	2	4	10% HCl leach; mixed with dead gas for counting; aragonitic.
145	**Balanus balanus**	83-BS-289+ 84-BS-160	TO – 71	–	7 640 ± 60	–	268.2				>20% HCl leach; 64.0 mg after pretreatment; 3 targets counted; calcitic.
79.0	basal organic pond sediment[2]	BS-81-3 (1:406-414cm)	GSC – 3970	-25.9	7 300 ±110	80.0 (dry)	–	2	2	3	NaOH leach omitted; slight reaction with HCl; some ice lenses; organic C content, 2.1-3.8%.
81.5-83.5	**Macoma calcarea**	BS-79-137+ BS-79-138	GSC – 2913	-0.5	8 190 ± 110	15.5	–	2	2	3	10% HCl leach; mixed with dead gas for counting; aragonitic.
78.0	**Clinocardium ciliatum**	BS-81-3 (1:532 cm)	TO – 115		8 510 ± 50	–	115.6				10% HCl leach; 104.0 mg after pretreatment; 2 targets counted.
390	aquatic moss	BS-79-27 (2:45-50cm)	GSC – 2934	-30.8	8 970 ±190	5.0 (dry)	–	2	2	4	NaOH + HCl leaches + distilled water rinses; mixed with dead gas for counting.
390	aquatic moss	BS-81-30 (7:52.5-53.0cm)	TO – 111		9 370 ± 110		118.2				NaOH + HCl leaches + distilled water rinses; 21.2 mg after pretreatment; 2 targets counted.

1   Marine molluscs and cirripeds identified by W. Blake, Jr. The moss at the base of the cores from Pim Island has proved to be difficult to identify but is a member of the Amblystegiaceae (J.A. Janssens, personal communication, 1980).

2   Samples from 398.5-400.5 cm, 406-408 cm, and 413-414 cm all contain freshwater diatoms of the genus **Fragilaria**; freshwater diatoms were not found below this level in the core (unpublished GSC Diatom Report No. 84-8 by S. Lichti-Federovich).

3   Laboratory designations: GSC – Geological Survey of Canada; TO – IsoTrace Laboratory, University of Toronto.

4   All age determinations from the Radiocarbon Dating Laboratory, Geological Survey of Canada, are based on a ¹⁴C half-life of 5568 ± 30 years and 0.95 of the activity of the NBS oxalic acid standard. Ages are quoted in conventional radiocarbon years before present (B.P.) where 'present' is taken to be 1950. All finite age determinations from this laboratory are based on the 2σ criterion; i.e., there is a 95% probability that the correct age in conventional radiocarbon years lies within the stated limits of error. ¹³C/¹²C ratios were determined at the Department of Earth Sciences, University of Waterloo, under the direction of P. Fritz and R.J. Drimmie. Relative to the PDB standard, it is GSC practice to normalize δ¹³C values on terrestrial organic materials and bones of all types to -25.0 ‰, whereas marine shells are normalized to 0.0 ‰ (Lowdon and Blake, 1970).

5   At IsoTrace all samples are normalized to -25.0 ‰, and all quoted errors are 68.3% confidence limits. Preparation of the machine-ready sample causes the fractionation of the sample material to vary systematically from the top to the bottom of the target. The computer analysis program uses the ¹³C/¹²C ratio obtained during the measurement, which is the product of this fractionation and the natural fractionation of the sample, to correct the ¹⁴C/¹²C ratio appropriately. While this procedure yields a highly reliable result for the ¹⁴C/¹²C ratio, at no time during the measurement is a value of the natural fractionation alone obtained (see IsoTrace Laboratory, 1984 Annual Report, 84.12.31, Chapter II.2, p. 31-64, Radiocarbon Analysis, by R.P. Beukens).

6   At IsoTrace each target is given 7 to 8 runs, and each run takes 22 minutes.

Figure 50.3. *Aerial view southeastward over the Cape Herschel peninsula, with Inglefield Land, Greenland, in the distance. Location of 'Moraine Pond' is indicated by the arrow, July 12, 1979. 201464-P*

whose surface is at an elevation of 83.0 m (above the level of the ice foot, as determined by an instrumental survey). As fragments of such rugged pelecypod species as **Hiatella arctica, Mya truncata,** and **Astarte borealis** are abundant in till all over the Cape Herschel peninsula, only thin and fragile shells of **Macoma calcarea** were used for dating. The result, on a 15.5 g sample, was 8190 ± 110 BP (GSC-2913).

In May 1981 a core of frozen sediment 5.85 m long was recovered from this shallow pond. This core was the longest taken from any site in the area, either of frozen pond sediment or unfrozen sediment from larger lakes (Blake, 1981, 1982a). Fragments of **Macoma calcarea** and other marine shells were noticed in the cuttings brought to the surface when coring was under way, and their presence was the first indication that a marine sand had been penetrated. Later, in the laboratory, fragments of marine shells were recovered as selected increments of the core were melted (Fig. 50.4). A hinge fragment (115.6 mg) of **Clinocardium ciliatum,** like **Macoma calcarea** a fragile pelecypod, was extracted from the core at a depth of 532 cm. The age of this fragment, weighing only 104.0 mg after pretreatment, was determined to be 8510 ± 50 BP (TO-115; Table 50.1).

This date shows that the sea was able to penetrate to the north side of Cape Herschel peninsula a little earlier than had been indicated by the previous determination (GSC-2913; 8190 ± 110 BP). The value obtained for TO-115 also indicates that the upper part of the marine sand unit (the marine sand extends from 415 to 585 cm in the core) is presumably comparable in age to the unit from which the surface shells derive. The basal organic material in the core, from the interval 406 to 414 cm, is 7300 ± 110 years old (GSC-3970; Table 50.1).

Figure 50.4. *Detail of the **Clinocardium ciliatum** shell fragment in stony sand at 532 cm depth in the 1981 core (7.5 cm diameter) of frozen sediment from 'Moraine Pond' at Cape Herschel. 201464-J*

427

The third site is Proteus Lake on Pim Island (Fig. 50.1, 50.5). A sample of aquatic moss at the base of the 50 cm-thick organic sequence gave an age of 8970 ± 190 years (GSC-2934; Blake, 1981; Hyvärinen, 1985). To obtain this age determination by conventional decay counting, it was necessary to use a 5 cm-thick increment, i.e., the entire thickness of the basal moss layer in a core collected in June 1979. A certain amount of time was necessary for the moss layer to build up to a thickness such that it would compress to a thickness of 5 cm under the load of the overlying organic lake sediments. Hence, for the accelerator a 0.5 cm-thick slice (utilizing only the central part of a core taken in June 1981) provided 118.2 mg of dry moss from immediately above the grey inorganic sediment of which the bottom 37 cm of the core is composed (Fig. 50.6). The new age determination, 9370 ± 110 years (TO-111), on a sample weighing only 21.2 mg after pretreatment, provides a much closer approximation for the onset of organic accumulation in Proteus Lake. At the time of writing this date is the oldest obtained from the basal organic sediment in any pond or lake in east-central Ellesmere Island.

Figure 50.5. *Aerial view northeastward at Proteus Lake (elevation 390 m), Pim Island. The coring site was located in the northern part of the lake (approximate position indicated by the arrow). There is still only a moat of open water around the edges of the lake when the photograph was taken on July 19, 1983. 201464-R*

Figure 50.6. *Detail of the moss layer at the base of the organic sequence in Proteus Lake. Sample BS-81-30 (core 7) was taken on June 10, 1981 under 25 cm of snow, 286 cm of ice, and in a water depth of approximately 5 m. The increment from 52.5 to 53.0 cm depth (arrow) was used for radiocarbon age determination TO-111, 9370 ± 110 years. 201464-Q*

Summary

These three examples give an indication of the great promise of the AMS dating method. There are obviously many applications. For example, marine geologists will be able to obtain ages on milligram-sized samples of foraminifera extracted from ocean-bottom cores; archeologists will be able to date irreplaceable artifacts or miniscule pieces of charcoal; and Quaternary geologists will be able to utilize individual shells, twigs, needles, leaves, fecal pellets, or tiny bone samples.

The capability of dating small samples, as demonstrated in the case of the MacMillan Glacier shells reported here, will permit the elimination of the perennial problem of mixing materials of different ages. Much greater precision can be achieved in dating pollen peaks or zone boundaries in lake sediment cores, for it will now be possible to determine the age of an organic-rich sediment slice only a millimetre or two in thickness, instead of 5 cm or even 10 cm. By way of contrast, in the early days of radiocarbon dating, on occasion it was necessary to use much longer increments. For example, in an early palynological study of lake sediments in central Labrador – Nouveau Québec (Grayson, 1956), 30 cm-long increments of the basal sediment were required for dating, and the resultant dates, of Holocene age, still had error terms of several hundred years.

References

Bennett, C.L., Beukens, R.P., Clover, M.R., Gove, H.E., Liebert, R.B., Litherland, A.E., Purser, K.H., and Sondheim, W.E.
1977: Radiocarbon dating using electrostatic accelerators: negative ions provide the key; Science, v. 198, p. 508-510.

Blake, W., Jr.
1978: Coring of Holocene pond sediments at Cape Herschel, Ellesmere Island, Arctic Archipelago; in Current Research, Part C, Geological Survey of Canada, Paper 78-1C, p. 119-122.

1981: Lake sediment coring along Smith Sound, Ellesmere Island and Greenland; in Current Research, Part A, Geological Survey of Canada, Paper 81-1A, p. 191-200.

1982a: Coring of frozen pond sediments, east-central Ellesmere Island: a progress report; in Current Research, Part C, Geological Survey of Canada, Paper 82-1C, p. 104-110.

Blake, W., Jr. (cont.)
1982b: Geological Survey of Canada radiocarbon dates XXII; Geological Survey of Canada, Paper 82-7, 22 p.

1984a: Post-Hypsithermal advance of Leffert Glacier, Ellesmere Island, Arctic Canada; American Quaternary Association (AMQUA), 8th Biennial Meeting (Boulder, Colorado, 1984), Program and Abstracts, p. 14.

1984b: Geological Survey of Canada radiocarbon dates XIV; Geological Survey of Canada, Paper 84-7, 35 p.

Doucas, G., Garman, E.F., Hyder, H.R.McK., Sinclair, D., Hedges, R.E.M., and White, N.R.
1978: Detection of ^{14}C using a small van de Graaff accelerator; Nature, v. 276, p. 253-255.

Dyck, W.
1967: The Geological Survey of Canada radiocarbon dating laboratory; Geological Survey of Canada, Paper 66-45, 45 p.

Grayson, J.F.
1956: The postglacial history of vegetation and climate in the Labrador-Quebec region as determined by palynology; unpublished Ph.D. dissertation, University of Michigan, Ann Arbor, 252 p.

Gribbin, J.
1979: Extending the radiocarbon calendar; New Scientist, v. 83, p. 98-100.

Haynes, C.V.
1978: Applications of radiocarbon dating with accelerators to archaeology and geology; in Proceedings of the First Conference on Radiocarbon Dating with Accelerators, ed. H.E. Gove; University of Rochester, Rochester, New York, p. 276-288.

Hyvärinen, H.
1985: Holocene pollen stratigraphy of Baird Inlet, east-central Ellesmere Island, arctic Canada; Boreas, v. 14, p. 19-32.

Litherland, A.E.
1984: Accelerator mass spectrometry; Nuclear Instruments and Methods in Physics Research, v. B5, p. 100-108.

Lowdon, J.A.
1985: The Geological Survey of Canada radiocarbon dating laboratory; Geological Survey of Canada, Paper 84-24, 16 p.

Lowdon, J.A. and Blake, W., Jr.
1970: Geological Survey of Canada radiocarbon dates IX; Radiocarbon, v. 12, p. 46-86.

Muller, R.A.
1977: Radioisotope dating with a cyclotron; Science, v. 196, p. 489-494.

Nelson, D.E., Korteling, R.G., and Stott, W.R.
1977: Carbon-14: direct detection at natural concentrations; Science, v. 198, p. 507-508.

Possnert, G. and Olsson, I.U.
1984: First Nordic colloquium on accelerators and dating, March 11th-12th, 1983; Boreas, v. 13, p. 365-375.

Smol, J.P.
1983: Paleophycology of a high arctic lake near Cape Herschel, Ellesmere Island; Canadian Journal of Botany, v. 61, p. 2195-2204.

Stuiver, M.
1978: Carbon-14 dating: a comparison of Beta and ion counting; Science, v. 202, p. 881-883.

Depressions in the bottom of Lac Megantic, Quebec - probable stagnant ice features

A.C.L. Larocque
Terrain Sciences Division

Abstract

Subbottom surveys using a low frequency acoustic profiler have been carried out on Lac Mégantic. The profiles reveal three acoustic units which have been interpreted as follows: 1) till and/or bedrock; 2) laminated proglacial lake sediment; and 3) organic sediment with a clastic component. The subbottom profiles intersect depressions, which are as deep as 20 m, in the upper two units. These depressions are thought to be partially filled kettle holes which formed when blocks of stagnant glacier ice prevented deposition of proglacial sediments; the ice was later removed by flotation and/or in situ melting. Kettles were partially or completely filled by proglacial and Holocene sediment during subsequent sedimentation.

Résumé

Des sondages sous-lacustres par profileur acoustique à basses fréquences ont été exécutés au lac Mégantic. Les profils mettent en évidence trois unités acoustiques que l'on interprète ainsi: 1) till ou socle rocheux, ou les deux; 2) sédiments laminés de lac proglaciaire; et 3) sédiments organiques avec une composante clastique. Les profils sous-lacustres rencontrent des dépressions qui atteignent 20 m de profondeur dans les deux unités supérieurs. On croit qu'il s'agit de dépressions glaciaires (kettles) partiellement comblées et dues à la présence de blocs de glacier stagnant à l'emplacement desquels les sédiments proglaciaires ne pouvaient se déposer; ces blocs auraient par la suite été délogés par flottation ou fusion sur place, ou les deux, laissant des creux qu'une sédimentation ultérieure a partiellement comblés de matériaux proglaciaires et holocènes.

Figure 51.1. *Approximate ice front position during formation of the Ditchfield Moraine complex. Raised delta is related to the 430 m proglacial lake which covered the Lac Mégantic basin. Ice front position and surficial deposits taken from Shilts (1981, Fig. 34, 51). Note locations of depressions and buried depressions in Lac Mégantic.*

Introduction

In June 1982 and July 1984 subbottom profiling was carried out on Lac Mégantic in the Eastern Townships of Quebec (Fig. 51.1) using a Raytheon RTT-1000 low frequency subbottom profiling system. Survey techniques, results of previous studies, and application of subbottom surveys have been discussed by Shilts et al. (1976), Klassen and Shilts (1982), Shilts and Farrell (1982), and Shilts (1984). Klassen and Shilts (1982) described coring and comparative studies which serve as the basis for interpretation of sonar records. This paper describes briefly some features observed in subbottom profiles of Lac Mégantic and discusses the processes which may have led to their formation. The features include depressions, buried depressions, and faults in sediments in the central part of the lake basin.

Bedrock and glacial geology of the Lac Mégantic basin

Lac Mégantic is approximately 15 km long, up to 4 km wide, and has an elevation of 395 m a.s.l. It occupies a deep bedrock basin, with more than 80 m of closure in places. The lake cuts across northeast-striking, steeply dipping Paleozoic metasediments (Lord, 1938; Marleau, 1968). The north end of the lake is underlain by slates and sandstones of the Compton Formation. The central part of the lake is underlain by Frontenac Formation quartzites and slates interbedded with greenstones. The greenstones form a prominent northwest facing escarpment along the south side of Rivière Victoria valley. The south end of the lake is underlain by granite (Marleau, 1968).

Figure 51.3 (below)

Profile 84-12 across north end of Lac Mégantic. A few metres of acoustically transparent material (organic sediment) overlies horizontally laminated clastic sediment which is relatively undisturbed. Note multiple reflection of bedrock surface (1), clastic sediment within organic layer (2), and 200 kHz reflection (3).

Figure 51.2. Subbottom profiles obtained from Lac Mégantic in 1982 and 1984. Heavy lines indicate profiles which appear in this paper as figures.

Figure 51.4. Profile 82-23 across south end of Lac Mégantic. No depressions are present but sediment is offset along normal fault (arrow). Fault may have been caused by letdown of sediment over a thin layer of melting ice or by compaction of sediment.

Figure 51.5. Profile 84-31 intersects depression with continuous layers of laminated sediment draping it. Profile also intersects buried depression (1). Hummocky surface deposit (2) at left end of profile is a modern sediment slump. Note parallel reflectors near sediment surface indicating a large clastic component in the modern organic layer.

Several authors have described the late glacial history and surficial geology of southern Quebec (e.g., McDonald, 1969; Shilts, 1970, 1981; Lamarche, 1971, 1974; McDonald and Shilts, 1971; Gadd et al., 1972). In the Lac Mégantic area, several deltas near 430 m elevation provide evidence of a major proglacial lake dammed by ice which blocked modern outlets to the north. Two possible outlets for the proglacial lake were located to the south on the Quebec-Maine border (Shilts, 1981, Fig. 52). A strongly developed ice front position across Lac Mégantic is marked by the Ditchfield Moraine complex (Fig. 51.1). The major rivers that contributed sediment to the 430 m proglacial lake were Victoria, Bergeron, and Clinton (Fig. 51.1). Rivière Arnold was also a source of sediment but entered the high level lake several kilometres south of its present mouth and consequently contributed little sediment to the area of the basin covered by modern Lac Mégantic. The major sources of modern sediment are Victoria and Arnold rivers.

Results of profiling

Ninety traverses totalling approximately 250 km were carried out on Lac Mégantic (Fig. 51.2). Three distinct acoustic units can be seen in the subbottom profiles. The terminology used here to describe the types of reflectors which make up these units has been adapted in part from

Figure 51.6. *Profile 84-28 across middle of Lac Mégantic intersects typical depressions. Apparent crossing of reflectors (arrow) below the depression is actually a diffraction pattern caused by steeply dipping sediment surface. True relief of lake bottom is shown in the cross-section below the subbottom profile.*

Bally (1983). The term "draping" is used to describe layers of sediment which follow the contours of an underlying sediment or bedrock surface and may or may not represent an unconformable relationship.

The <u>lowest acoustic unit</u> is marked by a well defined irregular upper surface which commonly produces multiple reflections (Fig. 51.3). There is no penetration of the acoustic signal below this surface, which represents till or bedrock, or both. The surface is usually steeply dipping and can be traced to depths of over 80 m on some profiles. In the north end of the lake, the surface forms shallow, less steeply dipping benches (Fig. 51.3).

The <u>middle acoustic unit</u> comprises two types of reflectors. Both types are parallel or subparallel, but the lower reflectors are poorly defined and the upper ones are well defined. This unit represents laminated, fine grained clastic sediments. It is found throughout the lake basin and is more than 30 m thick in some areas. In the north end of

the lake, over 20 m of horizontal, undisturbed reflectors fill deep depressions, whereas less than 6 m of well defined reflectors drape the surface of bedrock benches (Fig. 51.3). Profile 82-23 from the south end of the lake intersects approximately 20 m of well defined horizontal reflectors (Fig. 51.4). The reflectors are offset, indicating the presence of a fault. Underlying poorly defined reflectors appear to be highly disrupted.

Profiles from the central, deepest part of the lake (between Baie Victoria and Pointe Dollard) intersect more than 30 m of well defined and poorly defined reflectors. They are generally horizontal but in some areas continuous reflectors drape depressions up to 20 m deep (Figs. 51.5, 51.6). Some profiles also intersect reflectors draped over shallow depressions, which are overlain by horizontal reflectors (Figs. 51.5). A profile across Baie Victoria shows horizontal parallel reflectors ending abruptly on one side of a depression, and dipping parallel reflectors on the other side

Figure 51.7. *Profile 84-18 across Baie Victoria intersects an apparent ice-contact face. Note growth faults (arrows) which have been attenuated by continued sedimentation. Dipping sediments at the left side of the profile are thought to be a distal facies of the raised delta at the mouth of Rivière Victoria.*

(Fig. 51.7; a subbottom profile of a similar feature can be seen in Shilts, 1984, Fig. 76.1). The horizontal reflectors in Figure 51.7 are offset in several places indicating the presence of faults. Profile 84-37 (Fig. 51.8) is oriented parallel to the long axis of the lake and intersects many depressions similar to those in Figures 51.5 and 51.6.

The upper unit is acoustically transparent to the low frequency signal. Its upper surface is marked by the reflection from a 200 kHz signal (Fig. 51.3). This unit is at least 4 m thick and is found overlying the middle unit throughout the lake basin. It is interpreted as watery organic sediment deposited largely after Lac Mégantic had drained to its present level. In the central part of the lake, this unit contains horizontal reflectors, indicating that the organic layer has a major clastic component (Figs. 51.5, 51.6).

At least 34 depressions and buried depressions in the central part of Lac Mégantic (Fig. 51.1) are evident from the subbottom profiles. The depressions are up to 20 m deep and 250 m across and are variable in outline. They do not form a continuous trench but are closed and isolated. A bathymetric map of Lac Mégantic (Ministère des richesses naturelles du Québec, 1977) also shows closed-contour depressions in the same general locations as Figure 51.1.

Interpretation and discussion of results

The horizontal well defined reflectors observed in subbottom profiles are interpreted as laminated proglacial lake sediment. This interpretation is based on comparison with subbottom records from other lakes, coring to bedrock through similar sequences, and the fact that laminated silty clay is found, although rarely, onshore around the south end of the lake (Shilts, 1981). Underlying poorly defined reflectors are also interpreted as proglacial lake sediment. The transparency of these reflectors is probably caused by the loss of energy of the acoustic signal in the thick overlying sediments.

The acoustically transparent upper unit is interpreted as watery organic Holocene sediment. It is has a large clastic component, especially in the central part of the lake where profiles show the presence of horizontal reflectors near the sediment surface. The presence of clastic material makes it difficult to determine accurately the thickness of organic sediment from the subbottom profiles. It is possible that relatively thick Holocene sediments overlie the proglacial sediments. For example, organic detritus from the bottom of a 9 m core with significant clastic component from nearby Lac aux Araignées has been dated at 10 700 ± 310 BP (GSC-1353, Lowdon and Blake, 1979; Mott in Shilts, 1981).

Figure 51.8. *Profile 84-37 oriented parallel to the long axis of the lake, intersects many depressions and buried depressions (arrows). Hummocky surface deposit at the end of the profile is a modern sediment slump (1).*

The depressions in the central part of Lac Mégantic are thought to be kettle holes which have been draped with proglacial and modern sediment. The kettles formed when blocks of stagnant glacier ice, which were surrounded by and possibly buried under early proglacial lake sediment, either melted or floated to the surface. Evidence of sublacustrine buried ice has been documented by Gustavson (1975a) and by Shaw (1977). Gustavson (1975a) proved the existence of stagnant glacier ice buried under proglacial sediments in proglacial Malaspina Lake, Alaska, by coring through sediments into ice. He also observed floating icebergs covered with laminated proglacial sediments. Shaw (1977) described exposed terraces of laminated proglacial sediment in Okanagan Valley in British Columbia at elevations over 400 m a.s.l. He proposed that such terraces represent a former proglacial lake bed, part of which collapsed when underlying ice melted. He also proposed that lacustrine sediments at greater elevations than the major terrace were deposited in small lakes ponded between ice and the valley sides. When the ice melted, terraces with ice-contact faces remained.

Gustavson (1975b) has shown that turbidity currents entering Malaspina Lake from surface streams or from englacial or subglacial tunnels flowed to the lowest available depressions in the lake. Deposition of proglacial sediments took place as the turbidity currents slowed. Sedimentation in proglacial Lac Mégantic likely occurred in a similar manner. Stranded blocks of ice created topographic highs on the lake floor. Meltwater issuing from the ice front flowed as turbidity currents into the low areas around the blocks of ice. Ice would subsequently have been removed, creating an "ice-block cast" (Shilts, 1984). The pattern of sedimentation in Lac Mégantic was probably as complex as that in Malaspina Lake: "Sites of deposition changed as basins filled, as buried stagnant ice melted and made new basins available, and as the ice front retreated northward and made newer deeper basins available." (Gustavson, 1975a, p. 452).

Formation of the depressions in Lac Mégantic was likely initiated by the deposition of laminated proglacial lake sediments around and possibly over isolated blocks of stagnant glacier ice. Two possible mechanisms for ice removal will be discussed here. The first is that blocks of ice floated to the surface, creating a depression in the surrounding sediment. Continued proglacial sedimentation caused laminated sediments to be draped over the ice-contact faces with angular unconformity. Any sediment overlying the floating ice would have been suspended in the lake as the ice melted. Another possible mechanism for ice removal is in situ melting of the stranded ice blocks. Melting of stagnant ice and deposition of laminated sediments may have occurred contemporaneously. As a result, sediment draped in continuous layers over ice blocks and previously deposited sediments would have been deformed as the ice melted. This deformation would have consisted of faulting and folding associated with compressive stresses, as described by Klassen and Shilts (1982, p. 380-381). Successive layers of sediment would have been disrupted similarly until the ice had melted completely; continuous layers of undeformed proglacial and modern sediment were then draped over the depression. It should be noted that one mechanism does not necessarily preclude the other, and certain features may be associated with either process. For example, removal of ice by either melting or flotation could be expected to produce slumping on the ice-contact face and faults in the marginal sediments. The profile in Figure 51.7 intersects an apparent ice-contact face with growth faults which have been attenuated by continued sedimentation.

The models presented above are simplified and do not take into account factors such as thickness of ice, rate of ice melt, amount of sediment overlying the ice (if any),

and rate, amount, and source of sediment supply. The variety of contributing factors has resulting in the formation of several different types of depressions which may all be related to removal of ice blocks. For example, the profiles in Figures 51.5 and 51.6 intersect deep depressions draped with continuous layers of sediment as described specifically above. Some profiles also intersect shallow buried depressions (Figs. 51.5, 51.8) which probably formed when smaller blocks of stagnant ice were removed early during deposition of the laminated sediments. The depressions were then filled in during subsequent sedimentation. Profile 84-18 (Fig. 51.7) intersects one apparent ice-contact face that was not overlain unconformably by laminated sediments as described above. The other side of the depression is draped by laminated sediments. This probably reflects two periods of sedimentation. The horizontally laminated ice-contact sediments were deposited first between the north side of Baie Victoria and ice which occupied the other half of the bay. The dipping laminated sediments have not been deformed and appear to contain primary sedimentary structures. They are thought to have been deposited after the ice melted, and are possibly a distal facies of the raised proglacial delta at the mouth of Rivière Victoria (Fig. 1, from Shilts, 1981). The proportions of the sediment fill related to the modern delta and to the proglacial delta are not known. In any case, the sediments appear to have been deposited preferentially in the deep depression close to the source and did not cover the ice-contact sediments. If the dipping sediments are a distal facies of the raised delta, it would indicate that the ice block melted before the proglacial lake drained.

One of several other explanations for formation of the depressions is erosion by lateglacial or postglacial currents. This is unlikely, however, because the depressions are closed (Fig. 51.1), and in most cases continuous layers of fine grained sediment drape the depression rather than being cut. In light of Gustavson's work (1975a, b), nondeposition of proglacial sediments caused by the presence of stagnant blocks of ice remains the most probable explanation for formation of the depressions in Lac Mégantic.

Summary and conclusions

Several authors (Gustavson, 1975a; Shaw, 1977) have provided direct evidence of buried glacier ice in modern and Pleistocene proglacial lakes. Subbottom profiles from Lac Mégantic reveal a series of depressions in the central deeper part of the lake basin. The depressions are interpreted as having formed when blocks of stagnant ice that which were surrounded by and possibly buried under laminated proglacial sediments were removed. Removal may have been accomplished by flotation or melting. Either or both of the mechanisms may have created the depressions which were later draped unconformably with proglacial and/or Holocene sediments. The size and distribution of the depressions may have been determined by a number of factors such as thickness of ice, rate of ice melt, and source of sediment supply. It may also be significant that the depressions occur only beneath the area which was covered by a lobe of ice during the formation of the Ditchfield Moraine complex.

Acknowledgments

References

Bally, A.W. (editor)
1983: Seismic expression of structural styles – a picture and work atlas; American Association of Petroleum Geologists, Studies in Geology Series no. 15, v. 1.

Gadd, N.R., McDonald, B.C., and Shilts, W.W.
1972: Deglaciation of southern Quebec; Geological Survey of Canada, Paper 71-47, 19 p.

Gustavson, T.C.
1975a: Bathymetry and sediment distribution in proglacial Malaspina Lake, Alaska; Journal of Sedimentary Petrology, v. 45, no. 2, p. 450-461.

1975b: Sedimentation and physical limnology in proglacial Malaspina Lake, southeastern Alaska; in Glaciofluvial and Glaciolacustrine Sedimentation, ed. A.V. Jopling and B.C. McDonald; Society of Economic Paleontologists and Mineralogists, Special Publication 23, p. 249-263.

Klassen, R.A. and Shilts, W.W.
1982: Subbottom profiling of lakes of the Canadian Shield; in Current Research, Part A, Geological Survey of Canada, Paper 82-1A, p. 375-384.

Lamarche, R.Y.
1971: Northward moving ice in the Thetford Mines area of Southern Quebec; American Journal of Science, v. 271, p. 383-388.

1974: Southeastward, northward, and westward ice movement in the Asbestos area of southern Quebec; Geological Society of America Bulletin, v. 85, p. 465-470.

Lord, C.S.
1938: Mégantic Sheet (west half), Frontenac County, Quebec; Geological Survey of Canada, Map 379A, scale 1 inch to 1 mile.

Lowdon, J.A. and Blake, W., Jr.
1979: Geological Survey of Canada radiocarbon dates XIX; Geological Survey of Canada, Paper 79-7, 58 p.

Marleau, R.A.
1968: Woburn - East Mégantic - Armstrong area, Frontenac and Beauce Counties; Quebec Department of Natural Resources, Geological Report 131, 55 p.

McDonald, B.C.
1969: Surficial geology of La Patrie-Sherbrooke area, Quebec, including Eaton River watershed; Geological Survey of Canada, Paper 67-52, 21 p.

McDonald, B.C. and Shilts, W.W.
1971: Quaternary stratigraphy and events in southeastern Quebec; Geological Society of America Bulletin, v. 82, p. 683-698.

Ministère des richesses naturelles du Quebec
1977: Courbes bathymétriques du Lac Mégantic; Ministère des richesses naturelles, Direction générale des eaux, service des relevés.

Shaw, J.
1977: Sedimentation in an alpine lake during deglaciation, Okanagan Valley, British Columbia, Canada; Geografiska Annaler, v. 59A, p. 221-240.

Shilts, W.W.
1970: Pleistocene geology of the Lac Mégantic region, southeastern Quebec, Canada; unpublished Ph.D. dissertation, Department of Geology, Syracuse University, 154 p.

1981: Surficial geology of the Lac Mégantic area, Quebec; Geological Survey of Canada, Memoir 397, 102 p.

1984: Sonar evidence for postglacial tectonic instability of the Canadian Shield and Appalachians; in Current Research, Part A, Geological Survey of Canada, Paper 84-1A, p. 567-579.

Shilts, W.W. and Farrell, L.E.
1982: Subbottom profiling of Canadian Shield lakes – implications for interpreting effects of acid rain; in Current Research, Part B, Geological Survey of Canada, Paper 82-1B, p. 209-221.

Shilts, W.W., Dean, W.E., and Klassen, R.A.
1976: Physical, chemical, and stratigraphic aspects of sedimentation in lake basins of the eastern arctic shield; in Report of Activities, Part A, Geological Survey of Canada, Paper 76-1A, p. 245-254.

Revised lithostratigraphy of the Cambro-Ordovician Saint John Group, southern New Brunswick - a preliminary report

Project 730044

R.K. Pickerill [1] and S.K. Tanoli [1]
Precambrian Geology Division

Abstract

The Cambro-Ordovician Saint John Group has historically been subdivided into eleven formations. The existing scheme is, however, inappropriate as many of the formations, particularly those of Middle Cambrian-Early Ordovician age, were distinguished on a biostratigraphic rather than lithostratigraphic basis. We suggest the sequence can be more appropriately subdivided into seven formations, each of which can be clearly and easily identified by the field geologist. The Lower Cambrian formations comprise, from base to top, the Ratcliffe Brook, Glenn Falls and Hanford Brook formations, all of which are retained from the previous nomenclature. The Middle Cambrian strata comprise the Forest Hills Formation (to replace the Fossil Brook, Porter Road and Hastings Cove formations) and Upper Cambrian strata and King Square Formation (to replace the Black Shale Brook and Narrows formations). The Early Ordovician strata are referred to as the Reversing Falls Formation (to replace the Navy Island and Suspension Bridge formations). Brief descriptions of each formation are given.

Résumé

Dans les travaux antérieurs, le groupe cambro-ordovicien de Saint John, dans le sud du Nouveau-Brunswick, est divisé en onze formations. Or, cette division se révèle inappropriée puisque nombre de ces formations, en particulier celles qui datent du Cambrien moyen et du début de l'Ordovicien, ont été distinguées suivant des critères biostratigraphiques plutôt que lithostratigraphiques. Selon les auteurs, il serait plus juste de diviser la séquence en sept formations, dont chacune peut être reconnue clairement et facilement par le géologue sur place. Le Cambrien inférieur comprend, de la base au sommet, les formations de Ratcliffe Brook, de Glenn Falls et de Hanford Brook, qui étaient toutes présentes dans l'ancienne nomenclature. Le Cambrien moyen est représenté par la formation de Forest Hills (qui remplace les formations de Fossil Brook, de Porter Road et de Hastings Cove), et le Cambrien supérieur par les formations de King Square (au lieu de la formation de Agnostus Cove) et de Silver Falls (substituée aux formations de Black Shale Brook et de Narrows). Le début de l'Ordovicien comprend la formation de Reversing Falls (qui remplace les formations de Navy Island et de Suspension Bridge). Chacune de ces formations est décrite succinctement.

---

[1] Department of Geology, University of New Brunswick, Fredericton, New Brunswick E3B 5A3

Introduction

In the Saint John area of southern New Brunswick, the Cambro-Ordovician Saint John Group of Matthew (1963) outcrops in four broadly defined geographic areas, one north and three south of the Kingston Peninsula (Fig. 52.1). These are, north of the Kingston Peninsula, (i) the Long Reach area 40 km north-northwest of Saint John, and south, (ii) the Loch Lomond – Garnett Settlement – Ratcliffe Brook area approximately 25 km northeast of Saint John, (iii) the Hanford Brook-Hammond River area approximately 50 km northeast of Saint John, and (iv) in and around the city of Saint John itself (Fig. 52.1). Currie (1984) has recently demonstrated that south of the Kingston Peninsula the group occurs in a series of en echelon basins that trend north-northeast whereas to the north they trend east-northeast. Internally the basins are intricately folded and, in the case of the southerly basins, are fault-bounded on their northwest side.

Since the pioneering work on the Saint John Group by Matthew in the late nineteenth and early twentieth centuries (e.g. Matthew, 1963, 1888, 1890, 1891, 1892, 1893, 1895a, b, 1908 etc.) the most comprehensive stratigraphic scheme has been that proposed by Hayes and Howell (1937) and subsequently adopted by Alcock (1938) in two important and detailed publications on the geology of the Saint John area. Unfortunately, as also noted by North (1971), Landing (1980), Pickerill (1982) and Currie (1984), Hayes and Howell (1937) essentially subdivided the strata above their three basal formations (= Lower Cambrian) on a biostratigraphic rather than lithostratigraphic basis. Thus, the so-called Middle Cambrian-Lower Ordovician formations of Hayles and Howell (1937) are improperly defined as they are based on paleontological studies of discontinuous outcrops of similar and broadly monotonous lithology. As such, many are not mappable units and are in contravention to all stratigraphic codes; one, the Black Shale Brook Formation, was even based on a single and even biostratigraphically uncertain locality (see below)!

Figure 52.1. Distribution of the Saint John Group (stippled) in the Saint John – Long Reach – Ratcliffe Brook/Hanford Brook areas of southern New Brunswick.

Subsequent workers (e.g. Yoon, 1970; Richards, 1971; Ruitenberg et al., 1979; Currie et al., 1981; Currie, 1984) have therefore had great difficulty in using the nomenclature as proposed by Hayes and Howell (1937) particularly in the absence of good faunal control. This is particularly relevant as many of the outcrops of the Saint John Group are unfossiliferous (Currie, 1984). Even where fossils are present it is necessary to be an experienced systematic palaeontologist to determine exactly where in the sequence the outcrop is located. Thus, more recent workers have utilized the recognizable Lower Cambrian formations but have included all overlying strata into "undivided Cambro-Ordovician Saint John Group" (e.g. Ruitenberg et al., 1979; Currie et al., 1981; Currie, 1984).

This report revises the nomenclature of Hayes and Howell (1937) into more adequately defined and mappable units. In doing so, because of historical precedence and rules of priority, we have retained their Lower Cambrian formations as these are easily recognizable and mappable. However, their Middle Cambrian-Early Ordovician divisions have been grouped into newly defined formations, and in a single case a formational name has been revised because of its original inappropriate etymology.

Although the results presented herein represent mapping in the Saint John area from 1982-84 inclusive, research is still continuing. Thus, while we regard our nomenclatural scheme as finalized we refrain from detailed descriptions of individual formations and their geographic distribution. Rather, herein we simply define our formational stratigraphy, briefly describe the essential characteristics of each formation noting the location of proposed stratotypes, and relate the nomenclatural scheme to that previously proposed by Hayes and Howell (1937) and Alcock (1938).

Location and brief history of research

In southern New Brunswick outcrops of the Cambro-Ordovician Saint John Group studied in detail thus far lie between 65°35'-66°16'W and 45°15'-45°30'N (map areas 21H/5 and 21G/8 – Fig. 52.1). In the late nineteenth and early twentieth centuries the strata were studied by many well-known geologists including Dawson, Bailey, Ells, Walcott and, of course, Matthew (see Hayes and Howell, 1937 for review). Many of these early studies were paleontological although there was also considerable debate on the age of the basal sediments (= Ratcliffe Brook Formation) as either Precambrian or Lower Cambrian, Walcott (1900) finally suggesting an Early Cambrian age (see also Patel, 1973, 1975). By far the most important contributions with respect to the early stratigraphic studies of the Saint John Group were those of Matthew (1863-1908). Although Matthew made continual revisions to his stratigraphic scheme over a number of years his "final" version was summarized in 1895, as represented in Table 52.1. Matthew's (1895a) scheme was simplified in the sense that no formal nomenclature was adopted and he subdivided the strata paleontologically into a number of "divisions" and "bands" (Table 52.1).

In 1937 Hayles and Howell subdivided the strata into a number of "formational" divisions, which were subsequently adopted by Alcock (1938). It is notable that several of the "formational" boudaries proposed by Hayles and Howell (1937) correspond to the paleontological "divisions" of Matthew (1895); nevertheless, some of their boundaries clearly do not (Table 52.1) and therefore, were presumably made more on a lithological rather than paleontological basis. Indeed, it is apparent from our own research that the scheme proposed by Hayles and Howell (1937) was in all probability made utilizing both lithological but more particularly paleontological criteria. In any event, such a scheme is in contravention to all existing stratigraphic codes.

The difficulties in applying the stratigraphic scheme of Hayes and Howell (1937) were clearly recognize in unpublished theses by both Yoon (1970) and Richards (1971) who were both unable to distinguish the majority of so-called formational units, even including the more easily recognizable basal formations (Table 52.1). Both these authors subdivided the group into a number of more simplified divisions, the boundaries of which, however, varied quite considerably (Table 52.1). Although we regard both these schemes as totally unsatisfactory and extremely over-simplified, they do serve to illustrate the inherent difficulties involved in the lithostratigraphic subdivision of the group.

Finally, as noted above, most recent mapping projects in the Saint John area (Ruitenberg et al., 1979; Currie et al., 1981; Currie, 1984) also failed to adopt the stratigraphic nomenclature of Hayles and Howell (1937) apart from the recognition of the Lower Cambrian formations. Middle Cambrian – Lower Ordovician formations were simply lumped as undivided Saint John Group, thus again reflecting the nomenclatural difficulties of the scheme of Hayes and Howell (1937).

Lithostratigraphy

We propose that within the Saint John Group seven formations can clearly be recognized in the field. From base to top of the group these comprise the Ratcliffe Brook, Glen Falls and Hanford Brook Formations of Early Cambrian age; the Forest Hills Formation of Middle Cambrian age and the Reversing Falls Formation of Early Ordovician age (Table 52.1). In the following description emphasis is placed on newly proposed or redefined formations; for those that are retained reference can be made to Hayes and Howell (1937) and Alcock (1938) for more detailed descriptions. Palaeontological details of individual formations may be obtained in the previously referenced papers by Matthew, in McLearn (1915) and in Hayes and Howell (1937).

Lower Cambrian

Ratcliffe Brook Formation (retained)

The Ratcliffe Brook Formation consists of up to 285 m of maroon, purple-red or grey-green conglomerate, sandstone, siltstone and shale which disconformable overlie unnamed redbed sequences of Eocambrian age and or, Precambrian volcanics of the Coldbrook Group (Tanoli et al., 1985). The stratotype is in Ratcliffe Brook, though the best and most continuously exposed section is in Hanford Brook (Fig. 52.1), proposed as the "paratype" by Hayes and Howell (1937, p. 58). Although the full range of lithologies is not present in all available surface outcrops, allocation to the formation is relatively straightforward because of the distinctive composition and coloration (Tanoli et al., 1985). Detailed descriptions of the formation may be found in Hayes and Howell (1937) and Alcock (1938) and references therein. Upper contact of the formation is typically transitional, more rarely sharp, but obviously conformable with the Glenn Falls Formation.

Glenn Falls Formation (retained)

The Glenn Falls Formation consists of approximately 5-15 m of fine- to more typically coarse-grained white, greenish white or rarely pink quartzite overlain by coarse grained black sandstone which is typically very thin. More rarely, pebbly quartzite and thin pebble conglomerate lenses and layers are present. Lower and upper boundaries are conformable but typically transitional over a thickness of approximately 1 m. The stratotype is at Glen Falls, northeast of Saint John (Fig. 52.1).

Hanford Brook Formation (retained)

The Hanford Brook Formation comprises up to 23 m of olive-grey to grey or dark grey fine grained sandstone and minor shale. Shale increases in abundance in the upper 5 m. The sandstone can easily be distinguished by the presence of glauconite, chamosite and phosphate nodules and by the presence of the bivalved crustaceans **Beyrichona** and **Hipponicharion**, which are otherwise absent within the Saint John Group. The stratotpye is in Hanford Brook (Fig. 52.1), though many additional exposures exist in the Saint John region (see Hayes and Howell, 1937). The lower contact is conformable but gradational with the Glenn Falls Formation; the upper contact is marked by the base of a thin but variable 'rotten' limestone or fossiliferous calcareous shale of the Forest Hills Formation.

Middle Cambrian

Forest Hills Formation (new)

Stratotype. Cold Brook in the Glen Falls area, north-northeast of Saint John (45°19'05"N, 66°0'38"W). The best exposed and most complete section of the formation is present there; however, the descriptor Coldbrook has previously been utilized for the Precambrian Coldbrook Group volcanics and associated strata and therefore we have chosen Forest Hills, where the formation is also reasonably well-exposed (and is in the same area) as the most appropriate name. Additional exposures may be observed in Saint John itself along the exit of Highway 1, at Goodrich Street near the junction of Somerset Street and Winter Street, on the northeastern shore of Catons Island, on Long Island, in Ratcliffe Brook, in Hanford Brook and on Porter Road (Fig. 52.1).

Lithology. Basal fossiliferous calcareous grey shale or 'rotten' limestone with abundant disarticulated trilobite detritus, phosphate, chamosite and glauconite grains or nodules and shale clasts overlain by light grey or olive grey shale and then by dark or grey shale with thin and subordinate fine grained sandstone interbeds and fossiliferous lime-rich lenses. The basal layers were previously referred to by Hayes and Howell (1937) as the "Black Limestone" and are up to a maximum of 1.75 m thick, but are extremely distinctive.

Thickness. Variable but a maximum of approximately 45 m.

Lower boundary. Sharp, and represented by the 'rotten' limestones or fossiliferous calcareous grey shales which are interpreted to have been deposited during a depositional hiatus (cf. Hayes and Howell, 1937).

Upper boundary. Typically unexposed (see Hayes and Howell, 1937) but considered gradational and conformable with the overlying King Square Formation, the basal beds of which contain an increased proportion of thinly bedded fine grained sandstone relative to shale.

Table 52.1. Stratigraphy of the Cambro-Ordovician Saint John Group of southern New Brunswick, 1895-present.

Author		Matthew 1895			Hayes + Howell 1937, and Alcock 1938	Yoon 1970	Richards 1971	This Article	
	AGE	SERIES		BANDS	FORMATIONS	UNITS	FORMATIONS	FORMATIONS	AGE
SAINT JOHN GROUP	L.ORD.	Bretonian	DIVISION 3	Band d	Suspension Bridge	Upper Black Shale	Navy Island	Reversing Falls	L.ORD.
	U.CAMB.			Band c	Navy Island				U.CAMB.
				Band b	Narrows	Upper Sandstone		Silver Falls	
				Band a		Lower Black Shale			
		Johannian	DIVISION 2	Band c	Black Shale Brook		King Square	King Square	
				Band b	Agnostus Cove				
				Band a					
	M.CAMB.	Acadian	DIVISION 1	Band d	Hastings Cove	Lower Sandstone	Hanford Brook	Forest Hills	M.CAMB.
					Porter Road				
				Band c	Fossil Brook				
				Band b	Hanford Brook			Hanford Brook	
	L.CAMBRIAN			Band a	Glenn Falls		Glen Falls	Glen Falls	L.CAMBRIAN
		Etcheminian	DIVISION 0		Ratcliffe Brook	Redbed	Ratcliffe Brook	Ratcliffe Brook	
						Basal Conglomerate			

Remarks. This newly proposed formation comprises the Fossil Brook, Porter Road and Hastings Cove formations of Hayes and Howell (1937) and Alcock (1938) or Bands c and d, Division 1 of Matthew (1895a). Revision of the lighostratigraphy proposed by the former authors was considered necessary because:

(i) All three previously established formations are lithologically similar and were distinguished biostratigraphically mainly on the presence of different species of the Middle Cambrian trilobite **Paradoxides.** Even Hayes and Howell (1937) readily admitted (e.g. p. 72) that the boundaries between these formations were totally inter-gradational and could be distinguished by "an early recognizeable difference in fauna". What variation in lithology did exist was also present within each of the individual formations (e.g. Hayes and Howell, 1937, p. 71), and therefore the distinction between them is impossible unless faunal data are considered (cf. North, 1971).

(ii) All three formations are poorly exposed; indeed the Porter Road Formation is now only exposed in a small ditch on the southern side of Porter Road. Although Hayes and Howell (1937, p. 73) referred to a previous exposure on the southern bank of Hanford Brook, this is now covered. As such, this formation is not mappable, and in all probability never was even historically.

(iii) No stratotypes were originally designated for any of the three formations, merely locations where "fossils" could be collected.

(iv) Fossil Brook was supposedly a small tributary of Porter Brook (Hayes and Howell, 1937, p. 70) but all historical and existing maps do not name the small stream. As such, the name is inappropriate.

When combined, these observations suggest that a single, newly defined formation, herein termed the Forest Hills Formation, best describes and accommodates the previously established but erroneous lithostratigraphic nomenclature.

Exposures of the formation are few and are typically present in the lower few metres, where the 'rotten' limestones or fossiliferous calcareous shales may be observed. As briefly noted above, these 'rotten' limestones are believed to represent a depositional hiatus, similar to that previously reported between Lower and Upper Cambrian strata in Cape Breton and southeastern Newfoundland (see Hutchinson, 1962; Henningsmoen, 1969). Although the upper boundary is considered essentially gradational and conformable, there is a notable faunal gap between the Forest Hills and King Square formations (i.e. between the Middle and Upper Cambrian) similar to that observed, for example, in southeastern Newfoundland (see North, 1971). Whether or not this faunal break represents a sedimentological break or otherwise is, however, unknown at this time.

Upper Cambrian

King Square Formation (new)

Stratotype. The section exposed in King Square in the city of west Saint John, a small park bounded by Duke Street, Watson Street, Prince Street and Lancaster Street and overlooking the Saint John River just below Reversing Falls (Fig. 52.1, 52.2) (45°0'30"N, 66°04'40"W). The stratotype exposes approximately 80 m of the formation though upper and lower boundaries are unexposed. The formation is the most extensively exposed formation within the Saint John Group and many localities, too numerous to mention here, may be observed in Saint John as well as at Forest Hills, Loch Lomond Road, the Black River area, Ratcliffe Brook, Hammond River, Kennebecasis Bay and in the Long Reach (Fig. 52.1).

Lithology. Thinly interbedded (2-10 cm) grey fine grained sandstone (weathering pink to buff) and black and grey micaceous shale and siltstone passing upward into thicker bedded sandstone (20-70 cm) with a decreased proportion of interbedded shale and siltstone and in turn into thinly interbedded (5-20 cm) fine grained sandstone and extensively bioturbated shale and siltstone. Sandstones exhibit a variety of sedimentary structures including parallel lamination, ripple cross-lamination, wave- and current-formed symmetric and asymmetric ripples, interference and linguoid ripples, flute marks, ball and pillow structures and slump structures. Minor limestone nodules and lenses are sporadically developed.

Thickness. Variable, up to a maximum of 380-400 m.

Lower boundary. (see above – Forest Hill Formation).

Upper boundary. The upper boundary with the overlying Silver Falls Formation is only exposed on Little River in the Silver Falls area, at the falls itself (Fig. 52.1), where the contact is faulted but essentially conformable. Otherwise the upper boundary is only assumed to be conformable, though mapping would suggest this is the case.

Remarks. This newly proposed formation is equivalent to the Agnostus Cove Formation of Hayes and Howell (1937) and Alcock (1938) or Bands a and b and the lower part of c of Matthew's (1895a), Division 2. Revision of previous nomenclature was considered necessary because "Agnostus Cove" is not a geographic location. Instead, the formation was named based on the abundant trilobite **Agnostus** discovered in strata typical of the formation in a small unnamed cove on Long Island is Kennebecasis Bay (Fig. 52.1). Richards (1971) also noted this and informally proposed the descriptor King Square to replace the previous inappropriate nomenclature. We therefore follow Richards (1971) and formally revise the formation herein.

The King Square Formation is the most widely exposed, thickest, (excluding the Ratcliffe Brook Formation) and easily recognizeable formation within the Saint John Group. Thickness is variable but the estimate by Hayes and Howell (1937) as 200 feet is considered totally inappropriate. Maximum thickness is estimated from map extrapolation in the King Square area (Fig. 52.2) as between 380-400 m. Even single continuously exposed sections are up to 116 m, that is considerably greater than the estimate of Hayes and Howell (1937). Contained faunas are typically scarce apart from inarticulate brachiopods (particularly **Lingulella**), trace fossils and locally abundant medusoids (see Pickerill, 1982).

Silver Falls Formation (new)

Stratotype. On the northern bank of Little River at Silver Falls in the northeastern outskirts of Saint John (45°17'12"N, 66°01'02"W). There the stratotype exposes approximately 70 m (including a 7-8 m covered interval) though upper and lower contacts are unexposed. Additional exposures occur on the southwestern part of Navy Island, along the western bank of the Saint John River near the "Wharf Museum" at Reversing Falls and on Chesley Drive in Saint John itself (Fig. 52.2). An exposure previously recently reported by Landing (1980) at Germaine Street is now covered.

Figure 52.2. Outcrop geology of the Reversing Falls – Navy Island district, city of Saint John.

Lithology. Dark grey or more typically black shale with rare and thin calcareous and fossiliferous interbeds and calcareous nodules and rare and thin fine grained sandstone typically less than 5 cm thick. At the stratotype the succession is structurally overturned but two divisions are clearly recognized; a lower 11 m of black shale and an upper ca. 59 m (including the 7-8 m covered interval) of black and grey shale with thin sandstone interbeds. These two divisions cannot clearly be recognized elsewhere, however, and are regarded as informal.

Thickness. Minimum of 70 m.

Lower boundary. (see above – King Square Formation).

Upper boundary. Unexposed but on Navy Island (Fig. 52.2) at least is considered gradational and conformable. Elsewhere, such as at Chesley Drive and on the north shore of the Saint John River near Suspension Bridge the upper contact is faulted.

Remarks. This newly proposed formation is equivalent to the Black Shale Brook and Narrows formations of Hayes and Howell (1937) and Alcock (1938) or the upper part of Band c, Division 2 and Bands a and b, Division 3 of Matthew (1895a). Revision of the previous nomenclature was considered necessary because:

(i) Black Shale Brook does not exist on any topogrpahic maps; it was merely a name designated by Hayes and Howell (1937) for a small brook west of Porter Road.

Figure 52.2

(ii) The Black Shale Brook Formation was established on the discovery of the trilobites **Homoagnostus obesus** and **Olenus** in loose float near this stream (Hayes and Howell, 1937, p. 78). The only outcrop on the stream was 25 feet of black shales which, incidentally, were unfossiliferous! No other location in the Saint John region was allocated with certainty to the formation, although several were suspected. As such, therefore, the formation is unmappable.

(iii) Search by both the present authors and Landing (1980, p. 755) has indicated that the previously mentioned exposure of shales no longer exists. Indeed, the only outcrops in the area belong to the King Square Formation as defined herein.

Because of these factors we have combined the two previous formations into a newly proposed Silver Falls Formation whose definition conforms to existing stratigraphic codes. We have chosen to introduce the new terminology rather than to expand the previous definition of the Narrows Formation in order to avoid potential confusion of future workers in the region.

The formation can easily be distinguished from the underlying King Square Formation by the presence of many wave- and current-rippled sandstone surfaces and heavily bioturbated shales in the latter which are not present in the Silver Falls Formation. Indeed, shales of the Silver Falls Formation are decidedly non-bioturbated. Distinction from shales of the overlying Reversing Falls Formation is more difficult but can be made using the following criteria: shales in the Reversing Falls Formation are carbonaceous, pyritiferous, graptolite-bearing, extremely fissile and are only slightly calcareous containing very few carbonate concretions. Landing et al. (1978) were unable to diferentiate the Navy Island and Narrows Formations (= Silver Falls and Reversing Falls Formations herein) lithologically, but we feel that using these criteria their distinction is perfectly feasible.

Thickness of the Silver Falls Formation is difficult to estimate because of generally poor exposure and complex structural problems. Nevertheless we regard the thickness of "several hundred feet" by Hayes and Howell (1937, p. 56) as an overestimate. Map interpolation would indicate a thickness of between 60-80 m. Contained faunas are typically scarce, restricted essentially to the thin calcareous and fossiliferous interbeds and or, calcareous nodules and are listed and or, described in Hayes and Howell (1937), and more recently by Landing et al. (1978) and Landing (1980).

Reversing Falls Formation (new)

Stratotype. Along the north shore of the Narrows at the upper end of Saint John Harbour below the intersection of Douglas Avenue and Chesley Drive (45°15'38"N, 66°05'W). The only additional exposures are also in Saint John at the western part of the shale exposure on Chesley Drive in front of the Ocean Steel Corporation Building and at the north-western tip of Navy Island below the Harbour Bridge (Fig. 52.2).

Lithology. Black, carbonaceous, fissile shale with common reduction spots and pyrite blebs and nodules. Calcareous nodules are extremely rare and graptolites are reasonably common, locally abundant.

Thickness. Minimum 50 m.

Lower boundary. (see above – Silver Falls Formation).

Upper boundary. Unobserved.

Remarks. This newly proposed formation is equivalent to the Navy Island and Suspension Bridge formations of Hayes and Howell (1937) and Alcock (1938) of Bands c and d, Division 3 of Matthew (1895a). Revision of the previous nomenclature was considered necessary because there is no lithologic distinction between the two previously proposed formations, merely a change in faunas (cf. Landing, 1980). We therefore include these distinctive but monothonous black shales in a single newly defined formation. Unlike the underlying formations of the Saint John Group this formation cannot be mapped regionally and instead, is only exposed in the Reversing Falls area (Fig. 52.2). However, we do suspect that the strata are present at least elsewhere in the city of Saint John and probably underlie the low-lying ground of the core of the Saint John Syncline (see Hayes and Howell, 1937; Richards, 1971). Whether or not the formation is present elsewhere in the region is unknown; however, the suggestion by Currie (1984) that the Saint John Group formed in a single relatively large basin would certainly favour its previously widespread distribution.

Distinction of the Reversing Falls Formation from the underlying Silver Falls Formation has been noted above. Faunal lists may be found in McLearn (1915), Hayes and Howell (1937), Landing et al. (1978) and Landing (1980).

Conclusions

The Cambro-Ordovician Saint John Group of southern New Brunswick is composed of approximately 890 m of conglomerate and dominantly sandstone and shale. Seven distinctive formations can be clearly recognized and easily utilized by the field geologist. Lower Cambrian formations include the basal Ratcliffe Brook Formation, comprising maroon, purple-red or grey-green conglomerate, sandstone and shale; the Glen Falls Formation, comprising white, greenish white or rarely pink quartzite, pebbly quartzite or pebble conglomerate; and the Hanford Brook Formation, comprising olive-grey to grey or dark grey fine grained sandstone and minor shale. These Lower Cambrian formations are retained from the previously established nomenclature of Hayes and Howell (1937) and Alcock (1938). The Forest Hills Formation, of Middle Cambrian age, comprises a basal fossiliferous calcareous grey shale or 'rotten' limestone overlain by grey or olive grey shale and dark shale with thin and subordinate fine grained sandstone interbeds. Upper Cambrian strata are subdivided into the King Square and Silver Falls Formations. The King Square Formation consists of interbedded fine grained sandstone beds exhibiting a wide variety of sedimentary structures. In contract to underlying and overlying formations, the shale and siltstone in this formation is commonly extensively bioturbated. The Silver Falls Formation consists of dark grey or black shale with rare and thin fine grained sandstone interbeds and calcareous nodules. Lower Ordovician strata are all included in the Reversing Falls Formation which comprises black, carbonaceous, pyritiferous, graptolitic shale. All Middle Cambrian-Lower Ordovician formations are newly proposed.

Acknowledgments

We thank Ismail Patel for joining us in the field on several occasions and for his active and animated discussion on the internal stratigraphy of the Saint John Group and Les Fyffe for reviewing the manuscript. Special thanks also go to Ken Currie for his co-operation and interest in this project and Tom Bolton who kindly gave advie on stratigraphic nomenclature. Technical assistance was provided by Paul Chenard, Bob McCulloch and Sherri Townsend.

References

Alcock, F.J.
1938: Geology of the Saint John Region, New Brunswick; Geological Survey of Canada, Memoir 216, 65 p.

Currie, K.L.
1984: A reconsideration of some geological relationships near Saint John, New Brunswick; in Current Research, Part A, Geological Survey of Canada, Paper 84-1A, p. 29-36.

Currie, K.L., Nance, R.D., Pajari, G.E., and Pickerill, R.K.
1981: Some aspects of the Pre-Carboniferous geology of Saint John, New Brunswick; in Current Research, Part A, Geological Survey of Canada, Paper 81-1A, p. 23-30.

Hayes, A.O. and Howell, B.F.
1937: Geology of Saint John, New Brunswick; Geological Society of America, Special Paper 5, 146 p.

Henningsmoen, G.
1969: Short account of Cambrian and Tremadocian of Acado-Baltic province; in North Atlantic — geology and continental drift, ed. M.Kay; American Association of Petroleum Geologists, Memoir 12, p. 110-114.

Hutchinson, R.D.
1962: Cambrian stratigraphy and trilobite faunas of southeastern Newfoundland; Geological Survey of Canada, Bulletin 88, 156 p.

Landing, E.
1980: Late Cambrian-early Ordovician macrofaunas and phosphatic microfaunas, St. John Group, New Brunswick; Journal of Paleontology, v. 54, p. 752-761.

Landing, E., Taylor, M.E., and Erdtmann, B.D.
1978: Correlation of the Cambrian-Ordovician boundary between the Acado-Baltic and North American faunal provinces; Geology, v. 6, p. 75-78.

Matthew, G.F.
1963: Observations on the geology of St. John county, New Brunswick; Canadian Naturalist, v. 8, p. 241-260.

1888: On the classification of the Cambrian rocks in Acadia; Canadian Record of Science, v. 3, p. 71-81.

1890: Illustrations of the fauna of the St. John Group, No. 5; Transactions of the Royal Society of Canada, v. 8, Section 4, p. 123-166.

1891: Illustrations of the fauna of the St. John Group, No. 6; Transactions of the Royal Society of Canada, v. 9, Section 4, p. 33-65.

1892: Illustrations of the fauna of the St. John Group, No. 7; Transactions of the Royal Society of Canada, v. 10, Section 4, p. 95-109.

1893: Illustrations of the fauna of the St. John Group, No. 8; Transactions of the Royal Society of Canada, v. 11, Section 4, p. 85-129.

1895a: The Protolenus fauna; Transactions of the New York Academy of Sciences, v. 14, p. 101-153.

1895b: Two new Cambrian Graptolites with notes on other species of Graptolitidae of that age; Transactions of the New York Academy of Sciences, v. 14, p. 262-273.

1908: Geological cycles in the Maritime provinces of Canada; Transactions of the Royal Society of Canada, v. 26, section 4, p. 121-143.

McLearn, F.H.
  1915:   The Lower Ordovician (Tetragraptus Zone) at
          St. John, New Brunswick, and the new genus
          Protistograptus; American Journal of Science,
          v. 40, Series 4, p. 49-59.

North, F.K.
  1971:   The Cambrian of Canada and Alaska; in Cambrian
          of the New World, ed. C.H. Holland; John Wiley &
          Sons Ltd., Toronto, p. 219-324.

Patel, I.M.
  1973:   Sedimentology of the Ratcliffe Brook Formation
          (Lower   Cambrian?)   in   southeastern   New
          Brunswick; Geological Society of America,
          Abstracts with Programs, v. 5, p. 206.

  1975:   The Precambrian-Cambrian boundary in southern
          New Brunswick; Geological Society of America,
          Abstracts with Programs, v. 7, p. 104.

Pickerill, R.K.
  1982:   Cambrian Medusoids from the St. John Group,
          southern New Brunswick; in Current Research,
          Part B,   Geological · Survey   of   Canada,
          Paper 82-1B, p. 71-76.

Richards, N.A.
  1971:   Structure in the Precambrian and Paleozoic rocks
          at Saint John, New Brunswick; unpublished M.Sc.
          thesis, Carleton University, Ottawa, Ontario,
          73 p.

Ruitenberg, A.A., Giles, P.S., Venugopal, D.V.,
Buttimer, S.M., McCutcheon, S.R., and Chandra, J.
  1979:   Geology and mineral deposits, Caledonia area;
          Mineral   Resources   Branch,   New Brunswick
          Department of Natural Resources and Canada
          Department of Regional Economic Expansion,
          Memoir 1, 213 p.

Tanoli, S.K., Pickerill, R.K., and Currie, K.L.
  1985:   Distinction of Eocambrian and Lower Cambrian
          redbeds, Saint John area, southern New
          Brunswick;   in Current   Research,   Part A,
          Geological Survey of Canada, Paper 85-1A,
          p. 699-702.

Walcott, C.D.
  1900:   Lower Cambrian terrane in the Atlantic Province;
          Proceedings of the Washington Academy of
          Sciences, v. 1, p. 301-339.

Yoon, T.
  1970:   The Cambrian and Lower Ordovician stratigraphy
          of the Saint John area, New Brunswick;
          unpublished M.Sc. thesis, University of New
          Brunswick, Fredericton, New Brunswick, 92 p.

Use of multiple regression for petrophysical characterization of granites as a function of alteration

Project 690038

F.P. Agterberg, T.J. Katsube [1], and S.N. Lew
Economic Geology and Mineralogy Division

Abstract

Micropores of crystalline rocks potentially contribute to retarding the migration of radionuclides. In this paper the relation between porosity and formation factor (bulk rock resistivity over pore water resistivity) is statistically analyzed by multiple regression using dummy variables. The results show that a linear relationship exists between porosity and the reciprocal of the formation factor. It is also shown that pocket porosity first increases and later decreases with increasing degree of alteration. The tortuosity initially remains constant but becomes larger when the granites considered reach their highest degree of alteration. The average formation factor increases with the progress of alteration. These trends indicate the effect that alteration has on the pore structure.

Résumé

Les micropores des roches cristallines pourraient contribuer à retarder la migration des radionucléides. Dans le présent rapport, la relation entre la porosité et le facteur de formation (résistivité de la roche sur résistivité de l'eau interstitielle) est analysée statistiquement par régression multiple sur des variables simulées. Les résultats indiquent qu'il existe une relation linéaire entre la porosité et la réciproque du facteur de formation. Ils démontrent également que la porosité des poches commence par s'accroître pour ensuite diminuer avec l'augmentation du degré d'altération. Constante au début, la tortuosité augmente lorsque les granites considérés atteignent leur maximum d'altération. Le facteur de formation moyen s'accroît à mesure que progresse l'altération. Ces rapports donnent une idée des effects de l'altération sur la structure poreuse de la roche.

---

[1] Resource Geophysics and Geochemistry Division

Introduction

A study of the pore structure of crystalline rocks is being carried out under the Canadian Nuclear Fuel Waste Management Program. This is due to the potential for micropores to contribute to retarding the migration of radionuclides (Agterberg et al., 1984; Katsube and Kamineni, 1983). Porosity and formation factor (bulk electrical resistivity of the rock over pore fluid electrical resistivity) are important parameters used to characterize the pore structure. It is well known that the following empirical relationship exists between the formation factor (F) and porosity (ϕ) (Schlumberger, 1972),

$$F = a \phi^{-n} \tag{1}$$

The symbols a and n are coefficients that vary according to rock type. Equation (1) is known as the Archie formula (Archie, 1942). Various physical models have been proposed to explain this relationship, but none of them are totally satisfactory. Katsube et al. (1985) indicated that if the existence of pocket pores is considered in the tortuosity model commonly used to describe pore structure in crystalline rocks (Wadden and Katsube, 1982; Katsube and Kamineni, 1983; Walsh and Brace, 1984), as shown in Figure 53.1a, then the following relationship should exist between the effective porosity (ϕ_E) and formation factor,

$$\phi_E = \phi_P + \tau^2 (1/F) \tag{2}$$

where

ϕ_P = pocket porosity
τ = tortuosity

The effective porosity is the sum of the porosity of all interconnected pores. Isolated pores are excluded. The tortuosity is a parameter indicating how tortuous a pore is, and is larger than unity. If it is assumed that τ is constant, then equation (2) indicates that a linear relationship should exist between ϕ_E and $1/F$ (Fig. 53.1b).

The effective porosity and formation factor have been determined for 152 granitoid core samples. Katsube et al. (1985) showed that when ϕ_E is plotted against $1/F$ as in Figure 53.2, there is a general trend suggesting that τ is constant. This suggestion, however, could not be confirmed previously due to the scatter of the data. One of the main reasons for the scatter appears to be the difference in the degree of alteration. It was also proposed that τ and ϕ_P are constant within a group of rocks with similar degrees of alteration, but vary when the degree of alteration varies. However, this also could not be confirmed because of the scatter of the data. Consequently, the multiple regression analysis method was applied to determine, (1) whether τ can be considered constant and a linear relationship exists between ϕ_E and $1/F$, and (2) whether τ and ϕ_P vary with the degree of alteration. This paper discusses the results of this multiple regression analysis.

Description of data

The effective porosity is determined by measuring the difference in mass between vacuum-saturated and oven-dried rock samples. The formation factor is determined by taking the ratio of the bulk electrical resistivity of the rock sample to the electrical resistivity of the pore water for five different concentrations of pore water. The samples are 4.5 cm in diameter, and 1.0 cm in thickness. Details of the measuring and sampling methods are described in Katsube (1981). A total of 152 granitoid samples have been collected from Whiteshell (WN), Underground Research Laboratory (URL) at Lac du Bonnet, and Atikokan (ATK) research sites. The rock samples are divided into four groups designated 1-4 on the basis of the degree of pink coloration: grey (1); pinkish-grey (2); greyish-pink (3); pink (4), (Katsube and Kamineni, 1983). Grey and pink indicate the lowest and highest degree of alteration, respectively. The porosity, formation factor and alteration data are listed in Table 53.1.

Theory of multiple regression with dummy variables

Consider a dependent variable y which is related to p independent variables x_i (i=1,2,...,p) as:

$$y = \beta_0 + \beta_1 x_1 + ... + \beta_p x_p \tag{3}$$

where the β_k (k=0,1,...,p) are unknown parameters to be estimated.

Figure 53.1(a,b). *Theoretical relationship between effective porosity (ϕ_E) and formation factor (F). Parameters characterizing pore structure are: aperture (d), tortuosity ($\tau = \ell_P/\ell$), path density (n) and pocket porosity (ϕ_P) (after Katsube et al., in press).*

Figure 53.2. *Actual data for measurements of effective porosity (ϕ_E) plotted against reciprocal of formation factor (1/F). Final solution consisting of 4 straight lines for different degrees of alteration has been superimposed (also see Fig. 53.4).*

Suppose that we have n observations with each observation consisting of (p+1) numbers:

$$y_j, x_{1j}, ..., x_{pj} \quad \text{for } j = 1, 2, ..., n \tag{4}$$

Based upon the n observations, we want to estimate the unknown (p+1) parameters β_k (k=0,1,2,...,p).

In multiple regression, y in (3) is assumed to be the expected or 'true' value of a random variable Y with

$$\begin{aligned} Y &= y + \varepsilon \\ &= \beta_0 + \beta_1 x_1 + ... + \beta_p x_p + \varepsilon \end{aligned} \tag{5}$$

where ε is called the residual. The latter is the same random variable as Y except that its expected value is equal to zero. For each observation j (=1,2,...,n) as in (4), y_j is considered to be an observed value of the random variable Y_j with the expected value:

$$\begin{aligned} E(Y_j) &= y_j \\ &= \beta_0 + \beta_1 x_{1j} + ... + \beta_p x_{pj} \end{aligned} \tag{6}$$

However, the corresponding residual ε_j of Y_j has the same expected value, zero for all j=1,2,...,n.

In addition, the Y_j (j=1,2,...,n) are, as usually assumed to be normally distributed with identical variance in order to apply the standard statistical significance tests to the estimated parameters and residuals. Under the linear model in (5), the (p+1) parameters β_k (k=0,1,...,p) are estimated by the method of least squares (LS method) which minimizes the sum of squares of the residuals.

The preceding theory can be found in statistical textbooks (e.g., Kendall, 1980). Computer programs to carry out the estimation of the coefficients and residuals are available in statistical packages such as SPSS, SAS, and BMDP. The method of dummy variables used in this paper is a variant of multiple regression analysis and can be applied

using these same computer programs. We have used SPSS for calculations and DISSPLA for plotting of diagrams. Reviews of use of dummy variables have previously been given in Gujarati (1970) and Agterberg (1974).

In the present application, effective porosity (y) is related to reciprocal of formation factor (x) for granitic rocks with four different types of alteration (cf. Table 53.1). In the analysis of the data, we multiply the porosity and reciprocal of the formation factor by 100 and 1000, respectively. These four groups will as before be denoted by the index j = 1, ..., 4.

For each alteration j (j=1,2,3,4), we assume a linear equation, as in (6),

$$E(Y_j) = y_j = \alpha_j + \beta_j x_j \tag{7}$$

From the observations, α_j and β_j (j=1,2,3,4) in the preceding four equations can be estimated by a_j and b_j by applying the LS method four times separately.

However, suppose that $\beta_\ell = \beta_m$ but $\alpha_\ell \neq \alpha_m$ in the preceding equation (7). By applying the regressions separately, one for $j = \ell$ and the other for j=m, the estimators b_ℓ and b_m for β_ℓ and β_m would not be equal. Hence, we would obtain two estimators b_ℓ and b_m for a single parameter $\beta_\ell = \beta_m$. The technique of dummy variables permits us to obtain only one estimator for $\beta_\ell = \beta_m$ and one for each of α_ℓ and α_m. In addition, the hypothesis $\beta_\ell = \beta_m$ can be evaluated by the application of significance tests.

Consider two sets of observations, one for the ℓ-th alteration and the other for the m-th alteration, i.e.

$$(y_{\ell i}, x_{\ell i}) \quad i=1,2,...,n_\ell \qquad \text{and}$$

$$(y_{mj}, x_{mj}) \quad j=1,2,...,n_m.$$

Table 53.1. Physical properties of crystalline rocks from research areas: URL (Underground Research Laboratory in Lac du Bonnet), WN (Whiteshell Nuclear Research Establishment) and ATK (Atikokan)

Sample (Borehole)-(Depth in m)	Alteration	ϕ_E	F	Sample (Borehole)-(Depth in m)	Alteration	ϕ_E	F
URL1-46.25	4	0.30	8.79	WN1-460.4	4	0.37	1.67
URL1-68.35	4	0.22	8.03	WN2-24.55	4	0.26	5.24
URL1-100.3	3	0.24	6.78	WN2-55.25	1	0.16	16.4
URL1-131.2	3	0.28	2.81	WN2-85.10	1	0.18	10.5
URL1-177.0	1	0.31	2.35	WN2-98.30	4	0.26	5.02
URL1-230.4	1	0.31	2.05	WN2-124.5	4	0.28	4.13
URL1-254.2	1	0.34	1.29	WN2-145.6	4	0.28	4.00
URL1-302.3	1	0.33	1.47	WN4-408.8	4	0.28	2.70
URL1-357.1	1	0.37	0.75	WN4-468.8	4	0.38	3.30
URL1-397.7	1	0.38	1.32	WN4-482.2	4	0.32	3.20
URL1-433.1	1	0.61	0.61	WN4-505.3	3	0.33	4.40
URL1-496.6	1	0.36	0.65	WN4-551.0	3	0.32	2.70
URL1-527.3	1	0.35	0.72	WN4-564.2	3	0.32	2.60
URL1-592.5	1	0.42	0.78	WN4-603.7	4	0.30	3.60
URL1-615.8	2	0.36	0.83	WN4-631.3	2	0.39	1.50
URL1-662.3	1	0.46	0.73	WN4-659.9	2	0.46	1.80
URL2-256.2	1	0.32	0.82	WN4-692.5	2	0.41	3.00
URL2-448.2	1	0.41	0.64	WN4-719.4	2	0.43	1.50
URL2-586.1	1	0.49	0.50	WN4-746.8	2	0.45	1.80
URL2-705.8	1	0.40	0.58	WN4-789.5	1	0.47	2.10
URL2-798.8	2	0.37	0.58	WN4-809.3	1	0.48	1.40
URL2-871.7	2	0.55	0.44	WN4-540.8	1	0.54	1.20
URL2-1001.3	1	0.67	0.38	WN4-863.5	1	0.49	1.50
URL2-1095.0	1	0.57	0.38	WN4-906.4	1	0.40	1.80
URL5-16.5	2	0.40	1.78	WN4-928.2	1	0.51	1.60
URL5-77.0	2	0.33	4.02	ATK1-13.3	4	0.27	3.80
URL5-108.2	4	0.53	1.40	ATK1-39.9	3	0.20	4.10
URL5-126.8	1	0.38	2.54	ATK1-79.2	3	0.21	5.70
URL5-156.9	2	0.41	1.27	ATK1-94.4	3	0.34	3.60
URL5-199.3	4	0.34	1.98	ATK1-111.3	3	0.19	3.56
URL5-246.8	4	0.37	3.36	ATK1-128.3	3	0.25	6.00
URL5-239.8	1	0.43	1.17	ATK1-163.1	3	0.26	3.40
URL5-333.9	1	0.42	1.36	ATK1-174.1	3	0.28	4.70
URL5-370.1	1	0.56	0.64	ATK1-237.9	3	0.22	3.80
URL5-451.1	1	0.60	0.56	ATK1-283.4	3	0.19	6.30
URL5-497.0	1	0.58	0.54	ATK1-320.9	2	0.34	1.70
URL7-132.0	3	0.25	3.82	ATK1-361.2	2	0.25	4.10
URL7-134.1	3	0.31	3.46	ATK1-400.3	3	0.26	5.70
URL7-135.4	3	0.30	3.48	ATK1-433.3	2	0.28	3.00
URL7-137.2	3	0.27	4.47	ATK1-475.3	1	0.32	2.60
URL7-138.4	3	0.18	5.53	ATK1-505.2	1	0.31	1.50
URL7-139.7	4	0.17	11.5	ATK1-539.9	1	0.45	1.01
URL7-140.6	4	0.16	4.61	ATK1-594.0	1	0.45	0.63
URL7-143.2	4	0.19	9.56	ATK1-630.2	1	0.49	0.60
URL7-144.0	4	0.23	6.77	ATK1-671.0	1	0.43	1.00
URL7-145.7	4	0.22	5.02	ATK1-715.0	3	0.24	8.00
URL7-147.5	4	0.19	5.30	ATK1-747.1	2	0.39	1.10
URL7-147.7	4	0.19	4.71	ATK1-788.1	1	0.47	0.73
URL7-148.1	4	0.18	6.55	ATK1-812.3	1	0.35	0.81
URL7-150.2	4	0.18	5.17	ATK1-849.2	1	0.24	1.70
URL7-155.3	4	0.21	6.29	ATK1-901.9	1	0.34	1.10
URL7-157.6	4	0.17	7.21	ATK1-923.8	3	0.29	6.50
URL7-138.2	4	0.14	8.41	ATK1-979.7	1	0.29	1.50
URL7-159.2	4	0.17	9.36	ATK1-1021.2	1	0.46	7.50
URL7-161.7	4	0.20	5.81	ATK1-1034.2	4	0.34	3.80
URL7-161.3	4	0.22	4.95	ATK1-1063.4	1	0.49	0.97
URL7-163.7	4	0.23	2.65	ATK1-1079.4	3	0.23	2.00
URL7-166.5	4	0.29	2.35	ATK1-1097.2	4	0.29	6.80
URL7-170.7	4	0.23	2.84	ATK1-1121.6	4	0.46	4.60
URL7-174.3	3	0.28	1.55	ATK1-1140.4	1	0.64	0.54
URL7-177.6	3	0.27	1.43	ATK5-106.4	1	0.29	2.45
URL7-181.0	2	0.39	0.96	ATK5-224.3	4	0.22	4.96
URL7-181.8	2	0.37	1.25	ATK5-337.4	1	0.27	2.33
URL7-184.7	2	0.34	1.21	ATK5-423.9	2	0.26	4.38
URL7-188.0	1	0.31	1.75	ATK5-534.1	1	0.40	1.66
URL7-192.9	1	0.28	1.40	ATK5-625.7	1	0.29	4.28
URL7-197.8	1	0.28	1.42	ATK5-708.6	1	0.35	0.90
WN1-138.4	4	0.35	3.01	ATK5-817.9	1	0.40	0.45
WN1-160.7	4	0.29	3.31	ATK5-867.6	1	0.34	0.90
WN1-223.7	3	0.43	1.95	ATK5-918.3	1	0.34	0.86
WN1-245.8	3	0.36	2.14	ATK5-951.2	1	0.29	1.53
WN1-294.3	4	0.40	2.17	ATK5-975.5	1	0.37	0.91
WN1-303.3	4	0.33	1.83	ATK5-1050.2	1	0.37	0.70
WN1-345.3	3	0.35	2.08	ATK5-1107.8	1	0.44	0.67
WN1-384.6	4	0.31	2.30	ATK5-1228.5	1	0.29	1.96
WN1-410.5	4	0.34	2.27				

By combining the two sets of observations and defining two new dummy variables, we obtain:

$$
\begin{array}{llll}
y_{\ell 1} & 0 & x_{\ell 1} & 0 \\
\bullet & \bullet & \bullet & \bullet \\
\bullet & \bullet & \bullet & \bullet \\
\bullet & \bullet & \bullet & \bullet \\
y_{\ell n_\ell} & 0 & x_{\ell n_\ell} & 0 \\
y_{m1} & 1 & x_{m1} & x_{m1} \\
\bullet & \bullet & \bullet & \bullet \\
\bullet & \bullet & \bullet & \bullet \\
\bullet & \bullet & \bullet & \bullet \\
y_{mn_m} & 1 & x_{mn_m} & x_{mn_m}
\end{array}
\tag{8}
$$

Instead of two sets of observations, n_ℓ observations for the ℓ-th alteration and n_m observations for the m-th alteration, with one dependent variable and one independent variable, we now have a single set of $(n_\ell + n_m)$ observations with one dependent variable and three independent variables.

Consider now the following model:

$$Y_{\ell m} = \gamma_0 + \gamma_1 z_1 + \gamma_2 z_2 + \gamma_3 z_3 + \epsilon_{\ell m} \tag{9}$$

Using the data in (8) where the first column is considered as consisting of the expected values for $Y_{\ell m}$, and the second, third and fourth columns are representing z_1, z_2 and z_3, respectively, and using the LS method of multiple regression, LS estimators c_0, c_1, c_2 and c_3 are obtained for γ_0, γ_1, γ_2 and γ_3.

If c_3 is statistically significant (i.e., $\gamma_3 \neq 0$) according to the statistical significance test, the hypothesis $\beta_\ell = \beta_m$ should be rejected under the assumptions of the model. Otherwise, i.e. if γ_3 can be assumed to be zero, c_2 may be regarded as an estimator of $\beta_\ell = \beta_m$. However, a better estimator of γ_2 may be obtained by repeating the multiple regression after deleting z_3 as an independent variable. Similarly, we can test $\alpha_\ell = \alpha_m$ by examining c_1 following the same procedure as for c_3.

The model can be extended to incorporate more than two groups. A version in which all four groups are considered simultaneously will be introduced and used at the end of the next section.

Application of multiple regression with dummy variables

The four groups of Table 53.1 were compared pairwise according to the method explained in the previous section. The results are shown in Table 53.2. Each multiple regression run yielded 4 coefficients c_0 to c_3 which were evaluated for statistical significance according to an F-test as follows. Suppose that one of the coefficients and its corresponding independent variable x_{ij} are omitted. Then the squared multiple correlation coefficient R^2 which provides a measure of the total degree of fit provided by a multiple regression equation will be reduced. This difference is only statistically significant if it exceeds a critical value determined by the numbers of observations in the groups compared to one another. An F-value can be computed to evaluate this difference. If the contribution of the variable is not statistically significant, this F-value is equal to one on the average. Each estimated F-value can be transformed into a probability P that the contribution of the corresponding variable is not significant (Table 53.2).

The values of R^2 and estimated standard deviations of residuals s_e are also shown in Table 53.2 for the six multiple regressions performed. The s_e-values suggest that the average deviation from the fitted regression lines decreases slightly with increasing degree of alteration. Inspection of the coefficients of Table 53.2 illustrates that c_0, c_2, $(c_0 + c_1)$ and $(c_2 + c_3)$ are almost equal to one another for all four groups in the six different pairs. This allows us to extract the following four linear relationships:

Group 1: $y_1 = 0.256 + 0.138x_1$
Group 2: $y_2 = 0.326 + 0.117x_2$
Group 3: $y_3 = 0.214 + 0.165x_3$
Group 4: $y_4 = 0.157 + 0.431x_4$

These lines are shown graphically in Figure 53.3. They also represent the best-fitting lines of least squares resulting from bivariate regressions. We have approximately $\epsilon_{ij} = \epsilon_i = \epsilon_j$ where ϵ_{ij} represents the residuals for y_{ij} in a pairwise comparison (i, j); ϵ_i is for y_i and ϵ_j for y_j in corresponding bivariate regressions. Inspection of Table 53.2 shows that the coefficients c_0 and c_2 are statistically significant in all six solutions. The F-values are less than one for c_3 in the pairwise comparisons (1, 2), (1, 3) and (2, 3). This indicates that the slopes of the lines, for groups 1 to 3 are probably equal to one another. $P_3 = 0.000$, 0.000 and 0.004 for the 3 pairwise comparisons involving Group 4.

Table 53.2. Pairwise comparison of groups of samples with different degrees of alteration (i,j) using model of equations (8) and (9) in the text. Each coefficient c (c_0–c_4) is followed by its F-ratio which was converted into the probability P that the coefficient is equal to zero. The multiple correlation coefficient squared (R^2) and estimated standard deviation of residuals (s_e) are also listed for each regression solution.

(i, j)	(1, 2)	(1,3)	(1, 4)	(2, 3)	(2, 4)	(3, 4)
c_0	0.256	0.256	0.256	0.326	0.326	0.214
F_0	107.739	132.543	132.113	157.373	147.540	82.804
P_0	0.000	0.000	0.000	0.000	0.000	0.000
c_1	0.070	-0.042	-0.099	-0.112	-0.169	-0.057
F_1	3.136	1.425	10.515	9.443	25.446	3.688
P_1	0.082	0.237	0.000	0.004	0.000	0.059
c_2	0.138	0.138	0.138	0.117	0.117	0.165
F_2	51.913	63.865	63.658	16.574	15.538	5.695
P_2	0.000	0.000	0.000	0.000	0.000	0.020
c_3	-0.022	0.026	0.293	0.048	0.314	0.266
F_3	0.304	0.103	19.414	0.355	21.094	9.143
P_3	0.584	0.750	0.000	0.555	0.000	0.004
R^2	0.523	0.712	0.704	0.704	0.670	0.514
s_e	0.071	0.064	0.065	0.060	0.062	0.055

Figure 53.3. *Effect of degree of alteration on the $\emptyset_E$ versus 1/F relationship. Four straight lines fitted by pairwise comparison of groups with different degrees of alteration. Group means (diamonds) are also shown.*

Figure 53.4. *Schematic diagram for the different degrees of alteration 1-4. Final solution obtained by multiple regression with 3 dummy variables (see Table 53.3). Group means (diamonds) are also shown.*

It may therefore be concluded that Group 4 has a different slope. The coefficient c_1 is not statistically significant for level of significance $\alpha = 0.05$ in three pairwise comparisons: (1, 2) with $P_1 = 0.082$, (1, 3) with $P_1 = 0.237$ and (3, 4) with $P_1 = 0.059$. It is noted that from the pairwise comparisons (1,2) and (1,3), it could be inferred that $c_1 = 0$ suggesting the same intercept for alterations 1, 2 and 3. However, the results in Table 53.2 also indicate that the difference in intercept between alterations 2 and 3 is statistically significant. This inconsistency arises from the fact that only two alterations are compared in each regression of Table 53.2. It suggests that more than two groups should be compared simultaneously as will be done later in this section. In the final solution (Fig. 53.2, 53.4), the intercept of alteration 1 is between those of 2 and 3.

It was initially decided to rerun the multiple regressions for pairs (i, i + 1) which have one or more P-values greater than 0.05 in Table 53.2. Dropping the variable with least effect in each of the runs (1, 2), (2, 3) and (3, 4) gave the following results:

Pair (1, 2): $y_1 = 0.262 + 0.133x_1$; $y_2 = 0.314 + 0.133x_2$
Pair (2, 3): $y_2 = 0.322 + 0.123x_2$; $y_3 = 0.227 + 0.123x_3$
Pair (3, 4): $y_3 = 0.178 + 0.256x_3$; $y_4 = 0.178 + 0.374x_4$

All coefficients are statistically significant ($P > \alpha = 0.05$) in these new runs. Although this presents an advantage with respect to the earlier result shown in Figure 53.3, the new result has nine, instead of eight coefficients because there are now two different solutions for y_2 and y_3. Because the resulting lines for Groups 2 and 3 are not approximately coinciding, it was decided to perform a single multiple regression with 3 dummy variables separating all four groups but forcing the slopes of Groups 1, 2 and 3 to be equal to one another. The model for this run is:

$$y = \gamma_0 + \gamma_1 d_1 + \gamma_2 d_2 + \gamma_3 d_3 + \gamma_4 x + \gamma_5 d_3 x + \varepsilon \qquad (10)$$

where $y = y_j$, $x = x_j$ (j = 1, ..., 4); $d_1 = 0$ if $x = x_1$ (and 1 otherwise); $d_2 = 0$ is $x = x_1$ or x_2 (and 1 otherwise); and $d_3 = 0$ if $x = x_1$, x_2 or x_3 (and 1 if $x = x_4$).

The estimated coefficients for the new run are shown in Table 53.3. The R^2-value amounts to 0.703. The standard deviation of residuals amounts to $s_e = 0.062$. Assuming that this pooled value for s_e can be used for all four groups, the final solution becomes:

Group 1: $y_1 = 0.261 + 0.134x_1$
Group 2: $y_2 = 0.313 + 0.134x_2$
Group 3: $y_3 = 0.223 + 0.134x_3$
Group 4: $y_4 = 0.158 + 0.431x_4$

Table 53.3. Final multiple regression result using model of equation (10) in the text. F-ratios and corresponding probabilities P show that coefficients c probably differ from zero indicating that the effects of all variables used are statistically significant.

i	c_i	F_i	P_i
0	0.2611	183.8	0.000
1	-0.0656	7.1	0.009
2	-0.0899	18.6	0.000
3	0.0519	8.2	0.005
4	0.1341	86.0	0.000
5	0.2968	21.4	0.000

The F- and P-values in Table 53.2, show that the variables in this model all contribute significantly. The final result is shown graphically in Figures 53.2 and 53.4. In Figures 53.3 and 53.4, the average x- and y-values for the groups are also shown with

Group 1: $\bar{x}_1 = 1.163$; $\bar{y}_1 = 0.416$
Group 2: $\bar{x}_2 = 0.770$; $\bar{y}_2 = 0.416$
Group 3: $\bar{x}_3 = 0.296$; $\bar{y}_3 = 0.263$
Group 4: $\bar{x}_4 = 0.282$; $\bar{y}_4 = 0.291$

Discussion and conclusions

The multiple regression analysis consists of estimating 8 coefficients in 4 linear equations (one equation for each group of samples). The grouping is based on the degree of alteration 1-4. The results of the analysis indicate that while the intercept varies for different groups, the slope is identical for groups 1 to 3, but is larger for group 4. This confirms the assumption that ϕ_p (intercept) varies with alteration, but τ (square root of the slope) is independent of alteration until an alteration degree of 4 is reached. Since the values of ϕ_E and $1/F$ were multiplied by 10^2 and 10^3 for the analysis, the true values of the intercepts, slopes and averages for x and y are respectively 10^{-2}, 10, 10^{-3} times those shown in the solutions. Therefore, the values of τ for groups 1-3 is 1.16, and for group 4 is 2.08.

The value of ϕ_p increases as the degree of alteration progresses from 1 to 2, but then decreases with further progress of alteration. The mean of $1/F$ decreases as alteration progresses. These trends, as well as the trends observed for τ, are shown in Figure 53.4. Based on the model presented by Katsube et al. (1985), the changes in τ and ϕ_p in relation to alteration can be explained as follows. It is assumed the basic pore structure of an unaltered rock can be represented by alteration 1 in Figure 53.4. As the alteration progresses to degree 2, certain minerals along the connecting paths are leached, pocket pores form and the tortuosity remains constant. This explains the parallel shift of the lower line 1 to the upper line 2 in Figure 53.4. As alteration progresses to alteration 3, deposition takes place, the paths are narrowed (alteration 3) and some of the pocket pores are sealed off from the network of connecting pores. The tortuosity remains constant. When the paths are narrowed, the aperture decreases and the formation factor (F) will increase (equation 1). Thus, the average of $1/F$ shifts along the upper line towards the lower end of the abscissa, as shown in Figure 53.4. The sealing of the pocket pores results in the parallel shift of line 2 to the lower line 3 in Figure 53.4. As the alteration progresses to degree 4, the thickness of the deposition layer increases and finally some paths are sealed and more of the pocket pores are blocked off from the main connecting path. This results in an increase in tortuosity (τ) and a further decrease in pocket porosity (ϕ_p) as shown in the shift of data to a line with a larger gradient and a decrease in the intercept in Figure 53.4. This model is identical to that proposed by Katsube and Kamineni (1983).

The results of the multiple regression analysis provide a firm statistical basis which supports the physical model suggested by Katsube et al. (1985): τ and ϕ_p are constants that vary with the degree of alteration, and thus a linear relationship exists between ϕ_E and $1/F$. This physical model is very useful for characterizing the pore structure of rocks. This study shows that multiple regression analysis using dummy variables is very useful for analyzing the pore structure data. Previously it was shown that the statistical method for decomposition of mixtures of normal distributions was also an effective method for obtaining information on intermediate pores that were buried in data dominated by the effect of micro and nano pores (Agterberg et al., 1984). The use of statistical methods is becoming essential in the study of pore structure of crystalline rocks.

Acknowledgment

References

Agterberg, F.P.
1974: Geomathematics: Mathematical Background and Geo-Science Applications. Elsevier, Amsterdam, 596 p.

Agterberg, F.P., Katsube, T.J., and Lew, S.N.
1984: Statistical analysis of granite pore size distribution data, Lac du Bonnet batholith, eastern Manitoba; in Current Research, Part A, Geological Survey of Canada, Paper 84-1A, p. 29-38.

Archie, G.E.
1942: The electrical resistivity log as an aid in determining some reservoir characteristics; Trans. American Institute for Mining Engineers, 146: 54-67.

Gujarati, D.
1970: Use of dummy variables in testing for equality between sets of coefficients in linear regressions: A generalization; American Statistician, v. 24 (5), p. 18-21.

Katsube, T.J.
1981: Pore structure and pore parameters that control radionuclide transport in crystalline rocks; Proc. Tech. Prog. International Powder and Bulk Solids Handling and Processing, Rosemont, Ill., May 12-14, p. 394-409.

Katsube, T.J. and Kamineni, D.C.
1983: Effect of alteration on pore structure of crystalline rocks: core samples from Atikokan, Ontario. Canadian Mineralogist, v. 21, p. 637-644.

Katsube, T.J., Percival, J.B., and Hume, J.P.
1985: Characterization of the rock mass by pore structure parameters; Atomic Energy of Canada Limited, Technical Record TR-299.

Kendall, M.G.
1980: Multivariate Analysis (Second edition); Griffin, London, 210 p.

Schlumberger
1972: Log interpretation manual/principles, vol. I, Houston, Schlumberger Well Services, Inc.

Wadden, M.M. and Katsube, T.J.
1982: Radionuclide diffusion rates in crystalline rocks; Chemical Geology, v. 36, p. 191-214.

Walsh, J.B. and Brace, W.T.
1984: The effect of pressure on porosity and the transport properties of rock; Journal of Geophysical Research, v. 89, p. 9425-9431.

Establishment of coal logging field calibration facilities: a progress report

Project 820021

L.D. Schock and P.G. Killeen
Resource Geophysics and Geochemistry Division

Abstract

Considerable progress has been made towards the establishment of coal logging field calibration facilities in Eastern and Western Canada. Both sites have been selected and two large cylindrical in-ground tanks have been installed in Dartmouth, Nova Scotia, to house model boreholes assembled from precast calibration zones with known physical properties. The land allocated for the Dartmouth site was provided by the Nova Scotia Research Foundation Corporation which will oversee and maintain the facility upon its completion for their own and public use. The two fiber glass tanks, designed to meet numerous special requirements, will permit the addition of calibration zones as they are developed and tested in Ottawa. A similar calibration facility in Western Canada will be located in Calgary at the Institute of Sedimentary and Petroleum Geology. Two fiberglass tanks, already constructed, are expected to be installed in summer 1985. Delivery of the first calibration zones for density logging should begin later in the year.

Résumé

La mise en place d'installations régionales de calibrage sur le terrain des appareils servant à faire la diagraphie des sondages du charbon a franchi des étapes importantes tant dans l'Est que dans l'Ouest du pays. Deux emplacements ont été chosis et deux énormes réservoirs cylindriques ont été installés sous terre à Dartmouth, en Nouvelle-Écosse. Ils contiendront des trous de sondage modèles assemblés à partir de zones de calibrage préfabriquées aux propriétés physiques connues. À Dartmouth, le terrain a été fourni par la Nova Scotia Research Foundation Corporation qui surveillera et entretiendra l'installation pour ses propres besoins et ceux du public. Les deux réservoirs de fibre de verre, conçus pour satisfaire à un grand nombre d'exigences particulières permettra l'addition de zones de calibrage qui auront été mises au point et vérifiées à Ottawa. Une autre installation de calibrage semblable sera installée dans l'Ouest, à l'Institut de géologie sédimentaire et pétrolière de Calgary. La mise en place des deux réservoirs de fibre de verre, déjà construits, devrait avoir lieu au cours de l'été 1985 et la livraison des premières zones de calibrage relatives aux essais de densité devrait débuter plus tard cette année.

Introduction

A major step towards the completion of the coal logging field calibration facility for Eastern Canada was made in late March 1985. This consisted of the in-ground installation of two fiberglass tank assemblies at the site of the Nova Scotia Research Foundation Corporation (NSRFC) in Dartmouth, as part of a federal energy research and development project on 'Borehole Geophysics: Applications to Coal'. The tank assemblies designed by the Borehole Geophysics Section of the Geological Survey of Canada will eventually contain cylindrical calibration zones with an axial borehole. The zones will simulate the physical properties of rocks encountered during coal logging operations. Prior to delivery to the site the zones will be designed, tested and evaluated at the Ottawa primary calibration facility (Killeen et al., 1984).

These model borehole logging facilities are required for the proper calibration and standardization of borehole logging tools used to determine the location and thickness of coal seams as well as information on the quality of coal. They can also be used for research and development of new borehole geophysical techniques for measuring coal-related rock properties. The first zones to be provided are designed for the calibration of density logging tools, since density is the physical property which most uniquely defines coal and is the measurement most widely recorded in the coal industry. Calibration zones with other measured and documented physical properties such as porosity or magnetic susceptibility will be added to the model boreholes in the future.

Model boreholes: the field logging calibration facilities

The field calibration facilities for both Eastern and Western Canada will consist of a vertical stack of calibration zones, contained in an appropriate below-ground tank as shown in Figure 1 with provision for water saturation to simulate most field conditions. The central hole in each cylindrical zone is aligned such that the stack provides a continuous hole through all the zones, which is further aligned with a run pipe protruding below the tank. Some calibration measurements require that a steel drill rod (or pipe) be temporarily suspended in the model borehole to simulate logging inside the drill rod. For this reason the insulated fiberglass cover for the tank was designed to support the weight of two drill rod sections as well as a maximum of four workers. During the calibration procedure, logging tools would normally be lowered into the model borehole on a cable which runs over a pulley suspended by an overhead gantry assembly. Continuous logging through the entire simulated borehole during the calibration procedure is ensured by the 'run pipe' beneath the tank.

Two essential requirements for the facility were: (1) that it be watertight to prevent seepage of ground water into an empty tank or of water from a full tank into the environment, and (2) that it be free of metallic material to avoid electrical or magnetic interference during calibration of logging tools which measure electrical or magnetic properties of rocks. Upon consideration of these special requirements, a fiberglass tank with circular cross-section was selected.

Fiberglass has definite advantages, being low maintenance, nonmagnetic, strong, tough, resilient, waterproof and weathertight, capable of withstanding extreme weather conditions and rough handling. Also, construction problems associated with concrete forming on-site are minimized since the only requirement is for a level concrete base for the tanks. Freezing is precluded through the use of insulation around the upper section of the tank, eliminating the need for anti-freeze in the water in the tank.

FIBER GLASS TANK ASSEMBLY
G.S.C./SCHOCK 11/84

Figure 1. *Schematic diagram of the tank assembly used in the field calibration facilities showing a vertical stack of calibration zones aligned with the run pipe in the below-ground tank. The optional drill rod is shown suspended from the cover inside the model borehole formed by the zones. The reducer at the bottom allows smooth transition from the below-tank run pipe to the zone borehole.*

Components are designed and constructed at the fiberglass plant, shipped to the site and assembled with relative ease. Possible future damage to the fiberglass tank or run pipe is eliminated by the following precautions: 1) a concrete base is installed within the tank to absorb the shock during positioning of calibration zones or the impact of an inadvertently dropped object, such as a logging tool; 2) the bottom of the run pipe is filled with a 60 cm layer of silica sand to cushion the blow from a falling tool.

The fiberglass tank design was developed taking into consideration the particular conditions of each site. Considerations included the environment, type of material to be excavated, depth to bedrock, hydrostatic conditions, frost susceptibility of the soil, backfill pressures, settlement, tendency for flotation or leakage of tanks, ability to vary the borehole diameter in future, worker safety, and security against possible vandalism.

Four fiberglass tank assemblies comprising tank, cover, run pipe, reducer and overhead gantry were required, ie. two each for Eastern and Western Canada. As a result of the above-mentioned site considerations, the two sets differ slightly. In particular the Western tanks are more robust and the boreholes in the calibration zones are larger than those for Eastern Canada. The optimum borehole diameter was determined based on common regional coal drilling practice, to be 100 mm in Western Canada and 75 mm in Eastern Canada requiring an appropriate reducer allowing smooth transition from below-tank run pipe (200 mm diameter) to the borehole.

The installation of the Nova Scotia tank assemblies

The Eastern site at the Nova Scotia Research Foundation Corporation was selected for three main reasons: (1) it is the location of a group actively involved in coal logging and interested in the use of the facility, (2) a suitable tract of land was available and the NSRFC was willing to allocate it for the facility and (3) the NSRFC was willing to maintain a logging calibration facility. Maintenance includes providing access to the site upon reasonable notice, to people desiring to calibrate logging probes. The location was ideal with nearby electrical and water supplies, and a security fence surrounded the property. Preliminary subsurface soil test reports had indicated the area (a) was underlain by glacial till with extensive preconsolidation, (b) had a low water table, and (c) had bedrock well below the required excavation depth. The site also sloped slightly which simplified excavation.

As excavation proceeded, it became evident that the soil conditions were favourable, with the excavation walls remaining stable and no slumping occurring. Water was not encountered and the weather was co-operative. A large hole for the two tanks was excavated to a depth of about 6 m. On the downhill side of the excavation a ramp was formed by excavating one wall of the hole. A truck-mounted drill rig was backed down the ramp into the excavation to drill the holes and install the run pipes for the two tank assemblies (see Figure 2). Upon completion and removal of the drill rig from the excavation, a single continuous concrete base was prepared for the two tanks, being poured around the two

Figure 2. Installation of run pipes for the two tank assemblies involved backing a truck-mounted drill rig down the ramp into the excavation, drilling the holes and placing the run pipes.

Figure 3. A crane was used for positioning the tank over the run pipe and lowering it onto the concrete base.

461

Figure 4. *The completed coal logging field calibration facility at the Nova Scotia Research Foundation Corporation showing insulated tank and cover, and overhead gantry.*

protruding fiberglass run pipes. The tanks which had an appropriate hole in the bottom were positioned over the run pipes and lowered into place (see Figure 3). The fiberglass tank bottom was bonded to the run pipes. The additional layer of protective concrete was poured inside each tank and a fiberglass lip was bonded to the tank wall above it to prevent any possible upward movement of the tank bottom (the so-called "oil-can effect"). Backfilling, spreading and levelling were completed and the remaining fiberglass components (cover, overhead gantry, etc.) were assembled as shown in Figure 4.

Progress on the Western Canada coal logging facility

The Western site is to be located in Calgary at the Institute of Sedimentary and Petroleum Geology, adjacent to calibration pads for portable gamma-ray spectrometers which were constructed in 1977 (Killeen, 1979). At this location, the water table is variable and the ground is unstable, requiring an engineering site evaluation with appropriate recommendations prior to installation of the new fiberglass tanks. Although the details of the procedure for installation remain to be determined, the Western tanks have already been designed and constructed to withstand the extreme condition of saturated soil surrounding them to the top. These tanks are 60 cm longer than the Eastern tanks to allow a greater amount of concrete inside for additional load against uplift.

It is expected that the Calgary set of in-ground tanks will be installed in summer 1985. Calibration zones for both logging facilities will be delivered and installed shortly afterwards. Additional calibration zones will be added as they become available.

References

Killeen, P.G.
    1979:   Gamma ray spectrometric methods in uranium exploration – application and interpretation; in Geophysics and Geochemistry in the Search for Metallic Ores, ed. P.J. Hood; Geological Survey of Canada, Economic Geology Report 31, p. 163-229.

Killeen, P.G., Bernius, G.R., Schock, L.D., and Mwenifumbo, C.J.
    1984:   New developments in the GSC Borehole Geophysics Test Area and calibration facilities; in Current Research, Part B, Geological Survey of Canada, Paper 84-1B, p. 373-374.

A digital signal processing unit for the Geo Instruments magnetic susceptibility sensors, with analogue and RS-232C outputs

Q. Bristow
Resources Geophysics and Geochemistry Division

Abstract

A digital signal processing unit has been developed at the Geological Survey of Canada for use with magnetic susceptibility sensors made by Geo Instruments, the Finnish geophysical instrumentation manufacturer. An industry-standard RS-232C interface enables data acquisition and control by a personal computer or similar system.

Résumé

Un dispositif de traitement des signaux numériques compatible avec les capteurs magnétiques fabriqués par la Geo Instruments, fabricant finlandais d'instruments géophysiques, a été mis au point à la Commission géologique du Canada. Un interface RS-232C conforme aux normes de l'industrie permet à un ordinateur personnel ou à un système semblable de stocker et de contrôler les données. Le dispositif sera probablement mis sur le marché par l'agent nord-américain de la Geo Instruments, Urtec Instruments Sales de Toronto.

Introduction

Geo Instruments of Helsinki, Finland, produce instrumentation for making magnetic susceptibility measurements in both laboratory and field environments. A borehole logging magnetic susceptibility probe is included in the line of equipment and this was the subject of an evaluation which was reported previously by Bristow and Bernius (1984).

The sensors in these instruments transmit the susceptibility signal as a small deviation in a reference frequency, which is approximately 1450 Hz. The existing processing modules use frequency-to-voltage (F/V) converters to convert the small frequency changes, (30 Hz at most) to analogue signals suitable for driving a strip chart recorder.

In the case of field measurements these processing units are subject to considerable temperature variations and this has been known to cause some baseline drift which can introduce errors into the measurements. This is of particular concern in the case of borehole logging, where a continuous record is being acquired over a period of an hour or so.

An alternative processing unit has been developed at the Geological Survey of Canada, which processes the signal by digital techniques involving a crystal controlled clock. It will probably be manufactured by and be commercially available from Urtec Instrument Sales of Toronto, the North American agent for the Geo Instruments magnetic susceptibility instrumentation.

The development was aimed at finding a technique which offered better stability than the F/V converter in extracting the small frequency excursions containing the signal information, and which would at the same time provide both a digital interface and a "zero-signal-level-store" capability. The latter would enable susceptibility sensors with widely differing zero-signal frequencies to be used without any factory adjustments being required, while the digital interface would allow direct data acquisition by a micro-computer.

Principle of operation

The principle of operation is shown in the block diagram of Figure 1. It depends on the fact that a full scale susceptibility signal produces a frequency shift of 20 to 30 Hz, which is less than 3% of the zero level of approximately 1450 Hz. Under these conditions the period changes almost linearly with frequency.

The incoming sensor frequency is divided by 256 to produce a lower frequency with a period of about 180 ms. This is used as the basic period measurement gate time for a 15 MHz crystal controlled oscillator. It also sets the sample rate at between 5 and 6 measurements per second. When the zero or base-line signal level is being sampled, the counts from the 15 MHz oscillator are fed to a 12 bit DOWN counter. This counter over-ranges many times in the course of a single measurement and finally stores the least significant 12 bits of the total count, (total capacity 4095). When it is required to start signal measurements, (e.g. in the case of borehole measurements, after the probe has stabilized in the borehole fluid for about 30 minutes), then the oscillator pulse train is sent to the UP counter, which is now preset before each sample count with the zero-signal level previously stored in the DOWN counter. The 12 bit digital result is then latched out to the 12 bit digital-to-analogue converter, and to a UART (universal asynchronous receiver/transmitter) for transmission via the industry

Figure 1. *A block diagram of the digital signal processing unit showing the method used to store a zero signal level and subtract it from subsequent measurements.*

standard RS-232C protocol to a personal computer or other more elaborate data acquisition system. Subtraction of the large zero-level signal is thus accomplished by using a crystal, with a short term stability of 1 part in 10^7, rather than a voltage reference which is necessary when an F/V converter is used.

The DOWN counter is preset with a value of 512 (approximately 12% of full scale). This digital offset allows the signal measurements to fall below the stored zero level by up to 12% without the UP counter overranging. This offset is carried through to the digital-to-analogue converter and appears as a 12% of full scale offset in the analogue and digital outputs. It can be suppressed by the zero adjust control of the chart recorder if one is used, or by the digital data acquisition system.

The front panel "ZERO" switch initiates a zero-level store operation as described above, which takes an average value over approximately 3 seconds. Control logic provides the necessary signals to ensure proper sequencing of the various operations involved. A digital sensitivity control is implemented by changing the oscillator frequency with a four-position switch. This allows selection of four digital and analogue output scales each with a resolution of 1 part in 4096, and nominal ranges of 2000, 8000, 32000 and 128000 x 10^{-5} S.I. units.

Experimental

A prototype of the unit (Fig. 2) was constructed in "Euro-card" format with the RS-232C interface occupying one of the three 100 mm circuit cards which contain the circuitry. The recently available high-speed "CMOS" low power logic is used for most of the circuitry. The only exception is the UART chip required for the RS-232C interface. This allows for battery operation in a field environment if only analogue data are being recorded, since power to the UART can be disconnected by a switch mounted inside the unit.

In the manual or OFF-LINE mode of operation, the sensitivity range is switch selectable by the operator. In the ON-LINE mode the ranges are controlled by an external data acquisition system. In this mode front panel LED's indicate the range that has been selected.

Laboratory and field tests have confirmed that with the borehole version of the equipment, the use of the digital signal processing unit offers a substantial reduction in base-line drift. Test logs were run at the GSC test holes at Bells Corners, near Ottawa, a facility which has been described Bernius (1981). These holes intersect 65 m of sedimentary strata with very low magnetic susceptibility levels, (less than 500 x 10^{-5} S.I.), underlain by crystalline rock with levels exceeding 25 000 x 10^{-5} S.I. in places.

One test was run with the output from the borehole magnetic susceptibility probe being fed in parallel to two of the Geo Instruments processing modules and the digital signal processing unit. After the probe had been allowed to stabilize, the digital unit was set to zero and the readings on the other two units were recorded. A log was then made down to 300 m and back to the starting point. The elapsed time was approximately 1 hour and 40 muinutes. The net drifts shown by the three units with the probe back at the starting point were as follows: (S.I. x 10^{-5} units).

Geo Instruments Module 1	317
Geo Instruments Module 2	174
Digital Signal Processing Unit	31

Figure 2. *Prototype version of the digital signal processing unit. The circuitry is contained on three 100 mm "Eurocard" standard boards.*

While some baseline drift was still evident with the digital unit, it was down to 20% or less than that shown by the two other modules. This residual drift originates in the probe itself and cannot be removed by the processing unit.

In the borehole logging application an advantage of computer operation is the ability to make the sensitivity range adjust automatically to accommodate the widely varying signal levels received as the probe encounters different rock types along the borehole. The necessary software was written to test this idea using a data acquisition system based on a Data General Corp. NOVA mimicomputer (Bristow, 1979). The algorithm forced an automatic range change to the minimum sensitivity level if the received signal exceeded 50% of full scale, or to the next highest sensitivity level if the signal was less than 10% of full scale. This technique ensured that sudden large increases in signal would always be properly handled. The anticipated range changes were observed in test logs as the probe moved from sedimentary to crystalline rock and vice versa. The resulting log showed better resolution of the low level signals than a second one that had been made with the sensitivity fixed at the minimum of the four levels. This setting would be the only choice without the auto-ranging capability, since there would be a risk of over-ranging at a more sensitive setting.

Conclusions

A digital signal processing unit has been described which provides additional capability and versatility for the existing Geo Instruments magnetic susceptibility instrumentation. This unit offers a number of improvements and advantages, the main features being as follows:

* Digital auto-zero, whereby the incoming signal level at any time can be stored as the zero reference level at the push of a button.

* Essentially drift-free operation due to the inherent stability of the crystal reference oscillator. Any observed drift is due to the sensor alone.

* Choice of four sensitivity ranges, with the highest setting giving a measurement resolution of approximately 0.5 x 10^{-5} S.I. units.

* Analogue output, via a 12 bit digital-to-analogue converter from the digitally processed signal, for strip chart records.

* Digital output via an RS-232C interface, allowing for instant connection to almost any personal computer.

* The auto-zero and sensitivity settings can be operated remotely via the RS-232C interface, or manually by front panel controls. Selection of operating mode is by an ON-LINE/OFF-LINE switch.

The power consumption of the unit is low enough that it can be battery operated if necessary, and thus be compatible with the battery operated magnetic susceptibility sensors produced by Geo Instruments.

Acknowledgments

The author gratefully acknowledges the participation of staff technologist Y. Blanchard who built and tested the prototype unit and made substantial contributions of his own to the final design concept.

References

Bristow, Q. and Bernius, G.R.
1984: Field evaluation of a magnetic susceptibility logging tool; in Current Research, Part A, Geological Survey of Canada, Paper 84-1A, p. 453-462.

Bernius, G.R.
1981: Boreholes near Ottawa for the development and testing of borehole logging equipment – a preliminary report; in Current Research, Part C, Geological Survey of Canada, Paper 81-1C, p. 51-53.

Bristow, Q.
1979: NOVA-based airborne and vehicle mounted system for real-time acquisition, display and recording of geophysical data; in Proceedings of Data General Corp. Users Group Conference, New Orleans, Dec. 1979.

An index of commercially-acquired potential field data in the Canadian East Coast Offshore

Project 730081

R. Macnab, D. Plasse[1], and M. Graves[2]
Atlantic Geoscience Centre, Dartmouth

Abstract

A review of public reports held by the Canada Oil and Gas Lands Administration has led to the creation of a catalogue that describes commercial activity in the measurement of the gravity and magnetic fields of the East Coast Offshore prior to 1980. The catalogue has served to identify a number of projects in which commercial data might serve as a useful complement to similar data collected in the region during the course of government surveys.

Résumé

L'examen des rapports publics que possède l'Administration du pétrole et du gaz des terres du Canada a entraîné l'élaboration d'un catalogue descriptif des activités commerciales réalisées avant 1980 qui visaient à mesurer les champs gravimétrique et magnétique au large de la côte atlantique. Le catalogue a permis de repérer un certain nombre de projets dont les données commerciales pourraient judicieusement compléter les données qui ont été relevées dans cette région au cours de levés effectués par le gouvernement.

---

[1] Earth and Ocean Research Ltd., Dartmouth, N.S.
[2] Cuesta Research Ltd., Halifax, N.S.

Surveys in the Canadian East Coast Offshore

Government and industry have been involved in the measurement of gravity and magnetics in the Canadian East Coast Offshore for over 20 years. Government operations have been undertaken largely through collaboration between three federal agencies: the Canadian Hydrographic Service, the Earth Physics Branch, and the Geological Survey of Canada (Macnab, 1983; Miller et al., 1983; Macnab et al., 1985). These data have been collected for purposes relating to mapping and long-term scientific research; the data, as a rule, have been made public through various means such as scientific papers in the open literature, formal maps, and the Open File systems.

Industry operations, on the other hand, have been handled independently by a large number of oil companies and geophysical exploration firms. As these operators have concentrated on the search for exploitable hydrocarbon reserves, the data in general have been of a proprietary nature, and have thus received only restricted circulation.

There are requirements, however, for private operators to submit reports on certain aspects of their offshore activities to the Canada Oil and Gas Lands Administration (COGLA). In general, these reports are disclosed to the public five and a half years after completion of the field work. Taken together, such documents provide a good overview of industry activity in the region, because they chronicle the data-gathering operations that have occurred in various areas down through the years.

The index project

Under the auspices of the Frontier Geoscience Program, a project was undertaken recently to catalogue and to index the above-described commercial operations. The purpose of this project was to facilitate the identification of private data sets that could serve to complement or to improve the potential field data collected by government agencies. This approach has the potential for realizing significant economies because it is usually far less expensive to re-process and to consolidate existing data that it is to mount expeditions for the purpose of collecting new data. (Multiparameter operations carried out on large government survey vessels have been estimated to cost in the order of $25 000 per day.)

The index project was carried out in two phases by the consulting firm of Earth and Ocean Research Limited. In the first phase, a thorough search was conducted through public reports (i.e., those describing field operations prior to 1980) held on file by COGLA and relating to east coast projects. The objectives of this search were to identify all projects or operations that included the collection of gravity and/or magnetic data, and to extract significant pieces of information for tabulation: date of field operation, name of operator/contractor, locality, types and quantities of data collected, equipment used, method of navigation, general comments on data ownership and accessibility, etc.

In all, some 126 separate operations were identified and tabulated. Primary outputs of the first phase were a set of one-page project summaries, plus a set of annual index maps in which were plotted the different projects' work areas. Having all the information organized in this systematic fashion facilitated the extraction of data for various kinds of analyses. For instance, the histogram shown in Figure 1 provides a good historical view of the extent of industry involvement in the East Coast Offshore: one project in 1959 was the forerunner for a series of operations that began in 1964; these peaked in the years 1971-75, and tapered off rapidly in 1976-79.

In the second phase of the index preparation, a review of the project summaries and the annual maps was undertaken to pick out "target surveys", those with potential to enhance the data sets that had been collected and archived by government agencies. Of the 126 projects perused, 33 were deemed to qualify as target surveys. As far as could be determined from the information at hand, the data from these target surveys were held by 14 operators.

The shaded area in Figure 2 illustrates in a composite fashion the general area covered by the 33 target surveys. In fact, there is considerable overlap between many of the individual surveys, and the distribution of data is by no means uniform throughout. However, given the extent and quantity of data collected on these operations, it appeared worthwhile to consider an attempt at consolidation, followed by merging with other data sets.

The next step involved a series of interviews with representatives of the operators concerned to determine: a) the status of the data collected on each target survey, and b) the possibility of obtaining the data with a view to merging with government data sets.

Results of the project

Information obtained in the first and second phases of this project, plus interviews with industry personnel, was used to carry out a fairly objective assessment of the target data sets, and of the likelihood of making further use of them. This assessment was summarized by assigning each data set to one of the following categories:

1. Impossible: data lost or of hopeless quality.

2. Impractical: requiring excessive effort on account of quality or retrieval problems.

3. Possible: requiring some as yet undetermined effort to retrieve and to integrate with the existing government data base.

Figure 1. Number of industry operations in the years 1959-1979, during which gravity and magnetic data were collected in the East Coast Offshore.

Figure 2. *The shaded region is an approximate composite of the areas where gravity and magnetic data were collected by 33 commercial surveys out of the 126 that were catalogued.*

Several data sets were identified that, on the surface at least, fit into category number 3. Further discussion is underway between data specialists in government and industry in order to explore the feasibility of acquiring the data, and to work out a plan for transferring some of these holdings from the private to the public sector.

This project has been fully documented in a GSC Open File report (Plasse and Graves, 1985).

Acknowledgments

References

Macnab, R.F.
    1983: Multiparameter mapping off the east coast of Canada; in Current Research, Part A, Geological Survey of Canada, Paper 83-1A, p. 163-171.

Macnab, R., Loncarevic, B.D., Cooper, R.V., Girouard, P.R., Hughes, M.D., and Shouzhi, F.
    1985: A regional marine multiparameter survey south of Newfoundland; in Current Research, Part B, Geological Survey of Canada, Paper 85-1B, report 38.

Miller, R.O., Macnab, R.F., Amos, C.L., and Fader, G.B.
    1983: Canadian East Coast multiparameter surveys, 1982; in Current Research, Part B, Geological Survey of Canada, Paper 83-1B, p. 331-334.

Plasse, D. and Graves, M.
    1985: Index of commercially acquired potential field data in the Canadian East Coast Offshore; Geological Survey of Canada, Open File 1158.

The Geological Survey of Canada Date Locator File: a progress report

Project 590457

R. McNeely
Terrain Sciences Division

Abstract

A database of selected information on samples dated by the Geological Survey of Canada Radiocarbon Dating Laboratory has been developed as a service to Quaternary researchers. The information is as concise as possible and only minimal textual information is included on the microcomputer file. Database searches are facilitated by using indexed fields (KEYS). Retrieved information can be printed in a wide variety of formats including index cards for personal use and tables of data for publication. Data tables can be transmitted to word processors and incorporated directly into manuscripts. Future enhancements to the system will include the transfer of extracted data files to other locations and the generation of sample location overlays and maps.

Résumé

Une base de données contenant des renseignements choisis sur des échantillons datés par le Laboratoire de datation au carbone radioactif de la Commission géologique du Canada a été mise sur pied pour répondre aux besoins des spécialistes du Quaternaire. Les renseignements emmagasinés dans le micro-ordinateur sont aussi concis que possible et l'entrée de renseignements sous forme de textes y est restreinte. La consultation de la base de données est facilitée par l'utilisation de champs indexés (KEYS). Les renseignements peuvent être extraits diverses formes d'imprimés, y compris sous sur fiches-index pour usage personnel et sous forme de tableaux de données à publier. Le système permet la transmission des tableaux de données à des machines de traitement de textes de manière à les incorporer directement aux manuscrits. Des améliorations seront apportées au système, notamment le transfert de fichiers de données à d'autres endroits et la production de transparents et de cartes de l'emplacement des échantillons.

Introduction

As with most scientific disciplines, Quaternary research has undergone an information explosion in the last few decades. Since the inception of the radiocarbon dating technique more than 35 years ago, the number of samples dated by this technique has steadily increased. The large number of dates now available has made it increasingly difficult for Quaternary researchers to locate and manage the existing information.

Discussions amongst members of Terrain Sciences Division led to the recognition that the most efficient way to contend with the increasing number of dates would be to computerize the information. Following these preliminary discussions, Terrain Sciences Division undertook the development of a Geological Survey of Canada Date Locator File in order to improve the accessibility of dates on Canadian samples to Quaternary researchers.

The Date Locator File

The Date Locator File is a computerized database of selected information on published GSC-dated samples. Because the database has been developed as a service to the users, it has been based on the 'Geological Survey of Canada Radiocarbon Age Data Form' and contains primarily field parameters, rather than laboratory variables. The file does not attempt to mimic radiocarbon date lists or other types of descriptive reports, but instead provides the most pertinent information in as concise a format as possible with limited descriptive text. When a date of interest is identified by a search of the database, the user can consult both the references and the submitter to obtain additional information on the sample.

Historical Development

In 1982 an interactive, proto-database was developed on the mainframe computer (CYBER, model 730) of Energy, Mines and Resources using the SIR (Scientific Information Retrieval) database management system. Testing of the database on SIR revealed a variety of problems and certain limitations with this mainframe application. The increasing availability of microcomputers and associated database management programs provided an alternative mode for developing the database. By September 1983 a proto-database was installed on a VICTOR 9000 / SIRIUS micro-computer; testing of the database continued into early 1984. By the spring of 1985, in excess of 2600 records had been entered onto a file and edited. The database includes all dates published in the 'GSC Radiocarbon Date Lists' for the years 1962 to 1984 inclusive.

The database

File structure and data validity

The database is ordered (sorted) on laboratory number. Even though the information on file for each sample is as concise as possible in order to allow a maximum degree of flexibility when searching the database, each record requires about 1 k bytes of disk storage. Data verification is the responsibility of the submitter. The Radiocarbon Dating Laboratory will initiate the addition of new data records to the file, but the modification (editing) of existing data records will only be undertaken at the request of the submitter. Although the database has been developed as a service to the clientele, its completness and utility depend largely upon ongoing user involvement and a commitment to validate the data.

Data searches and retrievals

Certain fields such as the submitter's name, province, NTS map sheet, coordinates, locality, sample material, taxon, and significance of the sample have been designated as KEY fields and are indexed to facilitate data searches in an interactive mode. Most retrievals of data will be done in a 'batch' mode using defined links between the KEY and secondary fields. A retrieval request can be simple – for example, "All dates on Prince Edward Island" (one KEY) – or complex – "Only those dates on willow (**Salix**) in Nova Scotia related to deglaciation between 10 000 and 20 000 BP" (four KEYS).

Search limitations do exist but in most cases are acceptable. The more specific a request, the greater the likelihood that records will not be included because of missing data. The requested identifier must match the database term exactly or the record will not be retrieved, for example "paleo-" is not "palaeo-". Although a term of interest may occur in a text field, extensive text entries are not normally searched because of the inordinate amount of time required to process them; an example of this would be the simple request for "all Champlain Sea dates". "Champlain Sea" may occur in the comment field of some records but not necessarily all records related to the Champlain Sea. This request could be executed by defining the geographical and temporal extent of the Champlain Sea, retrieving the data, and then culling the non-Champlain Sea records from the extracted file.

Data reports

Once a retrieval has been made, the information can be printed in a wide variety of formats, including complete data records and tables of data for publication. In addition, the most pertinent information can be printed on index cards for the client's reference file. Although standard formats have been developed, special reports can be designed to fulfil most requirements. After a retrieval has been made and the organization of the table defined, the data can be transmitted directly to a word processor for final formatting and incorporation (camera-ready) into a manuscript. This facility eliminates the necessity for retyping the information, and proofreading and editing the table.

Future developments

Data transfers

Although the master Date Locator File will be maintained by Terrain Sciences Division, extracted subsets of the database (ASCII files) can be transmitted to other locations either by sending data diskettes for use on compatible microcomputers or by using the mainframe computer as an intermediary in the transmittal of the data. The responsibility for maintaining the subset of data rests

with the user. In order to avoid a multiplicity of databases which may not correspond to the master file, the wholesale transfer of the database will not be undertaken.

Plots

Once a retrieval has been made, the location of the sample sites along with the sample numbers can be plotted either as a UTM-grid overlay for maps at scales of 1:250 000 and larger, or a complete map can be drawn on a plotter when the map scale is smaller than 1:250 000. The latter plot will be developed from the World Data Bank II on the mainframe computer which will provide physiographic features and political boundaries for a base map; then the Date Locator File information will be superposed on this map.

Data storage and processing in Terrain Sciences Division

Project 690095

R.K. Burns
Terrain Sciences Division

Abstract

An extensive network of SIR computer databases has been developed by Terrain Sciences Division. The objective is to provide an accessible, organized, and secure data bank containing information pertaining to Quaternary samples. These data can be processed through a number of statistical and plotting programs for anlaysis and display.

Résumé

Un réseau étendu de bases de données informatisées, identifiées par le sigle SIR, a été mis au point par le Division de la science des terrains. Le but de ce système est de fournir les services d'une banque de données accessible, structurée et sécuritaire donnant des renseignements pertinents sur des échantillons quarternaires. Ces données peuvent-être traitées afin d'aboutir à des résultats statistiques et graphiques servant éventuellement à des analyses et à de l'affichage graphique et numérique.

Introduction

A substantial effort has been made to develop a computer system to store and process data for the large volume of Quaternary samples collected and analyzed by Terrain Sciences Division. At present the Division operates a number of SIR databases to organize and store data and a series of statistical and plotting programs to process and display data. These computer operations are processed through the Computer Science Centre's Control Data CYBER 730 computer system.

Data storage

Quaternary data are organized and stored using the SIR (Scientific Information Retrieval) data management system (Robinson et al., 1979). SIR is a hierarchical database, accessible in batch and interactive form, in which a variety of distinct data records are linked by a unique identifier — the sample number. The SIR data management system was selected for use by the Division for a number of reasons. For handling Quaternary data, its two most valuable assets are its flexibility for designing the database structure and the flexibility in defining variable formats. The ability to specify variable labels, value labels, data types (integer, real, or alphanumeric), valid values, missing values, and security passwords are features in SIR that are ideally suited to the numerous types of data collected by the Division.

Four levels of SIR databases have been created for use by the Division. Each level has an identical structure but contains a specific group of samples. The base level file is the project file used by the individual researcher to organize data related to a specific project. The other three levels of files — regional, local, and detailed — are general storage files. Regional samples are those collected at a density of 10 km or greater, local samples at 1-10 km, and detailed samples at a density greater than one per kilometre. One other SIR database has been developed for use by the Terrain Sciences sedimentological laboratories to keep track of sample storage. Each record contains information on the sample number, the fraction stored, storage tray, storage location, and the name of the field officer who collected or who is responsible for the sample.

SIR data bases of each level contain a large and varied amount of information. The data are organized in the form of records, which to date include location information, field and laboratory sample descriptions, plotting and statistical indicators, and the results of geochemical anlaysis (Table 1). A textural composition record is currently being developed. Indicators are used to identify the level of database for each sample as well as to designate samples for used in plotting and statistical data processing programs. In geochemical records, for example, indicators identify those samples selected for laboratory processing and analyses; where more than one set of analyses is available, indicators show which group should be used for map plotting and statistical manipulation. Plotting scale of each sample is controlled by the database level indicator. Regional, local, and detailed files are plotted at scales 1:250 000 (and smaller), 1:50 000 to 1:250 000, and larger than 1:25 000, respectively.

Figure 1. *Example of a report generated from a SIR database.*

GRAIN SIZE ANALYSIS

DATA

SAMPLE NUMBER HALFWAY K   LAB NUMBER 15507

TOTAL AIR-DRY WEIGHT   372.3000   SPLIT AIR-DRY WEIGHT   50.2500
WEIGHT SIEVED   25.8900   PERCENT MOISTURE   1.0000
PAN WEIGHT   .5100   DISPERSANT WEIGHT PER 25 ML   .1390
COLOUR OF SUSPENSION

COMPLETE ANALYSIS OF MATERIAL FINER THAN   2.0 MM

			WEIGHT IN RANGE	WEIGHT PERCENT IN RANGE	CUMULATIVE PERCENT COARSER THAN LOWER LIMIT
32.	+	MM	0.0000		
32.	- 16.	MM	0.0000		
16.	- 8.	MM	0.0000		
8.	- 4.	MM	0.0000		
4.	- 2.	MM	51.2000		
2.0	- 1.4	MM	1.3200	2.7085	2.7085
1.4	- 1.0	MM	1.2900	2.6469	5.3554
1.0	- 0.71	MM	1.4900	3.0573	6.4127
0.71	- 0.50	MM	1.8100	3.7139	12.1266
0.50	- 0.35	MM	2.2000	4.5141	16.6407
0.35	- 0.25	MM	2.7200	5.5811	22.2218
0.25	- 0.18	MM	2.6400	5.4169	27.6387
0.18	- 0.12	MM	3.5900	7.3662	35.0049
0.12	- 0.088	MM	2.8900	5.9299	40.9348
0.088	- 0.063	MM	2.5200	5.1707	46.1055
0.063	- 0.044	MM	3.0100	6.1761	52.2817
0.044	- 0.031	MM	2.5600	5.2528	57.5345
0.031	- 0.016	MM	4.2560	8.7328	66.2672
0.016	- 0.008	MM	3.2640	6.6973	72.9645
0.008	- 0.004	MM	3.2440	6.6563	79.6208
0.004	- 0.002	MM	2.2840	4.6865	84.3073
LESS THAN 0.002		MM	7.6480	15.6927	

MATERIAL FINER THAN 0.002 MM MAKES UP 15.69 PERCENT OF THE WEIGHT RECOVERED

METHOD LOSS = -.977

STATISTICS

SAMPLE NUMBER HALFWAY K

	MEAN	SORTING	SKEWNESS	KURTOSIS
FOLK (1968)	*****	*****	*****	*****
INMAN (1952)	*****	*****	*****	*****

MEDIAN   4.06

*****. MULTIMODAL DISTRIBUTION - STATISTICS NOT PRODUCED

GRAIN SIZE ANALYSIS

HALFWAY K :

Figure 2. *Example of output from grain size analysis program.*

Table 1. Records and variables defined in SIR databases used by the Terrain Sciences Division

```
                    LOCATION RECORD

Sample Number            UTM Zone
UTM Coordinates          NTS Sheet Number
Geographical Name

                SAMPLE DESCRIPTION RECORD

Sample Number            Field Officer
Regional Plotting Indicator  Local Plotting Indicator
Detailed Plotting Indicator  Stratigraphic Section Indicator
Oxidation State          Stratigraphic Unit
Depth of Sample          Inclusions in Sample*
Texture of Sample        Colour of Sample
Colour of Clay Fraction*  Comments
Original Sample Number   Field Notes Reference Number

                    COMMENTS RECORD

Sample Number            Run**
Comments

                 DUMMY VARIABLE RECORD

Sample Number            DUM1 to DUM10

(variables DUM1 to DUM10 are used for computations
during data retrieval and do not store data)

                  GEOCHEMICAL RECORD

Sample Number            Run**
Statistical Analysis Indicator  Plotting Indicator
VAR1 to VAR___

(Geochemical variable definitions are based on the size
fraction, method of analysis and chemical element. The
number of geochemical variables defined in each data base
is  open  ended  and  increases  to  include  new
fraction/method/element combinations)

Data retrievals can include any combination of variables.
```

```
 * up to three different observations can be included
** the Run indicator identifies duplicate analysis of the
   same sample
```

Data input in a SIR database allows the initial entry of data for any variable(s) defined in each record type. If a variable has a set of valid values or value ranges, only samples within those predetermined limits will be accepted. Rejected samples are identified by the SIR system for error checking. Data update includes data to be added to or modified in existing samples. SIR retrievals are used to create reports (Fig. 1), perform statistical analyses, and generate separate files of data for plotting. The ability to design retrieval programs that only retrieve samples that meet specific requirements is a valuable feature of the SIR system. By setting conditions on a key variable, for example location or sediment type, it is possible to retrieve data only from samples which satisfy the condition.

Data processing

A variety of programs are available for processing data. Textural composition data from a sample can be processed through a grain size analysis program to produce statistics, a histogram, and a cumulative plot (Fig. 2). Mapping of sample location and geochemical data is presently accomplished by two methods. One method uses a plotting program developed by members of the Division to produce line drawings on the Calcomp plotter. Another method uses a colour contour plotting package created by D.J. Ellwood of the Geological Survey to produce colour or black and white shaded plots on the Applicon plotter. This program has been used by Keetles and Wyatt (this volume) to plot sedimentological parameters of surficial sediments. A modified form of a program by D. Barry of the Computer Science Centre is being developed to produce three dimensional plots, in colour, of sedimentary units recorded through subbottom profiling of lakes.

Acknowledgments

References

Kettles, I.M. and Wyatt, P.H.
  1985: Applications of till geochemistry in southwestern New Brunswick – acid rain sensitivity and mineral exploration; in Current Research, Part B, Geological Survey of Canada, Paper 85-1B, p. 000-000.

Robinson, B.N., Anderson, G.D., Cohen, E., and Gazdzik, W.F.
  1979: Scientific Information Retrieval Users Manual, version 1.1; SIR Inc., Evanston, IL.

FEDERAL-PROVINCIAL MINERAL DEVELOPMENT PROGRAMS 1984-89 AND OTHER FEDERAL PROGRAMS

PROGRAMMES FÉDÉRAUX-PROVINCIAUX DE MISE EN VALEUR DES RESSOURCES MINÉRALES, 1984 à 1989, ET AUTRES PROGRAMMES FÉDÉRAUX

Upper Carboniferous strata of the Tatamagouche Syncline, Cumberland Basin, Nova Scotia[1]

R.J. Ryan[2]

Abstract

Geological investigations indicate that the Upper Carboniferous strata of the Tatamagouche Syncline can be divided into eight map units based on their lithologies and relative abundances.

Alluvial fans developed in the southern part of the study area originating from pre-Carboniferous rocks. In the north and central parts of the area sand and mud were deposited along low sinuosity, anastomosing rivers. In the eastern part of the Tatamagouche Syncline, strongly unimodal paleocurrent measurements indicate flow to the north-northwest. In the western part of the area, crossbeds on the northern limb of the syncline indicate flow to the south and east, suggesting that diapirism of the Windsor Group evaporites may have been contemporaneous with sedimentation.

Copper, silver, zinc, lead and uranium occurrences are numerous and are usually associated with carbonaceous conglomerates and sandstones within the channel lags.

Résumé

Les recherches géologiques indiquent que les couches du Carbonifère supérieur du synclinal Tatamagouche peuvent se subdiviser en huit unités cartographiques en fonction de leurs lithologies et de leur abondance relative.

Les cônes alluviaux qui se sont formés dans la partie sud de la zone à l'étude se composent de matériel provenant de roches antérieures au Carbonifère. Dans les parties nord et centrale de la zone étudiée, le sable et la boue se sont déposés le long de cours d'eau anastomosés mais peu sinueux. Dans la partie est du synclinal Tatamagouche, des mesures du paléocourant fortement unimodal indiquent un écoulement en direction nord-nord-ouest. Dans la partie ouest de la région, la présence de couches obliques sur le flanc nord du synclinal indique un écoulement vers le sud et l'est, phénomène qui semble indiquer la contemporanéité du diapirisme des évaporites du groupe de Windsor avec l'épisode de sédimentation.

Les venues de cuivre, d'argent, de zinc, de plomb et d'uranium sont nombreuses et sont habituellement associées aux conglomérats charbonneux et aux grès formés dans les dépôts fluviatiles.

Introduction

The post-Acadian Upper Paleozoic sedimentary rocks of the Atlantic region of Canada range in age from Middle Devonian to Early Permian. These rocks may be divided into four groups: the Horton, Windsor, Canso-Riversdale and the Cumberland-Pictou (Fig. 1).

The name Windsor Group was proposed by Bell (1929) for the Carboniferous marine limestones, evaporites and clastics within the Windsor District of Nova Scotia.

The Canso and Riversdale groups overlap in age, as discussed by Kelley (1967), and were considered as a separate division by Howie and Barss (1974). The Canso Group was defined by Bell (1944) as a sequence of Namurian A nonmarine red and grey shales and sandstones that overlies the marine beds of the Windsor Group. The Riversdale Group was defined by Bell (1944) as a sequence of Westphalian A continental strata that lie stratigraphically between the Canso and the Cumberland groups. Howie and Barss (1974) suggested that the Canso-Riversdale are regionally indivisible and range in age from late Visean to Westphalian A. Paleontological data and local distinctive lithostratigraphic units help in the definition of some formations.

Bell (1944) defined the Cumberland Group as those rocks between the Riversdale Group and overlying Pictou Group. The Cumberland Group is restricted to the Cumberland Basin of Nova Scotia and to a few areas in southern New Brunswick. Bell (1929) defined the Pictou Group as Westphalian C to Stephanian and the sandstone, shales, and mudstones are similar to those exposed on the West Branch of the River John, Nova Scotia. Because of the contemporaneous nature of the groups and the limited areal extent of the Cumberland Group, in particular, Howie and Barss (1974) referred to the Cumberland and the Pictou as one stratigraphic unit. Howie and Barss also suggested inclusion of the red beds of Prince Edward Island within the Pictou Group.

The Upper Carboniferous strata of the Tatamagouche Syncline area are folded into a gently plunging syncline trending northeast. The strata comprise red and grey conglomerates, sandstones and mudstones with minor limestones, totalling approximately 3400 m in thickness (Fig. 2, 3, Table 1).

Figure 2. *Stratigraphic column of the Carboniferous strata, Tatamagouche Syncline.*

Messervey (1929), Papenfus (1931), Schumway (1957), Brummer (1958), MacKay and Zentilli (1976), Dunsmore (1977) and van de Poll (1978), as well as numerous exploration companies, have all made significant contributions to the understanding of the mineralization processes within the Upper Carboniferous of northern Nova Scotia.

Present study

During the 1984 field season, geological investigations in the west half of the Tatamagouche Syncline were completed and integrated with the data from the eastern part of the syncline, investigated in 1983.

Stratigraphy

A compilation of the two field seasons' mapping and subsurface data is summarized in Table 1. Tables 2 to 4 summarize the detailed lithological information for each of the map units. Ages for the lower units are after Hacquebard (1972) and upper units from Ryan (1984).

Paleocurrent studies

Over 600 paleocurrent measurements were recorded, including ripple marks, parting lineations, crossbed truncation ridges, preferred plant fragment orientations, flute marks, tool marks, pebble imbrications, and crossbedding. The trough crossbeds gave the most consistent paleocurrent determinations (Fig. 4).

The paleocurrent data for the eastern part of the Tatamagouche Syncline exhibit strongly unimodal distributions with a modal trend of north-northwest (340°; Fig. 5). The low variance in the paleocurrent data indicates that deposition, for the most part, occurred as a result of low sinuosity flow, due, in part, to steeper gradients than those found elsewhere within the Upper Carboniferous rocks of the

Figure 1. *Generalized Carboniferous stratigraphy, Atlantic Canada.*

PICTOU GROUP

| 10 | Upper Red Beds |

| 9 | Middle Red Beds |

| 8 | Lower Red Beds |

| 7 | Grey Beds |

CUMBERLAND GROUP

| 6 | Fine Facies |

| 5 | Coarse Facies |

RIVERSDALE GROUP

| 4 | Boss Point Formation |

| 3 | Millsville Formation |

| 2 | WINDSOR GROUP |

| 1 | PRECARBONIFEROUS |

Figure 3. Generalized geological map of the Carboniferous rocks, Tatamagouche Syncline.

Atlantic region. The Pictou upper red beds and the Boss Point Formation exhibit significant variability in paleocurrent directions.

The north-northwest direction of flow was therefore dominant from Namurian to the early Permian in the eastern half of the Tatamagouche Syncline.

The data for the western part of the Tatamagouche Syncline indicate a division of flow at approximately the synclinal axis. On the southern limb the flow continues to be to the north-northwest. On the northern limb, flow is to the south-southeast, indicating a possible topographic high to the northwest.

The southerly flow directions observed on the northern limb are found in progressively older beds towards the west suggesting that diapirism of the Windsor Group evaporites was initiated in the west during the Westphalian B. The first

indication of topographic relief to the north within the eastern part of the Malagash Anticline is found within the Pictou upper red beds of Stephanian age, suggesting that the Windsor Group evaporite diapirism migrated through time from west to east. Further paleocurrent studies north of the Malagash Anticline may confirm this hypothesis.

Sedimentology

Riversdale Group. The Millsville Formation is characterized by pebble imbrication, coarse, poorly sorted boulder to pebble conglomerates and only rare evidence of cross stratification. The presence of planar beds supports the existence of episodic sheet flow. Some of the conglomerates appear to be matrix-supported and were probably the result of debris flows. The sedimentological factors together with geographical distribution of the formation indicate that the environment of deposition was a proximal alluvial fan.

Table 1. Generalized stratigraphy of the Carboniferous strata in Tatamagouche Syncline area, Cumberland Basin, N.S.

Age	Thickness	Sand:silt ratios	Bedforms	Lithologies	Map unit
Stephian to Early Permian	300 m+	1:5	Trough cross stratified conglomerates and sandstones, fining upward cycles, ripple drift and lunate rippled siltstone, planar mudstone and limestone.	Red to reddish-grey shale, mudstone, siltstone, medium grained subarkose, pebbly arkose, and mud chip conglomerate, thin laterally continuous grey micritic limestones.	Pictou. Upper red beds
Westphalian D to Stephanian	310 m	1:3	Trough crossbedded sandstones and conglomerates, most fine upward in cycles, planar siltstone, mudstone and limestone.	Red, coarse grained arkose, medium grained subarkose, calcareous mud chip conglomerate, siltstone and mudstone, minor thin grey limestone.	Pictou. Middle red beds
Westphalian C-D	800 to 900 m	1:1	Trough crossbedded sandstone and conglomerate, fining upward cycles, ripple drift and lunate ripple siltstone, planar mudstone.	Red calcareous mud chip conglomerate, arkose, subarkose siltstone, mudstone and shale, sandstones usually coarse grained.	Pictou. Lower red beds
Westphalian C	100 to 400 m	2:1	Trough cross stratified conglomerate and sandstone, ripple drift siltstone, planar mudstone and shale fining upward cycles.	Calcareous mud chip conglomerate, coarse grained arkose, fine grained subarkose, siltstone, mudstone and shale, reddish brown to grey, rare coal.	Pictou. Grey beds
Westphalian B?	0.0 (East) to 700 m (West)	(South) 15:1 to 8:1 (North)	Large trough cross stratification, crossbed imbrication, high flow planar beds.	Red polymictic cobble to pebble orthoconglomerate, red coarse grained pebbly arkose.	Cumberland. Coarse facies
Westphalian A	200 to 600 m	10:1	Trough crossbedded, sandstones, rare planar beds, ripple drift siltstones, low flow planar mudstones.	Greyish-brown coarse to fine grained subarkose, minor arkose, siltstone, thin interbedded red and green shale and mudstone.	Boss Point Formation
Namurian	0.0 to 700 m	25:1	Upper flow planar beds, some pebble imbrication, massive to thickly bedded.	Red, rarely grey, boulder to pebble conglomerate, polymictic, orthoconglomerates with rare paraconglomerates. Rare coarse grained sandstone interbeds.	Millsville Formation
Visean	1000 m ±	N/A	Planar accretion, salt tectonism obscures bedding.	Marine fossiliferous limestone, salt, gypsum and minor siltstone.	Windsor Group

The Boss Point Formation is sand-dominated with only thin interbeds of siltstone and shale. The sandstone and conglomerate beds are generally tabular and trough cross stratified. Deposition of the Boss Point Formation of the Tatamagouche area probably took place in moderate to low sinuosity, meandering, sand-dominated streams.

Cumberland Group. The Cumberland Group coarse facies, which is made up of polymictic conglomerates, exhibits both obscure cross stratification and planar graded beds. The presence of some trough cross stratification and the finer grain size of the conglomerates, suggest deposition in braided streams in a mid to distal alluvial fan environment. The existence of planar-bedded coarse sands and conglomerates indicates that during flood stage, sheet flow was dominant.

The conglomerates of the Cumberland fine facies are interpreted as being channel lag, traction load, deposits. The sandstones appear to be trough cross stratified and probably result from channel dune progradation. The red and grey shales and minor thin coals represent the flood plain and back swamp environments marginal to the fluvial channels.

Pictou Group. The Pictou grey beds exhibit unimodal paleocurrent data of low variance and fining upward sequences of conglomerate to sandstone which are similar in characteristics to sedimentary rocks which Campbell (1976) attributed to deposition in low sinuosity streams. The conglomerates constitute channel lags and the sandstones (arkoses), channel fill due to the migration of dunes, which resulted in trough cross stratification. The subarkoses were

Table 2. Lithological descriptions of the Riversdale and Cumberland groups, Tatamagouche Syncline, Cumberland Basin, N.S.

Map unit	%	Lithology	Colour	Grain size	Sorting	Roundness	Composition Qtz	Fld	Mic	Pl	Bedform
Millsville Formation	100	Ortho and para-conglomerate	Red	Boulder to pebble	V poor	Sub rd	Polymictic				Planar high flow regime
Boss Point Formation	10	Mud chip conglomerate	Brown grey	Pebble 25%	Poor	Sub rd	40	20	5	2	Large trough
	70	Subarkose	Grey brown	Fine-medium sand	Mod.	Sub ang	80	15	1-5	2	Large trough
	10	Siltstone	Light grey	Silt	Well	Sub rd	90	5	3	2	Planar
	10	Shale	Grey to black	Clay	-	-	Clay			5	Planar
Cumberland. Coarse facies	90	Conglomerate	Red brown	Cobble to pebble	Poor	Sub rd	Polymictic				Large trough
	10	Arkose	Red brown	Coarse sand	Poor	Sub ang	70	25	5	-	Trough cross
Cumberland. Fine facies	10	Mud chip conglomerate	Grey 26%	Pebble	Poor	Sub rd	40	20	5	2	Large trough
	10	Pebbly arkose	Grey	V coarse	Poor	Sub ang	65	25	6	4	Large trough
	30	Arkoses	Grey	Medium to coarse	Mod.	Sub ang	60	30	7	3	Large trough
	10	Subarkoses	Grey	Fine to medium	Well	Sub rd	75	15	8	2	Large trough
	40	Siltstones and shales	Black to red brown	Silt to clay	Well	Sub rd	Qtz and clay micromicaceous				Ripple drift and planar

Table 3. Lithological descriptions of the Pictou grey beds and the Pictou lower red beds, Tatamagouche Syncline, Cumberland Basin, N.S.

Map unit	%	Lithology	Colour	Grain size	Sorting	Roundness	Qtz	Composition Fld	Mic	Pl	Bedform
Pictou. Grey beds	3	Calcareous mud chip conglomerate	Grey with red and grey clasts	Pebble	Poor	Moderate	50	5 40%-clasts	2	2	Large trough
	3	Pebbly arkoses	Grey to brown	Pebbles in v. coarse ss	Poor	Sub ang	65	25	6	4	Large trough
	50	Arkose	Lt. pink grey	Coarse sand	Poor	Sub ang	70	25	2	2	Large and small troughs
	5	Subarkose	Lt. grey	Medium to fine sand	Moderate	Sub rd	75	15	7	2	Planar coarse upwards
	40	Siltstone and mudstone	Red-brown	Silt to clay	Moderate	-	Quartz and clay				Planar beds
Pictou. Lower red beds	2	Calcareous mud chip conglomerate	Red-grey to red-brown	Pebble	Poor	Moderate	50	5 40%-clasts	1	2	Large trough
	2	Pebbly arkose	Red-brown	Pebble in coarse sand	Poor	Sub ang	66	27	3	4	Large trough
	6	Arkose	Red-brown	V. coarse sand	Poor	Ang	63	30	5	2	Large trough
	15	Subarkose	Red-brown to red-grey	Coarse to fine sand	Moderate	Sub ang	80	12	6	2	Coarse large and small troughs, fine-planar
	76	Siltstone, mudstone, shale and limestone (thin)	Red to red-brown	Silt to clay	Moderate	-	Qtz + clay + calcite				Planar, ripples and ripple drift worm burrows

Table 4. Lithological descriptions of the Pictou middle red beds and the Pictou upper red beds, Tatamagouche Syncline, Cumberland Basin, N.S.

Map unit	%	Lithology	Colour	Grain size	Sorting	Roundness	Qtz	Composition Fld	Mic	Pl	Bedform
Pictou. Middle red beds	1	Calcareous mud chip conglomerate	Red-brown	Pebble	Poor	Sub rd	50	15 32%-clasts	2	1	Large trough
	1	Pebbly arkose	Red-brown	Pebbles in coarse sand	Poor	Angular	65	28	5	2	Large trough
	4	Arkose	Red-brown	Coarse sand	Poor	Sub ang	70	25	4	1	Large and small trough
	10	Subarkose	Red-brown	Coarse to fine sand	Moderate	Sub rd	80	15	4	1	Small trough and tabular cross strata
	83	Siltstone, mudstone and shale	Red-brown	Silt to clay	-	-	Quartz to clay				Planar, ripple & ripple drift, worm burrows abundant
	1	Limestone	Grey	Micrite	-	-	Calcite				Fossiliferous
Pictou. Upper red beds	2	Calcareous mud chip conglomerate	Grey to red-brown	Pebble	Poor	Sub rd	50	15 30%-clasts	2	1	Large trough
	3	Pebbly arkose	Red-brown to red-grey	Pebble in coarse sand	Poor	Sub ang	65	30	4	1	Large trough
	5	Arkose	Red-brown	Coarse sand	Poor	Sub ang	70	25	4	1	Large and small trough
	3	Subarkose	Red-brown to red-grey	Medium to fine sand	Moderate	Sub rd	80	15	4	1	Planar, small troughs, tabular cross strata
	86	Siltstone, mudstone, and shale	Red	Silt-clay	-	-	Quartz + clay				Planar, ripples and ripple drift
	1	Limestone	Grey	Micrite	-	-	Calcite				Fossiliferous

Figure 4. *Crossbed paleocurrent trends within the Upper Carboniferous strata, Tatamagouche Syncline.*

Figure 5. *Crossbed paleocurrent trends, Tatamagouche Syncline.*

deposited as coarsening upward cycles of levee and crevasse splay deposits and the finer grained sedimentary rocks were deposited on the flood plains.

The environment of deposition of the Pictou lower red beds is very similar to that of the Pictou grey beds. Low sinuosity, possibly anastomosing streams yielded channel lag conglomerates. The arkoses and coarse subarkoses were deposited in the channels by migrating dunes. The fine subarkoses represent levee and possibly crevasse splay deposition. The fine grained sediments were deposited on the flood plains, and the limestones resulted from lake deposition within back swamp areas.

The arkoses and coarse grained subarkoses of the Pictou middle red beds exhibit tabular crossbedding in addition to the more common trough crossbedding.

The paleocurrent data for this unit exhibit slightly more variance than the Pictou lower red beds and the Pictou grey beds. Therefore, although still within a low sinuosity stream system, some meandering is apparent for streams at the time of the Pictou middle red bed deposition. The increase is finer grained sedimentary rocks, and variance in paleocurrent data would indicate a lessening in the stream gradient.

Limestones were deposited in large lakes which periodically extended over most of the flood plain area. The existence of extensive lakes would further suggest a lower stream gradient within the Pictou middle red bed unit. The extensive channel sands are concave upward at their bases, suggesting low sinuosity streams. The great width of the streams is due in part to the lack of soil binding grasses during the Carboniferous (van de Poll, 1984).

The Pictou upper red beds have numerous mud-filled abandoned channels. Tabular cross stratification is present but trough crossbedding is the most common sedimentary structure in sandstone and conglomerate. Plant debris is abundant within most of the channel-sand units.

Reduction spheres up to 8 cm across are locally abundant within the siltstones and fine grained sandstones. The fine sandstones and siltstones almost always contain lunate ripples. Reverse graded bedding is common within the planar bedded fine grained subarkoses.

Limestone beds are common and are light to medium grey biomicrites with abundant ostracod, gastropod and algal remains. The upper limestones often are intraclastic and contain micritic clasts of ostracod limestones.

The paleocurrent directions of the upper red beds are much more varied than those for the underlying Upper Carboniferous strata of the Tatamagouche Syncline (Fig. 4). Direction reversals within a few tens of metres can be observed in the Cape John area. Although the paleocurrent data are polymodal, the north-northwest (340°) direction is still dominant.

The paleocurrent data suggest a meandering stream environment. Trough cross stratification is the most common bedform. Oxbow configurations are not present near the mud-filled abandoned channels as would be expected with meander cut offs.

The most likely configuration for the streams is therefore an anastomosing one. Divergent branches can easily explain paleocurrent reversals and channel abandonment.

Economic geology

In North America, the terms stratiform and stratabound are both used and are not necessarily synonymous. In Europe more emphasis is placed on the morphology than in America.

Figure 6. *Metallic mineral occurrences in the Carboniferous Tatamagouche Syncline. Triangle = copper, circle = uranium, square = lead.*

Pelissonier (1972) classified copper deposits with the use of the terms discordant (vein and multifissured), subconcordant and concordant.

In addition to morphological classification there are classifications based on genesis of the ore deposit. Lindgren (1933), Schneiderhohn (1962) and Gustafson and Williams (1981) have all proposed genetic classification schemes.

Within this paper, the mineral occurrences have a two fold classification, with the first part being the morphological character and the second being the genetic character of the mineralization.

I also adopt the definition of diagenetic ore deposits proposed by Gustafson and Williams (1981), that is, diagenetic ore mineralization results from the concentration of substances contained within the rock or sedimentary basin.

There are at least 40 mineral occurrences within the Tatamagouche Syncline (Fig. 6). Copper occurrences are most numerous, and several of these have associated uranium mineralization and high silver values (McNabb, 1977; MacDonald, 1978; Chatterjee, 1979). Lead mineralization was discovered in boulders near Skinner's Cove (Ryan, 1984; Fig. 6).

Copper usually occurs as malachite, nodules of chalcocite or chalcocite replacing both plant material and pyrite (Schumway, 1957). The copper was thought to be supergene enriched by Brummer (1958), but the existence of chalcocite in diamond drill core at depths of 300 m is not consistent with this interpretation.

Uranium occurrences can occur with little or no associated copper mineralization (McNabb, 1977). The uranium mineralization is, however, very closely associated with carbon and is bound in most cases by carbon. The uranium which was left behind by the migrating uranium-bearing solutions has undergone some remobilization within channel sandstone beds due to hydraulic pressures, resulting in uranium mineralization within carbon-deficient sandstones close to carbon-rich channel lags.

Dunsmore (1977) suggested that the uranium mineralization usually occurred near the base of fining-upward cycles in the Tatamagouche area. Almost all of the mineral occurrences are associated with carbon-rich channel lag sandstones within multistoried channels which usually, although not everywhere, occur near the base of the channel sandstone bodies. Because the lag sandstones are part of the overall channel sequence, it is necessary to follow such beds down channel, and not down dip, in order to delineate mineralized zones.

The mineralization within the Tatamagouche Syncline is polyphase.

Carbon from plant material provides a place for bacterial reduction to fix sulphur within the channel lag sandstones. The presence of the underlying evaporites of the Windsor Group may provide sulphur to the mineralizing solutions (Dunsmore, 1977). The first sulphide was pyrite replacing plant material in sandstones and conglomerates rich in organic matter (Schumway, 1957). The pyrite and plant material have been replaced by stratabound chalcocite and native silver during an early, pre-folding, low temperature, subsurface, diagenetic phase of mineralization, probably involving remobilization of copper from adjacent strata. Silver values of up to 470 ppm are usually associated with massive chalcocite.

The distribution of the uranium occurrences indicates that the uranium was deposited after folding in two phases (MacNabb, 1977). The original uranium mineralization was as stratiform low temperature subsurface epigenetic mineralization (trend type deposition). It is found close to original plant debris within channel sandstones. Evidence of secondary migration of this uranium by small roll fronts has been preserved on the lateral margins of several channel sands.

The timing of the lead mineralization is unknown. In the Tatamagouche area it is closely associated with carbon-rich channel lag-conglomerates, unlike the Yava Deposit, Cape Breton, which is of similar age but shows little correlation between lead mineralization and the presence of carbon (Bjørlykke and Sangster, 1981).

The nature of the mineralizing processes within these continental red beds is clearly dependent upon the composition, texture and morphology of the sedimentary units. It is, therefore, essential that investigations of mineralization within similar geological settings require concurrent detailed studies of stratigraphy, structure and sedimentology, in order to formulate a comprehensive exploration model.

References

Bell, W.A.
1929: Horton-Windsor District, Nova Scotia; Geological Survey of Canada, Memoir 155.

1944: Carboniferous Rocks and Fossil Floras of Northern Nova Scotia; Geological Survey of Canada, Memoir 238.

1958: Possibilities for occurrence of petroleum reservoirs in Nova Scotia; Nova Scotia Department of Mines, 177 p.

Bjørlykke, A. and Sangster, D.F.
1981: An Overview of Sandstone Lead Deposits and their Relation to Red-Bed Copper and Carbonated-Hosted Lead-Zinc Deposits; Economic Geology, 75th Anniversary Volume, 1981, p. 179-213.

Brummer, J.J.
1958: Supergene copper-uranium deposits in Northern Nova Scotia; Economic Geology, v. 53, p. 309-324.

Campbell, C.V.
1976: Reservoir geometry of fluvial sheet sandstone; Bulletin American Association of Petroleum Geologists, 60, p. 1009-1020.

Chatterjee, A.K.
1979: Metallogenic Map of Nova Scotia; Nova Scotia Department of Mines and Energy.

Dawson, J.W.
1855: Acadian Geology (1st Ed.); London, MacMillan and Co.

Dunsmore, H.E.
1977: A new genetic model for Uranium-Copper Mineralization, Permo-Carboniferous Basin, Northern Nova Scotia; in Report of Activities, Part B, Geological Survey of Canada, Paper 77-1B, (1977).

Fletcher, H.
1892: Report on Geological Surveys and Explorations in the Counties of Pictou and Colchester, Nova Scotia; Geological Survey of Canada Annual Report, 1889-1891, v. 5, pt. P, p. 5-193.

Gustafson, Lewis B. and Williams, Neil
1981: Sediment-Hosted Stratiform Deposits of Copper, Lead and Zinc; Economic Geology, 75th Anniversary Volume, p. 139-178.

Hacquebard, P.A.
1972: The Carboniferous of Eastern Canada; Compte Rendu, 7th International Carboniferous Congress, Krefeld 1971, tome I, p. 69-90.

Howie, R.D. and Barss, M.S.
1974: Upper Paleozoic Rocks of the Atlantic Provinces, Gulf of St. Lawrence, and adjacent continental shelf; Geological Survey of Canada, Paper 74-30, v. 2, p. 35-50.

Kelley, D.G.
1967: Some aspects of Carboniferous Stratigraphy and Depositional History in the Atlantic Provinces; Geological Association of Canada, Special Paper No. 4, p. 213-228.

Lindgren, A.
1933: Mineral Deposits; McGraw Hill, New York, 813 p.

MacDonald, C.J.D.
1978: Uranium, Tatamagouche Area, Nova Scotia; Noranda Exploration Co. Ltd., Assessment Report, Nova Scotia, 11E/11C 54-D-45 (11).

MacKay, R.M. and Zentilli, M.
1976: Mineralogical Observations on the Copper-Uranium occurrence at Black Brook, Nova Scotia; Geological Survey of Canada, Paper 76-1B.

MacNabb, B.E.
1977: Uranium, Tatamagouche Area, Nova Scotia; Lacana Exploration, Nova Scotia Assessment Report, 11E/NW 54-D-45 (01).

Messervey, J.P.
1929: Copper in Nova Scotia; Nova Scotia Department of Mines Publication 7.

Papenfus, E.B.
1931: "Red Bed" Copper Deposits in Nova Scotia and New Brunswick; Economic Geology, v. 26, p. 314-330.

Pelissonier, H.
1972: Les dimensions des gisements de cuivre du monde; Bureau de Recherches Geologiques et Minières, Mémoire 57, 403 p.

Ryan, R.J.
1984: Upper Carboniferous strata of the east half of the Tatamagouche Syncline; in Current Research, Part A, Geological Survey of Canada, Paper 84-1A, p. 473-476.

Schneiderhohn, H.
1962: Erzlagerstatten Kurzvorlesung Zur Einfuhrung und Weider-holung. 4 Auflage: Stuttgard, Fisher-Verlag.

Schumway, G.
1957: Sedimentary Copper, Tatamagouche Area, Nova Scotia; unpublished M.Sc. thesis, M.I.T.

van de Poll, H.W.
1978: Paleoclimatic Control and Stratigraphic Limits of Synsedimentary Mineral Occurrences in Mississippian-Early Pennsylvanian Strata of Eastern Canada; Economic Geology, v. 73, p. 1069-1081.

1984: Personal Communication.

Stratigraphy and sedimentology of the Cabano, Pointe aux Trembles, and Lac Raymond formations, Témiscouata and Rimouski counties, Quebec

Contract 12ST.23233-4-0047

Jean David[2], Nathalie Chabot[2], Claude Marcotte[2], Jean Lajoie[2], and Pierre J. Lespérance[2]
Precambrian Geology Division

Abstract

The Cabano Formation formerly considered early and middle Llandoverian is extended downward to the Ashgillian, and even possibly late Caradocian. The other two formations, the Pointe Aux Trembles and the Lac Raymond, are late Llandoverian (C_1 to C_5).

Fossils indicate that the environment of deposition was marine at least from the lower part of the Cabano up to the mid Pointe Aux Trembles. The upper part of the sequence could have accumulated in subaerial environments. The coarse sediments of the lower part of the section were transported by mass flows and accumulated in a calm, possibly deep marine environment.

The Cabano sediments were derived from the north, and possibly from the south from sedimentary nappes and from obducted ophiolites, a source similar in age and composition to that of the Honorat Group of Gaspé as well as other units of similar age in the Québec Appalachians.

The ensialic volcanic arc present in northwestern New Brunswick in the early Llandoverian did not contribute sediments to the trough until the late Llandoverian when it became a major source, suggesting northwestward convergence of the arc.

Résumé

La formation de Cabano, considérée antérieurement comme datant du Llandovérien inférieur et moyen, s'avère plus ancienne et date plutôt de l'Ashgillien, peut-être même du Caradocien supérieur. Les deux autres formations, soit Pointe Aux Trembles et Lac Raymond, sont d'âge Llandovérien supérieur (C_1 à C_5).

La présence de fossiles indique un milieu d'accumulation marin, au moins de la base de la formation de Cabano à la fin de la demie inférieure de la formation de Pointe Aux Trembles. La mise en place de la partie sommitale de la séquence aurait pu se produire en milieu subaérien. On estime qu'un mode de transport par épanchement de masse est responsable de l'accumulation des sédiments grossiers de la base de la section possiblement en un milieu marin profond et calme.

Les sédiments de la formation de Cabano sont dérivés du nord et, peut-être du sud, à partir de nappes sédimentaires et d'ophiolites obductées. Cette provenance est similaire en âge et en composition au groupe d'Honorat de la Gaspésie, aussi bien qu'à d'autres unités d'âge équivalent que l'on retrouve dans les Appalaches du Québec.

L'arc volcanique ensialique présent, au Llandovérien inférieur, dans la partie nord-ouest du Nouveau-Brunswick n'a fourni aucuns sédiments de la fosse avant le Llandovérien supérieur, époque à laquelle l'arc est devenu une source majeure; ce phénomène semble indiquer une convergence de l'arc vers le nord-ouest. Cet article est également disponible en français.

Introduction

The objectives of the 1984 field season were to study the age, provenance and environment of sedimentation of the Lower Silurian rocks of Témiscouata and Rimouski counties in the Québec Appalachians in order to arrive at a better paleogeographic understanding of these unique strata. Field work consisted of detailed measurement of bed thickness, grain size and primary structures on selected sections of the Cabano, Pointe Aux Trembles, and Lac Raymond formations, in map areas Cabano (21 N/10), Squateck (21 N/15), and Lac Prime (22 C/1; see Fig. 1), coupled with detailed sampling for petrographic and chemical analyses. The following progress report is essentially based on field data.

Stratigraphy

The stratigraphy of the area is summarized in Figure 2. The general geology was described by Lajoie et al. (1968). The Cabano Formation was considered by these authors to be early and middle Llandoverian (A_4-B_3). Deformed graptolites found last summer, 600 m above the base of the Cabano Formation along the Rimouski River (? **Orthograptus amplexicaulis**, and **Climacograptus** sp.; of the **typicalis**, **brevis-putillus** or **normalis** groups; J. Riva, personal communication, 1984) indicate that the formation extends down into the Ordovician Ashgillian (**G. persculptus** Zone), to possibly the late Caradocian (**D. clingani** Zone). The contact of the Cabano Formation with the underlying Trinité Group (Lajoie et al., 1968) has never been observed, although there are few beds missing in section I at Mount Longue-Vue (Fig. 1, 3). In this area, the Cabano is gently folded, with dips less than 20°, and overlies the tightly folded and slightly metamorphosed strata of the Trinité Group that contain a graptolite fauna of Caradocian age.

The Pointe Aux Trembles Formation extends northeastward from Témiscouata Lake area to the central part of the region where it intertongues with the Lac Raymond

Figure 1.   General geology, modified from Lajoie et al. (1968), with locations of stratigraphic sections.

492

Figure 2. Table of formations in the Témiscouata and Rimouski areas.

Figure 3. Stratigraphic sections of the Cabano Formation in the Rimouski River area; locations of sections on Figure 1.

Formation (Fig. 1). Lenses of Pointe Aux Trembles lithology persist for some distance within the Lac Raymond. Northeast of Lac des Echos (section IV, Fig. 1), a large lens of epiclastic and pyroclastic rocks has been named the Lac Castor Member by Lajoie et al. (1968). The contact of the Cabano Formation with the Pointe Aux Trembles and Lac Raymond formations is transitional and is placed at the first occurrence of volcanic detritus. Lajoie et al. (1968) assigned a late Llandoverian age (C_1 to C_5) to the Pointe Aux Trembles and Lac Raymond formations.

The Llandoverian Pointe Aux Trembles and Lac Raymond formations are overlain paraconformably by the Upper Silurian (Ludlovian) Mont Wissick Group and St-Léon Formation. Reassessment of the Asselin Formation of Lajoie et al. (1968) appears to indicate that these strata are best assigned to the St-Léon Formation of the Mont Wissick Group.

Cabano Formation

The Cabano Formation can be subdivided into a fine- and a coarse-grained facies. Its most distinctive rock is a dark grey lithic wacke that contains abundant slaty fragments which impart a foliation to the rock. In the fine grained facies, the wacke is interbedded with siltstone and mudstone, whereas in the coarse grained facies it is interbedded with conglomerate.

To study the petrography and sedimentology of the Cabano we chose two sections in the fine facies (sections II, and III; Fig. 1, 3), and three sections in the conglomerate facies (sections I, VII E, and W; Fig. 2, 4). Section I is on the slopes of Mount Longue-Vue, section II is along the Rimouski River, section III is on Orient Brook, NW of Echos Lake, and sections VII E and W are on the east and west shores of Témiscouata Lake respectively (Fig. 1).

The thickness of the Cabano Formation ranges from 1000 m on Témiscouata Lake and at Mount Longue-Vue, at both extremities of the studied area, to 2500 m near the centre of the sedimentary basin, at Biencourt Lake.

The fine grained facies of which the Rimouski River section (II) is typical, makes up most of the Cabano Formation. The mudstone beds are thin ($\bar{x}$: 4 cm), interbedded with very thin beds ($\bar{x}$: 2 cm) of fine grained wacke. The lower contact of sandstone beds is sharp, commonly erosive. These beds show primary structure sequences characteristic of so-called distal turbidites (**bcd, cde** of the turbidite model). Paleocurrents measured on crossbedding of the c division give a general W to E direction of transport in section III, and NW to SE direction in section II (Fig. 3).

Figure 4. Bed-thickness distribution for the Cabano conglomerate (A) and sandstone (B), in the Témiscouata Lake sections.

- **LAC TEMISCOUATA SECTION**
- ○ **ORIENT, RIMOUSKI, LONGUE-VUE SECTIONS**

Figure 5. Framework composition of the Cabano sandstone. Qm: monocrystalline quartz grains; K: potassic feldspar; P: monocrystalline plagioclase; Lt: total lithic fragments; Qp: unstable lithic plus stable quartzose lithic fragments.

Framework mineralogical composition of ten sandstone samples gives an average of 53% quartz, 42% rock fragments, and 5% feldspar (mostly plagioclase). The rock fragments are all sedimentary in origin, and are made of mudstone, siltstone, chert, quartzite, and limestone (Fig. 5).

The coarse grained facies of the Cabano is composed of granule to cobble lithic conglomerate in thick beds ($\bar{x}$: 76 cm; Fig. 6) interbedded with medium bedded ($\bar{x}$: 13 cm) coarse grained wacke similar to the sandstone described above in the fine facies, although much coarser. Figure 4 gives bed-thickness distribution for the Cabano sandstone and conglomerate. The beds of conglomerate are lenticular, and their lateral extent is commonly limited to 10 m. Soles are sharp and non-erosive, whereas the upper contact may show a thin transition with the overlying sandstone beds. The beds are massive (65%), inversely graded (19%), normally graded (13%), or rarely (3%) show a lower inversely graded division

overlain by a normally graded division. Clasts are generally matrix supported (25 to 35% sandy matrix), with a random fabric that may be perpendicular to the upper bedding plane, with clasts projecting into the overlying sandstone (Fig. 6). In a few beds there is an **a** fabric that is oriented ENE-WSW when the beds are restored to the horizontal.

Figure 6. Large clast at top of a conglomerate bed, projecting into overlying sandstone bed. Cabano Formation, section VII W.

Figure 7. Stratigraphic sections of Cabano conglomerate on Témiscouata Lake.

494

All the clasts in the conglomerate have a sedimentary origin. Quartzite, lithic and feldspathic sandstones, and limestone make up 95% of the clasts (Fig. 7); the remaining 5% are made up of siltstone, dolomite, and lithic conglomerate. Preliminary results show that there is little up-section variation of clast composition for the lower half of the studied sections, but there may be an up-section increase of quartzite fragments coupled with a decrease of lithic and feldspathic sandstones in the upper part of the section (Fig. 7). since the study was done on one granulo-metric class to avoid the possible effect of size on composition it suggests an up-section variation of the source area. Also, lateral variations suggest possible local influence for clast composition as limestone fragments are much more abundant on the eastern shore of Témiscouata Lake (15 to 30%), than on the western shore (0-15%).

The conglomeratic facies of the Cabano Formation is present in sections I, III and VII in variable proportions and at different stratigraphic horizons. At Mount Longue-Vue, most of the formation is composed of the coarse facies. In section III on Orient Brook the conglomerate facies crops out at the top but is at the base of the formation on Témiscouata Lake. At these last two localities the conglomeratic facies represents less than 30% of the formation. In all sections there is no systematic up-section variation of bed thickness and maximum grain size (Fig. 4). Maximum grain size (MGS) was used to get an approximation of the critical shear stress responsible for the transport of the coarse fraction (see Lajoie and St-Onge, 1985).

The fine grained facies of the Cabano Formation appears to consist of a series of fining-upward cycles (Fig. 3); they have not been analyzed yet.

Pointe Aux Trembles Formation

The Pointe Aux Trembles Formation is a volcaniclastic unit overlying the Cabano Formation in a monoclinal sequence. Its thickness increases from 300 m in the southwest to 900 m in the northeastern sections, near Pain de Sucre Lake. The formation shows important lateral variations, but it can generally be subdivided into three vertical facies: a basal transition with the underlying Cabano, overlain by a sequence of epiclastic and possibly pyroclastic rocks, which in turn is overlain by pyroclastic rocks. In a few sections thin vesiculated lava flows of intermediate composition crop out at the top of the formation (Gregory, 1900; Lespérance and Greiner, 1969).

The Pointe Aux Trembles-Cabano contact is placed at the first occurrence of feldspathic sandstone, a rock type that is interbedded with the various lithologies of the formation. Above that bed, the transitional facies varies much along strike in grain size and bed thickness, but it generally coarsens up-section with both grain size and sand-mud ratio increasing. On Témiscouata Lake (VI), the transition is 90 m thick. The base consists of very thin beds (1-3 cm) of mudstone locally interbedded with thin (3-10 cm) siltstone and fine arkosic sandstone beds. At the top of the transition, beds are thick (10 to 90 cm), and the sand medium grained. Most of the coarse detrital beds show character-istics of turbidites, the lower beds showing the **b-c** divisions, and the upper beds the **a-b-c** divisions of the turbidite model. Slumped beds are present at this locality where sole marks (flutes) suggest a SW to NE sediment transport.

The overlying epiclastic facies is characterized by a mixture of fragments that have both a sedimentary and a volcanic origin. Rocks consist of lithic sandstone in beds 10 to 100 cm thick, interbedded with rare irregular, massive beds of conglomerate, 10 to 30 cm thick, in which the main clasts are rounded, vesiculated, intermediate volcanic rocks

that float in the sandy matrix. The sandstone beds show primary structure sequences of classic turbidites, with the graded division at the base.

The pyroclastic sequence that tops the Pointe Aux Trembles Formation is composed of tuff and breccia (Fig. 8, 9). It has the coarsest sizes and the thickest beds found within the formation. At section V (Fig. 10), the tuff beds can be very thick (7.25 m). The interbedded breccia beds, with grain sizes ranging from 5 to 30 cm, are 50 to 660 cm thick. The beds are massive, normally or reversely graded. In section V, there is little evident up-section variation of maximum grain size, but the conglomerate thickness does seem to increase.

Various fossil fragments (mainly brachiopods) have been found in a few horizons of the two lower facies of the Pointe Aux Trembles Formation, but they do not occur in the upper pyroclastic facies.

The Pointe Aux Trembles Formation varies laterally in grain size and bed thickness. The coarsest fraction and the thicker beds occur near the Pain de Sucre Lake (section V); from there both parameters decrease to the SW and to the NE. Additional data must be gathered to document the lateral variations and to explain the paleocurrent directions.

The Lac Raymond Formation

Little work was done on the Lac Raymond Formation during the last field season. The formation is essentially a fine grained equivalent of the Pointe Aux Trembles Formation. In section IV, the Lac Raymond is composed mostly of mudstone and tuffs in beds ranging from 3 to

Figure 8. Pointe Aux Trembles breccia. Section V.

Figure 9. Tuff and feldspathic sandstone beds in Pointe Aux Trembles Formation. Section, southern shore of Témiscouata Lake.

Figure 10. *Pointe Aux Trembles Formation at Lac Pain de Sucre (V).*

10 cm, interbedded with siltstone and fine sandstone in beds 10 to 100 cm thick, and rare conglomerate. The sandstone and conglomerate beds are turbidites with a well developed graded division. The basal 300 m of this section are part of a 10 km-long lens of granule and pebble (2 to 64 mm) conglomerate that intertongues at both extremities with the finer clastics of the Lac Raymond. This large lens has been called the Lac Castor Member by Lajoie et al. (1968). Its composition is similar to that of the epiclastic facies of the Pointe Aux Trembles Formation. The primary structure sequences in the Lac Castor beds are characteristic of turbidity current deposition.

Discussion

Fossils found in the Cabano, Pointe Aux Trembles and Lac Raymond formations indicate that the environment of deposition was marine, in all probability from the base of the Cabano sedimentary sequence to perhaps the middle of the Pointe Aux Trembles Formation. There are no fossil occurrences in the upper part of the Pointe Aux Trembles, and volcanic rocks are massive with no apparent fragmentation suggesting accumulation in a subaerial environment. It could explain the large hiatus that there is between the late Llandoverian Pointe Aux Trembles and the Ludlovian Mont Wissick Group.

The primary structure sequences observed in the coarse clastics of the Cabano, Pointe Aux Trembles and Lac Raymond are characteristic of sediments transported by mass flows, that have accumulated at the base of slopes. Massive or reversely graded beds that have sharp non-erosive lower contacts, with large clasts projecting above the upper contact, and with no laminations are characteristic of debris flows in which mixtures of fine and coarse sediments moved downslope by laminar flow. The normally graded beds with sequences of traction structures accumulated from turbidity currents. Thin mud interbeds present at all levels in the Cabano and Lac Raymond formations accumulated from pelagic suspension, and show no evidence of erosion by bottom currents which suggests deposition in a calm, possibly deep, environment.

It is too early to arrive at definite conclusions on the source areas of the clastic fraction of the Cabano, Pointe Aux Trembles and Lac Raymond formations. Not enough data are available and only general considerations may be examined at this stage. The composition of the Cabano is very different from that of the other two units. Two very different petrographic provinces supplied the sediments for these two contrasting rock assemblages, one essentially sedimentary, and the other with a strong contribution from volcanic terranes.

There has been little or no work done on the Cabano Formation since Lajoie et al. (1968) proposed that the sediments had been derived from high relief sources essentially composed of sedimentary rocks and located in the general NW direction of the depositional basin. Our paleocurrent data do confirm the NW source, at least for the Rimouski region. Elsewhere the data suggest a W to E transport. There still is little evidence for the northwestern source other than that mentioned, and it is quite possible that some of the Cabano sediments were derived from the south, although there is as yet no evidence to support it. The distribution of the conglomeratic facies suggests two major distributary deep-sea channels, one in the vicinity of Témiscouata Lake, and a second in the vicinity of Mount Longue-Vue; from these, the finer fractions were distributed over the entire basin.

The Cabano sequence is not unique in these parts of the Appalachian Orogen. The Caradocian to Ashgillian fauna that was found last summer, coupled with its early Llandoverian fauna higher in the sequence, make the formation correlative with parts of the totally Ordovician Honorat Group of Gaspé (Béland and Vennat, 1979), and of the Matapédia Valley (Ducharme, 1979). The composition of the Honorat (Skidmore, 1965) is similar to that of the Cabano, although not identical. The major difference is that the Honorat contains some volcanic detritus and accessory chromite and picotite derived from ultramafic rocks (Vennat, 1979; Ducharme, 1979). According to Vennat (1979) and Ducharme (1979), the Honorat clastics that are exposed in the southern part of the Gaspé Peninsula were derived from Cambro-Ordovician sources located to the south of the depositional centres, in part from the Elmtree-Fournier assemblage of northern New Brunswick, which, according to Pajari et al. (1977) represents the crust of an inland sea. The Honorat, and possibly the Cabano sediments, have many characteristics similar to those derived from collision orogen sources (Dickinson and Suczek, 1979).

Our working hypothesis is that the Cabano sediments were derived from sources of similar tectonic history to that of the Honorat, possibly from the north as well as from the south. The Cabano mineralogy will therefore have to be evaluated in that perspective, considering that ultramafic rocks are present to the northwest of the Cabano Formation in the Cambro-Ordovician sequence of Lake Témiscouata (Lespérance and Grenier, 1969).

The Pointe Aux Trembles and Lac Raymond formations have a high proportion of volcanic material that had to be derived from the southeast since there are no known volcanic rocks of that age to the north and northwest. The lateral variation of the coarsest fraction suggests that there were two main submarine canyons feeding sediments to the trough. One was located in the vicinity of Pain de Sucre Lake, and the other near Castor Lake (section IV, Fig. 1). The general decrease in size eastward from the latter section would indicate that the volcanic vents were restricted to the southwestern portion of Figure 1. The upper part of the Pointe Aux Trembles Formation is pyroclastic in origin, and the presence of "andesitic" lavas at the top points to the proximity of the volcanic centres at that time.

Andesitic volcanoes existed in the northwestern region of New Brunswick from Ashgillian time, and they were source rocks for the Siegas Formation (Hamilton-Smith, 1971). Farther east, north of Bathurst, Pajari et al. (1977) reported andesitic volcanism of similar age that are representative of volcanic assemblages formed on continental crust. The volcanic centre located in northwestern New Brunswick did not contribute much if any detritus to the Ashgillian and early Llandoverian Cabano, perhaps because the axis of the volcanic centres was too far away, or the Cabano trough was isolated from the Siegas by a structural high. Hamilton-Smith (1971) proposed a northwestward migration of volcanic centres in northwest New Brunswick in late Llandoverian time. The transition from the Cabano to the Pointe Aux Trembles, coupled with the up-section increase of the volcanic end-members within the Pointe Aux Trembles with lavas at the top, support the northwestward progradation of the volcanic centres from early late Llandoverian (C_1) to late Llandoverian (C_5).

The working hypothesis that we propose is summarized in Figure 11. The Cabano sediments were derived from high-relief sedimentary nappes and possibly from obducted ophiolites, a source similar in age and composition to that of the Honorat of Gaspé as well as other lithological units of roughly the same age, such as the Nicolet River Formation of the autochthonous domain of the Quebec Appalachians (Beaulieu et al., 1980). These large blocks could have contributed detritus to northern as well as southern deep-sea basins. The ensialic volcanic arc did not contribute sediments to the trough until early Late Llandoverian and was the major contributor in Late Llandoverian suggesting northwestward convergence of the arc.

Figure 11. *Paleogeography of southwestern Québec and northwestern New Brunswick during Ashgillian and Llandoverian time. O.O.C.: obducted oceanic crust. Modified from Hamilton-Smith (1971).*

More fieldwork is needed before the facies distribution and the tectonic history of the Pointe Aux Trembles and Lac Raymond can be solved. Detailed petrography and geochemistry on the coarse and fine fractions of these formations and on the Cabano should confirm or modify the proposed history of the sources.

References

Beaulieu, J., Lajoie, J., and Hubert, C.
1980: Provenance et modèle de dépôt de la Formation de la Rivière Nicolet, flysch taconique du Domaine autochtone et du Domaine externe des Appalaches du Québec; Canadian Journal of Earth Sciences, v. 17, p. 855-865.

Béland, J. and Vennat, G.
1979: Notes sur les Groupes d'Honorat et de Matapédia dans la région de Carleton-St-Omer, Gaspésie, Québec; in Current Research, Part B, Geological Survey of Canada, Paper 79-1B, p. 13-15.

Dickinson, W.R. and Suczek, C.A.
1979: Plate tectonics and sandstone compositions; American Association of Petroleum Geologists, Bulletin, v. 63, p. 2164-2182.

Ducharme, D.
1979: Pétrographie d'une partie du Flysch de l'Ordovicien supérieur et du Silurien inférieur – Anticlinorium d'Aroostook-Percé, Gaspésie, Québec; Mémoire de maîtrise, Université de Montréal, Montréal, Québec; unpublished.

Gregory, H.W.
1900: Volcanic rocks from Témiscouata Lake; American Journal of Science, v. 10, p. 14-18.

Hamilton-Smith, T.
1971: Paleogeography of northwestern New Brunswick during the Llandovery: a study of provenance of the Siegas Formation; Canadian Journal of Earth Sciences, v. 8, p. 196-203.

Lajoie, J. and St-Onge, D.A.
– Characteristics of two Pleistocene channel-fill deposits and their implication on the interpretation of megasequences in ancient sediments; Sedimentology. (in press)

Lajoie, J., Lespérance, P.J., and Béland, J.
1968: Silurian stratigraphy and paleogeography of Matapedia-Témiscouata region, Québec; American Association of Petroleum Geologists, Bulletin, v. 52, p. 615-640.

Lespérance, P.J. and Grenier, H.R.
1969: Région de Squatek-Cabano, Comtés de Rimouski, Rivière-du-Loup et Témiscouata; Ministère des Richesses Naturelles du Québec, Rapport géologique 128.

Pajari, G.E., Rast, N., and Stringer, P.
1977: Paleozoic volcanicity along the Bathurst-Dalhousie geotraverse, New Brunswick, and its relations to structure; in Volcanic Regimes in Canada, ed. W.R.A. Baragar, L.C. Coleman, and J.H. Hall; Geological Association of Canada, Special Publication 16, p. 111-124.

Skidmore, W.B.
1965: Région d'Honorat-Reboul, Comté de Bonaventure; Ministère des Richesses Naturelles du Québec, Rapport géologique 107.

Vennat, G.
1979: Structure et stratigraphie de l'Anticlinorium d'Aroostook-Percé dans la région de St-Omer-Carleton-Gaspésie-Appalaches du Québec; Mémoire de maîtrise, Université de Montréal, Montréal, Québec; unpublished.

The geology of the Nicoba Zn-Cu deposit, Lynn Lake, Manitoba: preliminary results[1]

Project 800007

B.A. Barham[2]
Precambrian Geology Division

Abstract

The Nicoba Zn-Cu deposit, located in the Lynn Lake Greenstone Belt, is hosted by pyroclastic and epiclastic rocks of the Lynn Lake Rhyolitic Complex. Footwall lithologies contain lenticular units of felsic pyroclastic flows, volcanic breccia with mafic matrix, and other fragmental rocks. A massive porphyritic tuff forms the hangining wall. Thin stratiform layers of sulphide are interlayered with chemical and detrital sediments. Hydrothermal alteration, and subsequent medium grade metamorphism have resulted in a thick, nearly conformable footwall layer of porphyroblastic aluminous schist depleted in Na_2O and CaO. Minerals commonly developed in the schist include Mg-biotite, sericite, andalusite, kyanite, staurolite, plagioclase, garnet and gahnite. The schist layer is enveloped by sericitized felsic rocks. Metamorphosed equivalents of intensely chloritized rocks have not been identified.

Résumé

Le dépôt de Zn-Cu Nicoba, situé dans la zone Greenstone de Lynn Lake, s'encaisse dans les roches détritiques et pyroclastiques du complexe rhyolitique de Lynn Lake. Les lithologies reconnues comprennent des unités lenticulaires de coulées pyroclastiques de nature felsique, des brèches volcaniques à matrice mafique et d'autres roches détritiques. Le toit de la couche se compose d'un tuf porphyritique massif. Dans les minces couches stratiformes de sulfure s'intercalent des sédiments chimiques et détritiques. L'altération hydrothermale et le métamorphisme moyen subséquent ont entraîné la formation dans le mur d'une couche épaisse, presque concordante, de schiste alumineux porphyroblastique à faible teneur en Na_2O et CaO. Parmi les minéraux qui se sont développés dans le schiste, on compte la biotite-Mg, la séricite, l'andalousite, la kyanite, la staurolite, le plagioclase, le grenat et le gahnite. La couche de schiste est enveloppeé de roches felsiques séricitisées. Des équivalents métamorphisés de roches très chloritisées n'ont pas été identifiés.

Introduction

During the summer of 1984, the Nicoba massive sulphide deposit was investigated by mapping surface exposures and logging available drill core. An extensive zone of metamorphosed hydrothermally altered felsic volcanic fragmental rocks, now largely of pelitic composition, forms the footwall to thin stratiform, sphalerite-rich, sulphide lenses and other chemical sediments. The deposit, in general, fits the volcanogenic massive sulphide model as described by various authors (Franklin et al., 1981; Sangster, 1972; Lydon, 1984) but, in detail, the geological setting, the mineralogical and chemical manifestations of hydrothermal alteration and subsequent metamorphism, though not unique, present an interesting variant to other documented deposits.

Regional setting

The Lynn Lake Greenstone Belt of Aphebian age (1940 ± 75, 1825 ± 210 Ma, Clark, 1980) lies within the southern Churchill Structural Province of Manitoba. The belt is a domain of metamorphosed volcanic, sedimentary and plutonic rocks bounded by the Kisseynew Sedimentary Gneiss Belt to the south and the Southern Indian Gneiss Belt to the north. A portion of the Lynn Lake Greenstone Belt, including the Nicoba area, is shown in Figure 1.

Reconnaissance mapping in the Lynn Lake area led to the recognition of an older pre-Sickle Group of volcanic rocks unconformably overlain by the Sickle Series of quartzo-feldspathic sediments (Norman, 1934; Henderson et al., 1936; Downie, 1936). In a detailed study, Bateman (1942, 1945) used the term Wasekwan Series for pre-Sickle rocks in the vicinity of McVeigh Lake and recognized post-Wasekwan intrusive rocks, possibly of pre-Sickle age. In this locality, the predominantly volcanic sequence includes some interlayered sediments. The results of detailed mapping in the Lynn Lake area by various workers were compiled by Milligan (1960) into a comprehensive geological report. He accepted the stratigraphic subdivision into Wasekwan Series and Sickle Series and subdivided intrusive rocks into pre-Sickle and post-Sickle groups. Emslie and Moore (1961) mapped the area between Lynn Lake and Fraser Lake in detail and described the geology of the Ni-sulphide bearing gabbros of Sherritt Gordon Mines Limited. Campbell (1969) suggested that the Wasekwan and Sickle series be revised to Wasekwan and Sickle groups.

A four-year mapping program by the Manitoba Mineral Resources Division concentrating on the volcanic and sedimentary rocks of the Lynn Lake Greenstone Belt resulted in the publication of the report by Gilbert et al. (1980). They described the lithology and geological history of the belt and determined the grade of peak metamorphism as lower to upper amphibolite facies.

In 1982, the Manitoba Mineral Resources Division embarked on a program to document the geology of known mineral occurrences in the Lynn Lake Belt. Fedikow and Gale (1982) briefly mentioned the Nicoba deposit and recognized rocks of pelitic composition as metamorphosed hydrothermally altered rocks.

The Lynn Lake Rhyolitic Complex

The Nicoba deposit is located within a large body of felsic volcanic rocks centred near the townsite of Lynn Lake, Manitoba (Fig. 1). Norman (1934, p. 28) described rocks from this area as "well-banded, fine grained tuffs interbanded with coarse pyroclastics and lavas". Later workers considered the felsic rocks to be primarily epiclastic in origin (Allan, 1946; Ruttan, 1955). Milligan (1960, p. 35) included these rocks in a broadly defined sedimentary unit but also described rocks in the Lynn Lake area "and to the south, where pyroclastics, sediments, agglomerates, flow breccias and flows of varying composition appear to be intermixed in bewildering profusion". He further cited the influence of probable explosive volcanism.

Emslie and Moore (1961) recognized that the felsic rocks in the Lynn Lake and Frances Lake areas were predominantly volcanic in origin. The southern boundary of their rhyolite flow and/or tuff unit passes through the Nicoba outcrop area and a pyrrhotite-pyrite occurrence, first reported by Allan (1946) and later by Milligan (1960), is shown on their map and described briefly in the text (Emslie and Moore, 1961, p. 22).

Gilbert et al. (1980) introduced the term 'Lynn Lake Rhyolite' and extended its usage to include the felsic volcanic fragmental rocks south of the Nicoba deposit. Emslie and Moore (1961) considered these rocks to be part of a dominantly epiclastic unit but with a significant felsic volcanic component in this area. Fedikow and Gale (1982) renamed the body the 'Lynn Lake Rhyolitic Complex'. Baldwin (1983) extended the boundary of the complex some 750 m north of its previously recognized northern limit west of the townsite of Lynn Lake.

Baldwin (1983) also subdivided the complex into Southern, Central and Northern Units, thus recognizing a major change in lithological character at the stratigraphic position of the Nicoba deposit (Fig. 2). The Southern Unit consists of plagioclase- and quartz-phyric and aphyric tuffs, lapilli tuffs, minor pyroclastic breccia and lava flows, and heterogeneous epiclastic rocks. The Central Unit consists predominantly of plagioclase- and quartz-phyric tuff with lesser amounts of lapilli tuff. The Northern Unit consists primarily of aphyric tuff, massive biotite, quartz and plagioclase-phyric flows and interbedded and/or intruded amphibolite. East of the Lynn Lake townsite, exposure is poor and the stratigraphic subdivision remains uncertain (Baldwin, 1983).

As presently understood, the Lynn Lake Rhyolitic Complex is approximately 18 km long and up to 3 km thick with felsic pyroclastic rocks constituting about 75% of the body (Baldwin, 1983; Fig. 2). A rhyolite flow from this complex has a U-Pb age of 1910+15/-10 Ma (Baldwin et al., 1985). Norman (1934) described normally graded tuffs from this region and concluded that the northwesterly dipping rocks are upright. Emslie and Moore (1961), in a structural interpretation, suggested that the rocks in this area are south-facing. Gilbert et al. (1980) and Baldwin (1983) observed that rare younging criteria indicate stratigraphic tops to the northwest.

Besides the Nicoba deposit, two other deposits having the characteristics of volcanogenic massive sulphide deposits have been identified within the complex (Fedikow and Gale, 1982; Fig. 2). The Y deposit is underlain by a narrow crosscutting zone of sericitic alteration and is overlain by a zinc-rich layer of chemical and detrital sediments. All deposits within the Lynn Lake Rhyolitic Complex are zinc-rich relative to copper and lead. The Nicoba and Frances Lake deposits lie at or near the top of the major internal stratigraphic units (Baldwin, 1983). The Nicoba deposit has been previously described by Trinder (1983).

Geology of the Nicoba Zn–Cu deposit

Geological mapping in the Nicoba area is hampered by lack of outcrop, the lenticular nature of volcanic units of particularly the footwall sequence, and the imprint of locally pervasive retrograde metamorphism. Individual volcanic units in the footwall sequence rarely exceed a few metres in width and generally cannot be traced beyond one outcrop. However, on the basis of lithological similarity of rocks observed in drill core, a local stratigraphy for the Nicoba deposit can be established.
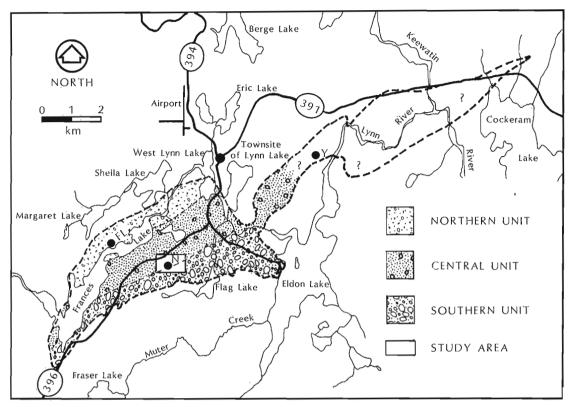
Figure 1. General geology of the Lynn Lake Greenstone Belt in the Lynn Lake-Sickle Lake area. Undifferentiated pre-Sickle Group intrusive rocks are largely diorite and quartz diorite (simplified after Gilbert et al., 1980; modified after Baldwin, 1983).

LEGEND

INTRUSIVE ROCKS

Post-Sickle Group
- Berge Lake pluton, granodiorite

Pre-Sickle Group
- undifferentiated
- granodiorite, quartz diorite
- gabbro, diorite

SICKLE GROUP
- meta-sandstone, meta-conglomerate

WASEKWAN GROUP
- Zed Lake meta-graywacke, migmatite (Wasekwan-?)
- meta-sedimentary rocks
- felsic meta-volcanic and meta-volcaniclastic rocks
- mafic and intermediate meta-volcanic and meta-volcaniclastic rocks
- W - Wasekwan undivided

- geologic contact
- fault
- N - Nicoba deposit (Zn-Cu)
- FL - Frances Lake deposit (Zn-Cu)
- Y - Y deposit (Zn-Cu)
- Ag - Agassiz deposit (Au)
- LL - Lynn Lake townsite
- provincial highway
- railway
- mine site (Ni-Cu-Co, closed)

KILOMETRES
1 0 1 2 3 4 5

501

Figure 2. *Preliminary stratigraphic subdivision of the Lynn Lake Rhyolitic Complex (N - Nicoba deposit, Y-Y deposit, FL-Frances Lake deposit, after Baldwin, 1983).*

The structure of the Nicoba deposit is simple. Volcanic and epiclastic units form a steeply north-dipping monocline. The regional, ENE-WSW foliation is parallel to, or shallowly crosscuts stratigraphic layering. Fragment elongations are within the plane of the regional foliation.

The following discussion of lithology and metamorphosed alteration products refers to Figure 3.

Footwall unit 1 is dominantly monolithologic with plagioclase-phyric felsic lapilli set in a biotite-rich plagioclase-phyric matrix which commonly contains some garnet (<5%). Fragments generally compose 70% of the rock but the fragment:matrix ratio can vary markedly. Subordinate amounts of other fragmental rocks are present.

Outcrops of unit 2 weather distinctly dark green and usually carry some buff, white or grey felsic fragments. The unit consists of a preponderance of heterolithologic lenses, some of which carry angular to subrounded felsic, intermediate and mafic blocks and smaller fragments in an amphibolitic matrix. Some lenses resemble the laharic breccias described from the Mattabi and other massive sulphide deposits (Franklin, 1976; Fig. 4). Monolithologic mafic lapilli tuff and finely bedded mafic sediments or tuff also occur.

Footwall unit 3 is composed of felsic pyroclastic flows with minor interbedded tuff. In the western outcrop area, the flows are monolithologic with corroded plagioclase-phyric fragments and matrix. One outcrop in this area contains 50% felsic bombs up to 2 m in length set in a matrix of tuff.

The eastern outcrop area of unit 3 is strongly altered and retrograded but quartz eyes and fragment shapes are recognizable. Here the rock is dominated by tightly packed

monolithologic fragments with matrix generally composing <10% of the rock. The overlying porphyroblastic schist is considered to be an intensely altered equivalent of this unit for reasons discussed in the section on alteration.

Footwall unit 4 marks the contact between the Southern and Central units of the Lynn Lake Rhyolitic Complex. In drill core, the unit is composed of thinly bedded tuffs and lapilli tuffs with quartz and/or feldspar phenocrysts, cherty fragmental rocks, bedded epiclastic rocks and sulphide-rich rocks.

In the eastern outcrop area, paucity of outcrop and retrogression make definition of this unit difficult. Consequently, the continuity of the unit as displayed in Figure 3 is highly schematic and in some places it may be missing. However, several unique and singular outcrops of thin epiclastic and primary volcanic rocks are present and included in unit 4. These include a thin greyish plagioclase-phyric ash-flow tuff which contains ragged and apparently flattened sericitic fragments. In thin section, the fragments can be seen to, in part, wrap around phenocrysts and are thus reminiscent of fiamme. However, primary features are obscured by alteration and a strong foliation.

This unit includes a variety of volcanic rocks and epiclastic and chemical sediments occurring between the upper, intensely altered rocks of unit 3, and the extensive, monotonous tuffs of unit 5 which form the hanging wall to the deposit and the bulk of the Central Unit of Baldwin (1983). A similar relationship exists about 1 km east of the Nicoba area, probably at the same stratigraphic level, where hydrothermally altered rocks of largely pelitic composition are overlain by rhyolitic fragmental rocks, a thin cherty, pyritic unit and massive rhyolite tuff (Fedikow and Gale, 1982).

Figure 3

Preliminary geology of the Nicoba Zn-Cu deposit.

Figure 4. *Felsic fragment-mafic matrix volcanic breccia from footwall unit 2.*

The sulphide lenses of unit 4 consist mainly of pyrite and pyrrhotite and, among the ore minerals, sphalerite is present in greater abundance than chalcopyrite. One thin galena veinlet was observed in core. Most intersectons consist of several closely spaced thin massive sulphide layers separated by intensely altered rock consisting of biotite, retrograde chlorite and disseminated sulphides. Some sulphide layers are mineralogically zoned with chalcopyrite-rich lower sections and sphalerite-rich upper sections.

The hanging wall (unit 5) is composed of massive tuffs carrying blue quartz and/or feldspar phenocrysts (An_7, Table 1) constituting as much as 10% of the rock. Plagioclase phenocrysts are subhedral to euhedral and commonly display albite twinning.

Rare intrusive rocks occur in the area as thin (0.3 to 2.0 m) mafic dykes, both in the footwall and hanging wall sequence.

Alteration

Based on field observations and relationships observed in drill core, several mappable alteration types have been identified. To some degree, the character of alteration has only become apparent through petrographic study and electron microprobe analysis.

Alteration and subsequent medium grade metamorphism at the Nicoba deposit have produced a distinct stratiform footwall zone of pelitic composition in which large porphyroblasts of aluminous minerals occur (Fig. 3). The zone extends at least 350 m beyond the western margin of Figure 3, below swamp, where drillholes have intersected the hanging wall tuffs, sulphide layers, and porphyroblastic schist.

In drill core, sulphide lenses are underlain by a thin (0.5-2.0 m) stratiform layer consisting almost entirely of biotite and carrying accessory amounts of sulphide, oxide and locally an aluminous silicate and gahnite. The altered rocks below this layer can be roughly divided into randomly distributed zones of sericite-rich or Mg-biotie-rich rocks (Table 1). Accompanying the micas and quartz are porphyroblasts of one or several of pink andalusite, kyanite, zinc-rich staurolite, and less commonly garnet or untwinned plagioclase (Table 1). Many of the zones contain the apparently stable assemblage andalusite-kyanite. Rocks in

drill core are fresh or moderately retrograded and the aluminous silicates are retrograded to chlorite-sericite assemblages. Textures in fresh samples suggest equilibrium at peak metamorphic conditions.

Amphiboles are conspicuously missing from the schists. Indeed, there is no indication of the metamorphosed equivalent of a Mg-enriched footwall zone in outcrop or in drill core intersections. At this grade of metamorphism, the development of cordierite-anthophyllite rocks could be expected in metamorphosed chloritic zones marked by magnesium and iron enrichment and alkali depletion (Froese, 1969; Franklin et al., 1981; Walford and Franklin, 1982; Lydon, 1984).

Gahnite is common in footwall schists and to a lesser degree in the hanging wall tuffs, and increases in abundance with proximity to mineralized unit 4. The sulphide minerals pyrrhotite and pyrite are common but rarely occur in more than trace amounts in the footwall schists along with sparse ilmenite and magnetite grains. A 4 cm band of massive fluorite was intersected within sercite-quartz schist.

In outcrop, porphyroblastic schist is pervasively retrograded to a chlorite + sericite + quartz assemblage. Pseudomorphs, however, are easily visible due to variable concentrations of retrograde products. Trinder (1983) suggested, on the basis of morphology, that the pseudomorphs probably represented cordierite or kyanite porphyroblasts. Cordierite has not been observed in the fresh rocks in drill core and the pseudomorphs probably represent andalusite, kyanite, staurolite and plagioclase (Fig. 5a).

Porphyroblasts are largely confined to the plane of regional foliation and are randomly oriented within that plane (Fig. 5b). This mineral fabric is commonly observed in porphyroblastic rocks in the Lynn Lake area (Jackson and Gordon, 1985). Retrograde chlorite and sericite are strongly foliated at an oblique angle to the regional trend. This NE-SW foliation is briefly mentioned by Gilbert et al. (1980) and is attributed, in the Lynn Lake area, to metamorphism contemporaneous with post-Sickle intrusive of the Berge Lake granodiorite (1765 ± 100 Ma, Clark, 1980; Fig. 1).

In fresh porphyroblastic schist, this late fabric results in a strong crenulation of micaceous minerals, pressure shadow recrystallization of micas and quartz and kink banding in biotite and kyanite.

Irregular fragments of aphyric and quartz- and/or plagioclase-phyric felsic rock are often observed within the schist unit in outcrop (Fig. 5c). On the basis of this observation, the schists are considered to be intensely altered equivalents of map unit 3.

In the eastern outcrop area, the lower half of unit 3 is highly altered but still retains the character of a felsic fragmental rocks. Replaced porphyroblasts are localized in the matrix surrounding clasts (Fig. 5d) and in intensely sericitic selvages mantling lenticular vein-like structures with cores generally composed of retrograde chlorite (Fig. 5e). They are oriented subparallel to layering and regional foliation. Towards the western margin of the eastern outcrop area, one of these vein-like structures contains a core of prograde biotite + anhedral plagioclase + minor pyrrhotite and is mantled by a concentration of subhedral untwinned plagioclase porphyroblasts.

Anastomosing veinlets almost totally composed of tremolite (Table 1) are confined to unit 2. The tremolite contrasts markedly in thin section with the strongly pleochroic amphibole common in weakly altered or unaltered rocks of this unit. In addition, garnet is more abundant in the areas surrounding these veinlets and may represent a metamorphosed alteration product of these rocks. The extent of this alteration is not well established.

Table 1. Selected mineral analyses

	Plagioclase phenocryst unit 5	Mg-biotite		Plagioclase porphyroblasts		Staurolite porphyroblasts		Tremolite porphyroblasts	
	unit 5	unit 3,	Alt.-A1	unit 3,	Alt.-A1	unit 3,	Alt.-A1	unit 2,	Alt.-D
SiO_2	66.69	38.72	39.19	61.50	61.19	27.64	27.49	54.77	55.08
TiO_2	-	0.94	0.80	-	-	0.42	0.41	0.01	0.08
Al_2O_3	20.91	16.63	16.47	24.46	24.86	54.52	54.08	2.93	4.72
$FeO_{(t)}$	-	11.04	10.61	-	-	9.64	10.17	3.75	3.79
MnO	-	0.24	0.22	-	-	0.57	0.54	0.90	0.51
MgO	-	17.75	17.39	-	-	1.93	2.19	21.63	20.47
CaO	1.55	0.01	0.02	6.21	6.83	-	-	12.51	12.12
Na_2O	10.87	0.43	0.55	8.30	7.95	-	-	0.31	0.41
K_2O	0.13	8.99	8.96	0.06	0.06	-	-	0.07	0.23
ZnO	-	-	-	-	-	4.41	3.56	-	-
	100.15	94.75	94.21	100.53	100.89	99.13	98.44	96.88	97.41
	n=3	n=3	n=2	n=3	n=3	n=3	n=3	n=3	n=2
	An_7			An_{29}	An_{32}				

Analytical procedure: Samples were analyzed at Carleton University using a Cambridge Microscan V electron probe operated at 15 kV gun potential and a specimen current of 60 nanoamperes measured on an amphibole standard.

Sericitic and pyritic alteration has been weakly to intensely imposed on some lapilli tuffs of unit 1, the pyroclastic flows in the western area of unit 3, and extensively, on the hanging wall tuffs. In addition, aluminous assemblages are developed in hanging wall rocks close to the ore-bearing strata. These thin fracture and foliation controlled zones commonly contain garnet.

A thick lens of the hanging wall tuffs appears cherty in outcrop and carries up to 5% pyrite as euhedral cubes. Petrographic work revealed that quartz and plagioclase phenocrysts occur in similar abundance and proportion as in rocks of unit 5. This lens is thus considered an extensively sheared and silicified equivalent. The silicification may represent silica freed through feldspar destruction rather than introduced silica.

In addition to the alteration types presented in Figure 3, a singular outcrop of heterolithic, volcanic fragment-bearing epiclastic rock in unit 4 contains large irregularly shaped, greenish patches which contain the calcic minerals clinozoisite, scapolite, titanite and fibrous rosettes of amphibole.

Trinder (1983) attempted to establish the chemical characteristics of the outcropping altered rocks at the Nicoba deposit. This, and any subsequent chemical study is inhibited by the inabilility to establish the background concentrations of elements within the footwall succession of the deposit. His work showed that the retrograded schists display very low concentrations of Na_2O and CaO and high concentrations of MgO and $Fe_2O_{3(t)}$ relative to less altered rocks of units 1, 2, 3 and 5.

Of more value are the analyses of fresh or weakly retrograded rocks of D.D.H. #378 (Fig. 3, 6; Trinder, 1983). While the chemical nature of the alteration zone awaits more complete study, the depicted variations warrant some preliminary comment.

The porphyroblastic schists display strong depletions in Na_2O and CaO. Walford and Franklin (1982) attributed the development of kyanite in altered rhyolite at the Anderson mine to alkali depletion rather than alumina enrichment. The Al_2O_3 pattern in the porphyroblstic schist of D.D.H. #378 is erratic but does not appear anomalous and the extensive development of metamorphic aluminous minerals is likely a consequence of alkali-depleted rocks.

Unit 4 displays distinctive compositional anomalies relative to the adjacent units, being enriched in MgO, $Fe_2O_{3(t)}$ and the metals Cu, Zn and Au. Depletion is evident in the case of Na_2O, CaO, K_2O and SiO_2. The chemical character here is reminiscent of the chloritic zones of classic deposits of the Abitibi Belt (Lydon, 1984; Knuckey et al., 1982; Knuckey and Watkins, 1982; Franklin et al., 1981).

Summary

The Nicoba Zn-Cu deposit occurs within an extensive Aphebian felsic volcanic complex of largely pyroclastic origin (Baldwin, 1983). The footwall to the ore lenses is composed of a thick sequence of weakly to intensely altered lensey felsic pyroclastic flows, volcanic breccias and epiclastic rocks. The hanging wall rocks form a relatively homogeneous sequence of porphyritic felsic tuffs.

The predominance of felsic fragmental rocks to the virtual exclusion of mafic rocks, is rare in host rocks of volcanogenic massive sulphide deposits of the Canadian Shield (Franklin and Thorpe, 1982). The Mattabi deposit of northwest Ontario is underlain by a thick sequence of lapilli tuffs and epiclastic and laharic fragmental rocks and, in this sense, is an analogue (Franklin et al., 1975, 1977). Similarly, the predominance of felsic pyroclastic rocks and the lensey nature of volcanic units bears resemblance to the geological setting of Kuroko deposits. However, the subvolcanic intrusions, common to many producing volcanogenic massive sulphide deposits (Franklin et al., 1981; Franklin and Thorpe, 1982), and evident in virtually all the Kuroko deposits (Ohmoto and Skinner, 1983; Urabe et al., 1983), are lacking in the Nicoba succession.

(a) Pseudohexagonal pseudomorphs and retrograde chlorite-rich lens (alteration-a2)

(b) Ragged pseudomorphs (kyanite ?) in random orientation in plane of regional foliation

(c) Retrograded porphyroblastic schist with preserved felsic rock

(d) Sericitic pseudomorphs and matrix surrounding felsic fragment (alteration-b,a2)

(e) Vein-like structure with chlorite core in sericite + pseudomorph-rich felsic rock

Figure 5. Some features of the altered rocks in the footwall of the Nicoba deposit.

Figure 6. *Variation in oxide and metal abundance in D.D.H. #378 (after Trinder, 1983).*

Hydrothermal alteration and subsequent medium grade metamorphism have resulted in the development of a nearly conformable layer of aluminous porphyroblastic schist depleted in Na_2O and CaO. The schist grades into an underlying zone of sericitic alteration with aluminous assemblages confined to fractures, regional foliation planes, and the matrix surrounding fragments. Mapping of alteration types suggests that alteration crosscuts stratigraphic layering at a shallow angle (Fig. 3). The conformity of lithological, mineral and structural fabric elements suggests that the nearly comformable shape of the alteration zone is a result of considerable strain and deformation.

No Mg-enriched crosscutting pipe has been identified at the Nicoba deposit, a feature it has in common with the Mattabi deposit (Franklin et al., 1975, Franklin et al., 1977). Weak to moderate sericitic and pyritic alteration is found extending into the hanging wall rocks. In the immediate hangining wall, minor amounts of aluminous, garnet-bearing rocks are confined to fractures and foliation planes.

Establishing the concentration gradients of elements in altered rocks at the Nicoba deposit and the extent of alteration in the Southern Unit of the Lynn Lake Rhyolitic Complex awaits further study.

Acknowledgments

References

Allan, J.D.
  1946: Geology of the Lynn Lake area, Granville Lake Division; Manitoba Mines Branch, Preliminary Report 46-2.

Baldwin, D.A.
  1983: Stratigraphic studies of felsic volcanic rocks associated with mineral occurrences in the Lynn Lake area, Manitoba; in Manitoba Mineral Resources Division, Report of Field Activities 1983, p. 88-93.

Baldwin, D.A., Syme, E.C., Zwanzig, H.V., Gordon, T.M., Hunt, P.A., and Stevens, R.D.
  1985: U/Pb zircon ages from the Lynn Lake and Rusty Lake metavolcanic belts, Manitoba: two ages of Proterozoic magmatism; Geological Association of Canada-Mineralogical Association of Canada, Joint Annual Meeting, Fredericton 1985, Program with Abstracts, v. 10, p. A3.

Bateman, J.D.
  1942: Geology and metamorphism in the McVeigh Lake area, northern Manitoba; American Journal of Science, v. 240, p. 789-808.

  1945: McVeigh Lake Area, Manitoba; Geological Survey of Canada, Paper 45-14.

Campbell, F.H.A.
  1969: Sickle-Wasekwan contact, Granville Lake; Manitoba Mines Branch, Summary of Geological Fieldwork 1969, Geological Paper 4/69, p. 9-14.

Clark, G.
  1980: Rubidium-strontium geochronology in the Lynn Lake Greenstone Belt, northwestern Manitoba; Manitoba Mineral Resources Division, Geological Paper GP80-2.

Downie, D.L.
  1936: Granville Lake Sheet (west half), Manitoba; Geological Survey of Canada, Map 343A with marginal notes.

Emslie, R.F. and Moore, J.M., Jr.
  1961: Geological studies of the area between Lynn Lake and Fraser Lake; Manitoba Mines Branch, Publication 59-4.

Fedikow, M.A.F. and Gale, G.H.
  1982: Mineral deposit studies in the Lynn Lake area; in Manitoba Mineral Resources Division, Report of Field Activities 1982, p. 44-53.

Franklin, J.M.
  1976: Role of laharic breccia in genesis of volcanogenic massive sulphide deposits; in Report of Activities, Part A, Geological Survey of Canada Paper 76-1A, p. 293-300.

Franklin, J.M. and Thorpe, R.I.
  1982: Comparative metallogeny of the Superior, Slave and Churchill provinces; in Precambrian Sulphide Deposits, ed. R.W. Hutchinson, C.D. Spence and J.M. Franklin; Geological Association of Canada, Special Paper 25, p. 3-90.

Franklin, J.M., Gibb, W., Poulsen, K.H., and Severin, P.
  1977: Archean metallogeny and stratigraphy of the South Sturgeon Lake area; Institute on Lake Superior Geology, 23rd Annual Meeting, Guidebook.

Franklin, J.M., Kasarda, J., and Poulsen, K.H.
  1975: Petrology and chemistry of the alteration zone of the Mattabi massive sulphide deposit; Economic Geology, v. 70, p. 63-79.

Franklin, J.M., Lydon, J.W., and Sangster, D.F.
  1981: Volcanic-associated massive sulphide deposits; Economic Geology, 75th Anniversary Volume, p. 485-627.

Froese, E.
  1969: Metamorphic rocks from the Coronation mine and surrounding area; Geological Survey of Canada, Paper 68-5, p. 55-77.

Gilbert, H.P., Syme, E.C., and Zwanzig, H.V.
  1980: Geology of the metavolcanic and volcaniclastic metasedimentary rocks in the Lynn Lake area; Manitoba Mineral Resources Division, Geological Paper GP80-1.

Henderson, J.E., Norman, G.W.H., and Downie, D.L.
  1936: Granville Lake Sheet (east half), Manitoba; Geological Survey of Canada, Geology, Map 344A with marginal notes.

Jackson, S.L. and Gordon, T.M.
  1985: Metamorphism and structure of the Laurie Lake region, Manitoba; in Current Research, Part A, Geological Survey of Canada, Paper 85-1A, p. 753-759.

Knuckey, M.J. and Watkins, J.J.
  1982: The geology of the Corbet massive sulphide deposit, Noranda district, Quebec, Canada; in Precambrian Sulphide Deposits, ed. R.W. Hutchinson, C.D. Spence and J.M. Franklin; Geological Association of Canada, Special Paper 25, p. 297-317.

Knuckey, M.H., Comba, C.D.A., and Riverin, G.
1982: Structure, metal zoning and alteration at the Millenbach deposit, Noranda, Quebec; in Precambrian Sulphide Deposits, ed. R.W. Hutchinson, C.D. Spence and J.M. Franklin; Geological Association of Canada, Special Paper 25, p. 255-295.

Lydon, J.W.
1984: Volcanogenic massive sulphide deposits part 1: a descriptive model; Geoscience Canada, v. 11, no. 4, p. 195-202.

Milligan, G.C.
1960: Geology of the Lynn Lake district; Manitoba Mines Branch, Publication 57-1.

Norman, G.W.H.
1934: Granville Lake District, northern Manitoba; Geological Survey of Canada, Summary Report 1933, Part C, p. 23-41.

Ohmoto, H. and Skinner, B.J.
1983: The Kuroko and related volcanogenic massive sulphide deposits: introduction and summary of new findings; in The Kuroko and Related Volcanogenic Massive Sulphide Deposits, ed. H. Ohmoto and B.J. Skinner; Economic Geology Monograph 5, p. 1-8.

Ruttan, G.D.
1955: Geology of Lynn Lake; Canadian Mining and Metallurgical, Bulletin, v. 48, p. 339-348.

Sangster, D.F.
1972: Precambrain volcanogenic massive sulphide deposits in Canada: a review; Geological Survey of Canada, Paper 72-22.

Trinder, I.D.
1983: The geology and geochemistry of the Nicoba alteration zone, Lynn Lake, Manitoba; unpublished B.Sc. thesis, University of Manitoba, Winnipeg, Manitoba.

Urabe, T., Scott, S.D., and Hattori, K.
1983: A comparison of footwall-rock alteration and geothermal systems beneath some Japanese and Canadian volcanogenic massive sulphide deposits; in The Kuroko and Related Volcanogenic Massive Sulphide Deposits, ed. H. Ohmoto and B.J. Skinner; Economic Geology Monograph 5, p. 345-364.

Walford, P.C. and Franklin, J.M.
1982: The Anderson Lake mine, Snow Lake, Manitoba; in Precambrian Sulphide Deposits, ed. R.W. Hutchinson, C.D. Spence and J.M. Franklin; Geological Association of Canada, Special Paper 25, p. 481-523.

Upper Carboniferous sedimentation in northern Nova Scotia and the origin of Stellarton Basin[1]

Project 840045

Gary M. Yeo
Precambrian Geology Division

Abstract

Stellarton Gap, a partly fault-bounded depression underlain by Carboniferous strata, separates the major basement complexes of northern Nova Scotia, the Cobequid and Antigonish highlands. Sedimentation in Stellarton Gap was largely controlled by fault movement. Late Carboniferous strike-slip movement resulted in a pull-apart graben, the Stellarton Basin. During the initial stages of basin subsidence, alluvial fan and fluvial clastics of the Cumberland Group (Westphalian B) were shed into Stellarton Gap from the northwest and south. Subsequently, fine grained clastics and organic material accumulated as the Stellarton Group (Westphalian B and C) in restricted lakes of Stellarton Basin. Simultaneously, Pictou Group sands were deposited in eastern Cumberland Basin by braided rivers flowing north and east. Cessation of strike-slip movement ended subsidence of Stellarton Basin, but Pictou sedimentation continued, eventually burying at least part of the basin.

Résumé

L'ouverture de Stellarton, dépression partiellement limitée par des failles, repose sur des couches carbonifères; elle sépare les hautes-terres de Cobequid et les hautes-terres d'Antigonish, qui sont les principaux socles métamorphiques du nord de la Nouvelle-Écosse. La sédimentation y a été largement contrôlée par le mouvement des failles. Au Carbonifère récent, le mouvement de décrochement a produit un graben de séparation, le bassin de Stellarton. Au cours des phases initiales d'affaissement du bassin, des sédiments clastiques de cônes alluviaux et des sédiments fluviatiles du groupe de Cumberland (Westphalien B) se sont accumulés dans l'ouverture de Stellarton à partir du nord-ouest et du sud. Plus tard, l'accumulation de sédiments clastiques fins et de matériaux organiques a donné le groupe de Stellarton (Westphalien B et C) dans les lacs à circulation restreinte du bassin de Stellarton. Les sables du groupe de Pictou ont été déposés en même temps dans la partie est du bassin de Cumberland par des rivières anastomosées coulant vers le nord et l'est. L'arrêt du mouvement de décrochement a mis fin à l'affaissement du bassin de Stellarton, mais la sédimentation du groupe de Pictou s'est poursuivie pour finalement enterrer au moins une partie du bassin.

---

[1] Contribution to Canada-Nova Scotia Mineral Development Agreement 1984-89. Project carried by Geological Survey of Canada

Introduction

Exploration and potential development of the various energy resources of Stellarton Basin, a fault-bounded Carboniferous basin containing the Pictou Coalfield, should be aided by more detailed understanding of its geometry and development. Consequently, a basin analysis of Stellarton Basin was begun during the 1984 field season. Preliminary field observations have been integrated with previous work (Bell, 1940; Donohoe and Wallace, 1982; Fletcher, 1902; Giles, 1982; Gillis, 1964; Haites, 1956; Maehl, 1961) into a 1:50 000 regional map of the surrounding New Glasgow – Toney River area (Yeo, in press).

The principal tectono-stratigraphic elements of this area are the Cobequid and Antigonish Highlands, and the Stellarton Gap, which separates them (Fig. 1). These three elements are delimited by the Cobequid, Hollow, and Chedabucto fault systems.

The Cobequid and Antigonish highlands are complex terranes of metamorphic, igneous, and sedimentary rocks ranging in age from late Proterozoic to Carboniferous. Both areas have been affected by at least three separate orogenic events. Although relationships between the Proterozoic rocks of these areas are still conjectural (Keppie, 1982), it is possible to correlate their Paleozoic strata with confidence (Fig. 2).

The Stellarton Gap is a broad, northeast-trending, partly fault-bounded depression underlain by Carboniferous rocks (Fig. 1). It lies between the two major basement complexes, Cobequid Highlands to the west and Antigonish Highlands to the east, and forms a link between the two chief Carboniferous basins of mainland Nova Scotia, Cumberland Basin to the north and Minas Basin to the southwest. The tectonic "keystone" of the Stellarton Gap is the Stellarton Basin.

General Geology

Antigonish Highlands

The oldest rocks in the Antigonish Highlands are assigned to the Georgeville Group, a late Proterozoic assemblage of volcanics and siliciclastics, currently interpreted to be a rifted craton margin sequence (Murphy, 1985). A K-Ar whole-rock age of 591 ± 33 Ma (corrected to 1976 IUGS standard from Wanless, 1967 in Murphy, 1984) from a gabbro, which apparently intrudes Georgeville rocks, provides a minimum age for at least part of this assemblage.

The upper Ordovician to lower Devonian Arisaig Group (Boucot et al., 1974; Maehl, 1961) unconformably overlies the Georgeville Group. A basal unit comprising mainly subaerial, andesitic flows, tuffs, and reddish volcaniclastic sediments, is unconformably overlain by a predominantly fine grained sequence of shallow marine siliciclastics. These coarsen upwards into predominantly red, fluviatile sandstones of the lower Devonian Knoydart Formation. The Knoydart may be correlated with the Old Red Sandstone of western Europe.

Basalts, felsic tuffs, and alluvial fan conglomerates of the Devono-Carboniferous McAras Brook Formation overlie pre-Devonian strata unconformably. These rocks are interpreted to have been emplaced along active fault zones which formed the southern boundary of the Devono-Carboniferous Fundy Basin (Bradley, 1982; Dostal et al., 1983; Fralick and Schenk, 1981). The conglomerates, which comprise mainly clasts of Knoydart sandstone, were shed towards the northwest (Fralick and Schenk, 1981).

The early Carboniferous Windsor Group is exposed at the western end of the Antigonish Highlands, where it lies unconformably on Devonian and older strata (Giles, 1982),

and in fault blocks along the eastern part of the Cobequid Fault system (Bell, 1940; Giles, 1979). Evaporites and carbonates of the Bridgeville Formation are unconformably overlain by local conglomerates, sandstones, siltstones, evaporites, and carbonates of the Forbes Lake and Churchville formations. The Windsor Group is interpreted as a series of major early Carboniferous transgression-regression cycles comparable to those recognized in the lower Carboniferous of western Europe (Giles, 1981).

Cobequid Highlands

The oldest rocks in the Cobequid Highlands are 934 ± 82 Ma (whole-rock Rb-Sr) granitic orthogneisses of the Mt. Thom Complex (Gaudette et al., 1984). Relationships between the Mt. Thom Complex and younger strata are obscured by several generations of granitoid intrusions.

Rhyolites, dacites, and minor andesites, which pass into shallow marine, fine-grained siliciclastics and tuffs of Silurian age, comprise the Earltown Formation (Donohoe, 1979; Wallace and Donohoe, 1977). These rocks are correlative with the Arisaig Group (Fig. 2).

In fault contact with, or unconformably above the Earltown Formation, are felsic and mafic terrestrial volcanics, and fluvial conglomerates, wackes, and siltstones of the Devonian to early Carboniferous Fountain Lake Group (Donohoe and Fralick, 1980). Quartz and metasedimentary clasts predominate in the sediments (Gillis, 1964). Like the correlative McAras Brook Formation (Fig. 2), the Fountain Lake Group was emplaced in the initial stages of the development of Fundy Basin (Dostal et al., 1983).

The late Devonian(?) to early Carboniferous Falls Formation (formerly included in the upper River John Group), a thick wedge of conglomeratic alluvial fan and fluvial molasse, overlies the Fountain Lake Group unconformably (Wallace and Donohoe, 1977). An increase in the proportion of metasedimentary clasts and a decrease in volcanic clast abundance compared to Fountain Lake sediments reflects unroofing of pre-Devonian rocks (Gillis, 1964). The Falls Formation is probably correlative with finer grained fluvial deposits of the early Carboniferous Nuttby Formation. The Falls and Nuttby formations may be assigned to the Horton Group. Devono-Carboniferous and older rocks at the eastern end of the Cobequid Highlands are unconformably overlain by middle Carboniferous and younger strata discussed below.

Stellarton Gap

As noted above, Windsor Group strata are exposed within the Stellarton Gap. These lower Carboniferous rocks are overlain by four diachronous successions of middle to late Carboniferous alluvial fan and fluvial sediments: the Canso, Riversdale, Cumberland, and Pictou groups.

The early Carboniferous Canso Group rests conformably on the upper Windsor Group between the Cobequid and Antigonish highlands. The Canso Group here consists predominantly of brownish fine grained sandstones (commonly quartz wackes) and mudstones (Bell, 1940; Gillis, 1964). North of the Hollow Fault, the Canso Group comprises lithic sandstones of the Lismore Formation, overlying and interfingering with the Hollow Conglomerate, from which it is largely reworked (Fralick and Schenk, 1981). Abundant Knoydart sandstone, metaquartzite, and igneous clasts in the latter suggest that the Hollow Conglomerate was shed northerly from the Antigonish Highlands. Paleocurrent measurements from the Lismore Formation indicate a source to the west (Fralick and Schenk, 1981) as well as to the southeast (Fig. 3). Late Visean foraminifera from a limestone bed in the Lismore Formation (Mamet, 1970) suggest a transitional relationship between the Windsor and Canso groups (Fralick and Schenk, 1981).
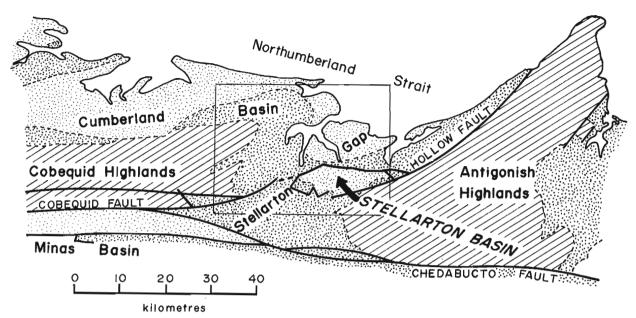
Figure 1. *Location map of northern Nova Scotia. Pre-Carboniferous rocks are indicated by the ruled pattern. Early and middle Carboniferous strata are shown in heavy stipple. Late Carboniferous strata (Pictou and Stellarton groups) are shown in light stipple. The area of Figure 3 is outlined.*

The early Middle Carboniferous Riversdale Group is in fault contact with or unconformably overlies older strata at the eastern end of the Cobequid Highlands. A lower unit, the Millsville Conglomerate, comprising predominantly reddish-brown conglomerate with minor lithic sandstone and siltstone, was shed east and north from the Cobequid Highlands as alluvial fan and braided gravelly river deposits (Gillis, 1964). Abundant feldspars and granitic rock fragments distinguish these conglomerates from others in Stellarton Gap area (Gillis, 1964). This unit is transitional to the overlying Boss Point Formation, a fluvial sequence of sublithic sandstone and conglomerate with minor mudstone and coal (Gillis, 1964). This also was shed outwards from the Cobequid Highlands (Fig. 3). Boss Point and Canso sandstones may be distinguished by the abundance of feldspars and granitic grains in the former (Gillis, 1964). Canso and Riversdale strata in the Stellarton Gap area are the youngest rocks in eastern Canada to have undergone metamorphism (to "slate grade") according to Belt (1968).

The early Upper Carboniferous Cumberland Group includes two formations in Stellarton Gap. The New Glasgow Conglomerate, a thick sequence of reddish-brown conglomerate with minor sandstone and siltstone, deposited in alluvial fans and braided stream systems during Westphalian B time, lies disconformably on the Boss Point Formation (Gillis, 1964). Other contacts are not exposed. In the west, the New Glasgow Conglomerate is very quartz-rich, with some feldspathic material, suggesting a Cobequid Highland source (Gillis, 1964). In the east it comprises mainly reworked Carboniferous sediments and green metaquartzite (Fralick and Schenk, 1981). Composition, reduction in clast size towards the north and east (Fralick and Schenk, 1981), and local clast imbrication (Fig. 3) indicate another source to the southwest. Grey and red sandstone, mudstone, and minor conglomerate of the Middle River Formation (middle Westphalian B) are interpreted to be meandering river deposits (Fralick and Schenk, 1981). The Middle River Formation appears to be in fault contact with older strata, except locally, where it rests disconformably on the Canso (Bell, 1940). Conglomerates exposed near the base of the Middle River Formation (Bell, 1940) suggest that it is transitional upwards from the New Glasgow Conglomerate.

Predominantly grey, coarse grained, lithic sandstones and siltstones with minor exposures of shale and conglomerate characterize the Pictou Group in eastern Cumberland Basin. In this area it is late Carboniferous (Westphalian C to Stephanian according to Barss and Hacquebard, 1967). Elsewhere, Pictou strata range from middle Carboniferous (e.g. south of the Cobequids) to Permian age (e.g. Prince Edward Island). In the New Glasgow – Toney River area, the Pictou Group comprises mainly sandy braided river deposits in basal sections, passing upwards into meandering river deposits (Fralick and Schenk, 1981). Fralick and Schenk (1981) distinguished two types of conglomerate in the Pictou Group, one rich in carbonate clasts, and the second comprising mainly quartz and green metaquartzite. Sediment transport was generally northerly (Fig. 3).

Geology of Stellarton Basin

The Stellarton Group, a thick (>2600 m) sequence of coal- and oil shale-bearing, grey and red, lacustrine and alluvial shales, lithic sandstones and conglomerates, is entirely confined to the fault-bounded Stellarton Basin. The area underlain by these coal-bearing rocks is known as the Pictou Coalfield. Fault blocks of Pictou, Cumberland, Canso, and Windsor strata are also included in Stellarton Basin. The Stellarton Group is late Westphalian B to Westphalian C in age (Barss and Hacquebard, 1967; Howie and Barss, 1975) and therefore partly time-correlative with the Pictou Group (Fig. 2). Locally, the Stellarton Group rests disconformably on the Cumberland Group or unconformably on the Canso Group (Bell, 1940). Highly variable transport directions in the Stellarton Group (Fig. 3) are indicative of a small restricted basin, separate from the major basin to the north in which Pictou sandstones accumulated at the same time.

Bell (1940) divided the Stellarton Group into two divisions, each of three members. The lower division, underlying the western and eastern parts of Pictou Coalfield, comprises two relatively coarse grained, redbed sequences, the Skinner Brook and Plymouth members, separated by a grey, shaly, coal-bearing unit, the Westville Member. Accumulation of these sequences was diachronous

Figure 2. Correlation of Paleozoic strata in the New Glasgow – Toney River area, Nova Scotia. Stratigraphic groups are indicated in upper case; formations in lower case. Relationships between units are shown schematically. Radiometric ages from: Cormier (1979, 1982) and Cormier and Murphy (personal communication, in Chandler et al., in press). Microfossil ages from: Barss and Hacquebard (1967), Boucot et al. (1974), Donohoe and Wallace (1982), Giles (1981), Mamet (1970), and Wallace and Donohoe (1977).

Figure 3. *Geological sketch map of the New Glasgow area (NTS 11E/10) showing Carboniferous sediment dispersal patterns.*

(Bell, 1940). The upper division, underlying the central part of Pictou Coalfield, comprises two predominantly fine grained, grey, coal-bearing sequences, the Albion and Thorburn members, separated by an oil shale-bearing unit, the Coal Brook Member. The redbed members which distinguish the lower division likely accumulated above water table along the margins of the developing basin, peripheral to the swamps and lakes of the Westville and Albion basins.

The Pictou Coalfield is probably the oldest continuously active mining district in Canada, and the most extensively exploited for its size (Hacquebard, 1979). Mining began early in the nineteenth century. About 53.5 million tonnes of coal have been produced since then (Hacquebard, 1979). Recent production (10 610 t in 1981) from one active mine has been very small, however. Total remaining resources are estimated to be as much as 63 million t. This coal, peripheral to mined-out zones, is generally of lower quality (Chesal, 1982). Ash contents are quite high (10.3-34.6%) compared to other Maritime coals, although sulphur contents are low (0.5-3.3%). With the exception of the Westville seams, the coal is of high volatile "A" bituminous rank, suitable for thermal power generation. The Westville coals are of medium volatile bituminous rank, and could be blended for use as a metallurgical coal as well as a high quality steam coal (Hacquebard, 1979).

Oil shales and torbanites occur throughout the upper division of the Stellarton Group, especially in the Coal Brook Member. Shale oil recoveries are quite variable, but generally less than 250 l/t (Macauley, 1984). The oil shales are considered to be uneconomic at present because of their general irregularity, low yield, and distribution beneath developed areas (Macauley and Ball, 1984; Macauley, 1984).

The highest heatflow values reported in the Maritimes (30-33°C/km) are found locally in Stellarton Basin (Nolan Davis Associates, 1984). Not only does this indicate a potential geothermal energy source, but it may explain the higher rank of the Westville coals.

Relationships between the Stellarton and Pictou groups are enigmatic. Although they are now locally in fault contact or separated by a narrow, easterly-trending, upthrown ridge of Cumberland and Canso Group rocks, the Stellarton Group was clearly deposited in a separate basin.

Structural Geology

Several workers have suggested that the Cobequid and Hollow Fault systems (Fig. 1), which separate Carboniferous strata of Stellarton Gap from Carboniferous and older rocks of Cobequid and Antigonish highlands respectively,

are related (Belt, 1968; Benson, 1974; Fralick and Schenk, 1981; Eisbacher, 1969, and others). The Chedabucto Fault system, which forms the southern boundary of the Antigonish Highlands and Stellarton Gap, is also related to the Cobequid Fault (Fig. 1). Movement on these three fault systems was the dominant control on regional sedimentation, especially during the late Paleozoic. Unfortunately, the extent and sense of such movement is not well constrained. Various interpretations have been made of the history of movement on these faults (Belt, 1968; Benson, 1974; Eisbacher, 1969; Donohoe and Wallace, 1982; Fralick and Schenk, 1981; Keppie, 1982; Webb, 1967, and others).

Cobequid Fault

Emplacement of the Fountain Lake volcanics in the Devonian is indicative of crustal extension, including probable movement on the Cobequid Fault system (Fig. 2). This event was related to the initial development of Fundy Basin (Belt, 1968; Bradley, 1982; Keppie, 1982, and others). The trend of the Scotsburn Anticline subparallel to the eastern Cobequid Fault suggests reverse movement on this part of the fault during the late Devonian. Webb (1967) interpreted the apparent refolding of the Scotsburn Anticline into a gentle "Z" shape to suggest dextral movement on the fault in late Devonian – early Carboniferous time. Normal faulting at the eastern end of the Cobequid Fault system in late Namurian time is suggested by normal fault movement on the subparallel, northeast-trending Loganville Fault, (Gillis, 1964). Eisbacher (1969) demonstrated convincingly, through tectonic fabric studies, that dextral movement took place on the Cobequid Fault south of the Cobequid Highlands during Westphalian B – Stephanian time. Normal faulting appears to have predominated on the eastern part of the Cobequid Fault system in the Mesozoic (although sinistral movement related to opening of the Bay of Fundy probably took place to the west).

Hollow Fault

The regional extension indicated by emplacement of the McAras Brook volcanics and conglomerates during the initial development of the Fundy Basin (Bradley, 1982, 1983; Dostal et al., 1983; Fralick and Schenk, 1981; Keppie, 1982) suggests movement on the Hollow Fault system. Deposition of the Hollow and Forbes Lake conglomerates suggests renewed activity in late Visean time (Fig. 2). Truncation of Canso strata east of Stellarton Basin by the Hollow Fault system suggests late Carboniferous reactivation. No direct evidence for the sense of this movement has been reported. If the late Westphalian-Stephanian dextral strain on the Cobequid Fault was transferred to the Hollow Fault, Stellarton Basin can be explained as a simple rhomb graben (Bradley, 1982, 1983; Fralick and Schenk, 1981; Yeo and Gillis, 1985).

Chedabucto Fault

Although the Chedabucto Fault lies south of the New Glasgow – Toney River map area (Fig. 1), its history is relevant to the regional geology. The Chedabucto Fault is the easterly extension of the Cobequid Fault. Together, these form the northern boundary of the St. Mary's Graben, the fundamental division between the Meguma Terrane of southern Nova Scotia and the Avalon Terrane of the north. As Keppie (1982) noted, there is no evidence for the existence of this fault system before the mid Devonian. Early movement was mainly dextral, related to the "docking" of the Meguma Terrane with eastern North America (Keppie, 1982). Reactivation of the Chedabucto Fault in the late Carboniferous is suggested by truncation of metamorphosed Horton strata on the southern edge of the Antigonish Highlands. Schistosity and minor folds are indicative of dextral movement. Sinistral movement related to the opening of the Bay of Fundy took place in the Mesozoic (Keppie, 1982).

Origin of Stellarton Basin

In spite of widespread agreement that Stellarton Basin developed as a pull-apart basin formed in response to strike-slip on the Hollow – Cobequid fault system (Bradley, 1982, 1983; Fralick and Schenk, 1981, and others), the only direct evidence so far reported in support of this hypothesis has been Eisbacher's (1969) detailed strain analyses of the Cobequid Fault. His conclusion that dextral movement took place in upper Westphalian time is supported by Yeo and Gillis' (1985) preliminary strain analyses of fractured conglomerates along the northern margin of Stellarton Basin. Other evidence in support of strike-slip movement along the northern margin of Stellarton Basin includes the juxtaposition of Pictou and Stellarton group strata, which belong to separate depositional basins although they overlap in age. An important piece of indirect evidence for pull-apart rifting is Bradley's (1982) estimated subsidence curve for Cumberland Basin, which shows that an episode of lithospheric stretching took place in early Upper Westphalian time.

Initially, coarse grained siliciclastics of the Cumberland Group were carried by low sinuosity rivers into the incipient Stellarton Basin from the northwest and south. Predominantly fine grained siliciclastics continued to be shed from the basin margins to accumulate with abundant organic material in lakes as the Stellarton Group. At the same time, Pictou Group sands were shed northerly into eastern Cumberland Basin. Significant strike-slip movement and consequent subsidence probably ceased before the end of the Westphalian. Pictou sedimentation continued, eventually overlapping and blanketing at least the western part of Stellarton Basin.

Details of the pull-apart hypothesis remain to be resolved. (1) It is not clear whether Stellarton Basin is a simple rhomb graben or whether subsidence was due to the divergence or curvature of the strike-slip fault systems. Late Carboniferous, left-lateral movement on the Hollow Fault, as suggested by Benson (1974), would favour an origin by diverging strike-slips. The distribution of lower Stellarton Group strata at the eastern and western extremities of the basin, rather than younging from one end of the basin to the other, supports the former alternative, however. (2) Evidence for some secondary faults is indirect (Bell, 1940). The existence and attitude of these should be investigated. (3) Late Carboniferous, counter-clockwise rotation of Stellarton Gap should have resulted from dextral movement on all of the bounding faults. This might be tested by determination of the sense of movement on secondary faults, such as those trending northwesterly.

A pull-apart origin for Stellarton Basin has some important consequences. (1) It is unlikely that any of the coal seams are offset by faulting outside the basin since the present fault boundaries must closely approximate the original basin margins. (2) Comparison of the geometry and development of Stellarton Basin with other pull-apart basins should help to predict the presence of coal at depth. (3) The persistence of anomalously high heat flow in a pull-apart basin suggests that the underlying crust has remained thin. (4) Finally, the tectonism which resulted in formation of the Stellarton Basin was probably also the cause of penetrative deformation and low grade metamorphism observed in the Riversdale – Canso strata of Stellarton Gap (Belt, 1968).

References

Barss, M.S. and Hacquebard, P.A.
1967: Age and stratigraphy of the Pictou Group in the Maritime Provinces as revealed by fossil spores; Geological Association of Canada, Special Paper No. 4, p. 267-283.

Bell, W.A.
1940: The Pictou coalfield, Nova Scotia; Geological Survey of Canada, Memoir 225, 160 p.

Belt, E.S.
1968: Post-Acadian rifts and related facies, Eastern Canada; in Studies of Appalachian Geology: Northern and Maritime; Interscience Publishers. p. 95-113.

Benson, D.G.,
1974: Geology of the Antigonish Highlands, Nova Scotia; Geological Survey of Canada, Memoir 376, 92 p.

Boucot, A.J., Dewey, J.F., Dineley, D.L., Fletcher, L., Fyson, W.K., Griffin, J.G., Hickox, C.F., McKerrow, W.S., and Ziegler, A.M.
1974: Geology of the Arisaig area, Antigonish County, Nova Scotia; Geological Society of America, Special Paper 139, 191 p.

Bradley, D.C.
1982: Subsidence in late Paleozoic basins in the northern Appalachians; Tectonics, v. 1, p. 107-123.

1983: Tectonics of the Acadian Orogeny in New England and adjacent Canada; Journal of Geology, v. 91, p. 381-400.

Chandler, F.W., Sullivan, R.W., and Currie, K.L.K
—   The Springdale Group and correlative rocks: a Llandoverian overlap sequence in the Canadian Appalachians; Canadian Journal of Earth Science. (in press)

Chesal, S.
1982: Pictou Coalfield Project: an evaluation of coal resources in the Westville, Stellarton, and Thorburn districts of the Pictou Coalfield; Nova Scotia Department of Mines and Energy, Report, 95 p.

Cormier, R.F.
1979: Rubidium/strontium isochron ages of Nova Scotian granitoid plutons; Nova Scotia Department of Mines and Energy, Report 79-1, p. 143-147.

1982: Rb/Sr age data for the Fountain Lake Group volcanics; Nova Scotia Department of Mines and Energy, Report 82-1, p.114-115.

Donohoe, H.V.
1979: The Cobequid Highlands – results and conclusions; Nova Scotia Department of Mines and Energy, Report 79-1, p. 149-150.

Donohoe, H.V. and Fralick, P.W.
1980: Syn-Acadian Orogeny molasse, Cobequid and Antigonish highlands, Nova Scotia; Geological Association of Canada Program with Abstracts, v. 5, p. 49 (abstract).

Donohoe, H.V. and Wallace, P.I.
1982: Debert-Mt. Thom region; Nova Scotia Department of Mines and Energy, Map 82-9, (1:50 000 scale).

Dostal, J., Keppie, J.D., and Dupuy, C.
1983: Petrology and geochemistry of Devono-Carboniferous volcanic rocks in Nova Scotia; Maritime Sediments and Atlantic Geology, v. 19, p. 59-71.

Eisbacher, G.H.
1969: Displacement and stress field along part of the Cobequid Fault, Nova Scotia; Canadian Journal of Earth Sciences, v. 6, p. 1095-1104.

Fletcher, H.
1902: Geological maps of Stellarton, New Glasgow, Pictou, and Westville; Geological Survey of Canada, Maps 598, 600, 609, and 610 (1 inch = 1 mile).

Fralick, P.W. and Schenk, P.E.
1981: Molasse deposition and basin evolution in a wrench tectonic setting: the late Paleozoic eastern Cumberland Basin, Maritime Canada; in Sedimentation and Tectonics in Alluvial Basins, ed. A.D. Miall; Geological Association of Canada, Special Paper 23, p. 77-98.

Gaudette, W.J., Olszewski, W.J., and Donohoe, H.V.
1984: Rb/Sr isochrons of Precambrian age from plutonic rocks in the Cobequid Highlands, Nova Scotia. Nova Scotia Department of Mines and Energy, Report 84-1, p. 285-292.

Giles, P.S.
1979: Upper Windsor limestone at Limerock, Pictou County; Nova Scotia Department of Mines and Energy Report 79-1, p. 79-80.

1981: Major transgressive-regressive cycles in middle to late visean rocks of Nova Scotia; Nova Scotia Department of Mines and Energy, Paper 81-2, 43 p.

1982: Geological map of the Eureka area, central Nova Scotia; Nova Scotia Department of Mines and Energy, Map, (1:50 000 scale).

Gillis, J. W.
1964: Geology of northwestern Pictou County, Nova Scotia, Canada; unpublished PhD thesis, Pennsylvania State University, 130 p.

Hacquebard, P.A.
1979: A geological appraisal of the coal resources of Nova Scotia; Canadian Institute of Mining and Metallurgy, Transactions, v. 82, p.48-59.

Hacquebard, P.A. and Donaldson, J.R.
1969: Carboniferous coal deposits associated with flood plain and limnic environments in Nova Scotia; Geological Society of America, Special Paper 114, p. 143-191.

Haites, T.B.
1956: Some geological aspects of the Pictou coalfield with reference to their influence on mining operations; in Third Conference on the Origin and Constitution of Coal, Crystal Cliffs, Nova Scotia, June 1956; Nova Scotia Department of Mines and Nova Scotia Research Foundation, Halifax, p. 39-93.

Howie, R.D. and Barss, M.S.
1975: Upper Paleozoic rocks of the Atlantic Provinces, Gulf of Saint Lawrence, and adjacent continental shelf; in Offshore Geology of Eastern Canada, Geological Survey of Canada, Paper 74-30, v. 2, p. 35-50.

Keppie, J.D.
1982: The Minas geofracture; in Major Structural Zones and Faults of the Northern Appalachians; ed. P. Saint Julien and J. Beland; Geological Association of Canada, Special Paper 24, p. 263-280.

Macauley, G.
1984: Geology of the oil shale deposits of Canada; Geological Survey of Canada, Paper 81-25, p. 40-41.

Macauley, G. and Ball, F.D.
1984: Oil shales of the Big Marsh and Pictou areas, Nova Scotia; Geological Survey of Canada, Open File Report 1037, 57 p.

Maehl, R.H.
1961: The older Paleozoic of Pictou County, Nova Scotia; Nova Scotia Department of Mines, Memoir 4, 112 p.

Mamet, B.L.
1970: Carbonate microfacies of the Windsor Group (Carboniferous), Nova Scotia and New Brunswick; Geological Survey of Canada, Paper 70-21, 121 p.

Murphy, J.B.
1984: Geology of the southern Antigonish Highlands, Nova Scotia; in Current Research, Part A, Geological Survey of Canada, Paper 84-1A, p. 587-595.

Murphy, J.B. (cont.)
1985: Geology of the southwestern part of the Antigonish Highlands; in Current Research, Part B, Geological Survey of Canada, Paper 85-1B.

Nolan Davis Associates Ltd.
1984: Groundwater flow patterns in Carboniferous sediments of Atlantic Canada. Earth Physics Branch, Open File Report 84-29.

Wallace, P.I. and Donohoe, H.V.
1977: The Cobequid Highlands survey; Nova Scotia Department of Mines and Energy, Report 77-1, p. 167-179.

Webb, G.W.
1967: Paleozoic wrench faults in Canadian Appalachians. American Association of Petroleum Geologists, Memoir 12, p. 754-786.

Yeo, G.M.
–   Geological map of the New Glasgow – Toney River area, Nova Scotia (NTS 11E/10 and 11E/15); Geological Survey of Canada, Open File. (in press)

Yeo, G.M. and Gillis, K.
1985: Origin of Stellarton Basin; Atlantic Geoscience Society, 1985 Symposium, Wolfville, Program with Abstracts.

Geology of the southwestern Antigonish Highlands, Nova Scotia[1]

J. Brendan Murphy[2]
Precambrian Geology Division

Abstract

The southwestern Antigonish Highlands are predominantly underlain by late Precambrian felsic to mafic volcanics and interlayered mudstones. This area is lithologically similar to the southern highlands but contrasts with younger late Precambrian rocks of the northern highlands. (Georgeville Group) which consist of turbidites and mafic volcanics.

Mapping in summer 1984 indicates that the contact between northern and southern sequences is transitional, that the Keppoch Formation is the oldest formation in the Georgeville Group, and that the entire sequence represents the progressive opening of a sedimentary basin.

Upper Ordovician-Silurian sequences consisting of bimodal volcanics and fluviatile to shallow marine sediments preferentially occur near fault zones. Pervasive shearing is common and is probably mid-Devonian (Acadian).

New localities containing pyritic zones have been found. They occur in both Precambrian and Ordovician-Silurian felsic volcanics. They may be stratabound, intrusive-related, fault-related or associated with the contact between subaerial and submarine volcanics.

Résumé

La partie sud-ouest des hautes-terres Antigonish repose sur des roches volcaniques, de nature felsique à mafique, dans lesquelles s'intercalent des couches de mudstone, le tout datant du Précambrien supérieur. La lithologie de cette région s'apparente à celle des hautes-terres au sud; elle diffère cependant des hautes-terres au nord caractérisées par la présence de roches plus récentes du Précambrien supérieur (groupe de Georgeville), soit des turbidites et des roches volcaniques mafiques.

Les travaux de cartographie effectués au cours de l'été 1984 indiquent que le contact entre les séquences sud et nord est transitoire, que la formation de Keppoch est la formation la plus ancienne du groupe de Georgeville et que la séquence entière représente l'ouverture progressive d'un bassin sédimentaire.

Les séquences datant de l'Ordovicien supérieur et du Silurien, séquences composées de roches volcaniques bimodales et de sédiments dont l'origine varie de fluviatile à marine de faible profondeur, se manifestent surtout près des zones de failles. Le cisaillement dont les effets sont répandus remonte probablement au Dévonien moyen (Acadien).

On a découvert d'autres zones pyriteuses dans les roches volcaniques felsiques qui datent du Précambrien ainsi que de l'Ordovicien et du Silurien. Elles sont soit limitées à certaines unités stratigraphiques, soit associées à des roches intrusives, soit associées à des failles ou soit associées au contact entre des roches volcaniques subaériennes et sous-marines.

Introduction

The Antigonish Highlands lie in northeastern mainland Nova Scotia. They predominantly consist of late Precambrian metavolcanics and metasediments that are unconformably overlain by lower Paleozoic rocks. The highlands are bounded to the north and west by the Hollow Fault, to the east by Devono-Carboniferous rocks, and to the south by the Chedabucto Fault (Fig. 1, 2). They form part of the Avalon "Composite" (Keppie, 1983a) or "Suspect" Terrane (Williams and Hatcher, 1982) that lies on the southeastern margin of the Appalachians.

Mapping in the southwestern Antigonish Highlands continued in summer 1984 and was concentrated between longitudes 62°15' and 62°30'W (see Fig. 2, 3). This mapping represents the continuation of a project initiated in 1978 (and continued in 1979) by the Nova Scotia Department of Mines and Energy in co-operation with the Canadian Department of Regional Economic Expansion. Work in 1978 and 1979 (in collaboration with J.D. Keppie and A.J. Hynes) concentrated on the northern part of the region. The project resumed in 1983 with the objective of mapping the southern highlands to determine the stratigraphy, geochemistry and petrology of the igneous rocks, the deformational and metamorphic histories, to interpret the geological history from the above, and to investigate the economic potential. In 1983, about 500 km^2 were mapped in the central and southeastern highlands. The current field season (in which 450 km^2 were mapped) represents the extension of that area to the west. The Antigonish Highlands in total comprise about 1500 km^2. To date, about 1050 km^2 have been mapped. This paper reports on the current field season's activities: details of earlier work are given by Murphy (1984) and Murphy et al. (1982).

Previous work

The Antigonish Highlands were first mapped in detail by Benson (1974) and were thought to represent a folded and faulted eugeosynclinal assemblage of probable Cambro-Ordovician age. Benson placed these rocks in the Brown's Mountain Group which was divided into four formations, in ascending order; the Keppoch Formation (dominated by rhyolites), the Baxter Brook Formation (mainly slates and greywackes), the Brierly Brook Formation (mafic to intermediate volcanics) and the Little Hollow Formation (dominated by red siltstones and quartzites).

Figure 1. *Location map of the Antigonish Highlands. A map of the darkened area is presented in Figure 2 HF-Hollow Fault, CF-Chedabucto Fault.*

Preliminary mapping by Keppie (1978) revealed that most of the rocks in the northern highlands were probably Precambrian and he recommended the abandonment of the Brown's Mountain Group and its formations. These findings prompted the remapping of the northern highlands in 1978 and 1979. Three new groups; Georgeville Group (Precambrian), MacDonald Brook Group and Iron Brook Group (both Cambrian) were defined to replace the Brown's Mountain Group (Murphy et al., 1979, 1982). Within each group a number of formations were defined. The stratigraphy and distribution of these units is given in Table 1 and Figure 2 respectively. Figure 2 is a composite map of the highlands showing work from 1978 to present.

The Georgeville Group in the northern Antigonish Highlands is at least 4000 m thick, though the base and top have not been documented. It is composed of seven formations which, in general, document a progressively deeper environment of deposition. Three of these formation are excellently exposed on the shoreline of the Northumberland Strait (Fig. 2). In ascending order they are the Chisholm Brook Formation (1G, basalt and marble), the Morar Brook Formation (2G1, mudstones, tuffs, chert and limestone), and the Livingstone Cove Formation (3G1, conglomerate, wacke and mudstone). The remaining formations are best exposed inland and correlation with the shoreline sections is made on lithological comparison.

The Maple Ridge Formation (2G, mudstone and greywacke) is probably laterally equivalent to the Morar Brook Formation. The overlying James River Formation (3G, conglomerate greywacke, mudstone and minor basalt) is thought to be in part laterally equivalent to the Livingstone Cove Formation. The Clydesdale Formation (4G), overlying the James River Formation, is dominated by basalt, minor greywacke and slate and is in turn overlain by the South Rights Formation (5G) which consists of mudstone and greywacke.

In the Georgeville area the Georgeville Group is post-tectonically intruded by appinitic gabbro (6A) and alaskitic granite (6B, Fig. 2). Both these intrusions are late Precambrian (P. Reynold personal communication, 1979, ^{40}Ar-^{39}Ar on hornblende in the appinite, and R.K. Wanless personal communication, 1980, K-Ar on muscovite in alaskite). The age of the James River and Ohio granites (6K) is less certain and they may be Cambrian (see Cormier, 1979).

The Georgeville Group is unconformably overlain by Cambrian-Lower Ordovician (Murphy et al., 1982) and by Upper Ordovician-Silurian successions (Murphy, 1984). Cambrian rocks occur only in the extreme northern highlands near Malignant Cove and are divided into two groups; the MacDonald Brook Group (7A) dominated by mafic and felsic volcanic rocks, and the Iron Brook Group (7B) consisting of fluviatile to shallow marine clastic rocks, fossiliferous lime-stones and ironstones (Fig. 2). These groups are related by lateral facies variations (Murphy et al., 1979). Upper Ordovician-Silurian rocks belong to the Bears Brook Group (Maehl, 1961) and consist of arkosic conglomerates to sand-stones, felsic and mafic volcanics, and fossiliferous green-blue siltstones and slates. Contacts between Cambro-Lower Ordovician and Upper Ordovician-Silurian sequences are not exposed but on structural arguments they are probably unconformable.

In 1983, mapping commenced in the southern highlands since the relationship between the Georgeville Group as defined in the northern highlands and the Keppoch Formation of Benson (1974) was unknown. The mapping showed that the Keppoch Formation is Precambrian (Murphy, 1984) and although the formation name was retained, its definition was

Figure 2. *Composite geological map of the Antigonish Highlands. The northern highlands are modified after Murphy et al. (1982), the southern highlands (east of 62°30') after Murphy, 1984. The area west of 62°30' (Fig. 3) is the subject of this report. Symbols to this map are given in the legend (Table 1).*

modified to include intermediate and mafic volcanics and sediment interlayered with the volcanics in the southern highlands. In detail, field relations show that the Keppoch Formation unconformably underlies the James River Formation of the Georgeville Group and that further mapping was required to document the relations between the Keppoch Formation and older formations of the Georgeville Group.

The major question left unanswered in Murphy (1984) was the detailed relationship between the Keppoch Formation and the Georgeville Group of the northern highlands. Given that the Keppoch Formation is older than the James River Formation, it may represent an early subaerial phase of the Georgeville Group or could document an earlier tectonic environment. This summers' mapping attempts a solution to this problem.

521

Figure 3. *Geological map of the southwestern Antigonish Highlands. Symbols are given in Table 1.*

Distribution of rock units

One of the major difficulties in establishing the distribution of lithologies in the present area is that faulting is more prevalent and more intense than in other parts of the highlands. For Precambrian rocks, correlation across fault blocks is made on lithological comparison and stratigraphic constraints. Evaluation of younger rocks is aided by fossils.

Within the area mapped in 1984 (see Fig. 3), Precambrian rocks are dominated by mudstones and greywackes to the north and mafic intermediate and felsic volcanics to the south. The mudstones and greywackes to the north of the Marshy Hope Fault (MHF) are isolated from other Precambrian exposures by a cover of Upper Ordovician to Silurian rocks. These lithologies in the north most closely resemble those of the James River Formation. Because of the uncertainty involved in this correlation the unit is left undivided on the map. To the south of the Marshy Hope Fault, however, the succession appears to be broadly continuous with that to the east and a James River Formation assignment is made with more confidence.

The Keppoch Formation (in the south of the map area) is generally E trending and is subdivided with the subaerial Frasers Brook member (1KA, B, C, D) overlain to the north and south by the submarine Moose River member (1KE). The contact between these members is defined by first appearance of thin plane-laminated mudstones interlayered with volcanic rocks. This relationship is extremely important to the geological history of the highlands since it indicates a transition from subaerial-type volcanism in the south to submarine sedimentation and volcanism in the north. It also indicates that the Keppoch Formation should be regarded as part of the Georgeville Group.

Precambrian sediments overlying the Keppoch Formation occur in a series of southward dipping monoclinal successions in the south of the map area. These sediments are also thin plane-laminated and resemble those of the Maple Ridge Formation, but at present they are mapped as "Georgeville undivided" since they are separated from the type section and exposure was not extensive enough to evaluate their stratigraphic context.

Late Precambrian intrusive rocks occur in the vicinity of Eden Lake, here termed the Eden Lake Complex (6A). The age of the complex is based on isotopic data, on comparison with similar Precambrian complexes in the northern highlands (see below), and in part on field relations. The complex intrudes the Keppoch Formation and is unconformably overlain by Upper Ordovician-Silurian (Fig. 3). It consists of hornblende gabbros (appinites) with quartzo-feldspathic pegmatic segregation.

Cambrian to Lower Ordovician rocks (7) are present only in the extreme north of the highlands. Upper Ordovician-Silurian rocks (8, 9, 10; Arisaig Group) consist of red arkoses, conglomerates and slates, felsic and subordinate mafic volcanics, blue-green siltstones and slates. These rocks are generally found on the flanks of the highlands and adjacent to faults (Fig. 2, 3). Sequences are generally monoclinal on the scale mapped. On the flanks, they consistently dip away from the basement rocks (Georgeville Group) and give the impression of draping the highlands. The stratigraphy is generally similar to that described in Murphy (1984). The Bears Brook Formation consists of arkoses and volcanics and its contact with the Beechill Cove Formation is based on the first appearance of blue-green fossiliferous siltstone (see Boucot et al., 1974). The most important difference between the stratigraphy of the northern and southern highlands is the hitherto unrecognized occurrence of thick felsic volcanics within the Beechill Cove Formation (9B). In general, felsic volcanic rocks in the Beechill Cove Formation thicken markedly to the south near Eden Lake (Fig. 3).

The base of the Ross Brook Formation (10) is defined by the first appearance of grey micaceous siltstones (see Boucot et al., 1974). In the northern part of Figure 3, the Ross Brook and Beechill Cove formations overstep the Bears Brook Formation onto "Georgeville" basement. The overall distribution of Upper Ordovician-Lower Silurian rocks in the norther part of the map area suggests an onlap relationship of these rocks onto basement.

Granitic plutons generally occur adjacent to, or south of the Brown's Mountain Fault. They intrude all lithologies, and are assigned a Devono-Carboniferous age on the basis of isotopic data (see Cormier, 1979). They are spatially associated with faults (see Fig. 2, 3).

Description of lithologies

A detailed description of the lithologies of the northern and southern highlands has been given elsewhere (Murphy et al., 1979; Murphy, 1984) and only formations that occur within the southwestern highlands (Fig. 3) are described here.

Precambrian

Greywackes and mudstones of the James River Formation in the map area (3G, Fig. 3) consist of poorly to moderately cleaved, green fine grained greywackes, commonly graded with slaty tops and interlayered green thinly laminated mudstones. Individual greywacke units are typically 1-2 m thick. These rocks are locally metamorphosed to chloritic schists adjacent to the Brown's Mountain Fault.

The unit named "Georgeville undivided" (G) is remarkably homogeneous throughout the map area and consists of grey and green thin plane-laminated mudstones. Although slump structures are common, facing criteria such as graded bedding or crossbedding were rarely observed. These rocks closely resemble the thinly laminated mudstones of the Morar Brook and Maple Ridge formations.

The Keppoch Formation is divided into two members on the absence or presence of thin laminated mudstones interlayered with the volcanics. The lower member is informally named the Fraser's Brook member after the section on, and adjacent to, Fraser's Brook to the east of the mapped area (see Murphy, 1984). These rocks consist of felsic volcanics dominated by ignimbrites and tuffs with minor flows, plagioclase porphyritic basaltic andesites, aphyric basalts, minor lahars and thin interflow sediments. With the exception of lahars, volcanic rocks of the Fraser's Brook member are remarkable fresh. Secondary alteration to chlorite, sericite, epidote and calcite is minor. Ignimbrites commonly exhibit a well developed banding in the field which in thin section is defined by flattened pumice fragments. Banding is generally parallel to bedding. True rhyolitic flows are relatively subordinate in volume. These red massive rocks are very fine grained, displaying subtrachytic texture defined by plagioclase and sericitized orthoclase with interstitial quartz and devitrified glass. Tuffs are generally pink to green massive rocks with angular lithic and crystal fragments up to 6 cm in length, in a fine grained crypto-crystalline quartzo-feldspathic matrix.

In the upper member (Moose River), felsic tuffs are especially common and are a distinctive apple-green in the field. They consist of little to intensely altered felsic fragments in a sericitized fine grained matrix. Lahars and ignimbrites do not occur in the Moose River member.

Basaltic andesites are deep green and contain plagioclase phenocrysts up to 1.5 cm long displaying subtrachytic texture in a matrix dominated by plagioclase

and minor augite, magnetite, sphene, ± actinolite. Calcite is generally rare although it may be present in significant amount adjacent to faults. Mudstones that are interlayered with the volcanic rocks of the Moose River member are very similar to those of the Maple Ridge or Morar Brook formations. They are green, moderately cleaved, thinly plane-laminated rocks that display some graded bedding and crossbedding on a fine scale.

Upper Ordovician-Silurian

Upper Ordovician-Silurian rocks consist of mafic and felsic volcanics, red conglomerates, arenaceous sandstones and fossiliferous blue-green siltstones and slates. Those in the north of the Brown's Mountain Fault, correlate favourable with the well known Arisaig section (Boucot et al., 1974) north of the Hollow Fault. Those successions south of Brown's Mountain Fault vary significantly particularly in the greater thicknesses of the felsic volcanics. The Bears Brook Formation consists of mafic and felsic volcanics underlain by, and interbedded with, arkosic sandstones and conglomerates.

Mafic volcanics are green, massive and fine grained. They commonly contain amygdules filled with quartz, calcite, pumpellyite or zeolites. In thin section, they contain saussuritized albite displaying flow alignment. Rare microphenocrysts of augite, partially altered to chlorite, may also be present. Epidote and chlorite are ubiquitous secondary minerals. Sphene, rutile, calcite, quartz and actinolite may be present.

Felsic volcanics are generally ignimbrites or tuffs. Their field and petrographic appearance closely resemble that of the Precambrian felsic rocks and they can only be reliably distinguished on stratigraphic context. Banding is well developed in the ignimbrites, and is defined by flattened pumic. In less welded zones, glass shards with angles close to 120° are preserved. Crystal fragments (quartz, serricitized feldspar) generally predominate over lithic fragments (rhyolite) in contast to felsic volcanics of the Keppoch Formation. Tuffs are pink, massive and fine grained containing angular fragments of rhyolite (up to 1 cm) in an ash matrix.

The arkoses and conglomerates are typically red but may contain large irregular green stained patches. They are generally polymictic containing angular to subrounded clasts of mafic and felsic volcanics, red slate and siltstones, granite, quartz and feldspar. In the field they display channels and many examples of normal and reverse grading.

Rocks of the Beechill Cove Formation are very similar to those of the type area near Arisaig that have been described in detail by Pickerill and Hurst (1983). They consist of red poorly sorted conglomerates with sandy and silty lenses, red shale and siltstone, moderately fossiliferous and micaceous blue-green mottled mudstone and layered siltstone. Pebbles in the conglomerate vary considerably in grain size (4-30 mm). The blue-green mudstones and siltstones have a distinctly rusty weathering colour.

The Ross Brook Formation consists of blue-grey fossiliferous moderately cleaved micaceous laminated mudstones, minor micaceous laminated siltstone and sandstone (see more detailed description in Maehl, 1961, and Hurst and Pickerill, in press).

Intrusive rocks

Within the map area (Fig. 3) two major types of plutonic rocks occur. The Gabbroic Complex located at Eden Lake which is Precambrian, and a number of isolated granitoid rocks that are probably mid-Devonian to Carboniferous.

The Eden Lake complex is dominated by a medium grained hornblende-plagioclase-bearing gabbro with minor pegmatitic hornblende gabbros, and irregularly defined felsic "sweaty" veinlets and pods. These lithologies are heterogeneously distributed on a hand specimen and outcrop scale. These lithologies and textures are typical of the appinitic suite and strongly resemble those of the Greendale Complex in the northern highlands.

Devonian-Carboniferous granites are typically orange to red in hand specimen and dominated by medium grained equigranular quartz, perthitic microcline, and plagioclase, with variable muscovite and biotite. In detail, many granites are locally internally heterogenous, showing abundant evidence for contamination. This contamination is usually manifest in discontinuous green chloritic pods and streaks throughout the rock.

Mafic dykes intrude all lithologies and hence may be of many phases and ages of intrusion. They are usually fresh with incipient alteration of mafic minerals to chlorite, and they are all fine grained, consisting of subophitic augite-plagioclase intergrowths with equant to skeletal magnetite. Hypersthene and hornblende are present in some dykes. Rarely, serpentine pseudomorphs after olivine occur.

Stratigraphy and age relationships

The Keppoch Formation has been interpreted (Murphy, 1984) to be Precambrian on the basis of regional stratigraphic arguments. This is because it unconformably underlies that James River Formation of the Georgeville Group. At that time it was not known whether the Keppoch Formation represented an entirely separate volcanic event that preceded the Georgeville Group, or whether it represented volcanism towards the base of the group. At present, no absolute age is known (quartz-eyed rhyolites, collected for U-Pb determinations on zircon, are currently being analyzed). The following evidence, however, supports the latter interpretation.

The Keppoch Formation has been traced into the present map area (Fig. 3) where it has been subdivided into two informal conformable members, the Frasers Brook member, and the overlying Moose River member. The presence of welded ignimbrites, lahars and the nature of the arkosic sediments in the Frasers Brook member, indicate a subaerial environment of deposition. The base of the overlying Moose River Formation is defined by the first appearance of grey and green thinly laminated mudstone that are interlayered with the volcanics. These mudstones are very similar to the thinly laminated mudstones that characterize the Morar Brook and Maple Ridge formations of the Georgeville Group in the northern highlands and suggest a low energy marine environment of deposition for the Moose River member. Units of 10-15 m of uninterrupted mudstone occur within the Moose River Formation. This suggests that volcanism was distal. The Moose River member of the Keppoch Formation is interpreted as transitional between older subaerial volcanics to the south (i.e. Frasers Brook member) and submarine sediments and relatively subordinate volcanics to the north (i.e. Georgeville Group as defined by Murphy et al., 1979). These age relationships indicate that the Keppoch Formation should be considered as part of Georgeville Group, approximately laterally equivalent to, or older than, the Chisholm Brook Formation on the northern highlands (see Table 1).

Mappable units of thin plane-laminated mudstones characteristics of the Georgeville Group, do occur at the southern margin of the area. They are commonly bounded to the north and south by fault slices that are presumably

Table 1. Generalized stratigraphy of the Antigonish Highlands (to accompany Fig. 2, 3).

	F = Fossils. Λ, ∇, V felsic, intermediate, mafic volcanic. X sediments �513 pyrite-bearing		
	NORTH	CENTRAL	SOUTH
Devono-Carb.		Undivided (see Boehner and Giles, 1982)	
	unconformity	11 Granite	11 Granite
		ARISAIG GROUP: (see Boucot et al.,1974)	
U. Ordovician-Silurian		10 Ross Brook Formation	10 Ross Brook Formation
		9A, 9B Beechill Cove Formation (sediment, volcanic)	9 Beechill Cove Formation
		8a, 8b, 8 Bears' Brook Formation (sediment, volcanic, undivided)	8 Bears' Brook Formation
	unconformity		
	7D Granite, Syenite		
	7B IRON BROOK GROUP: 7A MACDONALD BROOK GROUP:		
	Ferrona Fm. Arbuckle Fm.		
	Little Hollow Fm.	absent	absent
	Black John Fm. Malignant Cove Fm.		
Cambrian-L. Ordovician			
H?, C?	unconformity	6K Granite	6K Granite
	6B Akaskite		
	6A Greendale Appinite Complex		6A Eden Lake Appinite Complex
		GEORGEVILLE GROUP:	
		G Georgeville Group Undivided (sediments)	
		5G South Rights Formation	
		4G Clydesdale Formation	
Hadrynian	3G1 Livingstone Cove Formation	3G James River Formation	
	2G1 Morar Brook Formation	2G Maple Ridge Formation	Keppoch Formation
	1G Chisholm Brook Formation		1KE Moose River Member
			1KA, 1KB, 1KC Fraser's Brook Member (felsic, intermediate, mafic)

related to movement adjacent to the Chedabucto Fault. Since they are generally fault-bounded, they are mapped at present as undivided Georgeville Group. These occurrences may be traced to the east to Lochaber where they unconformably overlie the Keppoch Formation (Fig. 2).

The Eden Lake Complex intrudes Precambrian rocks. Although the contact is not exposed, the complex apparently truncates the contact between the Frasers Brook and Moose River members (see Fig. 3). Upper Ordovician-Silurian rocks unconformably overlie the complex. Thus, on field relationships alone, the Eden Lake complex could be from Late Precambrian to Upper Ordovician in age. However, several factors suggest that it is Late Precambrian. First, radiometric dating of the complex (Wanless et al., 1967, p. 129, K-Ar on hornblende) has yielded an age of 584 ± 28 Ma. Second, the complex is lithologically similar in part to the Greendale Complex of the Antigonish Highlands (see Murphy et al., 1982) and the Black Brook Pluton in the southern highlands (Murphy, 1984). The Greendale Complex has been radiometrically dated using the $^{39}Ar-^{40}Ar$ dating method on hornblende. This analysis yielded plateau ages of 653 ± 9 Ma, 629 ± 8 Ma, and 599 ± 9 Ma (P. Reynolds, personal communication, 1981). The above data suggest an important intrusive event of "appinitic" gabbro in the Antigonish Highlands in the latest Precambrian.

Upper Ordovician-Silurian rocks unconformably overlie the Keppoch Formation, the James River Formation and the Eden Lake Complex. The lowermost units in this sequence consist of arkosic sandstones and conglomerates and belong to the Bears Brook Formation as discussed by Maehl (1961) and Smith (1979). Mafic volcanic flows in the formation are not laterally continuous and only occur in the northwest of the map area (Fig. 3) where they may be up to 50 m thick.

The lack of continuity of these flows may indicate a strong paleotopographic control. Felsic volcanic rocks within the formation are present in all well exposed sections. Although these rhyolites are difficult to distinguish from those of the Keppoch Formation, their age is confirmed by its stratigraphic context, i.e. by the nature of the interlayered sediments (arkosic sandstones) and the overlying Beechill Cove Formation (see Boucot et al., 1974; Pickerill and Hurst, 1983).

The base of the overlying Beechill Cove Formation is defined at the first appearance of marine sediments. Fossils from blue-green siltstones in this sequence are lowermost Silurian and are similar to those from sections north of the Hollow Fault (Smith, 1979; R. Pickerill and J. Hurst, personal communication, 1984; A. Boucot and T. Bolton written communication, 1984). These age determinations also provide an upper age limit for the Bears Brook Formation. Felsic volcanics (9B), interlayered with the Beechill Cove Formation in the southern highlands are also assigned a Silurian age.

The age of the Ross Brook Formation in the southwestern Antigonish Highlands is early Silurian. Fossils similar to those in the type area north of the Antigonish Highlands (Hurst and Pickerill, in press) occur in the Ross Brook Formation in the Antigonish Highlands (R. Pickerill and J. Hurst, personal communication, 1984).

In the southern region of the area Maehl (1961) distinguished the Sunnybrae, Glencoe Brook and Kerrowgare formations as lateral equivalents to the Bears Brook, Beechill Cove and Ross Brook formations respectively. Those names were proposed because of the lack of continuity in exposure between the respective type localities. Although I found

these correlations to be generally correct, newly discovered exposures that occur between the type localities of the respective facies equivalents, and the overall similarity of these laterally equivalent formations, indicate that the names proposed by Maehl (1961) in the southern highlands may be redundant and should be replaced by their better known northern equivalents (see. Fig. 3). Further mapping to the west and systematic work on fossil assemblages are needed to substantiate this contention.

Granitic rocks intrude all lithologies (Fig. 2). Preliminary Rb-Sr age determinations (Cormier, 1979) indicate that they are broadly ranging, from middle to late Devonian. The age is consistent with the geology of the highlands since granites do not intrude the late Devonian(?)-Carboniferous Horton Group (see Boehner and Giles, 1982). These granites are spatially related to faults (Fig. 3).

The age of dykes is problematical. They are overwhelmingly mafic, although a few occurrences of quartz-eyed rhyolitic porphyry occur. Dykes are likely to be varied ages. From studies in the northern highlands, dykes are known to be related to mafic volcanics of the Chisholm Brook Formation (Precambrian) and the Arbuckle Formation (Cambrian; Murphy et al., 1979). Mafic volcanism is also evident in Upper Ordovician and Carboniferous rocks, and some dykes may be feeders. Mafic dykes also intrude the Devonian granites, indicating at least one post-Devonian phase of mafic intrusion. At present no systematic distinction has been attempted.

Structural geology

Murphy (1984) divided the Precambrian rocks in Antigonish into three regions on differing structural style (see Fig. 2):

1. North of the Brown's Mountain Fault, characterized by regional F_1 isoclinal folds.

2. Between Brown's Mountain Fault and the contact with the Keppoch Formation, in which isoclinal folds are absent or local

3. The Keppoch Formation, in which regional folding is absent.

Most of the map area of Figure 3 lies within region 3. There is no compelling evidence for regional folding within the map area. It is likely, since much of the Keppoch Formation was deposited subaerially, that the distribution of units was governed by paleotopography. Therefore the present distribution may be mainly governed by primary considerations. If regional folding did occur in region 3, it appears to have been supratenuous, i.e. antiformal fold hinges are located on paleotopographic highs and limbs are on paleoslopes. If this is true, then tectonic folding resulted in a tightening of the primary distribution. Further evidence for supratenuous folding is provided by the thinly laminated mudstones ("Georgeville undivided") that drape the southwestern and southern highlands (Fig. 2, 3) in a series of monoclinal successions consistently dipping away from the Keppoch Formation throughout the southern highlands.

Similarly, the structural style in Arisaig Group rocks is governed by local rather than regional factors. The rocks occur in monoclinal successions, in contrast to the relatively complex folded structures of probable mid-Devonian age that were reported by Boucot et al. (1974) in the Arisaig Group north of the Hollow Fault. It is likely, therefore that these rocks were protected from this deformation, possibly due to their proximity to basement (i.e. the Georgeville Group). These successions are spatially associated with faults. Due to limited exposures, Murphy (1984) was unable to deduce whether these rocks were deposited in active fault-troughs or

whether the spatial association was due to post-Silurian downthrow and preservation. The latter interpretation is preferred since facies variations do not occur as one approaches the fault margins.

Faults are an important structural feature in the southwestern Antigonish Highlands (Fig. 3). This is probably due to the highlands being bound in a "vice" by the Chedabucto Fault to the south and the Hollow Fault to the north. The faults in the present map area can be divided into two categories (Fig. 3):

1. Those that parallel the trends of the Hollow or Chedabucto Faults. Many of these faults, i.e. the Marshy Hope and Brown's Mountain faults, can be mapped into the southwestern highlands (Fig. 3) and can generally be traced from the highlands where they displace Devono-Carboniferous rocks, defining a minimum age for latest displacement (see Boehner and Giles, 1982). Where they are exposed, rocks adjacent to the fault have a local vertical fracture cleavage parallel to the strike of the fault.

2. The second category occurs mainly in the southern part of the map area, and is generally north to northwesterly trending in region 3. They are characterized by intense shearing that imparts a local schistosity in Precambrian, Upper Ordovician-Silurian successions and locally in some Devono-Carboniferous granites. This latter relationship defines a maximum age for latest movement on these faults. Pyritic zones in felsic volcanic and intrusive successions have been found adjacent to these faults. In general, these faults contain less offset. They are at a high angle to the Chedabucto and Hollow faults and, if motion on all these faults was contemporaneous, then minimal displacement might be expected (see Fig. 2).

Devonian plutons (11) tend to be spatially associated with faulting. Some of the intrusions appear to postdate these faults since they do not display any schistosity and the plutons appear to truncate the trace of the faults; others are truncated and sheared by these faults. It is suggested that shearing and intrusion of these plutons were roughly contemporaneous. This may explain the abundant streaky xenoliths and heterogeneity of many granites. Further, such an origin may explain the highly variable ^{87}Sr-^{86}Sr initial ratio (see Cormier, 1979) of contemporaneous plutons. Since these faults only occur in the southern part of the highlands, they are likely to be related to movements on the Chedabucto Fault. Since this age is generally thought to be about the time that the Meguma Terrane docked (e.g. Keppie, 1983a) detailed study on the geometry and displacement on these faults may provide significant information concerning this docking procedure. Further, it may be significant that many of the trends of these faults are found in the Meguma Terrane itself (see Keppie, 1982).

The earliest age of faulting is more problematic, and it is conceivable that many faults show a considerable degree of inheritance. For example, the rhomboidal outcrop pattern of the Cambrian rocks (Fig. 2) has been attributed to a pull-apart basin localized by Late Precambrian-Early Cambrian transcurrent movement along the Hollow Fault (Murphy et al., in press). There is some evidence that the Chedabucto Fault or an ancestral variety of the fault may have been present in Late Precambrian time. Firstly, in the southern margin of the highlands, southward-dipping, thin laminated slates drape the southern margin of the Keppoch Formations. This suggests that the present site of the Chedabucto Fault was then an important paleogeographic low. Secondly, the spatial association of the Late Precambrian appinitic complexes (6a) with the Chedabucto and Hollow faults would suggest that their intrusion was localized along these faults (Fig. 2, 3).

Table 2. Results of lithogeochemical survey of various pyritic zones in the Antigonish Highlands. Locations of samples are shown in Figure 2. Au, Pb, Zr, and Ag were analyzed at Technical University of Nova Scotia using an aqua regia leach and atomic absorbtion. Au was determined by X-ray Assay Laboratories, Toronto, by neutron activation.

Sample		Locality	Cu	ppm Pub	Zn	Ag	Au (ppb)
IRL	-1	A	161	55	109	1.1	8
	2	A	54	13	153	1.9	4
	3	A	7	> 2	29	> 0.2	8
	4	A	272	2	77	0.6	11
	5	A	82	21	99	1.4	5
	6	A	920	3	77	> 0.2	1
	7	A	6	> 2	18	> 0.2	4
	8	A	4	> 2	11	> 0.2	17
	9	A	71	18	40	5.7	7
	10	A	72	47	159	1.8	6
	10a	A	184	7	128	0.3	7
	11	A	216	8	109	0.3	13
	12	A	258	14	117	0.3	12
	13	A	187	10	119	> 0.2	1
E09	-950	B	7	20	56	> 0.2	3
	951	B	5	> 2	32	> 0.2	10
	952	B	3	25	30	> 0.2	18
	953	B	3	6	25	> 0.2	17
	954	B	6	14	44	> 0.2	14
	955	B	1	6	7	> 0.2	22
	956	B	5	6	24	> 0.2	10
	957	B	2	> 2	23	> 0.2	22
	958	B	3	2	35	> 0.2	13
MV I		B	79	480	168		-2
E09	-959	B	4	4	11	> 0.2	14
	960	B	12	5	29	0.2	42
	961	B	3	2	15	> 0.2	11
	962	B	2	2	16	> 0.2	29
900, 901		B	79	69	750	0.2	1
MC	-2	C	810	2	147	> 0.2	4
	3	C	267	2	160	> 0.2	4
WHCU-1A		D	25	> 2	10	> 0.2	4
	1C	D	9	> 2	13	> 0.2	7
	1D	D	3	7	11	> 0.2	13
	1E	D	11	4	19	> 0.2	1
	1H	D	14	> 2	27	> 0.2	7
	1I	D	19	5	15	> 0.2	2
TH05	-IR2	E	30	9	22	> 0.2	16
	IR3	E	60	15	35	> 0.2	13
DT9	-1	F	188	12	785	0.4	22
420-4AC		F	4	2	26	> 0.2	1
LUI	-1	G	2	9	19	> 0.2	11
LU3	-1	G	2	6	19	> 0.2	49
420	-2B	G	4	2	26	> 0.2	1
	-2B	G	64	18	25	> 0.2	28
	3	G	40	17	35	> 0.2	61
BMF	-1	H	1	12	43	> 0.2	4
	3	H	13	20	65	> 0.2	17
G05	-3	I	9	27	29	> 0.2	32
G08	-11	J	9	3	72	> 0.2	3
G12	-10	K	68	6	26	> 0.2	11
G14	-5C	L	3	2	20	> 0.2	12
G15	-2B	L	21	3	79	> 0.2	5
	-5B	L	267	273	2425	> 0.2	5
G21	-1C	L	3	10	18	> 0.2	6
21A	-4A	L	37	4	24	> 0.2	25
425	-7A	N	16	44	8	> 0.2	7
	7A1	N	12	29	10	> 0.2	17
	7A2	N	7	34	8	> 0.2	7
426	-2J	P	74	100	104	> 0.2	12
427	-5A	Q	5	9	23	> 0.2	14
405	-2	R	176	278	1755	> 0.2	2

Economic geology

During the summer of 1984 a reconnaissance lithogeochemical survey of selected pyritic zones of the central and southern highlands was undertaken. The following discussion is preliminary and speculative; nevertheless some useful points can be made.

Although previous work has documented numerous minor mineral occurrences (e.g. Bourque, 1981) major occurrences were unknown. Detailed mapping of the southwestern highlands has revealed many interesting pyritic zones both in Precambrian and Upper Ordovician-Silurian rocks. They are generally adjacent to, or within, felsic volcanics. In some zones intense silicification and basification has occurred. There appear, at present, to be four main modes of occurrence (Fig. 2):

1. Adjacent to the NW set of shear faults, mainly in the Precambrian volcanics (e.g. localities F, H, L, N and P on Fig. 2).

2. Near the contact between the Moose River and Fraser members of the Keppoch Formation (i.e. the contact between subaerial and submarine volcanics, e.g. L).

3. As discontinuous lenses stratabound and up to 250 m thick in the Keppoch Formation, (see Murphy, 1984; e.g. locality A) or in Ordovician-Silurian rocks (e.g. localities E and Q).

4. Adjacent to the Brown's Mountain Fault mainly in intrusive felsic porphyritic dykes of Ordovician-Silurian or Carboniferous age (localities B, C, G, I, and R).

The last may be particularly significant since at least six examples have been located, one of which (locality B) was previously reported by Fletcher (1886) and mined for silver in the 19th century. Here the pyritization appears to be related to the intrusion of a quartz-eyed felsic porphyry close to the fault plane. Other pyritic occurrences along the fault are also closely associated with a similar porphyry. Of further interest perhaps, is that Murphy (1984) suggested that the Brown's Mountain Fault may represent the contact between the Precambrian oceanic (north) and continental (south) domains, and it therefore represents an area of extreme competence contrast and a likely site for faults and magmatism. The age of these dykes is, at present, unknown. The youngest rocks they intrude are the Beechill Cove Formation. If their intrusion is related to felsic magmatism, then most likely ages are Lower Silurian or Carboniferous. Chemically they closely resemble Lower Silurian volcanics. The Brown's Mountain Fault exerts a significant facies control on Upper Ordovician to Silurian stratigraphy and may have been active at that time. Thus, if the quartz-eyed porphyries are Lower Silurian, these pyritic zones may be particularly attractive in view of the recent discoveries in rocks of a similar age in Newfoundland.

The results of the survey (Table 2) indicate some anomalous concentrations of base and precious metals. Of particular interest is the relatively high base-metal concentrations in some of the intrusive quartz-eyed porphyries. Values tend to be erratic suggesting that significant mobility may have occurred. Silver values are, however, low.

Generally speaking, the Precambrian volcanic rocks analyzed contain less gold than the younger felsic rocks. It is clear from the analyses that all four modes of occurrence have some interesting features and warrant further and more detailed investigation.

Discussion

Mapping the southern highlands (Murphy, 1984) revealed that the Keppoch Formation was Precambrian. Precambrian rocks were divided into two successions; the Georgeville

Group and the Keppoch Formation, that had distinct lithologies, stratigraphy, depositional environments, structural style and tectonic setting. At that time, the detailed relationship of the Keppoch Formation to the Georgeville Group, as defined in the northern highlands, was unknown save that it was older than the James River Formation. Thus, the Keppoch Formation could either represent an earlier stage of a major tectonic event in the Antigonish Highlands, or a completely separate and earlier Precambrian event. However, evidence from the southwestern highlands supports the former interpretation.

Mapping in the southwestern highlands revealed that the Keppoch Formation can be subdivided into the Frasers Brook member, which was deposited subaerially, and the Moose River member, which contains marine mudstones interlayered with volcanics. These mudstones resemble those of the Maple Ridge and Morar Brook formations of the northern highlands. These observations, together with regional stratigraphic considerations in the southern highlands (Murphy, 1984) indicate that the Keppoch Formation is part of the Georgeville Group, and that part of the Keppoch Formation is time-equivalent to the Chisholm Brook and Morar Brook formations. The thickness of uninterrupted units of mudstone in the Moose River member suggests that it represents a period of waning volcanism from a distal source. Decreasing heat flow in the southern highlands may have contributed to subsidence and draping of the Keppoch Formation by mudstones.

The thinly laminated mudstones that overlie the Keppoch Formation in the southern part of the Figure 3 (mapped as "Georgeville undivided") resemble those of the Maple Ridge Formation or Morar Brook Formations. If this is substantiated it would considerably strengthen the above correlations.

However, it is now clear that the Georgeville Group underlies much of the Antigonish Highlands. The group is dominated by subaerially deposited (continental) felsic and mafic volcanics in the south and by turbidites and mafic volcanics (oceanic) in the north. The Keppoch Formation should now be considered the oldest formation of the Georgeville Group. Thus the Georgeville Group probably records a history of change from a subaerially deposited (continental) felsic to mafic volcanic regime to a mafic-dominated, submarine (oceanic) environment and may comprehensively document magmatic processes during the genesis of an oceanic basin. Geochemical and petrological studies of the Keppoch Formation, will be extremely important in detailing this history. The proliferation of faults in the region denies the opportunity to view a complete stratigraphic transition from continental to oceanic domains. However, a comparison between the geochemistry of volcanics of the Chisholm Brook Formation and that of mafic volcanics of the Keppoch Formation should enable a further evaluation of this interpretation.

The transitional nature of the contact between continental and oceanic domains defined on the surface by the Moose River member of the Keppoch Formation (Fig. 3) does not necessarily imply such a transition between continental and oceanic sources at depth. The present contact between these sources is interpreted to be a combination of the Brown's Mountain and Marshy Hope faults. This is based on the distribution of Precambrian and Paleozoic granitic plutons and on the variations in Precambrian structural style (see Murphy 1984). The granitic plutons presumably have continental sources and are, generally close to, or south of, the Brown's Mountain Fault. The lack of regional F_1 isoclinal folds in region 2 and 3 (in contrast to region 1) may be due to protection by the Precambrian continental environment of the Keppoch Formation, and may also be accounted for by this interpretation.

Upper Ordovician to Silurian rocks of the Arisaig Group are far more widespread in the southwestern highlands than previously mapped (compare Benson, 1974). They are lithologically similar to equivalent sections to the north of the Hollow Fault and represent the oldest rocks occurring on both sides of this fault. This is particularly significant in view of the importance attached in regional tectonic modelling to the earliest overstep sequences across fault blocks (see Keppie, 1983a; Williams and Hatcher, 1982). However, some facies changes do occur across the Brown's Mountain Fault and these need further evaluation. The overall similarity indicates that the Bears Brook Formation is in part, time-equivalent to the Dunn Point Formation as suggested by Smith (1979). Since the Bears Brook Formation represents a significant lateral variation of the Dunn Point Formation, the term is useful and should be retained. However, the Glencoe Brook and Kerrowgare formations of Maehl (1961) are so similar to the Beechill Cove and Ross Brook formations respectively, that their usefulness is considered doubtful and needs further evaluation to the west of the map area.

The Arisaig Group is invariable spatially associated with faults that do not exert noticeable facies control, and the spatial association is attributed to post-Silurian downthrow and preservation. However, it is certainly conveivable that the Brown's Mountain Fault was active. Further evidence of this activity may be gained from the spatially associated quartz porphyries that may be Lower Silurian.

Mid-Devonian granitic plutons crosscut these shear zones suggesting that they may range from mid-Silurian to mid-Devonian. The shear zones may be related to the docking of the Megume Terrane to the south. The Hollow and Chedabucto faults have a long history of episodic movement, and there is evidence to suggest that they were at least locally important in the Late Precambrian.

Murphy (1984) stated that the presence of oceanic and continental domains may be reflected in the distribution of mineral deposits, and that the Brown's Mountain Fault may have special significance in this regard. To date, several promising pyritic zones have been identified along this fault. It was also stated that in general the southern highlands, may offer more potential than rocks in the northern highlands. This may be especially significant in the light of the spatial association of fault zones with many pyritic occurrences in felsic volcanic rocks in both Upper Ordovician-Silurian and Precambrian successions.

Results of mapping in the southwestern highlands

The following are the most important conclusions of the 1984 field season:

1. A map suitable for publication at 1:50 000 scale of the southwestern highlands was prepared. A summary of this is presented in Figure 3.

2. The Keppoch Formation in the southwestern highlands can be subdivided into two mappable members: a lower member of felsic to mafic volcanics, and an upper member where the volcanics are interlayered with thinly laminated slates similar to those of the Morar Brook and Maple Ridge formations of the Northern Antigonish Highlands.

3. The contact between these members defines a change from sub-aerial to marine environments of deposition. These members are informably defined here and termed the Frasers Brook and Moose River members respectively.

4. The stratigraphic context and depositional environment of the Moose River member indicate that the Keppoch Formation is in part laterally equivalent to the Chisholm Brook and Morar Brook formations of the northern highlands (Table 1). Thus, for the first time a link is established between southern and northern stratigraphic sequences.

5. The above observations imply that the Keppoch Formation should be considered as an early part of the Georgeville Group.

6. The transition from subaerial to submarine environments implies that the entire Georgeville sequence may fully document magmatic and sedimentological processes during an opening of an ocean basin.

7. Several pyritic zones were found which further attest to the encouraging economical potential of the Keppoch Formation. There are two modes of occurrence, i.e. stratabound and/or fault-related.

8. The extent of known Upper Ordovician-Silurian successions is considerably increased especially in the southern part of the map area in the vicinity of Eden Lake. In this area, thick rhyolitic flows occur within the Beechill Cove Formation, and some pyritic zones and new fossil localities in blue-green siltstones have been documented.

9. The Eden Lake Complex consists of hornblende porphyritic (appinitic) gabbros and is very similar to the Late Precambrian Greendale Complex of the northern highlands. These indicate that there may be an important phase of intrusion of "appinitic" magma in the late Precambrian.

10. Faulting in the southwestern highlands has been especially intense resulting in local penetrative schistosity and complete recrystallization of Precambrian to Silurian lithologies. Mafic and felsic volcanics are converted to chlorite-sericite schists respectively. Pyritic zones in felsic volcanics may be spatially associated with these faults.

11. Devono-Carboniferous plutonic rocks are variably affected by this style of faulting. Some granites are truncated by the faulting but others appear to be unaffected. This suggests that this faulting was roughly contemporaneous with Late Devonian plutonism.

12. There is evidence to suggest that the Hollow and Chedabucto faults had a long history of repeated movement and may have been at least locally important in the late Precambrian.

Acknowledgments

References

1974: Geology of the Antigonish Highlands, Nova Scotia; Geological Survey of Canada, Memoir 376, 92 p.

Boehner, R.C. and Giles, P.S.
1982: Geological map of the Antigonish Basin, Nova Scotia, scale 1:50 000; Nova Scotia Department of Mines and Energy, Map 82-2.

Boucot, A.J., Dewey, J.F., Dineley, D.L., Fletcher, R., Fyson, W.K., Griffin, J.G., Hiskox, C.F., McKerrow, W.S., and Zeigler, A.K.
1974: Geology of the Arisaig area, Antigonish County, Nova Scotia; Geological Survey of America, Special Paper 139, 191 p.

Bourque, P.D.
1981: A metallogenic study of the Antigonish area, Nova Scotia, with special reference to the copper occurrences of the Ohio-Sylvan Glen belt; unpublished M.Sc. thesis, Dalhousie University, 419 p.

Cormier, R.F.
1979: Rubidium-strontium isochron ages of Nova Scotian granitoid plutons; in Nova Scotia Department of Mines, Report of Activities, Report 79-1, p. 143-147.

Fletcher, H.
1886: Report on geological surveys and explorations in the counties of Guysborough, Antigonish and Pictou; Geological Survey of Canada, Annual Report for 1885, 2, p. 5-128.

Geological Survey of Canada
1982: Experimental colour compilation, high resolution aeromagnetic vertical gradient, parts of 11E/8, 11E/9, 11F/5, 11F/12, Nova Scotia; Geological Survey of Canada, Map 40 079G.

Hurst, J.M. and Pickerill, R.K.
— The relationship between sedimentary facies and faunal associations in the Llandovery siliciclastic Ross Brook Formation, Arisaig, Nova Scotia; Canadian Journal of Earth Sciences. (in press)

Keppie, J.D.
1978: Brown's Mountain Group, Antigonish Highlands, Nova Scotia – preliminary reassessment; Geological Society of America, Northeastern Section, Abstracts.

1982: Tectonic map of the Province of Nova Scotia, scale 1:500 000; Nova Scotia Department of Mines and Energy, Map 82-1.

1983a: The Appalachian collage; International Geological Correlation Program, Caledonide Orogen Volume, Uppsala meeting.

1983b: The Minas Geofracture; in Major Structural Zones and Faults of the Northern Appalachians, ed. P. St.-Julien and J. Beland; Geological Association of Canada, Special Paper 24, p. 263-279.

Keppie, J.D., Dostal, J., and Zentilli, M.
1978: Petrology of the Early Silurian Dunn Point and McGillivray Brook formations, Arisaig, Nova Scotia; Nova Scotia Department of Mines, Paper 78-5, 20 p.

Landing, E., Nowlan, G., and Fletcher, T.P.
1980: A microfauna associated with early Cambrian trilobites of the Callavia Zone, northern Antigonish Highlands, Nova Scotia; Canadian Journal of Earth Sciences, v. 17, p. 400-418.

Maehl, R.H.
1961: The older Paleozoic of Pictou County, Nova Scotia; Nova Scotia Department of Mines, Memoir 4, 112 p.

Murphy, J.B.
1961: Geology of the southern Antigonish Highlands, Nova Scotia; in Current Research, Part A, Geological Survey of Canada, Paper 84-1A, p. 587-595.

Murphy, J.B., Cameron, K., Dostal, J., Keppie, J.D., and Hynes, A.J.
— Cambrian volcanism in Nova Scotia; Canadian Journal of Earth Sciences. (in press)

Murphy, J.B., Keppie, J.D., and Hynes, A.J.
 1979: Geology of the northern Antigonish Highlands; in Nova Scotia Department of Mines, Report of Activities, Report 79-1, p. 105-107.

 1982: Geological map of the northern Antigonish Highlands; Nova Scotia Department of Mines and Energy, Map 82-3.

 — Geology of the northern Antigonish Highlands, Nova Scotia; Nova Scotia Department of Mines and Energy, Memoir. (in prep.)

Pickerill, R.K. and Hurst, J.M.
 1983: Sedimentary facies, depositional environments, and faunal association of lower Llandovery (Silurian) Beechill Cove Formation, Arisaig, Nova Scotia; Canadian Journal of Earth Sciences, v. 20, p. 1761-1779.

Smith, P.K.
 1979: Note on the geology and new Silurian fossil occurrences, south and east of Kenzieville, Antigonish Highlands; in Nova Scotia Department of Mines, Report of Activities, Report 79-1, p. 89-94.

Wanless, R.K., Stevens, R.D., Lachance, G.R., and Edmonds, C.M.
 1967: Age determinations and geological studies; Geological Survey of Canada, Paper 67-2, part A, p. 125-129.

Williams, H. and Hatcher, R.D. Jr.
 1982: Suspect terranes and accretionary history of the Appalachian Orogen; Geology, v. 10, p. 497-560.

Remarques sur les mouvements et la dispersion glaciaire du Wisconsinien en Gaspésie (Québec)[1]

Gilbert Prichonnet[2] et Luc Desmarais[2]
Division de la science des terrains

Résumé

Cette étude traite des événements glaciaires du secteur de Mont Joli – Matane-lac Matapédia et lac Humqui. Deux écoulements glaciaires attribués au Wisconsinien sont identifiés: le plus ancien, vers le sud-sud-est, est majeur; il est responsable de la mise en place d'une nappe de till irrégulière et de quelques formes fuselées; le deuxième, tardif, montre des marques d'écoulement rayonnant vers le sud-ouest, l'ouest et le nord-ouest à partir de la vallée de la Matapédia. La calotte glaciaire responsable de ces mouvements semble s'être dissociée du front de l'inlandsis (?) ou d'une autre masse de glace localisée vers la dépression de la rivière Mitis. Un modèle de retrait dans le sens de la pente a permis l'accumulation de complexes fluvio-glaciaires dans le val de la Matapédia.

Des débris précambriens et des ardoises rouges montrent un transport net vers le sud-sud-est jusqu'au delà des monts Notre-Dame. Le transport vers l'ouest, nord-ouest et le nord demeure problématique: une étude plus détaillée est en cours.

Des glaciers de cirque ont persisté dans quelques niches sur le versant nord des monts Notre-Dame, lors de le déglaciation.

Abstract

Two ice flows, believed to be Wisconsinan, were identified in the Mont Joli-Matane-Matapédia Lake, and Humqui Lake area. The oldest, and better recorded, occurred towards the south-southeast; this ice deposited an irregular till sheet and left a few streamlined forms. The second, more recent flow, shows traces of radial flow towards the southwest, west, and northwest from the Matapédia valley. The ice responsibility for these movements probably represents a discrete glacier originating from the main glacier or from another ice mass situated near the Mitis River valley. As the ice retreated downslope, glaciofluvial deposits accumulated in Matapedia syncline.

Precambrian erratics and red slates indicate a transport to the south-southeast, to beyond the Notre Dame Mountains. Transport towards the west, the northwest and the north remains problematic and is presently under study.

On the northern face of the Notre Dame Mountains, a few cirque glaciers remained active during the deglaciation.

Introduction

Un projet de caractérisation des tills par géochimie a été entrepris à l'été 1984, dans un secteur de la Gaspésie occidentale (fig. 1). La campagne d'échantillonnage a également permis un relevé des marques d'érosion glaciaire et des comptages pétrographiques sur le terrain, ou en laboratoire lors du traitement des échantillons pour séparer la fraction argileuse. Cette note a pour objectif de discuter les premiers résultats de ces deux approches, l'étude géochimique étant encore en cours.

Le projet général comprend aussi une étude plus systématique de la pétrographie des tills et des dépôts fluvioglaciaires (été 1985). Par ailleurs, une synthèse stratigraphique des évènements quaternaires dans la région de La Rédemption-Sayabec est menée parallèlement (L. Desmarais, en préparation).

Cadre physique

Du pointe de vue structural, tout le territoire d'étude (environ 50 x 50 km) appartient aux Appalaches: la côte, peu découpée, est sensiblement parallèle (240°-060°) au grain tectonique.

D'anciennes plate-formes structurales forment une série de terrasses étagées, sur 3 à 4 km de largeur, le long de l'estuaire du Saint-Laurent: elles sont recouvertes de dépôts récents de la mer de Goldthwait (Dionne, 1977; Locat, 1977; Martineau, 1980); en fait, des sédiments marins fossilifères s'étendent sur plus de 15 km dans certaines vallées profondes (rivières Mitis et Neigette, fig. 2), situation non signalée par certaines cartes du Quaternaire (ex. Locat, 1978).

Le plateau appalachien débute à quelques kilomètres de la côte. Il atteint 410 m dans le petit massif dit "collines de Chics-Chocs": voir les points cotés sur la figure 2. Ce plateau est fortement disséqué par le réseau fluviatile, et parsemé de petits lacs. Sur 20 km de largeur, cette zone est généralement pauvre en dépôts quaternaires.

Le val, ou synclinal de la Matapédia (WSW-ENE), forme une dépression relative entre la rivière Mitis et le lac Matapédia, dont le niveau se situe à environ 165 m. Dans le secteur de la Rédemption (fig. 2), la ligne de partage des eaux, entre les bassins de la Mitis et de la Matapédia, forme une dorsale nord-sud qui, on le verra plus loin, semble avoir joué un rôle dans l'écoulement glaciaire lors de la déglaciation. D'importants dépôts fluvio-glaciaires sont identifiés dans la zone centrale de cette dépression, tandis qu'une nappe de till importante recouvre la partie est.

Au sud, ce val s'appuie contre la chaîne des monts Notre-Dame culminant à 907 m d'altitude (mont Saint-Pierre). Ce prolongement occidental des monts Chics-Chocs domine le bassin versant vers les lacs à la Croix

Figure 1. *Cartes de localisation.*

et Humqui. On a noté, sur leur flanc nord, quelques formes en cirque avec moraine arquée frontale (L. Desmarais, en préparation), et, sur leur versant sud, une large traînée de till présentant quelques allongements sud-sud-est (fig. 2).

En se basant sur les subdivisions proposées par Poole et Rodgers (1972), on note 2 ensembles tectonostratigraphiques dans la zone d'étude: (1) au nord, l'anticlinorium de Québec; (2) au sud, le synclinorium de Gaspé (vallée du Connecticut).

Les roches variées (shales, grès, siltstones, conglomérats, ...) du premier ensemble sont d'âge cambro-ordovicien: les schistes argileux ou ardoises rougeâtres et violacées (Aubert de la Rue, 1941; Béland, 1960; Liard, 1972), semblent intéressants pour déterminer le sens du transport glaciaire. Des bandes de quartzites blanchâtres affleurent en particulier au sommet de cette séquence vers le sud: ce sont des roches de type Kamouraska qui ne devraient pas être confondues avec les grès quartzitiques de la Formation de Val-Brillant (Béland, 1960) à l'affleurement du moins; à l'état d'erratique leur distinction est plus délicate. Dans le deuxième ensemble, d'âge siluro-dévonien, les grès quartzitiques de Val-Brillant forment un horizon repère très important pour l'étude des dispersions glaciaires. Un petit lambeau de serpentinite diorite, à l'est de La Rédemption (fig. 2), constitue également un marqueur pour l'étude géochimique des tills.

Rappel sur les problèmes des glaciations dans les Appalaches

Les problèmes de zone non glacée en altitude au pléniglaciaire, dans le coeur de la Gaspésie, et d'écoulements radiaux à la fin de la glaciation, ont été évoqués dès le début du siècle (Chalmers, 1906) et discutés par Flint et al. (1942) et Alcock (1944). Pour la zone d'étude considérée ici, Coleman (1925) avait noté la présence de débris des Laurentides depuis le fleuve jusqu'à la baie des Chaleurs. McGerrigle (1952) a signalé l'abondance des débris erratiques provenant du plateau laurentien dans la vallée de la Matapédia.

Lebuis et David (1977) et David et Lebuis (1985) ont présenté une synthèse des évènements glaciaires identifiés sur un large secteur des Appalaches recouvrant d'ailleurs la bordure est de la présente zone d'étude. Ils suggèrent cinq évènements glaciaires successifs et définissent quatre unités de till ou diamictons d'origine glaciaire. L'un des points critiques nous paraît être l'importance et l'extension des mouvements vers le nord et le nord-ouest: on sait qu'un mouvement majeur avec transport vers le nord-est est clairement établi plus à l'est (Chauvin, 1984). L'auteur conclut prudemment qu'on ne peut donner un âge précis à ce (ou ces) transport(s).

Les marques d'érosion glaciaire et les formes fuselées

Près de 50 sites de stries ont été étudiés: certains trop rapprochés sont représentés par un seul point sur la figure 2. Les indices habituels de polarité et les quelques recoupements observés permettent de conclure que deux mouvements sûrs se sont succédés sur la région (fig. 3):

a) un écoulement sud-sud-est, avec quelques déviations locales — par exemple dans les cols des monts Notre-Dame — est identifié sur l'ensemble de la région; les marques sont généralement bien nettes dans les secteurs nord-ouest et sud;

b) un écoulement vers les secteurs sud-ouest, ouest et nord-ouest recoupe le précédent en quelques sites; en plusieurs sites l'érosion est très superficielle, et la polarité établie grâce à de très petites "queues de rat".

Dans le secteur entre la rivière Mitis et au nord-ouest de La Rédemption, deux indices pourraient indiquer une poussée vers le nord-est (fig. 3).

Figure 2. *Distribution des stries, des accumulations fluvio-glaciaires majeures et de quelques formes fuselées. Villages: A: Amqui; LR: La Rédemption; S: Savabec; VB: Val-Brillant.*

46 sites
111 mesures
classes de 5°

Au sud-est de Mont-Joli, quelques formes fuselées sont bien concordantes avec le mouvement sud-est. Également, au sud du lac Matapédia et à l'arrière de la chaîne des monts Notre-Dame, une traînée de till forme quelques fuselages orientés sud-sud-est: lors de la campagne de creusage pour échantillonner le till, il a été possible de constater une diminution progressive de l'épaisseur du till depuis le pied des reliefs vers le secteur sud-sud-est (de plus de 4 m à moins d'un mètre en 3,5 km).

Les dépôts fluvio-glaciaires du val de la Matapédia

Une série de complexes fluvio-glaciaires constituent des réserves d'importance variable entre la rivière Mitis, à l'ouest, et le lac Matapédia, à l'est: leur disposition spatiale a été simplifiée à l'extrême sur la figure 2; sur la figure 4, les principales formes sont représentées.

a) Le complexe situé à 3,5 km à l'est de La Rédemption, est extrêmement important pour comprendre le schéma de la déglaciation régionale. La masse principale présente une accumulation limitée par des côtés arqués et abrupts tant à l'ouest qu'à l'est: les concavités peuvent s'expliquer par une présence de glace sans doute puissante et active (?) de part et d'autre. Le complexe est situé sur la

Figure 3 (ci-contre). Diagramme des stries (classe de 5°) et mouvements glaciaires reconnus (1 et 2, ordre chronologique).

Figure 4 (ci-dessous). Les complexes fluvio-glaciaires principaux du val de la Matapédia. Géologie: voir figure 2. Photographies aériennes à 1/15 840 n^o: Q63316 – n°s 88 à 99; Q63324 – n°s 193 à 200; Q63314, n°s 108 à 110. (Photocartothèque de la province de Québec.) Les flèches doubles indiquent le sens d'écoulement des lobes après leur individualisation.

pente nord des monts Notre-Dame: il constitue probablement un complexe interlobaire. La glace encore active s'écoulant de l'ouest-sud-ouest et du nord-est, a érodé le massif de serpentinite-diorite localisé partiellement sous les dépôts: le pourcentage de galets de cette roche atteint 12% dans la gravière exploitée; cette concentration constitue une anomalie à l'échelle régionale. Une autre concentration de serpentinite (11% dans les graviers) est identifiée dans un till à 2 km au nord du massif. En fait, il est raisonnable de penser que cette roche fortement diaclasée a formé un talus d'éboulis dispersé par les petits torrents locaux avant la glaciation.

Le complexe se poursuit par une série de crêtes morainiques étagées parallèlement sur la pente, vers le nord-ouest: celles-ci marquent autant de position de recul du front glaciaire.

b) À 5 km au nord-est de La Rédemption débute un autre complexe fluvio-glaciaire dont les quatre moraines frontales n'ont été percées que tout récemment pour rectifier la route qui les contournait précédemment (Prichonnet, 1984, pl. I, 9). Ce complexe frontal (Lebuis et David, 1977) est très puissant et il se poursuit par des accumulations disposées également en crêtes parallèles sur les pentes des monts Notre-Dame.

c) Un troisième complexe important offre une disposition comparable, au sud-est de St-Cléophas, traduisant encore une fois un recul glaciaire dans le sens de la pente (fig. 4).

d) "L'esker" des lacs Awantjish. Ce "cordon" se poursuit sur près de 10 km en direction est-nord-est: Lebuis et David (1977) le considèrent comme un esker. Considérant les crêtes arquées et parallèles qui le jouxtent, côté amont et côté aval, il semble qu'il s'agisse plutôt d'une crevasse tardive qui a isolé le lobe résiduel glaciaire piégé dans l'axe du val. Ce cordon fluvio-glaciaire constituerait une sorte de moraine latérale, l'extension des dépôts étant limitée au nord par le glacier et au sud par les eaux de fonte et de ruissellement au pied des pentes.

Quelques contrôles sur le sens d'écoulement des eaux fluvio-glaciaires montrent un écoulement vers l'ouest-sud-ouest selon le gradient actuel du réseau fluviatile (fig. 4).

En conclusion, sur ce modèle de retrait glaciaire, on peut ajouter que la zone de séparation entre les deux lobes de glace qui ont occupé la partie nord-est du val (celui qui est évident) et la partie sud-ouest du val (celui qui a laissé moins de preuves) a été commandée par une série de reliefs disposés autour de la ligne de partage des eaux et par cette ondulation même. Les quelques indications d'écoulements vers le nord-est trouvées au nord-ouest de La Rédemption (fig. 2) s'expliqueraient bien par la présence d'un glacier épais et actif localisé dans la dépression de la rivière Mitis.

Une telle disposition du front de l'inlandsis s'harmoniserait avec les fronts et les écoulements des eaux fluvio-glaciaires identifiés dans la vallée de la rivière Mitis, plus au nord-ouest (fig. 2).

La dispersion des galets erratiques indicateurs

L'étude des pétrographies du till ou des dépôts fluvio-glaciaires a été effectuée sur 110 sites environ. Le choix du plus grand nombre est lié aux cibles choisies pour l'étude géochimique du till, soit dans les zones siluro-dévoniennes présentant des "roches-marqueurs" (serpentinite et formation de Val-Brillant), et au delà des monts Notre-Dame pour l'étude de la traînée vers le sud-est. Vers l'ouest, des aménagements routiers importants ont permis un bon accès à la nappe de till régionale. Enfin, vers le nord, les affleurements étant rares, quelques creusages à la pelle

mécanique avaient pour but de reconnaître les éléments métalliques caractérisant le till reposant sur les roches cambro-ordoviciennes.

Les figures 5, 6 et 7 présentent les pourcentages de trois types de roches. Compte tenu de l'état préliminaire de cette approche, ce sont des observations et conclusions le plus souvent qualitatives qui seront présentées. Elles sont toutefois basées sur le comptage de plus de 8000 galets (de 5 à 25 cm) et plus de 21,000 graviers et cailloux (de 0,4 à 5 cm environ).

Dispersion des ardoises rouges (fig. 5)

Cette roche-marqueur a été choisie empiriquement après avoir constaté que certaines bandes formaient de larges affleurements et que leur identification permettait un contrôle efficace et rapide.

Quelques conclusions générales découlent de l'analyse des pourcentages relevés tant dans la fraction grossière que dans la fraction fine:

1. les pourcentages d'ardoises rouges sont systématiquement élevés du côté sud-est des affleurements reconnus; cette approche sera approfondie;

2. cette roche fragile a tendance à s'effriter rapidement lors du transport glaciaire et son pourcentage diminue très vite vers le sud-est au delà des derniers affleurements reconnus;

3. une traînée faible mais relativement constante est identifiée jusqu'à la vallée de la rivière Humqui, traduisant un transport vers le "sud" certain, au delà de la barrière naturelle des monts Notre-Dame.

Dispersion des roches précambriennes (fig. 6)

La distribution dans 17 sites de ces débris demande une certaine prudence dans l'interprétation: il y a beaucoup plus de sites où ces roches sont absentes que de sites où elles sont présentes. Par ailleurs, les petits débris sont extrêmement rares. On constate néanmoins que les quelques valeurs relativement élevées dans les pourcentages de galets de till et de dépôts fluvio-glaciaires montrent une décroissance de type exponentielle depuis la zone nord vers le sud: la courbe de concentration de 4% passerait au nord du synclinal de la Matapédia, et celle de 2% se situerait sur le bassin versant de la rivière Humqui. Rappelons que le lac Humqui est à environ 100 km de la côte nord du Saint-Laurent (où affleurent les roches grenvilliennes), selon une direction NNW-SSE.

Cette distribution vers le sud-sud-est confirme la précédente, et appuie l'interprétation des marques d'érosion glaciaire (fig. 2 et 3). On peut également affirmer que les formes fuselées doivent avoir été façonnées par le même écoulement puisqu'elles sont parallèles à cette direction.

Dispersion des grès quartzitiques type Val-Brillant (fig. 7)

À cause des possibilités d'erreur d'identification des grès quartzitiques blancs affleurant au nord du synclinal de la Matapédia, tous les pourcentages situés sur le Cambro-Ordovicien seront réexaminés. Notons toutefois que le transport de galets et cailloux vers le nord de la zone d'affleurement du Val-Brillant ne devrait pas être un indice suffisant pour évoquer un transport glaciaire dans la même direction: les rivières appalachiennes sont très encaissées et elles ont pu transporter ces grès très résistants au cours de leur longue histoire; ces galets ont pu être repris par le mouvement sud-sud-est à partir de dépôts fluviatiles (ou encore à partir d'anciens dépôts glaciaires ?).

Figure 5. *La dispersion glaciaire des ardoises rouges, du Cambro-Ordovicien régional. Voir figure 2.*

Figure 6. *La dispersion glaciaire des roches précambriennes de la côte nord du Saint-Laurent. Voir figure 2.*

Figure 7. *La dispersion glaciaire des grès-quartzitiques de type formation de Val-Brillant. Voir figure 2.*

La distribution des mêmes "grès" dans et au sud du synclinal de la Matapédia nous paraît toutefois qualitativement significative. À l'exception d'un pourcentage anormal (80%) lié probablement à la destruction de l'affleurement par la pelle mécanique lors du creusage (3 km au sud-ouest de Sayabec – fig. 7), les concentrations observées sont faibles près du contact puis augmentent en direction sud-sud-est avant de diminuer à nouveau vers le sud-sud-est. De plus, vers la terminaison périclinale nord-est, les écoulements tant vers le sud-sud-est que vers le nord-ouest (fig. 3) ont pu concentrer les débris de cette roche mais sur de faibles distances. Enfin, la traînée de ces mêmes débris, dans les tills, au-delà des monts Notre-Dame, représente une persistance normale de cette roche dure (mais aux surfaces d'affleurement restreintes) dans le contexte régional; les concentrations de gros débris dans les dépôts fluvio-glaciaires de la vallée Humqui peuvent s'expliquer par une usure et une fragmentation moindre lors du transport fluvio-glaciaire; la pente naturelle a pu faciliter leur concentration dans la vallée.

La distribution des grès quartzitiques ne contredit pas les conclusions basées sur les autres approches; elle devra être précisée, en particulier par des comptages des gros débris (non effectués encore) dans ce que nous identifions comme la traînée sud-sud-est au-delà des monts Notre-Dame.

Conclusions

Une seule nappe de till a été identifiée dans l'ensemble de la région, mais plusieurs sous-faciès sont présents: en particulier, on a noté des diamictons plus lâches, dans les zones accidentées, qui correspondent, semble-t-il, aux faciès délavés accompagnant la déglaciation – ou la phase glaciaire tardive – en milieu montagneux, avec circulation plus abondante d'eau de fonte (faciès d'ablation). La nappe de till de fond aurait été mise en place lors du mouvement glaciaire vers le sud-sud-est, au pléniglaciaire: l'inlandsis provenait alors des Laurentides.

Le deuxième mouvement glaciaire de quelque importance correspondrait à l'isolement de masses de glace localisées sur les Appalaches, ici dans la dépression de la Matapédia, et assez épaisses pour amorcer un écoulement radial chenalisé par le val de la Matapédia vers le sud-ouest et l'ouest, et vers la rivière Tartigou en direction nord-ouest. Cet écoulement de courte durée n'aurait pas obligatoirement eu d'effet important sur la couverture de till; par contre, le lobe glaciaire aurait concentré ses effets au nord des monts Notre-Dame et l'essentiel de la charge glaciaire se serait manifestée sous la forme de dépôts fluvio-glaciaires de contact, particulièrement sur les pentes nord des monts Notre-Dame. Des glaciers de cirque ont persisté quelque temps sur ce versant nord, plus froid, de la chaîne (cf. les cirques des Chics-Chocs de Lebuis et David, 1977; Desmarais, en préparation).

En même temps que le lobe de la Matapédia s'individualisait, le front de l'inlandsis reculait vers le nord-nord-ouest, accumulant des dépôts de contact fluvio-glaciaires dans la basse vallée de la Mitis. Ce double retrait vers la baie des Chaleurs (Lebuis et David, 1977) et vers le Saint-Laurent, a pu faciliter le piégeage de lacs proglaciaires dans la dépression du lac Matapédia actuel, et dans la vallée de la Mitis où des talus d'érosion littorale ont été notés jusqu'à une altitude de 220 m.

Ce modèle permet d'expliquer la plupart des observations de terrain réalisées à ce jour.

On sait que des débris minéralisés ont été décelés dans un train de dispersion et leur source identifiée grâce à l'étude du transport glaciaire, plus à l'est en Gaspésie (Chauvin, 1984). Pour la région considérée ici de nombreux

indices de cuivre sont signalés dans la séquence cambro-ordovicienne (Aubert de la Rue, 1941). Les problèmes de transport glaciaire dans la zone d'étude sont donc intéressants du point de vue prospection minérale puisque plusieurs mouvements glaciaires successifs peuvent avoir transporté des blocs minéralisés ou des farines glaciaires chargées de métaux de base (étude en cours) dans des directions contradictoires: selon les hypothèses retenues (Lebuis et David, 1977; présente étude) 2 à 3 mouvements glaciaires d'importance variable ont affecté ce secteur des Appalaches. La prochaine étape de cette recherche s'attachera donc à préciser les faits et hypothèses proposés ici: les résultats seront testés grâce à quelques problèmes locaux (les minéralisations mentionnées ci-dessus et quelques anomalies géochimiques identifiées).

Bibliographie

Alcock, F.J.
  1944: "Further information on glaciation in Gaspé"; Trans. Royal Soc. Canada, series III, vol. 38, sec. IV, p. 15-21.

Aubert de la Rue, E.
  1941: "Région du lac Matapédia". Partie des comtés de Matane, Matapédia, Rimouski; Min. Mines Qué., Rapp. Géol. 9, 47 p., carte.

Béland, J.
  1960: "Rapport préliminaire sur la région de Rimouski, Matapédia, Bonaventure et Matane"; Min. Mines Qué., Rapp. prél. 430, carte no. 1342, 20 p.

Chalmers, R.
  1906: "Surface geology of eastern Quebec"; Geol. Surv. Can., Ann. Rep. (1904), part A, p. 250A-263A.

Chauvin, L.
  1984: "Géologie du Quaternaire et dispersion glaciaire en Gaspésie, Région de Mont-Louis-Rivière Madeleine"; MERQ. Et. 83-19, 60 p.

Coleman, A.P.
  1925: Physiographie et géologie glaciaire de la Péninsule de Gaspé, Québec; Commission géologique du Canada, Bulletin no. 34, série no. 41, 54 p.

David, P.P. et Lebuis, J.
  1985: Glacial maximum and deglaciation of Western Gaspé; Québec, Canada, Geol. Soc. of Am. Sp. Paper 197, p. 85-109.

Dionne, J.C.
  1977: La mer de Goldthwait au Québec; Géogr. phys. et Quat., Vol. XXXI, nos. 1-2, p. 61-80.

Flint, R.F., Demorest, M., and Washburn, A.L.
  1942: "Glaciation of Shickshock Mountains, Gaspé Peninsula"; Bull. of Geol. Soc. of America, Vol. 53, p. 1211-1230.

Lebuis, J. et David, P.P.
  1977: La stratigraphie et les évènements du Quaternaire de la partie occidentale de la Gaspésie, Québec; Géogr. phys. et Quat., Vol. XXXI, nos. 3-4, p. 275-296.

Liard, Ph.
  1972: "Géologie de la région de Mont-Joli-Matane. Comtés de Matane, Matapédia et Rimouski"; Min. Rich. Nat. Québec, Dir. Gén. Mines, D.P. 202, cartes, 7 p.

Locat, J.
  1977: L'émersion des terres dans la région de Baie-des-Sables/Trois-Pistoles; Géogr. phys. et Quat., Vol. XXXI, nos. 3-4, p. 297-306.

  1978: Le Quaternaire de la région de Baie-des-Sables/Trois-Pistoles; Ministère de l'Énergie et des Ressources du Québec, DPV. 605, 64 p.

Martineau, G.
  1980: Dépôts meubles de la région de Rimouski-Trois-Pistoles; Ministère de l'Énergie et des Ressources, Direction Générale de la Recherche Géologique et Minérale, Rapport préliminaire, DPV-717, 10 p.

McGerrigle, H.W.
  1952: "Pleistocene glaciation of Gaspe Peninsula"; Trans. Royal Soc. Canada, Vol. 46, series III, sec. IV, p. 37-51.

Poole, W.H. et Rodgers, J.
  1972: Appalachian geotectonic elements of the Atlantic Provinces and Southern Québec. congrès géologique international (21e) D.J. Glass, ed. Excursion A63-C63, 200 p.

Prichonnet, G.
  1984: Glaciations d'inlandsis: séquences glaciaires, proglaciaires et non glaciaires du Quaternaire de l'Est Canadien; Bull. Centres de Recherche et d'Exploration-Production. Elf Aquitaine, 8 (1), p. 105-133.

Anthophyllite-bearing rocks in the Flin Flon-Sherridon area, Manitoba[1]

Project 800007

E. Froese
Precambrian Geology Division

Abstract

In the Flin Flon-Sherridon area, anthophyllite-bearing rocks occur in mafic and felsic volcanic rocks of the Amisk Group and in quartz-rich gneisses of the Sherridon Group. These rocks probably indicate chlorite-rich precursors developed as in situ alteration zones in volcanic rocks and as sedimented altered material in the Sherridon Group. Alteration zones in volcanic rocks are commonly associated with sulphide mineralization, whereas many stratiform lenses of cordierite-anthophyllite rocks in the Sherridon Group occur far removed from sulphide deposits.

Résumé

Dans la région de Flin Flon et Sherridon, les roches contenant de l'anthophyllite se manifestent dans des roches volcaniques de nature mafique et felsique du groupe d'Amisk, et dans les gneiss riches en quartz du groupe de Sherridon. Ces roches indiquent probablement que les roches antérieures étaient riches en chlorite et qu'elles se sont formées sous forme de zones d'altération in situ dans des roches volcaniques et sous forme de matériaux altérés sédimentés dans le groupe de Sherridon. Les zones d'altération dans les roches volcaniques sont habituellement associées à la minéralisation en sulfures tandis que les nombreuses lentilles stratiformes de roches de cordiérite et antophyllite du groupe de Sherridon se trouvent à une très grande distance des dépôts de sulfure.

Figure 1. Regional geology of the Flin Flon–Sherridon area and location of anthophyllite-bearing rocks.

LEGEND

Granitic intrusions

Undifferentiated Kisseynew gneisses

Granitoid gneisses

Missi Group, Sherridon Group

Amisk sedimentary rocks, Nokomis Group

Amisk volcanic rocks

Anthophyllite-bearing rocks

★ In quartz-rich gneisses, Sherridon Group

■ In felsic volcanic rocks, Amisk Group

▶ In mafic volcanic rocks, Amisk Group

Km

0   5   10   15   20

A great deal of interest in anthophyllite-bearing rocks stems from the possibility that they could be formed by the metamorphism of chlorite-rich, hydrothermally altered rocks. As part of a study of metamorphosed alteration zones, several occurrences in the Fin Flon-Sherridon area were visited in 1984 in order to collect samples and gain a better understanding of their geological setting. In this area, anthophyllite-bearing rocks occur in three distinct lithological associations, as shown in Figure 1.

The geological sketch map (Fig. 1) is based mainly on the compilation by Bailes (1971) and on reports by Byers and Dahlstrom (1954) and Byers et al. (1965). More recent work in the area (Tuckwell, 1979; McRitchie, 1980; Froese and Gall, 1981; James, 1983; Zwanzig, 1983, 1984; Froese, 1984) and observations in 1984 led to some modifications. The Kisseynew gneisses are thought to be the metamorphosed equivalents of Amisk volcanic and sedimentary rocks and Missi sedimentary rocks. Many amphibolites within the Kisseynew gneisses, e.g. the layers at Tyrrell Lake and to the north, probably are metamorphosed Amisk volcanic rocks. The Kisseynew gneisses have been subdivided into the Nokomis and Sherridon groups (Robertson, 1953) and these have been correlated, respectively, with greywacke-shale of the Amisk Group and lithic arenite of the Missi Group (Bailes, 1971). A layer of Missi or Sherridon quartz-rich gneiss between Tyrrell Lake and Kisseynew Lake was erroneously mapped as granite by Byers and Dahlstrom (1954) and Byers et al. (1965).

Cordierite-anthophyllite rocks occur as an alteration zone in mafic volcanic rocks below the Coronation orebody, southwest of Flin Flon (Froese, 1969; Whitmore, 1969). At Vass Lake, north of Tyrrell Lake, anthophyllite has been reported from a quartz-garnet gneiss associated with sulphide mineralization in hornblende-garnet gneiss (Byers and Dahlstrom, 1954), which probably is a metamorphosed mafic volcanic rock.

Anthophyllite-bearing rocks, accompanied by small amounts of staurolite and cordierite, occur as irregular lenses and masses in felsic volcanic rocks east of Weldon Bay (Froese and Gall, 1981; Froese, 1984). There are some subeconomic sulphide deposits in the vicinity; however, the anthophyllite-bearing rocks are nearly free of sulphides.

In the Sherridon area, cordierite-anthophyllite rocks occur as stratiform lenses in quartz-rich gneisses of the Sherridon Group (Robertson, 1953; Froese and Goetz, 1981; Goetz and Froese, 1982). These rocks are present along the same stratigraphic horizon as stratiform massive sulphide deposits; however, many occurrences appear to be unrelated to sulphide mineralization. Garnet-anthophyllite rocks are associated with sulphide mineralization in Sherridon gneisses west of Sherridon and near the centre of Kississing Lake (Gale, 1980).

The unusual composition of cordierite-anthophyllite rocks led Eskola (1914) to account for their origin by high-temperature iron-magnesium metasomatism. However, Tilley and Flett (1930) suggested the possibility of pre-metamorphic, low-temperature alteration in view of the chemical similarity of cordierite-anthophyllite rocks and mixtures of chlorite and aluminous minerals. Many anthophyllite-bearing rocks do not contain cordierite, presumably reflecting a smaller proportion of aluminum minerals. In the search for chloritic precursors of anthophyllite-bearing rocks, two main processes of chloritization have been considered: hydrothermal alteration related to mineralization (Iwao, 1955; Koark, 1962; de Rosen-Spence, 1969; Froese, 1969; Whitmore, 1969) and chloritization as part of the complex alteration leading to the formation of spilites (Vallance, 1967, 1969). The essential requirement for spilitization, the interaction of rock and water, is realized in the sub-seafloor environment (Spooner and Fyfe, 1973). In addition to in situ chloritization, it has been suggested that chloritic rocks could be transported and sedimented as stratiform bodies (MacLean and MacGeehan, 1976; MacGeehan, 1978; Schermerhorn, 1978; Bernard et al., 1982). Warren (1979) applied the term distal to stratiform chlorite-rich rocks.

The cordierite-anthophyllite rocks in mafic and felsic volcanic rocks of the Amisk Group reflect in situ alteration; rocks displaying varying degrees of alteration, as well as nearly unaltered remnants, can be observed. In contrast, the cordierite-anthophyllite lenses in quartz-rich gneisses of the Sherridon Group have a uniform texture and composition and exhibit sharp contacts with adjacent rocks. It is more likely that these rocks represent transported and sedimented altered material, although the source remains unknown.

References

Bailes, A.H.
1971: Preliminary compilation of the geology of the Snow Lake-Flin Flon-Sherridon area; Manitoba Mines Branch, Geological Paper 1/71.

Bernard, A.J., Degallier, G., and Soler, E.
1982: The exhalative sediments linked to the volcanic exhalative massive sulphide deposits: a case study of European occurrences; in Ore Genesis: The State of the Art, ed. G.C. Amstutz et al.; Springer-Varlag, New York, p. 553-564.

Byers, A.R. and Dahlstrom, C.D.A.
1954: Geology and mineral deposits of the Amisk-Wildnest lakes area, Saskatchewan; Saskatchewan Department of Mineral Resources, Report 14.

Byers, A.R., Kirkland, S.J.T., and Pearson, W.J.
1965: Geology and mineral deposits of the Flin Flon area, Saskatchewan; Saskatchewan Department of Mineral Resources, Report 62.

Eskola, P.
1914: On the petrology of the Orijärvi region in south-western Finland; Bulletin de la Commission Géologique de Finlande, no. 40.

Froese, E.
1969: Metamorphic rocks of the Coronation mine and surrounding area; Geological Survey of Canada, Paper 68-5, p. 55-77.

1984: Geology of the Weldon Bay – Fay Lake area, Manitoba; in Current Research, Part B, Geological Survey of Canada, Paper 84-1B, p. 355-358.

Froese, E. and Gall, Q.
1981: Geology of the eastern vicinity of Kisseynew Lake, Manitoba; in Current Research, Part A, Geological Survey of Canada, Paper 81-1A, p. 311-313.

Froese, E. and Goetz, P.A.
1981: Geology of the Sherridon Group in the vicinity of Sherridon, Manitoba; Geological Survey of Canada, Paper 80-21.

Gale, G.H.
1980: Mineral deposit studies – Flin Flon/Kisseynew; Manitoba Mineral Resources Division, Report of Field Activities 1980, p. 51-64.

Goetz, P.A. and Froese, E.
1982: The Sherritt Gordon massive sulphide deposit; Geological Association of Canada, Special Paper 25, p. 557-569.

Iwao, S.
1955: Mg-enrichment around some ore-deposits in Japan – particularly with reference to hydrothermal gypsum and silica deposits; Geological Society of Japan, Journal, v. 61, p. 543-555 (in Japanese).

James, D.T.
1983: Origin and metamorphism of the Kisseynew gneisses, Kisseynew Lake – Cacholotte Lake area, Manitoba; unpublished M.Sc. thesis, Carleton University, Ottawa.

Koark, H.J.
1962: Zur Altersstellung und Entstehung der Sulfiderze vom Typus Falun; Geologische Rundschau, v. 52, p. 123-146.

MacGeehan, P.J.
1978: The geochemistry of altered volcanic rocks at Metagami, Quebec: a geothermal model for massive sulphide genesis; Canadian Journal of Earth Sciences, v. 15, p. 551-570.

MacLean, W.H. and MacGeehan, P.J.
1976: Garon Lake mine, Matagami, Quebec; Mineral Exploration Research Institute, Department of Geological Sciences, McGill University, Montreal, Case History 76-1.

McRitchie, W.D.
1980: Cacholotte Lake (parts of 63K/13, 14 and 63N/3, 4); Manitoba Mineral Resources Division, Report of Field Activities 1980, p. 65-69.

Robertson, D.S.
1953: Batty Lake map-area, Manitoba; Geological Survey of Canada, Memoir 271.

Rosen-Spence, A. de
1969: Genèse des roches à cordiérite-anthophyllite des gisements cupro-zincifères de la région de Rouyn-Noranda, Québec, Canada; Canadian Journal of Earth Sciences, v. 6, p. 1339-1345.

Schermerhorn, L.J.G.
1978: Epigenetic magnesium metasomatism or syngenetic chloritite metamorphism at Falun and Orijärvi; Institution of Mining and Metallurgy, Transactions, section B, v. 87, p. 162-167.

Spooner, E.T.C. and Fyfe, W.S.
1973: Sub-seafloor metamorphism, heat and mass transfer; Contributions to Mineralogy and Petrology, v. 42, p. 287-304.

Tilley, C.E. and Flett, J.S.
1930: Hornfelses from Kenidjack, Cornwall; Geological Survey of Great Britain, summary of progress for the year 1929, part II, p. 24-41.

Tuckwell, K.
1979: Stratigraphy and mineral deposits of the Sherridon area; Manitoba Mineral Resources Division, Report of Field Activities 1979, p. 42-45.

Vallance, T.G.
1967: Mafic rock alteration and isochemical development of some cordierite-anthophyllite rocks; Journal of Petrology, v. 8, p. 84-96.

1969: Spilites again: some consequences of the degradation of basalts; Linnean Society of New South Wales, Proceedings, v. 94, p. 8-51.

Warren, R.G.
1979: Sapphirine-bearing rocks with sedimentary and volcanogenic protoliths from the Arunta Block; Nature, v. 278, p. 159-161.

Whitmore, D.R.E.
1969: Geology of the Coronation copper deposit; Geological Survey of Canada, Paper 68-5, p. 37-53.

Zwanzig, H.V.
1983: Kisseynew project: Lobstick Narrows (parts of 63K/13, 14 and 63N/3, 4); Manitoba Mineral Resources Division, Report of Field Activities 1983, p. 15-22.

1984: Kisseynew project: Lobstick Narrows – Cleunion Lake, Puffy Lake and Nokomis Lake areas; Manitoba Mineral Resources Division, Report of Field Activities 1984, p. 38-45.

CANADA-NEWFOUNDLAND MINERAL DEVELOPMENT AGREEMENT 1884-89

ENTENTE DE MISE EN VALEUR DES MINÉRAUX CANADA-TERRE-NEUVE

Contents/Table des matières

GEOLOGY OF THE PARADISE RIVER REGION, GRENVILLE PROVINCE, EASTERN LABRADOR

Project J.1.9.2.

by

Charles F. Gower, Nathaniel Noel and Timothy Van Nostrand

ABSTRACT

The Paradise River region is located in the Lake Melville terrane of the Grenville Province, eastern Labrador. Four major lithological associations were mapped, namely (i) orthogneiss, (ii) metasedimentary gneiss, (iii) anorthositic-gabbroic-monzonitic rocks, (iv) granitoid plutons. Orthogneiss is found in discrete belts that flank, or occur within granitoid plutons, and above thrusts. It is, at least in part, the tectonized equivalent of the granitoid plutons. Metasedimentary gneiss is dominated by biotite-sillimanite-garnet bearing pelites, but psammitic gneiss, quartzite and calc-silicate rocks are locally present. Most anorthositic-gabbroic-monzonitic rocks are grouped as the White Bear Arm complex, which shows well preserved primary fabrics in its interior but has a highly tectonized, thrust-bound margin. A sheet of recrystallized anorthosite also occurs in the southwest quadrant of the study area. The granitoid plutons are divided into two groups, namely (i) diorite, monzonite and granodiorite belonging to the Earl Island domain (of the Groswater Bay Terrane), (ii) an intergradational plutonic package of megacrystic and non-megacrystic granodiorite, monzonite, granite and alkali-feldspar granite mostly in the Lake Melville terrane. In addition to these lithological associations, other rocks mapped include mafic intrusions of various ages, including Lower Phanerozoic north-northeast trending mafic dikes.

The regional structure is controlled by two major northwest trending zones of ductile deformation, and the thrust-bounded White Bear Arm complex. The departure of structures in the central and northwest parts of the region from the regional northwest trend is attributed to the collective effects of the strike dip and thrust faults. This interpretation is extended to a regional structural synthesis of the Lake Melville terrane. Faulting related to the newly recognized Sandwich Bay graben has little effect on earlier structural patterns.

Prospects for economic mineralization appear to be confined to sulfide-rich zones in metasedimentary gneiss, radioactive granitoid rocks and mica-rich pegmatite.

INTRODUCTION

A major 1:100,000 scale reconnaissance mapping program in the Grenville Province of eastern Labrador commenced in 1979 in the Makkovik Province and adjacent northern fringe of the Grenville Province and between 1979-1984 regional mapping coverage has gradually advanced southward. Mapping in the Paradise River region in 1984 (outlined in Figure 1), represents an extension of that coverage, and at the same time the start of a new 5-year Canada-Newfoundland joint project that will complete 1:100,000 scale geological mapping of an 80 km wide coastal fringe of the Grenville Province in eastern Labrador.

The Paradise River region comprises four NTS 1:50,000 sheets (13H/3,4,5,6) which encompass an area of approximately 3700 km^2. The only previously published geological map which includes the whole of the map area is that of Eade (1962) at 1:500,000 scale. Eade showed the area to be underlain mainly by granitic gneiss, lesser metasedimentary gneiss, granite to granodiorite plutons, and gabbroic to anorthositic intrusions. More recently, much of the northern part of the area was re-examined by Cherry (1978a,b). Cherry depicted the area as largely underlain by schlieric migmatite gneiss with the distribution of metasedimentary gneiss essentially unchanged from Eade's map.

Mineral exploration has been carried out intermittently by BRINEX Ltd. Initial geological mapping and mineral potential evaluation was carried out in 1954 by (Piloski, 1955) who recommended the area as favourable for U, Cu, Ni and Au mineralization. Airborne magnetic and electromagnetic surveys were flown in 1959 (Wilson, 1959) and a combined geological, lake sediment geochemical, ground electromagnetic and prospecting program was undertaken in 1965. Results are summarized in a report by Sutton (1965) with appendices by Juilland (geology), Meyer (geochemistry), Staub (ground geophysics), and Cote and Anderson (laboratory methods). Active interest by Brinex ceased after further reconnaissance geological mapping by Kranck (1966) although the Ni potential of the region was subsequently reviewed for BRINEX by Westoll (1971).

The present mapping, benefit from complete aeromagnetic map coverage (Geological Survey of Canada, 1974a,b,c,d,e) and mapping experience gained in similar rocks farther north (Gower et al., 1981, 1983a,c; Owen et al., 1983). Mapping has resulted in considerable refinement of rock type distribution and protolith identification, and has permitted an initial attempt at regional structural synthesis of the Lake Melville terrane.

REGIONAL SETTING

The study area is situated entirely within the Grenville Province and, except for the northeast corner, is an extension of the Lake Melville terrane (Gower, 1984; Gower and Owen, 1984). The northeast corner of the map area, a lithologically distinct part of the Groswater Bay terrane, is informally referred to in this paper as the Earl Island domain. The location of the study area and major (litho) tectonic subdivisions recognized in the Grenville Province of Labrador are shown in Figure 1. Ornamentation in Figure 1 is intended to depict lithotectonically correlative regions, although names of (litho) tectonic subdivisions are those used locally. Further reference is made to these areas with respect to structural synthesis.

Figure 1: *Major structural features of the Grenville Province, Labrador. Distribution and names of allochthons in central and western Labrador are from Ryan et al. (1982), Rivers and Nunn (in press) and Thomas et al. (in press). Location of paradise River region outlined.*

DESCRIPTION OF ROCK UNITS

Orthogneiss

All rocks mapped as orthogneiss are located in the western half of the study area and occur as narrow belts less than 4 km wide. These are marginal to other rock types, especially granitoid plutons, or to

major structures such as thrusts. In Figure 2 the orthogneisses have been subdivided into three units but all have, in part, a well-banded, migmatic aspect. The units are entirely intergradational, hence no boundaries are drawn on the map. Undoubtedly, in detail, the interfingering of the various orthogneiss types is more complex than shown but even where outcrop permits we do not believe that more detailed mapping will significantly change the regional distribution patterns depicted. These rocks are not necessarily the oldest in the area, as will become clear in the ensuing description.

The biotite hornblende granodiorite-diorite-amphibolite unit is characterized by ubiquitous hornblende. The amphibolites are amphibole-plagioclase±pyroxene rocks with local orthopyroxene bearing leucosome patches (Plate 1). They have a strongly foliated, lensy to well-banded appearance. The most extensive amphibolitic gneiss occurs marginal to a thrust northeast of Crooked Lake (Figure 2). The gabbroid rocks on the hanging wall of the thrust are amphibolite in part and it is quite probable that the underlying amphibolitic gneiss simply represents similar rocks which have experienced more intense strain and migmatization in a series of structurally lower thrust slices. Amphibolitic gneiss elsewhere is mostly restricted to single outcrop; rarely seen local discordance to an earlier fabric demonstrates that these gneisses are highly deformed mafic dikes.

The dioritic and hornblende-bearing granodiorite gneisses are medium grained, migmatitic, variably banded rocks. Northeast of Crooked Lake, these gneisses separate the amphibolites and quartzofeldspathic gneisses and are interpreted to result from the thorough interleaving and migmatization of the amphibolitic and quartzofeldspathic protoliths. Elsewhere, these gneisses occur in areas commonly less than a few km² and are interpreted as small deformed plutons or tectonized margins of larger hornblende-bearing intrusions.

Biotite granodiorite gneiss is the most extensive orthogneiss rock type. It is a creamy weathering, medium grained, weakly to well-banded rock, locally with common amphibolite lenses and crosscut by discordant minor granitic intrusions. Garnet occurs sporadically. The unit also includes minor tonalite, quartz diorite and quartz monzondiorite gneiss.

Biotite granite gneiss occurs as a pink to red weathering, fine to medium grained gneiss, locally with biotitic schlieren or amphibolite layers, which occurs principally in the central part of the map area. The unit is probably derived from minor

LEGEND

SYMBOLS

PHANEROZOIC

⬛ GABBRO, DIORITE DIKES

HELIKIAN OR OLDER

🔲 UNASSIGNED METAGABBRO, AMPHIBOLITE, MAFIC GRANULITE

GRANITOID PLUTONS

🔲 GRANITE, ALKALI FELDSPAR GRANITE

🔲 K-FELDSPAR MEGACRYSTIC GRANITOID ROCKS

🔲 BIOT. GRANODIORITE TO GRANITE

🔲 HBL. DIORITE TO GRANODIORITE

🔲 BIOT. HBL. MONZODIORITE TO GRANODIORITE

🔲 BIOT. HBL. DIORITE TO QUARTZ DIORITE

UNASSIGNED ANORTHOSITIC ROCKS

🔲 ANORTHOSITE, LEUCOGABBRO AND METAMORPHIC DERIVATIVES

HELIKIAN OR OLDER (CONTINUED)

WHITE BEAR ARM COMPLEX

🔲 FINE GRAINED GRANULITE, LEUCONORITE

🔲 MONZODIORITE, MONZONITE, QUARTZ SYENITE, GRANITE

🔲 GABBRO, TROCTOLITE, COMMONLY CORONITIC AND LAYERED

🔲 ANORTHOSITE, LEUCOGABBRO

METASEDIMENTARY GNEISS

🔲 PELITIC AND PSAMMITIC METASEDIMENTARY GNEISS, MINOR CALC-SILICATE ROCK

🔲 QUARTZITE

ORTHOGNEISS

🔲 BIOT. GRANITE GNEISS

🔲 BIOT. GRANODIORITE GNEISS

🔲 BIOT. HBL. GRANODIORITE-DIORITE AMPHIBOLITE GNEISS

GEOLOGICAL BOUNDARY; APPROXIMATE, DIFFUSE ....

NORMAL FAULT ....

THRUST ....

UNDIFFERENTIATED FAULTS, PROBABLY STRIKE SLIP ....

ANTIFORM ....

SYNFORM ....

GNEISSOSITY, FOLIATION ....

PYRITE .... py

ANOMALOUS RADIOACTIVITY .... U

MICA .... ml

0   4   8   12   16
kilometres

Figure 2: *Geology of the Paradise River region.*

Plate 1: *Orthopyroxene in quartzofelds-pathic leucosome patches in amphibolite associated with orthogneiss.*

granitoid intrusions or, less likely, arkosic metasediments.

Metasedimentary Gneiss

Metasedimentary gneiss occurs in three major linear zones in the northeast, central and southwest parts of the map area. All are dominated by sillimanite-garnet-biotite pelitic and semi-pelitic gneiss, but psammitic gneiss, diatexite, quartzite, and, rarely calc-silicate rocks and mafic supracrustal rocks are present. Pelitic gneiss is characteristically rusty, creamy or gray weathering, medium grained and well-banded. It is migmatitic with a restite comprising fibrous or prismatic sillimanite, mauve garnet, biotite, graphite and magnetite and leucosome pods or fine laminations of quartz + plagioclase + K-feldspar (Plate 2). Muscovite, probably retrograde is locally present in the pelitic gneiss (especially north of the community of Paradise River) and may also be found in late discordant pegmatites within the paragneiss. White weathering diatexite with abundant garnet is particularly common in the southwest metasedimentary gneiss belt and is interpreted as a partial melt product from the pelitic gneiss. The psammitic gneisses are closely

associated with the pelitic gneiss, differing mainly in having a slightly coarser grained, more sugary appearance and lacking sillimanite. Garnet is typically wine colored rather than the distinctive mauve as in the pelites.

Plate 2: *Sillimanite bearing metasedimentary gneiss showing tight folding and transposition of fold limbs.*

Quartzite is a major rock type in the central metasedimentary gneiss belt east of Crooked Lake (Figure 2). It was first reported by Piloski (1955) and subsequently mentioned by Eade (1962), Kranck (1966) and Cherry (1978a,b). Only Kranck made any attempt to show its distribution. The band shown on Figure 2 east of the south end of Crooked Lake corresponds to one of his mapped quartzite units. It occurs in white weathering, massive to thickly bedded layers interbanded with psammitic and pelitic gneiss. Although much of the unit is pure quartz it also contains magnetite, graphite, garnet, biotite and feldspar, especially in thin beds. Kranck also mapped quartzite just southwest of Crooked Lake. Present mapping indicates that quartzite is a subordinate rock in this area, occurring as thin beds within sillimanite-bearing pelitic gneiss. Quartzite is also found as thin layers associated with pelitic gneiss in the southwest metasedimentary gneiss belt and with probable mafic supracrustal rocks in the northeast belt.

The mafic supracrustal rocks are confined to one shoreline locality 4 km north of Paradise River (community). The rocks are fine grained amphibolites with epidote-plagioclase-diopside-grossularite pods and discontinuous melanocratic seams.

In less intensely metamorphosed and deformed rocks (e.g. some Archean greenstone belts) such calcic material and melanocratic seams can be identified as interpillow mesostasis and pillow margins respectively. A pillow-form mafic lava or hyaloclastite protolith may therefore be applicable to this locality. Similar rocks occur on the southeast shore of The Backway (see Gower et al., 1983b) and at Dead Islands (52°48'N, 55°55'W) (Gower, personal observation). These are the only known mafic supracrustal rock localities in eastern Labrador, and the occurrences appear to be confined to a single metasedimentary belt at the northern fringe of the Lake Melville terrane. As all three occurrences are shoreline outcrops it is possible that this recessive-weathering unit occurs inland and is a characteristic feature of this particular metasedimentary belt.

Fine grained schistose mafic rocks were also observed 4 km east of Crooked Lake, where the thrust crosses Paradise River. A mafic supracrustal protolith is conceivable for these rocks also, but their structural position, adjacent to a thrust, and association with tectonic enclaves of metamorphosed layered gabbro suggest derivation from a highly deformed metagabbro.

Calc-silicate rocks, noted previously by Eade (1962) and Cherry (1978a,b) are not abundant and were only observed on either side of the south end of Crooked Lake. The rocks consist of quartz + grossular/andradite + diopside + calcic plagioclase and most commonly are present as boudinaged pods.

White Bear Arm complex

The White Bear Arm complex (WBAC) is an informal name introduced here for an anorthositic-gabbroic-monzonitic layered intrusion and associated mafic granulite, the northwest end of which underlies much of the eastern part of the map area. The WBAC was first named White Bear Arm gabbro by Piloski (1955) and referred to as White Bear Arm norite and White Bear Arm pluton by Wardle (1976). The type locality is at White Bear Arm on the southeast Labrador coast. The continuity of the WBAC from the coast to the present area (approximately 125 km) was suggested by Piloski (1955). We have not examined the ground between the coast and the Paradise River map area, but by using geophysical data and earlier mapping it appears appropriate to apply the name in the Paradise River area. The WBAC is not well exposed and the distribution of the four lithological subdivisions shown in Figure 2 must be considered tentative.

The anorthosite/leucogabbro unit has been identified only on the southwest flank of the WBAC and is a white or grey weathering, medium grained recrytallized rock. The mineralogy consists of plagioclase, clinopyroxene, orthopyroxene and hornblende with minor garnet and quartz. Locally recrystallized clusters of mafic silicates attest to derivation from a much coarser-grained protolith. However, because of its position adjacent to a major thrust, intense deformation has obliterated original textures.

Gabbro-troctolite rocks were mapped mostly in the center zone of the WBAC and amphibolitic rocks, interpreted as metamorphosed equivalents, have been included under the same ornamentation in Figure 2. Amphibolite is most abundant on the northeast flank of the WBAC and at its northwest tip.

In the center of the complex, gabbroid rocks are massive and primary plagioclase, olivine, clinopyroxene and orthopyroxene are preserved. Well-developed double orthopyroxene-amphibole coronas marginal to olivine also occur. Igneous layering, rhythmic in places, is present, especially in the southeast corner of the study area. Retrogression of pyroxene to amphibole is evident, particularly in rocks injected by either pegmatite or quartz-feldspar veins, and in those rocks having a marked metamorphic fabric.

Rocks grouped in the legend as monzodiorite, monzonite, quartz syenite and granite are creamy-brown to pink weathering, fine to coarse grained rocks and grade into K-feldspar or plagioclase megacrystic varieties. In places the monzonite-syenite clearly intrudes earlier mafic rocks, producing an agmatite with well-defined reaction rims at felsic-mafic interfaces (Plate 3). Elsewhere the monzonites contain irregular mafic enclaves which show K-feldspar megacrysts rimmed by plagioclase and large quartz crystals identical to the host monzonite. Some of the enclaves have chilled margins (texturally distinct from the reaction rims alluded to earlier) and are almost certainly mafic dikes. These apparently contradictory intrusive relationships will be evaluated when petrographic data are available.

The "fine grained granulite, leuconorite" unit is shown as underlying large areas of the WBAC (Figure 2). However, because of the fine grain size and rectiplanar shape of many outcrops we suspect that they may be mafic dikes with a granulite facies mineralogy. As the fine-grained granulites occur as isolated, resistant outcrops without an intervening contrasting rock type we have little choice but to depict distribution as shown.

Plate 3: *Monzonite-syenite of White Bear Arm complex intruding earlier mafic rocks producing an agmatite with well-defined reaction rims of felsic-mafic interfaces. Reaction rims 2 cm wide.*

Plate 4: *Well-preserved primary layering in the unassigned anorthosite unit.*

Unassigned Anorthositic Rocks

Distinctive, recessive-weathering anorthositic rocks are well exposed between Eagle River and the southern map boundary. Northwest of Eagle River, because of thick surficial deposits, their distribution is larely conjectural. The rock type is white to grey weathering, medium grained, recyrstallized and commonly strongly foliated. It consists of plagioclase, amphibole, pyroxene, with minor garnet and biotite. Coarse grained to extremely coarse grained primary textures are preserved in places. Poikilitic crystals over a metre in diameter were seen on upper Paradise River and individual pyroxenes over 25 cm long are not unusual. Amphibole in places partially replaces primary pyroxene; elsewhere former primary mafic silicates are now aggregates of amphibole, epidote (rare) and biotite. Primary layering is well preserved at the nose of the antiform near the south boundary of the map area (Plate 4). The presence of biotite granodiorite gneiss and megacrystic granodiorite in the core of the antiform constrain the thickness of the anorthosite to a maximum of 3 km.

Identical rocks outcrop along Alexis River west of Port Hope Simpson (C. Gower, personal observation, 1984) and geophysical data indicate that this unit is continuous between Eagle River and the southeast Labrador coast.

Granitoid Plutons

The granitoid plutons are divided into two groups, namely (i) an association of relatively melanocratic diorite, monzodiorite and granodiorite belonging to the Earl Island domain in the northeast corner of the map area, (ii) an intergradational granodiorite to granite plutonic package subdivided into four units which occurs throughout the remainder of the map area.

The granitoid plutonic rocks of the Earl Island domain are medium grained, hornblende-biotite-plagioclase-quartz rocks with minor garnet and K-feldspar and are subdivided into two groups in Figure 2. Fabric varies from weakly foliated to gneissic, the latter being accompanied by a quartz-feldspar leucosome. Amphibolitic bands, probably representing deformed mafic dikes, are common. Quartz diorite is depicted north of lower Eagle River in Figure 2. These fine to medium grained recrystallized hornblende + biotite ± garnet rocks are mineralogically similar, but not obviously related to those in the Earl Island domain.

We describe the remaining granitoid plutons from northeast to southwest. The Paradise Arm pluton (new informal name), southwest of Paradise River (community), was first mapped on the Sandwich Bay 1:100,000 sheet area (Gower et al., 1983) and, with a length of at least 48 km, is the largest K-feldspar rich pluton mapped within the Grenville Province of eastern

Labrador. It is a medium to coarse grained K-feldspar megacrystic rock with a variable composition including granodiorite, granite, monzogranite or syenogranite. Much of this compositional range is due to variable megacryst abundance which locally exceeds 40% of the rock. Megacrysts exceed 7 cm long in places. Plagioclase also may occur as megacrysts, but rarely larger than 1 cm in diameter. Mafic phases are hornblende and garnet. The northeast side of the pluton is interpreted as a fault, based on a single mylonitized outcrop near Paradise River (community). The southwest side appears to be intrusive in the vicinity of Beaver Brook but close to Eagle River it is tectonic. There appears to be a complete lithological gradation between the monzonite of the White Bear Arm complex and the Paradise Arm pluton. Coupling this fact with their spatial juxtaposition leads us to suspect a genetic link.

The belt of granitoid plutons crossing the central part of the map area comprises dominantly K-feldspar megacrystic rocks. Specific granitoid types include granodiorite, monzogranite, granite and alkali feldspar granite. These rocks differ from the Paradise Arm pluton in having smaller K-feldspar megacrysts and lacking plagioclase megacrysts. The rocks are fine to medium grained, recrystallized, pink, creamy or brownish weathering rocks with biotite ± hornblende ± garnet as mafic phases. At many localities the rocks are strongly deformed, even mylonitic, and some rocks mapped as orthogneiss in the region are almost certainly extremely deformed and migmatized equivalents. For example, we infer that the biotite granodiorite gneiss on the hanging wall of the thrust west of Crooked Lake is correlative with the adjacent granitoid pluton and that the thrust transects a pluton that was formerly continuous across the map area.

The granitoid plutons in the northwest corner of the map area can be divided into two groups, alkali-feldspar granite in the east and amphibole-bearing K-feldspar megacrystic granitoid rocks farther west. The alkali-feldspar granite is a pink weathering, coarse grained rock with biotite schlieren, amphibolite enclaves and a few syenitic to granitic late stage dikes. It has a distinct radioactive element signature with total scintillometer counts usually 3 times normal background (200 cps) for such rocks and on one outcrop 20 times background.

The megacrystic granitoid plutons in the northwest corner consist of buff to pink weathering, medium grained, recrystallized biotite hornblende granodiorite to granite. Similar rocks were mapped in the Sandwich Bay 1:100,000 sheet (Gower et al., 1983) and are probably regionally correlative with those in the Paradise River area.

The large K-feldspar megacrystic granitoid pluton in the southwest part of the map area (Plate 5) is a pink weathering, medium to coarse grained, biotite-bearing granodiorite, granite or alkali-feldspar granite with common amphibolite enclaves. It is particularly characterized by abundant pegmatite with large magnetite crystals and books of biotite exceeding 10 cm across in places. It has a strongly deformed to mylonitic fabric.

Plate 5: *Strongly deformed K-feldspar megacrystic granitoid pluton and late pegmatite dike.*

The granitoid pluton in the southwest corner of the map area is a pink to rusty-cream weathering medium-grained, recrystallized rock with a biotite-dominant margin and hornblende bearing interior. A gneissic septum separates these two varieties but whether this represents older gneiss or merely a high-strain zone is unclear.

Unassigned Metagabbro, Amphibolite and Mafic Granulite

This variable group of mafic rocks includes fine grained amphibolite, coarse grained garnetiferous amphibolite, two-pyroxene mafic granulite, metagabbro with relict igneous textures and rare melanocratic diorite. Occurrence of the unit vary in size from enclaves within other rock types to the map-scale bodies depicted in Figure 2. The unit was probably derived from mafic intrusions that ranged from minor dikes to small plutons.

Lower Phanerozoic Gabbro, Diorite Dikes.

Three north-northwest trending mafic dikes were mapped in the Paradise River Map

Figure 3: *Generalized foliation trends and other structural features in the Paradise River region.*

area and are extensions to dikes known farther north. The characteristic lithology is a black or brown weathering, coarse grained ophitic-textured gabbro with common interstitial K-feldspar. Typically the mafic silicates have been partially hydrated but primary textures are well-preserved. The westernmost dike extends from north of Cape Porcupine to the south-west quadrant of the map area - a distance of about 100 km. The continuity of the other two dikes is less established but both extend for at least 50 km. K-Ar dates obtained farther north give ages of 514 ± 08 Ma (W.R.) (Grasty et al., 1969) and 553 ± 22 Ma (biotite) (Wanless et al., 1970). These intrusions are correlated with the Long Range dikes of similar trend and age on the Great Northern Peninsula of New-foundland.

STRUCTURE

For descriptive purposes the region is divided into four northwest-trending sectors. These are, (i) the northeastern area bounded by the southwestern margin of the Paradise Arm megacrystic granodiorite, (ii) the White Bear Arm complex, (iii) the northwestern and central zone, bounded on its southwest side by the unassigned anorthosite unit, and (iv) the southwestern area.

In the northeastern sector regional foliation and gneissosity have a consistent northwest trend (Figure 3). Foliations are steeply dipping (70°) and lineations steeply plunging (50°). Minor folds indi-cate tight folding, especially in the meta-sedimentary gneiss; associated lineations

554

define fold axes. The relative dispositions of quartz diorite and metasedimentary gneiss north of Paradise River are interpreted in terms of a regional west-plunging Z fold.

The White Bear Arm complex appears to have a half-basin form. Foliations mostly dip inward (i.e. east or northeast) at angles between 40-70°, although some inward dips of less than 10° were recorded; in the southeast corner, steep outward dips exist. Lineations also plunge radially inward and are interpreted as stretching lineations related to thrusting at the margins of the WBAC. The nature of the thrusting is not known in detail but there are probably several more thrust surfaces present than indicated on Figure 3. Broad zones of mylonite were mapped along Beaver Brook and locally noted elsewhere (Plate 6). Rotated K-feldspar megacrysts indicate that the hanging wall of the thrust has been transported westward. No field evidence for a fault was found between the WBAC and the Paradise Arm pluton despite their linear boundary which appears to truncate regional structural trends in the WBAC.

Plate 6: *Ultramylonite at strike-slip faulting flanking internal thrust.*

The northwest and central zone is characterized by north-northeast structural trends which gradually curve round into a northwest trend in the southern part of the sector. In the vicinity of Crooked Lake, dips are mostly steeply to the east and lineations consistently plunge moderately to the north. Minor folds indicate that lineations are parallel to fold axes and we suspect the presence of tight-to-isoclinal major folds, overturned to the west. The

folding becomes more open westward, and the regional plunge changes from north-northeast to southwest, accounting for a basinal structure adjacent to Eagle River. This basin is obvious from photolineaments and is shown on the map of Eade (1962). The isoclinal folds near Crooked Lake are interpreted as the result of west to northwest transport of the WBAC over the underlying gneisses and granitoid plutons.

The unassigned anorthosite which separates the central and western zones has been folded into a shallowly north-plunging antiform. On the northwest side of Eagle River we interpret the antiform axis as swinging north to pass through the circular alkali feldspar granite.

Southwest of the anorthosite, structures revert to a northwest trend with steep foliation dips and moderately plunging, poorly developed lineations. As in the northeast sector, map patterns indicate major Z folds. The large megacrystic granitoid pluton is interpreted to occupy a synform which, northwest of Eagle River, parallels the trend of the adjacent antiform through the anorthosite, and swings north to link up with a well-defined synform in the northwest corner of the study area.

Two post-Grenvillian northeast trending, normal faults, namely the Eagle River and Paradise River faults cross the map area (Figure 4). The faults are accompanied by zones of brecciation and low-grade alteration. The faults link up with similar structures, the Sandwich Bay map-area (Gower et al., 1983a). They define the newly recognized and informally named Sandwich Bay graben, which is probably of similar age to the Double Mer and Lake Melville grabens hosting Double Mer Formation farther northwest. One exposure of similar post-Grenvillian conglomerate was mapped by (Gower et al., 1983a) on the west side of Sandwich Bay.

METAMORPHISM

Metamorphic grade throughout the map area includes upper amphibolite to granulite facies. Garnet is a ubiquitous metamorphic mineral in the orthogneisses and granite plutons and orthopyroxene was observed in several localities in the quartzofeldspathic leucosome of associated mafic rocks. The metasedimentary gneisses are characterized by biotite + sillimanite + garnet + plagioclase - K-feldspar - quartz assemblages. Magnetite is a characteristic accessory phase and muscovite is a locally extensive retrograde mineral. In the northwest continuation of the metasedimentary belt near Paradise River (Gower et al., 1983a) kyanite, orthopyroxene and cordierite have been found in various

Figure 4: *Distribution of Lower Phanerozoic mafic dikes and outline of the Sandwich Bay graben.*

pelitic assemblages (Gower, unpublished data).

The anorthositic rocks partially retain primary mineralogies but they show extensive hydration to amphibole bearing assemblages and recrystallization of primary silicates. In the White Bear Arm complex primary olivine is preserved as a primary phase mantled by double hypersthene-amphibole coronas. Fine grained granulite is a widespread rock type.

A single K-Ar biotite age of 1105 Ma suggests that temperatures were elevated above 300°C (blocking temperature for biotite) until ca. 1.1 Ga.

REGIONAL STRUCTURAL SYNTHESIS OF THE LAKE MELVILLE TERRANE

Mapping in the Paradise River area, coupled with additional interpretation of previous mapping, allows a preliminary regional structural synthesis of the Lake Melville terrane to be presented here (Figure 5).

The synthesis is based on the premise that there was large-scale regional transport of the Lake Melville terrane in a northwest to north-northwest direction. Thus northeast or east-northeast trending

structures are either thrust slices or overturned isoclinal folds in contrast to northwest trending structures which are essentially right-lateral strike-slip faults, with a possible thrust component. Although the east-northeast trending margin of the Lake Melville terrane has been markedly modified by post-Grenvillian normal faults related to the formation of the Double Mer graben, one thrust lobe is preserved north of the graben in the Double Mer White Hills. This lobe has well-developed, shallowly south-plunging stretching lineations. Because of lithological and metamorphic contrasts with the surrounding rocks this lobe is taken as the boundary of the Lake Melville terrane. However the thrust slice is one of a package – some thrusts cross the southern Groswater Bay terrane – and there is evidence of structural repetition within the Double Mer White Hills thrust lobe.

The Double Mer White Hills lobe is one of several thrust sheets that occur across the Grenville Province of Labrador, as well as farther west. The Cape Caribou River allochthon (Ryan et al., 1982; Wardle and Ash, 1984), north of Goose Bay (Figure 1) is comparable to the Double Mer White Hills thrust sheet in lithological make-up, structural style and metamorphic grade. Larger allochthons farther west include the Wilson Lake and Lac Joseph allochthons (Figure 1).

Southeast of Rigolet, the northern boundary of the Lake Melville terrane has a regional northwest trend, which continues to the southeast Labrador coast (Figure 1). Most foliations dip steeply southwest along this section of the boundary, except near Rigolet where, as the regional trend changes to east-northeast, foliations are less steep and south plunging lineations are obvious. We suggest that the northwest trending part of the Lake Melville terrane boundary is a major right-lateral strike-slip fault and that there are many similar faults within the southeast Lake Melville terrane.

The English River fault bounding the northeastern side of the Mealy Mountains Intrusive Suite is interpreted as major right-lateral strike-slip fault. Sense of movement is based on limited observations in the English River area. This passes through the Paradise River as a diffuse zone of ductile deformation in the region of the unassigned anorthosite. The combined effect of movement along the English River fault and movement along the northeastern boundary of the Lake Melville terrane is to slice up the intervening region into a series of blocks with internal northwest facing, frontal thrusts and flanked by strike-slip faults.

Figure 5: *Regional geological synthesis of the Lake Melville terrane.*

Structurally underlying these 'internal' thrusts the rocks have been deformed into isoclinal, overturned northwest verging folds which, away from the thrust front become more open. The folds more distant from the internal thrusts are major regional structures which are unlikely to have a direct causal link with the thrusts.

Several major folds have been interpreted to occur between Eagle River and the Mealy Mountains. An antiform northwest of Eagle River is outlined by unassigned anorthosite and the core of the fold has been intruded by alkali feldspar granite. The synform farther west has been interpreted to extend from the southern boundary of the Paradise River area to west of Rigolet, a distance of approximately 150 km. The axial trace of the synform is defined by folded quartz diorite bodies in places. The antiform west and south of the synform is actually a domal structure outlined by metasedimentary gneiss. The core of this dome has been intruded by a clinopyroxene bearing quartz syenite to granite which gives a 1273 Ma (U-Pb zircon) age (Krogh, personal communication 1984). We suspect a similar age applies to the alkali-feldspar granite intruding the antiform near Eagle River.

The effect of northwest transport of the Mealy Mountains terrane has been to tighten the northwest end of the domal structure (north of Lake Melville) into a series of tight, overturned, north verging folds and to refold the regional synform in the Paradise River region into open Z structures.

ECONOMIC MINERAL POTENTIAL

The economic mineral potential of the area was assessed during reconnaissance surveys by British Newfoundland Corporation Ltd. (BRINCO), the results of which did not encourage continued activity. However, subsequent more comprehensive aeromagnetic coverage, as well as more detailed geological mapping and results from regional lake sediment surveys suggests, to us, that the area deserves reassessment.

Metasedimentary gneiss appears to be a unit with some economic potential (see Gower and Erdmer, 1984). Sulfide rich zones (mainly pyrite, but with minor chalcopyrite) are common especially in the metasedimentary gniess belts through Crooked Lake and 8 km west of Crooked Lake. Anomalously radioactive pegmatite (counts up to 20 times background) was discovered on the west side of Crooked Lake. The metasedimentary gneiss in the Crooked Lake region also hosts an abandoned mica quarry with biotite and muscovite books 15-20 cm in diameter.

Another major feature of potential economic interest is a granite in the northwest part of the map area. This has anomalous radioactivity, in one place reaching 20 times background, and may be a host to other lithophile element mineralization.

Lake sediment geochemical anomalies (especially U in water) are closely associated with this granite.

Other economic possibilities include Ni-Co-Cr-Cu mineralization within the White Bear Arm complex and LIL element mineralization in various pegmatiates associated with some of the K-rich megacrystic granitoid plutons.

REFERENCES

Cherry, M.
   1978a: Geological mapping in the Sandwich Bay area, southeastern Labrador. *In* Report of Activities for 1977. *Edited by* R.V. Gibbons. Newfoundland Department of Mines and Energy, Mineral Development Division, Report 78-1, pages 9-15.

   1978b: Sandwich Bay. Newfoundland Department of Mines and Energy, Mineral Development Division, Map 78176.

Eade, K.E.
   1962: Geology, Battle Harbour - Cartwright, Labrador. Geological Survey of Canada, Map 22-1962.

Geological Survey of Canada
   1974a: Aeromagnetic map 13H/4, Newfoundland. Geological Survey of Canada, Map 6028G, scale 1:63,360.

1974b: Aeromagnetic map 13H/3, Newfoundland. Geological Survey of Canada, Map 6029G, scale 1:63,360.

1974c: Aeromagnetic map 13H/6, Newfoundland. Geological Survey of Canada, Map 6036G, scale 1:63,360.

1974d: Aeromagnetic map 13H/5, Newfoundland. Geological Survey of Canada, Map 6037G, scale 1:63,360.

1974e: Aeromagnetic map 13H and 13E, Cartwright, Newfoundland. Geological Survey of Canada, Map 7389G, scale 1:250,000.

Gower, C.F.
1984: Geology of the Double Mer White Hills and surrounding region, Grenville Province, eastern Labrador. *In* Current Research, Part A, Geological Survey of Canada, Paper 84-1A, pp. 553-561.

Gower, C.F. and Erdmer, P.
1984: The Mineral potential of paragneiss in the Grenville Province in eastern Labrador. *In* Current Research. *Edited by* M.J. Murray, J.G. Whelan and R.V. Gibbons. Newfoundland Department of Mines and Energy, Mineral Development Division, Report 84-1, pp. 80-87.

Gower, C.F., Finn, G., Gillespie, R.T., Noel, N. and Owen, V.
1983a: Sandwich Bay 1:100,000 Map Sheet. Newfoundland Department of Mines and Energy, Mineral Development Division, Map 83-45.

Gower, C.F., Noel, N. and Gillespie, R.T.
1983b: Groswater Bay 1:100,000 Map Sheet. Newfoundland Department of Mines and Energy, Mineral Development Division, Map 83-43.

Gower, C.F., Noel, N., Gillespie, R.T., Finn, G. and Emslie, R.F.
1983c: English River 1:100,000 Map Sheet. Newfoundland Department of Mines and Energy, Mineral Development Division, Map 83-44.

Gower, C.F. and Owen, V.
1984: Pre-Grenvillian and Grenvillian lithotectonic regions in eastern Labrador - correlations with the Sveconorwegian Orogenic Belt in Sweden. Canadian Journal of Earth Sciences, Volume 21, pages 678-693.

Gower, C.F., Owen, V., and Finn, G.
1982: The geology of the Cartwright region, Labrador. *In* Current Research. *Edited by* C.F. O'Driscoll and R.V. Gibbons. Newfoundland Department of Mines and Energy, Mineral Development Division, Report 82-1, pages 122-130.

Kranck, S.H.
1966: Report on geology of the northern part of Sandwich Bay - Square Island joint venture area. Unpublished private report, BRINCO Ltd.

Owen, V., Gower, C.F. and Finn, G.
1983: Table Bay 1:100,000 Map Sheet. Newfoundland Department of Mines and Energy, Mineral Development Division, Map 83-46.

Piloski, M.J.
1955: Geological report on area 'E', Labrador concession. Unpublished private report, BRINCO Ltd.

Rivers, T. and Nunn, G.A.G.
in press: A reassessment of the Grenvillian Orogeny in Western Labrador *In* The Deep Proterozoic Crust in the North Atalntic Provinces. *Edited by* J. Tournet. Nato Advanced Study Institute.

Ryan, B., Neale, T., and McGuire, J.
1982: Descriptive notes to accompany geological maps of the Grand Lake area, Labrador 13F/10,11,14,15. Newfoundland Department of Mines and Energy, Mineral Development division, 14 pages.

Sutton, W.R.
1965: Report on Sandwich Bay - Square Island, southeast Labrador joint venture area. Unpublished private report, BRINCO Ltd.

Thomas, A., Nunn, G.A.G. and Wardle, R.J.
in press: A 1650 Ma Orogenic belt within the Grenville Province of Northeastern Canada. *In* The Deep Proterozoic Crust in the North Atlantic Provinces. *Edited by* J. Tournet. NATO Advanced Study Institute.

Wanless, R.K., Stevens, R.D., Lachance, G.R. and Delabio, R.N.
1970: Age determinations and geological studies. Geological Survey of Canada, Paper 69-2A, pages 71-78.

Wardle, R.J.
1976: Geology of the Francis Harbour - Snug Harbour Area. Newfoundland Department of Mines and Energy, Mineral Development Division, Map 771.

Wardle, R.J. and Ash, C.
1984: Geology of the North West River area. *In* Current Research for 1983. *Edited by* M.J. Murray, J.G. Whelan and R.V. Gibbons. Newfoundland Department of Mines and Energy, Mineral Development Division, Report 84-1, pages 53-67.

Westoll, N.D.S.
    1971: Summary of nickel exploration in
    southern Labrador. Unpublished private
    report, BRINCO Ltd.

Wilson, B.T.
    1959: Report on the geophysical survey
    of the Sandwich Bay area, Labrador by
    Lundberg Explorations Ltd. Unpublished
    private report for BRINCO.

METALLOGENY OF PERALKALINE ROCKS IN LABRADOR: STRANGE LAKE PERALKALINE GRANITE AND LETITIA LAKE (MANN #1) SHOWING

by

Randy Miller
Mineral Deposits Section

This year was the first of a five year project designed to study the metallogeny of the Strange Lake Zr-Y-Nb-REE mineralization and the Letitia Lake Be-Nb mineralization. To date, the preliminary field work has been completed for the Mann #1 showing at Letitia Lake, while the Strange Lake Alkalic Complex has been mapped and sampled. The available drill core from both of these showings has also been relogged.

The Strange Lake Alkalic Complex, located west of Nain on the Quebec-Labrador border, was mapped and sampled during the summer. A 1:10,000 scale bedrock geology map incorporating drill core and outcrop data will be completed in the near future. Samples collected for thin section, geochemical and mineralogical studies are presently being prepared; thus, results should be available in 1985. Planned laboratory studies include:

a) microprobe mineral analysis,
b) mineral separation and analysis,
c) major, minor and rare earth element whole rock analysis,
d) fluid inclusion study,
e) petrographic characterization of samples,
f) radiometric age dating.

These studies will help to characterize the ore minerals, some of which are unnamed minerals, and will help to establish the conditions and processes involved in ore formation.

The Mann #1 showing, located on Letitia Lake, 160 km northwest of Goose Bay, was visited this summer to collect samples and to identify geological problems. The study of both the field and drill core samples from the mineralized zones and host rocks will help to establish the ore-forming processes for this unusual type of deposit. Preliminary observations suggest that the Be-Nb mineralization is associated with peralkaline veins and sills, and with the metasomatism associated with their intrusion. Laboratory work this winter will include geochemical and mineralogical studies. The mineralization and host rocks will be mapped next summer to produce a 1:2,400 scale bedrock map.

It is hoped that the studies outlined above will aid in the further development of these deposits, as well as continued exploration for similar occurrences in other parts of Labrador.

GEOLOGICAL MAPPING OF CAMBRIAN AND ORDOVICIAN SEDIMENTARY ROCKS OF THE BELLBURNS (12I/5/6), PORTLAND CREEK (12I/4) AND INDIAN LOOKOUT (12I/3) MAP AREAS, GREAT NORTHERN PENINSULA, NEWFOUNDLAND

by

Ian Knight

ABSTRACT

Lower Paleozoic platformal, flyschoid and allochthonous rocks occur in the map area. Lower Cambrian siliciclastics and carbonates and Middle Cambrian to Middle Ordovician carbonates compose the generally conformable platformal sequence that sits unconformably upon Precambrian granitic basement. Regional subaerial exposure of the platform during sedimentation produced two disconformities at the middle and end of the Lower Ordovician. Paleokarst developed at the surfaces and a network of stratiform and discordant collapse breccias formed at selective lithostratigraphic horizons and close to northeast trending faults.

The platform plunges south beneath Middle Ordovician northeastward and eastward derived sandy flysch. Spectacular limestone breccias derived from destruction of uplifted Middle Ordovician platformal carbonates occur within the flysch. Allochthonous rocks include ribbon limestones and shale and limestone conglomerates and thin bedded fine grained sandstones and shales of unknown age.

The gently to moderately dipping autochthonous strata are transected by numerous long northeast trending and an important group of west trending faults. The Long Range Precambrian inlier is thrust westward over autochthonous strata. A narrow zone of strong deformation and extensive recrystallization of the carbonates occurs in platformal rocks west of the thrust. Inverted bedding, recumbent folds and thrust and reverse faults occur in the zone.

Numerous sphalerite showings occur in dolomites that replace Lower Ordovician limestones in the center of the area. The carbonate hosted Mississippi-valley type deposits form a zinc rich district centered around the Daniels Harbour Zinc Mine.

INTRODUCTION AND GEOLOGICAL SETTING

A large southward-narrowing wedge-shaped area of Cambrian and Ordovician platformal rocks was mapped between River of Ponds and Parsons Pond on the west side of the Great Northern Peninsula (Figure 1). The rocks include gently dipping to strongly deformed strata of the Lower Paleozoic autochthonous Humber Zone, which formed the northern Newfoundland part of the passive margin of Iapetus Ocean. These rocks lie west of uplifted Precambrian basement rocks of the Long Range Mountains and their outcrop narrows to the southwest as they plunge beneath autochthonous Middle Ordovician flyschoid formations and transported Lower Paleozoic deepwater sedimentary rocks of the northern edge of the Humber Arm Allochthon. The Lower Paleozoic autochthon lies unconformably upon Precambrian basement; this contact can be observed only in the northeastern part of the Bellburns map area on and near Blue Mountain.

The autochthonous sequence is essentially a conformable, platformal buildup. However, two intervals of erosion of middle and late Early Ordovician age occur within the carbonate succession. In the Middle Ordovician, the platform collapsed and was blanketed by thick Middle Ordovician flysch derived by erosion of Lower Paleozoic allochthons that were subsequently obducted onto the autochthon during the final phases of the Taconic orogeny. Severe folding and faulting affected the rocks that form the structurally lower parts of the Taconic allochthon. Deformation of the autochthon mainly resulted in many north to northeast and eastward trending faults but, close to the allochthon and near the uplifted Long Range Precambrian inlier, the platformal rocks are much more intensely deformed. The area provides an excellent opportunity to study the faulted contact relationships of the Long Range inlier and the Lower Paleozoic platformal rocks.

Field mapping was done along the Viking Highway, along extensive wood roads, and around many lakes to facilitate access by foot to all but the eastern areas near the Long Range Mountains, where a helicopter was used. Recently regenerated to mature evergreen forests and huge tracts of peat land, particularly in the western and southern parts of the area, characterize the low (60 to 180 m) coastal plain in the area. Only close to the Long Range Mountains, which overlook the plain at an elevation of 360 to 460 m, does topographic relief become rugged. Here, scarp-edged,

LEGEND

SEDIMENTARY ROCKS OF UNKNOWN AGE, POSSIBLY ALLOCHTHONOUS

Sh -   *Green, gray, black shale and mudstone, thin limestone, thin sandstone, red and black chert.*

Cgl -   *Limestone conglomerate, thin bedded limestone, shale, minor sandstone.*

AUTOCHTHONOUS ROCKS

MIDDLE ORDOVICIAN

Ss-2 -   *Unnamed upper green sandstone, pebbly sandstone, conglomerate, shale.*

Ls-Br - *Unnamed limestone breccia and minor calcarenite.*

Ss-1 -   *Unnamed lower green sandstones and interbedded shale, some pebbly sandstone.*

TH Table Head Group - *Limestone, minor dolomitic limestone, dolostone and shale.*

TH-2 - Table Cove and Black Cove Formations
TH-1 - Table Point Formation; THd - dolomitized

LOWER ORDOVICIAN

St. George Group (SG, WB, BH, C, A)

SG -   Undivided

A   Aguathuna Formation - *Dolostone, dolomitic shale, chert pebble conglomerate and pebbly dolostone.*

C   Catoche Formation - *Limestone, C_l, top extensively replaced by diagenetic dolostone C_d.*

BH   Boat Harbour Formation - *Limestone, dolomitic limestone, dolostone, diagenetic dolostone, collapse breccias.*

WB   Watts Bight Formation - *Diagenetic dolostone.*

MIDDLE TO UPPER CAMBRIAN

Port au Port Group (PP, MP, PJ)

PP   Undivided

PJ   Petit Jardin Formation - *Dolostone, minor shale and limestone.*

MP   March Point Formation - *Dolostone, minor shale, sandstone.*

LOWER CAMBRIAN

Labrador Group (L, B, F, HR)

L   Undivided

HB   Hawke Bay Formation - *White sandstone, minor shale.*

F   Forteau Formation - *Limestone, shale, sandstone.*

B   Bradore Formation - *Red and gray sandstone, minor conglomerate.*

PRECAMBRIAN

PE   Grenville Basement - *Granite, gneiss.*

SYMBOLS

sp   Sphalerite _ ⚲sp
sp   Sphalerite boulders _ _ _ _ _ _ _ _ _ _ _ _ _ _ _ _ _ _ ⬭sp

Figure 1: *Sketch map of the geology (in part), of the Bellburns, Indian Lookout and Portland Creek map sheets.*

north trending ridges and lake-filled valleys reflect the 3 km wide, folded and faulted zone of underlying platformal rocks.

The area is well known for the zinc mine at Daniels Harbour. The Mississippi Valley-type sphalerite mineralization in several closely grouped deposits forms the heart of this zinc-rich district.

STRATIGRAPHY

Three geologic terranes occur in the map area; namely, Precambrian basement, autochthonous Lower Paleozoic platformal and basinal sedimentary rocks and allochthonous Lower Paleozoic basinal sedimentary rocks.

Precambrian Basement Rocks: Uplifted Precambrian basement rocks form the Long Range inlier at the eastern edge of the map area. These rocks, mapped only in a reconnaissance fashion for less than 2 km east from their western contact, consist predominantly of massive, slightly foliated, equigranular, fine to coarse grained to megacrystic, pink to red, micaceous granites. Rafts and layers of hornblende-plagioclase and quartz- feldspar-mica gneiss are enclosed within the granites. Chlorite is ubiquitously developed through the granite, suggesting that the basement rocks have undergone greenschist grade metamorphism. Foliations measured in the outcrop generally dip at low to moderate angles to the east.

Lower Paleozoic Platformal Rocks: Lower Paleozoic platformal rocks approximately 1600 m thick in the map area are subdivided according to the nomenclature outlined previously in adjacent map areas by Knight and Boyce (1984). Additional nomenclature follows that of Klappa et al. (1980) for rocks of the Table Head Group. The succession is described in order of the four rock groups that comprise the platformal succession; namely, the Labrador, Port au Port, St. George and Table Head Groups.

Labrador Group (Lower Cambrian): This mixed siliciclastic-carbonate succession comprising the Bradore, Forteau and Hawke Bay Formations is exposed only along the eastern edge of the map area. There, it forms either fault-bounded wedges that are steeply dipping to overturned just west of the Long Range boundary fault or flat-lying, rounded to arrowhead-shaped outliers resting unconformably upon Precambrian basement rocks, as on and just north of Blue Mountain.

The succession is best exposed in a steep gulch on the northwest side of Blue Mountain, where it consists of poorly exposed basal pebbly, red arkosic sand-stones of the Bradore Formation (1a) overlain by thinly stratified gray, micaceous, sandstones and shales. These are capped by planar laminated and thinly stratified and crossbedded, slightly bioturbated red arkosic sandstones, similar to those described in other Long Range outliers of the Torrent River map area (Knight and Boyce, 1984).

A pink, crystalline dolomite(?) to nodular, shaly fossiliferous gray limestone conformably rests upon the topmost red sandstones of the Bradore Formation. It is correlative with the Devils Cove Member, Forteau Formation, Canada Bay and elsewhere in western Newfoundland (Knight and Saltman, 1980; James and Kobluk, 1978; James and Stevens, 1982). The remaining 110 m of the Forteau Formation (1b) consists of fossiliferous black shales that contain thin bioclastic limestones overlain by crossbedded and stratified, bioclastic and oolitic black limestones. The limestones are interbedded at intervals with cross laminated and laminated, often strongly bioturbated gray siltstones and shales. No evidence of archaeocyathid bioherms has been noted in the map area.

Resting conformably upon the Forteau Formation, are white to pinkish and massive weathering, flinty, white quartz arenites of the Hawke Bay Formation (1c) that form the contour-bedded tops of the outliers. The well sorted, unfossiliferous quartz arenites are crossbedded and commonly ripple marked, but are conspicuously bereft of bioturbation. This is in contrast to several intercalated units, 1-4 m thick, of thinly bedded, planar laminated and cross-laminated, argillaceous and shaly, gray and red quartzose sandstones. These are intensely ploughed by numerous u-shaped and tubular burrows and may contain layers of phosphatic intraclasts. Phosphate crusts on sandstone beds and phosphate, shale and sandstone intraclasts particularly characterize 10 cm thick, cross-laminated and laminated, sandstones that are interbedded with gray shales in a 2 to 3 m thick sequence at the top of the formation.

The characteristics of the Labrador Group support the interpretation of the depositional history of the group in nearby areas as proposed by Knight (in preparation). Braided stream sands deposited on a coastal plain, that lay west of a shallow siliciclastic shoreline, contributed the red and gray sandstones of the Bradore Formation. Widespread transgression established open marine shelf conditions in which accumulated the shallowing upward, low energy shale and high energy, grainy limestone succession of the Forteau Formation. Eastward prograding quartz sands blanketed the carbonate shelf in a complex of tidal sand bodies and related intertidal

facies, as the Hawke Bay Formation completed the succession. Abundant phosphate intraclasts and crusts at the top of the formation suggest exposure of the platform as sedimentation on the Early Cambrian shelf came to an end.

Port au Port Group (Middle to Late Cambrian): A poorly exposed succession of argillaceous dolostones, dolostones, shales and limestones forms the Port au Port Group. The basal March Point Formation (30 m) (2a) rests with sharp conformity upon the Hawke Bay sandstones. This formation consists of basal dark gray shales overlain by yellow weathering, bioturbated and vuggy, thinly stratified, dark gray argillaceous dolostones. Green, gray and reddish shales, yellow weathering, pale gray dolostones, and gray to blue-gray limestones comprise the overlying Petit Jardin Formation (2b). The shales are mostly low in the formation, intercalated with dolostones that exhibit cryptalgal structures and many other features of intertidal and supratidal carbonate flat deposition. Limestones and dolostones are important in a middle member that contains stromatolites, channel-bound and sheeted intraformational floatstones and rudstones, oolitic grainstones, burrowed, thinly bedded and parted limestones and muddy dolomitic carbonates as well as mudcracked horizons. Trilobites recovered from the member in two localities along the west shore and 1.4 km west of Western Blue Pond (known locally as John William's Bluey) include *Arapahoia* sp., *Coosella* sp. cf. *C. helena* Lochman, *Terranovella* sp. cf. *T. obscura* Lochman and *Welleraspis* sp.; they are indicative of the Dresbachian *Crepicephalus-Cedaria* zones which suggests the unit spans the early Late Cambrian (Boyce, this volume).

Buff weathering, thickly bedded, cherty dolostones form most of the upper half of the formation. Burrowed and stromatolitic beds alternate with wavy laminated and thinly bedded microcrystalline dolostones.

The rocks of the Port au Port Group accumulated within shallow subtidal to supratidal carbonate settings. Tidal flats accumulating cryptalgal laminites and mudrocks were established as deposition of the Petit Jardin Formation succeeded the shallow subtidal muds that formed much of the March Point Formation. Higher energy stromatolite buildups, fringed by oolite bodies, and tidal flat deposits crossed by conglomerate-filled tidal channels typify the middle of the formation. More open shelf conditions then produced repeated shoaling upward peritidal sequences, suggesting repeated migration of shallow shoreline conditions as mudflats or mudflat islands prograded seaward over subtidal or lagoonal muds.

St. George Group: The Lower Ordovician St. George Group is widely developed in the central, western and southern parts of the map area. It has been subdivided into four formations outlined previously by Knight and Boyce (1984) and Knight (in preparation) in the Port Saunders area. Lithologically, the basal Watts Bight Formation (3a) is composed of black, fine to medium crystalline diagenetic dolostones exhibiting extensive burrow-mottling of thinly stratified carbonates and lesser cryptalgal mounds; it remains consistent as elsewhere on the Northern Peninsula. It is best exposed around the western part of Eastern Blue Pond (locally called Western Bluey) and near Flat Pond. The overlying Boat Harbour Formation (3b) is not well exposed; it consists of a complex array of interbedded limestones, dolostones, shaly limestones, and diagenetic dolostones. Features of shallow peritidal deposition such as fossiliferous, bioturbated mudrocks, associated stromatolites, flaser bedded and laminated, locally mudcracked, dolomitic limestones were noted in better outcrops.

Highlighting the 1984 mapping in this formation, however, was the discovery of several exposures of the Boat Harbour "pebble bed" and exposure surface along the coast and along a woods road near Bateau Barrens. This interval, which occurs less than 30 m from the top of the formation where it is overlain by cyclically developed grainy and muddy limestones, is expressed slightly differently in the various localities. However, it is always typified by the presence of abundant chert that fulfills a replacing and cementing role within carbonates below the solution surface and is reworked as pebbles in the overlying beds. In the roadside outcrop, the pebbles are scattered in a 60 cm thick conglomerate also containing dolostone and limestone pebbles. In exposures along the shore at Bateau Barrens, chert pebbles are concentrated in the overlying bed and in pockets and fissures along the irregular exposure surface. The chert is typically oolitic, porcelaneous or white megaquartz. Silicified fossil fragments occur in the roadside outcrop within the conglomerate.

Dolomitization of underlying strata also occurs up to a metre thick in the roadside exposure where there are no later dolomite overprints. In the coastal sections, however, dolomitization is considerably thicker, but this is likely related to dolomitization within a complex fault zone that follows the coast from Bateau Barrens south to Deer and Freshwater Coves. There is no relief or evidence of solution in the roadside outcrops, but relief of tens of centimetres occurs in the coastal sections. Also present in the coastal exposures are narrow branching

hardrock fissures penetrating a few metres below the exposure surface as well as locally developed pockets of solution collapse breccias. Both are filled by a microcrystalline, vitreous black dolomite matrix or cement. Metre thick, concordant, stratabound breccias composed of blocky, dolostone fragments up to 20 cm in size and set in a black siliceous dolostone and small rock particle matrix also occur in the same coastal fault zone at the southern end of Bateau Barrens. This breccia rests upon black Watts Bight dolostones and is comparable to other similar breccias that occur in the same stratigraphic interval elsewhere on the Northern Peninsula (Knight, 1978, 1980, in preparation; Knight and Boyce, 1984).

The overlying Catoche Formation (4c) is a succession of well bedded, bioturbated and fossiliferous, gray limestones which are replaced extensively by secondary dolostones towards the top of the formation. The limestones consist mostly of wackestones and packstones that are argillaceous and unevenly thinly stratified; lenses of intraclastic and bioclastic mudstones and planar stratified and rippled marked grainstones also occur. Boundstone mounds occur towards the base of the formation. The secondary dolostones are gray to black, massive, vuggy, and fine to medium crystalline. Open spaces filled by white baroque dolomite occur in selected beds known as pseudobreccia. Limestones are interbedded with and pass laterally into the dolostones towards the top of the formation.

Buff to yellow weathering, microcrystalline, light to dark gray, dolostones and green dolomitic shales of the Aguathuna Formation (4d), form the top of the St. George Group. Lamination, cross-lamination, small tepee structures, intraformational breccias, and mudcracks typify the dololaminites that intercalate with burrow-mottled, and thinly bedded dolostones, and rarely stromatolitic dolostones. Sand and pebbles composed of chert and dolostone lithoclasts also occur in the upper 12 m of the formation where they form layers, a few centimetres thick, in planar laminated dolostone towards the base of shallowing-upward cycles. A number of crudely stratified beds, 40 cm to 3 m thick of chert-dolostone pebble conglomerate, again in the upper 12 m of the formation, occur on the north shore of River of Ponds Lake, the eastern island of Portland Creek Pond and in a fault-bounded wedge along the shore at Table Cove, Bellburns. Silicification, fracturing, post-depositional brecciation and irregular bedding surfaces occur near and below the chert pebble interval in the formation.

There is a major thickness difference of 45 m between sections in the Aguathuna Formation on the northwest (15 m) and northeast (60 m) shore of River of Ponds Lake. This suggests that major faults that transect the lake (Torrent River Fault) have either juxtaposed two different paleogeographical settings or were active during deposition of the formation. At the base of the thinner section, Aguathuna dolostones rest upon a very irregular surface with relief up to 40 cm sculptured in diagenetic dolostones of the Catoche Formation. Silicification and fracturing is common below the surface; depressions at the surface and cavities and fissures below are filled by Aguathuna dolostones and chert detritus.

A coherent part of the Aguathuna Formation are matrix breccia bodies such as described by Lane (1984). The largest exposed rock body at Mine Lake is several hundreds of metres across and contains variable bedding punctuated by zones of mostly dolostone rubble. However, a breccia zone composed of color banded, laminated and thin bedded, black and light gray limestone occurs in the centre of the breccia body that cuts down into the underlying Catoche dolostones and limestones.

Numerous oligo- and polymictic matrix breccia bodies lie along the trace of the Bateau Cove fault zone where it cuts dolomites of the middle of the St. George Group. Abundant spar breccias also occur individually, and overlying and peripheral to matrix breccias. Matrix breccias are both concordant and discordant to bedding. Preliminary studies suggest some of these breccias post-date deposition of the Catoche Formation, while others have been linked to events affecting the older Boat Harbour Formation. Similar breccias have been noted in the Aguathuna Formation west of Eastern Blue Pond.

The buildup of the Early Ordovician platform was accomplished by deposition of generally monotonous subtidal limestone and repeated sequences of peritidal carbonate in two megacycles of transgression and regression. Both Tremadocian (Watts Bight - Boat Harbour Formations) and Arenigian (Catoche - Aguathuna Formation) megacycles culminated in subaerial exposure of the platform which was accompanied by widespread diagenesis, solution and development of a karst cavern system. Areal development of the subterranean cavern systems, now filled by collapse breccias, was controlled by lithostratigraphy and structure. Widespread stratabound collapse brecias are consistently located in basal dolostones of the Boat Harbour Formation immediately above the Watts Bight Formation. The cavern system related to the late Arenig disconformity however, was partly controlled by northeast trending faults and fractures that also influenced the thickness of the

Aguathuna Formation. They also formed the channel ways for deep penetration of solutions through the platform (Knight and Boyce, 1984).

Table Head Group (Middle Ordovician): The Middle Ordovician Table Head Group was defined by Klappa et al. (1979) as consisting of the Table Point, Table Cove, Black Cove and Cape Cormorant Formations.

The Table Point Formation is well known as a highly fossiliferous, well bedded, blue gray to gray, subtidal limestone. This year's mapping has, however, continued to highlight the formation's diversity. The formation commences with a basal cyclic member of bioclastic and intraclastic grainy mudrocks intercalated with laminated, frequently mudcracked, dolomitic lime mudstones or dolostones. This is overlain by a light gray weathering, fine grained, fenestral limestone. The fenestral limestone contains cement-filled skeletal porosity after gastropods and cephalopods as well as tubular and laminar fenestra and "stromataoids" voids, the latter filled by geopetal muds and calcite cements. Although this member is readily distinguished over wide areas of the map area where it can reach 30 m thickness, it is not present at Table Point and in the northeast of the map area where dark gray, mottled wackestones dominate the section. This suggests that there are rapid lateral facies changes; similar conclusions have been reached based on the study of drill logs in the Bellburns map area (Lane, personal communication, 1984).

Fossiliferous and bioturbated subtidal, argilliaceous dark gray limestones overlie the fenestral carbonates. Slump breccias and folds deform the subtidal limestones 3 m below a succession, 23 m thick, of interbedded burrowed, bioclastic wackestones and scour-based, cross laminated grainstones. Some small boundstone mounds also occur and the wackestones and grainstones intercalate upwards with dololaminites. The dololaminites exhibit lamination, cross bedding, mudcracks and fissure cracks, scour-and-fill structures, and pockets of intraformational breccia typical of intertidal settings. A succession of similar lithologies, 19 m thick, occurs in the middle of a westward younging, partly inverted sequence of Table Point Formation west of the Bateau Cove Fault, south of Bateau Cove. The remaining 200 + m of the formation consists of highly fossiliferous, bioturbated, argillaceous limestones that contain abundant large cephalopods, gastropods, sponges, bryozoa, ostracods, trilobites and brachiopods. Nodular to planar, thin bedded, argillaceous, lime mudstones with thin gray shale interbeds characterize the conformably overlying Table Cove Formation. The formation is famous for its Toquima -

Table Head trilobite fauna (Ross and Ingham, 1970). Many beds in this formation are deformed by synsedimentary slump folds, thrust faults and rotational slides.

The Table Cove Formation is gradationally overlain by 17 to 27 m of black shales of the Black Cove Formation. A few discontinuous fine limestone beds occur at the base. The top of the formation is badly sheared at Table Cove where it is almost 10 m thinner than at a shoreline section opposite the Daniels Harbour mine road.

Limestone conglomerates intercalated with shales, limestones and sandstones, defined as the Cape Cormorant Formation by Klappa et al. (1980), do not occur in the map area. Limestone breccias occurring at Daniels Harbour, Cliffy Point and Eastern Head and the western island of Portland Creek Pond are believed to lie within a succession of green sandy flysch and are not included in the Table Head Group.

Lithofacies that comprise the Table Head Group were laid down in shallow peritidal to open shelf environments during the deposition of the Table Point Formation. Cyclical peritidal shoaling upward sequences of the basal member of the formation appear to be superceded by shallow water light-coloured, fenestral limestones. These accumulated possibly as dominantly intertidal carbonate mud mounds rich in fenestra and accreting adjacent to areas of shallow subtidal carbonate mud. Shallow sandy to muddy tidal flat carbonates that overlie these deposits were then blanketed by widespread subtidal shelf limestones that hosted a rich shelly fauna. Continued sea level rise drowned the platform margin leading to deposition of slope deposits of the Table Cove Formation and basinal shales of the Black Cove Formation.

Autochthonous Middle Ordovician siliciclastic rocks and limestone breccias: Green sandstones interbedded with black shales form a succession of turbidite sands of great but unknown thickness. The succession is essentially composed of metre-thick sequences of thick bedded sandstones, pebbly sandstones and conglomerates, regularly intercalated sandstones and shales, shales with thin sandstones and siltstones and rare shale-sandstone mixtites. Sandwiched in the middle of the formation is a remarkable sequence of limestone breccia composed of rubble and blocks of Table Head limestone mixed with large ripups of shale and green sandstone. Towards the top and overlying the breccias are some calcarenites composed of rounded limestone sand and granules. No contacts between the green sandstones and limestone breccias are exposed but, 1) the presence of sandstone lithoclasts, 2) the consistent structural position, and 3) the lack of evidence for

faults that might have uplifted and tecton-
ically disrupted Table Head Group, support
the interpretation that the breccias lie
stratigraphically within the flysch and not
at the base. Dolomitized limestone breccias
and limestone sandstones that form The
Arches south of Portland Creek, may be
equivalent to the breccias, later uplifted
by a northeast trending fault. If this
interpretation is true, then the sandstones
and conglomerates forming Portland Hill
possibly belong to the uplifted sequence
and repeat rocks that occur near and south
of Portland Creek.

The green sandstones display grading,
massive, laminated and cross-laminated
intervals typical of Bouma sequences, con-
volute bedding, vein networks of pillar
structures, shale ripups, allochthonous
shelly fossils, and flute and load casted
bases. Many of the thicker beds contain
pebbles of sandstone, shale, quartz, chert,
argillite, light gray to white limestone,
and are crossbedded. Conglomerates form a
major part of the succession on top of
Portland Head. They include pebbles up to
10 cm in size of massive to laminated,
sometimes dolomitic, muddy, pale gray,
limestone, some with quartz sand laminae,
crinoidal grainstone, yellow weathering
dolostone, rare black and red chert, green
sandstone, and larger intraclasts of intra-
formationally derived conglomerate. The
conglomerates form lenses and beds with
sandstone matrices within dominantly green
sandstones that are planar laminated or are
affected by a gently eastward dipping
foliation.

A mixtite composed of sandstone and
shale intraclasts in a shale-sand matrix
occurs towards the top of the coastal
section, 2 km north of the Arches. The
shale dominated sequences consist of finely
laminated mudrocks intercalated with 1 to
rarely 10 cm laminated and cross-laminated
siltstone and sandstone beds.

Cross-lamination and crossbeds in the
lower sandstones at Table Point suggest a
prevailing southward direction of sediment
transport. Crossbeds in sandstones near
Portland Creek indicate a southwestward to
westward paleocurrent direction.

The limestone breccia member of the
formation is of unknown thickness although
it is probably tens of metres thick. It
consists of indistinct, roughly bedded,
centimetre sized rubble enclosing blocks
that may approach the dimensions of a small
house. The lithoclasts in the breccia
include limestones of Table Point and Table
Cove Formation type as well as black and
green-gray shales and green sandstones com-
parable to the Black Cove Formation and
overlying sandstones. Exotic clasts include
white fenestral laminated limestones with

early geopetal fills and cements, bio-
clastic limestones and gray and white
mottled boundstones. Larger blocks exhibit
partial brecciation and buckling. Although
most of the breccias lack significant mud
matrix, one bed, several metres thick on
the western island of Portland Creek Pond,
contains limestone clasts floating in a
shale matrix. At the top of the unit, in
Portland Cove, the breccias are overlain by
granulose to fine grained calcarenites com-
posed of rounded gray limestone sand. They
are well bedded, graded, crossbedded and
internally convoluted. Channels within the
breccias north of Eastern Head, are also
filled with similar calcarenites that are
partly eroded by overlying breccia.

The unnamed Middle Ordovician sand-
stones and limestone breccias are generally
believed to have accumulated in a foreland
basin following collapse of the Lower
Paleozoic platform and east of advancing
Taconic allochthons. The green sandy
flysch, exhibiting sand and shale dominated
sequences and varieties of turbidites and
grainflows, probably formed upon deepwater
fans. The lower sandstones and shales
derived from the north, blanketed the
collapsed carbonate platform. However,
tectonic activity within the basin uplifted
both sands and parts of the underlying
platform which then disintegrated by mass
wastage and possibly tectonic disturbance.
Megabreccias accumulated in local areas of
the basin superceded by finer limestone
sand deposits as the uplifted platform
highs were reduced in size and/or blanketed
by the younger sequence of easterly derived
sandy flysch.

*Autochthonous or allochthonous sediments of
unknown age or affinity:* Limestone conglom-
erates, thin bedded limestones and shales
with minor sandstones form an unnamed rock
unit (map unit Cgl) on the ridge east of
Portland Hill. The unit is at least struc-
turally overlying the green sandstone of
Portland Hill, but no contact was observed
to prove stratigraphic continuity. A leafy,
gently eastward dipping lamination occurs
in the last observed outcrop of rotted
green sandstone before the limestone con-
glomerate is encountered. This fabric may
have been structurally produced however,
had the limestone conglomerate been thrust
over the sandstone. The limestone conglom-
erate unit has been mapped south of Five
Mile Road. The succession is dominated by
beds up to 4 m thick of pale gray, pebble-
to matrix-supported limestone conglomerate
composed of well sorted, rounded tabular
limestone lithoclasts. The lithoclasts
range up to 10 cm in size and include
laminated and thin bedded lime mudstones
and lesser oolitic and crinoidal grain-
stones. Some large limestone conglomerate
intraclasts also occur. The conglomerates
are intercalated with 2 to 10 m sequences

of shale and thin sandstones or laminated thin limestone beds intercalated with black shales, thin bioclastic limestones composed of crinoidal debris and 10 cm beds of calcareous siltstone and sandstone. Rare beds of sandstone which contain limestone intraclasts at the base, and grade up into thin planar stratification also occur in the thin bedded sequences. The unit resembles parts of the Cow Head Group. The presence of oolitic grainstones may suggest a Cambrian age since oolitic carbonates of platformal origin in western Newfoundland mostly occur in the rocks of Cambrian age.

The second sedimentary package of unknown affinity was mapped only in the southeastern part of the Portland Creek map sheet, north of Parsons Pond. It consists of a tightly folded sequence of black, gray, khaki and green .colored shales. Interbedded with the shales are nodular, laminated and massive, thinly bedded fine grained, gray limestones, and beds of laminated and cross-laminated, green-gray to buff calcareous siltstones and very fine grained micaceous sandstones. Sedimentary rocks exposed in rare outcrops within the large bogs and along some streams north of the centre of Parsons Pond include bedded gray and red cherts, green and red siltstones and mudstones as well as laminated, very fine grained sandstones. These fine grained sedimentary rocks which appear to structurally overlie unit Cgl are probably part of the Humber Arm Allochthon.

STRUCTURE

The map area like those to the north (Knight and Boyce, 1984), is dominated by a system of long, branching and anastomosing, curvilinear, high angle, north to northeast trending faults. These faults displace units vertically up to hundreds of metres and some are known to have strike-slip motion. Minor open to tight folds that parallel and trend oblique to faults have variable plunges. Locally steepened bedding and intense fracturing also characterize the fault zones.

On the Bellburns map area, particularly near and west of Eastern Blue Pond, a number of east-west faults that are generally downthrown to the northeast, cross-cut the stratigraphy and the northeast faults. In some instances, the latter offset, or terminate, against the west trending faults. An attractive structural interpretation of the area at the north end of Bateau Barrens, which is an alternative to that shown in figure 1, involves downthrowing north dipping Table Head rocks on the north side of west trending faults, against west dipping St. George Group.

Close to the Long Range Precambrian inlier near Western Blue Pond, bedding steepens and overturns in incompetent rocks such as the Forteau Formation and décollement occurs between the Forteau and the overlying Hawke Bay Formation. The Long Range western boundary fault has a sinuous to arcuate northeast trend from Parsons Pond north to Blue Mountain where the fault swings off almost eastward into the Precambrian inlier. This plus the presence of foliation and fracturing in chloritized granite and adjacent platformal rocks within a metre of the sharp fault plane suggests the fault is a thrust dipping at between 45 and 50° to the east. This conclusion is strengthened as the fault is traced south through the Indian Lookout and Portland Creek map sheets where intensity of deformation increases. Here inverted bedding, recumbent folds, eastward dipping reverse and thrust faults associated locally with recumbent west facing minor folds occur in autochthonous rocks in a zone up to 3 km wide within the adjacent platform. Older rock units override younger units westward in this zone. Caution is required in mapping the carbonates of this area, however, because most stratigraphic units have been recrystallized to a uniform fine, equigranular, vuggy, off-gray dolostone.

West of the 3 km zone of faulted platform, deformation of unnamed Middle Ordovician sandy and shaly flysch, is restricted to southeastward dipping monoclinal sequences. However, open, asymmetrical, southwest plunging folds with vertical to eastward dipping axial planes also affect the flysch along Western Feeder Brook and in Table Cove. A single cleavage occurs in interbedded shale beds.

Limestone conglomerates and thin bedded shales and limestones of unknown age structurally overlie the sandstones in a moderately dipping (12-29°) monoclinal southeastward filled sequence. However, allochthonous(?) fine siliciclastic rocks (Unit Cgl) in the southeast of the map area north of Parsons Pond are complexly deformed into a multitude of isoclinal to slightly recumbent folds that trend about 165°, and plunge gently (5 to 8°) to steeply (up to 75°) to the south. The folds which have a metre to decametre spacing, face westward with a well developed eastward dipping axial planar cleavage. Only one phase of deformation appears to have affected these rocks.

ECONOMIC GEOLOGY

The map area contains carbonate hosted Mississippi Valley-type sphalerite-rich district centred northeast of Daniels Harbour. The Daniels Harbour zinc mine, opened in 1975, recovers ore from several narrow, ribbon-like sphalerite lenses that occur in secondary dolostones that replace Catoche

limestones. The mineralization occurs adjacent to collapse breccia bodies associated with a regional late Arenigian disconformity near the top of the St. George Group. Description of host rocks and mineralization is given by Collins and Smith (1975), Lane (1984) and Crossley and Lane (1984). Sphalerite mineralization is also known in the area northeast and east of the mine and includes showings and prospects, such as the Trapper, in rocks of similar type and stratigraphic position.

Outside the district, mineralization is sparse. Some sphalerite crystals have been found in dolomite-cemented vugs along the shore near Deer Cove; black diagenetic dolomites of the Watts Bight Formation from a ridge 5 km west of Flat Pond responded to the application of a zinc reactive solution. However, no visible mineralization was seen.

ACKNOWLEDGEMENTS

REFERENCES

Boyce, W.D.
    1985: Cambro-Ordovician biostratigraphic investigations, Great Northern Peninsula, Western Newfoundland. *In* Current Research. *Edited by* R.V. Gibbons, Newfoundland Department of Mines and Energy, Mineral Development Division, Report 85-1.

Collins, J.A., and Smith, L.
    1975: Zinc deposits related to diagenesis and intrakarstic sedimentation in the Lower Ordovician St. George Formation, Western Newfoundland. Bulletin of Canadian Petroleum Geology, volume 23, pages 393-427.

Crossley, R.V., and Lane, T.E.
    1984: A guide to the Newfoundland Zinc Mines Limited ore bodies, Daniels Harbour. *In* Mineral Deposits of Newfoundland - A 1984 Perspective. *Edited by* H.S. Swinden and M.J. Murray, Newfoundland Department of Mines and Energy, Mineral Development Division, Report 84-3, pages 45-51.

Klappa, C.F., Opalinski, P.R., and James, N.P.
    1980: Middle Ordovician Table Head Group in western Newfoundland: a revised stratigraphy. Canadian Journal of Earth Sciences, volume 17, pages 1007-1019.

Knight, I.
    1977: Cambro-Ordovician platformal rocks of the Northern Peninsula, Newfoundland. Newfoundland Department of Mines and Energy, Mineral Development Division, Report 77-6, 27 pages.

    1978: Platformal sediments on the Great Northern Peninsula: Stratigraphic studies and geological mapping of the north St. Barbe District. *In* Report of Activities for 1977. *Edited by* R.V. Gibbons. Newfoundland Department of Mines and Energy, Mineral Development Division, Report 78-1, pages 140-150.

    1980: Cambro-Ordovician carbonate stratigraphy of western Newfoundland; sedimentation, diagenesis and zinc-lead mineralization. Newfoundland Department of Mines and Energy, Mineral Development Division, Open File Nfld. 1154, 43 pages.

    In preparation: Geology of Lower Paleozoic platformal rocks of the Port Saunders, St. John Island and parts of the Castors River map sheet. Newfoundland Department of Mines and Energy, Mineral Development Division.

Knight, I., and Boyce, W.D.
    1984: Geological mapping of the Port Saunders (12I/11), St. John Island (12I/14) and parts of the Torrent River (12I/10) and Bellburns (12I/6) map sheets, northwestern Newfoundland. *In* Current Research. *Edited by* M.J. Murray, J.G. Whelan and R.V. Gibbons, Newfoundland Department of Mines and Energy, Mineral Development Division, Report 84-1, pages 114-124.

Lane, T.E.
    1984: Preliminary classification of carbonate breccias, Newfoundland Zinc Mines, Daniel's Harbour, Newfoundland. *In* Current Research. *Edited by* M.J. Murray, J.G. Whelan and R.V. Gibbons, Newfoundland Department of Mines and Energy, Mineral Development Division, Report 84-1, pages 131-140. *Also in* Geological Survey of Canada, Paper 84-1A, pages 505-512.

Ross, R.J., and Ingham, J.K.
    1979: Distribution of the Toquima-Table Head (Middle Ordovician-Whiterock) faunal realm in the Northern Hemisphere. Geological Society of America Bulletin, volume 81, pages 393-408.

METALLOGENY OF THE TALLY POND VOLCANICS, VICTORIA LAKE GROUP, CENTRAL NEWFOUNDLAND

by

B.F. Kean
Mineral Deposits Section

ABSTRACT

The Victoria Lake Group in central Newfoundland is a thick sequence of volcanic, volcaniclastic and sedimentary rocks deposited during the development of an Early-Middle Ordovician island arc. Volcanic rocks occur within two principal volcanic units, informally termed the Tulks Hill and Tally Pond volcanics. The volcanic rocks consist of intercalated mafic and felsic rocks that are predominantly pyroclastic; mafic pillow lava is more common in the Tally Pond volcanics than in the Tulks Hill volcanics. The felsic volcanics occur as laterally extensive sheets of crystal and crystal-lithic tuff, breccia and minor flows. Sedimentary rocks consist of sandstone, siltstone, shale, argillite, chert and minor interbedded conglomerate. The clastic sedimentary rocks appear to be derived from the adjacent and underlying volcanic rocks of the Victoria Lake Group to the southwest.

Six volcanogenic sulfide occurrences are known in the Victoria Lake Group. Four occur in the Tulks Hill volcanics and two in the Tally Pond volcanics. The Tally Pond (Boundary) deposit and Burnt Pond project both occur in the felsic pyroclastics of the Tally Pond volcanics. The Tally Pond deposit comprises two zones of massive sulfides underlain by a zone of pervasive chlorite-pyrite (-chalcopyrite) alteration.

INTRODUCTION

Metallogenic studies, as part of a new five-year (1984-89) project designed to investigate the pre-Caradocian volcanogenic mineral deposits of central Newfoundland, were started in July, 1984. The 1984 studies concentrated on the Tally Pond Volcanics, and involved regional rock geochemistry and detailed stratigraphic, structural and geochemical studies in the area of the Tally Pond deposit.

Access to the area is provided by woods roads from Millertown and Grand Falls. The area is characterized by a heavily forested (fir, spruce), gently undulating landscape with extensive glacial till cover. Consequently, bedrock exposure is poor.

PREVIOUS WORK

Parts of the area have been mapped in detail by mineral exploration companies, including ASARCO, Abitibi-Price and Noranda. The first systematic geological mapping was done at 1:250,000 scale by the Geological Survey of Canada (Riley, 1957; Williams, 1970). The Newfoundland Department of Mines and Energy has done 1:50,000 scale regional mapping of the King George IV Lake (12A/4), Victoria Lake (12A/6), Star Lake (12A/11E), Lake Ambrose (12A/16), Noel Paul's Brook (12A/9), Buchans (12A/15), Badger (12A/16) and Grand Falls (2D/13) map areas (Kean, 1977, 1979a,b, 1983; Kean and Jayasinghe, 1980, 1982; Kean and Mercer, 1981).

Brown (1952) proposed the name 'Victoria River Series' for the volcanic and sedimentary rocks in the Lake Ambrose - Victoria River area. Riley (1957) proposed the name 'Strides Group' for similar rocks in the western half of the Red Indian Lake map area. Kean (1977) abandoned these names and proposed and defined the 'Victoria Lake Group' to include all the pre-Caradocian volcanic and sedimentary rocks in this area (Figure 1).

Volcanogenic sulfide mineralization in the rocks presently assigned to the Victoria Lake Group was first discovered in the early 1900's near the mouth of Victoria River. Subsequently, five other volcanogenic base metal deposits have been discovered, the Jacks Pond, Tulks East, Tulks Hill and Tally Pond (Boundary) deposits and the Burnt Pond prospect.

REGIONAL GEOLOGY

The Victoria Lake Group underlies that part of the Dunnage Zone of central Newfoundland which extends from Grand Falls in the northeast to King George IV Lake in the southwest; and from Red Indian Lake in the north to Noel Paul's Brook in the south.

The Ordovician geological development of the Dunnage Zone is recorded in three very broad geologic settings: (1) ophiolitic sequences which are interpreted to have formed as oceanic crust; where contacts are preserved, these are always the stratigraphically lowest units and they are believed to represent basement to most of

Figure 1: *Early to Middle Ordovician volcanic-dominated island arc sequences and massive sulfide deposits (solid squares) in central Newfoundland. A – Victoria Lake Group; B – Carter Lake Formation. Lines – felsic volcanic rocks; Vees – mafic and intermediate volcanic rocks; stippled – sedimentary rocks. Massive sulfide deposits: 1. Victoria Mine; 2. Jacks Pond; 3. Tulks East; 4. Tulks Hill; 5. Burnt Pond; 6. Tally Pond (after Swinden and Thorpe, in press).*

the younger rocks in the Dunnage Zone; (2) tholeiitic and calc-alkaline volcanic and subvolcanic rocks and related volcaniclastic rocks which stratigraphically overlie the ophiolites and range up to 8 km in total thickness. These units consist of mafic and felsic, dominantly submarine volcanic and volcaniclastic rocks, and are generally interpreted to represent the remains of one or more Early-Middle Ordovician island arcs; and (3) post-island arc flysch, argillite and conglomerate which stratigraphically overlie many of the island arc sequences and are mainly derived from them. These sedimentary rocks range in age from Middle Ordovician to Early Silurian and are succeeded by younger Silurian rocks consisting of subaerial, mainly felsic, volcanic rocks and terrestrial sediments.

In the south-central part of the Dunnage Zone, the ophiolite sequences are represented by the King George IV Lake, Annieopsquotch, Star Lake and Shanadithit Brook Complexes. The King George IV Lake and Annieopsquotch Complexes are faulted against the Early-Middle Ordovician

island arc sequences of the Victoria Lake Group to the southwest of Red Indian Lake, but are interpreted to have been in original stratigraphic continuity (Herd and Dunning, 1979).

The Victoria Lake Group is conformably overlain by Caradocian age black shales and cherts in the northeast which in turn are conformably overlain by Middle Ordovician to Early Silurian flysch, argillite and conglomerate. Siltstone and tuffaceous sandstone of the Harbour Round Formation overlie the Victoria Lake Group in the Red Indian Lake area. This assemblage of rocks is in fault contact with the Buchans Group and the Southwest Brook Complex along the Lloyds River - Red Indian Lake fault system to the northwest.

The southern and southeastern limits of the Victoria Lake Group are marked by the unconformably overlying, locally fault-modified, Rogerson Lake Conglomerate, which in turn is faulted against the mafic volcanics of the Pine Falls Formation and unnamed volcanic, sedimentary and metamorphic rocks south of Noel Paul's Brook.

Rocks of the study area occupy a regional northeast-trending anticlinorium (Victoria Anticlinorium). Regionally, the sequence youngs northwesterly on the north limb and southeasterly on the south limb of this structure; however, there are many smaller scale, first order and second order folds resulting in variable facing directions. Poor exposure, however, generally precludes deciphering the detailed structure.

GEOLOGY OF THE VICTORIA LAKE GROUP

The Victoria Lake Group is a sequence of volcanic, epiclastic and sedimentary rocks that has been dated by conodonts collected from limestone lenses near the stratigraphic top of the Group as Late Llanvirnian (Kean and Jayasinghe, 1982). It is also conformably overlain by Carodocian shale and chert (Kean and Jayasinghe, 1982). The thickness of the Group cannot be estimated with any degree of certainty because of folding and poor exposure.

The Victoria Lake Group can be divided into two major regional facies: (1) volcanic rocks in the southwest and along its southeastern margin, comprising approximately 60% of the group, and (2) a predominantly sedimentary facies to the northeast which is laterally equivalent and derived from the volcanic rocks.

Volcanic Rocks

Volcanic rocks predominate in the southwestern part of the Victoria Lake Group and along its southeastern margin. The two principal volcanic units are informally termed the Tulks Hill volcanics in the southwest and the Tally Pond volcanics in the southeast. Due to poor exposure and complicated structural relations, it is not known whether the Tally Pond volcanics are stratigraphically equivalent to the Tulks Hill volcanics. However, the types of felsic volcanic rocks and the relative proportions of felsic and mafic lithologies in the two units are similar. Small intercalations of volcanic rocks also occur within the clastic sedimentary rock facies of the Victoria Lake Group to the northeast. Similar rock units are sporadically present farther east and are assigned to the Carter Lake Formation (Kean and Jayasinghe, 1980).

Tulks Hill volcanics: The Tulks Hill volcanics, host to the Victoria mine and the Jacks Pond, Tulks East and Tulks Hill deposits, consist of mafic to felsic volcanic rocks. The mafic volcanic rocks are mainly pyroclastic, comprising mafic to intermediate aquagene tuff, reworked tuff, lapilli tuff, agglomerate and breccia. Mafic epiclastic volcanic rocks are also common. Mafic lavas are not common in this unit, but where present they exhibit small, commonly flattened, pillows with thin selvages and little interpillow material. Pillow breccias are present locally.

The felsic volcanic rocks occur as laterally extensive sheets of crystal and crystal-lithic tuff, breccias and minor porphyritic flows and shallow intrusions. The major significant mineralization occurs in the felsic volcanics.

Tally Pond volcanics: The Tally Pond volcanics consist of intercalated mafic and felsic volcanic rocks. The mafic volcanic rocks comprise vesicular and amygdaloidal, generally pillowed, flows and mafic to andesitic tuff, agglomerate and breccia. Mafic pillow lava is more common in the Tally Pond volcanics than in the Tulks Hill volcanics. The pillows are generally small and have little interpillow material; where present, the latter consists of mafic tuff (probably hyaloclastic) and minor green chert. The breccias contain mafic volcanic rock fragments that range up to 20 cm across. Some of the breccias contain pillow fragments and are interpreted to be pillow breccias.

The felsic volcanic rocks, which are host to the Tally Pond deposit and Burnt Pond prospect, consist of tuff, lapilli tuff and breccia. Flow-banded rhyolite and rhyolitic breccia are locally present and quartz-feldspar, generally black, subvolcanic porphyries are common. The lapilli tuff consists of subangular to rounded clasts of white, gray and green dacite and rhyolite, in places flow banded, in a fine grained to locally vitric, tuffaceous matrix. The breccias contain angular felsic volcanic fragments ranging from 3 to 45 cm in length in a tuffaceous matrix. Locally, gas breccias are developed and consists of flow-aligned, *in situ* brecciated clasts in an aphanitic to vitric, siliceous matrix.

Carter Lake Formation: The Carter Lake Formation consists of predominantly felsic volcanic rocks with fewer mafic volcanic rocks. It occurs intercalated with unnamed sedimentary and metasedimentary and metavolcanic rocks south of Noel Paul's Brook, and is not part of the Victoria Lake Group, but is interpreted to be age equivalent.

Mafic volcanic rocks consisting of pillow lava and pillow breccia are minor. The pillows range from 16 to 60 cm in size and contain calcite amygdules near their margins.

Quartz and quartz-feldspar porphyries and crystal tuffs, minor crystal-lithic, fine-grained silicic tuff and faintly flow-banded rhyolite comprise the felsic volcanic rocks.

Sedimentary Rocks

Clastic sedimentary rocks constitute most of the northeastern facies of the Victoria Lake Group (Kean and Jayasinghe, 1982). This facies consists of sandstone (graywacke) with interbedded siltstone, shale, argillite, conglomerate and rare limestone. Siliceous siltstone and chert are more common near the top of the sequence. Locally, there are thin inter calations of volcanic rocks.

The sequence generally displays cyclic bedding. A typical cycle consists of a lower unit of conglomerate and pebbly sandstone constituting almost 40% of the cycle. It generally has erosional bases with scour and fill structures, load casts and flame structures. It grades upwards into sandstone, which forms about 50% of the cycle. The sandstone grades from coarse at the bottom to fine towards the top, where faint laminations, crosslaminations or convolute laminations may be developed. The sandstone layer is overlain by thinly laminated siltstone, argillite or shale. The contact between the siltstone and underlying sandstone is sharp and free of erosional features. The cycles mainly include ABCE and ABE Bouma divisions (Bouma, 1962) and, locally, CE divisions.

These clastic sedimentary rocks contain a predominance of volcanic detritus and both the amount of pyroclastic material and the coarseness of pyroclastic and epiclastic material increase towards the volcanic rocks of the Victoria Lake Group to the southwest. This suggests that the clastic sedimentary rocks were derived from the adjacent and underlying volcanic rocks of the Victoria Lake Group.

Intrusive Rocks

The Victoria Lake Group is intruded by linear bodies of medium grained quartz monzonite, minor granite and granodiorite which appear to be related to volcanism. Fine to medium grained diorite and gabbro with rare coarse grained phases occur as small plugs to large bodies throughout the Victoria Lake Group.

VOLCANOGENIC SULFIDES

Six principal volcanogenic base metal sulfide occurrences are known in the Victoria Lake Group. They are the Victoria mine and the Jacks Pond, Tulks East and Tulks Hill deposits in the Tulks Hill volcanics and the Tally Pond (Boundary) deposit and Burnt Pond prospect in the Tally Pond volcanics. The locations of these deposits and prospects are shown on Figure 1. Of these, only the Tally Pond deposit will be discussed here.

Tally Pond (Boundary) deposit: The Tally Pond (Boundary) deposit, a significant Cu-Zn-Ag massive sulfide deposit, was discovered by Noranda Exploration Limited in 1982. Grades and tonnage figures are confidential at present.

The rocks near the deposit are poorly exposed and the massive sulfide body is exposed by trenching. Diamond drill core offers the best opportunity to study the mineralization.

The deposit occurs within a gently dipping sequence of felsic lapilli tuff on the south limb of a northeast-trending anticline developed on the south limb of the Victoria Anticlinorium. However, parasitic folds, probably on the scale of tens of metres, and possible minor cross-folds complicate the local structure. The deposit occurs in an inlier of the felsic volcanics which is overlain to the north and south by fine siliceous siltstone and interbedded sandstone.

The deposit actually consists of two zones, referred to as the North and South Zones. The North Zone dips gently northwards for the most part and the South Zone dips gently southeastward; however, dips in the eastern part of the South Zone appear to be to the north. There is no conclusive evidence that the North and South Zones are structural repeats of the same strati graphic horizon. Both zones have areas of alteration developed beneath them. Both the alteration areas extend or dip to the north. A rhyolite dome or plug with associated breccia is present in the South Zone.

The deposit mineralogy consists of fine grained pyrite and variable amounts of chalcopyrite, covellite and sphalerite; galena is present locally as a minor constituent. The contacts of the massive sulfides with the hanging wall and the footwall are sharp, although the footwall displays a zone of pervasive alteration that is generally present below the massive sulfides, in particular in the proximal facies. Also in the proximal facies, breccia textures are locally well developed. Distal parts of the massive sulfides generally display well developed bedding and laminations and, locally, graded bedding is apparent; there is generally very little alteration in the footwall in these areas.

The alteration consists mainly of variably intense chloritization accompanied by veinlets, blebs and disseminations of pyrite and lesser chalcopyrite. The chloritization is characterized by black chlorite which occurs in and replaces the matrix of the tuffs and locally completely replaces the rock. It also occurs as veins

and blebs. *In situ* gas(?) brecciation and veining by chlorite and minor graphite are locally developed. Sporadically and randomly developed in the alteration zones are white, bleached areas caused by sericitization and silicification; this type of alteration is well developed in parts of the South Zone. The alteration zones are interpreted to represent volcanogenic hydrothermal activity related to massive sulfide deposition.

ACKNOWLEDGEMENTS

Robert Lane of Buchans provided capable and cheerful assistance during the field season. J.E.S. James, Colin McKenzie and Dennis Fitzpatrick of Noranda Exploration and Geoff Thurlow of Abitibi-Price are thanked for help and stimulating discussion.

The manuscript has benefited from critical reading by Paul Dean and Cyril O'Driscoll.

REFERENCES

Brown, N.E.
1952: Geology of the Buchans Junction area, Newfoundland. M.Sc. thesis, McGill University, Montreal, Quebec, 83 pages.

Bouma, A.H.
1962: Sedimentology of some flysch deposits. A graphic approach to facies interpretation. Elsevier, Amsterdam, 168 pages.

Kean, B.F.
1977: Geology of the Victoria Lake map area (12A/6), Newfoundland. Newfoundland Department of Mines and Energy, Mineral Development Division, Report 77-4, 11 pages.

1979a: Star Lake map area, Newfoundland. Newfoundland Department of Mines and Energy, Mineral Development Division, Map 79-1.

1979b: Buchans map area, Newfoundland. Newfoundland Department of Mines and Energy, Mineral Development Division, Map 79-125.

1983: Geology of the King George IV Lake map area (12A/4), Newfoundland. Newfoundland Department of Mines and Energy, Mineral Development Division, Report 83-4, 67 pages.

Kean, B.F., and Jaysinghe, N.R.
1980: Geology of the Lake Ambrose (12A/10) - Noel Paul's Brook (12A/9) map area, central Newfoundland. Newfoundland Department of Mines and Energy, Mineral Development Division, Report 80-2, 29 pages.

1981: Geology of the Badger map area (12A/16), Newfoundland. Newfoundland Department of Mines and Energy, Mineral Development Division, Report 81-2, 37 pages.

Kean, B.F., and Mercer, N.L.
1981: Grand Falls map area (2D/13), Newfoundland. Newfoundland Department of Mines and Energy, Mineral Development Division, Map 8199.

Riley, G.C.
1957: Red Indian Lake (west half), Newfoundland. Geological Survey of Canada, Map 8-1957 with descriptive notes.

Williams, H.
1970: Red Indian (east half), Newfoundland. Geological Survey of Canada, Map 1196A.

GEOLOGY OF THE BURGEO MAP AREA
((11P/12), SOUTHWESTERN NEWFOUNDLAND

by

S.J. O'Brien and S.L. Tomlin
Newfoundland Mapping Section

ABSTRACT

The Burgeo map area lies within the southwestern segment of the Hermitage Flexure of the Newfoundland Appalachians. The area is underlain primarily by granitoid rocks of the synkinematic Burgeo granite and the late to posttectonic Chetwynd granite. Both plutons contain zones of earlier migmatite whose protoliths include sedimentary rocks of the mid-Ordovician Bay du Nord Group and gabbros of equivocal age and origin. The Burgeo granite is an extensive early to mid-Silurian, synkinematic, composite, granitoid pluton. Its earliest intrusive phases are diorite and xenolith-rich K-feldspar porphyritic granodiorite; subsequent phases are more granitic in composition. Field relationships indicate that magmatism produced distinct, albeit temporally overlapping, phases. The Chetwynd granite is a high level, siliceous granitoid that intruded the Burgeo granite after the culmination of the regional tectonothermal event. It has untested potential for economic concentrations of F-Sn-W-Mo and U.

INTRODUCTION

The Burgeo map area (Figure 1), bounded by north latitudes 47°30' and 47°45' and west longitudes 57°30' and 58°00', is centred approximately 8 km west of Burgeo, on the southwest coast of Newfoundland. Most of the Burgeo map area east of Grandy's Brook is accessible via route 480, a partially paved highway, which bisects the map area. The area west of Grandy's Brook is in part accessible from the coast; ready access to the remainder requires aircraft support.

Figure 1: *Location of the study area.*

Physiographically, the area forms part of the "Atlantic Uplands" of Twenhofel and McClintock (1940), and is characterized by a dissected peneplain surface marked by monadnocks at approximately 330 m to 350

m. Evidence of the Wisconsin glaciation is found in the wide variety of depositional and erosional glacial landforms and features. Geological control of topography is evident in the topographic contrast between areas underlain by the Burgeo and Chetwynd granites. Much of the area underlain by porphyritic phases of the Burgeo granite has an irregular, rugged topography, which southwards is further dissected by fault controlled valleys and gorges. In contrast the mainly equigranular Chetwynd granite and the lithologically similar parts of the Burgeo granite are characterized by a gentle, more rolling topography.

Previous systematic geological studies in the Burgeo area include the 1:250,000 scale mapping of Riley (1959); regional reconnaissance mapping was carried out by the Buchans Mining Company (Scott and Conn, 1950) and a 1:50,000 scale compilation of this work was published by Smyth (1979). Regional lake sediment geochemical studies by the Newfoundland Department of Mines and Energy (Butler and Davenport, 1980) led to follow-up exploration by Shell Canada Resources Ltd. and Falconbridge Nickel Co. Ltd. (Barry et al., 1981). Airborne gamma-ray spectrometric surveys of the region were carried out by the Geological Survey of Canada in 1984.

GENERAL GEOLOGY

The Burgeo map area is underlain by granite and migmatite, part of the Hermitage Flexure (Williams et al., 1970) of the southern Newfoundland Appalachians. The area contains three major geological elements:

1. An Ordovician or earlier suite of metasediment, paragneiss and migmatite,

2. The Burgeo granite, a large Silurian (?), mostly synkinematic, lithologically diverse pluton of mainly granodioritic to granitic composition, and

3. The Chetwynd granite, a Devonian (?), essentially posttectonic, high level, quartz rich pluton.

MIGMATITES AND METASEDIMENTARY ROCKS (Units 1 and 2)

These rocks include the migmatites, agmatites, metasedimentary rocks and paragneisses that are intruded by and form xenoliths within the Burgeo granite and, to a lesser degree, within the Chetwynd granite. Unit 1 consists mainly of migmatite and agmatite with amphibolite and minor paragneiss. Unit 2 is generally of metasedimentary origin but contains minor amphibolite.

Unit 1

Migmatite and agmatite of Unit 1 are exposed mainly along a 2 km wide coastal strip west of Burgeo, underlying much of the Sandbanks and the eastern part of the Big Barasway (Figure 2). A diagnostic feature of Unit 1 migmatite is that it forms well rounded, albeit knobby, gray weathering exposures that are largely devoid of any vegetation. Rocks of Unit 1 display a random gradation between agmatite and migmatite. The agmatites consist of dark green and gray to black, either massive or banded gabbro and diorite xenoliths in a granitoid host (Plate 1). The The orientation of banding within the blocks varies widely from that which is

Plate 1: *Gabbroic xenoliths in agmatite of Unit 1.*

developed in the surrounding granitoid. The granitoid is mainly equigranular but locally contains rare feldspar phenocrysts, and has a weakly developed to pronounced banding. The blocks are either flattened or subrounded to rounded and rarely angular; they range from a few centimetres to approximately 2 m in maximum dimension (Plate 2). Within the agmatite, the proportion of matrix to inclusion is highly variable, and the inclusions show varying degrees of migmatization or assimilation into the granitoid matrix (Plates 3 and 4). The true migmatites display raft textures, together with nebulitic and schlieren structures. Commonly, these migmatites are irregularly layered into biotite ± hornblende rich bands and granitoid bands. Orientation of the banding is quite variable. The banding itself is variably developed and the migmatite leucosome may be either gneissic or nebulitic and, locally, massive (Plate 5). In the nebulitic migmatite good equigranular texture is preserved; grain size is variable but usually about 1–2 mm. Very rarely, the granitoid contains isolated feldspar phenocrysts. Locally, the migmatite is cut by posttectonic coarse grained, muscovite rich, granitoid pegmatite.

Plate 2: *Large xenolith of banded gabbro, Unit 1.*

Unit 1a consists of the migmatite and agmatite which underlies an area of about 7 km^2 near the Wolf Hills, approximately 6 km north of Burgeo. The migmatite is designated as a separate subunit because it contains irregularly shaped and sized rafts and xenoliths of paragneiss, as well as amphibolite and gabbro. The migmatitic granitoid is well banded or nebulitic, and contains irregular shaped zones with a

LEGEND

PLEISTOCENE TO RECENT

12   *Unconsolidated sand and cobbles.*

DEVONIAN AND EARLIER

11   *Fine and medium grained diabase.*

10   *Pink, quartz-feldspar porphyry.*

CHETWYND GRANITE

9   *Pink, fine grained, equigranular or quartz porphyritic granite: coarse grained equigranular granite and minor K-feldspar porphyritic granite; 9a, pink equigranular granite with screens of rhyolite tuff.*

BURGEO GRANITE (Units 3 to 8)

8   *Pale pink to white, fine to locally coarse grained, equigranular biotite ± muscovite, rarely garnetiferous granite and adamellite; minor aplite; 8a, dark grey, foliated, equigranular biotite ± muscovite granite and granodiorite.*

7   *Pink, orange and red, coarse grained porphyritic adamellite and granite.*

6   *Pink, medium and coarse grained, phenocryst rich, K-feldspar porphyritic granite; 6a, aplite.*

5   *Grey and pale pink, variably porphyritic granite and adamellite; minor aplite; 5a, unseparated variably porphyritic and equigranular granite.*

4   *Grey, white and pale pink, foliated, coarse grained, K-feldspar porphyritic, xenolith bearing granodiorite; minor adamellite; 4a, xenolith rich porphyritic granodiorite; 4b, pink aplite; 4c, granite pegmatite.*

3   *Dark green and grey, fine to medium grained diorite; minor agmatite.*

ORDOVICIAN(?)

2   *Migmatized semi-pelitic schist; paragneiss; amphibolite; granite migmatite.*

1   *Migmatite, including agmatite, and associated granitoid; 1a, migmatite, biotite schist, amphibolite and metadiorite; minor peletic schist; 1b, grey migmatic to equigranular granitoid.*

Plate 3: *Partially assimilated diorite xenolith in migmatite of Unit 1.*

Plate 4: *Remnants of metabasic xenolith in migmatite of Unit 1.*

Figure 2: *Geology of the Burgeo Map area, southwestern Newfoundland.*

Plate 5: *Banding in leucosome of Unit 1 migmatite.*

Plate 6: *Migmatized metasedimentary raft in the Chetwynd granite.*

coarser grain size than that of the surrounding rock. As is the case with Unit 1, migmatites of Unit 1a are cut by posttectonic muscovite-bearing granite pegmatite dikes.

Unit 1b consists of fine to medium grained, gray, mainly equigranular to nebulitic granite, which borders Unit 1a to the south. It grades northwards into Unit 1a migmatite.

Unit 2

Unit 2 is a poorly exposed zone of metasedimentary rocks, granite and migmatite that is surrounded by equigranular and porphyritic phases of the Burgeo granite in the northeasternmost corner of the Burgeo map area. Similar metasedimentary migmatite occurs as inclusions in the Chetwynd granite, east of Connoire Bay. It consists of biotite schist associated with amphibolite, variably migmatized semipelite and associated psammite (Plate 6). Associated with, but not in contact with the metasediments, is a cataclastically foliated, locally migmatitic granitoid, containing xenoliths of paragneiss and amphibolite.

The origin of Unit 2 and its relationship to Unit 1 are uncertain. The migmatites and the metasedimentary rocks are probably equivalent to either the Ordovician La Poile or Bay du Nord Groups, exposed nearby (O'Brien, 1983; O'Brien and Tomlin, 1984; Blackwood, 1984). Presumably, the paragneiss has a similar protolith.

Burgeo granite (Units 3,4,5,6,7,8)

The Burgeo granite is a new name that is informally proposed to denote the large (approximately 3,000 km^2), roughly semicircular shaped, synkinematic granitoid pluton in southwestern Newfoundland, which is exposed between Connoire Bay and La Hune and whose northernmost extension lies near Top Pond (approximately 47°56' latitude). The new name Burgeo granite replaces the previously used name Burgeo Batholith (Williams, 1978; O'Brien, 1983; O'Brien and Tomlin, 1984).

U/Pb isotopic studies on the Burgeo granite are ongoing; finalized data are not available at the time of writing, but an early to mid-Silurian age is indicated by preliminary results (Krogh, personal communication, 1984).

The Burgeo granite underlies approximately 340 km^2 in the Burgeo map area, and represents almost 75 percent of the total land area there. On the basis of texture, lithology and field relationships, the granite has been divided into six distinctive phases. In order of decreasing age these include: fine and medium grained diorite (Unit 3), foliated, coarse grained porphyritic granodiorite (Unit 4), foliated, variably porphyritic granite and adamellite (Unit 5), locally foliated, pink, phenocryst rich, biotite granite (Unit 6), locally foliated, red, coarse grained, porphyritic adamellite and granite (Unit 7), and foliated and massive equi-

granular biotite ± muscovite granite (Unit 8).

Unit 3

Unit 3 is the least extensive phase of the Burgeo granite, underlying a total exposed area of less than 0.5 km^2. The unit is best exposed on several islands southwest of Burgeo. It consists of dark green and gray, fine to medium grained hornblende diorite. Near its contacts with porphyritic granodiorite (Unit 4), the diorite is agmatized.

The unit is not in contact with either of units 1 or 2, and the relationship between the diorite and the migmatites is unknown. Diorite underlies a small island several metres away from exposures of Unit 1 migmatite. If this diorite is part of Unit 3, then the close spatial association may indicate that the diorite and migmatites are related. Alternatively, it may be a large block within the agmatites, genetically unrelated to the later diorite of Unit 3.

Unit 4

Unit 4 is the most extensive phase of the Burgeo granite, constituting approximately 50 percent of the granite's area. Well exposed throughout, it underlies much of the area north of Connoire Bay, the area in and around Kings Harbour Brook, the area north and east of Big Barasway, and in and around the community of Burgeo.

Unit 4 contains a distinctive, xenolith-rich phase (subunit 4a). Pink aplite (4b) and granite pegmatite (4c) dikes are widespread and diagnostic of the unit.

Unit 4 consists mainly of biotite rich granodiorite and minor amounts of adamellite, which form characteristically knobby, white or gray weathering exposures. The granodiorite is either light to dark gray, mottled black and white, or pale red, with either white or pink phenocrysts (Plate 7). It is generally porphyritic, with 2-4 cm subhedral K-feldspar phenocrysts in a quartz, plagioclase, biotite ± sphene ± rare hornblende groundmass. Biotite is a major component, locally constituting up to 40% of the mode. The groundmass grain size is variable and gradationally between 2 mm and 1 cm. The proportion of phenocrysts to matrix is variable, with phenocrysts constituting between 10% and 30% of the rock. Rarely the granodiorite is essentially free of phenocrysts. Chloritized biotite, cloudy quartz and sericitized feldspar are typical alteration features. Unit 4 granodiorites and adamellites are either xenolith free or contain up to 5% xenoliths of either diorite, quartz diorite or gabbro. It is also weakly to strongly foliated, locally displaying a cataclastic fabric.

Plate 7: *K-feldspar porphyritic granodiorite, Unit 4 of the Burgeo granite.*

Unit 4a is a coarse grained, porphyritic granodiorite rich in mafic xenoliths. It forms a 0.5 to 1.0 km, roughly east-west trending zone within Unit 4 granodiorite; its contact with that phase is gradational. With the exception of the xenoliths, it is lithologically the same as Unit 4. The phase contains from 5 to 50 percent, characteristically flattened, gabbro, diorite and quartz diorite xenoliths from a few centimetres to 1 metre in length (Plate 8). While most xenoliths have sharp, rounded boundaries, some are partially assimilated into the granodiorite.

Plate 8: *Xenolith-rich granodiorite, Unit 4a of the Burgeo granite. Width of field of view is approximately 10 m.*

Units 4b and 4c are composed of dikes of aplite and pegmatite respectively, which intrude units 4 and 4a. The aplite is pink, fine grained and rarely quartz porphyritic, commonly sheared or brecciated, and form both distinct dikes and network vein systems. The pegmatite is composed of quartz and K-feldspar, with or without plagioclase, muscovite and biotite. They form pegmatitic or monomineralic segregations, veinlets and sharply bounded dikes.

Units 4 and 4a show both intrusive and gradational relationships with Units 1 and 1a and are intrusive into Units 2 and 3. The contact between Unit 4 and Unit 1 migmatite near Grandy's Brook is locally represented by a zone, several tens of metres wide, where the migmatite is cut by dikes and variably shaped plugs of porphyritic granite. In the same area, however, the granodiorite contains partially assimilated magnetite rich metabasic xenoliths near the contact. The granodiorite is gradational with finer grained, recrystallized, equigranular granitoid, similar to the migmatitic granitoids of Unit 1. This zone appears gradational into inclusion rich migmatite of Unit 1. The gradational nature of the contact between the granite and the migmatite suggests that migmatite formation and early plutonism are essentially contemporaneous, and that the migmatites may represent deep levels of the Burgeo granite.

The contact between Units 4 and 1a is marked by a hybrid zone of granodiorite, nebulitic migmatite and equigranular granite. The granodiorite locally grades into nebulitic granitoid migmatite (orthogneiss) over a distance of 1 m.

The contact between Units 4 and 2 is sharp and intrusive in nature. The contact of units 4 and 3 is similar, and is locally marked by a narrow (approximately 10 m) zone of agmatite.

Unit 5

Unit 5 is a granite-adamellite phase which is spatially associated with Unit 4. Unit 5 intrudes Unit 4 in most areas, but locally the contact is gradational. This phase includes equigranular biotite rich adamellite, equigranular granite, variably porphyritic granite and adamellite, and dikes of aplite and fine grained leucocratic adamellite. It differs from Unit 4 in that it: (1) is lithologically more diverse; (2) is more granitic in composition; (3) is either equigranular or more sparsely porphyritic; (4) generally contains less biotite; and (5) contains fewer xenoliths. Typical exposures are gray, pale pink or pale red and lack the knobby appearance of Unit 4. Porphyritic varieties usually contain either between 1 and 5 per-cent or 10 and 15 percent phenocrysts; rarely, up to 40 percent phenocrysts have been noted. The phenocrysts vary from 0.5 cm to 2 cm in length and are irregularly dispersed in a fine to medium grained groundmass of quartz plus K-feldspar, with or without biotite, sphene and rare muscovite. On average the unit is less melanocratic than Unit 4, with 3 percent to 5 percent biotite being characteristic. Equigranular varieties are medium to coarse grained and in many places are gradational into porphyritic granite. Locally the granite is more biotite rich, containing small (less than 50 cm^2) cognate zones of quartz diorite and tonalite. Unit 5 is pervasively foliated and metamorphosed.

Dikes of sparsely porphyritic aplite and granite, presumably related to Unit 5, cut porphyritic granodiorite of Unit 4. In other areas the contact appears to be gradational, and is based largely on a gradual decrease in phenocryst population from Unit 4 into Unit 5.

Unit 6

Unit 6 is a phenocryst-rich granite phase of the Burgeo granite, tentatively interpreted to be partly equivalent in age to Unit 5. It is exposed along the coast between Connoire Head and Big Barasway, northwards to Cobbler Hill, and in isolated stocks near Muddy Hole Bay and northeast of Connoire Bay. The granite is mainly medium to coarse grained, porphyritic, biotite-bearing and characteristically rich in euhedral, equant, 1-2 cm K-feldspar phenocrysts (Plate 9). It is pink or red, with diagnositc pink or pink and white, rapikivi-textured K-feldspar phenocrysts.

Plate 9: *K-feldspar porphyritic granite, Unit 6 of the Burgeo granite.*

Locally, textural variations occur, and the porphyritic phase is gradational into smaller zones of coarse grained equigranular granite. Pink, fine grained, equigranular granite and aplite dikes are widespread within the unit. Aside from a smaller modal proportion of biotite, Unit 6 is mineralogically similar to Units 4 and 5. The unit appears to lack the pervasive foliation and extensive metamorphism of earlier phases. It is, however, foliated locally, and is also sheared and brecciated along late northeast and northwest trending faults.

Unit 7

Unit 7 includes porphyritic granite and adamellite, that form a 10 km^2 boss east of Bay de Loup. Characteristically, it is either pink, orange or red, medium to coarse grained, K-feldspar porphyritic and generally phenocryst rich. The unit locally contains xenoliths and large (approximately 100 m^2), stoped rafts of diorite. It is foliated and brecciated along a major northeast trending fault which passes through Bay de Loup. This fault separates Unit 7 from the remainder of the Burgeo granite, thus its temporal relationship to Units 4, 5 and 6 is uncertain.

Unit 8

Unit 8 includes the equigranular — tured granitic phases of the Burgeo granite. These occur throughout the map area, forming more than a dozen separate bosses ranging in area from less than 1 km^2 to approximately 20 km^2. On the basis of color, biotite content and the presence or absence of xenoliths, the equigranular phases can be divided into two subunits.

Unit 8 consists of granite, adamellite, microgranite and aplite. These are either white to pink or light gray, and either fine, medium or coarse grained, and free of xenoliths (Plate 10). The granitoids are typically rich in K-feldspar and quartz, and contain variable amounts of biotite plus muscovite and garnet locally. Estimated modal biotite content is normally between 1 percent and 5 percent, but locally reaches up to 15 percent.

Unit 8 is typically equigranular; however, there is a slight, gradational increase in its K-feldspar phenocryst content towards the contact with Unit 5. Unit 8 lacks the ubiquitous foliation of Unit 4, but is affected locally by the regional deformation.

Unit 8a outcrops in the vicinity of Six Mile Hill, west of Grandy's Brook. It consists of light to dark gray, foliated, equigranular, biotite ± muscovite granite and granodiorite. Unit 8 contains numerous

Plate 10: *Equigranular granite, Unit 8 of the Burgeo granite.*

diorite xenoliths. Unit 8a is presumed to be intrusive into Unit 5; it intrudes and is in fault contact with Unit 4.

Unit 8 intrudes Units 1a, 4 and 5. Its contacts with 1a and 4 are sharp; both units are cut by narrow dikes of Unit 8. Both dikes and country rocks are at least locally affected by the same regional foliation. Although crosscutting relationships are seen locally, the contact of units 5 and 8 is generally gradational, marked by a gradual increase in phenocrysts from Unit 8 into Unit 5.

Chetwynd granite (Unit 9)

The name Chetwynd granite (Cooper, 1954) denotes the late to posttectonic granite which intrudes the Burgeo granite in the west-central parts of the map area. These rocks form the eastward extension of the granite from its type exposures in the La Poile area (Chorlton, 1978). The granite underlies approximately 75 km^2 of the Bureo area, and is intrusive into Units 4, 5 and 6 of the Burgeo granite.

The Chetwynd granite has yielded zircons dated at 377 ± 20 Ma (Dallmeyer, 1980). $^{40}Ar/^{39}Ar$ spectra for biotite from the granite in the adjacent La Poile area indicate a cooling age of 372 ± 5 Ma for the Chetwynd granite (Dallmeyer, 1980).

The Chetwynd granite, undivided in the Burgeo map area, is a high level, essentially massive, quartz rich granite. It is either pink or red and locally white weathering. It is texturally variable but mainly medium to coarse grained and equi-

granular. Locally, the granite contains zones that are fine grained quartz porphyritic, fine grained K-feldspar porphyritic, or rapikivi textured. The granite is characteristically leucocratic, with less than 1-2% modal biotite. It contains rare granitoid xenoliths and is, in places, miarolitic. The Chetwynd granite is essentially posttectonic, and intrudes the Burgeo granite after the main regional deformation. Structurally, it is characterized by a pronounced northeast trending parallel joint system;it is cut by several late faults which have little obvious displacement. The granite is intrusive into Units 4, 5 and 6 of the Burgeo granite and contains variably sized inclusions of Unit 1a metasediments, migmatites and diorite. Near the west boundary of the map area, the granite contains inclusions and small roof pendants of felsic tuff and tuffaceous sediments; these are presumably related to the La Poile Group to the west (e.g. Chorlton, 1978). A zone of network veins, dikes and stocks of Chetwynd granite intrude the Burgeo granite at the contact; the contact zone is of variable extent, in places over 1 km wide.

Units 10 and 11

These units consist of late, posttectonic dikes, which intrude the Chetwynd and Burgeo granites and the earlier migmatites. Unit 10 is composed of pink, leucocratic, fine grained, quartz and feldspar porphyritic, granite dikes. These are widely distributed and vary widely in orientation. They are locally continuous along strike for several hundreds of metres and have characteristically straight, sharp boundaries.

Unit 11 consists of diabase dikes. These are less widespread than the quartz-feldspar porphyry dikes and are dark gray, massive, and fine to medium grained.

MINERAL EXPLORATION POTENTIAL

Within the Burgeo map area, the Chetwynd granite has the greatest potential for granite hosted mineralization. It is high level, highly differentiated, potassic, and quartz rich, and thus potentially geochemically specialized. The Sn-W-F-Mo-U potential of the granite should be considered, especially since there are multi-element lake sediment geochemical anomalies near its margins (Butler and Davenport, 1980).

The latest phases of the Burgeo granite, particularly Unit 8, have a potential for molybdenite mineralization as well as related Sn-W-F mineralization. Molybdenite occurs in equivalent units in the adjacent Peter Snout map area (11P/13), two kilometers north of the Burgeo map area

(O'Brien, 1983). Elsewhere in the Burgeo granite, pegmatite dikes are widespread; these may be of some economic interest.

Screens of rhyolite tuff of the La Poile Group within the Chetwynd granite may indicate that volcanic rocks are present elsewhere within the granite, and are more extensive than previously thought. This is of particular interest in the light of recent gold discoveries within the La Poile Group, adjacent to the Chetwynd granite, 6 km west of the Burgeo map area (Northern Miner, August 30, 1984).

SUMMARY

The oldest rocks in the region are the migmatites. In the north they are metasedimentary in origin, related to the upper amphibolite facies metamorphism and local partial melting which accompanied the main regional deformation. Their protolith is presumably the metasedimentary rocks of the mid-Ordovician Bay du Nord Group or its equivalents. The southern migmatite zone has in part an igneous protolith; in the least remobilized zones, inclusions of layered and banded gabbro are recognizable. The protolith of the mafic rocks in the inclusions is equivocal and may be related to either early mafic phases of the Burgeo granite or to Lower Ordovician or earlier metagabbros interpreted as ophiolitic basement to the Bay du Nord Group in the White Bear River area to the north (O'Brien and Tomlin, 1984). The formation of the migmatites is considered to be essentially contemporaneous with early synkinematic plutonism of the Burgeo granite, in the early Silurian. The locally gradational contact between the migmatites and the earliest xenolith rich granodiorite phase of the Burgeo granite may indicate that these migmatites represent deep levels or parts of the root zone of the Burgeo granite.

Early to mid-Silurian magmatism produced several texturally and mineralogically distinct granitoid phases. In general, these become progressively more granitic with time. However, the existence locally of both crosscutting and gradational relationships between the same two phases indicate that some of the magmatic pulses are in part contemporaneous and of variable duration. The major phases are variably deformed, and in places relatively massive; this style of deformation is in keeping with the synkinematic nature of the Burgeo granite (e.g. Blackwood, 1984; O'Brien and Tomlin, 1984).

Late Silurian - Devonian magmatism resulted in the emplacement of essentially posttectonic quartz rich, potassic, high level granite, associated felsic porphyry dikes and diabase. The Chetwynd granite was

emplaced circa 372±5 Ma (Dallmeyer, 1980); this age date represents an upper time limit on the regional deformation and a minimum age for the Burgeo granite. The greatest potential for economic mineralization lies within the Chetwynd granite.

ACKNOWLEDGEMENTS

The authors wish to acknowledge the excellent assistance in the field provided by Messrs. Jacob Lushman and Richard Lushman of Grey River. A special vote of thanks is due Gerard Hartery of Universal Helicopters (Nfld.) Ltd., who cheerfully provided expert and obliging service throughout a field season marred by persistently inclement weather. Thanks also go to the Mineral Development Division Administrative Section for logistical support.

An initial draft of this manuscript was reviewed by R.F. Blackwood, S.P. Colman-Sadd, W.L. Dickson and P.W. Delaney.

REFERENCES

Barry, J.M., Trépanier, A. and MacLeod, R.
1981: Assessment report on the 1981 geology and geochemistry of the Connaire Bay area, Southwest Newfoundland. C.B. 1806-1808; Lic. 1737-1739. [11P/12 (93)].

Blackwood, R.F.
1984: Geology of the west half of the Dolland Brook map area (11P/15), Southern Newfoundland. *In* Current Research. *Edited by* M.J. Murray, J.G. Whelan and R.V. Gibbons. Newfoundland Department of Mines and Energy, Mineral Development Division, Report 84-1, pages 198-210.

Butler, A.J. and Davenport, P.H.
1980: Lake Sediment Geochemical Survey of Southwestern Newfoundland. Open File Nfld. (1150).

Chorlton, L.R.
1978: The geology of the La Poile map area (11O/9), Newfoundland. Newfoundland Department of Mines and Energy, Mineral Development Division, Report 78-5, 14 pages.

Cooper, J.R.
1954: The La Poile - Cinq Cerf map area, Newfoundland. Geological Survey of Canada, Memoir 256, 62 pages.

Dallmeyer, R.D.
1980: Subproject 1-20, Geochronology - Insular Newfoundland mapping. Progress report 10/31/79 - 9/1/80; Newfoundland Department of Mines and Energy, Mineral Development Division, unpublished report, 31 pages.

O'Brien, S.J.
1983: Geology of the eastern half of the Peter Snout map area (11P/13E), Newfoundland. *In* Current Research. *Edited by* M.J. Murray, P.D. Saunders, W.D. Boyce and R.V. Gibbons. Newfoundland Department of Mines and Energy, Mineral Development Division, Report 83-1, pages 57-67.

O'Brien, S.J. and Tomlin, S.L.,
1984: Geology of the White Bear River map area (11P/14). Southern Newfoundland. *In* Current Research. *Edited by* M.J. Murray, J.G. Whelan and R.V. Gibbons. Newfoundland Department of Mines and Energy, Mineral Development Division, Report 84-1, pages 220-231.

Riley, G.C.
1959: Burgeo - Ramea, Newfoundland. Geological Survey of Canada, Map 22-1959.

Scott, H.S., and Conn, H.K.
1950: Preliminary report of the geology of Buchans Mining Company concessions in central and south-central Newfoundland. Photographic Survey Corporation Ltd., Geological Division, unpublished report, 12 pages.

Smyth, W.R.
1979: Peter Snout, Newfoundland. Newfoundland Department of Mines and Energy, Mineral Development Division, Open File Map 7952.

Twenhofel, W.H. and McClintock, P.
1940: Surface of Newfoundland. Bulletin of the Geological Society of America, Volume 51, pages 1665-1728.

Williams, H.
1978: Tectonolithofacies map of the Appalachian Orogen. Memorial University of Newfoundland, Map 1.

Williams, H., Kennedy, M.J. and Neale, E.R.W.
1970: The Hermitage Flexure, the Cabot Fault, and the disappearance of the Newfoundland Central Mobile Belt. Geological Society of America Bulletin, Volume 81, pages 1563-1568.

GEOLOGY OF THE WEST HALF OF
THE BURNT POND MAP AREA (12A/3),
SOUTH-CENTRAL NEWFOUNDLAND

by

S.J. O'Brien and S.L. Tomlin

ABSTRACT

The map area lies within the Dunnage Zone of the Newfoundland Appalachians, and is located in the north-central part of the Hermitage Flexure. The oldest of the area's components are the mid-Ordovician polyphase deformed and metamorphosed sedimentary rocks of the Bay du Nord Group and migmatites of enigmatic origin. Both are intruded by the polyphase, Siluro-Devonian North Bay Granite. A major aeromagnetic linear separates the equigranular and earlier porphyritic phases of the granite. It is thought that the Bay du Nord Group was deformed and metamorphosed under upper greenschist to amphibolite facies conditions prior to and during the earliest magmatism of the North Bay Granite. Subsequent phases are late tectonic. The youngest equigranular granite phases are quartz rich and muscovite bearing, and have the potential of hosting Sn-W-Mo-U-F mineralization.

INTRODUCTION

The western half of the Burnt Pond map area is located in south-central Newfoundland and is bounded by 57°15' and 57°30' west longitudes and 48°00' and 48°15' north latitudes (Figure 1). From mid summer and autumn, the area is accessible by the private roads of Newfoundland and Labrador Hydro and Abitibi-Price Newfoundland Limited; access beyond the Granite Lake west dam requires the prior approval of Newfoundland and Labrador Hydro.

Figure 1: *Location of the study area.*

The area contains little bedrock exposure and is physiographically characterized by a boggy, flat to gently rolling topography (ca. 300-350 m), broken by widely scattered monadnocks (ca 450 m. asl.). The southern part of the area is topographically higher (350-450 m) and more irregular

than the north. Original drainage patterns have been drastically altered during flooding by Newfoundland and Labrador Hydro in the late 1960's.

Previous geological investigations in the area include reconnaissance mapping by the Buchans Mining Company (Scott and Conn, 1950) and 1:250,000 scale mapping by the Geological Survey of Canada (Riley, 1957). A project of limited geological reconnaissance together with map compilation was carried out by Smyth (1979). The area was covered by the regional lake bottom sediment sampling program of the Newfoundland Department of Mines and Energy (Butler and Davenport, 1980). The eastern half of the Burnt Pond map area was mapped at a scale of 1:50,000 by Dickson (1982) and 1:50,000 scale mapping of the westerly adjacent King George IV map area was completed by Kean (1983).

GENERAL GEOLOGY

The area forms part of the north-central Hermitage Flexure of the Dunnage Zone of the Newfoundland Appalachians, and is underlain by granitoid rocks of the North Bay Granite (Jewell, 1939) and metasedimentary rocks of the Bay du Nord Group (Dorf and Cooper, 1943; Cooper, 1954). The area can be divided into three components which form separate northeast to east trending belts (Figure 2). The southernmost component comprises mainly polydeformed, upper greenschist to amphibolite facies schists and metasediments (Units 1 and 2), which are intruded posttectonically by an equigranular granite stock (Unit 7). The central component comprises foliated, coarse grained, porphyritic granodiorite and granite (Unit 4) that intrude or are faulted against the metasedimentary rocks. In the contact zone, granites and metasediments are both affected by the regional foliation. A major aeromagnetic lineament separates the granitoids of the central

Figure 2: *Geological map of the western half of the Burnt Pond (12A/3) map area, New-foundland.*

LEGEND

DEVONIAN OR EARLIER

NORTH BAY GRANITE (Units 4 to 7)

7   *Buff to pink essentially massive, fine to medium grained, equigranular to quartz porphyritic, biotite ± muscovite granite.*

6   *Buff to pale pink massive to weakly foliated, fine to medium grained, equigranular, biotite ± muscovite granite; hornblende and tourmaline-muscovite-garnet bearing pegmatite; 6a, dark gray, fine to medium grained, equigranular, biotite-rich granite.*

5   *Buff to white, weakly foliated, medium to coarse grained, equigranular to sparsely porphyritic, biotite granite.*

4   *Gray and pale pink, foliated, coarse grained, K-feldspar porphyritic to megacrystic, biotite granite and granodiorite; 4a, unseparated, coarse grained porphyritic and equigranular biotite granite; 4b, coarse grained, K-feldspar porphyritic, biotite granodiorite containing cognate xenoliths of diorite; 4c, coarse grained, porphyritic, biotite granite with screens of paragneiss and metasedimentary rocks; 4d, fine to medium grained diabase; 4e, pink and gray aplite.*

ORDOVICIAN OR EARLIER

3   *Migmatite, psammite, paragneiss and granitoid.*

LOWER TO MIDDLE ORDOVICIAN

BAY DU NORD GROUP

2   *Gray to green shale, siltstone, sandstone, phyllite and psammite; minor thin tuff beds.*

1   *Pelite, semi-pelite and biotite schist with granitoid and quartz segregations.*

component from a northernmost component of porphyritic and equigranular granite and migmatite. In the northern zone, the migmatite and associated equigranular granitoids (Unit 3) are intruded by foliated porphyritic granodiorite and granite (Unit 4) and by foliated to massive equigranular to variably porphyritic granite and pegmatite (Units 5 and 6).

Bay du Nord Group (Units 1 and 2)

The Bay du Nord Group was defined by Dorf and Cooper (1943) and Cooper (1954) as the dominantly metasedimentary rocks exposed between La Poile Bay and Garia Bay on the southwest coast of Newfoundland. As originally defined, the group contained a fossiliferous sedimentary succession of Devonian age. Chorlton (1980) redefined the Bay du Nord Group, removing from it the fossiliferous section; the remaining metasedimentary and metavolcanic rocks were reassigned to the Ordovician. Subsequent mapping by Kean (1983), O'Brien (1983) and O'Brien and Tomlin (1984) has extended the group northeastwards into the present map area.

In the western half of the Burnt Pond area, the group is comprised mainly of pelitic to semi-pelitic, upper greenschist to amphibolite facies metasediments. On the basis of relative metamorphic grade, the group can be divided into two units.

Unit 1

Unit 1 consists mainly of highly contorted phyllites, semi-pelite, pelite and biotite schist, with minor siltstone and shale; quartz veining and incipient migmatization is widespread throughout. The metasediments are dark gray, black or green, locally rusty weathering, and either laminated, thinly bedded or massive. Quartzofeldspathic beds may be locally granoblastic. A fine penetrative foliation, often coplanar to bedding, is essentially ubiquitous. Locally, the fabric is parallel to the axes of early small scale folds. Refolding is widespread and accompanied locally by the transposition of S_1 by second generation cleavage. In places, granitic veins and quartz rich segregations impart a migmatitic appearance to Unit 1.

Unit 2

Unit 2 consists mainly of black, gray or locally buff, mainly fine grained clastic sedimentary rocks of lower to upper greenschist facies metamorphic grade. Shale, siltstone, sandstone, phyllite and psammite are diagnostic rock types; these occur together with rare coarse grained sandstone and conglomerate. Quartzofeldspathic arenite and lithic tuff in beds up to 20 cm thick are present, but uncommon. The sedimentary rocks are characteristically either black, gray or locally buff,

and fine grained. In most areas, the sediments form thin parallel beds and laminae; only rarely are they massive and thickly bedded (Plate 1). Sandy beds are locally cross-stratified. Adjacent to the granitoids, the sedimentary rocks are either massive, featureless hornfels or staurolite bearing schist. Unit 2 lacks the pervasive quartz veining and incipient migmatization diagnostic of Unit 1. Unit 2 is variably deformed, with an early fabric refolded on steep, upright, axial planes. The second deformation also produced a variety of kinks, crenulations and brittle structures within both Units 1 and 2.

Plate 1: *Thinly bedded sandstone and shale, Bay du Nord Group.*

The contact of Units 1 and 2 is gradational over a distance of several hundred metres, marked by a gradual decrease in metamorphic grade and the degree of metamorphic remobilization from Unit 1 into Unit 2.

Unit 3

Unit 3 denotes a zone of migmatite and associated granitoid rocks which is intruded by younger phases of the North Bay Granite. The zone is poorly exposed, and inferred to underlie approximately 20 km^2 north and east of Burnt Pond. Equivalent rocks underlie a narrow area immediately northwest of the steadies on Burnt Pond River.

The migmatites have irregularly developed stromatic and schlieren structures (Plate 2). Layering of biotite-rich, sillimanite-bearing bands and equigranular granitoid is of variable width, but is commonly between 2 and 5 mm. The proportion of

Plate 2: *Migmatized metasedimentary rocks, Unit 3.*

paleosome is variable, and the migmatites, in places, are comprised almost entirely of nebulitic granitoid leucosome. The migmatites contain psammitic xenoliths that display various degrees of assimilation with the leucosome. In places the xenoliths have polydeformed internal foliations (Plate 3); elsewhere they form indistinct zones within the migmatite, and have a fabric which is roughly concordant with that in the leucosome. The migmatites are intruded by the younger porphyritic and equigranular phases of the North Bay Granite.

Plate 3: *Refolded structures in psammitic xenolith, Unit 3.*

North Bay Granite (Units 4 to 7)

The name North Bay Granite (Jewell, 1939) denotes the large composite granitoid batholith which lies to the north of and intrudes the Bay du Nord Group along the central and eastern parts of the Hermitage Flexure. In the western half of the Burnt Pond area, the granite can be divided into four distinctive units, based on texture, mineralogy, degree of deformation and field relationships. These include: foliated porphyritic biotite granite and granodiorite (Unit 4); foliated coarse grained equigranular to variably porphyritic biotite granite (Unit 5); foliated to massive equigranular biotite ± muscovite granite (Unit 6), and massive, quartz-porphyritic to equigranular biotite ± muscovite granite (Unit 7).

Unit 4

Unit 4 comprises the foliated, coarse grained porphyritic, biotite granite and granodiorite that underlies much of the central part of the map area. Locally, it is divisible into subunits that are characterized by either: (a) their association with small amounts of equigranular granitoid (Unit 4a), (b) the presence of numerous diorite xenoliths (Unit 4b), or (c) the presence of screens of either metasediment or paragneiss (Unit 4c). Another diagnostic feature of Unit 4 is the presence of dikes of diabase (Unit 4d) and aplite (Unit 4e).

Unit 4 granite and granodiorite is either gray or very pale pink with pink or white K-feldspar phenocrysts and megacrysts (Plate 4). It is characteristically phenocryst rich, but may locally contain diffuse bands with relatively few phenocrysts. Grain size is characteristically coarse. Locally, two phenocryst size populations are developed: 1-2 cm and 4-5 cm. In places, megacrysts up to 8 cm were noted. Phenocrysts are either equant or subhedral to anhedral, and are zoned in places (Plate 5).

Diorite, metasediment and paragneiss are present as inclusions in the granite and granodiorite. The diorite xenoliths, presumably of cognate origin, vary from a few centimeters to 1.5 meters in maximum dimension (Plate 6). Their boundaries may be either sharp or diffuse, and the xenoliths have an internal foliation parallel to that in the enclosing granite. The metasedimentary inclusions are variable in size, and contain the regional foliation seen in the adjacent granite. The paragneiss has a previously deformed biotite rich banding and has undergone a different style of deformation than the surrounding granite.

Plate 4: *K-feldspar porphyritic, biotite granite, North Bay Granite (Unit 4).*

Plate 5: *Zoned K-feldspar megacryst in porphyritic, biotite granite, North Bay Granite (Unit 4).*

Unit 4 has a variably developed foliation which, although seen in most areas, is not everywhere penetrative. The regional foliation in the unit increases in intensity southwards, where it has a strong cataclastic component. Adjacent to the contact with the Bay du Nord Group, a protomylonite zone is developed in the granite. At the Granite Lake (west) Dam, the porphyritic granite and aplites which intrude

Plate 6: *Diorite xenoliths with K-feldspar porphyroblasts, North Bay Granite (Unit 4b).*

it are affected by brittle structures, and brecciation accompanied by extensive chlorite and hematite alteration is widespread.

Unit 4 posttectonically intrudes the migmatites of Unit 3. Although much of the contact between Units 2 and 4 is either faulted or unexposed, the presence of large xenoliths of metasediment in the granite immediately north of the assumed contact indicates an originally intrusive relationship. In the contact area, both granite and metasediment are affected by the regional deformation.

Unit 5

Unit 5 comprises the weakly foliated, medium to coarse grained, equigranular and medium grained, variably porphyritic biotite granite, which underlies the northernmost parts of the map area. Due to poor exposure, the unit cannot be further subdivided.

On the northern part of Burnt Ridge, the unit consists of weakly foliated, buff, medium grained, equigranular biotite granite. In places this granite contains 1–2 percent K-feldspar phenocrysts. A similar rock type forms the only exposure of this unit found west of Burnt Pond. Buff to white, medium grained, porphyritic, biotite-poor granite is exposed in the central part of the area underlain by Unit 5. Here, the granite is spatially associated with medium grained, sparsely por-

phyritic biotite granite. Coarse grained equigranular to sparsely porphyritic, biotite granite, exposed approximately 1 km northeast of the eastern end of Burnt Pond, is tentatively included with Unit 5.

The contact of Unit 5 with adjacent units is unexposed, thus the nature of its relationship to other phases of the North Bay Granite is uncertain. Its granitic composition and its spatial association with Unit 6 may indicate a genetic link with that phase.

Unit 6

Unit 6 is a fine to medium grained equigranular granite, which lies to the north of Units 3 and 4 and which is bounded to the north by Unit 5. It is exposed only on the southern part of Burnt Ridge and on the Victoria Dam access road. A distinctive aeromagnetic low over much of the area west of Burnt Pond is taken as evidence that Unit 6 underlies much of this drift and swamp covered area.

The typical rock type of this unit is a massive to weakly foliated, buff to pale pink, equigranular biotite ± muscovite granite. It is usually massive in outcrop but is locally foliated. In places it is cut by rare hornblende-bearing appinitic sweats and pegmatite dikes. Tourmaline-muscovite-garnet pegmatites are spatially associated with dikes of Unit 6 which intrude Units 3 and 4, near the eastern end of Burnt Pond (Plate 7). It is assumed that these latter pegmatites are also genetically related to Unit 6.

Plate 7: *Garnet-muscovite-tourmaline bearing granite pegmatite associated with Unit 6 of the North Bay Granite.*

Dikes of medium grained equigranular, biotite ± muscovite granite intrude the migmatites of Unit 3. These dikes are post-tectonic with respect to the deformation seen in the migmatites. Dikes of the same composition intrude porphyritic grano-diorite of Unit 4. Locally, both dike and host rock share the same regional foli-ation. The contact of Unit 6 with Unit 5 is unexposed and their relationship is unknown.

Unit 7

Unit 7 is a small granite plug, sepa-rate from the main body of the North Bay Granite, which intrudes the Bay du Nord Group. Its lithology is fine to medium grained buff to pink equigranular to quartz porphyritic leucocratic biotite ± muscovite granite. The granite lacks a pervasive foliation but is affected by narrow shear zones along which a cleavage is locally developed.

The unit has intruded the Bay du Nord Group after the first and main deformation. Dikes of this granite in the metasediments are affected only by the second phase folds of cleavage.

MINERAL POTENTIAL

The map area has potential for both sediment hosted and granitoid related mineralization. Within the Bay du Nord Group (Units 1 and 2), pyrite mineraliza-tion is widespread, and a potentially significant pyritiferous gossan is devel-oped over black slate and pelitic schist at Goodyears Dam on the south side of Granite Lake.

Uranium mineralization occurs in Bay du Nord Group sediments approximately 3 km south of the Burnt Pond map area (O'Brien and Tomlin, 1984, this volume). The uranium occurs in both pelitic schist and tuff-aceous metasediments. Both rock types occur within Units 1 and 2 in the Burnt Pond area, and these units have potential of hosting similar mineralization.

The North Bay Granite in the Burnt Pond area contains small showings of pyrite, chalcopyrite and molybdenite, and has a potential for tin, tungsten, fluorine and uranium mineralization. In the hydro canal immediately south of the dam on Burnt Pond, Unit 4 porphyritic granite is cut by dikes of Unit 6 equigranular granite. There, fractures in the porphyritic granite are partially coated by pyrite, chalco-pyrite and molybdenite mineralization.

Significant Mo-W mineralization occurs in the North Bay Granite near the eastern end of Granite Lake, approximately 40 km to the east (Dickson, 1982). There sparse, disseminated molybdenite occurs in granite dikes, quartz veins and pegmatites, which cut altered muscovite-biotite granite. Wolframite and scheelite (0.1 to 2 percent WO_3) occur in quartz veins near the contact between muscovite-biotite granite and biotite granodiorite. Immediately east of the western half of the Burnt Pond map area, lake sediment molybdenum anomalies occur over the equivalents of Unit 5 (Butler and Davenport, 1980). Boulders of equigranular granite with tourmaline and minor molybdenite disseminations were found in the easternmost part of the area, and suboutcrop of Unit 5 with minor tourmaline and molybdenite-coated fractures was seen approximately 500 m east of the map area. Tourmaline-muscovite-garnet pegmatites and quartz-rich segregations occur in Units 3 and 4 close to the contact with Unit 5 near the east end of Burnt Pond. These dikes are presumed to be related to Unit 5, and have good potential for tungsten mineralization.

SUMMARY

The major geological components of the map area are the Ordovician Bay du Nord Group, the Siluro-Devonian(?) North Bay Granite, and migmatites of equivocal age and origin. The Bay du Nord Group repre-sents a period of Middle Ordovician distal marine sedimentation accompanied by limited volcanism. These rocks were first deformed and metamorphosed under upper greenschist to amphibolite facies conditions prior to and in part during the intrusion of the early porphyritic phases of the North Bay Granite. Subsequent equigranular phases of the granite are late synkinematic to post-tectonic with respect to the major tectono-thermal event affecting the sedimentary rocks. The youngest phase of the granite cross cuts S_1 in the metasediments; dikes of this phase are affected by open upright F_2 folds.

The protolith of the migmatites in the North Bay Granite is uncertain. In the adjacent King George IV map area, Kean (1983) demonstrated that migmatites there were related to high grade metamorphism of the Bay du Nord Group. It is thought that the migmatites represent higher metamorphic equivalents of the Bay du Nord Group rocks to the south, although there is no evidence in the map area which rules out another source for these rocks.

In light of the known occurrences of molybdenite, scheelite and wolframite showings elsewhere in the North Bay Granite (e.g. Dickson, 1982), the area can be con-sidered to have good potential for granite hosted mineralization.

ACKNOWLEDGEMENTS

REFERENCES

Butler, A.J., and Davenport, P.H.
1980: Lake Sediment Geochemical Survey of Southwestern Newfoundland. Newfoundland Department of Mines and Energy, Mineral Development Division, Open File Nfld. 1150.

Chorlton, L.B.
1980: Geology of the La Poile River map area (11O/9), Newfoundland. Newfoundland Department of Mines and Energy, Mineral Development Division, Report 80-3, 85 pages.

Cooper, J.R.
1954: The La Poile - Cinq Cerf map area, Newfoundland. Geological Survey of Canada, Memoir 256, 62 pages.

Dickson, W.L.
1982: Geology of the Wolf Mountain (12A/2W) and Burnt Pond (12A/3E) Map Area, Newfoundland. Newfoundland Department of Mines and Energy, Mineral Development Division, Report 82-5, 43 pages.

Dorf, E., and Cooper, J.R.
1943: Early Devonian plant fossils from Newfoundland. Journal of Paleontology, volume 17, pages 264-270.

Jewell, W.B.
1939: Geology and Mineral Deposits of the Bay d'Espoir area. Newfoundland Geological Survey, Bulletin 17, 29 pages.

Kean, B.F.
1983: Geology of the King George IV Lake Map Area (12A/4). Newfoundland Department of Mines and Energy, Mineral Development Division, Report 83-4, 67 pages.

O'Brien, S.J.
1983: Geology of the eastern half of the Peter Snout map area (11P/13E), Newfoundland. *In* Current Research. *Edited by* M.J. Murray, P.D. Saunders, W.D. Boyce and R.V. Gibbons, Newfoundland Department of Mines and Energy, Mineral Development Division, Report 83-1, pages 57-67.

O'Brien, S.J., and Tomlin, S.L.
1984: Geology of the White Bear River map area (11P/14), Newfoundland. *In* Current Research. *Edited by* M.J. Murray, J.G. Whelan and R.V. Gibbons, Newfoundland Department of Mines and Energy, Mineral Development Division, Report 84-1, pages 220-230.

Riley, G.C.
1957: Red Indian Lake (west half). Geological Survey of Canada, Map 8-1957.

Scott, H.S., and Conn, H.K.
1950: Preliminary report of the geology of the Buchans Mining Company concessions in central and south-central Newfoundland. Photographic Survey Corporation Limited, Geological Division, unpublished report, 12 pages.

Smyth, W.R.
1979: Burnt Pond (12A/3), Newfoundland. Newfoundland Department of Mines and Energy, Mineral Development Division, Map 7955.

URANIUM MINERALIZATION IN THE BAY DU NORD GROUP, SOUTHWEST NEWFOUNDLAND: A BRIEF NOTE

by

S.J. O'Brien and S.L. Tomlin
Newfoundland Mapping Section

ABSTRACT

Recently discovered radioactive zones within the mid-Ordovician Bay du Nord Group have yielded assays up to 4,330 g/t U. The main uranium phase is uraninite; it is concentrated in fine grained pelitic bands in staurolite schist and also in coarse grained, porous layers in an unwelded epiclastic volcanic rock. These new discoveries of syngenetic uranium mineralization, coupled with the existence of stratiform uranium occurrences elsewhere in group, indicate that the Bay du Nord Group and the southwestern Newfoundland Hermitage Flexure form a potentially significant, previously unrecognized, uranium province.

INTRODUCTION

Uranium mineralization in the mid-Ordovician Bay du Nord Group of southwestern Newfoundland was discovered during 1:50,000 regional mapping of the White Bear River (11P/14) map area (O'Brien and Tomlin, 1984). Outcrops of radioactive staurolite schist and a zone of radioactive boulders and suboutcrop of tuffaceous sediment, which locally yielded in excess of 10,000 c.p.s. (BGS-1 scintillometer), were discovered at two localities (grid references 770122 and 731131 respectively). At that time, the origin of the mineralization was uncertain. The authors assumed that the mineralization at that locality was genetically related to granitoid rocks, as the mineralized schists were spatially associated with nearby two-mica leucogranite dikes.

REGIONAL GEOLOGY

The Bay du Nord Group (Dorf and Cooper, 1943; Cooper, 1954) is a thick and extensive succession of Mid-Ordovician, polydeformed, amphibolite facies metasedimentary and metavolcanic rocks, whose regional exposure pattern defines the west-central part of the Hermitage Flexure (Williams et al., 1970) of the Newfoundland Dunnage Zone (Figure 1). In the central parts of the Hermitage Flexure, the Bay du Nord Group is either bounded by faults or intruded by two major synkinematic to post-tectonic granitoid plutons, the Burgeo and North Bay Granites. The group is also intruded by a suite of smaller late to post tectonic granitoids, which are areally confined within the boundaries of the volcano-sedimentary belt. The Bay du Nord Group consists of dominantly silicic flows and volcaniclastic rocks in its lower stratigraphic levels, overlain by a dominantly metasedimentary succession, within which occurs distinct felsic volcanic units of variable thickness (O'Brien, 1983; O'Brien and Tomlin, 1984; Blackwood, 1984).

Figure 1: *Major geological elements of the Hermitage Flexure: 1: Bay du Nord Group - dominantly volcanic rocks, 2: Bay du Nord Group - dominantly sedimentary rocks, 3: Baie d'Espoir Group, 4: La Poile Group, 5: Undivided Paleozoic rocks, 6: Burgeo granite, 7: North Bay granite, 8: Post-tectonic granitoids.*

GEOLOGY OF THE SHOWINGS

Showing "A" (Figure 2) consists of radioactive staurolite bearing light to dark gray and black semi-pelitic schist of the Bay du Nord Group, exposed on the eastern shore of White Bear River. The radioactivity occurs over a width of approximately 30 cm, being concentrated in a zone of schist cut by quartz veins. The mineralized schists have a pronounced fabric defined by biotite and muscovite; quartzofeldspathic bands in the schist are granoblastically recrystallized. Staurolite porphyroblasts, up to 10 mm in length, overgrow the main fabric, but are affected by second generation folds and later quartz veining.

Showing "B" consists of large, tabular, radioactive boulders and radioactive suboutcrop located approximately four kilometres west-northwest of Showing "A". Several isolated radioactive boulders

---

LEGEND

7	Pink felsite and fine grained granite; minor muscovite bearing leucogranite.
6	Fine to medium grained equigranular to medium grained porphyritic granite.
5	Coarse grained K-feldspar porphyritic granite and granodiorite.
4	Black slate, graphitic schist, phyllite and minor semipelite.
3	Thickly to thinly bedded gray psammite, semipelite, phyllite, sandstone, siltstone and shale.
2	Rhyolite flows, massive and banded felsic tuff; 3a, bedded tuffs and tuffaceous sedimentary rocks.
1	Mafic tuff and tuffaceous sediment; amphibolite.

Figure 2: *Geology of the north-central White Bear River map area.*

were discovered over an area of a hundred or more square metres; the area of the main zone of boulders and suboutcrop is approximately 10 square metres. The mineralization occurs in fine to medium grained nonwelded quartz phyric tuffs which are either massive or display a crude primary layering of apparent epiclastic origin. They are dark gray on fresh surface, but previously buried boulders, when exposed for a period of a few months, have weathered yellow due to uranophane formation. The tuffs are recrystallized, and a granoblastic texture is developed. Subhedral, recrystallized quartz phenocrysts, from 1 to 2 mm in diameter, comprise up to 10% of the tuffs. The tuffs are biotite rich and fine grained biotite defines a weak foliation; coarser grained porphyroblasts are widespread.

The same tuffs, although not mineralized, are exposed approximately 1 km to the west of Showing "B". There, they form a distinct band, several tens of metres thick, associated with other rhyolitic tuffs. These volcanics are bounded stratigraphically by semipelitic schist of the Bay du Nord Group. The volcanic unit is exposed immediately north of Showing "B" and several tens of metres south of Showing "A" on White Bear River. The unit is very poorly exposed, but has been traced along strike for approximately 7 kilometres.

MINERALIZATION

Autoradiographs of mineralized samples from both showings indicate that the uranium mineralization is stratiform and strata-bound. In Showing "A", the uranium is concentrated in the finest grained pelitic bands of the staurolite schist (Figure 3a). Some remobilization of the uranium into quartz veins occurred during the deformation and accompanying metamorphism is evident. Uraninite is the main uranium phase; development of secondary uranophane is extensive. A grab sample of staurolite schist assayed 669 g/t U (Table 1).

In Showing "B", the uranium, although disseminated throughout much of the rock, is concentrated in the most porous zones of the tuff (Figure 3b). Further concentrations are parallel to primary banding in the tuff. The most radioactive boulders assayed 4330 g/t uranium (Table 1). No pitchblende was seen in hand specimen; x-ray diffraction studies, presently in progress, indicate that uraninite is probably the main uraniferous phase. Allanite is obvious in thin sections of the tuffs. As mentioned above, uranophane is also present.

A

B

Figure 3(a+b): *Autoradiographs of mineralized samples of the Bay du Nord Group, White Bear River map area. A: staurolite schist with quartz veins, B: nonwelded tuff.*

SAMPLE NO.	ROCK TYPE	SHOWING	U g/t
1940601	nonwelded tuff	"B"	3,990
1940602	staurolite schist	"A"	669
1940603	nonwelded tuff	"B"	4,290
1940604	nonwelded tuff	"B"	4,240
1940605	nonwelded tuff	"B"	4,330
1940606	nonwelded tuff	"B"	4,240

Table 1: *Uranium assays (N.A.A.) of grab samples from radioactive zones in the Bay du Nord Group, White Bear River map area.*

SUMMARY AND CONCLUSIONS

Recently discovered uranium mineralization in the mid-Ordovician Bay du Nord Group is stratiform in nature and is interpreted to be essentially syngenetic. The mineralization is present, locally, where felsic volcaniclastic rocks are interbedded with fine grained pelitic metasediments. The source of the uranium may lie within the volcanic rocks, possibly related to the liberation of U during devitrification of volcanic glasses (e.g. Rosholt et al., 1971). Locally, the uranium appears to have been remobilized from the volcanics into the overlying pelitic sediments. Within the unwelded tuffs, uranium is concentrated in the coarser grained, more porous zones. Some of the uranium has been remobilized during subsequent deformation and metamorphism of the pelitic rocks. It is possible that some remobilization of uranium has occurred during intrusion of the nearby granites.

Uranium mineralization is present in the Bay du Nord Group elsewhere in the Hermitage Flexure. Approximately 40 km to the west, in the Peter Snout map area, Shell Canada Resources discovered several showings of uranium in the late 1970's. The recorded mineralization occurs in numerous boulders and outcrop of fine grained metasediment and feldspathic schist of the Bay du Nord Group, and also in the Baggs Hill granite, an Ordovician, subvolcanic intrusion (Wells, 1981). Shell Canada Resources has reported up to 30,000 c.p.s. (Urtec UG-130) radioactivity from the Bay du Nord Group in that area. Several samples containing greater than 2,000 g/t U and one sample with greater than 5,000 g/t U have been reported (Wells, 1981). It was thought that the uranium mineralization was related to the intrusion of the Devonian Peter Snout Granite, and that U was remobilized from originally uraniferous sediments by heat associated with that intrusion (Wells, 1981). On the basis of investigations by one of us (S.J. O'Brien), it appears that while the above model may be partially applicable, not all the mineralization at Peter Snout is related to the granite. At least some of the observed mineralization is strata-bound and originally syngenetic, and is concentrated in zones where schistose tuff and pelitic schist are intercalated. It is possible that the granite intrusion results only in minor remobilization. Together with the strata-bound occurrences in the White Bear River area, these showings - regardless of their uncertain origin - serve to further demonstrate the obvious uranium potential of the entire Hermitage Flexure belt.

REFERENCES

Blackwood, R.F.
1984: Geology of the west half of the Dolland Brook map area (11P/15), Southern Newfoundland. *In* Current Research. *Edited by* M.J. Murray, J.G. Whelan and R.V. Gibbons. Newfoundland Department of Mines and Energy, Mineral Development Division, Report 84-1, pages 198-210.

Cooper, J.R.
1954: The La Poile-Cinq Cerf map area, Newfoundland. Geological Survey of Canada, Memoir 256, 62 pages.

Dorf, E., and Cooper, J.R.
1943: Early Devonian plant fossils from Newfoundland. Journal of Paleontology, volume 17, pages 264-270.

O'Brien, S.J.
1983: Geology of the eastern half of the Peter Snout map area (11P/13), Newfoundland. *In* Current Research. *Edited by* M.J. Murray, P.D. Saunders, W.D. Boyce and R.V. Gibbons. Newfoundland Department of Mines and Energy, Mineral Development Division, Report 83-1, pages 57-67.

O'Brien, S.J., and Tomlin, S.L.
1984: Geology of the White Bear River map area (11P/14), Newfoundland. *In* Current Research. *Edited by* M.J. Murray, J.G. Whelan and R.V. Gibbons. Newfoundland Department of Mines and Energy, Mineral Development Division, Report 84-1, pages 220-230.

Rosholt, J.N., Prijana, and Noble, D.C.
    1971: Mobility of uranium and thorium
    in glassy and crystallized volcanic
    rocks. Economic Geology, volume 66,
    pages 1061-1069.

Wells, S.
    1981: Assessment work report, geolog-
    ical and geochemical. License numbers
    1619 and 1620. Peter Snout, Quadrangle
    C-block VI. Shell Canada Resources
    Limited. [11P/13 (82)].

Williams, H., Kennedy, M.J., and Neale,
E.R.W.
    1970: The Hermitage Flexure, the Cabot
    Fault, and the disappearance of New-
    foundland Central Mobile Belt. Geolog-
    ical Society of America Bulletin,
    volume 81, pages 1563-1568.

GEOLOGY OF THE BURGEO GRANITE AND ASSOCIATED ROCKS IN THE RAMEA (11P/11) AND LA HUNE (11P/10) MAP AREAS, SOUTHERN NEWFOUNDLAND

by

W.L. Dickson, P.W. Delaney and J.C. Poole*

ABSTRACT

The La Hune (11P/10) and Ramea (11P/11) map areas are dominated by the Silurian-Devonian Gaultois, Burgeo, North Bay and François granites. A conformable sequence of metasediments and metavolcanics of probable Ordovician age occurs in the Grey River and Devil Bay - Hare Bay areas. Migmatites, metasediments and granitic gneisses occur in the northern part of the La Hune map area mainly as two northwest-trending belts.

The Gaultois Granite is a medium to coarse grained, strongly deformed to locally mylonitic, K-feldspar porphyritic, biotite-rich granite to granodiorite.

The Burgeo granite is an extensive, syntectonic, composite intrusion with a wide variation in textures and mafic mineral content. Generally it is a coarse grained, K-feldspar porphyritic, biotite ± hornblende granite to granodiorite. The Burgeo granite is weakly to moderately deformed but locally it is mylonitic near the contact with metasediments at Grey River and Hare Bay.

The North Bay Granite is a medium grained, massive to weakly foliated, K-feldspar porphyritic, biotite ± muscovite granite, with a U/Pb age date of 396 Ma.

The François granite is a posttectonic granite that intrudes the Gaultois and Burgeo granites. Dikes related to the François granite also intrude the North Bay Granite. The François granite occurs as two overlapping, circular lobes with concentric rings of fine and coarse grained, massive, K-feldspar ± quartz porphyritic, biotite granite which rarely contains muscovite.

Conglomerate, sandstone, shale and limestone nonconformably overlie the François granite near Cape La Hune.

East of Grey River, the Burgeo and Gaultois granites have been thrust southwards on north dipping fault planes. There is no evidence that this thrusting has affected the François granite. West of Grey River the Burgeo granite is extensively sheared in its southern regions, possibly as a result of thrusting. Northwest trending mylonitization occurs along the trace of the Dragon Bay Fault, near Dolland Brook, affecting the Burgeo and Gaultois granites and the migmatites, metasediments and granitic gneiss.

Only the François granite contains significant mineral potential. Some greisen veins were located and minor magnetite probably containing uranium was found in pegmatites. The entire François granite is 2 to 3 times more radioactive than the other granitoids in the area. Extensive silicification of the brecciated Burgeo granite occurs along the Bay de Loup Brook fault and thus may have some gold potential.

INTRODUCTION

The Ramea (11P/11) and La Hune (11P/10) map areas (Figure 1) are located along the south coast of Newfoundland between Burgeo (9 km to the west) and St. Alban's (70 km to the east) (Figure 1). The communities of Grey River, Ramea and François are serviced by coastal boat from Burgeo and Hermitage. Helicopter support is available in St. Alban's and Milltown. Access to the interior is restricted by high coastal cliffs and is best gained by helicopter. Coastal exposure is excellent but high seas often prevent boat work.

Inland exposure is excellent and the northern areas were mapped on foot from helicopter-placed fly camps with a base camp in Milltown. The extremely rugged coastal areas were mapped using a helicopter.

This report deals mainly with the Burgeo, North Bay and Gaultois Granites, and Ordovician migmatites in the Hare Bay area; only a brief description of the François granite is given in this report as a detailed description is given in Poole et al. (1985). The metasedimentary and metavolcanic rocks which occur to the east and

* Department of Earth Sciences, Memorial University of Newfoundland, St. John's, Newfoundland, A1B 3X5.

1

Figure 1: *Geology of the La Hune (11P/10) and Ramea (11P/11) map areas.*

west of the community of Grey River are described in detail by Blackwood (1985).

Prior to 1984, reconnaissance geological mapping was carried out by Buchan's Mining Company (Scott and Conn, 1950), Riley (1959), Williams (1971) and Smyth (1979a,b). A detailed report on the wolframite mineralization at Grey River is given in Higgins (1980). Reconnaissance lake sediment geochemistry was carried out by Butler and Davenport (1978, 1980) and Davenport and Butler (1981, 1982). Detailed follow-up work on rock geochemistry and surficial sediments in the northern part of the François granite are given in McConnell (1984) where a multi-element (U, F, Mo, Zn, Pb) lake sediment anomaly occurs.

An airborne radiometric survey was carried out over the granitoids of the south coast of Newfoundland including the La Hune and Ramea areas (Geological Survey of Canada, 1983a,b) which highlighted the François granite as highly radioactive with only local anomalies in the Burgeo and Gaultois Granites.

REGIONAL SETTING

The La Hune and Ramea map areas cover the southeastern corner of the 3000 km^2 Burgeo granite (informal name), which is dominated by variably deformed biotite granodiorite and granite. The Burgeo granite has intruded Ordovician and presumed Ordovician metasedimentary and metavolcanic rocks, which form a concave belt along the northern margin of the batholith, and an easterly trending belt along the southern margin in the Grey River and Devil Bay areas.

The relative age of the main plutonic units is based on contact relationships

and/or degree of deformation. Preliminary U/Pb isotopic work supports the geological interpretation. West of the eastern lobe of the François granite, medium grained equigranular biotite ± muscovite granite dikes from the Burgeo granite cut the Gaultois Granite. Furthermore, the Gaultois Granite is strongly deformed throughout the La Hune map area whereas the Burgeo granite is generally less deformed. This indicates that the Gaultois Granite is the older of the two. The North Bay Granite is only weakly deformed and intrudes a migmatite zone which separates the Burgeo and North Bay Granites. The Burgeo granite and the southwestern part of migmatite zone have been extensively mylonitized along the Dragon Bay Fault zone (Blackwood, 1983) in the Dolland Brook map area (Blackwood, 1984; Dickson and Delaney, 1984) whereas the North Bay Granite is essentially massive in this area and intrudes the migmatites. These relationships have been used by Blackwood (1984) and Dickson and Delaney (1984) to indicate that the North Bay Granite is the younger of the two.

The François granite is the youngest intrusive unit in the map area. It is entirely massive and crosscuts the tectonic fabric in the Gaultois and Burgeo granites. Quartz-feldspar porphyry dikes clearly related to the François granite intrude the North Bay Granite and fine grained dikes of François granite cut the Burgeo and Gaultois Granites.

Ongoing isotopic studies of zircons from the Burgeo granite in the White Bear River area (O'Brien and Tomlin, 1984) indicate an early to mid-Silurian age for this unit. Similarly, an early Devonian age of 396 Ma is indicated for medium to coarse grained, massive to weakly foliated, K-feldspar porphyritic, biotite granite, of

LEGEND

DEVONIAN?

19   *Red and green conglomerate, sandstone, shale and limestone.*

DEVONIAN

Francois granite (Units 14 to 18)

18   *Pink to red, fine grained, massive, equigranular, biotite granite dikes.*

17   *Pink to red, fine grained, massive, quartz-feldspar-biotite porphyritic granite.*

16   *Gray, medium grained, massive, quartz-K-feldspar porphyritic, biotite granodiorite.*

15   *Pink, fine to medium grained, K-feldspar porphyritic, biotite syenite.*

14   *Pink, coarse grained, massive, equigranular to K-feldspar porphyritic, biotite granite.*

DEVONIAN OR OLDER

13   *Gray, fine grained, massive diabase dikes.*

North Bay Granite (Unit 12)

12   *Pink to buff, medium grained, weakly foliated, equigranular to locally K-feldspar porphyritic, biotite ± muscovite granite.*

Burgeo granite (Units 6 to 11)

11   *Pink or buff to locally black, fine to medium grained, very strongly foliated proto-mylonitic and ultramylonitic, locally K-feldspar porphyritic, biotite granite.*

10   *Buff, medium grained, weakly foliated, equigranular to K-feldspar porphyritic, biotite ± muscovite granite.*

9   *Pink, coarse grained, massive, equigranular, biotite granite.*

8   *Pink to buff, coarse grained, massive to moderately foliated, K-feldspar porphyritic, biotite granite.*

7   *Buff to gray, medium grained, equigranular to locally K-feldspar porphyritic, moderately foliated, biotite granodiorite.*

6   *Buff to gray, coarse grained, K-feldspar porphyritic, moderately foliated, biotite grano-diorite.*

Gaultois Granite (Units 3 to 5)

5   *Buff, medium grained, K-feldspar porphyritic, strongly foliated to locally mylonitic, biotite granite and granodiorite.*

4   *Gray to buff, coarse grained, K-feldspar porphyritic, strongly foliated to locally mylonitic, biotite granite.*

3   *Gray, coarse grained, K-feldspar porphyritic, strongly foliated to mylonitic, biotite ± hornblende granodiorite.*

ORDOVICIAN?

2   *Gray to black, biotite ± muscovite psammitic schist, granitoid gneiss and migmatite.*

1   *Undivided psammitic to pelitic biotite schist, migmatitie, amphibolite and various foliated granitoids.* **1a**, *Hornblende metagabbro.*

the North Bay Granite, in the Dolland Brook area (Dickson and Delaney, 1984).

DESCRIPTION OF UNITS

Ordovician Metasediments and Metavolcanics (Unit 1)

An elongate belt of metasedimentary and metavolcanic rocks of presumed Ordovician age (Unit 1) occurs in the Bay de Vieux to La Hune Bay area and continues along the coast to the east of Devil Bay. This unit is described by Blackwood (1985) as a lower sequence of metavolcanics overlain to the south by a sequence of upper greenschist to lower amphibolite facies metasediments and migmatites. This sequence is in fault contact with the Burgeo granite with locally developed mylonite zones. Cordierite porphyroblasts and a hornfels texture are developed close to the contact with the Burgeo granite and indicate a possible intrusive relationship (Blackwood, 1985). The reader is referred to Blackwood (op cit.) for a detailed description of the southern metamorphic unit (Unit 1).

Ordovician Migmatite and Associated Granitoid Gneiss and Metasediments (Unit 2)

Unit 2 has been divided into two subunits. Subunit 2a outcrops in the northeast corner of the La Hune map area as a 1-4 km wide, northwest-trending belt of polydeformed, biotite ± muscovite psammitic migmatite with granitic and migmatitic gneiss which have been intruded by massive, equigranular, biotite-muscovite granite (Unit 12).

Unit 2b forms a 50-100 m wide northwest-trending belt in the north central part of the La Hune map area. It is mainly an equigranular to porphyroclastic, biotite-muscovite granite gneiss with minor convoluted migmatite. Deformation varies from strong to protomylonitic.

In the northwest corner of the La Hune map area, strongly foliated migmatite ocurs as locally abundant large (20 m^2) xenoliths in weakly foliated biotite granodiorite.

Devonian or Older Gaultois Granite (Units 3-5)

The Gaultois Granite outcrops on both sides of Hare Bay and continues along the coast to the mouth of Rencontre Bay. The Gaultois Granite also occurs northwest of the eastern portion of the François Granite. The main component of the Gaultois Granite is an intensely deformed, biotite-rich, K-feldspar porphyritic granitoid. On the coast between Devil Bay and Hare Bay, the Gaultois Granite is in contact with Ordovician metavolcanics (Unit 1) but the

nature of the contact is uncertain because of intense deformation.

Unit 3 of the Gaultois Granite is a coarse grained, K-feldspar porphyritic, strongly foliated to protomylonitic, biotite ± hornblende granodiorite. It is bordered on the south by Unit 4, a K-feldspar porphyritic, strongly foliated to mylonitic, biotite granite to granodiorite. Unit 5 is a medium grained, K-feldspar porphyritic, strongly foliated to mylonitic, biotite granite. A 10 m wide dike of massive, metamorphosed, coarse grained equigranular biotite granite of unknown origin cuts the Gaultois Granite east of Hare Bay.

Devonian or Older Burgeo granite (Units 6-11)

The oldest unit of the Burgeo granite is medium to coarse grained, commonly K-feldspar porphyritic, biotite granodiorite (Unit 6). Unit 7 is mainly medium grained, equigranular to locally K-feldspar porphyritic, biotite granodiorite which is commonly spatially associated with Unit 6. Both units are rich in biotite (around 10%) and locally may contain hornblende e.g. near Slopdish Lake (local name). K-feldspar phenocrysts range from 1 to 5 cm in length and may comprise up to 10% of the rock. The granodiorite is cut by dikes of coarse grained porphyritic granite (Unit 8).

Unit 8 is a coarse grained, porphyritic biotite granite with a highly variable proportion of biotite. The majority of this unit is buff with 2 to 5 cm long K-feldspar phenocrysts in an equigranular groundmass with 3 to 5% biotite. Along the coast, west of White Bear Bay, the granite is conspicuously pink to red and generally contains less than 2% biotite. Between Bay de Vieux and White Bear Bay, much of the area is underlain by pink, coarse grained K-feldspar porphyritic granite with less than 2% biotite.

Unit 9 also occurs in this area and is a coarse grained equigranular biotite granite with about 1 to 2% biotite. Dikes of this unit often exceed 50 m in width and have intruded coarse porphyritic biotite granite (Unit 8).

Medium grained, equigranular to K-feldspar porphyritic, biotite ± muscovite granite (Unit 10) underlies the northern parts of the map areas and also commonly occurs as dikes which intrude all other units of the Burgeo granite. Xenoliths of migmatite are locally abundant in this unit. Muscovite forms less than 1% of the rock and is commonly absent. K-feldspar phenocrysts vary in abundance up to 10% and are 1-2 cm in length.

The northeastern part of the Burgeo granite, in the La Hune map area, has been extensively deformed and mylonitized along the trace of a major fault which is a continuation of the Dragon Bay fault zone of Blackwood (1983). This zone of mylonitic granitoids extends from the contact with the mylonitic metasediments of Unit 2 into the Burgeo granite up to 3 km. Coarse and medium grained granites (Units 8 and 10) have been mylonitized and reduced to a very fine grained, K-feldspar porphyroclastic blastomylonite (Unit 11) near the contact with the metasediments. The fabric in the mylonitic and associated strongly deformed granite is defined by flattened quartz and fine grained biotite; feldspar augen up to 2 cm in length are common in the originally coarse porphyritic granites.

Diabase and gabbro xenoliths are common throughout the Burgeo granite and occur mainly in coarse grained, porphyritic biotite granite (Unit 8). Extensive areas of the Ramea Islands are underlain by mafic rocks. The xenoliths range in size from a few centimetres to over 500 m in length. In a few places, swarms of 30 cm long oval xenoliths are cut by thin aplite and pegmatite veins. In other places the more sizeable xenoliths are cut by granite dikes. These mafic xenoliths vary from fine grained diabase to coarse grained gabbro and all have been metamorphosed, with coarse actinolite prominent in the gabbroic xenoliths. The larger diabase and gabbro occurrences are not interpreted to be dikes because of the lack of chilled margins on the diabase. Furthermore, granite dikes cross-cutting the diabase are similar in composition and texture as the host granite.

O'Brien and Tomlin (1984) have interpreted an extensive area of layered peridotite, gabbro and diabase in the Burgeo granite in the White Bear River map area as having an ophiolitic origin. The diabase and gabbroic xenoliths in the Ramea and La Hune map areas have no apparent layering. However, the possibility exists of an ophiolitic source for the xenoliths.

Devonian or Older North Bay Granite (Unit 12)

The North Bay Granite (Unit 12), within the map area, consists of medium grained, equigranular to locally highly K-feldspar porphyritic, weakly foliated, biotite ± muscovite granite locally with large xenoliths (20 m^2) of migmatite derived from Unit 2. The North Bay Granite has intruded the strongly deformed migmatite terrane and clearly postdates the main deformational episodes. Biotite is more abundant than muscovite which may be absent. K-feldspar phenocrysts are locally abundant and are about 2 cm long. The North Bay Granite is cut by a prominent north-

west-trending fault but there is little evidence of deformation along the fault.

Devonian or Older Diabase Dikes (Unit 13)

Three southerly-trending diabase dikes were located in the La Hune and Ramea map areas. The dikes are fine grained, equigranular to slightly plagioclase porphyritic. Two dikes are less than 15 cm thick and the other is over 2 m thick. Chilled margins are prominent. No tectonic fabric is apparent in the dikes but the presence of minor epidote and chlorite indicates that the dikes have been metamorphosed in the lower greenschist facies.

Devonian François granite (Units 14-18)

A very brief description of the François granite is given here. For a more extensive description see Poole, Delaney and Dickson (1985).

The François granite is a posttectonic intrusion comprised mainly of coarse grained, porphyritic to equigranular, biotite granite, medium grained, porphyritic biotite granodiorite, fine grained quartz-feldspar-biotite porphyry, medium grained porphyritic biotite syenite and numerous fine grained granite dikes which have intruded the other plutonic units in the La Hune map area and the Dolland Brook map area (Dickson and Delaney, 1984). A 10 m thick north-northeast trending, massive, quality-feldspar porphyry dike has intruded the mylonites and migmatites, north of the François granite and west of Dolland Brook. This dike is a continuation of one mapped by Dickson and Delaney (1984) and thus the dike has a minimum length of 5 km. A conspicuous feature of the northeast part of the François granite is a series of concentric zones of the various units which range in width from 150 m to 2 km. Numerous faults have offset slightly the various concentric rings.

Devonian? Sediments (Unit 19)

A sequence of interbedded, red and green conglomerate with minor sandstone, shale and limestone is located to the southwest of La Hune Bay. This unit nonconformably overlies Unit 7 of the François granite (Blackwood, 1985). Williams (1971) reports that granite boulders occur near the base of this sequence. K/Ar dating of muscovite from this granite gave an age of 399 ± 17 Ma. Williams notes that the granite clasts do not resemble the nearby granites. A more detailed description of this unit is given in Blackwood (1985).

DEFORMATION AND METAMORPHISM

The metasedimentary Units 1 and 2 have been polydeformed. The structure and metamorphism of Unit 1 is described in detail

by Blackwood (1985), who describes a generally conformable sequence of metavolcanic and metasedimentary rocks which increase in metamorphic grade from lower amphibolite facies in the north to upper amphibolite facies with associated migmatization in the southern units.

Unit 2 has been polydeformed during two main regional events. The main deformation produced tight isoclinal folds with an axial planar schistosity. This has been recumbently folded with superimposed open, easterly trending, gently plunging folds and locally a steep crenulation cleavage. Metamorphism reached upper amphibolite facies and was accompanied by extensive migmatization.

The mylonitization which has affected the northern margin of the Burgeo granite (Unit 11) extends into Unit 2 but is generally restricted to a narrow marginal zone, probably less than 500 m in width. This has resulted in a strongly schistose rock with a steep, planar, northwest-trending fabric.

Throughout the map area, the Gaultois Granite is very strongly deformed with narrow zones of protomylonite. The granite commonly resembles an augen gneiss as the foliae are completely recrystallized. Near the entrance to Rencontre Bay the Gaultois Granite is extensively mylonitized to a black, very fine grained to glassy rock with 5 mm x 1 mm relict K-feldspar augen.

The Burgeo granite is variably deformed. Near the contact with Unit 1, easterly-trending narrow zones of mylonite (10 m wide) occur in strongly foliated granite. Narrow protomylonite zones occur throughout the coastal parts of the Burgeo granite where the rocks are also extensively faulted and brecciated. On Ramea Islands, the granitoids are strongly deformed to mylonitic and locally the main fabric is cut by a well developed crenulation cleavage. Northeast of the community of Grey River, in the La Hune map area, the granite has been thrust to the south in numerous low angle imbricate thrusts with arcuate fronts bordered by tear faults. The thrusting affects the granite for roughly 10 km to the north of the contact with Unit 1. The effects of this thrusting show a decreasing intensity and increasing dip angle towards the north. This style of deformation continues to the west into the Ramea map area.

The early mafic granitoids of the Burgeo granite are commonly more deformed than the later, less mafic granitoids. This indicates that the Burgeo granite is a syntectonic intrusion with an extensive range in ages of plutonism. An upper limit on the age of deformation in the La Hune - Ramea map areas would be given by dating the

François granite which, apart from minor brecciation along faults, is entirely massive. The posttectonic Chetwynd granite, which is lithologically similar to parts of the François granite, has been dated at 372 ± 5 Ma (Anonymous, 1980; O'Brien and Tomlin, 1985), and sets the upper limit for deformation in Burgeo map area.

Along the trace of the Bay de Loup Brook fault the granites are locally mylonitic. The foliation parallels the fault. A subsequent brittle deformation has produced a 100 to 500 m wide breccia zone with 2-10 cm long angular clasts of deformed granite. This breccia has been healed in places by extensive silicification.

MINERALIZATION

The Burgeo granite contains minor occurrences of pyrite. Large diabase xenoliths on Ramea were found to contain disseminated magnetite and tourmaline, and associated brecciated granite contained 1-2 mm thick veinlets of magnetite and tourmaline. Massive granite on Ramea also contained noticeable magnetite. Minor fluorite was found in a granite dike associated with massive quartz cutting diabase, also on Ramea.

The Burgeo granite is extensively brecciated along the Bay de Loup Brook fault. This breccia has subsequently been silicified initially by red jasper-like quartz and subsequently by white to clear vein quartz. This zone of silicification occurs throughout the fault zone and the proportion of quartz varies from 5% to 95%. The fault zone reaches 500 m in width but is generally 100 m wide. Only one minor occurrence of pyrite was discovered and one occurrence of vein calcite was also found. The granite appears highly altered to sericite in a few places. The possibility of gold mineralization exists in this area.

Blackwood (1985) discovered specular hematite along fractures in granite at the entrance to Southeast Arm. Also in the Grey River area there are sizeable subeconomic quartz veins containing wolframite, fluorite, barite and base metals (Higgins, 1980; Higgins and Smyth, 1980; Blackwood, 1985). These quartz veins are posttectonic and cut amphibolite and leucogranite in the Grey River enclave as well as porphyritic granite of the Burgeo granite. Pyrite was located on a joint surface in the North Bay Granite on Morgan Brook.

Lake sediment surveys conducted by Butler and Davenport (1978, 1980) and Davenport and Butler (1982) indicate anomalous W, Mo, Pb and F concentrations in the François granite, particularly in its eastern lobe and the southern part of its

western lobe. Anomalous Pb values are found in the vicinity of the Grey River tungsten deposit, and Co, F and Mo are marginally enriched in various parts of the Burgeo granite in the Ramea map area. Airborne radiometric surveys by the Geological Survey of Canada (1983a, 1983b) indicate high U and Th levels in the François granite. A more detailed account of the economic potential of the François granite is given in Poole et al. (1985).

SUMMARY

The oldest units in the La Hune and Ramea map areas are the sequences of probable Ordovician metasediments and metavolcanics that occur in the vicinity of the community of Grey River, along the coast west of Hare Bay, and in the Dolland Brook to Grey River area.

The Gaultois Granite is a medium to coarse grained, strongly deformed to protomylonitic, K-feldspar porphyritic, biotite granite to granodiorite. Dikes of Burgeo and François granite intrude the Gaultois Granite, which is also more intensely deformed than other granitoids in the area, and is thus considered to be the oldest granitoid unit.

The Burgeo granite is mainly a coarse grained, K-feldspar porphyritic, biotite ± hornblende granite to granodiorite. Medium grained biotite ± muscovite granite occurs along the northern parts of the map area and has intruded the coarse grained porphyritic granitoids. The Burgeo granite is weakly to moderately deformed with mylonitic deformation along its northern and southern contacts with the Ordovician units.

The North Bay Granite is a medium grained, massive to weakly foliated, K-feldspar porphyritic, biotite ± muscovite granite which has a U/Pb age date of 396 Ma. It intrudes a belt of migmatites near Dolland Brook.

The François granite is characterized by two overlapping circular lobes with concentric rings of fine and coarse grained, massive, leucocratic, K-feldspar ± quartz porphyritic to equigranular, biotite granites which very rarely contain muscovite. The François granite crosscuts the regional fabric in the Burgeo and Gaultois granites and dikes related to the François granite intrude the Gaultois, Burgeo and North Bay granites.

Near Cape La Hune, a Devonian (?) conglomerate sequence with minor layers of sandstone, shale and limestone, nonconformably overlies the François granite.

The Burgeo granite east of Grey River and the Gaultois Granite have been thrust southward on north dipping fault planes whose dip varies from subhorizontal in the south of the Burgeo granite to 45-60° further north and in the Gaultois Granite. The François granite, although locally brittly deformed along faults, does not appear to have been affected by this episode of thrusting. Further west, the Burgeo granite has been extensively sheared possibly in response to thrusting. A northwest-trending zone of mylonitization occurs along the trace of the Dragon Bay fault near Dolland Brook affecting the Burgeo and Gaultois granites and the migmatites, metasediments and granitic gneisses in the area. Extensive brittle deformation is superimposed on a mylonitic deformation along the Bay de Loup Brook Fault.

The François granite contains significant potential for Sn and U mineralization. Greisen veins were located in various parts of the granite and minor magnetite that likely contains uranium occurs in pegmatites near Sugarloaf. The radioactive background for the François granite is 2 to 3 times greater than that of the surrounding granitoids. In the Burgeo granite, extensive silicification occurs along the Bay de Loup Brook Fault and may have gold potential.

ACKNOWLEDGEMENTS

REFERENCES

Anonymous
    1980: Geochronology Report - Newfoundland and Labrador. *In* Current Research. *Edited by* C.F. O'Driscoll and R.V. Gibbons. Newfoundland Department of Mines and Energy, Mineral Development Division, Report 80-1, pages 143-146.

Blackwood, R.F.
    1983: Geology of the Facheux Bay (11P/9) area, Newfoundland. *In* Current Research. *Edited by* M.J. Murray, P.D. Saunders, W.D. Boyce and R.V. Gibbons. Newfoundland Department of Mines and Energy, Mineral Development Division, Report 83-1, pages 26-40.

1984: Geology of the west half of the Dolland Brook map area (11P/15), southern Newfoundland. *In* Current Research. *Edited by* M.J. Murray, J.G. Whelan and R.V. Gibbons. Newfoundland Department of Mines and Energy, Mineral Development Division, Report 84-1, pages 198-210.

1985: Geology of the Grey River area, south coast of Newfoundland. *In* Current Research. *Edited by* R.V. Gibbons. Newfoundland Department of Mines and Energy, Mineral Development Division, Report 85-1.

Butler, A.J., and Davenport, P.H.
1978: A lake sediment geochemical survey of the Meelpaeg Lake area, Central Newfoundland. Newfoundland Department of Mines and Energy, Mineral Development Division, Open File (Nfld) 986.

1980: Lake sediment geochemistry, Red Indian Lake area, Newfoundland. Newfoundland Department of Mines and Energy, Mineral Development Division, Open File Nfld. 12A (249).

Davenport, P.H., and Butler, A.J.
1981: Fluorine distribution in lake sediments in the Meelpaeg Lake area, Central Newfoundland. Newfoundland Department of Mines and Energy, Mineral Development Division, Open File 1222.

1982: Tungsten in lake sediment over granitoids in south-central Newfoundland - a pilot study. Newfoundland Department of Mines and Energy, Mineral Development Division, Open File (Nfld) 1302.

Dickson, W.L., and Delaney, P.W.
1984: Geology of the Wolf Mountain (east half) and Dolland Brook (east half) map areas, south-central Newfoundland. *In* Current Research. *Edited by* M.J. Murray, J.G. Whelan and R.V. Gibbons. Newfoundland Department of Mines and Energy, Mineral Development Division, Report 84-1, pages 232-241.

Geological Survey of Canada
1983a: Gamma Ray Spectrometry Survey, South Coast, Newfoundland. Geophysical Series Maps 36611 (10) G, 11P/10 La Hune.

1983b: Gamma Ray Spectrometry Survey, South Coast, Newfoundland. Geophysical Series Maps 36611(11)G, 11P/11 Ramea.

Higgins, N.C.
1980: The genesis of the Grey River tungsten prospect: a fluid inclusion,

geochemical and isotopic study. Unpublished Ph.D. thesis, Memorial University of Newfoundland, St. John's, Newfoundland, 540 pages.

McConnell, J.W.
1984: Geochemical Surveys over three tungsten anomalies in the North Bay batholith, southern Newfoundland. *In* Current Research. *Edited by* M.J. Murray, J.G. Whelan and R.V. Gibbons. Newfoundland Department of Mines and Energy, Mineral Development Division, Report 84-1, pages 126-131.

O'Brien, S.J., and Tomlin, S.
1984: Geology of the White Bear River map area (11P/14), southern Newfoundland. *In* Current Research. *Edited by* M.J. Murray, J.G. Whelan and R.V. Gibbons. Newfoundland Department of Mines and Energy, Mineral Development Division, Report 84-1, pages 220-231.

1985: Geology of the Burgeo map area (11P/12), southern Newfoundland. *In* Current Research. *Edited by* R.V. Gibbons. Newfoundland Department of Mines and Energy, Mineral Development Division, Report 85-1.

Poole, J., Delaney, P., and Dickson, W.
1985: Geology of the François granite, South Coast of Newfoundland. *In* Current Research. *Edited by* R.V. Gibbons. Newfoundland Department of Mines and Energy, Mineral Development Division, Report 85-1.

Riley, G.C.
1959: Geology Burgeo-Ramea, Newfoundland. Geological Survey of Canada, Map 22-1959.

Scott, H.S., and Conn, H.K.
1950: Preliminary report on the geology of the Buchans Mining Company concession in central and south-central Newfoundland. Photographic Survey Corporation Limited, Geological Division, unpublished report, 12 pages.

Smyth, W.R.
1979a: La Hune (11P/10), Newfoundland. Newfoundland Department of Mines and Energy, Mineral Development Division, Map 7950.

1979b: Ramea (11P/11), Newfoundland. Newfoundland Department of Mines and Energy, Mineral Development Division, Map 7951.

Williams, H.
1971: Burgeo (east half), Newfoundland. Geological Survey of Canada map 1280A, with descriptive notes.

GEOLOGY OF THE FRANÇOIS GRANITE, SOUTH COAST OF NEWFOUNDLAND

by

J.C. Poole*, P.W. Delaney and W.L. Dickson

ABSTRACT

The François granite is a posttectonic composite granite which has intruded the syn- to late tectonic Burgeo and Gaultois granites, their mylonitic equivalents and Ordovician migmatites. Dikes from the François granite have intruded the late tectonic North Bay Granite, a part of which has been dated at 396 Ma.

The Burgeo and Gaultois granites are dominantly coarse grained, K-feldspar porphyritic, variably foliated, biotite granite and granodiorite with extensive areas of younger medium grained biotite ± muscovite granite and granodiorite in the Burgeo granite.

The François granite is composed of two overlapping circular lobes which are composite. The northeastern lobe has a well developed concentric arrangement of intrusive units with a less well developed zonation in the southwestern lobe. The outer ring of the northeastern lobe has intruded the outer part of the southwestern lobe.

Rock types in each lobe are similar with an early outer zone of coarse grained, porphyritic biotite granite intruded successively by medium to locally coarse grained, porphyritic granite, medium grained porphyritic granite and granodiorite, and fine grained equigranular to quartz-feldspar porphyritic biotite granite which is locally granophyric and miarolitic. This sequence forms the rings in the northeastern lobe but generally forms isolated intrusions in the southwestern lobe. West of La Hune Bay, the southwestern lobe contains an area of syenite?, based on its low quartz and high K-feldspar content.

The François granite is distinctly leucocratic with less that 2% biotite and very rarely contains coarse muscovite. The potential for light-ion lithophile element associated mineralization such as tin and uranium is high. Siliceous greisened granite veins are small but locally abundant. Locally, K-feldspar phenocrysts are completely altered to kaolinite? and the entire intrusion is radiometrically anomalous. Minor uranium-bearing magnetite was located in coarse granite pegmatite near Sugarloaf and late magmatic fluorite is common as a coating on quartz phenocrysts. Molybdenite has been reported to occur in an aplite dike in the northern part of the François granite.

INTRODUCTION

Location and Access

The François granite (informal name) is located on the south coast of Newfoundland, approximately 70 km west of St. Albans (Figure 1). The community of François is served by CN Marine coastal boats from Burgeo and Hermitage. The coast in this area is deeply dissected by steep-sided fiords commonly with talus-covered lower slopes. The interior of the François granite, with some considerable effort, can be reached by foot from the head of these fiords but is best reached by helicopter from St. Albans or Milltown, the closest helicopter bases. The northern part of the François granite was traversed by foot but in the southwestern coastal areas the terrain is extremely rugged and sampling by helicopter was carried out. Most of the François granite is virtually devoid of vegetation, soil or till. Only in a few gulleys, where there are thin till deposits, does scrub spruce survive.

Previous Work

Mullins (1958) mapped part of the François granite west of La Hune Bay and described the rock as a porphyritic granite. The François area was mapped on a 1:250,000 scale by Williams (1971) who outlined the massive granitoids and syenite (granite of Mullins, 1958) which now comprise the François granite. Smyth (1979) produced a 1:50,000 scale compilation map of the area with little added detail.

The economic potential of the François granite was clearly indicated by Butler and Davenport (1978) and Davenport and Butler (1981, 1982) using lake sediment geochemical data. These indicated that the François granite contained anomalous U, Mo, F, Pb and W. Further geochemical and geological work by McConnell (1984a,b)

---

* Department of Earth Sciences, Memorial University of Newfoundland, St. John's, Newfoundland, A1B 3X5.

LEGEND

DEVONIAN

Francois granite (Units 5 to 15)

15   *Pink to red, fine grained, equigranular to slightly porphyritic, massive, biotite aplite dikes.*

14   *Pink, fine to medium grained, quartz and potassium feldspar porphyritic, massive, biotite granite.*

13   *Buff to gray, medium to medium-coarse grained, plagioclase ± potassium feldspar ± quartz porphyritic, massive, biotite granite and granodiorite.*

12   *Pink, fine to coarse grained, potassium feldspar ± quartz porphyritic, massive, biotite granite;* **12a** *— fine grained granite;* **12b** *— coarse grained granite.*

11   *Buff, coarse grained, potassium feldspar porphyritic, biotite granite.*

10   *Pink to buff, coarse grained, quartz rich, potassium feldspar porphyritic, massive, biotite granite.*

9   *Pink, fine to medium grained, quartz-potassium feldspar porphyritic, massive, biotite granite.*

8   *Buff to gray, medium to medium-coarse grained, feldspar ± quartz porphyritic, massive, biotite granite and granodiorite.*

7   *Pink to green, fine to coarse grained, equigranular to feldspar porphyritic, massive, biotite syenite?*

6   *Pink, coarse grained, potassium feldspar porphyritic, biotite granite.*

5   *Pink, coarse grained, equigranular to slightly potassium feldspar porphyritic, massive, biotite granite;* **5a** *— equigranular granite;* **5b** *— slightly porphyritic granite.*

DEVONIAN AND OLDER

4   *North Bay Granite: Buff, medium grained, equigranular to locally potassium feldspar porphyritic, weakly foliated, biotite ± muscovite granite.*

3   *Burgeo granite: Undivided, medium to coarse grained, equigranular to potassium feldspar porphyritic, weakly foliated to strongly mylonitized biotite granite and granodiorite.*

2   *Gaultois Granite: Pink to gray, medium to coarse grained, mainly potassium feldspar porphyritic, strongly foliated to mylonitic, biotite granite and granodiorite.*

ORDOVICIAN

1   *Undivided metasedimentary and metavolcanic rocks including migmatite and minor mylonitic equivalents.*

Figure 1: *Geological map of the François Granite.*

indicated anomalous Sn and the rock geochemistry indicated a highly siliceous, light-ion-lithophile (L.I.L.) element-enriched pluton with several varieties of granite and granodiorite. McConnell (1985) has carried out more detailed stream sediment sampling and prospecting in the northern part of the François granite. Airborne radiometric surveys by the Geological Survey of Canada (1983) indicated that the François granite is anomalously radioactive and that there is a zonal arrangement of the anomalies. The syenite of Williams (1971) contained the highest thorium anomaly and the highest U anomalies occur in the vicinity of Sugarloaf, north of Little Bay (Figure 1).

Regional Geology

The oldest rocks in the François area are probable Ordovician, strongly deformed and metamorphosed volcanic and sedimentary rocks (Unit 1) exposed along the coast and in the northern Hare Bay area. These rocks have been intruded by the strongly deformed Gaultois Granite (Unit 2), a medium to coarse grained, porphyritic, biotite granite. The Burgeo granite (Unit 3) is mainly a medium to coarse grained, porphyritic, biotite granite which has intruded the Gaultois Granite and is generally much less deformed than the Gaultois Granite. Thus the Burgeo granite is tentatively considered to be younger than the Gaultois Granite. The North Bay Granite (Unit 4) is mainly a medium grained, equigranular to porphyritic, biotite ± muscovite granite which is only weakly deformed. This granite has a preliminary U/Pb age of 396 Ma (see Dickson et al., 1985). More detailed descriptions of the pre-François units are given in Blackwood (1985) and Dickson et al. (1985).

Mylonitization is locally intense along the contact zones between the Ordovician metamorphic rocks, and the Burgeo and Gaultois Granites. The François granite cross cuts these mylonitic rocks and thus is the youngest intrusive unit in the map area. Posttectonic dikes of François granite also intrude the North Bay (Dickson and Delaney, 1984), Burgeo and Gaultois Granites. Contacts between the François granite and the older granitoid units are steeply dipping.

The term François granite (Units 5-14) is an informal name for a variety of massive, pink to gray, medium to coarse grained, porphyritic to equigranular, biotite granitoid phases located in the area between La Hune Bay and Hare Bay. No radiometric age dates are available for the François granite, but the presence of François granite dikes in the weakly deformed North Bay Granite, west of Dolland Brook (Dickson and Delaney, 1984), indi-

cates a maximum age of 396 Ma. The François granite consists of two overlapping circular complexes which trend towards the northeast. In the southwest of the complex, a small area of massive porphyritic syenite is included in the François granite. The two circular bodies which comprise the François granite are referred to as the northeast lobe and the southwest lobe. The northeast lobe is considered to be the younger of the two as one unit in the northeast lobe has intruded a unit of the southwest lobe. The relative age of the units within each lobe is known from intrusive relationships but the relative age between units in different lobes is not known.

FRANÇOIS GRANITE

Contact Relationships within the François granite

Contact relationships between each of the units indicate the sequence of intrusion. Unit 6 postdates subunit 5a as Unit 6 becomes finer grained adjacent to the contact and xenoliths of probable subunit 5a were found in Unit 6 within a hundred metres of the contact. Unit 7 postdates Unit 6 along a gradational contact (Blackwood, 1985). Unit 6 and subunit 5b are everywhere in fault contact. Unit 8 postdates subunit 5b with sharp intrusive contacts between finer grained Unit 8 adjacent to coarser grained Unit 5b. In one area the contact dips at 40° to 45° towards the north. The contact relationship between Unit 9 and Unit 6 is not known. Dikes of Unit 9 were found in all units except Unit 7. Thus Unit 9 is probably the youngest unit in the western lobe.

Unit 10 of the northeast lobe clearly postdates subunit 5a of the western lobe. This is indicated by a consistent zone, tens of metres wide, of fine grained, porphyritic granite which becomes coarser grained away from the contact with subunit 5a. The relationship between Unit 10 and Unit 11 is uncertain and may be transitional. The contact between Unit 10 and Unit 12 is often irregular and a sill-like intrusion of Unit 12 is indicated in some localities in the northern portions of the northeast lobe, by vertical textural variations in Unit 12. Unit 13 is a sill-like intrusion into Units 10 and 12, with sharp contacts dipping 40° south in the southern portion of the northeast lobe and 40° to 50° southwest in the southwestern portion of the northeast lobe. Thin, fine grained (chilled), biotite-rich margins occur within Unit 13 at the contacts with Units 10 and 12. Thin veins of Unit 13 intrude Units 10 and 12. Unit 14 probably postdates Unit 13 since fine grained, equigranular aplite dikes, similar to the main body of Unit 14, have intruded Unit 13.

Detailed description of the François granite (Units 5-15)

a. Southwest lobe - Units 5 to 9

Unit 5 is composed of pink, coarse grained, equigranular to slightly potassium feldspar porphyritic, massive, biotite granite, and has been divided into subunit 5a, which forms the northern arcuate margin of the southwestern lobe, and subunit 5b which forms the central part of the lobe. Subunit 5a is in sharp contact with the Burgeo granite and contains locally abundant xenoliths of migmatite and foliated granite close to the contact. The subunit is a homogeneous hypidiomorphic granular granite with approximately 1 to 2% biotite. Steeply dipping, medium grained, equigranular granite dikes have intruded subunit 5a. The dikes are commonly over 50 m in length and 1 m wide. Thin quartz veins are associated with easterly and northerly trending minor shear zones.

Subunit 5b is tentatively correlated with subunit 5a as both have a similar matrix texture, grainsize and mineralogy. However, subunit 5b is generally porphyritic with up to 10%, 1-3 cm long, potassium feldspar phenocrysts. Biotite forms 1% of the rock. The subunit is cut by thin shear zones which contain small barren quartz veins. In a few areas, very thin veins of dark coloured material is probably greisened granite.

Unit 6 is composed of pink, coarse grained, potassium feldspar porphyritic, biotite granite and forms a discontinuous circular zone, which separates subunits 5a and 5b, and forms most of the remaining parts of the outer ring of the southwest lobe. The marginal zones of Unit 6 are generally finer grained than the rest of the unit. Potassium feldspar phenocrysts are 1 to 3 cm in length and comprise 10 to 20% of the rock. The matrix contains varying proportions of potassium feldspar and plagioclase with 1 to 2% biotite. Small, dark, irregularly shaped, metadiorite (?) xenoliths, occur locally.

Unit 7 is composed of pink to green, fine to medium grained, equigranular to feldspar porphyritic, massive, biotite granite and medium to coarse grained, feldspar porphyritic, biotite syenite(?). The coarser grained component of this unit locally contains less than 10% quartz and thus has been termed a syenite, e.g. Williams (1971). Mullins (1958) records that in some areas the finer grained component contains up to 30% fine grained quartz in the matrix. Blackwood (1985) reports that the contact between Units 6 and 7 is gradational. Unit 7 contains 2 to 3 cm long potassium feldspar phenocrysts which form 2 to 20% of the rock and pale green plagioclase phenocrysts, about 1 cm in length are less abundant than the potassium feldspar. Biotite forms 2 to 5% of the rock. Aplite dikes up to 60 cm wide cut Unit 7 in a few places.

Unit 8 is composed of buff to gray, medium to medium-coarse grained, feldspar ± quartz porphyritic, massive, biotite granite and granodiorite. This distinctly more mafic unit is characterized by its generally darker colour and the presence of both plagioclase and potassium feldspar phenocrysts. The phenocrysts are 1 to 3 cm in length and form 10 to 20% of the rock. The matrix contains mainly plagioclase with smaller amounts of quartz and potassium feldspar and approximately 2 to 5% biotite.

Unit 9 is composed of pink, fine to medium grained, quartz - potassium feldspar porphyritic, massive, biotite granite. This unit forms small intrusions and dikes in the southwestern part of the southwest lobe. The granite is generally resistant to weathering and commonly has retained a glacial polish, perhaps as a result of a high quartz content. Potassium feldspar phenocrysts comprise 5 to 15% of the rock and are 5 to 20 mm in length. Quartz phenocrysts are commonly 5-7 mm in diameter and form 2 to 10% of the rock. The matrix contains 1-2 mm crystals of quartz, plagioclase and potassium feldspar with 1 to 3% biotite. Miarolitic cavities are common in this unit particularly near the margins and indicate that the unit was emplaced at a high structural level. Swarms of 10 to 50 cm wide quartz veins are common and cover areas of 3 to 5 m^2.

b. Northeast lobe - Units 10 to 14

Unit 10 is composed of pink to buff, coarse grained, quartz rich, potassium feldspar porphyritic, massive, biotite granite and forms most of the outer ring of the northeast lobe. In the central part of the lobe, similar granite is tentatively correlated with Unit 10. Within a few metres of the contact of Unit 10 with the country rocks, the granite becomes finer grained. Xenoliths of migmatite and foliated granite are common near the margin. Potassium feldspar phenocrysts, 2 to 3 cm in length, make up 5 to 20% of the rock. The matrix consists of quartz, plagioclase, and potassium feldspar, with 1 to 2% biotite. The finer grained varieties of Unit 10 are locally granophyric.

Steeply dipping aplite dikes, 20 to 50 cm wide, and aplite sills are common in the northern part of Unit 10. The dikes appear to have a radial arrangement about the center of the northeastern lobe. The dikes commonly contain a central zone of pegmatite and one sill was found to contain alternating layers of pegmatite and aplite.

Unit 11 is a buff, coarse grained, potassium feldspar porphyritic, biotite granite and forms an arcuate belt along the southeastern margin of the northeast lobe outside of Unit 10. This unit is distinguished in the field from Unit 10 by the buff colour, and higher proportion of plagioclase. Radioactivity is also higher in Unit 11 (see section on mineralization). Unit 11 contains about 10 to 20% potassium feldspar phenocrysts which are 1 to 2 cm in length. The matrix contains about 25% plagioclase with quartz and potassium feldspar and 1 to 3% biotite.

Unit 12 is composed of pink, fine to coarse grained, potassium feldspar ± quartz porphyritic, massive, biotite granite and forms a complete ring in the northeastern lobe. Mappable textural variants of Unit 12 are termed subunits 12a, a fine grained granite, and 12b a coarse grained granite. In general, Unit 12 is highly variable with common changes in grainsize, texture, and proportions of quartz and feldspar phenocrysts. Quartz and potassium feldspar phenocrysts are conspicuous in this unit. Quartz is generally dark gray to brown, subhedral, and 5 to 7 mm in diameter. The potassium feldspar phenocrysts are 1 to 2 cm in length and are locally highly altered to brown kaolinitic aggregates. The matrix of the granite is fine to coarse grained with minor plagioclase and less than 1% biotite.

Unit 13 is composed of buff to gray, medium to medium-coarse grained, plagioclase ± potassium feldspar ± quartz porphyritic, massive biotite granite and granodiorite. This distinctive gray to buff unit is similar to Unit 8 of the western lobe. Contacts are generally sharp and dip approximately 40°S, just north of Sugarloaf.

Unit 13 consists of 10 to 15% plagioclase phenocrysts, approximately 1 cm in length. Potassium feldspar phenocrysts 1 to 2 cm in length occur mainly in the coarser varieties of this unit and may comprise up to 10% of the rock. Phenocrysts of coarse subhedral to anhedral quartz also occur locally and comprise 5% of these rocks. The matrix consists of plagioclase, potassium feldspar, quartz, and 2 to 4% biotite. The proportion of potassium feldspar in the matrix is greater in the coarser varieties of this unit.

Unit 13 has been intruded by steeply dipping, northerly trending aplite dikes, 20-30 cm wide, in the northern portion of the eastern lobe. In one area, northerly trending, 2-4 cm wide greisen veins were observed adjacent to the contact with Unit 14.

Unit 14 is composed of pink, fine to medium grained, quartz and potassium feldspar porphyritic, massive, biotite granite and forms the core of the northeastern lobe. This unit is similar to Unit 12. In Unit 14, quartz phenocrysts are generally black to dark gray, anhedral to subhedral and 0.5 to 0.75 cm in diameter. Potassium feldspar phenocrysts are 1 to 2 cm in length. Combined phenocrysts comprise 10-25% of the rock. The matrix consists of fine to medium grained pink to red potassium feldspar, quartz ± plagioclase and less than 1% biotite.

In the eastern part of this unit the granite grades into a pink, coarse grained, potassium feldspar porphyritic, biotite granite which is tentatively included in Unit 10.

Unit 15 is composed of pink to red, fine grained, equigranular to slightly porphyritic, massive, biotite aplite dikes. To the northwest of the François granite, numerous thick red aplite dikes have intruded the Burgeo granite. The aplite dikes have a consistent northerly trend and are discontinuously exposed for up to 6 km from the edge of the François granite. The dikes range from 5 to 25 m in width and have exposed lengths of over 400 m. Contacts with the country rock are sharp and straight. Near the contact with the François granite, some of the dikes are medium to coarse grained and probably related to Unit 5a of the François granite.

The aplite contains 2 to 5% phenocrysts of feldspar, 2 to 3 mm in length. Biotite occurs as 1 to 2 mm flakes and forms 1% of the mode.

STRUCTURE

The northeastern lobe of the François granite is characterized by major ring structures. The outer margin of the lobe (Units 10 and 11) is 2-4 km wide with a diameter of 11-12 km and has been intruded by an irregular-shaped sill of Unit 12, a 0.5 to 1.25 km wide ring with a 6-7 km diameter. Unit 13 is generally 1-2 km wide but narrows to a true thickness of 60 m (horizontal width of 85 m x sine 45°) at the head of Devil Bay. The unit has a diameter of 4.5 to 5.5 km and has a 45° southward-dipping contact with Unit 12 in the southern and southwestern areas but the attitude of the contact in the north is unknown. The core of the lobe is elliptical and is occupied by Unit 14 in the west which grades into Unit 10 in the east. The elliptical core is 2 km by 4.5 km and at its western margin onlaps Unit 13 in possible lacolith fashion.

The southwestern lobe is not as obviously a ring structure as the northeastern lobe. Unit 5a and Unit 6 form an outer margin in most places. If the lobe was extended into the ocean to complete its circular shape then the youngest units would occur in the center.

Both lobes of the François granite are crosscut by faults. In most cases displacement is difficult to determine. A major northwest trending fault bisects the eastern lobe. Along this fault, the granite is brecciated and in some localities 1-10 m wide zones of 1-5 cm wide quartz veins are parallel to the fault. Displacement at the steeply dipping contact of the eastern lobe with the country rock is less than 200 m indicating a minimal strike slip component. North of this fault, the rings of the northeastern lobe have been offset by numerous faults but the ring structure is still apparent. The southwestern lobe is extensively faulted which may confuse identification of any rings in this lobe.

MINERALIZATION

Lake sediment surveys conducted by Butler and Davenport (1978) and Davenport and Butler (1981, 1982) indicated that the François granite contains anomalous W, Mo, Pb and F concentrations in the northeastern lobe and the southern part of the southwestern lobe. A follow-up stream sediment geochemical survey conducted by McConnell (1984a,b), produced very high Pb and U values as well as moderately high values for Sn, Zn and F, mainly in the vicinity of

Sugarloaf. No significant mineralization was found in the François granite and these anomalies may be partly the result of overall large-ion-lithophile enrichment in this highly siliceous granite.

Minor magnetite, probably containing uranium, occurs in pegmatite patches near Sugarloaf. One minor occurrence of possible topaz was located about 4 km north of Little Bay. McConnell (1984a,b) discovered topaz in a scree slope 1 km west of Devil Bay and trace molybdenite in an aplite dike near the northern contact between the François granite and the Burgeo granite. Fluorite occurs in the François granite as a coating on quartz crystals. This was most common in the fine grained version of Unit 12 where fine grained fluorite coats the quartz phenocrysts. This indicates a late magmatic origin for the fluorite and a system enriched in fluorine.

Airborne radiometric surveys by the Geological Survey of Canada (1983a) show the François granite to be enriched in U and Th. The radiometric anomalies were also able to pick out the concentric zones observed in the field. A hand-held GIS-4 Gamma Ray Spectrometer indicated lower anomalous radiometric values than expected but discerned relative differences between units and between the two lobes (Table 1).

SUMMARY AND CONCLUSIONS

The François granite is a Devonian, posttectonic, composite intrusion comprised of two overlapping ring complexes, each

Table 1: *Mean Gamma Radiation for each unit of the François granite. Values obtained using a Scintrex GIS-4 gamma ray spectrometer and reported in counts per second (c.p.s.).*

a. Western Lobe

	Total Counts	K+Th+U	Th+U	Th
Unit 5a	150	6	3	1
5b	260	8	4	2
6	190	7	3	1
7	315	11	6	1
8	190	7	4	2
9	250	9	5	2

b. Eastern Lobe

	Total Counts	K+Th+U	Th+U	Th
Unit 10	290	10	6	2
11	330	12	6	3
12	300	10	6	2
Units 12a,12b	310	11	6	2
13	200	7	5	1
14	310	11	6	2

approximately 12 to 15 km in diameter. The pluton has a northeasterly trend and part of the northeastern ring complex has intruded the southwestern ring complex. The sequence of intrusion in both complexes is similar with early coarse biotite granite intruded by medium grained granodiorite and subsequently by fine to medium grained granite. A small area of syenite at the southwest end of the complex is considered to be part of the François granite. Locally developed miarolitic cavities indicate that the François granite is a high level intrusion.

The ring structure is best developed in the northeastern part of the François granite where four distinctive rings have developed. Airborne radiometric surveys highlight these rings and also indicate that the entire François granite is three to five times more radioactive than the surrounding rocks. Highly radioactive magnetite was found in a few pegmatites north of Little Bay. The source of the Pb, Mo, Sn and W anomalies (Butler and Davenport, 1978; 1980; McConnell, 1984) is not apparent. Thin greisen veins are developed locally. Fluorite forms coatings on quartz crystals in a few places in the granite indicating a late magmatic origin for the fluorite and a system enriched in fluorine.

The François granite along with the other granites in the area have been geochemically sampled using a 2 km x 2 km grid system. Geologically complex areas were more intensively sampled. These samples will be analysed for major elements and trace elements including Sn, W, U, Mo, Li and Be. Samples have been collected for age dating.

ACKNOWLEDGEMENTS

REFERENCES

Blackwood, R.F.
    1985: Geology of the Grey River area, south coast of Newfoundland. *In* Current Research. *Edited by* R.V. Gibbons. Newfoundland Department of Mines and Energy, Report 85-1.

Butler, A.J., and Davenport, P.H.
    1978: A lake sediment geochemical survey of the Meelpaeg Lake area, Central Newfoundland. Newfoundland Department of Mines and Energy, Open File (Nfld) 986.

Davenport, P.H., and Butler, A.J.
    1981: Fluorine distribution in lake sediments in the Meelpaeg Lake area, Central Newfoundland. Newfoundland Department of Mines and Energy, Open File 1222.

    1982: Tungsten in lake sediment over granitoids in south-central Newfoundland – a pilot study. Newfoundland Department of Mines and Energy, Open File (Nfld) 1302.

Dickson, W.L., and Delaney, P.W.
    1984: Geology of the Wolf Mountain (east half) and Dolland Brook (east half) map areas, south-central Newfoundland. *In* Current Research. *Edited by* M.J. Murray, J.G. Whelan and R.V. Gibbons. Newfoundland Department of Mines and Energy, Report 84-1, pages 232-241.

Dickson, W.L., Delaney, P.W., and Poole, J.C.
    1985: Geology of the Burgeo granite and associated rocks in the Ramea (11P/11) and La Hune (11P/10) map areas, southern Newfoundland. *In* Current Research. *Edited by* R.V. Gibbons. Newfoundland Department of Mines and Energy, Report 85-1.

Geological Survey of Canada
    1983: Gamma Ray Spectrometry Survey, South Coast, Newfoundland. Geophysical Series Maps 36611(10)G, 11P/10 La Hune.

McConnell, J.W.
    1984a: Geochemical Surveys over three tungsten anomalies in the North Bay batholith, southern Newfoundland. *In* Current Research. *Edited by* M.J. Murray, J.G. Whelan and R.V. Gibbons. Newfoundland Department of Mines and Energy, Report 84-1, pages 126-131.

    1984b: Follow-up geochemistry over three mineralized granitoids in south-central Newfoundland. Newfoundland Department of Mines and Energy, Open File (Nfld) 1429.

Smyth, W.R.
    1979a: La Hune (11P/10), Newfoundland. Newfoundland Department of Mines and Energy, Map 7950.

Williams, H.
    1971: Burgeo (east half), Newfoundland. Geological Survey of Canada map 1280A, with descriptive notes.

GEOLOGY OF THE GREY RIVER AREA, SOUTHWEST COAST OF NEWFOUNDLAND

by

R. Frank Blackwood
Newfoundland Mapping Section

ABSTRACT

The Grey River enclave is an east-west trending belt of metamorphic rocks that straddles the Ramea (11P/11) and La Hune (11P/10) map areas; it is bounded to the north and west by the Burgeo granite and to the east-southeast by the Francois granite. Amphibolite facies metamorphism generally increases from north to south in the enclave, culminating in migmatite zones. Felsic metavolcanic and pelitic metasedimentary rocks suggest an affinity with lithologically similar Ordovician rocks found elsewhere along the Hermitage Flexure. Large, pretectonic quartz veins and much smaller, wolframite bearing, posttectonic quartz veins are special features of the Grey River area.

INTRODUCTION

Metamorphic rocks in the Grey River area straddle the Ramea (11P/11) and La Hune (11P/10) map areas on Newfoundland's southwest coast. The study area is located west of Francois and east of Burgeo and Ramea; these three communities, as well as Grey River, are regular stops on CN Marine's south coast ferry run. Burgeo, Ramea and Grey River are serviced by an additional ferry twice a week. A gravel road (route 460) links Burgeo to the Trans Canada Highway near Stephenville.

The present study involved systematic mapping of the metamorphic rocks and adjacent granitoids in the Grey River area on a 1:50,000 scale; it was completed during the 1984 field season. The remainder of the Ramea and La Hune map area was mapped by Dickson et al. (1985) and Poole et al. (1985). Exposure is continuous along the coast and excellent everywhere else in the Grey River area.

The Grey River area was first mapped by the Buchans Mining Company Limited (Bahyrycz, 1957) on a scale of 1 inch to 1320 feet after prospectors discovered quartz veins containing tungsten minerals. This mapping was extended to the La Hune Bay area (Mullins, 1958) and resulted in the definition of most of the major lithologic units, including quartz rich bands described as quartzites. A silica assessment study was done on the quartzites by the Newfoundland Department of Mines, Agriculture and Resources (Fleming, 1967; Bartlett, 1969; Butler and Greene, 1976). The Grey River area was also mapped on a 1 inch to 4 mile scale (Riley, 1959) and 1:250,000 scale (Williams, 1971) by the Geological Survey of Canada as part of the larger Burgeo (11P) map area. Higgins and Smyth (1980) did a regional summary of the area covered by Bahyrycz for the Newfoundland Department of Mines and Energy, partly in conjunction with a Ph.D. study of the tungsten bearing quartz veins by Higgins (1980a,b; Higgins and Kerich, 1982).

GENERAL GEOLOGY

The Grey River area is sited in the south-central part of the Hermitage Flexure (Williams et al., 1970), a generally west trending, sinuous configuration of rock units that occurs in southern Newfoundland. Structural and lithostratigraphic elements have an east-west trend in the map area. The metavolcanic, metasedimentary and migmatitic rocks are here informally referred to as the Grey River enclave and assigned a possible Ordovician age. These rocks are separated from the Ordovician Bay du Nord Group (Cooper, 1954; Chorlton, 1980a,b; Blackwood, 1984) to the north, and the Ordovician Baie d'Espoir Group (Jewell, 1939; Colman-Sadd, 1974, 1976) to the east, by Devonian or earlier granitoids.

Grey River enclave (Units 1-8)

The Grey River enclave is a zone of east-west trending units consisting of metavolcanic, metasedimentary and migmatitic rocks, together with pretectonic rocks of possible intrusive origin (Figure 1). The degree of partial melting and lit-par-lit granitoid veining generally increases from north to south.

Unit 1 is a band of felsic metavolcanic rocks that outcrops between the Gulch Cove area of Southeast Arm and La Hune Bay. A small area of Unit 1 outcrops at the western end of Big Pond, north of Grey River. The main area consists mostly of fine grained, pinkish white to grayish white weathering felsic tuffs with scattered 1 to 3 mm quartz and feldspar phenocrysts. The tuffs are commonly laminated with discontinuous 1 to 5 mm laminae defined by color and compositional variations, and accentuated by thin parallel quartz veins or segregations. Locally, 1 to 25 cm thick beds of felsic tuff contain interlayered 1 to 8 cm thick calcareous beds and lenses (Plate 1). Minor translucent quartz clasts occur in the carbonate; the associated volcanics generally contain a profusion of quartz clasts.

Figure 1: *Geology of the Grey River Area, southwest coast of Newfoundland.*

LEGEND

DEVONIAN OR LATER

Posttectonic quartz veins.

15　　*Red and green conglomerate, sandstone, shale and limestone.*

DEVONIAN OR EARLIER

14　　*Fine to medium grained, minor hornblende and biotite granite.*

FRANCOIS GRANITE (Units 12 and 13)

13　　*Fine to medium grained, feldspar porphyritic syenite.*

12　　*Coarse grained, feldspar porphyritic, biotite granite.*

BURGEO GRANITE (Units 10 and 11)

11　　*Fine to medium grained granite protomylonite, plus minor mylonite and ultramylonite.*

10　　*Commonly foliated, medium to coarse grained, feldspar porphyritic, biotite granite.*

9　　*Fine to coarse grained hornblende gabbro, including minor hornblendite, diorite and amphibolite.*

ORDOVICIAN (?)

GREY RIVER ENCLAVE (Units 1 — 8)

8　　*Agmatite. Hornblende ± biotite schist, migmatite, and amphibolite, intruded by foliated leucogranite.*

7　　*Fine to medium grained granite/granodiorite gneiss containing profuse mafic xenoliths.*

6　　*Fine to coarse grained amphibolite, including minor gabbro and hornblendite,* **6a,** *perido- tite,* **6b,** *hornblendite and gabbro.*

5　　*Amphibolite, hornblende ± biotite schist and hornblende diorite migmatite.*

4　　*Migmatized semipelitic, pelitic and psammitic schist, plus minor hornblende ± biotite schist.*

3　　*Pretectonic quartz veins (?).*

2　　*Pelitic to psammitic phyllite and schist, plus minor quartzite, banded amphibolite, and migmatite.*

1　　*Fine grained grayish white and pinkish white felsic tuff, locally containing minor carbonate lenses, medium to coarse grained quartz/feldspar lapilli tuff, and minor conglomerate, sandstone and phyllite.*

Locally, narrow zones of green phyllite occur in the volcanics in the Southeast Arm area. An area of enigmatic volcaniclastic rocks occurs in the eastern part of Unit 1 near La Hune Bay. Interpreted as coarse grained lapilli tuff or fine grained agglomerate/conglomerate, these rocks consist of lithic and crystal clasts in a pelitic matrix. The clasts are matrix supported, angular to round and poorly sorted. Pink feldspar clasts are 0.5 to 3 cm long, white feldspar clasts are 2 to 8 mm across and fine grained pink and gray felsic volcanic clasts are up to 7 cm long. The small area tentatively included in Unit 1 north of Grey River at Big Pond appears to be a large inclusion in the Burgeo Granite (Unit 10). It consists of granule to pebble conglomerate containing profuse felsic volcanic clasts, including quartz porphyry and jasper. Brownish red argillite containing grayish white carbonate lenses is associated with the conglomerate. Minor, possibly flow banded, red rhyolite and white weathering felsic tuff as well as greenish gray quartz and feldspar lapilli tuff also occur in the same small area.

Plate 1: *Felsic tuffs with calcareous interbeds are disposed in a recumbent isoclinal fold. Unit 1 west of La Hune Bay.*

The main regional foliation is penetratively developed throughout Unit 1 and locally is axial planar to isoclinal folds of bedding and laminae. Pretectonic granitoid veins are also folded by this deformation. These early folds are overturned to recumbent (Plate 1) and are commonly overprinted by relatively upright, open to moderately tight folds with a variably developed axial planar crenulation cleavage. The main fabric is a phyllitic foliation in the Southeast Arm and Big Pond

areas but fine to coarse grained biotite is developed on fabric planes near La Hune Bay. The volcanics are also recrystallized and contain biotite, muscovite and, locally, hornblende porphyroblasts in the eastern part of the unit.

Unit 2 consists mostly of metasedimentary rocks which occur along Southeast Arm and east of Gulch Cove. It is conformable with, and lies structurally below, Unit 1 felsic volcanics. In the Gulch Cove-Southeast Arm area these rocks are mostly gray or green phyllites and fine grained schists, interlayered with 0.5 to 10 cm wide semipelite, psammite and minor graphitic pelite bands. Locally, concordant, 1 to 8 cm thick, amphibolite layers have gradational boundaries with enclosing psammite, suggesting that originally these were beds of possible mafic to intermediate volcaniclastics. Also, 1 to 2 m zones of chlorite schist, and a more massive dark green rock containing profuse 1 to 4 mm epidote crystals may represent mafic volcanics. Pinkish white weathering felsic tuffs also occur locally in bands up to 60 cm wide and are best developed along the contact with Unit 1. Pink, siliceous lenses, 2 to 10 mm wide, may represent transposed cherty layers in phyllite along Southwest Arm; brownish red carbonate stringers are developed in the same area. Feldspathic quartzite and quartz mica schist occur with banded amphibolite (Plate 2) and pelite in Unit 2 at Gulch Cove.

Plate 2: *Primary (?) layering in amphibolite. Unit 2 at Gulch Cove.*

Locally, Unit 2 contains a profusion of 2 to 4 cm wide quartz segregations which, along with 1 to 2 mm granitoid sweats, developed parallel to the main

foliation, increase toward the southern contact with Unit 4 migmatite. Also, the quartzofeldspathic component of the semi-pelite becomes recrystallized into distinct quartz and feldspar crystals with proximity to the southern boundary. Muscovite porphyroblasts, common throughout Unit 2, are well developed in pelitic layers in this area and, along with biotite, are locally preferentially sited in pelitic laminae. Plagioclase porphyroblasts are selectively developed in pelitic layers north and east of Gulch Cove (Plate 3). Concordant, pre-tectonic amphibolite dikes and granite peg-matite are common in Unit 2 as are boudin-aged quartz veins and quartz plus white feldspar granitoid.

Plate 3: *Plagioclase porphyroblasts devel-oped in pelite/semipelite. Unit 2 east of Gulch Cove.*

The main fabric in Unit 2 is co-planar to bedding and locally appears composite where it is manifested as a fine but distinct 0.5 mm banding of alternating quartzofeldspathic layers and biotite rich layers in pelite-semipelite. It also appears to transpose an earlier foliation locally. However, no folding was observed associated with this earlier orientation and it may reflect a mimetically recrystal-lized primary anisotropy. The main foli-ation is schistose in the south but phyl-litic along Southeast Arm; the presence of concordant granitoid sweats at Gulch Cove, however, suggests that the phyllites repre-sent retrogressed amphibolite facies rocks, possibly due to movement along the faulted northern boundary of the Grey River enclave. Commonly the regional foliation is overprinted by a crenulation cleavage that is axial planar to moderately tight folds. Cordierite porphyroblasts, 1 to 4 cm

across, also overprint the main fabric at the entrance to Southwest Arm.

Unit 3, originally mapped as quartzite (Bahyrycz, 1957), is mostly confined to Unit 2 and the main zone occurs in the Gulch Cove area. It forms an approximately 350 m wide zone at the top of the cliff on the east side of Gulch Cove (Plate 4) and has an overall length of 5.8 km. It thins and pinches out in either direction along strike, bifurcating west of Gulch Cove. Other discontinuous, thinner bands occur east of the Gulch Cove zone and on an island in the southeast. Unit 3 consists mostly of white to grayish white weather-ing, fine to coarse grained quartz. Locally, it is coarsely recrystallized to granular translucent quartz. Minor, but conspicuous, coarse grained muscovite is common. Blebs and stringers of massive to disseminated magnetite, 1 to 6 mm wide and up to 50 mm long, occur locally. Dissemin-ated magnetite is also concentrated in 2 to 20 mm wide parallel bands that are contin-uous over tens of centimeters but end abruptly, e.g., on the eastern hill over-looking Gulch Cove. Distinct, mostly pink weathering feldspar occurs with the quartz in a number of places in Unit 3, particu-larly where the main zone tapers off along strike. The feldspars are 1 to 12 mm across and are either spottingly distributed or profuse enough that the rock resembles a leucogranite. This particular observation suggests an intrusive or quartz vein origin for Unit 3 and is consistent with a leuco-granite sill interpretation by Higgins and Smyth (1980). Also, discontinuous metasedi-mentary zones interpreted as rafts or xeno-liths are common in Unit 3 and consist mostly of pelitic to psammitic phyllite and schist. Interbedded quartzite, psammite, semipelite and amphibolite, with beds 1 to 10 cm wide, form a concordant zone in Unit 3 on the west side of Gulch Cove. These inclusions range from less than a metre across to several metres wide and tens of metres long. The smaller inclusions look convincingly like xenoliths although it could be argued that the larger ones repre-sent original interbedded material. The main contacts of Unit 3 are generally sharp and abrupt but locally interdigitating occurs and the quartz appears to form tongues that pervade the semipelite and psammite inclusions. Also, small quartz veins which cross-cut beds in Unit 2 adja-cent to Unit 3 locally contain minor feldspar and some are texturally identical to quartz in Unit 3.

A pronounced penetrative foliation is developed throughout most of Unit 3. It is commonly resolved as a 1 to 4 mm parting with minor muscovite concentrated on the fabric planes. Locally flecks of magnetite are oriented parallel to the main fabric. The foliation is also more intense along

Plate 4: *Looking east from Gulch Cove along the main quartz vein (Unit 3).*

the contact with Unit 2 and appears to be the same regional fabric in both. Minor, open to tight folds of the main fabric in the quartz unit are consistent with the later refolding observed in the metasedimentary rocks. Amphibolite and granite dikes intrude Unit 3 pretectonically in some places.

Unit 4 occurs throughout the enclave, generally structurally below and south of Unit 2. It is a migmatized metasedimentary unit that essentially is the higher grade metamorphic equivalent of Unit 2. Along its northern boundary with Unit 2, a clear gradation between the two units is evident. A crude migmatitic banding is developed in Unit 4, defined by granitoid sweats, lenses of metasedimentary protolith, granite veins and the penetrative foliation (Plate 5). The quartzofeldspathic component of the semipelite protolith becomes recrystallized such that the rock locally resembles a fine grained, strongly foliated, biotite ± minor hornblende granitoid. The discontinuous granitoid sweats are white weathering, wispy and truncated by granite ptygmas. Where the development of migma is greatest, the migmatite is a crudely banded tonalite containing muscovite and biotite rich schlieren. Pelitic portions are locally garnetiferous with some porphyroblasts up to 1 cm across. Plagioclase, muscovite and cordierite porphyroblasts are also developed in pelitic bands within the migmatite. Areas of less migmatized metasedimentary protolith, particularly the more siliceous material, occur throughout Unit 4. One such zone occurs on the coast west of Grey River Point where interbanded psammite and minor

quartzite, probably reflecting original bedding, are intruded by lit-par-lit granite veins. Concordant amphibolite bands occur throughout Unit 4 but increase in profusion towards its southern boundary. Some of these are clearly pretectonic dikes but bands marked by gradational boundaries with interlayered pelitic material are interpreted as primary in origin, i.e., mafic tuffs or flows.

Plate 5: *Quartz/granitoid segregations and veins in migmatite. Unit 4 on shore north of Grey River.*

The regional foliation is strongly developed throughout Unit 4 and most lithological elements in the migmatites are parallel to it. It is overprinted by a crenulation or strain-slip cleavage which is axial planar to moderately tight folds.

Amphibolite and mafic migmatite of Unit 5 form a linear zone south of and structurally below Unit 4; the contact between the two units is concordant and apparently conformable. Unit 5 is narrower east of Gulch Cove where it is limited southward by an agmatite zone. Fine grained banded amphibolite occurs in Unit 5 along its northern boundary where similar amphibolite layers also occur in Unit 4. The banding is interpreted as primary layering and is defined by variations in the color, grain size, and amount of amphibole. In hornblende-poor layers, plagioclase and minor quartz are strongly oriented along the layer parallel foliation. The banding is also accentuated by epidote rich lenses and concordant granite aplite or pegmatite veins. The amphibolites become more coarsely recrystallized and leucocratic to the south, a feature well displayed in the section south of Grey River harbour. The

leucocratic component consists of 2 to 6 cm plagioclase porphyroblasts and a profusion of 1 to 8 cm wide segregations of plagioclase plus quartz; these give the mostly dark weathering rock a streaky migmatitic appearance. Cross-cutting veinlets of epidote are also common. Towards Grey River Point, this rock grades into a crudely banded, fine to medium grained, hornblende ± minor biotite, diorite schist or migmatite. It contains 2 to 15 mm wide, hornblende rich lenses and bands as well as local welts of hornblendite several centimeters across. In places, patches of quartz and plagioclase granitoid, 1 to 4 cm across, have diffuse margins with the enclosing hornblende schist or gneiss and are interpreted as *in situ* granitoid sweats (Plate 6). Lit-par-lit granite veins add to the banded migmatitic aspect of Unit 5 in this area. These rocks also grade eastward into less migmatized amphibolite in the area west of Gulch Cove. Hornblende schist and migmatite characterize the unit east of Gulch Cove.

Plate 6: *In Situ granitoid welt of plagioclase and quartz in hornblende schist. Unit 5 north of Grey River Point.*

Unit 5, particularly in an area centered around the entrance to Grey River, is intruded by a profusion of dikes which locally may represent more than 50% of the sea cliff exposures. These include pretectonic, concordant to cross-cutting, amphibolite and granite aplite or pegmatite. The foliated amphibolite dikes generally predate the foliated granite dikes. Posttectonic granitic dikes cut the foliated dikes and are in turn intruded by fine grained, locally porphyritic, diabase dikes. The posttectonic mafic dikes are generally thinner than the early amphibo-

lites and locally form vertical pipes from which many offshoots follow internal contacts and other zones of weakness in the host rock.

A penetrative foliation, parallel to the crude migmatitic banding and well developed layering, occurs throughout Unit 5. It is locally axial planar to isoclinal folds of the banding. Variably oriented, minor shear zones, 1 to 4 cm wide, offset the banding or have the banding rotated into them in some areas. Amphibolite dikes, commonly at a high angle to the crude gneissic banding, have a margin parallel or slightly divergent foliation which locally is axial planar to folds in the adjacent migmatite. Granitoid segregations and quartz veins have developed parallel to the foliation in these dikes which were either intruded into active shear zones (Higgins and Smyth, 1980), or the dikes preferentially sited shearing after intrusion (Plate 7).

Plate 7: *Foliated amphibolite dike truncates banding in mafic migmatite. Note rim of leucogranite of enigmatic origin along the margins of the mafic dike. Unit 5 east of Grey River Point.*

Unit 6 forms a linear zone of amphibolite that is mostly surrounded by Unit 4 in the area west of Gulch Cove. It is generally greenish black weathering, and fine to coarse grained. Plagioclase crystals are 1 to 5 mm across and form augen in the foliation planes. Locally the feldspar exceeds hornblende in zones of leuco-amphibolite; variations in the hornblende/feldspar ratio also produce a crude banding in some areas. The more hornblende rich areas tend to be less well foliated and locally pods of coarse grained, dark green hornblendite

occur. Minor biotite was observed in a few places as was fine grained quartz in the groundmass. Locally, along its boundaries, the main amphibolite zone is fine grained with a 0.5 to 30 cm wide banding which appears concordant with the surrounding migmatized metasedimentary rocks. This might suggest a conformable relationship with the enclosing rocks and Unit 6 may have originated as a mafic volcaniclastic or flow. However, away from the margins it resembles a foliated medium grained gabbro including hornblendite pods. The occurrence of small mafic-ultramafic plugs (6a, 6b), here included with Unit 6, further suggests an intrusive origin. Subunit 6a is mostly variably foliated to massive, medium to coarse grained hornblendite, with variable amounts of gabbro. It is quite similar to small hornblendite pods in the main amphibolite zone. Subunit 6b is a coarse grained, relatively unfoliated, ultramafic containing 0.5 to 1 cm pyroxene crystals and minor biotite. Unit 6 is intruded by pretectonic leucogranite veins and both pretectonic and posttectonic mafic dikes; posttectonic quartz veins are common north of Grey River.

The penetrative regional foliation in Unit 6 is locally axial planar to folds of pretectonic dikes and minor banding in the amphibolite. A small zone of intensely foliated, grayish black weathering phyllite on the southeast side of Bay de Vieux contains scattered feldspar and quartz augen and is interpreted as mylonitized amphibolite. Within that zone, medium grained lenses of amphibolite protolith is preserved.

Unit 7 forms a small area west of Grey River Point. It consists of light gray to pinkish gray weathering, fine to medium grained, granite to granodiorite gneiss and migmatite. The banding is defined by discontinuous 1 to 5 mm wide layers, rich in biotite and/or hornblende. Commonly, biotite is the only dark mineral present. The banding or gneissosity either has a regular trend or is quite contorted with a diffuse schlieric outline. Profuse amphibolite lenses in the leucocratic gneiss are oriented parallel to the crude banding. Rarely, pelitic and quartz rich inclusions occur. Some of the amphibolite inclusions must represent mobilized pretectonic dikes since in detail they truncate the schlieric banding and are folded with it. However similar inclusions also truncate oriented mafic lenses that are interpreted as either restite or xenoliths of the hornblende schist/migmatite unit (5) to the north. The leucocratic gneiss is locally concordant with banding in the adjacent more mafic gneiss but locally intrudes and truncates the banding in the latter, e.g., east of Grey River Point (Plate 8). The myriad dikes which intrude Unit 5 also intrude Unit 7.

Plate 8: *Granodiorite migmatite (Unit 7) with schlieren structure intrudes regularly banded hornblende migmatite (Unit 5). Unit 5 at eastern entrance to Grey River harbour.*

Unit 8 is an agmatite zone which occurs east of Gulch Cove. Foliated amphibolite and hornblende ± biotite schist and migmatite of Unit 5 are intruded by fine to medium grained quartz and white feldspar granitoid. The intrusion breccia is accentuated by having black weathering, mafic rafts in the white weathering granitoid. Generally the granitoid predominates and locally contains minor biotite. The regional penetrative foliation is common to both rock types.

Gabbro (Unit 9)

Unit 9 is a fine to coarse grained, black weathering gabbro that intrudes the agmatite zone along its northern boundary. The contact is sharp and the gabbro is fine to medium grained along its margin. A moderate foliation is developed in the contact area where Unit 9 is locally amphibolitic. Generally, however, it is massive and where coarse grained, hornblende crystals are up to 1 cm long. Locally, zones of nearly hornblendite composition contain minor plagioclase; rare diorite also occurs in some places. The gabbro is intruded by pink granite aplite dikes.

Burgeo granite (Units 10 and 11)

The Burgeo granite, an informal name used here to replace the Burgeo batholith of Williams (1978), includes a vast area of granitoids to the north and west of the Grey River map area (Dickson et al., 1985; O'Brien and Tomlin, 1985). It intrudes the

Grey River enclave along its northern boundary. Unit 10 is a medium to coarse grained feldspar porphyritic biotite granite. Feldspar phenocrysts are 1 to 5 cm long. A penetrative foliation defined by oriented biotite and minor quartz elongation is commonly developed north of Southwest Arm and in the Bay de Vieux areas; however, local areas of weakly foliated to unfoliated biotite-poor granite also occur. The granite is dominated by cataclastic textures along its contact with the Grey River enclave. Narrow zones of protomylonite to mylonite occur where original feldspar phenocrysts are reduced to pink streaks. Commonly, however, the granite is brecciated or highly fractured, consisting of orange pink feldspar, 0.5 to 3 cm long, in a light to dark green weathering chloritized matrix. The fractures are anastomosing, locally chlorite filled, and cross-cut the penetrative foliation. The contact area west of Southwest Arm locally contains zones of dark gray weathering sheared granite/granodiorite that were originally mapped as metasedimentary rocks (Bahyrycz, 1957).

Unit 11 is a fine to medium grained granite protomylonite containing pink feldspar and minor biotite. It is tentatively included with the Burgeo granite and may represent a contact phase of the larger body. Feldspar porphyroclasts are 1 to 2 mm long and have a pronounced augen structure along with flattened quartz in zones of mylonite. Black weathering flinty zones of ultramylonite occur in some areas along the contact between Units 10 and 11. The protomylonite contains minor amphibolite xenoliths locally.

The relationship between the penetrative foliation in the Burgeo Granite and the main fabric in the Grey River enclave is not clearly understood. They are regionally concordant along part of the contact but the fabric in the granite appears to have a similar attitude to the strain-slip fabric in the metasedimentary rocks along part of Southwest Arm. Also, pelitic rocks at the entrance to Southwest Arm locally have a flinty hornfels texture and large cordierite porphyroblasts that overprint the main foliation. If the porphyroblasts are related to the Burgeo granite, it suggests that the granite in this area postdates the main deformation of the Grey River enclave.

Francois granite (Units 12 and 13)

The Francois granite (Poole et al., 1985) intrudes the Burgeo Granite, the Grey River enclave and Unit 9 gabbro in the eastern part of the map area. Granite similar to Unit 12 occurs on Gulch Cove Islands. The main area of the Francois granite is exposed east of the map area and is described by Poole et al. (1985). Unit 12 is a pink weathering, coarse grained, feldspar porphyritic, biotite granite. The feldspar phenocrysts are 0.5 to 3 cm long and biotite commonly forms 2 to 6 mm phenocrysts. Coarse grained quartz, 2 to 10 mm across, and finer grained white feldspar occur throughout. The granite is texturally uniform and apart from a local fracture cleavage, quite massive.

Unit 13 is a pink weathering, fine to medium grained, feldspar porphyritic, biotite syenite. Minor, fine grained quartz is locally visible in a pink feldspar-rich matrix which contains 0.4 to 2.0 cm long K-feldspar phenocrysts and 1 to 5 mm biotite phenocrysts. White to pale green plagioclase phenocrysts are smaller than the pink feldspar. A feldspar porphyry phase containing minor quartz phenocrysts occurs along the syenite's northern contact. The K-feldspar phenocrysts are commonly zoned and euhedral in the porphyry. Away from the contact, feldspar phenocrysts are profuse to sparsely developed. Locally some biotite is altered to chlorite. Along the eastern contact with Unit 12 granite, a porphyry phase included in Unit 13 contains conspicuous quartz phenocrysts 2 to 8 mm across with square to round cross-sections. The size and number of phenocrysts decrease away from the contact over several metres where it merges with the regular syenite. Unit 13 is unfoliated except for a locally developed contact parallel cleavage along its northern boundary.

Granite (Unit 14)

Unit 14 is a fine to medium grained, pinkish white weathering, granite plug that intrudes Unit 5 of the Grey River enclave on the hill above Grey River Point. It contains minor hornblende and even less biotite; locally pegmatitic patches occur. Completely unfoliated, it is a posttectonic granite of the same age and composition as many of the granite dikes in the same area.

Devonian(?) sedimentary rocks (Unit 15)

A small area of mostly gently dipping, upward facing, sedimentary rocks occurs on the western peninsula at the entrance to La Hune Bay. The most common rock type is pale green to gray weathering and minor reddish brown weathering granule to pebble conglomerate. Generally the conglomerate has a matrix of rounded pink feldspar and quartz granules which supports a variety of pebbles. Minor calcareous patches occur in the matrix locally. The pebbles consist of quartz and/or feldspar porphyry, pink, medium grained granite, flow banded rhyolite, red and purple fine grained felsic volcanics, argillite, sandstone, and quartz. Clasts range from 1.5 to 2.5 cm

across. Some of the argillite and felsic volcanic clasts have a parting or cleavage that predated incorporation into the conglomerate. Locally, trough cross-bedding occurs in the conglomerate and where interbedded with sandstone, the conglomerate beds range from 20 cm to 3.5 m thick. The interbedded sandstone and siltstone are reddish brown weathering, fine grained and graded. Commonly calcareous, they grade into white weathering carbonate rich layers containing interconnecting lenses of reddish brown siltstone; in other layers the clastic material dominates with anastomosing stringers and pods of carbonate (Plate 9). Interpreted as some type of caliche deposit, these rocks occur along the northern boundary of Unit 15 where it is in contact with the Francois granite (Unit 13).

Plate 9: *Carbonate pods in fine grained sandstone. Unit 15 near northern contact with Unit 14, western entrance to La Hune Bay.*

The contact between the sedimentary rocks and the Francois granite was originally interpreted as intrusive (Williams, 1971), but it appears, in fact, to be a nonconformity. The contact is steeply dipping and what appears to be a highly fractured "rubble" zone is developed in the underlying feldspar porphyry of Unit 13. Carbonate fills the fractures in the porphyry which is overlain by calcareous siltstone and sandstone with lenses of carbonate. The caliche-like zone directly overlies this and contains pebbles and boulders (up to 2 m across) of the porphyry; cracks in the boulders are also filled with carbonate. The sedimentary rocks are relatively unmetamorphosed but are overprinted by a slaty cleavage which locally is axial

planar to open to moderately tight folds. These rocks are posttectonic with respect to the deformation in the Grey River enclave and may be Devonian or later in age (Williams, 1971).

MINERALIZATION

Most of the known mineralization in the Grey River area occurs in association with posttectonic quartz veins (Bahyrycz, 1957; Higgins, 1980) that are chiefly concentrated in the amphibolite unit (6) north of the town of Grey River. The veins are of variable size, from 2 cm wide veinlets to large 1 m wide veins that are up to 400 m long. Two of the larger veins are shown on Figure 1. The veins follow north to northeast trending faults, joints and fissures that sharply truncate the foliation in the host rocks. Wolframite is the most important tungsten mineral but scheelite also occurs. Other ore minerals include pyrite, chalcopyrite, minor arsenopyrite, molybdenite, sphalerite, galena, bismuth and marcasite. Small, sulphide bearing quartz veins also cut sheared and mylonitized Burgeo granite (Unit 10) to the north, the largest of which on Dog Cove Brook contained pyrite, chalcopyrite, sphalerite and galena (Bahyrycz, 1957). Specular hematite forms thin coatings on fractures in the Burgeo Granite at the entrance to Southwest Arm.

A silica assessment (Bartlett, 1969) on the main quartz zone (Unit 3) east of Gulch Cove proved, by diamond drilling, a total tonnage of 12 million short tons with an average grade of 95.5 percent SiO_2 and 1.9 percent Al_2O_3 (Butler and Greene, 1976). The re-interpretation of the silica deposit as vein quartz could make it a possible target for gold exploration.

Disseminated pyrite mineralization occurs locally in the newly delineated felsic volcanic zone (Unit 1) and in metasedimentary rocks of Unit 2. Felsic volcanic and associated rocks are important hosts for gold and base metal mineralization throughout the Hermitage Flexure and represent the best potential in the Grey River map area.

SUMMARY AND CONCLUSION

Felsic metavolcanic rocks (Unit 1) and pelitic to psammitic metasedimentary rocks (Unit 2) form a conformable sequence in the northern part of the Grey River enclave. The volcanics structurally overlie the metasediments but their stratigraphic relationships are unknown; the presence of thin felsic volcanic bands in the underlying metasediments near the contact might suggest that Unit 1 volcanics are older and grade into Unit 2. Thick quartz rich bands (Unit 3), confined mostly to Unit 2, were

previously interpreted as bedded quartz-ites. However, field relationships suggest that these originated as pretectonic quartz veins, possibly from quartz released from the host rocks during regional metamor-phism. The metasedimentary rocks of Unit 2 are progressively metamorphosed southward and form the protolith for a zone of migma-tite (Unit 4). Banded amphibolite is con-cordant with the southern boundary of Unit 4 and grades through a zone (Unit 5) of granitoid segregation and *lit-par-lit* injection to a well banded migmatite at the entrance to Grey River harbour. The proto-lith for the hornblende migmatite may be mafic volcaniclastics and flows or a mafic intrusion, perhaps similar to the rela-tively homogeneous zone of amphibolite (Unit 6) that is confined mostly to Unit 4. The mafic migmatite is locally intruded by a granite to granodiorite gneiss or migma-tite (Unit 7) which contains profuse mafic inclusions. It is possible that this more leucocratic migmatite originated as an agmatite similar to Unit 8, where a mafic host is pervaded by leucogranite; sub-sequent or progressive deformation and metamorphism could produce the relation-ships seen in Unit 7.

Relatively massive gabbro (Unit 9) in the southeast intrudes the Grey River enclave, which is bounded to the north by the Burgeo granite (Units 10 and 11). A regional penetrative foliation in the Burgeo granite locally merges with mylonites in the contact between the granite and metamorphic rocks. Along this contact, the Grey River enclave appears retrogressed as chlorite and sericite phyl-lites contain remnant quartz and granitoid segregations, typical of the lower to upper amphibolite facies rocks to the south. Thus the final tectonic positioning of the granite postdates the main pulse of meta-morphism in the Grey River enclave. How-ever, displacement along the contact was probably not great since original intrusive relationships, indicated by xenoliths and porphyroblasts, are evident in the map area. The posttectonic Francois granite (Units 12 and 13) is mostly massive and truncates the eastward trace of the above units. A small plug of hornblende-biotite granite (Unit 14) is representative of the posttectonic granitoid veining in the mig-matite units. Finally, a mostly conglom-eratic sequence (Unit 15) was deposited nonconformably upon the Francois granite.

Felsic volcanic rocks occur with mostly pelitic rocks in the Grey River area. This is a common association through-out the Hermitage Flexure, particularly in the Baie d'Espoir and Bay du Nord Groups. The style of deformation and metamorphism (Blackwood, 1984) is also similar; the main period of folding in the Grey River area resulted in isoclinal, possibly recumbent

folds, although present attitudes may not reflect the original style. A crenulation cleavage, axial planar to upright, gently plunging folds overprints the earlier structures. Metamorphism increases south-ward or structurally downward, culminating in migmatites. These observations would tend to suggest that rocks of the Grey River enclave are the equivalent of Ordo-vician rocks that occur elsewhere along the Hermitage Flexure. A postulated Avalon Zone connection, based on correlating presumed orthoquartzites in the Grey River area with similar rocks elsewhere in the Avalon Zone (Smyth, 1981) is invalid if the present vein quartz interpretation is correct.

REFERENCES

Bahyrycz, G.A.
1957: Geology of the Grey River area, Newfoundland, with special reference to metamorphism. Unpublished M.Sc. thesis, McGill University, Montreal, 101 pages.

Bartlett, G.
1969: Silica assessment - Grey River area. Newfoundland Department of Mines, Agriculture and Resources, Mineral Resources Division, unpub-lished report, 15 pages.

Blackwood, R. F.
1984: Geology of the west half of the Dolland Brook map area (11P/15), southern Newfoundland. *In* Current Research. *Edited by* M.J. Murray, J.G. Whelan and R.V. Gibbons. Newfoundland Department of Mines and Energy, Mineral Development Division, Report 84-1, pages 198-209.

Butler, A.J., and Greene, B.A.
1976: Silica Resources of Newfound-land. Newfoundland Department of Mines and Energy, Mineral Development Divi-sion, Report 76-2, 68 pages.

Chorlton, L.B.
1980a: Notes on the geology of Peter Snout (11P/13, west half), Newfound-land, and accompanying Map 80201. New-foundland Department of Mines and Energy, Mineral Development Division, Map 80201 with marginal notes.

1980b: Geology of the La Poile River map area (110/16), Newfoundland. New-

foundland Department of Mines and Energy, Mineral Development Division, Report 80-3, 85 pages.

Colman-Sadd, S.P.
1974: The geological development of the Bay d'Espoir area, southeastern Newfoundland. Unpublished Ph.D. thesis, Memorial University of Newfoundland, St. John's, 271 pages.

1976: Geology of the St. Alban's Map-Area, Newfoundland (1M/13). Newfoundland Department of Mines and Energy, Mineral Development Division, Report 76-4, 19 pages.

Cooper, J.R.
1954: The La Poile - Cinq Cerf map area, Newfoundland. Geological Survey of Canada, Memoir 256, 62 pages.

Dickson, W., Delaney, P., and Poole, J.
1985: Geology of the Burgeo Granite and associated rocks in the Ramea (11P/11) and La Hune (11P/10) map areas, southern Newfoundland. *In* Current Research. *Edited by* R.V. Gibbons. Newfoundland Department of Mines and Energy, Mineral Development Division, Report 85-1.

Fleming, J.M.
1967: Grey River Silica Deposits: Assessment of sampling results. Newfoundland Department of Mines, Agriculture and Resources, Mineral Resources Division, unpublished report, 12 pages.

Higgins, Neville C.
1980: The genesis of the Grey River tungsten prospect: a fluid inclusion, geochemical and isotopic study. Unpublished Ph.D. thesis, Memorial University of Newfoundland, St. John's, 540 pages.

Higgins, N.C., and Smyth, W.R.
1980a: Geology of the Grey River area - regional summary. *In* Current Research. *Edited by* C.F. O'Driscoll and R.V. Gibbons. Newfoundland Department of Mines and Energy, Mineral Development Division, Report 80-1, pages 93-99.

1980b: Fluid-inclusion evidence for the transport of tungsten by carbonate complexes in hydrothermal solutions. Canadian Journal of Earth Sciences, Volume 17, pages 823-830.

Higgins, N.C., and Kerich, R.
1982: Progressive ^{18}O depletion during CO_2 separation from a carbon dioxide-rich hydrothermal fluid: evidence from

the Grey River tungsten deposit, Newfoundland. Canadian Journal of Earth Sciences, Volume 19, pages 2247-2257.

Jewell, W.B.
1939: Geology and mineral deposits of the Baie d'Espoir area. Geological Survey of Newfoundland, Bulletin 17, 29 pages.

Mullins, W.J.
1958: The Geology of the Cape La Hune area, southwest corner of Newfoundland, with special reference to igneous and metamorphic petrology. Unpublished B.Sc. thesis, Mount Allison University, 56 pages.

O'Brien, S.J., and Tomlin, S.L.
1985: Geology of the granitoid and associated rocks of the Burgeo map area (11P/12). *In* Current Research. *Edited by* R.V. Gibbons. Newfoundland Department of Mines and Energy, Mineral Development Division, Report 85-1.

Poole, J., Delaney, P., and Dickson, W.
1985: Geology of the Francois Granite, South Coast of Newfoundand. *In* Current Research. *Edited by* R.V. Gibbons. Newfoundland Department of Mines and Energy, Mineral Development Division, Report 85-1.

Riley, G.C.
1959: Burgeo - Ramea, Newfoundland. Geological Survey of Canada. Map 22-1959.

Smyth, W.R.
1981: The Grey River Orthoquartzites and related rocks, southern Newfoundland: a slice of Avalon Zone Precambrian basement tectonically positioned along the southern margin of the Central Mobile Belt? Geological Association of Canada, Mineralogical Association of Canada, Canadian Geophysical Union. Joint Annual Meeting, Program with abstracts, volume 6, page 52.

Williams, H.
1971: Burgeo (east half), Newfoundland. Geological Survey of Canada Map 1280A.

1978: Tectonic lithofacies map of the Appalachians. Memorial University of Newfoundland, Map 1.

Williams, H., Kennedy, M., and Neale, E.
1970: The Hermitage Flexure, the Cabot Fault, and the disappearance of the Newfoundland Central Mobile Belt. Geological Society of America Bulletin, volume 81, pages 1563-1568.

INDUSTRIAL MINERALS SURVEY - 1984

by

A.F. Howse and C.J. Collins*

INTRODUCTION

Attention again focused on barite during the 1984 field season. Activities were concentrated in two areas of southeastern Newfoundland, mainly as a follow-up to work done in the previous two field seasons. A brief survey was undertaken on the Isthmus of Avalon in an attempt to explain some of the barium anomalies revealed by a 1983 regional stream sediment survey (Howse et al., 1984). On the Burin Peninsula, a stream sediment survey was conducted in and around the St. Lawrence fluorspar district. Although that region has potential of hosting a wide range of mineral deposits (Strong et al., 1978), the primary objective of the survey was to help assess the potential for fluorite-barite minerali-zation in the outer fringe areas of the district. There, mineral occurrences in the form of fluorite-barite-galena veins and fluorite-barite float are well documented (Smith, 1957), and significant deposits of these minerals may be present. Other industrial mineral commodities briefly investigated in 1984 included a little known deposit of diatomaceous earth near the community of Victoria and brick shales on the Port au Port peninsula.

INDEX MAP

Figure 1: *Field study areas during 1984 field season (A) Avalon isthmus; (B) St. Lawrence area; (C) Shoal Point; and (D) Victoria/Carbonear areas.*

WESTERN AVALON PENINSULA

Previous Barite Assessment

Because of the wide distribution of vein deposits of barite throughout the western Avalon Peninsula, that area has been the focus of attention during the past three field seasons. Geologically, the region is underlain by a sequence of sedimentary and volcanic rocks belonging to the Upper Precambrian Connecting Point and Musgravetown Groups and to various Lower Cambrian formations. Barite, with or without quartz, occurs in veins cutting strata of all ages. On the eastern side of Placentia Bay, barite is present in the La Manche galena-calcite vein (Green, 1981), and as a very minor gangue mineral at the Silver Cliff lead-zinc-silver vein near Argentia (Chute, 1939). Specifically, the Isthmus of the Avalon and the St. Brides areas have been subjected to more intense investigations. Initially, the coastlines of both areas were surveyed by boat, inland areas were traversed by foot and highway and railway rock-cuts were examined. Numerous new, narrow, high grade veins of barite were discovered during the course of the 1982 project (Howse and French, 1983).

Typically these consist of salmon-pink, bladed or tabular crystal aggregates, occupying small fissures and commonly asso ciated with quartz and/or calcite. Faults which cross-cut the regional northeasterly structural trends are readily discernible on air photographs; those that parallel these trends are not as apparent. On the Bellevue Peninsula, several composite veins with varying proportions of barite, quartz and calcite were discovered. There, the most significant veins in terms of width and grade of barite occupy fractures that trend approximately north-south. The Colliers Point vein to the immediate south, first mined early in the century and sporadically reactivated in recent years, occupies an approximately north-south trending fault.

In 1983, the Mineral Deposits Section, in a coordinated effort with the Geochemical Section, carried out stream sediment surveys in two areas of the Western Avalon Peninsula. The projects conducted in the Isthmus of the Avalon and the St. Brides

* Department of Earth Sciences, Memorial University of Newfoundland, St. John's, A1B 3X5.

areas were aimed at assessing both indus-
trial mineral and base metal potential.
Prospecting for mineralized float and out-
crop was also an integral part of the
stream traverses. During the course of the
field work additional barite veins were
discovered on the Bellevue Peninsula, in
the northern part of the Isthmus near Jacks
Pond (Howse and Collins, 1984), and at
Cuslett, near St. Brides. A new barite-lead
vein was discovered near Southern Harbour.
Most of these deposits have subsequently
been staked and results of the stream
sediment surveys have been released on open
file (Howse et al., 1984).

Avalon Follow-up - 1984

A brief period in June was spent
traversing some of those streams, which
contained anomalous amounts of barium in
their stream sediments. Only a few streams
were traversed and water levels were high.
The aim was to examine the bedrock of the
immediate drainage area for barite mineral-
ization where it was located in four out of
the seven anomalous areas. The strongest
anomalies occur in streams which drain
areas underlain by rhyolitic rocks of the
Bull Arm Formation. In fact the concentra-
tion of barium in one stream, which flows
in a northeasterly direction into Broad
Lake, (maximum 24,964 g/t) suggests that
some form of physical concentration of the
barite is present in the stream sediment.
This is probably accomplished through
erosion of the host rock and the barite
followed by gravity settling of the denser
barite. Near the stream, barite and quartz
occur as films along fractures and joints
in rhyolite on the north side of the stream
valley. Because of its high specific
gravity, barite may have become segregated
into highly anomalous zones in the streams,
through the action of water.

An investigation of a barium stream
sediment anomaly near the Old Rantem
Station resulted in the discovery of barite
mineralization within a few metres of the
sample site. Stringers and veinlets of
gray-pink and reddish-pink barite cut red
medium-grained sandstone. The northeast
trending zone, which dips steeply to the
southeast, can be traced for about 5
metres. Hematite coated slikensides occur
in the footwall.

Barite was also found about 1 km
southwest and along strike from the Little
Southern Harbour barite-lead vein,
discovered in 1983 (Howse and Collins,
1983). The vein is about 15 cm wide and
consists of pink and reddish-pink bladed
crystals of barite. It is exposed in the
north bank (cliff) of the stream, strikes
028° and dips subvertically. The host rocks
are siltstones of the Connecting Point

Group. The stream sediments downstream of
the vein are anomalous in both barium and
lead, although no lead mineralization was
seen. Overburden covers the top of the 3
metre cliff in which the vein is exposed.

A barite occurrence at Bellevue
reported by McCartney (1956), was also
investigated. This was the only inland
occurrence of barite shown on McCartney's
map. The 20-50 cm wide vein consists of
pink, platy barite with numerous inclusions
of country rock. It strikes 020°, dips
vertically and can be traced 4 metres along
the stream bed in which it is exposed.
Stream sediment a few metres downstream
from the vein contain anomalous concentra-
tions of barium.

ST. LAWRENCE AREA

Fluorite-barite Mineralization - "Outer" Veins

A stream sediment survey was carried
out in the St. Lawrence fluorspar district
on the Burin Peninsula during the 1984
field season (Figure 2). Although the area
has potential for hosting a wide range of
mineral deposits (Strong et al., 1978) the
primary objective of the survey was to help
assess the potential for fluorite-barite
mineralization of the northern part of the
district. The project area is underlain by
Late Precambrian volcanic and sedimentary
rocks, Cambrian sedimentary rocks and the
Carboniferous St. Lawrence Granite, the
latter being the principal host rock for
the area's fluorite mineralization. Studies
of the genesis of the fluorite veins (Teng,
1974; Teng and Strong, 1976; Collins, 1984)
have supported hypotheses by Van Alstine
(1948) and Williamson (1956), that the
granite and fluorite had a common source,
i.e. a magma chamber that released ore
fluids during late stage differentiation.
These formed fluorite veins along faults
and shears in the granite as it cooled and
contracted. Veins of fluorite with an asso-
ciated barite content ranging up to 30 per-
cent, occur in a number of widely scattered
locations north of Lawn and St. Lawrence.
These, which include the Big Meadow Woods,
Anchor Drogue, Lunch Pond, Devils Kitchen,
Tilt Hill and Clam Pond veins, were collec-
tively referred to as "outer" veins by
Smith (1957) because of their location in
the peripheral region of the distinct. The
following arebrief descriptions of some of
these deposits based on the authors' own
field observations and experience in the
area, as well as data from the Department
of Mines and Energy geofiles. The descrip-
tion also includes that of the Lawn Barite
vein, a relatively newly (198^) discovered
vein uncovered by a road construction crew
in the community of Lawn.

LEGEND FOR FIGURE 2   Abbreviations

CARBONIFEROUS
    6   *St. Lawrence Granite*

CAMBRIAN
    5   *Inlet Group (clastic sedimentary rocks)*

PRECAMBRIAN
    4   *Marystown Group (subaerial volcanics)*
    3   *Burin Group (submarine basalts)*

INTRUSIVE ROCKS
    2   *Loughlins Hill Pluton (gabbro)*
    1   *Anchor Drogue Pluton (granodiorite)*

ba	Barite
dum	Dumortierite
fl	Fluorite
py	Pyrite
pph	Pyrophyllite
Cu	Copper
Pb	Lead
Mn	Manganese
Mo	Molybdenum
Ag	Silver
U	Uranium
Zn	Zinc

SYMBOLS

Fluorite vein xxxx
Mineral occurrence (dumortierite) . . . . ✗dum
Mineralized float . . . . △

Meadow Woods Vein

The Meadow Woods vein is by far the most important of the "outer" veins of the district. Discovered in 1944 by Aloysius Molloy and Louis Kelley, about 4 km north of Lawn, early workers traced it for approximately 600 m along its east-west strike. The width of the vein decreases eastward, averaging 3.6 m for 180 m, then 1.8 m for the next 180 m and gradually narrowing to about 1.2 m for the remaining strike length.

In the 1950's Newfoundland Fluorspar Limited sank a 12.2 m shaft into the vein to learn more about its characteristics at depth, and to establish the relative proportions of the different minerals (fluorite, barite, galena). The average analyses (Smith, 1957) of 12 run-of-mine samples taken while shaft-sinking were:

CaF_2	-	58.8%
$BaSO_4$	-	15.1%
$CaCO_3$	-	0.6%
SiO_2	-	19.5%
Pb	-	2.2%

Fluorite and barite was found to be mixed intimately but the galena was concentrated in a 15 cm wide band in the vein.

Alcan (1976) drilled eleven holes along the vein structure. Drilling confirmed the high fluorite content of the vein but the core was not assayed for $BaSO_4$.

The Big Meadow Woods trenches were examined by the authors in 1983. Rubble in the trenches consists of blocks of barite-rich, white fluorite; the barite is pink and salmon in color. The barite occurs as fine-grained bands and crystal aggregates

with fluorite and quartz. Malachite was also observed. Barite is estimated to comprise up to 20% of the vein. Smith (1957) concluded from his examination of the vein, as exposed in the trenches, that it contained barite sufficient to make up one-quarter to one-third run of the mine ore, and our observations tend to support that view.

Big Meadow Woods - East Extension Vein(s)

Extensive barite float was also noted in trenches about 6 km northeast of Lawn. The barite displays pink and white banding and has a bladed crystal texture. White, purple and green varieties of fluorite were noted. Minor galena and pyrite are associated with the barite and fluorite. The trenches were dug by David S. Robertson Associates Limited (1972), who explored a series of airborne VLF anomalies in the area. The anomalies trend toward the Meadow Woods vein, some 2.5 km to the west. These anomalies were tested by a series of three diamond drill holes in the immediate area of the trenches. Hole 72-4 (45°) intersected extensive barite-fluorite mineralization in granite from 13.9 m to 46.0 m. The hole log describes a system of parallel veins, up to 1.3 m thick, occurring in fractured, hematized, kaolinized, granite. Barite and fluorite occur in brecciated and silicified zones; galena was also noted. In most of the veins barite is the dominant mineral, but in some, fluorite is proportionally greater. The log notes several kaolinized zones, described as faults in the section, in which the rock was very incompetent and core recovery was extremely poor. The log also notes that the mineralized fault zone was intersected at a 45° angle. It is possible that this zone is an eastward extension of the Big Meadow Woods Structure.

Figure 2: *Geological map of St. Lawrence area.*

Anchor Drogue Vein

The Anchor Drogue vein lies 3.2 km west of Salmonier or about 20 km northeast of the town of St. Lawrence. The vein occurs along a fault which cuts volcanic rocks of the Marystown Group and granodiorite of the Anchor Drogue Pluton. Its attitude is 085/65°N and it has a maximum exposed width of 1.5 m. The vein is composed mainly of green-white coarsely crystalline fluorite, displaying prominent zoning with barite-rich bands on the hangingwall and footwall. Galena occurs as blebs and crystals scattered throughout the vein.

The Anchor Drogue vein was tested by 4 diamond drill holes in the 1950's (Newfoundland Fluorspar Limited) and 14 holes in the early 1970's (Allied Chemical Corp). The latter program indicated a reserve of about 15,000 tonnes of 40 - 50 percent CaF_2 and about 15 percent barite, in a shallow vein deposit.

Lunch Pond Vein

The Lunch Pond vein is located near the northern tip of Lunch Pond, about 11 km northwest of St. Lawrence. Discovered by Newfluor prospectors in 1950 the vein was trenched and diamond drilled. Although the trenching showed only a 60 cm wide vein, subsequent drilling indicated extensive mineralization. The best results from the holes drilled showed a cumulative total of 8.4 metres of fluorite contained in three sections of 1.2 m, 4.2 m, and 3.0 m respectively. The average grade was 58.8 percent CaF_2, including the 3 m section which averaged 66.5 percent CaF_2.

The vein which is hosted by St. Lawrence Granite, appears to strike about N65°E and dip 80°N; its strike length is unknown. The vein contains a mixture of fluorite, barite and calcite with minor galena. Barite is proportionally less than that contained in the Big Meadow Woods vein.

Clam Pond Vein

The Clam Pond vein outcrops on the west side of a stream which flows into the northeast end of the pond. Large angular chunks of red and salmon-pink barite with white and blue fluorspar were observed in the stream bed, near a small notch which marks the site of the vein. Van Alstine (1948) observed the vein in place and reported that much of it consisted of alternating bands (up to 1 cm wide) of red platy barite and white fluorite. Galena and sphalerite were also noted. The vein is hosted by the St. Lawrence Granite.

Devil's Kitchen Vein(s)

During the stream sediment survey numerous trenches containing large blocks of white and pink barite float were noted east of Main Brook Pond about 16 km north of St. Lawrence. These trenches are undoubtedly those described by Smith (1957) as containing extensive barite float. Host bedrock is visible in only one trench; there it consists of mineralized pink, medium to coarse-grained granite with finer aplitic zones. Green and white fluorite and pink platy barite, as well as minor galena, occur as float. Dimensions of the mineralized blocks indicate vein widths of 30 cm or more.

Lawn Barite Vein

The Lawn Barite vein was discovered in 1982 during road construction through the community of Lawn. The following description of the vein is a condensed version of an account by Collins (1984). The vein is located on the eastern side of Lawn Harbour and occurs in the Webbers Cove Conglomerate, part of the Upper Proterozoic Marystown Group, a sequence of dominantly subaerial volcanic rocks, which outcrop throughout the Grand Bank and Lamaline region. (O'Brien et al., 1977). The mineralization, exposed in a 25 m wide roadcut, consists of granite, fluorite, galena and sphalerite in two zones on either side of the road. The main vein, which is located on the southern side of the road, strikes 105°, dips almost vertically, and can be traced for about 25 meters along the outcrop. The vein widens with depth from only 15 cm at sub-outcrop level (1 m below surface) to 60 cm at the road level (about 4 m deeper). Two smaller veins (10 cm wide) were noted near the main vein and may be offshoots from it.

The mineralization in the main vein is primarily pink to white barite with intergrown fluorite and minor zones of galena and sphalerite. Some narrow zones of massive galena and sphalerite are also present. The more massive sections of the vein are characterized by banded white and pink barite, with intimately intergrown fluorite, together with minor bands of massive galena and sphalerite. Breccias are common, and consist of conglomerate fragments within banded crystalline barite and fluorite. Conglomerate with a matrix composed entirely or partially of barite, fluorite and calcite with or without veins or veinlets, is also common.

The conglomerate is relatively unaltered, coarse grained, and has a sandy matrix. Fragments are generally well rounded and include sedimentary and vol-

canic rocks together with fragments of granites or porphyry. Near the vein the conglomerate is altered over a 20 m width; the alteration zone consists of white to yellow clay minerals, presumably of hydrothermal origin.

Stream Sediment Survey

The stream sediment survey covered an area of about 200 km^2 and encompassed all of the fluorite and barite occurrences described above as well as a wide range of other metallic and non-metallic mineral occurrences (Figure 1) in the project area. The topography of the area is a reflection of bedrock type and the effects of glaciation. Volcanic and sedimentary rocks form high, rounded hills, while the granite usually underlies areas of low relief. Glacial features such as roche moutonnées, drumlins, and glacial till characterize the area, the latter having its greatest thickness in valleys and depressions. The region is generally dotted with small bogs and ponds. Wooded areas are sometimes present in stream valleys and on hillsides. The main drainage system is poorly developed and runs from north to south. However, many small streams run an irregular pattern between ponds and bogs.

Stream sediment samples were collected at 400 m intervals, however, this spacing varied considerably for some streams. The number of tributaries, connection between ponds and small brooks flowing into ponds sometimes resulted in more detailed sampling of an area than was originally planned.

Over 650 samples were collected. Descriptive data was routinely recorded for each sample and duplicates were taken for control purposes. The samples will be analyzed for a suite of elements including Ba, Sr, Cu, Pb, Zn, Ag, Fe, Mn, F, Co, Ni, Mo, U, Sn, W, and L.O.I. The results will be released on open file when they become available.

DIATOMACEOUS EARTH

Victoria – Carbonear

A cursory examination was made of the diatomaceous earth deposit which lies near Beaver Pond within the community of Victoria, Carbonear (Figure 3) This deposit was first recognized by N. Sutton, a resident of the area, who reported it to the Mineral Resources Division in 1963. The deposit was examined by Fletcher (1964) who, using a Swedish sampler (a device originally designed for testing peat), drilled 13 holes in the bog at the western end of the pond, and 7 holes in the pond itself. He estimated that there are approximately 65,700 tonnes of diatomaceous

earth under Beaver Pond and considerably less than that under the bog. Fletcher recommended more detailed logging with sub-surface contouring and laboratory testing.

The 1984 field work was aimed at obtaining samples of the deposit for laboratory tests. Using a Swedish sampler, samples were taken from the bog at the western end of Beaver Pond; as well as the pond itself (see Figure 2). Diatomaceous earth was encountered in all of the holes. Generally the deposit exhibits a fairly well defined layering with seemingly pure white material (30 - 60 cm thick) overlying a gray silty mixed layer (30 cm+). In some holes the white diatomaceous earth was encountered immediately on the surface and in others it was capped with peat. The test holes were limited to a depth of 3.6 m because of rod extensions. Descriptive logs were recorded for each hole and samples taken of the diatomaceous earth for laboratory tests.

BRICK SHALE

Shoal Point – Port au Port

A brief period was spent investigating shales of the Port au Port Peninsula in light of their potential industrial uses. The shales, together with minor sandstone and limy beds, form part of the lowest structural slice of the Humber Arm Supergroup (Williams et al., 1979). Shoal Point, on which the sampled shales are exposed, is a low-lying, uninhabited point of land projecting northwards for about 9 kilometers into Port au Port Bay (Figure 4). Its elevation does not exceed 15 m and most of the land averages about 3 - 4 meters above sea level. Harris (1962) sampled shales along the east shore of Shoal Point and concluded that the area had excellent potential for a brick shale quarry. He estimated a total reserve of about 7 million tonnes, assuming that 2.1 m of shale could be quarried above sea level. However, Harris's estimate is based on his observations of shale thickness on the east side of the point. On the west side there is much less exposure above sea level and most of the coastal exposures are covered at high tide. Correspondingly the thickness of peat on the west side of the point increases 3.6 m meters. Therefore, the reserve estimate of Harris (1962) may be too high, although substantial, amounts of quarryable material probably exist.

The shales in the Shoal Point section are red, green, black and highly fissile; minor sandstone and limy beds were also noted. Some of the beds contain large crystalline concretions of pyrite and marcasite. The shales are folded and faulted, and dips up to 50° were noted. The elevation of shale exposures averaged 2.2 m

● sample sites

Figure 3: *Location of the diatomaceous earth deposit near the town of Victoria. The deposit (shaded area) underlis Beaver Pond and the bog at its west end.*

above sea level in the sampled area on the east side of the point; exposures on the opposite shore are weathered down to sea level. The peat cover has a maximum thickness of 2.4 m on the east side of the point and 3.6 m on the west side. A total of six bulk samples were collected at 500 m intervals from both sides of the point. Chemical analyses and firing tests on the shales will be carried out in order to determine their suitability for the brick and cement industries.

ACKNOWLEDGEMENTS

REFERENCES

Chute, N.E.
    1939: Mineral Deposits of the Placentia Bay Area. Unpublished Report. Geological Survey of Newfoundland. Nfld. MDD File - 1N(11).

Collins, C.J.
    1984: Genesis of the St. Lawrence fluorite veins, as indicated by fluid inclusion and trace element data from three selected veins. Unpublished B.Sc. thesis, Memorial University of Newfoundland, St. John's, 103 pages.

David S. Robertson Associates Limited
    1972: St. Lawrence Area: 20 D.D.H. Logs, 1 Geology Map. Unpublished Report. Nfld. MDD File - 1L/14(43).

Fletcher, W.K.,
    1964: Report on the Diatomaceous Earth Field Party. Unpublished Report, Newfoundland Mineral Resources Division. Nfld. MDD File - Nfld (257).

Fogwill, W.D.
    1964: Diatomaceous earth survey. Unpublished Report, Newfoundland Mineral Resources Division. Nfld. MDD File - Nfld (348).

Green, R.E.
    1981: Genesis of the La Manche Vein and comparisons with similar Caledonide Deposits. Unpublished B.Sc. Thesis, Memorial University of Newfoundland, Nfld. MDD File - 1N/12 (426).

Figure 4: *Sketch map of the Shoal Point/ Port au Port Peninsula, showing sample site locations.*

Harris, I.
    1962: Report on the Limestone-Shale Survey in Newfoundland. Mineral Resources Division. Nfld. MDD File - Nfld (216).

Howse, A.F., Butler, A.J. and Collins, C.J.
    1984: Stream Sediment Geochemistry of the Bellevue Map Area (1N/12) Avalon Peninsula, Newfoundland. Newfoundland Department of Mines and Energy, Mineral Development Division. Nfld. MDD File - Nfld (452).

Howse, A.F., Butler, A.J. and Collins, C.J.,
    1984: Stream Sediment Geochemistry of the St. Brides Area (1L/16), Avalon Peninsula, Newfoundland. Newfoundland Department of Mines and Energy, Mineral Development Division. Nfld. MDD File - Nfld 1L/16 (91).

Howse, A.F., and Collins, C.J.
    1984: Barite Evaluation in Three Areas of Southeastern Newfoundland. *In* Current Research. *Edited by* M.J. Murray, J.G. Whelan and R.V. Gibbons. Newfoundland Department of Mines and Energy, Mineral Development Division, Report 84-1, pages 263-266.

Howse, A.F., and French, V.A.
    1983: Barite Evaluation Eastern and Western Newfoundland. *In* Current Research. *Edited by* M.J. Murray, P.D. Saunders, W.D. Boyce and R.V. Gibbons. Newfoundland Department of Mines and Energy. Mineral Development Division, Report 83-1, pages 150-156.

McCartney, W.D.
    1956: Dildo, Newfoundland. Geological Survey of Canada. Map 13-1956.

McCartney, W.D.
    1957: Whitbourne Map Area, Newfoundland. Geological Survey of Canada, Memoir 341, 135 pages.

O'Brien, S.J., Strong, P.C., and Evans, J.L.
    1977: The Geology of the Grand Bank (1M/4) and Lamaline (1L/13) Map areas, Burin Peninsula, Newfoundland. Newfoundland Department of Mines and Energy, Mineral Development Division, Report 77-7, 16 pages.

Strong, D.F., O'Brien, S.J., Strong, P.G., Taylor, S.W., and Wilton, D.H.
    1978: Geology of the Marystown (1M/3) and St. Lawrence (1L/14) map areas, Newfoundland. Newfoundland Department of Mines and Energy, Mineral Development Division, Report 77-8, 81 pages.

Smith, W.S.
    1957: St. Lawrence Area, Newfoundland - report on Fluorspar. Unpublished report for Newfoundland Fluorspar Limited Nfld. MDD File - 1L/14 (16).

Van Alstine, R.E.
    1948: Geology and Mineral Deposits of the St. Lawrence Area, Burin Peninsula, Newfoundland. Newfoundland Geological Survey, Bulletin, No. 23, 64 pages.

Teng, H.C.
  1974: A Lithogeochemical Study of the
  St. Lawrence Granite, Newfoundland.
  Unpublished M.Sc. thesis, Memorial
  University of Newfoundland, St.
  John's, 194 pages.

Teng, H.C. and Strong, D.F.
  1976: Geology and Geochemistry of the
  St. Lawrence Peralkaline Granite and
  Associated Fluorite Deposits, South-
  eastern Newfoundland. Canadian Journal
  of Earth Sciences, Volume 13, page
  1374-1385.

Author Index/Index des auteurs

NOTE TO CONTRIBUTORS

Submissions to the *Discussion* section of *Current Research* are welcome from both the staff of the Geological Survey and from the public. Discussions are limited to 6 double-spaced typewritten pages (about 1500 words) and are subject to review by the Chief Scientific Editor. Discussions are restricted to the scientific content of Geological Survey reports. General discussions concerning branch or government policy will not be accepted. Illustrations will be accepted only if, in the opinion of the editor, they are considered essential. In any case no redrafting will be undertaken and reproducible copy must accompany the original submissions. Discussion is limited to recent reports (not more than 2 years old) and may be in either English or French. Every effort is made to include both *Discussion* and *Reply* in the same issue. *Current Research* is published in January and July. Submissions should be sent to the Chief Scientific Editor, Geological Survey of Canada, 601 Booth Street, Ottawa, Canada, K1A 0E8.

AVIS AUX AUTEURS D'ARTICLES

Nous encourageons tant le personnel de la Commission géologique que le grand public à nous faire parvenir des articles destinés à la section *discussion* de la publication *Recherches en cours.* Le texte doit comprendre au plus six pages dactylographiées à double interligne (environ 1500 mots), texte qui peut faire l'objet d'un réexamen par le rédacteur en chef scientifique. Les discussions doivent se limiter au contenu scientifique des rapports de la Commission géologique. Les discussions générales sur la Direction ou les politiques gouvernementales ne seront pas acceptées. Les illustrations ne seront acceptées que dans la mesure où, selon l'opinion du rédacteur, elles seront considérées comme essentielles. Aucune retouche ne sera faite aux textes et dans tous les cas, une copie qui puisse être reproduite doit accompagner les textes originaux. Les discussions en français ou en anglais doivent se limiter aux rapports récents (au plus de 2 ans). On s'efforcera de faire coincider les articles destinés aux rubriques *discussions* et *reponses* dans le même numéro. La publication *Recherches en cours* paraît en janvier et en juillet. Les articles doivent être renvoyés au rédacteur en chef scientifique: Commission géologique du Canada, 601, rue Booth, Ottawa, Canada, K1A 0E8.